Determining Previously Undefined Immune Regulatory Networks in Regulatory T Cells and Innate Lymphoid Cells within the Tumour Microenvironment

Jing Xuan Lim

A thesis submitted for the degree of Doctor of Philosophy

Bioscience Institute

Newcastle University

March 2025

Abstract

Regulatory T cells (Tregs) are essential for immune suppression, employing multiple mechanisms, including co-inhibitory receptor expression. However, the role of the programmed cell death-1 receptor (PD-1) in Treg function remains controversial. Here, we identify PD-1 as a key checkpoint in Tregs, orchestrating a unique co-inhibitory receptor network that shapes their function in tumour immunity. We demonstrate that PD-1 regulates the expression and activity of CD30, a central driver of Treg suppressive function within the tumour microenvironment (TME). Mechanistically, PD-1 deficiency amplifies STAT5 signalling in Tregs, leading to upregulated CD30 expression and thus suppressive capacity. Consistently, in stage IV metastatic melanoma patients, anti-PD-1-resistant individuals exhibit increased CD30 expression on Tregs compared to responders. Thus, we uncover a novel role for PD-1 in restraining CD30 expression, thereby modulating Treg-mediated immunosuppression. These insights provide a rationale for targeting PD-1 and CD30 in combination therapies to improve cancer treatment outcomes. Innate lymphoid cells (ILCs) also play a crucial role in tissue immunity and are influenced by co-receptor signalling. Here, we define a subset of tumour-infiltrating ILCs characterised as $Tbet^{+}NK1.1^{-}$, which express PD-1 within the TME. We demonstrate that PD-1 profoundly regulates the function of $Tbet^{+}NK1.1^{-}$ ILCs in murine B16 melanoma. PD-1-deficient $Tbet^{+}NK1.1^{-}$ ILCs exhibit significantly increased production of IFN-γ, granzyme B, and granzyme K, correlating with diminished tumour growth. These findings highlight a novel regulatory axis through which PD-1 modulates anti-tumour responses in ILCs, suggesting potential therapeutic avenues to enhance immune-mediated tumour clearance.

Acknowledgement

First and foremost, I would like to express my deepest gratitude to my supervisor, Dr. Shoba Amarnath, for her invaluable guidance, unwavering support, and mentorship throughout my research journey. Her insights and encouragement have been instrumental in shaping this work. I am also immensely grateful to my co-supervisors, Dr. James Dawson and Prof. Marloes Peeters, for their constructive feedback, expertise, and continuous support.

I extend my sincere appreciation to my colleagues, Dr. Katie Smith, Tegan McTaggart and Bronagh Heaney for their camaraderie and technical assistance. I would also like to acknowledge Dr. Arian Laurence, Dr. John O'Shea, Prof. Graham Anderson, Dr. Hong-Wei Sun, and Dr. Jérémie Nsengimana for their valuable advice and suggestions, which have greatly enriched this research.

A special thank you to the Flow Cytometry Core Facility team for their technical expertise and support in flow cytometry techniques. I am also grateful to the Comparative Biology Centre team for their training and assistance with animal experimental techniques.

I am grateful to my PhD viva examiners, Prof. Graham Anderson and Prof. John Isaacs, for their insightful discussion, and to my progression panel, Dr. Amy Anderson and Dr. Lei Huang, for their thoughtful guidance over the past three years.

I am deeply grateful to my family—my father, Eng Lee Lim, my mother, Siew Seah Tan, my brother, Zheng Wei Lim, and my sister, Jing Yi Lim. Their belief in me has been my greatest source of strength. I would also like to acknowledge my friends, Jingyu Dong, Kexin See, Min Yu Yim and Xing Yee Low for their mental support and kindness, which have been invaluable throughout this journey. A special thanks to my partner and friend, Dr. Yuan Wang, for his thoughtful care and insightful discussions on code generation.

I would also like to acknowledge the financial support provided by the NC3Rs PhD studentship and the Newcastle University Overseas Research Scholarship, which made this research possible.

Lastly, I extend my gratitude to those individuals who have supported me in various ways throughout this journey, even if they are not mentioned by name. This thesis would not have been possible without the support of all these individuals, and I am truly thankful for their contributions to both my research and personal growth.

Declaration

I hereby declare that the work presented in this thesis is original and has not been submitted, in whole or in part, for the award of any other degree or professional qualification. All research and analysis contained within this thesis were conducted by me unless otherwise stated, and all sources of information have been properly acknowledged by reference. Collaborative contributions have been explicitly indicated and duly recognised.

Name: Jing Xuan Lim

Signature:

Date: 06/03/2025

Table of Contents

Abstract i

Acknowledgement ii

Declaration iii

Abbreviations xii

Chapter 1 Introduction 1

1.1 Principles of T cell-mediated immunity in cancer 1

1.2 Discovery and nomenclature of regulatory T cell 3

1.3 Thymic development of regulatory T cells 4

1.4 Peripheral development of regulatory T cells 6

1.5 Can tTregs be distinguished from pTregs? 7

1.6 Treg plasticity 8

1.6.1 Th1-like Treg 9

1.6.2 Th2-like Treg 11

1.6.3 Th17-like Treg 12

1.6.4 Tfh like-Treg 13

1.7 Regulation of Foxp3 expression and its epigenetic stability 15

1.7.1 T cell receptor signalling 16

1.7.2 IL-2-Induced JAK/STAT Signalling 18

1.7.3 TGF-β/Smad Signalling 19

1.7.4 Epigenetic Regulation of FoxP3 Expression 19

1.7.5 Post-translational modulation 20

1.8 Co-inhibitory receptors on Tregs 22

1.8.1 CTLA-4 24

1.8.2 PD-1 25

1.8.3 TIGIT 26

1.8.4 LAG-3 27

1.8.5 TIM3 28

1.8.6 GITR 29

1.8.7 CD30 30
1.8.8 GARP 31

Chapter 2 Materials and Methods 33

2.1 Mice 33

2.2 Patient characteristics 35

2.3 Reagents 35

2.4 B16F10 melanoma tumour model 36

2.5 Mouse tissue isolation and single cell preparation 36

2.5.1 Spleen and mesenteric lymph node 36
2.5.2 Liver 37
2.5.3 Bone marrow 37
2.5.4 Tumour-infiltrating lymphocyte isolation 37
2.5.5 Tumour-draining lymph nodes 38

2.6 Human peripheral blood mononuclear cell isolation 38

2.7 Flow cytometry and cell sorting 38

2.7.1 Cell viability staining 38
2.7.2 Surface staining 38
2.7.3 Intracellular staining for cytokines and transcription factors 39
2.7.4 Intracellular staining for phospho-proteins 39
2.7.5 Cell sorting 43
2.7.6 Data analysis 43

2.8 *In vitro* assays 43

2.8.1 Cell proliferation assay 43
2.8.2 Apoptotic assay 44
2.8.3 Treg suppressor assay 44
2.8.4 PD-L1 molecular mechanistic study 44
2.8.5 Phospho-STAT5 assay 45
2.8.6 In vitro culture of melanoma patient PBMCs 45

2.9 BD Rhapsody single-cell RNA sequencing 45

2.9.1 Cell preparation for scRNA-seq 45

2.9.2 Single cell library preparation and sequencing *46*
2.9.3 Preprocessing of scRNA-seq data *46*
2.9.4 Cell annotation for single-cell RNA-seq analysis *47*
2.9.5 Differential gene expression and pseudotime trajectory analysis *48*
2.9.6 Cell-cell communications *49*
2.10 NanoString CosMx™ Spatial Molecular Imaging **49**
2.10.1 Tissue processing *49*
2.10.2 Image acquisition and cell segmentation *50*
2.10.3 Pre-processing of spatial transcriptomics data *50*
2.10.4 Data analysis *50*
2.10.5 Spatially resolved cell-cell interaction analysis *51*
2.11 RT-qPCR **51**
2.11.1 RNA extraction from Tregs *51*
2.11.2 RT-qPCR assay *52*
2.11.3 RT-qPCR data analysis *52*
2.12 Chromatin immunoprecipitation sequencing analysis **52**
2.13 RNA Sequencing Analysis **52**
2.14 CD30 Biomarker Analysis **53**
2.15 ILC data analysis **53**
2.15.1 Analysis of scRNA-seq data *53*
2.15.2 Analysis of TIL immunobiology assay data *54*
2.15.3 Analysis of transwell assay data *54*
2.15.4 Analysis of in-vitro proliferation assay data *54*
2.15.5 Analysis of lactate assay data *54*
2.15.6 Analysis of Phospho-P70S6K data *55*
2.16 Statistical analysis **55**
2.17 Data availability statement **55**
2.18 Code availability statement **56**
Chapter 3 PD-1 dampens regulatory T cell function by controlling a unique co-inhibitory receptor landscape in steady state **57**

3.1 Introduction 57

3.2 Aims 58

3.3 Results 58

3.3.2 Pd1$^{-/-}$ Tregs do not differ in proliferation or apoptosis in steady state 62

3.3.3 PD-1 regulates a unique coreceptor network in Tregs in steady state 64

3.3.4 PD-1 intrinsically controls CD30 expression in Tregs 66

3.3.5 CD30 expression is driven by STAT5 signalling in Pd1$^{-/-}$ Treg 71

3.4 Discussion 75

3.5 Summary 76

Chapter 4 PD-1 deficiency enhances tumour-derived Treg function through the CD30/CD30L pathway 77

4.1 Introduction 77

4.2 Aims 77

4.3 Results 78

4.3.1 Pd1$^{-/-}$ Tregs possess greater suppressive capacity and promote tumour growth 78

4.3.2 BD Rhapsody single-cell analysis identifies CD30 as a potential candidate for enhanced Pd1$^{-/-}$ Treg function in melanoma 80

4.3.3 Functional validation of scRNA-seq analysis within the TME 84

4.3.4 Pd1$^{-/-}$ Treg exhibit several differentiation programs and enhanced crosstalk with NK cells within the TME 88

4.3.5 Functional validation of CellChat analysis within the TME 93

4.3.6 Spatial transcriptomics confirm Pd1$^{-/-}$ Treg differentiation states and communication network within the TME 94

4.3.7 PD-1 disruption, not the tumour microenvironment, drives CD30 expression in human Tregs 101

4.4 Discussion 107

4.5 Summary 110

Chapter 5 PD-1 negatively regulates the function of Tbet^{+}RORγt^{-}NK1.1^{-} NKp46^{-}EOMES^{-}ILCs in tumour microenvironment 112

5.1 Introduction 112

5.2 Aims 115

5.3 Results 116

5.3.1 BD Rhapsody single-cell RNA sequencing analysis reveals PD-1 expression in Tbet^{+}NK1.1^{-} ILC subpopulation in B16F10 melanoma tumour 116

5.3.2 Flow cytometry analysis reveals a novel Tbet^{+}NK1.1^{-}ILC subset in healthy WT and Pd1$^{-/-}$ mice 119

5.3.3 PD-1 deficiency specifically enhances Tbet^{+}NK1.1^{-}Eomes^{-}ILCs within the TME and TDLN. 121

5.3.4 PD-1 controls IFN-γ production in Tbet^{+}NK1.1^{-} ILCs within the TME..... 123

5.3.5 PD-1 controls proliferation of Tbet^{+}NK1.1^{-} ILCs within the TME..... 125

5.4 Discussion 129

5.5 Summary 133

Chapter 6 Discussion 134

6.1 Future directions 139

References 141

Appendix A 178

Appendix B 180

Appendix C 281

Appendix D 302

Appendix E 563

Appendix F 565

List of Figures

Figure 1.1 Overview of T cell subsets. 2
Figure 1.2 Developmental stages of thymocytes in thymus. 5
Figure 1.3 Development of tTregs, pTregs and iTregs from $CD4^+$ thymocytes. 6
Figure 1.4 Th-like Treg plasticity. 9
Figure 1.5 Transcriptional regulation and epigenetic modification of FoxP3. 15
Figure 1.6 TCR/CD3 complex and CD28 downstream signalling pathways. 17
Figure 1.7 Post-translational modifications of FOXP3 and their impact on Treg function. 21
Figure 1.8 Canonical co-inhibitory receptors on Tregs and their corresponding receptor-ligand interactions. 23
Figure 2.1 Breeding Scheme for *Pd1*$^{-/-}$*Foxp3*^{RFP}. 33
Figure 2.2 Generation of *Pd1*$^{fl/fl}$ and *Pd1*$^{fl/fl}$*Foxp3*^{ERT2Cre} mice. 34
Figure 3.1 PD-1 deficient Tregs exhibit an activated phenotype. 60
Figure 3.2 PD-1 deficient Tregs exhibit enhanced suppressive capacity. 62
Figure 3.3 PD-1 deficient Tregs do not differ in proliferation or apoptosis phenotype. 64
Figure 3.4 PD-1 deficient Tregs upregulates a unique network of co-inhibitory receptors. 65
Figure 3.5 Generation of mice inducibly ablating PD-1-expressing cells and selectively lacking PD-1 on Tregs. 66
Figure 3.6 PD-1 deficient Tregs upregulates a unique network of co-inhibitory receptors including CD30. 68
Figure 3.7 PD-1 deficient Tregs exhibit increased CD30 mRNA expression. 69
Figure 3.8 PD-1 intrinsically regulates CD30 expression in Treg. 71
Figure 3.9 PD-1 regulates IL-2-STAT5 driven CD30 expression in Tregs. 73
Figure 3.10 IL-2-STAT5 drives CD30 expression in $CD4^+$ T lymphocytes. 75
Figure 4.1 *Pd1*$^{-/-}$ Tregs possessed greater suppressive capacity in B16 *in vivo* model. 79
Figure 4.2 BD Rhapsody scRNA-seq reveals the presence of Tregs in WT and *Pd1*$^{-/-}$ cohorts in the B16 TME. 81
Figure 4.3 BD Rhapsody scRNA-seq analysis identifies CD30 as a potential marker for enhanced *Pd1*$^{-/-}$ Treg cell function within the TME. 83
Figure 4.4 CD30-expressing *Pd1*$^{-/-}$ Tregs enhances tumour burden in B16 *in vivo* model. 85
Figure 4.5 Blockade of CD30 in *Pd1*$^{-/-}$ Tregs reduces tumour burden in B16 *in vivo* model. 87
Figure 4.6 Pseudotime trajectory analysis of WT and *Pd1*$^{-/-}$ Tregs in murine B16 TME. 89

Figure 4.7 CellChat analysis reveals the communication network in WT and *Pd1*$^{-/-}$ TILs within the murine B16 TME. 91
Figure 4.8 CellChat analysis reveals the communication network of Tregs, NK cells and myeloid DCs with other TILs in the murine B16 TME. 92
Figure 4.9 *Pd1*$^{-/-}$ Tregs exhibit multiple differentiation states and are associated with altered NK cell and DC frequencies. 94
Figure 4.10 CosMx^{TM} spatial transcriptomics visualise cell-cell interaction within the B16 TME. 96
Figure 4.11 CosMx^{TM} spatial transcriptomics analysis reveals interaction network of Tregs within the B16 TME. 98
Figure 4.12 CosMx^{TM} spatial transcriptomics analysis reveals CD30L expression in TME cells and identifies Treg sub-states within the B16 TME. 100
Figure 4.13 BD Rhapsody scRNA-seq reveals cell cluster gene expression in human PBMCs from healthy controls and melanoma patients. 102
Figure 4.14 ScRNA-seq reveals cell cluster gene expression in human TILs from treatment naive melanoma patients. 104
Figure 4.15 Blockade of PD-1 signalling enhances CD30 expression in Tregs from melanoma patients *in vitro*. 105
Figure 4.16 ScRNA-seq reveals cell cluster gene expression in human TILs from baseline and anti-PD-1 treated melanoma patients. 106
Figure 4.17 CD30 as a predictive marker for poor survival in multiple cancers. 107
Figure 5.1 Single-cell RNA sequencing analysis reveals Tbet^{+}NK1.1^{-} ILCs within the tumour microenvironment. 117
Figure 5.2 Single-cell RNA sequencing analysis reveals PD-1 expression in Tbet^{+} NK1.1^{-} ILCs within the tumour microenvironment. 118
Figure 5.3 Frequency of Tbet^{+}NK1.1^{-} ILCs in WT and *Pd1*$^{-/-}$ mice under homeostatic conditions. 120
Figure 5.4 Frequency of Tbet^{+}NK1.1^{-} ILCs in WT TBG and *Pd1*$^{-/-}$ TBG mice within the TME. 122
Figure 5.5 PD-1 deficiency significantly increases IFN-γ^{+}Tbet^{+}NK1.1^{-} ILCs within the B16 melanoma TME. 124
Figure 5.6 Lactic acid derived from B16 melanoma tumours significantly increases PD-1 expression on Tbet^{+}NK1.1^{-} ILCs. 126

Figure 5.7 PD-1 inhibits the proliferative capacity of Tbet^{+}NK1.1^{-} ILCs within the B16 TME. 127
Figure 5.8 PD-1 deficiency significantly enhances fatty acid metabolism and glycolysis in Tbet^{+}NK1.1^{-} ILCs within the B16 melanoma TME. 129

Abbreviations

7AAD: 7-aminoactinomycin D

ADAM: a disintegrin and metalloproteinase

AEP: asparaginyl endopeptidase

AHR: aryl hydrocarbon receptor

AIRE: autoimmune regulator

Akt: protein kinase B

ALCL: anaplastic large cell lymphomas

AOM-DSS: azoxymethane-dextran sodium sulphate

AOM: azoxymethane

AP-1: activator protein 1

APC: antigen presenting cell

Areg: amphiregulin

BAT3: HLA-B-associated transcript 3

Bcl2: B-cell leukemia/lymphoma 2 protein

BM-APC: bone-marrow derived antigen-presenting cell

CDK2: cyclin-dependent kinase 2

CEACAM1: carcinoembryonic antigen-related cell adhesion molecule 1

ChIP-seq: chromatin immunoprecipitation sequencing

CNS: conserved non-coding DNA sequence

CpG: cytosine-phosphate-guanine

cSCC: cutaneous squamous cell carcinoma

cTEC: cortical thymic epithelial cells

CTL: cytotoxic T lymphocyte

CTLA-4: cytotoxic T lymphocyte antigen-4

CTV: cell trace violet

CXCR: CXC chemokine receptor

DAG: diacylglycerol

DC: dendritic cell

DGE analysis : differential gene expression analysis

DN: double-negative

DP: double-positive

DSS: dextran sulphate sodium

DT: diphtheria toxin

DTR: diphtheria toxin receptor

Eomes: eomesodermin

ERT2-Cre: Cre recombinase-mutated estrogen receptor

ES cell: embryonic stem cell

FACS buffer: flow cytometry staining buffer

FAO: fatty acid oxidation

FFPE: formalin-fixed paraffin-embedded

fl: flox

FMO: fluorescence minus one

FOV: field of view

FoxP3: transcription factor Forkhead box-p3

Foxp3^{ERT2Cre}: *Foxp3*$^{Ert2\text{-}Cre\text{-}GFP}$

FRT: flippase-recognition sites

Gal: galectin

GAP: GTPase-activating protein

GARP: Glycoprotein A repetitions predominant

GATA3: GATA binding protein 3

GEO: gene expression omnibus

GFP: green fluorescent protein

GITR: glucocorticoid-induced tumour necrosis factor receptor-related protein

GM-CSF: granulocyte macrophage colony-stimulating factor

GO: gene ontology

Grb2: growth factor receptor-bound protein-2

GSEA: gene set enrichment analysis

GvHD: graft versus host disease

Gzm: granzyme

H&E: haematoxylin and eosin

HRP: horseradish peroxidase

ICB: immune checkpoint blockade

Icos: inducible T-cell costimulator

IFN-γR: IFN-γ receptor

IFN: interferon

IGV: Integrated Genome Viewer

IKK: IκB kinase

IL-2R: IL-2 receptor

IL: interleukin

ILC: innate lymphoid cell

ILC1: group 1 ILC

ILC2: group 2 ILC

ILC3: group 3 ILC

ILCP: ILC precursor

IP: intraperitoneal

IP_3: inositol triphosphate

IRES: Internal ribosome entry sites

IRF8: interferon regulatory factor 8

ITAM: immunoreceptor tyrosine-based activation motifs

ITIM: immunoreceptor tyrosine-based inhibitory motif

iTregs: *in vitro*-generated Tregs

ITSM: immunoreceptor tyrosine-based switch motif

ITT: immunoglobulin tail tyrosine

IV: intravenous

Jak: Janus kinase

Ki67: Kiel 67

KNN: K-nearest neighbor graph

LA: lactic acid

LAG-3: lymphocyte-activation gene 3

LAP: latency associated peptide

LAT: linker for activated T cell

lg: ligand

LR: long range

LRR: leucine-rich repeat

LSECtin: lymph node sinusoidal endothelial cell C-type lectin

LSM: lymphocyte separation media

LTGF-β: latent TGF-β

LTi: lymphoid tissue inducing

LTiP: LTi precursor

mAb: monoclonal antibody

MAPK: mitogen-activated protein kinase

MCA: methylcholanthrene

Mel: Melanoma patient

MHC: major histocompatibility complex

mTEC: medullary thymic epithelial cells

mTOR: mammalian or mechanistic target of rapamycin

Natural killer cell: NK cell

NCBI: National Center for Biotechnology Information

NCR: natural cytotoxicity receptor

NEMO: NFκB essential modulator

Neo: neomycin

NFκB: nuclear factor kappa-B

NFAT: nuclear factor of activated T cells

NHSBT: NHS Blood and Transplant

NK: natural killer cell

NKP: NK precursor

Nrp-1: neuropilin-1

ORR: overall response rate

p-STAT5: phospho-STAT5

P2A: peptide 2A

PBMC: peripheral blood mononuclear cell

PBS: phosphate buffered saline

PCA: principal component analysis

PD-1: programmed cell death-1 receptor

PD-L1: programmed cell death ligand 1

PD-L2: programmed cell death ligand 2

Pd1: Pdcd1

$Pd1^{fl/fl}$: $Pdcd1^{fl/fl\text{-}DTR\text{-}tdTomato}$

$Pd1^{fl/fl}Foxp3^{ERT2Cre+/-}$: $Pd1^{fl/fl}Foxp3^{ERT2crehet}$

pDC: plasmacytoid dendritic cell

PI3K: phosphatidylinositol 3-kinase

PIP_2: phosphatidylinositol biphosphate

PKC-θ: protein kinase C

PLC-γ: Phospholipase C-γ

PP1: protein phosphatase 1

Pre-TCR: pre-T-cell receptor

pSTAT5: phospho-STAT5

PtdSer: phosphatidylserine

PTEN: Phosphatase and tensin homologue

PTM: post-translational modification

pTreg: peripherally derived Treg

RasGRP: Ras guanyl nucleotide releasing protein

RBC: red blood cell

rh: recombinant human

rmPD-L1 Fc: recombinant mouse PD-L1 Fc chimera protein

RNA-seq: RNA sequencing

RNA: ribonucleic acid

ROR: retinoic acid-related orphan receptor

ROS: high reactive oxygen species

RT-qPCR: real-time quantitative polymerase chain reaction

RT: room temperature

SC: subcutaneous

scRNA-seq: single-cell RNA sequencing

SEM: standard error of mean

SHIP1: SH2-containing inositol phosphatase 1

SHP: SH2-domain containing tyrosine phosphatase

SIRT1: sirtuin 1

sLAG-3: soluble LAG-3

SMAC: supramolecular activation cluster

SMI: Spatial Molecular Imaging

SP: single-positive

SR: short range

STAT: signal transducer and activator of transcription

Tbet: T-box-containing protein expressed in T cells

t-SNE: t-Distributed Stochastic Neighbour Embedding

TAP: Technology Access Program

TBG: Tbet-ZsGreen

Tconv: conventional T

TCR: T cell receptor

TDLN: tumour-draining lymph node

Teff cell: effector T cell

Tet: 10-11 translocation

Tfh: Follicular Th

Tfr: T follicular regulatory cell or Tfh-like Treg

TGF: transforming growth factor

Th cells: helper T cells

TIGIT: T-cell immunoreceptor with Ig and ITIM domains

TIL: tumour-infiltrating lymphocyte

TIM-3: T-cell immunoglobulin and mucin-domain containing-3

TME: tumour microenvironment

TNF: tumour necrosis factor

TNFR: tumour necrosis factor receptor

Tr1: T regulatory type 1

TRAF: TNF receptor-associated factors

Treg: regulatory T cell

TSDR: Treg specific demethylated region

TSLP: thymic stromal lymphopoietin

tTreg: thymically-derived Treg

TβRII: TGF-β type II receptor

UMAP: uniform manifold approximation and projection

UMI: unique molecular identifier

USP7: ubiquitin-specific peptidase

WT: wild type

α-syn: α-synuclein fibrils

α: antibody

Chapter 1 Introduction

1.1 Principles of T cell-mediated immunity in cancer

In the late nineteenth century, the concept of an epidemiological association between immunity and cancer was firstly conceived by Wilhelm Busch and Friedrich Fehleisen (Busch, 1868). This idea was further identified by William Coley who was also known as 'Father of Cancer Immunotherapy'. He demonstrated the effect of 'Coley's toxins' comprising of heat-inactivated *Streptococcus pyogenes* and *Serratia marcescens* to stimulate anti-cancer immunity, thereby achieving favourable responses in patients with various cancers (Nauts et al., 1946, Coley, 1893). Later, Lewis Thomas (Thomas, 1982) and Sir Frank Macfarlane Burnet (Burnet, 1970) formulated the cancer immunosurveillance hypothesis, proposing that cytotoxic lymphocytes are able to recognise tumour-associated neoantigens as foreign antigens and eradicate tumour cells. The validity of the immunosurveillance hypothesis was further supported by evidence from experimental murine models. Immunocompromised mice lacking a functional interferon-gamma (IFN-γ) receptor (i.e., IFN-γ receptor deficient mice and STAT-1 deficient mice) were more susceptible to methylcholanthrene (MCA)-induced carcinogenesis than wild type (WT) mice, leading to more rapid growth of tumours (Kaplan et al., 1998). In summary, unequivocal evidence showed the immune cells, especially T cells which can secrete IFN-γ, are capable of waging war against cancer.

T cells circulate through the bloodstream and tissue to defend against infection, disease and cancer. T cells can be divided into $CD8^+$ cytotoxic T lymphocytes (CTLs) and $CD4^+$ T cells. CTLs can kill infected cells directly via secretion of cytotoxic granules perforin and granzyme B. In response to T cell receptor (TCR) engagement, co-receptor stimulation and cytokine signals, $CD4^+$ T cells can differentiate into specific lineages including conventional T helper (Th) cells and regulatory T cells (Tregs), which are defined based on their patterns of cytokine production and master transcription factors (**Figure 1.1**).

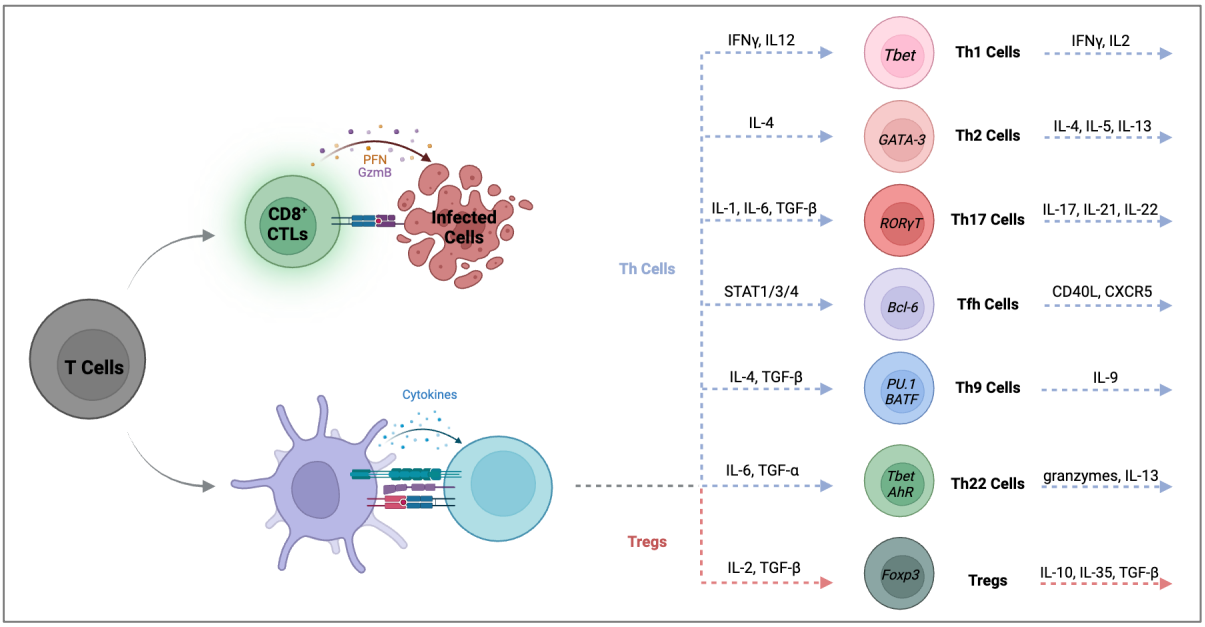

Figure 1.1 Overview of T cell subsets.
T cells consist of $CD8^+$ cytotoxic T lymphocytes (CTLs) and $CD4^+$ T cells. $CD8^+$ CTLs kill infected cells by releasing perforin (PFN) and granzyme B (GzmB). Upon TCR, co-stimulatory and cytokine signalling, $CD4^+$ T cells can further differentiate into either helper T (Th) cells: Th1, Th2, Th17, Tfh, Th9 and Th22, or Tregs based on the master transcription factor expressed and cytokines secreted.

The strength of the TCR signal and cytokines play a key role in Th cell polarisation, allowing Th cells to promote adaptive immunity and induce inflammation. In response to IFN-γ and interleukin-12 (IL-12), Tbet expression is promoted to form Th1 cells producing IFN-γ and IL-2 (Szabo et al., 2000). They are specialised in supporting the cytotoxic properties of CTLs, natural killer cells and macrophages against intracellular pathogen-infected cells. Th2 cells are characterised by GATA-3 expression (Zheng and Flavell, 1997) along with IL-4, IL-5 and IL-13 secretion upon IL-4 sensing. They are important for the elimination of helminths. Alongside the cytokine environment, van Panhuys *et al.* have shown that strong TCR signals drive the differentiation of Th1 cells, while weaker signals promote Th2 cell differentiation (van Panhuys et al., 2014). In the presence of IL-1, IL-6 and transforming growth factor β (TGF-β), RORγt expression is induced to generate Th17 cells secreting IL-17, IL-21 and IL-22 (Zheng and Flavell, 1997, Bettelli et al., 2006). These cytokines are required to control extracellular bacteria and fungi. Follicular Th (Tfh) cells are characterised by the expression of transcription factor Bcl-6, surface protein CD40L and CXC chemokine receptor 5 (CXCR5) in response to signal transducer and activator of transcription 1 (STAT1), STAT3 and STAT4 signals (Winstead, 2014). Of particular interest, CXCR5 promotes a migratory phenotype of Tfh cells towards follicle to interact with B cells through CD40L (Deenick and Ma, 2011). The crosstalk between Tfh cells and B cells results in germinal centre formation and B-cell isotype

switching. Th9 cells are characterised by two transcription factors PU.1 and BATF (Jabeen et al., 2013), alongside cytokine IL-9 secretion in response to IL-4 and TGF-β (Zhao et al., 2013, Li et al., 2017). Like Th2 cells, Th9 cells act against parasites. In the presence of IL-6 and TGF-α, the expression of transcription factors Tbet and AhR is induced, forming Th22 cells which can provide host defence in mucosal tissues and epithelia by secreting granzymes and IL-13 (Plank et al., 2017). Contrary to Th cells, Tregs suppress pathological immune responses directed against self-antigens, foreign antigens, and commensal microorganisms. Together with anti-CD3/28 signalling, TGF-β and IL-2 cytokines can initiate and maintain the transcription factor Forkhead box-p3 (FoxP3) expression, driving the differentiation of regulatory T cell (Treg) which secretes TGF-β and IL-10 (Chen et al., 1994, Levings et al., 2001). Further details on Treg development, differentiation, cytokine secretion, and plasticity will be discussed in this chapter.

1.2 Discovery and nomenclature of regulatory T cell

The concept of suppressor T cells was firstly proposed by Gershon and Kondo in 1970 (Gershon and Kondo, 1970). They demonstrated several types of suppressor T cells with different phenotypes and modes of actions (Green et al., 1983). However, a controversial atmosphere of using "suppressor T cells" to interpret suppressive immunological phenomena formed in late 1980s due to the lack of reliable markers. To distinguish suppressor T cells from other $CD4^+$ T cell subsets, number of attempts were carried out on naïve mice. Sakaguchi *et al.* and Sugihara *et al.* transferred $CD5^{low}CD4^+$ T cells to T cell-deficient BALB/c athymic nude mice (Sakaguchi et al., 1985) and T cell depleted C3H mice (Sugihara et al., 1988) respectively. Both mice developed autoimmune disease after cell transfer. This situation could be prevented when $CD5^{low}CD4^+$ T cells were co-transferred with normal untreated $CD4^+$ T cells (Sakaguchi et al., 1985). In 1990, Powrie and Mason showed that transfer of $CD45RC^{high}CD4^+$ T cells into PVG athymic nude rats could induce a severe wasting disease, leading to inflammation of multiple organs (Powrie and Mason, 1990). Furthermore, Powrie *et al.* transferred alternative $CD45RB^{high}CD4^+$ T cells to severe combined immunodeficient BALB/c mice, resulting in development of induced inflammatory bowel disease (Powrie et al., 1993). Again, co-transfer of the $CD45RB^{low}CD4^+$ T cells could prevent this autoimmune response, highlighting the regulatory relationship between the $CD45RB^{high}$ and $CD45RB^{low}$ $CD4^+$ T cell subsets.

In 1995, Sakaguchi *et al.* discovered CD25 which is a more ideal marker than CD5, CD45RB and CD45RC (Sakaguchi et al., 1995, Asano et al., 1996). It has been found to be specifically

expressed by 5-10% of peripheral $CD4^+$ T cells and less than 1% of peripheral $CD8^+$ T cells in normal naïve mice. In BALB/c athymic nude mice, transfer of $CD25^+CD4^+$ T cells elicited autoimmune disease at higher incidences than numerous $CD5^{low}$ or $CD45RB^{high}$ T cells, and this disease could be suppressed by co-transferring small number of $CD25^+CD4^+$ T cells (Suri-Payer et al., 1998, Asano et al., 1996, Sakaguchi et al., 1995). Without using $CD25^+CD4^+$ thymocytes, similar autoimmune diseases could be reproduced in syngeneic athymic nude mice (Itoh et al., 1999). Furthermore, removal of $CD25^+CD4^+$ T cells has been shown to enhance immune defences against non-self-antigens (Sakaguchi et al., 1995). Taken together, these phenomena revealed that thymic $CD25^+$ $CD4^+$ T cells play an indispensable role in maintaining self-tolerance and regulating immune responses towards foreign antigens, thus this specific subset of suppressive T cells was renamed as regulatory T cells (Tregs) (Sakaguchi et al., 2007). Significant advances in Treg biology were made with the identification of a gene located on the X chromosome, known as *foxp3*, which was discovered while investigating the genetic origins of autoimmune diseases, particularly in individuals with immune dysregulation, polyendocrinopathy, enteropathy, X-linked (IPEX) syndrome (Bennett et al., 2001, Chatila et al., 2000, Wildin et al., 2001) and in the scurfy mouse model (Brunkow et al., 2001). Mutations in *foxp3* that impair its function led to fatal, early-onset lymphoproliferative diseases in both humans and mice, causing widespread damage to various tissues and organs. Further studies demonstrated that Foxp3 is expressed at high levels specifically in Tregs, and its expression is crucial for Treg differentiation (Fontenot et al., 2003, Hori et al., 2003, Khattri et al., 2003, Wan and Flavell, 2007). Continuous expression of Foxp3 in mature Treg cells is required to preserve their phenotype and suppressive functions. A decrease or loss of Foxp3 expression in these cells leads to the acquisition of effector T cell-like characteristics, including the production of pro-inflammatory cytokines such as IL-2, IL-4, IL-17, and IFN-γ (Wan and Flavell, 2007, Williams and Rudensky, 2007). Collectively, these studies have underscored the pivotal role of Foxp3 in establishing the Treg lineage.

1.3 Thymic development of regulatory T cells

T cells originate from the multipotent hematopoietic stem cell in the bone marrow and migrate to the thymus to complete their development. At first, they enter the thymus via post-capillary venules located at cortico-medullary junction, the Notch ligand receptors expressed on the progenitors interacts with the Notch ligands expressed on the thymic stroma, promoting the transformation of progenitors into thymocytes committed to the T-cell lineage. The thymocytes express c-Kit and CD44 but not CD25 are known as double-negative 1 (DN1) cells. As the

thymocytes express the α chain of IL-2 receptor (IL-2R), CD25, they are considered as irreversibly committed to the T -cell lineage and are called DN2 cells. Then, the TCR β-chain locus is rearranged and results in a low expression of c-Kit and CD44, forming DN3 cells. DN4 cells appear when a β-chain pairs with a surrogate α-chain (pTα) to form a pre-T-cell receptor (pre-TCR), inducing rapid cell proliferation alongside the loss of CD25 expression. From DN1 stage to DN4 stage, thymocytes migrate outward through the cortico-medullary junction to the subcapsular region (**Figure 1.2**). Eventually, DN4 cells progress to large double-positive (DP) thymocytes expressing CD8 and CD4, which proliferate vigorously. Deeper in the cortex, they stop to proliferate and become small DP thymocytes.

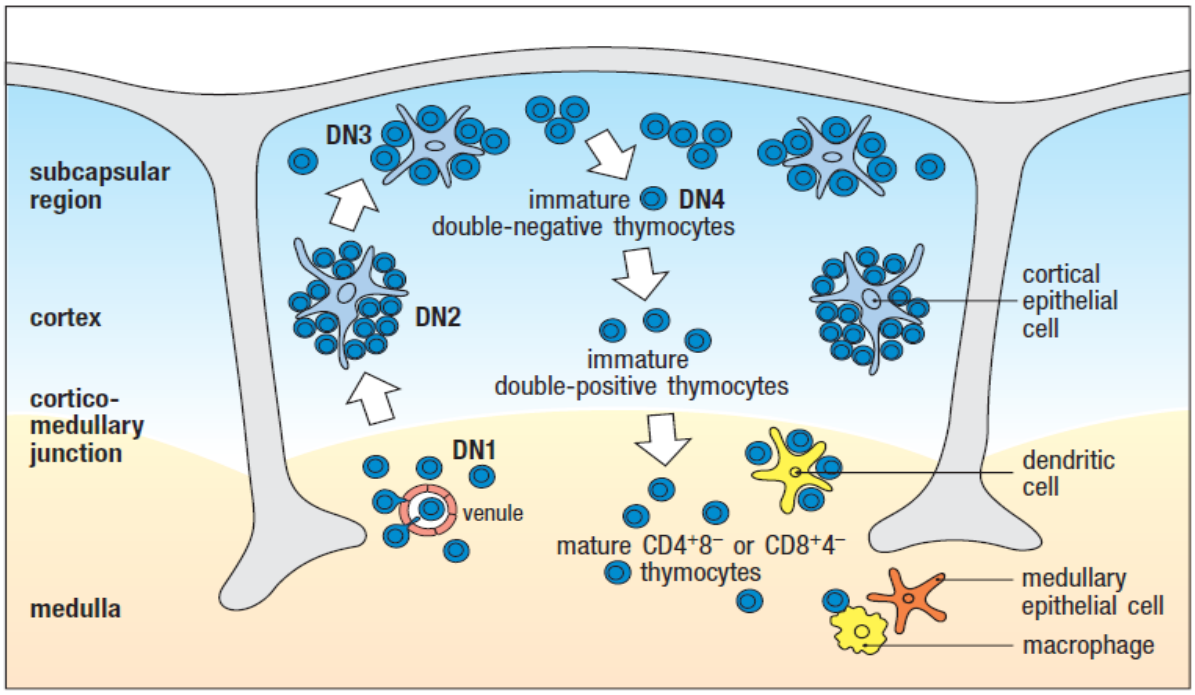

Figure 1.2 Developmental stages of thymocytes in thymus.
The precursor thymocytes enter the thymus via the venule near cortico-medullary junction. As described in text, $CD8^{-}CD4^{-}$ double-negative (DN) cells migrate through the cortico-medullary junction to the outer cortex upon T cell commitment. DN3 cells undergo proliferation in subcapsular region. The cells migrate back through the cortex once they differentiate into $CD8^{+}CD4^{+}$ double-positive thymocytes. After undergoing positive and negative selections, mature single-positive T cells egress from the thymus. Figure adapted from (MURPHY and WEAVER).

In cortical stroma, there are cortical thymic epithelial cells (cTECs) (**Figure 1.2**) expressing autoimmune regulator (AIRE), major histocompatibility complex (MHC) class I and MHC class II. The branching processes of cTECs allow the contact between MHC molecules and the TCR on DP thymocytes to undergo positive selection. Only about 10-30% of DP thymocytes that recognises self-peptide: self-MHC complexes are positively selected (MURPHY and WEAVER, Taniguchi et al., 2012, Hubert et al., 2011, Aschenbrenner et al., 2007). The

positively selected thymocytes then undergo negative selection either in the cortex or alternatively in the medullary region with the aid of medullary thymic epithelial cells (mTECs) (Takahama et al., 2017) and bone-marrow derived antigen-presenting cells (BM-APCs). During negative selection, single-positive (SP) thymocytes which have strong interaction with self-peptides are induced to undergo apoptosis; those that have intermediate interaction (Li and Rudensky, 2016) are further committed to thymically-derived Tregs (tTregs) precursors (Lee and Lee, 2018, Germain, 2002, Singer et al., 2008, Takahama et al., 2017, Cowan et al., 2015); those that have weak interaction develop into naïve conventional T (Tconv) cells (**Figure 1.3; upper left panel**). Finally, tTregs precursors become fully mature tTregs in the thymus, attributed to the constitutive expression of master transcription factor FoxP3, CD25 and high autoaffinity TCR (Sakaguchi et al., 2008). Consequently, naïve $CD8^+$ T cells, naïve $CD4^+$ Tconv cells and naïve $CD4^+$ tTregs ultimately egress from the thymus.

1.4 Peripheral development of regulatory T cells

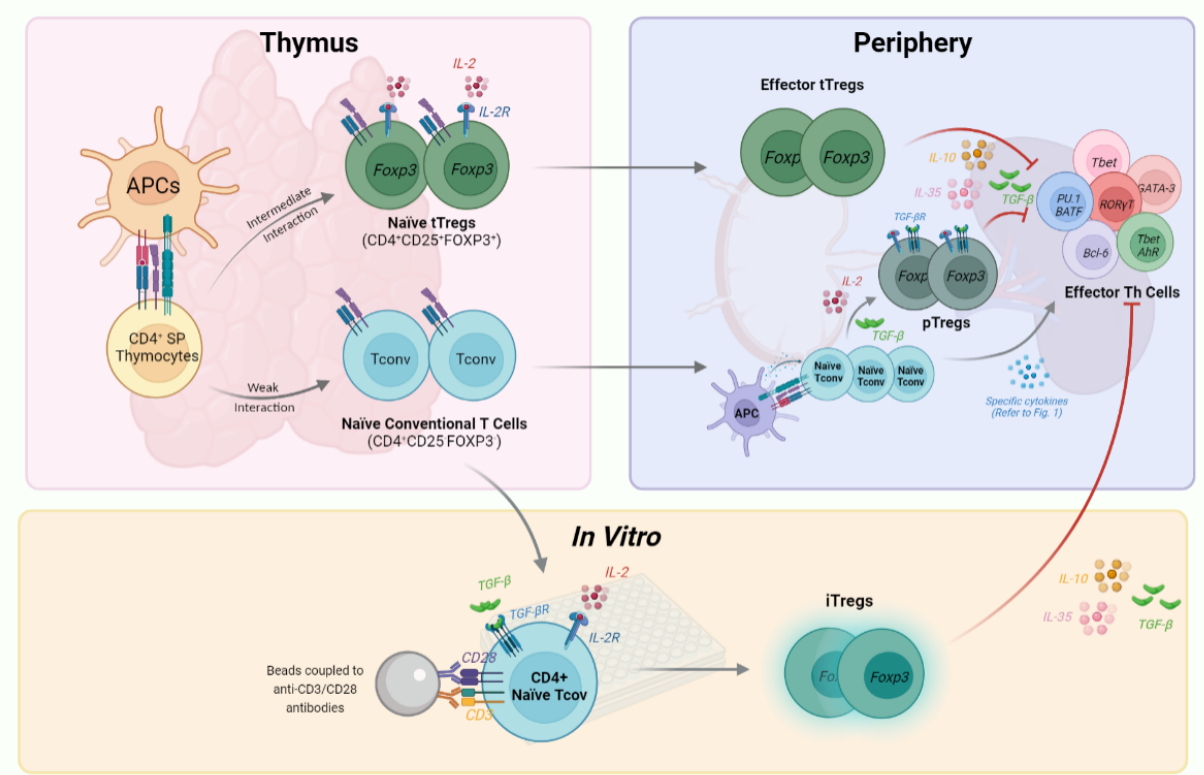

Figure 1.3 Development of tTregs, pTregs and iTregs from $CD4^+$ thymocytes.
During negative selection, $CD4^+$ single-positive (SP) thymocytes which have intermediate interaction with antigen presenting cells (APCs) are committed to develop into naïve tTregs whereas those with weak interaction are committed to become naïve conventional T cells. Upon maturation, both naïve tTregs and naïve conventional T cells egress from the thymus. Peripherally, APCs can provide various cytokines to induce differentiation of naïve $CD4^+$ Tconv cells into distinct Th subsets (refer to Figure1). The secretion of IL-2 and TGF-β can induce FoxP3 expression within $CD4^+$ Tconv cells, thus driving their differentiation into

peripherally derived Tregs (pTregs) with functional equivalent to that of tTregs. Both effector tTregs and pTregs regulate effector T cells through releasing inhibitory cytokines such as IL-10, IL-35 and TGF-β. In vitro, Tregs can be generated by stimulating naïve $CD4^+$ Tconv cells with anti-CD3/CD28, alongside cytokines IL-2 and TGF-β. This specific subset of Tregs is known as in vitro-generated Tregs (iTregs).

The priming of naive $CD4^+$ Tconv cells occurs within a secondary lymphoid organ **(Figure 1.3; upper right panel)**. At first, naive Tconv cells bind APCs transiently through interactions: LFA-1: ICAM-1/ICAM-2 and CD2: CD58. Subsequent binding of TCR to MHC II complex on APCs induces a conformational change in LFA-1, increasing its binding affinity toward ICAM-1/ICAM-2. Consequently, an immunological synapse known as supramolecular activation cluster (SMAC) is formed. To activate the clonal expansion and differentiation of Tconv cells, three kinds of signals are delivered by APCs: (1) activation signal generated upon the engagement of TCR with peptide: MHC II complex on APCs, (2) survival signal generated by interaction between costimulatory CD28 on T cells and B7 molecules on APCs, (3) differentiation signal promoted by cytokines that direct the differentiation of naive $CD4^+$ Tconv cells into several subsets of $CD4^+$ Th cells **(Figure 1.1)**. In this context, cytokines TGF-β and IL-2 can initiate and maintain FoxP3 expression, inducing differentiation of naive Tconv cells into Tregs in the periphery. Hence, these Tregs are known as peripherally derived Tregs (pTregs). Notably, there are two well-defined pTreg populations, Th3 and T regulatory type 1 (Tr1) in which both can secrete TGF-β and IL-10 (Chen et al., 1994, Levings et al., 2001).

In vitro, naïve Tconv cells can express FoxP3 under stimulation of anti-CD3/CD28 together with cytokines TGF-β and IL-2 (**Figure 1.3; bottom panel**). The resulting Tregs formed are known as *in vitro*-generated Tregs (iTregs) (Chen et al., 2003). Like tTregs and pTregs, iTregs are capable of suppressing effector T cells by releasing cytokines IL-10, IL-35 and TGF-β. However, it is worth noting that iTregs are relatively more labile than tTregs and pTregs, which could be due to rapid loss of FoxP3 expression when transferred in vivo (Selveraj and Geiger, 2008, Floess et al., 2007, Polansky et al., 2008).

1.5 Can tTregs be distinguished from pTregs?

Conventional wisdom holds that CD4, CD25 and transcription factor FoxP3 serve as phenotypic markers of Tregs in both mice and humans. However, these markers are not suitable for isolation of tTregs and pTregs with overlapping phenotype. Therefore, the relative contribution of tTregs and pTregs to immune homeostasis is insufficiently determined. To overcome this bottleneck, the use of Ikaros zinc finger transcription factor Helios as selective

tTregs marker has been proposed by Sugimoto *et al.* (Sugimoto et al., 2006). This was further supported by Shevach and Thornton *et al.* using three pieces of evidence: (1) both the earliest Tregs arising from the thymus and the earliest Tregs populating the mouse spleen expressed Helios, (2) iTregs generated from $CD4^+$ Tconv cells did not express Helios, (3) pTregs induced in model of oral tolerance did not express Helios (Shevach and Thornton, 2014). Nonetheless, the value of Helios to identify tTregs is excluded as it is widely expressed in naïve Tconv cells, pTregs and activated effector T cells in different circumstances (Gottschalk et al., 2012, Akimova et al., 2011, Shevach and Thornton, 2014). Also, the discovery of a $Helios^-$ tTreg population further refute the notion (Himmel et al., 2013).

Recently, an alternative surface antigen, neuropilin-1 (Nrp-1) has been claimed to distinguish tTregs from pTregs or iTregs (Yadav et al., 2012, Weiss et al., 2012). Although Nrp-1 was shown to be expressed by tTregs, but this remains equivocal due to several conditions. Firstly, Nrp-1 expression is positively regulated by TGF-β (Weiss et al., 2012), thus it can be found on TGF-β induced iTregs. Secondly, peripheral $FoxP3^+Helios^-$ T cells express significant level of Nrp-1 (Shevach and Thornton, 2014). Thirdly, pTregs obtained from highly inflammatory conditions express high level of Nrp1 (Weiss et al., 2012). Fourthly, the expression of Nrp-1 occurs at a later stage than Helios and FoxP3 in T cell development (Singh et al., 2015). Altogether, the usage of Helios and Nrp-1 to differentiate tTregs from pTregs still requires experimental approaches.

1.6 Treg plasticity

Tregs act as potent mediators of immune suppression and are vital for maintaining immune homeostasis. However, they are prone to plasticity in which they can alter their phenotype based on the environmental cues (Koch et al., 2009, Bailey-Bucktrout et al., 2013, Komatsu et al., 2014). Cumulative evidence suggests that Tregs not only express the key transcription factor Foxp3 but also have the capacity to co-express Th lineage-specific transcription factors, such as Tbet(Koch et al., 2009, Levine et al., 2017, Yu et al., 2015), GATA-3 (Yu et al., 2015), Bcl6 (Li et al., 2020), and RORγt (Steinmetz et al., 2011, Leppkes et al., 2009), which are essential for the Th1, Th2, Tfh, and Th17 effector phenotypes, respectively (**Figure 1.4**). These Tregs, which we refer to as Th-like Tregs, coexist with Th cells and retain the core characteristics of conventional Tregs, including Foxp3 expression, while also producing pro-inflammatory cytokines or transcription factors typically associated with $CD4^+$ Th cells

(Arterbery et al., 2016). The dynamic balance between Th-like Tregs and Th cells plays a critical role in maintaining immune homeostasis.

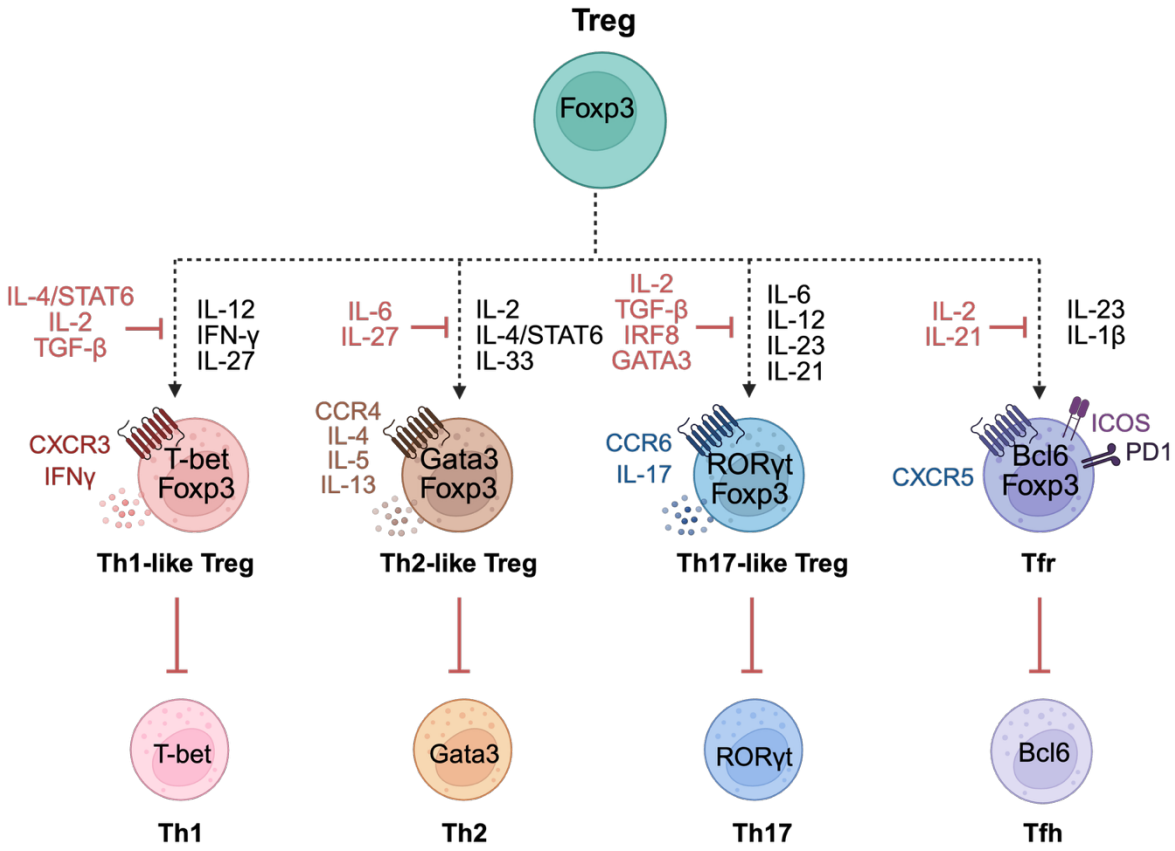

Figure 1.4 Th-like Treg plasticity.
The expression of Foxp3 alongside Th lineage-defining transcription factors enables Tregs to adapt to diverse inflammatory environments. By acquiring specific transcription factors, Tregs gain the ability to migrate to inflamed tissues and regulate immune activation in a context-dependent manner. For instance, Th1-like Tregs express Tbet and CXCR3, allowing them to control type 1 inflammation. Th2-like Tregs express GATA-3 and CCR4, facilitating the regulation of type 2 inflammation. Th17-like Tregs express RORγt and CCR6, enabling them to modulate type 3 inflammation. Additionally, T follicular regulatory (Tfr) cells express BCL6 and CXCR5, playing a crucial role in germinal center regulation and antibody production.

1.6.1 Th1-like Treg

Conventionally, the co-expression of transcription factor Tbet and cytokine IFN-γ in $CD4^+$ lymphocytes was thought to be exclusive to the Th1 effector cells. However, emerging evidence suggests that this is not the case, as Tbet and IFN-γ are also expressed in Tregs from both mice and humans, where it plays a crucial role in Treg suppression capacity in conjunction with FoxP3 (Koch et al., 2009, Zheng et al., 2011, Oldenhove et al., 2009). Furthermore, Tbet-induced chemokine receptor CXCR3 has been shown to facilitate the recruitment of Tregs to

sites of inflammation, and it has been used as a surface marker to identify Th1-like Tregs (Imanguli et al., 2014). The expression of Tbet in differentiated Tregs is modulated by various inflammatory signals, including IL-12, IFN-γ, and IL-27 (Hall et al., 2015, Gocher-Demske et al., 2023, Zhao et al., 2012) (**Figure 1.4**). The differentiation of Tregs into Th1-like cells is regulated by certain factors such as IL-4/STAT6 signalling, IL-2, TGF-β and immunosuppressive drugs (Wang et al., 2010, Li et al., 2016, Daniel et al., 2016), suggesting that these factors can potentially reverse the suppressive function and restore the inhibitory properties of Tregs.

It has been demonstrated that Tbet expression in Tregs is essential for regulating type 1 inflammation. This was first shown in a *Scurfy* mouse model, where the transfer of wildtype Tregs was sufficient to rescue the animal from inflammation and autoimmunity. In contrast, the transfer of Tbet–deficient Tregs, which have impaired suppressive capacities, failed to rescue the animal from inflammation (Zheng et al., 2011, Chang et al., 2009). Recent studies have further revealed that $CXCR3^+$ Th1-like Tregs regulates Th1-related pathogenic immune responses, which can be reversed by depleting interferon regulatory factor 8 (IRF8) (Lee et al., 2016, Hall et al., 2012) and can be induced by Tbet (Nosko et al., 2017, Levine et al., 2017). Additionally, IFN-γ^+ iTregs has been shown to downregulate Th1-type immune responses, proposing a self-regulatory mechanism in inflammatory processes (Venigalla et al., 2012). These anti-inflammatory IFN-γ^+ Th1-like Tregs were capable of inhibiting allograft rejection and a decrease in their proportion has been associated with a poor prognosis in chronic T cell-mediated rejection and ischemia-reperfusion injury (Xu et al., 2017).

In the tumour microenvironment (TME), Th1-like Tregs develop from Th1 cells via TGF signalling and PD-1 signalling in Th1 cells (Gianchecchi and Fierabracci, 2018, Stathopoulou et al., 2018, Amarnath et al., 2011). These $Tbet^+$ $CXCR3^+$ Th1-like Tregs are high proliferative and enriched in the tumour infiltrates, as seen in a mouse model of fibrosarcoma. $Tbet^+$ Tregs in the TME express perforin and antioxidant proteins, such as MT3. Perforin suppresses antitumor immunity while antioxidant proteins allows Treg localisation in tumour sites with high reactive oxygen species (ROS) (Okamoto et al., 2023). These Tregs play a key role in tumour immunity by suppressing the $CD8^+$ T cell activation, by disrupting interaction of conventional dendritic cells (DCs), DC1, and $CD8^+$ T cell. Blocking CXCR3 in Tregs enhances tumour antigen presentation by DC1 and $CD8^+$ T-cell priming. Furthermore, it has been reported that eliminating $Tbet^+$ Tregs alone can boost anti-tumour immunity (Okamoto et al.,

2023, Ayala et al., 2023, Zagorulya et al., 2023). Together, these findings underscore the ability of Tregs to suppress Th1 responses while simultaneously producing pro-inflammatory IFN-γ during their conversion into Th1-like cells.

1.6.2 Th2-like Treg

GATA-3 was initially described as a factor required for the differentiation of Th2 cells by inducing the expression of Th2 cytokines and negatively regulates Th1 differentiation by downregulating STAT4/IL-12Rβ2 chain (Usui et al., 2006). Nevertheless, co-expression of GATA-3 and FoxP3 has also been reported in Tregs (Wang et al., 2011). In Tregs, the expression of GATA-3 is positively regulated by TCR, IL-2, IL-4, and IL-33 and repressed by cytokines such as IL-27 and IL-6 (Wohlfert et al., 2011) (**Figure 1.4**). IL-4 signalling is a major driver of Th2-like Treg formation, as seen in *Il4ra*^{F709} mice, where increased IL-4R expression in Tregs promoted their reprogramming into Th2-like cells (Rivas et al., 2015). These IL-4-induced Tregs also express IL-5Rα, further supporting their Th2-like polarisation in response to IL-5 and other antigens (Hall et al., 2013, Yamada et al., 2015). GATA-3^{+} Tregs has also been found to express CCR4, allowing the Tregs to migrate to type 2 inflammation sites and attenuate Th2 responses (Faustino et al., 2013).

Th2-like Tregs play a key role in regulating type 2 immune responses, particularly in homeostasis and inflammation. They co-opt Th2-associated transcription factors like IRF4 and GATA-3 (Zheng et al., 2009). Notably, IRF4 expression in Tregs paradoxically inhibits Th2 immune responses while allowing IL-4-dependent immunoglobulin and plasma cells to infiltrate tissues, driving an atypical Th2 response (Zheng et al., 2009). Despite GATA-3 deletion reducing IL-4 expression in Tregs, it still results in impaired suppression of Th2 and other T-helper cells, contributing to inflammatory disease progression (Wang et al., 2011, Sawant and Vignali, 2014). Furthermore, GATA-3 also has been demonstrated to suppress Treg conversion into effector T cells and inhibits Teff-like cytokine secretion (Wohlfert et al., 2011). GATA-3 promotes ST2 expression in Tregs (Schiering et al., 2014), where ST2^{+} Tregs exhibit enhanced suppressive function, potentially via IL-33 signalling. ST2^{+} Tregs can express IL-5 and IL-13, and suppress CD4^{+} T-cell activation through IL-10 and TGF-β (Siede et al., 2016). However, IL-33 signalling in Tregs has been reported to play an opposing role in the lungs. Under homeostatic conditions, ST2^{+} Tregs suppress Th2 responses, while upon allergen exposure, IL-33 destabilises Tregs and enhance type 2 cytokine production (Chen et al., 2017). Th2-like Tregs contribute to controlling helminth infections (Li et al., 2018, Abdel Aziz et al.,

2018, Smith and Maizels, 2014), where IL-4 promotes their activation and migration to inflamed tissues (Abdel Aziz et al., 2018). Additionally, GATA-3$^+$ Tregs modulate lung inflammation in respiratory infections, including respiratory syncytial virus (Durant et al., 2013), and may be involved in immune dysfunction observed in severe SARS-CoV-2 cases (Xu et al., 2022). To summarise, both invasive and protective Th2-like Treg phenotypes have been observed, highlighting their dual role in immunity.

1.6.3 Th17-like Treg

RORγt is a key transcription factor for Th17 cells which involve in inflammatory responses in autoimmune diseases and infections (Zambrano-Zaragoza et al., 2014). Conventional wisdom held that RORγt had no functional role in Tregs, as studies showed that its transcriptional activity was inhibited through direct interaction with Foxp3. In the presence of IL-6, Foxp3 expression is diminished, enabling RORγt to become transcriptionally active and induce IL-17A production (Ichiyama et al., 2008). Contrary to earlier assumptions, RORγt$^+$ Tregs were later identified in various tissues (Koenen et al., 2008, Voo et al., 2009), including the gut, where they express CCR6 involved in migration and exhibit immunosuppressive properties (Yamazaki et al., 2008). The differentiation of Th17-like cells from Tregs primarily through IL-6, along with IL-21, IL-23 and IL-1β (Kryczek et al., 2011, Beriou et al., 2009) (**Figure 1.4**). Several studies have shown that Th17-like Treg conversion can be regulated by the decreased dependence of IL-6 on TGF-β and IL-2 (Massoud et al., 2016, Afzali et al., 2010), and its suppressive ability was impaired by a decrease in Th2 transcription factor GATA-3 (Wang et al., 2011). IFR8 which is a Th17 differentiation-inhibitory factor can also inhibit the IL-17A expression in Tregs (Ouyang et al., 2011, Zhong et al., 2017).

Th17-like Tregs can regulate type 3 inflammation in lymphoid and non-lymphoid tissues, including colon, small intestine and mesenteric lymph node. They can deplete IL-1 and IL-6 from the tissue by expressing IL-1R and IL-6R, both of which are critical for Th17 differentiation (Chaudhry et al., 2009). The presence of RORγt$^+$ Tregs has been found to directly proportional to the presence of microbiota in germ-free mice or antibiotic-treated mice (Sefik et al., 2015, Ohnmacht et al., 2015). Several studies have also demonstrated that Th17-like Tregs can be induced by several microbiota in small intestine and colon (Sefik et al., 2015). Apart from type 3 response, RORγt$^+$ Tregs can regulate type 2 responses, in which absence of the Th17-like cells enhances the Th2-driven defence against helminths (Ohnmacht et al., 2015). In non-lethal *Salmonella*-induced colitis model, Treg has been shown to adapt their phenotype

to regulate Th responses (Clay et al., 2020). This infection is characterised by an initial colonic Th17 response, which is later dominated by Th1 cells. During early infection, colonic Tregs upregulate Tbet to suppress Th1 responses while promoting Th17 bias. At later stages, RORγt$^+$ Tregs accumulate to dampen Th17 activity and sustain Th1 responses. These findings suggest that Tregs not only suppress CD4$^+$ T cells but also actively shape Th polarisation to control inflammation.

RORγt$^+$ Tregs have been identified in ovarian (Downs-Canner et al., 2017), lung (Phillips et al., 2015), and breast cancer (Seif et al., 2023) and are enriched in colon carcinoma (Lochner et al., 2008), where they contribute to an immunosuppressive microenvironment, likely through IL-10. However, their additional suppressive mechanisms remain unclear. In breast cancer, tumour-infiltrating Th17-like Tregs express CCR6 and CD73, with CD73 promoting the death of CD8$^+$ effector cell (Roy et al., 2021). Further research is needed to fully elucidate their role in tumour immunity.

1.6.4 Tfh like-Treg

Tfh cells are a subset of CD4$^+$ effector T cells that home to B cell follicles upon CXCR5 expression, facilitating B cell maturation in germinal centres (GC) (King, 2009). They are characterised by transcription factor Bcl6, along with inducible T cell co-stimulator (ICOS), and programmed cell death 1 receptor (PD-1). Tfh-like Tregs (Tfr) which differentiate from Tregs share key Tfh-associated factors such as Bcl6, ICOS and PD-1, but also co-express transcription factor FoxP3 (Chung et al., 2011, Linterman et al., 2011, Amé-Thomas et al., 2012) (**Figure 1.4**). Unlike Tfh cells, Tfr do not express IL-21, IL-4 or CD40L (Linterman et al., 2011, Chung et al., 2011, Wollenberg et al., 2011). While most Th-like Tregs arise from thymic-derived Tregs, Tfr can also differentiate from naïve cells in a PD-1/PD-L1-dependent manner (Aloulou et al., 2016). However, it remains unclear whether naïve cells first acquire a Tfh phenotype before differentiating into Tfr. IL-21 is known to promote Tfh cell generation, yet in Tregs, it negatively regulates Tfr development and impairs their suppressive function (Jandl et al., 2017, Ding et al., 2014). Paradoxically, IL-2 signalling inhibits the differentiation of Tregs into Tfr by promoting Blimp-1 expression in Tregs (Botta et al., 2017, Wing et al., 2017). When IL-2 levels are reduced, Tregs differentiate into Tfr and downregulate CD25 (Wing et al., 2017).

Within the GC, IL-1β promotes Tfh expansion while simultaneously inducing Tfr (Ritvo et al., 2017). In response, Tfr upregulate IL-1R2 and IL-1RA to regulate excessive Tfh expansion. To maintain homeostasis, Tfr employ a range of suppressive mechanisms to control Tfh responses and regulate GC reactions. These mechanisms include CTLA4, GITR, IL-10, TGFβ, neuritin, and Fgl2 secretion (Gonzalez-Figueroa et al., 2021, Sage et al., 2014, Wing et al., 2014, Sungnak et al., 2020). Additionally, Tfr can suppress T cells through direct cytolysis or by mechanically disrupting Tfh-B cell interactions (Sage and Sharpe, 2015). Beyond their immediate regulatory effects, Tfr-mediated suppression of B cells is long-lasting, persisting even in the absence of Tfr. Mechanistically, Tfr inhibits the Myc and mTOR pathways, altering B cell metabolism and inducing stable epigenetic modifications that reduce B cell effector activity. This mechanism can be reversed by IL-21 (Sage et al., 2016).

In addition to their role in GC dynamics, Tfr are critical in regulating allergic responses, primarily by controlling the IL-13 production in Tfh cells and limiting IgE secretion (Clement et al., 2019). Individuals with allergic rhinitis often exhibit reduced circulatory Tfr levels, along with impaired suppression of IgE production and diminished IL-10 secretion (Yao et al., 2021). Notably, allergy immunotherapy has shown promise in restoring Tfr levels, leading to reduced allergic reactions. These findings highlight the broader immunoregulatory functions of Tfr beyond GC homeostasis, extending their influence on various immune-related conditions. Given their ability to modulate Tfh responses and B cell activity, Tfr may also play a significant role in shaping immune dynamics within the TME. Multiple lines of evidence suggest that Tfh cells are crucial in orchestrating the tumour immune landscape. For instance, Tfh can regulate GC-like reactions within peritumoral tertiary lymphoid structures, a phenomenon correlated to improved prognosis (Gu-Trantien and Willard-Gallo, 2013). An increased frequency of suppressive Tfr has been observed in patients with various cancers including non–small cell lung carcinoma (Guo et al., 2017), ovarian cancer (Li et al., 2019), colorectal cancer (Li et al., 2020), and melanoma (Eschweiler et al., 2021), where their presence is associated with poorer prognosis. Tfr expansion has been noted in the blood of patients with follicular B lymphoma, potentially playing a beneficial role in suppressing B cell tumorigenesis (Amé-Thomas et al., 2012). This is particularly relevant given that diffuse large B-cell lymphoma can arise from B cells undergoing GC reactions, processes tightly regulated by Tfr (Cha et al., 2018). Further research is needed to fully elucidate the role of Tfr in these malignancies.

Despite their expression of Th-associated transcription factors and cytokines, Treg plasticity is characterised by a distinct immunosuppressive role in regulating Th cell responses while retaining Foxp3 expression. Unlike conventional Tregs, "plastic" Tregs do not provide broad suppression but instead selectively inhibit specific Th subsets (**Figure 1.4**). This adaptive plasticity may help restore immune balance, functioning as a negative feedback mechanism in disease progression.

1.7 Regulation of Foxp3 expression and its epigenetic stability

FoxP3 expression is closely linked to the stability of Treg, which serves as the master regulator of Treg identity and function (Fontenot et al., 2003). Its loss or downregulation can shift Tregs toward an alternative phenotype, diminishing their suppressive ability and promoting pro-inflammatory traits (Li and Zheng, 2015). Treg stability is governed by multiple regulatory mechanisms, including transcriptional regulations, epigenetic modifications and post-translational modifications. Therefore, understanding how FoxP3 expression is maintained is key to unravelling the balance between stable immunosuppression and functional reprogramming in Tregs.

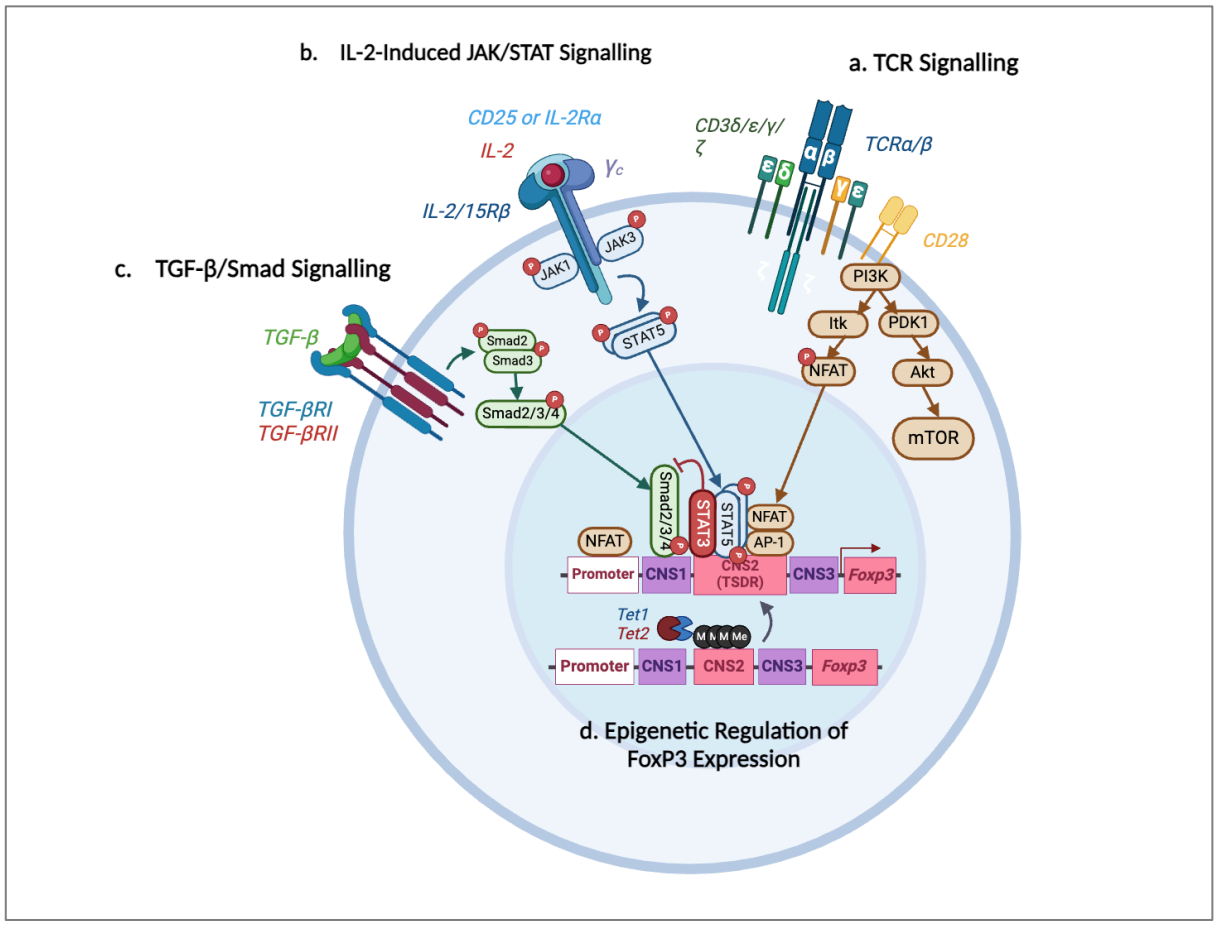

Figure 1.5 Transcriptional regulation and epigenetic modification of FoxP3.

Treg stability is regulated by several mechanisms, which act directly or indirectly on FoxP3 expression. **A,** T cell receptor (TCR) signalling. TCR signalling together with CD28 signalling activates phosphatidylinositol 3-kinase (PI3K), recruiting enzymes PDK-1 and Itk. PDK-1 activates serine/threonine kinase Akt, which in turn activates mammalian target of rapamycin (mTOR). Itk induces dephosphorylation of nuclear factor of activated T cells (NFAT), allowing its binding to the FoxP3 promoter and the conserved non-coding DNA sequence (CNS)2 region. **B,** IL-2 induced JAK/STAT signalling. Significant expression of IL-2Rα (CD25) confers high sensitivity towards IL-2. Through Janus kinase (Jak)1 and Jak 3, activated signal transducer and activator of transcription (STAT5) dimerises and binds to the CNS2 region. **C,** TGF-β/Smad signalling. Through transforming growth factor-β receptor (TGF-βR) I and TGF-BRII, Smad2/3 molecules are phosphorylated, which in turn form a Smad2/3/4 complex. The Smad2/3/4 complex then binds the CNS1 region and drives FoxP3 expression. TGF-β production is also autoregulated by Smad2/3. Notably, STAT3 acts antagonistically to STAT5 and Smad3. **D,** Epigenetic regulation of FoxP3 expression. The CNS2 enhancer region is also known as Treg-specific demethylated region (TSDR). Demethylation of TSDR by 10-11 translocation (Tet) family demethylases Tet1 and Tet2 is required to enable binding of transcription factors.

1.7.1 T cell receptor signalling

The TCR complex is comprised of TCRα/β chains and CD3δ/ε/γ/ζ subunits (**Figure 1.5a**). Upon engagement of antigen and TCR/CD3 complex, the cytoplasmic tyrosine kinase Lck attached to the intracellular portion of CD4 phosphorylates the immunoreceptor tyrosine-based activation motifs (ITAMs) in CD3δ/ε/γ/ζ. Tyrosine kinase ZAP-70 is then recruited by tandem SH2 domains to ITAMs before being activated by Lck. Accordingly, activated ZAP-70 further phosphorylates linker for activated T cells (LAT) and adaptor protein SLP-76, which are linked by adaptor protein Gads (**Figure 1.6**). Meanwhile, the engagement of CD28 with CD80 (B7.1) and CD86 (B7.2) initiates tyrosine phosphorylation and thus activates phosphatidylinositol 3-kinase (PI3K). PI3K produces PIP_3 which can recruit several enzymes, such as phosphoinositide-dependent protein kinase-1 (PDK-1) and kinase Itk to carry out the cascade of downstream signalling pathways. Phosphatase and tensin homologue (PTEN) acts antagonistically by mediating the reverse action of PI3K.

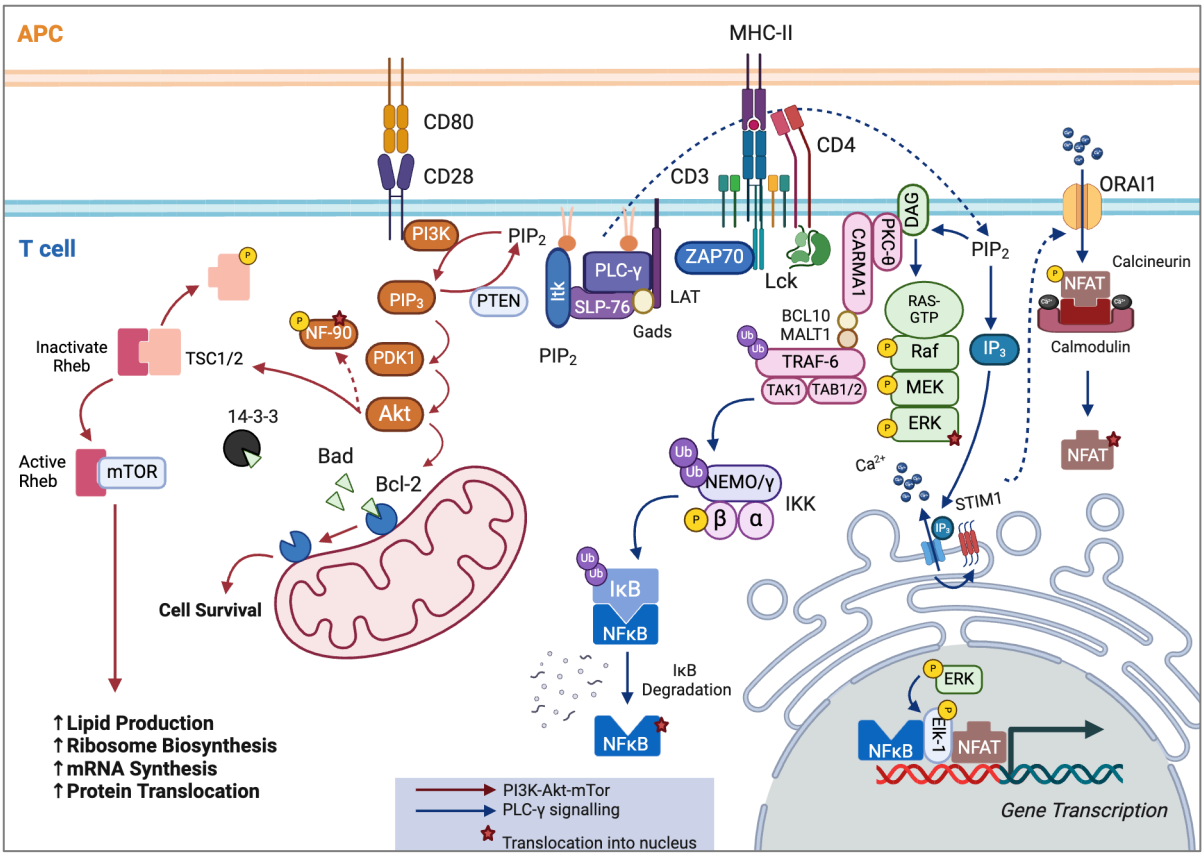

Figure 1.6 TCR/CD3 complex and CD28 downstream signalling pathways.
T cell receptor (TCR)/CD3 complex and CD28 signalling pathways activate multiple signalling cascades, leading to expression of transcription factors and gene transcription. Upon ligand engagement, the phosphatidylinositol 3-kinase (PI3K)-Akt-mammalian target of rapamycin (mTOR) pathway (red arrow) and phospholipase C-γ (PLC-γ) pathway (blue arrow) are activated. Finally, signalling cascades activate the transcription factors, allowing them to translocate into the nucleus (red star) and initiate subsequent gene transcription.

The first signalling module involving PDK1 is required to accommodate the energetic demand and cell survival of rapidly dividing cells by stimulating cellular metabolism. Activated PDK-1 phosphorylates a serine/threonine kinase known as Akt, which further phosphorylates a pro-apoptotic protein called Bad (**Figure 1.6; red arrow**). Upon binding, anti-apoptotic protein Bcl-2 is released from the mitochondrial membrane, promoting cell survival. Phosphorylated Bad binds to 14-3-3 and can no longer inhibit Bcl-2. Another function of Akt is to phosphorylate TSC1/2 complex which is a GTPase-activating protein (GAP) for the GTPase Rheb. Once phosphorylated, Rheb protein is released from TSC/12 complex, activating mammalian target of rapamycin (mTOR). mTOR can further work on multiple pathways to augment lipid production, ribosomal biosynthesis, mRNA synthesis and protein translocation. Of note, mTOR signalling has been studied to promote Th cell differentiation and suppress generation of iTregs (Chi, 2012, Powell et al., 2012). Additionally, CD28 co-stimulation can enhance IL-2 mRNA stability by activating Akt which phosphorylates RNA-binding protein

NF-90 (MURPHY and WEAVER). Specifically, phosphorylated NF-90 translocates from the nucleus to the cytoplasm and bind to the IL-2 mRNA, fostering IL-2 synthesis.

The second signal is carried out by LAT: Gads: SLP-76 scaffold complex together with Itk. After being activated by Itk, Phospholipase C-γ (PLC-γ) catalyses the breakdown of phosphatidylinositol biphosphate (PIP_2) into inositol triphosphate (IP_3) and diacylglycerol (DAG) (Fig1.5; blue arrow). IP_3 can induce the release of calcium stored in the endoplasmic reticulum, stimulating STIM1 aggregation and allowing extracellular calcium entry through ORAI1 channels. Ca^{2+} influx binds to calmodulin and activates calcineurin which dephosphorylates nuclear factor of activated T cells (NFAT). Eventually, NFAT enters the nucleus and stimulates transcription of genes participating in Tregs activation including FOXP3 and IL-2 in the presence of activator protein 1 (AP-1) and nuclear factor κB (NFκB). To be precise, NFAT transactivate FoxP3 expression by binding to the FoxP3 promoter and conserved non-coding DNA sequence 2 (CNS2) region within the FoxP3 locus.

A second branch of PLC-γ signalling leads to the activation of GTPAse Ras (**Figure 1.6; blue arrow**). Via DAG produced from PLC-γ, the expression of transcription factor AP-1 and activation of NFκB are promoted. For AP-1, DAG recruits Ras guanyl nucleotide releasing protein (RasGRP) to activate Ras. Activated Ras then triggers Raf which further phosphorylates Mek, leading to Erk phosphorylation. Activated Erk diffuses into the nucleus and phosphorylates transcription factor Elk-1, which further stimulates c-Fos transcription. Along with transcription factor c-Jun, c-Jun/Fos dimer promotes the AP-1 transcription. For NFκB signalling, DAG recruits protein kinase C (PKC-θ) to enable CARMA1 phosphorylation. Activated CARMA1 creates a scaffold to enable the binding of BCL10 and MALT1, successively recruiting the E3 ubiquitin ligase TRAF-6. After polyubiquitination on TRAF-6 itself and NFκB essential modulator (NEMO), TAB1/2 and TAK1 are recruited consecutively to phosphorylate IκB kinase (IKK) complex. Ultimately, IKK phosphorylates IκB to induce IκB ubiquitination and degradation, releasing NFκB.

1.7.2 IL-2-Induced JAK/STAT Signalling

In contrast to naïve T cells, Tregs constitutively express CD25 thereby possessing high-affinity IL-2R to outcompete other T cell subpopulations with low affinity IL-2R for the cytokine IL-2. IL-2 binding dimerises the IL-2R consisting of IL-2Rα/β/γ_c and brings associated cytoplasmic Janus kinase (JAK)1 and JAK3 together to phosphorylate each other (Johnston et

al., 1994, Rochman et al., 2009) (**Figure 1.5b**). The activated JAKs then phosphorylate specific tyrosine in the receptor tail, creating a binding site for signal transducers and activators of transcription 5 (STAT5) homodimers (Salas et al., 2020). Upon phosphorylation by JAKs, STAT5 reconfigures into a dimer and translocate into the nucleus. As a positive regulator (Yao et al., 2007), STAT5 complexes bind the enhancer element within the CNS2 region and drive FoxP3 expression, inducing differentiation of both tTregs and pTregs. In contrast to STAT5, STAT3 has an opposing role in FoxP3 regulation. STAT3 is a downstream target of cytokines IL-6, IL-21, and IL-23. Specifically, IL-6 shows its potential in regulating the appearance of iTregs (Chen et al., 2009). Moreover, the stability of FoxP3 expression within tTregs is also affected by STAT3 in inflammatory conditions (Laurence et al., 2012). These situations are contributed to the IL6/STAT3 pathway, in which binding of STAT3 to silencer elements within CNS2 region attenuates FoxP3 expression (Yao et al., 2007). Also, STAT3 can simultaneously prevent Smad3 binding to enhance elements, providing a framework for negative regulation of TGF-β induced FoxP3 transcription (Xu et al., 2010).

1.7.3 TGF-β/Smad Signalling

In conjunction with TCR signalling, cytokine transforming growth factor-β (TGF-β) can initiate the differentiation of naïve Tconv cells into pTregs (Amarnath et al., 2007). When TGF-β binds TGF-β type II receptor (TβRII), TβRII recruits and activates TβRI by phosphorylating its intracellular GS domain. Accordingly, TβRI phosphorylates Smad2 and Smad3 proteins, forming a Smad2/3: Smad4 complex (**Figure 1.5c**). The Smad2/3: Smad4 complex is then translocated into the nucleus and binds to the enhancer element within the CNS1 region of the *Foxp3* locus (Tone et al., 2008, Xu et al., 2010, Kashiwagi et al., 2015). Consequently, an autoregulation of TGF-β production is formed in which Smad3 drives FoxP3 expression and *Tgfb1* promoter activity, whereas Smad2 negatively regulates these activities (Kashiwagi et al., 2015). Notably, TGF-β-mediated signalling can also be depleted by STAT3 activation as stated. CNS1-deficient mice demonstrated the essential role of CNS1 region in inducing FoxP3 expression in pTregs but this was superfluous in tTregs (Josefowicz et al., 2012). However, this remains disputable due to compelling evidence showing the instability of tTreg development in the absence of TGFβRI (Liu et al., 2008, Konkel et al., 2014).

1.7.4 Epigenetic Regulation of FoxP3 Expression

Beyond cytokine-induced signalling, epigenetic modifications in the regulatory regions of the *FoxP3* locus are prominent in Treg commitment. Apart from the FoxP3 promoter, the two main

CNS elements within the locus are CNS1 and CNS2 (Zheng et al., 2010) (**Figure 1.5d**). CNS1 is indispensable for pTreg development. It is located upstream of the CNS2 and contains a Smad2/3 binding site, acting as a TGF-β-NFAT response element (Tone et al., 2008). CNS2 possesses regions with rich cytosine-phosphate-guanine (CpG) motifs, known as the Treg-specific demethylated region (TSDR). It can interact with transcription factors including STAT5, STAT3 and FoxP3 (Samstein et al., 2012, Xu et al., 2010, Yao et al., 2007, Zheng et al., 2010). In tTregs, enzymatic demethylation of the TSDR is vital for the expression of FoxP3 and thus favours lineage stability (Morikawa and Sakaguchi, 2014, Huehn and Beyer, 2015). This was further proved by the fact that iTregs demonstrate less demethylation on the same region along with unstable FoxP3 expression (Kim and Leonard 2007). Upon demethylation of CNS2, the sensitivity of Tregs towards IL-2 is enhanced significantly which is attributed to the significant level of CD25 expressed. Accordingly, STAT5 as the downstream target of IL-2 has greater occupancy of the CNS2 region (Feng et al., 2014). IL-2 has been reported to promote the demethylation of specific TSDR (Chen et al., 2011), likely through the indirect recruitment of Ten eleven translocation (Tet) family of demethylases Tet1 and Tet2 by STAT5 (Yang et al., 2015). In contrast, pro-inflammatory cytokines like IL-6 can trigger the methylation of CNS2 by recruiting DNA methyltransferase 1 (DNMT1), reducing Foxp3 transcription (Hodge et al., 2001, Lal et al., 2009, Zhang et al., 2005). This highlights the opposing effects of IL-2 and IL-6 on Foxp3 stability and Treg function. Notably, IL-6 along with other inflammatory cytokine such as IL-21 activates STAT3, which inhibits Foxp3 expression by suppressing IL-2-activated STAT5 binding to Foxp3 regulatory elements (Laurence et al., 2012). Furthermore, while TNF is generally considered antagonistic to Treg function in same contexts, it can also support STAT5-mediated expansion of certain Treg populations (Nguyen and Ehrenstein, 2016), indicating a complex interplay between stabilising and destabilising signalling pathways in Tregs exposed to inflammatory stimuli.

1.7.5 Post-translational modulation

Both mouse and human FOXP3 proteins are approximately 47 kDa in size and contain four key functional domains: the N-terminal repressor domain, zinc finger domain, leucine zipper domain, and C-terminal Forkhead domain (Bennett et al., 2001, Brunkow et al., 2001, Ziegler, 2006). In contrast to mice, freshly isolated human Tregs express two isoforms of FOXP3, which are FOXP3 and FOXP3Δ2 (Allan et al., 2005, Walker et al., 2003). Additionally, another isoform, FOXP3Δ2Δ7 has been reported (Mailer et al., 2009, Smith et al., 2006). The functional

activity of FoxP3 is finely tuned by various post-translational modifications (PTMs) including phosphorylation, acetylation and ubiquitinylation (**Figure 1.7**).

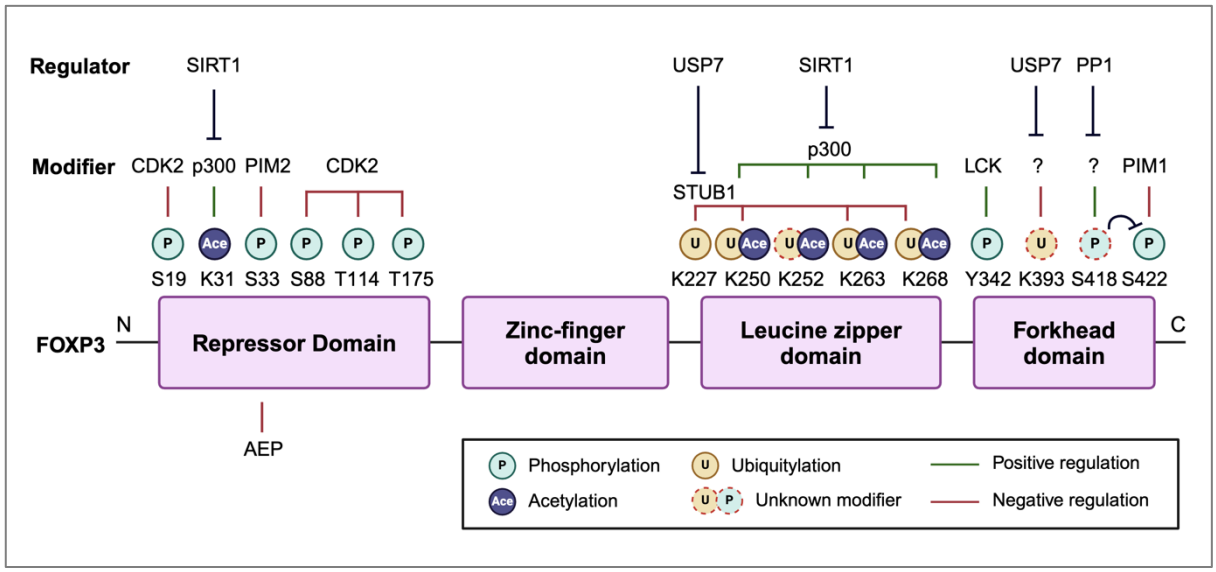

Figure 1.7 Post-translational modifications of FOXP3 and their impact on Treg function. The schematic representation of the mature FOXP3 protein, showing its functional domains including the repressor domain, zinc-finger domain, leucine zipper domain, forkhead domain, alongside key post-translational modification sites and their regulatory effects on Treg function.

FOXP3 acetylation at specific lysine residues including K63, K263 and K268 is catalysed by lysine acetyltransferases TIP60 and p300 (**Figure 1.7**), enhancing FOXP3 stability and target gene association (Xiao et al., 2014, Li et al., 2007, van Loosdregt et al., 2010, Samanta et al., 2008). Conversely, the histone deacetylases and lysine deacetylases including sirtuin 1 (SIRT1) removes these acetyl groups, promoting FOXP3 ubiquitylation and degradation, thereby reducing its expression (Tao et al., 2007, Li et al., 2007, van Loosdregt et al., 2010, Wang et al., 2009, van Loosdregt et al., 2011). Foxp3 phosphorylation can either enhance or inhibit its function. An unidentified kinase phosphorylates FOXP3 at S418, strengthening DNA binding and Treg gene regulation (Li et al., 2014). In arthritis, TNF-activated protein phosphatase 1 (PP1) dephosphorylates FOXP3, impairing its function and potentially contributing to Treg inefficacy in inflamed joints (Nie et al., 2013). By contrast, cyclin-dependent kinase 2 (CDK2) phosphorylates FOXP3 at multiple N-terminal residues including S19, S88, T114 and T175 (**Figure 1.7**), interfering FOXP3 stability and Treg suppressive function (Morawski et al., 2013). The kinase PIM1 phosphorylates FOXP3 at S422, inhibiting the expression of Treg-associated genes such as CD25 and CTLA-4 (Li et al., 2014). While TCR signalling limits PIM1 expression, IL-6 exerts the opposing effect. Notably, phosphorylation at S418 counteracts the inhibitory effect of S422 (Nie et al., 2013) (**Figure 1.7**). Similarly, PIM2 phosphorylates FOXP3 at N-terminal sites such as S33 and S41, disrupting Treg function while

potentially supporting Treg expansion (Deng et al., 2015, Basu et al., 2008). In cancer cells, LCK phosphorylates FOXP3 at Y342, leading to its upregulation, though its role in Tregs remains unclear (Nakahira et al., 2013).

K48-linked polyubiquitylation targets FOXP3 for proteasomal degradation, significantly impacting Treg function (Metzger et al., 2012, Ben-Neriah, 2002). HIF1 interacts and promotes FOXP3 degradation in differentiating $CD4^+$ T cells, while its inhibition stabilises FOXP3 levels (Dang et al., 2011). Inflammatory stress accelerates FOXP3 turnover in Tregs, with pro-inflammatory signals such as lipopolysaccharide, cytokines, heat shock, and psoriasis-associated CCL3 enhance FOXP3 degradation, driving Treg dysfunction and plasticity (Chen et al., 2013). The chaperone HSP70 recruits the E3 ubiquitin ligase, STUB1, which ubiquitylates FOXP3 at K227, K250, K263, and K268 (**Figure 1.7**), promoting its proteasomal degradation (Chen et al., 2013). STUB1 upregulation disrupts Treg function by reducing FOXP3 levels and suppressing Treg-associated genes while increasing effector cytokines like IL-2 and IFN-γ. In contrast, the deubiquitinases ubiquitin-specific peptidase (USP7) stabilises FOXP3 by catalysing its deubiquitylation, thereby enhancing Treg function (van Loosdregt et al., 2013). Additionally, recent study has revealed a protease called asparaginyl endopeptidase (AEP), which can negatively regulate Treg by direct binding and cleaving FOXP3 protein (Stathopoulou et al., 2018). Together, these PTMs provide a dynamic regulatory mechanism that integrates cellular signals to fine-tune Foxp3 activity, influencing Treg stability, differentiation and immune tolerance.

1.8 Co-inhibitory receptors on Tregs

Although the cytokines-induced signalling on Treg development is well-defined, the co-inhibitory receptor-induced signalling on Tregs remains unclear. Upon T-cell activation, co-inhibitory receptors are significantly upregulated on T cells to suppress T-cell activity and thus maintain a balance of immune homeostasis. Subsequently, the immune regulatory function of co-inhibitory receptors has been found to influence outcomes in autoimmune disease, tumour and chronic viral infection settings. Especially in the immunosuppressive tumour microenvironment (TME), most T cells a show dysfunctional and exhausted phenotype due to significant expression level of co-inhibitory receptors. In Tregs, co-inhibitory receptors promote suppressive function by interfering with the PI3K-Akt-mTOR pathway, which is an essential node in Treg development and stability (Pompura and Dominguez-Villar, 2018). Furthermore, inhibition of PI3K-Akt could lead to the nuclear retention of the transcription

factor FOXO1 which favours Tregs stability by stabilising FoxP3 expression and repressing pro-inflammatory genes encoding Tbet and IFN-γ (Kitz et al., 2016, Dominguez-Villar et al., 2011). In light of this function, the co-inhibitory receptors CTLA-4 (Brunet et al., 1987), PD-1 (Ishida et al., 1992), TIGIT (Yu et al., 2009), GITR (Sukumar et al., 2017), CD30 (Francisco et al., 2003) and GARP (de Streel et al., 2020) have been emerged and proposed as therapeutic targets in cancer. Here, we will focus on the downstream signalling pathway and resulting function of these co-inhibitory receptors upon ligand engagement in Tregs **(Figure 1.8)**.

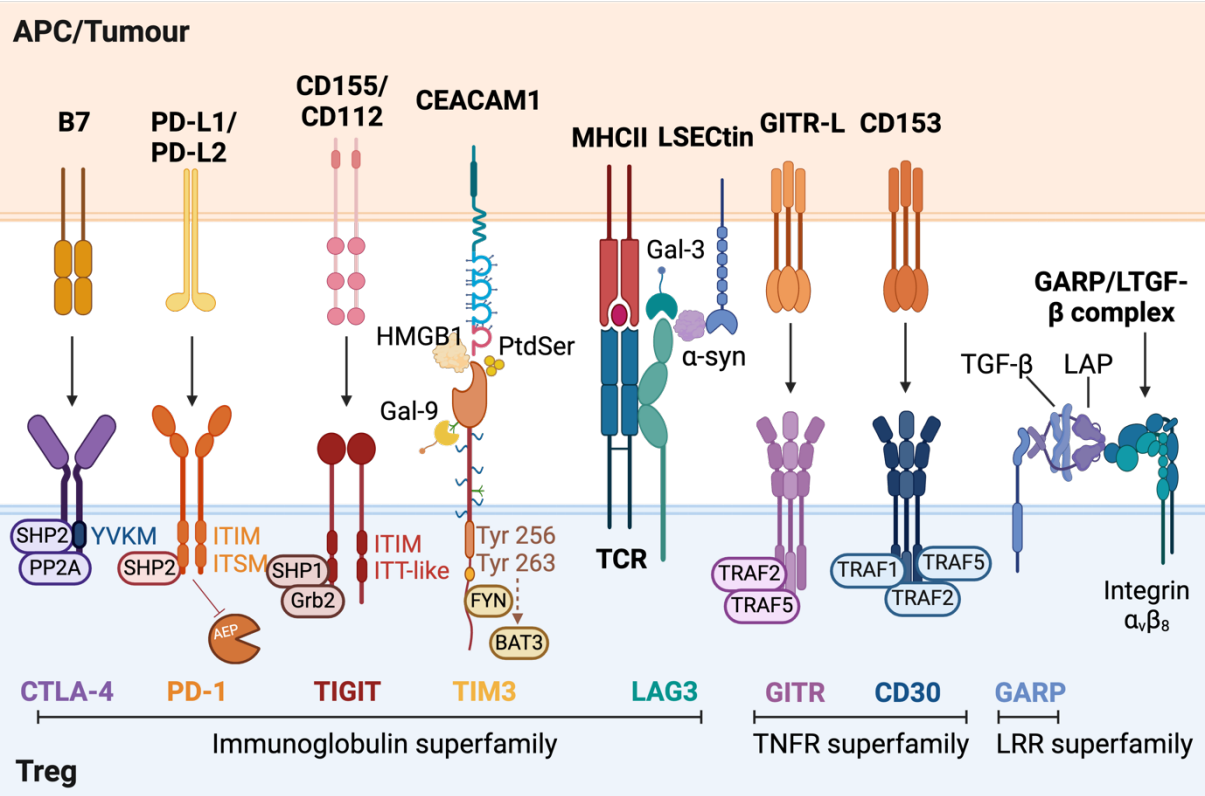

Figure 1.8 Canonical co-inhibitory receptors on Tregs and their corresponding receptor-ligand interactions.
Tregs express multiple co-inhibitory receptors that contribute to immune regulation by interacting with their respective ligands. CTLA-4 (cytotoxic T-lymphocyte antigen-4) binds to B7 (CD80/CD86) on antigen-presenting cells (APCs). PD-1 (programmed cell death receptor) interacts with PD-L1/PD-L2. TIGIT (T-cell immunoreceptor with immunoglobulin and ITIM domains) binds to CD155/CD112. LAG-3 (lymphocyte-activation gene 3) interacts with MHC class II molecules. TIM-3 (T-cell immunoglobulin and mucin-domain containing-3) binds to CEACAM1 and other ligands. GITR (glucocorticoid-induced tumour necrosis factor receptor-related protein) interacts with GITR ligand (GITRL). GARP (glycoprotein A repetitions predominant) is associated with TGF-β1 and its latent complex (LAP-TGF-β). CTLA-4, PD-1, TIGIT, TIM-3 and LAG-3 belong to immunoglobulin superfamily, GITR and CD30 belong to TNFR superfamily while GARP belongs to LRR (leucine-rich repeat) superfamily.

1.8.1 CTLA-4

Cytotoxic T-lymphocyte-associated protein 4 (CTLA-4), also known as CD152, is a CD28 homolog and is constitutively expressed on Tregs. The early stage of T-cell proliferation is believed to be regulated by CTLA-4 (Brunner et al., 1999). Like CD28, CTLA-4 binds B7-1 and B7-2 **(Figure 1.8)**. Due to the topology of its homodimer structure, CTLA-4 binds B7 ligands bivalently and hence has greater affinity to compete with monovalent CD28. Interaction between CTLA-4 and B7 ligands on APC counteracts the CD28-mediated costimulatory signals and prevents SMAC formation (Chunyang et al., 2013). Additionally, CTLA-4 on Tregs can entrap B7 ligands by trans-endocytosis in a cell-extrinsic manner for degradation (Qureshi et al., 2011), which further reduces the potency of APC to activate effector T cells. Notably, Tregs could outcompete CTLA-4^{+} effector T cells in capturing costimulatory ligands from APCs (Ovcinnikovs et al., 2019, Walker and Sansom, 2015), attributed to the higher level of CTLA-4 expression. Upon ligation of CTLA-4 on Tregs, TCRζ chain, CD28 and signalling molecules including CD3ε and ZAP70 are dephosphorylated. Therefore, an abrogation of the clustering of ZAP70 with LAT occurs which in turn inhibits the TCR signalling pathway. This could be mainly due to the recruitment of SH2-domain containing tyrosine phosphatase 2 (SHP2) to the YVKM motif, in which SHP2 is a downstream mediator of CTLA-4 (Rudd et al., 2009, Schneider et al., 1995). Besides that, the cytoplasmic domain of CTLA-4 can bind to the regulatory subunit of serine/threonine phosphatase PP2A which inhibits the PI3K-Akt pathway (Teft et al., 2009). In summary, consistent with the fact that suppression of PI3K-Akt pathway is required for Treg development, CTLA-4 demonstrates its role in Treg development by recruiting negative regulators of the PI3K-Akt pathway, SHP2 and PP2A.

Nonetheless, numerous studies have also demonstrated that kinases Fyn, Lyn and Lck can phosphorylate YVKM motif in cytoplasmic tail of CTLA-4, which in turn recruits and enhances PI3K activity (Hu et al., 2001, Hui et al., 2017, Ovcinnikovs et al., 2019, Rudd et al., 2009). Together with CD28 signalling, the migratory phenotype of Tregs into the TME is enhanced via activation of PI3K-mTOR pathway upon CTLA-4 engagement (Rudd et al., 2009, Kishore et al., 2017). Remarkably, B7-1 can interact with PD-L1 and deliver bidirectional inhibitory signals, proposing a crosstalk between PD-1 and CTLA-4 signalling pathways which exhibit synergistically inhibitory effect (Butte et al., 2007). Recent studies using *Ctla4*$^{fl/fl}$*Foxp3*^{Cre} mice have uncovered an unexpected role for CTLA-4 in Treg. Surprisingly, despite CTLA-4 deletion, Tregs retain their suppressive function, effectively protecting against experimental autoimmune encephalomyelitis (EAE) and dampening anti-tumour immunity in

MC38 tumours. This suggests that CTLA-4 is not essential for inducing T cell dysfunction within the TME. These findings offer additional insights into why Ipilimumab, a monoclonal antibody (mAb) targeting CTLA-4, is associated with immune-related adverse effects compared to traditional chemotherapies, despite its significant improvement in overall survival for patients with advanced-stage melanoma (FDA, 2011, Squibb, Savoia et al., 2016).

1.8.2 PD-1

Programmed cell death 1 (PD-1), also known as CD279, is expressed on activated T cells, B cells and monocytes. PD-1 can bind PD-1 ligands PD-L1 (B7-H1, CD274) and PD-L2 (B7-DC, CD273) **(Figure 1.8)**; the former is ubiquitously expressed on activated T cells, B cells and cancer cells, whereas the latter is specifically on APCs. Engagement of PD-1 with PD-L1 and PD-L2 can deliver an inhibitory signal to PD-1 expressing cells (Amarnath et al., 2010). Although PD-1 and CTLA-4 has been shown to use the same downstream signalling molecules, biased signal cascades can be observed upon activation (Parry et al., 2005). Differently from YVKM motifs in CTLA-4, the cytoplasmic tail of PD-1 contains an immunoreceptor tyrosine-based inhibitory motif (ITIM) and an immunoreceptor tyrosine-based switch motif (ITSM). Specifically, ITSM mutation reveals its prominent role in the inhibitory function of PD-1 (Chemnitz et al., 2004). In the presence of TCR signalling, the tail of PD-1 can be phosphorylated by Lck, which further recruits SHP1 and especially SHP2 with stronger interaction (Sheppard et al., 2004). SHP2 acts immediately by reducing phosphorylation of TCR proximal signalling molecules and attenuating the TCR signalling pathway (Yokosuka et al., 2012). PD-1 can also inhibit PI3K-Akt activity via ITSM motif in its cytoplasmic domain (Parry et al., 2005), suggesting a role for PD-1 in Treg development and stability. Simultaneously, intracellular anti-apoptotic signals can be delivered into PD-L1 overexpressing cancer cells, triggering tumour progression (Gato-Cañas et al., 2017). Pembrolizumab (Keytruda) was the first FDA approved drug targeting PD-1 following by Nivolumab (Opdivo). Both PD-1 antibodies show greater efficiency than ipilimumab against stage III and metastatic melanoma, attributed to the reinvigoration of exhausted CTLs which can kill cancer cells and thus restoration of anti-tumour immunity (Robert et al., 2015b, Wolchok et al., 2013).

Recently, the multifaceted roles of PD-1/PD-L1 pathway on Tregs have been explored and suggested to contribute to the complexity of PD-1 checkpoint inhibitor in melanoma TME. Firstly, PD-1 has been shown to maintain the suppressive function of Tregs through

upregulating PTEN and therefore antagonises PI3K signalling (Francisco et al., 2009). Secondly, our previous study demonstrated that PD-L1 engagement can orchestrate reprogramming of human PD-1^{+}Tbet^{+} Th1 cell to a regulatory phenotype (Amarnath et al., 2011). Via downstream SHP1/2 phosphatases, STATs and/or Akt are dephosphorylated and thus dampen the transcriptional signature of Th cell lineage (Amarnath et al., 2011, Franceschini et al., 2009, Francisco et al., 2009). This finding was consistent with the work in murine naïve T cells (Francisco et al., 2009). Thirdly, we also found that PD-1 can maintain FoxP3 stability by inhibiting an endo-lysosomal protease called AEP in a PD-L1-independent manner (Stathopoulou et al., 2018). AEP is known to be responsible for antigen processing in DCs (Manoury et al., 1998), but we found that it also destabilises FoxP3 expression in both iTregs and Tbet^{+} iTregs (Stathopoulou et al., 2018). Although the importance of PD-1 in iTreg development and FoxP3 stabilisation has been elucidated, recently PD-1 has been demonstrated to inhibit the activation and suppressive capacity of Tregs *in vivo* (Tan et al., 2020). PD-1-deficient Tregs have more capacity to inhibit effector T cell proliferation but along with less survival compared with PD-1^{+} Tregs, attributable to the reduced PI3K-Akt signalling (Tan et al., 2020). This indirectly revealed that PD-1 could promote activation of PI3K-Akt pathway in PD-1^{+} Tregs, thereby limiting Tregs activation. Overall, the above findings proposed a role of PD-1 in regulating suppressive function of Tregs and concurrently preserving Treg survival.

1.8.3 TIGIT

T cell immunoreceptor with Ig and ITIM domains (TIGIT), also known as WUCAM, VSIG9 and Vstm3, is widely expressed on T cells and NK cells (Manieri et al., 2017). Being one of the transcriptional targets of FoxP3, TIGIT is therefore constitutively upregulated on activated Tregs. Although TIGIT binds the ligands PVR (CD155) and nectin-2 (CD112) like CD226 **(Figure 1.8)**, but TIGIT and CD226 exert opposite effects in a competitive way. TIGIT binds CD155 with a higher affinity and exhibits its inhibitory function through interfering with co-stimulatory CD226 signalling (Sanchez-Correa et al., 2019). In *cis*, TIGIT harbours an ITIM and immunoglobulin tail tyrosine (ITT)-like motif on its cytoplasmic tail, which can mediate negative downstream signalling (Stanietsky et al., 2013, Liu et al., 2013). It has been demonstrated that the ITT-like motif has a major role in the TIGIT-mediated regulation of NK cells (Liu et al., 2013). TIGIT-CD155 engagement induces phosphorylation of the ITT-like motif, which in turn recruits growth factor receptor-bound protein-2 (Grb2) and SH2-containing inositol phosphatase 1 (SHIP1). Consequently, SHIP1 abrogates PI3K and mitogen-

activated protein kinase (MAPK) signalling, suppressing the cytotoxicity of NK cells. While the precise downstream mechanisms of TIGIT-CD155 interaction on Tregs remains to be defined, TIGIT could confer a superior suppressive capacity of Tregs by dampening PI3K signalling.

Compared to pTregs and effector T cells, TIGIT is more significantly expressed on tTregs (Fuhrman et al., 2015). High TIGIT expression together with low CD226 expression have been manifested to favour activation and expansion of tumour-infiltrating Tregs in melanoma (Fuhrman et al., 2015). This could be attributed to the TIGIT-mediated suppression of PI3K-Akt signalling in pTregs, which in turn inhibits the acquisition of a Th1 cell-like phenotype (Lucca et al., 2019). Despite high expression of TIGIT was found to associate with worse survival (Lee et al., 2019) in melanoma patients and blockade of TIGIT on $CD8^+$ T cells and Tregs was demonstrated to enhance anti-tumour function (Ge et al., 2021, Fourcade et al., 2018), no TIGIT checkpoint inhibitor has been approved by FDA for cancer immunotherapy.

1.8.4 LAG-3

Lymphocyte activating-3 (LAG-3), also known as CD223, is significantly found on tissue-infiltrating Tregs and tumour-infiltrating Tregs compared to effector T cells (Magnuson et al., 2018, Huang et al., 2004). The ligands of LAG3 are MHCII, FGL-1, α-synuclein fibrils (α-syn), lectins galectin-3 (Gal-3), and lymph node sinusoidal endothelial cell C-type lectin (LSECtin) **(Figure 1.8)**. Indeed, LAG-3 confers both intrinsic and extrinsic regulatory activity. In *trans*, LAG-3 delivers inhibitory signal to APCs by outcompeting with CD4 to bind MHCII (Liang et al., 2008); in *cis*, LAG-3 limits Tregs proliferation (Lucca and Dominguez-Villar, 2020). It is noteworthy that several studies showed LAG-3 acts functionally independent from CD4 (Xu et al., 2014, Wang et al., 2019, Kouo et al., 2015) and MHCII (Hannier et al., 1998, Tian et al., 2015), but relies on its cytoplasmic domain for suppressive function. Conventionally, LAG-3 is translated, resides in late endosomes and subsequent trafficked to cell surface upon TCR activation. Once LAG-3 binds to its ligand, an inhibitory signal is delivered through its unknown inhibitory motifs to counteract TCR downstream signalling pathway. Although three regions conserved between mice and humans: RRFSALE motif, KIEELE motif and EX/EP repeat motif, have been proposed to be potent in signal transduction, however all remained speculative due to the inconsistent perspectives (Graydon et al., 2021). Consequently, the expression of transcription factor including NFAT is downregulated, thereby reducing cytokine IL-2 production and T-cell proliferation. Inhibitory activity of surface LAG-3 is regulated by

a disintegrin and metalloproteinase (ADAM10 and ADAM17), particularly on plasmacytoid dendritic cells (pDCs) (Andrews et al., 2020), producing soluble LAG-3 (sLAG-3). While it remains unclear whether sLAG3 can bind and inhibit MHCII, studies indicate that non-cleavable LAG-3 or metalloproteinase inhibitor impairs T cell-mediated immunity in cancer patients, indirectly suggesting an inert role of sLAG-3 (Li et al., 2007, Andrews et al., 2020). Notably, LAG-3^{+}Tregs are more prevalent in the TME and circulation of cancer patients compared to healthy individuals (Camisaschi et al., 2010), supporting the notion that LAG-3 enhances the suppressive function of Tregs toward APCs.

LAG-3 has emerged as a promising target in cancer immunotherapy, while clinical trial evaluating its blockade in combination with PD-1 inhibitors showing encouraging result in advanced melanoma (Ascierto et al., 2017). The phase II/III RELATIVITY-047 trial showed that the anti-LAG-3 antibody (relatlimab), in combination with anti-PD-1 antibody (nivolumab), significantly improved progression-free survival in patients with advanced melanoma compared to nivolumab alone (Tawbi et al.). This led to the first FDA approval of a dual LAG-3/PD-1 checkpoint blockade. While the primary mechanism of LAG-3 inhibition is thought to reinvigorate exhausted effector T cells, emerging evidence suggests it may also modulate Treg function, warranting further investigation.

1.8.5 TIM3

T cell immunoglobulin and mucin domain-containing protein 3 (TIM3), encoded by *Havcr2*, is expressed on IFNγ-producing cells, Tregs and APCs. In fact, it is initially located in lipid rafts before being recruited to SMAC upon T-cell activation (Clayton et al., 2014). TIM3 can bind multiple ligands including galectin 9, phosphatidylserine (PtdSer), carcinoembryonic antigen-related cell adhesion molecule 1 (CEACAM1) and high mobility group protein B1 (HMGB1) (Wolf et al., 2020) **(Figure 1.8)**. Of note, only galectin 9 (Zhu et al., 2005) and CEACAM1 (Huang et al., 2015) can interact with TIM3 both in *trans* and in *cis*. Like LAG-3, the intracellular signalling upon TIM3 activation is not fully elucidated due to the lack of canonical inhibitory motifs. Nevertheless, it has been found that Tyr256 and Tyr263 on cytoplasmic tail can deliver downstream inhibitory signal through interaction with HLA-B-associated transcript 3 (BAT3) and tyrosine kinase FYN (Rangachari et al., 2012, Lee et al., 2011). In TIM3 inert state, there is a BAT3 attached on its cytoplasmic tail to recruit activated Lck. Upon binding of TIM3 with galectin 9, BAT3 is released from TIM3 while FYN induces the inhibitory phosphorylation of Lck (Davidson et al., 2007). In the aid of receptor

phosphatases CD45 and CD148, TIM3 can disrupt the formation of SMAC (Clayton et al., 2014). Collectively, these result in downregulation of TCR signalling cascade associated with PI3K-Akt pathway and T-cell proliferation.

High suppressor activity of TIM-3^{+}Tregs has been found both *in vitro* and *in vivo* (Gautron et al., 2014, Sakuishi et al., 2013), potentially due to diminished PI3K-Akt pathway. Besides that, TIM-3 is preferentially expressed on tumour-resident and tumour-infiltrating Tregs compared with circulating Tregs in human cancers (Gao et al., 2012, Yan et al., 2013). This enrichment in the immunosuppressive TME highlights TIM-3 as a marker of highly suppressive Tregs in tumours and a promising immunotherapeutic target. While TIM-3 blockade has demonstrated potential in enhancing anti-tumour immunity by revitalising effector T cells (Zeidan et al., 2023, Sakuishi et al., 2010, Ngiow et al., 2011, Zhou et al., 2011), no TIM-3-targeting therapy has been approved by FDA for cancer immunotherapy.

1.8.6 GITR

Glucocorticoid-induced tumour necrosis factor related protein (GITR) is encoded by *Tnfrsf18* and belongs to the tumour necrosis factor receptor (TNFR) superfamily. It is constitutively expressed on Tregs and can be found on Tconv cells and non-T cells at low to moderate levels (Shimizu et al., 2002, McHugh et al., 2002). GITR expression is increased upon several different stimulations within 24h on both Tregs and Teff cells (Shimizu et al., 2002, Krausz et al., 2007). In the context of Tregs, FoxP3 promotes GITR expression (Khattri et al., 2003) which is distinct from that of the Tconv cells which rely on canonical NF-kB signalling (Zhan et al., 2008). GITR binds to its ligand GITRL which is predominantly found on APCs and endothelial cells **(Figure 1.8)**. GITR-GITRL interaction recruits TNFR associated factors (TRAFs) 2 and 5, positively modulating downstream activation of the MAPK including p38, ERK1/2 and JNK, and canonical NF-kB signalling, promoting cell survival through upregulation of Bcl-xL and cytokine production (Snell et al., 2010, Esparza et al., 2006). Despite TRAF1 has been proposed to interact with GITR (Kwon et al., 1999), there is a study showing the activation of downstream canonical NF-kB pathway in TRAF1-deficienct primary T cells (Snell et al., 2010). Furthermore, GITR-GITRL stimulation in Tregs has been demonstrated to activate downstream canonical NF-kB and JNK pathway *in vitro*, but not ERK1/2 or p38, in which JNK signalling is vital in abrogation of Treg suppressive function upon GITR engagement (Kwon et al., 1999).

In general, GITR stimulated by GITRL or anti-GITR antibodies (DTA-1) can enhance TCR-induced T cell proliferation and cytokine production including IL-2 and IFN-γ (Tone et al., 2003, Stephens et al., 2004, Kanamaru et al., 2004, Igarashi et al., 2008, Kohm et al., 2004, Ronchetti et al., 2004, Ronchetti et al., 2007). However, the functional roles of GITR on Tregs are more complex with studies showing its positive role in promoting Treg expansion (van Olffen et al., 2009) and its negative role in dampening Treg suppressive function (Kanamaru et al., 2004, Ronchetti et al., 2004, Valzasina et al., 2005) and inducing Teff resistance to Treg suppression (Shimizu et al., 2002, Stephens et al., 2004, Ko et al., 2005, Nishikawa et al., 2008, Mitsui et al., 2010). Furthermore, DTA-1 agonist has been demonstrated to reduce FoxP3 expression, modify intracellular localisation of FoxP3 in tumour-infiltrating Tregs and deplete Tregs (Cohen et al., 2010, Coe et al., 2010). Whether the effect of DTA-1 agonist on FoxP3 expression was due to a direct effect of downstream GITR signalling in Tregs which leads to loss of Foxp3 or an indirect effect due to modified cytokine environment remained questionable.

1.8.7 CD30

CD30 is encoded by *Tnfrsf8* and belongs to the TNFR superfamily. CD30 was firstly discovered on Reed-Sternberg cells associated with Hodgkin's disease by promoting Reed-Sternberg proliferation and survival (Gruss et al., 1994, Gruss et al., 1996). Further studies have shown that it can be expressed on activated lymphoid cells and anaplastic large cell lymphomas (ALCL) (Hsu and Hsu, 2000, Gattei et al., 1997). In fact, *in vitro* stimulation of T cells with anti-CD3 antibodies has been reported to induce CD30 on various T cell subsets including Th0, Th1 and Th2 cell clones (Bengtsson et al., 1995, Hamann et al., 1996). CD30 binds to CD30L (also known as CD153) **(Figure 1.8)** which is expressed on APCs, activated T cells, granulocytes and resting B cells (Horie and Watanabe, 1998, Romagnani et al., 1998). CD30/CD30L engagement induces receptor trimerization and signal transduction via recruitment of TRAF including TRAF1, TRAF2 and TRAF5, along with TRAF-binding proteins (Smith et al., 1994, Duckett and Thompson, 1997). This signalling complex then activates downstream NF-kB pathway and MAPK pathway including ERK1/2, contributing to pro-survival and anti-apoptotic benefits (Duckett et al., 1997, Zheng et al., 2003, Krysov et al., 2007, Watanabe et al., 2011). Brentuximab vedotin (SGN-35) is an anti-CD30 mAb conjugated with a microtubule disrupting agent called monomethyl auristatin E (King et al., 2002, Francisco et al., 2003). It has been approved by FDA in treating relapsed CD30-expressing Classical Hodgkin, systemic anaplastic large cell lymphoma (ALCL) and adult T-cell leukaemia (Francisco et al., 2003, Maeda et al., 2010).

Although CD30 has been well studied in Hodgkin lymphoma and ALCL, its role in T cells including Treg is still not fully understood. Gerli R *et al.* have found the regulatory phenotype of CD30 on T cells in rheumatoid arthritis and accumulation of those CD30-expressing cells at the inflammatory sites of patients diagnosed with systemic sclerosis and chronic graft versus host disease (GvHD) (Gerli et al., 2000). Zeiser *et al.* have demonstrated that early CD30 signalling involves in Treg-mediated acute GvHD protection by blocking the CD30/CD153 pathway using anti-CD153 mAb during the early phase after major MHC-mismatch bone marrow transplantation (Zeiser et al., 2007). From here, whether CD30 contributes to Treg suppressive function and its role in Tregs in TME remains to be identified.

1.8.8 GARP

Glycoprotein A repetitions predominant (GARP) is encoded by *Lrrc32* and belongs to leucine-rich repeat (LRR) superfamily. Surface expression of GARP is detected on mesenchymal stromal cells, platelets and Tregs (Roubin et al., 1996, Macaulay et al., 2007, Li et al., 2015). Unlike constitutive expression of CTLA-4 and GITR on Tregs, the high expression of GARP is only restricted to those activated Tregs (Noyan et al., 2014, Zhou et al., 2013). GARP is responsible in TGF-β activation. In brief, a proprotein is first made up of mature TGF-β, latency associated peptide (LAP) and a signal peptide. The signal peptide was then cleaved by furin proteases, turning inactive TGF-β into mature TGF-β. Mature TGF-β binds LAP through disulfide bridges and non-covalent interactions, forming latent TGF-β (LTGF-β). GARP allows the binding of LTGF-β to the αVβ8 integrin to form a ring-like shape with TGF-β orientated towards the centre and this complex is known as GARP/LTGF-β complex **(Figure 1.8)**. TGF-β can be released either by metalloproteinases or serine proteases recruited by integrins that may cleave LAP from the GARP/LTGF-β complex, or through binding of the integrins to LTGF-β to result in deformation of the LAP and cell contraction. Mature TGF-β released from Tregs can act in both paracrine and autocrine manner. TGF-β downregulates Teff function by inhibiting their proliferation and cytokine production capability. In parallel, it is also able to induce FoxP3 expression and maintain Treg function via downstream Smad2/3 phosphorylation **(Figure 1.5c)**.

Tregs expressing GARP have been found to possess greater suppressive capacity in mice with colitis-associated colon cancer (Pastille et al., 2014). Those high suppressive Tregs isolated from head and neck squamous cell carcinoma patients also showed upregulated GARP and LAP expression, thereby suppressing anti-tumour responses and leading to recurrence of

cancer (Schuler et al., 2013). Depletion of $GARP^+CTLA\text{-}4^+$ Tregs has been shown to restore anti-tumour function of $CD8^+$ T cells (Kalathil et al., 2013). Thus, blockade of LTGF-β/GARP may represent a novel target to inhibit Treg function in cancer immunotherapy. Igney *et al.* have produced several batches of antibodies with distinct binding specificities that can interfere with active TGF-β formation and associated signalling, but these antibodies showed no effect on Treg function *in vitro* (Igney et al., 2023). Despite Cuende *et al.* has generated and found two anti-GARP antibodies which were able to inhibit the suppression capacity of human Tregs in both *in vitro and in vivo* (Cuende et al., 2015), no GARP ICB has been approved by FDA for cancer immunotherapy until now.

1.1 Hypothesis

While antibodies targeting PD-1/PDL1 pathway has been successful in treating several cancers, many cancer patients still fail to respond (Larkin et al., 2019) and in some cases PD-1 inhibition may even exacerbate cancer growth (Park et al., 2021). The mechanisms underlying this resistance remain unclear, but correlative studies in human cancers have suggested that Tregs play a central role in immune evasion following PD-1 therapy (Kamada et al., 2019). In this discussion, we focus on CTLA-4, CD30, GARP, and TIGIT, given their well-established roles in regulating Treg function and their potential impact on anti-PD-1 resistance. Although TIM-3 and LAG-3 are emerging immune checkpoints with stronger links to T effector cell biology, our focus remains on those with more defined mechanisms in Treg-mediated immunosuppression and their contribution to therapy resistance. Understanding how these key checkpoint receptors shape Treg function in the context of PD-1 blockade resistance will provide valuable insights into overcoming immune evasion in cancer immunotherapy.

1.2 Aims

This study aims to

- determine whether PD-1 regulates the co-inhibitory receptors on Tregs in mice.
- determine how alterations in the co-inhibitory receptor landscape influence Treg function.
- determine whether PD-1 regulates co-inhibitory receptor expression on Tregs in human.
- determine how alterations in the co-inhibitory receptor contribute to resistance against PD-1 blockade in cancer patients.

Chapter 2 Materials and Methods

2.1 Mice

C57BL/6, CD45.1 C57BL/6 and *Rag1*$^{-/-}$ mice were purchased from Charles River Laboratories while *Foxp3*^{RFP} and *Foxp3*$^{ERT2\text{-}Cre\text{-}GFP}$ mice were purchased from Jackson Laboratory. *Pdcd1*$^{-/-}$ (*Pd1*$^{-/-}$) C57BL/6 were provided by Dr Lieping Chen (Yale University School of Medicine, New Haven, CT). *Pd1*$^{-/-}$ mice were further bred to *Foxp3*^{RFP} mice to generate *Pd1*$^{-/-}$*Foxp3*^{RFP} mice as shown in **Figure 2.1**.

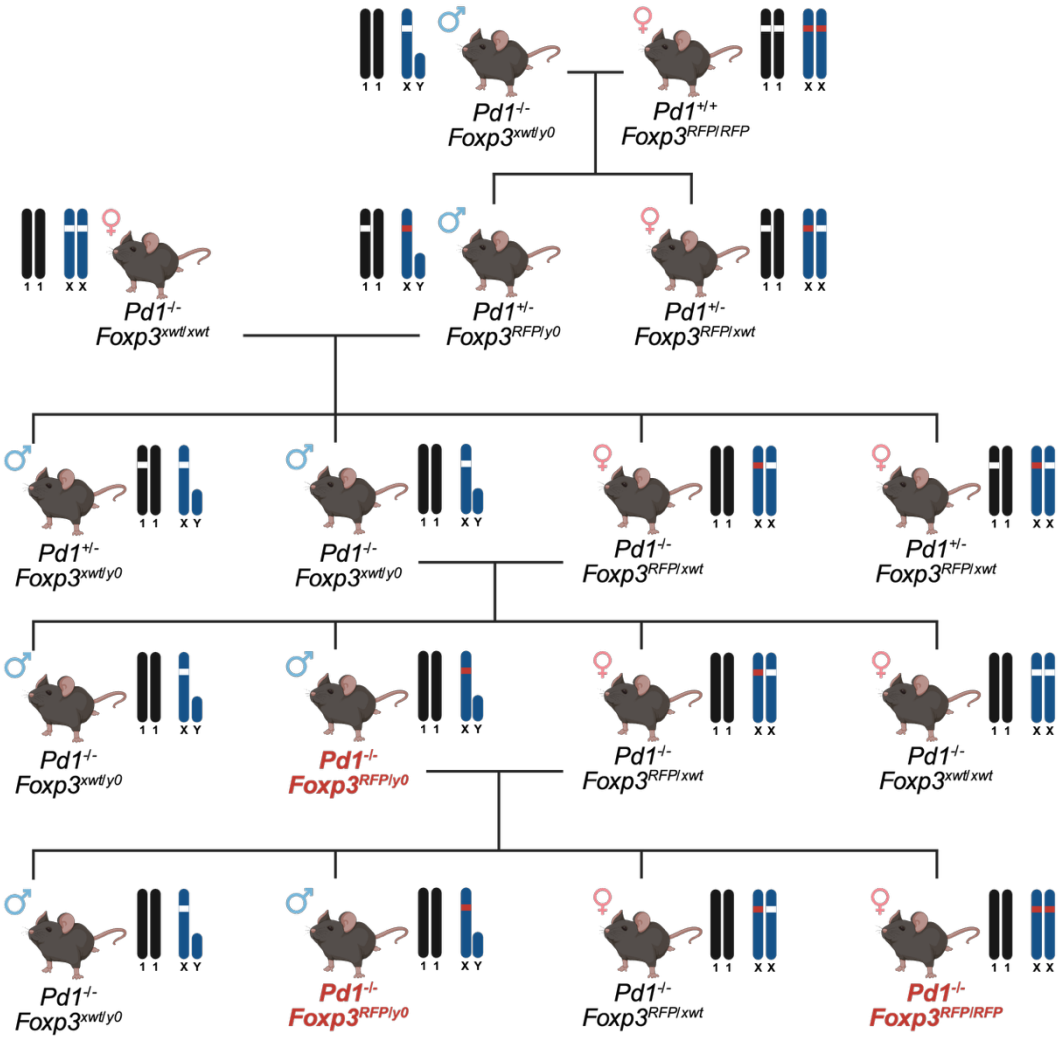

Figure 2.1 Breeding Scheme for *Pd1*$^{-/-}$*Foxp3*^{RFP}.
Pdcd1 gene locus is located in chromosome 1 while *Foxp3* gene locus is located in sex chromosome. A *Pdcd1*$^{-/-}$ (*Pd1*$^{-/-}$) male mouse was crossed with a *Foxp3*^{RFP} female mouse to generate *Pd1*$^{+/-}$*Foxp3*$^{RFP/y0}$ males, which were then backcrossed with *Pd1*$^{-/-}$ females to produce *Pd1*$^{-/-}$*Foxp3*$^{RFP/xwt}$ females. Backcrossing of *Pd1*$^{-/-}$*Foxp3*$^{RFP/xwt}$ females with *Pd1*$^{-/-}$ males resulted in generation of desired *Pd1*$^{-/-}$*Foxp3*$^{RFP/y0}$ males (highlighted in red). Desired

Pd1$^{-/-}$*Foxp3*$^{RFP/RFP}$ females (highlighted in red) were then produced by crossing the desired males with *Pd1*$^{-/-}$*Foxp3*$^{RFP/xwt}$ females. The line was maintained as homozygous for *Pd1*$^{-/-}$, along with hemizygous or homozygous for *Foxp3*^{RFP}.

Pdcd1$^{fl/fl\text{-}DTR\text{-}tdTomato}$ (*Pd1*$^{fl/fl}$) mice were generated in Ozgene using a PD-1 targeting vector containing neo flippase-recognition sites (FRT) on either side of neo cassette. Gene sequence encoding internal ribosome entry sites (IRES), reporter tdTomato, peptide 2A (P2A) and diphtheria toxin receptor (DTR) were knocked into exon 5 while loxP sites were inserted to be flanking exons 2 and 3 encoding transmembrane and first cytoplasmic exon of PD-1 respectively **(Figure 2.2a)**. Linearised vector DNA was electroporated into C57BL/6 embryonic stem (ES) cells and the resulting neomycin-resistant (neo) ES cells were screened for homologous recombination. ES cells carrying the desired recombinant event were microinjected into blastocysts, and the resulting chimeric mice produced germline transmission of the targeted PD-1 allele. Mice carrying the targeted allele were bred with flippase-expressing mice to delete neo, yielding *Pd1*$^{fl/fl}$ mice (**Figure 2.2b**). To inducibly ablating PD-1 expressing cells, *Pd1*$^{fl/fl}$ mice were given 10mg/kg of diphtheria toxin from *Corynebacterium diphtheriae* (Sigma-Aldrich, Dorset, UK) in PBS up to 10 dosages at two-day intervals via intraperitoneal (IP) injection. *Pd1*$^{fl/fl}$ males were further bred to *Foxp3*$^{Ert2\text{-}Cre\text{-}GFP}$ (*Foxp3*^{ERT2Cre}) females to generate *Pd1*$^{fl/fl}$*Foxp3*^{ERT2Cre} mice (**Figure 2.2c**) using the breeding strategy similar to that of the *Pd1*$^{-/-}$*Foxp3*^{RFP}. To selectively eliminate PD-1 in FoxP3-expressing regulatory T cells (Tregs), *Pd1*$^{fl/fl}$*Foxp3*^{ERT2Cre} mice were given 1mg tamoxifen (Sigma-Aldrich) in corn oil for 5 consecutive days via IP injection (**Figure 2.2c**).

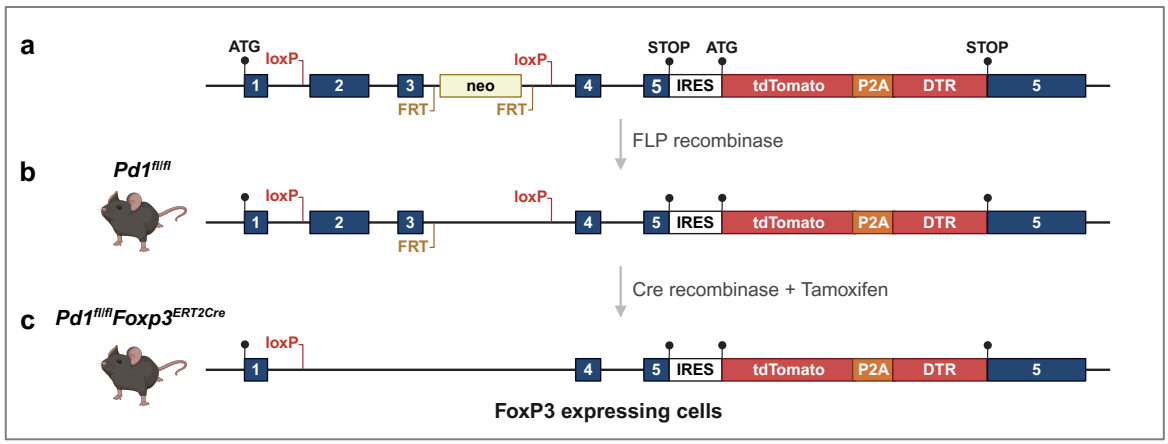

Figure 2.2 Generation of *Pd1*$^{fl/fl}$ and *Pd1*$^{fl/fl}$*Foxp3*^{ERT2Cre} mice.
(a) Gene targeted locus of the *Pd1* gene consisting of exon 1-5, FRT, neo cassette, IRES, tdTomato, P2A and DTR. **(b)** Schematic showing generation of PD-1 expressing cell-specific ablation mice, referred to as *Pd1*$^{fl/fl}$ mice. **(c)** Schematic showing generation of

inducible Treg-specific PD-1 conditional knockout mice, referred to as $Pd1^{fl/fl}Foxp3^{ERT2Cre}$ mice.

All mice were bred and maintained in a pathogen-free facility at Newcastle University under a home office-approved project license (PPL number: PBFB610F9). Ear notch samples from breeders and pups generated from heterozygous breeders were collected and sent to Transnetyx for genotyping to confirm the genetic background of the mice. All experimental animals were 8 to 12 weeks of age. All murine experimental procedures were performed at Newcastle University incorporating the NC3R guidelines for animal research, and the data were presented according to the ARRIVE guidelines.

2.2 Patient characteristics

Human PBMC from healthy donors were derived from NHS Blood and Transplant (NHSBT) in Newcastle upon Tyne. Stage IV metastatic melanoma patients were recruited from Royal Victoria Infirmary in Newcastle upon Tyne under ethics [REC reference 24/NE/0014]. Patients were treated with combination therapy of ipilimumab (anti-CTLA4) and pembrolizumab (anti-PD-1). Blood samples were collected on the subsequent clinic visit post treatment, at which point the antibody plasma concentration was three half-lives of both antibodies. Hence, in keeping with the literature (Brahmer et al., 2010) the effect of anti-PD-1 was deemed minimal in this cohort. Publicly mined dataset (Tirosh et al., 2016, Sade-Feldman et al., 2018) included tumour-infiltrating lymphocytes (TILs) from treatment naïve patients, and patients treated with anti-PD-1 including pre and post treatment. Patients who responded and not responded were also used from public dataset. For responders, only samples that contained post treatment biopsy dataset was utilised to match the non-responders. The characteristics of metastatic melanoma patients are shown in **Appendix Table D.1**.

2.3 Reagents

Mouse complete media was made up of DMEM (Gibco/Thermo Fisher Scientific) supplemented with 10% FBS, 2mM L-glutamine (Corning, Wales, UK), 0.1mM non-essential amino acids, 1mM sodium pyruvate (Sigma-Aldrich), 50µM 2-mercaptoethanol and penicillin and streptomycin (100 units/ml penicillin; 100µg/ml streptomycin, Corning). Melanoma culture media was made up of DMEM (Gibco) supplemented with 10% FBS and penicillin and streptomycin (100 units/ml penicillin; 100µg/ml streptomycin). Flow cytometry staining (FACS) buffer was made up of PBS supplemented with 0.5% BSA

(Sigma-Aldrich) and 0.01% sodium azide. HEPES buffer was made up of PBS supplemented with 1% HEPES (Sigma-Aldrich). Miltenyi buffer was made up of PBS supplemented with 0.5% BSA and 2mM EDTA (Sigma-Aldrich). Human peripheral blood mononuclear cell (PBMC) culture media was made up of X-VIVO^{TM} 15 with gentamicin and PR (Lonza, Berkshire, UK) formulated with 10% FBS.

2.4 B16F10 melanoma tumour model

B16 melanoma was set up using established protocols (Stathopoulou et al., 2018, Lim et al., 2023). B16F10 melanoma cells were cultured in melanoma culture media at 37 °C with 5% CO_2. Mice were inoculated with 3x10^5 B16F10 melanoma cells via subcutaneous (SC) injection into the flank as previously reported (Mallett et al., 2020). Tumour volume was measured daily from day 5 post inoculation and calculated by the following equation: tumour volume = π/6 x 0.5 x length x width^2 as described previously (Schatton et al., 2008). In certain experiments, *Pd1$^{fl/fl}$* and *Pd1$^{fl/fl}$Foxp3^{ERT2Cre}* mice were utilized and treated with PBS or 1mg tamoxifen in corn oil respectively via IP injection for 5 consecutive days prior of tumour reconstitution. For Treg adoptive transfer experiment, *Rag1$^{-/-}$* mice were re-constituted with 5x10^4 sorted CD4$^+$CD25$^-$ from CD45.1 WT mouse as Teff cells along with 5x10^4 sorted CD4$^+$Foxp3^{RFP} as Tregs from either Foxp3^{RFP} or *Pd1$^{-/-}$* Foxp3^{RFP} mice via intravenous (IV) injection at day 8 post inoculation. In certain experiments, mice were treated with with 0.1mg isotype control IgG2a (2A3, Bio X Cell, NH, USA) or anti-CD153 (RM153, 2BScientific, Oxfordshire, UK) via IP injection for 4 times at two-day intervals starting from day 9. Mice were euthanised when tumour volume reached 800mm^3-1500mm^3.

2.5 Mouse tissue isolation and single cell preparation

2.5.1 Spleen and mesenteric lymph node

Single-cell suspensions of spleen and lymph node were generated by mechanically disrupting tissue through a 40μm strainer into mouse complete media. For splenocytes, cells were incubated with 3mL red blood cell (RBC) lysis buffer (BioLegend, London, UK) for 3 min at room temperature (RT). Cells were washed with 10mL complete media for 5 min at 400 × g and resuspended in 10mL complete media.

2.5.2 Liver

Liver was perfused with PBS before harvesting. Liver tissue was incubated at 37ºC for 30 min in 2mL FBS free DMEM media containing liberase (0.25mg/mL; Roche, West Sussex, UK) and DNase I (0.5mg/mL; Roche). Single-cell suspensions were prepared by mechanically disrupting tissue through 100µm strainer into 5mL FBS. After washing with complete media for 5 min at 400 × g, the pellet was re-suspended in 10mL 40% Percoll solution (Sigma-Aldrich) and was centrifuged at 600 × g for 30 min with no brake. After centrifugation, the pellet containing lymphocytes and RBCs were isolated. RBCs were eliminated using 3mL RBC lysis buffer for 3 min at RT. Cells were then washed with 10mL complete media and resuspended in 10mL complete media.

2.5.3 Bone marrow

Bone marrow femurs were isolated into petri dish containing HEPES buffer and both femur ends were snapped using scalpels. The marrow was then flushed out into the petri dish with 10mL HEPES buffer using a syringe with 25-gauge needle attached. Repeat flushing was performed until the bone turned white, indicating that all the marrow was removed. Single-cell suspension was prepared by mechanically disrupting tissue through 70µm strainer into 10mL HEPES buffer. After centrifugation for 5 min at 400 × g, cells were incubated with 3mL RBC lysis buffer for 3 min at RT. Cells were washed with 10mL complete media for 5 min at 400 × g and resuspended in 10mL PBS.

2.5.4 Tumour-infiltrating lymphocyte isolation

Tumour tissue was incubated at 37ºC for 30 min in 2mL FBS free DMEM media containing liberase (0.25mg/mL; Roche) and DNase I (0.5mg/mL; Roche). Single-cell suspensions were prepared by mechanically disrupting tissue through 100µm strainer into 5mL FBS. After washing with 10mL complete media for 5 min at 400 × g, pellet was re-suspended into 5mL complete media and was layered on the top of 5mL lymphocyte separation media (LSM; PromoCell). After centrifugation for 20 min at 600 × g, the top-to-bottom layers consisting of plasma, tumour-infiltrating lymphocytes (TILs), LSM, and RBCs and/or tumour cells. TILs residing in the interphase were isolated using a transfer pipette. TILs were washed twice with 10mL complete media and centrifuged for 20 min at 600 × g to remove any residual LSM. After washing, TILs were resuspended in 5mL complete media.

2.5.5 Tumour-draining lymph nodes

Tumour-draining lymph nodes (TDLNs) were isolated from the inguinal draining lymph nodes. Single-cell suspension was generated by mechanically disrupting TDLNs through a 40μm strainer into complete media. Cells were washed with 10mL complete media for 5 min at 400 × g and resuspended in 1mL complete media.

2.6 Human peripheral blood mononuclear cell isolation

Human peripheral blood mononuclear cells (PBMCs) were isolated from whole blood using Leucosep method. 3mL of LSM were added into the Leucosep tube (Greiner) and the tube was centrifuged at RT for 30 s at 1000 × g to sediment the LSM below the porous membrane. Blood was diluted with PBS to 1:2 dilution. 3-8mL blood was distributed into the tube and was centrifuged at RT for 10 min at 1000 × g with no brake. After centrifugation, the top-to-bottom layers consisting of plasma, PBMCs, LSM, porous barrier, LSM and a pellet enriched with RBCs and granulocytes were observed. The plasma layer fraction up to a minimum remnant of 5-10 mm above the PBMC layer was discarded to prevent contamination of PBMCs. The PBMC layer was then isolated with a transfer pipette and was washed twice with PBS at RT for 10 min at 250 × g to remove any residual LSM. After washing, PBMCs were resuspended in 5mL PBS.

2.7 Flow cytometry and cell sorting

2.7.1 Cell viability staining

Single cell suspensions were generated from indicated tissues and washed with PBS prior to staining. Cells were stained with LIVE/DEAD™ Fixable Blue Dead Cell Stain Kit as per manufacturer's instructions (Invitrogen/Thermo Fisher Scientific, Scotland, UK).

2.7.2 Surface staining

For murine Treg study, single cell suspensions were stained with biotin-labelled CD30 antibody and CD16/32 at 4ºC for 20 min. Cells were washed with 1mL FACS buffer for 5 min at 400 × g and stained with streptavidin at 4ºC for 20 min in dark. After washing, cells were stained with a combination of surface markers including CD4, CD25, CD44, CD62L, CD45.1, CD45.2, Nrp1, Ki67, GARP, GITR, TIGIT, CD119, ST2, CD127 and CD16/32 at 4ºC for 30 min in dark. Control staining was performed using streptavidin alone or by staining the cells with fluorescence-minus-one (FMO) controls. For murine dendritic cell

(DC) and natural killer (NK) cell study, single cell suspensions were stained with a combination of surface markers including CD11b, CD11c, H-2K^b, I-A/I-E, NK1.1, PD-L1, PD-L2, CD86, CD80 and CD16/32 at 4ºC for 30 min dark. For murine innate lymphoid cell (ILC) study, single cell suspensions were stained with biotin-labelled lineage cocktail at 4ºC for 20 min as follows: CD3, CD4, CD5, CD8, CD11b, CD11c, CD19, CD49b, Ter119, F4/80, B220, NK1.1, BTLA, Gr1 and CD16/32 followed by streptavidin. After washing, cells were stained with a combination of surface markers including CD45, CD90.2, CD127, CD25, KLRG1, Nkp46, PD-1, PD-L1, PD-L2, ST2 and CD16/32 at 4ºC for 30 min in dark. After surface staining, cells were washed FACS buffer for 5 min at 400 × g, resuspend in 400μL FACS buffer and ran on flow cytometry on the same day, if cell fixation and permeabilization was not performed.

2.7.3 Intracellular staining for cytokines and transcription factors

Intracellular cytokine production of cells was induced by using stimulation cocktail containing protein transport inhibitors (eBioscience/Thermo Fisher Scientific) at 37°C for 4 hr. After washing with complete media for 5 min at 400 × g, cells were stained for viability and surface markers when necessary. Cells were fixed and permeabilized using Foxp3 Transcription Factor Staining Buffer Set (eBioscience/Thermo Fisher Scientific) for murine Treg, DC and NK cell study and BD Cytofix/Cytoperm Fixation/Permeabilization Kit (BD Biosciences) for murine ILC study as manufacturer's instructions. Intracellular staining was performed overnight in dark at 4ºC. For murine Treg study, cells were stained in 1X permeabilization buffer (eBioscience/Thermo Fisher Scientific) with the following antibodies: FoxP3, Tbet, RORγt, GATA3, Bcl2, Helios, CTLA4, IL-10, IL-17A, IFN-γ, GzmB and CD16/32. For murine ILC study, cells were stained in 1X Perm/Wash buffer (BD Biosciences) with the following antibodies: Tbet, RORγt, Eomes, IL-5, IL-13, IL-17A, IL-22, IFN-γ, TNF-α and CD16/32. After washing with 1X permeabilization buffer or 1X Perm/Wash buffer twice for 5 min at 400 × g, cells were resuspended in 400μL FACS buffer and ready to be analysed on flow cytometry within a week.

2.7.4 Intracellular staining for phospho-proteins

Cells were harvested and washed with complete media after a two-day culture period as described in **section 2.8.5**. After stimulating with 80 ng/mL murine IL-2 (Miltenyi Biotec, Bisley, Surrey) at 37°C for 15 min, cells were then immediately fixed using pre-warmed 1X BD Phosflow Lyse/Fix Buffer (BD Biosciences) at 37°C for 10 min. Following

centrifugation at 400 × g for 5 min, the cell pellet was loosened by vortexing, and cells were permeabilized for 20 min on ice with pre-chilled BD Phosflow Perm Buffer III (BD Biosciences). After three washes with 3 mL of FACS buffer for 5 min at 400 × g, cells were stained with biotin-conjugated CD30, followed by streptavidin, as described in **section 2.7.2**. Cells were then washed with 3 mL of FACS buffer and stained with the following antibodies at RT for 20 min in the dark: phospho-STAT5 (pSTAT5), CD4, FoxP3 and CD16/32. After two washes with 3 mL of FACS buffer, cells were analysed by flow cytometry within one week.

All flow antibodies used are listed in **Table 2.3**.

Marker	Fluorophore	Clone	Cat #	Company	Dilution
B220	Biotin	RA3-6B2	103204	BioLegend	1:200
Bcl2	FITC	10C4	11-6992-41	eBioscience	1:200
BTLA	APC	6A6	139109	BioLegend	1:200
CD119	PE	2E2	12-1191-82	eBioscience	1:200
CD11b	Biotin	M1/70	101204	BioLegend	1:200
CD11c	PE	N418	117307	BioLegend	1:200
CD11c	Biotin	N418	117304	BioLegend	1:200
CD152	BV605	UC10-4B9	106323	BioLegend	1:200
CD152	BV711	BNI3	369631	BioLegend	1:200
CD16/32	NA	3G8, FUN-2, 10.1	422301	BioLegend	1:100
CD16/32	NA	93	101320	BioLegend	1:100
CD19	Biotin	6D5	115504	BioLegend	1:200
CD223	BV786	C9B7W	125219	BioLegend	1:200
CD223	PECy7	11C3C65	369309	BioLegend	1:200
CD25	FITC	PC61	102005	BioLegend	1:200
CD25	BV785	PC61	102051	BioLegend	1:200
CD30	Biotin	mCD30.1	102303	BioLegend	1:200
CD30	APC	BY88	333909	BioLegend	1:200
CD3ε	Biotin	145-2C11	100304	BioLegend	1:200
CD3ε	PE/Dazz594	145-2C11	100347	BioLegend	1:200

CD4	Biotin	GK.15	100404	BioLegend	1:200
CD4	AF700	GK1.5	100429	BioLegend	1:200
CD4	BV510	GK1.5	100449	BioLegend	1:200
CD4	BV711	GK1.5	100447	BioLegend	1:200
CD4	AF700	RPA-T4	300526	BioLegend	1:200
CD44	APC/Cy7	IM7	103027	BioLegend	1:200
CD44	AF700	IM7	103025	BioLegend	1:200
CD45.1	FITC	A20	110705	BioLegend	1:200
CD45.2	AF700	104	109821	BioLegend	1:200
CD49b	Biotin	DX5	108904	BioLegend	1:200
CD5	Biotin	53-7.3	100604	BioLegend	1:200
CD62L	BV510	MEL-14	104441	BioLegend	1:200
CD62L	BV650	MEL-14	104453	BioLegend	1:200
CD8α	Biotin	53-6.7	100704	BioLegend	1:200
CD8α	PE/Dazz594	HIT8a	300929	BioLegend	1:200
CD8α	BV786	RPA-T8	563823	BD Biosciences	1:200
CD80	BV421	16-10A1	104725	BioLegend	1:200
CD86	AF700	A17199A	159213	BioLegend	1:200
CD90.2	AF700	30-H12	105320	BioLegend	1:400
Eomes	PECy7	Dan11mag	25-4875-82	eBioscience	1:100
F4/80	Biotin	BM8	123106	BioLegend	1:200
Foxp3	APC	FJK-16s	17-5773-80	eBioscience	1:200
Foxp3	PE	FJK-16s	12-5773-80	eBioscience	1:200
Foxp3	AF700	FJK-16s	56-5773-82	eBioscience	1:200
Foxp3	FITC	FJK-16s	11-5773-82	eBioscience	1:200
Foxp3	BV421	206D	320123	BioLegend	1:200
GARP	PECy7	YGIC86	25-9891-82	BioLegend	1:200
GARP	PerCP/Cy5.5	7B11	352513	BioLegend	1:200
GATA3	PECy7	TWAJ	25-9966-42	eBioscience	1:200
GITR	BV786	DTA-1	741020	BD Biosciences	1:200
GITR	APC/Fire750	108-17	371221	BioLegend	1:200

Gr1	Biotin	RB6-8C5	108404	BioLegend	1:200
GzmB	PerCP/Cy5.5	QA16A02	372211	BioLegend	1:100
H-2K^{b}	BV510	AF6-88.5	116523	BioLegend	1:200
Helios	AF700	22F6	137241	BioLegend	1:200
Helios	PE/Dazz594	22F6	137231	BioLegend	1:200
I-A/I-E	APC	M5/114.1 5.2	107613	BioLegend	1:200
IFN-γ	BV510	XMG1.2	505841	BioLegend	1:200
IL-10	BV605	JES5-16E3	505031	BioLegend	1:200
IL-10	PE	JES5-16E3	505007	BioLegend	1:200
IL-17A	APC/Cy7	TC11-18H10.1	506939	BioLegend	1:200
IL-22	APC	IL-22JOP	17-7222-80	eBioscience	1:200
IL-5	BV421	TRFK5	504311	BioLegend	1:200
Ki67	FITC	SolA15	11-5698-80	eBioscience	1:200
NK1.1	FITC	PK136	108706	BioLegend	1:200
NK1.1	BV650	PK136	108735	BioLegend	1:200
Nkp46	PE/Dazz594	29A1.4	137629	BioLegend	1:200
Nrp1	APC	3E12	145205	BioLegend	1:200
PD-1	APC/Cy7	29F.1A12	135223	BioLegend	1:200
PD-1	PE	29F.1A12	135205	BioLegend	1:200
PD-1	FITC	29F.1A12	135213	BioLegend	1:200
PD-1	PerCP/Cy5.5	29F.1A12	135207	BioLegend	1:200
PD-1	AF488	EH12.2H7	329935	BioLegend	1:200
PD-L1	BV785	10F.9G2	124331	BioLegend	1:200
PD-L2	PE/Dazz594	TY25	107215	BioLegend	1:200
pSTAT5	AF488	47	612598	BD Biosciences	1:5
RORγt	PE	B2D	12-6981-80	eBioscience	1:150
ST2	PE	DJ8	101001PE	MD Bioproducts	1:200

Tbet	FITC	4B10	644811	BioLegend	1:100
Ter119	Biotin	TER-119	116204	BioLegend	1:200
TIGIT	BV421	1G9	142111	BioLegend	1:200
TIGIT	BV510	A15153G	372737	BioLegend	1:200
TNF-α	BV786	MP6-XT22	506341	BioLegend	1:200

Table 2.3 List of antibodies used for flow cytometry experiments.

2.7.5 Cell sorting

CD90.2 T cells were enriched from splenocytes isolated from *Foxp3*^{RFP} or *Pd1*$^{-/-}$ *Foxp3*^{RFP} mice by using CD90.2 MicroBeads (Miltenyi Biotec) as per manufacturer's instruction. After centrifugation for 5 min at 400 × g, cells were stained in PBS with surface antibody cocktail at 4ºC for 15 min in dark as follows: CD4, CD25 and CD16/32. Cell viability was identified by DAPI prior sorting. CD4^{+}FoxP3^{RFP+} cells were sorted as Tregs and CD4^{+}CD25^{-}FoxP3^{RFP-} cells were sorted as naïve CD4 T cells (Teff). Sorted Tregs and Tnaïve cells were washed with PBS twice prior to be used in *in-vitro* or *in-vivo* experiments.

2.7.6 Data analysis

Flow cytometry was performed using a BD LSRFortessa X20. Sort purification was performed on a BD FACSAria Fusion. All data were analysed using FlowJo 10 (Tree Star). Graphs and statistical analyses were done with SPICE 6.1 (https://niaid.github.io/spice/) and GraphPad Prism 10.

2.8 *In vitro* assays

2.8.1 Cell proliferation assay

Isolated Tregs from *Foxp3*^{RFP} or *Pd1*$^{-/-}$ *Foxp3*^{RFP} mice were stained in PBS with Cell Trace Violet (CTV) (Invitrogen/Thermo Fisher Scientific) as per manufacturer's instruction. CTV-stained cells were plated at 1 x 10^6 cells/mL in 96-well U bottom plate and were cultured with 0.5µg/mL αCD3 (145-2C11, BioLegend), 2µg/mL anti-CD28 (37.51, BioLegend) and 80ng/ml human IL-2 (Miltenyi Biotec) for 72 h in a humidified incubator at 37 °C with 5% CO_2. After harvesting, cells were stained for viability and surface markers as described in **section 2.7.1** and **2.7.2** respectively. Cell proliferation was assessed through CTV dilution on flow cytometry.

2.8.2 Apoptotic assay

Isolated Tregs from *Foxp3*^{RFP} or *Pd1*$^{-/-}$*Foxp3*^{RFP} mice were plated at 1 x 10^6 cells/mL in 96-well U bottom plate and 0.5µg/mL αCD3 (145-2C11, BioLegend), 2µg/mL anti-CD28 (37.51, BioLegend) and 80ng/ml human IL-2 (Miltenyi Biotec) for 72 h in a humidified incubator at 37 °C with 5% CO_2. After washing with cold PBS, Tregs were stained with 5µl Annexin V (BD Biosciences) and 5µl 7-AAD (BD Biosciences) in 100µl 1X Annexin V binding buffer (BD Biosciences) at RT for 15 min in dark. 400µl binding buffer was added and Tregs were analysed by flow cytometry within 1 h.

2.8.3 Treg suppressor assay

Sorted Teff cells from *Foxp3*^{RFP} were stained in PBS with CTV. 5 x 10^4 Teff cells and the indicated ratios of sorted Tregs from either *Foxp3*^{RFP} or *Pd1*$^{-/-}$*Foxp3*^{RFP} mice were stimulated using 0.5µg/mL αCD3 (145-2C11, BioLegend) along with irradiated splenocytes from C57BL/6 WT mice as antigen-presenting cells (APCs) using a 4:1 ratio of APCs to Teff cells. Cells were cultured for 72 h in a humidified incubator at 37 °C with 5% CO_2 and proliferation was assessed on flow cytometry.

2.8.4 PD-L1 molecular mechanistic study

CD4 Teff cells ($CD4^+CD25^-$) and Tregs ($CD4^+CD25^+$) were isolated from WT or *Pd1*$^{-/-}$ mice using $CD4^+CD25^+$ Regulatory T Cell Isolation Kit (Miltenyi Biotec) as per manufacturer's instruction. Cell-culture 96-well plates were prepared by coating with either 5µg/ml anti-CD3 (145-2C11, BioLegend) alone or 5µg/ml of anti-CD3 and recombinant mouse PD-L1 Fc chimera protein (rmPDL1fc; R&D Systems/Bio-Techne, Leeds, UK) for 3 h at 37°C. The wells were washed with PBS three times. Tregs ($CD4^+CD25^+$) were isolated from WT mice or *Pd1*$^{-/-}$ mice using $CD4^+CD25^+$ Regulatory T Cell Isolation Kit (Miltenyi Biotec) as per manufacturer's instruction. Isolated Tregs were then seeded in the wells and cultured in mouse complete media at 1 x 10^6 cells/mL. 2µg/mL anti-CD28 (37.51, BioLegend) were added into the wells. In certain wells, 10µg/ml anti-PD-1 (RMP1.14, Bio X Cell) was added to block PD-1/PD-L1 interaction. After 72 h, cells were washed with complete media and further stimulated with either 10µg/ml anti-mouse IL-2 (S4B6, Invitrogen/Thermo Fisher Scientific) alone or 10µg/ml anti-IL-2 and 80ng/ml human IL-2 (Miltenyi Biotec) for 24 h in a humidified incubator at 37 °C with 5% CO_2. Cells were then harvested for flow cytometry and real-time quantitative polymerase chain reaction (RT-

qPCR) assays to investigate CD30 expression, as described in **section 2.7** and **2.11** respectively.

2.8.5 Phospho-STAT5 assay

Cell-culture 96-well plates were prepared by coating with either 5µg/ml anti-CD3 (145-2C11, BioLegend) alone or 5µg/ml of anti-CD3 and rmPDL1fc (R&D Systems/Bio-Techne) for 3 h at 37°C. The wells were washed with PBS three times. Tregs ($CD4^+CD25^+$) were isolated from WT mice or *Pd1*$^{-/-}$ mice using $CD4^+CD25^+$ Regulatory T Cell Isolation Kit (Miltenyi Biotec) as per manufacturer's instruction. Isolated Tregs were then cultured in complete media at 1 x 10^6 cells/mL and incubated with 2µg/mL anti-CD28 (37.51, BioLegend) and 10µg/mL anti-IL-2 (S4B6, Invitrogen) for 48 h in a humidified incubator at 37 °C with 5% CO2. In certain wells, 10µg/mL anti-PD-1 (RMP1.14, Bio X Cell) was added to block PD-1/PD-L1 interaction. After 48 h, cells were washed with 1 mL complete media for 3 min at 400 × g and further stimulated with 80ng/mL IL-2 (Miltenyi Biotec) for 15 min at 37°C. Cell fixation and permeabilization, alongside pSTAT5 staining were then performed as described in **section 2.7.4**.

2.8.6 In vitro culture of melanoma patient PBMCs

Human PBMCs derived from stage IV metastatic melanoma patients were plated at 1 x 10^6 cells/mL in 96-well U bottom plate. Cells were stimulated with 0.5µg/mL anti-CD3 (OKT3, BioLegend) along with either 20µg/mL isotype control IgG2b (MPC-11, BioLegend) or anti-PD-L1 (29E.2A3, BioLegend) for 72 h in a humidified incubator at 37 °C with 5% CO_2.

2.9 BD Rhapsody single-cell RNA sequencing

2.9.1 Cell preparation for scRNA-seq

Isolated B16F10 melanoma TILs from C57BL/6 WT and *Pd1*$^{-/-}$ mice were stained with lineage markers for 20 min at 4°C as follows: CD3ε (145-2C11, BioLegend), CD4 (GK1.5, BioLegend) , CD5 (53-7.3, BioLegend), CD8α (53-6.7, BioLegend), CD11b (M1/70, BioLegend), CD11c (N418, BioLegend), CD19 (6D5, BioLegend), CD49b (DX5, BioLegend), Ter119 (TER-119, BioLegend), F4/80 (BM8, BioLegend), B220 (RA3-6B2, BioLegend) and Gr1 (RB6-8C5, BioLegend). After washing with Miltenyi buffer, cells were incubated with anti-Thy1 (S20007C, BioLegend) and streptavidin (BioLegend) for 20 min at 4°C. After washing, cells were incubated with AbSeq antibodies and unique sample tags using BD Mouse Single-Cell Multiplexing Kit (BD Biosciences) for 60 min

on ice. AbSeq antibody-oligos used were as follows: CD25, CD103, CD119, CD37, CD223, CD272, CD273, CD274, CD278, CD279, IL-17Rb, IL-23R, IL-33R, CD335, CD3 and NK1.1. After washing three times, cells were stained with DAPI, and flow enriched for $Lineage^{+}Thy1^{+}$ population consisting of T cells, innate immune cells and NK cells. For human samples, PBMCs were thawed and stained with PE-conjugated anti-CD45 (BioLegend, clone; HI30) for 30 min at 4°C. Each sample was incubated with a unique sample tag using BD Human Single-Cell Multiplexing Kit (BD Biosciences) for 20 mins. Cells were then washed in PBS supplemented with FBS, stained with DAPI and sorted for $CD45^{+}$ cells. After sorting, cells were pooled and incubated with TruStain FcX (BioLegend) and BD AbSeq Immune Discovery Panel antibodies (BD Biosciences). AbSeq antibody-oligos used were as follows: CD3, CD4, CD8, CD11C, CD14, CD16, CD19, CD25, CD27, CD28, CD45RA, CD56, CD62L, CD127, CD134, CD137, CD161, CD183, CD185, CD186, CD196, CCR7, CD272, CD278, CD279, GITR, TIM3, HLA-DR, IgD and IgM. Both samples were then loaded onto primed BD rhapsody cartridges and incubated for 20 min at RT. Cell capture beads were washed and loaded onto the cartridge. Following cell capture bead incubation, the cartridge was washed twice, and the cells were lysed. The cell capture beads were then retrieved, and reverse transcription was performed. The bead suspension was treated with exonuclease I and subsequently stored at 4°C for ≤ 3 months.

2.9.2 Single cell library preparation and sequencing

The single-cell library preparation was performed according to the manufacturer's protocol provided by BD Biosciences. Briefly, pooled sample tag/AbSeq/mRNA library was sequenced with a read length minimum of 51bp R1 and 71bp R2 and a 200-cycle sequencing protocol was used. Sequencing libraries were sequenced on a NovaSeq 6000 (Illumina) using a S2 Reagent Kit v1.5 (200 cycles).

2.9.3 Preprocessing of scRNA-seq data

For murine and human scRNA-seq datasets, FastQ files were processed using the BD Rhapsody analysis pipeline (https://www.sevenbridges.com/bdgenomics), which generated unique molecular identifier (UMI) counts. In R software (v.3.3), the Seurat package (v5.0.3) was used to further analyse transcriptomic and protein expression data (AbSeq). For murine samples, cells were filtered for ≥ 10 UMIs and 20-300 genes detected per cell. For human samples, cells were filtered for 1200-60000 UMIs and 50-200 genes detected per cell. Multiplets and indeterminates were removed from downstream analysis.

Expression matrices were log-normalised, and the top 2000 variable features were identified. Samples were integrated using an anchor set and scaled by z-score conversion. Dimensionality reduction (npcs = 50) was performed using principal component analysis (PCA). The top 10 and the top 20 PCs were used to compute uniform manifold approximation and projection (UMAP) for murine and human scRNA-seq, respectively. A K-nearest neighbour graph (KNN) was constructed using the *FindNeighbors* function (k.param = 20, dims = 1:10 for murine and 1:20 for human, annoy.metric = 'euclidean'), and Louvain clustering (resolution = 0.6) was performed.

For publicly mined datasets, the data files were pre-processed by original authors(Sade-Feldman et al., 2018, Tirosh et al., 2016) and the processed gene expression data were retrieved from Gene Expression Omnibus (GEO) database. In RStudio, the Seurat package was used to identify the top 2000 variable features. Dimensionality reduction (npcs = 50) was performed using PCA. The top 10 PCs and the top 20 PCs were used to compute UMAP for scRNA-seq of treatment naive melanoma patients, and anti-PD-1 untreated/treated melanoma patients, respectively. A KNN graph was constructed using the *FindNeighbors* function (k.param = 20, dims = 1:10 for treatment-naïve melanoma patients and 1:20 for anti-PD-1 baseline/treated melanoma patients, annoy.metric = 'euclidean'). Louvain clustering was performed with a resolution = 0.2 for treatment-naïve melanoma patients and 0.1 for anti-PD-1 baseline/treated melanoma patients.

2.9.4 Cell annotation for single-cell RNA-seq analysis

Cluster identities of murine and human scRNA-seq data were assigned by using *ScType* function based on cell-type-specific gene sets **(Appendix Table B.1&C.1)**. Nine clusters (Basophil, T Effectors, Macrophage, Megakaryocyte, Myeloid DC, B cell, NK, pDC and Treg) were revealed in murine TILs. 'T Effectors' cluster was further subclustered into 'CD4 Tcm', 'CD4 Teff', 'CD8 Tcm' and 'CD8 Teff'. For scRNA-seq analysis of human PBMCs, cells were also annotated using a manual review process based on the algorithmically defined marker gene expression for each cluster with *FindAllMarkers* function (method = "Wilcoxon" with Bonferroni correction) along with protein expression data, revealing 16 clusters in human PBMCs (B cell, $CD8^+$ Tc1, $CD11c^+CD14^+$, $CD11c^+CD16^+$, $CD4^+$ Teff, $CD8^+$ Teff, γδ, $CD4^+$ Tmem, $CD8^+$ Tmem, $CD4^+$ Tnaive, $CD8^+$ Tnaive, $CD161^+$ NK, NK, $CD8^+$ Tc17, Treg and other). For publicly mined datasets, cluster identities were annotated based on the algorithmically defined marker gene expression for

each cluster with *FindAllMarkers* function (method = "Wilcoxon" with Bonferroni correction). This process revealed nine clusters (CD4 T, CD8 T, $CD4^{-}CD8^{-}$ T, B, macrophage, endothelial cell, CAFs, melanoma and NK) for treatment-naive patients and six clusters (CD4 T, CD8 T, B, monocyte and macrophage, DC and NK/NKT) for anti-PD-1 baseline/treated patients which the top preferentially expressed genes ($p<0.001$) included multiple known markers of particular cell types. The 'CD4 T' cluster was further divided into 'CD4 T' without FoxP3 expression and 'Treg' with FoxP3 expression in both datasets. Gene expression of clusters was visualised as either violin plot using *VlnPlot* function in Seurat package or dot plot using *JJDotPlot* function in scRNAtoolVis package (0.1.0).

2.9.5 Differential gene expression and pseudotime trajectory analysis

Differential gene expression was determined using the *FindMarkers* function (method = "Wilcoxon" with Bonferroni correction). For this analysis, Abseq antibodies were excluded. Genes were considered differentially expressed when they achieved $\log_2$ (fold change) $\geq$ |0.585| and an adjusted *p* value ≤ 0.05, illustrated as a volcano plot using *ggplot2* (v3.5.0) package. To overcome individual sample pooling, mRNA expression for the co-inhibitory receptors were obtained and plotted to show expression in each individual sample. The average mRNA expression of selected genes in Tregs across individuals was calculated using the mean function with *summarise* from the dplyr package (v1.1.4). An unpaired Student's *t-test* was performed to measure difference between groups. In addition, single-cell mRNA expression was visualized using violin plot generated with the *VlnPlot* function in the Seurat package and a clustered Wilcoxon rank-sum test (method = "ds) (Jiang et al., 2020) was performed using *clusWilcox.test* function in clusrank (v1.0-4) package to overcome sample pooling effects while measuring differences in co-inhibitory receptor expression between two groups. Gene ontology (GO) over representation analysis was performed using the *clusterProfiler* (v4.10.1) package. Gene symbol was converted into Entrez ID using *biomaRt* package (v3.18). The enriched GO terms were acquired from the list of differentially expressed genes by using *enrichGO* function and visualised as a dot plot using *dotplot* function. Gene set enrichment analysis (GSEA) was conducted using the *gseGO* function with the Kolmogorov-Smirnov test, ranking genes and applying a p-value cutoff of 0.05 to identify significant GO terms. Pseudotime single-cell trajectory analysis was performed using the Monocle2 plugin on SeqGeq^{TM} software.

2.9.6 Cell-cell communications

To determine cell-cell interactions and signalling patterns, we applied cell communications CellChat (v2) R package to our single-cell analysis (https://github.com/sqjin/CellChat) (Jin et al., 2021). CellChat cross-references a ligand-receptor interaction database (CellChatDB.mouse) including extracellular matrix (ECM)-receptor interactions, cell-cell contact interaction and secreted signalling. To identify significant cell-cell interactions, over-expressed ligands and receptors were identified by *identifyOverExpressedGenes* and *identifyOverExpressedInteractions* functions utilising default parameters. Communications with <3 cells were excluded with *filterCommunication* function. The communication probability was calculated with *computeCommunProbPathway* function and significant communications were determined using a permutation test. The aggregated cell-cell communication network was then compiled using *aggregateNet* function, visualised as a circle plot using *netVisual_circle* function and a chord plot using *netVisual_chord_gene* function. Network centrality scores were then calculated by using the *netAnalysis_computeCentrality* function, and the roles of each TIL group as signal senders or receivers within the inferred communication network were quantified using the *netAnalysis_signalingRole_heatmap* function. Cophenetic and Silhouette values were evaluated by using *selectK* function to identify the optimal number of communication patterns of TILs. Outgoing and incoming patterns were then determined by using *identifyCommunicationPatterns* function to reveal how the sender cells coordinated with certain outgoing signalling pathways to drive communication or how the target cells responded to incoming signalling pathways.

2.10 NanoString CosMx™ Spatial Molecular Imaging

2.10.1 Tissue processing

Tumours were harvested from B16F10 melanoma-bearing *Rag1*$^{-/-}$ mice reconstituted with CD45.1 WT Teff cells along with either WT Treg or *Pd1*$^{-/-}$ Treg and were fixed in 10% neutral buffered formalin (Sigma-Aldrich) overnight. Tumour tissues were embedded in paraffin, punched as 3mm biopsies and mounted onto center of the Leica Bond Plus slides. FFPE slides were air-dried at RT after sectioning for overnight and ready to be shipped to NanoString with desiccant and ice pack. Haematoxylin and eosin staining of slides was performed by NovoPath at Newcastle Hospitals, which was further observed under Zeiss Axio Imager 2 and analysed using ZEISS ZEN software to access tissue block quality and to select field of view (FOV).

2.10.2 Image acquisition and cell segmentation

CosMx™ experiments were performed by NanoString as part of the Technology Access Program (TAP). Briefly, standard methods performed for fluorescent in situ hybridization was applied by NanoString on FFPE tissue slide to expose RNA targets as previously described (He et al., 2022). Fluorescent bead-based fiducials fixed to the tissue were introduced to provide an optical reference for cyclic image acquisition, following by hybridization of RNA specific probes and antibodies. After washing, the sample was assembled into a flow cell and loaded onto a Spatial Molecular Imaging (SMI) instrument for RNA readout and morphological imaging. Raw images were transformed to decoded RNA transcripts at subcellular resolution through workflow including (1) three-dimensional primary image processing to identify and register reporter spots, (2) decoding of reporter spots to RNA transcripts with registered X, Y, Z spatial location, (3) outlining of nuclei and cell boundaries with DAPI and antibodies after cyclic reporter readout for morphology-based cell segmentation, and (4) assigning RNA transcripts to single cells.

2.10.3 Pre-processing of spatial transcriptomics data

CosMx™ SMI data and Flat File were exported from AtoMx SIP to a QWS S3 Bucket. The output of CosMx™ SMI data consisted of Seurat object, TileDB array and a folder 'Flow Cell ID' containing raw decoded files and images for each FOV while the output of Flat File was consisted of count matrix, cell metadata, global transcripts, global cell boundaries and global FOV position. Both output files were downloaded using the S3 console and used for data analysis. Sample was loaded into R software (v4.3.3) using *LoadNanostring* function and expression profiles of cells were clustered using the R software package Seurat (v.5.0.0). Briefly, data were normalised and scaled using the *SCTransform* function. Dimensionality reduction (npcs = 5) was performed using PCA and the top 5 PCs were used to compute UMAP. A KNN graph was constructed using the *FindNeighbors* function (k.param = 20, dims = 1:5, annoy.metric = 'euclidean'), and Louvain clustering (resolution = 0.2) was performed.

2.10.4 Data analysis

Clusters identities were assigned by using *ScType* function based on cell-type-specific gene sets **(Appendix Table D.1)** and published papers on cell identification in skin and tumour tissue (Jacob et al., 2023, Chu et al., 2022, Kim et al., 2022, Solé-Boldo et al., 2020, Ordovas-Montanes et al., 2018), revealing 5 clusters in murine TME (Basal cell, Immune

cells, Schwann cell, Tumour cell and Melanocyte). The 'Immune cells' cluster was further subclustered into 'Monocyte', 'DC', 'ILC', 'Mast cell', 'Treg', 'NK', 'Macrophage' and '$CD4^+$ T cell'. Each FOV region was zoomed in and visualised using *Crop* function. By using *ImageDimPlot* function, the cell identities were overlaid onto the FOV images. Spatial expression pattern of individual molecules was visualised using the *ImageFeaturePlot* function. Visualisation of gene expression, calculation of average gene expression, differential gene expression analysis and enrichment analysis were performed as described in scRNA-seq analysis in **section 2.9.5**. A clustered Wilcoxon rank-sum test was performed using *clusWilcox.test* function in clusrank (v1.0-4) to measure the differences in co-inhibitory receptor expression between two or more than two groups, FDR correction was applied when comparing more than two groups.

2.10.5 Spatially resolved cell-cell interaction analysis

Treg population was further divided into several groups based on their spatial location and cell interaction on FOVs by using their specific 'Cell_ID'. The number of physical interactions of Treg with alternative cell types on the FOV images was manually counted. By using *FindAllMarkers* function (method = "Wilcoxon"), specific genes in each Treg subsets interacting with neighbouring cells or alone within the FOV was determined by visually annotating cells. Treg-specific genes were further subdivided into either short-range (SR) or long-range (LR) communications based on biological function by manual curation. Genes involved in cell-cell contact were annotated as SR and secreted or signalling genes were annotated as LR. SR consisted of genes for cell surface receptors, proliferation markers, apoptotic markers and LR consisted of genes for cytokines, chemokines, transcription factors that can drive cytokine, chemokine production etc.

2.11 RT-qPCR

2.11.1 RNA extraction from Tregs

Treg cultures were performed as described in **section 2.8.4**. mRNA extraction from Tregs was done using the RNeasy Mini Kits (Qiagen) as per the manufacturer's protocol. cDNA synthesis for mRNA was carried out using the TaqMan Reverse Transcription Reagents (Applied Biosystems).

2.11.2 RT-qPCR assay

cDNAs were used as the template for RT-qPCR using LightCycler 480 II (Roche). TaqMan Gene Expression assays (FAM) were purchased from Life Technologies Thermo Fisher Scientific for the quantitation of mouse CD30 mRNA: Mm00437140_m1 (*Tnfrsf8*) along with actin mRNA: Mm00607939_s1 (*Actb*) which was used as a housekeeping control for quantitation in mouse. All TaqMan assay RT-qPCRs were performed using TaqMan Fast Advanced Master Mix (Applied Biosystems). The RT-qPCR reaction included an initial step of 10 min at 95 °C followed by 50 cycles of a 15 s denaturation at 95 °C and then 60 s annealing and extension at 60 °C.

2.11.3 RT-qPCR data analysis

Results were processed by LightCycler 480 software. Samples were assigned to control (WT Treg) and experimental (*Pd1*$^{-/-}$ Treg) groups. CT values were then normalized with Actb as a reference gene by using formula: ΔCt = Average Ct (*Tnfrsf8*) - Average Ct (*Actb*). The difference between the ΔCt values for the WT Treg and *Pd1*$^{-/-}$ Treg was calculated by using formula: ΔΔCt = ΔCt (*Pd1*$^{-/-}$ Treg) - ΔCt (WT Treg). The expression fold change was then calculated by using formula: Fold change = $2^{-\Delta\Delta Ct}$.

2.12 Chromatin immunoprecipitation sequencing analysis

STAT5 chromatin immunoprecipitation sequencing (ChIP-seq) dataset was derived from National Center for Biotechnology Information (NCBI) GEO under the accession number GSE207265 (Villarino et al., 2022). In brief, naïve WT CD4^{+} cells were stimulated with plate-bound 10μg/ml of anti-CD3 (17A2, Bio X Cell) and anti-CD28 (37.51, Bio X Cell) in the presence of anti-mouse IL-2 (S4B6) for 48 h. Cells were then washed and cultured with 100 U/mL human IL-2 (NIH/National Cancer Institute Biological Resources Branch Preclinical Repository) for 48 h. Genome browser files were rendered with Integrated Genome Viewer (IGV) similar to previously published analysis performed by our group (Amarnath et al., 2017).

2.13 RNA Sequencing Analysis

RNA sequencing dataset was derived from NCBI GEO under the accession number GSE207265 (Villarino et al., 2022). In brief, naïve WT and *Stat5*$^{-/-}$ CD4^{+} cells were cultured with plate-bound 10μg/mL of anti-CD3 (17A2, Bio X Cell) and anti-CD28 (37.51, Bio X Cell) in the presence of anti-mouse IL-2 (S4B6) for 72 h. Cells were then washed and re-stimulated with agonist anti-TCR along with either anti-IL-2 (S4B6) or 100 U/mL

human IL-2 (NIH/National Cancer Institute Biological Resources Branch Preclinical Repository) for 4 d. For GSEA, transcriptomes of TNF family including *Tnfrsf8, Tnfrsf4, Tnfrsf13b, Tnfrsf11b, Tnfrsf18, Tnfrsf21, Tnfrsf1b, Tnfrsf9, Tnfrsf17, Tnfrsf19, Ltbr, Eda2r, Tnfrsf11a, Ngfr, Tnfrsf1a, Tnfrsf12a, Tnfrsf10a, Cd40, Tnfrsf13c, Fas, Tnfrsf25, Cd27* and *Tnfrsf14* were ranked by rank metric score.

2.14 CD30 Biomarker Analysis

CD30 as a biomarker in different cancers was performed on R2 Genomics Analysis and Visualization Platform. The dataset analysed was derived from TCGA and NCBI GEO under accession number GSE42568 (Clarke et al., 2013) and GSE33114 (de Sousa et al., 2011). Kaplan-Meier survival analysis with default log-rank test was used to determine the optimum expression cutoff and compare the survival between two groups.

2.15 ILC data analysis

The murine ILC scRNA-seq and flow cytometry data, initially generated by Dr. Stephanie Laba and Dr. Grace Mallet as part of their study on NK1.1-NKp46+ ILCs, were reanalysed to further investigate the $NK1.1^{-}NKp46^{-}Tbet^{+}PD\text{-}1^{+}$ ILC subset identified in Figure 1 of the PNAS paper (Lim et al., 2023). This reanalysis coupled with additional experiments outlined in **sections 2.4**, **2.5** and **2.7**, aims to determine the regulatory role of PD-1 in this ILC subset and its contribution to driving anti-tumour responses in melanoma.

2.15.1 Analysis of scRNA-seq data

ILC scRNA-seq data was generated using BD Rhapsody platform. In brief, TILs were isolated from tumours established on WT and $Pd1^{-/-}$ mice as previously described in **section 2.5.4.** Murine TILs were then stained with lineage markers, anti-Thy1 antibody, streptavidin, Abseq antibodies and sample tags as described in **section 2.9.1**. After washing three times, cells were stained with DAPI, and flow enriched for $Lineage^{-}Thy1^{+}$ population. Samples were then pooled and loaded on to the rhapsody cartridges. Experiment was performed as described in **section 2.9.1 and 2.9.2**. Analysis of ILC scRNA-seq was done using SeqGeq software. Quality control was performed to exclude doublets and genes that were expressed at low levels. Indeterminates were removed from downstream analysis. Expression matrices were log normalised. Dimensionality reduction (npcs = 15) was performed using PCA. The top 15 PCs were used to compute t-Distributed Stochastic Neighbour Embedding (t-SNE). An unsupervised clustering of data was then performed by using PhenoGraph plugin in SeqGeq with a k value of 87 applied. Gene expression was

illustrated as violin plots using ViolinBox plugin. By using iCellR plugin, differential expression analysis was performed between cell clusters, and genes were considered differentially expressed when they achieved fold change ≥ 1.5 and a q-value cutoff of 0.05.

2.15.2 Analysis of TIL immunobiology assay data

B16F10 melanoma cells were established on WT *TbetZsGreen* (TBG) mice and *Pd1*$^{-/-}$ TBG mice via SC injection as previously described (Stathopoulou et al., 2018, Lim et al., 2023). Mice were euthanised on day 12 unless otherwise stated for TIL immunobiology assays. In some experiments, mice were injected with 200μg/mL BODIPY or vehicle before harvest. All flow cytometry data were analysed using FlowJo 10 (Tree Star). Graphs and statistical analyses were done with GraphPad Prism 9.

2.15.3 Analysis of transwell assay data

Splenocytes from WT TBG were plated at a concentration of 5 x 10^5 cells/mL. Transwell inserts were seeded with B16 melanoma cells and cultured with splenocytes at 0:1, 1:1, 1:10 and 1:100 ratios. Cultures were stimulated with 40ng/mL IL-2 and 40ng/mL IL-7 for 24 h. PD-1 expression was measured by flow cytometry and analysed using FlowJo 10 (Tree Star). Graphs and statistical analyses were done with GraphPad Prism 9.

2.15.4 Analysis of in-vitro proliferation assay data

Splenocytes from WT TBG mice and *Pd1*$^{-/-}$ TBG mice were stained in PBS with CTV (Invitrogen/Thermo Fisher Scientific) as per manufacturer's instruction. Cells were cultured with 40ng/mL IL-2, 40ng/mL IL-7, 20μg/mL anti-PD-1 (RMP1-14) or 20μg/mL isotype control IgG2a (2A3) for 5 d. Cytokines were replenished on day 2 and 4, and proliferation was assessed on day 5. For human studies, PBMCs derived from healthy donors were stained in PBS with CTV (Invitrogen/Thermo Fisher Scientific) as per manufacturer's instruction. Cells were cultured with 40ng/mL IL-2, 40ng/mL IL-7, 20μg/mL anti-PD-1 (EH12.2H7) or 20μg/mL isotype control IgG1 (MG1-45) for 7 d. Cytokines were replenished on day 2 and 4, and proliferation was assessed on day 7. Cell proliferation was assessed by flow cytometry and analysed using FlowJo 10 (Tree Star). Graphs and statistical analyses were done with GraphPad Prism 9.

2.15.5 Analysis of lactate assay data

Splenocytes from WT TBG mice and *Pd1*$^{-/-}$ TBG mice were incubated with 100ng/mL IL-2 and 100ng/mL IL-7 or in combination with 20mM lactic acid for 24 h. PD-1 expression

on Lineage$^-$CD45$^+$CD127$^+$CRTh2$^-$CD117$^-$Tbet$^+$ was measured by flow cytometry and analysed using FlowJo 10 (Tree Star). Graphs and statistical analyses were done with GraphPad Prism 9.

2.15.6 Analysis of Phospho-P70S6K data

Tumours reached >600mm^3 were harvested and TILs were isolated. TILs were stimulated with 80ng/mL IL-2 and 40ng/mL IL-7 for 15 min and stained with phospho-P70S6K (pP70S6K) antibody (cupk43k). In some experiments, TILs were enriched using CD90.2 microbeads (Miltenyi Biotec) as per manufacturer's instructions and cultured for 3 d with 80ng/mL IL-2 and 40ng/mL IL-7 alone or in combination with 20µg/ml anti-PD-1 antibody (RMP1-14) or isotype control IgG2a (2A3). Cells were then washed, restimulated with IL-2 and IL-7 for 15 min and stained with pP70S6K antibody (cupk43k). pP70S6K expression was assessed by flow cytometry and analysed using FlowJo 10 (Tree Star). Graphs and statistical analyses were done with GraphPad Prism 9.

2.16 Statistical analysis

Statistical analysis was performed using GraphPad Prism 10, RStudio or SeqGeq. All data shown were expressed as individual data points with the line at the mean unless otherwise stated. Error bars on graphs showed the standard error of the mean (SEM). Two groups were compared with two-tailed paired or unpaired Student's t-test, or Wilcoxon rank-sum test or clustered Wilcoxon rank-sum test. Multiple groups were compared using one- or two-way ANOVA analysis corrected by Sidak's multiple comparison test or the Kruskal-Wallis test followed by pairwise comparisons using the Dunn's test, or with clustered Wilcoxon rank-sum test for single-cell analysis with FDR correction or Wilcoxon rank-sum test for differential gene expression analysis with Bonferroni correction for multiple testing. P-values of ≤0.05 were defined as statistically significant (*p≤0.05, **p≤0.01, ***p≤0.001 and ****p≤0.0001). P-values >0.05 were defined as statistically not significant (ns or not shown).

2.17 Data availability statement

ScRNA-seq data of treatment naive and anti-PD-1 treated melanoma patients used in this paper are available under accession numbers GSE72056 and GSE120575 (Tirosh et al., 2016, Sade-Feldman et al., 2018). All the raw data from the mouse BD Rhapsody scRNA-seq experiments for ILC and Treg studies, human BD Rhapsody scRNA-seq experiments along with the NanoString CosMx^{TM} experiment have been uploaded to the NCBI GEO,

and deposited under GSE229288, GSE273532, GSE280319 and GSE273530 respectively (Lim et al., 2025). The CellChat database for mouse datasets used in the cell–cell communication analysis is available via GitHub at https://github.com/sqjin/CellChat.

2.18 Code availability statement

The code used in analysing the dataset was deposited into the GitHub website. The URL for the code is https://github.com/JXLIM99/scRNAseq-and-Nanostring-Cosmx-SMI.

Chapter 3 PD-1 dampens regulatory T cell function by controlling a unique co-inhibitory receptor landscape in steady state

3.1 Introduction

Tregs are essential for maintaining immune homeostasis, exerting their function through multiple pathways, including the expression of co-inhibitory receptors such as PD-1. While the function of PD-1 inhibitory signals in effector $CD4^+$ and $CD8^+$ T cells are well-documented (Freeman et al., 2000, Barber et al., 2006, Parry et al., 2005, Wherry and Kurachi, 2015, Pardoll, 2012, McLane et al., 2019), its role in regulating Treg function remains controversial. PD-1 signalling is mediated through its ITSM motif, which recruits and activates SHP1/2 phosphatases, leading to the dephosphorylation and inactivation of downstream signalling pathways (Okazaki et al., 2001, Chemnitz et al., 2004, Yokosuka et al., 2012). In $CD8^+$ T cells and, to some extent, in Tregs, PD-1 has been shown to inhibit TCR and CD28 signalling, including the PI3K/Akt pathway, thereby influencing cellular function and plasticity (Kamphorst et al., 2017, Hui et al., 2017, Francisco et al., 2009). However, the role of PI3K/Akt signalling in Tregs remains complex. While PD-1-mediated inhibition of this pathway has been associated with functional plasticity, unchecked PI3K/Akt activation has also been shown to enhance Treg proliferation and function in the absence of PD-1 (Tan et al., 2021).

Beyond the PI3K/Akt pathway, PD-1 has also been implicated in regulating STAT5 signalling downstream of cytokines such as IL-2 (Franceschini et al., 2009, Laba et al., 2022). Previous work has demonstrated that PD-1 can dampen STAT1/4/5 phosphorylation (Amarnath et al., 2011, Taylor et al., 2017), with the PD-1/STAT5 axis playing a role in Tregs during viral infections (Franceschini et al., 2009). While PD-1 has been shown to enhance and maintain FoxP3 expression in stimulated murine $CD4^+$ Th cells (Francisco et al., 2009) and human and murine $Tbet^+$ Th1 cells (Amarnath et al., 2011, Stathopoulou et al., 2018), it remains unclear whether PD-1-mediated STAT5 suppression affects Treg function independent of FoxP3. Additionally, within the TME, PD-L1 expression correlates with an increase in intra-tumoral $FoxP3^+$ T cells, suggesting that PD-1 signalling contributes to Treg maintenance in this context (Dong et al., 2002). PD-1 blockade has been shown to restore the proliferative capacity of exhausted $CD8^+$ T cells while also increasing their apoptosis (Barber et al., 2006). In the absence of PD-1, $CD8^+$ T cells can also

upregulate multiple co-inhibitory receptors (Odorizzi et al., 2015). Whether a similar regulatory mechanism exists in Tregs is not well understood.

Given the emerging evidence that PD-1 can negatively regulate Treg function as observed in $CD8^+$ T cells (Tan et al., 2020), this chapter aims to investigate how PD-1 influences Treg behaviour under steady-state conditions. Specifically, we will examine three key aspects of Treg function: (1) suppressive capacity, (2) proliferation and apoptosis, and (3) the co-inhibitory receptor landscape, with a particular focus on understanding how PD-1-STAT5 interactions shape Treg biology.

3.2 Aims

The aim of this chapter is to investigate the role of PD-1 in regulating Treg function under steady-state-conditions. Specifically, we aim to determine:

1. whether PD-1 control Treg suppressive capacity, proliferation and apoptosis;
2. whether PD-1 regulates Treg function via canonical co-inhibitory receptors and, if so, which receptors are involved; and
3. the molecular mechanisms underlying PD-1-mediated regulation of these co-inhibitory receptors in Tregs.

3.3 Results

The results and analyses presented in this chapter have been published in *Nature Immunology*, June 02, 2025. DOI: 10.1038/s41590-025-02172-0.

3.3.1 PD-1 dampens Treg function in in-vitro cell culture

In order to assess the role of PD-1 on Tregs, splenocytes from WT and *Pd1*$^{-/-}$ mice were characterised for $CD4^+FoxP3^+$ using flow cytometry (**Figure 3.1a-b**). We found a significant increase in $FoxP3^+$ Treg frequency in the splenocytes from *Pd1*$^{-/-}$*FoxP3*^{RFP} mice compared to WT animals (**Figure 3.1c**), consistent with recently published data (Tan et al., 2021). Next, we investigated whether this increase was attributed to thymically derived Tregs (tTregs) or peripherally induced Tregs (pTregs). To distinguish between these subsets, we assessed the expression of Nrp1 and Helios, potential markers associated with tTregs (Weiss et al., 2012, Yadav et al., 2012, Thornton et al., 2010), and found no significant differences between WT and *Pd1*$^{-/-}$ Tregs (**Figure 3.1d-f**). Additionally, there were no changes in the expression of CD25, Tbet, GATA-3 or RORγt in *Pd1*$^{-/-}$ Tregs (**Figure 3.1g-j**), suggesting that the expansion of Treg population is not driven by

alterations in tTreg or pTreg proportions. Tregs can be divided into naïve and effector subsets based on their marker expression. In line with Perry *et al.* (Perry et al., 2022), we

observed an increase in CD62L^{-}CD44^{+} effector Tregs and a corresponding decrease in CD62L^{+}CD44^{-} naïve Tregs (**Figure 3.1k-m**).

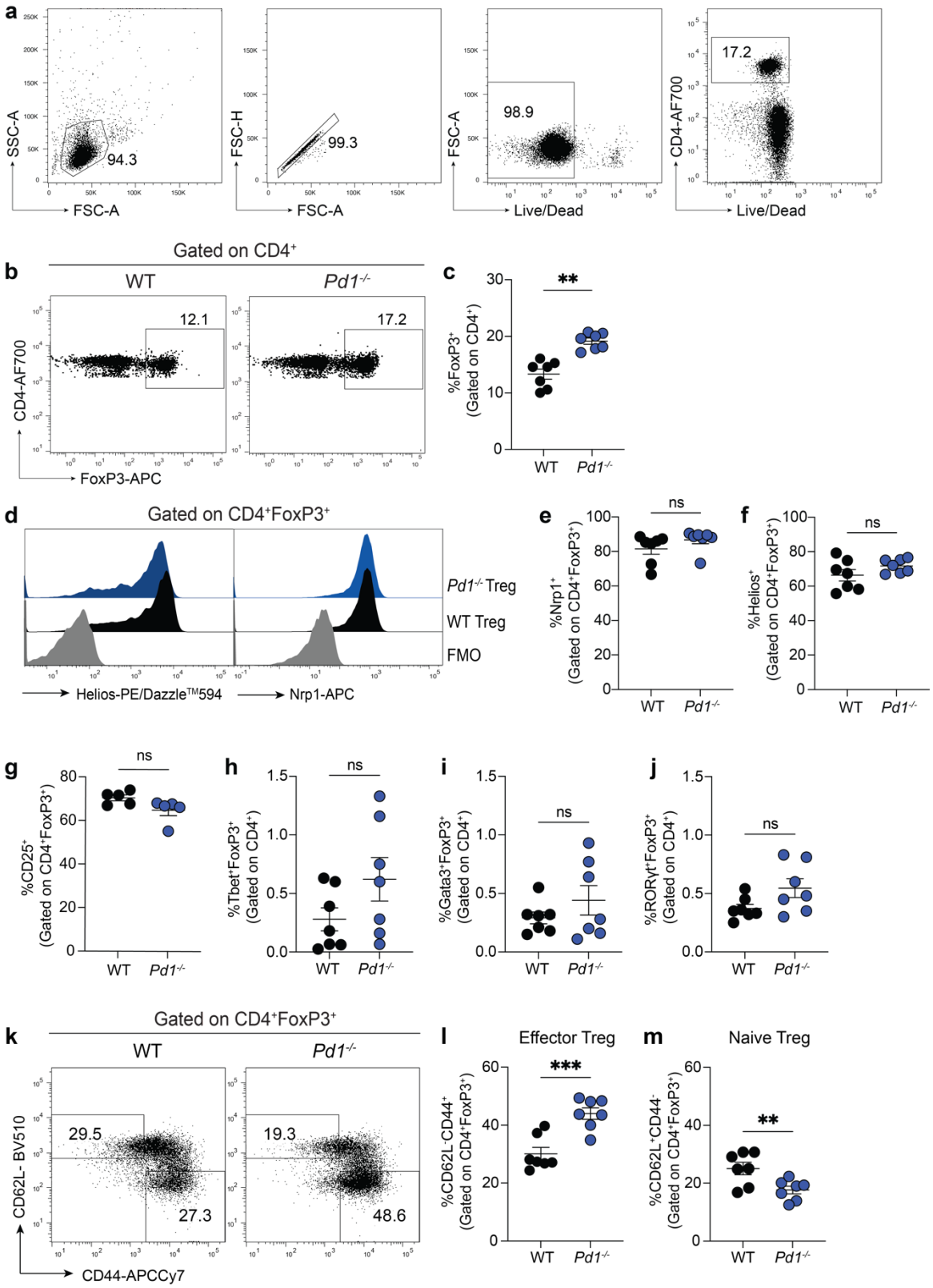

Figure 3.1 PD-1 deficient Tregs exhibit an activated phenotype.

Foxp3^{RFP} (WT) and *Pd1*$^{-/-}$*Foxp3*^{RFP} (*Pd1*$^{-/-}$) spleens were harvested and immunophenotyped using flow cytometry. **A,** Representative flow cytometric plots demonstrating the gating strategy for CD4^{+} T cells from murine splenocytes. **B,** Representative flow cytometry plots and **C**, summary data of FoxP3 expression in CD4^{+} T cells in WT and *Pd1*$^{-/-}$ mice. **D,** Representative flow cytometry plots and summary of **E,** Neuropilin-1 (Nrp1) and **F,** Helios expression in Tregs from WT and *Pd1*$^{-/-}$ mice. **G**, Frequency of CD25^{+} Tregs. **H-J**, Frequency of Tbet^{+}FoxP3^{+}, GATA3^{+}FoxP3^{+} and RORγt^{+}FoxP3^{+} on CD4^{+} T cells. **K**, Representative flow plots of CD44 and CD62L expression in Tregs. **L-M**, Summary of the frequency of CD62L^{-}CD44^{+} and CD62L^{+}CD44^{-} Tregs. Data shown are Mean±SEM from seven independent experiments. An unpaired Student's t-test was performed. ****P < 0.01, ***P < 0.001. FMO, fluorescence minus one; NS, not significant.**

Next, we investigated whether *Pd1*$^{-/-}$ Tregs exhibited enhanced suppressive function under steady-state conditions *in vitro* (Thornton and Shevach, 1998). CD90.2 T cells were enriched from murine splenocytes. CD4^{+}FoxP3^{RFP+} cells were sorted as Tregs from *Foxp3*^{RFP} and *Pd1*$^{-/-}$*Foxp3*^{RFP} mice, while CD4^{+}CD25^{-}FoxP3^{RFP-} cells were sorted as naïve CD4^{+} T cells (Teff) from *Foxp3*^{RFP} mice. The purity of sorted Tregs and WT Teff cells was confirmed by flow cytometry (**Figure 3.2a**). Sorted WT Teff cells were stained with CTV and co-cultured with sorted Tregs from either *Foxp3*^{RFP} or *Pd1*$^{-/-}$*Foxp3*^{RFP} mice at the indicated ratios. Cells were stimulated with 0.5μg/mL anti-CD3 in the presence of irradiated C57BL/6 WT splenocytes as antigen presenting cells (APCs) at a 4:1 APC-to-Teff ratio. After 72 h of culture, cell proliferation was assessed through cell trace violet (CTV) dilution by flow cytometry (**Figure 3.2b-c**). This analysis revealed that *Pd1*$^{-/-}$ Tregs were significantly more suppressive than WT Tregs *in vitro*. In summary, these findings demonstrate that PD-1 deficiency leads to an expansion of Treg populations specifically effector Treg subset and enhances Treg suppressive function *in vitro*.

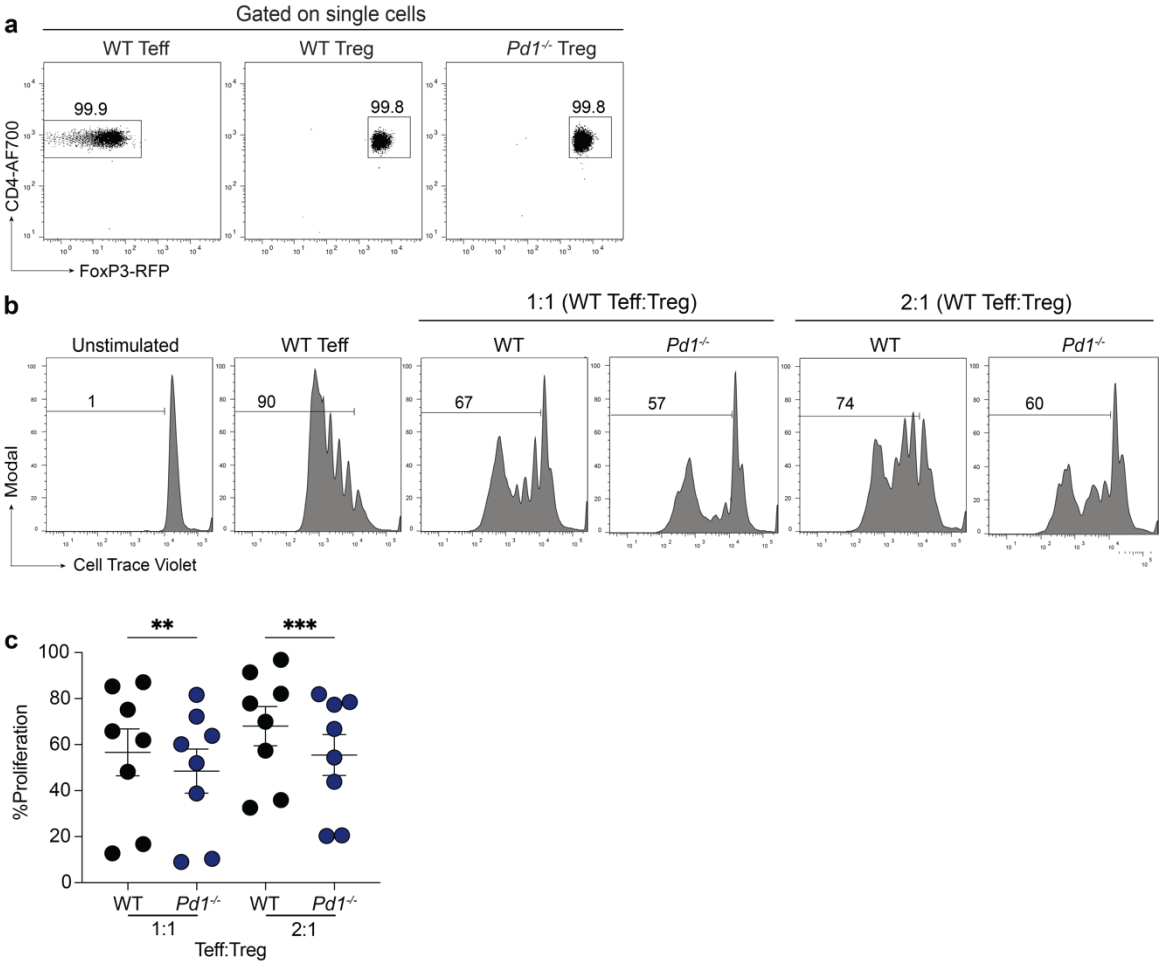

Figure 3.2 PD-1 deficient Tregs exhibit enhanced suppressive capacity.
Tregs were sorted from *Foxp3*^{RFP} (WT) and *Pd1*$^{-/-}$*Foxp3*^{RFP} (*Pd1*$^{-/-}$) murine splenocytes and cultured with CD4^{+}CD25^{-}FoxP3^{-} WT Teff cells, irradiated splenocytes as APCs and αCD3 at 1:1 and 2:1 Teff to Treg ratios. **A.** Flow cytometry plots showing the purity of sorted WT Teff cells, WT Tregs and *Pd1*$^{-/-}$ Tregs. **B.** After 72 h, Teff cell proliferation was measured by cell trace violet (CTV) dilution. **C**, Percentage of Teff cell proliferation is shown. A one-way ANOVA with multiple Sidak's comparison was performed. Data shown are Mean±SEM from eight independent experiments. **P < 0.01, ***P < 0.001.

3.3.2 Pd1$^{-/-}$ *Tregs do not differ in proliferation or apoptosis in steady state*

Since PD-1 has been shown to regulate the proliferative capacity and apoptosis of CD8^{+} T cells, we investigated whether a similar mechanism operates in Tregs. We first assessed the expression of proliferation marker Ki67 in Tregs isolated from *Foxp3*^{RFP} or *Pd1*$^{-/-}$ *Foxp3*^{RFP} murine splenocytes (**Figure 3.3a**). Contrary to previous reports (Tan et al., 2021, Perry et al., 2022), we found no significant difference in the proportion of Ki67^{+} cells between WT and *Pd1*$^{-/-}$ Tregs, although a trend toward higher Ki67 expression was observed in the absence of PD-1 (**Figure 3.3b**). Next, we tested whether *Pd1*$^{-/-}$ Tregs exhibited enhanced proliferation in response to TCR stimulation *in vitro*. CD4^{+}FoxP3^{RFP+} cells were sorted and stained with CTV before being stimulated with 0.5µg/mL anti-CD3, 2µg/mL anti-CD28

and 80ng/ml human IL-2. After 72 h of culture, proliferation was assessed by CTV dilution using flow cytometry (**Figure 3.3c**). No differences in proliferation were observed between WT and *Pd1*$^{-/-}$ Tregs (**Figure 3.3d**), indicating that PD-1 deficiency does not affect the proliferative capacity of Tregs. To assess whether PD-1 regulates Treg survival, we examined Bcl-2 expression and found no significant differences in Tregs between the WT and *Pd1*$^{-/-}$ cohort (**Figure 3.3e-f**). Additionally, an Annexin V assay was performed to evaluate apoptosis in *Pd1*$^{-/-}$ Tregs. After 72 h of culture, no change in Annexin V staining was noted between WT and *Pd1*$^{-/-}$ Tregs, and the frequency of live cells remained unchanged (**Figure 3.3g-i**). In overall, these findings suggest that PD-1 does not regulate the proliferation and apoptosis of Tregs.

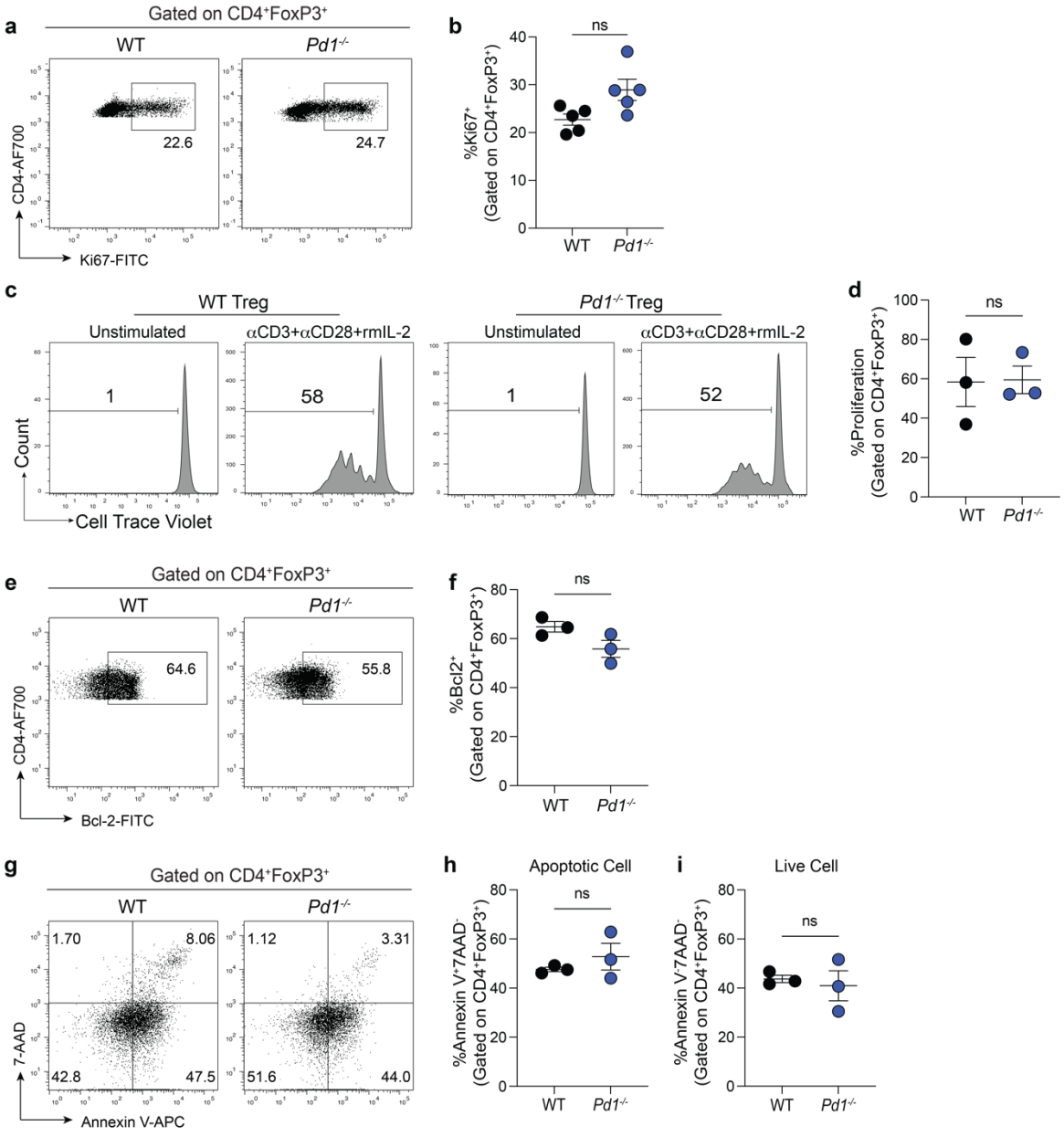

Figure 3.3 PD-1 deficient Tregs do not differ in proliferation or apoptosis phenotype. Analysis of $CD4^+FoxP3^+$ Tregs in spleens of healthy C57BL/6 (WT) and *Pd1*$^{-/-}$ mice. **A,** Representative flow cytometry plot and **B**, Summary data of Ki67 expression in Tregs. **C,** Representative flow cytometry plots showing CTV dilution in isolated WT and *Pd1*$^{-/-}$ Tregs at 72 h post *in-vitro* stimulation with αCD3/28 and rmIL-2. **D**, Summary data showing Treg proliferation. **E,** Representative flow cytometry plot and **F**, Summary data of Bcl-2 expression in Tregs. **G,** Representative flow cytometry plot and summary data of **H,** $AnnexinV^+7AAD^-$ apoptotic Tregs and **I,** $AnnexinV^-7AAD^-$ live Tregs. Data shown are Mean±SEM with each datapoint represents an independent experiment. Statistical analyses were performed using an unpaired Student's t-test. NS, not significant.

3.3.3 PD-1 regulates a unique coreceptor network in Tregs in steady state

In the absence of PD-1, $CD8^+$ T cells has been shown to upregulate multiple co-inhibitory receptors (Odorizzi et al., 2015). Based on this, we investigated whether Tregs similarly upregulate other canonical co-inhibitory receptors when PD-1 is absent. Specifically, we assessed the expression of CD30, CTLA-4, GARP, GITR, and TIGIT on Tregs isolated from isolated from *Foxp3*^{RFP} or *Pd1*$^{-/-}$ *Foxp3*^{RFP} murine splenocytes (**Figure 3.4a**). To accurately determine changes in co-inhibitory receptor expression, we quantified absolute numbers rather than frequencies. This approach provides a direct assessment of whether PD-1 deficiency leads to a true expansion of co-inhibitory receptor-expressing Tregs in spleen, without being influenced by shifts in the broader immune cell populations. We observed a significant increase in the absolute numbers of all measured coreceptors in *Pd1*$^{-/-}$ Tregs compared to WT Tregs, except for TIGIT which remained unchanged (**Figure 3.4b-f**). Odorizzi et al. also demonstrated that PD-1 shapes the co-inhibitory receptor expression landscape in $CD8^+$ T cells under steady-state conditions (Odorizzi et al., 2015). To determine whether PD-1 plays a similar role in Tregs, we analysed co-inhibitory receptor networks using Boolean analysis (**Figure 3.4g**). This revealed a significant increase in the $CD30^+GITR^+CTLA\text{-}4^+TIGIT^+$ subset within *Pd1*$^{-/-}$ Tregs (**Figure 3.4h, Appendix Table A.1**). These alterations in co-inhibitory receptor expression suggest a compensatory adaptation in Treg phenotype in response to PD-1 deficiency, highlighting a sophisticated regulatory network controlled by PD-1 similar to what has been observed in $CD8^+$ T cells. We next investigated whether similar changes were noted in $CD4^+FoxP3^-$ T cells. Neither a change in frequency nor alterations in the co-receptor landscape was observed (**Figure 3.4i-k**), suggesting that PD-1-mediated regulation of co-inhibitory receptor expression is specific to Tregs. Finally, we assessed the cytokine profile of Tregs

in WT and *Pd1*$^{-/-}$ mice and found no differences in IL-10, IFN-γ and IL-17 expression (**Figure 3.4l-n**).

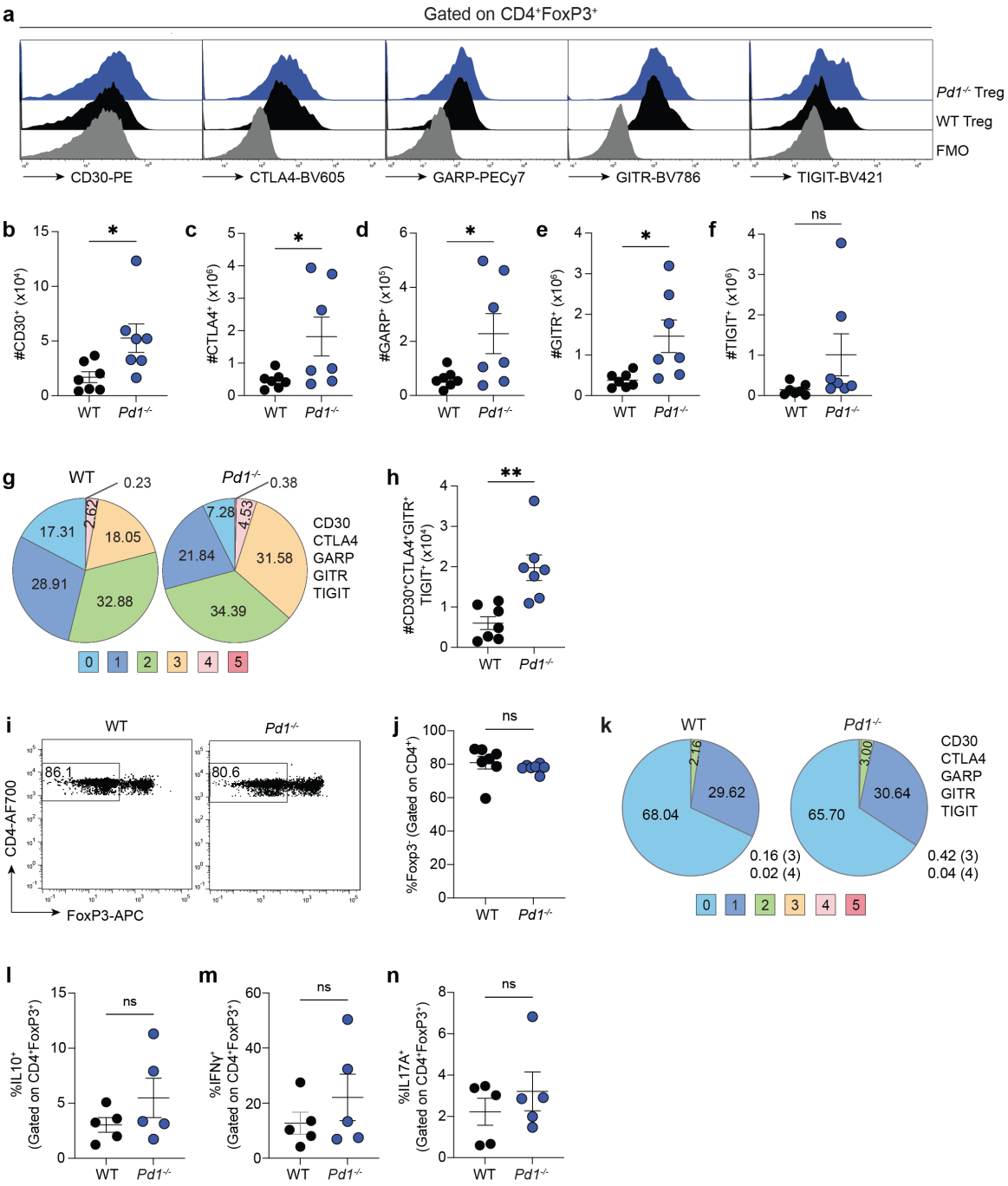

Figure 3.4 PD-1 deficient Tregs upregulates a unique network of co-inhibitory receptors.

Foxp3^{RFP} (WT) and *Pd1*$^{-/-}$*Foxp3*^{RFP} (*Pd1*$^{-/-}$) spleens were harvested and immunophenotyped using flow cytometry. **A,** Representative flow cytometry plots of CD30, CTLA4, GARP, GITR and TIGIT expression in Tregs. **B-F**, Absolute numbers of CD30, CTLA4, GARP, GITR and TIGIT in WT and *Pd1*$^{-/-}$ Tregs. **G,** Boolean analysis of 5 different co-inhibitory receptor expression in WT and *Pd1*$^{-/-}$ Tregs. **H,** Linear analysis of CD30 network of coreceptors in WT and *Pd1*$^{-/-}$ Tregs. **I**, Representative flow cytometry

plots and **J**, summary of the frequency of $CD4^+FoxP3^-$ T cells. **K**, Boolean analysis of 5 different co-inhibitory receptor expression in WT and *Pd1*$^{-/-}$ $CD4^+FoxP3^-$ T cells. **L-N**, Summary of IL10, IFNγ and IL17A expression in Tregs. Data shown are Mean±SEM with each datapoint represents an independent experiment, an unpaired Student's t-test was performed. *P < 0.05, **P < 0.01. FMO, fluorescence minus one; NS, not significant.

3.3.4 PD-1 intrinsically controls CD30 expression in Tregs

We next investigated whether the upregulation of co-inhibitory receptors in effector Tregs was due to an intrinsic or extrinsic requirement for PD-1. To address this, we generated *Pd1*$^{fl/fl\text{-}DTR\text{-}Tdtomato}$ mice (abbreviated as *Pd1*$^{fl/fl}$), in which *loxP* sites flank exons 2 and 3 of the *Pd1* gene (**Figure 3.5a**) as previously reported (Strauss et al., 2020). This model also includes an IRES-driven tdTomato reporter and the diphtheria toxin receptor (DTR). To inducibly ablating PD-1 expressing cells, *Pd1*$^{fl/fl}$ mice were administered 10mg/kg of diphtheria toxin from *Corynebacterium diphtheriae* in PBS via IP injection, with up to 10 doses given at two-day intervals (**Figure 3.5b**). We then crossed *Pd1*$^{fl/fl}$ mice with *Foxp3*$^{ERT2\text{-}Cre\text{-}eGFP}$ (Rubtsov et al., 2010) to generate *Pd1*$^{fl/fl}$*Foxp3*$^{ERT2\text{-}Cre\text{-}eGFP}$ (abbreviated as *Pd1*$^{fl/fl}$*Foxp3*^{ERT2Cre}) mice. To selectively knock out PD-1 in FoxP3-expressing Tregs, *Pd1*$^{fl/fl}$*Foxp3*^{ERT2Cre} mice were administered 1mg of tamoxifen in corn oil via IP injection for five consecutive days (**Figure 3.5c**).

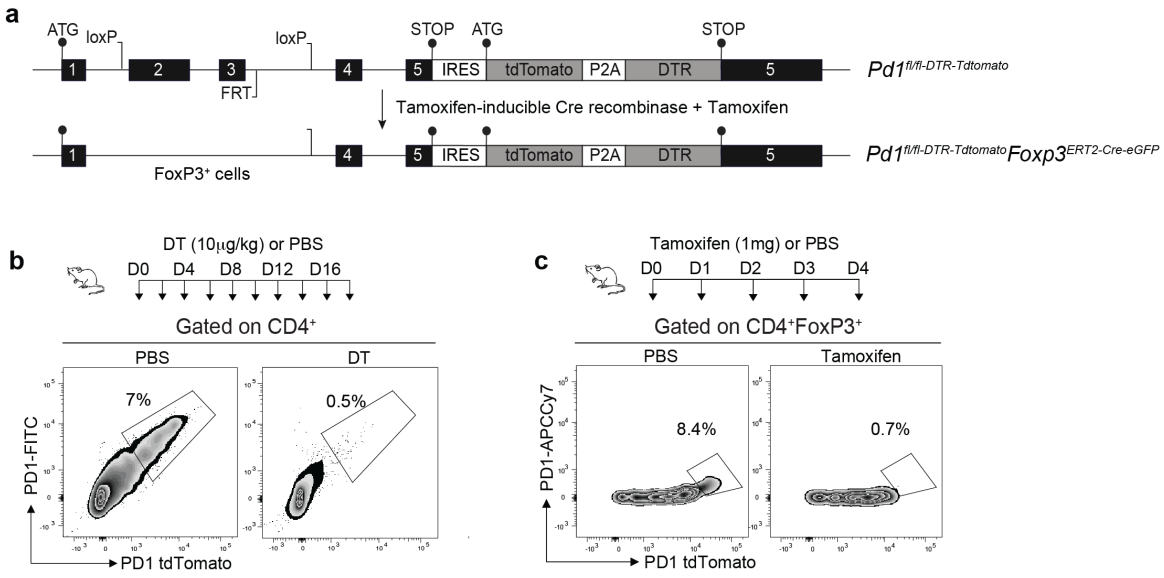

Figure 3.5 Generation of mice inducibly ablating PD-1-expressing cells and selectively lacking PD-1 on Tregs.

A, Schematic representation of *Pd1* gene locus in *Pd1*$^{fl/fl}$ mice generated by Ozgene (**top panel**) and in *Pd1*$^{fl/fl}$*Foxp3*^{ERT2Cre} mice upon tamoxifen treatment (**bottom panel**). **B,** *Pd1*$^{fl/fl}$ mice were administered with PBS or 10μg/kg body weight of diphtheria toxin (DT) for up to 10 dosages via IP injection. Representative flow cytometric plots showing PD-1 antibody versus tdTomato gated on $CD4^+$ cells, with either PBS **(left panel)** or DT treatment (**right panel**). **C,** *Pd1*$^{fl/fl}$*Foxp3*^{ERT2Cre} mice were administered PBS or 1mg tamoxifen for 5

consecutive days. Flow cytometric plots of PD-1 antibody versus tdTomato expression in Tregs from PBS (**left panel**) or tamoxifen-treated mice (**right panel**).

Using the *Pd1*$^{fl/fl}$*Foxp3*^{ERT2Cre} inducible conditional knockout model, we repeated the experiments previously performed in global *Pd1*$^{-/-}$*FoxP3*^{RFP} mice, following tamoxifen treatment. Similar to global *Pd1*$^{-/-}$ mice, we observed an increase in FoxP3^{+} Tregs (**Figure 3.6a-b**), with no changes in CD25, Helios, Tbet, GATA-3 or RORγt expression (**Figure 3.6c-g**). However, unlike the global *Pd1*$^{-/-}$*FoxP3*^{RFP} mice, the frequencies of CD62L^{-}CD44^{+} effector Tregs or CD62L^{+}CD44^{-} naïve Tregs remained unchanged (**Figure 3.6h-i**). Notably, only CD30 expression was significantly increased in conditional knock out Tregs, with no alterations in CTLA-4, GARP, GITR or TIGIT (**Figure 3.6j-o**). A compensatory increase in the co-inhibitory receptor network was again observed (**Figure 3.6p-q, Appendix Table A.2**), further supporting a regulatory adaptation in response to PD-1 loss. Consistent with *Pd1*$^{-/-}$*FoxP3*^{RFP} mice, cytokine expression remained unchanged (**Figure 3.5r-t**).

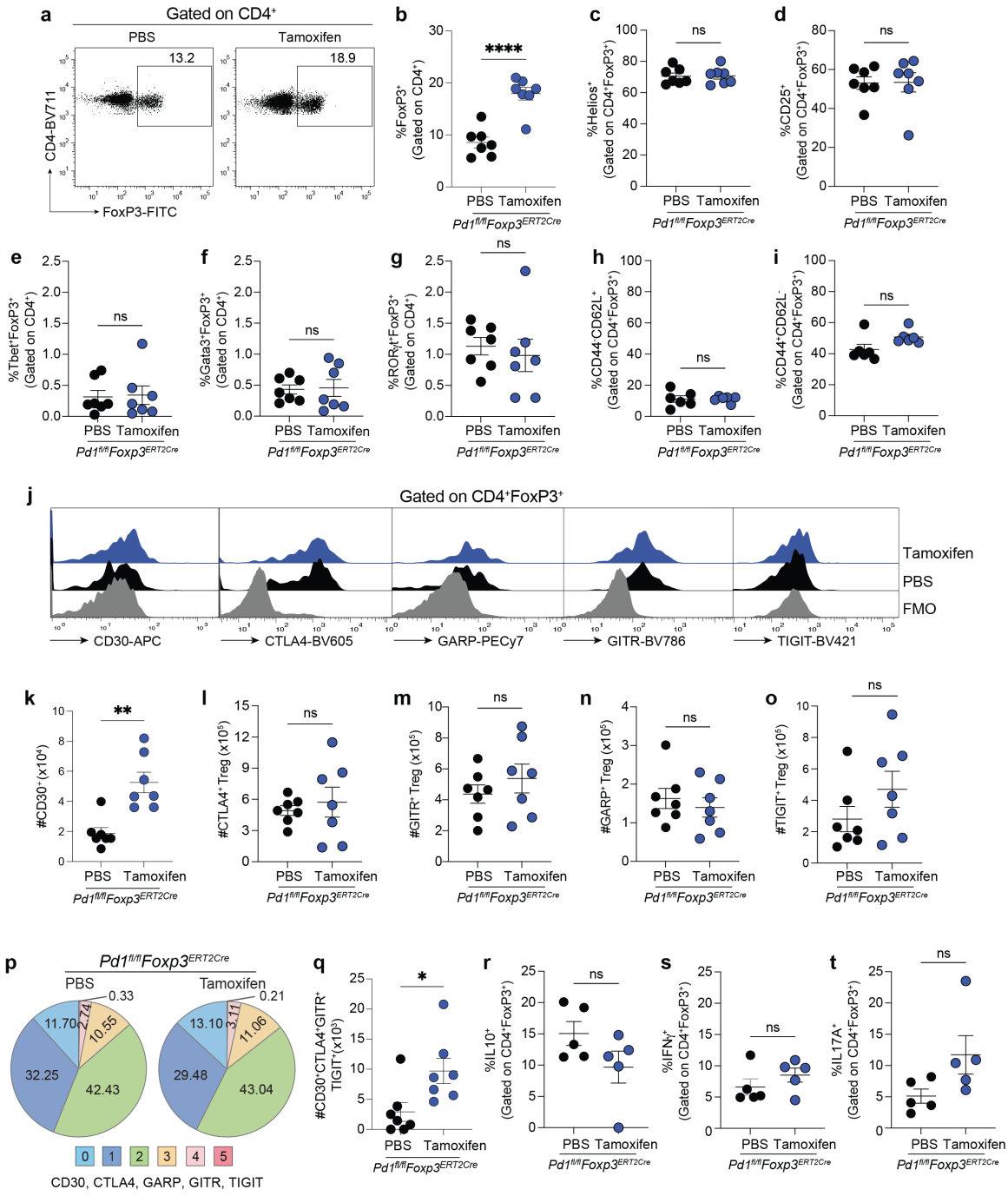

Figure 3.6 PD-1 deficient Tregs upregulates a unique network of co-inhibitory receptors including CD30.

Immunophenotyping of Tregs from PBS and tamoxifen treated *Pd1*$^{fl/fl}$*Foxp3*^{ERT2Cre} murine splenocytes. **A,** Representative flow cytometry plots and **B**, summary data of FoxP3 expression in CD4$^+$ T cells. **C-D**, Summary data showing Helios and CD25 expression in Tregs. **E-G**, Frequency of Tbet$^+$FoxP3$^+$ cells, GATA3$^+$FoxP3$^+$ cells and RORγt$^+$FoxP3$^+$ cells. **H-I,** Summary of the frequency of CD62L$^-$CD44$^+$ and CD62L$^+$CD44$^-$ Tregs. **J,** Representative flow cytometry plots of CD30, CTLA4, GARP, GITR and TIGIT expression in Tregs. Absolute counts of **K**, CD30$^+$ Tregs, **L**, CTLA4$^+$ Tregs, **M**, GARP$^+$ Tregs, **N**, GITR$^+$ Tregs and **O**, TIGIT$^+$ Tregs. **P,** Boolean analysis of 5 different co-inhibitory receptor expression in Tregs. **Q,** Linear analysis of CD30 network of coreceptors in Tregs. **R-T**, Summary showing expression of intracellular cytokines including IL10,

IFNγ and IL17A in Tregs. Data shown are Mean±SEM with each data point represents an independent experiment. An unpaired Student's t-test was performed. *P < 0.05, ****P < 0.0001. NS, not significant.

To determine whether CD30 regulation occurred at the transcription level, we assessed CD30 mRNA expression in Tregs from *Pd1*$^{-/-}$*FoxP3*^{RFP} and tamoxifen-treated *Pd1*$^{fl/fl}$*Foxp3*^{ERT2Cre} mice. Tregs were isolated from murine splenocytes using the Miltenyi Treg Isolation kit based on CD4^{+}CD25^{+} expression. The purity of isolated Tregs was confirmed by flow cytometry (**Figure 3.7a-b**) with minor contamination from CD4^{+}Foxp3^{-} cells, likely due to the expression of CD25 on activated non-Treg CD4^{+} T cells. mRNA was extracted from Tregs using the Qiagen RNeasy Mini Kits. cDNA synthesis was performed using the TaqMan Reverse Transcription Reagents, followed by reverse transcription quantitative polymerase chain reaction (RT-qPCR) for the quantitation of mouse CD30 mRNA (*Tnfrsf8*), with actin mRNA (*Actb*) serving as a housekeeping control. Our analysis revealed a significant upregulation of CD30 mRNA in Tregs from both *Pd1*$^{-/-}$*FoxP3*^{RFP} and tamoxifen-treated *Pd1*$^{fl/fl}$*Foxp3*^{ERT2Cre} mice (**Figure 3.7c-d**), proposing that PD-1 deficiency directly influences CD30 transcription in Tregs.

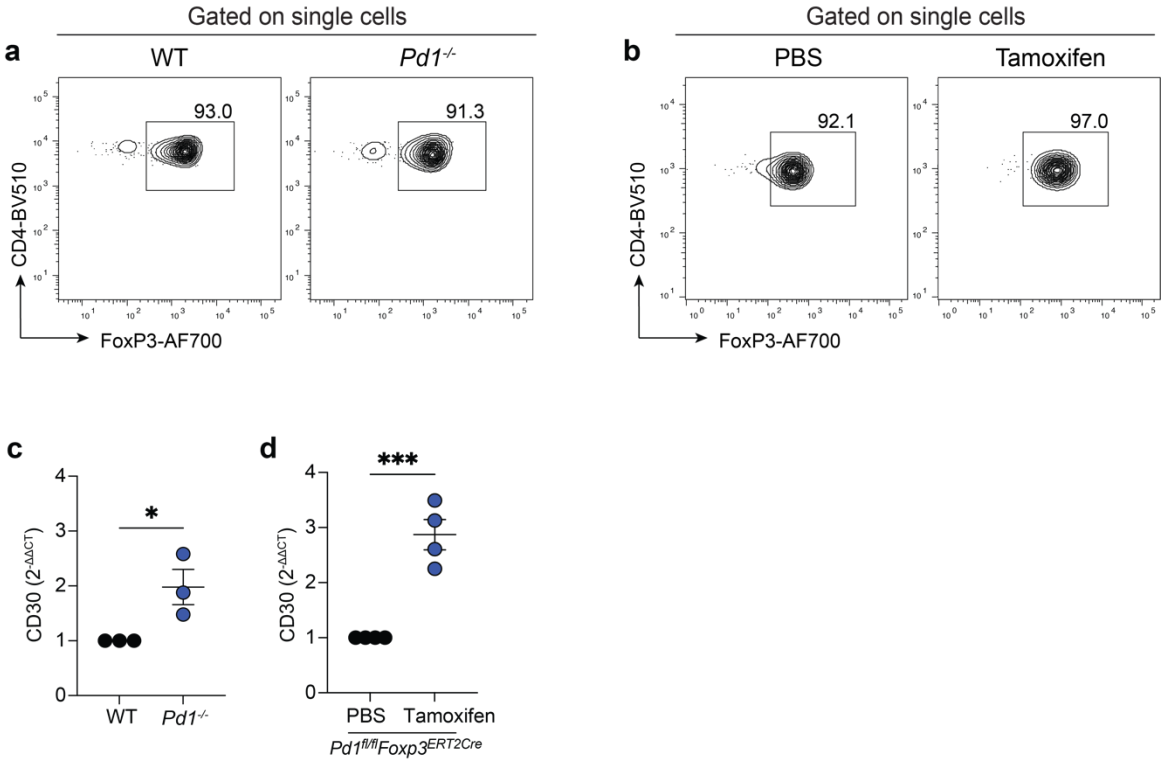

Figure 3.7 PD-1 deficient Tregs exhibit increased CD30 mRNA expression.
Tregs were isolated from *Foxp3*^{RFP} (WT), *Pd1*$^{-/-}$*Foxp3*^{RFP} (*Pd1*$^{-/-}$), PBS and tamoxifen-treated *Pd1*$^{fl/fl}$*Foxp3*^{ERT2Cre} murine splenocytes using Miltenyi Treg Isolation kit. **A,** Flow cytometry plots showing the purity of isolated WT Tregs and *Pd1*$^{-/-}$ Tregs. **B,** Flow cytometry plots showing the purity of isolated PBS and tamoxifen-treated

Pd1$^{fl/fl}$*Foxp3*^{ERT2Cre} Tregs. **C,** RT-qPCR analysis of CD30 mRNA expression in Tregs from *Foxp3*^{RFP} and *Pd1*$^{-/-}$*Foxp3*^{RFP}. **D,** RT-qPCR analysis of CD30 mRNA expression in Tregs from PBS and tamoxifen-treated *Pd1*$^{fl/fl}$*Foxp3*^{ERT2Cre} mice. Data shown are Mean±SEM with each data point represents an independent experiment, an unpaired Student's t-test was performed. *P < 0.05, ***P < 0.001.

Finally, we investigated whether PD-1 intrinsically regulates CD30 expression in Tregs. To determine which co-inhibitory receptors are intrinsically controlled by PD-1, we utilised *Pd1*$^{fl/fl}$*Foxp3*^{ERT2crehet} (abbreviated as *Pd1*$^{fl/fl}$*Foxp3*$^{ERT2Cre+/-}$) female mice, in which approximately half of the Tregs are PD-1 deficient upon tamoxifen treatment while the remaining Tregs retain PD-1 expression due to the FoxP3 X chromosome inactivation (Tommasini et al., 2002) (**Figure 3.8a**). This model is analogous to the reported *Ctla4*$^{fl/fl}$*Foxp3*$^{ERT2Cre+/}$ mice (Ding et al., 2024). This experimental design allowed us to compare PD-1-deficient and PD-1-expressing Tregs within the same environment. We analysed Tregs in the spleen by first gating on CD44^{+} Tregs to select activated Tregs that would have upregulated PD-1 in response to activating signals. Then, within this CD44^{+} Treg population, we further gated on PD-1^{+} and PD-1^{-} cells (**Figure 3.8b**). This strategy enabled us to isolate Tregs that lost PD-1 due to tamoxifen administration, rather than those that were PD-1^{-} because they had never been activated as previously described (Tan et al., 2021). Using this approach, we found that PD-1 intrinsically inhibited CD30 expression in effector Tregs (**Figure 3.8c**). Taken together, these data suggest that PD-1 intrinsically restrains CD30 expression in Tregs under steady-state conditions. No changes were observed in GARP or TIGIT expression but an intrinsic upregulation of GITR and CTLA-4 was noted (**Figure 3.8d-g**).

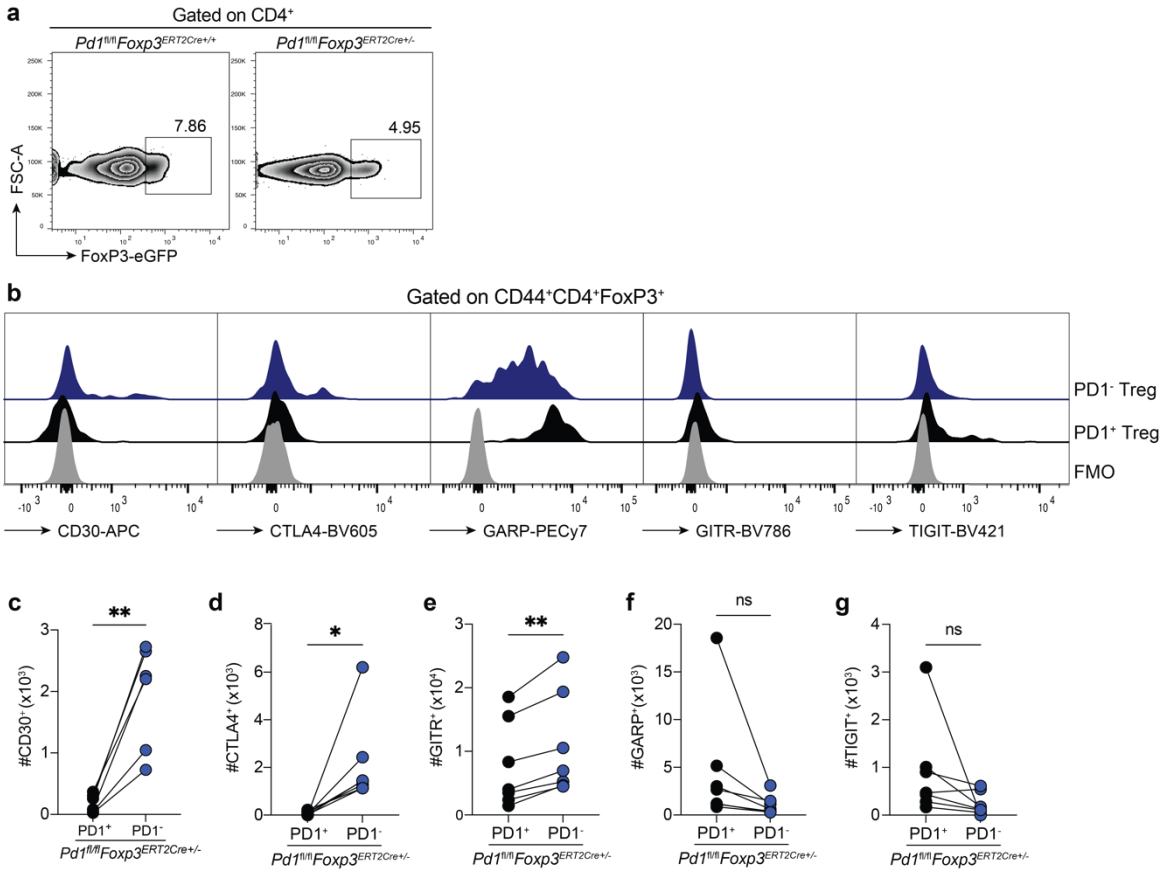

Figure 3.8 PD-1 intrinsically regulates CD30 expression in Treg.
Analysis of spleens of *Pd1*$^{fl/fl}$*Foxp3*$^{ERT2Cre+/-}$ female mice pre-administered with 1mg tamoxifen for 5 consecutive days via IP injection. **A,** Representative flow cytometry plots of Foxp3$^{ERT2Cre\text{-}eGFP}$ expression in CD4^{+} T cells from *Pd1*$^{fl/fl}$*Foxp3*$^{ERT2Cre+/+}$ and *Pd1*$^{fl/fl}$*Foxp3*$^{ERT2Cre+/-}$ female mice. **B,** Representative flow cytometry plots of CD30, CTLA4, GARP, GITR and TIGIT expression in PD-1^{-} and PD-1^{+} effector Tregs from *Pd1*$^{fl/fl}$*Foxp3*$^{ERT2Cre+/-}$ mice. Absolute counts of **C,** CD30^{+} Tregs, **D**, CTLA4^{+} Tregs, **E**, GARP^{+} Tregs, **F**, GITR^{+} Tregs and **G**, TIGIT^{+} Tregs. Data shown are Mean±SEM from 6 independent experiments, a paired Student's t-test was performed. *P < 0.05, **P < 0.01. FMO, fluorescence minus one; NS, not significant.

3.3.5 CD30 expression is driven by STAT5 signalling in Pd1$^{-/-}$ Treg

PD-1 has been reported to inhibit PI3K/Akt signalling (Tan et al., 2021) and STAT5 (Taylor et al., 2017) downstream of TCR and IL-2 stimulation. To assess whether PD-1 regulates CD30 expression, we stimulated WT FoxP3^{+} T cells with anti-CD3/28 in the presence or absence of PD-1 signalling. Tregs were isolated from WT murine splenocytes using Miltenyi Treg Isolation kit and activated with plate-bound 5µg/ml anti-CD3 and recombinant mouse PD-L1 Fc chimera protein (rmPD-L1 Fc), along with 2µg/ml anti-CD28. PD-1 signalling was blocked with 10µg/ml anti-PD-1. After 72 h, cells were washed and cultured for an additional 24 h with 10µg/ml anti-mouse IL-2 in the presence or absence of 80ng/ml recombinant human IL-2 (rhIL-2) (**Figure 3.9a**). In the absence of IL-2, PD-1

signalling had no effect on CD30 expression (**Figure 3.9b, left panel)**. However, under IL-2 stimulation, PD-1 inhibition led to a significant increase in both CD30 protein (**Figure 3.9b, right panel)** and mRNA expression (**Figure 3.9c)** compared to the rmPD-L1 Fc condition. This suggested that PD-1 restrains CD30 expression in response to IL-2 signalling. To further investigate whether IL-2 induces CD30 expression, we stimulated Tregs isolated from *Foxp3*^{RFP} or *Pd1*$^{-/-}$ *Foxp3*^{RFP} mice with plate-bound 5µg/ml anti-CD3 and 2µg/ml anti-CD28, alongside either 10µg/ml anti-mouse IL-2 or 80ng/ml rhIL-2. Cells were harvested at various time points and CD30 expression was assessed using flow cytometry. We observed a significant increase in CD30 expression in both WT and *Pd1*$^{-/-}$ Tregs following IL-2 stimulation compared to anti-IL-2 conditions (**Figure 3.9d)**. Given the established role of PD-1 in inhibiting STAT5 signalling, we next investigated whether PD-1 regulates STAT5 phosphorylation in Tregs. *Foxp3*^{RFP} Tregs were stimulated with plate-bound 5µg/ml anti-CD3 and rmPD-L1 Fc, along with 2µg/ml anti-CD28 and 10µg/ml anti-mouse IL-2 for 48 h. 10µg/ml anti-PD-1 was added to block the PD-1/PDL1 interaction. Cells were then washed and re-stimulated with 80ng/ml rhIL-2 for 15 min and p-STAT5 expression was measured by flow cytometry (**Figure 3.9e, left panel)**. We found that PD-1 activation through PD-L1 downregulated STAT5 phosphorylation, while PD-1 blockade enhanced p-STAT5 expression (**Figure 3.9e, right panel)**, confirming that PD-1 negatively regulates STAT5 signalling in Tregs.

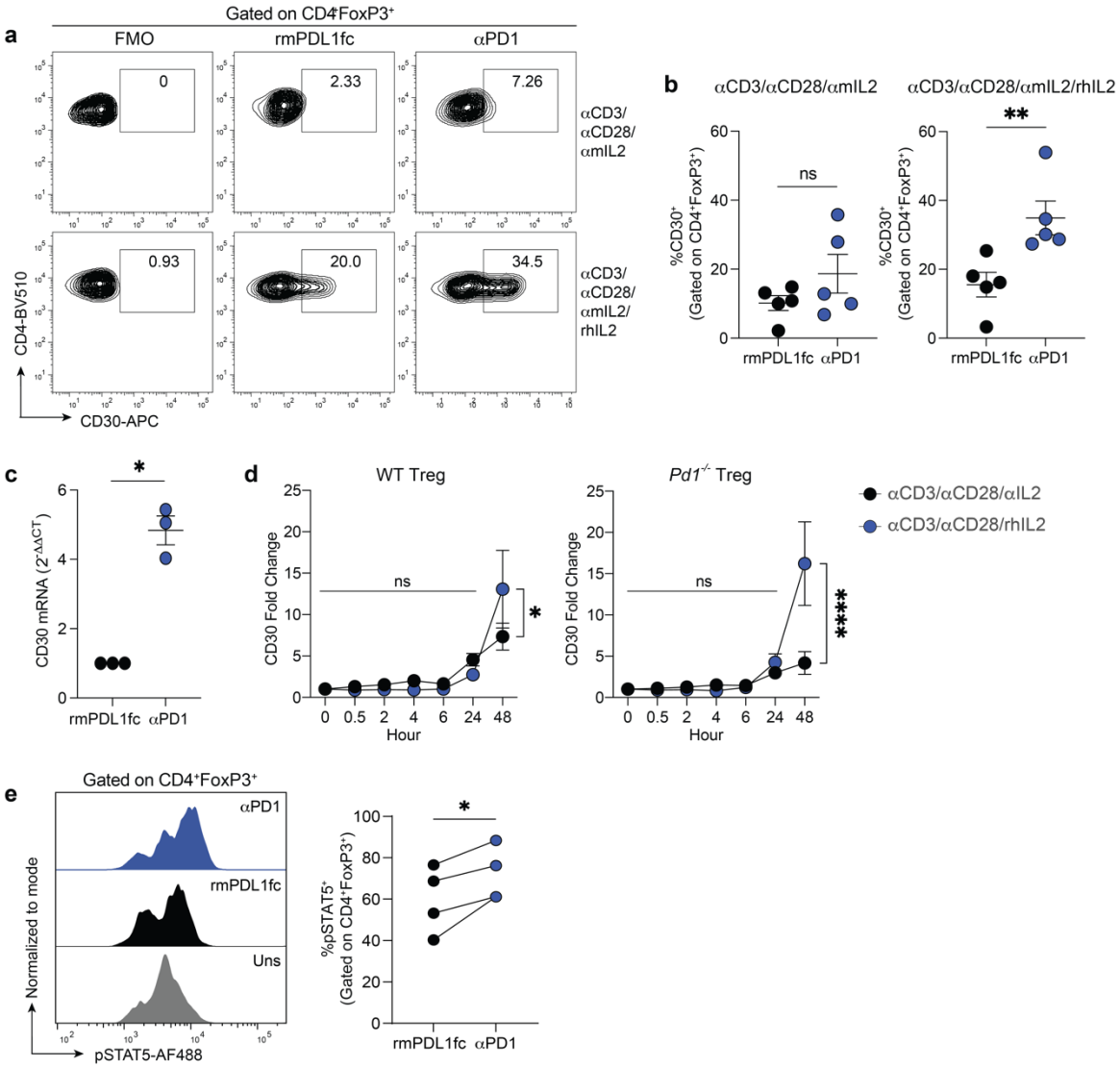

Figure 3.9 PD-1 regulates IL-2-STAT5 driven CD30 expression in Tregs.
WT Tregs from C57BL/6 (WT) mice were stimulated with αCD3/28 and cultured with either αIL-2 or IL-2 in rmPDL1 Fc-coated well plate. αPD-1 was added to block the PD-1/PDL1 interaction. **A,** Representative flow cytometry plots showing CD30 expression. **B,** Summary of CD30 expression in Tregs cultured with either αIL-2 or αIL-2 plus rhIL-2 across five independent experiments. **C,** CD30 mRNA expression in Tregs from three independent experiments. **D,** Tregs from WT and *Pd1*$^{-/-}$ mice were stimulated with αCD3/28 and cultured with either αIL-2 or rhIL-2. At the indicated time points, CD30 expression on Tregs were plotted as fold change of expression at specific time point compared to unstimulated condition (0 h). Data are shown from seven independent experiments. **E,** Tregs from WT mice were stimulated with αCD3/28 and αIL-2 in rmPD-L1 Fc-coated plate. αPD-1 was added to block the PD-1/PDL1 interaction. After 48 h, cells were washed and stimulated with rhIL-2 for 15 min to allow p-STAT5 staining (**left panel**). Expression of p-STAT5 in CD30^{+} Tregs (**right panel**) across four independent experiments. Data shown are Mean±SEM. Statistical analyses were performed using a paired Student's t-test in **B** and **E**, an unpaired Student's t-test in **C,** or two-way ANOVA with multiple Sidak's comparison in **D**. *P < 0.05, **P < 0.01, ****P < 0.0001, NS, not significant. Uns, unstimulated.

To explore whether STAT5 directly regulates CD30 expression, we analysed our previously published ChIP-seq data set (Villarino et al., 2022). Naïve WT $CD4^+$ cells were stimulated with plate-bound 10μg/ml of anti-CD3 and anti-CD28 in the presence of anti-mouse IL-2 for 48 h, then cultured with 100 U/ml human IL-2 for an additional 48 h. We found that STAT5 bound to the *Tnfrsf8* (CD30) gene locus in WT $CD4^+$ T lymphoblasts stimulated with IL-2 for 48 h (**Figure 3.10a, top panel)**. Notably, STAT5 occupancy overlapped with two p300-binding sites flanking the gene, suggesting a potential role in CD30 transcriptional regulation (**Figure 3.10a, bottom panel)**. To confirm STAT5 positively regulated CD30 expression, we performed a GSEA analysis on our previously published RNA-seq datasets (Villarino et al., 2022). Naïve WT and *Stat5*$^{-/-}$ $CD4^+$ T cells were cultured with plate-bound 10μg/ml of anti-CD3 and anti-CD28 in the presence of anti-mouse IL-2 for 72 h, then re-stimulated with agonist anti-TCR in the presence of either anti-IL-2 or 100 U/ml human IL-2 for 4 d. Differential gene expression was ranked comparing WT $CD4^+$ T cells in response to IL-2 stimulation compared to anti-IL-2 condition, or in IL-2 stimulated WT $CD4^+$ T cells compared to *Stat5*$^{-/-}$ $CD4^+$ T cells. Within this dataset, we specifically examined TNFR family members, including *Tnfrsf8, Tnfrsf4, Tnfrsf13b, Tnfrsf11b, Tnfrsf18, Tnfrsf21, Tnfrsf1b, Tnfrsf9, Tnfrsf17, Tnfrsf19, Ltbr, Eda2r, Tnfrsf11a, Ngfr, Tnfrsf1a, Tnfrsf12a, Tnfrsf10a, Cd40, Tnfrsf13c, Fas, Tnfrsf25, Cd27* and *Tnfrsf14.* Among these, *Tnfrsf8* was highly ranked as an IL-2-induced gene in the presence of STAT5 (**Figure 3.10b)**. However, the TNFR family as a whole was not significantly enriched in either condition. Finally, we examined whether STAT5 regulates other co-inhibitory receptors associated with checkpoint therapy. Unlike CD30, no significant STAT5-dependent regulation was observed for clinically relevant co-inhibitory receptors (**Figure 3.10c)**, indicating that STAT5-mediated CD30 induction is a specific effect rather than a general feature of TNFR family members.

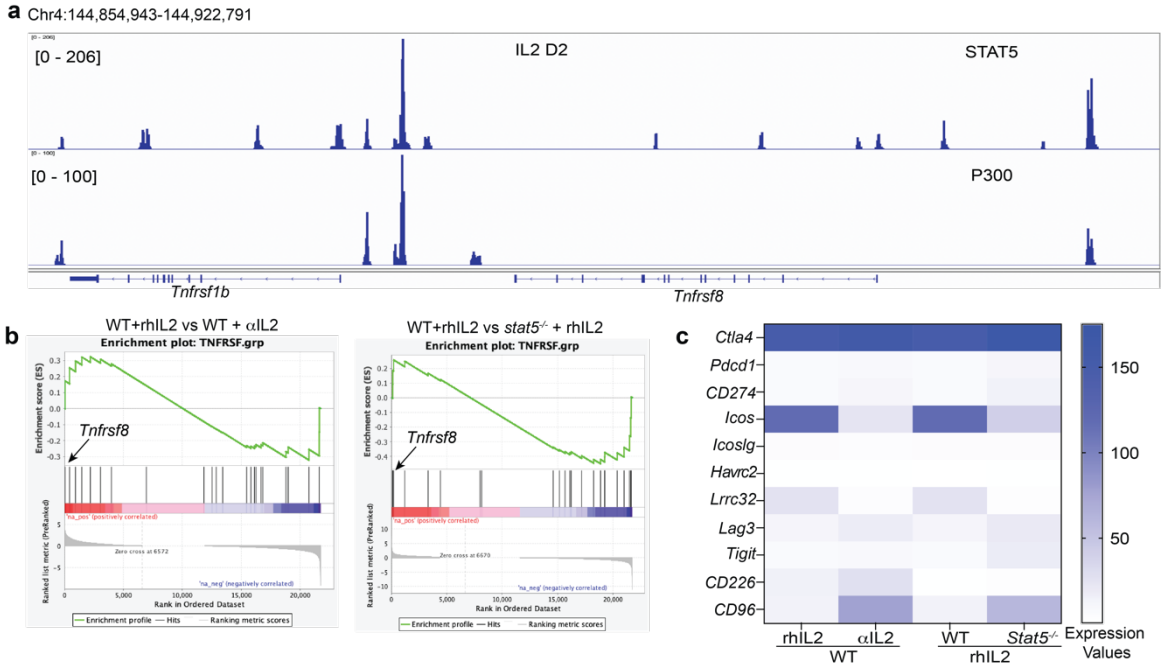

Figure 3.10 IL-2-STAT5 drives CD30 expression in CD4$^+$ T lymphocytes.
A, Representative ChIP-seq tracks and peaks detected by STAT5 **(top panel)** and p300 **(bottom panel)** at the *Tnfrsf8* gene locus of naïve WT CD4$^+$ cells stimulated with αCD3/28 and rhIL-2 for 3 d. **B,** Naïve WT and *Stat5*$^{-/-}$ CD4$^+$ cells were stimulated with αCD3/28 in the presence of αIL-2 for 72 h, washed and re-stimulated with αTCR along with either αIL-2 or rhIL-2 for 4 d. GSEA plots showing *Tnfrsf* family gene ranking in IL-2-treated WT CD4$^+$ cells compared to either αIL-2-treated WT CD4$^+$ cells (**left panel**) or *Stat5*$^{-/-}$ CD4$^+$ cells (**right panel**). **C,** Heatmap showing expression of co-receptors and ligands in WT and *Stat5*$^{-/-}$ CD4$^+$ cells.

3.4 Discussion

This chapter focused on the role of PD-1 specifically in murine Tregs, focusing on its impact on suppressive capacity, proliferation, apoptosis, and the broader co-inhibitory receptor landscape. Our findings demonstrate that *Pd1*$^{-/-}$ Tregs exhibit enhanced suppressive function compared to WT Tregs, aligning with previous studies in autoimmunity and infectious diseases (Tan et al., 2021, Perry et al., 2022). Interestingly, while *Pd1*$^{-/-}$ Tregs displayed an effector-like phenotype, this did not correspond to dysfunction (Brunkow et al., 2001) but rather to improved regulatory function. Notably, this enhancement was not attributed to increased proliferation, reduced apoptosis or alterations in cytokine production. To explore alternative mechanisms, we examined the role of other well-known co-inhibitory receptors, including CD30, GITR, CTLA-4, TIGIT and GARP. Although CTLA-4 and GITR expression increased, our data identified CD30 as the primary receptor intrinsically regulated by PD-1. CD30 has been previously implicated in immunotherapy and Treg biology, particularly in graft-versus-host disease,

where it plays a crucial role in Treg-mediated suppression (Zeiser et al., 2007). These findings highlight a novel compensatory pathway in Tregs, suggesting that CD30 may function as an adaptive regulator in the absence of PD-1.

Furthermore, our data highlight the interplay between PD-1 and STAT5 signalling in regulating co-inhibitory receptor expression across different T effector subsets. Previous work in our lab demonstrated that PD-1 inhibits STAT5 signalling in group 2 innate lymphoid cells (Franceschini et al., 2009, Taylor et al., 2017, Laba et al., 2022, Amarnath et al., 2011) and our findings extend this regulatory mechanism to Tregs. While the effect is subtle, we show that PD-1 suppresses STAT5 phosphorylation in Tregs, thereby restricting CD30 expression. The downstream consequences of PD-1 signalling in T cells including Tregs remain complex and context-dependent, with conflicting reports suggesting inhibition of either CD28 signalling or TCR activation (Kamphorst et al., 2017, Hui et al., 2017). Notably, many of these studies do not account for the presence of IL-2, which can be present in the culture system or produced by contaminating T cells and functionally plastic Tregs. By incorporating an anti-IL-2 blocking antibody, we demonstrate that CD30 is not induced in Tregs in the absence of IL-2. Thus, our findings suggest that IL-2-driven STAT5 activation promotes CD30 expression, a process that can be suppressed by PD-1.

3.5 Summary

In summary, our study underscores the critical role of PD-1 in regulating Treg function, highlighting its ability to modulate suppressive capacity through mechanisms beyond proliferation, apoptosis or cytokine production. We identify CD30 as a key co-inhibitory receptor intrinsically regulated by PD-1, suggesting a novel compensatory pathway that maintains Treg function in the absence of PD-1. Additionally, we demonstrate that PD-1 suppresses STAT5 phosphorylation, thereby restricting IL-2 driven CD30 expression in Tregs. These findings provide new insights into the interplay between PD-1, STAT5 and co-inhibitory receptor networks in Tregs, with potential implications for understanding immune regulation and designing targeted immunotherapies.

Chapter 4 PD-1 deficiency enhances tumour-derived Treg function through the CD30/CD30L pathway

4.1 Introduction

The use of antibodies against the PD-1/PD-L1 pathway has been successful in the treatment of several cancers, yet many cancer patients do not respond (Larkin et al., 2019) and in some cases PD-1 inhibition may enhance cancer growth (Park et al., 2021). The mechanisms underlying this resistance within the immune system is unclear. Correlative studies in human cancers suggest that Tregs contribute to immune resistance following PD-1 blockade (Kamada et al., 2019). More recently, these observational reports have been superseded by mechanistic tumour studies, where it has been shown that PD-1 is important in functional plasticity of Tregs within tumour-infiltrating lymphocytes (TILs), with PD-1-deficient Tregs displaying dysfunction (Kim et al., 2023). These findings (Tan et al., 2021, van Gulijk et al., 2023, Perry et al., 2022) align with Chen *et al* (Chen et al., 2014), who showed that PD-1 deficiency has an impact in peripheral Treg generation. Collectively, several reports demonstrate that PD-1 can negatively regulate Treg function in autoimmunity and infections, potentially contributing to immunotherapy resistance in cancer and driving hyper-progressive disease (Kamada et al., 2019, van Gulijk et al., 2023). However, the literature presents conflicting views on PD-1's role in Tregs (Francisco et al., 2009, Amarnath et al., 2011, Asano et al., 2017), highlighting both negative and positive regulatory function for PD-1 in Tregs, with a lack of consensus on the role of PD-1 in driving Treg function. These discrepancies likely stem from the lack of an unbiased analysis of *Pd1*$^{-/-}$ Tregs in steady-state conditions and within the TME. Additionally, how Tregs communicate with neighbouring cells in the TME and how PD-1 deficiency alters this communication remains poorly understood. Historically, PD-1 on CD8^{+} T cells was thought to suppress anti-tumour immunity through PD-L1 interactions on tumour cells. However, with the advent of single-cell analysis and spatial transcriptomics, it remains to be determined whether PD-1^{+} Tregs exhibit an altered cell communication program compared to their PD-1^{-} counterparts.

4.2 Aims

In the previous chapter, we demonstrated that PD-1-deficient Tregs exhibit enhanced suppressive capacity and upregulate a co-inhibitory receptor landscape in steady state.

Additionally, our data showed that PD-1 blockade increases IL-2-STAT5 driven CD30 expression on Tregs. However, the functional significance of this unique co-receptor network, particularly the role of CD30 remains unclear. Here, we investigated whether CD30 contributes to enhanced Treg function within the TME during PD-1 deficiency. We hypothesised that in the absence of PD-1, Tregs could enhance their suppressive function via (a) upregulating CD30 expression and (b) altering their communication programme within the TME, contributing to anti-PD-1 resistance. To test this hypothesis, we pursued the following objectives:

1. To investigate the suppressive function of WT and *Pd1*$^{-/-}$ Tregs *in vivo*.
2. To compare the transcriptomics profile of WT and *Pd1*$^{-/-}$ Tregs using BD Rhapsody single-cell RNA sequencing (scRNA-seq).
3. To assess the communication network of WT and *Pd1*$^{-/-}$ Tregs within TME using CellChat analysis
4. To visualise the physical interaction between WT or *Pd1*$^{-/-}$ Tregs and TILs within TME using NanoString CosMx^{TM} spatial molecular imaging.
5. To characterise the co-receptor landscape of Tregs derived from treatment naïve and anti-PD-1-treated stage IV metastatic melanoma patient.

4.3 Results

The results and analyses presented in this chapter have been published in *Nature Immunology*, June 02, 2025. DOI: 10.1038/s41590-025-02172-0.

4.3.1 Pd1$^{-/-}$ Tregs possess greater suppressive capacity and promote tumour growth

We validated our previous findings on the suppressive function of WT and *Pd1*$^{-/-}$ Tregs *in vitro* using an *in vivo* B16F10 melanoma model. *Rag1*$^{-/-}$ mice, which lack mature T cells, were subcutaneously inoculated with B16F10 melanoma cells and subsequently reconstituted with either WT or *Pd1*$^{-/-}$ CD45.2^{+} Tregs alongside WT CD45.1^{+}CD4^{+} T effector (Teff) cells **(Figure 4.1a)**. Tumour growth was significantly enhanced in mice receiving *Pd1*$^{-/-}$ Tregs compared to those reconstituted with WT Tregs, with differences emerging from day 17 post-inoculation **(Figure 4.1b)**. To determine whether the increased tumour burden observed in the *Pd1*$^{-/-}$ Treg cohort was driven by alterations in T cell frequency or cytokine profiles within the TME, we analysed the immunobiology of the TILs by flow cytometry **(Figure 4.1c)**. Both cohorts possessed comparable absolute counts of Tregs and CD4^{+} Teff cells **(Figure 4.1d-e)**. Additionally, we observed no significant

differences in IL-10 production in Tregs or IFNγ expression in CD4$^+$ Teff cells within the TME **(Figure 4.1f-g)**. These findings suggest that the enhanced suppressive capacity of *Pd1*$^{-/-}$ Tregs is not attributable to the changes in T cell frequency or cytokine profiles.

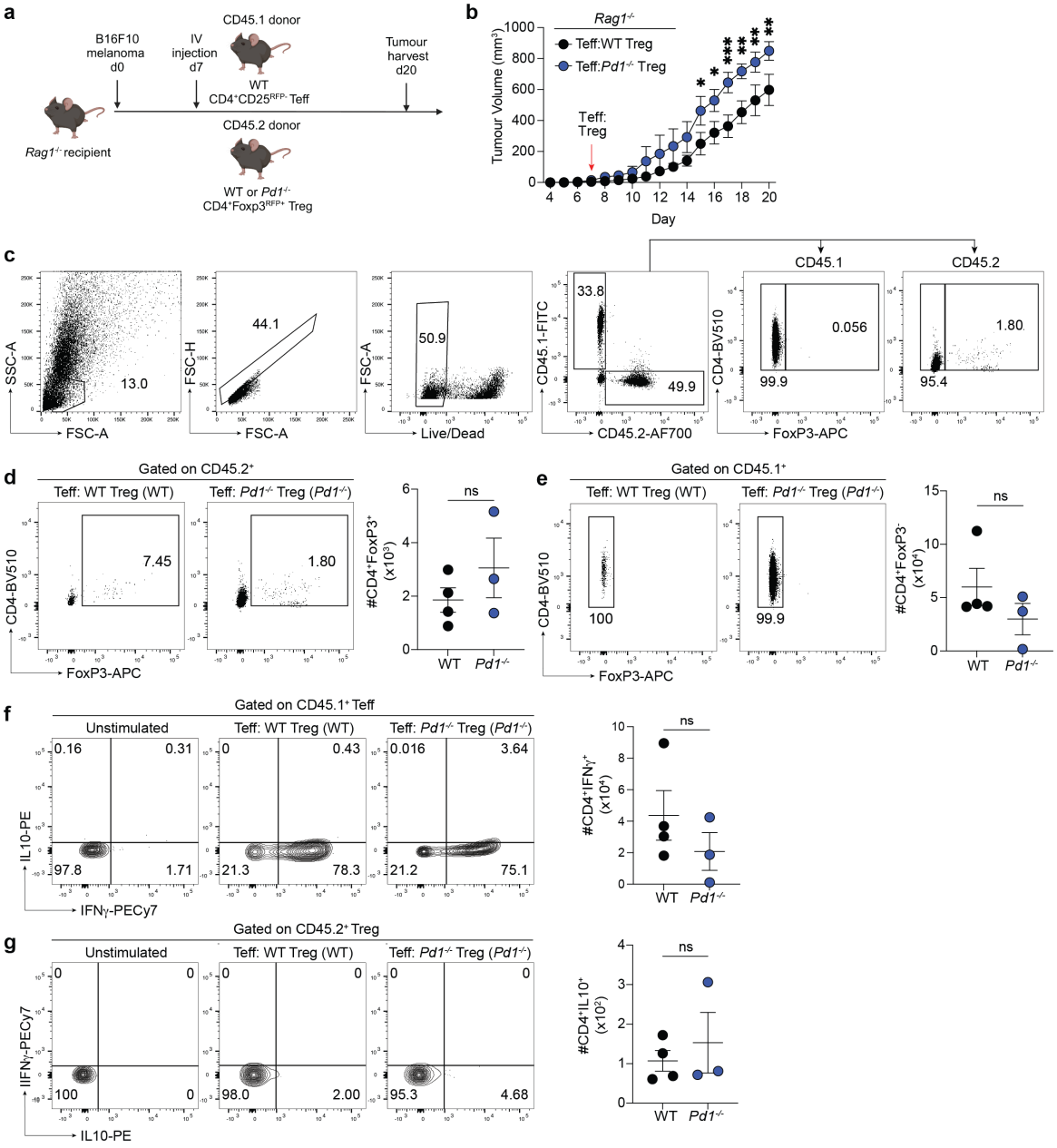

Figure 4.1 *Pd1*$^{-/-}$ Tregs possessed greater suppressive capacity in B16 *in vivo* model. **A,** *Rag1*$^{-/-}$ mice were subcutaneously inoculated with B16F10 melanoma cells on d0 and further reconstituted with CD45.1$^+$ Teff cells and CD45.2$^+$ Tregs sorted from either *Foxp3*^{RFP} (WT) or *Pd1*$^{-/-}$*Foxp3*^{RFP} (*Pd1*$^{-/-}$) mice via IV injection on d7. **B,** Tumour volume was monitored (n=8 mice in WT Treg group and n=6 in *Pd1*$^{-/-}$ Treg cohort). **C,** Flow cytometry plots demonstrating gating strategy applied on TIL immunobiology analysis. **D,** Flow cytometry plots showing Treg (CD4$^+$FoxP3$^+$) frequency gated on CD45.2$^+$ **(left panel)** and summary of its absolute count **(right panel)**. **E,** Flow cytometry plots showing Teff cell (CD4$^+$FoxP3$^-$) frequency gated on CD45.1$^+$ **(left panel)** and summary of its absolute count **(right panel)**. **F,** Flow cytometry plots showing IFN-γ$^+$IL-10$^-$ frequency gated on

Teff cell **(left panel)** and summary of its absolute count **(right panel)**. **G,** Flow cytometry plots showing IFN-γ^{-}IL-10^{+} frequency gated on Treg **(left panel)** and summary of its absolute count **(right panel)**. Data shown are Mean±SEM. Each datapoint represents an independent experiment in **D-G**. Statistical analyses were performed using a two-way ANOVA with multiple Sidak's comparison in **B** and an unpaired Student's t-test in **D-G**. *P < 0.05, **P < 0.01, ***P < 0.001. NS, not significant.

4.3.2 BD Rhapsody single-cell analysis identifies CD30 as a potential candidate for enhanced Pd1$^{-/-}$ Treg function in melanoma

To investigate the co-inhibitory receptor landscape in Tregs within the TME, we established B16 tumours in WT and *Pd1*$^{-/-}$ mice **(Figure 4.2a)**. We utilised the germline *Pd1*$^{-/-}$ mice to generate a resource relevant to clinical settings. Tumour growth was monitored and showed no significant difference between groups at the time of harvest **(Figure 4.2b)**. TILs were enriched from the tumour tissues for BD Rhapsody scRNA-seq analysis. We first performed Louvain clustering on merged WT and *Pd1*$^{-/-}$ TILs and visualised the immune cell clusters within each cohort separately **(Figure 4.2c-d)**. The cell identities were then assigned based on cell-type-specific gene sets **(Appendix Table B.1)**, with Treg identified by the expression of *Cd4* and *Foxp3* **(Figure 4.2e-f)**. The frequency of each immune cell cluster across individual mouse was determined, confirming the presence of Tregs in both groups **(Figure 4.2g)**.

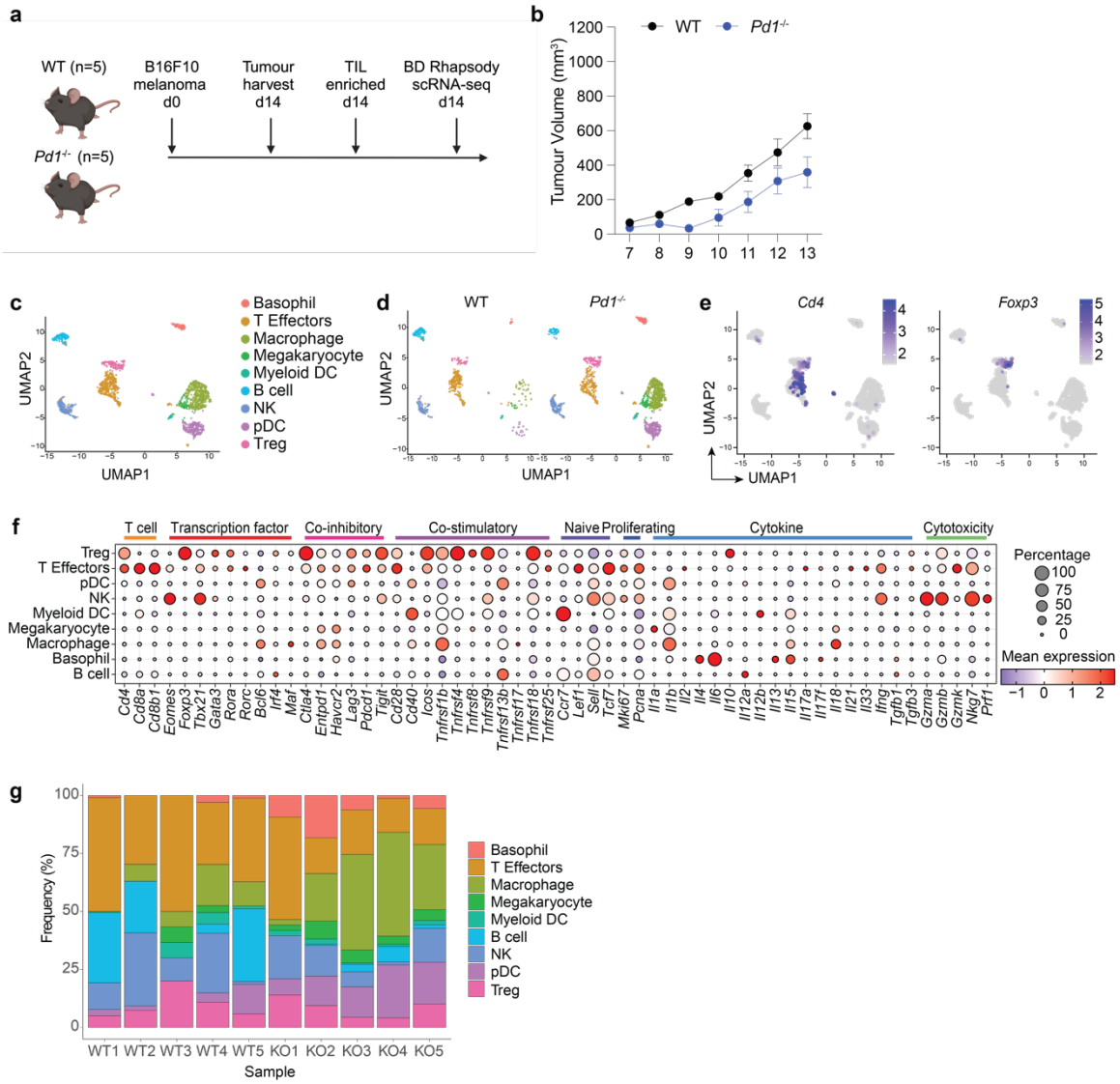

Figure 4.2 BD Rhapsody scRNA-seq reveals the presence of Tregs in WT and *Pd1*$^{-/-}$ cohorts in the B16 TME.

A, C57BL/6 WT and *Pd1*$^{-/-}$ (KO) mice were subcutaneously injected with B16F10 melanoma cells (n=5/cohort). **B,** Tumour growth was investigated and TILs were harvested on d14 for BD Rhapsody scRNA-seq. **C,** A uniform manifold approximation and projection (UMAP) plot of 1,810 enriched TILs derived from WT and *Pd1*$^{-/-}$ cohorts, color-coded by assigned cell type. **D,** UMAP plots showing separately visualised WT and *Pd1*$^{-/-}$ TILs, highlighting similar clustering patterns between cohorts. **E,** UMAP representation of *Cd4* and *Foxp3* expression, identifying the presence of Tregs. **F,** Dot plot depicting the expression of candidate genes across various immune cell clusters. **G,** Sample tag-based identification of individual mice, showing the distribution of cell clusters across each sample.

Differential gene expression (DGE) analysis, illustrated as a volcano plot **(Figure 4.3a, Appendix Table B.2)**, revealed that among the canonical co-inhibitory receptors examined in the previous chapter including *Ctla4*, *Tnfrsf18* (GITR), *Lrrc32* (GARP) and *Tigit,* only *Tnfrsf8* (CD30) was significantly upregulated in *Pd1*$^{-/-}$ TILs. Within the effector CD4^{+} and

$CD8^+$ T cell subsets of the T Effector cluster, we found an increase in *Gzm* transcripts in *Pd1*$^{-/-}$ TILs compared with WT TILs **(Figure 4.3b-c, Appendix Table B.3-4)**. Since the DGE analysis was performed using the *FindMarkers* function with the standard Wilcoxon rank-sum test, which treats the Treg population from different individuals with the same genotype as a whole before statistical analysis, the observed significance could be influenced by batch effects. To account for this, we also performed a clustered Wilcoxon rank-sum test when comparing coreceptor expression in Tregs (Datta and Satten, 2005), incorporating individual mice as clusters to account for the hierarchical structure of the data **(Figure 4.3d)**. This approach reduced the risk of false positives arising from inter-sample variability rather than biological differences. Additionally, we assessed the mean expression of co-inhibitory receptors in Tregs from each mouse individually, using an unpaired Student's t-test to compare expression levels across genotypes, ensuring the observed differences were not driven by a single outlier or batch-specific effects. Consistent with our initial findings, *Tnfrsf8* remained the only receptor significantly upregulated in both single-cell and bulk-level analyses, reinforcing its potential role as a PD-1 regulated co-inhibitory receptor in the TME **(Figure 4.3e)**. Further supporting this, Boolean analysis confirmed that the altered co-inhibitory receptor network observed in steady-state *Pd1*$^{-/-}$ Tregs was preserved at the transcript level in *Pd1*$^{-/-}$ TILs, with the most significant changes occurring in cells co-expressing three or more coinhibitory receptors **(Figure 4.3f)**. These findings suggest that PD-1 plays a key role in shaping the co-inhibitory landscape in Tregs, mirroring its function in $CD8^+$ T cells during chronic viral infection (Odorizzi et al., 2015). Additionally, gene ontology (GO) and gene set enrichment analysis (GSEA) indicated enhanced cytokine signalling in *Pd1*$^{-/-}$ Tregs, further highlighting the broader impact of PD-1 loss on Treg function within the TME **(Figure 4.3g-h, Appendix Table B.5-6)**.

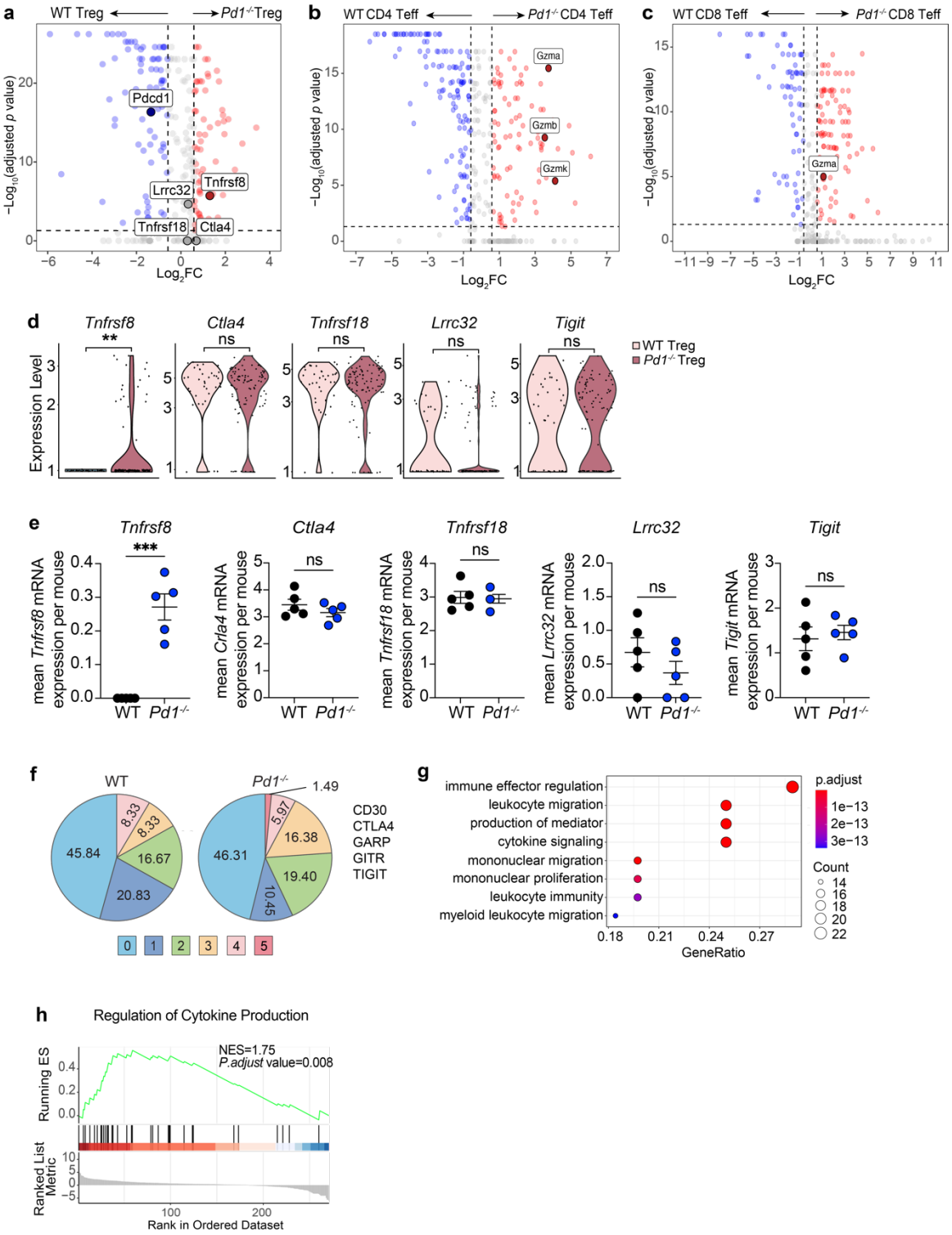

Figure 4.3 BD Rhapsody scRNA-seq analysis identifies CD30 as a potential marker for enhanced *Pd1*$^{-/-}$ Treg cell function within the TME.

C57BL/6 WT and *Pd1*$^{-/-}$ mice were subcutaneously injected with B16F10 melanoma cells (n=5/cohort). **A,** Differential gene expression (DGE) analysis of *Pd1*$^{-/-}$ Tregs compared to that of the WT Tregs. **B,** DGE analysis of *Pd1*$^{-/-}$ effector CD4^{+} (Teff) compared to that of the WT CD4^{+} Teff. **C,** DGE analysis of *Pd1*$^{-/-}$ effector CD8^{+} (Teff) compared to that of the WT CD8^{+} Teff. **D-E,** mRNA expression of transcripts *Tnfrsf8* (CD30), *Ctla4*, *Tnfrsf18* (GITR), *Lrrc32* (GARP) and *Tigit* within WT and *Pd1*$^{-/-}$ Tregs at **D,** single-cell level and **E,** bulk-level. **F,** Average percentage of Tregs expressing 0-5 transcripts encoding *Tnfrsf8*

(CD30), *Ctla4*, *Tnfrsf18* (GITR), *Lrrc32* (GARP) and *Tigit* in WT and *Pd1*$^{-/-}$ Tregs in TME. **G,** GO analysis identified the functions of upregulated genes within *Pd1*$^{-/-}$ Tregs. **H,** GSEA showing enhanced regulation of cytokine production of *Pd1*$^{-/-}$ Tregs involved in immune response. Data shown are Mean±SEM in **E**. Each datapoint represents a single cell in **D** or an independent animal in **E**. Statistical analyses were performed using Wilcoxon rank-sum test with Bonferroni's correction in **A-C**, clustered Wilcoxon rank-sum test in **D**, an unpaired Student's t-test in **E**, Fisher's exact test with FDR correction in **G** and Kolmogorov-Smirnov test with FDR correction in **H**.

4.3.3 Functional validation of scRNA-seq analysis within the TME

We next aimed to validate our scRNA-seq findings on CD30 expression and its functional role in *Pd1*$^{-/-}$ Tregs. First, we tested whether the absence of PD-1 intrinsically enhances CD30 expression in Treg TILs. Using the same *Rag1*$^{-/-}$ B16 melanoma model, we observed a significant increase in CD30 frequency in Tregs, but not in CD45.1^{+} T effector cells within TIL population **(Figure 4.4a-b)**. Next, we sought to determine whether Tregs in *Pd1*$^{fl/fl}$*Foxp3*^{ERT2Cre} mice exhibit a tumour-protective role similar to global *Pd1*$^{-/-}$ Tregs. To test this, we established B16 tumours in control *Pd1*$^{fl/fl}$ mice treated with PBS and *Pd1*$^{fl/fl}$*Foxp3*^{ERT2Cre} mice treated with tamoxifen **(Figure 4.4c)**. Tumour growth was significantly increased in the cohort with PD-1 specifically deficient in Tregs **(Figure 4.4d)**. Consistent with our findings in germline *Pd1*$^{-/-}$ mice, we observed a significant increase in Foxp3^{+} Tregs while Foxp3^{-} Tconv cell frequency remained unchanged **(Figure 4.4e)**. Next, we observed the PD-1 expression on Tregs and Tconv cells. PD-1 expression was significantly reduced in Tregs but not in Tconv cells in *Pd1*$^{fl/fl}$*Foxp3*^{ERT2Cre} mice pre-treated with tamoxifen **(Figure 4.4f-g)**, showing that the enrichment of Tregs in tumours was attributable to the inducible deletion of PD-1 in Tregs. Furthermore, *Pd1*$^{fl/fl}$*Foxp3*^{ERT2Cre} mice exhibited a significant increase in absolute numbers of CD30^{+} Tregs compared to *Pd1*$^{fl/fl}$ control mice **(Figure 4.4h),** whereas no significant differences were observed in the absolute counts of GITR^{+}, CTLA-4^{+}, IFN-γ^{+} and IL-10^{+} Tregs **(Figure 4.4i-l)**. Taken together, these findings suggest that the increased tumour burden was not driven by alterations in the Tconv compartment or Treg cytokine profile but rather by the expansion of CD30^{+} Tregs.

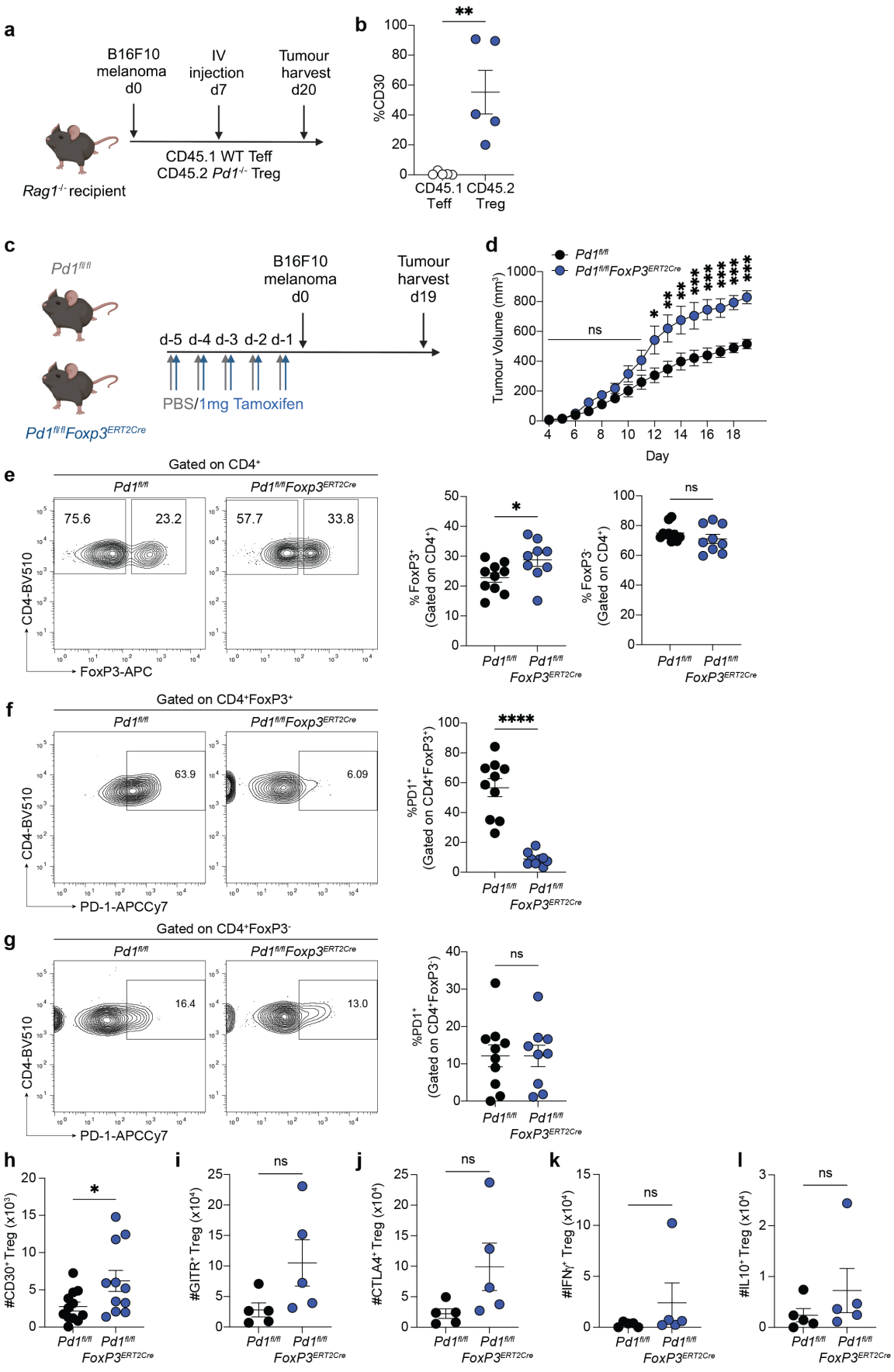

Figure 4.4 CD30-expressing *Pd1*$^{-/-}$ Tregs enhances tumour burden in B16 *in vivo* model.

A, *Rag1*$^{-/-}$ mice were subcutaneously inoculated with B16F10 melanoma cells on d0 and further reconstituted with CD45.1^{+} Teff cells and CD45.2^{+} Tregs sorted from *Pd1*$^{-/-}$ *Foxp3*^{RFP} (*Pd1*$^{-/-}$) mice via IV injection on d7. **B,** Summary of CD30 expression on CD4^{+} Teff cells and Tregs. **C,** *Pd1*$^{fl/fl}$ and *Pd1*$^{fl/fl}$*Foxp3*^{ERT2Cre} pre-administered with PBS and 1mg tamoxifen respectively were subcutaneously injected with B16F10 melanoma cells. **D**, Tumour volume was monitored (n=10 for *Pd1*$^{fl/fl}$ and n=9 for *Pd1*$^{fl/fl}$*Foxp3*^{ERT2Cre}). **E-L,** TILs were harvested for immunophenotyping on d19 by using flow cytometry. **E,** Flow cytometry plots **(left panel)** and quantifications of FoxP3^{+} Treg and FoxP3^{-} Tconv cell frequency **(right panel)**. **F,** Flow cytometry plots **(left panel)** and summary of PD-1 expression on Tregs **(right panel)**. **G,** Flow cytometry plots **(left panel)** and summary of PD-1 expression on Tconv cells **(right panel)**. Absolute counts of **H,** CD30^{+} Tregs, **I,** GITR^{+} Tregs, **J,** CTLA4^{+} Tregs, **K,** IFNγ^{+} Tregs and **L,** IL10^{+} Tregs. Data shown are Mean±SEM, with each datapoint represents an independent experiment in **B, E-L**. Statistical analyses were performed using a paired Student's t-test in **B,** a two-way ANOVA with multiple Sidak's comparison in **D** and an unpaired Student's t-test in **E-L**. *P < 0.05, **P < 0.01, ***P < 0.001, ****P < 0.0001. NS, not significant.

Confident that CD30 expression was specifically enriched in the Treg compartment and enhanced in the absence of PD-1, we used the *Rag1*$^{-/-}$ B16 melanoma model to investigate the functional consequence of CD30 on tumour growth **(Figure 4.5a)**. *Rag1*$^{-/-}$ mice were reconstituted with either WT or *Pd1*$^{-/-}$ CD45.2^{+} Tregs along with WT CD45.1^{+}CD4^{+} T cells, with the *Pd1*$^{-/-}$ CD45.2^{+} Treg cohort receiving either an isotype control or anti-CD30L (anti-CD153) treatment. We found that blocking the CD30 pathway with anti-CD153 significantly inhibited tumour growth in the *Pd1*$^{-/-}$ CD45.2^{+} Treg cohort on day 16, compared to cohort receiving the isotype control **(Figure 4.5b)**. This reduction in tumour growth with anti-CD153 treatment largely reversed the differences in tumour growth observed between mice reconstituted with WT or *Pd1*$^{-/-}$ CD45.2^{+} Tregs. Next, we tested whether anti-CD153 treatment also impacted the pro-tumour function of WT Tregs **(Figure 4.5c)**. Notably, no difference in tumour growth was observed when *Rag1*$^{-/-}$ mice were reconstituted with WT Tregs followed by treatment with either isotype or anti-CD153 **(Figure 4.5d)**. Taken together, these results indicate that the CD30/CD30L pathway specifically regulates PD-1-deficient Treg function while playing a minimal role in WT Tregs. Remarkably, in contrast to previous reports (Gaspal et al., 2011), our immunophenotyping of these mice revealed that anti-CD153 treatment did not deplete the absolute counts of either Tregs or Teff cells across all conditions **(Figure 4.5e-f, i-j)**. Furthermore, no difference was observed in IL-10 production by Tregs or IFN-γ expression in CD4^{+} Teff cells **(Figure 4.5g-h, k-l)**.

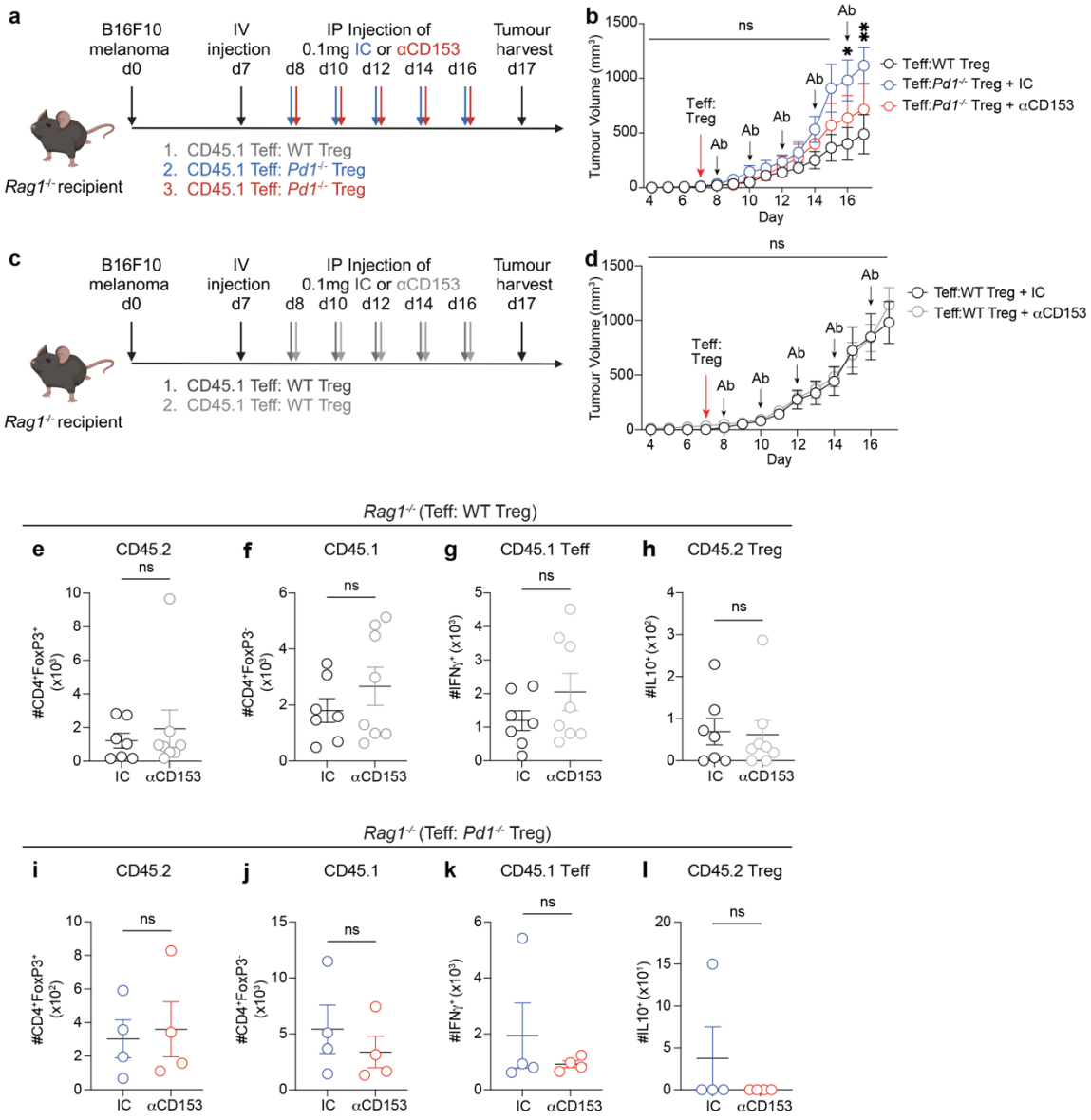

Figure 4.5 Blockade of CD30 in *Pd1*$^{-/-}$ Tregs reduces tumour burden in B16 *in vivo* model.

A, *Rag1*$^{-/-}$ mice were subcutaneously inoculated with B16F10 melanoma cells on d0 and further reconstituted with CD45.1^{+} Teff cells and CD45.2^{+} Tregs sorted from either *Foxp3*^{RFP} (WT) or *Pd1*$^{-/-}$*Foxp3*^{RFP} (*Pd1*$^{-/-}$) mice via IV injection on d7, with or without treatment (n=3 for Teff: WT Treg cohort). Mice reconstituted with *Pd1*$^{-/-}$ Treg were further treated with either 0.1mg anti-IgG2a isotype control (n=8) or anti-CD153 (n=9) via IP injection for 5 dosage at two-day intervals. **B,** Tumour volume was measured. **C,** *Rag1*$^{-/-}$ mice were subcutaneously inoculated with B16F10 melanoma cells on d0 and further reconstituted with CD45.1^{+} Teff cells and CD45.2^{+} Tregs sorted from WT mice via IV injection on d7. Mice were further treated with either 0.1mg anti-IgG2a isotype control (n=7) or anti-CD153 (n=8) via IP injection for 5 dosage at two-day intervals. **D,** Tumour volume was measured. **E-H,** Immunophenotyping of TILs derived from *Rag1*$^{-/-}$ mice reconstituted with WT Tregs, showing the absolute counts of **E,** Treg, **F,** Tconv cells, **G,** IFNγ^{+} Tconv cells and **H,** IL10^{+} Tregs. **I-L,** Immunophenotyping of TILs derived from *Rag1*$^{-/-}$ mice reconstituted with *Pd1*$^{-/-}$ Tregs, showing the absolute counts of **I,** Treg, **J,** Tconv cells, **K,** IFNγ^{+} Tconv cells and **L,** IL10^{+} Tregs. Data shown are Mean±SEM, with each datapoint represents an independent experiment in **E-L**. Statistical analyses were

performed using a two-way ANOVA with multiple Sidak's comparison in **B&D** and an unpaired Student's t-test in **E-L**. *P < 0.05, **P < 0.01, NS, not significant.

4.3.4 Pd1$^{-/-}$ Treg exhibit several differentiation programs and enhanced crosstalk with NK cells within the TME

Next, we performed pseudotime and trajectory analysis on BD Rhapsody scRNA-seq data from murine TILs using the Monocle plugin in SeqGeq™ software. This revealed that, when combined, WT and *Pd1*$^{-/-}$ Tregs exhibited seven distinct differentiation states **(Figure 4.6a-b, Appendix Table D.7)**. In line with observations of Kim *et al.* (Kim et al., 2023), we found that in the absence of PD-1, pseudotime trajectory analysis of Treg TILs from B16 melanoma tumours revealed five differentiation states, compared to three in WT Treg TILs **(Figure 4.6c-d, Appendix Table D.8-9)**. Further analysis of enriched genes in each state showed that WT Tregs differentiated into three differentiation states: a tissue-resident state (state 1), an immunosuppressive phenotype marked by *Tigit* (state 2) and a cytotoxic state (state 3) **(Figure 4.6e)**. In contrast, *Pd1*$^{-/-}$ Tregs exhibited five differentiation states: a type 1 phenotype characterised either by either IFN-γR (CD119) expression (state 1) or STAT1 expression (state 3), a cytotoxic phenotype (state 2), an immune-regulatory phenotype (state 4) and a TNFR-enriched differentiation program (state 5) **(Figure 4.6f)**. PD-1 has been reported to imprint a Treg phenotype and prevent the emergence of a type 1 phenotype in both murine and human Tregs (Amarnath et al., 2011, Stathopoulou et al., 2018). Our unbiased analysis suggests that multiple shifts occur in *Pd1*$^{-/-}$ Tregs, where a subset acquires enhanced suppressor or cytotoxic function, driven by *Tigit, Gzmb, Tnfr* and *Il10* (state 2,4 & 5). Meanwhile, another subset exhibits functional plasticity through type 1-associated receptors and transcription factors (state 1 & 3).

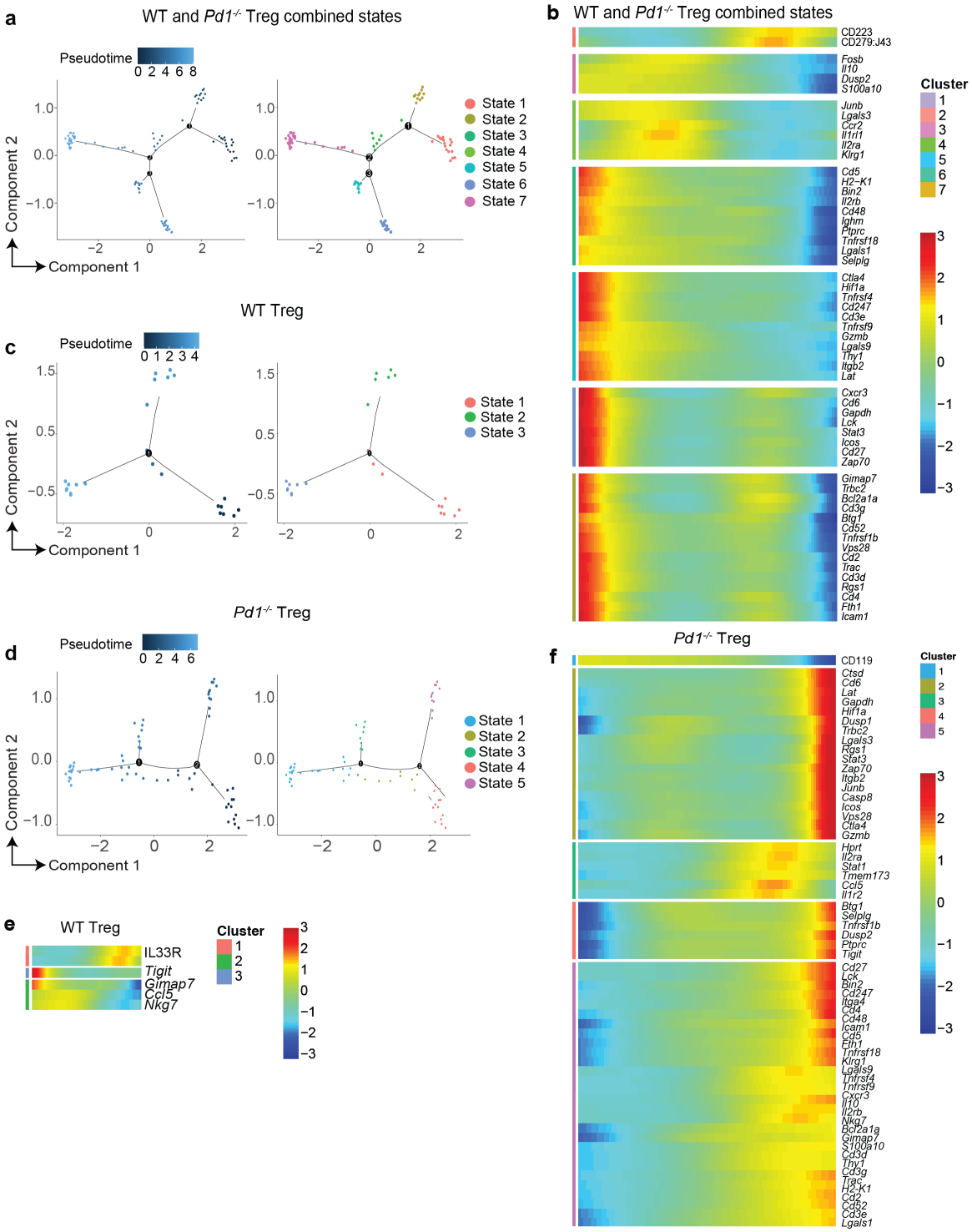

Figure 4.6 Pseudotime trajectory analysis of WT and *Pd1*$^{-/-}$ Tregs in murine B16 TME. BD Rhapsody scRNA-seq data of **A,** merged WT and *Pd1*$^{-/-}$ Tregs or **C&D,** separately were analysed using pseudotime trajectory inference to examine the dynamic progression of Tregs in the TME. Cells are coloured by pseudotime **(left panel)** and cell state **(right panel)**, illustrating the transition of Tregs along the inferred differentiation trajectory. Distinct states along the trajectory indicate potential functional heterogeneity, with key branch points suggesting divergent regulatory programs. **B&E-F,** Heatmaps illustrating gene expression dynamics along the pseudotime trajectory, highlighting key transcriptional

changes associated with differentiation and functional specialisation of **B,** merged WT and *Pd1*$^{-/-}$ Tregs or **E-F,** separately. Data shown are from n=5 WT and n=5 *Pd1*$^{-/-}$ mice.

Using CellChat analysis of scRNA-seq data, we examined the communication program of Tregs within the TME. Cell-cell communication is mediated through ligand-receptor interactions, where a ligand expressed by one cell binds to a receptor on a target cell, triggering downstream signalling **(Figure 4.7a)**. Incoming signalling refers to signals received by Tregs through their surface receptors from other immune cells, while outgoing signalling represents ligands expressed by Tregs that interact with receptors on other immune cells. In WT Tregs, we identified a single incoming signalling pattern predominantly mediated by the ligand CD86 (binding to CTLA-4) and PD-L1 (binding to PD-1) **(Figure 4.7b)**. In contrast, *Pd1*$^{-/-}$ Tregs exhibited dual incoming signalling patterns, primarily driven by CD86 and TNF (binding to TNF receptors) respectively **(Figure 4.7c)**. To further explore immune cell interactions within TILs, we analysed outgoing signalling patterns and found no significant differences between WT and *Pd1*$^{-/-}$ cells **(Figure 4.7e)**. However, *Pd1*$^{-/-}$ NK cells contributed less to outgoing signalling while maintaining comparable levels of incoming signalling **(Figure 4.7d)**.

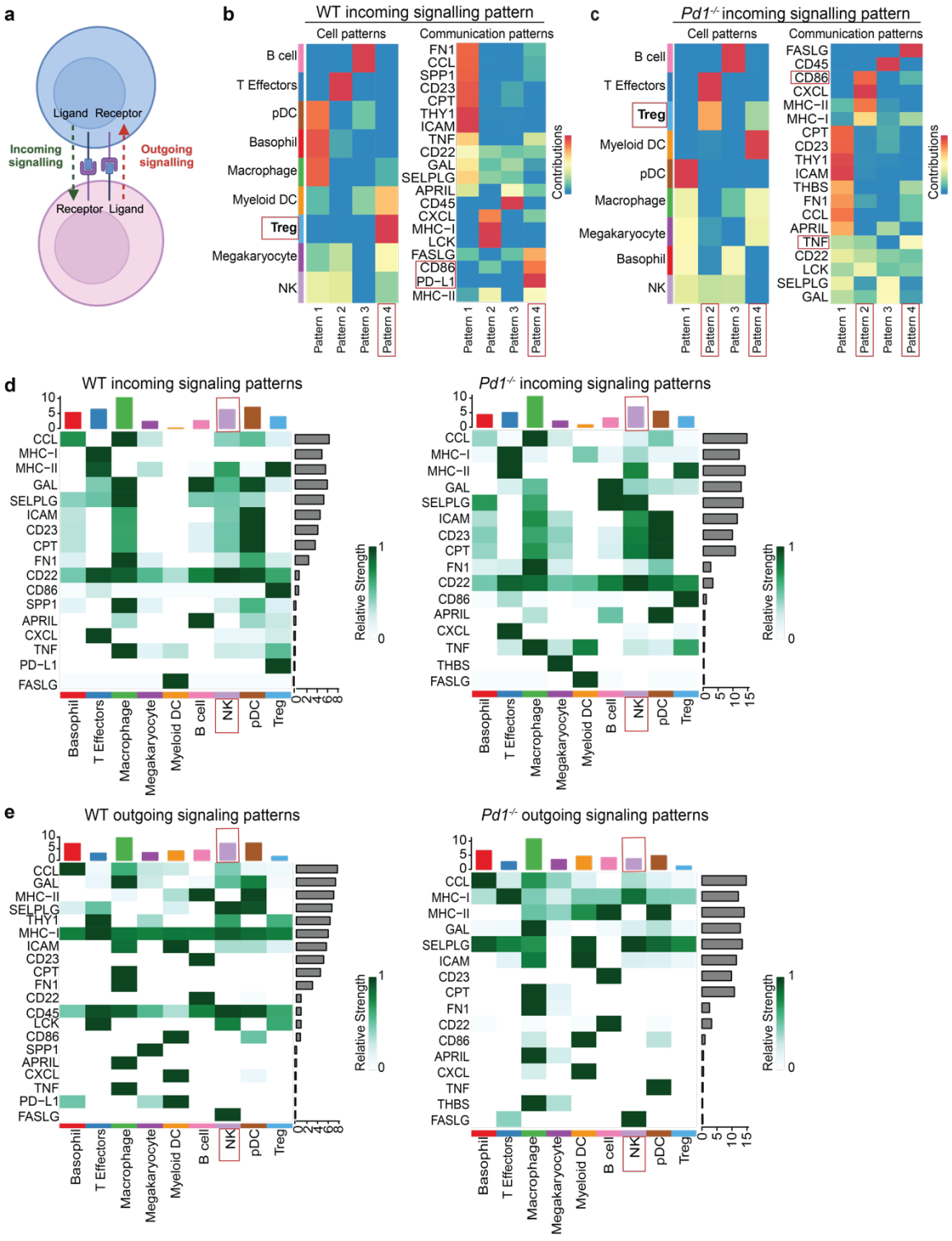

Figure 4.7 CellChat analysis reveals the communication network in WT and *Pd1*$^{-/-}$ TILs within the murine B16 TME.

A, Schematic diagram illustrating the CellChat analysis framework for evaluating cell-cell interactions through receptor-ligand pairs. **B-C,** Heatmap showing cell communication patterns and receiving signalling patterns in WT and *Pd1*$^{-/-}$ TILs. **D**, Incoming signalling patterns in WT and *Pd1*$^{-/-}$ TILs. **E**, Outgoing signalling patterns in WT and *Pd1*$^{-/-}$ TILs, with NK cell signalling patterns highlighted by a red box. CellChat models the communication probability based on the law of mass action and identifies significant communications using permutation tests. Data shown are from n=5 WT and n=5 *Pd1*$^{-/-}$ mice.

Next, we assessed Treg crosstalk with other immune cells in the TME. *Pd1*$^{-/-}$ Tregs were highly interacting with NK cells and myeloid DCs compared to WT Tregs **(Figure 4.8a)**. Notably, this enhanced Treg-NK cell interaction was associated with diminished NK cell communication with T effectors **(Figure 4.8b)**, whereas myeloid DC communication remained unchanged **(Figure 4.8c)**. This predictive analysis suggests that *Pd1*$^{-/-}$ Tregs may influence NK cell interaction with T effectors within the TME, though experimental validation is required and remains beyond the scope of this study.

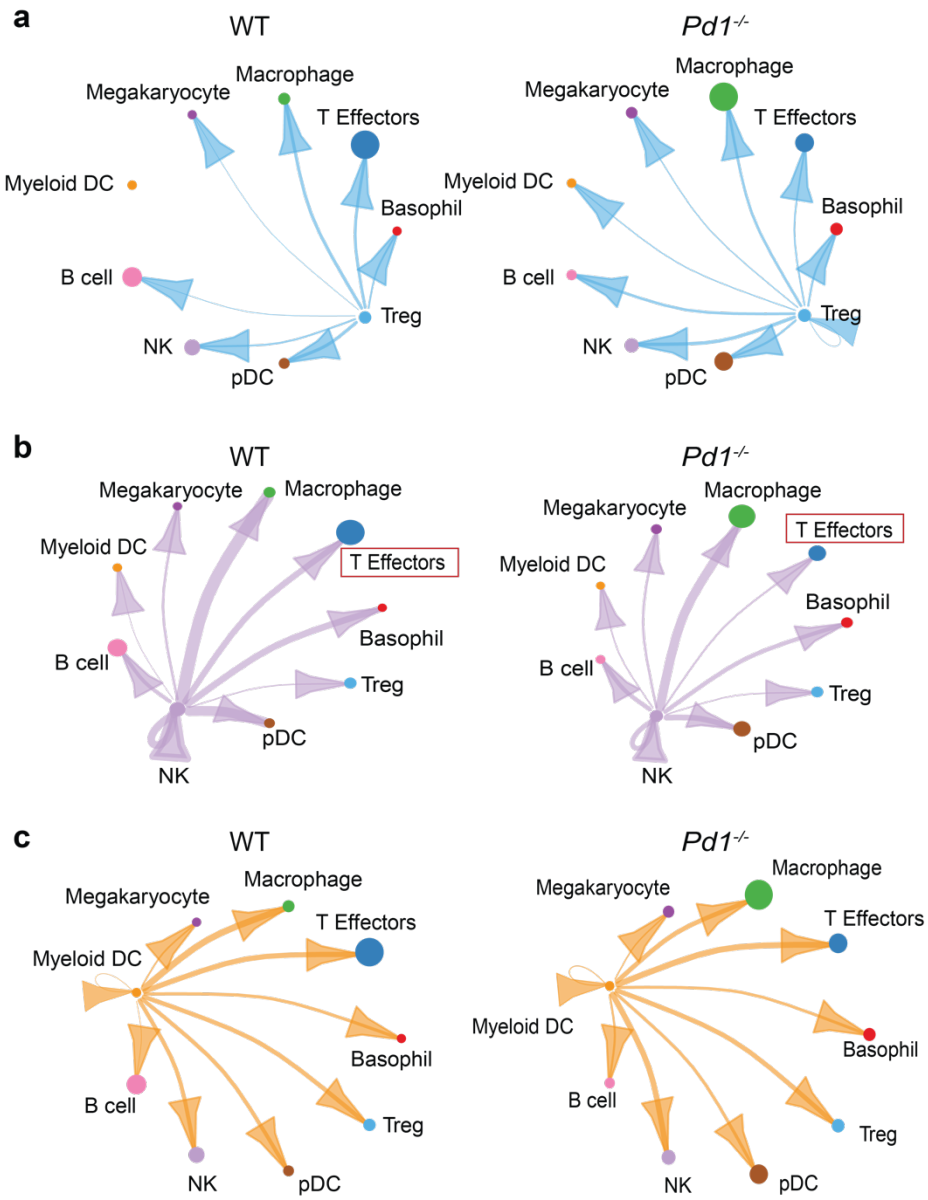

Figure 4.8 CellChat analysis reveals the communication network of Tregs, NK cells and myeloid DCs with other TILs in the murine B16 TME.
Circle plots visualise the interactions of **A,** Tregs (blue), **B,** NK cells (purple) and **C,** myeloid DCs (orange) with other TILs in WT and *Pd1*$^{-/-}$ cohort. The edge width represents the strength of interactions., while edge colours correspond to sending cell population. Data represent n=5 WT and n=5 *Pd1*$^{-/-}$ mice.

Collectively, our data suggest that *Pd1*$^{-/-}$ Tregs exhibit multiple differentiation programs within the TME. Specifically, *Tnfrsf, Il10 and Tigit* expression marks regulatory Treg subsets, whereas other states align with a type 1 Treg phenotype. However, it is important to note that the CellChat analysis provides only predictive insights into Treg, NK cell and DC interactions.

4.3.5 Functional validation of CellChat analysis within the TME

To validate our pseudotime differentiation states predicted using Monocle and the CellChat communication analysis, we assessed Tregs in *Pd1*$^{fl/fl}$*Foxp3*^{ERT2Cre} mice following tamoxifen treatment and tumour reconstitution **(Figure 4.9a)**, characterising them via flow cytometry. To further examine Treg heterogeneity, we subcategorised Tregs based on our pseudotime trajectory analysis. In WT TILs, we identified three distinct Treg sub-states, whereas PD-1-deficient TILs exhibited five different Treg sub-states **(Figure 4.9b-c)**. Of note, the frequency of type 1 Tregs (state 1 and 3) was significantly reduced in PD-1-deficient TILs in this experimental setting. Next, we tested whether PD-1 deficiency in Tregs influenced NK and DC populations within TILs, as predicted by our CellChat analysis. Indeed, we observed a significant reduction in NK and DC frequencies within the TILs **(Figure 4.9d-e)**. However, no changes were detected in other functional markers **(Figure 4.9f-l)**. Taken together, these findings validate our predictive analyses, demonstrating that PD-1-deficient Tregs impact NK and DC subset frequencies within the TILs.

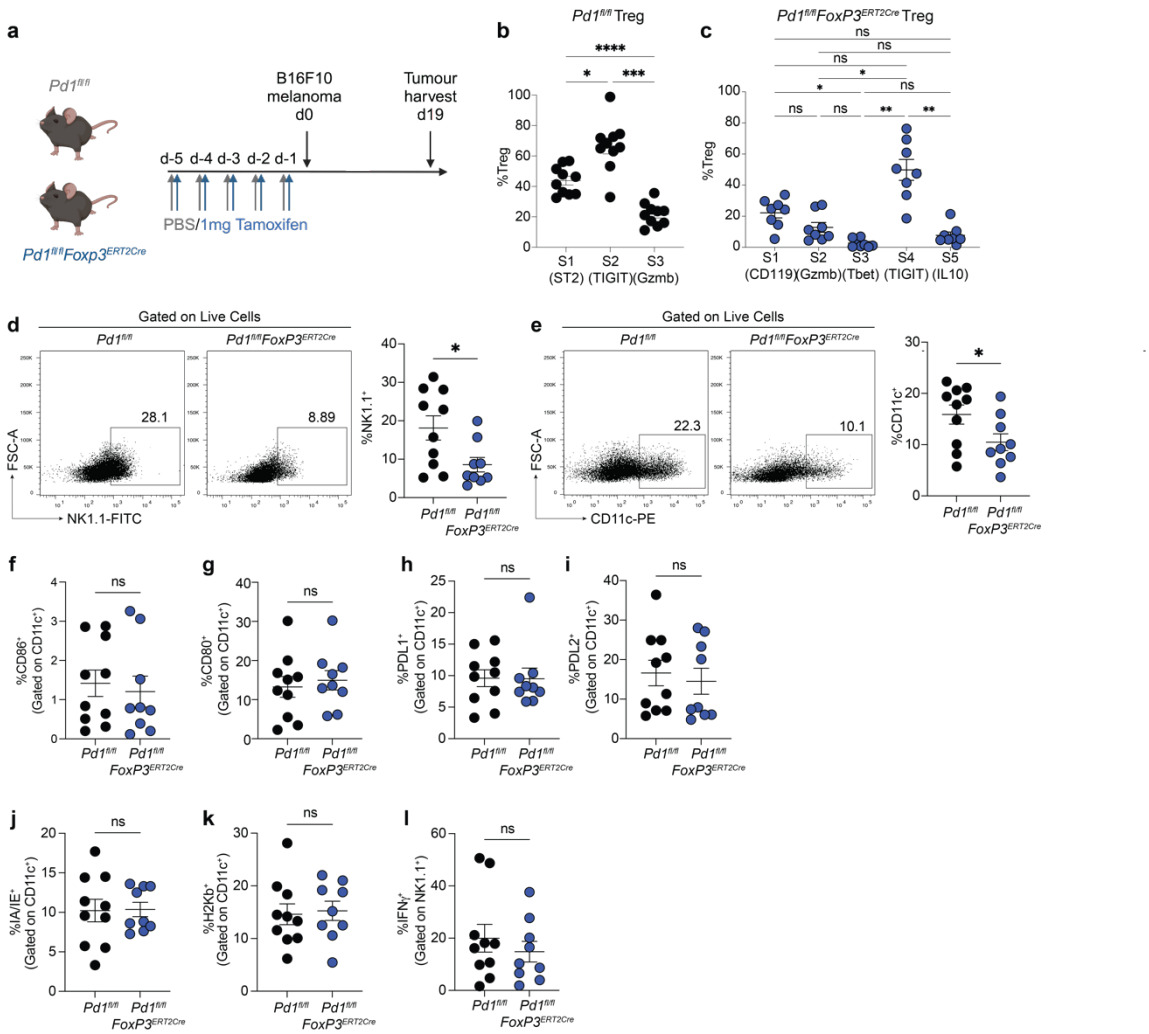

Figure 4.9 *Pd1*$^{-/-}$ Tregs exhibit multiple differentiation states and are associated with altered NK cell and DC frequencies.

A, *Pd1*$^{fl/fl}$ and *Pd1*$^{fl/fl}$*Foxp3*^{ERT2Cre} pre-administered with PBS or 1mg tamoxifen were subcutaneously injected with B16F10 melanoma cells. Tumour immunophenotyping was performed on day 19. **B,** Differentiation states of WT Tregs in *Pd1*$^{fl/fl}$ mice, characterised by ST2, TIGIT and GzmB expression. **C,** Differentiation states of *Pd1*$^{-/-}$ Tregs in *Pd1*$^{fl/fl}$*Foxp3*^{ERT2Cre}, characterised by IFNγR (CD119), GzmB, Tbet, TIGIT and IL10 expression. **D-E,** Flow cytometry plots and summary of **D,** NK cell and **E,** DC frequencies. **F-K,** Frequency of CD86, CD80, PDL1, PDL2, MHC class II (IA/IE) and MHC class I (H2Kb) expression in CD11c^{+} DCs. **L,** IFNγ expression in NK1.1^{+} cells. Data shown are Mean±SEM, with data points within each group are matched to the same individual mouse in **B-C**, while each data point represents an individual mouse in **D-L**. Statistical analyses were performed using a matched one-way ANOVA using a Sidak's multiple comparison test in **B-C** and an unpaired Student's t-test in **D-L**. *P < 0.05, **P < 0.01, ***P < 0.001, ****P < 0.0001, NS, not significant.

4.3.6 Spatial transcriptomics confirm Pd1$^{-/-}$ *Treg differentiation states and communication network within the TME*

To determine whether the predictive pseudotime trajectory analysis and CellChat communication networks of Treg subsets could be visualised within the TME, we

performed CosMx™ spatial transcriptomics with 1000 plex mouse panel. *Rag1*$^{-/-}$ mice were injected with B16 melanoma cells and reconstituted with either WT or *Pd1*$^{-/-}$ CD45.2^{+} Tregs, along with WT CD45.1^{+} naive CD4^{+} T cells **(Figure 4.10a)**. H&E staining of tumour sections from both groups was evaluated and identical tissues were selected for CosMx™ analysis **(Figure 4.10b)**. Fields of view (FOVs) enriched for immune infiltration and surrounding tumour tissue were chosen for further analysis. Single-cell segmentation and immune cell profiling enabled precise identification of individual cells and their corresponding cell types within the tissue. Immune cell profiling was performed using Louvain clustering analysis, integrating RNA transcript data across all FOVs to improve resolution **(Figure 4.10c, Appendix Table C.1)**. The frequency of identified cell clusters was shown **(Figure 4.10d)**. This approach allowed us to subdivide and classify the 'Immune cells' cluster based on specific immune cell markers **(Figure 4.10e-f)**, which were subsequently mapped to individual cells within the tissue **(Figure 4.10g)**.

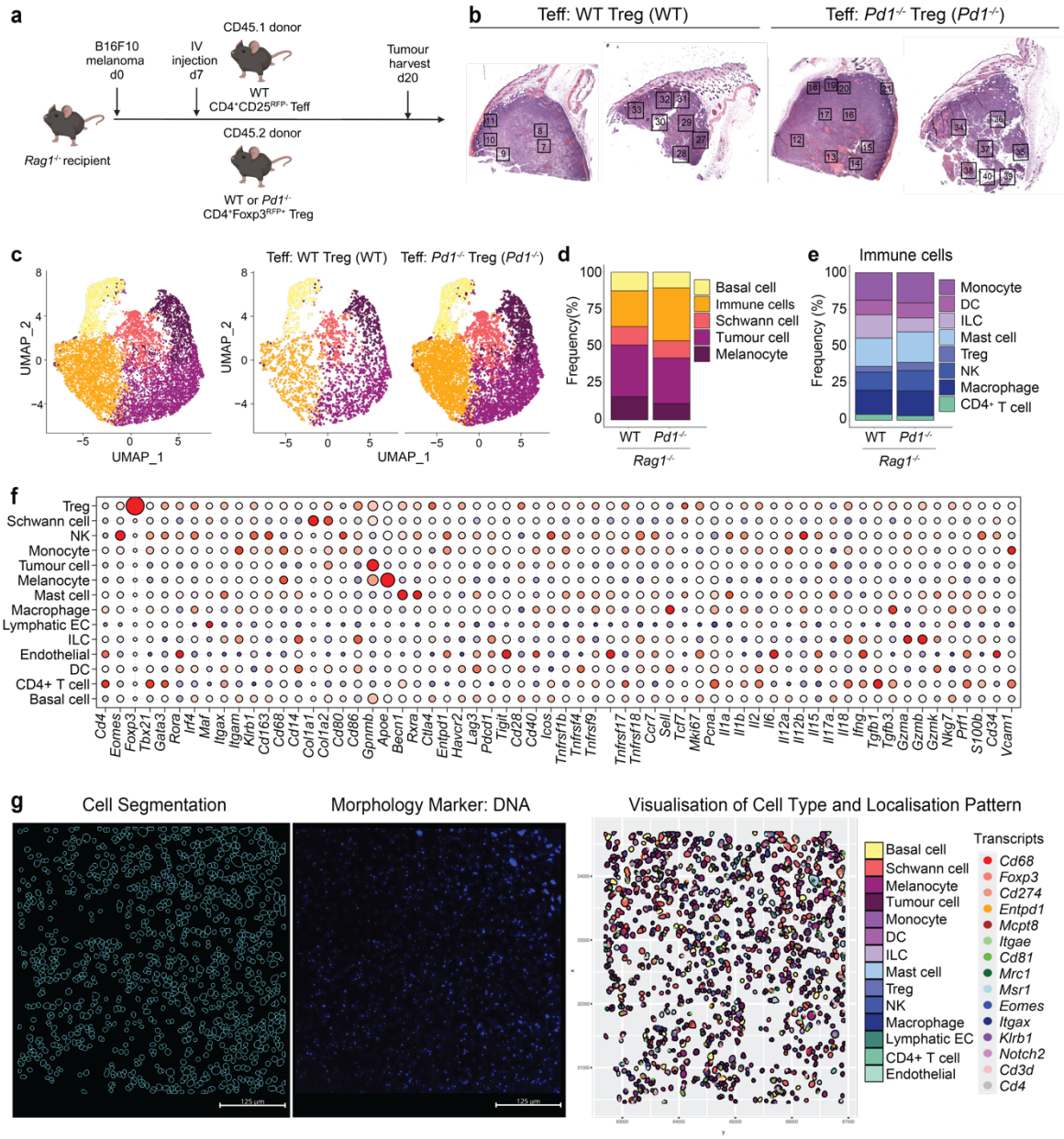

Figure 4.10 CosMx™ spatial transcriptomics visualise cell-cell interaction within the B16 TME.

A, *Rag1*$^{-/-}$ mice were subcutaneously inoculated with B16F10 melanoma cells on d0 and further reconstituted with CD45.1^{+} Teff cells and CD45.2^{+} Tregs sorted from either *Foxp3*^{RFP} (WT, n=2) or *Pd1*$^{-/-}$*Foxp3*^{RFP} (*Pd1*$^{-/-}$, n=2) mice via IV injection on d7. Tumours were harvested for CosMx spatial transcriptomics analysis on d20. **B,** H&E stain of FFPE punch biopsies derived from *Rag1*$^{-/-}$ mice reconstituted with WT Teff: WT Treg (**left panel**) and WT Teff: *Pd1*$^{-/-}$ Treg (**right panel**), with field of views (FOVs) annotated. **C,** A uniform manifold approximation and projection (UMAP) view of 9,231 heterogenous cells derived from WT Teff: WT Treg and WT Teff: *Pd1*$^{-/-}$ Treg cohorts, colour-coded by assigned cell type (**left panel**). WT and *Pd1*$^{-/-}$ Treg cohorts were decoupled to assess homogeneity in cell clusters (**middle and right panel**). **D**, Frequency of tissue-derived cells, tumour-derived cells and immune cells within each cluster. **E,** Subclustering of immune cells, showing the frequency of immune cell subsets between WT and *Pd1*$^{-/-}$ Treg cohorts. **F**, Dot plot showing identification markers of all the clusters. **G,** Representative

FOV showing cell segmentation (**left panel**), DNA staining **(middle panel)** and cell identities with transcripts overlays (**right panel**).

Next, we performed pathway analysis and found that leukocyte migration pathways were upregulated in *Pd1*$^{-/-}$ Tregs compared with WT Tregs **(Figure 4.11a)**. The CosMx™ dataset was then used for descriptive spatial analyses to examine Treg interactions with other cells in the TME. Treg cell IDs and spatial coordinates were extracted from the FOV object in RStudio **(Appendix Table C.2)**. Each Treg interaction with neighbouring cells was recorded as an event, and these interactions were manually annotated and classified as single, dual or multiple interactive events **(Figure 4.11b)**. We found that *Pd1*$^{-/-}$ Tregs were more interactive than WT Tregs. To systematically analyse Treg interactions with tumour and immune cells, we categorised Tregs based on their interactions within the FOV. This was done by identifying Tregs interacting with specific neighbouring cell types **(Appendix Table C.3)**, grouping Tregs by unique Cell IDs based on their interactions with a given cell type, performing DGE analysis to determine enriched transcripts within each group **(Appendix Table C.4-5)**, identifying short-range (SR) and long-range (LR) communication signals in Tregs. In line with our CellChat analysis, we found that Tregs exhibited SR communication signals (ligand-receptor interactions) with CD4^{+} T effector cells, NK cells, DCs and macrophages, as well as with tissue-resident cells within the TME **(Figure 4.11c)**. However, it is important to note that these are descriptive analyses through manual annotation that suggest a possible interaction with other immune cells rather than definitive functional relationship. Similar to our CellChat findings, we observed potential interactions between Tregs, NK cells and DCs, mediated through SR or LR communication signals. Next, we analysed the mRNA of DCs and NK cells for functional changes. Here, although a slight increase in *Il10* was noted in the DCs and a slight increase in *Gzmb* was noted in NK cells **(Figure 4.11d-e)**, on validating these outputs in the murine tumour model using *Pd1* $^{fl/fl}$ and *Pd1*$^{fl/fl}$*FoxP3*^{ERT2Cre} mice, we did not see any difference in IL-10 expression in DCs or GzmB expression in NK cells within the TME **(Figure 4.11f-g)**. Hence, we conclude that *Pd1*$^{-/-}$ Tregs can decrease the frequency of NK and DCs within the TME but do not change IL-10 or GzmB protein expression.

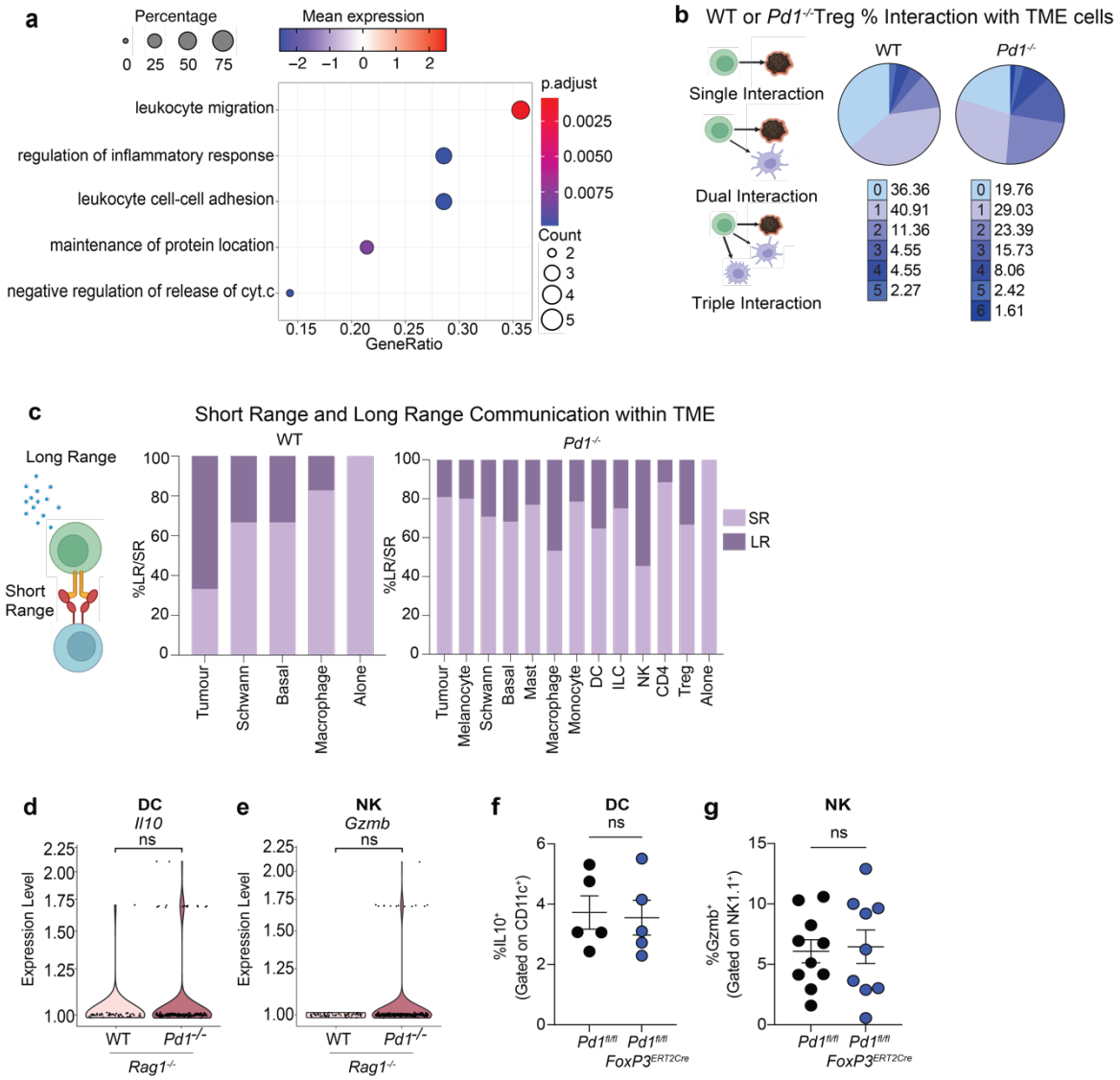

Figure 4.11 CosMx™ spatial transcriptomics analysis reveals interaction network of Tregs within the B16 TME.

Rag1$^{-/-}$ mice were subcutaneously inoculated with B16F10 melanoma cells on d0 and further reconstituted with CD45.1^{+} Teff cells and CD45.2^{+} Tregs sorted from either *Foxp3*^{RFP} (WT, n=2) or *Pd1*$^{-/-}$*Foxp3*^{RFP} (*Pd1*$^{-/-}$, n=2) mice via IV injection on d7. Tumours were harvested for CosMx spatial transcriptomics analysis on d20. **A,** Gene ontology (GO) analysis of *Pd1*$^{-/-}$ Tregs. **B,** Graphical representation of analysis of cell-cell interactions (**left panel**), number of interactions involving WT Tregs (**middle panel**) or *Pd1*$^{-/-}$ Tregs (**right panel**) with other cells in the TME. **C,** Graphical representation of definition of SR and LR genes (**left panel**), and frequency of LR/SR interactions of either WT Tregs (**middle panel**) or *Pd1*$^{-/-}$ Tregs (**right panel**) with other cells in the TME. **D-E**, Single-cell gene expression of *Il10* in DCs and *Gzmb* in NK cells. **F-G,** *Pd1*$^{fl/fl}$ and *Pd1*$^{fl/fl}$*Foxp3*^{ERT2Cre} pre-administered with PBS or 1mg tamoxifen were subcutaneously injected with B16F10 melanoma cells. Tumor immunophenotyping was performed on day 19. **F-G**, Frequency of IL-10 expression within DCs and GzmB expression in NK cells. Data shown are Mean±SEM, with each data point represents a single cell in **D-E**, while each data point represents an individual mouse in **F-G**. Statistical analyses were performed using a clustered Wilcoxon rank-sum test in **D-E** and an unpaired Student's t-test in **F-G**. NS, not significant.

We next aimed to confirm the role of CD30/CD30L in the TME. Since our CosMx^{TM} panel did not include *Tnfrsf8* (CD30), we investigated which cell types within the TME predominantly communicated with Tregs via *Tnfsf8* (CD30L), as CD30 is the exclusive receptor for CD30L. We observed ubiquitous CD30L expression in tissue-resident cells, tumour cells and immune cells in the cohort treated with WT or *Pd1*$^{-/-}$ Treg **(Figure 4.12a)**. Next, we visualised CD30L-expressing cells in contact with Tregs across all the FOVs. The frequency of each cell type was visualised and we identified potential interactions of all cells with Tregs via CD30L within the TME **(Figure 4.12b)**. We next sought to visualise and validate our pseudotime trajectory analysis within the TME, which revealed three distinct subsets of Tregs in the WT Treg-treated cohorts and five subsets in the *Pd1*$^{-/-}$ Treg-treated cohorts **(Figure 4.12c)**. Taken together, the descriptive analysis of CosMx™ data highlighted the presence of CD30L in all cells within the TME and identified different Treg subsets in both WT and *Pd1*$^{-/-}$ cohorts. To further validate which *Pd1*$^{-/-}$ Treg subsets are primarily involved in the CD30/CD30L pathway, we assessed CD30 expression within Treg subsets in a murine B16 melanoma model using tamoxifen-treated *Pd1*$^{fl/fl}$*Fox*p3^{ERT2Cre} mice. We observed CD30 expression in both regulatory and cytotoxic Treg subsets **(Figure 4.12d-e)**. These validation studies suggest that CD30 is expressed predominantly in the regulatory subsets within the *Pd1*$^{-/-}$ Treg population in the TME and that blocking the CD30/CD30L interaction may unleash a regulatory axis within the TME.

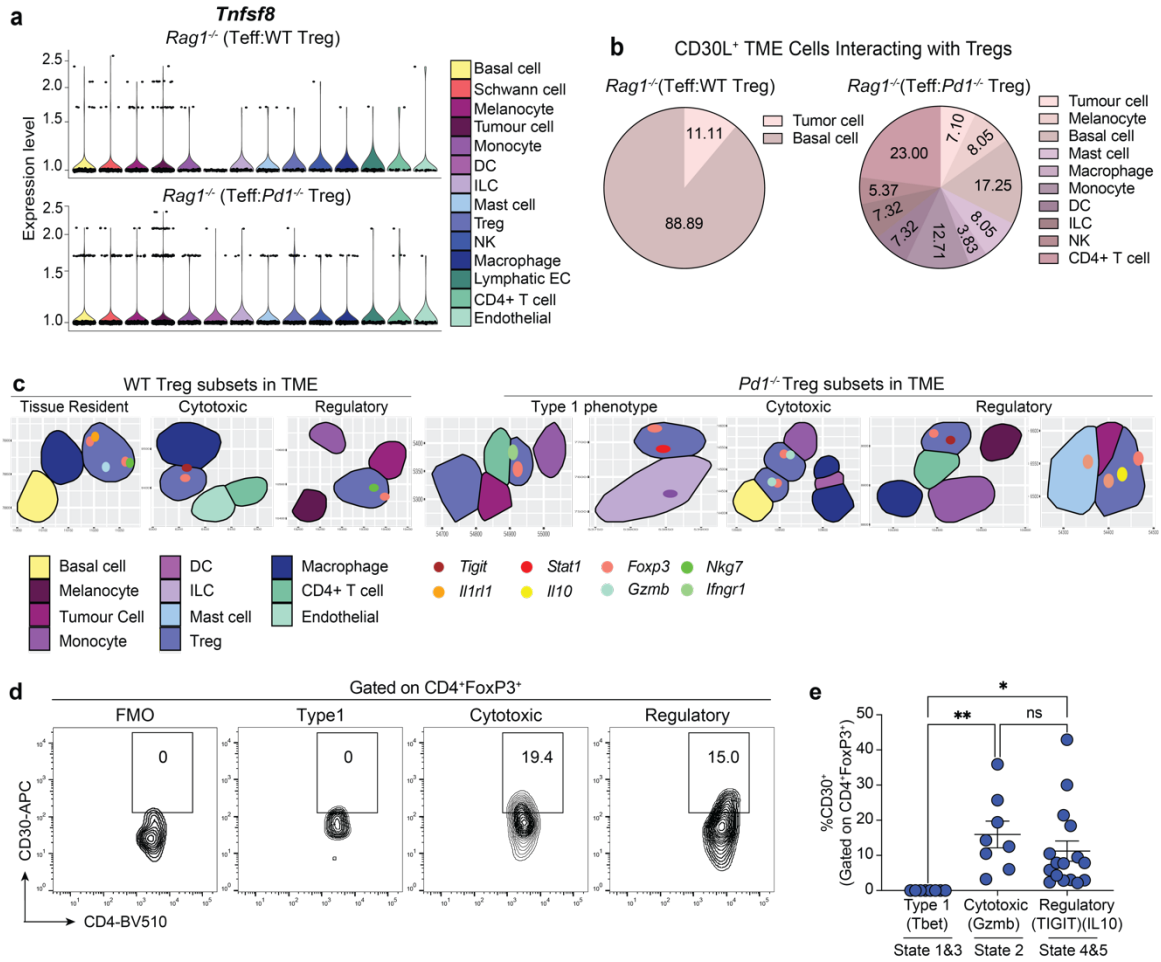

Figure 4.12 CosMx™ spatial transcriptomics analysis reveals CD30L expression in TME cells and identifies Treg sub-states within the B16 TME.

Rag1$^{-/-}$ mice were subcutaneously inoculated with B16F10 melanoma cells on d0 and further reconstituted with CD45.1^{+} Teff cells and CD45.2^{+} Tregs sorted from either *Foxp3*^{RFP} (WT, n=2) or *Pd1*$^{-/-}$*Foxp3*^{RFP} (*Pd1*$^{-/-}$, n=2) mice via IV injection on d7. Tumours were harvested for CosMx spatial transcriptomics analysis on d20. **A,** Expression of *Tnfsf8* within the TME in *Rag1*$^{-/-}$ mice reconstituted with either WT **(top panel)** or *Pd1*$^{-/-}$ Tregs **(bottom panel)** with CD4^{+} T eff cells. **B,** Pie chart showing frequency of *Tnfsf8*$^{+}$ TME cells interacting with WT or *Pd1*$^{-/-}$ Tregs. **C,** Field of views (FOVs) of colocalization of different WT and *Pd1*$^{-/-}$ Treg states interacting with distinct cell types in the TME. **D-E,** *Pd1*$^{fl/fl}$*Foxp3*^{ERT2Cre} pre-administered with 1mg tamoxifen were subcutaneously injected with B16F10 melanoma cells. Tumour immunophenotyping was performed on d19. Representative flow cytometry plots and summary of CD30 expression in various *Pd1*$^{-/-}$ Treg subsets within the TME. Data shown represent individual cells in **A** and individual mice in **E**. Statistical analyses was performed using clustered Wilcoxon rank-sum test with FDR correction in **A** and a one-way ANOVA using Sidak's multiple comparison test was performed in **E**.

4.3.7 PD-1 disruption, not the tumour microenvironment, drives CD30 expression in human Tregs

We next examined whether CD30 expression was conserved in human Tregs and whether the TME or anti-PD-1 treatment drove CD30 expression in human melanoma Tregs. For this analysis, in-house BD Rhapsody scRNA-seq of peripheral blood mononuclear cells (PBMCs) from Stage IV human melanoma patients and healthy controls (HC) was performed by Ms. Tegan McTaggart, using a panel of 30 AbSeq antibodies and a human immune response gene panel **(Figure 4.13a)**. We also used a publicly available scRNA-seq dataset on melanoma TILs to validate this finding in naïve melanoma TILs. Immune cell clusters in PBMCs from HC and melanoma patients were defined based on AbSeq protein expression and the top 5 gene transcripts enriched in each cluster **(Figure 4.13b-f, Table 2.6, Appendix Table D.2-3)**. The frequency of each immune cell cluster was assessed for each individual **(Figure 4.13c)**.

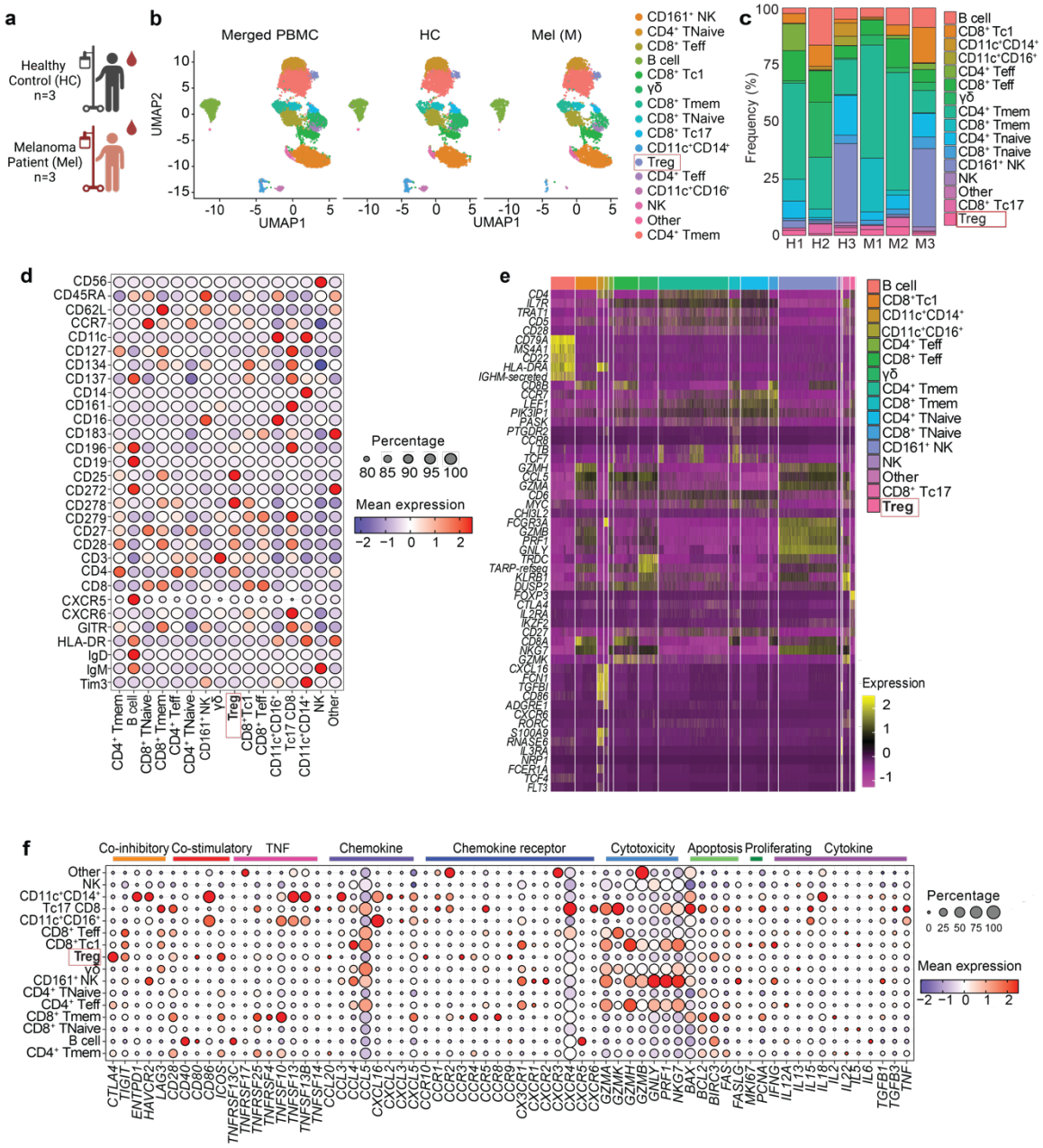

Figure 4.13 BD Rhapsody scRNA-seq reveals cell cluster gene expression in human PBMCs from healthy controls and melanoma patients.

A, PBMCs from healthy controls (HC, n=3) and stage IV melanoma patients (Mel, n=3) were subjected to BD Rhapsody single-cell analysis. Each individual patient sample was tagged with a unique identifier. **B,** A uniform manifold approximation and projection (UMAP) view of 11,634 cells, coloured by cell type **(left panel)**. UMAPs of HC **(middle panel)** and Mel **(right panel)** PBMCs showing cluster homogeneity between the two cohorts. **C,** Frequency of each cell cluster within individual samples. **D,** AbSeq protein expression for each cell type, with dot size and colour representing the percentage of protein expression and the averaged scaled expression value, respectively. **E,** Unbiased transcript analysis showing a heatmap of the top 5 enriched gene transcripts per cell type. **F**, Dot plot showing expression of candidate marker genes across all immune clusters. Statistical analysis was performed using the Wilcoxon rank-sum test with Bonferroni's correction in **E.**

Additionally, the publicly available dataset on naïve melanoma TILs was analysed using gene expression data **(Figure 4.14a)**. Immune cell profiling was performed based on the significantly enriched genes in each cluster, with Tregs annotated by the expression of *CD4* and *FOXP3* **(Figure 4.14b-d, Appendix Table D.4)**. The frequency of each immune cell cluster was also assessed for each individual in this dataset **(Figure 4.14e)**. We next evaluated CD30 expression in Tregs from HC PBMC, melanoma PBMC (Mel) and melanoma TILs at both the single-cell and bulk level. At the single-cell level, we found that CD30 mRNA expression, along with other co-receptors, was not significantly altered in Tregs from either TILs or PBMCs **(Figure 4.14f)**. However, at the bulk level, which refers to mean mRNA expression per individual, *TIGIT* expression was significantly elevated in melanoma TILs, suggesting that TIGIT is regulated by the TME **(Figure 4.14g)**. We were unable to assess GITR expression in this dataset because the PBMC scRNA-seq included the GITR Abseq, while the publicly available dataset did not contain AbSeq or CiteSeq antibodies, preventing a direct comparison. However, overall, this analysis suggests that the TME alone does not drive enhanced CD30 expression in Tregs within PBMCs or TILs in melanoma.

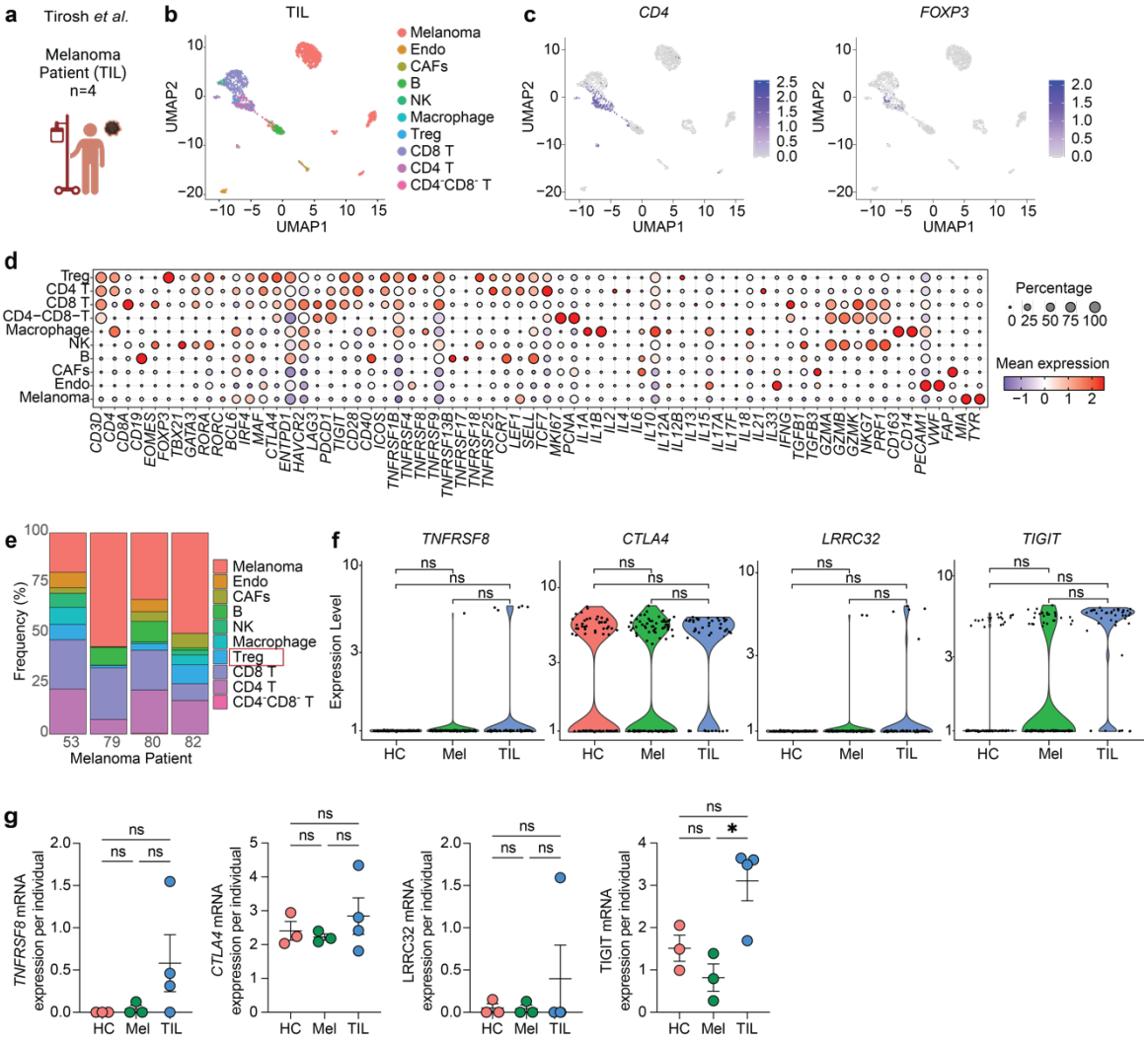

Figure 4.14 ScRNA-seq reveals cell cluster gene expression in human TILs from treatment naive melanoma patients.
A, CD45^{+} and CD45^{-} tumours from treatment naive melanoma patient dataset (TIL, n=4) was publicly mined and analysed using RStudio. **B,** A uniform manifold approximation and projection (UMAP) view of 1,603 cells, coloured by cell type. **C,** A UMAP view of *CD4* and *FOXP3* expression. **D,** Dot plot showing expression of candidate marker genes across all immune clusters. **E,** Frequency of each cell cluster within individual patients. **F-G**, mRNA expression of transcripts *TNFRSF8* (CD30), *CTLA4, LRRC32* (GARP), *TNFRSF18* (GITR) and *TIGIT* within HC, Mel and TIL at **F,** single-cell and **G,** bulk level. Data shown are Mean±SEM in **G**. Each datapoint represents a single cell in **F** or an individual patient in **G**. Statistical analyses were performed using the clustered Wilcoxon rank-sum test corrected with FDR correction in **F** and a one-way ANOVA using Sidak's multiple comparison test in **G.**

We next tested the effect of blocking the PD-1 pathway on CD30 expression in Tregs. For this, we performed *in-vitro* cultures of PBMCs from three Stage IV human melanoma patients. The cells were stimulated with 0.5µg/mL anti-CD3 in the presence of either 20µg/mL isotype control IgG2b or anti-PD-L1 for 72 h **(Figure 4.15a)**. We found that culturing Tregs in the presence of anti-PD-L1 upregulated CD30 in all three human

melanoma patients, further suggesting that it is not the TME, but rather anti-PD-1, that drives CD30 expression in tumour Tregs **(Figure 4.15b)**. This phenomenon has been independently confirmed by other groups and a Phase II clinical trial investigating the use of anti-CD30 in PD-1 resistant melanoma patients is currently ongoing [NCT04609566].

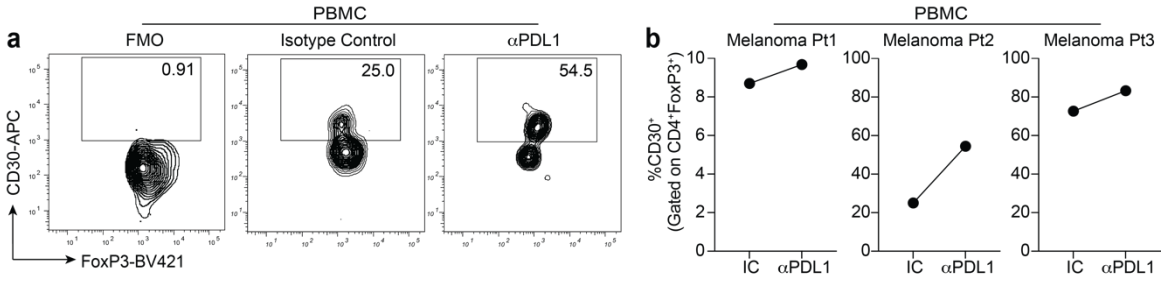

Figure 4.15 Blockade of PD-1 signalling enhances CD30 expression in Tregs from melanoma patients *in vitro*.
PBMCs from melanoma patients (Mel, n=3) were cultured for 72 h with an isotype control or anti-PDL1 antibody to block PD-1/PDL1 interactions. **A,** Representative flow plots showing CD30 expression in Tregs treated with either isotype control or anti-PDL1. **B,** Summary of CD30 expression in Tregs from individual patients under both conditions.

We next analysed a public dataset to assess CD30 expression in Tregs from a cohort of anti-PD-1 treated melanoma patients **(Figure 4.16a)**. First, we performed Louvian clustering analysis, classified the cell clusters and assessed the frequency of each cell cluster for each individual **(Figure 4.16b-e, Appendix Table D.5)**. After confirming the presence of Tregs based on the expression of *CD4* and *FOXP3* in the patient samples **(Figure 4.16c)**, we conducted two types of analysis. In the first analysis, we examined CD30 expression alongside other co-receptors in patient samples, both at baseline and after anti-PD-1 therapy. When individual patient data were analysed separately (rather than pooled), we observed that *Tnfrsf8* (CD30) mRNA expression was significantly increased post-therapy, with no changes observed in *CTLA4*, *LRRC32* (GARP), *TNFRSF18* (GITR) and *TIGIT* **(Figure 4.16f)**. The significant difference in CD30 was consistent in single-cell analysis, with no differences noted in other coreceptors **(Figure 4.16g)**. In the second analysis, we compared CD30 expression in Tregs from responders and non-responders to anti-PD-1 therapy. We found that CD30 mRNA was predominantly expressed in Tregs in the non-responder cohort and no significance was noted with other co-inhibitory receptors **(Figure 4.16h)**. It is important to note that this analysis was based on a small population and requires validation in a larger cohort.

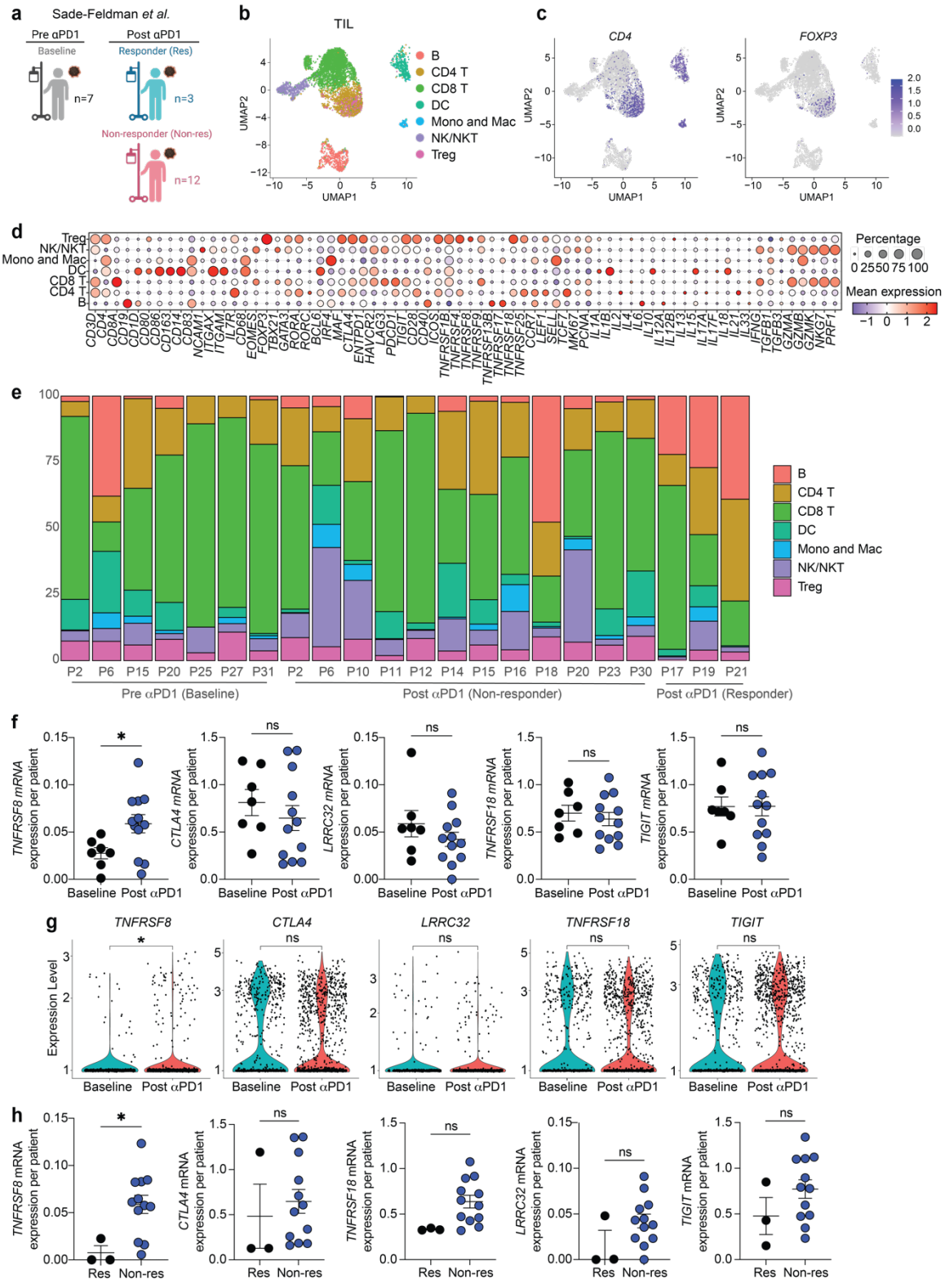

Figure 4.16 ScRNA-seq reveals cell cluster gene expression in human TILs from baseline and anti-PD-1 treated melanoma patients.

A, A publicly available dataset of TILs from melanoma patients at baseline (n=7) or post anti-PD-1 therapy (n=12 non-responders, n=3 responders) was publicly mined and analysed using RStudio. **B,** A uniform manifold approximation and projection (UMAP) view of 7,564 cells, coloured by cell type. **C**, A UMAP view of *CD4* and *FOXP3* expression. **D**, Dot plot showing expression of candidate marker genes across all immune clusters. **E**,

Frequency of each cluster within individual patients. **F-G**, mRNA expression of transcripts *TNFRSF8* (CD30), *CTLA4, LRRC32* (GARP), *TNFRSF18* (GITR) and *TIGIT* in Tregs from individual patients at baseline and post αPD-1 therapy at **F,** bulk and **G,** single-cell level. **H,** Bulk-level mRNA expression of transcripts *TNFRSF8* (CD30), *CTLA4, LRRC32* (GARP), *TNFRSF18* (GITR) and *TIGIT* in Tregs from αPD-1-treated patients who either responded (Res) or did not respond (Non-res). Data shown are Mean±SEM in **F&H**. Statistical analyses were performed using an unpaired Student's t-test in **F&H** and the clustered Wilcoxon rank-sum test in **G**.

Finally, we explored whether CD30 could serve as a biomarker for predicting cancer-free survival across various cancers including melanoma. We found that elevated CD30 expression in PBMCs is associated with poor survival in patients with uveal melanoma, breast, lung, and colon cancer (**Figure 4.17**), identifying CD30 as a potential biomarker and therapeutic target for post-checkpoint therapy outcomes. Thus, using both our data and publicly available datasets, we demonstrate that human Tregs within TILs and PBMCs upregulate CD30 in response to PD-1 inhibition, which could drive anti-PD-1 resistance in melanoma.

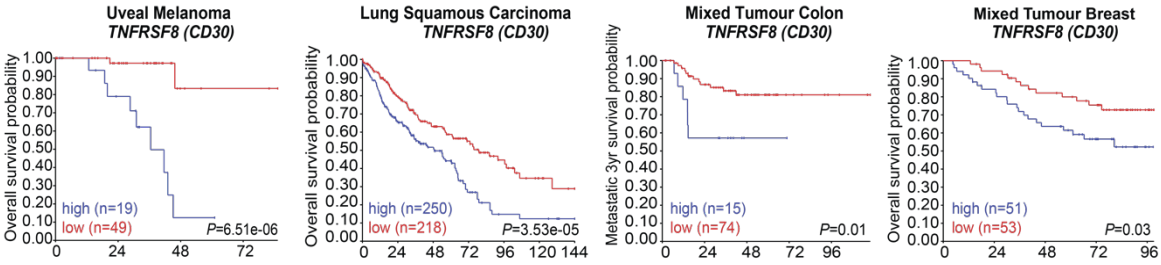

Figure 4.17 CD30 as a predictive marker for poor survival in multiple cancers. Kaplan-Meier analysis of overall survival of patients diagnosed with uveal melanoma, lung squamous carcinoma, mixed tumour colon, or mixed tumour breast, stratified by CD30 expression levels. *P* values are indicated for each comparison. Survival curve analysis was performed using R2 Genomics Analysis and Visualization Platform.

4.4 Discussion

The use of antibodies against PD-1 and CTLA-4 has revolutionised cancer treatment, particularly in melanoma. However, despite their success, many patients either fail to respond, do not respond at all or develop hyper-progressive disease, where PD-1 inhibition paradoxically accelerates tumour growth (Larkin et al., 2019, Park et al., 2021). Emerging evidence suggests that anti-PD-1 immunotherapy may increase Treg populations in some patients, contributing to resistance to immunotherapy (Kamada et al., 2019). In this chapter, we investigate three key aspects of PD-1 biology in Tregs within the TME using clinically relevant global *Pd1*$^{-/-}$ and biologically specific *Pd1*$^{fl/fl}$*Foxp3*^{ERT2Cre} mouse models. We demonstrate that (1) PD-1 regulates the expression of the CD30 co-inhibitory receptor in

Tregs, (2) CD30-expressing Tregs exhibit enhanced suppressive function following PD-1 blockade and (3) PD-1 regulates the differentiation and communication network of Tregs. Our findings offer valuable insights into the complex interplay between PD-1 and Treg function in the context of cancer immunotherapy resistance.

Our observation that *Pd1*$^{-/-}$ Tregs exhibit superior function compared to WT Tregs in an *in vivo* B16F10 melanoma model aligns with recent reports demonstrating a similar phenotype in autoimmunity and infectious diseases (Tan et al., 2021, Perry et al., 2022). Within our dataset, CD30 emerged as the dominant co-inhibitory receptor intrinsically regulated by PD-1 deficiency in Tregs within the TME. This unexpected finding identifies a novel regulatory pathway in Tregs that could be leveraged to enhance checkpoint therapies. The role of CD30 in immunotherapy and Treg biology has been previously explored, with studies showing that CD30 plays a crucial role in Treg suppressive function in graft versus host disease (Zeiser et al., 2007). Our data complement these observations and offer potential therapeutic implications for overcoming anti-PD-1 resistance. Specifically, patients exhibiting increased Treg numbers following PD-1 blockade may benefit from anti-CD30 antibody therapy. While murine studies have shown that targeting CD30 in combination with other co-receptors can lead to Treg depletion (Gaspal et al., 2011), our findings did not support this, as blocking the CD30/CD30L axis preserved Treg numbers within the TME while significantly reducing tumour burden.

The functional plasticity of Tregs has been well established, with cytokines (Laurence et al., 2012) and co-receptors (Amarnath and Brown, 2020) playing a significant role in shaping their behaviour. Previously, we have shown that PD-1 is vital for maintaining FoxP3 expression in both human (Amarnath et al., 2011) and murine Tbet^{+} Tregs (Stathopoulou et al., 2018). Additionally, a recent study suggests *Pd1*$^{-/-}$ Tregs exhibit increased functional plasticity within the TME (Kim et al., 2023). Kim *et al.* further demonstrated that *Pd1*$^{-/-}$ Tregs acquire an altered metabolic phenotype that drives their functional plasticity in the TME, supporting earlier findings by us and others that PD-1 induces a glycolytic phenotype in T cells and innate immune cells (ILC2/ILC1) (Lim et al., 2023, Helou et al., 2020). Using predictive pseudotime trajectory analysis, we identified a similar phenotype in *Pd1*$^{-/-}$ Tregs, where our unbiased analysis revealed a shift toward type 1 differentiation states in Tregs. These findings suggest that while PD-1 regulates the emergence of Tregs with type 1-like Tregs, it simultaneously enhances regulatory subsets

that drive immune suppression via TNFRs, TIGIT and IL-10. Integrating unbiased computational analysis with functional validation studies may help resolve the diverse findings reported in Treg biology. Within the TME, multiple Treg states co-exist and their function is influenced by the predominant state in a given spatial and temporal context. To explore this, we employed spatial transcriptomics to determine which Treg states are associated with immune or tumour cells. We found that *Ifngr*-expressing Tregs were localised near fibroblasts, blood vessels and monocytes, whereas *Il10-, Tigit-, Tnfrsf*-expressing Tregs were predominantly found in close proximity to tumour cells. These findings suggest that *Pd1*$^{-/-}$ Tregs exhibit functional plasticity and adapt their immune suppressive function within the TME based on their local communication networks. Further validation in murine models confirmed an increase in CD30 expression within the regulatory Treg subsets within the TME.

The altered communication programs driven by various Treg differentiation states prompted us to investigate Treg crosstalk with immune cells within the TME. Our CellChat analysis revealed that *Pd1*$^{-/-}$ Tregs exhibited enhanced interaction with myeloid DCs and NK cells within the TME. Validation studies further showed a decrease in NK and DC frequencies, suggesting that Tregs regulate these immune subsets. However, our validation studies cannot determine whether this downregulation occurs through direct or indirect communication within the TME.

Beyond the crosstalk phenotype, we also examined the distinct communication patterns of WT and *Pd1*$^{-/-}$ Tregs in TME. Our data suggests that in relation to co-inhibitory receptors, WT Tregs predominantly rely on CTLA-4 and PD-1, whereas PD-1 deletion enhances an alternative communication program primarily driven by TNFR. Although GITR appears to contribute to this process, CD30 is the predominant signalling pathway activated. These findings may explain the lack of success in combination trials using anti-PD-1 and GITR agonists (Heinhuis et al., 2020). Similarly, anti-LAG-3 combination trials have been proposed to overcome resistance (Aggarwal et al., 2023), but our single-cell analysis indicates that LAG3 expression is not universally altered across all T cell subsets. These findings underscore the importance of conducting unbiased analyses of T cell populations in clinical models of established, large tumours before designing combination therapy trials with checkpoint inhibitors.

Our spatial transcriptomics and immunobiology data further suggest that multiple Treg differentiation states coexist within the TME and the predominant phenotype should be targeted in order to overcome tumour resistance. We show that the Treg subset most closely associated with tumour cells exhibits an immunosuppressive phenotype characterised by TNFR and IL-10 expression, along with CD30. This finding underscores the potential of targeting $CD30^+$ Tregs to overcome Treg-mediated resistance to tumour growth. Indeed, clinical trials investigating the conjugated anti-CD30 therapy, brentuximab vedotin [NCT04609566] in anti-PD-1 resistant patients are ongoing, with preliminary interim analysis reporting a 24% overall response rate (ORR) compared to 11% in anti-LAG-3 combination trials for this patient cohort (Ascierto et al., 2023). Notably, combination trials using anti-GITR and anti-PD-1 have shown a lack of response in this population (Papadopoulos et al., 2021, Comito et al., 2022). Hence, our findings highlight a key role for $CD30^+$ Tregs in driving anti-PD-1 resistance in melanoma and suggest that targeting this subset may be a promising therapeutic strategy to enhance immunotherapy efficacy.

In this study, we also confirm that our findings in the murine melanoma model are reproducible in melanoma patients, demonstrating that CD30 expression in Tregs is not induced by the TME but rather by anti-PD-1 blockade. Our unbiased single-cell analysis reveals that CD30 expression following PD-1/PD-L1 inhibition is preserved in human Tregs, supporting the translational relevance of our murine data. However, a limitation of our human study is the sample size. While our dataset provides proof-of-principle confirmation, further phenotypic validation is necessary to strengthen the case for targeting CD30 as a combination therapy in melanoma patients who develop resistance. To address this limitation, we investigated whether CD30 could serve as a predictive biomarker for survival across multiple solid cancers. In silico analysis of published datasets indicates that CD30 is indeed a prognostic marker for survival in human cancers.

4.5 Summary

In summary, through unbiased analyses and murine validation studies, we demonstrate that PD-1-deficient Tregs possess enhanced suppressive capacity, primarily driven by CD30 expression within the melanoma TME. Additionally, PD-1 regulates Treg differentiation and alters their communication programs, particularly via TNFR signalling, which may underlie the ineffectiveness of certain checkpoint inhibitor combinations. These findings provide mechanistic insights into the role of Tregs in melanoma patients who develop

resistance to anti-PD-1 therapy. Notably, we confirm the relevance of our murine results in melanoma patients, demonstrating that PD-1 blockade, rather than the TME, induces CD30 expression in Tregs. Additionally, in silico analysis supports the potential of CD30 as a prognostic biomarker for survival across multiple solid cancers. Collectively, this study consolidates previous contradictory findings and highlights $CD30^+$ Tregs as a promising therapeutic target to overcome resistance to anti-PD-1 therapy.

Chapter 5 PD-1 negatively regulates the function of Tbet^{+}RORγt^{-}NK1.1^{-} NKp46^{-}EOMES^{-}ILCs in tumour microenvironment

5.1 Introduction

Innate lymphoid cells (ILCs) are tissue-resident innate immune cells which are involved in the first line of defence against cancer and infection. Under inflammatory conditions, ILCs upregulate migratory capacity in response to cytokine stimulation within and between the organs like other immune cells. Natural killer (NK) cells and lymphoid tissue inducing (LTi) cells are the first two ILC subsets to be identified (Kiessling et al., 1975, Mebius et al., 1997). ILCs can be classified into three distinct groups which are group 1 ILC (ILC1), group 2 ILC (ILC2) and group 3 ILC (ILC3). ILC1 is consisted of NK cells and helper-like ILC1(Cortez et al., 2015, Sojka et al., 2014) whereas ILC3 is consisted of LTi cells and helper-like ILC3 (Almeida and Belz, 2016). NK cells share similarities with CD8^{+} cytotoxic T cells in their capability of releasing cytotoxic granules to kill the cancer cells without prior sensitisation. Helper-like ILC1, ILC2 and ILC3 mirror the phenotype and function of CD4^{+} helper T (Th) cells, Th1, Th2 and Th17 cells respectively (Spits et al., 2013). LTi cells are important in lymphoid tissue development (Van de Pavert and Mebius, 2010). ILC1s and NK cells possess several common features: (a) functional dependence on the transcription factor Tbet, (b) activation via type 1 cytokines namely interleukin-12 (IL-12), IL-15 and IL-18, and (c) production of effector cytokines including interferon-γ (IFN-γ) and tumour necrosis factor-α (TNF-α) to exert anti-tumour immunity (Bernink et al., 2013, Fuchs et al., 2013, Klose et al., 2014) **(Figure 5.1)**. In general, ILC1s and NK cells are identified as Lineage^{-}NKp46^{+}NK1.1^{+}CD49a^{+}CD49b^{-} and Lineage^{-} NKp46^{+}NK1.1^{+}CD49b^{+} respectively. The expression of transcription factor Eomes also enables the differentiation of NK cells from helper-like ILC1s (Daussy et al., 2014, Peng et al., 2013). ILC2s are characterised by the transcription factor GATA3 and are activated by cytokines IL-25, IL-33 and thymic stromal lymphopoietin (TSLP) to exert parasitic defence and allergic responses by producing type 2 cytokines IL-5, IL-9, IL-13 and other factor like amphiregulin (Areg) (Mjosberg et al., 2011, Monticelli et al., 2011, Moro et al., 2010, Neill et al., 2010, Klose and Artis, 2016). ILC3s are characterised by the transcription factor RORγt and are activated by IL-23 and IL-1β to develop immunity against extracellular bacterial infection by producing IL-17, IL-22 and granulocyte macrophage colony-stimulating factor (GM-CSF). It can be further divided based on NKp46 (NCR) expression (Cella et al., 2009, Sonnenberg et al., 2011, Sawa et al., 2010, Satoh-Takayama

et al., 2008, Buonocore et al., 2010, Sanos et al., 2009, Cupedo et al., 2009, Crellin et al., 2010). Unlike T cells and B cells, ILCs do not express antigen-specific receptor but they can react to infection or insults through the generation of cytokines and secreted proteins, which can further direct and enhance T cell and myeloid responses. Furthermore, it has been shown that ILCs can interact with $CD4^+$ T cells via major histocompatibility complex (MHC) class II molecules and exhibit high plasticity capabilities depending on their tissue environment as $CD4^+$ T cells (Klose and Artis, 2020).

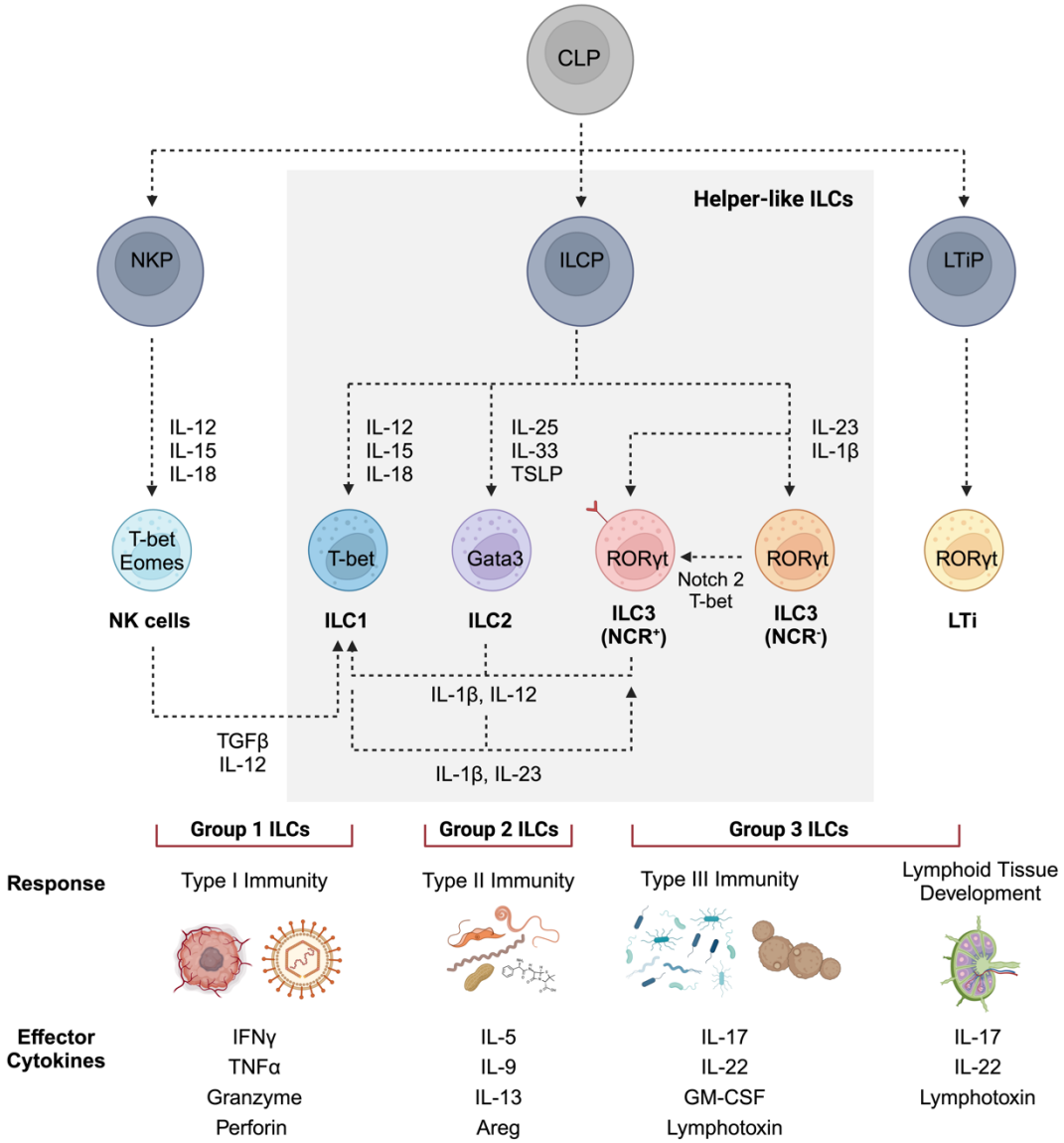

Figure 5.1 Function and plasticity of ILC subsets. All ILCs originate from common lymphoid progenitors (CLPs). NK cells are developed from NK precursor (NKP), helper-like ILC1-ILC3 are developed from ILC precursor (ILCP) while LTi cells are developed from LTi precursor (LTiP). ILC subsets are classified based on their differential expression of cell surface markers, transcription factors and effector cytokines. ILCs contribute to diverse range of immunity and show high plasticity under inflammatory conditions.

Although the function of NK cells in eradicating tumours has been well studied within the tumour microenvironment (TME), the role of helper ILCs are yet to be clarified. Paradoxically ILC1s have been shown to engage in both tumour suppressing and tumour promoting activities (Gao et al., 2017). Indeed, intratumoural IL-15 and transforming growth factor β (TGFβ) were suggested to determine ILC1 to establish either pro- or anti-tumour responses. IL-15 which has been shown to be secreted by tumour cells, can potentially induce the production of granzyme B by $CD103^+$ cytotoxic ILC1 against the tumour cells (Dadi et al., 2016). In contrast, TGF-β contributes to the conversion of NK cells into intermediate ILC1 and non-cytotoxic ILC1, which in turn reduce immunosurveillance and obtain pro-tumorigenic phenotype (Gao et al., 2017). Furthermore, ILC1 can transdifferentiate into ILC3s in the presence of IL-1β and IL-23 **(Figure 5.1)**, leading to enhanced tumour growth (Koh et al., 2019, Liu et al., 2019). The function of ILC2s in pro- and anti-tumorigenic responses has also been explored by a few reports (Jovanovic et al., 2014, Li et al., 2014). Like NK cells, in the presence of IL-1β and IL-12, ILC2s can transdifferentiate into ILC1s which induces downregulation of both GATA3 expression and IL-5 production and promotes upregulation of Tbet expression and IFN-γ secretion (Ohne et al., 2016, Lim et al., 2016, Zhang et al., 2017). In addition, TGF-β signalling has been shown to convert ILC2 into ILC3-like cells by upregulating expression of IL-23 receptor, which in turn promote the development of IL-17-producing ILCs (Bal et al., 2016). Although the ILC2 conversion into ILC1-like cells and ILC3-like cells has been studied, however whether ILC1s can transdifferentiate into ILC-2 like cells and the role of ILC3-like cells in the TME upon conversion still yet to be understood. The anti-tumour responses of ILC3s have been studied in malignant melanoma while the pro-tumour responses of IL-22 expressing ILC3s have been shown in bacteria-induced colon cancer (Kirchberger et al., 2013, Chan et al., 2014, Eisenring et al., 2010). As mentioned, helper-like ILC3s can be divided into NCR^- and NCR^+ subsets which depend on the Tbet expression under Notch2 ligand signalling **(Figure 5.1)**, with study showing that TGF-β could also play a role (Viant et al., 2016). In the presence of IL-12, the expression of RORγt is downregulated in NCR^+ ILC3 and allow its conversion into $Tbet^+$ "ex-ILC3s" thereby resembling ILC1s in phenotype (Raykova et al., 2017). In order to limit the ILC3 plasticity, transcription factor c-MAF allows ILC3s to restrain the expression of both Tbet and IFN-γ expression at steady state (Parker et al., 2020, Tizian et al., 2020). Moreover, the expression of aryl hydrocarbon receptor (AHR) has also been reported to limit the ILC3s to develop into $EOMES^+Tbet^+$ NK-like cells in response to IL-12 and IL-15 (Hughes et al., 2014).

Taken together, it is now clear that the function and plasticity of ILCs within the TME is mainly dependent on the microenvironmental signals and cytokine availability (Nussbaum et al., 2017).

Despite the role of cytokine in shaping ILC phenotype has been widely reported, the role of co-receptor in regulating ILC function is less studied. The expression of several coreceptors on ILCs within the TME has been reported including programmed cell death-1 receptor (PD-1) (Taylor et al., 2017) and its ligand PD-L1 (Schwartz et al., 2017). Recent literature has revealed that in the presence of exogenous IL-33, PD-1 plays a role in ILC2 regulation within the TME (Moral et al., 2020, Jacquelot et al., 2021). Apart from ILC2, PD-1 expression has been found to be upregulated in ILC1 in both murine tumours (Gao et al., 2017, Salimi et al., 2018) and human hepatocellular carcinomas (Heinrich et al., 2022). While the functional implications of co-receptors within ILCs remain unclear, co-receptor expression offers an avenue to enhance ILC responses in cancer (Salimi et al., 2018, Klose and Artis, 2020, Moral et al., 2020), which potentially overcoming the current gap in therapeutic efficacy.

5.2 Aims

Previous work in our laboratory has shown the role of PD-1 in regulating KLRG1^{+} ILC2 and blockade of PD-1 can induce the expansion and also the protective function of ILC2 against helminthic infection (Taylor et al., 2017). Although PD-1 expression has been noted on all ILC subsets in the TME, the functional consequence of PD-1 within ILC biology within the TME is not fully elucidated. Therefore, the first question we postulated was: does PD-1 regulate ILC subsets in the TME. We hypothesised that PD-1 would specifically regulate ILC function in the TME and disrupting PD-1 signalling would boost the number and function of ILC against cancer. The main objectives were:

1. To identify PD-1 expression in ILC populations within the B16 melanoma TME.
2. To characterise the presence and phenotype of ILC in healthy WT and *Pdcd1*$^{-/-}$ (*Pd1*$^{-/-}$) mice.
3. To determine the impact of PD-1 deficiency on ILC within the B16 melanoma TME of WT and *Pd1*$^{-/-}$ mice.
4. To investigate the role of PD-1 on cytokine secretion profile of ILC within the B16 melanoma TME.

5. To investigate the role of PD-1 on proliferation of ILC within the B16 melanoma TME.

5.3 Results

The results and analyses presented in this chapter have been published in *Proceedings of the National Academy of Sciences (PNAS)*, April 25, 2023. DOI: 10.1073/pnas.221658712.

5.3.1 BD Rhapsody single-cell RNA sequencing analysis reveals PD-1 expression in Tbet^{+}NK1.1^{-} ILC subpopulation in B16F10 melanoma tumour

Despite PD-1 being shown to have an essential role in exogenous IL-33 driven ILC2 anti-tumour responses in both pancreatic cancer (Moral et al., 2020) and metastatic melanoma models (Jacquelot et al., 2021), it still remains unascertained whether PD-1 function is relevant without the presence of exogenous IL-33; given that IL-33 is not produced within the melanoma TME. To examine whether PD-1 regulates ILC subsets within the TME, B16F10 melanoma tumour in WT and *Pd1*$^{-/-}$ mice was established, and tumour growth was monitored. Significant lower tumour burden was noted in *Pd1*$^{-/-}$ cohort than that of the WT cohort starting from day 10 post-inoculation **(Figure 5.1a)**. On day 14, the tumours were harvested and the tumour-infiltrating lymphocytes (TILs) were isolated as single cell suspension. To investigate the distribution of Lineage^{-}Thy1^{+} subsets and their relative PD-1 expression within the TME, we utilised BD Rhapsody single-cell RNA sequencing (scRNA-seq) platform which allows to study both PD-1 protein expression along with transcriptomics using an unbiased approach. In order to do this, enriched Lineage^{-}Thy1^{+} ILCs derived from the isolated TILs in WT and *Pd1*$^{-/-}$ mice (n=5 per cohort) were subjected to scRNA-seq analysis. As a result, 13 clusters were identified within the enriched TILs and visualised by using an t-distributed Stochastic Neighbour Embedding (t-SNE) plot **(Figure 5.1b)**, with WT TILs and *Pd1*$^{-/-}$ TILs sharing a similar clustering fashion **(Figure 5.1c)**. It is worth noting that several *Pd1*$^{-/-}$ TIL clusters had more cell numbers than that of the WT TIL clusters.

To further identify immune populations occupying the TME, we next performed differential gene expression analysis of the TIL clusters, complemented by referencing AbSeq protein expression visualised on the t-SNE plot. Notably, cluster 1 and cluster 5 significantly express NK1.1 (AbSeq) and CD3 (AbSeq) proteins, respectively **(Figure 5.1d, Appendix Table E.1-2)**. Cluster 10 exhibited a type 1 phenotype but did not express NK1.1 (AbSeq) or NKp46 (CD335, AbSeq) proteins **(Figure 5.1d, Appendix Table E.3)**.

Transcriptomic analysis revealed that cluster 10 was enriched for genes associated with ILC1 signature, including *Tbx21* (Tbet), *Ifng* and *Stat4*, compared to cluster 1 and 5 **(Figure 5.1e, Appendix Table E.1-3)**. Furthermore, cluster 10 expressed *Gzmb* and *Gzmk* transcripts, indicative of its cytotoxic potential **(Figure 5.1e, Appendix Table E.3)**.

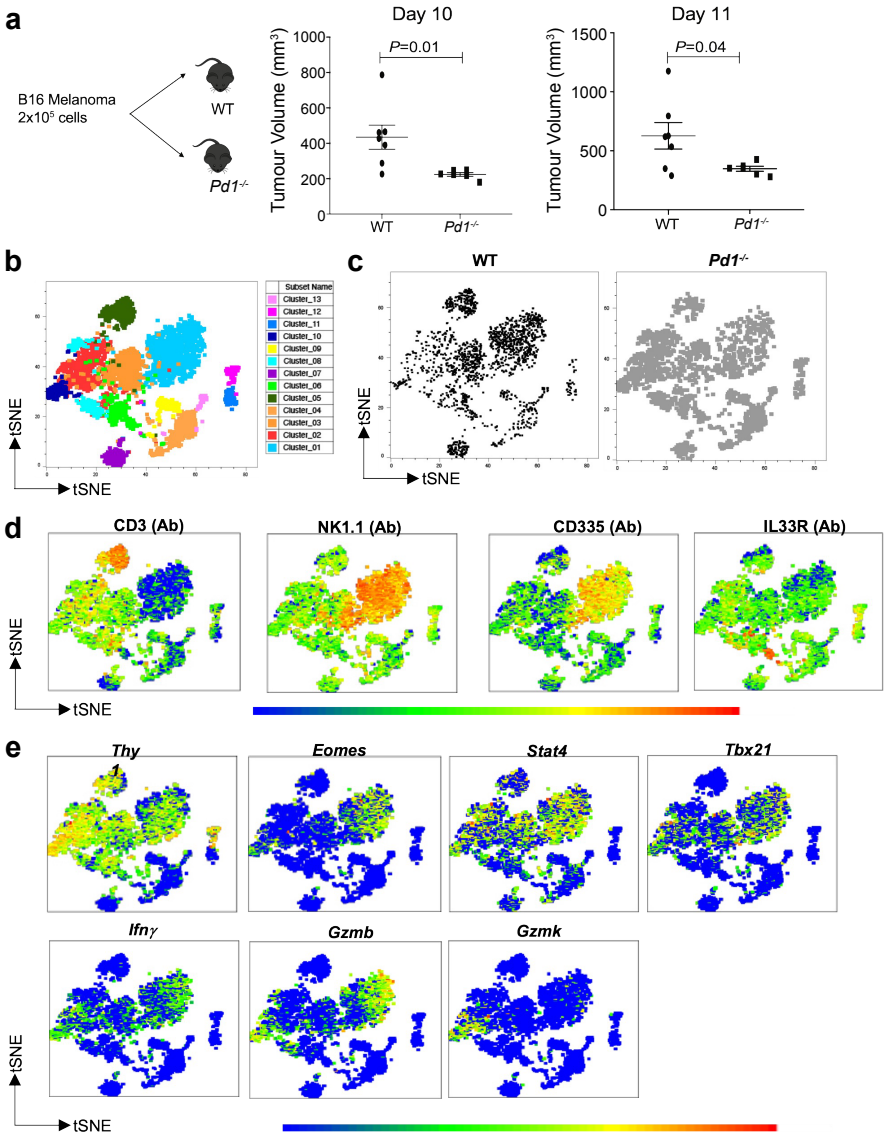

Figure 5.1 Single-cell RNA sequencing analysis reveals Tbet^{+}NK1.1^{-} ILCs within the tumour microenvironment.
A, WT and *Pd1*$^{-/-}$ mice were inoculated with B16F10 melanoma cells via subcutaneous injection. Tumour volume was measured. Tumour infiltrating lymphocytes were subjected to single-cell RNA sequencing analysis. Analysis of protein and gene expression was performed in SeqGeq software with inserted plugins. **B,** t-distributed Stochastic Neighbour Embedding (t-SNE) was computed and clustering was performed by using the PhenoGraph plugin with various populations highlighted. **C,** t-SNE plots of WT and *Pd1*$^{-/-}$ samples were decoupled to show similar clustering between the samples. **D,** t-SNE plots of protein CD3, NK1.1, NKp46 and IL33R detected by AbSeq. **E,** t-SNE plots of type 1 gene transcripts within the various clusters. Data shown are from n=5 WT and n=5 *Pd1*$^{-/-}$ mice.

These findings were supported by quantitative analysis, which demonstrated that cluster 10 expressed significantly higher levels of CD25 protein, along with transcripts *Tbx21*, *Stat4*, *Ifng*, *Gzmk* and *Gzmb*, compared to cluster 1 (NK1.1^{+}) and/or cluster 5 (CD3^{+}) (**Figure 5.2a**). Conversely, cluster 10 exhibited significant low expression of CD335 (NKp46 AbSeq), NK1.1 (AbSeq), and *Gzma* (**Figure 5.2b**). No significant difference in *Eomes* expression was observed between cluster 1 and 10 (**Figure 5.2c**). Of note, PD-1 (Abseq) protein was significantly upregulated in cluster 10 compared to cluster 1 and 5, suggesting a potential regulatory role of PD-1 in this ILC population within the TME (**Figure 5.2d**).

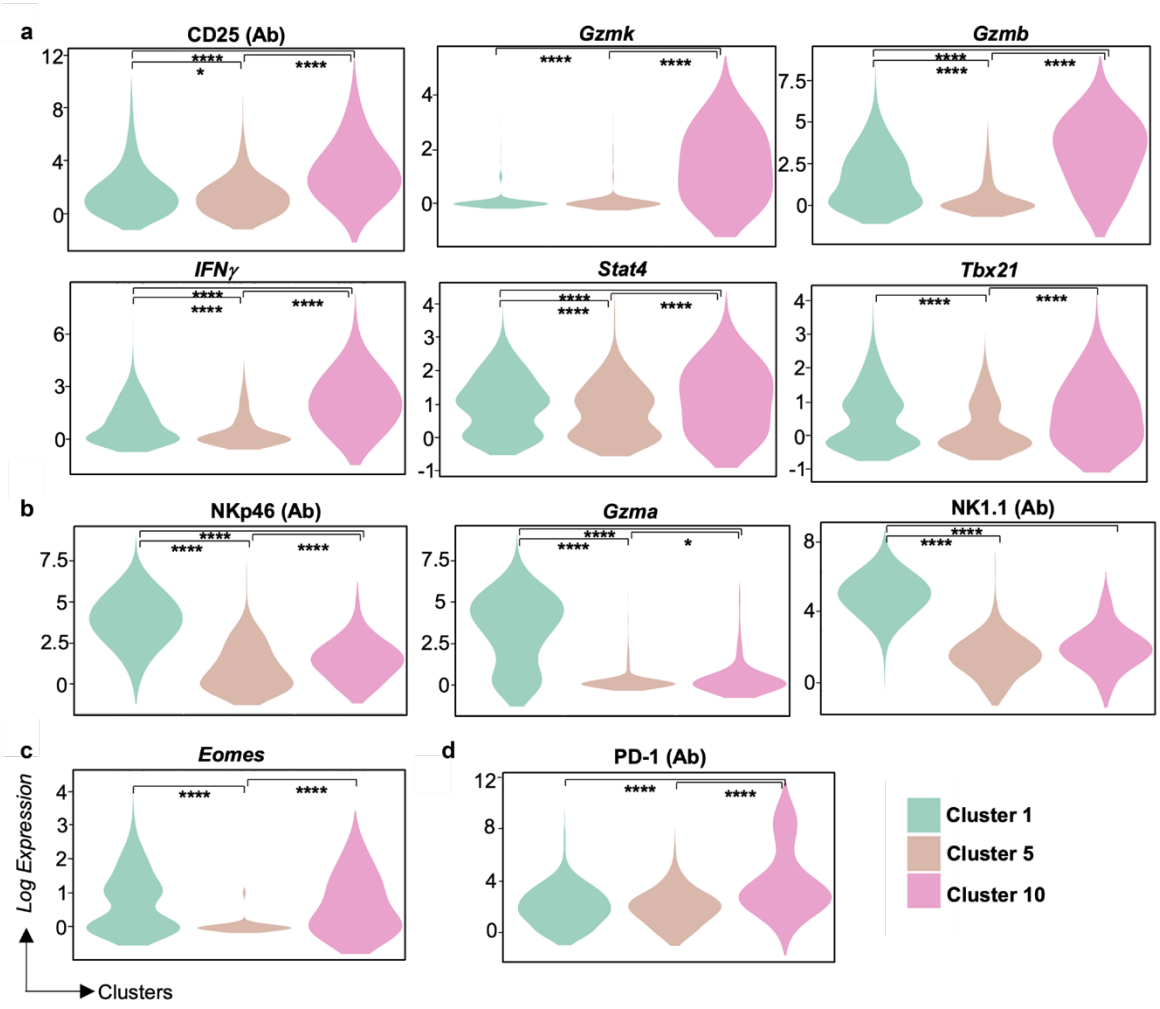

Figure 5.2 Single-cell RNA sequencing analysis reveals PD-1 expression in Tbet^{+} NK1.1^{-} ILCs within the tumour microenvironment.
WT and *Pd1*$^{-/-}$ mice were inoculated with B16F10 melanoma cells via subcutaneous injection. Tumour infiltrating lymphocytes were subjected to single-cell RNA sequencing analysis. Violin plots comparing cluster 1 (NK cell), cluster 5 (T cell) and cluster 10 (Tbet^{+} ILC) were generated in SeqGeq software using the ViolinBox plugin. **A,** Significantly upregulated protein and gene transcripts in cluster 10. **B,** Significantly downregulated proteins and gene transcripts in cluster 10. **C,** Expression of Eomes transcript. **D,** Expression of PD-1 (AbSeq) protein. Data shown are from n=5 WT and n=5 *Pd1*$^{-/-}$ mice.

Statistical analysis applied within violin plots were Kruskal-Wallis test followed by pairwise comparisons using Dunn's test with Bonferroni correction.

5.3.2 Flow cytometry analysis reveals a novel Tbet^{+}NK1.1^{-}ILC subset in healthy WT and Pd1$^{-/-}$ mice

We next investigated whether the Tbet^{+}NK1.1^{-} ILCs observed within the TME also existed in normal homeostatic condition or if their phenotype results from NK1.1 downregulation within the TME. To address this, we characterised the helper ILC1 subset using surface markers consistent with our scRNA-seq data in healthy, non-tumour-bearing WT and *Pd1*$^{-/-}$ mice. A similar ILC subset was defined as Tbet^{+}RORγt^{-}NK1.1^{-}NKp46^{-} and further categorised based on Eomes expression **(Figure 5.3a)**. Specifically, Tbet^{+}RORγt^{-}NK1.1^{-}NKp46^{-} ILCs were divided into Tbet^{+}RORγt^{-}NK1.1^{-}NKp46^{-}Eomes^{+} and Tbet^{+}RORγt^{-}NK1.1^{-}NKp46^{-}Eomes^{-} subsets. These three ILC populations were found in the bone marrow **(Figure 5.3b-d)**, liver **(Figure 5.3e-g)** and spleen **(Figure 5.3h-j)**. In overall, our data demonstrate that this novel ILC population is present not only in the TME of both WT and *Pd1*$^{-/-}$ mice but also under steady-state conditions.

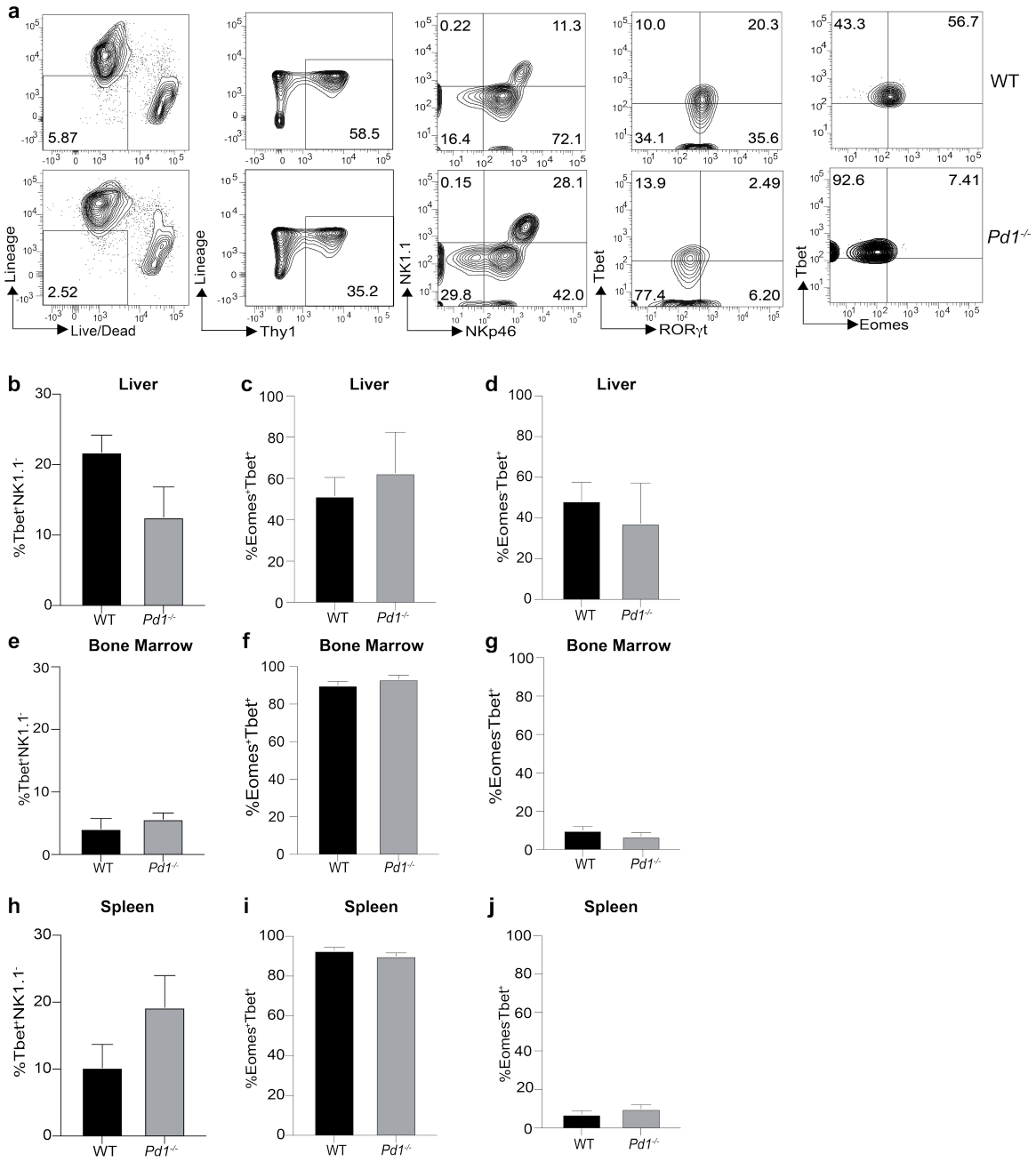

Figure 5.3 Frequency of Tbet^{+}NK1.1^{-} ILCs in WT and *Pd1*$^{-/-}$ mice under homeostatic conditions.

Liver, bone marrow and spleen tissues were harvested from healthy WT and Pd1$^{-/-}$ mice. **A,** Representative flow cytometric contour plots illustrating the gating strategy for identifying Tbet^{+}NK1.1^{-} ILCs. **B-D,** Frequencies of Tbet^{+}NK1.1^{-} ILCs, Tbet^{+}NK1.1^{-}Eomes^{+} ILCs and Tbet^{+}NK1.1^{-}Eomes^{-} ILCs in the liver, respectively. **E-G,** Frequencies of Tbet^{+}NK1.1^{-} ILCs, Tbet^{+}NK1.1^{-}Eomes^{+} ILCs and Tbet^{+}NK1.1^{-}Eomes^{-} ILCs in the bone marrow, respectively. **H-J,** Frequencies of Tbet^{+}NK1.1^{-} ILCs, Tbet^{+}NK1.1^{-}Eomes^{+} ILCs and Tbet^{+}NK1.1^{-}Eomes^{-} ILCs in the spleen, respectively. Data are presented as mean±SEM of n=4 mice, with statistical significance performed using an unpaired Student's t-test.

5.3.3 PD-1 deficiency specifically enhances Tbet^{+}NK1.1^{-}Eomes^{-}ILCs within the TME and TDLN.

Pd1$^{-/-}$TbetZsGreen (*Pd1$^{-/-}$* TBG) mice were generated to further investigate the Tbet^{+}NK1.1^{-} ILC subpopulation. B16F10 melanoma cells were established on both WT TBG and *Pd1$^{-/-}$* TBG mice, and tumour growth was monitored **(Figure 5.4a)**. Consistent with previous observations, *Pd1$^{-/-}$TBG* mice exhibited a significantly lower tumour burden compared to WT *TBG* mice starting on day 14 **(Figure 5.4b)**. Tumours were harvested on day 14 **(Figure 5.4c)** to perform immunophenotyping and to obtain detectable number of helper ILCs. First, we assessed the expression of PD-1 in Tbet^{+}NK1.1^{-} ILCs and ILC2s, revealing that both subsets expressed PD-1 **(Figure 5.4d-e)**. Next, we examined which ILC population was modulated by PD-1 within the melanoma TME (**Figure 5.4f**). The frequency of Tbet^{+}NK1.1^{-}Eomes^{-} ILCs was significantly increased in the absence of PD-1 within the TME (**Figure 5.4g**). Notably, no significant changes were observed in other ILC subsets, including Eomes^{+} and RORγt^{+}NKp46^{+} (**Figure 5.4h-i**). To further explore this subset, we analysed additional tissues, including the lungs, small intestine, skin, spleen and tumour-draining lymph nodes (TDLNs). Tbet^{+}NK1.1^{-}Eomes^{-} ILCs were specifically enriched in the TDLNs in the absence of PD-1 but not in other examined tissues (**Figure 5.4j-n**). Collectively, these findings propose a regulatory role of PD-1 in controlling Tbet^{+}NK1.1^{-}Eomes^{-} ILCs within the melanoma TME and TDLNs.

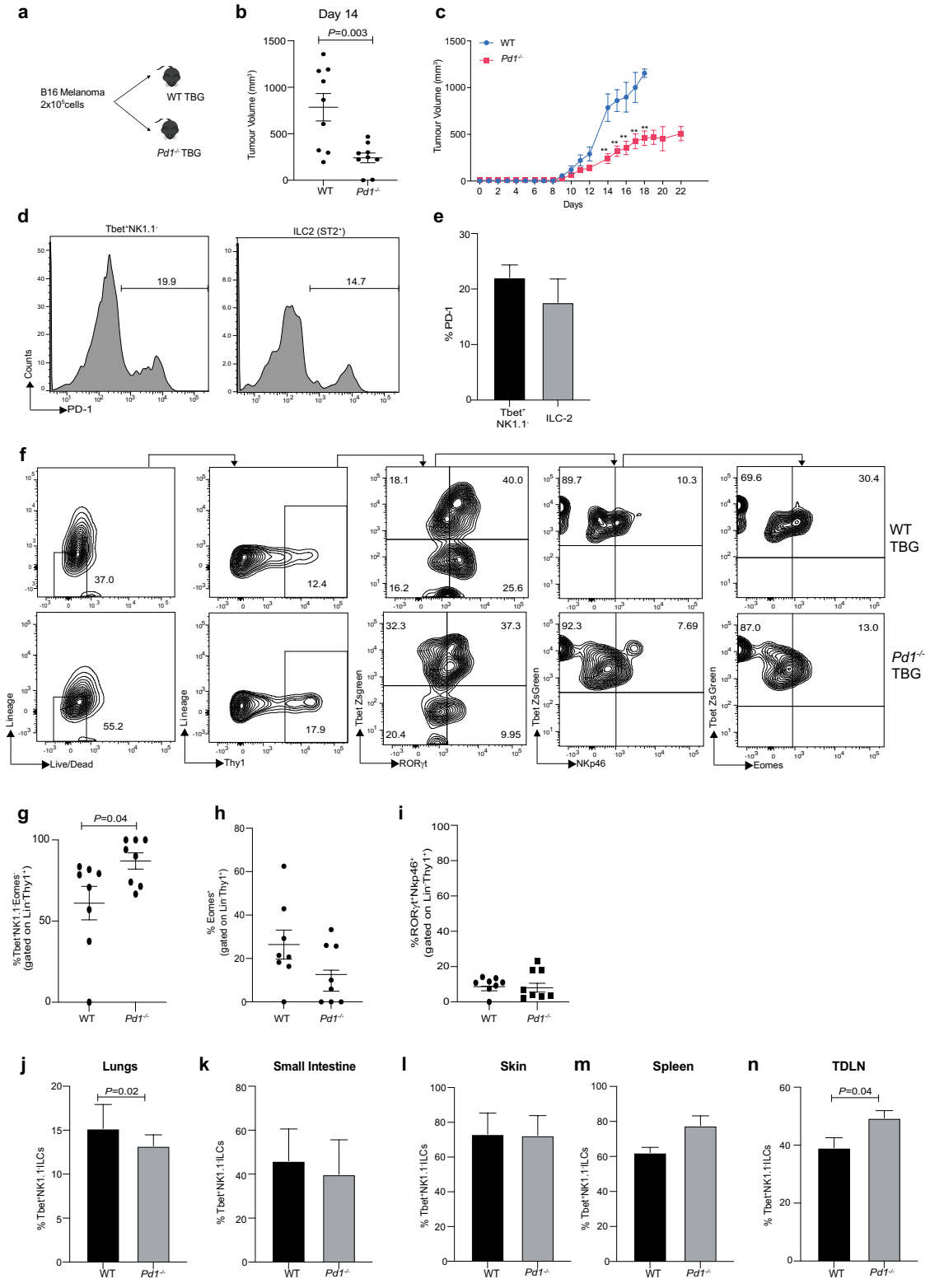

Figure 5.4 Frequency of Tbet^{+}NK1.1^{-} ILCs in WT TBG and *Pd1*$^{-/-}$ TBG mice within the TME.

A, WT TBG and *Pd1*$^{-/-}$ TBG mice were inoculated with B16F10 melanoma cells via subcutaneous injection. Tumour volume was measured in the both cohorts on **(B)** day 14 (n = 9, unpaired Student's t-test) and **(C)** indicated time points (n = 9, two-way ANOVA). On day 14, TILs were isolated and characterised by flow cytometry. Representative flow

cytometry plots and summary showing PD-1 expression on **(D)** Tbet^{+}NK1.1^{-} ILCs and **(E)** ST2^{+} ILC2s within the TME. **F,** Representative flow cytometry plots and gating strategy for identifying ILC subsets. Frequencies of **(G)** Tbet^{+}NK1.1^{-}Eomes^{-} ILCs, **(H)** Eomes^{+} ILCs and **(I)** NKp46^{+} ILCs in TILs (n = 8, unpaired Student's t-test). Frequencies of Tbet^{+}NK1.1^{-} ILC in **(J)** lungs, **(K)** small intestine**, (L)** skin, **(M)** spleen and **(N)** tumour-draining lymph node (TDLN) (n = 5, unpaired Student's t-test). Data are presented as mean±SEM.

5.3.4 PD-1 controls IFN-γ production in Tbet^{+}NK1.1^{-} ILCs within the TME.

Since previous work in our lab demonstrated that PD-1 regulate cytokine secretion in ILC2 (Taylor et al., 2017), we sought to identify whether PD-1 plays a same role in tumour-infiltrating Tbet^{+}NK1.1^{-} ILCs. PD-1 deficiency led to a significant increase in IFN-γ production in Tbet^{+}NK1.1^{-} ILCs and no significant changes were observed in the secretion of IL-17A, IL-22 and TNF-α **(Figure 5.5a-g)**. Next, we assessed whether the IFN-γ production in Lineage^{+}NKp46^{+} cells exhibited changes similar to those in Tbet^{+}NK1.1^{-} ILCs in the absence of PD-1 within the TME. Given that NK1.1 and CD49b were included in the lineage panel, we postulated that the NKp46^{+} population within the lineage gate may have reflected NK1.1^{+} cells. Despite this, no significant changes in IFN-γ production were observed in the Lineage^{+}NKp46^{+} population **(Figure 5.5h)**. Notably, Lineage^{+}NKp46^{-} population significantly increased IFN-γ secretion in the absence of PD-1, which could be attributable to T cells within the TME **(Figure 5.5i)**. Overall, these findings suggest that PD-1 regulates IFN-γ production specifically in the Tbet^{+}NK1.1^{-} ILC population, which exhibits a "helper-like ILC1" phenotype.

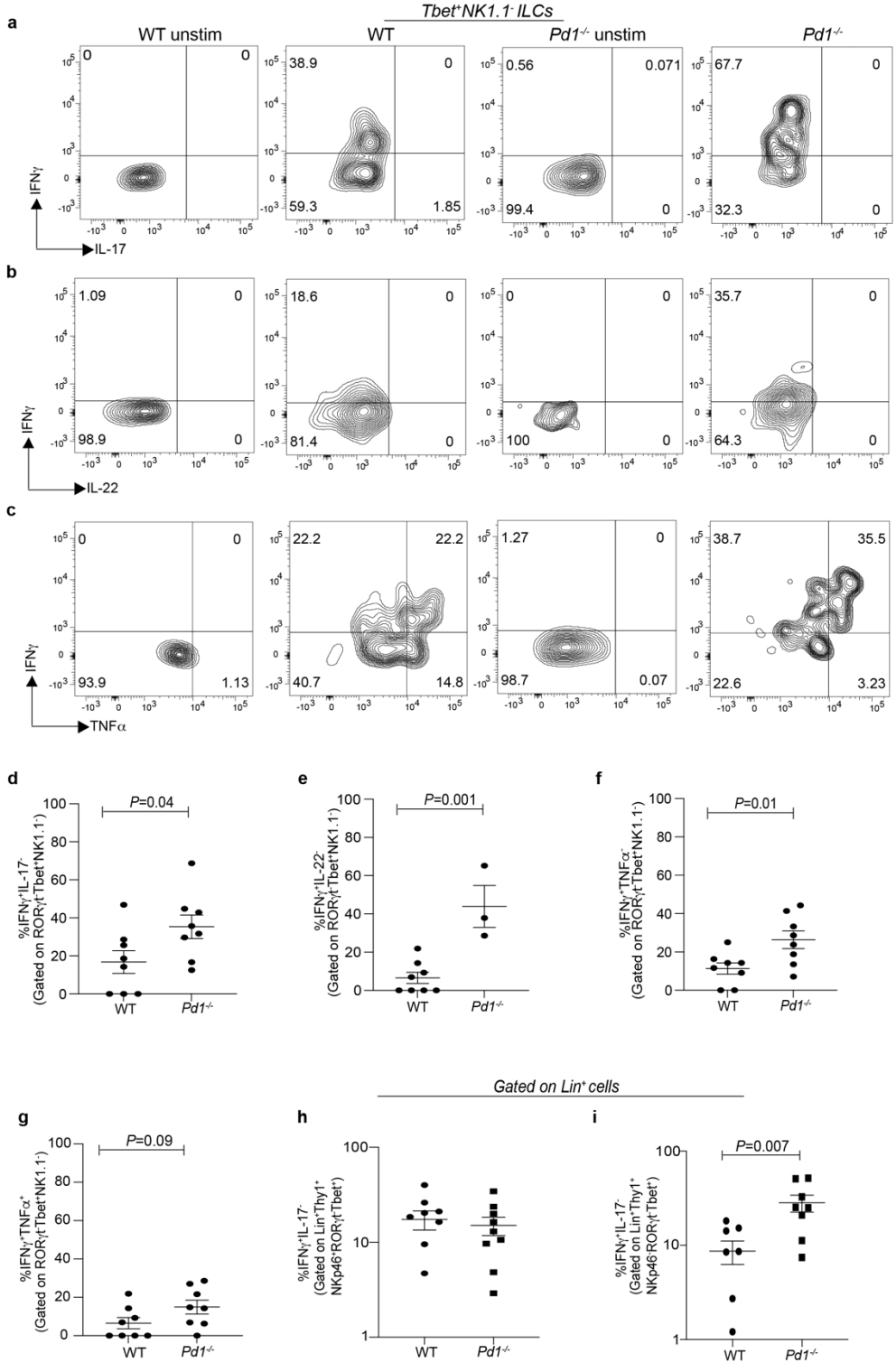

Figure 5.5 PD-1 deficiency significantly increases IFN-γ$^+$Tbet$^+$NK1.1$^-$ ILCs within the B16 melanoma TME.

C57BL6 WT TBG or *Pd1*$^{-/-}$ TBG were inoculated with B16F10 melanoma cells via subcutaneous injection. Tumour infiltrating lymphocytes were isolated, stimulated for 4 h with cytokine stimulation cocktail and then characterised by flow cytometry. ILCs were identified as Lineage$^-$Thy1$^+$. **A&D**, Representative flow plots and summary data for IFN-γ

and IL-17 expression. **B&E,** Representative flow plots and summary data for IFN-γ and IL-22 expression. **C,** Representative flow plots and **F-G,** summary data for IFN-γ and TNF-α. **H,** Expression of IFN-γ in Lineage$^+$NKp46$^+$ TILs and **I,** Lineage$^+$NKp46$^-$ TILs. Data shown are mean±SEM, with each data point representing the number of mice per cohort used in each experiment. Statistical significance was determined using an unpaired Student's t-test.

5.3.5 PD-1 controls proliferation of Tbet$^+$NK1.1$^-$ ILCs within the TME.

The molecular mechanism by which PD-1 regulates the frequency of Tbet$^+$NK1.1$^-$ ILCs within the TME was next investigated. First, PD-1 expression on Tbet$^+$NK1.1$^-$ ILCs within the TME and surrounding normal skin was assessed. Tbet$^+$NK1.1$^-$ ILCs in the TME exhibited significantly higher PD-1 expression compared to their counterparts in normal skin (**Figure 5.6a-b**), suggesting that PD-1 expression is selectively upregulated in Tbet$^+$NK1.1$^-$ ILCs within the TME. Next, the ability of tumour cells to induce PD-1 expression on Tbet$^+$NK1.1$^-$ ILCs was evaluated. In transwell co-culture experiments, B16 melanoma cells induced PD-1 expression in ILCs, with a significant increase in the frequency of PD-1$^+$ ILCs observed at a 1:1 tumour-to-lymphocyte ratio after 6h**.** A similar trend was noted at 1:10 ratio, but this effect was completely abrogated at a 1:100 ratio (**Figure 5.6c-d).** Since tumour-derived lactate has been reported to suppress ILC2 proliferation (Wagner et al., 2020), it was next investigated whether lactic acid (LA) is produced by B16 tumours and whether it contributes to PD-1 induction in Tbet$^+$NK1.1$^-$ ILCs. *In-vitro* experiments confirmed that B16 tumour supernatants contained significant levels of LA at 24 hour (**Figure 5.6e**) and the addition of LA significantly increased PD-1 expression on Tbet$^+$NK1.1$^-$ ILCs (**Figure 5.6f-h).**

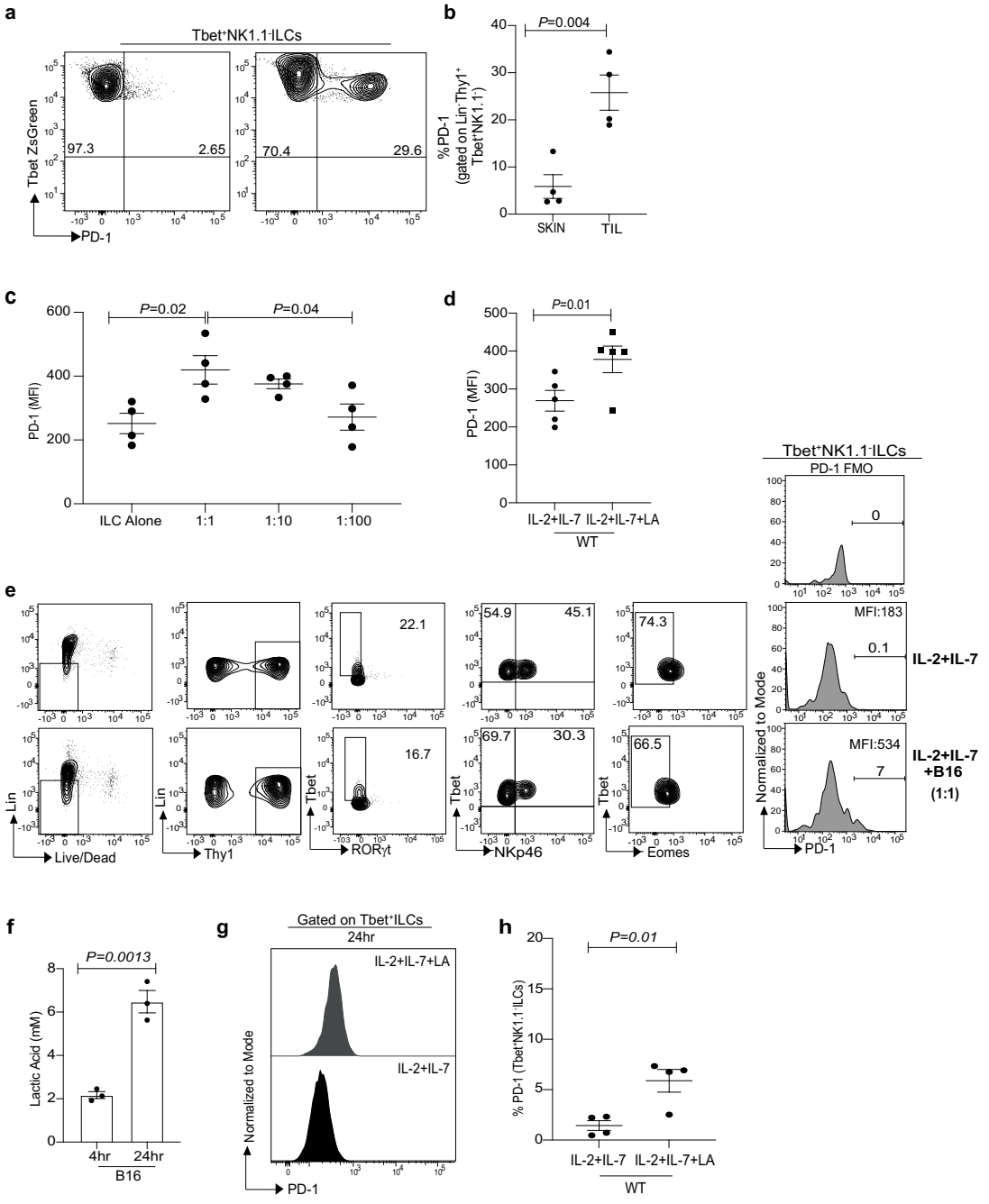

Figure 5.6 Lactic acid derived from B16 melanoma tumours significantly increases PD-1 expression on Tbet$^+$NK1.1$^-$ ILCs.

A-B, C57BL6 WT TBG was reconstituted with B16F10 melanoma cells via subcutaneous injection. On day 14, Tbet$^+$NK1.1$^-$ ILCs were characterised by flow cytometry. PD-1 expression was measured in skin-derived and tumour-derived Tbet$^+$RORγt$^-$NK1.1$^-$ ILCs. **C-D**, PD-1 expression was assessed in splenocyte cultures stimulated with cytokines IL-2 and IL-7 alone or in the presence of B16 melanoma cell line at melanoma cell-to-lymphocyte ratios of 1:1, 1:10 and 1:100 after 6 h. **E**, B16 melanoma cells were expanded in media for 4 h or 24 h and the supernatant was collected. Lactic acid (LA) levels were measured in the supernatant **F-H**, Splenocytes were incubated for 24 h with IL-2 and IL-7 alone or with LA, and PD-1 expression on Tbet$^+$NK1.1$^-$ ILCs were measured. Data shown are mean±SEM, with each data point representing the number of mice per cohort used in

each experiment or the number of individuals in *in-vitro* experiments performed. Statistical significance was determined using an unpaired Student's t-test for comparison of two groups and a one-way ANOVA was performed for comparison of three or more groups.

We next examined whether tumour cell supernatant regulated the proliferative capacity of ILCs through PD-1. To assess this, we measured the proliferation of WT Tbet^{+}NK1.1^{-} ILC in the presence of tumour cell supernatant and compared it to the proliferation of *Pd1*$^{-/-}$ Tbet^{+}NK1.1^{-} ILCs. Our results showed that B16 tumour supernatant significantly inhibited proliferation of WT Tbet^{+}NK1.1^{-} ILCs compared to PD-1-deficient cells (**Figure 5.7a-b**). In fresh cell culture media, *Pd1*$^{-/-}$ Tbet^{+}NK1.1^{-} ILCs exhibited reduced proliferation relative to WT cells in response to IL-2 and IL-7. Furthermore, within the B16 TME *in-vivo*, *Pd1*$^{-/-}$ cohorts displayed a significantly higher proliferative potential of Tbet^{+}NK1.1^{-} ILCs, as indicated by increased Ki67 expression (**Figure 5.7c-d**).

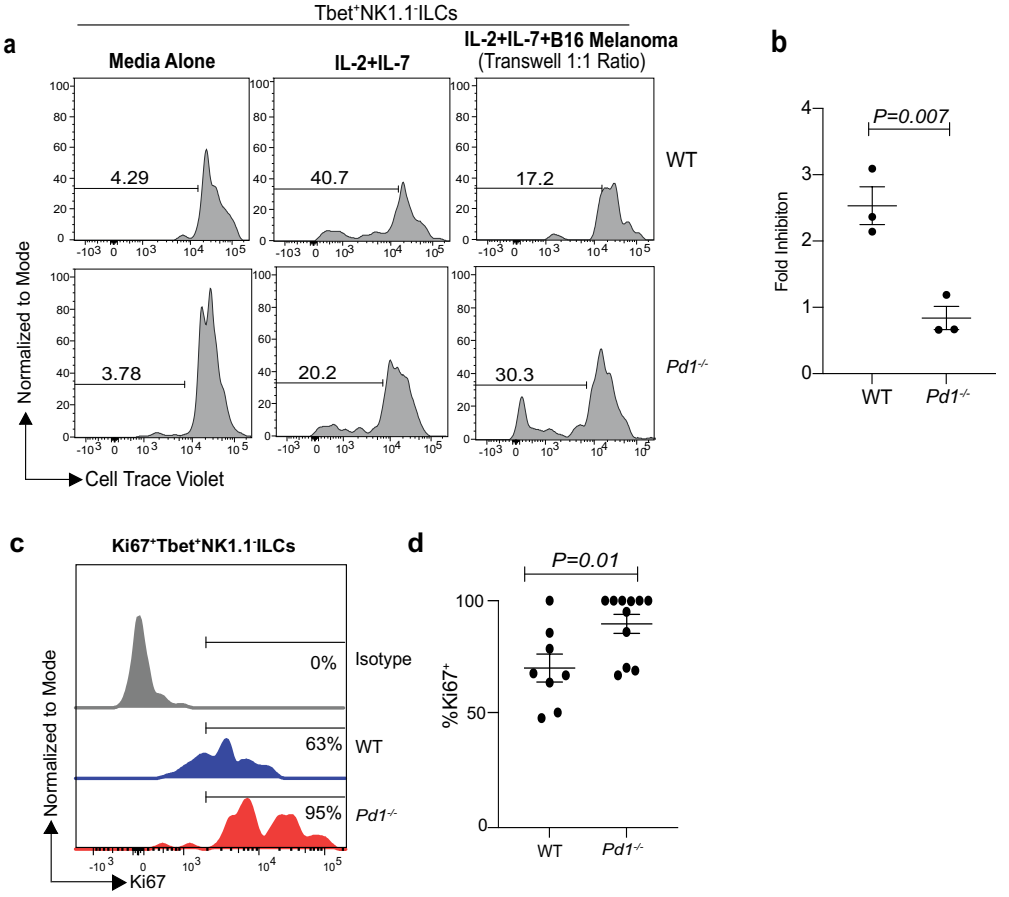

Figure 5.7 PD-1 inhibits the proliferative capacity of Tbet^{+}NK1.1^{-} ILCs within the B16 TME.

A, Representative flow plots showing proliferation of Tbet^{+}RORγt^{-}NK1.1^{-} ILCs from WT and *Pd1*$^{-/-}$ splenocytes in transwell experiments at melanoma cell-to-lymphocyte ratios of 1:1. **B,** Fold inhibition of proliferation in response to melanoma supernatant in WT and *Pd1*$^{-/-}$ Tbet^{+}NK1.1^{-} ILCs. Proliferation in the presence of IL-2 and IL-7 was first measured in WT ILCs, followed by proliferation in the presence of B16 melanoma supernatant. Fold

inhibition was calculated by comparing proliferation rates between two conditions and then plotted for both WT and *Pd1*$^{-/-}$ ILCs. **C,** Representative flow cytometry plots showing Ki67 expression in Tbet^{+}RORγt^{-}NK1.1^{-} tumour-derived ILCs from C57BL6 WT TBG and *Pd1*$^{-/-}$ TBG cohorts. **D,** Cumulative data showing Ki67 expression across cohorts. Data shown are mean±SEM, with each data point representing the number of mice per cohort used in each experiment. *In-vivo* experiments were repeated twice, and *in-vitro* experiments were repeated three times. Statistical significance was determined using an unpaired Student's t-test.

We next investigated the molecular mechanism through which PD-1 suppresses proliferation in ILC subsets. Recent studies have demonstrated that PD-1 alters the metabolic phenotype of T cells (Patsoukis et al., 2015) and myeloid cells (Strauss et al., 2020), with PD-1-mediated metabolic regulation of myeloid cells in the TME shown to enhance anti-tumour responses. Additionally, PD-1 has been implicated in modulating ILC2 metabolism during allergic inflammation (Helou et al., 2020). Consistent with these findings, we observed that PD-1 significantly regulated fatty acid metabolism and glycolysis in WT mice (**Figure 5.8a-d**). To further explore metabolic changes at a single-cell level, we examined the metabolic signatures of WT and *Pd1*$^{-/-}$ ILC populations within the TME. Notably, *Pd1*$^{-/-}$ type I ILCs from cluster 10 had significantly reduced *Apoe* transcript levels compared to WT cohorts (**Figure 5.8e**). Further analysis of *Apoe* expression in PD-1^{+} and PD-1^{-} cells from cluster 10 confirmed that *Apo*e expression was predominantly restricted to PD-1^{+} cells (**Figure 5.8f**). In line with increased glycolysis, PD-1 deficiency also increased mTOR signalling in Tbet^{+}NK1.1^{-} ILC TILs within the B16 TME, as indicated by increased phosphorylation of p70S6K (**Figure 5.8g-h**). This molecular mechanism was further validated in WT Tbet^{+} ILC TILs whereby PD-1 blockade similarly enhanced mTOR signalling and p70S6K phosphorylation (**Figure 5.8i-j)**. Taken together, these findings suggest a molecular mechanism by which PD-1 regulates ILCs within the TME. Depending on the prevailing alarmins, PD-1 expression is induced in specific ILC subsets (exogenous IL-33 in ILC2s and melanoma-derived lactate in Tbet^{+}NK1.1^{-} ILCs). PD-1 blockade enhances ILC proliferative capacity by promoting glycolysis and upregulating the mTOR signalling pathway, thereby shaping their metabolic and functional responses within the TME.

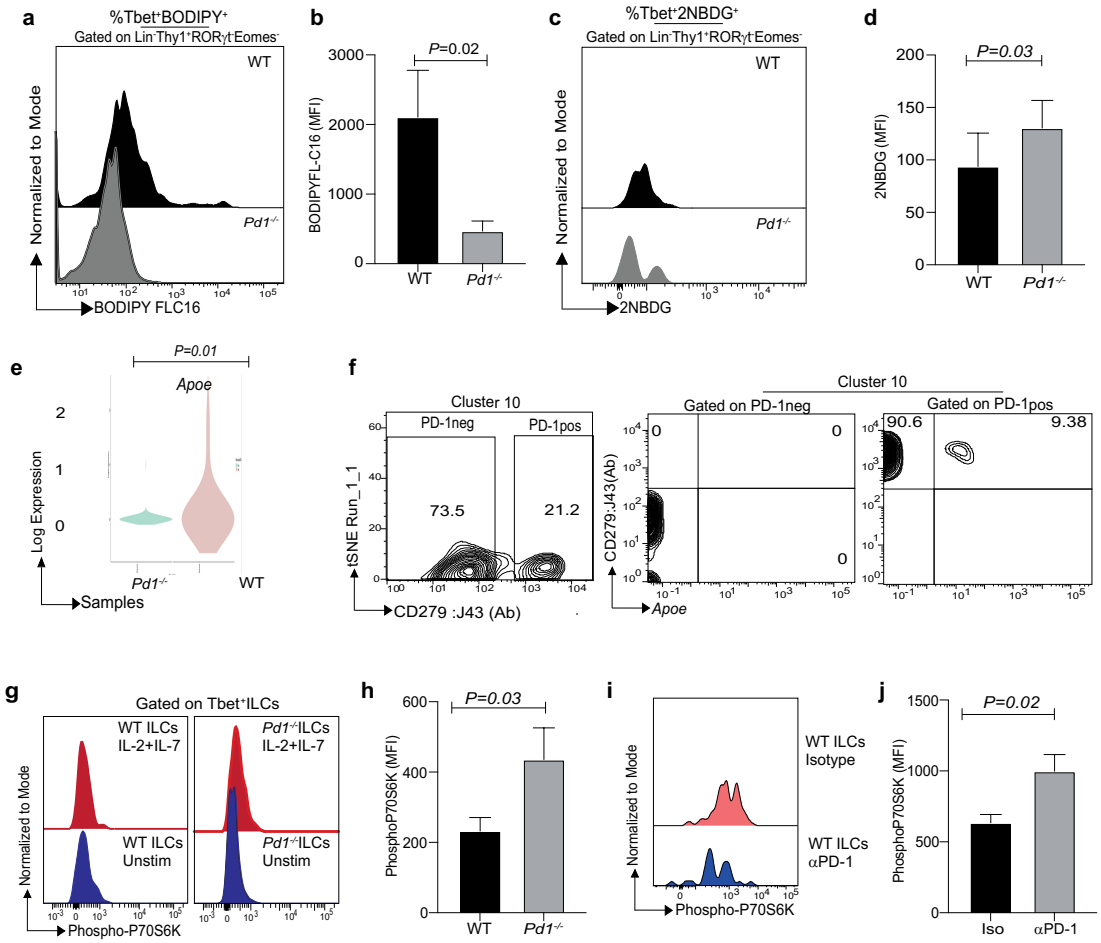

Figure 5.8 PD-1 deficiency significantly enhances fatty acid metabolism and glycolysis in Tbet^{+}NK1.1^{-} ILCs within the B16 melanoma TME.
WT TBG or *Pd1*$^{-/-}$ TBG mice were reconstituted with B16 melanoma cells via subcutaneous injection. On day 14, TILs were harvested. **A-B,** MFI of BODIPY (4,4-difluoro-5,7-dimethyl-4-bora-3a,4a-diaza-s-indacene-3-hexadecanoic acid) indicating fatty acid uptake in WT and *Pd1*$^{-/-}$ Tbet^{+}NK1.1^{-} ILCs (n = 5, paired one-tailed Student's *t*-test). **C-D**, 2NBDG uptake reflecting glucose metabolism in WT and *Pd1*$^{-/-}$ Tbet^{+}NK1.1^{-} ILCs (n = 4, paired one-tailed Student's *t*-test). **E**, *Apoe* gene expression in WT and *Pd1*$^{-/-}$ Tbet^{+}NK1.1^{-} ILCs within the TME. **F**, scRNA-seq contour plot showing the gating strategy for *Apoe* transcript levels in PD-1^{-} (PD-1neg) and PD-1^{+} (PD-1pos) subsets within Cluster 10 (Tbet^{+}NK1.1^{-} ILCs) in the TME. **G-H**, TILs were harvested and cultured with IL-2 and IL-7 for 15 min, followed by measurement of phosphoP70S6Kinase (phospho-P70S6K) (n = 4, paired one-tailed Student's *t*-test). **I-J**, WT TILs were stimulated for 3 d with either an isotype control or anti-PD-1 antibody (αPD-1). On day 3, TILs were stimulated with IL-2 and IL-7 for 15 min, and phospho-P70S6K levels were measured (n = 3, paired one-tailed Student's *t*-test). Data shown are mean±SEM.

5.4 Discussion

Anti-PD-1-based immunotherapies have shown remarkable effect in treatment of multiple cancers including melanoma, bladder cancer, lung cancer and Hodgkin lymphoma. The current paradigm dictates that anti-PD-1 therapies are able to rejuvenate exhausted

cytotoxic $CD8^+$ T cell by blocking engagement of $PD\text{-}1^+$ cytotoxic T cell from $PD\text{-}L1^+$ tumour cells within the TME, which in turn induces robust anti-tumour immunity. Recent studies demonstrated that PD-1 blockade can also enhance anti-tumour property of innate immune cells including NK cells and myeloid cells within the TME (Hsu et al., 2018, Gordon et al., 2017). Evidence that PD-1 can be expressed on innate immune cells including ILCs implicate the possible use of PD-1 checkpoint inhibitors in eliciting tissue-mediated immunity within the TME impoverished in inflammatory infiltrates. This is further confirmed by reports demonstrating that PD-1 blockade can enhance anti-tumour effects of IL-33 primed ILC2 in pancreatic and metastatic TME (Moral et al., 2020, Jacquelot et al., 2021).

Since numerous studies demonstrate that all helper-like ILCs can elicit both pro- and anti-tumorigenic activity, the role of ILCs in tumour biology have remained controversial. Moreover, whether ILCs participate in the clinical benefit of checkpoint inhibitors are not known. Here, we found a previously undefined ILC subset, defined as $Tbet^+NK1.1^-$ ILCs, which can be specifically regulated by PD-1 within the TME. PD-1 expression was noted on $Tbet^+NK1.1^-$ ILCs and PD-1 deficiency specifically enhanced frequency of $Tbet^+NK1.1^-$ ILCs in the melanoma TME. $Tbet^+NK1.1^-$ ILCs possess type 1 signature and PD-1/PD-L1 signalling in this ILC subpopulation can dampen its anti-tumour properties in the TME.
The anti-tumour properties of ILC2s against B16 has been extensively reported (Saranchova et al., 2018b, Wagner et al., 2020, Kim et al., 2016, Long et al., 2018). However, these reports have consistently shown the function of ILC2 within the context of exogenous IL-33 addition and whether PD-1 can regulate ILCs in the absence of the exogenous cytokines is not known. Here, using a single-cell approach on experimental murine models, we found that PD-1-deficient mice had significantly a greater number of $Tbet^+NK1.1^-$ ILC in various TMEs including B16. Of note, this ILC population was found in both WT and PD-1-deficient mice in similar frequency within steady state. Taken together, these data demonstrate that although healthy tissues are enriched in different ILC subsets, when perturbed with tumour, anti-PD-1 treatment can expand $Tbet^+NK1.1^-$ ILC in different tumour types which in turn enhance IFN-γ production. These data also propose the possibility of uniform treatment strategies for multiple solid cancers which are not enriched for inflammatory infiltrates whereby anti-PD-1 immunotherapy could be administered to boost anti-tumour responses of tissue resident $Tbet^+NK1.1^-$ ILC which possesses an immune type 1 phenotype.

Our previous study on host-pathogen responses (Taylor et al., 2017) showed different immune dynamics compared to melanoma, where ILC2 numbers are significantly reduced due to elevated lactate production (Wagner et al., 2020). This immunosuppressive effect exerted by melanoma can be mitigated through IL-33 administration (Wagner et al., 2020). Additionally, a combination of PD-1 blockade and exogenous IL-33 has been shown to boost ILC2-driven chemokine secretion, facilitating DC recruitment and consequently enhancing $CD8^+$ T cell responses in pancreatic cancer (Moral et al., 2020). Herein lies the importance of our current study which specifically investigates how PD-1 regulates $Tbet^+NK1.1^-$ ILCs within the TME. By uncoupling the effect of PD-1 and exogenous IL-33, our findings reveal that PD-1 selectively regulates $Tbet^+NK1.1^-$ ILC within the TME. The molecular mechanism by which PD-1 regulates $Tbet^+NK1.1^-$ ILC populations within the TME remains unknown. Our findings reveal a unique expression pattern of PD-1 on ILCs, where its expression is restricted to TME-resident ILCs and absent in the surrounding normal skin. Furthermore, within the TME, PD-1 expression is selectively upregulated on $Tbet^+NK1.1^-$ ILCs, suggesting that tumour-derived factors drive immune activation within the TME, leading to PD-1 expression (Kumagai et al., 2022). Consistent with previous studies (Wagner et al., 2020, Kumagai et al., 2022), we found that lactate, a metabolic byproduct of tumour cells, induces PD-1 expression on $Tbet^+NK1.1^-$ ILCs. Blocking PD-1 specifically enhanced proliferation of $Tbet^+NK1.1^-$ ILC in *in vivo* murine tumour models. These findings uncover a novel tumour-driven immune evasion mechanism in which lactate promotes PD-1 expression, thereby inhibiting $Tbet^+NK1.1^-$ ILC-mediated anti-tumour responses. We propose that, consistent with tumour-infiltrating Tregs, tumour-associated ILCs metabolize LA into phosphoenolpyruvate, which subsequently increases cytoplasmic calcium ion concentration. This rise in calcium levels facilitates NFAT translocation into the nucleus, where it may enhance PD-1 expression (Kumagai et al., 2022).

We next investigated whether the proliferation of $Tbet^+NK1.1^-$ ILCs is regulated by PD-1-mediated metabolic control. In line with established ILC2 biology (Wilhelm et al., 2016), we found that within the TME, $Tbet^+NK1.1^-$ ILCs primarily rely on fatty acid oxidation (FAO) to meet their metabolic demands. However, in the absence of PD-1, FAO was significantly downregulated, accompanied by a metabolic shift toward glycolysis, mirroring metabolic adaptions observed in ILC2s (Helou et al., 2020). Our findings align with previous reports on PD-1's role in T-cell metabolism (Patsoukis et al., 2015) and ILC2 function. Wilhelm et al. first described that ILC2s predominantly depend on FAO, with its

inhibition impairing their effector functions. Subsequent study (Helou et al., 2020) in airway hyperreactivity models demonstrated that PD-1 deficiency leads to enhanced aerobic glycolysis in ILC2s upon IL-33 stimulation, accompanied by increased amino acid catabolism, including glutamine and methionine degradation, which supports ILC proliferation. Notably, similar metabolic adaptations in tumour-associated ILC2s (Moral et al., 2020, Jacquelot et al., 2021) were evident only under IL-33 priming, suggesting that IL-25 and TSLP (other ILC2 alarmins) may not induce the same metabolic reprogramming in PD-1-deficient ILC2s. This distinction highlights the need for further investigation into how different alarmins shape ILC metabolism in the absence of PD-1. A key limitation of studies relying on exogenous IL-33 is that they may primarily reflect the effects of IL-33-PD-1 interactions, rather than capturing PD-1's broader role in activated ILCs within the tumour or tissue microenvironment. Our study overcomes this limitation by demonstrating a tumour-intrinsic role for PD-1 in regulating $Tbet^{+}NK1.1^{-}$ ILC metabolism in response to tumour-derived alarmins. Specifically, we show that PD-1 intrinsically modulates the metabolic switch in $Tbet^{+}NK1.1^{-}$ ILCs within the TME, leading to increased mTOR pathway activation. Importantly, our findings reveal a tumour-driven mechanism in which PD-1, induced by tumour-derived lactate, selectively suppresses $Tbet^{+}NK1.1^{-}$ ILC proliferation through metabolic reprogramming.

Although the presence of and expression of coinhibitory receptors ILC1s in tumour has been characterised in multiple studies, the role of ILC1 acting as pro- or anti-tumorigenic is still difficult to discern due to its heterogeneity. The three most significant caveats in this field are as follows: 1) Transcriptomes rarely correlate well with proteomes (for example: Tbet protein which define a type 1 function in both innate and adaptive immune cells), 2) most ILC1 identification are restricted to surface receptor proteins including CD49, c-kit, CRTH2, CD5, and CD127 in both mice and humans, and 3) despite co-inhibitory receptor expression was analysed, none of the studies demonstrate whether the co-inhibitory receptors are co-expressed with Tbet or render a functional change to the ILC subsets. We have tried to resolve some of these issues in this work by identifying ILCs based on existing literature but with further analysis of Tbet protein co-expression with PD-1 protein via BD Rhapsody scRNA-seq and flow cytometry analysis. In parallel, we also revealed the presence of a type 1 ILC population in human cutaneous squamous cell carcinoma (cSCC) similar to our murine study (Lim et al., 2023). This type 1 ILC population can be characterised as $CRTH2^{-}CD117^{-}CD127^{+}Tbet^{+}$ and is regulated by PD-1. Of note, this population is characteristically divergent from the one described in cSCC by Luci et al.

(Luci et al., 2021), based on CD56 and Tbet expression and its responsiveness towards anti-PD-1 immunotherapy. Consequently, we have found and defined a PD-1-dependent ILC subset participating in anti-tumour immunity.

5.5 Summary

In summary, these results demonstrate that PD-1 can control the anti-tumour function of $Tbet^{+}NK1.1^{-}$ ILCs by regulating its frequency and IFN-γ production within the tumour micro-environment. Despite these data, it still remains to be deciphered to what extent this ILC subset can be harnessed for enhancing anti-tumour responses by using anti-PD-1 immunotherapy. In any case, this study clearly highlights the importance of understanding the regulatory function of PD-1 in ILC subsets to fully harness the potential of PD-1 in modulating immune responses through ILC biology.

Chapter 6 Discussion

The role of PD-1 in negative regulation of T cell responses was initially discovered in late 1990s (Agata et al., 1996, Nishimura et al., 1999, Nishimura et al., 2001, Okazaki et al., 2001). Since then, the development of anti-PD-1 monoclonal antibodies (mAbs), nivolumab and pembrolizumab, revolutionised the treatment of human cancers(Baumeister et al., 2016, Ribas and Wolchok, 2018, Chamoto et al., 2020) including malignant melanoma. The central premise of anti-PD-1 mAbs suggest that these interventions act in the TME by blocking interaction of PD-1 on $CD8^+$ T cells with PD-L1 on tumour cells, promoting the expansion and differentiation of anti-tumour $CD8^+$ T cells (Ribas and Wolchok, 2018, Arlauckas et al., 2017, Garris et al., 2018, Oh et al., 2020, Peng et al., 2020, Waldman et al., 2020). Despite a significant clinical benefit of PD-1 inhibitors in melanoma patients (Larkin et al., 2015), a substantial proportion of advanced melanoma patients either fail to response, develop hyper-progressive disease or acquire resistance to anti-PD-1 therapy (Topalian et al., 2012, Hamid et al., 2013, Robert et al., 2015a, Robert et al., 2015b). The mechanisms underlying this resistance remain unclear, with no reliable biomarkers currently available for predicting treatment failure. Recent study (Kamada et al., 2019) suggest that tumour-associated Tregs may contribute to immune resistance following anti-PD-1 therapy.

Current literatures highlight both positive (Amarnath et al., 2011, Kim et al., 2023, Stathopoulou et al., 2018) and negative (Tan et al., 2021, van Gulijk et al., 2023, Perry et al., 2022, Chen et al., 2014) roles of PD-1 in Tregs with a lack of consensus on its role in driving Treg function, which could be due to the lack of unbiased analysis of $Pd1^{-/-}$ Tregs in steady state and TME. To address these discrepancies, Tregs from PD-1-deficient mice were characterised and the importance of PD-1 in Treg suppressive function was assessed in both *in vitro* and *in vivo* studies. These experiments showed that $Pd1^{-/-}$ mice had greater number of Tregs compared to WT mice, which was mainly attributed to an increase in effector-like Treg populations. *In vitro*, $Pd1^{-/-}$ Tregs exhibited enhanced suppressive capacity compared to WT Tregs. *In vivo*, $Rag1^{-/-}$ mice reconstituted with $Pd1^{-/-}$ Tregs exhibited greater melanoma tumour burden compared to those mice receiving WT Tregs.
From here, we hypothesised that the superior function of $Pd1^{-/-}$ Tregs could be rendered through increase in the expression of alternative co-receptors. This hypothesis was reinforced by using $Foxp3^{Ert2CreHet}Pd1^{fl/fl}$ mice where it was shown that CD30 was dominantly upregulated in $Pd1^{-/-}$ Tregs compared to PD-1^+ Tregs, suggesting an intrinsic

regulation of CD30 by PD-1 in steady state. By using B16F10 melanoma bearing *Pd1*$^{-/-}$ mice and *Pd1*$^{fl/fl}$*Foxp3*^{ERT2Cre} mice, upregulation of CD30 transcript and protein was further confirmed and found to be restricted on *Pd1*$^{-/-}$ Tregs. Treatment of *Rag1*$^{-/-}$ mice reconstituted with Teff cells and *Pd1*$^{-/-}$ Tregs with CD30/CD30L blockade led to significantly reduction in tumour burden with preserved Treg numbers within the TME which was not corroborated in previous study (Gaspal et al., 2011). Collectively, our work offers a novel combination therapy of anti-PD-1 and anti-CD30 towards PD-1 refractory melanoma patients who have enriched Treg numbers post-PD-1 therapy. Similar to our work, recent report has shown that ICOS can replace PD-1 and enhance Treg function (Geels et al., 2024, McGee et al., 2022). Hence, our observation is similar to recently published work on how other coreceptors can enhance Treg function in the absence of PD-1.

Having established that PD-1 can affect Treg and ILC plasticity in the TME (Kim et al., 2023, Lim et al., 2023, Helou et al., 2020), the effect of PD-1 towards Treg differentiation and communication programme in TME was then investigated. Pseudotime trajectory analysis revealed several differentiation states in *Pd1-/-* Tregs compared to WT Tregs, highlighting the importance of PD-1 in regulation of Treg functional plasticity (Kim et al., 2023) and thus function within the TME. We noted *Pd1-/-* Tregs contained type 1 differentiation state and high immunosuppressive state expressing TNFRs and IL10, which were not found in WT Tregs. Therefore, we conclude that PD-1 controls the development of Tregs with type 1 phenotype and immune regulatory phenotype, aligning with our previous work (Amarnath et al., 2011) and recently published work (Lim et al., 2023). Our spatial analysis further validated the presence of these Treg differentiation states within the TME, with *Pd1*$^{-/-}$ Treg expressing TNFR and IL-10 being the most predominant tumour-interacting and immunosuppressive subset. This suggests that the potential of this particular Treg subset may contribute to anti-PD-1 resistance in melanoma. These findings help resolve inconsistencies in Treg characterisation, demonstrating that multiple Treg states with distinct functions and phenotypes exist in the TME in the absence of PD-1. Traditional suspension flow cytometry of TILs often categorises Tregs as either functional or dysfunctional, whereas our study underscores the value of spatial transcriptomics in identifying tumour-associated Treg subsets and their role in tumour regulation. While Tregs are highly dynamic within the TME and our spatial analysis provides key insights into their distribution and interactions over time, it does not fully capture the complexity of Treg

function. Nevertheless, it enables the visualisation of Treg subsets in relation to tumour growth, offering a more comprehensive perspective on their spatial and temporal dynamics. Based on CellChat and spatial analysis, the enhanced crosstalk of *Pd1*$^{-/-}$ Tregs was identified with myeloid DCs and NK cells being the two most Treg-interacting cell types, suggesting that interaction of *Pd1*$^{-/-}$ Tregs with NK cells and myeloid DCs may affect Teff cell function within the TME. Overall, our work demonstrates that PD-1-deficient Tregs could be more amenable to functional plasticity and at the same time enhance immune suppressive function within the TME based on their communication programs. However, while computational predictions provide valuable insights, they require functional validation. Our melanoma experiments in the *Pd1*$^{fl/fl}$*Foxp3*^{ERT2Cre} mice further address this problem whereby we saw a differential frequency in DCs and NK cells within the TME. Again, it should be noted that whether these observations are an outcome of direct Treg-DC or Treg-NK interactions or indirectly through other immune cells. *In-vitro* experiments could clarify this but would not fully recapitulate the complexities of the TME, therefore was not utilised in this study.

In addition to the PI3K/Akt pathway (Francisco et al., 2009), PD-1 can downregulate STAT5 which is downstream of IL-2 receptor signalling in Tregs (Franceschini et al., 2009, Laba et al., 2022, Amarnath et al., 2011, Taylor et al., 2017). To assess whether PD-1 regulates CD30 expression, we first assessed the CD30 expression on isolated WT Tregs stimulated with rmPD-L1 Fc in the presence or absence of anti-PD-1. PD-1 blockade significantly enhanced CD30 expression in an IL-2-dependent manner, with *Pd1*$^{-/-}$ Tregs exhibiting an even greater CD30 fold change. By performing pSTAT5 assay, we found that PD-1 can inhibit STAT5 phosphorylation in IL-2 stimulated Tregs, which in turn suppressing CD30 expression. Next, based on our previously published ChIP-seq datasets (Villarino et al., 2022), we found that STAT5 binds to the CD30 gene locus and shared two sites with p300, suggesting positive regulatory role of STAT5 in CD30 expression. GSEA of our previously published RNA-seq dataset (Villarino et al., 2022) further confirmed CD30 as the most upregulated TNFRSF family member in IL-2-stimulated Tregs. Hence, we conclude that PD-1-mediated inhibition of IL-2/STAT5 signalling suppresses CD30 expression, highlighting a potential rationale for combination therapies targeting checkpoint receptors driven by IL-2 signalling.

Our findings in the murine melanoma model are consistent with those in melanoma patients, demonstrating that CD30 expression in Tregs is induced by anti-PD-1 blockade rather than by the TME. We further confirmed the persistence of the CD30-mediated Treg phenotype in human melanoma patients post PD-1/PD-L1 blockade, with CD30 being significantly upregulated in anti-PD-1-treated non-responders. Furthermore, we identified CD30 can be used as a biomarker for predicting survival not only in melanoma but also in other solid cancers such as squamous carcinoma and uveal melanoma, reinforcing its role as a predictive biomarker of survival in human cancers.

Similar to T cells, PD-1 expression was noted on activated ILC1, ILC2, ILC3 and LTi (Vacca et al., 2019, Oldenhove et al., 2018, Yu et al., 2016), proposing its role in regulation of ILC function. Previously, our group have shown that PD-1 can regulate ILC2 function by dampening ILC2 proliferation and cytokine production during parasitic helminth infections (Taylor et al., 2017). Recent studies have demonstrated an improved anti-tumour immunity associated with PD-1 blockade of IL-33 primed ILC2 in melanoma TME by enhancing chemokine production (Wagner et al., 2020). Despite that, the role of ILCs in promoting antitumour responses remains inconclusive since all helper-like ILCs have been elicited both pro and anti-tumorigenic functions within the literature (Wagner et al., 2020, Moral et al., 2020, Chan et al., 2014, Gao et al., 2017, Jovanovic et al., 2014, Li et al., 2014, Ikutani et al., 2012, Saranchova et al., 2018a, Kirchberger et al., 2013, Eisenring et al., 2010). In addition, whether these ILC populations can be harnessed by using anti-PD-1 treatment is unclear.

To understand the role of PD-1 on ILC subset in TME, TILs were isolated from B16F10 melanoma-bearing WT and *Pd1*$^{-/-}$ mice. By using single cell approach, we found a novel Tbet^{+}NK1.1^{-} ILC subset expressing PD-1 and possessing type 1 phenotype in the TME (Lim et al., 2023). Frequency of Tbet^{+}NK1.1^{-} ILC subset was significantly enhanced in the absence of PD-1. Such significant changes were also noted between WT and *Pd1*$^{-/-}$ mice in azoxymethane-dextran sodium sulphate (AOM-DSS) induced colorectal cancer and metastatic B16 melanoma model, accompanying with a significant reduction in tumour burden (Lim et al., 2023). From here, we hypothesised that PD-1 can regulate Tbet^{+}NK1.1^{-} ILC subset possessing anti-tumour phenotype. This hypothesis was reinforced by using *Rag*$^{-/-}$ mice established with B16 tumour. In line with previous study (Wagner et al., 2020), we found that NK cell depletion *Rag*$^{-/-}$ mice did not affect tumour progression, instead only

concomitant NK cell depletion and anti-PD-1 antibodies enhanced survival and reduced tumour volume of *Rag*$^{-/-}$ mice, highlighting partly the anti-tumour property of Tbet^{+}NK1.1^{-} ILCs (Lim et al., 2023). This was further confirmed by the loss of protection when ILCs were depleted in *Rag*$^{-/-}$ mice while other innate immune cell compartments retained (Lim et al., 2023). This observation appeared to conflict with published reports suggesting anti-PD-1 therapy in cancer treatment may function through NK cells or macrophage-dependent fashion (Gordon et al., 2017, Hsu et al., 2018).

Furthermore, we have shown that enhanced PD-1 expression is restricted to Tbet^{+} ILCs within the TME but not in other tissues, proposing that such situation could be attributed to the tumour-derived products activating the immune compartment. By performing transwell experiments, we found that lactate produced by tumour cells can induce PD-1 expression on Tbet^{+} ILCs (Lim et al., 2023) which is in line with previous studies (Wagner et al., 2020, Kumagai et al., 2022). PD-1 deficiency or blockade specifically enhanced proliferation of Tbet^{+} ILC in both *in vivo* murine and *in vitro* human tumour models (Lim et al., 2023). Our data demonstrate a new tumour-derived immune evasion program driven by lactate and PD-1 by which Tbet^{+} ILC driven anti-tumour responses are suppressed. We propose that consistent with tumour-derived Tregs, tumour-derived ILCs metabolise lactic acid into phosphoenolpyruvate which increases calcium ion concentration within the cytoplasm, thereby promoting NFAT translocation into the nucleus and could enhance the expression of PD-1 (Kumagai et al., 2022).

Our findings highlight a key role for PD-1 in regulating the metabolic switch of Tbet+ ILCs within the TME. Consistent with ILC2 biology (Wilhelm et al., 2016), we found that Tbet^{+}NK1.1^{-} ILCs primarily rely on FAO for their metabolic demands. However, in the absence of PD-1, this balance shifted towards increased glycolysis, mirroring PD-1's metabolic influence in ILC2s (Helou et al., 2020) and T cells (Patsoukis et al., 2015). While previous studies have shown that PD-1 loss enhances glycolysis and amino acid catabolism in IL-33-driven ILC2 activation (Moral et al., 2020, Jacquelot et al., 2021), our results emphasise that tumour-derived alarmins, rather than exogenous IL-33 alone, can induce similar metabolic reprogramming in Tbet^{+} ILCs. This distinction underscores the importance of PD-1 in modulating ILC metabolism within the TME. We further demonstrated that tumour-derived lactate upregulates PD-1 expression on Tbet^{+} ILCs, subsequently limiting their proliferative capacity by regulating glycolysis and the mTOR

pathway. Taken together, these findings provide mechanistic insight into how PD-1 restricts ILC expansion in tumours, reinforcing its role as a metabolic checkpoint in the TME.

In summary, by using unbiased analysis, this study comprehensively demonstrated the mechanistic insight into the functional role of PD-1 in both Tregs and $Tbet^{+}NK1.1^{-}$ ILCs in TME. This definitive report consolidates previous contradictory findings and highlights the critical need to understand regulatory function of PD-1 on Tregs and ILCs in order to fully harness the potential of anti-PD-1 therapy in boosting anti-tumour immunity and to avoid anti-PD-1 resistance concomitantly. The concept of reinvigorating anti-tumour activity of $CD8^{+}$ T cell and $Tbet^{+}NK1.1^{-}$ ILCs by using anti-PD-1 treatment, alongside depleting highly suppressive $CD30^{+}$ Tregs by using anti-CD30 treatment within the TME might aid in achieving this goal.

6.1 Future directions

Our study focused on the mechanisms occur within Treg and ILC after PD-1 blockade. However, several questions regarding the functional and molecular consequences of PD-1 deficiency in Tregs and ILCs remain to be explored.

One critical aspect requiring further investigation is the signalling output of CD30 in PD-1-deficient Tregs and its impact on their function and stability. To elucidate the downstream pathways activated by CD30 in the absence of PD-1 signalling, Tregs could be isolated from murine splenocytes or human PBMCs. Following stimulation and expansion, Tregs could be stimulated with IL-2 in combination with anti-PD-1 and/or anti-CD30 antibodies. Subsequent analysis of key downstream signalling proteins such as TNF receptor-associated factors (TRAF) and nuclear factor kappa-B (NF-κB), could be performed using techniques such as western blotting or flow cytometry. Investigating these molecular pathways could provide crucial insights into the role of CD30-mediated signalling in Tregs and its potential in modulating immune responses.

Furthermore, identifying novel NF-κB-specific targets within PD-1-deficient Tregs may offer a new therapeutic strategy to overcome anti-PD-1 resistance in melanoma. Understanding how CD30 signalling influences NF-κB activation and its downstream effects could pave the way for rational combination therapies designed to enhance Treg-

mediated immune regulation while overcoming immune evasion mechanisms employed by tumours.

Despite our data has shown valuable insights into the role of PD-1 in Tbet^{+} ILC regulation, the extent to which these cells can be leveraged to enhance anti-tumour responses through anti-PD-1 immunotherapy remains to be fully understood. Given their metabolic reprogramming in the absence of PD-1, future studies should explore whether modulating metabolic pathways in these cells can enhance their functionality within the TME. Additionally, determining how PD-1 blockade affects ILC crosstalk with other immune subsets, such as cytotoxic T cells and APCs, will be essential to fully understand their therapeutic potential. Exploring whether ILC subsets can be utilised as direct effector cells in tumour control or as modulators of broader immune responses could help guide the development of novel combinatory strategies to enhance the efficacy of immune checkpoint blockade.

Finally, future translational studies should focus on optimising therapeutic strategies involving CD30 and PD-1 blockade. A key question to address is whether a concomitant or sequential treatment schedule would be most effective in enhancing anti-tumour immunity. Additionally, determining the optimal frequency and dosing regimen of anti-CD30 therapy relative to anti-PD-1 therapy will be crucial for maximising therapeutic efficacy while minimising potential adverse effects. Answering these questions will be essential for refining combination immunotherapy strategies and improving clinical outcomes in melanoma patients.

References

ABDEL AZIZ, N., NONO, J. K., MPOTJE, T. & BROMBACHER, F. 2018. The Foxp3+ regulatory T-cell population requires IL-4Rα signaling to control inflammation during helminth infections. *PLoS biology,* 16**,** e2005850.

AFZALI, B., MITCHELL, P., LECHLER, R. I., JOHN, S. & LOMBARDI, G. 2010. Translational mini-review series on Th17 cells: induction of interleukin-17 production by regulatory T cells. *Clin Exp Immunol,* 159**,** 120-30.

AGATA, Y., KAWASAKI, A., NISHIMURA, H., ISHIDA, Y., TSUBATA, T., YAGITA, H. & HONJO, T. 1996. Expression of the PD-1 antigen on the surface of stimulated mouse T and B lymphocytes. *Int Immunol,* 8**,** 765-72.

AGGARWAL, V., WORKMAN, C. J. & VIGNALI, D. A. A. 2023. LAG-3 as the third checkpoint inhibitor. *Nat Immunol,* 24**,** 1415-1422.

AKIMOVA, T., BEIER, U. H., WANG, L., LEVINE, M. H. & HANCOCK, W. W. 2011. Helios expression is a marker of T cell activation and proliferation. *PloS one,* 6**,** e24226.

ALLAN, S. E., PASSERINI, L., BACCHETTA, R., CRELLIN, N., DAI, M., ORBAN, P. C., ZIEGLER, S. F., RONCAROLO, M. G. & LEVINGS, M. K. 2005. The role of 2 FOXP3 isoforms in the generation of human CD4+ Tregs. *J Clin Invest,* 115**,** 3276-84.

ALMEIDA, F. F. & BELZ, G. T. 2016. Innate lymphoid cells: models of plasticity for immune homeostasis and rapid responsiveness in protection. *Mucosal Immunology,* 9**,** 1103-1112.

ALOULOU, M., CARR, E. J., GADOR, M., BIGNON, A., LIBLAU, R. S., FAZILLEAU, N. & LINTERMAN, M. A. 2016. Follicular regulatory T cells can be specific for the immunizing antigen and derive from naive T cells. *Nature Communications,* 7**,** 10579.

AMARNATH, S. & BROWN, M. L. 2020. Harnessing proteases for T regulatory cell immunotherapy. *Eur J Immunol,* 50**,** 770-778.

AMARNATH, S., COSTANZO, C. M., MARIOTTI, J., ULLMAN, J. L., TELFORD, W. G., KAPOOR, V., RILEY, J. L., LEVINE, B. L., JUNE, C. H. & FONG, T. 2010. Regulatory T cells and human myeloid dendritic cells promote tolerance via programmed death ligand-1. *PLoS biology,* 8**,** e1000302.

AMARNATH, S., DONG, L., LI, J., WU, Y. & CHEN, W. 2007. Endogenous TGF-β activation by reactive oxygen species is key to Foxp3 induction in TCR-stimulated and HIV-1-infected human CD4+CD25-T cells. *Retrovirology,* 4**,** 57.

AMARNATH, S., LAURENCE, A., ZHU, N., CUNHA, R., ECKHAUS, M. A., TAYLOR, S., FOLEY, J. E., GHOSH, M., FELIZARDO, T. C. & FOWLER, D. H. 2017. Tbet is a critical modulator of FoxP3 expression in autoimmune graft-versus-host disease. *Haematologica,* 102**,** 1446-1456.

AMARNATH, S., MANGUS, C. W., WANG, J. C., WEI, F., HE, A., KAPOOR, V., FOLEY, J. E., MASSEY, P. R., FELIZARDO, T. C., RILEY, J. L., LEVINE, B. L., JUNE, C. H., MEDIN, J. A. & FOWLER, D. H. 2011. The PDL1-PD1 axis converts human TH1 cells into regulatory T cells. *Sci Transl Med,* 3**,** 111ra120.

AMé-THOMAS, P., LE PRIOL, J., YSSEL, H., CARON, G., PANGAULT, C., JEAN, R., MARTIN, N., MARAFIOTI, T., GAULARD, P., LAMY, T., FEST, T., SEMANA, G. & TARTE, K. 2012. Characterization of intratumoral follicular helper T cells in follicular lymphoma: role in the survival of malignant B cells. *Leukemia,* 26**,** 1053-63.

ANDREWS, L. P., SOMASUNDARAM, A., MOSKOVITZ, J. M., SZYMCZAK-WORKMAN, A. L., LIU, C., CILLO, A. R., LIN, H., NORMOLLE, D. P., MOYNIHAN, K. D., TANIUCHI, I., IRVINE, D. J., KIRKWOOD, J. M., LIPSON, E. J., FERRIS, R. L., BRUNO, T. C., WORKMAN, C. J. & VIGNALI, D. A. A. 2020. Resistance to PD1 blockade in the absence of metalloprotease-mediated LAG3 shedding. *Science Immunology,* 5**,** eabc2728.

ARLAUCKAS, S. P., GARRIS, C. S., KOHLER, R. H., KITAOKA, M., CUCCARESE, M. F., YANG, K. S., MILLER, M. A., CARLSON, J. C., FREEMAN, G. J. & ANTHONY, R. M. 2017. In vivo imaging reveals a tumor-associated macrophage–mediated resistance pathway in anti–PD-1 therapy. *Science translational medicine,* 9**,** eaal3604.

ARTERBERY, A. S., OSAFO-ADDO, A., AVITZUR, Y., CIARLEGLIO, M., DENG, Y., LOBRITTO, S. J., MARTINEZ, M., HAFLER, D. A., KLEINEWIETFELD, M. & EKONG, U. D. 2016. Production of Proinflammatory Cytokines by Monocytes in Liver-Transplanted Recipients with De Novo Autoimmune Hepatitis Is Enhanced and Induces TH1-like Regulatory T Cells. *J Immunol,* 196**,** 4040-51.

ASANO, M., TODA, M., SAKAGUCHI, N. & SAKAGUCHI, S. 1996. Autoimmune disease as a consequence of developmental abnormality of a T cell subpopulation. *J Exp Med,* 184**,** 387-96.

ASANO, T., MEGURI, Y., YOSHIOKA, T., KISHI, Y., IWAMOTO, M., NAKAMURA, M., SANDO, Y., YAGITA, H., KORETH, J., KIM, H. T., ALYEA, E. P., ARMAND, P., CUTLER, C. S., HO, V. T., ANTIN, J. H., SOIFFER, R. J., MAEDA, Y., TANIMOTO, M., RITZ, J. & MATSUOKA, K.-I. 2017. PD-1 modulates regulatory T-cell homeostasis during low-dose interleukin-2 therapy. *Blood,* 129**,** 2186-2197.

ASCHENBRENNER, K., D'CRUZ, L. M., VOLLMANN, E. H., HINTERBERGER, M., EMMERICH, J., SWEE, L. K., ROLINK, A. & KLEIN, L. 2007. Selection of Foxp3+ regulatory T cells specific for self antigen expressed and presented by Aire+ medullary thymic epithelial cells. *Nature immunology,* 8**,** 351-358.

ASCIERTO, P. A., LIPSON, E. J., DUMMER, R., LARKIN, J., LONG, G. V., SANBORN, R. E., CHIARION-SILENI, V., DRENO, B., DALLE, S., SCHADENDORF, D., CALLAHAN, M. K., NYAKAS, M., ATKINSON, V., GOMEZ-ROCA, C. A., YAMAZAKI, N., TAWBI, H. A., SARKIS, N., WARAD, D., DOLFI, S., MITRA, P., SURYAWANSHI, S. & GROB, J. J. 2023. Nivolumab and Relatlimab in Patients With Advanced Melanoma That Had Progressed on Anti-Programmed Death-1/Programmed Death Ligand 1 Therapy: Results From the Phase I/IIa RELATIVITY-020 Trial. *J Clin Oncol,* 41**,** 2724-2735.

ASCIERTO, P. A., MELERO, I., BHATIA, S., BONO, P., SANBORN, R. E., LIPSON, E. J., CALLAHAN, M. K., GAJEWSKI, T., GOMEZ-ROCA, C. A. & HODI, F. S. 2017. Initial efficacy of anti-lymphocyte activation gene-3 (anti–LAG-3; BMS-986016) in combination with nivolumab (nivo) in pts with melanoma (MEL) previously treated with anti–PD-1/PD-L1 therapy. American Society of Clinical Oncology.

AYALA, M. A. M., CAMPBELL, T. F., ZHANG, C., DAHAN, N., BOCKMAN, A., PRAKASH, V., FENG, L., SHER, T. & DUPAGE, M. 2023. CXCR3 expression in regulatory T cells drives interactions with type I dendritic cells in tumors to restrict CD8+ T cell antitumor immunity. *Immunity,* 56**,** 1613-1630. e5.

BAILEY-BUCKTROUT, S. L., MARTINEZ-LLORDELLA, M., ZHOU, X., ANTHONY, B., ROSENTHAL, W., LUCHE, H., FEHLING, H. J. & BLUESTONE, J. A. 2013. Self-antigen-driven activation induces instability of regulatory T cells during an inflammatory autoimmune response. *Immunity,* 39**,** 949-62.

BAL, S. M., BERNINK, J. H., NAGASAWA, M., GROOT, J., SHIKHAGAIE, M. M., GOLEBSKI, K., VAN DRUNEN, C. M., LUTTER, R., JONKERS, R. E. & HOMBRINK, P. 2016. IL-1β, IL-4 and IL-12 control the fate of group 2 innate lymphoid cells in human airway inflammation in the lungs. *Nature immunology,* 17**,** 636-645.

BARBER, D. L., WHERRY, E. J., MASOPUST, D., ZHU, B., ALLISON, J. P., SHARPE, A. H., FREEMAN, G. J. & AHMED, R. 2006. Restoring function in exhausted CD8 T cells during chronic viral infection. *Nature,* 439**,** 682-687.

BASU, S., GOLOVINA, T., MIKHEEVA, T., JUNE, C. H. & RILEY, J. L. 2008. Cutting edge: Foxp3-mediated induction of pim 2 allows human T regulatory cells to preferentially expand in rapamycin. *J Immunol,* 180**,** 5794-8.

BAUMEISTER, S. H., FREEMAN, G. J., DRANOFF, G. & SHARPE, A. H. 2016. Coinhibitory Pathways in Immunotherapy for Cancer. *Annu Rev Immunol,* 34**,** 539-73.

BEN-NERIAH, Y. 2002. Regulatory functions of ubiquitination in the immune system. *Nat Immunol,* 3**,** 20-6.

BENGTSSON, Å., JOHANSSON, C., LINDER, M. T., HALLDéN, G., VAN DER PLOEG, I. & SCHEYNIUS, A. 1995. Not only Th2 cells but also Th1 and Th0 cells express CD30 after activation. *Journal of Leucocyte Biology,* 58**,** 683-689.

BENNETT, C. L., CHRISTIE, J., RAMSDELL, F., BRUNKOW, M. E., FERGUSON, P. J., WHITESELL, L., KELLY, T. E., SAULSBURY, F. T., CHANCE, P. F. & OCHS, H. D. 2001. The immune dysregulation, polyendocrinopathy, enteropathy, X-linked syndrome (IPEX) is caused by mutations of FOXP3. *Nat Genet,* 27**,** 20-1.

BERIOU, G., COSTANTINO, C. M., ASHLEY, C. W., YANG, L., KUCHROO, V. K., BAECHER-ALLAN, C. & HAFLER, D. A. 2009. IL-17–producing human peripheral regulatory T cells retain suppressive function. *Blood,* 113**,** 4240-4249.

BERNINK, J. H., PETERS, C. P., MUNNEKE, M., TE VELDE, A. A., MEIJER, S. L., WEIJER, K., HREGGVIDSDOTTIR, H. S., HEINSBROEK, S. E., LEGRAND, N., BUSKENS, C. J., BEMELMAN, W. A., MJOSBERG, J. M. & SPITS, H. 2013. Human type 1 innate lymphoid cells accumulate in inflamed mucosal tissues. *Nat Immunol,* 14**,** 221-9.

BETTELLI, E., CARRIER, Y., GAO, W., KORN, T., STROM, T. B., OUKKA, M., WEINER, H. L. & KUCHROO, V. K. 2006. Reciprocal developmental pathways for the generation of pathogenic effector TH17 and regulatory T cells. *Nature,* 441**,** 235-238.

BOTTA, D., FULLER, M. J., MARQUEZ-LAGO, T. T., BACHUS, H., BRADLEY, J. E., WEINMANN, A. S., ZAJAC, A. J., RANDALL, T. D., LUND, F. E., LEóN, B. & BALLESTEROS-TATO, A. 2017. Dynamic regulation of T follicular regulatory cell responses by interleukin 2 during influenza infection. *Nature Immunology,* 18**,** 1249-1260.

BRAHMER, J. R., DRAKE, C. G., WOLLNER, I., POWDERLY, J. D., PICUS, J., SHARFMAN, W. H., STANKEVICH, E., PONS, A., SALAY, T. M. & MCMILLER, T. L. 2010. Phase I study of single-agent anti–programmed death-1 (MDX-1106) in refractory solid tumors: safety, clinical activity, pharmacodynamics, and immunologic correlates. *Journal of clinical oncology,* 28**,** 3167-3175.

BRUNET, J.-F., DENIZOT, F., LUCIANI, M.-F., ROUX-DOSSETO, M., SUZAN, M., MATTEI, M.-G. & GOLSTEIN, P. 1987. A new member of the immunoglobulin superfamily—CTLA-4. *Nature,* 328**,** 267-270.

BRUNKOW, M. E., JEFFERY, E. W., HJERRILD, K. A., PAEPER, B., CLARK, L. B., YASAYKO, S. A., WILKINSON, J. E., GALAS, D., ZIEGLER, S. F. &

RAMSDELL, F. 2001. Disruption of a new forkhead/winged-helix protein, scurfin, results in the fatal lymphoproliferative disorder of the scurfy mouse. *Nat Genet,* 27**,** 68-73.

BRUNNER, M. C., CHAMBERS, C. A., CHAN, F. K., HANKE, J., WINOTO, A. & ALLISON, J. P. 1999. CTLA-4-Mediated inhibition of early events of T cell proliferation. *J Immunol,* 162**,** 5813-20.

BUONOCORE, S., AHERN, P. P., UHLIG, H. H., IVANOV, II, LITTMAN, D. R., MALOY, K. J. & POWRIE, F. 2010. Innate lymphoid cells drive interleukin-23-dependent innate intestinal pathology. *Nature,* 464**,** 1371-5.

BURNET, F. M. 1970. The concept of immunological surveillance. *Prog Exp Tumor Res,* 13**,** 1-27.

BUSCH, W. 1868. Aus der Sitzung der medicinischen Section vom 13 November 1867. *Berl Klin Wochenschr,* 5**,** 137.

BUTTE, M. J., KEIR, M. E., PHAMDUY, T. B., SHARPE, A. H. & FREEMAN, G. J. 2007. Programmed death-1 ligand 1 interacts specifically with the B7-1 costimulatory molecule to inhibit T cell responses. *Immunity,* 27**,** 111-22.

CAMISASCHI, C., CASATI, C., RINI, F., PEREGO, M., DE FILIPPO, A., TRIEBEL, F., PARMIANI, G., BELLI, F., RIVOLTINI, L. & CASTELLI, C. 2010. LAG-3 Expression Defines a Subset of CD4⁺CD25^{high}Foxp3⁺ Regulatory T Cells That Are Expanded at Tumor Sites. *The Journal of Immunology,* 184**,** 6545-6551.

CELLA, M., FUCHS, A., VERMI, W., FACCHETTI, F., OTERO, K., LENNERZ, J. K., DOHERTY, J. M., MILLS, J. C. & COLONNA, M. 2009. A human natural killer cell subset provides an innate source of IL-22 for mucosal immunity. *Nature,* 457**,** 722-5.

CHA, Z., GU, H., ZANG, Y., WANG, Z., LI, J., HUANG, W., QIN, A., ZHU, L., TU, X., CHENG, N., SONG, H. & QIAN, B. 2018. The prevalence and function of CD4+CXCR5+Foxp3+ follicular regulatory T cells in diffuse large B cell lymphoma. *International Immunopharmacology,* 61**,** 132-139.

CHAMOTO, K., HATAE, R. & HONJO, T. 2020. Current issues and perspectives in PD-1 blockade cancer immunotherapy. *Int J Clin Oncol,* 25**,** 790-800.

CHAN, I. H., JAIN, R., TESSMER, M. S., GORMAN, D., MANGADU, R., SATHE, M., VIVES, F., MOON, C., PENAFLOR, E., TURNER, S., AYANOGLU, G., CHANG, C., BASHAM, B., MUMM, J. B., PIERCE, R. H., YEARLEY, J. H., MCCLANAHAN, T. K., PHILLIPS, J. H., CUA, D. J., BOWMAN, E. P., KASTELEIN, R. A. & LAFACE, D. 2014. Interleukin-23 is sufficient to induce rapid de novo gut tumorigenesis, independent of carcinogens, through activation of innate lymphoid cells. *Mucosal Immunol,* 7**,** 842-56.

CHANG, J. H., KIM, Y. J., HAN, S. H. & KANG, C. Y. 2009. IFN-γ-STAT1 signal regulates the differentiation of inducible Treg: Potential role for ROS-mediated apoptosis. *European journal of immunology,* 39**,** 1241-1251.

CHATILA, T. A., BLAESER, F., HO, N., LEDERMAN, H. M., VOULGAROPOULOS, C., HELMS, C. & BOWCOCK, A. M. 2000. JM2, encoding a fork head-related protein, is mutated in X-linked autoimmunity-allergic disregulation syndrome. *J Clin Invest,* 106**,** R75-81.

CHAUDHRY, A., RUDRA, D., TREUTING, P., SAMSTEIN, R. M., LIANG, Y., KAS, A. & RUDENSKY, A. Y. 2009. CD4+ regulatory T cells control TH17 responses in a Stat3-dependent manner. *Science,* 326**,** 986-91.

CHEMNITZ, J. M., PARRY, R. V., NICHOLS, K. E., JUNE, C. H. & RILEY, J. L. 2004. SHP-1 and SHP-2 associate with immunoreceptor tyrosine-based switch motif of programmed death 1 upon primary human T cell stimulation, but only receptor ligation prevents T cell activation. *J Immunol,* 173**,** 945-54.

CHEN, C.-C., KOBAYASHI, T., IIJIMA, K., HSU, F.-C. & KITA, H. 2017. IL-33 dysregulates regulatory T cells and impairs established immunologic tolerance in the lungs. *Journal of Allergy and Clinical Immunology,* 140**,** 1351-1363. e7.

CHEN, Q., KIM, Y. C., LAURENCE, A., PUNKOSDY, G. A. & SHEVACH, E. M. 2011. IL-2 controls the stability of Foxp3 expression in TGF-β–induced Foxp3+ T cells in vivo. *The Journal of Immunology,* 186**,** 6329-6337.

CHEN, W., JIN, W., HARDEGEN, N., LEI, K.-J., LI, L., MARINOS, N., MCGRADY, G. & WAHL, S. M. 2003. Conversion of peripheral CD4+ CD25− naive T cells to CD4+ CD25+ regulatory T cells by TGF-β induction of transcription factor Foxp3. *The Journal of experimental medicine,* 198**,** 1875-1886.

CHEN, X., DAS, R., KOMOROWSKI, R., BERES, A., HESSNER, M. J., MIHARA, M. & DROBYSKI, W. R. 2009. Blockade of interleukin-6 signaling augments regulatory T-cell reconstitution and attenuates the severity of graft-versus-host disease. *Blood, The Journal of the American Society of Hematology,* 114**,** 891-900.

CHEN, X., FOSCO, D., KLINE, D. E., MENG, L., NISHI, S., SAVAGE, P. A. & KLINE, J. 2014. PD-1 regulates extrathymic regulatory T-cell differentiation. *Eur J Immunol,* 44**,** 2603-16.

CHEN, Y., KUCHROO, V. K., INOBE, J.-I., HAFLER, D. A. & WEINER, H. L. 1994. Regulatory T cell clones induced by oral tolerance: suppression of autoimmune encephalomyelitis. *Science,* 265**,** 1237-1240.

CHEN, Z., BARBI, J., BU, S., YANG, H. Y., LI, Z., GAO, Y., JINASENA, D., FU, J., LIN, F., CHEN, C., ZHANG, J., YU, N., LI, X., SHAN, Z., NIE, J., GAO, Z., TIAN, H., LI, Y., YAO, Z., ZHENG, Y., PARK, B. V., PAN, Z., ZHANG, J., DANG, E., LI, Z., WANG, H., LUO, W., LI, L., SEMENZA, G. L., ZHENG, S. G., LOSER, K., TSUN, A., GREENE, M. I., PARDOLL, D. M., PAN, F. & LI, B. 2013. The ubiquitin ligase Stub1 negatively modulates regulatory T cell suppressive activity by promoting degradation of the transcription factor Foxp3. *Immunity,* 39**,** 272-85.

CHI, H. 2012. Regulation and function of mTOR signalling in T cell fate decisions. *Nature Reviews Immunology,* 12**,** 325-338.

CHU, T. H., BARAL, K., LABIT, E., ROSIN, N., SINHA, S., UMANSKY, D., ALZAHRANI, S., ARORA, R., CAO, L. & RANCOURT, D. 2022. Comparison of human skin‐and nerve‐derived Schwann cells reveals many similarities and subtle genomic and functional differences. *Glia,* 70**,** 2131-2156.

CHUNG, Y., TANAKA, S., CHU, F., NURIEVA, R. I., MARTINEZ, G. J., RAWAL, S., WANG, Y. H., LIM, H., REYNOLDS, J. M., ZHOU, X. H., FAN, H. M., LIU, Z. M., NEELAPU, S. S. & DONG, C. 2011. Follicular regulatory T cells expressing Foxp3 and Bcl-6 suppress germinal center reactions. *Nat Med,* 17**,** 983-8.

CHUNYANG, L., WANG, H. & WEI, B. 2013. PD-1 and CTLA-4 Mediated Inhibitory Signaling for T cell Exhaustion during Chronic Viral Infections. *Journal of Clinical & Cellular Immunology,* 01.

CLARKE, C., MADDEN, S. F., DOOLAN, P., AHERNE, S. T., JOYCE, H., O'DRISCOLL, L., GALLAGHER, W. M., HENNESSY, B. T., MORIARTY, M., CROWN, J., KENNEDY, S. & CLYNES, M. 2013. Correlating transcriptional networks to breast cancer survival: a large-scale coexpression analysis. *Carcinogenesis,* 34**,** 2300-8.

CLAY, S. L., BRAVO-BLAS, A., WALL, D. M., MACLEOD, M. K. & MILLING, S. W. 2020. Regulatory T cells control the dynamic and site-specific polarization of total CD4 T cells following Salmonella infection. *Mucosal immunology,* 13**,** 946-957.

CLAYTON, K. L., HAALAND, M. S., DOUGLAS-VAIL, M. B., MUJIB, S., CHEW, G. M., NDHLOVU, L. C. & OSTROWSKI, M. A. 2014. T cell Ig and mucin Domain–Containing protein 3 is recruited to the immune synapse, disrupts stable synapse formation, and associates with receptor phosphatases. *The Journal of Immunology,* 192**,** 782-791.

CLEMENT, R. L., DACCACHE, J., MOHAMMED, M. T., DIALLO, A., BLAZAR, B. R., KUCHROO, V. K., LOVITCH, S. B., SHARPE, A. H. & SAGE, P. T. 2019. Follicular regulatory T cells control humoral and allergic immunity by restraining early B cell responses. *Nature Immunology,* 20**,** 1360-1371.

COE, D., BEGOM, S., ADDEY, C., WHITE, M., DYSON, J. & CHAI, J.-G. 2010. Depletion of regulatory T cells by anti-GITR mAb as a novel mechanism for cancer immunotherapy. *Cancer Immunology, Immunotherapy,* 59**,** 1367-1377.

COHEN, A. D., SCHAER, D. A., LIU, C., LI, Y., HIRSCHHORN-CYMMERMAN, D., KIM, S. C., DIAB, A., RIZZUTO, G., DUAN, F. & PERALES, M. A. 2010. Agonist anti-GITR monoclonal antibody induces melanoma tumor immunity in mice by altering regulatory T cell stability and intra-tumor accumulation. *PloS one,* 5**,** e10436.

COLEY, W. B. 1893. *A preliminary note on the treatment of inoperable sarcoma by the toxic products of erysipelas*, Meriden Gravure Company.

COMITO, F., PAGANI, R., GRILLI, G., SPERANDI, F., ARDIZZONI, A. & MELOTTI, B. 2022. Emerging Novel Therapeutic Approaches for Treatment of Advanced Cutaneous Melanoma. *Cancers (Basel),* 14.

CORTEZ, V. S., ROBINETTE, M. L. & COLONNA, M. 2015. Innate lymphoid cells: new insights into function and development. *Current opinion in immunology,* 32**,** 71-77.

COWAN, J. E., JENKINSON, W. E. & ANDERSON, G. 2015. Thymus medulla fosters generation of natural Treg cells, invariant γδ T cells, and invariant NKT cells: what we learn from intrathymic migration. *European journal of immunology,* 45**,** 652-660.

CRELLIN, N. K., TRIFARI, S., KAPLAN, C. D., SATOH-TAKAYAMA, N., DI SANTO, J. P. & SPITS, H. 2010. Regulation of cytokine secretion in human CD127(+) LTi-like innate lymphoid cells by Toll-like receptor 2. *Immunity,* 33**,** 752-64.

CUENDE, J., LIéNART, S., DEDOBBELEER, O., VAN DER WONING, B., DE BOECK, G., STOCKIS, J., HUYGENS, C., COLAU, D., SOMJA, J., DELVENNE, P., HANNON, M., BARON, F., DUMOUTIER, L., RENAULD, J. C., DE HAARD, H., SAUNDERS, M., COULIE, P. G. & LUCAS, S. 2015. Monoclonal antibodies against GARP/TGF-β1 complexes inhibit the immunosuppressive activity of human regulatory T cells in vivo. *Sci Transl Med,* 7**,** 284ra56.

CUPEDO, T., CRELLIN, N. K., PAPAZIAN, N., ROMBOUTS, E. J., WEIJER, K., GROGAN, J. L., FIBBE, W. E., CORNELISSEN, J. J. & SPITS, H. 2009. Human fetal lymphoid tissue-inducer cells are interleukin 17-producing precursors to RORC+ CD127+ natural killer-like cells. *Nat Immunol,* 10**,** 66-74.

DADI, S., CHHANGAWALA, S., WHITLOCK, B. M., FRANKLIN, R. A., LUO, C. T., OH, S. A., TOURE, A., PRITYKIN, Y., HUSE, M. & LESLIE, C. S. 2016. Cancer immunosurveillance by tissue-resident innate lymphoid cells and innate-like T cells. *Cell,* 164**,** 365-377.

DANG, E. V., BARBI, J., YANG, H. Y., JINASENA, D., YU, H., ZHENG, Y., BORDMAN, Z., FU, J., KIM, Y., YEN, H. R., LUO, W., ZELLER, K., SHIMODA, L.,

TOPALIAN, S. L., SEMENZA, G. L., DANG, C. V., PARDOLL, D. M. & PAN, F. 2011. Control of T(H)17/T(reg) balance by hypoxia-inducible factor 1. *Cell,* 146**,** 772-84.

DANIEL, V., TROJAN, K. & OPELZ, G. 2016. Immunosuppressive drugs affect induction of IFNy+ Treg in vitro. *Human Immunology,* 77**,** 146-152.

DATTA, S. & SATTEN, G. A. 2005. Rank-Sum Tests for Clustered Data. *Journal of the American Statistical Association,* 100**,** 908-915.

DAUSSY, C., FAURE, F., MAYOL, K., VIEL, S., GASTEIGER, G., CHARRIER, E., BIENVENU, J., HENRY, T., DEBIEN, E., HASAN, U. A., MARVEL, J., YOH, K., TAKAHASHI, S., PRINZ, I., DE BERNARD, S., BUFFAT, L. & WALZER, T. 2014. T-bet and Eomes instruct the development of two distinct natural killer cell lineages in the liver and in the bone marrow. *J Exp Med,* 211**,** 563-77.

DAVIDSON, D., SCHRAVEN, B. & VEILLETTE, A. 2007. PAG-associated FynT regulates calcium signaling and promotes anergy in T lymphocytes. *Molecular and cellular biology,* 27**,** 1960-1973.

DE SOUSA, E. M. F., COLAK, S., BUIKHUISEN, J., KOSTER, J., CAMERON, K., DE JONG, J. H., TUYNMAN, J. B., PRASETYANTI, P. R., FESSLER, E., VAN DEN BERGH, S. P., RODERMOND, H., DEKKER, E., VAN DER LOOS, C. M., PALS, S. T., VAN DE VIJVER, M. J., VERSTEEG, R., RICHEL, D. J., VERMEULEN, L. & MEDEMA, J. P. 2011. Methylation of cancer-stem-cell-associated Wnt target genes predicts poor prognosis in colorectal cancer patients. *Cell Stem Cell,* 9**,** 476-85.

DE STREEL, G., BERTRAND, C., CHALON, N., LIéNART, S., BRICARD, O., LECOMTE, S., DEVREUX, J., GAIGNAGE, M., DE BOECK, G., MARIëN, L., VAN DE WALLE, I., VAN DER WONING, B., SAUNDERS, M., DE HAARD, H., VERMEERSCH, E., MAES, W., DECKMYN, H., COULIE, P. G., VAN BAREN, N. & LUCAS, S. 2020. Selective inhibition of TGF-β1 produced by GARP-expressing Tregs overcomes resistance to PD-1/PD-L1 blockade in cancer. *Nature Communications,* 11**,** 4545.

DEENICK, E. K. & MA, C. S. 2011. The regulation and role of T follicular helper cells in immunity. *Immunology,* 134**,** 361-367.

DENG, G., NAGAI, Y., XIAO, Y., LI, Z., DAI, S., OHTANI, T., BANHAM, A., LI, B., WU, S. L., HANCOCK, W., SAMANTA, A., ZHANG, H. & GREENE, M. I. 2015. Pim-2 Kinase Influences Regulatory T Cell Function and Stability by Mediating Foxp3 Protein N-terminal Phosphorylation. *J Biol Chem,* 290**,** 20211-20.

DING, R., YU, X., HU, Z., DONG, Y., HUANG, H., ZHANG, Y., HAN, Q., NI, Z. Y., ZHAO, R., YE, Y. & ZOU, Q. 2024. Lactate modulates RNA splicing to promote CTLA-4 expression in tumor-infiltrating regulatory T cells. *Immunity,* 57**,** 528-540.e6.

DING, Y., LI, J., YANG, P., LUO, B., WU, Q., ZAJAC, A. J., WILDNER, O., HSU, H.-C. & MOUNTZ, J. D. 2014. Interleukin-21 Promotes Germinal Center Reaction by Skewing the Follicular Regulatory T Cell to Follicular Helper T Cell Balance in Autoimmune BXD2 Mice. *Arthritis & Rheumatology,* 66**,** 2601-2612.

DOMINGUEZ-VILLAR, M., BAECHER-ALLAN, C. M. & HAFLER, D. A. 2011. Identification of T helper type 1-like, Foxp3+ regulatory T cells in human autoimmune disease. *Nat Med,* 17**,** 673-5.

DONG, H., STROME, S. E., SALOMAO, D. R., TAMURA, H., HIRANO, F., FLIES, D. B., ROCHE, P. C., LU, J., ZHU, G. & TAMADA, K. 2002. Tumor-associated B7-H1 promotes T-cell apoptosis: a potential mechanism of immune evasion. *Nature medicine,* 8**,** 793-800.

DOWNS-CANNER, S., BERKEY, S., DELGOFFE, G. M., EDWARDS, R. P., CURIEL, T., ODUNSI, K., BARTLETT, D. L. & OBERMAJER, N. 2017. Suppressive IL-17A(+)Foxp3(+) and ex-Th17 IL-17A(neg)Foxp3(+) T(reg) cells are a source of tumour-associated T(reg) cells. *Nat Commun,* 8**,** 14649.

DUCKETT, C. S., GEDRICH, R. W., GILFILLAN, M. C. & THOMPSON, C. B. 1997. Induction of nuclear factor κB by the CD30 receptor is mediated by TRAF1 and TRAF2. *Molecular and cellular biology,* 17**,** 1535-1542.

DUCKETT, C. S. & THOMPSON, C. B. 1997. CD30-dependent degradation of TRAF2: implications for negative regulation of TRAF signaling and the control of cell survival. *Genes & development,* 11**,** 2810-2821.

DURANT, L. R., MAKRIS, S., VOORBURG, C. M., LOEBBERMANN, J., JOHANSSON, C. & OPENSHAW, P. J. 2013. Regulatory T cells prevent Th2 immune responses and pulmonary eosinophilia during respiratory syncytial virus infection in mice. *Journal of virology,* 87**,** 10946-10954.

EISENRING, M., VOM BERG, J., KRISTIANSEN, G., SALLER, E. & BECHER, B. 2010. IL-12 initiates tumor rejection via lymphoid tissue-inducer cells bearing the natural cytotoxicity receptor NKp46. *Nat Immunol,* 11**,** 1030-8.

ESCHWEILER, S., CLARKE, J., RAMíREZ-SUáSTEGUI, C., PANWAR, B., MADRIGAL, A., CHEE, S. J., KARYDIS, I., WOO, E., ALZETANI, A., ELSHEIKH, S., HANLEY, C. J., THOMAS, G. J., FRIEDMANN, P. S., SANCHEZ-ELSNER, T., AY, F., OTTENSMEIER, C. H. & VIJAYANAND, P. 2021. Intratumoral follicular regulatory T cells curtail anti-PD-1 treatment efficacy. *Nature Immunology,* 22**,** 1052-1063.

ESPARZA, E. M., LINDSTEN, T., STOCKHAUSEN, J. M. & ARCH, R. H. 2006. Tumor necrosis factor receptor (TNFR)-associated factor 5 is a critical intermediate of costimulatory signaling pathways triggered by glucocorticoid-induced TNFR in T cells. *Journal of Biological Chemistry,* 281**,** 8559-8564.

FAUSTINO, L., FONSECA, D. M. D., TAKENAKA, M. C., MIROTTI, L., FLORSHEIM, E. B., GUERESCHI, M. G., SILVA, J. S., BASSO, A. S. & RUSSO, M. 2013. Regulatory T cells migrate to airways via CCR4 and attenuate the severity of airway allergic inflammation. *The Journal of Immunology,* 190**,** 2614-2621.

FDA, F. 2011. Approves New Treatment for a Type of Late-Stage Skin Cancer. *Media Release,* 25.

FENG, Y., ARVEY, A., CHINEN, T., VAN DER VEEKEN, J., GASTEIGER, G. & RUDENSKY, ALEXANDER Y. 2014. Control of the Inheritance of Regulatory T Cell Identity by a cis Element in the Foxp3 Locus. *Cell,* 158**,** 749-763.

FLOESS, S., FREYER, J., SIEWERT, C., BARON, U., OLEK, S., POLANSKY, J., SCHLAWE, K., CHANG, H.-D., BOPP, T. & SCHMITT, E. 2007. Epigenetic control of the foxp3 locus in regulatory T cells. *PLoS biology,* 5**,** e38.

FONTENOT, J. D., GAVIN, M. A. & RUDENSKY, A. Y. 2003. Foxp3 programs the development and function of CD4+CD25+ regulatory T cells. *Nature Immunology,* 4**,** 330-336.

FOURCADE, J., SUN, Z., CHAUVIN, J.-M., KA, M., DAVAR, D., PAGLIANO, O., WANG, H., SAADA, S., MENNA, C., AMIN, R., SANDER, C., KIRKWOOD, J. M., KORMAN, A. J. & ZAROUR, H. M. 2018. CD226 opposes TIGIT to disrupt Tregs in melanoma. *JCI Insight,* 3.

FRANCESCHINI, D., PAROLI, M., FRANCAVILLA, V., VIDETTA, M., MORRONE, S., LABBADIA, G., CERINO, A., MONDELLI, M. U. & BARNABA, V. 2009. PD-L1 negatively regulates CD4+ CD25+ Foxp3+ Tregs by limiting STAT-5

phosphorylation in patients chronically infected with HCV. *The Journal of clinical investigation,* 119**,** 551-564.

FRANCISCO, J. A., CERVENY, C. G., MEYER, D. L., MIXAN, B. J., KLUSSMAN, K., CHACE, D. F., REJNIAK, S. X., GORDON, K. A., DEBLANC, R. & TOKI, B. E. 2003. cAC10-vcMMAE, an anti-CD30–monomethyl auristatin E conjugate with potent and selective antitumor activity. *Blood,* 102**,** 1458-1465.

FRANCISCO, L. M., SALINAS, V. H., BROWN, K. E., VANGURI, V. K., FREEMAN, G. J., KUCHROO, V. K. & SHARPE, A. H. 2009. PD-L1 regulates the development, maintenance, and function of induced regulatory T cells. *Journal of Experimental Medicine,* 206**,** 3015-3029.

FREEMAN, G. J., LONG, A. J., IWAI, Y., BOURQUE, K., CHERNOVA, T., NISHIMURA, H., FITZ, L. J., MALENKOVICH, N., OKAZAKI, T., BYRNE, M. C., HORTON, H. F., FOUSER, L., CARTER, L., LING, V., BOWMAN, M. R., CARRENO, B. M., COLLINS, M., WOOD, C. R. & HONJO, T. 2000. Engagement of the Pd-1 Immunoinhibitory Receptor by a Novel B7 Family Member Leads to Negative Regulation of Lymphocyte Activation. *Journal of Experimental Medicine,* 192**,** 1027-1034.

FUCHS, A., VERMI, W., LEE, J. S., LONARDI, S., GILFILLAN, S., NEWBERRY, R. D., CELLA, M. & COLONNA, M. 2013. Intraepithelial type 1 innate lymphoid cells are a unique subset of IL-12- and IL-15-responsive IFN-gamma-producing cells. *Immunity,* 38**,** 769-81.

FUHRMAN, C. A., YEH, W. I., SEAY, H. R., SAIKUMAR LAKSHMI, P., CHOPRA, G., ZHANG, L., PERRY, D. J., MCCLYMONT, S. A., YADAV, M., LOPEZ, M. C., BAKER, H. V., ZHANG, Y., LI, Y., WHITLEY, M., VON SCHACK, D., ATKINSON, M. A., BLUESTONE, J. A. & BRUSKO, T. M. 2015. Divergent Phenotypes of Human Regulatory T Cells Expressing the Receptors TIGIT and CD226. *J Immunol,* 195**,** 145-55.

GAO, X., ZHU, Y., LI, G., HUANG, H., ZHANG, G., WANG, F., SUN, J., YANG, Q., ZHANG, X. & LU, B. 2012. TIM-3 expression characterizes regulatory T cells in tumor tissues and is associated with lung cancer progression. *PloS one,* 7**,** e30676.

GAO, Y., SOUZA-FONSECA-GUIMARAES, F., BALD, T., NG, S. S., YOUNG, A., NGIOW, S. F., RAUTELA, J., STRAUBE, J., WADDELL, N. & BLAKE, S. J. 2017. Tumor immunoevasion by the conversion of effector NK cells into type 1 innate lymphoid cells. *Nature immunology,* 18**,** 1004-1015.

GARRIS, C. S., ARLAUCKAS, S. P., KOHLER, R. H., TREFNY, M. P., GARREN, S., PIOT, C., ENGBLOM, C., PFIRSCHKE, C., SIWICKI, M. & GUNGABEESOON, J. 2018. Successful anti-PD-1 cancer immunotherapy requires T cell-dendritic cell crosstalk involving the cytokines IFN-γ and IL-12. *Immunity,* 49**,** 1148-1161. e7.

GASPAL, F., WITHERS, D., SAINI, M., BEKIARIS, V., MCCONNELL, F. M., WHITE, A., KHAN, M., YAGITA, H., WALKER, L. S., ANDERSON, G. & LANE, P. J. 2011. Abrogation of CD30 and OX40 signals prevents autoimmune disease in FoxP3-deficient mice. *J Exp Med,* 208**,** 1579-84.

GATO-CAñAS, M., ZUAZO, M., ARASANZ, H., IBAñEZ-VEA, M., LORENZO, L., FERNANDEZ-HINOJAL, G., VERA, R., SMERDOU, C., MARTISOVA, E. & AROZARENA, I. 2017. PDL1 signals through conserved sequence motifs to overcome interferon-mediated cytotoxicity. *Cell reports,* 20**,** 1818-1829.

GATTEI, V., DEGAN, M., GLOGHINI, A., DE IULIIS, A., IMPROTA, S., ROSSI, F. M., ALDINUCCI, D., PERIN, V., SERRAINO, D. & BABARE, R. 1997. CD30 ligand is frequently expressed in human hematopoietic malignancies of myeloid and

lymphoid origin. *Blood, The Journal of the American Society of Hematology,* 89**,** 2048-2059.

GAUTRON, A. S., DOMINGUEZ-VILLAR, M., DE MARCKEN, M. & HAFLER, D. A. 2014. Enhanced suppressor function of TIM-3+ FoxP3+ regulatory T cells. *European journal of immunology,* 44**,** 2703-2711.

GE, Z., ZHOU, G., CARRASCOSA, L. C., GAUSVIK, E., BOOR, P. P., NOORDAM, L., DOUKAS, M., POLAK, W. G., TERKIVATAN, T. & PAN, Q. 2021. TIGIT and PD1 co-blockade restores ex vivo functions of human tumor-infiltrating CD8+ T cells in hepatocellular carcinoma. *Cellular and molecular gastroenterology and hepatology,* 12**,** 443-464.

GEELS, S. N., MOSHENSKY, A., SOUSA, R. S., MURAT, C., BUSTOS, M. A., WALKER, B. L., SINGH, R., HARBOUR, S. N., GUTIERREZ, G., HWANG, M., MEMPEL, T. R., WEAVER, C. T., NIE, Q., HOON, D. S. B., GANESAN, A. K., OTHY, S. & MARANGONI, F. 2024. Interruption of the intratumor CD8⁺ T cell:Treg crosstalk improves the efficacy of PD-1 immunotherapy. *Cancer Cell,* 42**,** 1051-1066.e7.

GERLI, R., PITZALIS, C., BISTONI, O., FALINI, B., COSTANTINI, V., RUSSANO, A. & LUNARDI, C. 2000. CD30+ T cells in rheumatoid synovitis: mechanisms of recruitment and functional role. *The Journal of Immunology,* 164**,** 4399-4407.

GERMAIN, R. N. 2002. T-cell development and the CD4-CD8 lineage decision. *Nat Rev Immunol,* 2**,** 309-22.

GERSHON, R. K. & KONDO, K. 1970. Cell interactions in the induction of tolerance: the role of thymic lymphocytes. *Immunology,* 18**,** 723-737.

GIANCHECCHI, E. & FIERABRACCI, A. 2018. Inhibitory Receptors and Pathways of Lymphocytes: The Role of PD-1 in Treg Development and Their Involvement in Autoimmunity Onset and Cancer Progression. *Front Immunol,* 9**,** 2374.

GOCHER-DEMSKE, A. M., CUI, J., SZYMCZAK-WORKMAN, A. L., VIGNALI, K. M., LATINI, J. N., PIEKLO, G. P., KIMBALL, J. C., AVERY, L., CIPOLLA, E. M. & HUCKESTEIN, B. R. 2023. IFNγ-induction of TH1-like regulatory T cells controls antiviral responses. *Nature immunology,* 24**,** 841-854.

GONZALEZ-FIGUEROA, P., ROCO, J. A., PAPA, I., NúñEZ VILLACíS, L., STANLEY, M., LINTERMAN, M. A., DENT, A., CANETE, P. F. & VINUESA, C. G. 2021. Follicular regulatory T cells produce neuritin to regulate B cells. *Cell,* 184**,** 1775-1789.e19.

GORDON, S. R., MAUTE, R. L., DULKEN, B. W., HUTTER, G., GEORGE, B. M., MCCRACKEN, M. N., GUPTA, R., TSAI, J. M., SINHA, R., COREY, D., RING, A. M., CONNOLLY, A. J. & WEISSMAN, I. L. 2017. PD-1 expression by tumour-associated macrophages inhibits phagocytosis and tumour immunity. *Nature,* 545**,** 495-499.

GOTTSCHALK, R. A., CORSE, E. & ALLISON, J. P. 2012. Expression of Helios in peripherally induced Foxp3+ regulatory T cells. *J Immunol,* 188**,** 976-80.

GRAYDON, C. G., MOHIDEEN, S. & FOWKE, K. R. 2021. LAG3's Enigmatic Mechanism of Action. *Frontiers in Immunology,* 11.

GREEN, D. R., FLOOD, P. M. & GERSHON, R. K. 1983. Immunoregulatory T-cell pathways. *Annu Rev Immunol,* 1**,** 439-63.

GRUSS, H.-J., PINTO, A., GLOGHINI, A., WEHNES, E., WRIGHT, B., BOIANI, N., ALDINUCCI, D., GATTEI, V., ZAGONEL, V. & SMITH, C. A. 1996. CD30 ligand expression in nonmalignant and Hodgkin's disease-involved lymphoid tissues. *The American journal of pathology,* 149**,** 469.

GRUSS, H. J., DASILVA, N., HU, Z. B., UPHOFF, C. C., GOODWIN, R. G. & DREXLER, H. G. 1994. Expression and regulation of CD30 ligand and CD30 in human leukemia-lymphoma cell lines. *Leukemia,* 8**,** 2083-94.

GU-TRANTIEN, C. & WILLARD-GALLO, K. 2013. Tumor-infiltrating follicular helper T cells: The new kids on the block. *OncoImmunology,* 2**,** e26066.

GUO, Z., LIANG, H., XU, Y., LIU, L., REN, X., ZHANG, S., WEI, S. & XU, P. 2017. The Role of Circulating T Follicular Helper Cells and Regulatory Cells in Non-Small Cell Lung Cancer Patients. *Scandinavian Journal of Immunology,* 86**,** 107-112.

HALL, A. O. H., BEITING, D. P., TATO, C., JOHN, B., OLDENHOVE, G., LOMBANA, C. G., PRITCHARD, G. H., SILVER, J. S., BOULADOUX, N. & STUMHOFER, J. S. 2012. The cytokines interleukin 27 and interferon-γ promote distinct Treg cell populations required to limit infection-induced pathology. *Immunity,* 37**,** 511-523.

HALL, B. M., TRAN, G. T., ROBINSON, C. M. & HODGKINSON, S. J. 2015. Induction of antigen specific CD4+ CD25+ Foxp3+ T regulatory cells from naïve natural thymic derived T regulatory cells. *International Immunopharmacology,* 28**,** 875-886.

HALL, B. M., TRAN, G. T., VERMA, N. D., PLAIN, K. M., ROBINSON, C. M., NOMURA, M. & HODGKINSON, S. J. 2013. Do natural T regulatory cells become activated to antigen specific T regulatory cells in transplantation and in autoimmunity? *Frontiers in immunology,* 4**,** 208.

HAMANN, D., HILKENS, C., GROGAN, J. L., LENS, S., KAPSENBERG, M. L., YAZDANBAKHSH, M. & VAN LIER, R. 1996. CD30 expression does not discriminate between human Th1-and Th2-type T cells. *Journal of immunology (Baltimore, Md.: 1950),* 156**,** 1387-1391.

HAMID, O., ROBERT, C., DAUD, A., HODI, F. S., HWU, W. J., KEFFORD, R., WOLCHOK, J. D., HERSEY, P., JOSEPH, R. W., WEBER, J. S., DRONCA, R., GANGADHAR, T. C., PATNAIK, A., ZAROUR, H., JOSHUA, A. M., GERGICH, K., ELASSAISS-SCHAAP, J., ALGAZI, A., MATEUS, C., BOASBERG, P., TUMEH, P. C., CHMIELOWSKI, B., EBBINGHAUS, S. W., LI, X. N., KANG, S. P. & RIBAS, A. 2013. Safety and tumor responses with lambrolizumab (anti-PD-1) in melanoma. *N Engl J Med,* 369**,** 134-44.

HANNIER, S., TOURNIER, M., BISMUTH, G. & TRIEBEL, F. 1998. CD3/TCR complex-associated lymphocyte activation gene-3 molecules inhibit CD3/TCR signaling. *The Journal of Immunology,* 161**,** 4058-4065.

HE, S., BHATT, R., BROWN, C., BROWN, E. A., BUHR, D. L., CHANTRANUVATANA, K., DANAHER, P., DUNAWAY, D., GARRISON, R. G., GEISS, G., GREGORY, M. T., HOANG, M. L., KHAFIZOV, R., KILLINGBECK, E. E., KIM, D., KIM, T. K., KIM, Y., KLOCK, A., KORUKONDA, M., KUTCHMA, A., LEWIS, Z. R., LIANG, Y., NELSON, J. S., ONG, G. T., PERILLO, E. P., PHAN, J. C., PHAN-EVERSON, T., PIAZZA, E., RANE, T., REITZ, Z., RHODES, M., ROSENBLOOM, A., ROSS, D., SATO, H., WARDHANI, A. W., WILLIAMS-WIETZIKOSKI, C. A., WU, L. & BEECHEM, J. M. 2022. High-plex imaging of RNA and proteins at subcellular resolution in fixed tissue by spatial molecular imaging. *Nature Biotechnology,* 40**,** 1794-1806.

HEINHUIS, K. M., CARLINO, M., JOERGER, M., DI NICOLA, M., MENIAWY, T., ROTTEY, S., MORENO, V., GAZZAH, A., DELORD, J. P., PAZ-ARES, L., BRITSCHGI, C., SCHILDER, R. J., O'BYRNE, K., CURIGLIANO, G., ROMANO, E., PATAH, P., WANG, R., LIU, Y., BAJAJ, G. & SIU, L. L. 2020. Safety, Tolerability, and Potential Clinical Activity of a Glucocorticoid-Induced TNF Receptor-Related Protein Agonist Alone or in Combination With Nivolumab

for Patients With Advanced Solid Tumors: A Phase 1/2a Dose-Escalation and Cohort-Expansion Clinical Trial. *JAMA Oncol,* 6**,** 100-107.

HEINRICH, B., GERTZ, E. M., SCHAFFER, A. A., CRAIG, A., RUF, B., SUBRAMANYAM, V., MCVEY, J. C., DIGGS, L. P., HEINRICH, S., ROSATO, U., MA, C., YAN, C., HU, Y., ZHAO, Y., SHEN, T. W., KAPOOR, V., TELFORD, W., KLEINER, D. E., STOVROFF, M. K., DHANI, H. S., KANG, J., FISHBEIN, T., WANG, X. W., RUPPIN, E., KROEMER, A., GRETEN, T. F. & KORANGY, F. 2022. The tumour microenvironment shapes innate lymphoid cells in patients with hepatocellular carcinoma. *Gut,* 71**,** 1161-1175.

HELOU, D. G., SHAFIEI-JAHANI, P., LO, R., HOWARD, E., HURRELL, B. P., GALLE-TREGER, L., PAINTER, J. D., LEWIS, G., SOROOSH, P., SHARPE, A. H. & AKBARI, O. 2020. PD-1 pathway regulates ILC2 metabolism and PD-1 agonist treatment ameliorates airway hyperreactivity. *Nat Commun,* 11**,** 3998.

HIMMEL, M. E., MACDONALD, K. G., GARCIA, R. V., STEINER, T. S. & LEVINGS, M. K. 2013. Helios+ and Helios- cells coexist within the natural FOXP3+ T regulatory cell subset in humans. *J Immunol,* 190**,** 2001-8.

HODGE, D. R., XIAO, W., CLAUSEN, P. A., HEIDECKER, G., SZYF, M. & FARRAR, W. L. 2001. Interleukin-6 regulation of the human DNA methyltransferase (HDNMT) gene in human erythroleukemia cells. *Journal of Biological Chemistry,* 276**,** 39508-39511.

HORI, S., NOMURA, T. & SAKAGUCHI, S. 2003. Control of regulatory T cell development by the transcription factor Foxp3. *Science,* 299**,** 1057-61.

HORIE, R. & WATANABE, T. CD30: expression and function in health and disease. Seminars in immunology, 1998. Elsevier, 457-470.

HSU, J., HODGINS, J. J., MARATHE, M., NICOLAI, C. J., BOURGEOIS-DAIGNEAULT, M. C., TREVINO, T. N., AZIMI, C. S., SCHEER, A. K., RANDOLPH, H. E., THOMPSON, T. W., ZHANG, L., IANNELLO, A., MATHUR, N., JARDINE, K. E., KIRN, G. A., BELL, J. C., MCBURNEY, M. W., RAULET, D. H. & ARDOLINO, M. 2018. Contribution of NK cells to immunotherapy mediated by PD-1/PD-L1 blockade. *J Clin Invest,* 128**,** 4654-4668.

HSU, P.-L. & HSU, S.-M. 2000. Autocrine growth regulation of CD30 ligand in CD30-expressing Reed-Sternberg cells: distinction between Hodgkin's disease and anaplastic large cell lymphoma. *Laboratory investigation,* 80**,** 1111-1119.

HU, H., RUDD, C. E. & SCHNEIDER, H. 2001. Src kinases Fyn and Lck facilitate the accumulation of phosphorylated CTLA-4 and its association with PI-3 kinase in intracellular compartments of T-cells. *Biochem Biophys Res Commun,* 288**,** 573-8.

HUANG, C.-T., WORKMAN, C. J., FLIES, D., PAN, X., MARSON, A. L., ZHOU, G., HIPKISS, E. L., RAVI, S., KOWALSKI, J., LEVITSKY, H. I., POWELL, J. D., PARDOLL, D. M., DRAKE, C. G. & VIGNALI, D. A. A. 2004. Role of LAG-3 in Regulatory T Cells. *Immunity,* 21**,** 503-513.

HUANG, Y.-H., ZHU, C., KONDO, Y., ANDERSON, A. C., GANDHI, A., RUSSELL, A., DOUGAN, S. K., PETERSEN, B.-S., MELUM, E. & PERTEL, T. 2015. CEACAM1 regulates TIM-3-mediated tolerance and exhaustion. *Nature,* 517**,** 386-390.

HUBERT, F. X., KINKEL, S. A., DAVEY, G. M., PHIPSON, B., MUELLER, S. N., LISTON, A., PROIETTO, A. I., CANNON, P. Z., FOREHAN, S., SMYTH, G. K., WU, L., GOODNOW, C. C., CARBONE, F. R., SCOTT, H. S. & HEATH, W. R. 2011. Aire regulates the transfer of antigen from mTECs to dendritic cells for induction of thymic tolerance. *Blood,* 118**,** 2462-72.

HUEHN, J. & BEYER, M. Epigenetic and transcriptional control of Foxp3+ regulatory T cells. Seminars in immunology, 2015. Elsevier, 10-18.

HUGHES, T., BRIERCHECK, E. L., FREUD, A. G., TROTTA, R., MCCLORY, S., SCOVILLE, S. D., KELLER, K., DENG, Y., COLE, J. & HARRISON, N. 2014. The transcription factor AHR prevents the differentiation of a stage 3 innate lymphoid cell subset to natural killer cells. *Cell reports,* 8**,** 150-162.

HUI, E., CHEUNG, J., ZHU, J., SU, X., TAYLOR, M. J., WALLWEBER, H. A., SASMAL, D. K., HUANG, J., KIM, J. M. & MELLMAN, I. 2017. T cell costimulatory receptor CD28 is a primary target for PD-1–mediated inhibition. *Science,* 355**,** 1428-1433.

ICHIYAMA, K., YOSHIDA, H., WAKABAYASHI, Y., CHINEN, T., SAEKI, K., NAKAYA, M., TAKAESU, G., HORI, S., YOSHIMURA, A. & KOBAYASHI, T. 2008. Foxp3 inhibits RORgammat-mediated IL-17A mRNA transcription through direct interaction with RORgammat. *J Biol Chem,* 283**,** 17003-8.

IGARASHI, H., CAO, Y., IWAI, H., PIAO, J., KAMIMURA, Y., HASHIGUCHI, M., AMAGASA, T. & AZUMA, M. 2008. GITR ligand-costimulation activates effector and regulatory functions of CD4+ T cells. *Biochemical and Biophysical Research Communications,* 369**,** 1134-1138.

IGNEY, F. H., EBENHOCH, R., SCHIELE, F. & NAR, H. 2023. Anti-GARP Antibodies Inhibit Release of TGF-β by Regulatory T Cells via Different Modes of Action, but Do Not Influence Their Function In Vitro. *ImmunoHorizons,* 7**,** 200-212.

IKUTANI, M., YANAGIBASHI, T., OGASAWARA, M., TSUNEYAMA, K., YAMAMOTO, S., HATTORI, Y., KOURO, T., ITAKURA, A., NAGAI, Y. & TAKAKI, S. 2012. Identification of innate IL-5–producing cells and their role in lung eosinophil regulation and antitumor immunity. *The Journal of Immunology,* 188**,** 703-713.

IMANGULI, M. M., COWEN, E. W., ROSE, J., DHAMALA, S., SWAIM, W., LAFOND, S., YAGI, B., GRESS, R. E., PAVLETIC, S. Z. & HAKIM, F. T. 2014. Comparative analysis of FoxP3(+) regulatory T cells in the target tissues and blood in chronic graft versus host disease. *Leukemia,* 28**,** 2016-27.

ISHIDA, Y., AGATA, Y., SHIBAHARA, K. & HONJO, T. 1992. Induced expression of PD-1, a novel member of the immunoglobulin gene superfamily, upon programmed cell death. *The EMBO journal,* 11**,** 3887-3895.

ITOH, M., TAKAHASHI, T., SAKAGUCHI, N., KUNIYASU, Y., SHIMIZU, J., OTSUKA, F. & SAKAGUCHI, S. 1999. Thymus and autoimmunity: production of CD25+CD4+ naturally anergic and suppressive T cells as a key function of the thymus in maintaining immunologic self-tolerance. *J Immunol,* 162**,** 5317-26.

JABEEN, R., GOSWAMI, R., AWE, O., KULKARNI, A., NGUYEN, E. T., ATTENASIO, A., WALSH, D., OLSON, M. R., KIM, M. H., TEPPER, R. S., SUN, J., KIM, C. H., TAPAROWSKY, E. J., ZHOU, B. & KAPLAN, M. H. 2013. Th9 cell development requires a BATF-regulated transcriptional network. *J Clin Invest,* 123**,** 4641-53.

JACOB, T., ANNUSVER, K., CZARNEWSKI, P., DALESSANDRI, T., KALK, C., LEVRON, C. L., SANZ, N. C., KASTRITI, M. E., MIKKOLA, M. L. & RENDL, M. 2023. Molecular and spatial landmarks of early mouse skin development. *Developmental Cell,* 58**,** 2140-2162. e5.

JACQUELOT, N., SEILLET, C., WANG, M., PIZZOLLA, A., LIAO, Y., HEDIYEH-ZADEH, S., GRISARU-TAL, S., LOUIS, C., HUANG, Q., SCHREUDER, J., SOUZA-FONSECA-GUIMARAES, F., DE GRAAF, C. A., THIA, K., MACDONALD, S., CAMILLERI, M., LUONG, K., ZHANG, S., CHOPIN, M.,

MOLDEN-HAUER, T., NUTT, S. L., UMANSKY, V., CIRIC, B., GROOM, J. R., FOSTER, P. S., HANSBRO, P. M., MCKENZIE, A. N. J., GRAY, D. H. D., BEHREN, A., CEBON, J., VIVIER, E., WICKS, I. P., TRAPANI, J. A., MUNITZ, A., DAVIS, M. J., SHI, W., NEESON, P. J. & BELZ, G. T. 2021. Blockade of the co-inhibitory molecule PD-1 unleashes ILC2-dependent antitumor immunity in melanoma. *Nat Immunol,* 22**,** 851-864.

JANDL, C., LIU, S. M., CAñETE, P. F., WARREN, J., HUGHES, W. E., VOGELZANG, A., WEBSTER, K., CRAIG, M. E., UZEL, G., DENT, A., STEPENSKY, P., KELLER, B., WARNATZ, K., SPRENT, J. & KING, C. 2017. IL-21 restricts T follicular regulatory T cell proliferation through Bcl-6 mediated inhibition of responsiveness to IL-2. *Nature Communications,* 8**,** 14647.

JIANG, Y., LEE, M.-L. T., HE, X., ROSNER, B. & YAN, J. 2020. Wilcoxon rank-based tests for clustered data with R package clusrank. *Journal of Statistical Software,* 96**,** 1-26.

JIN, S., GUERRERO-JUAREZ, C. F., ZHANG, L., CHANG, I., RAMOS, R., KUAN, C. H., MYUNG, P., PLIKUS, M. V. & NIE, Q. 2021. Inference and analysis of cell-cell communication using CellChat. *Nat Commun,* 12**,** 1088.

JOHNSTON, J. A., KAWAMURA, M., KIRKEN, R. A., CHEN, Y. Q., BLAKE, T. B., SHIBUYA, K., ORTALDO, J. R., MCVICAR, D. W. & O'SHEA, J. J. 1994. Phosphorylation and activation of the Jak-3 Janus kinase in response to interleukin-2. *Nature,* 370**,** 151-3.

JOSEFOWICZ, S. Z., NIEC, R. E., KIM, H. Y., TREUTING, P., CHINEN, T., ZHENG, Y., UMETSU, D. T. & RUDENSKY, A. Y. 2012. Extrathymically generated regulatory T cells control mucosal TH2 inflammation. *Nature,* 482**,** 395-399.

JOVANOVIC, I. P., PEJNOVIC, N. N., RADOSAVLJEVIC, G. D., PANTIC, J. M., MILOVANOVIC, M. Z., ARSENIJEVIC, N. N. & LUKIC, M. L. 2014. Interleukin-33/ST2 axis promotes breast cancer growth and metastases by facilitating intratumoral accumulation of immunosuppressive and innate lymphoid cells. *Int J Cancer,* 134**,** 1669-82.

KALATHIL, S., LUGADE, A. A., MILLER, A., IYER, R. & THANAVALA, Y. 2013. Higher frequencies of GARP(+)CTLA-4(+)Foxp3(+) T regulatory cells and myeloid-derived suppressor cells in hepatocellular carcinoma patients are associated with impaired T-cell functionality. *Cancer Res,* 73**,** 2435-44.

KAMADA, T., TOGASHI, Y., TAY, C., HA, D., SASAKI, A., NAKAMURA, Y., SATO, E., FUKUOKA, S., TADA, Y., TANAKA, A., MORIKAWA, H., KAWAZOE, A., KINOSHITA, T., SHITARA, K., SAKAGUCHI, S. & NISHIKAWA, H. 2019. PD-1(+) regulatory T cells amplified by PD-1 blockade promote hyperprogression of cancer. *Proc Natl Acad Sci U S A,* 116**,** 9999-10008.

KAMPHORST, A. O., WIELAND, A., NASTI, T., YANG, S., ZHANG, R., BARBER, D. L., KONIECZNY, B. T., DAUGHERTY, C. Z., KOENIG, L. & YU, K. 2017. Rescue of exhausted CD8 T cells by PD-1–targeted therapies is CD28-dependent. *Science,* 355**,** 1423-1427.

KANAMARU, F., YOUNGNAK, P., HASHIGUCHI, M., NISHIOKA, T., TAKAHASHI, T., SAKAGUCHI, S., ISHIKAWA, I. & AZUMA, M. 2004. Costimulation via glucocorticoid-induced TNF receptor in both conventional and CD25+ regulatory CD4+ T cells. *The Journal of Immunology,* 172**,** 7306-7314.

KAPLAN, D. H., SHANKARAN, V., DIGHE, A. S., STOCKERT, E., AGUET, M., OLD, L. J. & SCHREIBER, R. D. 1998. Demonstration of an interferon γ-dependent tumor surveillance system in immunocompetent mice. *Proceedings of the National Academy of Sciences,* 95**,** 7556-7561.

KASHIWAGI, I., MORITA, R., SCHICHITA, T., KOMAI, K., SAEKI, K., MATSUMOTO, M., TAKEDA, K., NOMURA, M., HAYASHI, A., KANAI, T. & YOSHIMURA, A. 2015. Smad2 and Smad3 Inversely Regulate TGF-β Autoinduction in Clostridium butyricum-Activated Dendritic Cells. *Immunity,* 43**,** 65-79.

KHATTRI, R., COX, T., YASAYKO, S. A. & RAMSDELL, F. 2003. An essential role for Scurfin in CD4+CD25+ T regulatory cells. *Nat Immunol,* 4**,** 337-42.

KIESSLING, R., KLEIN, E., PROSS, H. & WIGZELL, H. 1975. „Natural" killer cells in the mouse. II. Cytotoxic cells with specificity for mouse Moloney leukemia cells. Characteristics of the killer cell. *European journal of immunology,* 5**,** 117-121.

KIM , H.-P. & LEONARD , W. J. 2007. CREB/ATF-dependent T cell receptor–induced FoxP3 gene expression: a role for DNA methylation. *Journal of Experimental Medicine,* 204**,** 1543-1551.

KIM, J., KIM, W., MOON, U. J., KIM, H. J., CHOI, H. J., SIN, J. I., PARK, N. H., CHO, H. R. & KWON, B. 2016. Intratumorally Establishing Type 2 Innate Lymphoid Cells Blocks Tumor Growth. *J Immunol,* 196**,** 2410-23.

KIM, M. J., KIM, K., PARK, H. J., KIM, G. R., HONG, K. H., OH, J. H., SON, J., PARK, D. J., KIM, D., CHOI, J. M., LEE, I. & HA, S. J. 2023. Deletion of PD-1 destabilizes the lineage identity and metabolic fitness of tumor-infiltrating regulatory T cells. *Nat Immunol,* 24**,** 148-161.

KIM, Y.-S., SHIN, S., YIN, J. H., PARK, J., JUNG, S.-H. & CHUNG, Y.-J. 2022. Single-cell RNA sequencing reveals the existence of pro-metastatic subpopulation within a parental B16 murine melanoma cell line. *Biochemical and Biophysical Research Communications,* 613**,** 120-126.

KING, C. 2009. New insights into the differentiation and function of T follicular helper cells. *Nat Rev Immunol,* 9**,** 757-66.

KING, H. D., DUBOWCHIK, G. M., MASTALERZ, H., WILLNER, D., HOFSTEAD, S. J., FIRESTONE, R. A., LASCH, S. J. & TRAIL, P. A. 2002. Monoclonal antibody conjugates of doxorubicin prepared with branched peptide linkers: inhibition of aggregation by methoxytriethyleneglycol chains. *Journal of medicinal chemistry,* 45**,** 4336-4343.

KIRCHBERGER, S., ROYSTON, D. J., BOULARD, O., THORNTON, E., FRANCHINI, F., SZABADY, R. L., HARRISON, O. & POWRIE, F. 2013. Innate lymphoid cells sustain colon cancer through production of interleukin-22 in a mouse model. *J Exp Med,* 210**,** 917-31.

KISHORE, M., CHEUNG, K. C. P., FU, H., BONACINA, F., WANG, G., COE, D., WARD, E. J., COLAMATTEO, A., JANGANI, M., BARAGETTI, A., MATARESE, G., SMITH, D. M., HAAS, R., MAURO, C., WRAITH, D. C., OKKENHAUG, K., CATAPANO, A. L., DE ROSA, V., NORATA, G. D. & MARELLI-BERG, F. M. 2017. Regulatory T Cell Migration Is Dependent on Glucokinase-Mediated Glycolysis. *Immunity,* 47**,** 875-889.e10.

KITZ, A., DE MARCKEN, M., GAUTRON, A. S., MITROVIC, M., HAFLER, D. A. & DOMINGUEZ-VILLAR, M. 2016. AKT isoforms modulate Th1-like Treg generation and function in human autoimmune disease. *EMBO Rep,* 17**,** 1169-83.

KLOSE, C. S. & ARTIS, D. 2020. Innate lymphoid cells control signaling circuits to regulate tissue-specific immunity. *Cell research,* 30**,** 475-491.

KLOSE, C. S. N. & ARTIS, D. 2016. Innate lymphoid cells as regulators of immunity, inflammation and tissue homeostasis. *Nature Immunology,* 17**,** 765-774.

KLOSE, C. S. N., FLACH, M., MOHLE, L., ROGELL, L., HOYLER, T., EBERT, K., FABIUNKE, C., PFEIFER, D., SEXL, V., FONSECA-PEREIRA, D., DOMINGUES, R. G., VEIGA-FERNANDES, H., ARNOLD, S. J., BUSSLINGER,

M., DUNAY, I. R., TANRIVER, Y. & DIEFENBACH, A. 2014. Differentiation of type 1 ILCs from a common progenitor to all helper-like innate lymphoid cell lineages. *Cell,* 157**,** 340-356.

KO, K., YAMAZAKI, S., NAKAMURA, K., NISHIOKA, T., HIROTA, K., YAMAGUCHI, T., SHIMIZU, J., NOMURA, T., CHIBA, T. & SAKAGUCHI, S. 2005. Treatment of advanced tumors with agonistic anti-GITR mAb and its effects on tumor-infiltrating Foxp3+ CD25+ CD4+ regulatory T cells. *The Journal of experimental medicine,* 202**,** 885-891.

KOCH, M. A., TUCKER-HEARD, G., PERDUE, N. R., KILLEBREW, J. R., URDAHL, K. B. & CAMPBELL, D. J. 2009. The transcription factor T-bet controls regulatory T cell homeostasis and function during type 1 inflammation. *Nat Immunol,* 10**,** 595-602.

KOENEN, H. J. P. M., SMEETS, R. L., VINK, P. M., VAN RIJSSEN, E., BOOTS, A. M. H. & JOOSTEN, I. 2008. Human CD25highFoxp3pos regulatory T cells differentiate into IL-17–producing cells. *Blood,* 112**,** 2340-2352.

KOH, J., KIM, H. Y., LEE, Y., PARK, I. K., KANG, C. H., KIM, Y. T., KIM, J.-E., CHOI, M., LEE, W.-W. & JEON, Y. K. 2019. IL23-producing human lung cancer cells promote tumor growth via conversion of innate lymphoid cell 1 (ILC1) into ILC3. *Clinical Cancer Research,* 25**,** 4026-4037.

KOHM, A. P., WILLIAMS, J. S. & MILLER, S. D. 2004. Cutting edge: ligation of the glucocorticoid-induced TNF receptor enhances autoreactive CD4+ T cell activation and experimental autoimmune encephalomyelitis. *The Journal of Immunology,* 172**,** 4686-4690.

KOMATSU, N., OKAMOTO, K., SAWA, S., NAKASHIMA, T., OH-HORA, M., KODAMA, T., TANAKA, S., BLUESTONE, J. A. & TAKAYANAGI, H. 2014. Pathogenic conversion of Foxp3+ T cells into TH17 cells in autoimmune arthritis. *Nat Med,* 20**,** 62-8.

KONKEL, J. E., JIN, W., ABBATIELLO, B., GRAINGER, J. R. & CHEN, W. 2014. Thymocyte apoptosis drives the intrathymic generation of regulatory T cells. *Proc Natl Acad Sci U S A,* 111**,** E465-73.

KOUO, T., HUANG, L., PUCSEK, A. B., CAO, M., SOLT, S., ARMSTRONG, T. & JAFFEE, E. 2015. Galectin-3 shapes antitumor immune responses by suppressing CD8+ T cells via LAG-3 and inhibiting expansion of plasmacytoid dendritic cells. *Cancer immunology research,* 3**,** 412-423.

KRAUSZ, L. T., BIANCHINI, R., RONCHETTI, S., FETTUCCIARI, K., NOCENTINI, G. & RICCARDI, C. 2007. GITR-GITRL system, a novel player in shock and inflammation. *The Scientific World Journal,* 7**,** 533-566.

KRYCZEK, I., WU, K., ZHAO, E., WEI, S., VATAN, L., SZELIGA, W., HUANG, E., GREENSON, J., CHANG, A., ROLIńSKI, J., RADWAN, P., FANG, J., WANG, G. & ZOU, W. 2011. IL-17+ regulatory T cells in the microenvironments of chronic inflammation and cancer. *J Immunol,* 186**,** 4388-95.

KRYSOV, S. V., ROWLEY, T. F. & AL-SHAMKHANI, A. 2007. Inhibition of p38 mitogen-activated protein kinase unmasks a CD30-triggered apoptotic pathway in anaplastic large cell lymphoma cells. *Molecular Cancer Therapeutics,* 6**,** 703-711.

KUMAGAI, S., KOYAMA, S., ITAHASHI, K., TANEGASHIMA, T., LIN, Y. T., TOGASHI, Y., KAMADA, T., IRIE, T., OKUMURA, G., KONO, H., ITO, D., FUJII, R., WATANABE, S., SAI, A., FUKUOKA, S., SUGIYAMA, E., WATANABE, G., OWARI, T., NISHINAKAMURA, H., SUGIYAMA, D., MAEDA, Y., KAWAZOE, A., YUKAMI, H., CHIDA, K., OHARA, Y., YOSHIDA, T., SHINNO, Y., TAKEYASU, Y., SHIRASAWA, M., NAKAMA, K., AOKAGE,

K., SUZUKI, J., ISHII, G., KUWATA, T., SAKAMOTO, N., KAWAZU, M., UENO, T., MORI, T., YAMAZAKI, N., TSUBOI, M., YATABE, Y., KINOSHITA, T., DOI, T., SHITARA, K., MANO, H. & NISHIKAWA, H. 2022. Lactic acid promotes PD-1 expression in regulatory T cells in highly glycolytic tumor microenvironments. *Cancer Cell,* 40**,** 201-218.e9.

KWON, B., YU, K.-Y., NI, J., YU, G.-L., JANG, I.-K., KIM, Y.-J., XING, L., LIU, D., WANG, S.-X. & KWON, B. S. 1999. Identification of a novel activation-inducible protein of the tumor necrosis factor receptor superfamily and its ligand. *Journal of Biological Chemistry,* 274**,** 6056-6061.

LABA, S., MALLETT, G. & AMARNATH, S. The depths of PD-1 function within the tumor microenvironment beyond CD8+ T cells. Seminars in Cancer Biology, 2022. Elsevier, 1045-1055.

LAL, G., ZHANG, N., VAN DER TOUW, W., DING, Y., JU, W., BOTTINGER, E. P., REID, S. P., LEVY, D. E. & BROMBERG, J. S. 2009. Epigenetic regulation of Foxp3 expression in regulatory T cells by DNA methylation. *The Journal of Immunology,* 182**,** 259-273.

LARKIN, J., CHIARION-SILENI, V., GONZALEZ, R., GROB, J. J., COWEY, C. L., LAO, C. D., SCHADENDORF, D., DUMMER, R., SMYLIE, M., RUTKOWSKI, P., FERRUCCI, P. F., HILL, A., WAGSTAFF, J., CARLINO, M. S., HAANEN, J. B., MAIO, M., MARQUEZ-RODAS, I., MCARTHUR, G. A., ASCIERTO, P. A., LONG, G. V., CALLAHAN, M. K., POSTOW, M. A., GROSSMANN, K., SZNOL, M., DRENO, B., BASTHOLT, L., YANG, A., ROLLIN, L. M., HORAK, C., HODI, F. S. & WOLCHOK, J. D. 2015. Combined Nivolumab and Ipilimumab or Monotherapy in Untreated Melanoma. *New England Journal of Medicine,* 373**,** 23-34.

LARKIN, J., CHIARION-SILENI, V., GONZALEZ, R., GROB, J. J., RUTKOWSKI, P., LAO, C. D., COWEY, C. L., SCHADENDORF, D., WAGSTAFF, J., DUMMER, R., FERRUCCI, P. F., SMYLIE, M., HOGG, D., HILL, A., MARQUEZ-RODAS, I., HAANEN, J., GUIDOBONI, M., MAIO, M., SCHOFFSKI, P., CARLINO, M. S., LEBBE, C., MCARTHUR, G., ASCIERTO, P. A., DANIELS, G. A., LONG, G. V., BASTHOLT, L., RIZZO, J. I., BALOGH, A., MOSHYK, A., HODI, F. S. & WOLCHOK, J. D. 2019. Five-Year Survival with Combined Nivolumab and Ipilimumab in Advanced Melanoma. *N Engl J Med,* 381**,** 1535-1546.

LAURENCE, A., AMARNATH, S., MARIOTTI, J., KIM, Y. C., FOLEY, J., ECKHAUS, M., O'SHEA, J. J. & FOWLER, D. H. 2012. STAT3 transcription factor promotes instability of nTreg cells and limits generation of iTreg cells during acute murine graft-versus-host disease. *Immunity,* 37**,** 209-222.

LEE, J., SU, E. W., ZHU, C., HAINLINE, S., PHUAH, J., MOROCO, J. A., SMITHGALL, T. E., KUCHROO, V. K. & KANE, L. P. 2011. Phosphotyrosine-dependent coupling of Tim-3 to T-cell receptor signaling pathways. *Molecular and cellular biology,* 31**,** 3963-3974.

LEE, W., KIM, H. S., BAEK, S. Y. & LEE, G. R. 2016. Transcription factor IRF8 controls Th1-like regulatory T-cell function. *Cellular & molecular immunology,* 13**,** 785-794.

LEE, W. & LEE, G. R. 2018. Transcriptional regulation and development of regulatory T cells. *Experimental & Molecular Medicine,* 50**,** e456-e456.

LEE, W. J., LEE, Y. J., CHOI, M. E., YUN, K. A., WON, C. H., LEE, M. W., CHOI, J. H. & CHANG, S. E. 2019. Expression of lymphocyte-activating gene 3 and T-cell immunoreceptor with immunoglobulin and ITIM domains in cutaneous melanoma and their correlation with programmed cell death 1 expression in tumor-infiltrating lymphocytes. *Journal of the American Academy of Dermatology,* 81**,** 219-227.

LEPPKES, M., BECKER, C., IVANOV, I. I., HIRTH, S., WIRTZ, S., NEUFERT, C., POULY, S., MURPHY, A. J., VALENZUELA, D. M. & YANCOPOULOS, G. D. 2009. RORγ-expressing Th17 cells induce murine chronic intestinal inflammation via redundant effects of IL-17A and IL-17F. *Gastroenterology,* 136**,** 257-267.

LEVINE, A. G., MENDOZA, A., HEMMERS, S., MOLTEDO, B., NIEC, R. E., SCHIZAS, M., HOYOS, B. E., PUTINTSEVA, E. V., CHAUDHRY, A., DIKIY, S., FUJISAWA, S., CHUDAKOV, D. M., TREUTING, P. M. & RUDENSKY, A. Y. 2017. Stability and function of regulatory T cells expressing the transcription factor T-bet. *Nature,* 546**,** 421-425.

LEVINGS, M. K., SANGREGORIO, R., GALBIATI, F., SQUADRONE, S., DE WAAL MALEFYT, R. & RONCAROLO, M.-G. 2001. IFN-α and IL-10 induce the differentiation of human type 1 T regulatory cells. *The Journal of Immunology,* 166**,** 5530-5539.

LI, J., CHEN, S., XIAO, X., ZHAO, Y., DING, W. & LI, X. C. 2017. IL-9 and Th9 cells in health and diseases—From tolerance to immunopathology. *Cytokine & Growth Factor Reviews,* 37**,** 47-55.

LI, J., RAZUMILAVA, N., GORES, G. J., WALTERS, S., MIZUOCHI, T., MOURYA, R., BESSHO, K., WANG, Y.-H., GLASER, S. S. & SHIVAKUMAR, P. 2014. Biliary repair and carcinogenesis are mediated by IL-33–dependent cholangiocyte proliferation. *The Journal of clinical investigation,* 124**,** 3241-3251.

LI, L., MA, Y. & XU, Y. 2019. Follicular regulatory T cells infiltrated the ovarian carcinoma and resulted in CD8 T cell dysfunction dependent on IL-10 pathway. *International Immunopharmacology,* 68**,** 81-87.

LI, L., YANG, S.-H., YAO, Y., XIE, Y.-Q., YANG, Y.-Q., WANG, Y.-H., YIN, X.-Y., MA, H.-D., GERSHWIN, M. & LIAN, Z.-X. 2016. Block of both TGF-β and IL-2 signaling impedes Neurophilin-1+ regulatory T cell and follicular regulatory T cell development. *Cell Death & Disease,* 7**,** e2439-e2439.

LI, M. O. & RUDENSKY, A. Y. 2016. T cell receptor signalling in the control of regulatory T cell differentiation and function. *Nature reviews. Immunology,* 16**,** 220-233.

LI, N., WANG, Y., FORBES, K., VIGNALI, K. M., HEALE, B. S., SAFTIG, P., HARTMANN, D., BLACK, R. A., ROSSI, J. J. & BLOBEL, C. P. 2007. Metalloproteases regulate T-cell proliferation and effector function via LAG-3. *The EMBO journal,* 26**,** 494-504.

LI, X. & ZHENG, Y. 2015. Regulatory T cell identity: formation and maintenance. *Trends in immunology,* 36**,** 344-353.

LI, Y., GUAN, X., LIU, W., CHEN, H.-L., TRUSCOTT, J., BEYATLI, S., METWALI, A., WEINER, G. J., ZAVAZAVA, N. & BLUMBERG, R. S. 2018. Helminth-induced production of TGF-β and suppression of graft-versus-host disease is dependent on IL-4 production by host cells. *The Journal of Immunology,* 201**,** 2910-2922.

LI, Y., KIM, B. G., QIAN, S., LETTERIO, J. J., FUNG, J. J., LU, L. & LIN, F. 2015. Hepatic Stellate Cells Inhibit T Cells through Active TGF-β1 from a Cell Surface-Bound Latent TGF-β1/GARP Complex. *J Immunol,* 195**,** 2648-56.

LI, Y., WANG, Z., LIN, H., WANG, L., CHEN, X., LIU, Q., ZUO, Q., HU, J., WANG, H. & GUO, J. 2020. Bcl6 preserves the suppressive function of regulatory T cells during tumorigenesis. *Frontiers in immunology,* 11**,** 806.

LIANG, B., WORKMAN, C., LEE, J., CHEW, C., DALE, B. M., COLONNA, L., FLORES, M., LI, N., SCHWEIGHOFFER, E. & GREENBERG, S. 2008. Regulatory T cells inhibit dendritic cells by lymphocyte activation gene-3 engagement of MHC class II. *The Journal of Immunology,* 180**,** 5916-5926.

LIM, A. I., MENEGATTI, S., BUSTAMANTE, J., LE BOURHIS, L., ALLEZ, M., ROGGE, L., CASANOVA, J.-L., YSSEL, H. & DI SANTO, J. P. 2016. IL-12 drives functional plasticity of human group 2 innate lymphoid cells. *Journal of Experimental Medicine,* 213**,** 569-583.

LIM, J. X., LAI, C. Y., MALLETT, G. E., MCDONALD, D., HULME, G., LABA, S., SHAPANIS, A., PAYNE, M., PATTERSON, W. & ALEXANDER, M. 2023. Programmed cell death-1 receptor-mediated regulation of Tbet+ NK1. 1− innate lymphoid cells within the tumor microenvironment. *Proceedings of the National Academy of Sciences,* 120**,** e2216587120.

LIM, J. X., MCTAGGART, T., JUNG, S. K., SMITH, K. J., HULME, G., LABA, S., NG, Y. Q., WILLIAMS, A., HUSSAIN, R., COXHEAD, J., COSGAREA, I., ARDEN, C., NSENGIMANA, J., LOVAT, P., ANDERSON, G., SUN, H.-W., LAURENCE, A. & AMARNATH, S. 2025. PD-1 receptor deficiency enhances CD30+ Treg cell function in melanoma. *Nature Immunology*.

LINTERMAN, M. A., PIERSON, W., LEE, S. K., KALLIES, A., KAWAMOTO, S., RAYNER, T. F., SRIVASTAVA, M., DIVEKAR, D. P., BEATON, L., HOGAN, J. J., FAGARASAN, S., LISTON, A., SMITH, K. G. & VINUESA, C. G. 2011. Foxp3+ follicular regulatory T cells control the germinal center response. *Nat Med,* 17**,** 975-82.

LIU, S., ZHANG, H., LI, M., HU, D., LI, C., GE, B., JIN, B. & FAN, Z. 2013. Recruitment of Grb2 and SHIP1 by the ITT-like motif of TIGIT suppresses granule polarization and cytotoxicity of NK cells. *Cell Death Differ,* 20**,** 456-64.

LIU, Y., SONG, Y., LIN, D., LEI, L., MEI, Y., JIN, Z., GONG, H., ZHU, Y., HU, B. & ZHANG, Y. 2019. NCR− group 3 innate lymphoid cells orchestrate IL-23/IL-17 axis to promote hepatocellular carcinoma development. *EBioMedicine,* 41**,** 333-344.

LIU, Y., ZHANG, P., LI, J., KULKARNI, A. B., PERRUCHE, S. & CHEN, W. 2008. A critical function for TGF-beta signaling in the development of natural CD4+CD25+Foxp3+ regulatory T cells. *Nat Immunol,* 9**,** 632-40.

LOCHNER, M., PEDUTO, L., CHERRIER, M., SAWA, S., LANGA, F., VARONA, R., RIETHMACHER, D., SI-TAHAR, M., DI SANTO, J. P. & EBERL, G. 2008. In vivo equilibrium of proinflammatory IL-17+ and regulatory IL-10+ Foxp3+ RORgamma t+ T cells. *J Exp Med,* 205**,** 1381-93.

LONG, A., DOMINGUEZ, D., QIN, L., CHEN, S., FAN, J., ZHANG, M., FANG, D., ZHANG, Y., KUZEL, T. M. & ZHANG, B. 2018. Type 2 Innate Lymphoid Cells Impede IL-33-Mediated Tumor Suppression. *J Immunol,* 201**,** 3456-3464.

LUCCA, L. E., AXISA, P. P., SINGER, E. R., NOLAN, N. M., DOMINGUEZ-VILLAR, M. & HAFLER, D. A. 2019. TIGIT signaling restores suppressor function of Th1 Tregs. *JCI Insight,* 4.

LUCCA, L. E. & DOMINGUEZ-VILLAR, M. 2020. Modulation of regulatory T cell function and stability by co-inhibitory receptors. *Nature Reviews Immunology,* 20**,** 680-693.

LUCI, C., BIHL, F., BOURDELY, P., KHOU, S., POPA, A., MEGHRAOUI-KHEDDAR, A., VERMEULEN, O., ELALDI, R., POISSONNET, G., SUDAKA, A., BOZEC, A., BEKRI, S., CAZARETH, J., PONZIO, G., BARBRY, P., REZZONICO, R., MARI, B., BRAUD, V. M. & ANJUèRE, F. 2021. Cutaneous Squamous Cell Carcinoma Development Is Associated with a Temporal Infiltration of ILC1 and NK Cells with Immune Dysfunctions. *J Invest Dermatol,* 141**,** 2369-2379.

MACAULAY, I. C., TIJSSEN, M. R., THIJSSEN-TIMMER, D. C., GUSNANTO, A., STEWARD, M., BURNS, P., LANGFORD, C. F., ELLIS, P. D., DUDBRIDGE, F., ZWAGINGA, J. J., WATKINS, N. A., VAN DER SCHOOT, C. E. & OUWEHAND,

W. H. 2007. Comparative gene expression profiling of in vitro differentiated megakaryocytes and erythroblasts identifies novel activatory and inhibitory platelet membrane proteins. *Blood,* 109**,** 3260-9.

MAEDA, N., MUTA, H., OFLAZOGLU, E. & YOSHIKAI, Y. 2010. Susceptibility of human T-cell leukemia virus type I-infected cells to humanized anti-CD30 monoclonal antibodies in vitro and in vivo. *Cancer science,* 101**,** 224-230.

MAGNUSON, A. M., KINER, E., ERGUN, A., PARK, J. S., ASINOVSKI, N., ORTIZ-LOPEZ, A., KILCOYNE, A., PAOLUZZI-TOMADA, E., WEISSLEDER, R. & MATHIS, D. 2018. Identification and validation of a tumor-infiltrating Treg transcriptional signature conserved across species and tumor types. *Proceedings of the National Academy of Sciences,* 115**,** E10672-E10681.

MAILER, R. K., FALK, K. & RöTZSCHKE, O. 2009. Absence of leucine zipper in the natural FOXP3Delta2Delta7 isoform does not affect dimerization but abrogates suppressive capacity. *PLoS One,* 4**,** e6104.

MALLETT, G., PATTERSON, W., PAYNE, M. & AMARNATH, S. 2020. Isolation and Characterization of Innate Lymphoid Cells within the Murine Tumor Microenvironment. *Methods Mol Biol,* 2121**,** 153-164.

MANIERI, N. A., CHIANG, E. Y. & GROGAN, J. L. 2017. TIGIT: A Key Inhibitor of the Cancer Immunity Cycle. *Trends Immunol,* 38**,** 20-28.

MANOURY, B., HEWITT, E. W., MORRICE, N., DANDO, P. M., BARRETT, A. J. & WATTS, C. 1998. An asparaginyl endopeptidase processes a microbial antigen for class II MHC presentation. *Nature,* 396**,** 695-699.

MASSOUD, A. H., CHARBONNIER, L. M., LOPEZ, D., PELLEGRINI, M., PHIPATANAKUL, W. & CHATILA, T. A. 2016. An asthma-associated IL4R variant exacerbates airway inflammation by promoting conversion of regulatory T cells to TH17-like cells. *Nat Med,* 22**,** 1013-22.

MCGEE, M. C., ZHANG, T., MAGAZINE, N., ISLAM, R., CAROSSINO, M. & HUANG, W. 2022. PD-1 and ICOS counter-regulate tissue resident regulatory T cell development and IL-10 production during flu. *Front Immunol,* 13**,** 984476.

MCHUGH, R. S., WHITTERS, M. J., PICCIRILLO, C. A., YOUNG, D. A., SHEVACH, E. M., COLLINS, M. & BYRNE, M. C. 2002. CD4+ CD25+ immunoregulatory T cells: gene expression analysis reveals a functional role for the glucocorticoid-induced TNF receptor. *Immunity,* 16**,** 311-323.

MCLANE, L. M., ABDEL-HAKEEM, M. S. & WHERRY, E. J. 2019. CD8 T Cell Exhaustion During Chronic Viral Infection and Cancer. *Annu Rev Immunol,* 37**,** 457-495.

MEBIUS, R. E., RENNERT, P. & WEISSMAN, I. L. 1997. Developing lymph nodes collect CD4+ CD3− LTβ+ cells that can differentiate to APC, NK cells, and follicular cells but not T or B cells. *Immunity,* 7**,** 493-504.

METZGER, M. B., HRISTOVA, V. A. & WEISSMAN, A. M. 2012. HECT and RING finger families of E3 ubiquitin ligases at a glance. *J Cell Sci,* 125**,** 531-7.

MITSUI, J., NISHIKAWA, H., MURAOKA, D., WANG, L., NOGUCHI, T., SATO, E., KONDO, S., ALLISON, J. P., SAKAGUCHI, S. & OLD, L. J. 2010. Two distinct mechanisms of augmented antitumor activity by modulation of immunostimulatory/inhibitory signals. *Clinical Cancer Research,* 16**,** 2781-2791.

MJOSBERG, J. M., TRIFARI, S., CRELLIN, N. K., PETERS, C. P., VAN DRUNEN, C. M., PIET, B., FOKKENS, W. J., CUPEDO, T. & SPITS, H. 2011. Human IL-25- and IL-33-responsive type 2 innate lymphoid cells are defined by expression of CRTH2 and CD161. *Nat Immunol,* 12**,** 1055-62.

MONTICELLI, L. A., SONNENBERG, G. F., ABT, M. C., ALENGHAT, T., ZIEGLER, C. G., DOERING, T. A., ANGELOSANTO, J. M., LAIDLAW, B. J., YANG, C. Y., SATHALIYAWALA, T., KUBOTA, M., TURNER, D., DIAMOND, J. M., GOLDRATH, A. W., FARBER, D. L., COLLMAN, R. G., WHERRY, E. J. & ARTIS, D. 2011. Innate lymphoid cells promote lung-tissue homeostasis after infection with influenza virus. *Nat Immunol,* 12**,** 1045-54.

MORAL, J. A., LEUNG, J., ROJAS, L. A., RUAN, J., ZHAO, J., SETHNA, Z., RAMNARAIN, A., GASMI, B., GURURAJAN, M., REDMOND, D., ASKAN, G., BHANOT, U., ELYADA, E., PARK, Y., TUVESON, D. A., GöNEN, M., LEACH, S. D., WOLCHOK, J. D., DEMATTEO, R. P., MERGHOUB, T. & BALACHANDRAN, V. P. 2020. ILC2s amplify PD-1 blockade by activating tissue-specific cancer immunity. *Nature,* 579**,** 130-135.

MORAWSKI, P. A., MEHRA, P., CHEN, C., BHATTI, T. & WELLS, A. D. 2013. Foxp3 protein stability is regulated by cyclin-dependent kinase 2. *J Biol Chem,* 288**,** 24494-502.

MORIKAWA, H. & SAKAGUCHI, S. 2014. Genetic and epigenetic basis of Treg cell development and function: from a FoxP3-centered view to an epigenome-defined view of natural Treg cells. *Immunological reviews,* 259**,** 192-205.

MORO, K., YAMADA, T., TANABE, M., TAKEUCHI, T., IKAWA, T., KAWAMOTO, H., FURUSAWA, J., OHTANI, M., FUJII, H. & KOYASU, S. 2010. Innate production of T(H)2 cytokines by adipose tissue-associated c-Kit(+)Sca-1(+) lymphoid cells. *Nature,* 463**,** 540-4.

MURPHY, K. & WEAVER, C. JANEWAY'S 9TH EDITION.

NAKAHIRA, K., MORITA, A., KIM, N. S. & YANAGIHARA, I. 2013. Phosphorylation of FOXP3 by LCK downregulates MMP9 expression and represses cell invasion. *PLoS One,* 8**,** e77099.

NAUTS, H. C., SWIFT, W. E. & COLEY, B. L. 1946. The treatment of malignant tumors by bacterial toxins as developed by the late William B. Coley, MD, reviewed in the light of modern research. *Cancer research,* 6**,** 205-216.

NEILL, D. R., WONG, S. H., BELLOSI, A., FLYNN, R. J., DALY, M., LANGFORD, T. K., BUCKS, C., KANE, C. M., FALLON, P. G., PANNELL, R., JOLIN, H. E. & MCKENZIE, A. N. 2010. Nuocytes represent a new innate effector leukocyte that mediates type-2 immunity. *Nature,* 464**,** 1367-70.

NGIOW, S. F., VON SCHEIDT, B., AKIBA, H., YAGITA, H., TENG, M. W. & SMYTH, M. J. 2011. Anti-TIM3 antibody promotes T cell IFN-γ–mediated antitumor immunity and suppresses established tumors. *Cancer research,* 71**,** 3540-3551.

NGUYEN, D. X. & EHRENSTEIN, M. R. 2016. Anti-TNF drives regulatory T cell expansion by paradoxically promoting membrane TNF-TNF-RII binding in rheumatoid arthritis. *J Exp Med,* 213**,** 1241-53.

NIE, H., ZHENG, Y., LI, R., GUO, T. B., HE, D., FANG, L., LIU, X., XIAO, L., CHEN, X., WAN, B., CHIN, Y. E. & ZHANG, J. Z. 2013. Phosphorylation of FOXP3 controls regulatory T cell function and is inhibited by TNF-α in rheumatoid arthritis. *Nat Med,* 19**,** 322-8.

NISHIKAWA, H., KATO, T., HIRAYAMA, M., ORITO, Y., SATO, E., HARADA, N., GNJATIC, S., OLD, L. J. & SHIKU, H. 2008. Regulatory T cell–resistant CD8+ T cells induced by glucocorticoid-induced tumor necrosis factor receptor signaling. *Cancer research,* 68**,** 5948-5954.

NISHIMURA, H., NOSE, M., HIAI, H., MINATO, N. & HONJO, T. 1999. Development of lupus-like autoimmune diseases by disruption of the PD-1 gene encoding an ITIM motif-carrying immunoreceptor. *Immunity,* 11**,** 141-51.

NISHIMURA, H., OKAZAKI, T., TANAKA, Y., NAKATANI, K., HARA, M., MATSUMORI, A., SASAYAMA, S., MIZOGUCHI, A., HIAI, H., MINATO, N. & HONJO, T. 2001. Autoimmune dilated cardiomyopathy in PD-1 receptor-deficient mice. *Science,* 291**,** 319-22.

NOSKO, A., KLUGER, M. A., DIEFENHARDT, P., MELDERIS, S., WEGSCHEID, C., TIEGS, G., STAHL, R. A., PANZER, U. & STEINMETZ, O. M. 2017. T-bet enhances regulatory T cell fitness and directs control of Th1 responses in crescentic GN. *Journal of the American Society of Nephrology,* 28**,** 185-196.

NOYAN, F., LEE, Y. S., ZIMMERMANN, K., HARDTKE‐WOLENSKI, M., TAUBERT, R., WARNECKE, G., KNOEFEL, A. K., SCHULDE, E., OLEK, S. & MANNS, M. P. 2014. Isolation of human antigen‐specific regulatory T cells with high suppressive function. *European journal of immunology,* 44**,** 2592-2602.

NUSSBAUM, K., BURKHARD, S. H., OHS, I., MAIR, F., KLOSE, C. S. N., ARNOLD, S. J., DIEFENBACH, A., TUGUES, S. & BECHER, B. 2017. Tissue microenvironment dictates the fate and tumor-suppressive function of type 3 ILCs. *J Exp Med,* 214**,** 2331-2347.

ODORIZZI, P. M., PAUKEN, K. E., PALEY, M. A., SHARPE, A. & WHERRY, E. J. 2015. Genetic absence of PD-1 promotes accumulation of terminally differentiated exhausted CD8+ T cells. *J Exp Med,* 212**,** 1125-37.

OH, S. A., WU, D.-C., CHEUNG, J., NAVARRO, A., XIONG, H., CUBAS, R., TOTPAL, K., CHIU, H., WU, Y. & COMPS-AGRAR, L. 2020. PD-L1 expression by dendritic cells is a key regulator of T-cell immunity in cancer. *Nature Cancer,* 1**,** 681-691.

OHNE, Y., SILVER, J. S., THOMPSON-SNIPES, L., COLLET, M. A., BLANCK, J. P., CANTAREL, B. L., COPENHAVER, A. M., HUMBLES, A. A. & LIU, Y.-J. 2016. IL-1 is a critical regulator of group 2 innate lymphoid cell function and plasticity. *Nature immunology,* 17**,** 646-655.

OHNMACHT, C., PARK, J.-H., CORDING, S., WING, J. B., ATARASHI, K., OBATA, Y., GABORIAU-ROUTHIAU, V., MARQUES, R., DULAUROY, S., FEDOSEEVA, M., BUSSLINGER, M., CERF-BENSUSSAN, N., BONECA, I. G., VOEHRINGER, D., HASE, K., HONDA, K., SAKAGUCHI, S. & EBERL, G. 2015. The microbiota regulates type 2 immunity through RORγt⁺ T cells. *Science,* 349**,** 989-993.

OKAMOTO, M., SASAI, M., KURATANI, A., OKUZAKI, D., ARAI, M., WING, J. B., SAKAGUCHI, S. & YAMAMOTO, M. 2023. A genetic method specifically delineates Th1-type Treg cells and their roles in tumor immunity. *Cell Reports,* 42.

OKAZAKI, T., MAEDA, A., NISHIMURA, H., KUROSAKI, T. & HONJO, T. 2001. PD-1 immunoreceptor inhibits B cell receptor-mediated signaling by recruiting src homology 2-domain-containing tyrosine phosphatase 2 to phosphotyrosine. *Proceedings of the National Academy of Sciences,* 98**,** 13866-13871.

OLDENHOVE, G., BOUCQUEY, E., TAQUIN, A., ACOLTY, V., BONETTI, L., RYFFEL, B., LE BERT, M., ENGLEBERT, K., BOON, L. & MOSER, M. 2018. PD-1 Is Involved in the Dysregulation of Type 2 Innate Lymphoid Cells in a Murine Model of Obesity. *Cell Rep,* 25**,** 2053-2060.e4.

OLDENHOVE, G., BOULADOUX, N., WOHLFERT, E. A., HALL, J. A., CHOU, D., DOS SANTOS, L., O'BRIEN, S., BLANK, R., LAMB, E., NATARAJAN, S., KASTENMAYER, R., HUNTER, C., GRIGG, M. E. & BELKAID, Y. 2009. Decrease of Foxp3+ Treg cell number and acquisition of effector cell phenotype during lethal infection. *Immunity,* 31**,** 772-86.

ORDOVAS-MONTANES, J., DWYER, D. F., NYQUIST, S. K., BUCHHEIT, K. M., VUKOVIC, M., DEB, C., WADSWORTH, M. H., HUGHES, T. K., KAZER, S. W.

& YOSHIMOTO, E. 2018. Allergic inflammatory memory in human respiratory epithelial progenitor cells. *Nature,* 560**,** 649-654.

OUYANG, X., ZHANG, R., YANG, J., LI, Q., QIN, L., ZHU, C., LIU, J., NING, H., SHIN, M. S., GUPTA, M., QI, C. F., HE, J. C., LIRA, S. A., MORSE, H. C., 3RD, OZATO, K., MAYER, L. & XIONG, H. 2011. Transcription factor IRF8 directs a silencing programme for TH17 cell differentiation. *Nat Commun,* 2**,** 314.

OVCINNIKOVS, V., ROSS, E. M., PETERSONE, L., EDNER, N. M., HEUTS, F., NTAVLI, E., KOGIMTZIS, A., KENNEDY, A., WANG, C. J. & BENNETT, C. L. 2019. CTLA-4–mediated transendocytosis of costimulatory molecules primarily targets migratory dendritic cells. *Science immunology,* 4**,** eaaw0902.

PAPADOPOULOS, K. P., AUTIO, K., GOLAN, T., DOBRENKOV, K., CHARTASH, E., CHEN, Q., WNEK, R. & LONG, G. V. 2021. Phase I Study of MK-4166, an Anti-human Glucocorticoid-Induced TNF Receptor Antibody, Alone or with Pembrolizumab in Advanced Solid Tumors. *Clin Cancer Res,* 27**,** 1904-1911.

PARDOLL, D. M. 2012. The blockade of immune checkpoints in cancer immunotherapy. *Nature Reviews Cancer,* 12**,** 252-264.

PARK, H. J., KIM, K. W., WON, S. E., YOON, S., CHAE, Y. K., TIRUMANI, S. H. & RAMAIYA, N. H. 2021. Definition, Incidence, and Challenges for Assessment of Hyperprogressive Disease During Cancer Treatment With Immune Checkpoint Inhibitors: A Systematic Review and Meta-analysis. *JAMA Netw Open,* 4**,** e211136.

PARKER, M. E., BARRERA, A., WHEATON, J. D., ZUBERBUEHLER, M. K., ALLAN, D. S., CARLYLE, J. R., REDDY, T. E. & CIOFANI, M. 2020. c-Maf regulates the plasticity of group 3 innate lymphoid cells by restraining the type 1 program. *Journal of Experimental Medicine,* 217.

PARRY, R. V., CHEMNITZ, J. M., FRAUWIRTH, K. A., LANFRANCO, A. R., BRAUNSTEIN, I., KOBAYASHI, S. V., LINSLEY, P. S., THOMPSON, C. B. & RILEY, J. L. 2005. CTLA-4 and PD-1 receptors inhibit T-cell activation by distinct mechanisms. *Mol Cell Biol,* 25**,** 9543-53.

PASTILLE, E., BARDINI, K., FLEISSNER, D., ADAMCZYK, A., FREDE, A., WADWA, M., VON SMOLINSKI, D., KASPER, S., SPARWASSER, T., GRUBER, A. D., SCHULER, M., SAKAGUCHI, S., ROERS, A., MüLLER, W., HANSEN, W., BUER, J. & WESTENDORF, A. M. 2014. Transient ablation of regulatory T cells improves antitumor immunity in colitis-associated colon cancer. *Cancer Res,* 74**,** 4258-69.

PATERSON, A. M., LOVITCH, S. B., SAGE, P. T., JUNEJA, V. R., LEE, Y., TROMBLEY, J. D., ARANCIBIA-CáRCAMO, C. V., SOBEL, R. A., RUDENSKY, A. Y., KUCHROO, V. K., FREEMAN, G. J. & SHARPE, A. H. 2015. Deletion of CTLA-4 on regulatory T cells during adulthood leads to resistance to autoimmunity. *J Exp Med,* 212**,** 1603-21.

PATSOUKIS, N., BARDHAN, K., CHATTERJEE, P., SARI, D., LIU, B., BELL, L. N., KAROLY, E. D., FREEMAN, G. J., PETKOVA, V., SETH, P., LI, L. & BOUSSIOTIS, V. A. 2015. PD-1 alters T-cell metabolic reprogramming by inhibiting glycolysis and promoting lipolysis and fatty acid oxidation. *Nat Commun,* 6**,** 6692.

PENG, H., JIANG, X., CHEN, Y., SOJKA, D. K., WEI, H., GAO, X., SUN, R., YOKOYAMA, W. M. & TIAN, Z. 2013. Liver-resident NK cells confer adaptive immunity in skin-contact inflammation. *J Clin Invest,* 123**,** 1444-56.

PENG, Q., QIU, X., ZHANG, Z., ZHANG, S., ZHANG, Y., LIANG, Y., GUO, J., PENG, H., CHEN, M., FU, Y. X. & TANG, H. 2020. PD-L1 on dendritic cells attenuates T

cell activation and regulates response to immune checkpoint blockade. *Nat Commun,* 11**,** 4835.

PERRY, J. A., SHALLBERG, L., CLARK, J. T., GULLICKSRUD, J. A., DELONG, J. H., DOUGLAS, B. B., HART, A. P., LANZAR, Z., O'DEA, K., KONRADT, C., PARK, J., KUCHROO, J. R., GRUBAUGH, D., ZARETSKY, A. G., BRODSKY, I. E., MALEFYT, R. W., CHRISTIAN, D. A., SHARPE, A. H. & HUNTER, C. A. 2022. PD-L1-PD-1 interactions limit effector regulatory T cell populations at homeostasis and during infection. *Nat Immunol,* 23**,** 743-756.

PHILLIPS, J. D., KNAB, L. M., BLATNER, N. R., HAGHI, L., DECAMP, M. M., MEYERSON, S. L., HEIFERMAN, M. J., HEIFERMAN, J. R., GOUNARI, F., BENTREM, D. J. & KHAZAIE, K. 2015. Preferential expansion of pro-inflammatory Tregs in human non-small cell lung cancer. *Cancer Immunol Immunother,* 64**,** 1185-91.

PLANK, M. W., KAIKO, G. E., MALTBY, S., WEAVER, J., TAY, H. L., SHEN, W., WILSON, M. S., DURUM, S. K. & FOSTER, P. S. 2017. Th22 Cells Form a Distinct Th Lineage from Th17 Cells In Vitro with Unique Transcriptional Properties and Tbet-Dependent Th1 Plasticity. *The Journal of Immunology,* 198**,** 2182-2190.

POLANSKY, J. K., KRETSCHMER, K., FREYER, J., FLOESS, S., GARBE, A., BARON, U., OLEK, S., HAMANN, A., VON BOEHMER, H. & HUEHN, J. 2008. DNA methylation controls Foxp3 gene expression. *European journal of immunology,* 38**,** 1654-1663.

POMPURA, S. L. & DOMINGUEZ-VILLAR, M. 2018. The PI3K/AKT signaling pathway in regulatory T-cell development, stability, and function. *Journal of Leukocyte Biology,* 103**,** 1065-1076.

POWELL, J. D., POLLIZZI, K. N., HEIKAMP, E. B. & HORTON, M. R. 2012. Regulation of immune responses by mTOR. *Annu Rev Immunol,* 30**,** 39-68.

POWRIE, F., LEACH, M. W., MAUZE, S., CADDIE, L. B. & COFFMAN, R. L. 1993. Phenotypically distinct subsets of CD4+ T cells induce or protect from chronic intestinal inflammation in C. B-17 scid mice. *International Immunology,* 5**,** 1461-1471.

POWRIE, F. & MASON, D. 1990. OX-22high CD4+ T cells induce wasting disease with multiple organ pathology: prevention by the OX-22low subset. *Journal of Experimental Medicine,* 172**,** 1701-1708.

QURESHI, O. S., ZHENG, Y., NAKAMURA, K., ATTRIDGE, K., MANZOTTI, C., SCHMIDT, E. M., BAKER, J., JEFFERY, L. E., KAUR, S. & BRIGGS, Z. 2011. Trans-endocytosis of CD80 and CD86: a molecular basis for the cell-extrinsic function of CTLA-4. *Science,* 332**,** 600-603.

RANGACHARI, M., ZHU, C., SAKUISHI, K., XIAO, S., KARMAN, J., CHEN, A., ANGIN, M., WAKEHAM, A., GREENFIELD, E. A. & SOBEL, R. A. 2012. Bat3 promotes T cell responses and autoimmunity by repressing Tim-3–mediated cell death and exhaustion. *Nature medicine,* 18**,** 1394-1400.

RAYKOVA, A., CARREGA, P., LEHMANN, F. M., IVANEK, R., LANDTWING, V., QUAST, I., LüNEMANN, J. D., FINKE, D., FERLAZZO, G. & CHIJIOKE, O. 2017. Interleukins 12 and 15 induce cytotoxicity and early NK-cell differentiation in type 3 innate lymphoid cells. *Blood advances,* 1**,** 2679-2691.

RIBAS, A. & WOLCHOK, J. D. 2018. Cancer immunotherapy using checkpoint blockade. *Science,* 359**,** 1350-1355.

RITVO, P.-G. G., CHURLAUD, G., QUINIOU, V., FLOREZ, L., BRIMAUD, F., FOURCADE, G., MARIOTTI-FERRANDIZ, E. & KLATZMANN, D. 2017.

T_{fr} cells lack IL-2Rα but express decoy IL-1R2 and IL-1Ra and suppress the IL-1–dependent activation of T_{fh} cells. *Science Immunology,* 2**,** eaan0368.

RIVAS, M. N., BURTON, O. T., WISE, P., CHARBONNIER, L.-M., GEORGIEV, P., OETTGEN, H. C., RACHID, R. & CHATILA, T. A. 2015. Regulatory T cell reprogramming toward a Th2-cell-like lineage impairs oral tolerance and promotes food allergy. *Immunity,* 42**,** 512-523.

ROBERT, C., LONG, G. V., BRADY, B., DUTRIAUX, C., MAIO, M., MORTIER, L., HASSEL, J. C., RUTKOWSKI, P., MCNEIL, C., KALINKA-WARZOCHA, E., SAVAGE, K. J., HERNBERG, M. M., LEBBé, C., CHARLES, J., MIHALCIOIU, C., CHIARION-SILENI, V., MAUCH, C., COGNETTI, F., ARANCE, A., SCHMIDT, H., SCHADENDORF, D., GOGAS, H., LUNDGREN-ERIKSSON, L., HORAK, C., SHARKEY, B., WAXMAN, I. M., ATKINSON, V. & ASCIERTO, P. A. 2015a. Nivolumab in previously untreated melanoma without BRAF mutation. *N Engl J Med,* 372**,** 320-30.

ROBERT, C., SCHACHTER, J., LONG, G. V., ARANCE, A., GROB, J. J., MORTIER, L., DAUD, A., CARLINO, M. S., MCNEIL, C., LOTEM, M., LARKIN, J., LORIGAN, P., NEYNS, B., BLANK, C. U., HAMID, O., MATEUS, C., SHAPIRA-FROMMER, R., KOSH, M., ZHOU, H., IBRAHIM, N., EBBINGHAUS, S. & RIBAS, A. 2015b. Pembrolizumab versus Ipilimumab in Advanced Melanoma. *New England Journal of Medicine,* 372**,** 2521-2532.

ROCHMAN, Y., SPOLSKI, R. & LEONARD, W. J. 2009. New insights into the regulation of T cells by gamma(c) family cytokines. *Nat Rev Immunol,* 9**,** 480-90.

ROMAGNANI, P., ANNUNZIATO, F., MANETTI, R., MAVILIA, C., LASAGNI, L., MANUELLI, C., VANNELLI, G. B., VANINI, V., MAGGI, E. & PUPILLI, C. 1998. High CD30 ligand expression by epithelial cells and Hassal's corpuscles in the medulla of human thymus. *Blood, The Journal of the American Society of Hematology,* 91**,** 3323-3332.

RONCHETTI, S., NOCENTINI, G., BIANCHINI, R., KRAUSZ, L. T., MIGLIORATI, G. & RICCARDI, C. 2007. Glucocorticoid-induced TNFR-related protein lowers the threshold of CD28 costimulation in CD8+ T cells. *The Journal of Immunology,* 179**,** 5916-5926.

RONCHETTI, S., ZOLLO, O., BRUSCOLI, S., AGOSTINI, M., BIANCHINI, R., NOCENTINI, G., AYROLDI, E. & RICCARDI, C. 2004. Frontline: GITR, a member of the TNF receptor superfamily, is costimulatory to mouse T lymphocyte subpopulations. *European journal of immunology,* 34**,** 613-622.

ROUBIN, R., PIZETTE, S., OLLENDORFF, V., PLANCHE, J., BIRNBAUM, D. & DELAPEYRIERE, O. 1996. Structure and developmental expression of mouse Garp, a gene encoding a new leucine-rich repeat-containing protein. *Int J Dev Biol,* 40**,** 545-55.

ROY, D., BOSE, S., PATI, S., GUIN, A., BANERJEE, K., SAHA, S., SINGHAL, A. K., CHAKRABORTY, J., SARKAR, D. K. & SA, G. 2021. GFI1/HDAC1-axis differentially regulates immunosuppressive CD73 in human tumor-associated FOXP3(+) Th17 and inflammation-linked Th17 cells. *Eur J Immunol,* 51**,** 1206-1217.

RUBTSOV, Y. P., NIEC, R. E., JOSEFOWICZ, S., LI, L., DARCE, J., MATHIS, D., BENOIST, C. & RUDENSKY, A. Y. 2010. Stability of the regulatory T cell lineage in vivo. *Science,* 329**,** 1667-71.

RUDD, C. E., TAYLOR, A. & SCHNEIDER, H. 2009. CD28 and CTLA-4 coreceptor expression and signal transduction. *Immunological reviews,* 229**,** 12-26.

SADE-FELDMAN, M., YIZHAK, K., BJORGAARD, S. L., RAY, J. P., DE BOER, C. G., JENKINS, R. W., LIEB, D. J., CHEN, J. H., FREDERICK, D. T. & BARZILY-ROKNI, M. 2018. Defining T cell states associated with response to checkpoint immunotherapy in melanoma. *Cell,* 175**,** 998-1013. e20.

SAGE, PETER T., PATERSON, ALISON M., LOVITCH, SCOTT B. & SHARPE, ARLENE H. 2014. The Coinhibitory Receptor CTLA-4 Controls B Cell Responses by Modulating T Follicular Helper, T Follicular Regulatory, and T Regulatory Cells. *Immunity,* 41**,** 1026-1039.

SAGE, P. T., RON-HAREL, N., JUNEJA, V. R., SEN, D. R., MALERI, S., SUNGNAK, W., KUCHROO, V. K., HAINING, W. N., CHEVRIER, N., HAIGIS, M. & SHARPE, A. H. 2016. Suppression by TFR cells leads to durable and selective inhibition of B cell effector function. *Nature Immunology,* 17**,** 1436-1446.

SAGE, P. T. & SHARPE, A. H. 2015. T follicular regulatory cells in the regulation of B cell responses. *Trends in Immunology,* 36**,** 410-418.

SAKAGUCHI, S., FUKUMA, K., KURIBAYASHI, K. & MASUDA, T. 1985. Organ-specific autoimmune diseases induced in mice by elimination of T cell subset. I. Evidence for the active participation of T cells in natural self-tolerance; deficit of a T cell subset as a possible cause of autoimmune disease. *J Exp Med,* 161**,** 72-87.

SAKAGUCHI, S., SAKAGUCHI, N., ASANO, M., ITOH, M. & TODA, M. 1995. Immunologic self-tolerance maintained by activated T cells expressing IL-2 receptor alpha-chains (CD25). Breakdown of a single mechanism of self-tolerance causes various autoimmune diseases. *J Immunol,* 155**,** 1151-64.

SAKAGUCHI, S., WING, K. & MIYARA, M. 2007. Regulatory T cells - a brief history and perspective. *Eur J Immunol,* 37 Suppl 1**,** S116-23.

SAKAGUCHI, S., YAMAGUCHI, T., NOMURA, T. & ONO, M. 2008. Regulatory T cells and immune tolerance. *cell,* 133**,** 775-787.

SAKUISHI, K., APETOH, L., SULLIVAN, J. M., BLAZAR, B. R., KUCHROO, V. K. & ANDERSON, A. C. 2010. Targeting Tim-3 and PD-1 pathways to reverse T cell exhaustion and restore anti-tumor immunity. *Journal of Experimental Medicine,* 207**,** 2187-2194.

SAKUISHI, K., NGIOW, S. F., SULLIVAN, J. M., TENG, M. W., KUCHROO, V. K., SMYTH, M. J. & ANDERSON, A. C. 2013. TIM3+ FOXP3+ regulatory T cells are tissue-specific promoters of T-cell dysfunction in cancer. *Oncoimmunology,* 2**,** e23849.

SALAS, A., HERNANDEZ-ROCHA, C., DUIJVESTEIN, M., FAUBION, W., MCGOVERN, D., VERMEIRE, S., VETRANO, S. & VANDE CASTEELE, N. 2020. JAK–STAT pathway targeting for the treatment of inflammatory bowel disease. *Nature Reviews Gastroenterology & Hepatology,* 17**,** 323-337.

SALIMI, M., WANG, R., YAO, X., LI, X., WANG, X., HU, Y., CHANG, X., FAN, P., DONG, T. & OGG, G. 2018. Activated innate lymphoid cell populations accumulate in human tumour tissues. *BMC Cancer,* 18**,** 341.

SAMANTA, A., LI, B., SONG, X., BEMBAS, K., ZHANG, G., KATSUMATA, M., SAOUAF, S. J., WANG, Q., HANCOCK, W. W., SHEN, Y. & GREENE, M. I. 2008. TGF-beta and IL-6 signals modulate chromatin binding and promoter occupancy by acetylated FOXP3. *Proc Natl Acad Sci U S A,* 105**,** 14023-7.

SAMSTEIN, R. M., ARVEY, A., JOSEFOWICZ, S. Z., PENG, X., REYNOLDS, A., SANDSTROM, R., NEPH, S., SABO, P., KIM, J. M. & LIAO, W. 2012. Foxp3 exploits a pre-existent enhancer landscape for regulatory T cell lineage specification. *Cell,* 151**,** 153-166.

SANCHEZ-CORREA, B., VALHONDO, I., HASSOUNEH, F., LOPEZ-SEJAS, N., PERA, A., BERGUA, J. M., ARCOS, M. J., BAñAS, H., CASAS-AVILéS, I., DURáN, E., ALONSO, C., SOLANA, R. & TARAZONA, R. 2019. DNAM-1 and the TIGIT/PVRIG/TACTILE Axis: Novel Immune Checkpoints for Natural Killer Cell-Based Cancer Immunotherapy. *Cancers (Basel),* 11.

SANOS, S. L., BUI, V. L., MORTHA, A., OBERLE, K., HENERS, C., JOHNER, C. & DIEFENBACH, A. 2009. RORgammat and commensal microflora are required for the differentiation of mucosal interleukin 22-producing NKp46+ cells. *Nat Immunol,* 10**,** 83-91.

SARANCHOVA, I., HAN, J., ZAMAN, R., ARORA, H., HUANG, H., FENNINGER, F., CHOI, K. B., MUNRO, L., PFEIFER, C. G. & WELCH, I. 2018a. Type 2 innate lymphocytes actuate immunity against tumours and limit cancer metastasis. *Scientific Reports,* 8**,** 2924.

SARANCHOVA, I., HAN, J., ZAMAN, R., ARORA, H., HUANG, H., FENNINGER, F., CHOI, K. B., MUNRO, L., PFEIFER, C. G., WELCH, I., TAKEI, F. & JEFFERIES, W. A. 2018b. Type 2 Innate Lymphocytes Actuate Immunity Against Tumours and Limit Cancer Metastasis. *Sci Rep,* 8**,** 2924.

SATOH-TAKAYAMA, N., VOSSHENRICH, C. A., LESJEAN-POTTIER, S., SAWA, S., LOCHNER, M., RATTIS, F., MENTION, J. J., THIAM, K., CERF-BENSUSSAN, N., MANDELBOIM, O., EBERL, G. & DI SANTO, J. P. 2008. Microbial flora drives interleukin 22 production in intestinal NKp46+ cells that provide innate mucosal immune defense. *Immunity,* 29**,** 958-70.

SAVOIA, P., ASTRUA, C. & FAVA, P. 2016. Ipilimumab (Anti-Ctla-4 Mab) in the treatment of metastatic melanoma: Effectiveness and toxicity management. *Human Vaccines & Immunotherapeutics,* 12**,** 1092-1101.

SAWA, S., CHERRIER, M., LOCHNER, M., SATOH-TAKAYAMA, N., FEHLING, H. J., LANGA, F., DI SANTO, J. P. & EBERL, G. 2010. Lineage relationship analysis of RORgammat+ innate lymphoid cells. *Science,* 330**,** 665-9.

SAWANT, D. V. & VIGNALI, D. A. 2014. Once a Treg, always a Treg? *Immunological reviews,* 259**,** 173-191.

SCHATTON, T., MURPHY, G. F., FRANK, N. Y., YAMAURA, K., WAAGA-GASSER, A. M., GASSER, M., ZHAN, Q., JORDAN, S., DUNCAN, L. M., WEISHAUPT, C., FUHLBRIGGE, R. C., KUPPER, T. S., SAYEGH, M. H. & FRANK, M. H. 2008. Identification of cells initiating human melanomas. *Nature,* 451**,** 345-9.

SCHIERING, C., KRAUSGRUBER, T., CHOMKA, A., FRöHLICH, A., ADELMANN, K., WOHLFERT, E. A., POTT, J., GRISERI, T., BOLLRATH, J., HEGAZY, A. N., HARRISON, O. J., OWENS, B. M. J., LöHNING, M., BELKAID, Y., FALLON, P. G. & POWRIE, F. 2014. The alarmin IL-33 promotes regulatory T-cell function in the intestine. *Nature,* 513**,** 564-568.

SCHNEIDER, H., PRASAD, K., SHOELSON, S. E. & RUDD, C. E. 1995. CTLA-4 binding to the lipid kinase phosphatidylinositol 3-kinase in T cells. *The Journal of experimental medicine,* 181**,** 351-355.

SCHULER, P. J., HARASYMCZUK, M., SCHILLING, B., SAZE, Z., STRAUSS, L., LANG, S., JOHNSON, J. T. & WHITESIDE, T. L. 2013. Effects of adjuvant chemoradiotherapy on the frequency and function of regulatory T cells in patients with head and neck cancer. *Clin Cancer Res,* 19**,** 6585-96.

SCHWARTZ, C., KHAN, A. R., FLOUDAS, A., SAUNDERS, S. P., HAMS, E., RODEWALD, H. R., MCKENZIE, A. N. J. & FALLON, P. G. 2017. ILC2s regulate adaptive Th2 cell functions via PD-L1 checkpoint control. *J Exp Med,* 214**,** 2507-2521.

SEFIK, E., GEVA-ZATORSKY, N., OH, S., KONNIKOVA, L., ZEMMOUR, D., MCGUIRE, A. M., BURZYN, D., ORTIZ-LOPEZ, A., LOBERA, M., YANG, J., GHOSH, S., EARL, A., SNAPPER, S. B., JUPP, R., KASPER, D., MATHIS, D. & BENOIST, C. 2015. MUCOSAL IMMUNOLOGY. Individual intestinal symbionts induce a distinct population of RORγ^{+} regulatory T cells. *Science,* 349**,** 993-7.

SEIF, F., TORKI, Z., ZALPOOR, H., HABIBI, M. & PORNOUR, M. 2023. Breast cancer tumor microenvironment affects Treg/IL-17-producing Treg/Th17 cell axis: Molecular and therapeutic perspectives. *Mol Ther Oncolytics,* 28**,** 132-157.

SELVERAJ, R. & GEIGER, T. 2008. Mitigation of experimental allergic encephalomyelitis by TGF-β induced Foxp3+ regulatory lymphocytes through the induction of anergy and infectious tolerance. *J Immunol,* 180**,** 2830-2838.

SHEPPARD, K. A., FITZ, L. J., LEE, J. M., BENANDER, C., GEORGE, J. A., WOOTERS, J., QIU, Y., JUSSIF, J. M., CARTER, L. L., WOOD, C. R. & CHAUDHARY, D. 2004. PD-1 inhibits T-cell receptor induced phosphorylation of the ZAP70/CD3zeta signalosome and downstream signaling to PKCtheta. *FEBS Lett,* 574**,** 37-41.

SHEVACH, E. M. & THORNTON, A. M. 2014. tTregs, pTregs, and iTregs: similarities and differences. *Immunological reviews,* 259**,** 88-102.

SHIMIZU, J., YAMAZAKI, S., TAKAHASHI, T., ISHIDA, Y. & SAKAGUCHI, S. 2002. Stimulation of CD25+ CD4+ regulatory T cells through GITR breaks immunological self-tolerance. *Nature immunology,* 3**,** 135-142.

SIEDE, J., FRöHLICH, A., DATSI, A., HEGAZY, A. N., VARGA, D. V., HOLECSKA, V., SAITO, H., NAKAE, S. & LöHNING, M. 2016. IL-33 receptor-expressing regulatory T cells are highly activated, Th2 biased and suppress CD4 T cell proliferation through IL-10 and TGFβ release. *PloS one,* 11**,** e0161507.

SINGER, A., ADORO, S. & PARK, J.-H. 2008. Lineage fate and intense debate: myths, models and mechanisms of CD4- versus CD8-lineage choice. *Nature Reviews Immunology,* 8**,** 788-801.

SINGH, K., HJORT, M., THORVALDSON, L. & SANDLER, S. 2015. Concomitant analysis of Helios and Neuropilin-1 as a marker to detect thymic derived regulatory T cells in naïve mice. *Scientific Reports,* 5**,** 7767.

SMITH, C. A., FARRAH, T. & GOODWIN, R. G. 1994. The TNF receptor superfamily of cellular and viral proteins: activation, costimulation, and death. *Cell,* 76**,** 959-962.

SMITH, E. L., FINNEY, H. M., NESBITT, A. M., RAMSDELL, F. & ROBINSON, M. K. 2006. Splice variants of human FOXP3 are functional inhibitors of human CD4+ T-cell activation. *Immunology,* 119**,** 203-11.

SMITH, K. A. & MAIZELS, R. M. 2014. IL-6 controls susceptibility to helminth infection by impeding Th2 responsiveness and altering the Treg phenotype in vivo. *European journal of immunology,* 44**,** 150-161.

SNELL, L. M., MCPHERSON, A. J., LIN, G. H., SAKAGUCHI, S., PANDOLFI, P. P., RICCARDI, C. & WATTS, T. H. 2010. CD8 T cell-intrinsic GITR is required for T cell clonal expansion and mouse survival following severe influenza infection. *The Journal of Immunology,* 185**,** 7223-7234.

SOJKA, D. K., PLOUGASTEL-DOUGLAS, B., YANG, L., PAK-WITTEL, M. A., ARTYOMOV, M. N., IVANOVA, Y., ZHONG, C., CHASE, J. M., ROTHMAN, P. B. & YU, J. 2014. Tissue-resident natural killer (NK) cells are cell lineages distinct from thymic and conventional splenic NK cells. *elife,* 3**,** e01659.

SOLé-BOLDO, L., RADDATZ, G., SCHüTZ, S., MALLM, J.-P., RIPPE, K., LONSDORF, A. S., RODRíGUEZ-PAREDES, M. & LYKO, F. 2020. Single-cell transcriptomes of the human skin reveal age-related loss of fibroblast priming. *Communications biology,* 3**,** 188.

SONNENBERG, G. F., MONTICELLI, L. A., ELLOSO, M. M., FOUSER, L. A. & ARTIS, D. 2011. CD4(+) lymphoid tissue-inducer cells promote innate immunity in the gut. *Immunity,* 34**,** 122-34.

SPITS, H., ARTIS, D., COLONNA, M., DIEFENBACH, A., DI SANTO, J. P., EBERL, G., KOYASU, S., LOCKSLEY, R. M., MCKENZIE, A. N. & MEBIUS, R. E. 2013. Innate lymphoid cells—a proposal for uniform nomenclature. *Nature reviews immunology,* 13**,** 145-149.

SQUIBB, B.-M. Press Release. FDA Approves YERVOY (Tm)(ipilimumab) for the treatment of patients with newly diagnosed or previously-treated unresectable or metastatic melanoma, the deadliest form of skin cancer.

STANIETSKY, N., ROVIS, T. L., GLASNER, A., SEIDEL, E., TSUKERMAN, P., YAMIN, R., ENK, J., JONJIC, S. & MANDELBOIM, O. 2013. Mouse TIGIT inhibits NK-cell cytotoxicity upon interaction with PVR. *Eur J Immunol,* 43**,** 2138-50.

STATHOPOULOU, C., GANGAPLARA, A., MALLETT, G., FLOMERFELT, F. A., LINIANY, L. P., KNIGHT, D., SAMSEL, L. A., BERLINGUER-PALMINI, R., YIM, J. J., FELIZARDO, T. C., ECKHAUS, M. A., EDGINGTON-MITCHELL, L., MARTINEZ-FABREGAS, J., ZHU, J., FOWLER, D. H., VAN KASTEREN, S. I., LAURENCE, A., BOGYO, M., WATTS, C., SHEVACH, E. M. & AMARNATH, S. 2018. PD-1 Inhibitory Receptor Downregulates Asparaginyl Endopeptidase and Maintains Foxp3 Transcription Factor Stability in Induced Regulatory T Cells. *Immunity,* 49**,** 247-263.e7.

STEINMETZ, O. M., SUMMERS, S. A., GAN, P.-Y., SEMPLE, T., HOLDSWORTH, S. R. & KITCHING, A. R. 2011. The Th17-defining transcription factor RORγt promotes glomerulonephritis. *Journal of the American Society of Nephrology,* 22**,** 472-483.

STEPHENS, G. L., MCHUGH, R. S., WHITTERS, M. J., YOUNG, D. A., LUXENBERG, D., CARRENO, B. M., COLLINS, M. & SHEVACH, E. M. 2004. Engagement of glucocorticoid-induced TNFR family-related receptor on effector T cells by its ligand mediates resistance to suppression by CD4+ CD25+ T cells. *The Journal of Immunology,* 173**,** 5008-5020.

STRAUSS, L., MAHMOUD, M. A. A., WEAVER, J. D., TIJARO-OVALLE, N. M., CHRISTOFIDES, A., WANG, Q., PAL, R., YUAN, M., ASARA, J., PATSOUKIS, N. & BOUSSIOTIS, V. A. 2020. Targeted deletion of PD-1 in myeloid cells induces antitumor immunity. *Sci Immunol,* 5.

SUGIHARA, S., IZUMI, Y., YOSHIOKA, T., YAGI, H., TSUJIMURA, T., TARUTANI, O., KOHNO, Y., MURAKAMI, S., HAMAOKA, T. & FUJIWARA, H. 1988. Autoimmune thyroiditis induced in mice depleted of particular T cell subsets. I. Requirement of Lyt-1 dull L3T4 bright normal T cells for the induction of thyroiditis. *J Immunol,* 141**,** 105-13.

SUGIMOTO, N., OIDA, T., HIROTA, K., NAKAMURA, K., NOMURA, T., UCHIYAMA, T. & SAKAGUCHI, S. 2006. Foxp3-dependent and-independent molecules specific for CD25+ CD4+ natural regulatory T cells revealed by DNA microarray analysis. *International immunology,* 18**,** 1197-1209.

SUKUMAR, S., WILSON, D. C., YU, Y., WONG, J., NARAVULA, S., ERMAKOV, G., RIENER, R., BHAGWAT, B., NECHEVA, A. S., GREIN, J., CHURAKOVA, T., MANGADU, R., GEORGIEV, P., MANFRA, D., PINHEIRO, E. M., SRIRAM, V., BAILEY, W. J., HERZYK, D., MCCLANAHAN, T. K., WILLINGHAM, A., BEEBE, A. M. & SADEKOVA, S. 2017. Characterization of MK-4166, a Clinical

Agonistic Antibody That Targets Human GITR and Inhibits the Generation and Suppressive Effects of T Regulatory Cells. *Cancer Research,* 77**,** 4378-4388.

SUNGNAK, W., WAGNER, A., KOWALCZYK, M. S., BOD, L., KYE, Y.-C., SAGE, P. T., SHARPE, A. H., SOBEL, R. A., QUINTANA, F. J., ROZENBLATT-ROSEN, O., REGEV, A., WANG, C., YOSEF, N. & KUCHROO, V. K. 2020. T Follicular Regulatory Cell–Derived Fibrinogen-like Protein 2 Regulates Production of Autoantibodies and Induction of Systemic Autoimmunity. *The Journal of Immunology,* 205**,** 3247-3262.

SURI-PAYER, E., AMAR, A. Z., THORNTON, A. M. & SHEVACH, E. M. 1998. CD4+CD25+ T cells inhibit both the induction and effector function of autoreactive T cells and represent a unique lineage of immunoregulatory cells. *J Immunol,* 160**,** 1212-8.

SZABO, S. J., KIM, S. T., COSTA, G. L., ZHANG, X., FATHMAN, C. G. & GLIMCHER, L. H. 2000. A Novel Transcription Factor, T-bet, Directs Th1 Lineage Commitment. *Cell,* 100**,** 655-669.

TAKAHAMA, Y., OHIGASHI, I., BAIK, S. & ANDERSON, G. 2017. Generation of diversity in thymic epithelial cells. *Nature Reviews Immunology,* 17**,** 295-305.

TAN, C. L., KUCHROO, J. R., SAGE, P. T., LIANG, D., FRANCISCO, L. M., BUCK, J., THAKER, Y. R., ZHANG, Q., MCARDEL, S. L., JUNEJA, V. R., LEE, S. J., LOVITCH, S. B., LIAN, C., MURPHY, G. F., BLAZAR, B. R., VIGNALI, D. A. A., FREEMAN, G. J. & SHARPE, A. H. 2020. PD-1 restraint of regulatory T cell suppressive activity is critical for immune tolerance. *Journal of Experimental Medicine,* 218.

TAN, C. L., KUCHROO, J. R., SAGE, P. T., LIANG, D., FRANCISCO, L. M., BUCK, J., THAKER, Y. R., ZHANG, Q., MCARDEL, S. L., JUNEJA, V. R., LEE, S. J., LOVITCH, S. B., LIAN, C., MURPHY, G. F., BLAZAR, B. R., VIGNALI, D. A. A., FREEMAN, G. J. & SHARPE, A. H. 2021. PD-1 restraint of regulatory T cell suppressive activity is critical for immune tolerance. *J Exp Med,* 218.

TANIGUCHI, R. T., DEVOSS, J. J., MOON, J. J., SIDNEY, J., SETTE, A., JENKINS, M. K. & ANDERSON, M. S. 2012. Detection of an autoreactive T-cell population within the polyclonal repertoire that undergoes distinct autoimmune regulator (Aire)-mediated selection. *Proc Natl Acad Sci U S A,* 109**,** 7847-52.

TAO, R., DE ZOETEN, E. F., OZKAYNAK, E., CHEN, C., WANG, L., PORRETT, P. M., LI, B., TURKA, L. A., OLSON, E. N., GREENE, M. I., WELLS, A. D. & HANCOCK, W. W. 2007. Deacetylase inhibition promotes the generation and function of regulatory T cells. *Nat Med,* 13**,** 1299-307.

TAWBI, H. A., HODI, F. S., LIPSON, E. J., SCHADENDORF, D., ASCIERTO, P. A., MATAMALA, L., GUTIéRREZ, E. C., RUTKOWSKI, P., GOGAS, H., LAO, C. D., MENEZES, J. J. D., DALLE, S., ARANCE, A. M., GROB, J.-J., RATTO, B., RODRIGUEZ, S., MAZZEI, A., DOLFI, S. & LONG, G. V. Three-Year Overall Survival With Nivolumab Plus Relatlimab in Advanced Melanoma From RELATIVITY-047. *Journal of Clinical Oncology,* 0**,** JCO.24.01124.

TAYLOR, S., HUANG, Y., MALLETT, G., STATHOPOULOU, C., FELIZARDO, T. C., SUN, M. A., MARTIN, E. L., ZHU, N., WOODWARD, E. L., ELIAS, M. S., SCOTT, J., REYNOLDS, N. J., PAUL, W. E., FOWLER, D. H. & AMARNATH, S. 2017. PD-1 regulates KLRG1(+) group 2 innate lymphoid cells. *J Exp Med,* 214**,** 1663-1678.

TEFT, W. A., CHAU, T. A. & MADRENAS, J. 2009. Structure-Function analysis of the CTLA-4 interaction with PP2A. *BMC Immunol,* 10**,** 23.

THOMAS, L. 1982. On immunosurveillance in human cancer. *Yale J Biol Med,* 55**,** 329-33.

THORNTON, A. M., KORTY, P. E., TRAN, D. Q., WOHLFERT, E. A., MURRAY, P. E., BELKAID, Y. & SHEVACH, E. M. 2010. Expression of Helios, an Ikaros transcription factor family member, differentiates thymic-derived from peripherally induced Foxp3+ T regulatory cells. *The Journal of Immunology,* 184**,** 3433-3441.

THORNTON, A. M. & SHEVACH, E. M. 1998. CD4+CD25+ immunoregulatory T cells suppress polyclonal T cell activation in vitro by inhibiting interleukin 2 production. *J Exp Med,* 188**,** 287-96.

TIAN, X., ZHANG, A., QIU, C., WANG, W., YANG, Y., QIU, C., LIU, A., ZHU, L., YUAN, S. & HU, H. 2015. The upregulation of LAG-3 on T cells defines a subpopulation with functional exhaustion and correlates with disease progression in HIV-infected subjects. *The Journal of Immunology,* 194**,** 3873-3882.

TIROSH, I., IZAR, B., PRAKADAN, S. M., WADSWORTH, M. H., TREACY, D., TROMBETTA, J. J., ROTEM, A., RODMAN, C., LIAN, C. & MURPHY, G. 2016. Dissecting the multicellular ecosystem of metastatic melanoma by single-cell RNA-seq. *Science,* 352**,** 189-196.

TIZIAN, C., LAHMANN, A., HöLSKEN, O., COSOVANU, C., KOFOED-BRANZK, M., HEINRICH, F., MASHREGHI, M.-F., KRUGLOV, A., DIEFENBACH, A. & NEUMANN, C. 2020. c-Maf restrains T-bet-driven programming of CCR6-negative group 3 innate lymphoid cells. *Elife,* 9**,** e52549.

TOMMASINI, A., FERRARI, S., MORATTO, D., BADOLATO, R., BONIOTTO, M., PIRULLI, D., NOTARANGELO, L. & ANDOLINA, M. 2002. X-chromosome inactivation analysis in a female carrier of FOXP3 mutation. *Clinical & Experimental Immunology,* 130**,** 127-130.

TONE, M., TONE, Y., ADAMS, E., YATES, S. F., FREWIN, M. R., COBBOLD, S. P. & WALDMANN, H. 2003. Mouse glucocorticoid-induced tumor necrosis factor receptor ligand is costimulatory for T cells. *Proceedings of the National Academy of Sciences,* 100**,** 15059-15064.

TONE, Y., FURUUCHI, K., KOJIMA, Y., TYKOCINSKI, M. L., GREENE, M. I. & TONE, M. 2008. Smad3 and NFAT cooperate to induce Foxp3 expression through its enhancer. *Nat Immunol,* 9**,** 194-202.

TOPALIAN, S. L., HODI, F. S., BRAHMER, J. R., GETTINGER, S. N., SMITH, D. C., MCDERMOTT, D. F., POWDERLY, J. D., CARVAJAL, R. D., SOSMAN, J. A., ATKINS, M. B., LEMING, P. D., SPIGEL, D. R., ANTONIA, S. J., HORN, L., DRAKE, C. G., PARDOLL, D. M., CHEN, L., SHARFMAN, W. H., ANDERS, R. A., TAUBE, J. M., MCMILLER, T. L., XU, H., KORMAN, A. J., JURE-KUNKEL, M., AGRAWAL, S., MCDONALD, D., KOLLIA, G. D., GUPTA, A., WIGGINTON, J. M. & SZNOL, M. 2012. Safety, activity, and immune correlates of anti-PD-1 antibody in cancer. *N Engl J Med,* 366**,** 2443-54.

USUI, T., PREISS, J. C., KANNO, Y., YAO, Z. J., BREAM, J. H., O'SHEA, J. J. & STROBER, W. 2006. T-bet regulates Th1 responses through essential effects on GATA-3 function rather than on IFNG gene acetylation and transcription. *The Journal of experimental medicine,* 203**,** 755-766.

VACCA, P., PESCE, S., GREPPI, M., FULCHERI, E., MUNARI, E., OLIVE, D., MINGARI, M. C., MORETTA, A., MORETTA, L. & MARCENARO, E. 2019. PD-1 is expressed by and regulates human group 3 innate lymphoid cells in human decidua. *Mucosal Immunol,* 12**,** 624-631.

VALZASINA, B., GUIDUCCI, C., DISLICH, H., KILLEEN, N., WEINBERG, A. D. & COLOMBO, M. P. 2005. Triggering of OX40 (CD134) on CD4+ CD25+ T cells

blocks their inhibitory activity: a novel regulatory role for OX40 and its comparison with GITR. *Blood,* 105**,** 2845-2851.

VAN DE PAVERT, S. A. & MEBIUS, R. E. 2010. New insights into the development of lymphoid tissues. *Nature Reviews Immunology,* 10**,** 664-674.

VAN GULIJK, M., VAN KRIMPEN, A., SCHETTERS, S., ETERMAN, M., VAN ELSAS, M., MANKOR, J., KLAASE, L., DE BRUIJN, M., VAN NIMWEGEN, M., VAN TIENHOVEN, T., VAN IJCKEN, W., BOON, L., VAN DER SCHOOT, J., VERDOES, M., SCHEEREN, F., VAN DER BURG, S. H., LAMBRECHT, B. N., STADHOUDERS, R., DAMMEIJER, F., AERTS, J. & VAN HALL, T. 2023. PD-L1 checkpoint blockade promotes regulatory T cell activity that underlies therapy resistance. *Sci Immunol,* 8**,** eabn6173.

VAN LOOSDREGT, J., BRUNEN, D., FLESKENS, V., PALS, C. E., LAM, E. W. & COFFER, P. J. 2011. Rapid temporal control of Foxp3 protein degradation by sirtuin-1. *PLoS One,* 6**,** e19047.

VAN LOOSDREGT, J., FLESKENS, V., FU, J., BRENKMAN, A. B., BEKKER, C. P., PALS, C. E., MEERDING, J., BERKERS, C. R., BARBI, J., GRöNE, A., SIJTS, A. J., MAURICE, M. M., KALKHOVEN, E., PRAKKEN, B. J., OVAA, H., PAN, F., ZAISS, D. M. & COFFER, P. J. 2013. Stabilization of the transcription factor Foxp3 by the deubiquitinase USP7 increases Treg-cell-suppressive capacity. *Immunity,* 39**,** 259-71.

VAN LOOSDREGT, J., VERCOULEN, Y., GUICHELAAR, T., GENT, Y. Y., BEEKMAN, J. M., VAN BEEKUM, O., BRENKMAN, A. B., HIJNEN, D. J., MUTIS, T., KALKHOVEN, E., PRAKKEN, B. J. & COFFER, P. J. 2010. Regulation of Treg functionality by acetylation-mediated Foxp3 protein stabilization. *Blood,* 115**,** 965-74.

VAN OLFFEN, R. W., KONING, N., VAN GISBERGEN, K. P., WENSVEEN, F. M., HOEK, R. M., BOON, L., HAMANN, J. R., VAN LIER, R. A. & NOLTE, M. A. 2009. GITR triggering induces expansion of both effector and regulatory CD4+ T cells in vivo. *The Journal of Immunology,* 182**,** 7490-7500.

VAN PANHUYS, N., KLAUSCHEN, F. & GERMAIN, RONALD N. 2014. T-Cell-Receptor-Dependent Signal Intensity Dominantly Controls CD4+ T Cell Polarization In Vivo. *Immunity,* 41**,** 63-74.

VENIGALLA, R. K. C., GUTTIKONDA, P. J., ECKSTEIN, V., HO, A. D., SERTEL, S., LORENZ, H.-M. & TRETTER, T. 2012. Identification of a human Th1-like IFNγ-secreting Treg subtype deriving from effector T cells. *Journal of autoimmunity,* 39**,** 377-387.

VIANT, C., RANKIN, L. C., GIRARD-MADOUX, M. J., SEILLET, C., SHI, W., SMYTH, M. J., BARTHOLIN, L., WALZER, T., HUNTINGTON, N. D. & VIVIER, E. 2016. Transforming growth factor–β and Notch ligands act as opposing environmental cues in regulating the plasticity of type 3 innate lymphoid cells. *Science signaling,* 9**,** ra46-ra46.

VILLARINO, A. V., LAURENCE, A. D., DAVIS, F. P., NIVELO, L., BROOKS, S. R., SUN, H. W., JIANG, K., AFZALI, B., FRASCA, D., HENNIGHAUSEN, L., KANNO, Y. & O'SHEA, J. J. 2022. A central role for STAT5 in the transcriptional programing of T helper cell metabolism. *Sci Immunol,* 7**,** eabl9467.

VOO, K. S., WANG, Y.-H., SANTORI, F. R., BOGGIANO, C., WANG, Y.-H., ARIMA, K., BOVER, L., HANABUCHI, S., KHALILI, J., MARINOVA, E., ZHENG, B., LITTMAN, D. R. & LIU, Y.-J. 2009. Identification of IL-17-producing FOXP3⁺ regulatory T cells in humans. *Proceedings of the National Academy of Sciences,* 106**,** 4793-4798.

WAGNER, M., EALEY, K. N., TETSU, H., KINIWA, T., MOTOMURA, Y., MORO, K. & KOYASU, S. 2020. Tumor-Derived Lactic Acid Contributes to the Paucity of Intratumoral ILC2s. *Cell Rep,* 30**,** 2743-2757.e5.

WALDMAN, A. D., FRITZ, J. M. & LENARDO, M. J. 2020. A guide to cancer immunotherapy: from T cell basic science to clinical practice. *Nat Rev Immunol,* 20**,** 651-668.

WALKER, L. S. K. & SANSOM, D. M. 2015. Confusing signals: recent progress in CTLA-4 biology. *Trends in immunology,* 36**,** 63-70.

WALKER, M. R., KASPROWICZ, D. J., GERSUK, V. H., BENARD, A., VAN LANDEGHEN, M., BUCKNER, J. H. & ZIEGLER, S. F. 2003. Induction of FoxP3 and acquisition of T regulatory activity by stimulated human CD4+CD25- T cells. *J Clin Invest,* 112**,** 1437-43.

WAN, Y. Y. & FLAVELL, R. A. 2007. Regulatory T-cell functions are subverted and converted owing to attenuated Foxp3 expression. *Nature,* 445**,** 766-70.

WANG, J., SANMAMED, M. F., DATAR, I., SU, T. T., JI, L., SUN, J., CHEN, L., CHEN, Y., ZHU, G. & YIN, W. 2019. Fibrinogen-like protein 1 is a major immune inhibitory ligand of LAG-3. *Cell,* 176**,** 334-347. e12.

WANG, L., DE ZOETEN, E. F., GREENE, M. I. & HANCOCK, W. W. 2009. Immunomodulatory effects of deacetylase inhibitors: therapeutic targeting of FOXP3+ regulatory T cells. *Nat Rev Drug Discov,* 8**,** 969-81.

WANG, Y., SOUABNI, A., FLAVELL, R. A. & WAN, Y. Y. 2010. An intrinsic mechanism predisposes Foxp3-expressing regulatory T cells to Th2 conversion in vivo. *The Journal of Immunology,* 185**,** 5983-5992.

WANG, Y., SU, M. A. & WAN, Y. Y. 2011. An essential role of the transcription factor GATA-3 for the function of regulatory T cells. *Immunity,* 35**,** 337-348.

WATANABE, M., NAKANO, K., TOGANO, T., NAKASHIMA, M., HIGASHIHARA, M., KADIN, M. E., WATANABE, T. & HORIE, R. 2011. Targeted repression of overexpressed CD30 downregulates NF-kappaB and ERK1/2 pathway in Hodgkin lymphoma cell lines. *Oncology research,* 19**,** 463-469.

WEISS, J. M., BILATE, A. M., GOBERT, M., DING, Y., CUROTTO DE LAFAILLE, M. A., PARKHURST, C. N., XIONG, H., DOLPADY, J., FREY, A. B., RUOCCO, M. G., YANG, Y., FLOESS, S., HUEHN, J., OH, S., LI, M. O., NIEC, R. E., RUDENSKY, A. Y., DUSTIN, M. L., LITTMAN, D. R. & LAFAILLE, J. J. 2012. Neuropilin 1 is expressed on thymus-derived natural regulatory T cells, but not mucosa-generated induced Foxp3+ T reg cells. *J Exp Med,* 209**,** 1723-42, s1.

WHERRY, E. J. & KURACHI, M. 2015. Molecular and cellular insights into T cell exhaustion. *Nature Reviews Immunology,* 15**,** 486-499.

WILDIN, R. S., RAMSDELL, F., PEAKE, J., FARAVELLI, F., CASANOVA, J. L., BUIST, N., LEVY-LAHAD, E., MAZZELLA, M., GOULET, O., PERRONI, L., BRICARELLI, F. D., BYRNE, G., MCEUEN, M., PROLL, S., APPLEBY, M. & BRUNKOW, M. E. 2001. X-linked neonatal diabetes mellitus, enteropathy and endocrinopathy syndrome is the human equivalent of mouse scurfy. *Nat Genet,* 27**,** 18-20.

WILHELM, C., HARRISON, O. J., SCHMITT, V., PELLETIER, M., SPENCER, S. P., URBAN, J. F., JR., PLOCH, M., RAMALINGAM, T. R., SIEGEL, R. M. & BELKAID, Y. 2016. Critical role of fatty acid metabolism in ILC2-mediated barrier protection during malnutrition and helminth infection. *J Exp Med,* 213**,** 1409-18.

WILLIAMS, L. M. & RUDENSKY, A. Y. 2007. Maintenance of the Foxp3-dependent developmental program in mature regulatory T cells requires continued expression of Foxp3. *Nat Immunol,* 8**,** 277-84.

WING, JAMES B., ISE, W., KUROSAKI, T. & SAKAGUCHI, S. 2014. Regulatory T Cells Control Antigen-Specific Expansion of Tfh Cell Number and Humoral Immune Responses via the Coreceptor CTLA-4. *Immunity,* 41**,** 1013-1025.

WING, J. B., KITAGAWA, Y., LOCCI, M., HUME, H., TAY, C., MORITA, T., KIDANI, Y., MATSUDA, K., INOUE, T., KUROSAKI, T., CROTTY, S., COBAN, C., OHKURA, N. & SAKAGUCHI, S. 2017. A distinct subpopulation of CD25[−] T-follicular regulatory cells localizes in the germinal centers. *Proceedings of the National Academy of Sciences,* 114**,** E6400-E6409.

WINSTEAD, C. J. 2014. Follicular helper T cell-mediated mucosal barrier maintenance. *Immunol Lett,* 162**,** 39-47.

WOHLFERT, E. A., GRAINGER, J. R., BOULADOUX, N., KONKEL, J. E., OLDENHOVE, G., RIBEIRO, C. H., HALL, J. A., YAGI, R., NAIK, S. & BHAIRAVABHOTLA, R. 2011. GATA3 controls Foxp3+ regulatory T cell fate during inflammation in mice. *The Journal of clinical investigation,* 121**,** 4503-4515.

WOLCHOK, J. D., KLUGER, H., CALLAHAN, M. K., POSTOW, M. A., RIZVI, N. A., LESOKHIN, A. M., SEGAL, N. H., ARIYAN, C. E., GORDON, R.-A. & REED, K. 2013. Nivolumab plus ipilimumab in advanced melanoma. *New England Journal of Medicine,* 369**,** 122-133.

WOLF, Y., ANDERSON, A. C. & KUCHROO, V. K. 2020. TIM3 comes of age as an inhibitory receptor. *Nature Reviews Immunology,* 20**,** 173-185.

WOLLENBERG, I., AGUA-DOCE, A., HERNáNDEZ, A., ALMEIDA, C., OLIVEIRA, V. G., FARO, J. & GRACA, L. 2011. Regulation of the Germinal Center Reaction by Foxp3+ Follicular Regulatory T Cells. *The Journal of Immunology,* 187**,** 4553-4560.

XIAO, Y., NAGAI, Y., DENG, G., OHTANI, T., ZHU, Z., ZHOU, Z., ZHANG, H., JI, M. Q., LOUGH, J. W., SAMANTA, A., HANCOCK, W. W. & GREENE, M. I. 2014. Dynamic interactions between TIP60 and p300 regulate FOXP3 function through a structural switch defined by a single lysine on TIP60. *Cell Rep,* 7**,** 1471-1480.

XU, F., LIU, J., LIU, D., LIU, B., WANG, M., HU, Z., DU, X., TANG, L. & HE, F. 2014. LSECtin expressed on melanoma cells promotes tumor progression by inhibiting antitumor T-cell responses. *Cancer research,* 74**,** 3418-3428.

XU, L., KITANI, A., STUELTEN, C., MCGRADY, G., FUSS, I. & STROBER, W. 2010. Positive and Negative Transcriptional Regulation of the Foxp3 Gene is Mediated by Access and Binding of the Smad3 Protein to Enhancer I. *Immunity,* 33**,** 313-325.

XU, X., HUANG, H., WANG, Q., CAI, M., QIAN, Y., HAN, Y., WANG, X., GAO, Y., YUAN, M. & XU, L. 2017. IFN-γ-producing Th1-like regulatory T cells may limit acute cellular renal allograft rejection: Paradoxical post-transplantation effects of IFN-γ. *Immunobiology,* 222**,** 280-290.

XU, Z., JIANG, X., DAI, X. & LI, B. 2022. The dynamic role of FOXP3+ tregs and their potential therapeutic applications during SARS-CoV-2 infection. *Frontiers in Immunology,* 13**,** 916411.

YADAV, M., LOUVET, C., DAVINI, D., GARDNER, J. M., MARTINEZ-LLORDELLA, M., BAILEY-BUCKTROUT, S., ANTHONY, B. A., SVERDRUP, F. M., HEAD, R. & KUSTER, D. J. 2012. Neuropilin-1 distinguishes natural and inducible regulatory T cells among regulatory T cell subsets in vivo. *Journal of Experimental Medicine,* 209**,** 1713-1722.

YAMADA, A., USHIO, A., ARAKAKI, R., TSUNEMATSU, T., KUDO, Y., HAYASHI, Y. & ISHIMARU, N. 2015. Impaired expansion of regulatory T cells in a neonatal thymectomy-induced autoimmune mouse model. *The American Journal of Pathology,* 185**,** 2886-2897.

YAMAZAKI, T., YANG, X. O., CHUNG, Y., FUKUNAGA, A., NURIEVA, R., PAPPU, B., MARTIN-OROZCO, N., KANG, H. S., MA, L., PANOPOULOS, A. D., CRAIG, S., WATOWICH, S. S., JETTEN, A. M., TIAN, Q. & DONG, C. 2008. CCR6 regulates the migration of inflammatory and regulatory T cells. *J Immunol,* 181**,** 8391-401.

YAN, J., ZHANG, Y., ZHANG, J.-P., LIANG, J., LI, L. & ZHENG, L. 2013. Tim-3 expression defines regulatory T cells in human tumors. *PloS one,* 8**,** e58006.

YANG, R., QU, C., ZHOU, Y., KONKEL, J. E., SHI, S., LIU, Y., CHEN, C., LIU, S., LIU, D., CHEN, Y., ZANDI, E., CHEN, W., ZHOU, Y. & SHI, S. 2015. Hydrogen Sulfide Promotes Tet1- and Tet2-Mediated Foxp3 Demethylation to Drive Regulatory T Cell Differentiation and Maintain Immune Homeostasis. *Immunity,* 43**,** 251-263.

YAO, Y., CHEN, C.-L., YU, D. & LIU, Z. 2021. Roles of follicular helper and regulatory T cells in allergic diseases and allergen immunotherapy. *Allergy,* 76**,** 456-470.

YAO, Z., KANNO, Y., KERENYI, M., STEPHENS, G., DURANT, L., WATFORD, W. T., LAURENCE, A., ROBINSON, G. W., SHEVACH, E. M. & MORIGGL, R. 2007. Nonredundant roles for Stat5a/b in directly regulating Foxp3. *Blood,* 109**,** 4368-4375.

YOKOSUKA, T., TAKAMATSU, M., KOBAYASHI-IMANISHI, W., HASHIMOTO-TANE, A., AZUMA, M. & SAITO, T. 2012. Programmed cell death 1 forms negative costimulatory microclusters that directly inhibit T cell receptor signaling by recruiting phosphatase SHP2. *J Exp Med,* 209**,** 1201-17.

YU, F., SHARMA, S., EDWARDS, J., FEIGENBAUM, L. & ZHU, J. 2015. Dynamic expression of transcription factors T-bet and GATA-3 by regulatory T cells maintains immunotolerance. *Nat Immunol,* 16**,** 197-206.

YU, X., HARDEN, K., GONZALEZ, L. C., FRANCESCO, M., CHIANG, E., IRVING, B., TOM, I., IVELJA, S., REFINO, C. J. & CLARK, H. 2009. The surface protein TIGIT suppresses T cell activation by promoting the generation of mature immunoregulatory dendritic cells. *Nature immunology,* 10**,** 48-57.

YU, Y., TSANG, J. C., WANG, C., CLARE, S., WANG, J., CHEN, X., BRANDT, C., KANE, L., CAMPOS, L. S. & LU, L. 2016. Single-cell RNA-seq identifies a PD-1hi ILC progenitor and defines its development pathway. *Nature,* 539**,** 102-106.

ZAGORULYA, M., YIM, L., MORGAN, D. M., EDWARDS, A., TORRES-MEJIA, E., MOMIN, N., MCCREERY, C. V., ZAMORA, I. L., HORTON, B. L. & FOX, J. G. 2023. Tissue-specific abundance of interferon-gamma drives regulatory T cells to restrain DC1-mediated priming of cytotoxic T cells against lung cancer. *Immunity,* 56**,** 386-405. e10.

ZAMBRANO-ZARAGOZA, J. F., ROMO-MARTíNEZ, E. J., DURáN-AVELAR MDE, J., GARCíA-MAGALLANES, N. & VIBANCO-PéREZ, N. 2014. Th17 cells in autoimmune and infectious diseases. *Int J Inflam,* 2014**,** 651503.

ZEIDAN, A. M., GIAGOUNIDIS, A., SEKERES, M. A., XIAO, Z., SANZ, G. F., HOEF, M. V., MA, F., HERTLE, S. & SANTINI, V. 2023. STIMULUS-MDS2 design and rationale: a phase III trial with the anti-TIM-3 sabatolimab (MBG453) + azacitidine in higher risk MDS and CMML-2. *Future Oncol,* 19**,** 631-642.

ZEISER, R., NGUYEN, V., HOU, J.-Z., BEILHACK, A., ZAMBRICKI, E., BUESS, M., CONTAG, C. & NEGRIN, R. 2007. Early CD30 signaling is critical for adoptively transferred CD4+CD25+ regulatory T cells in prevention of acute graft-versus-host disease. *Blood,* 109**,** 2225-33.

ZHAN, Y., GERONDAKIS, S., COGHILL, E., BOURGES, D., XU, Y., BRADY, J. L. & LEW, A. M. 2008. Glucocorticoid-induced TNF receptor expression by T cells is

reciprocally regulated by NF-κB and NFAT. *The Journal of Immunology,* 181**,** 5405-5413.

ZHANG, K., XU, X., PASHA, M. A., SIEBEL, C. W., COSTELLO, A., HACZKU, A., MACNAMARA, K., LIANG, T., ZHU, J. & BHANDOOLA, A. 2017. Cutting edge: notch signaling promotes the plasticity of group-2 innate lymphoid cells. *The Journal of Immunology,* 198**,** 1798-1803.

ZHANG, Q., WANG, H. Y., MARZEC, M., RAGHUNATH, P. N., NAGASAWA, T. & WASIK, M. A. 2005. STAT3-and DNA methyltransferase 1-mediated epigenetic silencing of SHP-1 tyrosine phosphatase tumor suppressor gene in malignant T lymphocytes. *Proceedings of the National Academy of Sciences,* 102**,** 6948-6953.

ZHAO, J., ZHAO, J. & PERLMAN, S. 2012. Differential effects of IL-12 on Tregs and non-Treg T cells: roles of IFN-γ, IL-2 and IL-2R.

ZHAO, P., XIAO, X., GHOBRIAL, R. M. & LI, X. C. 2013. IL-9 and Th9 cells: progress and challenges. *Int Immunol,* 25**,** 547-51.

ZHENG, B., FIUMARA, P., LI, Y. V., GEORGAKIS, G., SNELL, V., YOUNES, M., VAUTHEY, J. N., CARBONE, A. & YOUNES, A. 2003. MEK/ERK pathway is aberrantly active in Hodgkin disease: a signaling pathway shared by CD30, CD40, and RANK that regulates cell proliferation and survival. *Blood,* 102**,** 1019-1027.

ZHENG, J., LIU, Y., QIN, G., LAM, K. T., GUAN, J., XIANG, Z., LEWIS, D. B., LAU, Y. L. & TU, W. 2011. Generation of human Th1-like regulatory CD4+ T cells by an intrinsic IFN-γ-and T-bet-dependent pathway. *European journal of immunology,* 41**,** 128-139.

ZHENG, W. & FLAVELL, R. A. 1997. The transcription factor GATA-3 is necessary and sufficient for Th2 cytokine gene expression in CD4 T cells. *Cell,* 89**,** 587-96.

ZHENG, Y., CHAUDHRY, A., KAS, A., DEROOS, P., KIM, J. M., CHU, T.-T., CORCORAN, L., TREUTING, P., KLEIN, U. & RUDENSKY, A. Y. 2009. Regulatory T-cell suppressor program co-opts transcription factor IRF4 to control TH2 responses. *Nature,* 458**,** 351-356.

ZHENG, Y., JOSEFOWICZ, S., CHAUDHRY, A., PENG, X. P., FORBUSH, K. & RUDENSKY, A. Y. 2010. Role of conserved non-coding DNA elements in the Foxp3 gene in regulatory T-cell fate. *Nature,* 463**,** 808-812.

ZHONG, W., XU, X., ZHU, Z., DU, Q., DU, H., YANG, L., LING, Y., XIONG, H. & LI, Q. 2017. Increased expression of IRF8 in tumor cells inhibits the generation of Th17 cells and predicts unfavorable survival of diffuse large B cell lymphoma patients. *Oncotarget,* 8**,** 49757-49772.

ZHOU, A. X., KOZHAYA, L., FUJII, H. & UNUTMAZ, D. 2013. GARP–TGF-β Complexes Negatively Regulate Regulatory T Cell Development and Maintenance of Peripheral CD4+ T Cells In Vivo. *The Journal of Immunology,* 190**,** 5057-5064.

ZHOU, Q., MUNGER, M. E., VEENSTRA, R. G., WEIGEL, B. J., HIRASHIMA, M., MUNN, D. H., MURPHY, W. J., AZUMA, M., ANDERSON, A. C. & KUCHROO, V. K. 2011. Coexpression of Tim-3 and PD-1 identifies a CD8+ T-cell exhaustion phenotype in mice with disseminated acute myelogenous leukemia. *Blood, The Journal of the American Society of Hematology,* 117**,** 4501-4510.

ZHU, C., ANDERSON, A. C., SCHUBART, A., XIONG, H., IMITOLA, J., KHOURY, S. J., ZHENG, X. X., STROM, T. B. & KUCHROO, V. K. 2005. The Tim-3 ligand galectin-9 negatively regulates T helper type 1 immunity. *Nature immunology,* 6**,** 1245-1252.

ZIEGLER, S. F. 2006. FOXP3: of mice and men. *Annu Rev Immunol,* 24**,** 209-26.

Appendix A

Boolean linear analysis of coreceptor expression on WT and *Pd1*$^{-/-}$ Tregs in murine splenocytes. Conventionally, single coreceptor expression was assessed on cells which lead to an issue where some cells could co-express more than one coreceptor. To avoid the circumstances, Boolean analysis was performed on FlowJo which allows the inspection of protein co-expression. Statistical analysis was done using an unpaired Student's t-test. **Table A.1** and **Table A.2** show the mean, standard deviation (SD) and standard error of mean (SEM) in Tregs from WT versus *Pd1*$^{-/-}$ mice and *Pd1*$^{fl/fl}$*Foxp3*^{ERT2Cre} treated with PBS or tamoxifen, respectively.

	WT			*Pd1-/-*					
	Mean	**SD**	**SEM**	**Mean**	**SD**	**SEM**	**p value**	**Sample Number**	**Statistical Analysis**
All 5 co-inhibitory receptor positive subset									
CD30+CTLA4+GARP+GITR+TIGIT+	1529	2546	962.2	3280	1831	692.1	0.0690	7	Unpaired Student's t test
4 co-inhibitory receptor positive subset									
CD30+CTLA4+GARP+GITR+TIGIT-	1745	2363	893.2	2080	1988	751.3	0.7191	7	Unpaired Student's t test
CD30+CTLA4+GARP+GITR-TIGIT+	507.9	1330	502.9	893.4	1614	610.1	0.6770	7	Unpaired Student's t test
CD30+CTLA4+GARP-GITR+TIGIT+	6027	4245	1604	19752	8351	3156	**0.0107**	7	Unpaired Student's t test
CD30+CTLA4-GARP+GITR+TIGIT+	66	75.78	28.64	271.1	311.1	117.6	0.0877	7	Unpaired Student's t test
CD30-CTLA4+GARP+GITR+TIGIT+	13358	16940	6403	91000	121779	46028	0.1375	7	Unpaired Student's t test
3 co-inhibitory receptor positive subset									
CD30+CTLA4+GARP+GITR-TIGIT-	4.286	11.34	4.286	56.29	107.7	40.69	0.2608	7	Unpaired Student's t test
CD30+CTLA4+GARP-GITR+TIGIT-	7348	9493	3588	10307	9730	3678	0.3729	7	Unpaired Student's t test
CD30+CTLA4+GARP-GITR-TIGIT+	3463	5100	1927	4869	6771	2559	0.4122	7	Unpaired Student's t test
CD30+CTLA4-GARP+GITR+TIGIT-	277.9	397.8	150.3	304.7	512.2	193.6	0.9119	7	Unpaired Student's t test
CD30+CTLA4-GARP+GITR-TIGIT+	274.9	658.5	248.9	7	18.52	7	0.3257	7	Unpaired Student's t test
CD30+CTLA4-GARP-GITR+TIGIT+	210.7	314.1	118.7	612	650.2	245.7	0.0728	7	Unpaired Student's t test
CD30-CTLA4+GARP+GITR+TIGIT-	25064	16390	6195	40189	24209	9150	0.1386	7	Unpaired Student's t test
CD30-CTLA4+GARP+GITR-TIGIT+	8131	13531	5114	27533	42766	16164	0.2515	7	Unpaired Student's t test
CD30-CTLA4-GARP+GITR+TIGIT+	1145	905.2	342.1	4380	2485	939.1	**0.0208**	7	Unpaired Student's t test
2 co-inhibitory receptor positive subset									
CD30+CTLA4+GARP-GITR-TIGIT-	1890	4156	1571	1991	3124	1181	0.9470	7	Unpaired Student's t test
CD30+CTLA4-GARP+GITR-TIGIT-	16	31.18	11.78	32	54.65	20.66	0.3933	7	Unpaired Student's t test
CD30-CTLA4+GARP+GITR-TIGIT-	7774	12789	4834	9614	14208	5370	0.5879	7	Unpaired Student's t test
CD30-CTLA4+GARP-GITR+TIGIT-	165056	115755	43751	269820	116352	43977	**0.0436**	7	Unpaired Student's t test
CD30+CTLA4-GARP-GITR+TIGIT-	1773	2157	815.4	2566	2595	980.7	0.4266	7	Unpaired Student's t test
CD30+CTLA4-GARP-GITR-TIGIT+	531	1322	499.5	305.1	807.3	305.1	0.2911	7	Unpaired Student's t test
CD30-CTLA4+GARP-GITR-TIGIT+	60215	76357	28860	273813	436815	165101	0.1988	7	Unpaired Student's t test
CD30-CTLA4-GARP+GITR+TIGIT-	6033	2379	899.1	6257	3422	1293	0.8833	7	Unpaired Student's t test
CD30-CTLA4-GARP+GITR-TIGIT+	1220	1551	586.1	1166	3084	1166	0.9609	7	Unpaired Student's t test
CD30-CTLA4-GARP-GITR+TIGIT+	6722	3275	1238	40069	21975	8306	**0.0075**	7	Unpaired Student's t test

Table A.1 Detailed analysis of co-receptor expression patterns in WT and *Pd1*$^{-/-}$ Tregs using Boolean linear analysis.

	PD1fl/flFoxP3ERT2CRE with PBS			PD1fl/flFoxP3ERT2CRE with Tamoxifen					
	Mean	SD	SEM	Mean	SD	SEM	P value	ample Numb	Statistical Analysis
All 5 co-inhibitory receptor positive subset									
CD30+CTLA4+GARP+GITR+TIGIT+	1141	1434	542.1	4006	3181	1202	0.0506	7	Unpaired Student's t test
4 co-inhibitory receptor positive subset									
CD30+CTLA4+GARP+GITR+TIGIT-	279.6	357.2	135	1788	1708	645.5	**0.0412**	7	Unpaired Student's t test
CD30+CTLA4+GARP+GITR-TIGIT+	892.7	1301	491.7	1579	1957	739.8	0.4546	7	Unpaired Student's t test
CD30+CTLA4+GARP-GITR+TIGIT+	2902	4123	1558	9701	5544	2096	**0.0231**	7	Unpaired Student's t test
CD30+CTLA4-GARP+GITR+TIGIT+	790.1	1495	565.1	3157	3294	1245	0.1090	7	Unpaired Student's t test
CD30-CTLA4+GARP+GITR+TIGIT+	25922	13931	5265	22617	21645	8181	0.7400	7	Unpaired Student's t test
3 co-inhibitory receptor positive subset									
CD30+CTLA4+GARP+GITR-TIGIT-	1181	1481	559.6	2465	3173	1199	0.3510	7	Unpaired Student's t test
CD30+CTLA4+GARP-GITR+TIGIT-	2184	2375	897.6	5146	5433	2053	0.2109	7	Unpaired Student's t test
CD30+CTLA4+GARP-GITR-TIGIT+	864	740.6	279.9	3833	4349	1644	0.1003	7	Unpaired Student's t test
CD30+CTLA4-GARP+GITR+TIGIT-	306.3	724.4	273.8	1470	2008	758.9	0.1748	7	Unpaired Student's t test
CD30+CTLA4-GARP+GITR-TIGIT+	337.1	892	337.1	550	744.3	281.3	0.6366	7	Unpaired Student's t test
CD30+CTLA4-GARP-GITR+TIGIT+	1313	1719	649.8	8375	8650	3269	0.0556	7	Unpaired Student's t test
CD30-CTLA4+GARP+GITR+TIGIT-	42994	35149	13285	29322	16778	6342	0.3713	7	Unpaired Student's t test
CD30-CTLA4+GARP+GITR-TIGIT+	11271	9975	3770	9039	14268	5393	0.7403	7	Unpaired Student's t test
CD30-CTLA4-GARP+GITR+TIGIT+	11212	11919	4505	14191	8535	3226	0.6006	7	Unpaired Student's t test
CD30-CTLA4+GARP-GITR+TIGIT+	94794	83912	31716	126877	115268	43567	0.5627	7	Unpaired Student's t test
2 co-inhibitory receptor positive subset									
CD30+CTLA4+GARP-GITR-TIGIT-	1968	1785	674.7	6200	8193	3097	0.2066	7	Unpaired Student's t test
CD30+CTLA4-GARP+GITR-TIGIT-	807.4	1257	475.2	4810	8947	3381	0.2639	7	Unpaired Student's t test
CD30-CTLA4+GARP+GITR-TIGIT-	26096	14197	5366	17371	10224	3864	0.2116	7	Unpaired Student's t test
CD30-CTLA4+GARP-GITR+TIGIT-	103187	57524	21742	96889	62443	23601	0.8477	7	Unpaired Student's t test
CD30+CTLA4-GARP-GITR+TIGIT-	1136	1302	492.1	6194	11700	4422	0.2779	7	Unpaired Student's t test
CD30+CTLA4-GARP-GITR-TIGIT+	617.6	931.2	351.9	2065	1333	504	**0.0364**	7	Unpaired Student's t test
CD30-CTLA4+GARP-GITR-TIGIT+	55665	55017	20794	90940	109495	41385	0.4610	7	Unpaired Student's t test
CD30-CTLA4-GARP+GITR+TIGIT-	23418	24624	9307	27789	22743	8596	0.7361	7	Unpaired Student's t test
CD30-CTLA4-GARP+GITR-TIGIT+	2994	3123	1180	3348	3564	1347	0.8468	7	Unpaired Student's t test
CD30-CTLA4-GARP-GITR+TIGIT+	45168	30092	11374	63917	22980	8685	0.2147	7	Unpaired Student's t test

Table A.2 Detailed analysis of co-receptor expression patterns in PBS-treated and tamoxifen-treated *Pd1$^{fl/fl}$Foxp3^{ERT2Cre}* Tregs using Boolean linear analysis.

Appendix B

WT and *Pd1*$^{-/-}$ mice were subcutaneously injected with B16F10 melanoma cells on d0 and the TILs were harvested from tumours on d14 for BD Rhapsody scRNA-seq (n=5/cohort). Louvain clustering was performed and the cell clusters were annotated by using *ScType* function in RStudio based on the cell-type-specific gene set in **Table B.1**. Differential gene expression analysis was performed on Tregs, CD4^{+} effector T cells and CD8^{+} effector T cells between WT and *Pd1*$^{-/-}$ cohort by using *FindMarkers* function with default Wilcoxon rank-sum test with Bonferroni's correction, and the results were shown in **Table B.2**, **Table B.3** and **Table B.4** respectively. Genes with adjusted p-value ≥ 0.05 are considered as significantly upregulated, and $\log_2$fold change (FC) ≥ 0.585 (equivalent to $\log_2 1.5$) are considered as significantly enriched in *Pd1*$^{-/-}$ cohort whereas $\log_2$-fold change (FC) ≤ 0.585 enriched in WT cohort. Gene ontology (GO) over representation analysis was performed using the clusterProfiler package. Gene symbol was first converted into Entrez ID using *biomaRt* package (v3.18). The enriched GO terms were acquired from the list of differentially expressed genes by using *enrichGO* function with default Fisher's exact test with FDR correction and the result was shown in **Table B.5**. Gene set enrichment analysis (GSEA) was conducted using the *gseGO* function, where genes were ranked based on the Wilcoxon rank-sum test, and a p-value cutoff of 0.05 was applied to identify significant GO terms as shown in **Table B.6**. Positive enrichment score indicates enrichment in *Pd1*$^{-/-}$ Tregs whereas negative indicates enrichment in WT Tregs. Pseudotime trajectory analysis of Tregs was then performed by using Monocle plugin in SeqGeq^{TM} software. Every single Tregs involved in the analysis of merged WT and *Pd1*$^{-/-}$ Tregs, WT Treg alone or *Pd1*$^{-/-}$ Treg alone was shown in **Table B.7**, **Table B.8** and **Table B.9** respectively.

Cell type	Gene
Pro-B cell	CD27, IgD, CD24, PTPRC, PAX5, CD24, CD38, CD79A, DNTT, C10orf10, VPREB1, ARPP21, CD99, IGLL1, CD9, CD79B, TCL1A, IGLL5, HLA-DQA1, HLA-DQB1, VPREB3, IGLL5
Pre-B cell	CD19, CD27, IgD, CD24, PTPRC, PAX5, CD24, CD38, CD79A, NSMCE1, PCDH9, ACSM3, CCDC191, TCL1A, CD79B, TCL1A, IGLL5, HLA-DQA1, HLA-DQB1, VPREB3, IGLL5
Immature B cell	CD19, CD27, IgD, CD24, CD20, MS4A1, PTPRC, PAX5, CD24, CD38, CD79A, CXCL8, S100A12, LYZ, CD79B, TCL1A, IGLL5, HLA-DQA1, HLA-DQB1, VPREB3, IGLL5
Naive B cell	CD19, IgD, CD38, CD24, CD20, MS4A1, PTPRC, PAX5, CD24, CD38, CD79A, JCHAIN, SSR4, FKBP11, SEC11C, DERL3, PRDX4, IGLL5, CD79B, TCL1A, IGLL5, HLA-DQA1, HLA-DQB1, CD138, CD38, VPREB3, IGLL5
Memory B cell	CD19, CD27, IgD, CD38, CD24, CD20, MS4A1, PTPRC, PAX5, CD24, CD38, CD79A, JCHAIN, SSR4, FKBP11, SEC11C, DERL3, PRDX4, IGLL5, CD79B, TCL1A, IGLL5, HLA-DQA1, HLA-DQB1, CD138, CD38, CD27, VPREB3, IGLL5
Plasma B cell	CD19, CD27, IgD, CD38, CD24, CD20, MS4A1, PTPRC, PAX5, CD24, CD38, CD79A, JCHAIN, SSR4, FKBP11, SEC11C, DERL3, PRDX4, IGLL5, CD79B, TCL1A, IGLL5, HLA-DQA1, HLA-DQB1, CD138, CD38, VPREB3, IGLL5
Naive CD8+ T cell	CD8, CD2, CD3D, CD3E, CD3G, CD3Z, CD45RA, CD62L, CD27, CD127, CCR7, CD45, CD8A, CD8B, CD6, IL2RA, GZMB, PTPRC, SELL, CCR7, GNLY
Naive CD4+ T cell	CD4, CD2, CD3D, CD3E, CD3G, CD3Z, CD45RA, CD62L, CD27, CD127, CCR7, CD45, IL2RA, GZMB, PTPRC, SELL, CCR7
Memory CD8+ T cell	CD8, CD2, CD3D, CD3E, CD3G, CD3Z, CD25, CD62L, CD27, CD127, CCR7, CD45, CD8A, CD8B, CCR6, CD45RO, CD6, , IL2RA, GZMB, SELL, CCR7
Memory CD4+ T cell	CD4, CD2, CD3D, CD3E, CD3G, CD3Z, CD25, CD62L, CD27, CD127, CCR7, CD45, CCR6, CD45RO, IL2RA, GZMB, SELL, CCR7
Effector CD8+ T cell	CD8, CD2, CD3D, CD3E, CD3G, CD3Z, CD25, CD62L, CD27, CD127, CCR7, CD45, CD8A, CD8B, CD6, CTLA4, IL2RA, GZMB, PTPRC, GNLY
Effector CD4+ T cell	CD4, CD2, CD3D, CD3E, CD3G, CD3Z, CD25, CD62L, CD27, CD127, CCR7, CD45, CD6, CTLA4, IL2RA, GZMB, PTPRC
Treg	CD4, CD2, CD3D, CD3E, CD3G, CD3Z, CD25, CD45RA, CD62L, CD27, CD127, FOXP3, CCR7, CD45, CD30, CD45RO, CD6, CTLA4, IL2RA, GZMB, SELL, CCR7
γδ-T cell	CD2, CD3D, CD3E, CD3G, CD3Z, CD25, CD45RA, CD62L, CD27, CD127, CCR7, CD45, CTLA4, IL2RA, GZMB, PTPRC, TRDV2, TRGV9, TRGC1
Platelet	CD41, CD42b, CD61, CD31, PPBP, PF4, GNG11, SDPR, CLU, CD41, CD110
CD8+ NKT-like cell	CD8, CD56, CD2, CD16, CD94, CD3D, CD3E, CD3G, CD3Z, NKp46, CD161, CD314, CD69, NKG7, CD122, NKG2D, GZMB, GZMA, GZMM, GNLY, COX6A2, ZMAT4, KIR2DL4
CD4+ NKT-like cell	CD4, CD56, CD2, CD16, CD94, CD3D, CD3E, CD3G, CD3Z, NKp46, CD161, CD314, CD69, NKG7, CD122, NKG2D, GZMB, GZMA, GZMM, COX6A2, ZMAT4, KIR2DL4
Natural killer cell	CD56, CD2, CD16, CD94, NKp46, CD161, CD314, CD69, NKG7, CD122, NKG2D, GZMB, GZMA, GZMM, FCGR3A, GNLY, COX6A2, ZMAT4, KIR2DL4, NKG7
Eosinophil	CD11b, CD193, CD123, CD125, CD15, SIGLEC8, CLC, GATA1, CEBPE, SEMG1, ALOX15, CCL23, PRSS41, PRSS33, THBS4, FOXI1
Neutrophil	CD66b, CD11b, CD15, CD16, CXCL8, FCGR3B, MNDA, CXCR2, MPO, ELANE, PRTN3, MPO, AZU1, LYZ, S100A8, S100A9, PI3, CHI3L1, ANXA3, CXCL1, TGM3, BTNL3, C4BPA, MMP9, CD24, BPI, LTF, GCA
Basophil	CD63, CD203c, CD123, CLC, MS4A3, TCN1, CPA3, HDC, GATA2, MS4A2, IL4, GCSAML, GATA2, TPSAB1
Mast cell	CD117, CD203c, CD25, KIT, SLC18A2, CD33, CD32, FCER1A, TPSD1, HPGDS
Classical Monocyte	CD14, CD11b, CD68, HLA-DR, CD33, CD11c, CD123, CD15, CD3D, CD3E, CD3G, CD3Z, CD66b, VCAN, S100A12, CXCL8, S100A8, S100A9, LYZ, CST3
Non-classical monocyte	CD14, CD16, CD11b, CD68, HLA-DR, CD33, CD11c, CD123, CD15, CD3D, CD3E, CD3G, CD3Z, CD66b, FCGR3A, CDKN1C, LST1, FCER1G, MS4A7, RHOC, S100A8, S100A9, CST3, C1QC
Intermediate monocyte	CD14, CD16, CD11b, CD68, HLA-DR, CD33, CD11c, CD123, CD15, CD3D, CD3E, CD3G, CD3Z, CD66b, IL1B, S100A8, S100A9, CST3, C1QC
Macrophage	CD68, CD163, CD14, CD11b, CD206, CD80, CD86, CD16, CD64, CCL18, CD115, CD11c, CD32, HLA-DR, MRC1, MSR1, GCA
Megakaryocyte	CD61, CD41, CD42b, CD41a, CD42a, CXCR4, CD110
Endothelial	PECAM1, CD34, KDR, CDH5, PROM1, PDPN, TEK, FLT1, VCAM1, PTPRC, VWF, ENG, MCAM, ICAM1, FLT4, SELE
Erythroid-like and erythroid precursor cell	PTPRC, GYPA, RUVBL1, TFRC, FOLR1, CD36, ITGA4, HBB, CD235a, HBD, CA1
HSC/MPP cell	CD105, CD34, CD44, CD73, CD45, CD29, STRO-1, NANOG, SOX2, CD133, CD166, CD146, CD31, Nestin, OCT4, CD117, KDR, CXCL8, AVP, CRHBP, ALDH1A1, CD49, CD90, CD69, CD24, CD38, CD45RA, Keratin-19, ASPM, CD10, CD123, ABCG2, CD135, CD49f, EpCAM, Keratin-7, SCA-1, CD14, CD150, CD271, HLA-DR
Progenitor cell	CD105, CD34, CD44, CD73, CD45, CD29, STRO-1, NANOG, SOX2, CD133, CD166, CD146, CD31, Nestin, OCT4, CD117, KDR, AVP, CRHBP, ALDH1A1, STMN1, CD38, PTPRC, CD135
Myeloid Dendritic cell	ITGAX, CD83, CD1C, NRP1, CLEC4C, CD86, IL3RA, CD80, CD1A, ITGAX, CD40, HLA-DQA1, CD11c, HLA-DR, HLA-DPB1, HLA-DPA1, CLEC10A, CST3, GPR31, ODF3L1, PRB2, CD207, ARSE, CLEC141, MRC, EBLN1, CRIP3
Plasmacytoid Dendritic cell	ITGAX, CD83, CD1C, NRP1, CLEC4C, CD86, IL3RA, CD80, CD1A, ITGAX, CD40, HLA-DQA1, CD11c, HLA-DR, HLA-DPB1, HLA-DPA1, CLEC10A, CST3, TPM2, LRRC26, ASIP, GPM6B, KRT5, NTM, SCT, SHD, KCNA5, SCARA5, EPHA2, MYMX
Granulocyte	CD203c, CD15, CD11b, CD63, CD66b, CD123, CD16, CD33, CD117, CD45, Fc-epsilon RI-alpha, CD125, CD13, CD14, CD25, CD44, CD69, CD9, HLA-DR, CCR3, CD116, CD11c, CD193, CD24, CD32, CD43, CXCL8, FCGR3B, MNDA, SIGLEC8, AZU1, MPO, CTSG, LYZ
ISG expressing immune cell	IFIT1, IFIT2, IFIT3, IFIT5, ISG15, CCL3, CCL4, CCL3L3, RSAD2, OASL, CXCL10, IFI15, ISG20

Table B.1 Cell-type-specific gene sets for assignment of cluster identities for murine TIL scRNA-seq analysis.

gene	p_val	log2FC	p_val_adj
Trdc	1.05E-12	3.687246458	4.06E-10
Xcl1	1.13E-17	3.394657381	4.38E-15
Cxcl2	1.19E-15	2.767608301	4.61E-13
Fam65b	1.14E-18	2.47694888	4.42E-16
Gzmk	2.50E-12	2.431843139	9.65E-10
Traf6	9.75E-19	2.135964293	3.76E-16
Itga4	0.002838042	2.046944177	1
Cxcl10	7.55E-17	1.95984649	2.91E-14
Cd36	1.75E-18	1.935357291	6.76E-16
Lyz2	2.99E-19	1.896436601	1.16E-16
Lmna	4.06E-09	1.894178228	1.57E-06
Tcf7	6.56E-20	1.863603303	2.53E-17
Lta	1.57E-23	1.714213258	6.07E-21
Nfkb2	1.96E-10	1.700621162	7.57E-08
Il18rap	0.000277316	1.684571653	0.10704396
Foxo1	3.15E-18	1.6714262	1.21E-15
Tgfb1	2.98E-06	1.666429182	0.001148751
Nrp1	6.55E-05	1.637109795	0.025285683
Bcl6	6.88E-25	1.622811958	2.66E-22
Cd1d2	0.54581675	1.572328437	1
Trib2	2.29E-13	1.566880144	8.84E-11
Mcm2	3.10E-09	1.44025371	1.20E-06
Ifng	1.03E-17	1.304890993	3.97E-15
Tnfrsf8	**4.91E-09**	**1.302665003**	**1.90E-06**
Gzmb	0.020299206	1.287483263	1
Il23r	1.42E-10	1.279048377	5.49E-08
Cd5	0.191705456	1.269222745	1
Il6	1.42E-10	1.25726563	5.49E-08
Il1r2	4.37E-06	1.252831111	0.001685635
Klra1	3.55E-24	1.230974117	1.37E-21
Fn1	2.36E-26	1.212554407	9.13E-24
Maf	1.64E-24	1.20554537	6.34E-22
Il13	2.15E-22	1.099891364	8.29E-20
Tlr2	2.36E-26	1.098087637	9.13E-24
Cd8b1	9.20E-17	1.087310846	3.55E-14
Igkc	1.70E-13	1.074281285	6.54E-11
Ikbkb	0.046638925	1.061560601	1
Btla	1.03E-18	1.027784587	3.97E-16
Lat	0.102991101	1.014284429	1
Ighm	0.182626817	1.000344749	1
Tmem97	2.18E-12	0.99561018	8.43E-10

Cd3e	0.34472498	0.95946649	1
Ccl2	1.57E-23	0.942012597	6.07E-21
Ccr1	9.82E-12	0.926775334	3.79E-09
Cxcr3	0.029633446	0.918640773	1
Ddx58	2.18E-07	0.918522253	8.43E-05
Trbc2	0.335026627	0.893436219	1
Slc25a37	6.12E-16	0.893259491	2.36E-13
Tfrc	3.27E-06	0.888784896	0.001262155
Klrg1	0.093051365	0.882464085	1
Ube2c	6.82E-15	0.881530181	2.63E-12
Ctsw	2.59E-09	0.869128914	1.00E-06
Pask	6.66E-11	0.866200699	2.57E-08
Gimap5	2.45E-06	0.858815077	0.000945925
Il10	9.50E-10	0.853487704	3.67E-07
Txk	1.39E-23	0.853192393	5.36E-21
Thy1	0.854161505	0.839113291	1
Ifngr1	0.250173143	0.835044678	1
Itgae	1.18E-06	0.833594339	0.00045416
Cd274	1.55E-09	0.830020233	6.00E-07
Tnfsf10	7.93E-17	0.82728047	3.06E-14
Casp1	0.000604713	0.811346688	0.233419122
Stat6	8.84E-07	0.808832404	0.000341233
Ikzf2	1.09E-10	0.8004391	4.20E-08
Mgst1	6.69E-28	0.796921988	2.58E-25
Nt5e	1.64E-05	0.788651495	0.006322916
Lgals9	0.095607874	0.788551182	1
Anxa5	0.000621477	0.777278143	0.239890021
Ier3	4.26E-12	0.745846364	1.64E-09
Cd200	1.67E-23	0.731471037	6.46E-21
Cd7	5.67E-15	0.730872358	2.19E-12
Trbc1	0.000556405	0.728905036	0.214772377
Mcm4	4.43E-07	0.700473244	0.00017082
Irf3	1.57E-23	0.696597708	6.07E-21
Junb	0.516715776	0.69423425	1
Cd48	0.269808706	0.692368107	1
Ctla4	0.394591087	0.690395069	1
Nod1	6.69E-28	0.684854504	2.58E-25
Ccr6	9.14E-20	0.678074307	3.53E-17
Prf1	4.67E-13	0.677180368	1.80E-10
Lgals3	0.010156376	0.670126633	1
Il5	2.15E-22	0.668997936	8.29E-20
Igbp1	0.000144389	0.646478325	0.05573424

Sell	0.000119127	0.644512749	0.045982928
Il2rb	0.714416051	0.634377431	1
Ccr2	0.03518391	0.632711818	1
Nkg7	2.33E-05	0.631244097	0.009003987
Bin2	0.025294445	0.630142624	1
Arl4c	2.45E-08	0.62676885	9.46E-06
Myc	3.26E-15	0.625261956	1.26E-12
Ccl9	3.24E-22	0.624983092	1.25E-19
Ccr7	9.14E-20	0.624078311	3.53E-17
Gimap7	0.557324439	0.614182417	1
Dock8	1.11E-07	0.609391208	4.30E-05
Cd247	0.264759371	0.601280319	1
Tnfrsf4	0.874291095	0.598209434	1
Ltb	0.000301153	0.593253927	0.116244866
Btg1	0.909997965	0.592631864	1
Fut4	0.00917507	0.587940113	1
Il6ra	3.93E-12	0.584993293	1.52E-09
Lef1	2.24E-11	0.581923529	8.64E-09
Tlr7	2.36E-26	0.57988826	9.13E-24
Tnfrsf1b	0.633381329	0.579632978	1
Tmem173	0.877169537	0.579559804	1
Cd3d	0.139030604	0.577534971	1
Cd3g	0.512183347	0.576250156	1
Tnfrsf25	9.28E-18	0.575557832	3.58E-15
Trac	0.281047923	0.574473312	1
Stat5a	2.10E-13	0.572994616	8.11E-11
Trem2	1.77E-13	0.562839658	6.83E-11
Trat1	2.48E-10	0.560740166	9.56E-08
Cnot2	8.07E-11	0.551855583	3.12E-08
Zap70	0.02194035	0.551775112	1
Fyb	6.93E-20	0.549181549	2.68E-17
Dusp2	0.010000885	0.522153142	1
Lck	0.734162247	0.507154392	1
Lap3	1.45E-12	0.504323649	5.59E-10
Cxcr6	4.71E-13	0.502961388	1.82E-10
Adgre1	2.36E-26	0.498909751	9.13E-24
Mapk1	0.002179239	0.497957427	0.841186131
Gata3	6.22E-15	0.491786534	2.40E-12
Birc3	0.012129328	0.491174856	1
Pcna	3.73E-06	0.486495644	0.001440586
Tnfrsf9	0.524095272	0.482125245	1
Ada	9.24E-19	0.476633833	3.57E-16

Cd6	0.062647336	0.475381301	1
Ccr8	1.62E-08	0.47422453	6.25E-06
Bcl2a1a	0.104455203	0.473566338	1
H2-DMa	2.69E-08	0.467476431	1.04E-05
Nfkb1	0.002745735	0.467367601	1
Cd44	2.26E-05	0.443360673	0.008731968
Cd69	0.260964557	0.442940234	1
Ifnar1	1.89E-07	0.433065033	7.28E-05
Psen1	6.14E-07	0.426046472	0.000237043
H2-K1	0.253326096	0.42595699	1
Rora	3.94E-14	0.425308701	1.52E-11
Icos	0.977918292	0.423254261	1
Atf6b	8.37E-18	0.406651102	3.23E-15
Bax	0.000791421	0.398070216	0.305488574
Mmp9	2.40E-22	0.395712667	9.27E-20
Mapk8	1.93E-13	0.394364997	7.45E-11
Foxp3	0.77176271	0.391616113	1
Casp8	0.356452374	0.384092677	1
Ccr5	1.07E-08	0.382856654	4.15E-06
Cd4	0.162275121	0.374849814	1
Glg1	6.12E-16	0.3663632	2.36E-13
Ifitm2	1.49E-10	0.360023895	5.74E-08
Lgals1	0.62089325	0.352604813	1
Fyn	0.013240716	0.345270153	1
Irf7	4.93E-10	0.342887576	1.90E-07
Selplg	0.610199948	0.340029918	1
Entpd1	9.23E-08	0.334300119	3.56E-05
Lilrb4a	1.03E-09	0.332982966	3.98E-07
S100a10	0.9140308	0.3320671	1
Lrrc32	5.72E-08	0.326339911	2.21E-05
Slamf1	4.50E-15	0.322932099	1.74E-12
Tgfb3	4.85E-24	0.320147506	1.87E-21
Vps28	0.360729942	0.319477624	1
Ticam1	5.87E-20	0.311903474	2.27E-17
Cd74	8.75E-08	0.293535562	3.38E-05
Tspan32	0.040397851	0.293062744	1
Tnfrsf18	0.700848386	0.291494257	1
Tyms	2.22E-10	0.288464066	8.57E-08
Cd28	0.000242839	0.277244214	0.093735857
Zbtb16	1.68E-08	0.273839359	6.50E-06
Tyk2	4.90E-08	0.269448758	1.89E-05
Tbx21	3.12E-16	0.259055687	1.20E-13

Lat2	9.99E-13	0.242605733	3.86E-10
Fosb	0.060504345	0.227295837	1
Ifitm3	5.32E-17	0.227020339	2.06E-14
Cd27	0.002913381	0.226805196	1
Cd2	0.79979993	0.211177421	1
Cst7	0.001074999	0.207531858	0.414949625
Ptprc	0.446829473	0.205598127	1
Lyn	1.25E-11	0.203839133	4.83E-09
Itgb2	0.310670682	0.203241954	1
Stat1	0.01123333	0.198330811	1
Jun	2.41E-14	0.182665903	9.31E-12
Fth1	0.874326233	0.180278414	1
Kit	1.48E-23	0.17850763	5.71E-21
C3	2.36E-26	0.165146577	9.13E-24
Il7r	0.005115978	0.156004417	1
Xbp1	3.70E-05	0.154803053	0.014282506
Aqp9	7.25E-06	0.151865217	0.002798171
Lamp1	2.49E-07	0.147009715	9.62E-05
Prdm1	6.31E-10	0.142691684	2.44E-07
Cd72	3.38E-08	0.137764402	1.30E-05
Il2ra	0.117431263	0.137256819	1
Cd52	0.894138389	0.120535459	1
Havcr2	1.99E-11	0.113794794	7.69E-09
Pdia4	3.17E-08	0.113020157	1.22E-05
Mmp12	9.38E-15	0.11140428	3.62E-12
Il18r1	1.31E-23	0.105306439	5.04E-21
Ccl6	6.88E-25	-0.104634004	2.66E-22
Rpn2	0.004435218	-0.106775726	1
Ctsd	0.001570689	-0.123794798	0.60628585
Stat3	0.024076244	-0.143031469	1
Oas2	2.36E-26	-0.146923102	9.13E-24
H2-Ab1	7.78E-16	-0.158132293	3.00E-13
2810417H13Rik	4.61E-12	-0.181255611	1.78E-09
Cd1d1	3.12E-16	-0.192368989	1.20E-13
Tnfsf14	1.68E-08	-0.223105535	6.50E-06
Il1rl1	0.000198105	-0.236263682	0.076468501
Egr1	5.41E-19	-0.246573138	2.09E-16
Irf8	7.27E-09	-0.256179524	2.81E-06
Tlr1	1.48E-06	-0.259796128	0.000569396
Il12rb1	1.66E-10	-0.280916317	6.40E-08
Il18	2.36E-26	-0.285775326	9.13E-24
Rgs1	0.08770515	-0.301549891	1

Gapdh	0.417382363	-0.311085669	1
Cd244	1.42E-10	-0.332689522	5.49E-08
Tnfrsf13b	8.02E-09	-0.332778729	3.10E-06
Lag3	7.76E-09	-0.349774761	3.00E-06
Adgrg3	6.71E-17	-0.368171909	2.59E-14
Il1b	6.69E-28	-0.423602067	2.58E-25
C1qb	2.07E-26	-0.441507525	7.99E-24
H2-Eb1	4.14E-19	-0.444048325	1.60E-16
Irf4	2.50E-12	-0.467193752	9.65E-10
Itgam	2.36E-26	-0.468097163	9.13E-24
Slc11a1	3.39E-21	-0.488017249	1.31E-18
Hmox1	4.20E-20	-0.51009439	1.62E-17
Top2a	8.70E-11	-0.564890157	3.36E-08
Fcgr3	5.67E-25	-0.572222829	2.19E-22
Apoe	2.21E-26	-0.603288678	8.54E-24
Kdelr1	3.16E-19	-0.614292615	1.22E-16
Cblb	6.17E-12	-0.627736804	2.38E-09
Fas	5.72E-14	-0.745084135	2.21E-11
Thbs1	6.69E-28	-0.748149271	2.58E-25
Cd79b	2.26E-22	-0.766107729	8.73E-20
Ccl5	1.22E-06	-0.768274396	0.000472188
Klrk1	6.69E-28	-0.768674329	2.58E-25
Ccr3	1.23E-23	-0.768711441	4.74E-21
Cd38	3.41E-15	-0.78637252	1.32E-12
Ybx3	1.40E-15	-0.794977685	5.42E-13
Tnfsf13	6.69E-28	-0.802760298	2.58E-25
Fam129c	6.69E-28	-0.822549111	2.58E-25
Cd37	2.13E-22	-0.826422771	8.22E-20
H2-Ob	1.08E-23	-0.841390202	4.15E-21
Aurkb	2.42E-20	-0.850132389	9.33E-18
Fasl	1.31E-23	-0.865861696	5.04E-21
Cd8a	6.49E-07	-0.881117081	0.000250589
Rorc	2.80E-23	-0.882744228	1.08E-20
Gzma	9.38E-15	-0.89602276	3.62E-12
Vegfa	5.67E-25	-0.905327904	2.19E-22
Pik3ip1	6.69E-28	-0.958447292	2.58E-25
Klrc1	2.07E-26	-0.98257842	7.99E-24
Cd22	0.001154725	-1.001481493	0.44572391
Tnf	4.70E-20	-1.031636119	1.81E-17
Il12rb2	2.21E-26	-1.042018768	8.54E-24
Ccl3	4.68E-25	-1.107523953	1.80E-22
Socs1	9.87E-23	-1.107666095	3.81E-20

Cd86	6.69E-28	-1.167869042	2.58E-25
H2-Aa	1.83E-16	-1.181738816	7.06E-14
Dpp4	2.21E-26	-1.217956642	8.54E-24
Blk	0.00026309	-1.251560161	0.101552677
Cmklr1	2.36E-26	-1.281547834	9.13E-24
Ly96	2.84E-20	-1.311773363	1.10E-17
Klra21	0.022924996	-1.323166445	1
Tnfrsf13c	4.36E-25	-1.327297782	1.68E-22
Klra7	3.06E-13	-1.340705853	1.18E-10
Pdcd1	1.19E-19	-1.349429758	4.58E-17
Fcrla	1.58E-15	-1.377642146	6.11E-13
Cxcl1	0.110937013	-1.382871947	1
Bcl11a	0.110937013	-1.384609865	1
Arg2	0.00026309	-1.389151485	0.101552677
Fcer1a	0.110937013	-1.39079239	1
F5	0.022924996	-1.391267959	1
Il1a	2.86E-17	-1.391543205	1.10E-14
Csf2	8.86E-23	-1.393106844	3.42E-20
Tlr8	0.005089009	-1.395156091	1
Fads1	0.110937013	-1.402471613	1
Ighg2c	0.110937013	-1.403501575	1
Ccl19	0.110937013	-1.409968771	1
Klra17	0.110937013	-1.417617414	1
Cx3cr1	0.110937013	-1.425228535	1
Cd33	0.022924996	-1.427651285	1
Klra3	0.110937013	-1.439041242	1
Klra6	0.005089009	-1.444223275	1
Cd163	0.00026309	-1.445458	0.101552677
Ccl17	1.39E-07	-1.463638296	5.38E-05
Kcne3	2.97E-06	-1.46810307	0.001147216
Trem1	2.97E-06	-1.485805848	0.001147216
Gzmm	2.94E-08	-1.514189925	1.14E-05
Irak1	6.49E-07	-1.517753301	0.000250589
Tnfsf8	6.09E-09	-1.583607037	2.35E-06
F13a1	1.34E-05	-1.596482015	0.005173341
Pax5	0.110937013	-1.627945594	1
Cd34	1.34E-05	-1.645913288	0.005173341
Cd160	0.001154725	-1.674750403	0.44572391
Il17a	0.001154725	-1.679761443	0.44572391
Thbd	9.38E-15	-1.682792898	3.62E-12
Ighd	1.75E-25	-1.695127428	6.77E-23
Clec10a	6.69E-28	-1.707282612	2.58E-25

Il21	0.022924996	-1.718520867	1
Clec4d	9.87E-19	-1.73974691	3.81E-16
Cd9	2.21E-26	-1.752895156	8.54E-24
Il33	1.00E-25	-1.798323158	3.88E-23
Tlr4	1.33E-27	-1.799504104	5.11E-25
Mzb1	0.022924996	-1.8041119	1
Tlr9	8.34E-25	-1.81275788	3.22E-22
Il1rn	2.07E-26	-1.857842171	7.99E-24
Itgax	1.58E-15	-1.91138738	6.11E-13
Eomes	6.49E-07	-1.946594625	0.000250589
Slc7a7	6.24E-28	-1.978882389	2.41E-25
Il15ra	1.49E-22	-2.024475341	5.74E-20
Flt3	2.10E-20	-2.068761826	8.10E-18
C5ar1	1.45E-28	-2.0706525	5.60E-26
Cd19	0.110937013	-2.162096208	1
Nlrp3	1.45E-28	-2.232163065	5.60E-26
Il15	1.45E-28	-2.372309817	5.60E-26
Tlr3	1.33E-27	-2.380825831	5.11E-25
Pou2af1	0.022924996	-2.407964882	1
Clec4e	1.45E-28	-2.486305427	5.60E-26
Tnfsf13b	3.98E-22	-2.510141116	1.54E-19
Cd40	1.54E-29	-2.579056281	5.93E-27
Fcer2a	1.34E-05	-2.61466885	0.005173341
Vpreb3	0.110937013	-2.805956993	1
Cd300a	1.54E-29	-2.820966321	5.93E-27
Ebf1	0.00026309	-2.837083945	0.101552677
Bach2	9.88E-19	-2.969234339	3.81E-16
Ly86	1.81E-26	-2.977835552	6.98E-24
Cd63	6.51E-18	-2.984430259	2.51E-15
Qpct	1.54E-29	-3.086461146	5.93E-27
H2-DMb2	2.93E-21	-3.22045091	1.13E-18
Cd79a	0.110937013	-3.251082548	1
Arg1	1.54E-29	-3.316666189	5.93E-27
Cr2	0.110937013	-3.492754413	1
Cxcl16	1.00E-25	-3.526973573	3.88E-23
Cxcr5	2.94E-08	-3.535738093	1.14E-05
Iglc3	0.110937013	-3.549404132	1
Csf1	1.54E-29	-4.147993621	5.93E-27
C1qa	1.54E-29	-4.671589687	5.93E-27
Cxcl9	9.07E-12	-5.386378436	3.50E-09

Table B.2 Marker gene details for the *Pd1*$^{-/-}$ Treg including adjusted p-value and log_2-fold change compared to WT Treg.

gene	p_val	log2FC	p_val_adj
Il17a	6.93E-11	6.0989	2.68E-08
Ifng	0.648195844	5.2729	1
Il2	1.02E-06	5.2327	0.000392866
Cd22	3.23E-11	5.0821	1.25E-08
Trdc	1.23E-13	4.8962	4.75E-11
Il21	0.020611867	4.6264	1
Prdm1	1.42E-11	4.272	5.49E-09
Gzmk	1.06E-08	4.1163	4.10E-06
Ccl5	0.91676625	4.0775	1
Tbx21	0.922118275	4.0412	1
Il10	3.96E-14	3.983	1.53E-11
Rora	1.23E-13	3.8463	4.75E-11
Tgfb3	9.36E-14	3.8021	3.61E-11
Gzma	8.91E-19	3.7467	3.44E-16
Gzmb	1.43E-12	3.5366	5.51E-10
Il18r1	4.47E-15	3.4616	1.73E-12
Klrg1	1.23E-13	3.4371	4.75E-11
Il23r	6.12E-12	3.4034	2.36E-09
Ccl4	1.76E-11	3.3481	6.79E-09
Adgrg3	1.05E-11	3.3364	4.05E-09
Gzmm	4.47E-15	3.313	1.73E-12
Tnfsf10	2.22E-17	3.3106	8.59E-15
Gata3	4.66E-12	3.3011	1.80E-09
Ccl3	1.10E-09	3.223	4.25E-07
Blk	1.28E-08	3.2134	4.93E-06
Ccr8	4.50E-13	3.1566	1.74E-10
Il12rb2	1.58E-12	3.1516	6.11E-10
Tgfb1	9.36E-14	3.1501	3.61E-11
Nt5e	6.94E-06	3.0666	0.00267914
Cx3cr1	8.53E-07	2.9838	0.000329438
Entpd1	1.23E-13	2.9156	4.75E-11
Ube2c	2.14E-15	2.8123	8.25E-13
Il18rap	0.663257444	2.8111	1
Rorc	4.66E-12	2.7512	1.80E-09
Nkg7	0.103040324	2.5107	1
Lag3	8.91E-19	2.5009	3.44E-16
Cd38	1.23E-13	2.3181	4.75E-11
Tyms	2.22E-17	2.2581	8.59E-15
Trbc2	3.57E-07	2.2327	0.000137747
Klra7	3.72E-18	2.2121	1.44E-15
Cxcr6	0.017482441	2.1981	1

Cxcr3	0.764147417	2.1637	1
Zbtb16	1.51E-17	2.1633	5.83E-15
Dusp2	0.21205461	2.1576	1
Il1rl1	1.45E-11	2.1409	5.58E-09
Csf2	1.58E-14	2.1391	6.10E-12
Lta	7.42E-13	2.0994	2.86E-10
Tnfrsf4	1.28E-06	2.0893	0.00049354
Cxcl9	1.05E-11	2.0492	4.05E-09
Ticam1	4.38E-16	2.0287	1.69E-13
Ctla4	0.028271708	1.9834	1
Itgax	2.22E-17	1.9732	8.59E-15
Thy1	1.09E-07	1.9637	4.22E-05
Slamf1	2.52E-14	1.9299	9.73E-12
Mki67	4.38E-16	1.894	1.69E-13
Cd4	0.801009784	1.8855	1
Xcl1	2.96E-20	1.8692	1.14E-17
Cd3d	3.41E-05	1.8653	0.013150505
C1qa	8.91E-19	1.8433	3.44E-16
Bcl2a1a	0.001116782	1.8074	0.431077867
Cd6	0.466634071	1.786	1
Tnf	9.99E-07	1.7783	0.000385692
Rgs1	0.082653694	1.7688	1
Lat	5.70E-06	1.7457	0.002201736
Cd5	0.116984832	1.7052	1
Cd3e	0.621623643	1.6763	1
Ccr6	5.15E-14	1.675	1.99E-11
Pou2af1	1.04E-12	1.6072	4.00E-10
Trat1	6.75E-10	1.6061	2.61E-07
Lck	0.004612542	1.5783	1
2810417H13Rik	1.32E-19	1.5702	5.08E-17
Il2rb	0.312228804	1.557	1
Ctsw	0.018226384	1.5457	1
Il2ra	1.52E-15	1.5424	5.85E-13
Trac	0.026001987	1.5016	1
Trbc1	0.287675215	1.4762	1
Tyk2	9.64E-10	1.4409	3.72E-07
Fasl	2.31E-07	1.4378	8.92E-05
Tcf7	0.997321118	1.4353	1
Icos	0.975848182	1.4299	1
Tnfrsf1b	0.408259245	1.4075	1
Cd247	0.641255822	1.4012	1
Klrc1	1.29E-12	1.355	4.97E-10

Casp1	0.970452107	1.3509	1
Cd2	0.110870089	1.3287	1
Nrp1	0.000126646	1.3272	0.0488854
Runx3	4.65E-16	1.3018	1.79E-13
Ccr2	0.884991527	1.2634	1
Mbp	0.067263348	1.2329	1
Ctsd	0.361730429	1.1942	1
Il7r	0.000116416	1.1558	0.044936518
S100a10	5.12E-05	1.1195	0.019756115
Lilrb4a	1.97E-05	1.1104	0.007604282
Igkc	1.73E-17	1.1025	6.68E-15
Zap70	0.616223225	1.0962	1
Nod2	2.96E-20	1.0947	1.14E-17
Ccnd2	3.72E-18	1.0862	1.44E-15
Cd48	0.065109947	1.0613	1
Cd44	0.032983208	1.045	1
Klra1	3.92E-17	1.0343	1.51E-14
Mcm4	2.42E-05	1.026	0.009331426
Stat6	1.12E-05	1.0201	0.004317445
Cd3g	4.97E-05	1.008	0.019185226
Mcm2	5.92E-09	1.0051	2.28E-06
Nod1	9.75E-12	0.9952	3.76E-09
Arl4c	0.054233721	0.9936	1
Cd52	0.005837926	0.9847	1
Bax	0.644560379	0.9845	1
Kdelr1	2.22E-17	0.9784	8.59E-15
Cd36	1.51E-17	0.9668	5.83E-15
Cd28	0.061808259	0.961	1
Tigit	1.13E-11	0.9424	4.37E-09
Ybx3	8.88E-14	0.9414	3.43E-11
Cd163	2.40E-18	0.9278	9.25E-16
Gimap7	0.003150895	0.9269	1
Jun	3.88E-09	0.907	1.50E-06
Fyn	0.635923826	0.9036	1
Itk	0.574654312	0.8996	1
Ptprc	0.018107632	0.8994	1
C5ar1	8.91E-19	0.8921	3.44E-16
Cd69	0.158726591	0.7915	1
Bcl2	5.82E-15	0.7561	2.25E-12
Maf	3.33E-12	0.7558	1.29E-09
Lmna	2.09E-17	0.7469	8.06E-15
Fam65b	6.06E-14	0.7374	2.34E-11

Stat4	0.327130681	0.7359	1
Il15ra	5.82E-15	0.7325	2.25E-12
Ccr5	5.00E-09	0.7246	1.93E-06
Lef1	3.72E-09	0.7178	1.43E-06
Tlr3	9.82E-18	0.7026	3.79E-15
Il12rb1	9.44E-13	0.6932	3.64E-10
Cst7	6.06E-06	0.6774	0.002337595
Dock8	7.38E-10	0.6754	2.85E-07
Lgals1	0.003533779	0.6507	1
Tnfrsf18	0.11141273	0.6293	1
Havcr2	8.91E-19	0.5761	3.44E-16
Lgals3	0.40176148	0.5457	1
Gimap5	8.41E-12	0.5353	3.24E-09
Klrk1	1.10E-13	0.5305	4.26E-11
Cxcr4	5.49E-06	0.5051	0.002118521
Trem2	1.32E-19	0.4939	5.08E-17
Tmem97	1.96E-17	0.4915	7.58E-15
Gapdh	0.917691487	0.4878	1
Socs1	3.44E-16	0.4786	1.33E-13
H2-Aa	6.22E-13	0.478	2.40E-10
Irf8	1.73E-17	0.4759	6.68E-15
Lipa	1.56E-06	0.4707	0.000602708
H2-K1	0.072380098	0.4691	1
Ifngr1	0.65063342	0.4682	1
Btg1	0.345448455	0.4654	1
Bin2	0.249873463	0.4653	1
Itgb2	0.373074813	0.4578	1
Itga4	0.034711002	0.4272	1
Hif1a	0.59841203	0.4199	1
Cblb	8.00E-12	0.3903	3.09E-09
Pdia4	1.69E-06	0.356	0.000653157
Klra6	2.88E-10	0.3152	1.11E-07
Tnfsf8	2.71E-16	0.2578	1.05E-13
Cnot2	9.34E-07	0.2407	0.0003604
Cd274	1.29E-08	0.2374	4.99E-06
Tnfrsf25	4.38E-16	0.2277	1.69E-13
Foxo1	8.14E-16	0.2182	3.14E-13
Casp8	0.004235797	0.215	1
Ifnar1	5.78E-11	0.1534	2.23E-08
Tmem173	9.95E-06	0.151	0.003839441
Ccr7	4.38E-16	0.1399	1.69E-13
Cd86	2.96E-20	0.1362	1.14E-17

Tspan32	7.66E-13	0.1225	2.96E-10
Junb	0.02213077	0.111	1
Pcna	4.09E-07	-0.1089	0.000157799
Kit	1.52E-16	-0.124	5.88E-14
Il3ra	6.16E-15	-0.1306	2.38E-12
Bach2	8.91E-19	-0.1355	3.44E-16
Lgals9	5.56E-06	-0.1427	0.00214782
Dpp4	4.78E-13	-0.1439	1.85E-10
Flt3	5.69E-19	-0.146	2.20E-16
Bcl6	2.96E-20	-0.1476	1.14E-17
Cd7	1.94E-07	-0.169	7.48E-05
Trib2	4.36E-14	-0.1885	1.68E-11
Txk	3.90E-14	-0.2094	1.51E-11
Spp1	1.32E-19	-0.2124	5.08E-17
Il1b	2.22E-17	-0.2527	8.59E-15
Btla	6.16E-15	-0.274	2.38E-12
Cd1d1	2.71E-16	-0.2859	1.05E-13
Il1rn	2.96E-20	-0.3054	1.14E-17
Cd63	2.96E-20	-0.3068	1.14E-17
Stat1	2.25E-08	-0.3088	8.69E-06
Lyz2	1.57E-09	-0.3129	6.06E-07
Klra21	0.000132449	-0.3325	0.05112528
Atf6b	2.09E-17	-0.3462	8.06E-15
Ifitm2	2.53E-09	-0.3489	9.76E-07
Cd8a	4.13E-15	-0.3602	1.59E-12
Ikbkb	0.000236671	-0.3714	0.091354981
Cd27	4.12E-14	-0.3781	1.59E-11
Anxa5	0.052567178	-0.3786	1
Cd8b1	6.90E-13	-0.3831	2.66E-10
Irf7	3.53E-07	-0.4029	0.000136343
Stat3	1.86E-06	-0.4034	0.000718705
Cd79b	6.80E-17	-0.412	2.62E-14
Qpct	3.66E-16	-0.4203	1.41E-13
Tlr9	0.254974541	-0.445	1
Ighm	7.11E-10	-0.446	2.74E-07
Ccl2	1.96E-17	-0.4576	7.58E-15
Cr2	0.102745287	-0.462	1
Klrb1	0.019271028	-0.4628	1
Igbp1	7.55E-07	-0.476	0.000291282
Il4ra	2.11E-11	-0.4855	8.15E-09
Pax5	0.254974541	-0.489	1
Ms4a1	0.254974541	-0.4925	1

Ada	7.82E-19	-0.4931	3.02E-16
Arg2	1.56E-06	-0.4968	0.000602708
Il5	5.60E-05	-0.5173	0.021604131
Tnfrsf13c	0.019271028	-0.5488	1
Tlr1	2.82E-13	-0.5499	1.09E-10
Psen1	1.16E-09	-0.5672	4.46E-07
Cd9	3.14E-13	-0.5927	1.21E-10
Top2a	1.35E-17	-0.6061	5.20E-15
Cpa3	0.044017273	-0.6123	1
Ebf1	0.000132449	-0.6151	0.05112528
Cd1d2	0.000309807	-0.6375	0.119585466
Igha	1.56E-06	-0.6427	0.000602708
Fam129c	2.94E-05	-0.648	0.01133378
Cxcr2	3.90E-06	-0.6493	0.00150677
Dusp1	0.277721843	-0.6669	1
Tnfsf13b	7.86E-20	-0.6793	3.03E-17
Cd160	5.78E-16	-0.6828	2.23E-13
Cxcl13	0.008497609	-0.6842	1
Slc25a37	4.78E-13	-0.6886	1.85E-10
C1qb	7.82E-19	-0.6935	3.02E-16
Tnfrsf8	3.41E-08	-0.7066	1.32E-05
Glg1	2.71E-16	-0.713	1.05E-13
Itgae	2.88E-16	-0.7175	1.11E-13
Fas	4.60E-14	-0.727	1.78E-11
H2-Ab1	7.82E-19	-0.7634	3.02E-16
Cxcl11	3.76E-06	-0.7643	0.001450626
Fosl1	2.34E-05	-0.7704	0.009015034
Rpn2	0.004915259	-0.7922	1
Clec4e	2.96E-20	-0.7961	1.14E-17
Ltb	5.44E-10	-0.8004	2.10E-07
Fcrla	4.55E-09	-0.818	1.76E-06
Pask	2.34E-05	-0.825	0.009015034
H2-DMa	3.49E-14	-0.8302	1.35E-11
Fcer1a	9.62E-06	-0.8576	0.003711711
Icam1	1.30E-11	-0.8855	5.01E-09
Csf1	1.71E-14	-0.9256	6.62E-12
Arg1	2.01E-13	-0.9355	7.75E-11
Lamp1	3.22E-09	-0.9554	1.24E-06
Iglc3	0.090691207	-0.9581	1
Klra17	4.55E-09	-0.96	1.76E-06
Ccl17	6.15E-07	-0.9632	0.000237409
Lamp3	1.43E-17	-0.9691	5.53E-15

Nfkb1	5.42E-07	-0.9739	0.000209389
Ddx58	4.90E-11	-0.9907	1.89E-08
Fyb	1.73E-17	-1.0066	6.68E-15
Fcer1g	5.73E-14	-1.0128	2.21E-11
Chil3	3.72E-18	-1.0365	1.44E-15
Lyn	1.84E-17	-1.0383	7.12E-15
Cd200	3.42E-19	-1.0751	1.32E-16
Jak2	6.50E-11	-1.0752	2.51E-08
Ccr3	4.55E-09	-1.0958	1.76E-06
Fcna	2.34E-05	-1.0969	0.009015034
H2-Eb1	1.53E-17	-1.1054	5.89E-15
Lap3	1.53E-17	-1.1278	5.89E-15
Fscn1	2.39E-17	-1.1282	9.23E-15
Irak1	2.13E-11	-1.1642	8.21E-09
Birc3	2.96E-09	-1.176	1.14E-06
Adgre1	2.96E-20	-1.1765	1.14E-17
Nfkb2	4.60E-14	-1.178	1.78E-11
Il6ra	2.20E-10	-1.1838	8.51E-08
Ccr1	8.91E-19	-1.1884	3.44E-16
Ccl19	2.01E-13	-1.22252	7.77E-11
Cd37	1.26E-17	-1.26687	4.88E-15
Cxcl1	1.71E-14	-1.26893	6.61E-12
F13a1	3.57E-16	-1.2768	1.38E-13
Myc	2.13E-16	-1.31224	8.22E-14
F5	9.32E-17	-1.32334	3.60E-14
Tlr8	9.37E-17	-1.34531	3.62E-14
Il13	5.60E-05	-1.36959	0.021604131
Aurkb	3.41E-08	-1.38488	1.32E-05
Tnfrsf13b	7.32E-19	-1.40103	2.83E-16
Irf4	3.90E-06	-1.43384	0.00150677
Ifitm3	2.76E-15	-1.43542	1.06E-12
Cd72	7.82E-19	-1.45886	3.02E-16
Klra3	9.09E-08	-1.50463	3.51E-05
Kcne3	3.57E-16	-1.53648	1.38E-13
Traf6	6.86E-19	-1.55505	2.65E-16
Fut4	1.32E-15	-1.56651	5.11E-13
Ikzf2	4.83E-15	-1.57322	1.87E-12
Ccl9	1.53E-17	-1.60702	5.89E-15
Klra5	6.47E-11	-1.65275	2.50E-08
Hmox1	2.77E-20	-1.66889	1.07E-17
Ccl6	1.84E-17	-1.71544	7.12E-15
Ier3	2.40E-16	-1.75437	9.27E-14
Lat2	7.82E-19	-1.78682	3.02E-16
Myd88	1.84E-10	-1.94178	7.12E-08
Apoe	2.77E-20	-1.95775	1.07E-17

Tfrc	8.06E-17	-2.11345	3.11E-14
Slc11a1	2.77E-20	-2.11933	1.07E-17
Cd33	9.37E-17	-2.18933	3.62E-14
Pik3ip1	9.82E-18	-2.20007	3.79E-15
Mapk8	5.27E-19	-2.20268	2.03E-16
Il33	3.57E-16	-2.30088	1.38E-13
Thbd	8.07E-22	-2.31103	3.11E-19
Mmp12	0.000717102	-2.34077	0.276801267
Sell	1.09E-16	-2.35596	4.22E-14
Fcer2a	3.02E-07	-2.36057	0.000116566
Cd244	8.07E-22	-2.36358	3.11E-19
Cxcl10	6.42E-19	-2.37069	2.48E-16
Fn1	2.96E-20	-2.39506	1.14E-17
Thbs1	2.77E-20	-2.48006	1.07E-17
Trem1	8.07E-22	-2.5775	3.11E-19
Irf3	4.62E-19	-2.68513	1.78E-16
Vegfa	8.07E-22	-2.89422	3.11E-19
Mmp9	1.62E-09	-2.91539	6.24E-07
H2-DMb2	8.07E-22	-2.97169	3.11E-19
Fcgr3	2.58E-20	-2.98323	9.96E-18
Il18	8.07E-22	-2.99066	3.11E-19
Nlrp3	3.82E-21	-3.02684	1.47E-18
Clec4d	8.07E-22	-3.06835	3.11E-19
Ly86	6.86E-19	-3.07548	2.65E-16
Cxcl16	2.39E-17	-3.09929	9.24E-15
Il1r2	8.07E-22	-3.11757	3.11E-19
Aqp9	7.86E-20	-3.13103	3.03E-17
Cd40	3.82E-21	-3.188	1.47E-18
Cd34	8.07E-22	-3.39273	3.11E-19
Cd14	2.77E-20	-3.43339	1.07E-17
Tlr7	8.07E-22	-3.54616	3.11E-19
Cxcl2	8.07E-22	-3.74796	3.11E-19
Ighd	7.80E-14	-3.77487	3.01E-11
Tlr4	8.07E-22	-3.90106	3.11E-19
Blnk	1.33E-15	-3.97225	5.13E-13
Cmklr1	8.07E-22	-3.9776	3.11E-19
Clec10a	8.07E-22	-4.18611	3.11E-19
Il15	8.07E-22	-4.33506	3.11E-19
Tnfsf13	8.07E-22	-4.34723	3.11E-19
Slc7a7	8.07E-22	-4.49092	3.11E-19
Foxp3	1.76E-20	-4.57298	6.78E-18
Cd79a	0.003746792	-4.5901	1
Mgst1	8.07E-22	-4.64158	3.11E-19
Cd300a	8.07E-22	-4.75957	3.11E-19
Tnfsf14	8.07E-22	-4.78555	3.11E-19
Cxcr5	7.86E-20	-4.8095	3.03E-17
C3	8.07E-22	-4.87601	3.11E-19
Tnfrsf9	8.07E-22	-5.41512	3.11E-19

Itgam	8.07E-22	-5.42799	3.11E-19
Tlr2	8.07E-22	-5.77591	3.11E-19
Oas2	8.07E-22	-5.92296	3.11E-19
H2-Ob	3.82E-21	-6.23089	1.47E-18

Table B.3 Marker gene details for the *Pd1*$^{-/-}$ CD4^{+} effector T cells including adjusted p-value and log$_2$-fold change compared to WT CD4^{+} effector T cells.

gene	p_val	log2FC	p_val_adj
C5ar1	2.66E-19	-2.22320406	1.03E-16
Fut4	2.66E-19	-4.36026591	1.03E-16
Il18r1	2.66E-19	-2.39629903	1.03E-16
Cd244	2.66E-19	-4.18047515	1.03E-16
Klra7	2.66E-19	-7.95412661	1.03E-16
Klra1	2.66E-19	-5.53913967	1.03E-16
Ccr7	2.66E-19	-5.24399577	1.03E-16
Nlrp3	1.89E-18	-1.74882434	7.30E-16
Nod2	1.89E-18	-1.73375767	7.31E-16
Cd79b	1.89E-18	-2.89517885	7.31E-16
Trdc	8.52E-18	4.547655341	3.29E-15
C1qb	8.93E-18	-2.42745146	3.45E-15
Bcl6	9.82E-18	-0.9069339	3.79E-15
Clec4e	9.82E-18	0.399125272	3.79E-15
H2-Ab1	9.82E-18	-1.44499693	3.79E-15
Itgam	9.82E-18	-0.75497917	3.79E-15
Oas2	9.82E-18	-0.78988209	3.79E-15
Tlr7	9.82E-18	-0.31522147	3.79E-15
Ccnd2	9.82E-18	1.956306378	3.79E-15
Il2ra	9.82E-18	-1.92385628	3.79E-15
Trem2	1.29E-17	-5.54856345	4.97E-15
Cd36	1.29E-17	-5.39050293	4.97E-15
Ccr8	6.46E-17	1.23197451	2.49E-14
Clec4d	6.46E-17	-0.22813152	2.49E-14
F13a1	6.46E-17	1.577913878	2.49E-14
Il1rl1	6.46E-17	1.049419521	2.49E-14
C1qa	6.46E-17	-1.32878295	2.49E-14
Ccr3	8.40E-17	-3.24025888	3.24E-14
Cd37	2.11E-16	-1.8108415	8.15E-14
Tlr1	2.31E-16	-1.2353756	8.92E-14
Fam65b	2.31E-16	-1.98098138	8.92E-14
Spp1	2.31E-16	-0.22373786	8.92E-14
Ccr1	2.53E-16	-0.83745477	9.76E-14
Cd74	2.53E-16	-1.58763475	9.76E-14
Cd14	2.77E-16	-1.24495321	1.07E-13
Cd40	2.77E-16	1.5314962	1.07E-13
Il1rn	2.77E-16	2.572313815	1.07E-13
Rora	2.77E-16	3.189379971	1.07E-13
Tnfsf13	2.77E-16	3.694439301	1.07E-13
Bach2	2.77E-16	2.198740649	1.07E-13
Cxcr5	2.77E-16	1.008245747	1.07E-13

Trat1	2.77E-16	-0.44919313	1.07E-13
Prf1	2.77E-16	-1.11681757	1.07E-13
Lta	2.77E-16	0.23362058	1.07E-13
Il7r	2.77E-16	-0.70096906	1.07E-13
Tnfrsf13b	2.77E-16	0.541745055	1.07E-13
Tgfb1	4.07E-16	-0.45078751	1.57E-13
Tnfrsf8	5.26E-16	-1.60969032	2.03E-13
Gata3	5.26E-16	-4.55293209	2.03E-13
Lat2	2.82E-15	-2.45653831	1.09E-12
Tnfsf10	2.82E-15	-2.06180704	1.09E-12
Arg1	3.16E-15	-1.69854103	1.22E-12
Blnk	3.16E-15	-1.9431183	1.22E-12
Klra21	3.16E-15	-3.61903041	1.22E-12
Cd86	3.98E-15	-0.95319107	1.54E-12
Lyn	4.72E-15	-1.36576281	1.82E-12
Xcl1	4.72E-15	1.171512482	1.82E-12
Il15	5.14E-15	1.897503786	1.98E-12
Cmklr1	5.60E-15	1.315500088	2.16E-12
Adgre1	6.10E-15	1.128906078	2.35E-12
Chil3	6.10E-15	1.683423103	2.35E-12
Clec10a	6.10E-15	1.199383766	2.35E-12
Ly86	6.10E-15	-0.46744526	2.35E-12
Slc11a1	6.10E-15	0.946397733	2.35E-12
Tlr4	6.10E-15	2.820920751	2.35E-12
Traf6	6.10E-15	2.075469214	2.35E-12
Zbtb16	6.10E-15	3.330818036	2.35E-12
Tlr2	6.10E-15	1.777845291	2.35E-12
Fam129c	1.43E-14	1.913029244	5.53E-12
Mmp12	1.43E-14	1.00231287	5.53E-12
Irf4	1.43E-14	0.545875438	5.53E-12
Flt3	1.82E-14	-2.22263235	7.04E-12
Trem1	1.82E-14	-1.72280405	7.04E-12
Foxo1	3.40E-14	2.234402524	1.31E-11
Tnfrsf13c	5.46E-14	1.508043602	2.11E-11
Fyb	6.62E-14	-1.72327568	2.55E-11
Nt5e	6.62E-14	-0.98190758	2.55E-11
Btla	7.78E-14	-0.27412055	3.00E-11
Ighm	7.78E-14	-0.55400497	3.00E-11
Tnf	7.78E-14	-0.78152049	3.00E-11
Fcgr3	9.14E-14	0.508160279	3.53E-11
Il12rb2	9.14E-14	0.654758367	3.53E-11
Slc7a7	9.91E-14	2.997542367	3.82E-11

Il6ra	1.07E-13	2.625261922	4.14E-11
Slamf1	1.07E-13	0.884640896	4.14E-11
Il21	1.82E-13	3.331172994	7.04E-11
Tgfb3	2.94E-13	3.415369827	1.13E-10
Tnfsf14	2.94E-13	2.597800615	1.13E-10
Igkc	4.17E-13	-1.58949183	1.61E-10
Irak1	4.30E-13	1.051359755	1.66E-10
Sell	8.36E-13	-0.93348745	3.23E-10
Cd4	1.23E-12	0.770455819	4.73E-10
Itgax	1.32E-12	0.729232065	5.11E-10
Runx3	1.43E-12	1.293375229	5.51E-10
Socs1	1.43E-12	1.736674046	5.51E-10
Fcna	1.52E-12	3.085465484	5.86E-10
Cxcl2	1.54E-12	3.335965971	5.94E-10
Tlr3	1.54E-12	2.80995169	5.94E-10
Klrg1	1.54E-12	0.90287823	5.94E-10
Ikzf2	1.54E-12	1.97410646	5.94E-10
S100a8	2.80E-12	-1.51223679	1.08E-09
H2-DMa	6.63E-12	-0.56755555	2.56E-09
Itgae	1.11E-11	1.051575121	4.30E-09
Cd200	1.27E-11	0.901938608	4.92E-09
Il4ra	1.27E-11	0.632840258	4.92E-09
Cd274	1.27E-11	1.292123195	4.92E-09
Prdm1	1.37E-11	0.183400962	5.29E-09
F5	1.39E-11	-1.24801692	5.38E-09
Csf2	1.39E-11	-1.19507797	5.38E-09
Tspan32	1.47E-11	1.599090487	5.68E-09
Ccl6	1.58E-11	1.812420024	6.11E-09
Tnfsf13b	1.58E-11	1.174460596	6.11E-09
Ccl2	1.83E-11	3.284866303	7.05E-09
H2-Eb1	1.83E-11	1.002489402	7.05E-09
Il18	1.83E-11	2.90237301	7.05E-09
Irf3	1.83E-11	3.498761477	7.05E-09
Ccr2	4.61E-11	-0.63367813	1.78E-08
Csf1	7.91E-11	3.29290296	3.05E-08
Il12rb1	8.59E-11	-0.12494053	3.32E-08
Ccl9	9.86E-11	-0.15757324	3.81E-08
Bcl2	1.21E-10	1.180024342	4.67E-08
Cd72	1.21E-10	1.141452015	4.67E-08
Tcf7	1.39E-10	1.566597494	5.35E-08
Fas	1.48E-10	2.081598369	5.73E-08
Trib2	1.48E-10	1.778020644	5.73E-08

Ticam1	1.59E-10	2.044271274	6.13E-08
Il10	1.70E-10	2.293911291	6.56E-08
Cd1d1	1.70E-10	2.229777826	6.56E-08
Thbs1	1.82E-10	5.48600311	7.02E-08
Kit	1.82E-10	4.536892059	7.02E-08
Txk	2.65E-10	-0.9815091	1.02E-07
Adgrg3	3.12E-10	-1.47415903	1.20E-07
Tnfsf8	4.52E-10	4.079131964	1.74E-07
Rorc	7.49E-10	2.33724146	2.89E-07
Pou2af1	7.49E-10	3.438873407	2.89E-07
Nfkb2	8.64E-10	0.807803569	3.34E-07
Fads1	1.12E-09	0.788059213	4.33E-07
Ighg2c	1.12E-09	0.716864643	4.33E-07
Mzb1	1.12E-09	0.788059213	4.33E-07
Ada	1.27E-09	1.838511042	4.91E-07
Ltb	2.14E-09	-0.24251294	8.25E-07
Cd22	4.88E-09	1.796375831	1.88E-06
Lyz2	5.42E-09	3.083125625	2.09E-06
Il1r2	9.94E-09	3.330645109	3.84E-06
Il18rap	1.45E-08	-1.07544169	5.61E-06
Klra6	1.76E-08	-3.1324505	6.78E-06
Ccl3	2.24E-08	0.169428284	8.63E-06
H2-DMb2	2.59E-08	-2.36346238	9.98E-06
Kcne3	2.59E-08	-2.07748171	9.98E-06
Gzma	2.60E-08	1.139786819	1.01E-05
Cd160	3.01E-08	0.128790446	1.16E-05
Tnfrsf4	3.19E-08	1.744831586	1.23E-05
Nod1	3.79E-08	1.077140245	1.46E-05
Cxcr4	4.25E-08	1.166975563	1.64E-05
Klrk1	7.25E-08	0.133686231	2.80E-05
Klra3	7.78E-08	-2.74679207	3.00E-05
Irf8	8.72E-08	-0.51647473	3.37E-05
Cd33	1.06E-07	-1.35544965	4.10E-05
Tlr9	1.06E-07	-2.05255531	4.10E-05
Slc25a37	1.41E-07	0.426674788	5.44E-05
Irf7	1.85E-07	1.284619478	7.15E-05
Tnfrsf9	2.19E-07	0.214776675	8.47E-05
Klrc1	2.85E-07	0.684810575	0.00011011
Glg1	3.93E-07	2.214606866	0.00015156
Fosl1	4.23E-07	-1.27132034	0.00016346
Gzmm	4.23E-07	-4.5525307	0.00016346
Havcr2	5.56E-07	-0.11237988	0.0002148

Dock8	5.68E-07	-0.18581449	0.00021924
Ccl4	6.50E-07	-0.21785446	0.00025096
Cd69	1.34E-06	-0.70887378	0.00051698
Lamp3	1.35E-06	1.822562605	0.00052288
Lilrb4a	1.41E-06	-0.23975642	0.00054348
Icos	1.41E-06	0.390239641	0.00054348
Ighd	1.64E-06	-4.79002763	0.00063467
Aqp9	1.64E-06	-4.63164679	0.00063467
Cd7	1.86E-06	-1.15180888	0.00071791
Vegfa	1.92E-06	5.00235434	0.00074183
Arl4c	2.42E-06	0.614534152	0.00093598
Pask	2.53E-06	2.230348512	0.00097668
Eomes	3.85E-06	0.335449946	0.00148449
Mapk8	5.24E-06	1.767120863	0.00202162
Tbx21	5.89E-06	0.29946099	0.00227223
Arg2	6.22E-06	-1.12688913	0.00240155
Cxcl9	6.22E-06	-1.06853417	0.00240155
Trbc1	7.43E-06	0.249252833	0.00286898
Cblb	7.90E-06	0.155622097	0.00304976
Gimap5	1.03E-05	0.906518708	0.0039609
Pik3ip1	1.55E-05	5.92118774	0.00597892
Cxcr6	2.10E-05	-0.23869473	0.00812444
Tyk2	2.11E-05	0.995593307	0.00813628
Igha	2.30E-05	-1.49949554	0.00887084
Fasl	2.54E-05	-0.33818012	0.00981569
Qpct	2.74E-05	3.551154332	0.01059181
Tnfrsf18	2.77E-05	0.181186872	0.01068577
Jak2	2.89E-05	0.485765542	0.0111466
Ly96	3.27E-05	3.742293561	0.01260428
Birc3	4.43E-05	0.856729431	0.01711465
Kdelr1	5.71E-05	1.694027496	0.02203794
Aurkb	6.59E-05	0.514178585	0.02542571
Cxcl10	7.96E-05	2.086882167	0.03071313
Lag3	0.000126305	0.312234519	0.04875391
Ccl5	0.000129374	-0.84098683	0.04993834
Ccr5	0.000149686	0.345315991	0.05777884
Cd38	0.000176679	-0.32912941	0.06819817
Tigit	0.000253478	-0.22182137	0.0978425
Cd163	0.00029404	-1.37823737	0.11349962
Lrrc32	0.00029414	-0.86852399	0.11353803
Ifng	0.000362306	0.161726558	0.13985002
Dpp4	0.000581187	2.446871173	0.22433815

Ifnar1	0.000602501	1.488827669	0.23256553
Cd6	0.000693503	0.188420917	0.26769214
Cst7	0.000713798	-0.20247636	0.27552603
Bcl2a1a	0.000871026	-0.45690433	0.33621598
Gzmb	0.000917379	0.790278939	0.3541084
Cxcr3	0.000927482	0.430970303	0.3580081
Tnfrsf1b	0.000967901	-0.16459278	0.37360978
Thbd	0.001006786	7.389134166	0.38861956
Cd5	0.001028088	0.35758507	0.39684213
Ddx58	0.001138714	0.185662197	0.43954369
Atf6b	0.001192007	1.409231312	0.46011477
Tnfrsf25	0.001209509	2.888519054	0.46687055
Dusp2	0.001359513	0.111713408	0.52477202
Il15ra	0.001381006	0.638750512	0.53306826
Itgb2	0.001515469	-0.73541927	0.58497089
Entpd1	0.001645309	0.172248533	0.63508915
Cd34	0.001867541	10.41759084	0.7208707
Mbp	0.00192351	0.369738518	0.74247474
Cd8a	0.001957023	-0.10527723	0.75541088
Gzmk	0.002018844	0.306364442	0.7792739
Myc	0.00203343	2.34747068	0.78490381
Itk	0.002084841	-0.34661536	0.80474847
Junb	0.002190691	1.40450575	0.8456067
Cd28	0.002352441	0.728879373	0.90804209
Fth1	0.002621152	1.830664661	1
Lmna	0.002806894	4.803170251	1
Itga4	0.002846434	-0.20882142	1
Bin2	0.002856778	-0.30402085	1
Lgals1	0.003332622	0.62561796	1
Bcl11a	0.003534069	-1.1285639	1
Il17a	0.003534069	-1.18681237	1
Mmp9	0.003534069	-0.99314905	1
Nfkb1	0.00365228	0.726331439	1
Icam1	0.004265702	1.443805474	1
Casp1	0.004297983	-0.59094999	1
Il33	0.004308863	7.901868251	1
Egr1	0.005236723	5.552049024	1
Cd3e	0.005386844	-0.55652141	1
Rpn2	0.005611815	1.808085172	1
Mki67	0.005681155	0.237216847	1
Cd247	0.006439813	-0.24319765	1
C3	0.006830486	9.83618963	1

Cd48	0.006842985	-0.40789904	1
Maf	0.007563397	3.918171942	1
Ctla4	0.007567929	0.535002658	1
Il2rb	0.007612956	-0.21638179	1
Ptprc	0.010849652	-0.48565191	1
Anxa5	0.011349902	2.264530195	1
Cd3g	0.011760479	-0.313554	1
Il23r	0.01215075	-1.10807732	1
Hmox1	0.01411364	1.522158393	1
Cd52	0.014740659	-0.36978692	1
Ctsw	0.015060884	0.102684451	1
Cd8b1	0.018182866	0.454353934	1
Il3ra	0.02342422	0.732094453	1
Ccr6	0.023761766	3.290536594	1
Top2a	0.029450265	0.349480105	1
Cxcl13	0.03023902	8.266618389	1
Ikbkb	0.033965531	0.419145708	1
Ube2c	0.035252798	1.056016387	1
Lamp1	0.037187627	1.822164012	1
Stat6	0.037932309	0.703048346	1
Cnot2	0.038824465	1.07177677	1
Blk	0.042388117	-1.16428584	1
Ccl17	0.042388117	-1.07135859	1
Cx3cr1	0.042388117	-1.12734957	1
Cxcr2	0.042388117	-1.08781301	1
Il13	0.042388117	-1.20480043	1
Il5	0.042388117	-1.13623493	1
Tlr8	0.042388117	-1.11741249	1
Cd2	0.048499513	0.193195112	1
Thy1	0.053106264	1.044187756	1
Lap3	0.067024633	1.122123852	1
Pdia4	0.080429281	3.154139254	1
Cd3d	0.08494425	0.205057368	1
Trac	0.092749262	0.135782804	1
Stat1	0.098464813	-0.2417957	1
Ier3	0.101711766	3.973755817	1
Ifngr1	0.104255551	0.409859519	1
Vps28	0.108460789	0.826056608	1
Tfrc	0.112967215	1.928245904	1
2810417H13Rik	0.126731865	0.571542565	1
Lgals9	0.128691847	1.208692822	1
Dusp1	0.138838823	1.049660626	1

Tyms	0.143923882	0.655262487	1
Cd1d2	0.15723532	-1.05633793	1
Cxcl1	0.161011092	7.501952179	1
Il6	0.173289993	6.656697567	1
Tmem97	0.179434998	2.395972955	1
Apoe	0.184426246	5.286753071	1
Ccl19	0.187917778	7.958734685	1
Casp8	0.18892105	0.680877802	1
Btg1	0.190787247	-0.31939636	1
Ctsd	0.215124238	0.897640367	1
Trbc2	0.219065141	0.157452189	1
Lgals3	0.219084108	0.368959991	1
S100a10	0.232565963	0.567735057	1
Mcm2	0.247611036	1.11060772	1
Mcm4	0.256910512	0.345220487	1
Hprt	0.258649891	0.536820598	1
Jun	0.269024419	4.411876551	1
H2-K1	0.274795861	-0.12702301	1
Mgst1	0.29011543	6.708358151	1
Lat	0.302426037	0.280319398	1
Bax	0.317162273	0.13659526	1
Nrp1	0.321465168	0.687269636	1
Ebf1	0.331687213	4.930542673	1
Ifitm2	0.334162017	4.434681025	1
Hif1a	0.343809873	1.009100366	1
Psen1	0.413497764	0.381146873	1
Fn1	0.429450452	8.977885335	1
Tmem173	0.433541818	0.869667206	1
Cd44	0.468125298	1.104671557	1
Gapdh	0.589795101	0.746127531	1
Igbp1	0.619771884	1.002210571	1
Stat3	0.626642433	0.734302275	1
Mapk1	0.63841835	1.312915568	1
Ifitm3	0.66333045	5.301634296	1
Ybx3	0.671155157	0.95889079	1
Xbp1	0.741976758	0.809103459	1
Fosb	0.75337218	4.364672227	1
Pcna	0.77017986	0.40876609	1
Cd63	0.825554856	6.008312167	1
Fyn	0.96659971	0.874296018	1

Table B.4 Marker gene details for the *Pd1*$^{-/-}$ CD8^{+} effector T cells including adjusted p-value and log$_2$-fold change compared to WT CD8^{+} effector T cells.

ID	Description	GeneRatio	BgRatio	FoldEnrichment	pvalue	p.adjust
GO:0002699	positive regulation of immune effector process	20/76	315/28905	24.14786967	1.91E-22	4.81E-19
GO:0002697	regulation of immune effector process	22/76	473/28905	17.68971848	1.00E-21	1.26E-18
GO:0002700	production of molecular mediator of immunity	17/76	233/28905	27.74932234	3.56E-20	2.98E-17
GO:0002702	positive regulation of molecular production	15/76	169/28905	33.75700716	3.53E-19	2.22E-16
GO:0050900	leukocyte migration	19/76	402/28905	17.97574627	6.39E-19	3.21E-16
GO:0002440	production of molecular mediator of immune	19/76	423/28905	17.08333333	1.65E-18	6.92E-16
GO:0007159	leukocyte cell-cell adhesion	19/76	445/28905	16.23876404	4.24E-18	1.52E-15
GO:0002685	regulation of leukocyte migration	16/76	253/28905	24.05242355	4.99E-18	1.57E-15
GO:0071674	mononuclear cell migration	15/76	203/28905	28.10312419	5.76E-18	1.61E-15
GO:0019221	cytokine-mediated signalling pathway	19/76	471/28905	15.34235669	1.21E-17	3.05E-15
GO:0046631	alpha-beta T cell activation	15/76	223/28905	25.58266462	2.38E-17	5.44E-15
GO:0002460	somatic recombination of immune receptors	19/76	494/28905	14.62803644	2.92E-17	5.65E-15
GO:0002367	cytokine production involved in immune	14/76	176/28905	30.253439	2.82E-17	5.65E-15
GO:0002687	positive regulation of leukocyte migration	14/76	179/28905	29.74639812	3.58E-17	6.01E-15
GO:0070661	leukocyte proliferation	18/76	420/28905	16.29981203	3.36E-17	6.01E-15
GO:0051251	positive regulation of lymphocyte activation	17/76	360/28905	17.95997807	5.62E-17	8.82E-15
GO:0070663	regulation of leukocyte proliferation	16/76	307/28905	19.8217041	1.08E-16	1.60E-14
GO:0046651	lymphocyte proliferation	17/76	378/28905	17.10474102	1.27E-16	1.77E-14

GO:0072676	lymphocyte migration	12/76	112/28905	40.74953008	1.58E-16	2.08E-14
GO:0002718	regulation of cytokine production	13/76	153/28905	32.31553148	1.75E-16	2.09E-14
GO:0032943	mononuclear cell proliferation	17/76	385/28905	16.79374573	1.72E-16	2.09E-14
GO:0002696	positive regulation of leukocyte activation	17/76	397/28905	16.28612621	2.86E-16	3.27E-14
GO:0071677	positive regulation of mononuclear cell	11/76	84/28905	49.8049812	3.11E-16	3.40E-14
GO:1903037	regulation of leukocyte adhesion	17/76	405/28905	15.96442495	3.98E-16	4.17E-14
GO:0050727	regulation of inflammatory response	17/76	411/28905	15.73136765	5.07E-16	5.10E-14
GO:0050670	regulation of lymphocyte proliferation	15/76	280/28905	20.37476504	7.13E-16	6.90E-14
GO:0050867	positive regulation of cell activation	17/76	421/28905	15.35770096	7.55E-16	7.03E-14
GO:0032944	regulation of mononuclear proliferation	15/76	285/28905	20.01731302	9.27E-16	8.32E-14
GO:0071675	regulation of mononuclear cell migration	12/76	133/28905	34.31539375	1.31E-15	1.14E-13
GO:0002822	Regulation of adaptive immune response	14/76	237/28905	22.46668887	1.85E-15	1.50E-13
GO:1903039	regulation of leukocyte cell-cell adhesion	15/76	298/28905	19.14407453	1.79E-15	1.50E-13
GO:0072678	T cell migration	10/76	69/28905	55.1201373	2.56E-15	2.01E-13
GO:0002703	regulation of leukocyte immunity	15/76	311/28905	18.34383991	3.37E-15	2.56E-13
GO:0001818	negative regulation of cytokine	15/76	312/28905	18.28504555	3.53E-15	2.61E-13
GO:0006935	chemotaxis	17/76	465/28905	13.90449915	3.87E-15	2.78E-13
GO:0042330	taxis	17/76	467/28905	13.84495097	4.16E-15	2.90E-13
GO:0002819	regulation of adaptive immune response	14/76	253/28905	21.04587061	4.58E-15	3.11E-13

GO:0097529	myeloid leukocyte migration	14/76	255/28905	20.88080495	5.11E-15	3.38E-13
GO:0002637	regulation of immunoglobulin production	11/76	111/28905	37.69025605	7.49E-15	4.83E-13
GO:0042098	T cell proliferation	14/76	265/28905	20.09285005	8.70E-15	5.47E-13
GO:0050863	regulation of T cell activation	16/76	408/28905	14.91486068	9.27E-15	5.69E-13
GO:0060326	cell chemotaxis	15/76	334/28905	17.08064135	9.60E-15	5.75E-13
GO:0022409	positive regulation of cell-cell adhesion	15/76	349/28905	16.34651636	1.83E-14	1.07E-12
GO:0002824	positive regulation of adaptive immune response based on somatic recombination of immune receptors built from immunoglobulin superfamily domains	12/76	167/28905	27.32902616	2.09E-14	1.19E-12
GO:0050921	positive regulation of chemotaxis	12/76	168/28905	27.16635338	2.24E-14	1.25E-12
GO:0002821	positive regulation of adaptive immune response	12/76	175/28905	26.07969925	3.67E-14	2.01E-12
GO:0030595	leukocyte chemotaxis	13/76	242/28905	20.43089387	6.88E-14	3.60E-12
GO:0035710	CD4-positive, alpha-beta T cell activation	11/76	135/28905	30.98976608	6.74E-14	3.60E-12
GO:1990266	neutrophil migration	11/76	140/28905	29.88298872	1.01E-13	5.19E-12
GO:0002449	lymphocyte mediated immunity	16/76	482/28905	12.6250273	1.21E-13	6.07E-12
GO:0002237	response to molecule of bacterial origin	15/76	422/28905	13.51880145	2.88E-13	1.42E-11
GO:0050870	positive regulation of T cell activation	13/76	272/28905	18.17748646	3.07E-13	1.48E-11
GO:1903708	positive regulation of hemopoiesis	12/76	217/28905	21.03201552	4.80E-13	2.24E-11
GO:1902107	positive regulation of leukocyte differentiation	12/76	217/28905	21.03201552	4.80E-13	2.24E-11
GO:1903555	regulation of tumour necrosis factor superfamily cytokine production	12/76	219/28905	20.83994232	5.35E-13	2.45E-11
GO:0042129	regulation of T cell proliferation	12/76	221/28905	20.65134556	5.96E-13	2.68E-11

GO:0071706	tumour necrosis factor superfamily cytokine production	12/76	226/28905	20.19445738	7.77E-13	3.43E-11
GO:0097530	granulocyte migration	11/76	169/28905	24.75513859	8.10E-13	3.45E-11
GO:1902105	regulation of leukocyte differentiation	14/76	369/28905	14.42982456	8.02E-13	3.45E-11
GO:2000404	regulation of T cell migration	8/76	51/28905	59.65944272	9.09E-13	3.81E-11
GO:0002639	positive regulation of immunoglobulin production	9/76	82/28905	41.74342105	9.25E-13	3.81E-11
GO:0002285	lymphocyte activation involved in immune response	12/76	230/28905	19.84324943	9.57E-13	3.88E-11
GO:2000514	regulation of CD4-positive, alpha-beta T cell activation	9/76	83/28905	41.24048827	1.03E-12	4.13E-11
GO:0050671	positive regulation of lymphocyte proliferation	11/76	176/28905	23.77055921	1.26E-12	4.97E-11
GO:0032946	positive regulation of mononuclear cell	11/76	179/28905	23.37216995	1.52E-12	5.80E-11
GO:0002706	regulation of lymphocyte mediated immunity	12/76	239/28905	19.09601409	1.51E-12	5.80E-11
GO:0050920	regulation of chemotaxis	12/76	246/28905	18.55263158	2.12E-12	7.94E-11
GO:0032496	response to lipopolysaccharide	14/76	402/28905	13.24528672	2.54E-12	9.40E-11
GO:0050871	positive regulation of B cell activation	9/76	94/28905	36.41447368	3.27E-12	1.19E-10
GO:0002520	immune system development	12/76	256/28905	17.82791941	3.38E-12	1.21E-10
GO:0070665	positive regulation of leukocyte proliferation	11/76	195/28905	21.45445344	3.88E-12	1.37E-10
GO:0002705	positive regulation of leukocyte mediated immunity	11/76	196/28905	21.34499194	4.10E-12	1.43E-10
GO:0046632	alpha-beta T cell differentiation	10/76	142/28905	26.78372869	4.30E-12	1.46E-10
GO:0032760	positive regulation of tumour necrosis factor production	10/76	142/28905	26.78372869	4.30E-12	1.46E-10
GO:0002366	leukocyte activation involved in immune response	13/76	336/28905	14.71510808	4.44E-12	1.49E-10

GO:0007249	canonical NF-kappaB signal transduction	12/76	264/28905	17.28767943	4.85E-12	1.60E-10
GO:1903557	positive regulation of tumour necrosis factor superfamily cytokine production	10/76	144/28905	26.41173246	4.95E-12	1.62E-10
GO:0002263	cell activation involved in immune response	13/76	340/28905	14.54198916	5.15E-12	1.66E-10
GO:0032655	regulation of interleukin-12 production	8/76	63/28905	48.29573935	5.39E-12	1.72E-10
GO:0050864	regulation of B cell activation	10/76	147/28905	25.87271751	6.08E-12	1.89E-10
GO:0046634	regulation of alpha-beta T cell activation	10/76	147/28905	25.87271751	6.08E-12	1.89E-10
GO:0032615	interleukin-12 production	8/76	65/28905	46.8097166	7.00E-12	2.14E-10
GO:0002377	immunoglobulin production	12/76	275/28905	16.59617225	7.81E-12	2.37E-10
GO:2000401	regulation of lymphocyte migration	8/76	66/28905	46.10047847	7.94E-12	2.38E-10
GO:0002274	myeloid leukocyte activation	12/76	281/28905	16.24180558	1.01E-11	2.97E-10
GO:0001906	cell killing	12/76	285/28905	16.01385042	1.19E-11	3.43E-10
GO:0032680	regulation of tumour necrosis factor production	11/76	216/28905	19.3686038	1.18E-11	3.43E-10
GO:1903706	regulation of hemopoiesis	14/76	457/28905	11.65121502	1.41E-11	4.02E-10
GO:0030593	neutrophil chemotaxis	9/76	112/28905	30.56214756	1.63E-11	4.55E-10
GO:0002720	positive regulation of cytokine production involved in immune response	9/76	112/28905	30.56214756	1.63E-11	4.55E-10
GO:0032640	tumour necrosis factor production	11/76	223/28905	18.76062072	1.66E-11	4.59E-10
GO:0043123	positive regulation of canonical NF-kappaB signal transduction	10/76	164/28905	23.19078947	1.81E-11	4.95E-10
GO:0032735	positive regulation of interleukin-12 production	7/76	44/28905	60.50687799	2.32E-11	6.27E-10
GO:0002708	positive regulation of lymphocyte mediated immunity	10/76	169/28905	22.50467144	2.44E-11	6.54E-10

GO:0051091	positive regulation of DNA-binding transcription factor activity	11/76	238/28905	17.57822866	3.35E-11	8.86E-10
GO:1990869	cellular response to chemokine	8/76	80/28905	38.03289474	3.89E-11	1.01E-09
GO:1990868	response to chemokine	8/76	80/28905	38.03289474	3.89E-11	1.01E-09
GO:0042113	B cell activation	12/76	319/28905	14.30704504	4.38E-11	1.12E-09
GO:0071347	cellular response to interleukin-1	8/76	82/28905	37.10526316	4.77E-11	1.21E-09
GO:0071219	cellular response to molecule of bacterial origin	12/76	322/28905	14.17374959	4.88E-11	1.23E-09
GO:0032635	interleukin-6 production	10/76	182/28905	20.89719491	5.09E-11	1.27E-09
GO:0042088	T-helper 1 type immune response	7/76	53/28905	50.23212512	9.16E-11	2.26E-09
GO:0071621	granulocyte chemotaxis	9/76	137/28905	24.98511333	1.01E-10	2.46E-09
GO:0048247	lymphocyte chemotaxis	7/76	54/28905	49.30190058	1.05E-10	2.54E-09
GO:0071216	cellular response to biotic stimulus	12/76	350/28905	13.03984962	1.28E-10	3.05E-09
GO:0070555	response to interleukin-1	8/76	96/28905	31.69407895	1.72E-10	4.08E-09
GO:0043370	regulation of CD4-positive, alpha-beta T cell differentiation	7/76	58/28905	45.90176951	1.77E-10	4.15E-09
GO:0002312	B cell activation involved in immune response	8/76	97/28905	31.36733587	1.87E-10	4.36E-09
GO:0002889	regulation of immunoglobulin mediated immune response	8/76	99/28905	30.73365231	2.21E-10	5.05E-09
GO:0002712	regulation of B cell mediated immunity	8/76	99/28905	30.73365231	2.21E-10	5.05E-09
GO:0032609	type II interferon production	9/76	150/28905	22.81973684	2.27E-10	5.14E-09
GO:0070371	ERK1 and ERK2 cascade	12/76	371/28905	12.30174493	2.48E-10	5.53E-09
GO:0002573	myeloid leukocyte differentiation	11/76	287/28905	14.57706767	2.47E-10	5.53E-09

GO:0043367	CD4-positive, alpha-beta T cell differentiation	8/76	103/28905	29.54011242	3.04E-10	6.71E-09
GO:0002548	monocyte chemotaxis	7/76	65/28905	40.95850202	4.03E-10	8.82E-09
GO:0045088	regulation of innate immune response	13/76	486/28905	10.17340806	4.27E-10	9.24E-09
GO:0051090	regulation of DNA-binding transcription factor activity	12/76	391/28905	11.67249966	4.52E-10	9.71E-09
GO:0050729	positive regulation of inflammatory response	9/76	167/28905	20.49676962	5.91E-10	1.25E-08
GO:2000406	positive regulation of T cell migration	6/76	37/28905	61.67496444	5.89E-10	1.25E-08
GO:0071222	cellular response to lipopolysaccharide	11/76	312/28905	13.4090334	5.97E-10	1.25E-08
GO:0030099	myeloid cell differentiation	13/76	500/28905	9.888552632	6.02E-10	1.25E-08
GO:0043122	regulation of canonical NF-kappaB signal transduction	10/76	235/28905	16.18421053	6.22E-10	1.27E-08
GO:0061082	myeloid leukocyte cytokine production	7/76	69/28905	38.58409611	6.20E-10	1.27E-08
GO:0002690	positive regulation of leukocyte chemotaxis	8/76	114/28905	26.68975069	6.88E-10	1.37E-08
GO:0070098	chemokine-mediated signalling pathway	7/76	70/28905	38.03289474	6.87E-10	1.37E-08
GO:0032731	positive regulation of interleukin-1 beta production	7/76	70/28905	38.03289474	6.87E-10	1.37E-08
GO:0070374	positive regulation of ERK1 and ERK2 cascade	10/76	240/28905	15.84703947	7.63E-10	1.51E-08
GO:0032675	regulation of interleukin-6 production	9/76	173/28905	19.785899	8.07E-10	1.59E-08
GO:0002381	immunoglobulin production involved in immunoglobulin-mediated immune response	7/76	73/28905	36.46989906	9.28E-10	1.81E-08
GO:0046637	regulation of alpha-beta T cell differentiation	7/76	78/28905	34.13208502	1.49E-09	2.79E-08
GO:0016444	somatic cell DNA recombination	7/76	78/28905	34.13208502	1.49E-09	2.79E-08
GO:0002891	positive regulation of immunoglobulin mediated immune response	7/76	78/28905	34.13208502	1.49E-09	2.79E-08

GO:0002714	positive regulation of B cell mediated immunity	7/76	78/28905	34.13208502	1.49E-09	2.79E-08
GO:0002562	somatic diversification of immune receptors via germline recombination within a single locus	7/76	78/28905	34.13208502	1.49E-09	2.79E-08
GO:2000403	positive regulation of lymphocyte migration	6/76	43/28905	53.06915545	1.52E-09	2.84E-08
GO:0070372	regulation of ERK1 and ERK2 cascade	11/76	343/28905	12.19713825	1.61E-09	2.96E-08
GO:0030217	T cell differentiation	11/76	343/28905	12.19713825	1.61E-09	2.96E-08
GO:0002294	CD4-positive, alpha-beta T cell differentiation involved in immune response	7/76	79/28905	33.70003331	1.63E-09	2.97E-08
GO:0032652	regulation of interleukin-1 production	8/76	128/28905	23.77055921	1.74E-09	3.14E-08
GO:0002293	alpha-beta T cell differentiation involved in immune response	7/76	80/28905	33.27878289	1.78E-09	3.20E-08
GO:0002287	alpha-beta T cell activation involved in immune response	7/76	81/28905	32.86793372	1.95E-09	3.47E-08
GO:0010935	regulation of macrophage cytokine production	6/76	45/28905	50.71052632	2.03E-09	3.59E-08
GO:0032732	positive regulation of interleukin-1 production	7/76	82/28905	32.46710526	2.13E-09	3.74E-08
GO:0042102	positive regulation of T cell proliferation	8/76	133/28905	22.87692917	2.36E-09	4.11E-08
GO:0032612	interleukin-1 production	8/76	134/28905	22.70620581	2.50E-09	4.30E-08
GO:0002286	T cell activation involved in immune response	8/76	134/28905	22.70620581	2.50E-09	4.30E-08
GO:2000516	positive regulation of CD4-positive, alpha-beta T cell activation	6/76	47/28905	48.55263158	2.66E-09	4.55E-08
GO:0032649	regulation of type II interferon production	8/76	136/28905	22.37229102	2.81E-09	4.77E-08

GO:0002200	somatic diversification of immune receptors	7/76	86/28905	30.95700734	2.98E-09	5.03E-08
GO:0002292	T cell differentiation involved in immune response	7/76	87/28905	30.60117967	3.23E-09	5.42E-08
GO:0002688	regulation of leukocyte chemotaxis	8/76	140/28905	21.73308271	3.54E-09	5.89E-08
GO:0010818	T cell chemotaxis	5/76	23/28905	82.68020595	3.56E-09	5.90E-08
GO:0045621	positive regulation of lymphocyte differentiation	8/76	143/28905	21.27714391	4.18E-09	6.87E-08
GO:0010934	macrophage cytokine production	6/76	52/28905	43.88410931	5.00E-09	8.16E-08
GO:0051345	positive regulation of hydrolase activity	12/76	488/28905	9.352351165	5.47E-09	8.87E-08
GO:0030098	lymphocyte differentiation	12/76	490/28905	9.314178303	5.72E-09	9.22E-08
GO:0034341	response to type II interferon	8/76	149/28905	20.42034617	5.78E-09	9.26E-08
GO:0002764	immune response-regulating signaling pathway	12/76	497/28905	9.182992693	6.70E-09	1.07E-07
GO:0002695	negative regulation of leukocyte activation	9/76	221/28905	15.48850917	6.93E-09	1.10E-07
GO:0061756	leukocyte adhesion to vascular endothelial cell	6/76	56/28905	40.74953008	7.90E-09	1.24E-07
GO:1904996	positive regulation of leukocyte adhesion to vascular	5/76	27/28905	70.43128655	8.48E-09	1.32E-07
GO:0045619	regulation of lymphocyte differentiation	9/76	227/28905	15.07912126	8.75E-09	1.36E-07
GO:0045089	positive regulation of innate immune response	11/76	404/28905	10.35549114	8.81E-09	1.36E-07
GO:0071887	leukocyte apoptotic process	8/76	159/28905	19.13604767	9.64E-09	1.48E-07
GO:0045190	isotype switching	6/76	59/28905	38.67752007	1.09E-08	1.64E-07
GO:0002208	somatic diversification of immunoglobulins involved	6/76	59/28905	38.67752007	1.09E-08	1.64E-07
GO:0002204	somatic recombination of immunoglobulin genes	6/76	59/28905	38.67752007	1.09E-08	1.64E-07

GO:0032651	regulation of interleukin-1 beta production	7/76	107/28905	24.88133301	1.38E-08	2.07E-07
GO:0050866	negative regulation of cell activation	9/76	241/28905	14.20315571	1.47E-08	2.19E-07
GO:0060907	positive regulation of macrophage cytokine production	5/76	30/28905	63.38815789	1.49E-08	2.20E-07
GO:0002833	positive regulation of response to biotic stimulus	11/76	431/28905	9.706771279	1.71E-08	2.52E-07
GO:0032653	regulation of interleukin-10 production	6/76	64/28905	35.65583882	1.79E-08	2.62E-07
GO:0032755	positive regulation of interleukin-6 production	7/76	113/28905	23.56020028	2.02E-08	2.92E-07
GO:0032611	interleukin-1 beta production	7/76	113/28905	23.56020028	2.02E-08	2.92E-07
GO:0048535	lymph node development	5/76	32/28905	59.42639803	2.09E-08	3.01E-07
GO:0032613	interleukin-10 production	6/76	67/28905	34.05930872	2.37E-08	3.39E-07
GO:0016447	somatic recombination of immunoglobulin gene segments	6/76	68/28905	33.55843653	2.60E-08	3.69E-07
GO:0002828	regulation of type 2 immune response	5/76	34/28905	55.93072755	2.88E-08	4.07E-07
GO:0043372	positive regulation of CD4-positive, alpha-beta T cell	5/76	35/28905	54.33270677	3.36E-08	4.71E-07
GO:0071346	cellular response to type II interferon	7/76	122/28905	21.82215272	3.44E-08	4.81E-07
GO:0030888	regulation of B cell proliferation	6/76	73/28905	31.25991348	4.00E-08	5.55E-07
GO:0045580	regulation of T cell differentiation	8/76	193/28905	15.76493046	4.37E-08	6.04E-07
GO:0045582	positive regulation of T cell differentiation	7/76	127/28905	20.96301285	4.55E-08	6.25E-07
GO:0045428	regulation of nitric oxide biosynthetic process	6/76	75/28905	30.42631579	4.71E-08	6.40E-07
GO:0016445	somatic diversification of immunoglobulins	6/76	75/28905	30.42631579	4.71E-08	6.40E-07
GO:1904994	regulation of leukocyte adhesion to vascular endothelial cell	5/76	38/28905	50.04328255	5.16E-08	6.97E-07

GO:0002763	positive regulation of myeloid leukocyte differentiation	6/76	77/28905	29.63602187	5.52E-08	7.43E-07
GO:0007204	positive regulation of cytosolic calcium ion concentration	8/76	200/28905	15.21315789	5.76E-08	7.70E-07
GO:0002757	immune response-activating signalling pathway	11/76	486/28905	8.608268356	5.81E-08	7.73E-07
GO:0010819	regulation of T cell chemotaxis	4/76	15/28905	101.4210526	5.89E-08	7.80E-07
GO:0080164	regulation of nitric oxide metabolic process	6/76	78/28905	29.25607287	5.97E-08	7.82E-07
GO:0042093	T-helper cell differentiation	6/76	78/28905	29.25607287	5.97E-08	7.82E-07
GO:0051092	positive regulation of NF-kappaB transcription factor activity	7/76	136/28905	19.57575464	7.29E-08	9.49E-07
GO:0045191	regulation of isotype switching	5/76	41/28905	46.38157895	7.65E-08	9.86E-07
GO:0002418	immune response to tumour cell	5/76	41/28905	46.38157895	7.65E-08	9.86E-07
GO:0097696	receptor signalling pathway via STAT	8/76	213/28905	14.2846553	9.35E-08	1.19E-06
GO:0001776	leukocyte homeostasis	7/76	141/28905	18.88157895	9.34E-08	1.19E-06
GO:0061081	positive regulation of myeloid leukocyte cytokine production involved in immune response	5/76	43/28905	44.22429621	9.79E-08	1.24E-06
GO:0016064	immunoglobulin mediated immune response	9/76	302/28905	11.33430638	1.02E-07	1.28E-06
GO:0019724	B cell mediated immunity	9/76	305/28905	11.2228214	1.11E-07	1.39E-06
GO:0048872	homeostasis of number of cells	10/76	408/28905	9.321787926	1.17E-07	1.47E-06
GO:0006809	nitric oxide biosynthetic process	6/76	88/28905	25.93151914	1.23E-07	1.54E-06
GO:0001771	immunological synapse formation	4/76	18/28905	84.51754386	1.31E-07	1.63E-06
GO:0031341	regulation of cell killing	7/76	153/28905	17.40067079	1.63E-07	2.01E-06
GO:0001562	response to protozoan	5/76	48/28905	39.61759868	1.72E-07	2.10E-06

GO:0046209	nitric oxide metabolic process	6/76	93/28905	24.53735144	1.72E-07	2.10E-06
GO:2001057	reactive nitrogen species metabolic process	6/76	95/28905	24.02077562	1.95E-07	2.36E-06
GO:0002761	regulation of myeloid leukocyte differentiation	7/76	157/28905	16.9573416	1.95E-07	2.36E-06
GO:0042092	type 2 immune response	5/76	50/28905	38.03289474	2.12E-07	2.55E-06
GO:0006310	DNA recombination	9/76	331/28905	10.34127047	2.21E-07	2.64E-06
GO:0006909	phagocytosis	8/76	239/28905	12.73067606	2.26E-07	2.69E-06
GO:1902624	positive regulation of neutrophil migration	5/76	51/28905	37.2871517	2.35E-07	2.79E-06
GO:0043270	positive regulation of monoatomic ion transport	8/76	241/28905	12.6250273	2.41E-07	2.84E-06
GO:1901623	regulation of lymphocyte chemotaxis	4/76	21/28905	72.44360902	2.55E-07	3.00E-06
GO:0002456	T cell mediated immunity	7/76	164/28905	16.23355263	2.62E-07	3.06E-06
GO:0048245	eosinophil chemotaxis	4/76	22/28905	69.1507177	3.11E-07	3.62E-06
GO:0046635	positive regulation of alpha-beta T cell activation	6/76	103/28905	22.15508431	3.16E-07	3.64E-06
GO:0002347	response to tumour cell	5/76	54/28905	35.21564327	3.14E-07	3.64E-06
GO:0046638	positive regulation of alpha-beta T cell differentiation	5/76	55/28905	34.57535885	3.45E-07	3.96E-06
GO:0055074	calcium ion homeostasis	9/76	354/28905	9.669380018	3.88E-07	4.43E-06
GO:0002369	T cell cytokine production	5/76	57/28905	33.36218837	4.14E-07	4.71E-06
GO:0045591	positive regulation of regulatory T cell differentiation	4/76	24/28905	63.38815789	4.50E-07	5.10E-06
GO:0141061	disruption of cell in another organism	6/76	110/28905	20.74521531	4.66E-07	5.23E-06
GO:0031640	killing of cells of another organism	6/76	110/28905	20.74521531	4.66E-07	5.23E-06

GO:0001909	leukocyte mediated cytotoxicity	7/76	179/28905	14.87319906	4.74E-07	5.29E-06
GO:0050731	positive regulation of peptidyl-tyrosine phosphorylation	7/76	182/28905	14.62803644	5.30E-07	5.89E-06
GO:0042116	macrophage activation	6/76	114/28905	20.01731302	5.75E-07	6.37E-06
GO:1902622	regulation of neutrophil migration	5/76	62/28905	30.6716893	6.33E-07	6.95E-06
GO:0072677	eosinophil migration	4/76	26/28905	58.51214575	6.31E-07	6.95E-06
GO:0009615	response to virus	9/76	377/28905	9.079470892	6.55E-07	7.16E-06
GO:0045639	positive regulation of myeloid cell differentiation	6/76	118/28905	19.33876004	7.05E-07	7.67E-06
GO:0051051	negative regulation of transport	10/76	497/28905	7.652493911	7.14E-07	7.74E-06
GO:0070498	interleukin-1-mediated signaling pathway	4/76	27/28905	56.34502924	7.40E-07	7.98E-06
GO:0071356	cellular response to tumor necrosis factor	7/76	193/28905	13.79431415	7.86E-07	8.44E-06
GO:0048660	regulation of smooth muscle cell proliferation	7/76	194/28905	13.72320944	8.14E-07	8.70E-06
GO:0090026	positive regulation of monocyte chemotaxis	4/76	28/28905	54.33270677	8.61E-07	9.17E-06
GO:0051250	negative regulation of lymphocyte activation	7/76	197/28905	13.51422656	9.02E-07	9.49E-06
GO:0050764	regulation of phagocytosis	6/76	123/28905	18.55263158	9.00E-07	9.49E-06
GO:0042100	B cell proliferation	6/76	123/28905	18.55263158	9.00E-07	9.49E-06
GO:1905517	macrophage migration	5/76	67/28905	28.38275727	9.35E-07	9.79E-06
GO:0042063	gliogenesis	9/76	397/28905	8.622066817	1.01E-06	1.05E-05
GO:2000106	regulation of leukocyte apoptotic process	6/76	126/28905	18.11090226	1.04E-06	1.08E-05
GO:0048145	regulation of fibroblast proliferation	6/76	127/28905	17.96829673	1.09E-06	1.12E-05

GO:0048659	smooth muscle cell proliferation	7/76	203/28905	13.11479129	1.10E-06	1.14E-05
GO:0007259	receptor signaling pathway via JAK-STAT	7/76	205/28905	12.98684211	1.18E-06	1.21E-05
GO:0006109	regulation of carbohydrate metabolic process	7/76	206/28905	12.92379918	1.22E-06	1.24E-05
GO:0045830	positive regulation of isotype switching	4/76	31/28905	49.07470289	1.32E-06	1.34E-05
GO:0034612	response to tumor necrosis factor	7/76	213/28905	12.49907339	1.52E-06	1.54E-05
GO:0002825	regulation of T-helper 1 type immune response	4/76	33/28905	46.10047847	1.70E-06	1.72E-05
GO:0002768	immune response-regulating cell surface receptor signaling pathway	8/76	313/28905	9.720867664	1.72E-06	1.73E-05
GO:0051928	positive regulation of calcium ion transport	6/76	138/28905	16.53604119	1.76E-06	1.76E-05
GO:0051607	defense response to virus	8/76	314/28905	9.689909487	1.76E-06	1.76E-05
GO:0030316	osteoclast differentiation	6/76	139/28905	16.41707686	1.84E-06	1.83E-05
GO:0046633	alpha-beta T cell proliferation	5/76	77/28905	24.69668489	1.87E-06	1.85E-05
GO:1901342	regulation of vasculature development	8/76	317/28905	9.598206874	1.89E-06	1.86E-05
GO:0071353	cellular response to interleukin-4	4/76	34/28905	44.74458204	1.93E-06	1.89E-05
GO:0042742	defense response to bacterium	9/76	430/28905	7.960373317	1.94E-06	1.90E-05
GO:0010959	regulation of metal ion transport	9/76	431/28905	7.941903773	1.98E-06	1.93E-05
GO:2001233	regulation of apoptotic signaling pathway	9/76	436/28905	7.850826895	2.17E-06	2.11E-05
GO:0009306	protein secretion	9/76	438/28905	7.814978371	2.25E-06	2.18E-05
GO:0035592	establishment of protein localization to extracellular region	9/76	439/28905	7.797176598	2.30E-06	2.21E-05
GO:0090025	regulation of monocyte chemotaxis	4/76	36/28905	42.25877193	2.44E-06	2.32E-05

GO:0070670	response to interleukin-4	4/76	36/28905	42.25877193	2.44E-06	2.32E-05
GO:0006874	intracellular calcium ion homeostasis	8/76	328/28905	9.276315789	2.44E-06	2.32E-05
GO:0071692	protein localization to extracellular region	9/76	445/28905	7.692046127	2.56E-06	2.41E-05
GO:0045123	cellular extravasation	5/76	82/28905	23.19078947	2.56E-06	2.41E-05
GO:0050769	positive regulation of neurogenesis	8/76	330/28905	9.220095694	2.55E-06	2.41E-05
GO:0050708	regulation of protein secretion	8/76	333/28905	9.137031769	2.72E-06	2.55E-05
GO:0141060	disruption of anatomical structure in another organism	6/76	150/28905	15.21315789	2.86E-06	2.68E-05
GO:0022408	negative regulation of cell-cell adhesion	7/76	236/28905	11.28094335	3.00E-06	2.79E-05
GO:0070228	regulation of lymphocyte apoptotic process	5/76	85/28905	22.37229102	3.06E-06	2.84E-05
GO:0048144	fibroblast proliferation	6/76	152/28905	15.01298476	3.09E-06	2.86E-05
GO:0006959	humoral immune response	8/76	339/28905	8.975314392	3.11E-06	2.86E-05
GO:1904064	positive regulation of cation transmembrane transport	6/76	153/28905	14.91486068	3.21E-06	2.95E-05
GO:0045637	regulation of myeloid cell differentiation	7/76	239/28905	11.13934155	3.26E-06	2.98E-05
GO:0001773	myeloid dendritic cell activation	4/76	39/28905	39.00809717	3.38E-06	3.08E-05
GO:0050777	negative regulation of immune response	7/76	241/28905	11.04689889	3.44E-06	3.11E-05
GO:0150076	neuroinflammatory response	5/76	87/28905	21.85798548	3.43E-06	3.11E-05
GO:0097191	extrinsic apoptotic signalling pathway	7/76	243/28905	10.95597791	3.63E-06	3.27E-05
GO:0050901	leukocyte tethering or rolling	4/76	40/28905	38.03289474	3.75E-06	3.35E-05
GO:0045672	positive regulation of osteoclast differentiation	4/76	40/28905	38.03289474	3.75E-06	3.35E-05

GO:0045589	regulation of regulatory T cell differentiation	4/76	40/28905	38.03289474	3.75E-06	3.35E-05
GO:0002361	regulatory T cell differentiation	3/76	12/28905	95.08223684	3.78E-06	3.36E-05
GO:0032102	negative regulation of response to external stimulus	9/76	470/28905	7.282894737	4.00E-06	3.54E-05
GO:0050868	negative regulation of T cell activation	6/76	162/28905	14.08625731	4.47E-06	3.94E-05
GO:0008037	cell recognition	6/76	163/28905	13.99983855	4.63E-06	4.07E-05
GO:0014015	positive regulation of gliogenesis	5/76	93/28905	20.44779287	4.77E-06	4.18E-05
GO:0060759	regulation of response to cytokine stimulus	6/76	164/28905	13.91447368	4.79E-06	4.18E-05
GO:0097028	dendritic cell differentiation	4/76	43/28905	35.37943696	5.04E-06	4.34E-05
GO:0045622	regulation of T-helper cell differentiation	4/76	43/28905	35.37943696	5.04E-06	4.34E-05
GO:0042832	defense response to protozoan	4/76	43/28905	35.37943696	5.04E-06	4.34E-05
GO:0032733	positive regulation of interleukin-10 production	4/76	43/28905	35.37943696	5.04E-06	4.34E-05
GO:0050730	regulation of peptidyl-tyrosine phosphorylation	7/76	256/28905	10.39961965	5.12E-06	4.39E-05
GO:1900180	regulation of protein localization to nucleus	6/76	166/28905	13.74682942	5.14E-06	4.39E-05
GO:0032660	regulation of interleukin-17 production	4/76	44/28905	34.57535885	5.53E-06	4.71E-05
GO:0034767	positive regulation of monoatomic ion transmembrane	6/76	169/28905	13.50280287	5.69E-06	4.84E-05
GO:0045066	regulatory T cell differentiation	4/76	45/28905	33.80701754	6.06E-06	5.11E-05
GO:0002724	regulation of T cell cytokine production	4/76	45/28905	33.80701754	6.06E-06	5.11E-05
GO:0010820	positive regulation of T cell chemotaxis	3/76	14/28905	81.49906015	6.23E-06	5.24E-05
GO:0042060	wound healing	8/76	373/28905	8.15718922	6.26E-06	5.25E-05

GO:0002269	leukocyte activation involved in inflammatory response	4/76	54/28905	28.17251462	1.26E-05	9.92E-05
GO:0032965	regulation of collagen biosynthetic process	4/76	55/28905	27.66028708	1.36E-05	0.00010646
GO:0140131	positive regulation of lymphocyte chemotaxis	3/76	18/28905	63.38815789	1.39E-05	0.00010817
GO:0097553	calcium ion transmembrane import into cytosol	6/76	198/28905	11.52511962	1.41E-05	0.00010939
GO:0048661	positive regulation of smooth muscle cell proliferation	5/76	117/28905	16.25337382	1.46E-05	0.00011328
GO:0060251	regulation of glial cell proliferation	4/76	56/28905	27.16635338	1.46E-05	0.00011328
GO:0050830	defense response to Gram-positive bacterium	6/76	201/28905	11.35310291	1.53E-05	0.00011729
GO:0002429	immune response-activating cell surface receptor signaling	7/76	303/28905	8.786477332	1.53E-05	0.00011729
GO:0002218	activation of innate immune response	7/76	303/28905	8.786477332	1.53E-05	0.00011729
GO:0032700	negative regulation of interleukin-17 production	3/76	19/28905	60.05193906	1.64E-05	0.00012397
GO:0032695	negative regulation of interleukin-12 production	3/76	19/28905	60.05193906	1.64E-05	0.00012397
GO:0002827	positive regulation of T-helper 1 type immune response	3/76	19/28905	60.05193906	1.64E-05	0.00012397
GO:0002295	T-helper cell lineage commitment	3/76	19/28905	60.05193906	1.64E-05	0.00012397
GO:0050678	regulation of epithelial cell proliferation	8/76	426/28905	7.14232765	1.64E-05	0.00012397
GO:0018108	peptidyl-tyrosine phosphorylation	7/76	309/28905	8.615866122	1.73E-05	0.00013052
GO:0045765	regulation of angiogenesis	7/76	310/28905	8.588073005	1.77E-05	0.00013285
GO:2000351	regulation of endothelial cell apoptotic process	4/76	59/28905	25.78501338	1.80E-05	0.00013385
GO:0061900	glial cell activation	4/76	59/28905	25.78501338	1.80E-05	0.00013385
GO:0032945	negative regulation of mononuclear cell proliferation	5/76	122/28905	15.58725194	1.79E-05	0.00013385

GO:0018212	peptidyl-tyrosine modification	7/76	311/28905	8.560458622	1.81E-05	0.00013403
GO:0031348	negative regulation of defense response	7/76	312/28905	8.533021255	1.84E-05	0.00013642
GO:0045058	T cell selection	4/76	61/28905	24.93960311	2.06E-05	0.00015152
GO:0072577	endothelial cell apoptotic process	4/76	62/28905	24.53735144	2.19E-05	0.00016118
GO:0070230	positive regulation of lymphocyte apoptotic process	3/76	21/28905	54.33270677	2.25E-05	0.00016361
GO:0051770	positive regulation of nitric-oxide synthase biosynthetic process	3/76	21/28905	54.33270677	2.25E-05	0.00016361
GO:0031334	positive regulation of protein-containing complex assembly	6/76	215/28905	10.61383109	2.24E-05	0.00016361
GO:0070664	negative regulation of leukocyte proliferation	5/76	128/28905	14.85659951	2.26E-05	0.00016381
GO:0048534	hematopoietic or lymphoid organ development	5/76	128/28905	14.85659951	2.26E-05	0.00016381
GO:0045912	negative regulation of carbohydrate metabolic process	4/76	63/28905	24.14786967	2.34E-05	0.00016832
GO:0010712	regulation of collagen metabolic process	4/76	63/28905	24.14786967	2.34E-05	0.00016832
GO:1904035	regulation of epithelial cell apoptotic process	5/76	130/28905	14.62803644	2.44E-05	0.000175
GO:0006816	calcium ion transport	8/76	451/28905	6.746411483	2.46E-05	0.00017632
GO:1904062	regulation of monoatomic cation transmembrane transport	7/76	328/28905	8.116776316	2.54E-05	0.00018146
GO:0043373	CD4-positive, alpha-beta T cell lineage commitment	3/76	22/28905	51.86303828	2.59E-05	0.00018428
GO:0032693	negative regulation of interleukin-10 production	3/76	22/28905	51.86303828	2.59E-05	0.00018428
GO:0000018	regulation of DNA recombination	5/76	132/28905	14.40639952	2.62E-05	0.00018568
GO:0060760	positive regulation of response to cytokine stimulus	4/76	65/28905	23.4048583	2.65E-05	0.00018628
GO:0032964	collagen biosynthetic process	4/76	65/28905	23.4048583	2.65E-05	0.00018628

GO:0046822	regulation of nucleocytoplasmic transport	5/76	135/28905	14.08625731	2.92E-05	0.00020512
GO:0045624	positive regulation of T-helper cell differentiation	3/76	23/28905	49.60812357	2.98E-05	0.000208
GO:0002922	positive regulation of humoral immune response	3/76	23/28905	49.60812357	2.98E-05	0.000208
GO:0051209	release of sequestered calcium ion into cytosol	5/76	136/28905	13.98268189	3.03E-05	0.00021075
GO:0030100	regulation of endocytosis	7/76	339/28905	7.853400093	3.13E-05	0.00021709
GO:0051283	negative regulation of sequestering of calcium ion	5/76	137/28905	13.88061852	3.13E-05	0.00021709
GO:0071622	regulation of granulocyte chemotaxis	4/76	68/28905	22.37229102	3.16E-05	0.00021846
GO:0007162	negative regulation of cell adhesion	7/76	342/28905	7.784510619	3.31E-05	0.00022832
GO:0051282	regulation of sequestering of calcium ion	5/76	139/28905	13.68089739	3.36E-05	0.00023079
GO:1903236	regulation of leukocyte tethering or rolling	3/76	24/28905	47.54111842	3.40E-05	0.00023085
GO:0097398	cellular response to interleukin-17	3/76	24/28905	47.54111842	3.40E-05	0.00023085
GO:0043011	myeloid dendritic cell differentiation	3/76	24/28905	47.54111842	3.40E-05	0.00023085
GO:0002363	alpha-beta T cell lineage commitment	3/76	24/28905	47.54111842	3.40E-05	0.00023085
GO:0051208	sequestering of calcium ion	5/76	141/28905	13.48684211	3.60E-05	0.00024379
GO:0050679	positive regulation of epithelial cell proliferation	6/76	235/28905	9.710526316	3.68E-05	0.00024889
GO:1904892	regulation of receptor signaling pathway via STAT	5/76	142/28905	13.39186434	3.72E-05	0.00025082
GO:0002224	toll-like receptor signaling pathway	4/76	71/28905	21.42698295	3.75E-05	0.00025216
GO:0014013	regulation of gliogenesis	5/76	143/28905	13.29821494	3.85E-05	0.000258
GO:0046640	regulation of alpha-beta T cell proliferation	4/76	72/28905	21.12938596	3.96E-05	0.00026365

GO:0045911	positive regulation of DNA recombination	4/76	72/28905	21.12938596	3.96E-05	0.00026365
GO:0007160	cell-matrix adhesion	6/76	238/28905	9.588124724	3.95E-05	0.00026365
GO:1904894	positive regulation of receptor signalling pathway via STAT	4/76	73/28905	20.83994232	4.19E-05	0.00027764
GO:0043369	CD4-positive or CD8-positive, alpha-beta T cell lineage commitment	3/76	26/28905	43.88410931	4.35E-05	0.00028765
GO:0034764	positive regulation of transmembrane transport	6/76	243/28905	9.390838207	4.44E-05	0.00029282
GO:0050767	regulation of neurogenesis	8/76	494/28905	6.159173237	4.69E-05	0.00030845
GO:0097396	response to interleukin-17	3/76	27/28905	42.25877193	4.88E-05	0.00031963
GO:0035743	CD4-positive, alpha-beta T cell cytokine production	3/76	27/28905	42.25877193	4.88E-05	0.00031963
GO:1904951	positive regulation of establishment of protein localization	7/76	364/28905	7.314018219	4.92E-05	0.00032107
GO:0034765	regulation of monoatomic ion transmembrane transport	7/76	366/28905	7.274050906	5.09E-05	0.00033148
GO:0050852	T cell receptor signalling pathway	5/76	152/28905	12.51082064	5.15E-05	0.00033445
GO:0045063	T-helper 1 cell differentiation	3/76	28/28905	40.74953008	5.46E-05	0.00035363
GO:0001959	regulation of cytokine-mediated signalling pathway	5/76	154/28905	12.34834245	5.48E-05	0.00035407
GO:2001234	negative regulation of apoptotic signalling pathway	6/76	253/28905	9.019658831	5.55E-05	0.00035779
GO:0048146	positive regulation of fibroblast proliferation	4/76	79/28905	19.25716189	5.71E-05	0.00036616
GO:0014009	glial cell proliferation	4/76	79/28905	19.25716189	5.71E-05	0.00036616
GO:0042306	regulation of protein import into nucleus	4/76	80/28905	19.01644737	6.00E-05	0.00038369
GO:0051769	regulation of nitric-oxide synthase biosynthetic process	3/76	29/28905	39.34437387	6.08E-05	0.00038671
GO:0051767	nitric-oxide synthase biosynthetic process	3/76	29/28905	39.34437387	6.08E-05	0.00038671

GO:0022612	gland morphogenesis	5/76	158/28905	12.03572618	6.19E-05	0.00039284
GO:0051279	regulation of release of sequestered calcium ion into cytosol	4/76	81/28905	18.78167641	6.30E-05	0.00039776
GO:0009988	cell-cell recognition	4/76	81/28905	18.78167641	6.30E-05	0.00039776
GO:0060252	positive regulation of glial cell proliferation	3/76	30/28905	38.03289474	6.74E-05	0.00042351
GO:0002837	regulation of immune response to tumor cell	3/76	30/28905	38.03289474	6.74E-05	0.00042351
GO:0033198	response to ATP	3/76	31/28905	36.80602716	7.45E-05	0.00046567
GO:0002834	regulation of response to tumor cell	3/76	31/28905	36.80602716	7.45E-05	0.00046567
GO:1904019	epithelial cell apoptotic process	5/76	166/28905	11.45569119	7.82E-05	0.00048766
GO:0032722	positive regulation of chemokine production	4/76	86/28905	17.68971848	7.96E-05	0.00049521
GO:0002698	negative regulation of immune effector process	5/76	167/28905	11.38709423	8.04E-05	0.00049921
GO:0001780	neutrophil homeostasis	3/76	32/28905	35.65583882	8.20E-05	0.00050782
GO:2001236	regulation of extrinsic apoptotic signaling pathway	5/76	169/28905	11.25233572	8.51E-05	0.00052546
GO:2000108	positive regulation of leukocyte apoptotic process	3/76	33/28905	34.57535885	9.00E-05	0.00055345
GO:0045662	negative regulation of myoblast differentiation	3/76	33/28905	34.57535885	9.00E-05	0.00055345
GO:0050728	negative regulation of inflammatory response	5/76	172/28905	11.05607405	9.24E-05	0.00056671
GO:0002726	positive regulation of T cell cytokine production	3/76	34/28905	33.55843653	9.86E-05	0.0006
GO:0002360	T cell lineage commitment	3/76	34/28905	33.55843653	9.86E-05	0.0006
GO:0002313	mature B cell differentiation involved in immune response	3/76	34/28905	33.55843653	9.86E-05	0.0006
GO:0050766	positive regulation of phagocytosis	4/76	91/28905	16.71775593	9.92E-05	0.0006022

GO:1903034	regulation of response to wounding	5/76	176/28905	10.80479964	0.00010298	0.00062382
GO:0036336	dendritic cell migration	3/76	35/28905	32.59962406	0.00010761	0.00064873
GO:0002719	negative regulation of cytokine production involved in immune	3/76	35/28905	32.59962406	0.00010761	0.00064873
GO:0060249	anatomical structure homeostasis	6/76	286/28905	7.978928966	0.00010893	0.00065358
GO:0001894	tissue homeostasis	6/76	286/28905	7.978928966	0.00010893	0.00065358
GO:0032729	positive regulation of type II interferon production	4/76	95/28905	16.01385042	0.00011719	0.00069815
GO:0050869	negative regulation of B cell activation	3/76	36/28905	31.69407895	0.00011717	0.00069815
GO:0010574	regulation of vascular endothelial growth factor production	3/76	36/28905	31.69407895	0.00011717	0.00069815
GO:0006606	protein import into nucleus	5/76	182/28905	10.44859746	0.00012052	0.00071627
GO:1904427	positive regulation of calcium ion transmembrane transport	4/76	96/28905	15.84703947	0.00012204	0.00072363
GO:0032386	regulation of intracellular transport	6/76	293/28905	7.788306089	0.00012429	0.00073519
GO:0090023	positive regulation of neutrophil chemotaxis	3/76	37/28905	30.83748222	0.00012726	0.00074752
GO:0045670	regulation of osteoclast differentiation	4/76	97/28905	15.68366793	0.00012704	0.00074752
GO:1903169	regulation of calcium ion transmembrane transport	5/76	184/28905	10.33502574	0.00012685	0.00074752
GO:1904018	positive regulation of vasculature development	5/76	185/28905	10.27916074	0.00013011	0.00076243
GO:1903531	negative regulation of secretion by cell	5/76	187/28905	10.16922319	0.00013681	0.00079802
GO:0051170	import into nucleus	5/76	187/28905	10.16922319	0.00013681	0.00079802
GO:0010506	regulation of autophagy	6/76	300/28905	7.606578947	0.00014131	0.00082236
GO:0120162	positive regulation of cold-induced thermogenesis	4/76	101/28905	15.06253257	0.00014852	0.00086032

GO:0007229	integrin-mediated signaling pathway	4/76	101/28905	15.06253257	0.00014852	0.00086032
GO:0071624	positive regulation of granulocyte chemotaxis	3/76	40/28905	28.52467105	0.00016091	0.0009278
GO:0010573	vascular endothelial growth factor production	3/76	40/28905	28.52467105	0.00016091	0.0009278
GO:0050851	antigen receptor-mediated signalling pathway	5/76	194/28905	9.802292458	0.0001624	0.00093427
GO:0051222	positive regulation of protein transport	6/76	309/28905	7.385028104	0.00016587	0.00094986
GO:0043087	regulation of GTPase activity	6/76	309/28905	7.385028104	0.00016587	0.00094986
GO:1900182	positive regulation of protein localization to nucleus	4/76	104/28905	14.62803644	0.00016627	0.00094999
GO:0001659	temperature homeostasis	5/76	196/28905	9.702269066	0.00017034	0.00097106
GO:0071634	regulation of transforming growth factor beta production	3/76	41/28905	27.82894737	0.00017328	0.0009856
GO:0062197	cellular response to chemical stress	6/76	313/28905	7.290650748	0.00017781	0.00100906
GO:0060485	mesenchyme development	6/76	314/28905	7.267432115	0.0001809	0.00102428
GO:0051281	positive regulation of release of sequestered calcium ion into cytosol	3/76	42/28905	27.16635338	0.00018626	0.00104991
GO:0032689	negative regulation of type II interferon production	3/76	42/28905	27.16635338	0.00018626	0.00104991
GO:0043254	regulation of protein-containing complex assembly	7/76	453/28905	5.877047752	0.00019098	0.00107412
GO:0042267	natural killer cell mediated cytotoxicity	4/76	108/28905	14.08625731	0.00019225	0.00107885
GO:0071604	transforming growth factor beta production	3/76	43/28905	26.53457772	0.00019985	0.00111157
GO:0043277	apoptotic cell clearance	3/76	43/28905	26.53457772	0.00019985	0.00111157
GO:0002335	mature B cell differentiation	3/76	43/28905	26.53457772	0.00019985	0.00111157
GO:0046032	ADP catabolic process	4/76	109/28905	13.95702559	0.00019918	0.00111157

GO:0051054	positive regulation of DNA metabolic process	6/76	321/28905	7.108952287	0.00020373	0.00113065
GO:0002228	natural killer cell mediated immunity	4/76	111/28905	13.70554765	0.00021358	0.00118266
GO:0043368	positive T cell selection	3/76	44/28905	25.93151914	0.00021407	0.0011828
GO:0035303	regulation of dephosphorylation	4/76	112/28905	13.58317669	0.00022105	0.001216
GO:0016525	negative regulation of angiogenesis	4/76	112/28905	13.58317669	0.00022105	0.001216
GO:0090022	regulation of neutrophil chemotaxis	3/76	45/28905	25.35526316	0.00022893	0.00124573
GO:0046031	ADP metabolic process	4/76	113/28905	13.46297159	0.00022871	0.00124573
GO:0043255	regulation of carbohydrate biosynthetic process	4/76	113/28905	13.46297159	0.00022871	0.00124573
GO:0009181	purine ribonucleoside diphosphate catabolic process	4/76	113/28905	13.46297159	0.00022871	0.00124573
GO:0009137	purine nucleoside diphosphate catabolic process	4/76	113/28905	13.46297159	0.00022871	0.00124573
GO:1901652	response to peptide	7/76	467/28905	5.700862166	0.00022986	0.00124807
GO:2000181	negative regulation of blood vessel morphogenesis	4/76	114/28905	13.34487535	0.00023655	0.00128166
GO:0051048	negative regulation of secretion	5/76	211/28905	9.012534298	0.00023977	0.00129628
GO:1901343	negative regulation of vasculature development	4/76	115/28905	13.22883295	0.00024459	0.00131671
GO:0048147	negative regulation of fibroblast proliferation	3/76	46/28905	24.80406178	0.00024444	0.00131671
GO:0032642	regulation of chemokine production	4/76	117/28905	13.00269906	0.00026126	0.00139447
GO:0009191	ribonucleoside diphosphate catabolic process	4/76	117/28905	13.00269906	0.00026126	0.00139447
GO:0048246	macrophage chemotaxis	3/76	47/28905	24.27631579	0.00026061	0.00139447
GO:0002701	negative regulation of production of molecular mediator of immune response	3/76	47/28905	24.27631579	0.00026061	0.00139447

GO:0034504	protein localization to nucleus	6/76	337/28905	6.771435265	0.0002645	0.00140878
GO:0048771	tissue remodeling	5/76	216/28905	8.803910819	0.00026712	0.00141974
GO:0070588	calcium ion transmembrane transport	6/76	338/28905	6.751401433	0.00026872	0.00142524
GO:0009179	purine ribonucleoside diphosphate metabolic process	4/76	118/28905	12.89250669	0.00026989	0.00142541
GO:0009135	purine nucleoside diphosphate metabolic process	4/76	118/28905	12.89250669	0.00026989	0.00142541
GO:0070542	response to fatty acid	3/76	48/28905	23.77055921	0.00027746	0.00145929
GO:0046636	negative regulation of alpha-beta T cell activation	3/76	48/28905	23.77055921	0.00027746	0.00145929
GO:0043280	positive regulation of cysteine-type endopeptidase activity	4/76	119/28905	12.7841663	0.00027872	0.00146285
GO:0050672	negative regulation of lymphocyte proliferation	4/76	120/28905	12.67763158	0.00028776	0.00150402
GO:0009134	nucleoside diphosphate catabolic process	4/76	120/28905	12.67763158	0.00028776	0.00150402
GO:0002709	regulation of T cell mediated immunity	4/76	121/28905	12.57285776	0.00029701	0.00154593
GO:0002262	myeloid cell homeostasis	5/76	221/28905	8.604727316	0.00029678	0.00154593
GO:0071447	cellular response to hydroperoxide	2/76	10/28905	76.06578947	0.00030285	0.00155063
GO:0071223	cellular response to lipoteichoic acid	2/76	10/28905	76.06578947	0.00030285	0.00155063
GO:0070391	response to lipoteichoic acid	2/76	10/28905	76.06578947	0.00030285	0.00155063
GO:0070092	regulation of glucagon secretion	2/76	10/28905	76.06578947	0.00030285	0.00155063
GO:0070091	glucagon secretion	2/76	10/28905	76.06578947	0.00030285	0.00155063
GO:0032667	regulation of interleukin-23 production	2/76	10/28905	76.06578947	0.00030285	0.00155063
GO:0032627	interleukin-23 production	2/76	10/28905	76.06578947	0.00030285	0.00155063

GO:0002604	regulation of dendritic cell antigen processing and	2/76	10/28905	76.06578947	0.00030285	0.00155063
GO:1901653	cellular response to peptide	6/76	346/28905	6.595299665	0.00030446	0.00155571
GO:0019722	calcium-mediated signaling	5/76	223/28905	8.527554874	0.00030932	0.00157737
GO:0070232	regulation of T cell apoptotic process	3/76	50/28905	22.81973684	0.00031324	0.00159409
GO:0032963	collagen metabolic process	4/76	124/28905	12.26867572	0.00032604	0.00165587
GO:0043547	positive regulation of GTPase activity	5/76	226/28905	8.414357243	0.00032888	0.00166361
GO:0015833	peptide transport	6/76	351/28905	6.501349528	0.00032862	0.00166361
GO:0031331	positive regulation of cellular catabolic process	6/76	352/28905	6.482879785	0.00033363	0.00168424
GO:0038061	non-canonical NF-kappaB signal transduction	4/76	125/28905	12.17052632	0.00033615	0.00169354
GO:0061138	morphogenesis of a branching epithelium	5/76	229/28905	8.304125488	0.00034937	0.00175662
GO:0032602	chemokine production	4/76	127/28905	11.97886448	0.00035704	0.00179162
GO:0045862	positive regulation of proteolysis	6/76	357/28905	6.392083149	0.00035958	0.00180077
GO:0046034	ATP metabolic process	5/76	232/28905	8.196744555	0.0003708	0.00181362
GO:0051169	nuclear transport	6/76	359/28905	6.356472658	0.00037039	0.00181362
GO:0006913	nucleocytoplasmic transport	6/76	359/28905	6.356472658	0.00037039	0.00181362
GO:1903242	regulation of cardiac muscle hypertrophy in response to	2/76	11/28905	69.1507177	0.00036952	0.00181362
GO:0071635	negative regulation of transforming growth factor beta	2/76	11/28905	69.1507177	0.00036952	0.00181362
GO:0071351	cellular response to interleukin-18	2/76	11/28905	69.1507177	0.00036952	0.00181362
GO:0060385	axonogenesis involved in innervation	2/76	11/28905	69.1507177	0.00036952	0.00181362

GO:0051712	positive regulation of killing of cells of another organism	2/76	11/28905	69.1507177	0.00036952	0.00181362
GO:0035744	T-helper 1 cell cytokine production	2/76	11/28905	69.1507177	0.00036952	0.00181362
GO:0032661	regulation of interleukin-18 production	2/76	11/28905	69.1507177	0.00036952	0.00181362
GO:0002676	regulation of chronic inflammatory response	2/76	11/28905	69.1507177	0.00036952	0.00181362
GO:0002317	plasma cell differentiation	2/76	11/28905	69.1507177	0.00036952	0.00181362
GO:0002920	regulation of humoral immune response	3/76	53/28905	21.52805362	0.00037227	0.00181373
GO:0002507	tolerance induction	3/76	53/28905	21.52805362	0.00037227	0.00181373
GO:0051098	regulation of binding	6/76	361/28905	6.321256743	0.00038146	0.00185491
GO:0009185	ribonucleoside diphosphate metabolic process	4/76	130/28905	11.70242915	0.0003901	0.00189328
GO:0098586	cellular response to virus	3/76	54/28905	21.12938596	0.00039343	0.00189841
GO:0042307	positive regulation of protein import into nucleus	3/76	54/28905	21.12938596	0.00039343	0.00189841
GO:0010823	negative regulation of mitochondrion organization	3/76	54/28905	21.12938596	0.00039343	0.00189841
GO:0061041	regulation of wound healing	4/76	131/28905	11.61309763	0.00040159	0.00193411
GO:0051235	maintenance of location	6/76	366/28905	6.234900777	0.00041026	0.00197205
GO:0035306	positive regulation of dephosphorylation	3/76	55/28905	20.74521531	0.00041534	0.00199267
GO:0034599	cellular response to oxidative stress	5/76	238/28905	7.990103936	0.00041665	0.00199513
GO:0031589	cell-substrate adhesion	6/76	369/28905	6.184210526	0.00042833	0.0020472
GO:2000551	regulation of T-helper 2 cell cytokine production	2/76	12/28905	63.38815789	0.00044267	0.00206467
GO:1904417	positive regulation of xenophagy	2/76	12/28905	63.38815789	0.00044267	0.00206467

GO:1904415	regulation of xenophagy	2/76	12/28905	63.38815789	0.00044267	0.00206467
GO:0051709	regulation of killing of cells of another organism	2/76	12/28905	63.38815789	0.00044267	0.00206467
GO:0045348	positive regulation of MHC class II biosynthetic process	2/76	12/28905	63.38815789	0.00044267	0.00206467
GO:0032650	regulation of interleukin-1 alpha production	2/76	12/28905	63.38815789	0.00044267	0.00206467
GO:0010612	regulation of cardiac muscle adaptation	2/76	12/28905	63.38815789	0.00044267	0.00206467
GO:0002579	positive regulation of antigen processing and presentation	2/76	12/28905	63.38815789	0.00044267	0.00206467
GO:0002420	natural killer cell mediated cytotoxicity directed against tumour	2/76	12/28905	63.38815789	0.00044267	0.00206467
GO:0001781	neutrophil apoptotic process	2/76	12/28905	63.38815789	0.00044267	0.00206467
GO:0000727	double-strand break repair via break-induced replication	2/76	12/28905	63.38815789	0.00044267	0.00206467
GO:0042531	positive regulation of tyrosine phosphorylation of STAT protein	3/76	56/28905	20.37476504	0.00043802	0.00206467
GO:0046425	regulation of receptor signalling pathway via JAK-STAT	4/76	134/28905	11.35310291	0.00043752	0.00206467
GO:0019882	antigen processing and presentation	4/76	135/28905	11.26900585	0.00044998	0.00209105
GO:0001910	regulation of leukocyte mediated cytotoxicity	4/76	135/28905	11.26900585	0.00044998	0.00209105
GO:0034113	heterotypic cell-cell adhesion	3/76	57/28905	20.01731302	0.00046149	0.00214054
GO:0009132	nucleoside diphosphate metabolic process	4/76	136/28905	11.18614551	0.0004627	0.00214223
GO:1902895	positive regulation of miRNA transcription	3/76	58/28905	19.67218693	0.00048574	0.00222432
GO:0033121	regulation of purine nucleotide catabolic process	3/76	58/28905	19.67218693	0.00048574	0.00222432
GO:0032757	positive regulation of interleukin-8 production	3/76	58/28905	19.67218693	0.00048574	0.00222432
GO:0030811	regulation of nucleotide catabolic process	3/76	58/28905	19.67218693	0.00048574	0.00222432

GO:0006110	regulation of glycolytic process	3/76	58/28905	19.67218693	0.00048574	0.00222432
GO:1903828	negative regulation of protein localization	5/76	246/28905	7.730263158	0.00048428	0.00222432
GO:0051651	maintenance of location in cell	5/76	247/28905	7.698966546	0.00049328	0.00225473
GO:0001763	morphogenesis of a branching structure	5/76	249/28905	7.637127457	0.00051166	0.00233027
GO:0001961	positive regulation of cytokine-mediated signaling pathway	3/76	59/28905	19.33876004	0.0005108	0.00233027
GO:2000510	positive regulation of dendritic cell chemotaxis	2/76	13/28905	58.51214575	0.00052226	0.00233622
GO:1902170	cellular response to reactive nitrogen species	2/76	13/28905	58.51214575	0.00052226	0.00233622
GO:0071863	regulation of cell proliferation in bone marrow	2/76	13/28905	58.51214575	0.00052226	0.00233622
GO:0045625	regulation of T-helper 1 cell differentiation	2/76	13/28905	58.51214575	0.00052226	0.00233622
GO:0032621	interleukin-18 production	2/76	13/28905	58.51214575	0.00052226	0.00233622
GO:0032610	interleukin-1 alpha production	2/76	13/28905	58.51214575	0.00052226	0.00233622
GO:0014745	negative regulation of muscle adaptation	2/76	13/28905	58.51214575	0.00052226	0.00233622
GO:0002756	MyD88-independent toll-like receptor signaling pathway	2/76	13/28905	58.51214575	0.00052226	0.00233622
GO:0002423	natural killer cell mediated immune response to tumor cell	2/76	13/28905	58.51214575	0.00052226	0.00233622
GO:0051224	negative regulation of protein transport	4/76	140/28905	10.86654135	0.00051615	0.00233622
GO:0045599	negative regulation of fat cell differentiation	3/76	60/28905	19.01644737	0.00053667	0.00238794
GO:0043030	regulation of macrophage activation	3/76	60/28905	19.01644737	0.00053667	0.00238794
GO:0006826	iron ion transport	3/76	60/28905	19.01644737	0.00053667	0.00238794
GO:0042886	amide transport	6/76	386/28905	5.911848923	0.00054286	0.00241121

GO:2001056	positive regulation of cysteine-type endopeptidase activity	4/76	144/28905	10.56469298	0.00057385	0.00254439
GO:0033619	membrane protein proteolysis	3/76	62/28905	18.40301358	0.0005909	0.00260616
GO:0030225	macrophage differentiation	3/76	62/28905	18.40301358	0.0005909	0.00260616
GO:0009205	purine ribonucleoside triphosphate metabolic process	5/76	257/28905	7.399395863	0.00059039	0.00260616
GO:0072683	T cell extravasation	2/76	14/28905	54.33270677	0.00060826	0.00265943
GO:0070673	response to interleukin-18	2/76	14/28905	54.33270677	0.00060826	0.00265943
GO:0045628	regulation of T-helper 2 cell differentiation	2/76	14/28905	54.33270677	0.00060826	0.00265943
GO:0002468	dendritic cell antigen processing and presentation	2/76	14/28905	54.33270677	0.00060826	0.00265943
GO:0009154	purine ribonucleotide catabolic process	4/76	146/28905	10.41997116	0.00060436	0.00265943
GO:0010821	regulation of mitochondrion organization	4/76	147/28905	10.349087	0.00062004	0.0027062
GO:0090303	positive regulation of wound healing	3/76	64/28905	17.82791941	0.0006485	0.00282555
GO:0009199	ribonucleoside triphosphate metabolic process	5/76	264/28905	7.203199761	0.00066645	0.0028987
GO:2000630	positive regulation of miRNA metabolic process	3/76	65/28905	17.55364372	0.0006786	0.00293633
GO:0002861	regulation of inflammatory response to antigenic stimulus	3/76	65/28905	17.55364372	0.0006786	0.00293633
GO:0090276	regulation of peptide hormone secretion	5/76	265/28905	7.176017875	0.00067789	0.00293633
GO:0120161	regulation of cold-induced thermogenesis	4/76	151/28905	10.074939	0.00068564	0.00296169
GO:0009144	purine nucleoside triphosphate metabolic process	5/76	266/28905	7.149040364	0.00068947	0.00297312
GO:2000508	regulation of dendritic cell chemotaxis	2/76	15/28905	50.71052632	0.00070065	0.00299054
GO:0072540	T-helper 17 cell lineage commitment	2/76	15/28905	50.71052632	0.00070065	0.00299054

GO:0071838	cell proliferation in bone marrow	2/76	15/28905	50.71052632	0.00070065	0.00299054
GO:0046643	regulation of gamma-delta T cell activation	2/76	15/28905	50.71052632	0.00070065	0.00299054
GO:0045586	regulation of gamma-delta T cell differentiation	2/76	15/28905	50.71052632	0.00070065	0.00299054
GO:0045188	regulation of circadian sleep/wake cycle, non-REM sleep	2/76	15/28905	50.71052632	0.00070065	0.00299054
GO:1901136	carbohydrate derivative catabolic process	5/76	268/28905	7.095689317	0.00071308	0.00303845
GO:0001936	regulation of endothelial cell proliferation	4/76	153/28905	9.943240454	0.00072022	0.00306368
GO:0002791	regulation of peptide secretion	5/76	270/28905	7.043128655	0.0007373	0.00313101
GO:0106106	cold-induced thermogenesis	4/76	155/28905	9.814940577	0.00075602	0.00319971
GO:0009261	ribonucleotide catabolic process	4/76	155/28905	9.814940577	0.00075602	0.00319971
GO:0090087	regulation of peptide transport	5/76	272/28905	6.991340944	0.00076212	0.00322011
GO:1904950	negative regulation of establishment of protein localization	4/76	156/28905	9.752024291	0.00077438	0.00326096
GO:0046427	positive regulation of receptor signaling pathway via JAK-STAT	3/76	68/28905	16.77921827	0.0007742	0.00326096
GO:1903798	regulation of miRNA processing	2/76	16/28905	47.54111842	0.00079938	0.00332171
GO:1902969	mitotic DNA replication	2/76	16/28905	47.54111842	0.00079938	0.00332171
GO:1901722	regulation of cell proliferation involved in kidney development	2/76	16/28905	47.54111842	0.00079938	0.00332171
GO:0046642	negative regulation of alpha-beta T cell proliferation	2/76	16/28905	47.54111842	0.00079938	0.00332171
GO:0045346	regulation of MHC class II biosynthetic process	2/76	16/28905	47.54111842	0.00079938	0.00332171
GO:0042748	circadian sleep/wake cycle, non-REM sleep	2/76	16/28905	47.54111842	0.00079938	0.00332171
GO:0014004	microglia differentiation	2/76	16/28905	47.54111842	0.00079938	0.00332171

GO:0002467	germinal center formation	2/76	16/28905	47.54111842	0.00079938	0.00332171
GO:0070231	T cell apoptotic process	3/76	69/28905	16.53604119	0.00080787	0.00335147
GO:0006195	purine nucleotide catabolic process	4/76	158/28905	9.628580946	0.00081205	0.00336324
GO:0010508	positive regulation of autophagy	4/76	160/28905	9.508223684	0.00085099	0.00351873
GO:0043467	regulation of generation of precursor metabolites and energy	4/76	161/28905	9.449166394	0.00087095	0.00359534
GO:0045806	negative regulation of endocytosis	3/76	71/28905	16.07023721	0.00087797	0.00360656
GO:0042509	regulation of tyrosine phosphorylation of STAT protein	3/76	71/28905	16.07023721	0.00087797	0.00360656
GO:0008347	glial cell migration	3/76	71/28905	16.07023721	0.00087797	0.00360656
GO:0009141	nucleoside triphosphate metabolic process	5/76	281/28905	6.767418992	0.00088163	0.00361571
GO:0098792	xenophagy	2/76	17/28905	44.74458204	0.00090442	0.00367319
GO:0070920	regulation of regulatory ncRNA processing	2/76	17/28905	44.74458204	0.00090442	0.00367319
GO:0045342	MHC class II biosynthetic process	2/76	17/28905	44.74458204	0.00090442	0.00367319
GO:0031053	primary miRNA processing	2/76	17/28905	44.74458204	0.00090442	0.00367319
GO:0007252	I-kappaB phosphorylation	2/76	17/28905	44.74458204	0.00090442	0.00367319
GO:0007096	regulation of exit from mitosis	2/76	17/28905	44.74458204	0.00090442	0.00367319
GO:0010634	positive regulation of epithelial cell migration	4/76	163/28905	9.333225702	0.00091185	0.00369741
GO:0043470	regulation of carbohydrate catabolic process	3/76	72/28905	15.84703947	0.00091442	0.00370185
GO:0072523	purine-containing compound catabolic process	4/76	164/28905	9.276315789	0.0009328	0.00376415
GO:0010950	positive regulation of endopeptidase activity	4/76	164/28905	9.276315789	0.0009328	0.00376415

GO:0051347	positive regulation of transferase activity	6/76	431/28905	5.294602516	0.00096267	0.00387845
GO:0140895	cell surface toll-like receptor signaling pathway	3/76	74/28905	15.41874111	0.00099017	0.00398284
GO:0035745	T-helper 2 cell cytokine production	2/76	18/28905	42.25877193	0.00101574	0.00406619
GO:0032966	negative regulation of collagen biosynthetic process	2/76	18/28905	42.25877193	0.00101574	0.00406619
GO:0002830	positive regulation of type 2 immune response	2/76	18/28905	42.25877193	0.00101574	0.00406619
GO:0032677	regulation of interleukin-8 production	3/76	75/28905	15.21315789	0.00102948	0.00410161
GO:0007260	tyrosine phosphorylation of STAT protein	3/76	75/28905	15.21315789	0.00102948	0.00410161
GO:0006879	intracellular iron ion homeostasis	3/76	75/28905	15.21315789	0.00102948	0.00410161
GO:2000377	regulation of reactive oxygen species metabolic process	4/76	169/28905	9.001868577	0.00104267	0.00414758
GO:0046824	positive regulation of nucleocytoplasmic transport	3/76	76/28905	15.01298476	0.00106977	0.00424197
GO:0032637	interleukin-8 production	3/76	76/28905	15.01298476	0.00106977	0.00424197
GO:1904036	negative regulation of epithelial cell apoptotic process	3/76	77/28905	14.81801094	0.00111105	0.00439179
GO:0002752	cell surface pattern recognition receptor signaling pathway	3/76	77/28905	14.81801094	0.00111105	0.00439179
GO:1904406	negative regulation of nitric oxide metabolic process	2/76	19/28905	40.03462604	0.0011333	0.00444482
GO:0045019	negative regulation of nitric oxide biosynthetic process	2/76	19/28905	40.03462604	0.0011333	0.00444482
GO:0042492	gamma-delta T cell differentiation	2/76	19/28905	40.03462604	0.0011333	0.00444482
GO:0033194	response to hydroperoxide	2/76	19/28905	40.03462604	0.0011333	0.00444482
GO:0010713	negative regulation of collagen metabolic process	2/76	19/28905	40.03462604	0.0011333	0.00444482
GO:1902893	regulation of miRNA transcription	3/76	78/28905	14.62803644	0.00115332	0.00451627

GO:1990845	adaptive thermogenesis	4/76	174/28905	8.743194192	0.00116133	0.00454057
GO:0001935	endothelial cell proliferation	4/76	175/28905	8.693233083	0.00118615	0.00463041
GO:0035304	regulation of protein dephosphorylation	3/76	79/28905	14.44287142	0.00119659	0.00466392
GO:0009166	nucleotide catabolic process	4/76	176/28905	8.643839713	0.00121134	0.0047141
GO:0033157	regulation of intracellular protein transport	4/76	177/28905	8.59500446	0.0012369	0.00479873
GO:0007596	blood coagulation	4/76	177/28905	8.59500446	0.0012369	0.00479873
GO:0061614	miRNA transcription	3/76	80/28905	14.26233553	0.00124088	0.00480672
GO:2000679	positive regulation of transcription regulatory region DNA binding	2/76	20/28905	38.03289474	0.00125709	0.0048249
GO:0035821	modulation of process of another organism	2/76	20/28905	38.03289474	0.00125709	0.0048249
GO:0030889	negative regulation of B cell proliferation	2/76	20/28905	38.03289474	0.00125709	0.0048249
GO:0006268	DNA unwinding involved in DNA replication	2/76	20/28905	38.03289474	0.00125709	0.0048249
GO:0002923	regulation of humoral immune response mediated by circulating	2/76	20/28905	38.03289474	0.00125709	0.0048249
GO:0002643	regulation of tolerance induction	2/76	20/28905	38.03289474	0.00125709	0.0048249
GO:1903036	positive regulation of response to wounding	3/76	81/28905	14.08625731	0.00128618	0.00492154
GO:0045453	bone resorption	3/76	81/28905	14.08625731	0.00128618	0.00492154
GO:0002753	cytosolic pattern recognition receptor signalling pathway	4/76	179/28905	8.498970891	0.00128916	0.00492545
GO:0050817	coagulation	4/76	180/28905	8.451754386	0.00131586	0.00501983
GO:1903578	regulation of ATP metabolic process	3/76	82/28905	13.91447368	0.00133251	0.00507566
GO:0007599	hemostasis	4/76	181/28905	8.40505961	0.00134294	0.00510764

GO:0045766	positive regulation of angiogenesis	4/76	182/28905	8.358877964	0.00137041	0.00520425
GO:0045064	T-helper 2 cell differentiation	2/76	21/28905	36.22180451	0.00138705	0.00522794
GO:0042953	lipoprotein transport	2/76	21/28905	36.22180451	0.00138705	0.00522794
GO:0002839	positive regulation of immune response to tumor cell	2/76	21/28905	36.22180451	0.00138705	0.00522794
GO:0002836	positive regulation of response to tumor cell	2/76	21/28905	36.22180451	0.00138705	0.00522794
GO:0002577	regulation of antigen processing and presentation	2/76	21/28905	36.22180451	0.00138705	0.00522794
GO:1901292	nucleoside phosphate catabolic process	4/76	184/28905	8.268020595	0.00142652	0.00536869
GO:0140888	interferon-mediated signaling pathway	3/76	85/28905	13.42337461	0.00147778	0.00554496
GO:0032091	negative regulation of protein binding	3/76	85/28905	13.42337461	0.00147778	0.00554496
GO:0001667	ameboidal-type cell migration	6/76	470/28905	4.855263158	0.00149813	0.00561297
GO:0043281	regulation of cysteine-type endopeptidase activity involved in	4/76	187/28905	8.135378553	0.00151368	0.00566277
GO:0072111	cell proliferation involved in kidney development	2/76	22/28905	34.57535885	0.00152316	0.00567291
GO:0071731	response to nitric oxide	2/76	22/28905	34.57535885	0.00152316	0.00567291
GO:0044872	lipoprotein localization	2/76	22/28905	34.57535885	0.00152316	0.00567291
GO:0045661	regulation of myoblast differentiation	3/76	86/28905	13.26728886	0.00152831	0.0056753
GO:0032481	positive regulation of type I interferon production	3/76	86/28905	13.26728886	0.00152831	0.0056753
GO:0010952	positive regulation of peptidase activity	4/76	188/28905	8.092105263	0.00154353	0.00572336
GO:0042269	regulation of natural killer cell mediated cytotoxicity	3/76	87/28905	13.11479129	0.00157992	0.00584967
GO:0030072	peptide hormone secretion	5/76	322/28905	5.905728996	0.00161027	0.00595326

GO:0060333	type II interferon-mediated signaling pathway	2/76	23/28905	33.07208238	0.00166538	0.00612101
GO:0046629	gamma-delta T cell activation	2/76	23/28905	33.07208238	0.00166538	0.00612101
GO:0002693	positive regulation of cellular extravasation	2/76	23/28905	33.07208238	0.00166538	0.00612101
GO:0002544	chronic inflammatory response	2/76	23/28905	33.07208238	0.00166538	0.00612101
GO:0002220	innate immune response activating cell surface receptor signaling	3/76	89/28905	12.82007688	0.00168639	0.00618917
GO:0010721	negative regulation of cell development	5/76	326/28905	5.833266064	0.00169962	0.00622865
GO:0030198	extracellular matrix organization	5/76	327/28905	5.81542733	0.00172252	0.00630337
GO:0002715	regulation of natural killer cell mediated immunity	3/76	90/28905	12.67763158	0.00174127	0.00636271
GO:0045229	external encapsulating structure organization	5/76	328/28905	5.797697368	0.00174564	0.00636944
GO:0043062	extracellular structure organization	5/76	329/28905	5.780075188	0.00176899	0.00644529
GO:0002790	peptide secretion	5/76	330/28905	5.762559809	0.00179257	0.00652175
GO:1901317	regulation of flagellated sperm motility	2/76	24/28905	31.69407895	0.00181369	0.00655118
GO:0045838	positive regulation of membrane potential	2/76	24/28905	31.69407895	0.00181369	0.00655118
GO:0034755	iron ion transmembrane transport	2/76	24/28905	31.69407895	0.00181369	0.00655118
GO:0001768	establishment of T cell polarity	2/76	24/28905	31.69407895	0.00181369	0.00655118
GO:0001767	establishment of lymphocyte polarity	2/76	24/28905	31.69407895	0.00181369	0.00655118
GO:0002711	positive regulation of T cell mediated immunity	3/76	92/28905	12.40203089	0.00185434	0.00668839
GO:0045732	positive regulation of protein catabolic process	4/76	199/28905	7.644802962	0.00189954	0.0068416
GO:0050709	negative regulation of protein secretion	3/76	93/28905	12.26867572	0.00191255	0.00687863

GO:0042391	regulation of membrane potential	6/76	495/28905	4.610047847	0.00194507	0.00698558
GO:0033209	tumor necrosis factor-mediated signaling pathway	3/76	94/28905	12.13815789	0.0019719	0.00702174
GO:0045807	positive regulation of endocytosis	4/76	201/28905	7.568735271	0.00196988	0.00702174
GO:2000353	positive regulation of endothelial cell apoptotic process	2/76	25/28905	30.42631579	0.00196805	0.00702174
GO:0071800	podosome assembly	2/76	25/28905	30.42631579	0.00196805	0.00702174
GO:0050765	negative regulation of phagocytosis	2/76	25/28905	30.42631579	0.00196805	0.00702174
GO:0010759	positive regulation of macrophage chemotaxis	2/76	25/28905	30.42631579	0.00196805	0.00702174
GO:0046883	regulation of hormone secretion	5/76	339/28905	5.609571495	0.00201529	0.00716612
GO:2000628	regulation of miRNA metabolic process	3/76	95/28905	12.01038781	0.00203238	0.00720648
GO:0002260	lymphocyte homeostasis	3/76	95/28905	12.01038781	0.00203238	0.00720648
GO:0045913	positive regulation of carbohydrate metabolic process	3/76	96/28905	11.88527961	0.002094	0.0074041
GO:0043299	leukocyte degranulation	3/76	96/28905	11.88527961	0.002094	0.0074041
GO:2000561	regulation of CD4-positive, alpha-beta T cell proliferation	2/76	26/28905	29.25607287	0.00212843	0.00748375
GO:0070168	negative regulation of biomineral tissue development	2/76	26/28905	29.25607287	0.00212843	0.00748375
GO:0051043	regulation of membrane protein ectodomain proteolysis	2/76	26/28905	29.25607287	0.00212843	0.00748375
GO:0016045	detection of bacterium	2/76	26/28905	29.25607287	0.00212843	0.00748375
GO:0051384	response to glucocorticoid	3/76	97/28905	11.76275095	0.00215678	0.00757281
GO:0046683	response to organophosphorus	3/76	98/28905	11.64272288	0.00222071	0.00778642
GO:1901857	positive regulation of cellular respiration	2/76	27/28905	28.17251462	0.0022948	0.00794646

GO:0051969	regulation of transmission of nerve impulse	2/76	27/28905	28.17251462	0.0022948	0.00794646
GO:0046716	muscle cell cellular homeostasis	2/76	27/28905	28.17251462	0.0022948	0.00794646
GO:0045821	positive regulation of glycolytic process	2/76	27/28905	28.17251462	0.0022948	0.00794646
GO:0035739	CD4-positive, alpha-beta T cell proliferation	2/76	27/28905	28.17251462	0.0022948	0.00794646
GO:0033123	positive regulation of purine nucleotide catabolic process	2/76	27/28905	28.17251462	0.0022948	0.00794646
GO:0032740	positive regulation of interleukin-17 production	2/76	27/28905	28.17251462	0.0022948	0.00794646
GO:0030813	positive regulation of nucleotide catabolic process	2/76	27/28905	28.17251462	0.0022948	0.00794646
GO:0002523	leukocyte migration involved in inflammatory response	2/76	27/28905	28.17251462	0.0022948	0.00794646
GO:0140747	regulation of ncRNA transcription	3/76	100/28905	11.40986842	0.00235209	0.00808912
GO:0046888	negative regulation of hormone secretion	3/76	100/28905	11.40986842	0.00235209	0.00808912
GO:0034446	substrate adhesion-dependent cell spreading	3/76	100/28905	11.40986842	0.00235209	0.00808912
GO:0002704	negative regulation of leukocyte mediated immunity	3/76	100/28905	11.40986842	0.00235209	0.00808912
GO:0001912	positive regulation of leukocyte mediated cytotoxicity	3/76	100/28905	11.40986842	0.00235209	0.00808912
GO:0051146	striated muscle cell differentiation	5/76	353/28905	5.387095572	0.00240111	0.00824644
GO:1900542	regulation of purine nucleotide metabolic process	3/76	101/28905	11.29689943	0.00241954	0.0082984
GO:2000273	positive regulation of signalling receptor activity	2/76	28/28905	27.16635338	0.00246713	0.00839291
GO:0060713	labyrinthine layer morphogenesis	2/76	28/28905	27.16635338	0.00246713	0.00839291
GO:0060445	branching involved in salivary gland morphogenesis	2/76	28/28905	27.16635338	0.00246713	0.00839291
GO:0035308	negative regulation of protein dephosphorylation	2/76	28/28905	27.16635338	0.00246713	0.00839291

GO:0006925	inflammatory cell apoptotic process	2/76	28/28905	27.16635338	0.00246713	0.00839291
GO:0002407	dendritic cell chemotaxis	2/76	28/28905	27.16635338	0.00246713	0.00839291
GO:2001237	negative regulation of extrinsic apoptotic signalling pathway	3/76	102/28905	11.18614551	0.00248819	0.0084417
GO:0006140	regulation of nucleotide metabolic process	3/76	102/28905	11.18614551	0.00248819	0.0084417
GO:0016051	carbohydrate biosynthetic process	4/76	215/28905	7.075887393	0.0025135	0.00851608
GO:0000041	transition metal ion transport	3/76	103/28905	11.07754216	0.00255803	0.00865529
GO:0098543	detection of other organism	2/76	29/28905	26.22958258	0.00264538	0.0088555
GO:0061440	kidney vasculature development	2/76	29/28905	26.22958258	0.00264538	0.0088555
GO:0061437	renal system vasculature development	2/76	29/28905	26.22958258	0.00264538	0.0088555
GO:0060964	regulation of miRNA-mediated gene silencing	2/76	29/28905	26.22958258	0.00264538	0.0088555
GO:0048634	regulation of muscle organ development	2/76	29/28905	26.22958258	0.00264538	0.0088555
GO:0045187	regulation of circadian sleep/wake cycle, sleep	2/76	29/28905	26.22958258	0.00264538	0.0088555
GO:0031100	animal organ regeneration	2/76	29/28905	26.22958258	0.00264538	0.0088555
GO:0001938	positive regulation of endothelial cell proliferation	3/76	104/28905	10.97102733	0.00262907	0.0088555
GO:0042130	negative regulation of T cell proliferation	3/76	105/28905	10.86654135	0.00270132	0.00901875
GO:0006096	glycolytic process	3/76	105/28905	10.86654135	0.00270132	0.00901875
GO:0042176	regulation of protein catabolic process	5/76	363/28905	5.238690735	0.00270784	0.00902852
GO:2000116	regulation of cysteine-type endopeptidase activity	4/76	220/28905	6.91507177	0.00273034	0.00909149
GO:0002437	inflammatory response to antigenic stimulus	3/76	106/28905	10.76402681	0.00277479	0.00922727

GO:1900368	regulation of post-transcriptional gene silencing by regulatory RNA	2/76	30/28905	25.35526316	0.00282952	0.00937208
GO:0061298	retina vasculature development in camera-type eye	2/76	30/28905	25.35526316	0.00282952	0.00937208
GO:0006929	substrate-dependent cell migration	2/76	30/28905	25.35526316	0.00282952	0.00937208
GO:0046849	bone remodelling	3/76	108/28905	10.56469298	0.0029254	0.00967692
GO:1905523	positive regulation of macrophage migration	2/76	31/28905	24.53735144	0.00301952	0.00992298
GO:0090594	inflammatory response to wounding	2/76	31/28905	24.53735144	0.00301952	0.00992298
GO:0060147	regulation of post-transcriptional gene silencing	2/76	31/28905	24.53735144	0.00301952	0.00992298
GO:0050802	circadian sleep/wake cycle, sleep	2/76	31/28905	24.53735144	0.00301952	0.00992298
GO:0010458	exit from mitosis	2/76	31/28905	24.53735144	0.00301952	0.00992298
GO:0010586	miRNA metabolic process	3/76	110/28905	10.37260766	0.00308096	0.01011166
GO:0090316	positive regulation of intracellular protein transport	3/76	111/28905	10.27916074	0.00316061	0.0103326
GO:0031960	response to corticosteroid	3/76	111/28905	10.27916074	0.00316061	0.0103326
GO:0007006	mitochondrial membrane organization	3/76	111/28905	10.27916074	0.00316061	0.0103326
GO:1903055	positive regulation of extracellular matrix organization	2/76	32/28905	23.77055921	0.00321536	0.01041676
GO:0060966	regulation of gene silencing by regulatory ncRNA	2/76	32/28905	23.77055921	0.00321536	0.01041676
GO:0060384	innervation	2/76	32/28905	23.77055921	0.00321536	0.01041676
GO:0043032	positive regulation of macrophage activation	2/76	32/28905	23.77055921	0.00321536	0.01041676
GO:0042749	regulation of circadian sleep/wake cycle	2/76	32/28905	23.77055921	0.00321536	0.01041676
GO:0031295	T cell costimulation	2/76	32/28905	23.77055921	0.00321536	0.01041676

GO:0010810	regulation of cell-substrate adhesion	4/76	230/28905	6.614416476	0.0032019	0.01041676
GO:0019364	pyridine nucleotide catabolic process	3/76	113/28905	10.09722869	0.00332368	0.01075384
GO:2000352	negative regulation of endothelial cell apoptotic process	2/76	33/28905	23.05023923	0.00341699	0.01091527
GO:1902019	regulation of cilium-dependent cell motility	2/76	33/28905	23.05023923	0.00341699	0.01091527
GO:0072575	epithelial cell proliferation involved in liver morphogenesis	2/76	33/28905	23.05023923	0.00341699	0.01091527
GO:0072574	hepatocyte proliferation	2/76	33/28905	23.05023923	0.00341699	0.01091527
GO:0060669	embryonic placenta morphogenesis	2/76	33/28905	23.05023923	0.00341699	0.01091527
GO:0060295	regulation of cilium movement involved in cell motility	2/76	33/28905	23.05023923	0.00341699	0.01091527
GO:0014898	cardiac muscle hypertrophy in response to stress	2/76	33/28905	23.05023923	0.00341699	0.01091527
GO:0006270	DNA replication initiation	2/76	33/28905	23.05023923	0.00341699	0.01091527
GO:0003299	muscle hypertrophy in response to stress	2/76	33/28905	23.05023923	0.00341699	0.01091527
GO:0031507	heterochromatin formation	3/76	114/28905	10.00865651	0.00340712	0.01091527
GO:0045666	positive regulation of neuron differentiation	3/76	116/28905	9.836093466	0.00357782	0.01138561
GO:0033138	positive regulation of peptidyl-serine phosphorylation	3/76	116/28905	9.836093466	0.00357782	0.01138561
GO:0014074	response to purine-containing compound	3/76	116/28905	9.836093466	0.00357782	0.01138561
GO:0006979	response to oxidative stress	5/76	388/28905	4.901146229	0.00359802	0.01143544
GO:0031294	lymphocyte costimulation	2/76	34/28905	22.37229102	0.00362439	0.01146128
GO:0022410	circadian sleep/wake cycle process	2/76	34/28905	22.37229102	0.00362439	0.01146128
GO:0014887	cardiac muscle adaptation	2/76	34/28905	22.37229102	0.00362439	0.01146128

GO:0010758	regulation of macrophage chemotaxis	2/76	34/28905	22.37229102	0.00362439	0.01146128
GO:0062012	regulation of small molecule metabolic process	5/76	389/28905	4.888546881	0.00363751	0.01148832
GO:0072526	pyridine-containing compound catabolic process	3/76	117/28905	9.752024291	0.0036651	0.01156092
GO:0010639	negative regulation of organelle organization	5/76	390/28905	4.876012146	0.00367731	0.01158491
GO:0008637	apoptotic mitochondrial changes	3/76	119/28905	9.588124724	0.00384354	0.01203319
GO:0002275	myeloid cell activation involved in immune response	3/76	119/28905	9.588124724	0.00384354	0.01203319
GO:0072539	T-helper 17 cell differentiation	2/76	35/28905	21.73308271	0.00383753	0.01203319
GO:0071404	cellular response to low-density lipoprotein particle stimulus	2/76	35/28905	21.73308271	0.00383753	0.01203319
GO:0002902	regulation of B cell apoptotic process	2/76	35/28905	21.73308271	0.00383753	0.01203319
GO:0060562	epithelial tube morphogenesis	5/76	395/28905	4.814290473	0.00388102	0.01213542
GO:0051101	regulation of DNA binding	3/76	120/28905	9.508223684	0.00393471	0.01228802
GO:1901889	negative regulation of cell junction assembly	2/76	36/28905	21.12938596	0.00405638	0.01260535
GO:0090183	regulation of kidney development	2/76	36/28905	21.12938596	0.00405638	0.01260535
GO:0072576	liver morphogenesis	2/76	36/28905	21.12938596	0.00405638	0.01260535
GO:0055094	response to lipoprotein particle	2/76	36/28905	21.12938596	0.00405638	0.01260535
GO:0046434	organophosphate catabolic process	4/76	246/28905	6.184210526	0.00406736	0.01262387
GO:0033044	regulation of chromosome organization	4/76	247/28905	6.159173237	0.00412619	0.01279068
GO:2000515	negative regulation of CD4-positive, alpha-beta T cell	2/76	37/28905	20.55832148	0.0042809	0.0131246
GO:0097242	amyloid-beta clearance	2/76	37/28905	20.55832148	0.0042809	0.0131246

GO:0090322	regulation of superoxide metabolic process	2/76	37/28905	20.55832148	0.0042809	0.0131246
GO:0070306	lens fiber cell differentiation	2/76	37/28905	20.55832148	0.0042809	0.0131246
GO:0033260	nuclear DNA replication	2/76	37/28905	20.55832148	0.0042809	0.0131246
GO:0032967	positive regulation of collagen biosynthetic process	2/76	37/28905	20.55832148	0.0042809	0.0131246
GO:0030431	sleep	2/76	37/28905	20.55832148	0.0042809	0.0131246
GO:0010614	negative regulation of cardiac muscle hypertrophy	2/76	37/28905	20.55832148	0.0042809	0.0131246
GO:0007435	salivary gland morphogenesis	2/76	37/28905	20.55832148	0.0042809	0.0131246
GO:0010632	regulation of epithelial cell migration	4/76	250/28905	6.085263158	0.00430614	0.01318591
GO:0046879	hormone secretion	5/76	405/28905	4.695419103	0.00431254	0.01318946
GO:1902106	negative regulation of leukocyte differentiation	3/76	125/28905	9.127894737	0.00441034	0.01345583
GO:0045445	myoblast differentiation	3/76	125/28905	9.127894737	0.00441034	0.01345583
GO:1904646	cellular response to amyloid-beta	2/76	38/28905	20.01731302	0.00451106	0.01371319
GO:0098581	detection of external biotic stimulus	2/76	38/28905	20.01731302	0.00451106	0.01371319
GO:0045577	regulation of B cell differentiation	2/76	38/28905	20.01731302	0.00451106	0.01371319
GO:0048762	mesenchymal cell differentiation	4/76	254/28905	5.989432242	0.00455423	0.01382769
GO:0009914	hormone transport	5/76	413/28905	4.604466675	0.00468166	0.01419747
GO:0071402	cellular response to lipoprotein particle stimulus	2/76	39/28905	19.50404858	0.00474684	0.01434322
GO:0051491	positive regulation of filopodium assembly	2/76	39/28905	19.50404858	0.00474684	0.01434322
GO:0014741	negative regulation of muscle hypertrophy	2/76	39/28905	19.50404858	0.00474684	0.01434322

GO:0001952	regulation of cell-matrix adhesion	3/76	130/28905	8.776821862	0.00491942	0.01484685
GO:0045936	negative regulation of phosphate metabolic process	5/76	419/28905	4.538531592	0.00497291	0.01497232
GO:0010563	negative regulation of phosphorus metabolic process	5/76	419/28905	4.538531592	0.00497291	0.01497232
GO:0035305	negative regulation of dephosphorylation	2/76	40/28905	19.01644737	0.00498821	0.0149825
GO:0010714	positive regulation of collagen metabolic process	2/76	40/28905	19.01644737	0.00498821	0.0149825
GO:1903707	negative regulation of hemopoiesis	3/76	131/28905	8.709823222	0.00502531	0.01507592
GO:0072593	reactive oxygen species metabolic process	4/76	262/28905	5.806548815	0.00507897	0.01521876
GO:0002040	sprouting angiogenesis	3/76	133/28905	8.578848437	0.00524119	0.0156118
GO:0042745	circadian sleep/wake cycle	2/76	41/28905	18.55263158	0.00523513	0.0156118
GO:0032885	regulation of polysaccharide biosynthetic process	2/76	41/28905	18.55263158	0.00523513	0.0156118
GO:0032872	regulation of stress-activated MAPK cascade	2/76	41/28905	18.55263158	0.00523513	0.0156118
GO:0032743	positive regulation of interleukin-2 production	2/76	41/28905	18.55263158	0.00523513	0.0156118
GO:0050829	defense response to Gram-negative bacterium	3/76	134/28905	8.51482718	0.0053512	0.01592061
GO:0051968	positive regulation of synaptic transmission, glutamatergic	2/76	42/28905	18.11090226	0.00548757	0.01624941
GO:0044786	cell cycle DNA replication	2/76	42/28905	18.11090226	0.00548757	0.01624941
GO:0010464	regulation of mesenchymal cell proliferation	2/76	42/28905	18.11090226	0.00548757	0.01624941
GO:0007431	salivary gland development	2/76	42/28905	18.11090226	0.00548757	0.01624941
GO:0032479	regulation of type I interferon production	3/76	136/28905	8.389609133	0.00557537	0.01648998
GO:0006090	pyruvate metabolic process	3/76	137/28905	8.32837111	0.00568954	0.01680788

GO:0002526	acute inflammatory response	3/76	138/28905	8.268020595	0.00580511	0.01712917
GO:0006898	receptor-mediated endocytosis	4/76	273/28905	5.572585309	0.00586472	0.01728477
GO:2000677	regulation of transcription regulatory region DNA binding	2/76	44/28905	17.28767943	0.00600891	0.01754518
GO:1904645	response to amyloid-beta	2/76	44/28905	17.28767943	0.00600891	0.01754518
GO:1903580	positive regulation of ATP metabolic process	2/76	44/28905	17.28767943	0.00600891	0.01754518
GO:0050918	positive chemotaxis	2/76	44/28905	17.28767943	0.00600891	0.01754518
GO:0035196	miRNA processing	2/76	44/28905	17.28767943	0.00600891	0.01754518
GO:0032508	DNA duplex unwinding	2/76	44/28905	17.28767943	0.00600891	0.01754518
GO:0006953	acute-phase response	2/76	44/28905	17.28767943	0.00600891	0.01754518
GO:0003352	regulation of cilium movement	2/76	44/28905	17.28767943	0.00600891	0.01754518
GO:0021782	glial cell development	3/76	140/28905	8.149906015	0.00604046	0.01761685
GO:0009150	purine ribonucleotide metabolic process	5/76	441/28905	4.312119585	0.00615139	0.01791958
GO:0032606	type I interferon production	3/76	141/28905	8.092105263	0.00616025	0.01792462
GO:0010811	positive regulation of cell-substrate adhesion	3/76	142/28905	8.035118606	0.00628146	0.01819306
GO:0070302	regulation of stress-activated protein kinase signalling cascade	2/76	45/28905	16.90350877	0.00627775	0.01819306
GO:0050691	regulation of defence response to virus by host	2/76	45/28905	16.90350877	0.00627775	0.01819306
GO:0002863	positive regulation of inflammatory response to antigenic stimulus	2/76	45/28905	16.90350877	0.00627775	0.01819306
GO:0034614	cellular response to reactive oxygen species	3/76	143/28905	7.978928966	0.00640408	0.01852687
GO:0033028	myeloid cell apoptotic process	2/76	46/28905	16.53604119	0.00655199	0.01888956

GO:0030279	negative regulation of ossification	2/76	46/28905	16.53604119	0.00655199	0.01888956
GO:0001783	B cell apoptotic process	2/76	46/28905	16.53604119	0.00655199	0.01888956
GO:0072594	establishment of protein localization to organelle	5/76	452/28905	4.207178621	0.00680896	0.01960793
GO:0010543	regulation of platelet activation	2/76	47/28905	16.18421053	0.0068316	0.01965063
GO:0033135	regulation of peptidyl-serine phosphorylation	3/76	148/28905	7.709370555	0.00703863	0.02019992
GO:0014902	myotube differentiation	3/76	148/28905	7.709370555	0.00703863	0.02019992
GO:0048873	homeostasis of number of cells within a tissue	2/76	48/28905	15.84703947	0.00711657	0.02033074
GO:0043507	positive regulation of JUN kinase activity	2/76	48/28905	15.84703947	0.00711657	0.02033074
GO:0043388	positive regulation of DNA binding	2/76	48/28905	15.84703947	0.00711657	0.02033074
GO:0006509	membrane protein ectodomain proteolysis	2/76	48/28905	15.84703947	0.00711657	0.02033074
GO:0045598	regulation of fat cell differentiation	3/76	149/28905	7.657629813	0.00716986	0.02045974
GO:0060560	developmental growth involved in morphogenesis	4/76	290/28905	5.245916515	0.00723224	0.02061435
GO:0009259	ribonucleotide metabolic process	5/76	460/28905	4.134010297	0.00731717	0.0208328
GO:1904037	positive regulation of epithelial cell apoptotic process	2/76	49/28905	15.5236305	0.00740685	0.02094579
GO:0072538	T-helper 17 type immune response	2/76	49/28905	15.5236305	0.00740685	0.02094579
GO:0050856	regulation of T cell receptor signaling pathway	2/76	49/28905	15.5236305	0.00740685	0.02094579
GO:0032881	regulation of polysaccharide metabolic process	2/76	49/28905	15.5236305	0.00740685	0.02094579
GO:0014003	oligodendrocyte development	2/76	49/28905	15.5236305	0.00740685	0.02094579
GO:0009595	detection of biotic stimulus	2/76	49/28905	15.5236305	0.00740685	0.02094579

GO:0016055	Wnt signalling pathway	5/76	462/28905	4.116114149	0.00744826	0.02103923
GO:0071900	regulation of protein serine/threonine kinase activity	4/76	294/28905	5.174543502	0.00758209	0.02132145
GO:0198738	cell-cell signalling by wnt	5/76	464/28905	4.098372278	0.00758098	0.02132145
GO:0098781	ncRNA transcription	3/76	152/28905	7.506492382	0.00757224	0.02132145
GO:0032388	positive regulation of intracellular transport	3/76	152/28905	7.506492382	0.00757224	0.02132145
GO:1900544	positive regulation of purine nucleotide metabolic process	2/76	50/28905	15.21315789	0.00770241	0.02153934
GO:0090199	regulation of release of cytochrome c from mitochondria	2/76	50/28905	15.21315789	0.00770241	0.02153934
GO:0048483	autonomic nervous system development	2/76	50/28905	15.21315789	0.00770241	0.02153934
GO:0045981	positive regulation of nucleotide metabolic process	2/76	50/28905	15.21315789	0.00770241	0.02153934
GO:0007157	heterophilic cell-cell adhesion via plasma membrane cell adhesion	2/76	50/28905	15.21315789	0.00770241	0.02153934
GO:0031346	positive regulation of cell projection organization	5/76	467/28905	4.072044404	0.00778315	0.02174093
GO:0061844	antimicrobial humoral immune response mediated by antimicrobial	3/76	154/28905	7.409005468	0.00784779	0.02189716
GO:0097300	programmed necrotic cell death	2/76	51/28905	14.91486068	0.00800324	0.02213437
GO:0048010	vascular endothelial growth factor receptor signalling pathway	2/76	51/28905	14.91486068	0.00800324	0.02213437
GO:0046641	positive regulation of alpha-beta T cell proliferation	2/76	51/28905	14.91486068	0.00800324	0.02213437
GO:0036230	granulocyte activation	2/76	51/28905	14.91486068	0.00800324	0.02213437
GO:0032392	DNA geometric change	2/76	51/28905	14.91486068	0.00800324	0.02213437
GO:0007520	myoblast fusion	2/76	51/28905	14.91486068	0.00800324	0.02213437
GO:0051100	negative regulation of binding	3/76	155/28905	7.361205433	0.00798776	0.02213437

GO:0045814	negative regulation of gene expression, epigenetic	3/76	155/28905	7.361205433	0.00798776	0.02213437
GO:0019693	ribose phosphate metabolic process	5/76	474/28905	4.011908728	0.00826946	0.02284553
GO:0032728	positive regulation of interferon-beta production	2/76	52/28905	14.62803644	0.00830929	0.02293037
GO:0042692	muscle cell differentiation	5/76	476/28905	3.995051968	0.00841221	0.02318891
GO:0070828	heterochromatin organization	3/76	161/28905	7.086874796	0.00885855	0.02439255
GO:0051403	stress-activated MAPK cascade	2/76	54/28905	14.08625731	0.00893698	0.02447447
GO:0045773	positive regulation of axon extension	2/76	54/28905	14.08625731	0.00893698	0.02447447
GO:0045124	regulation of bone resorption	2/76	54/28905	14.08625731	0.00893698	0.02447447
GO:0032715	negative regulation of interleukin-6 production	2/76	54/28905	14.08625731	0.00893698	0.02447447
GO:0010718	positive regulation of epithelial to mesenchymal transition	2/76	54/28905	14.08625731	0.00893698	0.02447447
GO:0071902	positive regulation of protein serine/threonine kinase activity	3/76	162/28905	7.043128655	0.00900888	0.02461774
GO:0016052	carbohydrate catabolic process	3/76	162/28905	7.043128655	0.00900888	0.02461774
GO:0018105	peptidyl-serine phosphorylation	4/76	310/28905	4.907470289	0.00909283	0.02482015
GO:0071453	cellular response to oxygen levels	3/76	163/28905	6.999919277	0.0091607	0.0249783
GO:0001503	ossification	5/76	487/28905	3.904814655	0.00922805	0.02513468
GO:0043029	T cell homeostasis	2/76	55/28905	13.83014354	0.00925855	0.02516323
GO:0035272	exocrine system development	2/76	55/28905	13.83014354	0.00925855	0.02516323
GO:0072006	nephron development	3/76	165/28905	6.91507177	0.00946883	0.02570694
GO:0140374	antiviral innate immune response	2/76	56/28905	13.58317669	0.00958523	0.02585545

GO:0043300	regulation of leukocyte degranulation	2/76	56/28905	13.58317669	0.00958523	0.02585545
GO:0036037	CD8-positive, alpha-beta T cell activation	2/76	56/28905	13.58317669	0.00958523	0.02585545
GO:0014888	striated muscle adaptation	2/76	56/28905	13.58317669	0.00958523	0.02585545
GO:0010463	mesenchymal cell proliferation	2/76	56/28905	13.58317669	0.00958523	0.02585545
GO:0048732	gland development	5/76	491/28905	3.873003537	0.00953783	0.02585545
GO:0015850	organic hydroxy compound transport	4/76	317/28905	4.799103437	0.00981131	0.02643692
GO:0006111	regulation of gluconeogenesis	2/76	57/28905	13.34487535	0.00991701	0.02666455
GO:0061448	connective tissue development	4/76	318/28905	4.784011917	0.00991688	0.02666455
GO:0043405	regulation of MAP kinase activity	3/76	168/28905	6.791588346	0.00994229	0.02670396
GO:0048511	rhythmic process	4/76	320/28905	4.754111842	0.01013022	0.0271797
GO:0051489	regulation of filopodium assembly	2/76	58/28905	13.11479129	0.01025384	0.02739442
GO:0045687	positive regulation of glial cell differentiation	2/76	58/28905	13.11479129	0.01025384	0.02739442
GO:0002675	positive regulation of acute inflammatory response	2/76	58/28905	13.11479129	0.01025384	0.02739442
GO:0018209	peptidyl-serine modification	4/76	321/28905	4.739301525	0.01023801	0.02739442
GO:0030010	establishment of cell polarity	3/76	170/28905	6.711687307	0.01026547	0.02739639
GO:0016311	dephosphorylation	4/76	322/28905	4.724583197	0.01034653	0.02758343
GO:0071103	DNA conformation change	2/76	59/28905	12.89250669	0.0105957	0.02809872
GO:0046902	regulation of mitochondrial membrane permeability	2/76	59/28905	12.89250669	0.0105957	0.02809872
GO:0043536	positive regulation of blood vessel endothelial cell migration	2/76	59/28905	12.89250669	0.0105957	0.02809872

GO:0031663	lipopolysaccharide-mediated signalling pathway	2/76	59/28905	12.89250669	0.0105957	0.02809872
GO:0002455	humoral immune response mediated by circulating immunoglobulin	2/76	59/28905	12.89250669	0.0105957	0.02809872
GO:0070482	response to oxygen levels	4/76	325/28905	4.68097166	0.01067658	0.02828338
GO:0031099	regeneration	3/76	173/28905	6.595299665	0.01076162	0.02847865
GO:0060443	mammary gland morphogenesis	2/76	60/28905	12.67763158	0.01094256	0.02889664
GO:0031342	negative regulation of cell killing	2/76	60/28905	12.67763158	0.01094256	0.02889664
GO:0010631	epithelial cell migration	4/76	329/28905	4.62406015	0.01112716	0.02935329
GO:2001238	positive regulation of extrinsic apoptotic signalling pathway	2/76	61/28905	12.46980155	0.0112944	0.02960805
GO:0060632	regulation of microtubule-based movement	2/76	61/28905	12.46980155	0.0112944	0.02960805
GO:0045954	positive regulation of natural killer cell mediated cytotoxicity	2/76	61/28905	12.46980155	0.0112944	0.02960805
GO:0001974	blood vessel remodelling	2/76	61/28905	12.46980155	0.0112944	0.02960805
GO:0001755	neural crest cell migration	2/76	61/28905	12.46980155	0.0112944	0.02960805
GO:2001235	positive regulation of apoptotic signalling pathway	3/76	176/28905	6.482879785	0.01127148	0.02960805
GO:0090132	epithelium migration	4/76	331/28905	4.59612021	0.01135699	0.02974112
GO:0090130	tissue migration	4/76	333/28905	4.568515884	0.01158987	0.03031938
GO:0070301	cellular response to hydrogen peroxide	2/76	62/28905	12.26867572	0.01165118	0.03041648
GO:0060711	labyrinthine layer development	2/76	62/28905	12.26867572	0.01165118	0.03041648
GO:0052548	regulation of endopeptidase activity	4/76	336/28905	4.527725564	0.01194492	0.03115096
GO:0006839	mitochondrial transport	3/76	180/28905	6.338815789	0.01197272	0.03119112

GO:0090497	mesenchymal cell migration	2/76	63/28905	12.07393484	0.01201289	0.03119875
GO:0043457	regulation of cellular respiration	2/76	63/28905	12.07393484	0.01201289	0.03119875
GO:0002717	positive regulation of natural killer cell mediated immunity	2/76	63/28905	12.07393484	0.01201289	0.03119875
GO:1900015	regulation of cytokine production involved in inflammatory response	2/76	64/28905	11.88527961	0.01237948	0.03195278
GO:0060324	face development	2/76	64/28905	11.88527961	0.01237948	0.03195278
GO:0046850	regulation of bone remodelling	2/76	64/28905	11.88527961	0.01237948	0.03195278
GO:0010921	regulation of phosphatase activity	2/76	64/28905	11.88527961	0.01237948	0.03195278
GO:0046496	nicotinamide nucleotide metabolic process	3/76	182/28905	6.269158473	0.01233257	0.03195278
GO:0030183	B cell differentiation	3/76	182/28905	6.269158473	0.01233257	0.03195278
GO:0051961	negative regulation of nervous system development	3/76	183/28905	6.234900777	0.01251481	0.03226896
GO:0019362	pyridine nucleotide metabolic process	3/76	184/28905	6.201015446	0.0126986	0.03270929
GO:0043506	regulation of JUN kinase activity	2/76	65/28905	11.70242915	0.01275093	0.03274346
GO:0034142	toll-like receptor 4 signaling pathway	2/76	65/28905	11.70242915	0.01275093	0.03274346
GO:0006911	phagocytosis, engulfment	2/76	65/28905	11.70242915	0.01275093	0.03274346
GO:0001822	kidney development	4/76	343/28905	4.435323001	0.01280042	0.03283698
GO:1903053	regulation of extracellular matrix organization	2/76	66/28905	11.52511962	0.01312723	0.03353846
GO:0050854	regulation of antigen receptor-mediated signalling pathway	2/76	66/28905	11.52511962	0.01312723	0.03353846
GO:0002762	negative regulation of myeloid leukocyte differentiation	2/76	66/28905	11.52511962	0.01312723	0.03353846
GO:0001836	release of cytochrome c from mitochondria	2/76	66/28905	11.52511962	0.01312723	0.03353846

GO:0062013	positive regulation of small molecule metabolic process	3/76	188/28905	6.069078947	0.013449222	0.034326238
GO:0070918	regulatory ncRNA processing	2/76	67/28905	11.35310291	0.013508327	0.034337648
GO:0048512	circadian behaviour	2/76	67/28905	11.35310291	0.013508327	0.034337648
GO:0030193	regulation of blood coagulation	2/76	67/28905	11.35310291	0.013508327	0.034337648
GO:0001658	branching involved in ureteric bud morphogenesis	2/76	67/28905	11.35310291	0.013508327	0.034337648
GO:0050714	positive regulation of protein secretion	3/76	189/28905	6.036967419	0.013640761	0.034639267
GO:0050878	regulation of body fluid levels	4/76	350/28905	4.346616541	0.013694237	0.034704952
GO:0009410	response to xenobiotic stimulus	4/76	350/28905	4.346616541	0.013694237	0.034704952
GO:0140253	cell-cell fusion	2/76	68/28905	11.18614551	0.01389421	0.035000043
GO:0032663	regulation of interleukin-2 production	2/76	68/28905	11.18614551	0.01389421	0.035000043
GO:0031098	stress-activated protein kinase signalling cascade	2/76	68/28905	11.18614551	0.01389421	0.035000043
GO:0001954	positive regulation of cell-matrix adhesion	2/76	68/28905	11.18614551	0.01389421	0.035000043
GO:0000768	syncytium formation by plasma membrane fusion	2/76	68/28905	11.18614551	0.01389421	0.035000043
GO:0000271	polysaccharide biosynthetic process	2/76	68/28905	11.18614551	0.01389421	0.035000043
GO:0048754	branching morphogenesis of an epithelial tube	3/76	191/28905	5.9737531	0.014028511	0.035302978
GO:1903556	negative regulation of TNF superfamily cytokine production	2/76	69/28905	11.02402746	0.014284847	0.035876228
GO:1900046	regulation of haemostasis	2/76	69/28905	11.02402746	0.014284847	0.035876228
GO:0072524	pyridine-containing compound metabolic process	3/76	193/28905	5.911848923	0.014422499	0.036113706
GO:0042552	myelination	3/76	193/28905	5.911848923	0.014422499	0.036113706

GO:0000302	response to reactive oxygen species	3/76	193/28905	5.911848923	0.014422499	0.036113706
GO:0030522	intracellular receptor signaling pathway	4/76	356/28905	4.273358959	0.014491301	0.036249881
GO:0007622	rhythmic behavior	2/76	70/28905	10.86654135	0.014680211	0.036613145
GO:0006949	syncytium formation	2/76	70/28905	10.86654135	0.014680211	0.036613145
GO:0002534	cytokine production involved in inflammatory response	2/76	70/28905	10.86654135	0.014680211	0.036613145
GO:0051897	positive regulation of phosphatidylinositol 3-kinase/protein kinase B	3/76	195/28905	5.851214575	0.014822738	0.036931975
GO:0072001	renal system development	4/76	359/28905	4.237648439	0.014900652	0.037052661
GO:0045787	positive regulation of cell cycle	4/76	359/28905	4.237648439	0.014900652	0.037052661
GO:0043393	regulation of protein binding	3/76	196/28905	5.821361439	0.015025205	0.037215139
GO:0021915	neural tube development	3/76	196/28905	5.821361439	0.015025205	0.037215139
GO:0008366	axon ensheathment	3/76	196/28905	5.821361439	0.015025205	0.037215139
GO:0007272	ensheathment of neurons	3/76	196/28905	5.821361439	0.015025205	0.037215139
GO:0098900	regulation of action potential	2/76	71/28905	10.71349148	0.015080276	0.037278086
GO:0050688	regulation of defense response to virus	2/76	71/28905	10.71349148	0.015080276	0.037278086
GO:1901224	positive regulation of non-canonical NF-kappaB signal transduction	2/76	72/28905	10.56469298	0.015485015	0.038016921
GO:0090559	regulation of membrane permeability	2/76	72/28905	10.56469298	0.015485015	0.038016921
GO:0090278	negative regulation of peptide hormone secretion	2/76	72/28905	10.56469298	0.015485015	0.038016921
GO:0050818	regulation of coagulation	2/76	72/28905	10.56469298	0.015485015	0.038016921
GO:0032648	regulation of interferon-beta production	2/76	72/28905	10.56469298	0.015485015	0.038016921

GO:0032608	interferon-beta production	2/76	72/28905	10.56469298	0.015485015	0.038016921
GO:0006801	superoxide metabolic process	2/76	72/28905	10.56469298	0.015485015	0.038016921
GO:1905330	regulation of morphogenesis of an epithelium	2/76	73/28905	10.41997116	0.015894401	0.038945929
GO:0061035	regulation of cartilage development	2/76	73/28905	10.41997116	0.015894401	0.038945929
GO:0099024	plasma membrane invagination	2/76	74/28905	10.27916074	0.016308407	0.039805181
GO:0060675	ureteric bud morphogenesis	2/76	74/28905	10.27916074	0.016308407	0.039805181
GO:0048662	negative regulation of smooth muscle cell proliferation	2/76	74/28905	10.27916074	0.016308407	0.039805181
GO:0002792	negative regulation of peptide secretion	2/76	74/28905	10.27916074	0.016308407	0.039805181
GO:0030308	negative regulation of cell growth	3/76	205/28905	5.565789474	0.016918089	0.041253225
GO:0032623	interleukin-2 production	2/76	76/28905	10.00865651	0.017150177	0.041697818
GO:0009620	response to fungus	2/76	76/28905	10.00865651	0.017150177	0.041697818
GO:0006919	activation of cysteine-type endopeptidase activity involved in	2/76	76/28905	10.00865651	0.017150177	0.041697818
GO:1990138	neuron projection extension	3/76	208/28905	5.485513664	0.01757741	0.042695274
GO:0072171	mesonephric tubule morphogenesis	2/76	78/28905	9.752024291	0.018010112	0.04366193
GO:0046847	filopodium assembly	2/76	78/28905	9.752024291	0.018010112	0.04366193
GO:0051402	neuron apoptotic process	4/76	381/28905	3.992954828	0.018127129	0.043903277
GO:0061180	mammary gland epithelium development	2/76	79/28905	9.628580946	0.018446827	0.044591657
GO:0045669	positive regulation of osteoblast differentiation	2/76	79/28905	9.628580946	0.018446827	0.044591657
GO:0098742	cell-cell adhesion via plasma-membrane adhesion molecules	3/76	212/28905	5.382013406	0.018478636	0.044625639

GO:0043524	negative regulation of neuron apoptotic process	3/76	213/28905	5.356745738	0.018707899	0.045135949
GO:0007517	muscle organ development	4/76	385/28905	3.951469583	0.018756911	0.04521081
GO:0016239	positive regulation of macroautophagy	2/76	80/28905	9.508223684	0.018888005	0.045396219
GO:0007492	endoderm development	2/76	80/28905	9.508223684	0.018888005	0.045396219
GO:0002673	regulation of acute inflammatory response	2/76	80/28905	9.508223684	0.018888005	0.045396219
GO:1905475	regulation of protein localization to membrane	3/76	215/28905	5.306915545	0.01917118	0.046032805
GO:0097194	execution phase of apoptosis	2/76	81/28905	9.390838207	0.019333621	0.046334341
GO:0001913	T cell mediated cytotoxicity	2/76	81/28905	9.390838207	0.019333621	0.046334341
GO:1903532	positive regulation of secretion by cell	4/76	389/28905	3.910837505	0.019400175	0.046449562
GO:0010611	regulation of cardiac muscle hypertrophy	2/76	82/28905	9.276315789	0.019783649	0.047277655
GO:0010324	membrane invagination	2/76	82/28905	9.276315789	0.019783649	0.047277655
GO:0001960	negative regulation of cytokine-mediated signaling pathway	2/76	83/28905	9.164552949	0.020238063	0.048271812
GO:0006887	exocytosis	4/76	394/28905	3.861207587	0.020223327	0.048271812
GO:0050796	regulation of insulin secretion	3/76	222/28905	5.13958037	0.020842632	0.049619674
GO:0019730	antimicrobial humoral response	3/76	222/28905	5.13958037	0.020842632	0.049619674

Table B.5 GO pathway analysis of genes enriched in *Pd1*$^{-/-}$ Tregs.

ID	Description	setSize	enrichmentScore	NES	pvalue	p.adjust	rank
GO:0070372	regulation of ERK1 and ERK2 cascade	28	0.713549537	2.179303844	2.0089E-05	2.0089E-05	38
GO:0070374	positive regulation of ERK1 and ERK2 cascade	24	0.71977033	2.152441768	5.755E-05	5.755E-05	38
GO:0070371	ERK1 and ERK2 cascade	31	0.669168993	2.091134848	3.7859E-05	3.7859E-05	38
GO:0061082	myeloid leukocyte cytokine production	17	0.744920848	2.022207902	0.00027136	0.00027136	43
GO:0010934	macrophage cytokine production	13	0.806902191	2.011292819	0.00022607	0.00022607	33
GO:0002720	positive regulation of cytokine production involved in immune response	22	0.679969803	1.974007984	0.00042638	0.00042638	58
GO:0051092	positive regulation of NF-kappaB transcription factor activity	18	0.716955165	1.970718303	0.00053958	0.00053958	33
GO:0043410	positive regulation of MAPK cascade	36	0.607030438	1.954761674	0.00027978	0.00027978	38
GO:0010935	regulation of macrophage cytokine production	12	0.792548968	1.925895232	0.00034757	0.00034757	33

GO:0003008	system process	38	0.584776265	1.911289352	0.00079	0.00079	60
GO:0051091	positive regulation of DNA-binding transcription factor activity	24	0.638231292	1.908602833	0.00278455	0.00278455	38
GO:0043408	regulation of MAPK cascade	45	0.563266937	1.904425375	0.00045622	0.00045622	38
GO:0042742	defence response to bacterium	20	0.664428804	1.884515916	0.00343641	0.00343641	37
GO:0002381	immunoglobulin production involved in immunoglobulin-mediated immune response	13	0.750349912	1.870330019	0.00222843	0.00222843	44
GO:0000165	MAPK cascade	50	0.546287375	1.856306464	0.00071898	0.00071898	38
GO:0061081	positive regulation of myeloid leukocyte cytokine production involved in immune response	12	0.763170594	1.854505737	0.00129245	0.00129245	37
GO:0032735	positive regulation of interleukin-12 production	9	0.811706336	1.848691855	0.00247981	0.00247981	34
GO:0060907	positive regulation of macrophage cytokine production	10	0.790396242	1.843339155	0.00460181	0.00460181	32
GO:0050764	regulation of phagocytosis	16	0.669397957	1.790202923	0.00542068	0.00542068	37

GO:0033554	cellular response to stress	52	0.517381374	1.783869467	0.00120632	0.00120632	66
GO:0007249	canonical NF-kappaB signal transduction	25	0.588235921	1.773885943	0.00462942	0.00462942	84
GO:0051090	regulation of DNA-binding transcription factor activity	31	0.567032572	1.771961319	0.00486513	0.00486513	62
GO:0002702	positive regulation of production of molecular mediator of immune response	37	0.544435818	1.767811835	0.00400676	0.00400676	44
GO:0006310	DNA recombination	15	0.676220622	1.757977935	0.00892938	0.00892938	48
GO:0032655	regulation of interleukin-12 production	13	0.704990519	1.757266722	0.00915327	0.00915327	34
GO:0032615	interleukin-12 production	13	0.704990519	1.757266722	0.00915327	0.00915327	34
GO:0002367	cytokine production involved in immune response	34	0.550552802	1.750625389	0.00562142	0.00562142	59
GO:0002718	regulation of cytokine production involved in immune response	32	0.557664397	1.749914837	0.00800805	0.00800805	59
GO:0032755	positive regulation of interleukin-6 production	21	0.609999978	1.74903674	0.01257764	0.01257764	38

GO:0016444	somatic cell DNA recombination	12	0.715720374	1.739201629	0.00739951	0.00739951	44
GO:0002562	somatic diversification of immune receptors via germline recombination within a single locus	12	0.715720374	1.739201629	0.00739951	0.00739951	44
GO:0002200	somatic diversification of immune receptors	12	0.715720374	1.739201629	0.00739951	0.00739951	44
GO:0060341	regulation of cellular localization	37	0.530628332	1.7229782	0.00631691	0.00631691	65
GO:0042088	T-helper 1 type immune response	17	0.628071839	1.705002402	0.01463711	0.01463711	58
GO:0032880	regulation of protein localization	34	0.535924081	1.704109577	0.00863996	0.00863996	65
GO:1990266	neutrophil migration	26	0.556850559	1.685914091	0.01737875	0.01737875	37
GO:1902533	positive regulation of intracellular signal transduction	64	0.467787832	1.68234086	0.00379595	0.00379595	38
GO:0045190	isotype switching	10	0.720135268	1.679478553	0.03078688	0.03078688	44
GO:0016447	somatic recombination of immunoglobulin gene segments	10	0.720135268	1.679478553	0.03078688	0.03078688	44

GO:0016445	somatic diversification of immunoglobulins	10	0.720135268	1.679478553	0.03078688	0.03078688	44
GO:0002208	somatic diversification of immunoglobulins involved in immune response	10	0.720135268	1.679478553	0.03078688	0.03078688	44
GO:0002204	somatic recombination of immunoglobulin genes involved in immune response	10	0.720135268	1.679478553	0.03078688	0.03078688	44
GO:0006109	regulation of carbohydrate metabolic process	10	0.719811106	1.678722551	0.03078688	0.03078688	61
GO:0032653	regulation of interleukin-10 production	14	0.660634679	1.676371264	0.01989632	0.01989632	84
GO:0032613	interleukin-10 production	14	0.660634679	1.676371264	0.01989632	0.01989632	84
GO:0050830	defense response to Gram-positive bacterium	13	0.671525921	1.673852515	0.02356622	0.02356622	70
GO:0060485	mesenchyme development	14	0.6586233	1.671267355	0.02051324	0.02051324	38
GO:0006909	phagocytosis	22	0.575510196	1.670753196	0.01294862	0.01294862	37
GO:0051962	positive regulation of nervous system development	15	0.642597449	1.670567415	0.01975669	0.01975669	49

GO:0050769	positive regulation of neurogenesis	15	0.642597449	1.670567415	0.01975669	0.01975669	49
GO:0032612	interleukin-1 production	21	0.582089701	1.669010344	0.02587082	0.02587082	38
GO:0071347	cellular response to interleukin-1	17	0.613384877	1.665132273	0.01995757	0.01995757	38
GO:0070555	response to interleukin-1	17	0.613384877	1.665132273	0.01995757	0.01995757	38
GO:0032731	positive regulation of interleukin-1 beta production	16	0.622320395	1.664301149	0.0207217	0.0207217	38
GO:0032635	interleukin-6 production	28	0.543401842	1.659643321	0.01707651	0.01707651	38
GO:0072359	circulatory system development	40	0.502945858	1.6537071	0.01437636	0.01437636	61
GO:1903829	positive regulation of protein localization	23	0.556770449	1.651751648	0.03886719	0.03886719	41
GO:0007254	JNK cascade	9	0.72432072	1.649667814	0.02395482	0.02395482	30
GO:0048762	mesenchymal cell differentiation	11	0.68429245	1.645579326	0.02533431	0.02533431	38

GO:0002548	monocyte chemotaxis	12	0.676947261	1.644982903	0.02200112	0.02200112	35
GO:0032611	interleukin-1 beta production	19	0.584088593	1.637027596	0.02250074	0.02250074	38
GO:1900180	regulation of protein localization to nucleus	13	0.655454497	1.633792716	0.03453096	0.03453096	59
GO:0030593	neutrophil chemotaxis	23	0.550691913	1.633718665	0.04429042	0.04429042	37
GO:0033036	macromolecule localization	61	0.456507418	1.630155089	0.00635219	0.00635219	90
GO:0032675	regulation of interleukin-6 production	26	0.536729904	1.624997036	0.02674796	0.02674796	38
GO:0061912	selective autophagy	4	0.891385768	1.624768549	0.01256802	0.01256802	33
GO:0072679	thymocyte migration	3	0.959842517	1.622916151	0.00333319	0.00333319	6
GO:0001667	ameboidal-type cell migration	17	0.597377953	1.621678894	0.02971445	0.02971445	33
GO:0072594	establishment of protein localization to organelle	12	0.667331748	1.621617191	0.02715993	0.02715993	57
GO:0044087	regulation of cellular component biogenesis	25	0.536959828	1.619257607	0.01929943	0.01929943	33
GO:0002292	T cell differentiation involved in immune response	19	0.577201029	1.617723793	0.02637498	0.02637498	61
GO:0061919	process utilizing autophagic mechanism	18	0.587745996	1.615556799	0.02661997	0.02661997	57
GO:0006914	autophagy	18	0.587745996	1.615556799	0.02661997	0.02661997	57
GO:0006606	protein import into nucleus	9	0.707446717	1.611236633	0.03219619	0.03219619	57

GO:0043123	positive regulation of canonical NF-kappaB signal transduction	18	0.585489102	1.609353199	0.02780968	0.02780968	32
GO:0098542	defense response to other organism	92	0.426972036	1.606967554	0.00442157	0.00442157	39
GO:0034504	protein localization to nucleus	14	0.632229811	1.604293446	0.03812921	0.03812921	59
GO:0070727	cellular macromolecule localization	55	0.458255911	1.60208883	0.0106006	0.0106006	90
GO:0008104	protein localization	55	0.458255911	1.60208883	0.0106006	0.0106006	90
GO:0032732	positive regulation of interleukin-1 production	17	0.589065261	1.599112748	0.03595253	0.03595253	38
GO:0016236	macroautophagy	8	0.725208	1.597867016	0.02532491	0.02532491	57
GO:0032386	regulation of intracellular transport	14	0.629595424	1.597608646	0.03998913	0.03998913	65
GO:0050920	regulation of chemotaxis	25	0.528873388	1.594872118	0.0213939	0.0213939	35
GO:0006886	intracellular protein transport	15	0.611860375	1.590659919	0.03910228	0.03910228	81
GO:0097398	cellular response to interleukin-17	4	0.872659176	1.590634756	0.01772408	0.01772408	38
GO:0097396	response to interleukin-17	4	0.872659176	1.590634756	0.01772408	0.01772408	38
GO:0060041	retina development in camera-type eye	5	0.82671108	1.590434335	0.02671556	0.02671556	33
GO:0032965	regulation of collagen biosynthetic process	7	0.747067416	1.590414236	0.03751508	0.03751508	58
GO:0010712	regulation of collagen metabolic process	7	0.747067416	1.590414236	0.03751508	0.03751508	58

GO:0001568	blood vessel development	35	0.496917588	1.589837775	0.02453799	0.02453799	61
GO:1903532	positive regulation of secretion by cell	16	0.593311715	1.586721852	0.03455915	0.03455915	65
GO:0051047	positive regulation of secretion	17	0.582665761	1.581740272	0.04130073	0.04130073	65
GO:0050727	regulation of inflammatory response	43	0.472074223	1.580022433	0.0153178	0.0153178	61
GO:0043122	regulation of canonical NF-kappaB signal transduction	22	0.544093607	1.579548266	0.02751226	0.02751226	84
GO:0002726	positive regulation of T cell cytokine production	8	0.716168504	1.577950093	0.0303049	0.0303049	58
GO:0050921	positive regulation of chemotaxis	21	0.550075819	1.577217789	0.04189497	0.04189497	35
GO:0002687	positive regulation of leukocyte migration	27	0.515126748	1.57669101	0.03773766	0.03773766	35
GO:0002824	positive regulation of adaptive immune response based on somatic recombination of immune receptors built from immunoglobulin superfamily domains	37	0.484615881	1.573573341	0.02260152	0.02260152	63
GO:0001944	vasculature development	36	0.487721214	1.570561666	0.01962312	0.01962312	61
GO:0032700	negative regulation of interleukin-17 production	4	0.861161719	1.569677828	0.02442283	0.02442283	33
GO:0046822	regulation of nucleocytoplasmic transport	9	0.68751145	1.565833309	0.04578325	0.04578325	60
GO:0044419	biological process involved in interspecies interaction between organisms	114	0.405753959	1.564139907	0.00310283	0.00310283	39

GO:0033157	regulation of intracellular protein transport	11	0.649674249	1.562329837	0.04670075	0.04670075	65
GO:1902531	regulation of intracellular signal transduction	81	0.41746615	1.552050853	0.00619727	0.00619727	64
GO:0032103	positive regulation of response to external stimulus	63	0.431304736	1.551408827	0.01629555	0.01629555	38
GO:0009617	response to bacterium	53	0.445846224	1.548431063	0.01629555	0.01629555	38
GO:0009991	response to extracellular stimulus	16	0.576535044	1.5418552	0.04282953	0.04282953	59
GO:0006259	DNA metabolic process	28	0.504639201	1.541255502	0.03978872	0.03978872	66
GO:0006954	inflammatory response	89	0.410383273	1.539781539	0.00727613	0.00727613	61
GO:0007267	cell-cell signalling	38	0.469721691	1.535243682	0.02591045	0.02591045	57
GO:0002821	positive regulation of adaptive immune response	39	0.468593556	1.534763449	0.02454266	0.02454266	63
GO:0002827	positive regulation of T-helper 1 type immune response	8	0.696283554	1.534137138	0.03795446	0.03795446	58
GO:0002440	production of molecular mediator of immune response	52	0.443308158	1.528473825	0.02063014	0.02063014	44
GO:0002708	positive regulation of lymphocyte mediated immunity	34	0.478424853	1.521275873	0.04206122	0.04206122	58
GO:1904417	positive regulation of xenophagy	3	0.899253731	1.520471721	0.02984633	0.02984633	30
GO:1904415	regulation of xenophagy	3	0.899253731	1.520471721	0.02984633	0.02984633	30
GO:0098792	xenophagy	3	0.899253731	1.520471721	0.02984633	0.02984633	30

GO:0098543	detection of other organism	3	0.899253731	1.520471721	0.02984633	0.02984633	30
GO:0016045	detection of bacterium	3	0.899253731	1.520471721	0.02984633	0.02984633	30
GO:0006952	defense response	133	0.390078289	1.518085024	0.0023569	0.0023569	44
GO:0006950	response to stress	164	0.38481211	1.514969489	0.00346232	0.00346232	61
GO:0090304	nucleic acid metabolic process	95	0.399604073	1.509879472	0.00851801	0.00851801	62
GO:0002700	regulation of production of molecular mediator of immune response	46	0.444361781	1.509421757	0.02498566	0.02498566	59
GO:0051707	response to other organism	106	0.394611111	1.50867001	0.00657811	0.00657811	39
GO:0043207	response to external biotic stimulus	106	0.394611111	1.50867001	0.00657811	0.00657811	39
GO:0009607	response to biotic stimulus	106	0.394611111	1.50867001	0.00657811	0.00657811	39
GO:0045806	negative regulation of endocytosis	3	0.888059701	1.501544687	0.03821425	0.03821425	33
GO:0051093	negative regulation of developmental process	52	0.435123944	1.500255627	0.02913403	0.02913403	62
GO:0009605	response to external stimulus	149	0.38108733	1.497035144	0.00238076	0.00238076	41
GO:0051668	localization within membrane	18	0.543548732	1.494070322	0.04970179	0.04970179	84
GO:0071495	cellular response to endogenous stimulus	42	0.448270088	1.490201896	0.04600597	0.04600597	58
GO:0046483	heterocycle metabolic process	102	0.388685556	1.484994788	0.01064454	0.01064454	62

GO:0002705	positive regulation of leukocyte mediated immunity	40	0.423058383	1.391033728	0.04901961	0.04901961	58
GO:0032101	regulation of response to external stimulus	88	0.365838429	1.379933484	0.04116996	0.04116996	49
GO:0023056	positive regulation of signaling	82	0.370194189	1.375546115	0.04771467	0.04771467	38
GO:0010647	positive regulation of cell communication	82	0.370194189	1.375546115	0.04771467	0.04771467	38
GO:0034641	cellular nitrogen compound metabolic process	106	0.355877833	1.360585646	0.03550291	0.03550291	62
GO:0009967	positive regulation of signal transduction	78	0.366492949	1.358117264	0.03705088	0.03705088	38
GO:0009653	anatomical structure morphogenesis	77	0.364332613	1.342869361	0.04928876	0.04928876	61
GO:0035556	intracellular signal transduction	104	0.350992547	1.342016876	0.03904712	0.03904712	81
GO:0001816	cytokine production	101	0.351118276	1.339200828	0.03122138	0.03122138	63
GO:0001817	regulation of cytokine production	96	0.351862714	1.331259599	0.0465211	0.0465211	63
GO:0007165	signal transduction	184	0.32411879	1.279950729	0.03859005	0.03859005	44
GO:0042221	response to chemical	156	0.325891057	1.273419838	0.0464353	0.0464353	59
GO:0006955	immune response	178	-0.348511995	-1.39546923	0.00810626	0.00810626	54
GO:0002376	immune system process	210	-0.364688518	-1.42098788	0.00568936	0.00568936	44
GO:0030183	B cell differentiation	23	-0.530408347	-1.53628967	0.02870196	0.02870196	37
GO:0050853	B cell receptor signaling pathway	12	-0.654448617	-1.62328898	0.0236609	0.0236609	37

Table B.6 GSEA of genes enriched in WT and *Pd1*$^{-/-}$ Tregs.

CellId	Size_Factor	Genes_Expressed	Pseudotime	Monocle_State
1_75997	2.89684653	97	6.053805283	6
1_321616	1.569102191	90	6.232210154	6
1_259827	2.595287291	85	3.887363092	3
1_568645	1.3155936	86	2.077211671	2
1_502918	1.267542952	74	0.964224882	1
1_35982	1.407276446	77	6.059340077	6
1_474124	1.51111003	64	4.89567604	5
1_127128	0.64288453	64	6.331036427	6
1_502154	2.174429893	59	4.993574094	5
1_515094	1.096328	63	6.08593444	6
1_180074	0.78758878	58	6.166715028	6
1_191622	0.584340063	57	0.774609672	1
1_113053	1.442071742	64	4.911743694	5
1_93207	1.198504665	51	6.615675004	7
1_352955	2.53287668	57	7.997325847	7
1_789617	2.076671678	51	7.917197896	7
1_835366	1.784501647	60	4.959940582	5
1_556623	1.611629776	52	7.904756027	7
1_180170	0.628524566	37	4.922224209	5
1_259228	0.313709977	42	6.209769534	6
1_234421	1.301233637	41	7.91902437	7
1_16759	1.276379853	37	7.94175752	7
1_737448	0.569427793	36	5.457347265	7
1_529153	1.070369604	34	7.99620701	7
2_653480	2.44340306	115	0.487097194	1
2_338365	1.693371108	97	2.283905043	2
2_823995	2.895741917	93	4.760392704	5
2_253296	1.417217959	74	2.184828844	2
2_144923	1.073683442	76	0.370658824	1
2_447028	1.789472404	96	6.025570144	6
2_132221	0.748927339	89	0.14728788	1
2_131160	1.547562245	75	2.00754446	2
2_719454	0.677679827	81	0.298683586	1
2_265864	1.507243886	81	3.886871043	3
2_418708	1.971733482	68	5.881697007	7
2_368523	0.652273737	64	6.327107093	6
2_175860	0.814099482	74	0.260501171	1
2_681695	0.439083506	59	0.231526254	1
2_732783	1.733689467	66	6.949812755	7
2_351458	0.584892369	55	0.582553591	1
2_872859	0.521377145	65	2.160726865	2

2_691651	0.509778712	59	2.265342044	2
2_807144	0.560038586	70	0.151343419	1
2_85268	0.614716909	68	0.274621518	1
2_550944	2.738334622	74	7.783069136	7
2_217286	0.549544766	57	2.35726623	2
2_560052	1.447594805	75	3.760886114	3
2_44138	2.447269204	60	7.829298698	7
2_104963	0.963774489	64	6.01140288	6
2_85740	0.886451607	65	6.165435433	6
2_452457	0.631286098	64	2.129338716	2
2_565796	0.834534815	62	2.041294068	2
2_327883	1.371376536	68	3.541100669	3
2_98580	0.655587575	58	0.637717728	1
2_586835	0.83232559	54	6.013432884	6
2_523941	0.425828155	65	0.079555351	1
2_312382	2.582584247	59	7.936903738	7
2_255260	1.234956881	59	3.644428474	3
2_822565	0.350714499	60	0	1
2_800646	1.233852268	64	5.932001149	6
2_28691	0.928979192	61	5.991589768	6
2_390246	2.047951751	58	7.864284196	7
2_640634	0.5876539	55	2.057595588	2
2_587164	1.516633093	61	4.870677753	5
2_516137	0.954385282	54	6.029971729	7
2_362840	0.581578531	52	0.543257093	1
2_116722	2.116437732	51	7.928952902	7
2_138782	0.663319863	44	2.695310572	3
2_529423	0.448472713	50	6.140800591	6
2_237815	2.070044003	46	8.097932967	7
2_145884	0.743956583	37	3.793438057	3
2_140710	1.107374126	45	7.735475641	7
2_707653	1.413904121	44	7.937695858	7
2_402714	0.61305999	42	3.816578266	3
2_760586	1.249316845	47	7.88741376	7
2_308010	0.31923304	36	1.939821477	2
2_390779	0.700324385	44	5.786211218	7
2_49142	0.367283688	42	0.445905407	1
2_325291	1.047725046	40	7.814539033	7
2_677455	1.64090201	45	7.942830664	7
2_100074	1.204580035	44	7.840085984	7
2_410327	0.541812478	42	4.835427628	5
2_226752	0.730701231	34	7.298143549	7

2_3813	0.822384077	47	4.930951593	5
2_318270	0.492104911	39	4.854845831	5
2_310297	0.830668671	31	7.737839581	7
2_816406	0.288303887	39	0.697019138	1
2_797338	1.091357244	36	7.882828442	7
2_111088	0.651169125	33	7.788475097	7
2_114987	0.79200723	35	7.866675842	7
2_477770	0.929531498	35	7.932706839	7

Table B.7 Details of every all WT and *Pd1*$^{-/-}$ Tregs involved in pseudotime trajectory analysis using Monocle. The cell ID of WT Treg started with "1_" while the *Pd1*$^{-/-}$ Treg started with "2_".

CellId	Size_Factor	Genes_Expressed	Pseudotime	Monocle_State
1_75997	2.348451112	97	0.460708245	1
1_321616	1.272059029	90	0.379272317	1
1_35982	1.140868147	77	0.361112663	1
1_474124	1.225045232	64	1.877021062	1
1_127128	0.521181524	64	0	1
1_515094	0.888784644	63	0.389470568	1
1_180074	0.638492142	58	0.28680064	1
1_113053	1.169076426	64	2.129865704	1
1_180170	0.509540012	37	2.318789444	1
1_259228	0.254322256	42	0.053949382	1
1_259827	2.103979366	85	3.599053725	2
1_568645	1.066541573	86	3.711649712	2
1_502918	1.027587284	74	3.630505281	2
1_191622	0.473719976	57	3.766525987	2
1_93207	0.971618477	51	3.041231555	2
1_737448	0.461630714	36	3.494361859	2
1_502154	1.762793523	59	4.101880486	3
1_352955	2.053383565	57	4.356271129	3
1_789617	1.683541693	51	4.276549774	3
1_835366	1.446681705	60	3.896065227	3
1_556623	1.306535814	52	4.281034654	3
1_234421	1.054900061	41	4.274093405	3
1_16759	1.034751291	37	4.342546876	3
1_529153	0.867740373	34	4.334669709	3

Table B.8 Details of every single WT Tregs involved in pseudotime trajectory analysis using Monocle.

CellId	Size_Factor	Genes_Expressed	Pseudotime	Monocle_State
2_418708	2.125674659	68	2.209959012	1
2_732783	1.86904559	66	1.777334186	1
2_550944	2.95212744	74	0.324138625	1
2_560052	1.560614365	75	2.804588784	1
2_44138	2.638337371	60	0.561532471	1
2_312382	2.784217005	59	0.16613714	1
2_390246	2.207843596	58	0.233843978	1
2_587164	1.635042749	61	2.366575721	1
2_516137	1.028897986	54	2.427694912	1
2_116722	2.281676553	51	0.178477457	1
2_237815	2.231660679	46	0	1
2_140710	1.193831286	45	1.272400991	1
2_707653	1.524293313	44	0.141008421	1
2_402714	0.660924054	42	2.170641048	1
2_760586	1.346856045	47	0.202713989	1
2_390779	0.755001532	44	2.135541722	1
2_325291	1.129525162	40	0.292969161	1
2_677455	1.769013841	45	0.117394847	1
2_100074	1.298626451	44	0.240674904	1
2_226752	0.787750021	34	1.204063125	1
2_3813	0.886590915	47	2.148824396	1
2_318270	0.530525524	39	2.683058439	1
2_310297	0.895522321	31	0.999212024	1
2_797338	1.176563901	36	0.189623068	1
2_111088	0.702008522	33	0.353300157	1
2_114987	0.853842426	35	0.212505309	1
2_477770	1.002103768	35	0.14601819	1
2_823995	3.121824156	93	3.050290113	2
2_131160	1.668386665	75	3.418843217	2
2_265864	1.624920489	81	3.039317478	2
2_327883	1.478445428	68	3.226378463	2
2_255260	1.331374941	59	3.147947684	2
2_640634	0.633534408	55	3.509050259	2
2_138782	0.715107918	44	3.335549569	2
2_145884	0.802040271	37	3.438782004	2
2_447028	1.929183724	96	4.285695266	3
2_104963	1.039020247	64	4.291368094	3
2_85740	0.955660456	65	4.90020881	3
2_586835	0.897308603	54	4.714855663	3
2_800646	1.330184086	64	3.513855943	3
2_28691	1.001508341	61	3.919149929	3
2_529423	0.483486785	50	4.77065403	3
2_410327	0.584113961	42	3.010018108	3

2_144923	1.157510235	76	6.337176178	4
2_132221	0.807399114	89	6.721631119	4
2_719454	0.730589022	81	6.353563904	4
2_368523	0.703199376	64	6.488731282	4
2_175860	0.877659509	74	6.41529985	4
2_681695	0.473364525	59	6.47747142	4
2_872859	0.562083159	65	6.189220486	4
2_807144	0.603763054	70	6.651241239	4
2_85268	0.662710335	68	6.453326645	4
2_523941	0.459074275	65	6.678800646	4
2_822565	0.378096193	60	6.87553223	4
2_362840	0.62698471	52	5.653631329	4
2_49142	0.395959005	42	6.290700588	4
2_653480	2.634169382	115	5.860225662	5
2_338365	1.825579413	97	6.437299176	5
2_253296	1.527865875	74	6.413853749	5
2_351458	0.630557273	55	5.985033084	5
2_691651	0.549579191	59	6.428819972	5
2_217286	0.59244994	57	6.501550934	5
2_452457	0.680573147	64	6.263180442	5
2_565796	0.899690311	62	6.221832051	5
2_98580	0.706771938	58	6.140115132	5
2_308010	0.34415685	36	6.182453076	5
2_816406	0.310812933	39	6.130569768	5

Table B.9 Details of every single *Pd1*$^{-/-}$ Tregs involved in pseudotime trajectory analysis using Monocle.

Appendix C

Rag1$^{-/-}$ mice were subcutaneously injected with B16F10 melanoma cells on d0 and reconstituted with CD45.1 CD4^{+} WT Teff, alongside WT or *Pd1*$^{-/-}$ Tregs (n=2/cohort) on d7. Tumours were harvested for CosMx spatial transcriptomics analysis on d20. Louvain clustering was performed and the cell clusters were annotated by using *ScType* function in RStudio based on the cell-type-specific gene set in **Table C.1** and published papers on cell identification in skin and tumour tissue (Jacob et al., 2023, Chu et al., 2022, Kim et al., 2022, Solé-Boldo et al., 2020, Ordovas-Montanes et al., 2018). Treg cell IDs and spatial coordinates were extracted from the FOV object in RStudio **(Table C.2)**. To systematically analyse Treg interactions with tumour and immune cells, Treg population was further divided into several groups based on their spatial location and cell interaction on FOVs by using their specific 'Cell_ID' **(Table C.3)**. The number of physical interactions of Treg with alternative cell types on the FOV images was manually counted. By using *FindAllMarkers* function (method = "Wilcoxon"), specific genes in each Treg subsets interacting with neighbouring cells or alone within the FOV was determined as shown in **Table C.4** and **Table C.5** for WT and *Pd1*$^{-/-}$ Treg treated cohort respectively. Treg-specific genes were further subdivided into either short-range (SR) or long-range (LR) communications based on biological function by manual curation. Genes involved in cell-cell contact were annotated as SR and secreted or signalling genes were annotated as LR. SR consisted of genes for cell surface receptors, proliferation markers, and apoptotic markers, whereas LR consisted of genes for cytokines, chemokines, transcription factors that can drive cytokine, chemokine production and etc.

Cell type	Gene
CD4+ T cells	CD4,CD2,CD3D,CD3E,CD3G,CD3Z,CD62L,CD27,CD127,CCR7,CD45,CCR6,IL2RA,GZMB,PTPRC,SELL,CCR7, CD25,CD62L,CTLA4
Tregs	FOXP3,CD4,CD2,CD3D,CD3E,CD3G,CD3Z,CD25,CD62L,CTLA4,IL2RA,CCR7
Platelets	CD41,CD42b,CD61,CD31,PPBP,PF4,GNG11,SDPR,CLU,CD41,CD110
CD4+ NKT-like cells	CD4,KLRB1C,CD2,CD16,CD94,CD3D,CD3E,CD3G,CD3Z,IL7R,CD314,CD69, NKG7, CD122,NKG2D,GZMB,GZMA,GZMM, COX6A2, ZMAT4, KIR2DL4
Natural killer cells	EOMES, KLRB1C, CD314,CD69,NKG7,CD122,NKG2D,GZMB,GZMA, GZMM, FCGR3A, GNLY,COX6A2,ZMAT4,KIR2DL4,NKG7
Eosinophils	CD125,CD15,CLC,GATA1,CEBPE,SEMG1,ALOX15,CCL23,PRSS41,PRSS33,THBS4, FOXI1,SIGLEC8
Neutrophils	CD66b,CD15,CD16,CXCL8,FCGR3B,MNDA,CXCR2,MPO,ELANE,PRTN3,MPO, AZU1,LYZ,S100A8,S100A9,PI3,CHI3L1,ANXA3, CXCL1, TGM3, BTNL3, C4BPA, MMP9,CD24,BPI,LTF,GCA
Basophils	CD63,CD203C,CD123,CLC,MS4A3,TCN1,CPA3,HDC,GATA2,MS4A2,IL4,GCS AML, GATA2,TPSAB1
Mast cells	CD117,CD203C,CD25,KIT,SLC18A2,CD33,CD32,FCER1A,TPSD1,HPGDS
Classical Monocytes	CD14,CD11B,CD68,HLA-DR,CD33,CD11C,CD123,CD15,CD66b,VCAN,S100A12,CXCL8,S100A8,S100A9,LYZ, CST3
Non-classical monocytes	CD14,CD16,CD11B,CD68,HLA-DR,CD33, CD11C, CD123, CD15,CD66b, FCGR3A, CDKN1C, LST1,FCER1G,MS4A7,RHOC,S100A8,S100A9,CST3,C1QC
Intermediate monocytes	CD14,CD16,CD11B,CD68,HLA-DR,CD33,CD11C, CD123,CD15,CD3D, CD3E, CD3G,CD3Z,CD66b,IL1B,S100A8,S100A9,CST3, C1QC
Macrophages	CD163,CD14,CD11B,CD206,CD80,CD86,CD16,CD64,CCL18,CD115,CD11C, CD32,HLA-DR,MRC1,MSR1,GCA
Megakaryocyte	CD61,CD41,CD42B,CD41A,CD42A,CXCR4,CD110
ILC	KLRB1C, IL7R, CD127
Endothelial	PECAM1,CD34,KDR,CDH5,PROM1,PDPN,TEK,FLT1,VCAM1,PTPRC,VWF, ENG,MCAM,ICAM1,FLT4,SELE
Erythroid-like and erythroid precursor cells	PTPRC,GYPA,RUVBL1,TFRC,FOLR1,CD36,ITGA4,HBB,CD235a,HBD,CA1
HSC/MPP cells	CD105,CD34,CD44,CD73,CD45,CD29,STRO-1, NANOG, SOX2, CD133, CD166, CD146, CD31, NES, OCT4, CD117, KDR, CXCL8, AVP, CRHBP, ALDH1A1, CD49, CD90,CD69,CD24,CD38, KRT19, ASPM, CD10, CD123, ABCG2, CD135, CD49F, EPCAM, KRT7, SCA1, CD14,CD150,CD271,HLA-DR
Progenitor cells	CD105,CD34,CD44,CD73,CD45,CD29,STRO-1,NANOG,SOX2, CD133,CD166, CD146,CD31,NES,OCT4,CD117,KDR,AVP,CRHBP,ALDH1A1,STMN1,CD38, PTPRC,CD135
Myeloid Dendritic cells	ITGAX,CD83,CLEC4C,CD86,IL3RA,CD80,ITGAX,CD40,HLA-DQA1, CD11C, CLEC10A, CST3, GPR31, ODF3L1,PRB2, CD207, ARSE, CLEC141, MRC, EBLN1,CRIP3
Plasmacytoid Dendritic cells	ITGAX,CD83,CLEC4C,CD86,IL3RA,CD80,ITGAX,CD40,CD11C,CLEC10A, CST3,TPM2,LRRC26,ASIP,GPM6B,KRT5,NTM,SCT,SHD, KCNA5, SCARA5, EPHA2,MYMX
Granulocytes	CD203C,CD15,CD11B,CD63,CD66b,CD123,CD16,CD33,CD117,CD45,FCER1, CD125,CD13,CD14,CD25,CD44,CD69,CD9,HLA-DR, CCR3, CD116, CD11C, CD193,CD24,CD32,CD43,CXCL8,FCGR3B,MNDA,SIGLEC8,AZU1,MPO,CTSG ,LYZ
ISG expressing immune cells	IFIT1,IFIT2,IFIT3,IFIT5,ISG15,CCL3,CCL4,CCL3L3,RSAD2,OASL,CXCL10, IFI15,ISG20
Keratinocytes	KRT1,KRT10,KRTDAP,KRT14,COL17A1,KRT2,KRT5
Vessel mural cells	COX4I2,RGS5,NDUFA4L2,IGFBP7, ITGA1,VTN,TM4SF1,GM13889,CCL11, ESAM,PDGFRa, PDGFRb
Melanocytes	PTGDS,GPNMB,CYSTM1,PMEL,MLANA,TYRP1,DCT,STMN1,CD59,KIT, APOE,GPR1,GSTP1
Fibroblasts	COL1A1,LUM,COL1A2,COL3A1,TWIST2,MEG3,DCN,TWIST1,VCAM1, COL6A2,COL6A1,CD34, PDGFRA,FBN1
Epidermis	KRT14,KRT5,SFN,KRT15,MT2,MT1,KRT17, TFAP2B,HSPB1, EPCAM, PDGFA, IFITM3, FABP5, TACSTD2,
Smooth muscle	MYL2,NR2F2,MYL9,CELSR2, ACTA2, MYH11, TAGLN,CALD1
Neuroactivity	CTSG,FPR1,GCG,GZMA,IAPP,LEP,NR3C1,P2RX5,PRSS2,SST
Pericytes	ACTA2,PRGS5,PDGFRB
Lymphatic endothelial cells	MRC1,MAF,CCL21,EFNA5,LYVE1,IGF1,PDGFC,CD74,EPHA4,CLDN5
Blood endothelial cells	MRC1,MAF,CCL21,EFNA5,LYVE1,IGF1,PDGFC,CD74,EPHA4,CLDN5
Schwann cells	S100B,S100A4,CD74,COL4A1,COL4A2,COL5A1,COL5A2,COL5A3,COL11A1, COL18A1
Submucosal secretory cell	LYZ,LTF,ZG16B,STATH,AZGP1,BPIFB1,SLP1,BPIFA1,TCN1,PIGR,DMBTA, PIP,ODAM,RNASE1,SLP1,AZGP1,XBP1,CXCL17, NUCB2,CCL28,NDFG2,
Melanoma tumour cell	CD63,KDM5B,GAL3,SPARS,MET,TMSB4X,BTF3,ACP5,VIM,HPGDS,ATP5b, FABP5

Table C.1 Cell-type-specific gene sets for assignment of cluster identities for CosMx™ analysis.

Sample	Cell ID	x	y
WT Treg	8_7	10848.66882	20050.9
WT Treg	15_7	11704.66882	19067.9
WT Treg	27_7	10199.66882	17817.9
WT Treg	70_7	11386.66882	19833.9
WT Treg	163_7	10488.66882	19344.9
WT Treg	225_7	12992.66882	19148.9
WT Treg	277_7	13020.66882	18952.9
WT Treg	380_7	11912.66882	18476.9
WT Treg	462_7	12151.66882	18015.9
WT Treg	468_7	10352.66882	17984.9
WT Treg	472_7	13041.66882	17947.9
WT Treg	50_8	17424.66875	16815.41
WT Treg	62_8	16905.66875	16654.41
WT Treg	171_8	16780.66875	18313.41
WT Treg	220_8	16653.66875	18100.41
WT Treg	276_8	18011.66875	17821.41
WT Treg	364_8	15620.66875	17284.41
WT Treg	411_8	18207.66875	16944.41
WT Treg	451_8	17572.66875	16561.41
WT Treg	525_8	17295.66875	14997.41
WT Treg	6_9	8776.335837	7208.974
WT Treg	11_9	9412.335837	6357.974
WT Treg	43_9	10768.33584	7349.974
WT Treg	117_9	9710.335837	6302.974
WT Treg	134_9	8392.335837	5983.974
WT Treg	149_9	8620.335837	5495.974
WT Treg	66_27	62771.00069	120383.8
WT Treg	203_27	64526.00069	118080.8
WT Treg	74_31	76475.66802	117633.3
WT Treg	105_31	76211.66802	117478.3
WT Treg	115_31	79003.66802	117432.3
WT Treg	164_31	78269.66802	117222.3
WT Treg	331_31	77032.66802	115730.3
WT Treg	350_31	78585.66802	115410.3
WT Treg	369_31	76474.66802	115140.3
WT Treg	390_31	79074.66802	114581.3
WT Treg	5_32	77758.66802	111911.3
WT Treg	12_32	79401.66802	111485.3
WT Treg	80_32	78693.66802	111757.3
WT Treg	147_32	78882.66802	110228.3
WT Treg	227_32	76426.66802	108974.3

WT Treg	246_32	78629.66802	108650.3
WT Treg	292_32	78761.66802	108236.3
WT Treg	43_33	74997.0001	101414.8
Pd1$^{-/-}$ Treg	85_12	9877.335863	49249.97
Pd1$^{-/-}$ Treg	99_12	9219.335863	49141.97
Pd1$^{-/-}$ Treg	147_12	9172.335863	48800.97
Pd1$^{-/-}$ Treg	164_12	9211.335863	48674.97
Pd1$^{-/-}$ Treg	169_12	10189.33586	48655.97
Pd1$^{-/-}$ Treg	186_12	9066.335863	48519.97
Pd1$^{-/-}$ Treg	210_12	10242.33586	48271.97
Pd1$^{-/-}$ Treg	259_12	7268.335863	46658.97
Pd1$^{-/-}$ Treg	260_12	6560.335863	46647.97
Pd1$^{-/-}$ Treg	20_13	6086.665963	57597.22
Pd1$^{-/-}$ Treg	22_13	8293.665963	57629.22
Pd1$^{-/-}$ Treg	26_13	6218.665963	57572.22
Pd1$^{-/-}$ Treg	91_13	5522.665963	57306.22
Pd1$^{-/-}$ Treg	154_13	5129.665963	56957.22
Pd1$^{-/-}$ Treg	170_13	6359.665963	56922.22
Pd1$^{-/-}$ Treg	173_13	4568.665963	56915.22
Pd1$^{-/-}$ Treg	209_13	4561.665963	56725.22
Pd1$^{-/-}$ Treg	218_13	6138.665963	56721.22
Pd1$^{-/-}$ Treg	268_13	5178.665963	56504.22
Pd1$^{-/-}$ Treg	295_13	4510.665963	56406.22
Pd1$^{-/-}$ Treg	316_13	5254.665963	56321.22
Pd1$^{-/-}$ Treg	321_13	4902.665963	56325.22
Pd1$^{-/-}$ Treg	370_13	5775.665963	56062.22
Pd1$^{-/-}$ Treg	406_13	4328.665963	55932.22
Pd1$^{-/-}$ Treg	426_13	4402.665963	55837.22
Pd1$^{-/-}$ Treg	432_13	5606.665963	55804.22
Pd1$^{-/-}$ Treg	467_13	5700.665963	55653.22
Pd1$^{-/-}$ Treg	574_13	4775.665963	55198.22
Pd1$^{-/-}$ Treg	577_13	4602.665963	55177.22
Pd1$^{-/-}$ Treg	637_13	6029.665963	54951.22
Pd1$^{-/-}$ Treg	643_13	5367.665963	54933.22
Pd1$^{-/-}$ Treg	657_13	6288.665963	54872.22
Pd1$^{-/-}$ Treg	681_13	5319.665963	54744.22
Pd1$^{-/-}$ Treg	770_13	6537.665963	54425.22
Pd1$^{-/-}$ Treg	771_13	5502.665963	54434.22

Pd1$^{-/-}$ Treg	772_13	5235.665963	54429.22
Pd1$^{-/-}$ Treg	784_13	4626.665963	54392.22
Pd1$^{-/-}$ Treg	793_13	6179.665963	54331.22
Pd1$^{-/-}$ Treg	797_13	5261.665963	54354.22
Pd1$^{-/-}$ Treg	829_13	4861.665963	54227.22
Pd1$^{-/-}$ Treg	855_13	6373.665963	54135.22
Pd1$^{-/-}$ Treg	863_13	4307.665963	54104.22
Pd1$^{-/-}$ Treg	943_13	5030.665963	53868.22
Pd1$^{-/-}$ Treg	954_13	7704.665963	53856.22
Pd1$^{-/-}$ Treg	983_13	7934.665963	53766.22
Pd1$^{-/-}$ Treg	984_13	4384.665963	53760.22
Pd1$^{-/-}$ Treg	987_13	5579.665963	53741.22
Pd1$^{-/-}$ Treg	991_13	4784.665963	53720.22
Pd1$^{-/-}$ Treg	53_15	8060.665954	71119.46
Pd1$^{-/-}$ Treg	10_16	18324.33572	64243.97
Pd1$^{-/-}$ Treg	22_16	18006.33572	64160.97
Pd1$^{-/-}$ Treg	42_16	18124.33572	63842.97
Pd1$^{-/-}$ Treg	49_16	18643.33572	63761.97
Pd1$^{-/-}$ Treg	73_16	18659.33572	63543.97
Pd1$^{-/-}$ Treg	82_16	18132.33572	63358.97
Pd1$^{-/-}$ Treg	125_16	18205.33572	62715.97
Pd1$^{-/-}$ Treg	127_16	18328.33572	62701.97
Pd1$^{-/-}$ Treg	171_16	18619.33572	62156.97
Pd1$^{-/-}$ Treg	192_16	18114.33572	61896.97
Pd1$^{-/-}$ Treg	214_16	21002.33572	61619.97
Pd1$^{-/-}$ Treg	248_16	18317.33572	61272.97
Pd1$^{-/-}$ Treg	278_16	18460.33572	60935.97
Pd1$^{-/-}$ Treg	286_16	17646.33572	60806.97
Pd1$^{-/-}$ Treg	295_16	18266.33572	60608.97
Pd1$^{-/-}$ Treg	10_17	18561.33571	53588.97
Pd1$^{-/-}$ Treg	25_17	18553.33571	52828.97
Pd1$^{-/-}$ Treg	26_17	18773.33571	52800.97
Pd1$^{-/-}$ Treg	34_17	18587.33571	52107.97
Pd1$^{-/-}$ Treg	88_17	18843.33571	53495.97
Pd1$^{-/-}$ Treg	110_17	19108.33571	53190.97
Pd1$^{-/-}$ Treg	113_17	18717.33571	53159.97
Pd1$^{-/-}$ Treg	123_17	19242.33571	53013.97

Pd1$^{-/-}$ Treg	133_17	19408.33571	52836.97
Pd1$^{-/-}$ Treg	172_17	19045.33571	52419.97
Pd1$^{-/-}$ Treg	182_17	19333.33571	52327.97
Pd1$^{-/-}$ Treg	212_17	20275.33571	52116.97
Pd1$^{-/-}$ Treg	234_17	20253.33571	51959.97
Pd1$^{-/-}$ Treg	282_17	20043.33571	51664.97
Pd1$^{-/-}$ Treg	296_17	18781.33571	51566.97
Pd1$^{-/-}$ Treg	299_17	19320.33571	51581.97
Pd1$^{-/-}$ Treg	310_17	18682.33571	51462.97
Pd1$^{-/-}$ Treg	317_17	20902.33571	51451.97
Pd1$^{-/-}$ Treg	6_18	34647.66564	54628.1
Pd1$^{-/-}$ Treg	21_18	31828.66564	52557.1
Pd1$^{-/-}$ Treg	25_18	31518.66564	52275.1
Pd1$^{-/-}$ Treg	36_18	33093.66564	51797.1
Pd1$^{-/-}$ Treg	62_18	34252.66564	55333.1
Pd1$^{-/-}$ Treg	110_18	34255.66564	55089.1
Pd1$^{-/-}$ Treg	119_18	33778.66564	55040.1
Pd1$^{-/-}$ Treg	128_18	33516.66564	55006.1
Pd1$^{-/-}$ Treg	148_18	33771.66564	54898.1
Pd1$^{-/-}$ Treg	150_18	33928.66564	54883.1
Pd1$^{-/-}$ Treg	298_18	32411.66564	54099.1
Pd1$^{-/-}$ Treg	353_18	33583.66564	53744.1
Pd1$^{-/-}$ Treg	354_18	33149.66564	53738.1
Pd1$^{-/-}$ Treg	358_18	34355.66564	53714.1
Pd1$^{-/-}$ Treg	382_18	33633.66564	53544.1
Pd1$^{-/-}$ Treg	462_18	31185.66564	53143.1
Pd1$^{-/-}$ Treg	586_18	32698.66564	52372.1
Pd1$^{-/-}$ Treg	600_18	34642.66564	52344.1
Pd1$^{-/-}$ Treg	615_18	33680.66564	52270.1
Pd1$^{-/-}$ Treg	641_18	33736.66564	52135.1
Pd1$^{-/-}$ Treg	645_18	33809.66564	52115.1
Pd1$^{-/-}$ Treg	685_18	34724.66564	51931.1
Pd1$^{-/-}$ Treg	706_18	34467.66564	51836.1
Pd1$^{-/-}$ Treg	742_18	32764.66564	51693.1
Pd1$^{-/-}$ Treg	770_18	32626.66564	51588.1
Pd1$^{-/-}$ Treg	802_18	34725.66564	51360.1
Pd1$^{-/-}$ Treg	13_19	32423.66563	60348.08

Pd1$^{-/-}$ Treg	17_19	32466.66563	59981.08
Pd1$^{-/-}$ Treg	38_19	33038.66563	58846.08
Pd1$^{-/-}$ Treg	41_19	34935.66563	58631.08
Pd1$^{-/-}$ Treg	45_19	33713.66563	58351.08
Pd1$^{-/-}$ Treg	73_19	33482.66563	60986.08
Pd1$^{-/-}$ Treg	88_19	34731.66563	60880.08
Pd1$^{-/-}$ Treg	105_19	31927.66563	60741.08
Pd1$^{-/-}$ Treg	158_19	31651.66563	60354.08
Pd1$^{-/-}$ Treg	182_19	34546.66563	60182.08
Pd1$^{-/-}$ Treg	187_19	34026.66563	60168.08
Pd1$^{-/-}$ Treg	228_19	31241.66563	59968.08
Pd1$^{-/-}$ Treg	279_19	32836.66563	59700.08
Pd1$^{-/-}$ Treg	313_19	34777.66563	59574.08
Pd1$^{-/-}$ Treg	334_19	35330.66563	59504.08
Pd1$^{-/-}$ Treg	340_19	34877.66563	59460.08
Pd1$^{-/-}$ Treg	375_19	35016.66563	59311.08
Pd1$^{-/-}$ Treg	406_19	33179.66563	59176.08
Pd1$^{-/-}$ Treg	407_19	33311.66563	59180.08
Pd1$^{-/-}$ Treg	462_19	33371.66563	58969.08
Pd1$^{-/-}$ Treg	492_19	34275.66563	58894.08
Pd1$^{-/-}$ Treg	505_19	34353.66563	58819.08
Pd1$^{-/-}$ Treg	515_19	31592.66563	58785.08
Pd1$^{-/-}$ Treg	547_19	34832.66563	58651.08
Pd1$^{-/-}$ Treg	549_19	34266.66563	58631.08
Pd1$^{-/-}$ Treg	590_19	35087.66563	58511.08
Pd1$^{-/-}$ Treg	599_19	34586.66563	58471.08
Pd1$^{-/-}$ Treg	603_19	34117.66563	58453.08
Pd1$^{-/-}$ Treg	636_19	33037.66563	58305.08
Pd1$^{-/-}$ Treg	664_19	33892.66563	58193.08
Pd1$^{-/-}$ Treg	678_19	33672.66563	58157.08
Pd1$^{-/-}$ Treg	679_19	34473.66563	58135.08
Pd1$^{-/-}$ Treg	736_19	32784.66563	57868.08
Pd1$^{-/-}$ Treg	746_19	33165.66563	57842.08
Pd1$^{-/-}$ Treg	793_19	35123.66563	57643.08
Pd1$^{-/-}$ Treg	822_19	32761.66563	57547.08
Pd1$^{-/-}$ Treg	888_19	34905.66563	57295.08
Pd1$^{-/-}$ Treg	898_19	34613.66563	57263.08

Pd1$^{-/-}$ Treg	961_19	31823.66563	57080.08
Pd1$^{-/-}$ Treg	992_19	34408.66563	57003.08
Pd1$^{-/-}$ Treg	1_20	31522.66564	66760.05
Pd1$^{-/-}$ Treg	8_20	34443.66564	66221.05
Pd1$^{-/-}$ Treg	11_20	34653.66564	65605.05
Pd1$^{-/-}$ Treg	32_20	32552.66564	66909.05
Pd1$^{-/-}$ Treg	104_20	34480.66564	66648.05
Pd1$^{-/-}$ Treg	105_20	33229.66564	66644.05
Pd1$^{-/-}$ Treg	108_20	33799.66564	66659.05
Pd1$^{-/-}$ Treg	126_20	33011.66564	66525.05
Pd1$^{-/-}$ Treg	195_20	34274.66564	66302.05
Pd1$^{-/-}$ Treg	233_20	32800.66564	66153.05
Pd1$^{-/-}$ Treg	244_20	31703.66564	66110.05
Pd1$^{-/-}$ Treg	245_20	32911.66564	66121.05
Pd1$^{-/-}$ Treg	312_20	33539.66564	65881.05
Pd1$^{-/-}$ Treg	357_20	33396.66564	65677.05
Pd1$^{-/-}$ Treg	367_20	32206.66564	65638.05
Pd1$^{-/-}$ Treg	560_20	33092.66564	64762.05
Pd1$^{-/-}$ Treg	564_20	31997.66564	64775.05
Pd1$^{-/-}$ Treg	567_20	34515.66564	64746.05
Pd1$^{-/-}$ Treg	576_20	31365.66564	64737.05
Pd1$^{-/-}$ Treg	582_20	30877.66564	64702.05
Pd1$^{-/-}$ Treg	701_20	33720.66564	64254.05
Pd1$^{-/-}$ Treg	775_20	31533.66564	63917.05
Pd1$^{-/-}$ Treg	810_20	30934.66564	63782.05
Pd1$^{-/-}$ Treg	836_20	33761.66564	63717.05
Pd1$^{-/-}$ Treg	873_20	31759.66564	63556.05
Pd1$^{-/-}$ Treg	896_20	30992.66564	63458.05
Pd1$^{-/-}$ Treg	899_20	34068.66564	63458.05
Pd1$^{-/-}$ Treg	907_20	33481.66564	63417.05
Pd1$^{-/-}$ Treg	940_20	33956.66564	63290.05
Pd1$^{-/-}$ Treg	964_20	34205.66564	63172.05
Pd1$^{-/-}$ Treg	1009_20	30521.66564	62946.05
Pd1$^{-/-}$ Treg	1046_20	32688.66564	62781.05
Pd1$^{-/-}$ Treg	3_21	23650.66575	77293.39
Pd1$^{-/-}$ Treg	8_21	22112.66575	76948.39
Pd1$^{-/-}$ Treg	55_21	25012.66575	77320.39

Pd1$^{-/-}$ Treg	66_21	22910.66575	77301.39
Pd1$^{-/-}$ Treg	134_21	21746.66575	77126.39
Pd1$^{-/-}$ Treg	159_21	23153.66575	77056.39
Pd1$^{-/-}$ Treg	393_21	22247.66575	76412.39
Pd1$^{-/-}$ Treg	427_21	24911.66575	76289.39
Pd1$^{-/-}$ Treg	488_21	24070.66575	76038.39
Pd1$^{-/-}$ Treg	571_21	22923.66575	75673.39
Pd1$^{-/-}$ Treg	706_21	21969.66575	74616.39
Pd1$^{-/-}$ Treg	29_34	23301.99975	100471.4
Pd1$^{-/-}$ Treg	70_34	20943.99975	99682.44
Pd1$^{-/-}$ Treg	81_34	22131.99975	99465.44
Pd1$^{-/-}$ Treg	82_34	22285.99975	99476.44
Pd1$^{-/-}$ Treg	105_34	20583.99975	98927.44
Pd1$^{-/-}$ Treg	146_34	22751.99975	101110.4
Pd1$^{-/-}$ Treg	174_34	22210.99975	100603.4
Pd1$^{-/-}$ Treg	176_34	22531.99975	100592.4
Pd1$^{-/-}$ Treg	213_34	23088.99975	100187.4
Pd1$^{-/-}$ Treg	224_34	20876.99975	100111.4
Pd1$^{-/-}$ Treg	226_34	21828.99975	100100.4
Pd1$^{-/-}$ Treg	244_34	22858.99975	99912.44
Pd1$^{-/-}$ Treg	248_34	24301.99975	99904.44
Pd1$^{-/-}$ Treg	264_34	22463.99975	99760.44
Pd1$^{-/-}$ Treg	267_34	21128.99975	99728.44
Pd1$^{-/-}$ Treg	275_34	22609.99975	99596.44
Pd1$^{-/-}$ Treg	279_34	22212.99975	99580.44
Pd1$^{-/-}$ Treg	301_34	21190.99975	99372.44
Pd1$^{-/-}$ Treg	308_34	20600.99975	99247.44
Pd1$^{-/-}$ Treg	313_34	20778.99975	99164.44
Pd1$^{-/-}$ Treg	3_36	18876.33573	112584
Pd1$^{-/-}$ Treg	2_37	12117.33579	110658
Pd1$^{-/-}$ Treg	35_37	14517.33579	109512
Pd1$^{-/-}$ Treg	57_37	12464.33579	110455
Pd1$^{-/-}$ Treg	70_37	14475.33579	110268
Pd1$^{-/-}$ Treg	94_37	14526.33579	109899
Pd1$^{-/-}$ Treg	99_37	13882.33579	109844
Pd1$^{-/-}$ Treg	127_37	14464.33579	109481
Pd1$^{-/-}$ Treg	131_37	14110.33579	109402

Pd1$^{-/-}$ Treg	26_38	9455.999917	105645.3
Pd1$^{-/-}$ Treg	43_38	10421.99992	105471.3
Pd1$^{-/-}$ Treg	45_38	9184.999917	105432.3
Pd1$^{-/-}$ Treg	48_38	9652.999917	105420.3
Pd1$^{-/-}$ Treg	52_38	9538.999917	105396.3
Pd1$^{-/-}$ Treg	73_38	9513.999917	105216.3
Pd1$^{-/-}$ Treg	85_38	10554.99992	105087.3
Pd1$^{-/-}$ Treg	86_38	9199.999917	105072.3
Pd1$^{-/-}$ Treg	99_38	9840.999917	104943.3
Pd1$^{-/-}$ Treg	107_38	8578.999917	104887.3
Pd1$^{-/-}$ Treg	124_38	8763.999917	104763.3
Pd1$^{-/-}$ Treg	127_38	9136.999917	104730.3
Pd1$^{-/-}$ Treg	130_38	8327.999917	104705.3
Pd1$^{-/-}$ Treg	179_38	9018.999917	104420.3
Pd1$^{-/-}$ Treg	189_38	7179.999917	104384.3
Pd1$^{-/-}$ Treg	199_38	8199.999917	104287.3
Pd1$^{-/-}$ Treg	207_38	10296.99992	104277.3
Pd1$^{-/-}$ Treg	231_38	7356.999917	104184.3
Pd1$^{-/-}$ Treg	236_38	6937.999917	104131.3
Pd1$^{-/-}$ Treg	250_38	10789.99992	104093.3
Pd1$^{-/-}$ Treg	252_38	9087.999917	104060.3
Pd1$^{-/-}$ Treg	277_38	10576.99992	103976.3
Pd1$^{-/-}$ Treg	9_39	5723.999949	118073.5
Pd1$^{-/-}$ Treg	23_39	6689.999949	117869.5
Pd1$^{-/-}$ Treg	28_39	6187.999949	117852.5
Pd1$^{-/-}$ Treg	35_40	5590.335875	109414
Pd1$^{-/-}$ Treg	37_40	5855.335875	109369
Pd1$^{-/-}$ Treg	44_40	6160.335875	109176

Table C.2 Treg Cell ID and coordinates on FOV images.

Alone	Tumour	Melanocyte	Schwann	Basal	Monocyte	DC	ILC	Mast cell	Treg	NK	Macrophage	LEC	CD4	Endothelial
15_7	27_7	411_8*	105_31	8_7	50_8*	784_13	169_12	357_20	127_16	260_12	11_9	331_31*	643_13	6_9*
462_7	70_7	771_13	115_31	62_8	85_12	299_17	199_38	248_34	641_18	295_13	74_31		829_13	210_12*
468_7	163_7	855_13	369_31	66_27	20_13	23_39	131_37	130_38	645_18	863_13	147_32		133_17	
220_8	277_7	128_18	987_13	246_32	22_13	991_13	29_34	252_38	41_19	110_17	259_12		105_20	
364_8	380_7	148_18	88_17	80_32	91_13	984_13	793_13	171_16	547_19	182_17	173_13		70_34	
43_9	225_7	353_18	21_18	147_12	406_13	224_34	49_16	170_13	549_19	212_17	218_13		81_34	
117_9	472_7	187_19	62_18	164_12	426_13	664_19	954_13	797_13	35_37	45_19	574_13		179_38	
134_9	276_8	313_19	110_18	186_12	125_16	99_12	192_16	370_13	127_37	736_19	22_16			
149_9	171_8	406_19	340_19	26_13	10_17	770_13	577_13	772_13		896_20	73_16			
203_27	451_8	492_19	462_19	42_16	34_17	234_17	154_13	310_17		82_34	25_17			
164_31	525_8	505_19	590_19	278_16	810_20	248_16	316_13	10_16		176_34	113_17			
390_31	350_31	515_19	599_19	26_17	226_34			983_13		213_34	615_18			
5_32	292_32	108_20	636_19	172_17	275_34			681_13		99_38	685_18			
12_32	268_13	560_20	898_19	150_18	279_34			73_38		277_38	907_20			
227_32	637_13	701_20	104_20	382_18	301_34			282_17		44_40	244_34			
43_33	943_13	873_20	244_20	888_19	26_38			321_13			264_34			
467_13	82_16	8_21	55_21	961_19	45_38			678_19			313_34			
657_13	295_16	706_21	134_21	57_37	231_38			209_13			94_37			
53_15	6_18	427_21	488_21	37_40	236_38			296_17			43_38			
214_16	36_18	836_20	571_21		250_38			432_13			48_38			
286_16	119_18	245_20	127_38								52_38			
123_17	298_18										107_38			
317_17	358_18										124_38			
25_18	600_18										207_38			
354_18	706_18													
462_18	742_18													
586_18	802_18													
770_18	73_19													
13_19	182_19													
17_19	228_19													
38_19	334_19													
88_19	375_19													
105_19	407_19													
158_19	603_19													
279_19	793_19													
746_19	679_19													
822_19	992_19													
1_20	11_20													
8_20	233_20													
32_20	312_20													
126_20	775_20													
195_20	66_21													
367_20	159_21													
564_20	174_34													
567_20	189_38													
576_20	2_37													
582_20	9_39													
899_20														
940_20														
964_20														
1009_20														
1046_20														
3_21														
393_21														
105_34														
146_34														
267_34														
308_34														
3_36														
70_37														
99_37														
85_38														
86_38														
28_39														
35_40														

Table C.3 Grouping of Treg subsets by using specific Cell ID based on physical cell-cell interaction on FOVs.

gene	p_val	log2FC	cluster	signalling
G0s2	8.00923E-05	4.548436625	Treg_Basal	SR
Ifi27	8.00923E-05	4.548436625	Treg_Basal	LR
Klf2	8.00923E-05	4.548436625	Treg_Basal	LR
Bst2	0.002316579	3.548436625	Treg_Basal	SR
Ephb6	0.002316579	3.548436625	Treg_Basal	SR
Hdac1	0.002316579	3.548436625	Treg_Basal	SR
Il17ra	0.002316579	3.548436625	Treg_Basal	SR
Map1lc3b	0.002316579	3.548436625	Treg_Basal	SR
Rac2	0.002316579	3.548436625	Treg_Basal	SR
Rigi	0.002316579	3.548436625	Treg_Basal	SR
Sod1	0.002316579	3.548436625	Treg_Basal	SR
Selplg	0.002340948	2.641546029	Treg_Basal	LR
Adgre5	0.003053991	2.963474124	Treg_Basal	SR
Itgb6	0.003053991	2.963474124	Treg_Basal	SR
Angpt2	0.006503821	3.963474124	Treg_Basal	LR
Areg	0.006503821	3.963474124	Treg_Basal	LR
Btk	0.006503821	3.963474124	Treg_Basal	LR
Ccl22	0.006503821	3.963474124	Treg_Basal	LR
Cd22	0.006503821	3.963474124	Treg_Basal	SR
Cd33	0.006503821	3.963474124	Treg_Basal	SR
Cd36	0.006503821	3.963474124	Treg_Basal	SR
Cdh1	0.006503821	3.963474124	Treg_Basal	SR
Cldn4	0.006503821	3.963474124	Treg_Basal	SR
Clec1a	0.006503821	3.963474124	Treg_Basal	SR
Ctsg	0.006503821	3.963474124	Treg_Basal	SR
Cuzd1	0.006503821	3.963474124	Treg_Basal	SR
Cxcl1	0.006503821	3.963474124	Treg_Basal	LR
Cxcl2	0.006503821	3.963474124	Treg_Basal	LR
Igfbp6	0.006503821	3.963474124	Treg_Basal	SR
Igkc	0.006503821	4.548436625	Treg_Basal	LR
Il23a	0.006503821	3.963474124	Treg_Basal	LR
Itk	0.006503821	4.548436625	Treg_Basal	LR
Krt8	0.006503821	3.963474124	Treg_Basal	SR
Lamp3	0.006503821	3.963474124	Treg_Basal	SR
Map2k1	0.006503821	3.963474124	Treg_Basal	LR
Mmp14	0.006503821	3.963474124	Treg_Basal	SR
Msmb	0.006503821	3.963474124	Treg_Basal	LR
Nrxn3	0.006503821	3.963474124	Treg_Basal	SR
Pgr	0.006503821	3.963474124	Treg_Basal	SR
Pparg	0.006503821	3.963474124	Treg_Basal	SR
Rarres1	0.006503821	3.963474124	Treg_Basal	SR

Rbpj	0.006503821	3.963474124	Treg_Basal	SR
Slc2a1	0.006503821	3.963474124	Treg_Basal	SR
Sorbs1	0.006503821	3.963474124	Treg_Basal	LR
Spry2	0.006503821	3.963474124	Treg_Basal	SR
Stmn1	0.006503821	3.963474124	Treg_Basal	SR
Tshz2	0.006503821	3.963474124	Treg_Basal	SR
Vcam1	0.006503821	3.963474124	Treg_Basal	LR
Cd27	0.006631037	3.129283017	Treg_Alone	SR
Gpnmb	0.001587229	2.253756592	Treg_Tumor	LR
Twist2	0.006765479	3.838719093	Treg_Tumor	LR
Fau	0.006775673	3.253756592	Treg_Tumor	SR
Ttr	2.561E-05	4.772589504	Treg_Macrophage	SR
Csf1	3.24853E-05	4.357552005	Treg_Macrophage	LR
NLRp2	3.24853E-05	4.357552005	Treg_Macrophage	SR
Acvr1b	0.000310141	4.772589504	Treg_Macrophage	SR
Ccr10	0.000310141	4.772589504	Treg_Macrophage	LR
Col12a1	0.000310141	4.772589504	Treg_Macrophage	SR
Col8a1	0.000310141	4.772589504	Treg_Macrophage	SR
Dcn	0.000310141	4.772589504	Treg_Macrophage	SR
Flt1	0.000310141	5.357552005	Treg_Macrophage	LR
Fzd7	0.000310141	4.772589504	Treg_Macrophage	SR
H2-Ob	0.000310141	4.772589504	Treg_Macrophage	SR
Il1r1	0.000310141	4.772589504	Treg_Macrophage	SR
Il1rl1	0.000310141	4.772589504	Treg_Macrophage	SR
Il36g	0.000310141	5.357552005	Treg_Macrophage	LR
Itga1	0.000310141	4.772589504	Treg_Macrophage	SR
Krt10	0.000310141	4.772589504	Treg_Macrophage	SR
Krt6b	0.000310141	4.772589504	Treg_Macrophage	SR
Mmp12	0.000310141	5.357552005	Treg_Macrophage	LR
Myh6	0.000310141	4.772589504	Treg_Macrophage	SR
Myl9	0.000310141	4.772589504	Treg_Macrophage	SR
Notch2	0.000310141	4.772589504	Treg_Macrophage	SR
Nusap1	0.000310141	4.772589504	Treg_Macrophage	SR
Pdgfb	0.000310141	4.772589504	Treg_Macrophage	SR
Ramp2	0.000310141	5.357552005	Treg_Macrophage	SR
Tnxb	0.000310141	4.772589504	Treg_Macrophage	SR
Wnt11	0.000310141	4.772589504	Treg_Macrophage	SR
Col4a2	0.000322912	4.187627003	Treg_Macrophage	SR
Ffar2	0.000463869	3.772589504	Treg_Macrophage	SR
SRsf2	0.007092156	3.03562391	Treg_Macrophage	SR
Clu	1.75026E-07	5.357552005	Treg_Schwann	SR
Tek	3.24853E-05	4.357552005	Treg_Schwann	LR

Abl1	0.000310141	4.772589504	Treg_Schwann	LR
Bmp5	0.000310141	4.772589504	Treg_Schwann	LR
C1qc	0.000310141	4.772589504	Treg_Schwann	SR
Calm1	0.000310141	4.772589504	Treg_Schwann	SR
Camp	0.000310141	4.772589504	Treg_Schwann	LR
Cd200r3	0.000310141	5.357552005	Treg_Schwann	SR
Cd24a	0.000310141	5.357552005	Treg_Schwann	SR
Cd69	0.000310141	4.772589504	Treg_Schwann	SR
Crp	0.000310141	4.772589504	Treg_Schwann	LR
Cxcr4	0.000310141	4.772589504	Treg_Schwann	LR
Fzd8	0.000310141	4.772589504	Treg_Schwann	SR
Gzmf	0.000310141	4.772589504	Treg_Schwann	SR
H2-Q1	0.000310141	4.772589504	Treg_Schwann	SR
Hilpda	0.000310141	4.772589504	Treg_Schwann	SR
Hmgcs1	0.000310141	4.772589504	Treg_Schwann	SR
Il1a	0.000310141	5.357552005	Treg_Schwann	LR
Kit	0.000310141	4.772589504	Treg_Schwann	SR
Myl12a	0.000310141	4.772589504	Treg_Schwann	SR
Myl7	0.000310141	4.772589504	Treg_Schwann	SR
NLRc4	0.000310141	4.772589504	Treg_Schwann	LR
NLRp3	0.000310141	4.772589504	Treg_Schwann	LR
Rgs2	0.000310141	4.772589504	Treg_Schwann	SR
Tpm1	0.000310141	4.772589504	Treg_Schwann	SR
Rarg	0.000322912	4.187627003	Treg_Schwann	SR

Table C.4 Enriched genes in WT Treg subsets.

gene	p_val	log2FC	cluster	signalling
Havcr2	0.000283243	2.743279368	Treg_Monocyte	SR
Flt3l	0.001192827	3.328241869	Treg_Monocyte	SR
Nosip	0.001313445	3.006313774	Treg_Monocyte	SR
Notch3	0.001313445	3.006313774	Treg_Monocyte	SR
Gzmb	0.001513533	2.328241869	Treg_Monocyte	SR
Abl1	0.00298624	3.105849447	Treg_Monocyte	LR
Itgb2	0.003304791	2.783921353	Treg_Monocyte	SR
Smo	0.003304791	2.783921353	Treg_Monocyte	SR
Syk	0.003467674	2.591276275	Treg_Monocyte	SR
Wnt9a	0.004282947	2.368883853	Treg_Monocyte	LR
Sat1	0.00489746	2.150703683	Treg_Monocyte	LR
Mrc2	0.006242439	2.91320437	Treg_Monocyte	SR
Bmp1	0.00625719	3.176238775	Treg_Monocyte	SR
S100a8	0.007938162	1.91320437	Treg_Monocyte	SR
Cxcr4	0.000336087	3.42931163	Treg_DC	LR
Sell	0.000469545	4.107383535	Treg_DC	LR
Krt14	0.000941931	2.728871912	Treg_DC	SR
Fzd5	0.002246224	2.943884803	Treg_DC	SR
Cdkn1a	0.002857569	2.050800007	Treg_DC	SR
Irf4	0.002906068	2.522421035	Treg_DC	LR
Ephb4	0.003719411	3.621956708	Treg_DC	LR
S100a4	0.003719411	3.621956708	Treg_DC	SR
Col6a1	0.004255877	3.206919209	Treg_DC	SR
Hmgcs1	0.004645207	2.84434913	Treg_DC	SR
Il34	0.006358097	2.522421035	Treg_DC	LR
Il10ra	0.006609809	2.341848789	Treg_DC	SR
Krt80	0.008599566	3.014274131	Treg_DC	SR
Snai2	0.008599566	3.014274131	Treg_DC	LR
Bag3	0.008930144	2.84434913	Treg_DC	SR
Adgrg5	0.009194333	2.42931163	Treg_DC	SR
Npr1	0.009194333	2.42931163	Treg_DC	SR
Wif1	3.76291E-07	2.975546956	Treg_Basal	SR
Jun	6.80488E-06	3.384937892	Treg_Basal	LR
Fasn	7.4874E-06	3.215012891	Treg_Basal	SR
Cd79a	1.62208E-05	3.741081703	Treg_Basal	SR
Gzma	2.38463E-05	3.063009798	Treg_Basal	SR
Gata3	5.89228E-05	3.063009798	Treg_Basal	LR
Casr	0.000137966	2.925506274	Treg_Basal	SR
Ido1	0.000160164	2.684498174	Treg_Basal	SR
Jak2	0.000260095	3.255654875	Treg_Basal	LR
Sorbs1	0.000260095	3.255654875	Treg_Basal	SR

Ikzf3	0.000278062	3.063009798	Treg_Basal	LR
Scgb3a1	0.00033131	2.57758297	Treg_Basal	LR
Cd3e	0.000585435	2.57758297	Treg_Basal	SR
Cxcl5	0.000733326	2.741081703	Treg_Basal	LR
H2-Q1	0.000814807	3.647972298	Treg_Basal	SR
Ifitm1	0.001171763	2.215012891	Treg_Basal	LR
Anxa1	0.001626386	2.741081703	Treg_Basal	SR
Osmr	0.001626386	2.741081703	Treg_Basal	SR
Tap2	0.001626386	2.741081703	Treg_Basal	SR
Ccdc80	0.001711725	2.384937892	Treg_Basal	SR
Psca	0.0018166	2.297475051	Treg_Basal	LR
Ddc	0.002692018	2.215012891	Treg_Basal	SR
Il23a	0.002723763	2.925506274	Treg_Basal	SR
Chek1	0.003020368	2.741081703	Treg_Basal	SR
Cd8b1	0.003062726	3.326044203	Treg_Basal	SR
Nfkbia	0.003062726	3.326044203	Treg_Basal	SR
Cd164	0.00316636	2.603578179	Treg_Basal	SR
Tubb5	0.00316636	2.603578179	Treg_Basal	SR
Oas1a/g	0.003331174	2.478047297	Treg_Basal	SR
Blk	0.003805497	2.815082284	Treg_Basal	LR
Il7r	0.004563007	2.925506274	Treg_Basal	SR
Gm13889	0.005342191	2.603578179	Treg_Basal	none
Tyrobp	0.005342191	2.603578179	Treg_Basal	LR
Slc2a1	0.005574889	2.478047297	Treg_Basal	LR
Cd38	0.005839711	2.362570079	Treg_Basal	SR
Stat5a	0.00611503	2.255654875	Treg_Basal	LR
Gper1	0.007961523	3.063009798	Treg_Basal	SR
Il17rb	0.007961523	3.063009798	Treg_Basal	SR
Itga2	0.007961523	3.063009798	Treg_Basal	LR
Itgav	0.007961523	3.063009798	Treg_Basal	SR
Ramp3	0.008598923	1.99262047	Treg_Basal	SR
Bmpr2	0.009067856	2.362570079	Treg_Basal	SR
Osm	0.009463341	2.255654875	Treg_Basal	LR
Lair1	0.009696041	2.94753258	Treg_Basal	SR
Myh11	0.009872968	2.156119202	Treg_Basal	SR
Epha4	1.23954E-09	4.84434913	Treg_ILC	SR
Birc3	6.00935E-05	3.206919209	Treg_ILC	SR
Lefty1	9.27454E-05	2.663776884	Treg_ILC	SR
Arg1	0.000411478	3.107383535	Treg_ILC	SR
Mmp19	0.000530129	3.692346036	Treg_ILC	SR
Clec10a	0.000562481	3.42931163	Treg_ILC	SR
Fzd1	0.000838513	2.969880012	Treg_ILC	SR

Upk3a	0.000886365	2.84434913	Treg_ILC	SR
Fgf13	0.000941931	2.728871912	Treg_ILC	LR
Rspo3	0.001062249	2.42931163	Treg_ILC	LR
Itgb6	0.001720796	2.621956708	Treg_ILC	SR
Fzd8	0.001735481	3.42931163	Treg_ILC	SR
Il6ra	0.001735481	3.42931163	Treg_ILC	SR
Gas6	0.003391258	2.943884803	Treg_ILC	SR
Col6a2	0.003719411	3.621956708	Treg_ILC	SR
Nlrp1a	0.004203921	2.621956708	Treg_ILC	LR
Dcn	0.004255877	3.206919209	Treg_ILC	SR
Xcl1	0.004255877	3.206919209	Treg_ILC	LR
Stat1	0.004443466	3.014274131	Treg_ILC	LR
Hdac11	0.006358097	2.522421035	Treg_ILC	SR
Il34	0.006358097	2.522421035	Treg_ILC	LR
Atf3	0.008599566	3.014274131	Treg_ILC	LR
Iapp	0.008599566	3.014274131	Treg_ILC	SR
Il1r2	0.008599566	3.014274131	Treg_ILC	SR
Il1rap	0.008599566	3.014274131	Treg_ILC	SR
Pdgfrb	0.008599566	3.014274131	Treg_ILC	SR
Acvrl1	0.008930144	2.84434913	Treg_ILC	SR
Cd200r3	0.008930144	2.84434913	Treg_ILC	SR
Ctsg	0.008930144	2.554842512	Treg_ILC	SR
Cd93	1.2888E-07	3.434231065	Treg_Macrophage	LR
Vegfb	0.000172549	2.69726547	Treg_Macrophage	LR
Ccr2	0.000228337	3.434231065	Treg_Macrophage	LR
Selenop	0.000228337	3.434231065	Treg_Macrophage	LR
Il7	0.00024475	3.11230297	Treg_Macrophage	LR
Nlrc4	0.000377341	2.559761947	Treg_Macrophage	LR
Hsp90ab1	0.000417029	1.960299876	Treg_Macrophage	SR
Fzd8	0.000957916	3.11230297	Treg_Macrophage	SR
Ifnl2/3	0.000957916	3.11230297	Treg_Macrophage	SR
Il20ra	0.000957916	3.11230297	Treg_Macrophage	SR
Il17b	0.001015291	2.849268564	Treg_Macrophage	LR
Bmp7	0.002116135	2.334695391	Treg_Macrophage	LR
Fgf18	0.002588054	3.171196659	Treg_Macrophage	LR
Ccl26	0.002748916	3.434231065	Treg_Macrophage	LR
Cd80	0.002748916	3.434231065	Treg_Macrophage	SR
Tgfbr1	0.002748916	3.434231065	Treg_Macrophage	SR
Acvr1b	0.002821654	2.849268564	Treg_Macrophage	SR
S100b	0.002821654	2.849268564	Treg_Macrophage	SR
Cd276	0.003121267	2.434231065	Treg_Macrophage	LR
Tek	0.003280225	2.171196659	Treg_Macrophage	LR

Inhbb	0.003461725	2.171196659	Treg_Macrophage	LR
Rnf43	0.005855917	2.171196659	Treg_Macrophage	SR
Lyve1	0.005990485	2.948804237	Treg_Macrophage	SR
Mlh1	0.006151908	2.055719441	Treg_Macrophage	SR
Adgrg3	0.006559299	2.626876142	Treg_Macrophage	SR
Il1r2	0.006559299	2.626876142	Treg_Macrophage	SR
Sec23a	0.006559299	2.626876142	Treg_Macrophage	SR
Map2k1	0.006848295	2.434231065	Treg_Macrophage	LR
Rigi	0.007160881	2.11230297	Treg_Macrophage	SR
Cd86	0.008601714	1.931730724	Treg_Macrophage	SR
Btf3	5.12844E-05	3.109298642	Treg_NK	LR
Ifng	0.000139049	3.694261143	Treg_NK	LR
Nosip	0.000157411	3.372333048	Treg_NK	SR
Stat4	0.000493499	3.149940627	Treg_NK	LR
Il27ra	0.000525101	2.957295549	Treg_NK	SR
Dusp2	0.000576774	2.694261143	Treg_NK	SR
Snai1	0.00102118	2.220329955	Treg_NK	SR
Krt6b	0.00123574	2.957295549	Treg_NK	SR
Nell2	0.00123574	2.957295549	Treg_NK	LR
Casp8	0.002904052	2.49786393	Treg_NK	LR
Tgfbi	0.004724613	3.220329955	Treg_NK	LR
Cd68	0.004933909	2.635367454	Treg_NK	SR
Icam2	0.004933909	2.635367454	Treg_NK	LR
Msr1	0.005402342	2.372333048	Treg_NK	SR
Nr1h2	0.005402342	2.372333048	Treg_NK	SR
Irf3	0.006585082	2.191760803	Treg_NK	LR
Itgax	0.008427172	2.49786393	Treg_NK	LR
Twist2	0.008427172	2.49786393	Treg_NK	LR
Krt17	0.008766597	2.372333048	Treg_NK	SR
Sfn	0.008766597	2.372333048	Treg_NK	SR
Cdkn3	0.009302037	3.957295549	Treg_NK	LR
Stat5a	0.009548765	2.149940627	Treg_NK	LR
Birc5	0.000188284	4.09592442	Treg_Mast	SR
Col4a5	0.000188284	4.09592442	Treg_Mast	SR
Ms4a4b	0.000349065	2.230854	Treg_Mast	SR
Nusap1	0.000442753	2.832890014	Treg_Mast	SR
Efnb2	0.0019612	2.925999419	Treg_Mast	SR
Il33	0.0019612	2.925999419	Treg_Mast	LR
Adgrg6	0.002066697	2.703606997	Treg_Mast	SR
Etv5	0.002093848	2.510961919	Treg_Mast	LR
Ace	0.002206675	2.373458396	Treg_Mast	SR
Fap	0.002206675	2.373458396	Treg_Mast	SR

Il7r	0.002206675	2.373458396	Treg_Mast	SR
Rela	0.004954324	2.510961919	Treg_Mast	LR
Serpina1a	0.005830534	2.008461579	Treg_Mast	SR
Tpi1	0.000302021	1.654004145	Treg_Tumor	SR
Ccl21a/b/d	0.000533953	2.291434066	Treg_Tumor	LR
Vsir	0.000688008	2.654004145	Treg_Tumor	SR
Cyp1b1	0.000731767	2.97593224	Treg_Tumor	SR
Ezh2	0.000731767	2.97593224	Treg_Tumor	LR
Cd59a	0.001397219	1.953564427	Treg_Tumor	SR
Pgk1	0.001424731	1.869732836	Treg_Tumor	SR
Celsr1	0.001806509	2.431611724	Treg_Tumor	LR
Il10rb	0.002457018	3.069041644	Treg_Tumor	SR
Sox2	0.002457018	3.069041644	Treg_Tumor	LR
P2rx5	0.0025048	2.654004145	Treg_Tumor	SR
Ndrg1	0.004028269	2.238966646	Treg_Tumor	SR
Ptgs1	0.006126113	2.654004145	Treg_Tumor	SR
Sqle	0.006515105	2.390969739	Treg_Tumor	SR
Gpnmb	0.008183384	1.213431554	Treg_Tumor	SR
Hdac3	0.00877763	2.97593224	Treg_Tumor	SR
Cd55	0.009162096	2.654004145	Treg_Tumor	SR
Chek2	0.009162096	2.654004145	Treg_Tumor	SR
Plac9	0.000338498	2.191839778	Treg_Alone	SR
Bmp5	0.003603594	2.758880371	Treg_Alone	SR
Igfbp3	0.006506129	2.021914776	Treg_Alone	SR
Itga3	4.43415E-07	4.690496915	Treg_CD4	SR
Sostdc1	5.4042E-06	4.36856882	Treg_CD4	LR
Oasl1	9.45824E-06	3.198643819	Treg_CD4	SR
Cryab	1.6356E-05	3.520571913	Treg_CD4	SR
Prss34	2.59276E-05	3.727022791	Treg_CD4	SR
Cx3cl1	3.53206E-05	3.883141993	Treg_CD4	LR
Angpt2	0.000126638	3.883141993	Treg_CD4	SR
Elane	0.000246586	3.105534414	Treg_CD4	SR
Snai2	0.000366171	3.690496915	Treg_CD4	SR
Acvrl1	0.000389057	3.520571913	Treg_CD4	SR
Atr	0.000860698	3.520571913	Treg_CD4	SR
Tnfsf13b	0.000860698	3.520571913	Treg_CD4	SR
Mx1	0.000961337	3.105534414	Treg_CD4	SR
Il22ra1	0.001424338	4.520571913	Treg_CD4	SR
Ackr3	0.001739305	3.36856882	Treg_CD4	SR
Itgb8	0.001739305	3.36856882	Treg_CD4	SR
Notch1	0.001739305	3.36856882	Treg_CD4	SR
Camp	0.001921632	2.990057197	Treg_CD4	SR

Arg1	0.003136919	3.231065296	Treg_CD4	SR
Pld3	0.003136919	3.231065296	Treg_CD4	SR
S100a10	0.003136919	3.231065296	Treg_CD4	SR
Tyms	0.004494466	1.990057197	Treg_CD4	SR
Ccnd1	0.00518209	3.105534414	Treg_CD4	SR
Tigit	0.00518209	3.105534414	Treg_CD4	SR
Cd8a	0.005390832	2.990057197	Treg_CD4	SR
Ctla4	0.005390832	2.883141993	Treg_CD4	SR
Epha2	0.005390832	2.990057197	Treg_CD4	LR
Wnt7a	0.005390832	2.990057197	Treg_CD4	SR
Itm2b	0.005629487	2.883141993	Treg_CD4	SR
Smad2	0.007313831	4.105534414	Treg_CD4	LR
Fkbp5	0.007585056	3.783606319	Treg_CD4	SR
Ctsw	0.00798822	2.990057197	Treg_CD4	SR
Hdac5	0.00798822	2.990057197	Treg_CD4	SR
Rnf43	0.008281161	2.883141993	Treg_CD4	SR
Foxp3	0.000203342	0.528520291	Treg_Melanocyte	LR
Gpx3	0.001991382	3.510961919	Treg_Melanocyte	SR
Sparcl1	0.003952313	2.288569498	Treg_Melanocyte	LR
Timp1	0.00404646	2.132450296	Treg_Melanocyte	SR
Uba52	0.005853386	1.703606997	Treg_Melanocyte	SR
Rgs1	0.008358886	3.09592442	Treg_Melanocyte	SR
Tpt1	0.009184236	1.684991319	Treg_Melanocyte	SR
Krt6b	0.009604866	2.510961919	Treg_Melanocyte	SR
Spry4	0.009730902	2.773996325	Treg_Melanocyte	SR
Cntfr	0.009996373	2.341036918	Treg_Melanocyte	SR
Pdgfb	4.43822E-06	4.412530644	Treg_Schwann	SR
Epcam	4.74941E-06	4.090602549	Treg_Schwann	LR
Pdgfd	9.9561E-06	3.897957471	Treg_Schwann	SR
Pigr	0.000140459	3.090602549	Treg_Schwann	SR
Ccr1	0.000427753	2.67556505	Treg_Schwann	LR
Nr1h3	0.001479641	2.67556505	Treg_Schwann	SR
Cd209a	0.001570538	2.560087832	Treg_Schwann	SR
Epor	0.001993025	3.190138222	Treg_Schwann	SR
Csf1	0.002219358	2.868210127	Treg_Schwann	LR
Iapp	0.002219358	2.868210127	Treg_Schwann	SR
Stat4	0.002219358	2.868210127	Treg_Schwann	LR
Col1a1	0.002462464	2.505640048	Treg_Schwann	SR
Lgals3bp	0.002910792	2.412530644	Treg_Schwann	SR
Cav1	0.003056057	2.297053426	Treg_Schwann	SR
Mif	0.004224034	1.277015673	Treg_Schwann	LR
Lama4	0.004321934	2.997493144	Treg_Schwann	SR

Apoa1	0.004542138	3.26052755	Treg_Schwann	SR
Ddr2	0.004542138	3.26052755	Treg_Schwann	LR
Cspg4	0.004744175	2.938599455	Treg_Schwann	SR
Cdkn1a	0.007008699	1.897957471	Treg_Schwann	SR
Camp	0.007289383	3.31299497	Treg_Schwann	SR
Lgals1	0.008075402	1.817584054	Treg_Schwann	SR
Ccr7	0.008520619	2.67556505	Treg_Schwann	LR
Fn1	0.008644893	2.801095932	Treg_Schwann	SR
Ccl5	2.39274E-06	3.321928095	Treg_Treg	LR
Zfp36	4.23285E-06	3.736965594	Treg_Treg	LR
Il12rb1	8.32212E-05	3.206450877	Treg_Treg	SR
Lyn	0.000126554	3.906890596	Treg_Treg	SR
Mt1	0.000184138	2.473931188	Treg_Treg	LR
Wnt5a	0.000199922	4.321928095	Treg_Treg	SR
Kdr	0.00041975	3.684498174	Treg_Treg	SR
Tlr1	0.000474301	3.321928095	Treg_Treg	SR
Il16	0.001073398	3.491853096	Treg_Treg	LR
Spry2	0.002286474	3.321928095	Treg_Treg	LR
Col3a1	0.002517048	3.032421478	Treg_Treg	SR
Tpsb2	0.003314325	3.906890596	Treg_Treg	SR
Atp5e	0.004262161	3.169925001	Treg_Treg	SR
Glud1	0.004262161	3.169925001	Treg_Treg	SR
Clec2d	0.004444508	3.032421478	Treg_Treg	SR
Clock	0.004444508	3.032421478	Treg_Treg	SR
Ly6d	0.004444508	3.032421478	Treg_Treg	SR
Smarcb1	0.004444508	3.032421478	Treg_Treg	SR
Tap2	0.004444508	3.032421478	Treg_Treg	SR
Txk	0.004444508	3.032421478	Treg_Treg	LR
Il15ra	0.004783416	2.263034406	Treg_Treg	SR
Il2	0.006094508	3.321928095	Treg_Treg	LR
Tnfrsf9	0.006094508	3.321928095	Treg_Treg	SR
Btf3	0.00718573	3.032421478	Treg_Treg	LR
Ifitm3	0.00718573	3.032421478	Treg_Treg	SR
Inhba	0.007462338	2.906890596	Treg_Treg	LR
Npr3	0.007462338	2.906890596	Treg_Treg	SR
H2-DMb2	0.007772673	2.791413378	Treg_Treg	SR
Il23a	0.007772673	2.791413378	Treg_Treg	LR
Cd70	0.009096753	3.321928095	Treg_Treg	SR

Table C.5 Enriched genes in *Pd1*$^{-/-}$ Treg subsets.

Appendix D

Human PBMCs from healthy donors were derived from NHS Blood and Transplant (NHSBT) in Newcastle upon Tyne. Stage IV metastatic melanoma patients were recruited from Royal Victoria Infirmary in Newcastle upon Tyne under ethics [REC reference 24/NE/0014]. Publicly mined dataset (Tirosh et al., 2016, Sade-Feldman et al., 2018) included tumour-infiltrating lymphocytes (TILs) from treatment naïve patients, and patients treated with anti-PD-1 including pre and post treatment. The characteristics of metastatic melanoma patients used are shown in **Table D.1**. In-house BD Rhapsody scRNA-seq of peripheral blood mononuclear cells (PBMCs) from Stage IV human melanoma patients and healthy controls (HC) was performed by Ms. Tegan McTaggart, using a panel of 30 AbSeq antibodies and a human immune response gene panel. According to cell-type-specific gene list shown in **Table D.2**, immune cell clusters in PBMCs from HC and melanoma patients were defined based on AbSeq protein expression and a manual review process based on the algorithmically defined marker gene expression for each cluster with *FindAllMarkers* function with default Wilcoxon rank-sum test with Bonferroni's correction with results shown in **Table D.3**. We also used publicly available scRNA-seq datasets on TILs from treatment-naïve melanoma patients alongside melanoma patients at baseline or anti-PD-1-treated conditions. Cluster identities were annotated based on the algorithmically defined marker gene expression for each cluster with *FindAllMarkers* function, which the top preferentially expressed genes ($p<0.001$) included multiple known markers of particular cell types. The results were shown in **Table D.4** for treatment-naïve TILs and in **Table D.5** for baseline/anti-PD-1-treated TILs.

Cohort	Sample	Patient ID	Age	Sex	Treatment	Lesion Type	Biopsy Site
In this Paper	Patient 1	P1	26	F	baseline blood draw	metastasis	Blood
	Patient 2	P2	54	F	basleine blood draw	metastasis	Blood
	Patient 3	P3	55	M	baseline blood draw	metastasis	Blood
Tirosh et al, 2016	Mel79	Mel79	74	M	Naïve	metastasis	LN
	Mel80	Mel80	86	F	Naïve	metastasis	LN
	Mel82	Mel82	81	M	Naïve	metastasis	LN
	Mel53	Mel53	77	F	Naïve	metastasis	Subcutaneous cancer
Sade-Feldman et al, 2018	P2	Pre_P2	75	M	baseline biopsy pre anti-PD1	metastasis	Small bowel
	P6	Pre_P6	66	F	baseline biopsy pre anti-PD1	metastasis	Left upper back
	P15	Pre_P15	72	M	baseline biopsy pre anti-PD1	metastasis	Right back subcutaneous
	P20	Pre_P20	64	F	baseline biopsy pre anti-PD1	metastasis	Right inguinoiliac lymphadenectomy
	P25	Pre_P25	74	M	baseline biopsy pre anti-PD1	metastasis	Adrenal gland
	P27	Pre_P27	62	F	baseline biopsy pre anti-PD1	metastasis	Upper abdomen
	P31	Pre_P31	65	F	baseline biopsy pre anti-PD1	metastasis	Left axillary lymph node
	P2	Post_P2	75	M	αPD1	metastasis	Left axilla
	P6	Post_P6	66	F	αPD1	metastasis	Right colectomy mass in caecum
	P10	Post_P10	60	F	αPD1	metastasis	Small bowel mass
	P11	Post_P11	68	F	αPD1	metastasis	Lymph node
	P12	Post_P12	68	M	αPD1	metastasis	Left anterior shoulder
	P14	Post_P14	70	M	αPD1	metastasis	Left axilla lesion
	P15	Post_P15	72	M	αPD1	metastasis	Left lower back
	P16	Post_P16	62	M	αPD1	metastasis	Right abdomen soft tissue
	P17	Post_P17	68	F	αPD1	metastasis	Lymph node
	P18	Post_P18	79	M	αPD1	metastasis	Lymph node
	P19	Post_P19	53	M	αPD1	metastasis	Lymph node
	P20	Post_P20	64	F	αPD1	metastasis	Right pelvic mass
	P21	Post_P21	75	F	αPD1	metastasis	Jejunum
	P23	Post_P23	62	M	αPD1	metastasis	Left frontal craniotomy
	P30	Post_P30	64	M	αPD1	metastasis	Left laparoscopic adrenalectomy

Table D.1 Clinical characteristics of the metastatic melanoma patients and information of samples used in the scRNA-seq analysis.

Cell type	Gene
Pro-B cell	CD27, IgD, CD24, PTPRC, PAX5, CD24, CD38, CD79A, DNTT, C10orf10, VPREB1, ARPP21, CD99, IGLL1, CD9, CD79B, TCL1A, IGLL5, HLA-DQA1, HLA-DQB1, VPREB3, IGLL5
Pre-B cell	CD19, CD27, IgD, CD24, PTPRC, PAX5, CD24, CD38, CD79A, NSMCE1, PCDH9, ACSM3, CCDC191, TCL1A, CD79B, TCL1A, IGLL5, HLA-DQA1, HLA-DQB1, VPREB3, IGLL5
Immature B cell	CD19, CD27, IgD, CD24, CD20, MS4A1, PTPRC, PAX5, CD24, CD38, CD79A, CXCL8, S100A12, LYZ, CD79B, TCL1A, IGLL5, HLA-DQA1, HLA-DQB1, VPREB3, IGLL5
Naive B cell	CD19, IgD, CD38, CD24, CD20, MS4A1, PTPRC, PAX5, CD24, CD38, CD79A, JCHAIN, SSR4, FKBP11, SEC11C, DERL3, PRDX4, IGLL5, CD79B, TCL1A, IGLL5, HLA-DQA1, HLA-DQB1, CD138, CD38, VPREB3, IGLL5
Memory B cell	CD19, CD27, IgD, CD38, CD24, CD20, MS4A1, PTPRC, PAX5, CD24, CD38, CD79A, JCHAIN, SSR4, FKBP11, SEC11C, DERL3, PRDX4, IGLL5, CD79B, TCL1A, IGLL5, HLA-DQA1, HLA-DQB1, CD138, CD38, CD27, VPREB3, IGLL5
Plasma B cell	CD19, CD27, IgD, CD38, CD24, CD20, MS4A1, PTPRC, PAX5, CD24, CD38, CD79A, JCHAIN, SSR4, FKBP11, SEC11C, DERL3, PRDX4, IGLL5, CD79B, TCL1A, IGLL5, HLA-DQA1, HLA-DQB1, CD138, CD38, VPREB3, IGLL5
Naive CD8+ T cell	CD8, CD2, CD3D, CD3E, CD3G, CD3Z, CD45RA, CD62L, CD27, CD127, CCR7, CD45, CD8A, CD8B, CD6, IL2RA, GZMB, PTPRC, SELL, CCR7, GNLY
Naive CD4+ T cell	CD4, CD2, CD3D, CD3E, CD3G, CD3Z, CD45RA, CD62L, CD27, CD127, CCR7, CD45, IL2RA, GZMB, PTPRC, SELL, CCR7
Memory CD8+ T cell	CD8, CD2, CD3D, CD3E, CD3G, CD3Z, CD25, CD62L, CD27, CD127, CCR7, CD45, CD8A, CD8B, CCR6, CD45RO, CD6, , IL2RA, GZMB, SELL, CCR7
Memory CD4+ T cell	CD4, CD2, CD3D, CD3E, CD3G, CD3Z, CD25, CD62L, CD27, CD127, CCR7, CD45, CCR6, CD45RO, IL2RA, GZMB, SELL, CCR7
Effector CD8+ T cell	CD8, CD2, CD3D, CD3E, CD3G, CD3Z, CD25, CD62L, CD27, CD127, CCR7, CD45, CD8A, CD8B, CD6, CTLA4, IL2RA, GZMB, PTPRC, GNLY
Effector CD4+ T cell	CD4, CD2, CD3D, CD3E, CD3G, CD3Z, CD25, CD62L, CD27, CD127, CCR7, CD45, CD6, CTLA4, IL2RA, GZMB, PTPRC
Treg	CD4, CD2, CD3D, CD3E, CD3G, CD3Z, CD25, CD45RA, CD62L, CD27, CD127, FOXP3, CCR7, CD45, CD30, CD45RO, CD6, CTLA4, IL2RA, GZMB, SELL, CCR7
γδ-T cell	CD2, CD3D, CD3E, CD3G, CD3Z, CD25, CD45RA, CD62L, CD27, CD127, CCR7, CD45, CTLA4, IL2RA, GZMB, PTPRC, TRDV2, TRGV9, TRGC1
Platelet	CD41, CD42b, CD61, CD31, PPBP, PF4, GNG11, SDPR, CLU, CD41, CD110
CD8+ NKT-like cell	CD8, CD56, CD2, CD16, CD94, CD3D, CD3E, CD3G, CD3Z, NKp46, CD161, CD314, CD69, NKG7, CD122, NKG2D, GZMB, GZMA, GZMM, GNLY, COX6A2, ZMAT4, KIR2DL4
CD4+ NKT-like cell	CD4, CD56, CD2, CD16, CD94, CD3D, CD3E, CD3G, CD3Z, NKp46, CD161, CD314, CD69, NKG7, CD122, NKG2D, GZMB, GZMA, GZMM, COX6A2, ZMAT4, KIR2DL4
Natural killer cell	CD56, CD2, CD16, CD94, NKp46, CD161, CD314, CD69, NKG7, CD122, NKG2D, GZMB, GZMA, GZMM, FCGR3A, GNLY, COX6A2, ZMAT4, KIR2DL4, NKG7
Eosinophil	CD11b, CD193, CD123, CD125, CD15, SIGLEC8, CLC, GATA1, CEBPE, SEMG1, ALOX15, CCL23, PRSS41, PRSS33, THBS4, FOXI1
Neutrophil	CD66b, CD11b, CD15, CD16, CXCL8, FCGR3B, MNDA, CXCR2, MPO, ELANE, PRTN3, MPO, AZU1, LYZ, S100A8, S100A9, PI3, CHI3L1, ANXA3, CXCL1, TGM3, BTNL3, C4BPA, MMP9, CD24, BPI, LTF, GCA
Basophil	CD63, CD203c, CD123, CLC, MS4A3, TCN1, CPA3, HDC, GATA2, MS4A2, IL4, GCSAML, GATA2, TPSAB1
Mast cell	CD117, CD203c, CD25, KIT, SLC18A2, CD33, CD32, FCER1A, TPSD1, HPGDS
Classical Monocyte	CD14, CD11b, CD68, HLA-DR, CD33, CD11c, CD123, CD15, CD3D, CD3E, CD3G, CD3Z, CD66b, VCAN, S100A12, CXCL8, S100A8, S100A9, LYZ, CST3
Non-classical monocyte	CD14, CD16, CD11b, CD68, HLA-DR, CD33, CD11c, CD123, CD15, CD3D, CD3E, CD3G, CD3Z, CD66b, FCGR3A, CDKN1C, LST1, FCER1G, MS4A7, RHOC, S100A8, S100A9, CST3, C1QC
Intermediate monocyte	CD14, CD16, CD11b, CD68, HLA-DR, CD33, CD11c, CD123, CD15, CD3D, CD3E, CD3G, CD3Z, CD66b, IL1B, S100A8, S100A9, CST3, C1QC
Macrophage	CD68, CD163, CD14, CD11b, CD206, CD80, CD86, CD16, CD64, CCL18, CD115, CD11c, CD32, HLA-DR, MRC1, MSR1, GCA
Megakaryocyte	CD61, CD41, CD42b, CD41a, CD42a, CXCR4, CD110
Endothelial	PECAM1, CD34, KDR, CDH5, PROM1, PDPN, TEK, FLT1, VCAM1, PTPRC, VWF, ENG, MCAM, ICAM1, FLT4, SELE
Erythroid-like and erythroid precursor cell	PTPRC, GYPA, RUVBL1, TFRC, FOLR1, CD36, ITGA4, HBB, CD235a, HBD, CA1
HSC/MPP cell	CD105, CD34, CD44, CD73, CD45, CD29, STRO-1, NANOG, SOX2, CD133, CD166, CD146, CD31, Nestin, OCT4, CD117, KDR, CXCL8, AVP, CRHBP, ALDH1A1, CD49, CD90, CD69, CD24, CD38, CD45RA, Keratin-19, ASPM, CD10, CD123, ABCG2, CD135, CD49f, EpCAM, Keratin-7, SCA-1, CD14, CD150, CD271, HLA-DR
Progenitor cell	CD105, CD34, CD44, CD73, CD45, CD29, STRO-1, NANOG, SOX2, CD133, CD166, CD146, CD31, Nestin, OCT4, CD117, KDR, AVP, CRHBP, ALDH1A1, STMN1, CD38, PTPRC, CD135
Myeloid Dendritic cell	ITGAX, CD83, CD1C, NRP1, CLEC4C, CD86, IL3RA, CD80, CD1A, ITGAX, CD40, HLA-DQA1, CD11c, HLA-DR, HLA-DPB1, HLA-DPA1, CLEC10A, CST3, GPR31, ODF3L1, PRB2, CD207, ARSE, CLEC141, MRC, EBLN1, CRIP3
Plasmacytoid Dendritic cell	ITGAX, CD83, CD1C, NRP1, CLEC4C, CD86, IL3RA, CD80, CD1A, ITGAX, CD40, HLA-DQA1, CD11c, HLA-DR, HLA-DPB1, HLA-DPA1, CLEC10A, CST3, TPM2, LRRC26, ASIP, GPM6B, KRT5, NTM, SCT, SHD, KCNA5, SCARA5, EPHA2, MYMX
Granulocyte	CD203c, CD15, CD11b, CD63, CD66b, CD123, CD16, CD33, CD117, CD45, Fc-epsilon RI-alpha, CD125, CD13, CD14, CD25, CD44, CD69, CD9, HLA-DR, CCR3, CD116, CD11c, CD193, CD24, CD32, CD43, CXCL8, FCGR3B, MNDA, SIGLEC8, AZU1, MPO, CTSG, LYZ
ISG expressing immune cell	IFIT1, IFIT2, IFIT3, IFIT5, ISG15, CCL3, CCL4, CCL3L3, RSAD2, OASL, CXCL10, IFI15, ISG20

Table D.2 Cell-type-specific gene sets for assignment of cluster identities for human PBMC scRNA-seq analysis.

gene	p_val	log2FC	p_val_adj	cluster
CD4	0	2.24762663	0	CD4+ Tmem
KLRK1	0	-4.5100897	0	CD4+ Tmem
CD8A	0	-5.0337944	0	CD4+ Tmem
IL7R	0	1.07480774	0	CD4+ Tmem
GZMB	0	-5.5577623	0	CD4+ Tmem
NKG7	0	-4.8651833	0	CD4+ Tmem
PRF1	0	-4.3674059	0	CD4+ Tmem
CTSW	0	-2.6583373	0	CD4+ Tmem
CST7	0	-3.1135052	0	CD4+ Tmem
FCGR3A	3.47E-282	-5.4550162	1.29E-279	CD4+ Tmem
GZMH	2.38E-274	-4.6199233	8.83E-272	CD4+ Tmem
CCL5	8.76E-242	-2.5053086	3.25E-239	CD4+ Tmem
CD8B	8.11E-226	-4.847407	3.01E-223	CD4+ Tmem
TRAC	5.88E-219	0.70304883	2.18E-216	CD4+ Tmem
IL23R	1.83E-196	0.72127345	6.79E-194	CD4+ Tmem
TRAT1	1.09E-187	1.44732046	4.06E-185	CD4+ Tmem
CD5	9.03E-187	1.11191329	3.35E-184	CD4+ Tmem
PIK3AP1	3.56E-182	-4.3602872	1.32E-179	CD4+ Tmem
GZMA	8.52E-177	-1.9213419	3.16E-174	CD4+ Tmem
GNLY	2.68E-176	-4.23853	9.95E-174	CD4+ Tmem
TARP-refseq	3.72E-167	-2.3789329	1.38E-164	CD4+ Tmem
LYN	1.32E-157	-4.8146347	4.89E-155	CD4+ Tmem
CD6	3.64E-155	0.78443708	1.35E-152	CD4+ Tmem
ITGAM	5.64E-155	-3.2726701	2.09E-152	CD4+ Tmem
HLA-DPA1	1.25E-148	-2.696911	4.64E-146	CD4+ Tmem
CD28	2.54E-143	1.42267408	9.43E-141	CD4+ Tmem
TBX21	3.37E-140	-2.6874794	1.25E-137	CD4+ Tmem
IL2RB	5.52E-138	-2.3121851	2.05E-135	CD4+ Tmem
KLRF1	1.08E-132	-4.4369565	4.02E-130	CD4+ Tmem
LTB	1.07E-131	1.75096484	3.98E-129	CD4+ Tmem
RUNX3	1.05E-129	-1.2963277	3.90E-127	CD4+ Tmem
S100A10	8.26E-129	0.46417749	3.07E-126	CD4+ Tmem
TRDC	3.46E-124	-4.5124632	1.28E-121	CD4+ Tmem
CD300A	2.31E-121	-2.3453557	8.59E-119	CD4+ Tmem
ITGB2	1.19E-118	-1.1251241	4.41E-116	CD4+ Tmem
CD74	4.83E-118	-2.3280216	1.79E-115	CD4+ Tmem
CD2	1.35E-117	0.51942247	5.00E-115	CD4+ Tmem
FCER1G	1.06E-116	-5.3818093	3.91E-114	CD4+ Tmem
CCL4	5.03E-114	-4.9822815	1.87E-111	CD4+ Tmem
LEF1	4.82E-110	0.66402175	1.79E-107	CD4+ Tmem
CD244	4.06E-108	-4.8964027	1.51E-105	CD4+ Tmem

IL32	3.42E-105	0.37566187	1.27E-102	CD4+ Tmem
FYB	1.44E-103	0.85897852	5.35E-101	CD4+ Tmem
YBX3	1.28E-99	-3.3955479	4.73E-97	CD4+ Tmem
TNFRSF25	5.23E-99	1.55426033	1.94E-96	CD4+ Tmem
CD44	2.59E-96	0.51225254	9.59E-94	CD4+ Tmem
TNFSF8	3.65E-93	1.13607575	1.36E-90	CD4+ Tmem
ITGAX	2.34E-91	-4.105551	8.69E-89	CD4+ Tmem
CX3CR1	1.77E-90	-4.3783592	6.56E-88	CD4+ Tmem
TCF7	5.72E-90	1.22669194	2.12E-87	CD4+ Tmem
LAT2	8.23E-88	-3.8207261	3.05E-85	CD4+ Tmem
KLRC1	1.33E-86	-4.5371341	4.94E-84	CD4+ Tmem
ZNF683	1.85E-78	-3.94322	6.85E-76	CD4+ Tmem
MYC	2.01E-78	0.84260899	7.47E-76	CD4+ Tmem
CD52	2.12E-77	0.26615656	7.88E-75	CD4+ Tmem
RORC	8.01E-76	1.58449479	2.97E-73	CD4+ Tmem
TNFSF10	6.84E-74	1.0509602	2.54E-71	CD4+ Tmem
NCR3	2.96E-68	-2.3798057	1.10E-65	CD4+ Tmem
IRF8	6.84E-67	-3.7626631	2.54E-64	CD4+ Tmem
HLA-DRA	6.73E-65	-3.8849611	2.50E-62	CD4+ Tmem
HLA-DMA	7.04E-65	-2.4721861	2.61E-62	CD4+ Tmem
IL18RAP	3.67E-64	-2.5084469	1.36E-61	CD4+ Tmem
B3GAT1	2.86E-63	-4.2888486	1.06E-60	CD4+ Tmem
ICOS	6.62E-63	1.32442729	2.45E-60	CD4+ Tmem
CCR4	3.78E-62	2.2495084	1.40E-59	CD4+ Tmem
PTPRC	2.39E-61	-0.541193	8.85E-59	CD4+ Tmem
CD160	4.50E-59	-6.6963627	1.67E-56	CD4+ Tmem
CD63	1.25E-57	-1.1213519	4.64E-55	CD4+ Tmem
PASK	1.78E-56	0.77936569	6.61E-54	CD4+ Tmem
CD3E	1.87E-56	0.24697685	6.95E-54	CD4+ Tmem
TRBC2	1.47E-55	0.40108691	5.45E-53	CD4+ Tmem
ANXA5	5.92E-54	0.38807406	2.20E-51	CD4+ Tmem
CD3D	2.67E-52	0.17251071	9.91E-50	CD4+ Tmem
KIR2DL1	3.45E-51	-5.258333	1.28E-48	CD4+ Tmem
CD27	4.65E-51	0.56645689	1.73E-48	CD4+ Tmem
KLRC3	3.94E-50	-4.429923	1.46E-47	CD4+ Tmem
TSPAN32	2.95E-49	-1.4374556	1.10E-46	CD4+ Tmem
DPP4	3.37E-48	1.03325698	1.25E-45	CD4+ Tmem
CD38	5.62E-47	-5.21807	2.08E-44	CD4+ Tmem
CD22	7.58E-47	-3.1391406	2.81E-44	CD4+ Tmem
JUNB	7.86E-47	0.51005665	2.92E-44	CD4+ Tmem
PIK3IP1	1.36E-45	0.2943268	5.06E-43	CD4+ Tmem
FAS	1.58E-45	1.03077883	5.86E-43	CD4+ Tmem

CTLA4	4.59E-45	1.35855045	1.70E-42	CD4+ Tmem
CCL3	3.68E-44	-4.395311	1.36E-41	CD4+ Tmem
BCL11B	7.00E-43	0.46758458	2.60E-40	CD4+ Tmem
CD3G	8.79E-43	0.49143211	3.26E-40	CD4+ Tmem
BIRC3	1.68E-42	0.72430343	6.22E-40	CD4+ Tmem
HAVCR2	2.22E-42	-3.3595585	8.22E-40	CD4+ Tmem
CD79A	2.27E-42	-3.8318879	8.43E-40	CD4+ Tmem
CD69	7.08E-41	0.39080092	2.63E-38	CD4+ Tmem
KIT	7.23E-38	1.96769375	2.68E-35	CD4+ Tmem
LGALS3	2.33E-36	0.66156062	8.63E-34	CD4+ Tmem
DUSP4	3.48E-36	1.92335304	1.29E-33	CD4+ Tmem
LAT	3.67E-36	0.33865633	1.36E-33	CD4+ Tmem
LY86	1.36E-35	-4.1821289	5.04E-33	CD4+ Tmem
IL2RA	4.19E-35	1.43882807	1.56E-32	CD4+ Tmem
IGHD-membrane	1.66E-34	-3.6862309	6.15E-32	CD4+ Tmem
CXCR3	2.52E-34	1.18837237	9.36E-32	CD4+ Tmem
DUSP2	5.92E-34	-1.085707	2.20E-31	CD4+ Tmem
MS4A1	9.33E-34	-2.7102683	3.46E-31	CD4+ Tmem
HLA-DQB1	1.40E-33	-2.308661	5.20E-31	CD4+ Tmem
GIMAP5	2.91E-33	0.57139292	1.08E-30	CD4+ Tmem
KLRC4	1.80E-32	-4.6848743	6.68E-30	CD4+ Tmem
CD247	1.16E-31	-1.0338048	4.30E-29	CD4+ Tmem
APOBEC3G	2.13E-31	-1.2246183	7.90E-29	CD4+ Tmem
IGHM-membrane	3.36E-31	-3.3053171	1.25E-28	CD4+ Tmem
TRIB2	4.41E-31	0.52713385	1.64E-28	CD4+ Tmem
KLRG1	6.92E-31	-1.4463987	2.57E-28	CD4+ Tmem
CCR2	1.51E-30	0.78586973	5.61E-28	CD4+ Tmem
PAX5	1.73E-30	-2.7064306	6.41E-28	CD4+ Tmem
IGHM-secreted	3.15E-30	-3.1854508	1.17E-27	CD4+ Tmem
BCL2	4.15E-30	0.60278694	1.54E-27	CD4+ Tmem
TNFRSF4	4.80E-30	1.96198919	1.78E-27	CD4+ Tmem
IRF4	2.03E-29	-2.5108536	7.54E-27	CD4+ Tmem
GIMAP2	2.65E-29	0.36863167	9.82E-27	CD4+ Tmem
POU2AF1	7.39E-28	-2.8030292	2.74E-25	CD4+ Tmem
CD86	1.54E-27	-5.5050672	5.72E-25	CD4+ Tmem
BIN2	2.70E-27	-0.5676734	1.00E-24	CD4+ Tmem
ZBTB16	8.35E-27	-2.0692765	3.10E-24	CD4+ Tmem
PRDM1	9.45E-27	0.29437002	3.51E-24	CD4+ Tmem
VNN2	1.13E-26	-1.9216644	4.19E-24	CD4+ Tmem
VPREB3	1.68E-25	-3.4564657	6.24E-23	CD4+ Tmem
LAG3	1.85E-25	-2.0265942	6.86E-23	CD4+ Tmem
IFNGR1	2.34E-25	-1.3358879	8.69E-23	CD4+ Tmem

CD7	6.98E-24	-1.2197091	2.59E-21	CD4+ Tmem
BLNK	8.52E-24	-3.7532583	3.16E-21	CD4+ Tmem
CBLB	1.13E-23	-0.8814542	4.19E-21	CD4+ Tmem
TXK	6.27E-23	-1.0747642	2.33E-20	CD4+ Tmem
FCER2	1.37E-22	-2.5423161	5.10E-20	CD4+ Tmem
CCND2	2.07E-21	0.28083016	7.69E-19	CD4+ Tmem
CD40	3.81E-21	-2.6977643	1.41E-18	CD4+ Tmem
LAIR2	5.77E-21	-2.3690494	2.14E-18	CD4+ Tmem
CD24	8.66E-21	-3.5056667	3.21E-18	CD4+ Tmem
MZB1	1.12E-20	-3.2767279	4.14E-18	CD4+ Tmem
SLC7A7	3.26E-20	-4.9057278	1.21E-17	CD4+ Tmem
CCR7	3.88E-20	0.11259942	1.44E-17	CD4+ Tmem
STAT1	6.07E-20	0.39982567	2.25E-17	CD4+ Tmem
CTSD	6.49E-20	-1.3166176	2.41E-17	CD4+ Tmem
HLA-A	9.17E-20	-0.2704614	3.40E-17	CD4+ Tmem
DUSP1	9.19E-20	-0.7210796	3.41E-17	CD4+ Tmem
CXCR2	4.52E-19	-5.6559117	1.68E-16	CD4+ Tmem
CMKLR1	5.29E-19	-6.06102	1.96E-16	CD4+ Tmem
CD1C	2.63E-18	-3.6635565	9.75E-16	CD4+ Tmem
FCN1	1.13E-17	-5.5699456	4.19E-15	CD4+ Tmem
CD33	4.22E-17	-5.2012541	1.57E-14	CD4+ Tmem
FOSB	5.99E-17	-0.492116	2.22E-14	CD4+ Tmem
CD48	8.04E-17	0.12406791	2.98E-14	CD4+ Tmem
RORA	1.05E-16	0.19501621	3.91E-14	CD4+ Tmem
FYN	3.47E-16	-0.5049124	1.29E-13	CD4+ Tmem
KDELR1	4.62E-16	0.67054527	1.71E-13	CD4+ Tmem
LAMP1	5.71E-16	-0.4489589	2.12E-13	CD4+ Tmem
IGHG1-secreted	6.37E-16	-4.8053011	2.37E-13	CD4+ Tmem
IGKC	8.55E-16	-4.1076672	3.17E-13	CD4+ Tmem
JCHAIN	1.84E-15	-5.3120193	6.83E-13	CD4+ Tmem
TCF4	5.30E-15	-4.1566262	1.97E-12	CD4+ Tmem
FOXP1	6.87E-15	0.29572743	2.55E-12	CD4+ Tmem
KLRB1	1.21E-14	-0.4134865	4.50E-12	CD4+ Tmem
FASLG	1.26E-14	-2.716086	4.68E-12	CD4+ Tmem
IGLC3	1.35E-14	-4.210092	5.01E-12	CD4+ Tmem
F5	2.35E-14	1.6442452	8.72E-12	CD4+ Tmem
IGBP1	2.74E-14	0.29433341	1.02E-11	CD4+ Tmem
IKZF2	8.73E-14	-2.1316297	3.24E-11	CD4+ Tmem
TGFBI	3.42E-13	-2.8401856	1.27E-10	CD4+ Tmem
CXCL16	1.14E-12	-2.2333971	4.23E-10	CD4+ Tmem
RNASE6	1.46E-12	-2.0512019	5.43E-10	CD4+ Tmem
CD79B	4.10E-12	-1.2871016	1.52E-09	CD4+ Tmem

IFNG	8.12E-12	-1.7878949	3.01E-09	CD4+ Tmem
FAM129C	2.62E-11	-2.2315211	9.71E-09	CD4+ Tmem
CHI3L2	4.44E-11	-1.3990936	1.65E-08	CD4+ Tmem
LGALS9	4.90E-11	-0.8960428	1.82E-08	CD4+ Tmem
S100A12	1.75E-10	-5.5432618	6.49E-08	CD4+ Tmem
KCNE3	1.80E-10	-3.1347633	6.66E-08	CD4+ Tmem
CD36	1.82E-10	-4.3755966	6.74E-08	CD4+ Tmem
LILRB4	2.14E-10	-2.7395218	7.95E-08	CD4+ Tmem
EBF1	2.76E-09	-4.3499348	1.03E-06	CD4+ Tmem
LTA	5.13E-09	0.68192918	1.90E-06	CD4+ Tmem
CD163	7.23E-09	-5.9062834	2.68E-06	CD4+ Tmem
FCER1A	1.93E-08	-5.5543195	7.17E-06	CD4+ Tmem
CD72	2.06E-08	-1.5100579	7.64E-06	CD4+ Tmem
FOXO1	2.84E-08	0.45712201	1.05E-05	CD4+ Tmem
S100A9	4.17E-08	-4.9020941	1.55E-05	CD4+ Tmem
TIAF1	5.37E-08	0.17496923	1.99E-05	CD4+ Tmem
IL3RA	5.42E-08	-3.1603573	2.01E-05	CD4+ Tmem
CD37	9.36E-08	-0.36617	3.47E-05	CD4+ Tmem
IKZF1	1.12E-07	0.20494978	4.14E-05	CD4+ Tmem
NCAM1	1.12E-07	-5.3157924	4.16E-05	CD4+ Tmem
ZAP70	2.02E-07	0.18819978	7.49E-05	CD4+ Tmem
TNFRSF13C	2.22E-07	-1.8114748	8.23E-05	CD4+ Tmem
TNFSF13	2.75E-07	-1.4339366	0.0001022	CD4+ Tmem
CLEC10A	3.03E-07	-4.7903294	0.00011256	CD4+ Tmem
MGST1	3.54E-07	-3.9104948	0.00013115	CD4+ Tmem
ENTPD1	4.84E-07	-1.213318	0.00017957	CD4+ Tmem
TNF	9.77E-07	0.27840282	0.00036244	CD4+ Tmem
CLEC4E	1.99E-06	-4.3157531	0.00073718	CD4+ Tmem
CR2	2.16E-06	-1.5457677	0.00079965	CD4+ Tmem
VEGFA	2.46E-06	-3.9702768	0.00091348	CD4+ Tmem
CD14	3.16E-06	-4.3440923	0.00117073	CD4+ Tmem
TLR8	3.18E-06	-2.7812415	0.00117927	CD4+ Tmem
LGALS1	3.75E-06	-0.154124	0.00139165	CD4+ Tmem
ITGAE	3.86E-06	-0.4906719	0.00143258	CD4+ Tmem
CXCL8	5.12E-06	-4.4774262	0.00189838	CD4+ Tmem
CD200	5.29E-06	-1.3298172	0.00196131	CD4+ Tmem
SELL	5.72E-06	-0.3178683	0.00212148	CD4+ Tmem
IL12A	7.58E-06	-1.9405831	0.00281078	CD4+ Tmem
TLR2	8.28E-06	-1.7179185	0.00307367	CD4+ Tmem
IL4R	1.31E-05	-0.1048272	0.00485318	CD4+ Tmem
ARL4C	1.32E-05	-0.4614572	0.0048979	CD4+ Tmem
LIPA	3.23E-05	-0.4100095	0.01197244	CD4+ Tmem

NT5E	3.43E-05	-0.9532709	0.01273796	CD4+ Tmem
IFITM3	3.57E-05	-0.4130509	0.01326167	CD4+ Tmem
STAT6	5.51E-05	0.10042747	0.02043598	CD4+ Tmem
ADA	9.57E-05	-0.6063926	0.03551886	CD4+ Tmem
IGHA1-secreted	0.00010418	-4.8919623	0.03865161	CD4+ Tmem
IL12RB2	0.00011087	-1.5954134	0.04113433	CD4+ Tmem
EOMES	0.00020572	-1.4355648	0.07632224	CD4+ Tmem
IER3	0.00027689	-1.060772	0.1027272	CD4+ Tmem
LAMP3	0.00028213	1.13856487	0.10466935	CD4+ Tmem
TNFSF13B	0.00034783	0.23553309	0.12904309	CD4+ Tmem
CD274	0.00035169	0.76473908	0.13047565	CD4+ Tmem
CASP5	0.00049104	-0.3611973	0.182177	CD4+ Tmem
CCR8	0.00115539	0.19528083	0.42865091	CD4+ Tmem
CXCR5	0.00159379	-0.5575627	0.59129567	CD4+ Tmem
CNOT2	0.00177927	-0.3328716	0.6601084	CD4+ Tmem
PTGDR2	0.00209966	-1.4835546	0.77897227	CD4+ Tmem
NINJ2	0.00283682	0.28478213	1	CD4+ Tmem
GAB2	0.00344873	-0.6626199	1	CD4+ Tmem
CCR5	0.00368017	-1.0830914	1	CD4+ Tmem
ICAM1	0.00385308	-0.7796182	1	CD4+ Tmem
STAT4	0.00409281	-0.4556175	1	CD4+ Tmem
XBP1	0.00562473	-0.3914634	1	CD4+ Tmem
TGFB3	0.0058162	-1.0203796	1	CD4+ Tmem
MCM2	0.00754843	-0.7481375	1	CD4+ Tmem
THBS1	0.008171	-1.2313203	1	CD4+ Tmem
CD79A	0	6.61559813	0	B cells
MS4A1	0	5.6127152	0	B cells
CD22	0	5.7126517	0	B cells
HLA-DRA	0	2.94961768	0	B cells
IGHM-secreted	0	5.80968377	0	B cells
HLA-DQB1	0	2.90840907	0	B cells
CD3E	0	-4.6678462	0	B cells
HLA-DMA	0	2.76658649	0	B cells
IGHD-membrane	0	6.52521784	0	B cells
CD3D	0	-4.8424656	0	B cells
CD79B	0	4.09099552	0	B cells
IGHM-membrane	0	5.95338776	0	B cells
TRAC	0	-4.4453611	0	B cells
POU2AF1	0	5.88159353	0	B cells
PAX5	0	5.69543728	0	B cells
IRF8	0	2.44977163	0	B cells
HLA-DPA1	0	2.19436862	0	B cells

IGLC3	0	5.85404851	0	B cells
IGKC	0	6.52867701	0	B cells
IL32	0	-4.5057226	0	B cells
VPREB3	0	6.21097543	0	B cells
FCER2	0	5.20211831	0	B cells
CD24	0	6.54251176	0	B cells
IGHG1-secreted	0	7.80484824	0	B cells
LY86	0	3.36715475	0	B cells
BLNK	0	5.32674387	0	B cells
MZB1	0	4.05818227	0	B cells
CD40	0	4.37186438	0	B cells
JCHAIN	0	5.23304782	0	B cells
CXCR5	0	4.24676944	0	B cells
FAM129C	0	4.86998509	0	B cells
CD74	0	2.96798316	0	B cells
HLA-A	0	-1.3841749	0	B cells
ITGB2	7.67E-299	-2.7208305	2.85E-296	B cells
SELPLG	3.93E-295	-4.1429681	1.46E-292	B cells
TCF4	1.20E-292	4.48570017	4.45E-290	B cells
CD37	8.53E-290	1.7054304	3.16E-287	B cells
LCK	3.56E-285	-3.9665203	1.32E-282	B cells
TCL1A	6.14E-279	3.2184583	2.28E-276	B cells
CR2	3.93E-277	4.69810226	1.46E-274	B cells
TRBC2	5.09E-274	-2.69728	1.89E-271	B cells
CD2	1.21E-269	-4.6583859	4.50E-267	B cells
S100A10	3.20E-265	-2.4462933	1.19E-262	B cells
FYN	5.11E-239	-2.9525885	1.90E-236	B cells
EBF1	5.19E-238	5.88499593	1.93E-235	B cells
IGHA1-secreted	9.19E-231	7.33659571	3.41E-228	B cells
TNFRSF13C	1.23E-229	4.64308482	4.55E-227	B cells
BTLA	1.26E-223	2.93133215	4.68E-221	B cells
CTSW	5.24E-223	-4.9067317	1.94E-220	B cells
ARL4C	3.08E-208	-3.9697831	1.14E-205	B cells
GAPDH	3.42E-203	-1.7548061	1.27E-200	B cells
CD200	1.48E-202	4.4621626	5.50E-200	B cells
IL7R	5.12E-200	-4.3079983	1.90E-197	B cells
CD1C	1.33E-196	2.4803819	4.92E-194	B cells
CST7	1.89E-196	-4.9551862	7.03E-194	B cells
LYN	1.25E-194	1.2329359	4.64E-192	B cells
CD6	9.72E-193	-3.9271396	3.61E-190	B cells
CCL5	1.90E-191	-4.1691321	7.04E-189	B cells
BIN2	1.05E-185	-2.3577066	3.91E-183	B cells

PTPRC	7.45E-177	-1.4501717	2.77E-174	B cells
IL2RB	4.27E-171	-5.0080158	1.58E-168	B cells
NKG7	6.67E-171	-5.2462911	2.48E-168	B cells
LAT	1.92E-166	-3.7974495	7.12E-164	B cells
RUNX3	1.16E-160	-2.5365482	4.32E-158	B cells
GZMA	2.23E-158	-5.3462735	8.28E-156	B cells
CD72	2.02E-141	3.11223246	7.50E-139	B cells
DUSP2	1.93E-135	-3.7427385	7.15E-133	B cells
TARP-refseq	7.19E-133	-5.0464526	2.67E-130	B cells
KLRK1	6.38E-132	-4.2682156	2.37E-129	B cells
IL23R	1.00E-130	-1.7914009	3.72E-128	B cells
FYB	7.93E-121	-4.3918427	2.94E-118	B cells
YBX3	5.74E-118	1.74443464	2.13E-115	B cells
CD247	1.65E-117	-4.3273965	6.12E-115	B cells
PRF1	4.11E-114	-4.9683253	1.53E-111	B cells
C10orf54	2.24E-112	-2.766901	8.33E-110	B cells
CD8A	6.29E-112	-5.0411232	2.33E-109	B cells
LAT2	6.84E-111	1.41653237	2.54E-108	B cells
AIM2	1.94E-110	3.66260103	7.18E-108	B cells
CD48	4.45E-106	-1.0775501	1.65E-103	B cells
BCL11B	1.19E-105	-4.0055074	4.42E-103	B cells
KLRB1	1.14E-101	-5.1712395	4.21E-99	B cells
CD5	7.48E-99	-3.8960086	2.78E-96	B cells
CD44	2.91E-98	-1.7760934	1.08E-95	B cells
RNASE6	3.56E-98	1.75888705	1.32E-95	B cells
NT5E	5.94E-96	2.42896691	2.20E-93	B cells
GNLY	6.18E-95	-4.8567214	2.29E-92	B cells
CD63	1.59E-94	-2.2370864	5.89E-92	B cells
LEF1	5.38E-94	-3.6502723	1.99E-91	B cells
GZMB	1.23E-93	-5.2396406	4.58E-91	B cells
BIRC3	2.11E-92	1.37510997	7.81E-90	B cells
GZMH	2.00E-91	-5.1195904	7.44E-89	B cells
PIK3IP1	1.17E-90	-1.6046775	4.35E-88	B cells
IFITM2	8.84E-90	-1.4680956	3.28E-87	B cells
IFITM3	8.01E-89	-1.6063988	2.97E-86	B cells
CD4	3.62E-88	-5.3486652	1.34E-85	B cells
LGALS1	1.96E-87	-2.2340441	7.28E-85	B cells
BACH2	8.78E-84	1.95833031	3.26E-81	B cells
CD3G	1.58E-77	-5.1646888	5.88E-75	B cells
CD300A	3.76E-77	-4.0706116	1.40E-74	B cells
IGHG1-membrane	4.88E-76	6.10792365	1.81E-73	B cells
FCGR3A	2.83E-74	-5.0307635	1.05E-71	B cells

IGHG4-secreted	2.41E-72	7.21196533	8.96E-70	B cells
CD8B	2.42E-72	-5.2494033	9.00E-70	B cells
RORA	2.90E-71	-3.6287564	1.08E-68	B cells
GIMAP2	7.40E-70	-3.0361786	2.75E-67	B cells
TBX21	9.04E-69	-4.3117164	3.35E-66	B cells
LAMP1	3.39E-66	-1.3837143	1.26E-63	B cells
GIMAP5	1.10E-63	-4.1694113	4.08E-61	B cells
PRDM1	2.00E-63	-3.0389131	7.43E-61	B cells
XBP1	6.21E-63	-1.9349846	2.30E-60	B cells
IL4R	1.07E-62	1.7989525	3.96E-60	B cells
RPN2	7.20E-61	-1.3397433	2.67E-58	B cells
PIK3AP1	1.48E-57	0.60234487	5.50E-55	B cells
TRAT1	1.08E-53	-4.3174444	4.00E-51	B cells
STAT4	9.66E-51	-3.867421	3.58E-48	B cells
CD7	2.62E-49	-4.3616515	9.72E-47	B cells
KLRG1	4.74E-47	-4.8140055	1.76E-44	B cells
CCND2	1.01E-45	-3.2490189	3.74E-43	B cells
ADA	7.53E-43	-2.5550044	2.79E-40	B cells
TRDC	1.14E-42	-4.7191917	4.22E-40	B cells
GZMK	2.66E-42	-4.7929179	9.87E-40	B cells
TNFRSF17	1.95E-41	5.72297677	7.22E-39	B cells
IL18RAP	8.99E-40	-4.1893895	3.34E-37	B cells
TCF7	1.45E-39	-3.0689866	5.38E-37	B cells
TSPAN32	7.38E-39	-2.6301113	2.74E-36	B cells
TXK	2.31E-38	-2.9088613	8.56E-36	B cells
JUNB	2.93E-38	-1.6101602	1.09E-35	B cells
FCER1G	2.78E-37	-5.6064154	1.03E-34	B cells
ENTPD1	3.37E-36	1.70267619	1.25E-33	B cells
KLRF1	1.04E-35	-4.152889	3.87E-33	B cells
CD28	1.45E-35	-4.0996772	5.37E-33	B cells
CD27	1.30E-34	-1.5853613	4.83E-32	B cells
ITGAM	2.23E-34	-2.5419907	8.26E-32	B cells
IGHG3-secreted	1.47E-33	7.29457517	5.45E-31	B cells
STAT1	1.04E-32	-2.3359745	3.84E-30	B cells
BLK	1.14E-32	3.71892265	4.25E-30	B cells
CD9	4.41E-32	2.80671969	1.64E-29	B cells
CD244	6.41E-32	-4.4936522	2.38E-29	B cells
GNAI2	2.84E-31	-1.2469336	1.05E-28	B cells
ZAP70	8.11E-31	-3.9758973	3.01E-28	B cells
CCL4	1.70E-30	-4.2609571	6.33E-28	B cells
TNFSF8	2.11E-30	-2.8944425	7.84E-28	B cells
IL6	2.77E-29	4.80542168	1.03E-26	B cells

CX3CR1	2.00E-27	-4.4535371	7.41E-25	B cells
ZNF683	5.56E-26	-4.9378564	2.06E-23	B cells
KLRC1	2.58E-25	-4.0872299	9.56E-23	B cells
TNFSF10	9.90E-25	-1.9701058	3.67E-22	B cells
IGHE-secreted	1.14E-24	5.63131792	4.22E-22	B cells
IL3RA	3.42E-24	1.0480971	1.27E-21	B cells
LGALS3	4.62E-24	-2.7728957	1.72E-21	B cells
PDIA6	1.22E-23	-1.0604518	4.54E-21	B cells
ANXA5	1.56E-21	-1.2108445	5.80E-19	B cells
DPP4	1.93E-21	-4.6023331	7.17E-19	B cells
CD86	2.97E-21	0.73564327	1.10E-18	B cells
CTSD	6.41E-21	-2.8309449	2.38E-18	B cells
IL18R1	9.18E-21	-3.134952	3.40E-18	B cells
APOBEC3G	1.05E-20	-1.4991248	3.91E-18	B cells
VPS28	1.67E-20	-1.0258464	6.19E-18	B cells
CD69	3.38E-20	-0.9698661	1.25E-17	B cells
ICOS	4.79E-20	-3.7576086	1.78E-17	B cells
LGALS9	8.52E-20	0.16428124	3.16E-17	B cells
PASK	2.03E-19	-1.5647757	7.54E-17	B cells
B3GAT1	2.13E-19	-4.5639851	7.89E-17	B cells
LAG3	3.03E-19	-6.1493153	1.12E-16	B cells
TNFRSF25	7.67E-19	-3.0286579	2.85E-16	B cells
RGS1	2.05E-18	-2.4775059	7.60E-16	B cells
CD160	2.96E-18	-6.4132509	1.10E-15	B cells
TIGIT	1.26E-17	-3.8096294	4.67E-15	B cells
CD80	1.41E-16	3.48692966	5.25E-14	B cells
IL12RB1	3.58E-16	-2.4393476	1.33E-13	B cells
ITGA4	3.67E-16	-0.9227123	1.36E-13	B cells
ZBTB16	2.15E-15	-2.8862083	7.96E-13	B cells
ITGAX	5.10E-15	-2.2787804	1.89E-12	B cells
LAIR2	1.33E-14	-5.3223307	4.92E-12	B cells
CASP5	2.69E-14	-0.7814917	9.99E-12	B cells
KIR2DL1	3.01E-14	-4.3818529	1.12E-11	B cells
HAVCR2	7.13E-14	-2.9879347	2.65E-11	B cells
TLR7	7.82E-14	3.07201172	2.90E-11	B cells
CD1A	8.60E-14	3.44909038	3.19E-11	B cells
KLRC3	8.99E-14	-4.08665	3.34E-11	B cells
SLC7A7	1.23E-13	0.24026177	4.58E-11	B cells
CCL3	1.25E-13	-5.1532239	4.64E-11	B cells
IRF4	2.13E-13	1.01171897	7.90E-11	B cells
STAT5A	6.29E-13	-1.3956543	2.33E-10	B cells
PDIA4	7.13E-13	-0.9960706	2.65E-10	B cells

CBLB	8.36E-13	-1.0615529	3.10E-10	B cells
BAX	1.02E-12	-0.7134768	3.77E-10	B cells
CTLA4	1.14E-12	-3.1317872	4.24E-10	B cells
PCNA	1.22E-12	-2.1909946	4.52E-10	B cells
MME	2.54E-12	2.44702139	9.42E-10	B cells
IKZF1	2.60E-12	-0.8873215	9.64E-10	B cells
ITGAE	5.03E-12	0.28898367	1.87E-09	B cells
IFNG	1.22E-11	-4.9894866	4.53E-09	B cells
CD70	2.92E-11	1.69084968	1.08E-08	B cells
STAT3	5.53E-11	-0.9266418	2.05E-08	B cells
SLC25A37	2.11E-10	0.46350777	7.84E-08	B cells
LIPA	2.51E-10	-0.8361858	9.30E-08	B cells
TLR9	3.10E-10	2.20155829	1.15E-07	B cells
FAS	3.11E-10	-2.0386839	1.15E-07	B cells
IL12A	3.28E-10	1.01256379	1.22E-07	B cells
CCR5	5.57E-10	-5.3925624	2.07E-07	B cells
IFNGR1	3.37E-09	-1.4457671	1.25E-06	B cells
RORC	3.49E-09	-5.1748268	1.29E-06	B cells
CCR2	4.07E-09	-3.4459011	1.51E-06	B cells
LAP3	4.87E-09	-0.9660397	1.81E-06	B cells
KLRC4	4.97E-09	-2.8490747	1.84E-06	B cells
TNFSF13B	6.83E-09	-3.3773392	2.53E-06	B cells
CCR4	3.19E-08	-5.2707258	1.19E-05	B cells
EGR3	3.82E-08	3.21896056	1.42E-05	B cells
TGFBI	8.56E-08	-4.0692124	3.18E-05	B cells
FASLG	1.14E-07	-4.0869768	4.21E-05	B cells
CXCR3	1.55E-07	-2.3323931	5.74E-05	B cells
NCR3	1.78E-07	-1.4683734	6.61E-05	B cells
BTG1	1.99E-07	-0.2675431	7.39E-05	B cells
DUSP4	2.60E-07	-5.3982223	9.65E-05	B cells
ADGRE1	3.16E-07	-5.0969408	0.00011726	B cells
TNF	5.43E-07	-2.2453642	0.00020136	B cells
BCL2	1.16E-06	-0.9671473	0.00043156	B cells
IGBP1	2.13E-06	-0.7986448	0.00079126	B cells
CXCR2	2.31E-06	-4.3915965	0.00085559	B cells
ICAM1	3.73E-06	-1.58906	0.00138529	B cells
CD33	4.14E-06	-4.9708573	0.00153432	B cells
PTGDR2	4.59E-06	-5.5122178	0.00170182	B cells
MCM2	5.26E-06	0.30665433	0.00195034	B cells
EOMES	5.85E-06	-5.0280081	0.00217005	B cells
IL12RB2	6.68E-06	-4.3264294	0.00247919	B cells
CMKLR1	7.08E-06	-3.79089	0.00262649	B cells

FOXP3	7.12E-06	-4.279996	0.00264206	B cells
FCN1	7.60E-06	-5.1264417	0.00282031	B cells
IKZF2	8.90E-06	-2.1248363	0.00330142	B cells
IER3	9.50E-06	-3.9248547	0.00352526	B cells
LTB	1.38E-05	-0.7852813	0.00510851	B cells
FOSB	2.97E-05	-0.909564	0.01100194	B cells
CD52	3.21E-05	-0.1821721	0.01191743	B cells
NINJ2	3.78E-05	-1.7166018	0.01403962	B cells
FOXP1	4.42E-05	0.28190352	0.01638526	B cells
KIT	4.97E-05	-4.4871986	0.01845298	B cells
LILRB4	5.24E-05	-2.8714411	0.01944222	B cells
IL15RA	6.60E-05	-1.5303664	0.02447603	B cells
F5	7.66E-05	-4.0639412	0.02842741	B cells
CD14	0.000124	-5.4247014	0.04600219	B cells
CD36	0.00013192	-4.8284274	0.04894131	B cells
CXCR6	0.00013852	-4.9925732	0.05139094	B cells
KCNE3	0.00019364	-4.1369922	0.0718407	B cells
TGFB1	0.00026414	-1.9436574	0.09799779	B cells
TNFRSF4	0.00033394	-3.5132011	0.1238907	B cells
KDELR1	0.00035424	-1.3197811	0.13142247	B cells
S100A9	0.00036659	-5.4183193	0.13600512	B cells
FTH1	0.00037185	-1.0761033	0.1379568	B cells
THBS1	0.00047112	-4.6332041	0.17478585	B cells
BCL2A1	0.00060465	-0.7809434	0.22432377	B cells
CLEC10A	0.00089318	-5.9519847	0.33137127	B cells
CCR8	0.00108811	-3.7373215	0.40368749	B cells
CD163	0.001262	-4.8645291	0.46820088	B cells
TNFSF14	0.00144738	-3.6553818	0.53697972	B cells
CD274	0.00196431	-2.8366412	0.72875772	B cells
FCER1A	0.00229259	-4.7874365	0.85054959	B cells
TLR2	0.00246569	-1.4220998	0.9147727	B cells
FUT4	0.00264786	-2.6117614	0.98235431	B cells
IL15	0.00288826	0.12680513	1	B cells
LAMP3	0.00373941	-2.9408892	1	B cells
CNOT2	0.00390161	-0.4891122	1	B cells
DOCK8	0.00406553	-0.612196	1	B cells
S100A12	0.00471351	-4.7867182	1	B cells
CXCL16	0.00968089	-0.5076747	1	B cells
CD8B	8.27E-196	2.09218742	3.07E-193	CD8+ TNaive
CCR7	2.41E-194	2.66007389	8.93E-192	CD8+ TNaive
LEF1	1.79E-135	1.86530942	6.66E-133	CD8+ TNaive
PIK3IP1	3.57E-88	1.42230188	1.32E-85	CD8+ TNaive

PASK	3.72E-74	1.62595454	1.38E-71	CD8+ TNaive
NT5E	6.78E-72	2.40626613	2.52E-69	CD8+ TNaive
CST7	2.27E-71	-4.9131245	8.43E-69	CD8+ TNaive
CCL5	1.28E-57	-3.4804236	4.76E-55	CD8+ TNaive
CD8A	4.13E-54	0.44391337	1.53E-51	CD8+ TNaive
GZMA	5.94E-54	-4.4227768	2.20E-51	CD8+ TNaive
LGALS1	5.60E-51	-3.6346721	2.08E-48	CD8+ TNaive
MYC	1.16E-50	1.48086705	4.31E-48	CD8+ TNaive
NKG7	1.40E-49	-4.7617066	5.21E-47	CD8+ TNaive
SELL	3.75E-46	0.86150345	1.39E-43	CD8+ TNaive
ARL4C	1.08E-43	-2.3416772	4.00E-41	CD8+ TNaive
CD27	1.63E-42	1.13596556	6.05E-40	CD8+ TNaive
IL23R	6.15E-41	0.75588724	2.28E-38	CD8+ TNaive
HLA-A	7.73E-41	-0.7154042	2.87E-38	CD8+ TNaive
ITGB2	3.04E-38	-1.5055816	1.13E-35	CD8+ TNaive
PRF1	5.16E-37	-4.4243826	1.91E-34	CD8+ TNaive
RUNX3	1.10E-35	-1.7459016	4.08E-33	CD8+ TNaive
KLRB1	1.24E-35	-5.1338885	4.61E-33	CD8+ TNaive
CD74	1.68E-35	-2.6616731	6.25E-33	CD8+ TNaive
CD52	4.82E-35	-0.8577816	1.79E-32	CD8+ TNaive
CD4	1.28E-33	-5.2580626	4.74E-31	CD8+ TNaive
GZMH	4.77E-33	-4.8052875	1.77E-30	CD8+ TNaive
KLRK1	9.09E-33	0.49198406	3.37E-30	CD8+ TNaive
GZMB	1.03E-30	-4.6042715	3.82E-28	CD8+ TNaive
GNLY	6.98E-30	-4.6819837	2.59E-27	CD8+ TNaive
HLA-DPA1	1.66E-29	-3.2179863	6.17E-27	CD8+ TNaive
CD300A	8.48E-29	-4.1870195	3.15E-26	CD8+ TNaive
TXK	8.07E-28	0.99435774	2.99E-25	CD8+ TNaive
DUSP2	8.12E-28	-2.7051134	3.01E-25	CD8+ TNaive
FCGR3A	1.75E-27	-4.6405368	6.49E-25	CD8+ TNaive
IL2RB	1.85E-27	-2.6336388	6.85E-25	CD8+ TNaive
TARP-refseq	1.03E-26	-2.9498811	3.82E-24	CD8+ TNaive
CD63	1.62E-26	-1.8560708	6.02E-24	CD8+ TNaive
PRDM1	2.97E-26	-3.8400629	1.10E-23	CD8+ TNaive
TBX21	2.08E-24	-3.9530001	7.72E-22	CD8+ TNaive
TSPAN32	3.99E-24	0.86623773	1.48E-21	CD8+ TNaive
ITGAM	6.62E-24	-4.9072072	2.46E-21	CD8+ TNaive
S100A10	3.21E-22	-1.1596124	1.19E-19	CD8+ TNaive
FYN	1.01E-21	-1.1601589	3.75E-19	CD8+ TNaive
PIK3AP1	1.45E-21	-4.7731108	5.37E-19	CD8+ TNaive
BCL11B	7.32E-21	0.75504696	2.71E-18	CD8+ TNaive
YBX3	1.60E-20	0.69210797	5.95E-18	CD8+ TNaive

TCF7	4.39E-20	0.89587513	1.63E-17	CD8+ TNaive
GAPDH	4.63E-19	-0.8658906	1.72E-16	CD8+ TNaive
CD48	8.30E-19	0.44902052	3.08E-16	CD8+ TNaive
IFITM2	2.14E-18	-1.1337602	7.93E-16	CD8+ TNaive
BACH2	3.73E-18	1.54019872	1.38E-15	CD8+ TNaive
LYN	4.26E-17	-4.2472579	1.58E-14	CD8+ TNaive
PDIA6	5.29E-16	-1.4738382	1.96E-13	CD8+ TNaive
TRDC	1.57E-15	-4.3333395	5.83E-13	CD8+ TNaive
KLRG1	4.04E-15	-3.5581163	1.50E-12	CD8+ TNaive
APOBEC3G	5.55E-15	-2.3005443	2.06E-12	CD8+ TNaive
IL32	8.72E-15	-0.8783634	3.23E-12	CD8+ TNaive
KLRC4	3.02E-14	1.1300041	1.12E-11	CD8+ TNaive
CCL4	3.94E-14	-5.2747686	1.46E-11	CD8+ TNaive
ANXA5	7.80E-14	-1.9312044	2.90E-11	CD8+ TNaive
IL18RAP	9.13E-14	-4.0678932	3.39E-11	CD8+ TNaive
LGALS3	6.15E-13	-5.2820615	2.28E-10	CD8+ TNaive
GZMK	7.17E-13	-3.6279708	2.66E-10	CD8+ TNaive
KLRF1	1.44E-12	-3.6986048	5.33E-10	CD8+ TNaive
HLA-DRA	2.54E-12	-4.3790793	9.41E-10	CD8+ TNaive
GIMAP5	3.50E-12	0.6994357	1.30E-09	CD8+ TNaive
FOXP1	4.25E-12	0.78076466	1.58E-09	CD8+ TNaive
HLA-DQB1	5.42E-12	-3.5037295	2.01E-09	CD8+ TNaive
CX3CR1	9.29E-12	-4.2330599	3.45E-09	CD8+ TNaive
IFITM3	9.66E-12	-0.9815274	3.58E-09	CD8+ TNaive
ZNF683	1.65E-11	-5.7060828	6.14E-09	CD8+ TNaive
LAT2	2.50E-11	-4.0854385	9.26E-09	CD8+ TNaive
BIN2	3.42E-11	-0.7350195	1.27E-08	CD8+ TNaive
HLA-DMA	4.84E-11	-2.7675102	1.79E-08	CD8+ TNaive
ITGAX	2.33E-10	-3.7183084	8.65E-08	CD8+ TNaive
TNFSF8	1.13E-09	0.5678738	4.17E-07	CD8+ TNaive
CD244	2.35E-09	-2.6784574	8.73E-07	CD8+ TNaive
TRAC	5.28E-09	0.15514395	1.96E-06	CD8+ TNaive
GNAI2	1.55E-08	-0.9742851	5.76E-06	CD8+ TNaive
CD247	1.84E-08	-1.3100249	6.81E-06	CD8+ TNaive
TNFSF10	2.38E-08	-1.6826645	8.82E-06	CD8+ TNaive
KLRC1	3.22E-08	-3.3263564	1.19E-05	CD8+ TNaive
LAMP1	4.83E-08	-0.7698719	1.79E-05	CD8+ TNaive
LGALS9	5.61E-08	-1.8440769	2.08E-05	CD8+ TNaive
RGS1	6.06E-08	-2.3467445	2.25E-05	CD8+ TNaive
SELPLG	6.46E-08	-0.6952139	2.40E-05	CD8+ TNaive
BCL2	6.49E-08	0.61072276	2.41E-05	CD8+ TNaive
MS4A1	1.25E-07	-3.231217	4.62E-05	CD8+ TNaive

CD79B	1.43E-07	-2.4520754	5.29E-05	CD8+ TNaive
IL18R1	1.55E-07	-2.3425535	5.74E-05	CD8+ TNaive
EGR1	2.69E-07	1.24193186	9.98E-05	CD8+ TNaive
CXCR4	3.52E-07	-0.6477321	0.00013046	CD8+ TNaive
CD22	3.79E-07	-3.3443395	0.00014051	CD8+ TNaive
LCK	4.89E-07	0.17973848	0.00018139	CD8+ TNaive
CD3E	5.60E-07	0.17504087	0.00020767	CD8+ TNaive
B3GAT1	5.87E-07	-3.1650839	0.00021779	CD8+ TNaive
FYB	6.99E-07	0.29940948	0.00025939	CD8+ TNaive
CD7	7.71E-07	0.43953237	0.00028613	CD8+ TNaive
KIR2DL1	8.29E-07	-4.3498673	0.00030754	CD8+ TNaive
TIGIT	8.33E-07	-2.6638601	0.00030886	CD8+ TNaive
CD160	1.17E-06	-3.9311291	0.0004354	CD8+ TNaive
ZBTB16	2.14E-06	-2.641302	0.00079266	CD8+ TNaive
CD69	2.24E-06	-0.9088242	0.00082981	CD8+ TNaive
DUSP1	2.28E-06	-0.7972928	0.00084649	CD8+ TNaive
NCR3	3.18E-06	-1.7463483	0.00117849	CD8+ TNaive
PAX5	4.32E-06	-3.7131293	0.00160372	CD8+ TNaive
IFNGR1	8.18E-06	-1.4953027	0.00303307	CD8+ TNaive
IGHM-secreted	8.86E-06	-3.2356756	0.00328805	CD8+ TNaive
STAT1	1.51E-05	0.62157744	0.00558439	CD8+ TNaive
LAIR2	1.54E-05	-4.2203568	0.00571569	CD8+ TNaive
IRF8	1.75E-05	-2.792615	0.00649551	CD8+ TNaive
LAG3	3.88E-05	-2.4805404	0.0143969	CD8+ TNaive
IFNG	4.65E-05	-4.352722	0.01724649	CD8+ TNaive
CCL3	5.32E-05	-3.6100316	0.01975113	CD8+ TNaive
CTLA4	6.13E-05	-2.5422313	0.02272721	CD8+ TNaive
TIAF1	6.40E-05	-0.9642454	0.02372616	CD8+ TNaive
FAS	6.66E-05	-2.1115223	0.02469304	CD8+ TNaive
IRF4	7.45E-05	-2.3462514	0.0276383	CD8+ TNaive
HAVCR2	9.78E-05	-2.0608441	0.03628784	CD8+ TNaive
LAP3	0.00012023	-1.1594226	0.04460429	CD8+ TNaive
TGFBI	0.00014104	-4.928439	0.05232636	CD8+ TNaive
CCR5	0.00014402	-4.6517854	0.05343211	CD8+ TNaive
ITGA4	0.00014771	-0.6381859	0.0547988	CD8+ TNaive
CASP5	0.00015401	-0.7756613	0.05713825	CD8+ TNaive
GIMAP2	0.00020307	0.34740464	0.07533797	CD8+ TNaive
BLNK	0.00021113	-4.1623169	0.07832919	CD8+ TNaive
VPREB3	0.00023546	-2.711978	0.08735534	CD8+ TNaive
POU2AF1	0.0002527	-2.6150665	0.09375091	CD8+ TNaive
CCR2	0.00026424	-3.8234258	0.09803152	CD8+ TNaive
RORC	0.00028251	-4.5454671	0.10481144	CD8+ TNaive

CD86	0.00032089	-4.6071042	0.11904984	CD8+ TNaive
MZB1	0.00048187	-3.4344199	0.1787739	CD8+ TNaive
IGHM-membrane	0.00052253	-3.0759584	0.19385697	CD8+ TNaive
IGHD-membrane	0.00055258	-3.3456386	0.20500685	CD8+ TNaive
FCER2	0.00056975	-2.2634402	0.21137597	CD8+ TNaive
BAX	0.00061848	-0.6152427	0.22945425	CD8+ TNaive
RNASE6	0.00083187	-3.4997725	0.30862362	CD8+ TNaive
CD37	0.00088127	-0.4352324	0.32695198	CD8+ TNaive
ADA	0.00098899	-0.8444287	0.36691372	CD8+ TNaive
CD24	0.00107011	-3.2921078	0.39701207	CD8+ TNaive
FTH1	0.00113077	-1.0286295	0.41951653	CD8+ TNaive
FOXO1	0.00113922	0.46577652	0.42264981	CD8+ TNaive
CXCR5	0.00114735	-2.7514039	0.42566723	CD8+ TNaive
NINJ2	0.00122203	-1.5647391	0.45337303	CD8+ TNaive
LIPA	0.00141532	-0.6761562	0.52508417	CD8+ TNaive
DPP4	0.00160962	0.44529746	0.59716854	CD8+ TNaive
LY86	0.00175566	-2.4158521	0.65134967	CD8+ TNaive
SLC7A7	0.00177559	-4.3753996	0.6587454	CD8+ TNaive
FASLG	0.00203363	-3.0326645	0.75447659	CD8+ TNaive
ADGRE1	0.00229217	-3.6054281	0.8503953	CD8+ TNaive
LAT	0.0025176	0.16132951	0.93402808	CD8+ TNaive
IGLC3	0.00255562	-4.1819255	0.94813333	CD8+ TNaive
CNOT2	0.00284097	0.14117058	1	CD8+ TNaive
CCR4	0.0029525	-2.4859696	1	CD8+ TNaive
CXCR2	0.0031846	-3.7016271	1	CD8+ TNaive
IL12RB2	0.0031846	-3.9455506	1	CD8+ TNaive
CMKLR1	0.00324337	-3.8063261	1	CD8+ TNaive
GAB2	0.00367668	-2.434698	1	CD8+ TNaive
IL15	0.00372469	-2.5949488	1	CD8+ TNaive
CD33	0.00396672	-4.1349367	1	CD8+ TNaive
IL12RB1	0.00400234	-1.5028262	1	CD8+ TNaive
CTSD	0.00402662	-1.0840994	1	CD8+ TNaive
STAT5A	0.00407824	0.16195504	1	CD8+ TNaive
LILRB4	0.00484243	-2.4350703	1	CD8+ TNaive
SLC25A37	0.00487416	0.51341112	1	CD8+ TNaive
TLR2	0.00512768	-3.4832298	1	CD8+ TNaive
ENTPD1	0.0052227	-3.3185652	1	CD8+ TNaive
FAM65B	0.00597927	0.22414179	1	CD8+ TNaive
DUSP4	0.00625806	-3.1729136	1	CD8+ TNaive
IGKC	0.00710694	-3.5230692	1	CD8+ TNaive
RORA	0.0076839	-0.6801386	1	CD8+ TNaive
TCF4	0.00782928	-3.2006434	1	CD8+ TNaive

FOSB	0.00800885	0.34262297	1	CD8+ TNaive
BCL6	0.0082711	-2.4513219	1	CD8+ TNaive
PTGDR2	0	5.92020015	0	CD8+ Tmem
CCR8	9.33E-187	5.34910952	3.46E-184	CD8+ Tmem
LTB	8.25E-186	3.1409062	3.06E-183	CD8+ Tmem
TCF7	1.63E-136	2.55167527	6.03E-134	CD8+ Tmem
IL7R	2.07E-136	1.67184348	7.69E-134	CD8+ Tmem
CD8B	2.90E-135	1.75117933	1.08E-132	CD8+ Tmem
CCR4	3.69E-123	3.49729492	1.37E-120	CD8+ Tmem
IL32	8.88E-111	1.24317752	3.30E-108	CD8+ Tmem
LEF1	9.22E-104	1.65412377	3.42E-101	CD8+ Tmem
SELL	3.72E-98	1.83089833	1.38E-95	CD8+ Tmem
MYC	3.78E-91	2.05930541	1.40E-88	CD8+ Tmem
TRAC	7.82E-88	1.15933273	2.90E-85	CD8+ Tmem
CD3E	4.88E-87	1.12779927	1.81E-84	CD8+ Tmem
TNFSF10	4.98E-85	2.06339558	1.85E-82	CD8+ Tmem
GIMAP2	6.14E-84	1.85379859	2.28E-81	CD8+ Tmem
CD52	2.12E-80	0.91323145	7.87E-78	CD8+ Tmem
CD48	4.53E-77	1.02878065	1.68E-74	CD8+ Tmem
IL23R	9.15E-73	1.09692413	3.39E-70	CD8+ Tmem
CD8A	1.46E-71	0.69465025	5.41E-69	CD8+ Tmem
CD3G	3.16E-70	1.60920094	1.17E-67	CD8+ Tmem
S100A10	5.20E-63	1.01307433	1.93E-60	CD8+ Tmem
IL2RA	5.39E-62	3.08339498	2.00E-59	CD8+ Tmem
IL4R	2.68E-59	1.5226841	9.95E-57	CD8+ Tmem
CD3D	6.69E-59	0.92910832	2.48E-56	CD8+ Tmem
YBX3	1.88E-56	1.82831959	6.98E-54	CD8+ Tmem
GIMAP5	1.89E-55	1.5863656	7.00E-53	CD8+ Tmem
TRAT1	3.56E-54	1.60939888	1.32E-51	CD8+ Tmem
GZMA	7.62E-51	-2.618396	2.83E-48	CD8+ Tmem
CD27	1.34E-50	1.4551477	4.99E-48	CD8+ Tmem
CD2	1.02E-48	0.91107798	3.80E-46	CD8+ Tmem
CD44	1.75E-46	1.12348653	6.48E-44	CD8+ Tmem
CD5	3.71E-45	1.3172229	1.38E-42	CD8+ Tmem
PASK	4.12E-45	1.55610391	1.53E-42	CD8+ Tmem
GZMB	9.30E-41	-4.9044987	3.45E-38	CD8+ Tmem
BIRC3	2.35E-38	1.79292011	8.72E-36	CD8+ Tmem
FCGR3A	3.76E-38	-5.1463174	1.40E-35	CD8+ Tmem
ZAP70	6.10E-38	1.49615922	2.26E-35	CD8+ Tmem
FYB	6.57E-38	1.35125986	2.44E-35	CD8+ Tmem
LGALS1	3.35E-37	1.08951806	1.24E-34	CD8+ Tmem
ANXA5	1.61E-36	1.14249359	5.98E-34	CD8+ Tmem

GAPDH	4.69E-35	0.5847817	1.74E-32	CD8+ Tmem
TNFRSF4	9.27E-34	2.7069861	3.44E-31	CD8+ Tmem
GNAI2	1.67E-33	1.04082744	6.20E-31	CD8+ Tmem
IKZF1	1.03E-32	1.28775916	3.82E-30	CD8+ Tmem
KDELR1	1.17E-31	2.1394925	4.34E-29	CD8+ Tmem
PRF1	3.33E-31	-3.2729214	1.24E-28	CD8+ Tmem
GZMH	2.61E-30	-4.1690433	9.67E-28	CD8+ Tmem
KLRK1	9.04E-30	0.81590038	3.35E-27	CD8+ Tmem
SELPLG	1.62E-29	0.70313299	6.00E-27	CD8+ Tmem
CLC	1.73E-29	5.45639335	6.42E-27	CD8+ Tmem
HLA-A	1.80E-29	0.40555037	6.67E-27	CD8+ Tmem
LAT	2.43E-29	0.92734706	9.00E-27	CD8+ Tmem
RPN2	2.48E-29	0.97695887	9.22E-27	CD8+ Tmem
KIT	1.03E-27	2.4183593	3.84E-25	CD8+ Tmem
CCR2	6.87E-27	2.18123924	2.55E-24	CD8+ Tmem
TBX21	1.56E-26	-3.1038777	5.77E-24	CD8+ Tmem
TNFRSF25	3.79E-26	1.60037818	1.40E-23	CD8+ Tmem
NKG7	4.68E-25	-3.5091287	1.74E-22	CD8+ Tmem
LCK	1.19E-24	0.66680946	4.42E-22	CD8+ Tmem
LYN	1.66E-23	-5.2648157	6.15E-21	CD8+ Tmem
CCR7	4.50E-23	0.8794587	1.67E-20	CD8+ Tmem
IGBP1	4.70E-23	1.23699169	1.75E-20	CD8+ Tmem
CD28	6.05E-22	1.37381336	2.25E-19	CD8+ Tmem
TRBC2	7.32E-22	0.70963467	2.71E-19	CD8+ Tmem
KLRB1	2.27E-21	-2.005775	8.43E-19	CD8+ Tmem
FOSB	4.61E-21	-1.6591109	1.71E-18	CD8+ Tmem
CD37	5.99E-21	0.44965312	2.22E-18	CD8+ Tmem
PIK3IP1	6.45E-21	0.69230658	2.39E-18	CD8+ Tmem
CD4	1.60E-20	-1.9430058	5.95E-18	CD8+ Tmem
CD7	6.73E-20	1.17412775	2.50E-17	CD8+ Tmem
CCL5	5.80E-19	-2.1043555	2.15E-16	CD8+ Tmem
XBP1	7.63E-19	0.85566575	2.83E-16	CD8+ Tmem
CCND2	3.11E-17	0.95020273	1.16E-14	CD8+ Tmem
TRDC	1.05E-16	-3.4053087	3.88E-14	CD8+ Tmem
STAT5A	1.07E-16	1.24829747	3.96E-14	CD8+ Tmem
KLRF1	2.41E-16	-3.3145381	8.95E-14	CD8+ Tmem
PDIA6	4.40E-16	0.83186606	1.63E-13	CD8+ Tmem
PRDM1	7.16E-16	0.8806993	2.66E-13	CD8+ Tmem
TARP-refseq	7.46E-16	-1.1911578	2.77E-13	CD8+ Tmem
JUNB	9.62E-16	0.79534274	3.57E-13	CD8+ Tmem
DOCK8	1.93E-15	1.12649917	7.18E-13	CD8+ Tmem
TNFSF8	3.35E-15	1.13739536	1.24E-12	CD8+ Tmem

CD6	5.81E-15	0.64178742	2.16E-12	CD8+ Tmem
CD69	7.99E-15	0.82072332	2.96E-12	CD8+ Tmem
CXCL5	1.74E-14	0.96986196	6.47E-12	CD8+ Tmem
FAM65B	1.81E-14	0.82895921	6.73E-12	CD8+ Tmem
FCER1G	1.92E-14	-4.3994254	7.10E-12	CD8+ Tmem
CST7	3.29E-14	-1.7617127	1.22E-11	CD8+ Tmem
STAT6	3.52E-14	1.02318863	1.30E-11	CD8+ Tmem
ITGAM	4.30E-14	-1.8061769	1.60E-11	CD8+ Tmem
CD244	8.64E-14	-3.4840825	3.21E-11	CD8+ Tmem
IL18RAP	1.03E-13	-2.8724527	3.81E-11	CD8+ Tmem
IFITM2	1.75E-13	0.57218517	6.50E-11	CD8+ Tmem
DUSP1	5.46E-13	-0.848829	2.03E-10	CD8+ Tmem
CX3CR1	6.44E-13	-4.1854085	2.39E-10	CD8+ Tmem
DUSP2	8.21E-13	-0.9809716	3.05E-10	CD8+ Tmem
NT5E	1.14E-12	1.71710663	4.24E-10	CD8+ Tmem
ITGAX	5.38E-12	-3.7892266	2.00E-09	CD8+ Tmem
ICOS	5.74E-12	1.44504767	2.13E-09	CD8+ Tmem
CCL4	5.93E-12	-3.6448639	2.20E-09	CD8+ Tmem
DPP4	1.27E-11	0.98788477	4.70E-09	CD8+ Tmem
LTA	4.77E-11	1.27411452	1.77E-08	CD8+ Tmem
TSPAN32	6.49E-11	0.70833098	2.41E-08	CD8+ Tmem
GZMK	9.21E-11	-3.1308271	3.42E-08	CD8+ Tmem
IFITM3	3.01E-10	0.47541629	1.12E-07	CD8+ Tmem
B3GAT1	3.36E-10	-4.2801638	1.25E-07	CD8+ Tmem
BCL2	3.56E-10	1.06406618	1.32E-07	CD8+ Tmem
PDIA4	4.73E-10	0.71036392	1.75E-07	CD8+ Tmem
PIK3AP1	6.63E-10	-1.0213315	2.46E-07	CD8+ Tmem
VPS28	6.98E-10	0.61824109	2.59E-07	CD8+ Tmem
KLRC1	1.08E-09	-2.9332073	4.00E-07	CD8+ Tmem
CD160	3.54E-09	-6.1772281	1.31E-06	CD8+ Tmem
PCNA	3.88E-09	0.98050764	1.44E-06	CD8+ Tmem
BAX	7.66E-09	0.59938872	2.84E-06	CD8+ Tmem
IRF8	8.27E-09	-2.863673	3.07E-06	CD8+ Tmem
C10orf54	2.27E-08	0.34853374	8.44E-06	CD8+ Tmem
FOXP1	4.04E-07	0.58988378	0.0001497	CD8+ Tmem
HLA-DPA1	8.41E-07	-1.5816855	0.00031217	CD8+ Tmem
CCL3	9.70E-07	-3.8926896	0.00035984	CD8+ Tmem
CD63	9.99E-07	0.30689422	0.00037068	CD8+ Tmem
CD38	1.05E-06	-3.3874493	0.00039011	CD8+ Tmem
KIR2DL1	1.36E-06	-3.3692917	0.00050542	CD8+ Tmem
JUN	1.76E-06	-0.5983172	0.00065285	CD8+ Tmem
F5	2.20E-06	1.88109366	0.00081606	CD8+ Tmem

ADGRE1	2.34E-06	1.48307718	0.00086822	CD8+ Tmem
FOXO1	2.90E-06	0.81886427	0.00107743	CD8+ Tmem
IL18	2.98E-06	0.69419151	0.00110464	CD8+ Tmem
IL18R1	3.49E-06	-1.3967444	0.00129308	CD8+ Tmem
HLA-DRA	3.87E-06	-3.0160515	0.00143398	CD8+ Tmem
BTG1	5.66E-06	0.29154821	0.00209829	CD8+ Tmem
STAT1	5.79E-06	0.88719513	0.00214682	CD8+ Tmem
ATF6B	6.82E-06	0.60257389	0.00252874	CD8+ Tmem
FAS	7.40E-06	0.89431901	0.00274394	CD8+ Tmem
HAVCR2	8.82E-06	-2.261243	0.00327186	CD8+ Tmem
GAB2	1.31E-05	1.45370157	0.00487508	CD8+ Tmem
CD22	1.37E-05	-2.0089562	0.00508877	CD8+ Tmem
LAIR2	1.39E-05	-3.5130085	0.00515258	CD8+ Tmem
LY86	2.25E-05	-3.1934337	0.0083552	CD8+ Tmem
KLRC3	3.19E-05	-1.863756	0.01182629	CD8+ Tmem
BCL11B	3.78E-05	0.40926537	0.01402095	CD8+ Tmem
CD74	4.62E-05	-1.7102246	0.01714209	CD8+ Tmem
IL2RB	4.66E-05	-1.2931364	0.0172795	CD8+ Tmem
CBLB	8.88E-05	-0.7132118	0.03292763	CD8+ Tmem
FCER2	0.00011201	-2.451647	0.041554	CD8+ Tmem
BCL2A1	0.00011907	0.45614163	0.04417443	CD8+ Tmem
CD9	0.00013548	1.90642268	0.05026244	CD8+ Tmem
IGHM-membrane	0.00014644	-2.7357151	0.054329	CD8+ Tmem
LIPA	0.00015789	0.56204421	0.05857588	CD8+ Tmem
ITGB2	0.00015984	-0.5940227	0.05930243	CD8+ Tmem
CD86	0.00016322	-4.2393488	0.0605534	CD8+ Tmem
PAX5	0.00022327	-1.9804132	0.08283476	CD8+ Tmem
EGR1	0.00025428	-1.9004651	0.09433909	CD8+ Tmem
KLRC4	0.00026521	0.7158589	0.09839286	CD8+ Tmem
HLA-DMA	0.00029027	-1.3055438	0.10768986	CD8+ Tmem
FYN	0.0003557	-0.3356666	0.13196616	CD8+ Tmem
CD24	0.00041257	-2.9366918	0.15306414	CD8+ Tmem
SLC7A7	0.00046319	-4.7029948	0.17184366	CD8+ Tmem
IL15	0.0006494	-2.0593458	0.24092771	CD8+ Tmem
BIN2	0.00070163	0.25598062	0.26030354	CD8+ Tmem
BLNK	0.0007286	-2.6297783	0.27031227	CD8+ Tmem
VPREB3	0.00086827	-2.2027029	0.32212896	CD8+ Tmem
CXCR2	0.00095334	-4.0292223	0.3536907	CD8+ Tmem
STAT4	0.00109896	0.45215485	0.40771353	CD8+ Tmem
TIAF1	0.00156251	0.51809624	0.57969231	CD8+ Tmem
STAT3	0.00194685	0.53649214	0.72227999	CD8+ Tmem
KLRG1	0.00204074	-1.0200352	0.75711406	CD8+ Tmem

TGFBI	0.00246565	-2.6679258	0.91475592	CD8+ Tmem
S100A9	0.00248002	-4.7211288	0.92008894	CD8+ Tmem
IL12RB2	0.00281144	-3.4517278	1	CD8+ Tmem
CMKLR1	0.00286402	-3.5796199	1	CD8+ Tmem
TCF4	0.00289105	-3.5282386	1	CD8+ Tmem
BACH2	0.00368671	0.6780252	1	CD8+ Tmem
CD33	0.00377207	-2.9120228	1	CD8+ Tmem
FAM129C	0.00408108	-2.7054528	1	CD8+ Tmem
VNN2	0.00409144	-1.4567465	1	CD8+ Tmem
BTLA	0.00412673	0.32363227	1	CD8+ Tmem
IFNGR1	0.00468379	-0.5349814	1	CD8+ Tmem
TLR2	0.00513128	-2.9450053	1	CD8+ Tmem
FCN1	0.00601311	-3.7658572	1	CD8+ Tmem
TLR9	0.0061982	1.74028792	1	CD8+ Tmem
KCNE3	0.00754201	-3.3009574	1	CD8+ Tmem
CXCR5	0.0086911	-1.2084263	1	CD8+ Tmem
IFNG	0.00871568	-2.0060444	1	CD8+ Tmem
TNFSF14	0.00885098	1.07296037	1	CD8+ Tmem
POU2AF1	0.0089763	-1.7405515	1	CD8+ Tmem
GZMH	6.07E-79	1.97666785	2.25E-76	CD4+ Teff
CD4	4.85E-43	1.79731984	1.80E-40	CD4+ Teff
CCL5	1.28E-35	1.10471277	4.76E-33	CD4+ Teff
NKG7	5.56E-35	0.94546621	2.06E-32	CD4+ Teff
CST7	5.51E-30	0.88854834	2.04E-27	CD4+ Teff
GZMA	1.51E-29	1.09271993	5.62E-27	CD4+ Teff
CD6	3.15E-27	1.28319874	1.17E-24	CD4+ Teff
LAIR2	9.55E-27	2.1802537	3.54E-24	CD4+ Teff
KLRG1	3.34E-26	1.68511569	1.24E-23	CD4+ Teff
IL32	2.52E-25	0.72166103	9.34E-23	CD4+ Teff
GNLY	1.27E-22	0.64980418	4.70E-20	CD4+ Teff
TARP-refseq	2.73E-22	0.84679947	1.01E-19	CD4+ Teff
CD2	1.82E-19	0.87115253	6.75E-17	CD4+ Teff
CD52	2.21E-19	0.63680905	8.18E-17	CD4+ Teff
PRF1	1.27E-16	0.33274471	4.71E-14	CD4+ Teff
CX3CR1	1.98E-16	1.33228045	7.35E-14	CD4+ Teff
ITGB2	2.45E-16	0.42938117	9.08E-14	CD4+ Teff
GZMB	4.59E-16	0.46324468	1.70E-13	CD4+ Teff
CD3E	6.77E-15	0.6808169	2.51E-12	CD4+ Teff
KLRK1	1.59E-14	-2.3196489	5.92E-12	CD4+ Teff
HLA-A	2.57E-14	0.3872907	9.53E-12	CD4+ Teff
TRAC	8.55E-14	0.56640455	3.17E-11	CD4+ Teff
CD3D	4.49E-13	0.58415758	1.67E-10	CD4+ Teff

RUNX3	1.18E-12	0.5161139	4.38E-10	CD4+ Teff
TBX21	2.97E-12	0.80783884	1.10E-09	CD4+ Teff
S100A10	6.21E-12	0.51849289	2.30E-09	CD4+ Teff
SELL	8.99E-12	-1.3546098	3.33E-09	CD4+ Teff
DUSP2	1.07E-11	0.49600341	3.97E-09	CD4+ Teff
CD8B	2.24E-11	-4.0839918	8.33E-09	CD4+ Teff
CD5	2.91E-11	1.13229068	1.08E-08	CD4+ Teff
CD3G	2.95E-11	1.11428306	1.09E-08	CD4+ Teff
GAPDH	2.21E-10	0.44900325	8.18E-08	CD4+ Teff
CTLA4	4.11E-10	1.67613788	1.53E-07	CD4+ Teff
CCR7	4.42E-10	-2.7342166	1.64E-07	CD4+ Teff
GNAI2	9.69E-10	0.79435995	3.59E-07	CD4+ Teff
CD8A	1.27E-09	-2.5277216	4.70E-07	CD4+ Teff
LEF1	1.35E-09	-1.8395291	5.00E-07	CD4+ Teff
PTPRC	2.06E-09	0.4155644	7.66E-07	CD4+ Teff
CD27	7.23E-09	-1.5366051	2.68E-06	CD4+ Teff
APOBEC3G	1.29E-08	0.93582977	4.78E-06	CD4+ Teff
LGALS1	3.08E-08	0.60142698	1.14E-05	CD4+ Teff
CCL4	4.62E-08	0.59159396	1.72E-05	CD4+ Teff
DUSP1	1.35E-07	-1.2522851	5.01E-05	CD4+ Teff
JUNB	1.52E-07	-1.1552216	5.64E-05	CD4+ Teff
TRDC	2.58E-07	-2.2786381	9.58E-05	CD4+ Teff
CD300A	3.00E-07	0.65794367	0.00011141	CD4+ Teff
SELPLG	3.40E-07	0.3614612	0.00012631	CD4+ Teff
MYC	3.46E-07	-1.9283129	0.00012845	CD4+ Teff
PIK3AP1	5.42E-07	-1.7897206	0.00020102	CD4+ Teff
YBX3	9.52E-07	-3.2744043	0.00035329	CD4+ Teff
HLA-DPA1	1.32E-06	-0.3276335	0.00048863	CD4+ Teff
TXK	2.29E-06	-2.154903	0.00084806	CD4+ Teff
PRDM1	2.33E-06	0.70017931	0.00086398	CD4+ Teff
CCR5	2.99E-06	1.23324011	0.00111101	CD4+ Teff
PASK	3.27E-06	-2.0908765	0.00121199	CD4+ Teff
AURKB	3.32E-06	2.7137581	0.00123343	CD4+ Teff
IL23R	4.40E-06	-0.7230311	0.00163216	CD4+ Teff
LAT2	9.69E-06	-3.2833349	0.00359616	CD4+ Teff
FOSB	1.41E-05	-2.0163487	0.00524904	CD4+ Teff
FYN	1.73E-05	0.53117071	0.00641538	CD4+ Teff
ZAP70	2.24E-05	0.89586388	0.00831245	CD4+ Teff
NCR3	2.27E-05	-1.9456474	0.00843262	CD4+ Teff
LGALS9	2.76E-05	-1.7440026	0.01025178	CD4+ Teff
FCER1G	2.92E-05	-3.3496236	0.01081732	CD4+ Teff
FOXP1	4.08E-05	-1.1516268	0.01513994	CD4+ Teff

ITGAM	5.23E-05	0.40004542	0.01938844	CD4+ Teff
BIN2	5.70E-05	0.33956524	0.02115897	CD4+ Teff
KLRC1	8.10E-05	-3.2841014	0.03004017	CD4+ Teff
PIK3IP1	0.00010127	-0.6768652	0.03757087	CD4+ Teff
IFITM2	0.00010354	0.32216723	0.03841174	CD4+ Teff
LGALS3	0.00024881	-0.9605794	0.09230939	CD4+ Teff
CD79A	0.00029172	-3.3608529	0.10822814	CD4+ Teff
B3GAT1	0.0003185	0.91352075	0.11816382	CD4+ Teff
JUN	0.0003938	-1.1463572	0.14609994	CD4+ Teff
ITGAX	0.00045023	-2.4035501	0.16703695	CD4+ Teff
CD28	0.00050117	-1.451667	0.18593315	CD4+ Teff
ZBTB16	0.00065257	-2.5164166	0.24210497	CD4+ Teff
CD74	0.00076796	-0.9214574	0.28491385	CD4+ Teff
FCGR3A	0.00086087	-1.4159602	0.31938397	CD4+ Teff
TNFSF8	0.00088423	-1.2591096	0.32804983	CD4+ Teff
BIRC3	0.00097354	-1.1635763	0.36118382	CD4+ Teff
KLRC3	0.00113092	-3.2552317	0.41957081	CD4+ Teff
CD79B	0.00126046	-0.9888538	0.4676307	CD4+ Teff
EOMES	0.00146375	1.5116311	0.54305056	CD4+ Teff
LCK	0.00162588	0.32266206	0.60320084	CD4+ Teff
TRBC2	0.00176575	0.24596451	0.65509472	CD4+ Teff
DPP4	0.0018573	-2.3444097	0.68905749	CD4+ Teff
LY86	0.00188402	-3.9564533	0.69897298	CD4+ Teff
ARL4C	0.00266652	0.15708546	0.98927847	CD4+ Teff
CD69	0.00293925	-0.7083734	1	CD4+ Teff
LAMP1	0.00304465	0.35524767	1	CD4+ Teff
VNN2	0.0032481	-2.27437	1	CD4+ Teff
IL18RAP	0.00344135	0.12952821	1	CD4+ Teff
PDIA6	0.00395883	0.36530565	1	CD4+ Teff
CXCL16	0.00427658	-4.2796116	1	CD4+ Teff
CD22	0.00454329	-2.5925257	1	CD4+ Teff
IGHD-membrane	0.00514301	-2.48093	1	CD4+ Teff
IGHG1-secreted	0.00607335	-5.0528317	1	CD4+ Teff
LAT	0.00684201	0.44458097	1	CD4+ Teff
IFITM3	0.00692995	0.18094075	1	CD4+ Teff
NT5E	0.00764662	-2.44247	1	CD4+ Teff
IRF8	0.00806359	-2.0040579	1	CD4+ Teff
ITGA4	0.00873209	0.28551974	1	CD4+ Teff
LYN	0.00926363	-1.2509887	1	CD4+ Teff
CCR7	0	2.16636058	0	CD4+ TNaive
LEF1	0	1.59289001	0	CD4+ TNaive
HLA-A	0	-1.2372757	0	CD4+ TNaive

CCL5	2.52E-244	-5.1596494	9.33E-242	CD4+ TNaive
CST7	5.48E-230	-5.5146496	2.03E-227	CD4+ TNaive
RUNX3	2.15E-201	-2.8751128	7.98E-199	CD4+ TNaive
PIK3IP1	3.55E-189	1.07198801	1.32E-186	CD4+ TNaive
GZMA	1.94E-185	-5.7351233	7.20E-183	CD4+ TNaive
NKG7	1.39E-184	-5.611049	5.15E-182	CD4+ TNaive
CD74	1.17E-180	-3.1565306	4.33E-178	CD4+ TNaive
ITGB2	2.02E-164	-1.8532246	7.49E-162	CD4+ TNaive
KLRK1	6.99E-163	-4.847455	2.60E-160	CD4+ TNaive
LGALS1	5.60E-160	-4.1694301	2.08E-157	CD4+ TNaive
S100A10	3.02E-156	-1.8101337	1.12E-153	CD4+ TNaive
CD52	1.77E-149	-1.0671704	6.57E-147	CD4+ TNaive
CTSW	2.02E-145	-3.2381594	7.49E-143	CD4+ TNaive
CD63	7.22E-140	-3.0400132	2.68E-137	CD4+ TNaive
PRF1	8.86E-133	-5.1872865	3.29E-130	CD4+ TNaive
CD8A	1.34E-132	-5.4335534	4.98E-130	CD4+ TNaive
IL2RB	6.48E-131	-3.7138187	2.40E-128	CD4+ TNaive
IL32	6.44E-117	-1.5020397	2.39E-114	CD4+ TNaive
TARP-refseq	5.08E-115	-4.0924445	1.89E-112	CD4+ TNaive
SELL	5.67E-112	0.60442742	2.10E-109	CD4+ TNaive
HLA-DPA1	5.72E-108	-3.8145572	2.12E-105	CD4+ TNaive
GZMB	1.38E-104	-5.4507804	5.11E-102	CD4+ TNaive
MYC	1.81E-102	1.04234339	6.70E-100	CD4+ TNaive
CD4	4.84E-102	0.53205039	1.80E-99	CD4+ TNaive
GZMH	1.25E-100	-5.2097201	4.64E-98	CD4+ TNaive
KLRB1	3.29E-98	-4.3552157	1.22E-95	CD4+ TNaive
GNLY	1.10E-96	-5.3488101	4.09E-94	CD4+ TNaive
GAPDH	5.26E-93	-1.152095	1.95E-90	CD4+ TNaive
ARL4C	1.56E-91	-2.058343	5.79E-89	CD4+ TNaive
IL23R	2.85E-90	0.6296509	1.06E-87	CD4+ TNaive
CD27	6.16E-90	0.72563963	2.28E-87	CD4+ TNaive
BCL11B	2.52E-89	0.81985399	9.34E-87	CD4+ TNaive
DUSP2	5.74E-88	-2.9320827	2.13E-85	CD4+ TNaive
FCGR3A	9.87E-86	-5.2608383	3.66E-83	CD4+ TNaive
TBX21	1.36E-79	-4.5921043	5.04E-77	CD4+ TNaive
CD8B	1.14E-78	-5.0005185	4.23E-76	CD4+ TNaive
CD300A	2.57E-78	-3.854933	9.53E-76	CD4+ TNaive
TCF7	2.38E-71	0.73740055	8.82E-69	CD4+ TNaive
GIMAP5	4.70E-68	0.75282062	1.74E-65	CD4+ TNaive
ITGAM	5.26E-68	-4.3561618	1.95E-65	CD4+ TNaive
IFITM2	3.70E-67	-1.3379349	1.37E-64	CD4+ TNaive
PIK3AP1	2.40E-66	-5.1382967	8.91E-64	CD4+ TNaive

PRDM1	1.88E-62	-3.1182235	6.97E-60	CD4+ TNaive
SELPLG	1.85E-58	-1.1874803	6.86E-56	CD4+ TNaive
ANXA5	2.40E-54	-2.3889699	8.89E-52	CD4+ TNaive
LYN	6.48E-54	-5.0314177	2.40E-51	CD4+ TNaive
TXK	1.66E-52	0.56820273	6.17E-50	CD4+ TNaive
CXCR4	4.41E-51	-1.1026804	1.64E-48	CD4+ TNaive
IFITM3	1.54E-50	-1.2688436	5.72E-48	CD4+ TNaive
PASK	1.99E-50	0.74787565	7.39E-48	CD4+ TNaive
APOBEC3G	3.79E-49	-2.7346172	1.40E-46	CD4+ TNaive
KLRG1	5.99E-49	-4.3653572	2.22E-46	CD4+ TNaive
PDIA6	6.86E-46	-1.7850517	2.54E-43	CD4+ TNaive
GZMK	1.51E-45	-5.3950497	5.61E-43	CD4+ TNaive
IL18RAP	2.59E-45	-4.7014653	9.62E-43	CD4+ TNaive
TRDC	2.06E-43	-4.8519195	7.65E-41	CD4+ TNaive
HLA-DRA	7.87E-43	-4.9310344	2.92E-40	CD4+ TNaive
BIN2	1.12E-42	-1.027106	4.15E-40	CD4+ TNaive
FCER1G	2.76E-42	-5.4976336	1.02E-39	CD4+ TNaive
TRAT1	1.25E-41	0.51099508	4.65E-39	CD4+ TNaive
HLA-DQB1	1.15E-40	-4.2729741	4.27E-38	CD4+ TNaive
CCL4	2.85E-40	-5.4898528	1.06E-37	CD4+ TNaive
FOSB	5.20E-40	0.69652216	1.93E-37	CD4+ TNaive
NCR3	4.43E-39	-3.5710287	1.64E-36	CD4+ TNaive
CD6	7.88E-39	0.21842972	2.92E-36	CD4+ TNaive
LGALS3	3.58E-38	-5.5052675	1.33E-35	CD4+ TNaive
CHI3L2	8.21E-38	1.10061228	3.05E-35	CD4+ TNaive
KLRF1	1.45E-37	-4.0067448	5.40E-35	CD4+ TNaive
FYN	7.10E-37	-0.9841825	2.63E-34	CD4+ TNaive
CD244	3.46E-34	-3.9203007	1.28E-31	CD4+ TNaive
RPN2	9.20E-34	-1.1050343	3.41E-31	CD4+ TNaive
BAX	9.23E-34	-1.2198728	3.43E-31	CD4+ TNaive
LAMP1	1.07E-33	-1.0623884	3.96E-31	CD4+ TNaive
ZNF683	1.11E-32	-5.5152366	4.10E-30	CD4+ TNaive
LAT2	1.17E-32	-4.2945184	4.35E-30	CD4+ TNaive
CX3CR1	2.13E-32	-4.9087049	7.92E-30	CD4+ TNaive
IL7R	2.18E-31	-0.1171017	8.08E-29	CD4+ TNaive
KLRC1	4.16E-30	-4.4448742	1.55E-27	CD4+ TNaive
FYB	1.79E-29	0.35815662	6.66E-27	CD4+ TNaive
BCL2	2.85E-29	0.5475343	1.06E-26	CD4+ TNaive
ITGAX	1.19E-28	-4.0132426	4.40E-26	CD4+ TNaive
FOXP1	9.61E-27	0.34774817	3.57E-24	CD4+ TNaive
PTPRC	2.11E-26	-0.5587552	7.84E-24	CD4+ TNaive
CD28	2.85E-26	0.30070533	1.06E-23	CD4+ TNaive

HLA-DMA	2.98E-26	-2.7539888	1.11E-23	CD4+ TNaive
C10orf54	3.96E-26	-1.4109822	1.47E-23	CD4+ TNaive
BTG1	1.34E-25	-0.5873828	4.96E-23	CD4+ TNaive
GNAI2	6.07E-25	-1.2489504	2.25E-22	CD4+ TNaive
ITGA4	1.64E-24	-1.0588898	6.10E-22	CD4+ TNaive
B3GAT1	5.06E-22	-4.4970804	1.88E-19	CD4+ TNaive
CASP5	5.61E-22	-1.2242292	2.08E-19	CD4+ TNaive
CD37	1.66E-21	-0.6768808	6.15E-19	CD4+ TNaive
ZBTB16	1.02E-20	-3.2750067	3.77E-18	CD4+ TNaive
DUSP1	1.26E-20	-1.1483994	4.69E-18	CD4+ TNaive
IL4R	1.45E-20	0.15359183	5.39E-18	CD4+ TNaive
BACH2	5.45E-20	0.76519995	2.02E-17	CD4+ TNaive
IRF8	7.55E-20	-3.5320071	2.80E-17	CD4+ TNaive
YBX3	1.60E-19	-2.3059774	5.92E-17	CD4+ TNaive
ICOS	2.71E-19	0.60091355	1.00E-16	CD4+ TNaive
CD160	8.28E-19	-4.6775977	3.07E-16	CD4+ TNaive
IFNGR1	1.44E-18	-2.1502345	5.34E-16	CD4+ TNaive
CD79A	1.51E-18	-4.0839721	5.60E-16	CD4+ TNaive
MS4A1	1.80E-18	-3.1613794	6.68E-16	CD4+ TNaive
CD79B	6.18E-18	-2.530093	2.29E-15	CD4+ TNaive
IGHM-secreted	1.85E-17	-3.6965203	6.87E-15	CD4+ TNaive
IL18R1	3.64E-17	-2.8433444	1.35E-14	CD4+ TNaive
KIR2DL1	5.19E-17	-4.5933112	1.93E-14	CD4+ TNaive
RGS1	1.21E-16	-2.0402985	4.50E-14	CD4+ TNaive
LAG3	1.65E-16	-3.6067578	6.10E-14	CD4+ TNaive
CD2	4.18E-16	-0.8245682	1.55E-13	CD4+ TNaive
KLRC3	4.24E-16	-3.9982089	1.57E-13	CD4+ TNaive
FAS	6.08E-16	-2.7299332	2.26E-13	CD4+ TNaive
CCL3	1.08E-15	-4.5364135	4.01E-13	CD4+ TNaive
TRIB2	7.06E-15	0.24105656	2.62E-12	CD4+ TNaive
HAVCR2	1.05E-14	-3.4866614	3.90E-12	CD4+ TNaive
IGHM-membrane	2.10E-14	-3.4493552	7.78E-12	CD4+ TNaive
TSPAN32	1.93E-13	-1.5042525	7.15E-11	CD4+ TNaive
CD22	6.55E-13	-2.7378952	2.43E-10	CD4+ TNaive
KLRC4	7.20E-13	-5.3302613	2.67E-10	CD4+ TNaive
IGHD-membrane	9.17E-13	-3.8203215	3.40E-10	CD4+ TNaive
LAIR2	1.25E-12	-3.6442723	4.65E-10	CD4+ TNaive
TIGIT	3.31E-12	-2.3112284	1.23E-09	CD4+ TNaive
RORA	4.73E-12	-1.186951	1.75E-09	CD4+ TNaive
ADA	5.80E-12	-1.3193854	2.15E-09	CD4+ TNaive
LY86	5.90E-12	-3.262859	2.19E-09	CD4+ TNaive
PAX5	6.11E-12	-3.0961234	2.27E-09	CD4+ TNaive

CCR5	8.80E-12	-6.3405106	3.26E-09	CD4+ TNaive
MZB1	1.48E-11	-4.9013458	5.48E-09	CD4+ TNaive
CCR2	1.84E-11	-5.5469666	6.81E-09	CD4+ TNaive
TGFBI	2.23E-11	-5.0678094	8.28E-09	CD4+ TNaive
CTSD	2.81E-11	-1.8277316	1.04E-08	CD4+ TNaive
CXCR3	8.95E-11	-2.962528	3.32E-08	CD4+ TNaive
IFNG	1.33E-10	-3.3343969	4.93E-08	CD4+ TNaive
LTA	1.88E-10	0.60138016	6.97E-08	CD4+ TNaive
RNASE6	2.55E-10	-4.3560246	9.47E-08	CD4+ TNaive
CD86	3.28E-10	-5.2676412	1.22E-07	CD4+ TNaive
POU2AF1	4.32E-10	-2.8186859	1.60E-07	CD4+ TNaive
ITGAE	4.72E-10	-1.4329673	1.75E-07	CD4+ TNaive
VPREB3	5.89E-10	-3.5426541	2.19E-07	CD4+ TNaive
RORC	6.48E-10	-5.0377487	2.41E-07	CD4+ TNaive
IGKC	2.75E-09	-3.6774126	1.02E-06	CD4+ TNaive
CD24	3.83E-09	-4.3002093	1.42E-06	CD4+ TNaive
CD247	4.75E-09	-1.1150065	1.76E-06	CD4+ TNaive
CD1C	5.12E-09	-5.0067221	1.90E-06	CD4+ TNaive
BLNK	6.33E-09	-3.6741465	2.35E-06	CD4+ TNaive
FCER2	6.64E-09	-2.7272799	2.46E-06	CD4+ TNaive
LAP3	7.71E-09	-1.3307272	2.86E-06	CD4+ TNaive
CCR4	1.01E-08	-4.3475103	3.74E-06	CD4+ TNaive
IKZF2	1.32E-08	-3.2164123	4.90E-06	CD4+ TNaive
FASLG	8.17E-08	-3.5954928	3.03E-05	CD4+ TNaive
CD5	1.14E-07	-0.2821032	4.24E-05	CD4+ TNaive
CXCR2	1.19E-07	-5.3903523	4.40E-05	CD4+ TNaive
JCHAIN	1.19E-07	-6.0461388	4.43E-05	CD4+ TNaive
CD44	2.05E-07	-0.6528115	7.59E-05	CD4+ TNaive
DUSP4	3.24E-07	-4.042444	0.00012027	CD4+ TNaive
CMKLR1	3.85E-07	-4.6362063	0.00014297	CD4+ TNaive
LILRB4	3.87E-07	-3.7246231	0.00014368	CD4+ TNaive
FOXO1	4.36E-07	0.34159066	0.00016192	CD4+ TNaive
CD33	7.24E-07	-4.5013614	0.00026854	CD4+ TNaive
IGLC3	8.72E-07	-4.2431722	0.00032355	CD4+ TNaive
EOMES	1.22E-06	-5.2252205	0.00045267	CD4+ TNaive
TRAC	1.40E-06	-0.1360063	0.00051782	CD4+ TNaive
LGALS9	1.54E-06	-1.4028788	0.00057117	CD4+ TNaive
CXCL16	1.71E-06	-2.7852497	0.00063382	CD4+ TNaive
NINJ2	2.90E-06	-2.0855564	0.00107463	CD4+ TNaive
CD72	2.97E-06	-3.4751242	0.0011005	CD4+ TNaive
GAB2	3.20E-06	-3.0685075	0.00118738	CD4+ TNaive
LIPA	3.22E-06	-0.8507318	0.00119422	CD4+ TNaive

IGHG1-secreted	3.86E-06	-4.6746596	0.00143046	CD4+ TNaive
PDIA4	4.85E-06	-1.1941369	0.00179934	CD4+ TNaive
ENTPD1	4.92E-06	-3.5430528	0.00182368	CD4+ TNaive
ICAM1	6.07E-06	-2.0281901	0.00225153	CD4+ TNaive
FCN1	7.31E-06	-5.2067559	0.00271165	CD4+ TNaive
EGR1	9.66E-06	0.36162315	0.00358498	CD4+ TNaive
TCF4	1.65E-05	-3.6577853	0.00613301	CD4+ TNaive
FAM129C	2.09E-05	-2.6227175	0.00775009	CD4+ TNaive
IL12RB2	2.13E-05	-3.4953196	0.00791756	CD4+ TNaive
PTGDR2	2.34E-05	-4.2316491	0.00867769	CD4+ TNaive
AIM2	2.37E-05	-3.6731456	0.00878316	CD4+ TNaive
TCL1A	2.40E-05	-1.5490871	0.00889469	CD4+ TNaive
IL15	2.88E-05	-1.8639726	0.01066986	CD4+ TNaive
CBLB	3.25E-05	-1.0169047	0.01206853	CD4+ TNaive
IL12RB1	3.95E-05	-1.3017369	0.01463969	CD4+ TNaive
PCNA	4.37E-05	-1.545072	0.0161985	CD4+ TNaive
CXCR6	4.50E-05	-5.1897856	0.01668173	CD4+ TNaive
TNFSF13	5.39E-05	-2.0930221	0.01999509	CD4+ TNaive
KCNE3	5.70E-05	-4.1322837	0.02116333	CD4+ TNaive
SLC7A7	5.73E-05	-3.2341586	0.02126131	CD4+ TNaive
PSEN1	6.28E-05	-1.3829106	0.02329647	CD4+ TNaive
BCL6	6.30E-05	-2.6203716	0.02337961	CD4+ TNaive
TNFSF13B	8.89E-05	-1.7349404	0.03297521	CD4+ TNaive
CD70	9.80E-05	-4.7525213	0.03637011	CD4+ TNaive
TNFRSF4	0.00010536	-3.8194894	0.03908962	CD4+ TNaive
KIT	0.00012947	-2.837673	0.04803413	CD4+ TNaive
IL3RA	0.00020252	-5.0483951	0.07513418	CD4+ TNaive
LAMP3	0.0003533	0.47414733	0.13107418	CD4+ TNaive
CD36	0.00038543	-3.529143	0.14299629	CD4+ TNaive
CCND2	0.00039111	-0.9245247	0.14510226	CD4+ TNaive
CD3D	0.00043578	-0.4997338	0.16167501	CD4+ TNaive
CCR8	0.00046915	-3.934534	0.17405365	CD4+ TNaive
S100A12	0.00052874	-4.9832741	0.1961639	CD4+ TNaive
IL15RA	0.00055523	-1.7239602	0.20599117	CD4+ TNaive
CD163	0.00055525	-5.0617415	0.20599617	CD4+ TNaive
THBS1	0.00056265	-3.9924083	0.2087441	CD4+ TNaive
TNFSF14	0.00056372	-3.5303687	0.20914038	CD4+ TNaive
TIAF1	0.00074024	-0.8817519	0.27463	CD4+ TNaive
NAMPT	0.00091757	-1.504468	0.3404195	CD4+ TNaive
IL12A	0.00110461	-2.6026859	0.40981143	CD4+ TNaive
EBF1	0.00123682	-3.2990266	0.45886101	CD4+ TNaive
STAT5A	0.00137064	-0.1158481	0.50850852	CD4+ TNaive

CD69	0.00146242	-0.7013503	0.54255757	CD4+ TNaive
S100A9	0.00158799	-5.0871699	0.58914461	CD4+ TNaive
IRF4	0.00159023	-1.3763857	0.58997431	CD4+ TNaive
TNF	0.00185399	-1.1229087	0.68782998	CD4+ TNaive
CD38	0.00196316	-1.4753761	0.72833184	CD4+ TNaive
KDELR1	0.00285661	-1.4393583	1	CD4+ TNaive
CLEC4E	0.00344575	-3.0701654	1	CD4+ TNaive
NT5E	0.00351569	-1.4899662	1	CD4+ TNaive
F5	0.00386594	0.1193264	1	CD4+ TNaive
TRBC2	0.00404666	-0.3778248	1	CD4+ TNaive
BTLA	0.00423893	-0.8721282	1	CD4+ TNaive
CD40	0.00498182	-1.1142182	1	CD4+ TNaive
VNN2	0.0056596	-0.3152759	1	CD4+ TNaive
IL2RA	0.00694451	-1.4107062	1	CD4+ TNaive
CD3G	0.00702463	-0.8690083	1	CD4+ TNaive
CLEC10A	0.00863256	-4.7671765	1	CD4+ TNaive
IL18	0.0087856	-1.0498212	1	CD4+ TNaive
FCGR3A	0	2.99525164	0	CD161+ NK
GZMB	0	3.22583605	0	CD161+ NK
PRF1	0	3.2958875	0	CD161+ NK
GNLY	0	4.18541831	0	CD161+ NK
GZMH	0	2.14169905	0	CD161+ NK
KLRF1	0	4.30529142	0	CD161+ NK
GZMA	0	1.82784346	0	CD161+ NK
IL7R	0	-3.3899336	0	CD161+ NK
TBX21	0	2.54439829	0	CD161+ NK
CD300A	0	2.50296801	0	CD161+ NK
ITGAM	0	2.75428927	0	CD161+ NK
CST7	0	1.97673162	0	CD161+ NK
IL2RB	0	3.0471438	0	CD161+ NK
KLRK1	0	1.48220603	0	CD161+ NK
NKG7	0	2.65038569	0	CD161+ NK
CTSW	0	2.12767226	0	CD161+ NK
FCER1G	0	2.58106685	0	CD161+ NK
CD63	0	1.77333862	0	CD161+ NK
TRDC	0	1.67213387	0	CD161+ NK
CD247	0	1.97476671	0	CD161+ NK
CD244	0	3.03759907	0	CD161+ NK
ITGAX	0	2.64003855	0	CD161+ NK
RUNX3	0	1.51740367	0	CD161+ NK
KIR2DL1	0	5.30965181	0	CD161+ NK
B3GAT1	0	3.35064036	0	CD161+ NK

CD160	0	4.2592345	0	CD161+ NK
ITGB2	0	1.42604128	0	CD161+ NK
KLRC1	5.87E-300	2.44404752	2.18E-297	CD161+ NK
IL18RAP	4.03E-292	2.26534936	1.49E-289	CD161+ NK
CX3CR1	9.24E-274	2.41201023	3.43E-271	CD161+ NK
HLA-A	1.63E-269	0.55905495	6.04E-267	CD161+ NK
CCL4	1.39E-261	2.08805863	5.16E-259	CD161+ NK
KLRC3	1.01E-260	3.08369119	3.74E-258	CD161+ NK
CCL5	8.18E-257	1.00438187	3.03E-254	CD161+ NK
HAVCR2	1.55E-256	3.36002909	5.75E-254	CD161+ NK
NCR3	2.48E-252	1.99019205	9.20E-250	CD161+ NK
IL23R	3.20E-242	-1.4487051	1.19E-239	CD161+ NK
CD4	1.67E-233	-4.5512559	6.18E-231	CD161+ NK
CD38	4.66E-233	3.72175443	1.73E-230	CD161+ NK
CD5	6.59E-230	-3.2030083	2.45E-227	CD161+ NK
LAT2	8.63E-223	2.4068411	3.20E-220	CD161+ NK
ARL4C	3.81E-205	0.97112342	1.41E-202	CD161+ NK
PTPRC	1.28E-201	0.71991163	4.76E-199	CD161+ NK
PIK3AP1	2.47E-200	1.48489997	9.17E-198	CD161+ NK
IFITM3	5.43E-199	1.04338171	2.01E-196	CD161+ NK
CD27	1.16E-198	-3.6796742	4.32E-196	CD161+ NK
IFITM2	1.13E-194	1.00105133	4.21E-192	CD161+ NK
LYN	7.71E-188	1.00651491	2.86E-185	CD161+ NK
BIN2	6.92E-184	0.94641053	2.57E-181	CD161+ NK
TRAC	7.39E-175	-1.074839	2.74E-172	CD161+ NK
ZNF683	1.15E-174	1.78730179	4.26E-172	CD161+ NK
CCR7	7.05E-168	-3.1892383	2.61E-165	CD161+ NK
TXK	4.35E-162	2.0015078	1.61E-159	CD161+ NK
MYC	3.73E-161	-3.3499818	1.38E-158	CD161+ NK
CD6	3.95E-159	-1.4625326	1.47E-156	CD161+ NK
LEF1	1.88E-158	-2.1940101	6.97E-156	CD161+ NK
CD7	3.40E-156	1.84815502	1.26E-153	CD161+ NK
CD8A	7.44E-147	0.84721637	2.76E-144	CD161+ NK
CXCR2	2.28E-145	4.48301138	8.44E-143	CD161+ NK
TRAT1	1.50E-142	-4.2094346	5.57E-140	CD161+ NK
ZBTB16	4.62E-136	2.05536906	1.71E-133	CD161+ NK
FYN	5.48E-128	0.74574243	2.03E-125	CD161+ NK
CMKLR1	8.66E-126	3.80479049	3.21E-123	CD161+ NK
CD3D	5.79E-125	-0.7569197	2.15E-122	CD161+ NK
CD44	4.59E-123	-1.0632927	1.70E-120	CD161+ NK
APOBEC3G	1.22E-118	1.27483979	4.52E-116	CD161+ NK
LAIR2	3.42E-118	2.58573741	1.27E-115	CD161+ NK

LGALS1	8.53E-114	0.64400143	3.17E-111	CD161+ NK
LAMP1	2.80E-111	0.79554658	1.04E-108	CD161+ NK
TSPAN32	5.54E-110	1.3455149	2.06E-107	CD161+ NK
SELPLG	1.11E-109	0.65047713	4.12E-107	CD161+ NK
CTSD	8.56E-109	1.82474582	3.17E-106	CD161+ NK
TARP-refseq	1.34E-106	0.12659948	4.95E-104	CD161+ NK
PIK3IP1	1.12E-100	-1.0119916	4.15E-98	CD161+ NK
CD28	4.94E-100	-4.5072795	1.83E-97	CD161+ NK
PASK	2.35E-98	-2.3324829	8.71E-96	CD161+ NK
TCF7	1.75E-95	-3.1583854	6.49E-93	CD161+ NK
TNFSF8	4.31E-94	-3.0691012	1.60E-91	CD161+ NK
KLRB1	5.06E-90	0.59598457	1.88E-87	CD161+ NK
BIRC3	1.19E-86	-2.5712975	4.42E-84	CD161+ NK
IFNG	1.17E-82	2.10536974	4.34E-80	CD161+ NK
IKZF2	9.00E-77	2.20686965	3.34E-74	CD161+ NK
FASLG	2.75E-75	2.69133907	1.02E-72	CD161+ NK
CCL3	1.76E-67	1.62015412	6.51E-65	CD161+ NK
LTB	3.57E-66	-4.5077881	1.33E-63	CD161+ NK
GZMK	5.45E-64	-2.6525084	2.02E-61	CD161+ NK
CD48	4.14E-57	-0.5460211	1.53E-54	CD161+ NK
BCL11B	1.00E-56	-1.0749194	3.72E-54	CD161+ NK
CD3G	1.67E-55	-1.3094658	6.20E-53	CD161+ NK
HLA-DQB1	4.08E-55	-2.6158852	1.51E-52	CD161+ NK
ADA	8.95E-55	1.07021467	3.32E-52	CD161+ NK
DPP4	1.31E-52	-4.1371236	4.85E-50	CD161+ NK
NCAM1	4.98E-52	4.59202216	1.85E-49	CD161+ NK
CXCR4	7.14E-50	-0.6881936	2.65E-47	CD161+ NK
CD3E	5.67E-49	-0.4551682	2.10E-46	CD161+ NK
FYB	1.84E-48	-0.9037986	6.81E-46	CD161+ NK
XBP1	3.77E-47	0.85491707	1.40E-44	CD161+ NK
YBX3	9.24E-47	-1.8484248	3.43E-44	CD161+ NK
MS4A1	6.25E-46	-2.9245029	2.32E-43	CD161+ NK
CD79A	8.26E-45	-3.5702005	3.07E-42	CD161+ NK
TNFRSF25	1.40E-43	-2.0811302	5.20E-41	CD161+ NK
LGALS9	4.98E-43	0.98481322	1.85E-40	CD161+ NK
ANXA5	4.20E-42	-0.9874699	1.56E-39	CD161+ NK
ICOS	2.16E-41	-2.4463448	8.02E-39	CD161+ NK
IRF4	4.20E-39	1.33869257	1.56E-36	CD161+ NK
GAPDH	1.01E-37	0.21925277	3.76E-35	CD161+ NK
FOXP1	9.96E-37	-0.8430809	3.69E-34	CD161+ NK
BTLA	4.23E-36	-3.0433327	1.57E-33	CD161+ NK
HLA-DMA	1.67E-35	-1.7140043	6.21E-33	CD161+ NK

POU2AF1	3.76E-35	-3.3737423	1.40E-32	CD161+ NK
IL18R1	1.05E-34	1.19017154	3.91E-32	CD161+ NK
GIMAP5	9.75E-34	-0.9515455	3.62E-31	CD161+ NK
IGHD-membrane	1.05E-33	-3.418771	3.88E-31	CD161+ NK
CD52	1.79E-33	-0.2787366	6.64E-31	CD161+ NK
BCL2	2.13E-33	-1.047802	7.90E-31	CD161+ NK
CXCR1	3.96E-31	3.34880636	1.47E-28	CD161+ NK
BCL2A1	5.16E-31	-1.7919468	1.91E-28	CD161+ NK
STAT4	4.50E-30	0.76675639	1.67E-27	CD161+ NK
CD22	4.65E-30	-2.3145632	1.73E-27	CD161+ NK
DUSP1	1.38E-29	0.21714758	5.10E-27	CD161+ NK
CTLA4	3.62E-29	-2.6756505	1.34E-26	CD161+ NK
HLA-DRA	3.94E-29	-3.0254638	1.46E-26	CD161+ NK
IL32	7.20E-29	-0.3453566	2.67E-26	CD161+ NK
CD2	8.37E-29	-0.4437586	3.11E-26	CD161+ NK
GIMAP2	8.88E-29	-0.6930135	3.29E-26	CD161+ NK
CBLB	1.64E-28	0.72711519	6.08E-26	CD161+ NK
IL12RB1	2.70E-28	1.02021368	1.00E-25	CD161+ NK
IL4R	6.96E-28	-0.9026583	2.58E-25	CD161+ NK
IGHM-secreted	2.50E-27	-2.64636	9.29E-25	CD161+ NK
NT5E	7.52E-26	-3.2943155	2.79E-23	CD161+ NK
CCR2	1.74E-25	-4.5706662	6.47E-23	CD161+ NK
KLRC4	2.08E-25	1.42193081	7.73E-23	CD161+ NK
LCK	4.77E-25	0.29184698	1.77E-22	CD161+ NK
CD8B	5.90E-25	0.22363728	2.19E-22	CD161+ NK
LIPA	2.56E-24	0.57553104	9.49E-22	CD161+ NK
TGFBI	4.29E-24	-3.9939342	1.59E-21	CD161+ NK
LY86	4.66E-24	-2.480719	1.73E-21	CD161+ NK
CXCL16	7.91E-24	-3.5438879	2.93E-21	CD161+ NK
PAX5	1.21E-23	-2.2500172	4.49E-21	CD161+ NK
RORC	1.63E-23	-6.8752858	6.05E-21	CD161+ NK
BACH2	7.41E-23	-1.2859156	2.75E-20	CD161+ NK
VPREB3	3.47E-22	-3.0124203	1.29E-19	CD161+ NK
CD79B	7.01E-22	-1.3097397	2.60E-19	CD161+ NK
IL2RA	1.51E-21	-5.0161582	5.60E-19	CD161+ NK
CD86	1.87E-21	-4.866292	6.95E-19	CD161+ NK
BAX	1.22E-20	0.43670747	4.52E-18	CD161+ NK
SELL	6.82E-20	-0.3642398	2.53E-17	CD161+ NK
JUNB	7.19E-20	-0.5837671	2.67E-17	CD161+ NK
IFNGR1	9.62E-20	0.79158931	3.57E-17	CD161+ NK
CD24	1.10E-19	-3.5503212	4.09E-17	CD161+ NK
PRDM1	1.27E-19	0.39313734	4.71E-17	CD161+ NK

CCR4	1.43E-19	-5.6784098	5.30E-17	CD161+ NK
RNASE6	5.92E-19	-2.919606	2.20E-16	CD161+ NK
TCL1A	1.37E-18	-1.1406149	5.07E-16	CD161+ NK
TNFSF10	1.97E-18	-0.7860782	7.31E-16	CD161+ NK
BLNK	3.92E-18	-2.7051201	1.46E-15	CD161+ NK
FOXO1	1.33E-17	-1.2234694	4.93E-15	CD161+ NK
CD1C	2.03E-17	-3.78152	7.54E-15	CD161+ NK
CXCR5	2.54E-17	-3.0735119	9.44E-15	CD161+ NK
LILRB4	6.08E-17	-4.8810864	2.25E-14	CD161+ NK
RPN2	1.41E-16	0.28116569	5.23E-14	CD161+ NK
SLC7A7	4.48E-16	-4.8046725	1.66E-13	CD161+ NK
NAMPT	6.14E-16	-1.3249335	2.28E-13	CD161+ NK
KLRG1	1.49E-15	0.30795737	5.51E-13	CD161+ NK
FCER2	1.83E-15	-1.8481261	6.77E-13	CD161+ NK
FOXP3	2.19E-15	-4.5416231	8.13E-13	CD161+ NK
FAS	5.69E-15	-1.1998744	2.11E-12	CD161+ NK
JCHAIN	6.20E-15	-5.0485847	2.30E-12	CD161+ NK
IGHA1-secreted	6.29E-15	-5.3250661	2.33E-12	CD161+ NK
ADGRE1	1.01E-14	-3.3953393	3.74E-12	CD161+ NK
STAT1	1.38E-14	-0.6989866	5.11E-12	CD161+ NK
PDIA4	2.16E-14	0.7377574	8.01E-12	CD161+ NK
IGBP1	2.98E-14	-0.4847387	1.11E-11	CD161+ NK
S100A10	4.78E-14	-0.5141557	1.77E-11	CD161+ NK
LGALS3	1.82E-13	-1.3325269	6.76E-11	CD161+ NK
FAM65B	2.13E-13	-0.341747	7.92E-11	CD161+ NK
CR2	3.95E-13	-2.8509882	1.46E-10	CD161+ NK
LTA	6.75E-13	-1.2926023	2.51E-10	CD161+ NK
SLC25A37	8.44E-13	-0.7614831	3.13E-10	CD161+ NK
CD37	1.11E-12	-0.3921798	4.12E-10	CD161+ NK
FCN1	1.44E-12	-4.7572857	5.36E-10	CD161+ NK
CD33	1.45E-12	-3.8448584	5.38E-10	CD161+ NK
F5	2.53E-12	-5.8603406	9.40E-10	CD161+ NK
DUSP4	4.66E-12	-2.6649757	1.73E-09	CD161+ NK
TNFSF13B	6.61E-12	-1.4185262	2.45E-09	CD161+ NK
PTGDR2	1.20E-11	-3.970317	4.45E-09	CD161+ NK
STAT5A	1.64E-11	-0.4293962	6.08E-09	CD161+ NK
IL12RB2	1.95E-11	1.31411519	7.22E-09	CD161+ NK
IGKC	2.19E-11	-3.6196558	8.11E-09	CD161+ NK
TNFSF13	2.55E-11	-1.3676644	9.45E-09	CD161+ NK
PDIA6	3.94E-11	0.36673079	1.46E-08	CD161+ NK
CD69	5.36E-11	-0.4871972	1.99E-08	CD161+ NK
TCF4	5.86E-11	-3.1012973	2.17E-08	CD161+ NK

ZAP70	7.54E-11	0.79439251	2.80E-08	CD161+ NK
FAM129C	7.81E-11	-1.9301372	2.90E-08	CD161+ NK
ENTPD1	1.00E-10	-2.6930799	3.73E-08	CD161+ NK
TGFB1	1.17E-10	1.43872785	4.33E-08	CD161+ NK
S100A9	1.93E-10	-4.3981171	7.14E-08	CD161+ NK
KIT	1.96E-10	-3.9061431	7.29E-08	CD161+ NK
KCNE3	3.66E-10	-4.6696511	1.36E-07	CD161+ NK
IGHM-membrane	4.21E-10	-2.6759826	1.56E-07	CD161+ NK
STAT3	4.44E-10	0.5255168	1.65E-07	CD161+ NK
IGHG1-secreted	6.39E-10	-4.0497841	2.37E-07	CD161+ NK
TLR2	7.26E-10	-2.5028193	2.69E-07	CD161+ NK
CXCR3	1.76E-09	-1.0162711	6.53E-07	CD161+ NK
TNFRSF13C	2.68E-09	-2.5534664	9.93E-07	CD161+ NK
CXCR6	2.97E-09	-4.3707024	1.10E-06	CD161+ NK
FTH1	3.50E-09	-0.7201578	1.30E-06	CD161+ NK
CD40	4.77E-09	-1.2722704	1.77E-06	CD161+ NK
S100A12	5.54E-09	-3.9402426	2.05E-06	CD161+ NK
AIM2	7.84E-09	-2.3502566	2.91E-06	CD161+ NK
CD36	8.57E-09	-4.1879244	3.18E-06	CD161+ NK
GAB2	1.01E-08	-1.6549575	3.73E-06	CD161+ NK
MZB1	1.03E-08	-1.6119917	3.83E-06	CD161+ NK
KDELR1	2.34E-08	-0.9996753	8.68E-06	CD161+ NK
CASP5	3.81E-08	0.3332408	1.41E-05	CD161+ NK
CD200	4.92E-08	-2.2669541	1.83E-05	CD161+ NK
CCR8	5.69E-08	-5.2026333	2.11E-05	CD161+ NK
EOMES	1.06E-07	1.06091181	3.93E-05	CD161+ NK
CD163	3.00E-07	-5.1452089	0.00011126	CD161+ NK
CLEC4E	4.01E-07	-5.8815368	0.00014895	CD161+ NK
CCND2	6.99E-07	0.44341158	0.00025922	CD161+ NK
LAMP3	8.99E-07	-3.3287926	0.00033349	CD161+ NK
CLEC10A	1.31E-06	-5.1278653	0.00048443	CD161+ NK
CD14	1.80E-06	-4.0500101	0.00066928	CD161+ NK
FCER1A	2.31E-06	-4.6651301	0.00085535	CD161+ NK
MGST1	2.42E-06	-4.289811	0.00089649	CD161+ NK
GNAI2	3.92E-06	0.1491262	0.00145415	CD161+ NK
EBF1	4.70E-06	-1.8965704	0.00174462	CD161+ NK
TLR8	5.29E-06	-3.7038888	0.00196382	CD161+ NK
CD9	9.29E-06	-3.2398952	0.00344704	CD161+ NK
RGS1	1.12E-05	-0.9428449	0.00415601	CD161+ NK
MCM2	1.33E-05	1.20708918	0.00494333	CD161+ NK
C10orf54	5.90E-05	-0.1254598	0.02188912	CD161+ NK
IGLC3	6.18E-05	-3.6363395	0.02291435	CD161+ NK

ATF6B	9.74E-05	0.71472775	0.03615289	CD161+ NK
TNFRSF4	0.00011483	-0.6325995	0.0426009	CD161+ NK
IL3RA	0.00014516	-2.4915936	0.05385487	CD161+ NK
THBS1	0.00018403	0.74925838	0.06827635	CD161+ NK
DUSP2	0.00039731	-0.4516247	0.14740154	CD161+ NK
LAT	0.00049935	-0.2285684	0.18525825	CD161+ NK
CNOT2	0.00066873	0.38095526	0.24810049	CD161+ NK
TRBC2	0.00095647	-0.2079468	0.3548504	CD161+ NK
TMEM97	0.00139819	1.3086153	0.51872912	CD161+ NK
IER3	0.00171192	0.85354699	0.63512212	CD161+ NK
VPS28	0.00202796	0.22668293	0.75237269	CD161+ NK
RORA	0.00271834	0.13842613	1	CD161+ NK
CD70	0.00361388	-0.9515618	1	CD161+ NK
TRDC	0	3.70072916	0	gammadelta
TARP-refseq	0	2.85439807	0	gammadelta
KLRB1	5.93E-226	1.90932454	2.20E-223	gammadelta
CCL5	6.09E-212	1.48589682	2.26E-209	gammadelta
DUSP2	4.11E-161	1.52163659	1.53E-158	gammadelta
CST7	1.63E-159	1.21079372	6.04E-157	gammadelta
KLRG1	2.11E-154	2.01943954	7.83E-152	gammadelta
KLRC1	5.67E-138	2.35222967	2.10E-135	gammadelta
IL18RAP	3.88E-126	1.72777197	1.44E-123	gammadelta
NKG7	5.68E-95	0.49657309	2.11E-92	gammadelta
IL12RB2	3.04E-78	3.06846093	1.13E-75	gammadelta
GZMA	9.36E-78	0.73126753	3.47E-75	gammadelta
KLRK1	2.41E-77	0.88482264	8.93E-75	gammadelta
GZMK	1.65E-72	1.4275551	6.14E-70	gammadelta
ZBTB16	2.93E-70	1.6947354	1.09E-67	gammadelta
CTSW	1.69E-69	0.66188034	6.28E-67	gammadelta
CD4	2.51E-62	-3.297232	9.33E-60	gammadelta
IL32	1.42E-59	0.54106738	5.27E-57	gammadelta
CD300A	3.18E-59	1.07697526	1.18E-56	gammadelta
LEF1	7.24E-58	-2.0745699	2.68E-55	gammadelta
CD8B	1.76E-51	-3.7232576	6.53E-49	gammadelta
CD3D	7.44E-50	0.60752658	2.76E-47	gammadelta
TRAC	9.83E-50	-1.0540175	3.65E-47	gammadelta
CCR7	4.66E-46	-2.7895047	1.73E-43	gammadelta
CD8A	5.73E-44	-2.3022972	2.13E-41	gammadelta
LAG3	2.50E-41	1.69906744	9.26E-39	gammadelta
TBX21	2.03E-40	0.8052063	7.52E-38	gammadelta
RUNX3	3.51E-39	0.59725321	1.30E-36	gammadelta
ITGAM	1.32E-33	0.87317068	4.90E-31	gammadelta

ARL4C	4.98E-32	0.67173557	1.85E-29	gammadelta
TRBC2	7.78E-32	-0.9254445	2.89E-29	gammadelta
FCER1G	2.16E-31	-5.0032621	8.01E-29	gammadelta
IFNGR1	2.34E-30	1.29478809	8.66E-28	gammadelta
HLA-A	5.25E-30	0.26975858	1.95E-27	gammadelta
ITGB2	2.87E-27	0.26138084	1.06E-24	gammadelta
JUNB	1.27E-26	-0.9314702	4.70E-24	gammadelta
FOSB	5.40E-26	-2.1953892	2.00E-23	gammadelta
CD247	1.13E-25	0.67769766	4.18E-23	gammadelta
PRF1	1.86E-25	-0.2443252	6.90E-23	gammadelta
PASK	2.48E-25	-1.9527651	9.20E-23	gammadelta
CD3E	7.05E-23	0.37811179	2.61E-20	gammadelta
FYB	9.68E-23	-1.0503544	3.59E-20	gammadelta
APOBEC3G	1.39E-22	0.92249399	5.16E-20	gammadelta
RORA	8.68E-22	0.89810258	3.22E-19	gammadelta
LAT2	1.80E-21	-2.9301231	6.68E-19	gammadelta
IL18R1	3.31E-21	1.10156692	1.23E-18	gammadelta
MYC	3.90E-21	-1.4189979	1.45E-18	gammadelta
BIRC3	9.41E-21	-1.6360168	3.49E-18	gammadelta
CASP5	2.28E-20	0.76146375	8.48E-18	gammadelta
TCF7	2.43E-20	-2.0211405	9.00E-18	gammadelta
LGALS9	3.01E-19	-1.6613206	1.12E-16	gammadelta
IL4R	4.46E-19	-1.0105859	1.66E-16	gammadelta
LGALS1	6.16E-19	-1.134579	2.29E-16	gammadelta
PIK3AP1	4.57E-18	0.73943506	1.70E-15	gammadelta
FYN	5.28E-18	0.47433201	1.96E-15	gammadelta
NCR3	1.42E-17	0.8864852	5.28E-15	gammadelta
LGALS3	1.89E-16	-2.0206016	7.00E-14	gammadelta
HLA-DRA	3.35E-16	-3.2341157	1.24E-13	gammadelta
CD79A	1.36E-15	-3.5249699	5.04E-13	gammadelta
CD79B	5.23E-15	-2.0788088	1.94E-12	gammadelta
LTB	1.53E-14	-2.5873846	5.67E-12	gammadelta
IL7R	1.62E-14	0.32100737	6.01E-12	gammadelta
BIN2	1.77E-14	0.43078957	6.56E-12	gammadelta
TXK	1.93E-14	-1.3322687	7.16E-12	gammadelta
CD22	3.25E-14	-2.8623355	1.20E-11	gammadelta
CXCR6	4.31E-14	1.42340597	1.60E-11	gammadelta
IRF8	2.46E-13	-2.5043697	9.11E-11	gammadelta
PIK3IP1	9.34E-13	-0.4973049	3.46E-10	gammadelta
RGS1	1.53E-12	-1.566418	5.67E-10	gammadelta
JUN	1.60E-12	-0.9839069	5.92E-10	gammadelta
CBLB	2.77E-12	0.75835997	1.03E-09	gammadelta

BCL2	3.28E-12	-0.9190069	1.22E-09	gammadelta
CXCR4	3.43E-12	0.19042564	1.27E-09	gammadelta
CD3G	4.20E-12	0.66664983	1.56E-09	gammadelta
IGHM-secreted	5.42E-12	-2.7542187	2.01E-09	gammadelta
HLA-DMA	5.55E-12	-1.5174751	2.06E-09	gammadelta
CCR5	9.84E-12	1.28404255	3.65E-09	gammadelta
PAX5	2.11E-11	-3.8593362	7.82E-09	gammadelta
LY86	5.33E-11	-4.8014268	1.98E-08	gammadelta
POU2AF1	6.80E-11	-3.0480898	2.52E-08	gammadelta
ITGAX	7.90E-11	-1.8247944	2.93E-08	gammadelta
LYN	1.09E-10	-1.5344834	4.04E-08	gammadelta
CTLA4	3.46E-10	-2.586581	1.29E-07	gammadelta
CCL4	1.32E-09	0.36295463	4.90E-07	gammadelta
MS4A1	1.55E-09	-2.0486437	5.76E-07	gammadelta
IGHG1-secreted	1.71E-09	-5.8492548	6.36E-07	gammadelta
TRIB2	2.44E-09	-0.6349391	9.05E-07	gammadelta
HAVCR2	2.47E-09	-2.2937296	9.16E-07	gammadelta
IRF4	3.05E-09	-2.1486483	1.13E-06	gammadelta
FCGR3A	3.17E-09	-0.4443916	1.17E-06	gammadelta
ITGA4	4.18E-09	0.42048157	1.55E-06	gammadelta
TGFBI	5.06E-09	-5.0893232	1.88E-06	gammadelta
HLA-DQB1	1.72E-08	-1.8479901	6.36E-06	gammadelta
ICOS	1.88E-08	-1.1540163	6.98E-06	gammadelta
RNASE6	2.66E-08	-4.8016469	9.87E-06	gammadelta
CD38	3.28E-08	-2.1367479	1.22E-05	gammadelta
DOCK8	8.15E-08	-0.4753321	3.02E-05	gammadelta
IGHD-membrane	8.43E-08	-2.8038661	3.13E-05	gammadelta
CD28	1.14E-07	-0.7184041	4.22E-05	gammadelta
FCER2	2.26E-07	-2.1239498	8.39E-05	gammadelta
CD86	2.98E-07	-4.2080406	0.00011041	gammadelta
CX3CR1	3.10E-07	0.705828	0.00011483	gammadelta
TNFSF13B	3.33E-07	-2.0241103	0.00012371	gammadelta
CD44	6.44E-07	0.27649702	0.00023892	gammadelta
CXCL16	8.16E-07	-3.054751	0.00030259	gammadelta
GIMAP5	8.83E-07	-0.3344287	0.00032741	gammadelta
CD1C	9.15E-07	-3.8346813	0.00033942	gammadelta
BLNK	1.05E-06	-2.9280485	0.00038995	gammadelta
CXCR5	1.28E-06	-1.8325466	0.00047622	gammadelta
FCN1	1.42E-06	-5.2901745	0.00052586	gammadelta
VPREB3	1.82E-06	-2.0648701	0.00067384	gammadelta
TNFSF13	2.31E-06	-1.5370017	0.00085694	gammadelta
KLRC4	2.42E-06	0.79890565	0.00089781	gammadelta

LILRB4	2.85E-06	-5.2579877	0.00105768	gammadelta
KIR2DL1	2.94E-06	-1.8099414	0.001089	gammadelta
IGLC3	3.06E-06	-3.771851	0.00113686	gammadelta
BACH2	6.81E-06	-0.9469784	0.00252757	gammadelta
TIGIT	7.76E-06	-1.1358704	0.00287844	gammadelta
IL2RA	9.36E-06	-2.4167924	0.00347397	gammadelta
SLC7A7	1.08E-05	-4.5815878	0.00402269	gammadelta
BCL11B	1.30E-05	-0.3600704	0.00483193	gammadelta
EGR1	1.44E-05	-2.0743037	0.00534657	gammadelta
NT5E	1.68E-05	-1.6088443	0.00622669	gammadelta
CD33	1.94E-05	-5.2712267	0.00721509	gammadelta
TNFSF14	1.97E-05	1.52993845	0.00729849	gammadelta
S100A9	2.11E-05	-5.0367623	0.00782884	gammadelta
TNFRSF25	2.23E-05	-0.7687465	0.00825772	gammadelta
LAMP1	2.30E-05	0.26410331	0.00855067	gammadelta
LAIR2	2.43E-05	-2.0182278	0.00899691	gammadelta
CCR4	2.56E-05	-2.5968724	0.0094789	gammadelta
ENTPD1	3.46E-05	-4.4548552	0.01283329	gammadelta
B3GAT1	4.35E-05	-1.0624666	0.01613937	gammadelta
CD24	4.50E-05	-1.7993981	0.01670189	gammadelta
JCHAIN	4.53E-05	-4.9126736	0.01680635	gammadelta
FOXP1	4.98E-05	-0.2444696	0.01847427	gammadelta
CCL3	6.52E-05	0.31942951	0.02419091	gammadelta
ZAP70	6.59E-05	-0.6133453	0.02443153	gammadelta
TLR2	0.00010067	-3.8165896	0.0373485	gammadelta
PTGDR2	0.00015435	-4.1475267	0.0572625	gammadelta
ANXA5	0.00015571	-0.3903535	0.05776801	gammadelta
STAT6	0.00018746	-0.3650322	0.06954773	gammadelta
IL23R	0.00019247	-0.2760073	0.07140726	gammadelta
FAM129C	0.00020133	-2.020783	0.0746935	gammadelta
MZB1	0.00020911	-1.9147728	0.07758086	gammadelta
TCF4	0.00024527	-3.4871474	0.09099676	gammadelta
GAB2	0.00025599	-2.1739052	0.09497368	gammadelta
CD37	0.00030199	-0.2605553	0.11203809	gammadelta
CMKLR1	0.00030408	-2.4602865	0.11281245	gammadelta
PTPRC	0.00034925	0.1512936	0.12957187	gammadelta
ADGRE1	0.00039394	-1.9126772	0.1461504	gammadelta
KCNE3	0.00040582	-4.1096521	0.15055936	gammadelta
BTG1	0.00041662	0.15072274	0.15456524	gammadelta
CTSD	0.00048748	-0.4510749	0.18085333	gammadelta
CD200	0.00051039	-3.2192779	0.18935554	gammadelta
IGKC	0.00051419	-3.3290627	0.19076378	gammadelta

TNFSF8	0.00051536	-0.4836371	0.19119965	gammadelta
S100A12	0.00055142	-5.0137432	0.20457766	gammadelta
BAX	0.00056398	0.26165483	0.20923489	gammadelta
F5	0.00060651	-1.9708687	0.22501641	gammadelta
TNFRSF4	0.00062082	-3.9088586	0.23032519	gammadelta
CD7	0.00063532	-0.3572989	0.23570212	gammadelta
IFITM3	0.00069629	-0.2800197	0.2583238	gammadelta
NAMPT	0.00076066	-0.7689411	0.2822058	gammadelta
ITGAE	0.00079566	0.55059821	0.2951914	gammadelta
TNF	0.00081275	-1.4562893	0.30153184	gammadelta
BTLA	0.00081656	-0.4481199	0.30294447	gammadelta
FOXP3	0.00083741	-2.6188962	0.3106788	gammadelta
TNFSF10	0.00084775	-0.3548907	0.31451537	gammadelta
CD72	0.0009104	-1.9079232	0.33775911	gammadelta
STAT4	0.00099359	0.40399581	0.36862014	gammadelta
CD14	0.00105139	-4.6272693	0.39006648	gammadelta
CD40	0.00108104	-0.9473525	0.40106711	gammadelta
CR2	0.00108359	-2.1160594	0.40201227	gammadelta
PSEN1	0.00135139	0.68746542	0.50136599	gammadelta
CD5	0.001641	0.26818627	0.60881177	gammadelta
FCER1A	0.00175837	-4.4406658	0.65235519	gammadelta
IL3RA	0.0021523	-4.4959599	0.79850444	gammadelta
CD36	0.00222308	-3.222965	0.82476365	gammadelta
GNAI2	0.00237826	-0.1550671	0.88233537	gammadelta
CCND2	0.00262848	-0.2619743	0.97516786	gammadelta
TCL1A	0.00270986	-0.4263618	1	gammadelta
ICAM1	0.0029219	-1.1468142	1	gammadelta
CXCR3	0.00299367	-0.6608366	1	gammadelta
CLEC10A	0.00331033	-5.596762	1	gammadelta
IFNG	0.00367057	-1.2462862	1	gammadelta
IL18	0.00370264	-0.3617465	1	gammadelta
IGHA1-secreted	0.00416894	-4.5461674	1	gammadelta
FASLG	0.00421812	0.67103257	1	gammadelta
CD163	0.00435858	-4.5093063	1	gammadelta
IER3	0.00581393	-0.3676847	1	gammadelta
DPP4	0.00603511	0.74150988	1	gammadelta
SELL	0.00607918	-0.280805	1	gammadelta
PDIA6	0.0061765	0.27396347	1	gammadelta
FOXO1	0.00704991	-0.223788	1	gammadelta
MCM2	0.00912419	-0.7333035	1	gammadelta
TNFRSF13C	0.00996634	-1.2418314	1	gammadelta
FOXP3	0	7.46832303	0	Treg

CTLA4	8.06E-120	3.37595871	2.99E-117	Treg
IL2RA	2.97E-65	3.150425	1.10E-62	Treg
IKZF2	1.16E-44	2.610404	4.31E-42	Treg
CD27	6.17E-38	1.40903527	2.29E-35	Treg
F5	8.95E-37	3.00382188	3.32E-34	Treg
CTSW	4.05E-33	-3.7090367	1.50E-30	Treg
CCL5	1.35E-31	-4.1025023	5.01E-29	Treg
DUSP4	6.95E-31	2.24046517	2.58E-28	Treg
NKG7	1.11E-30	-5.365881	4.11E-28	Treg
CCR3	3.15E-26	3.85528646	1.17E-23	Treg
RUNX3	5.99E-26	-2.2420096	2.22E-23	Treg
ITGB2	1.71E-25	-1.6729067	6.33E-23	Treg
RGS1	1.96E-25	1.49272421	7.26E-23	Treg
GZMA	1.82E-24	-3.538213	6.74E-22	Treg
LEF1	2.58E-24	1.18455292	9.59E-22	Treg
KLRK1	1.34E-23	-3.9328737	4.99E-21	Treg
CD4	8.19E-22	0.87907433	3.04E-19	Treg
TARP-refseq	1.07E-20	-3.7476845	3.99E-18	Treg
PRF1	5.97E-19	-4.473642	2.21E-16	Treg
GZMH	7.42E-19	-5.6930708	2.75E-16	Treg
CD8A	2.52E-18	-3.5913951	9.34E-16	Treg
CST7	7.85E-18	-3.0796679	2.91E-15	Treg
LGALS3	3.23E-17	1.1454073	1.20E-14	Treg
FCGR3A	9.20E-17	-5.0397973	3.41E-14	Treg
GZMB	9.24E-17	-4.8148015	3.43E-14	Treg
CD300A	1.14E-16	-4.8438273	4.23E-14	Treg
SELL	5.93E-16	0.7224796	2.20E-13	Treg
IFITM2	1.54E-14	-1.2928483	5.70E-12	Treg
IFITM3	9.67E-14	-1.3700157	3.59E-11	Treg
TIGIT	2.77E-13	1.26517381	1.03E-10	Treg
CD63	1.06E-12	-1.8098813	3.94E-10	Treg
ICOS	1.51E-12	1.71799747	5.59E-10	Treg
DUSP2	2.16E-12	-2.277349	8.00E-10	Treg
PIK3AP1	5.85E-12	-5.0798703	2.17E-09	Treg
ARL4C	1.50E-11	-1.4099697	5.55E-09	Treg
BIRC3	1.88E-11	1.12036649	6.98E-09	Treg
CD8B	3.20E-11	-2.6364771	1.19E-08	Treg
TRAC	9.03E-11	0.39624292	3.35E-08	Treg
LYN	1.46E-10	-5.1254235	5.41E-08	Treg
TBX21	4.18E-10	-2.5648117	1.55E-07	Treg
GNLY	3.39E-09	-4.2748086	1.26E-06	Treg
KLRG1	4.37E-09	-3.4227325	1.62E-06	Treg

CCR10	7.54E-09	3.19593975	2.80E-06	Treg
BTG1	1.40E-08	-0.6145005	5.21E-06	Treg
NINJ2	5.71E-08	1.47889542	2.12E-05	Treg
KLRF1	7.27E-08	-3.9123594	2.70E-05	Treg
FCER1G	8.29E-08	-4.610938	3.08E-05	Treg
XBP1	1.17E-07	-1.4438961	4.36E-05	Treg
LAMP1	1.93E-07	-0.8404012	7.16E-05	Treg
ITGAM	3.00E-07	-2.5173058	0.00011128	Treg
TRDC	3.14E-07	-4.5019372	0.00011645	Treg
LAT2	3.99E-07	-4.9137947	0.00014812	Treg
YBX3	4.73E-07	-3.8749627	0.00017555	Treg
IL7R	7.03E-07	-1.298418	0.00026065	Treg
APOBEC3G	8.32E-07	-1.914206	0.00030855	Treg
CD74	8.71E-07	-1.9595252	0.00032309	Treg
CCR9	8.90E-07	2.75700738	0.00033009	Treg
ITGA4	1.00E-06	-0.7970031	0.00037175	Treg
CCL4	1.21E-06	-3.3782394	0.00045051	Treg
ITGAX	1.43E-06	-4.0057995	0.00052909	Treg
KLRC1	1.54E-06	-4.8390439	0.00056956	Treg
CCR4	1.77E-06	1.54412526	0.00065655	Treg
LGALS1	1.89E-06	-1.2293114	0.00070064	Treg
STAT4	2.62E-06	-1.9784447	0.00097063	Treg
CX3CR1	3.06E-06	-4.192103	0.00113569	Treg
TRBC2	3.37E-06	0.33430348	0.00125091	Treg
LAMP3	3.81E-06	2.45001994	0.00141335	Treg
PIK3IP1	3.97E-06	0.43655032	0.00147124	Treg
CD244	4.36E-06	-3.2527081	0.00161799	Treg
TRIB2	4.71E-06	0.74721079	0.00174751	Treg
GZMK	4.88E-06	-3.0879198	0.00181138	Treg
PTPRC	5.92E-06	-0.5391922	0.00219558	Treg
CD28	6.90E-06	0.58012098	0.00255964	Treg
IL32	7.64E-06	0.26298471	0.00283413	Treg
HLA-A	1.61E-05	-0.3511773	0.00598753	Treg
ZBTB16	4.00E-05	-3.8201469	0.01482794	Treg
IRF8	4.96E-05	-3.1491866	0.0183992	Treg
ZNF683	5.31E-05	-3.2225588	0.01970344	Treg
HLA-DPA1	6.55E-05	-2.0372532	0.02430813	Treg
CD80	7.08E-05	3.15473138	0.02624851	Treg
IFNGR1	9.14E-05	-2.0819854	0.03392176	Treg
IL18RAP	0.00012348	-2.2489372	0.04581127	Treg
PDIA4	0.00015375	-1.781759	0.05704057	Treg
CD160	0.00018083	-4.8631347	0.06708905	Treg

CD44	0.00023705	0.30853091	0.08794527	Treg
LRRC32	0.0002614	3.84209814	0.09697945	Treg
ADA	0.00027786	-1.3993423	0.10308508	Treg
CCL3	0.00050487	-4.7328354	0.18730662	Treg
B3GAT1	0.00058818	-2.879159	0.21821632	Treg
CCR7	0.00064318	0.23125381	0.23861968	Treg
KIR2DL1	0.00074298	-4.017115	0.27564706	Treg
FAS	0.00078782	0.45676503	0.2922825	Treg
RPN2	0.00095437	-0.605534	0.35406944	Treg
DUSP1	0.0009697	-0.8761308	0.35975974	Treg
BCL2	0.00105511	0.28039244	0.39144697	Treg
LY86	0.00125649	-4.0637998	0.46615831	Treg
CD3D	0.00132719	0.12805779	0.49238884	Treg
CD5	0.00142463	0.18261246	0.52853712	Treg
IGLC3	0.00152036	-4.1354245	0.56405321	Treg
NCR3	0.00162835	-1.5239917	0.60411773	Treg
TGFBI	0.00230857	-5.1103343	0.85647936	Treg
CD22	0.00236148	-2.453672	0.87610743	Treg
CD48	0.00289612	-0.3699401	1	Treg
EGR1	0.00298397	1.70210572	1	Treg
KLRB1	0.00302431	-1.5348281	1	Treg
CD79A	0.00345767	-3.1416771	1	Treg
LIPA	0.0034785	-0.8123059	1	Treg
ITGAE	0.0035341	-0.7420317	1	Treg
IGHG1-secreted	0.00399976	-5.4912651	1	Treg
KLRC3	0.00422126	-2.9474048	1	Treg
IGHM-membrane	0.00423444	-3.0407991	1	Treg
IL4R	0.00504452	-0.9204719	1	Treg
CD37	0.00514717	-0.4528287	1	Treg
RNASE6	0.00582222	-3.8161971	1	Treg
MS4A1	0.00584503	-2.5223091	1	Treg
ENTPD1	0.00644394	1.14172481	1	Treg
PAX5	0.00739364	-2.3709577	1	Treg
HAVCR2	0.00811624	-2.3298881	1	Treg
PTTG2	0.00821729	1.30771333	1	Treg
PDIA6	0.00866673	-0.7880976	1	Treg
CXCL16	0.00890499	-3.4793588	1	Treg
KLRC4	0.00912516	-2.8592151	1	Treg
GZMH	0	2.40850903	0	CD8+ Tc1
CD8A	0	2.47175059	0	CD8+ Tc1
CD8B	1.24E-255	2.13556489	4.62E-253	CD8+ Tc1
NKG7	6.38E-219	1.41801539	2.37E-216	CD8+ Tc1

CCL5	3.82E-215	1.41610565	1.42E-212	CD8+ Tc1
GZMB	5.20E-165	1.23728279	1.93E-162	CD8+ Tc1
CST7	1.87E-159	1.15095707	6.92E-157	CD8+ Tc1
GZMA	5.70E-133	1.20029285	2.12E-130	CD8+ Tc1
PRF1	1.43E-129	0.81503901	5.29E-127	CD8+ Tc1
TARP-refseq	3.07E-128	1.21466945	1.14E-125	CD8+ Tc1
KLRK1	3.46E-119	1.23995853	1.28E-116	CD8+ Tc1
ZNF683	3.39E-115	2.28086738	1.26E-112	CD8+ Tc1
CD3D	2.66E-102	1.04656879	9.87E-100	CD8+ Tc1
ITGB2	1.69E-97	0.7774275	6.25E-95	CD8+ Tc1
HLA-A	2.28E-95	0.55156789	8.45E-93	CD8+ Tc1
CTSW	3.62E-85	0.7917952	1.34E-82	CD8+ Tc1
CX3CR1	5.42E-74	1.87849675	2.01E-71	CD8+ Tc1
TRAC	9.11E-70	0.7434609	3.38E-67	CD8+ Tc1
CD4	1.69E-69	-3.3347666	6.26E-67	CD8+ Tc1
IL32	1.96E-66	0.59191263	7.29E-64	CD8+ Tc1
IL7R	2.54E-64	-1.5975687	9.42E-62	CD8+ Tc1
CD2	1.22E-62	0.94992139	4.53E-60	CD8+ Tc1
CCL4	7.33E-62	1.97477685	2.72E-59	CD8+ Tc1
RUNX3	4.98E-61	0.68588401	1.85E-58	CD8+ Tc1
SELL	2.41E-60	-1.3814105	8.95E-58	CD8+ Tc1
IL23R	3.70E-59	-1.0831984	1.37E-56	CD8+ Tc1
CCR7	2.72E-55	-3.3796858	1.01E-52	CD8+ Tc1
MYC	3.17E-54	-3.1512775	1.18E-51	CD8+ Tc1
TBX21	9.70E-54	0.97414543	3.60E-51	CD8+ Tc1
CD52	1.56E-51	0.54073676	5.79E-49	CD8+ Tc1
LEF1	9.81E-51	-1.8972793	3.64E-48	CD8+ Tc1
PTPRC	5.17E-50	0.62892034	1.92E-47	CD8+ Tc1
TRBC2	1.85E-42	0.72865777	6.88E-40	CD8+ Tc1
KLRG1	1.67E-38	1.22253822	6.19E-36	CD8+ Tc1
LAIR2	1.14E-34	1.87158214	4.21E-32	CD8+ Tc1
TCF7	8.56E-33	-2.8715357	3.17E-30	CD8+ Tc1
TXK	9.80E-32	-2.3828464	3.64E-29	CD8+ Tc1
FYN	9.37E-31	0.56165255	3.48E-28	CD8+ Tc1
DUSP2	9.73E-31	0.41288915	3.61E-28	CD8+ Tc1
CD3E	1.89E-30	0.44911733	7.00E-28	CD8+ Tc1
LAG3	1.42E-29	1.61759981	5.28E-27	CD8+ Tc1
CD28	5.15E-29	-2.7951028	1.91E-26	CD8+ Tc1
CD27	1.09E-28	-1.140085	4.04E-26	CD8+ Tc1
SELPLG	1.38E-28	0.56708561	5.13E-26	CD8+ Tc1
HLA-DPA1	1.48E-28	-0.2001579	5.51E-26	CD8+ Tc1
LCK	1.52E-28	0.57982189	5.63E-26	CD8+ Tc1

TRDC	1.90E-28	-2.7397346	7.03E-26	CD8+ Tc1
FCER1G	2.05E-27	-3.6417888	7.61E-25	CD8+ Tc1
BIN2	2.42E-26	0.54817966	8.96E-24	CD8+ Tc1
TIGIT	2.86E-25	1.45922905	1.06E-22	CD8+ Tc1
LGALS9	3.53E-25	-1.9324329	1.31E-22	CD8+ Tc1
TNFSF8	6.82E-25	-2.1642641	2.53E-22	CD8+ Tc1
B3GAT1	1.16E-24	1.36990691	4.29E-22	CD8+ Tc1
PASK	9.66E-24	-1.6022877	3.58E-21	CD8+ Tc1
LAT2	1.36E-23	-2.8010852	5.05E-21	CD8+ Tc1
LGALS1	2.07E-23	0.51700258	7.68E-21	CD8+ Tc1
LTB	6.75E-23	-4.506292	2.51E-20	CD8+ Tc1
JUNB	1.56E-22	-0.7888529	5.77E-20	CD8+ Tc1
BIRC3	6.94E-22	-1.4466285	2.58E-19	CD8+ Tc1
ZBTB16	1.55E-19	-3.8141576	5.75E-17	CD8+ Tc1
CD6	3.34E-19	0.64444846	1.24E-16	CD8+ Tc1
CD79A	3.82E-18	-3.6428928	1.42E-15	CD8+ Tc1
TRAT1	6.51E-18	-1.1758107	2.42E-15	CD8+ Tc1
IL4R	1.44E-17	-0.9112216	5.35E-15	CD8+ Tc1
ITGA4	1.88E-17	0.60225899	6.96E-15	CD8+ Tc1
LGALS3	1.34E-16	-1.7819047	4.99E-14	CD8+ Tc1
GAPDH	1.36E-16	0.32612477	5.05E-14	CD8+ Tc1
TNFSF10	1.71E-16	-1.098748	6.35E-14	CD8+ Tc1
LAMP1	1.54E-15	0.5818859	5.72E-13	CD8+ Tc1
MS4A1	3.68E-15	-2.5042543	1.37E-12	CD8+ Tc1
ITGAX	1.21E-14	-2.1793481	4.48E-12	CD8+ Tc1
ARL4C	1.27E-14	0.36520276	4.71E-12	CD8+ Tc1
CD37	1.82E-14	-0.4416619	6.77E-12	CD8+ Tc1
IL18RAP	4.21E-14	-1.5524651	1.56E-11	CD8+ Tc1
PIK3IP1	6.77E-14	-0.5390875	2.51E-11	CD8+ Tc1
CD79B	7.88E-14	-1.640171	2.93E-11	CD8+ Tc1
LAT	1.98E-13	0.63198628	7.34E-11	CD8+ Tc1
ITGAM	3.03E-13	0.56497631	1.13E-10	CD8+ Tc1
DPP4	8.56E-13	-2.1687576	3.18E-10	CD8+ Tc1
IFNG	1.17E-12	2.00561453	4.33E-10	CD8+ Tc1
IRF8	1.36E-12	-2.3149258	5.05E-10	CD8+ Tc1
LY86	3.44E-12	-4.8936585	1.28E-09	CD8+ Tc1
CD22	4.94E-12	-2.4162054	1.83E-09	CD8+ Tc1
IGHM-secreted	5.20E-12	-2.4504546	1.93E-09	CD8+ Tc1
POU2AF1	1.44E-11	-2.7446274	5.36E-09	CD8+ Tc1
IGHD-membrane	1.52E-11	-3.0111783	5.63E-09	CD8+ Tc1
CD3G	3.48E-11	0.85217412	1.29E-08	CD8+ Tc1
APOBEC3G	5.98E-11	0.76996987	2.22E-08	CD8+ Tc1

PAX5	6.28E-11	-2.3047252	2.33E-08	CD8+ Tc1
FOXP1	2.23E-10	-0.421225	8.27E-08	CD8+ Tc1
KLRB1	2.35E-10	-0.8266606	8.72E-08	CD8+ Tc1
PRDM1	3.71E-10	0.69158441	1.38E-07	CD8+ Tc1
CD7	4.82E-10	-0.6938879	1.79E-07	CD8+ Tc1
GZMK	5.39E-10	-1.8180011	2.00E-07	CD8+ Tc1
FTH1	5.61E-10	-0.7356008	2.08E-07	CD8+ Tc1
NT5E	1.03E-09	-3.0089324	3.82E-07	CD8+ Tc1
LYN	1.31E-09	-1.2961231	4.84E-07	CD8+ Tc1
VPREB3	1.36E-09	-3.1470173	5.05E-07	CD8+ Tc1
TRIB2	1.38E-09	-0.422083	5.12E-07	CD8+ Tc1
IGHG1-secreted	2.59E-09	-4.8370449	9.62E-07	CD8+ Tc1
BACH2	7.44E-09	-1.3152116	2.76E-06	CD8+ Tc1
NCR3	9.67E-09	-0.9208069	3.59E-06	CD8+ Tc1
HLA-DQB1	1.12E-08	-1.5807082	4.17E-06	CD8+ Tc1
TNFRSF25	1.15E-08	-0.9576591	4.27E-06	CD8+ Tc1
CXCL16	1.33E-08	-2.9101559	4.95E-06	CD8+ Tc1
KIR2DL1	1.46E-08	-2.1483399	5.40E-06	CD8+ Tc1
KLRF1	2.10E-08	-1.3784103	7.81E-06	CD8+ Tc1
DUSP1	2.40E-08	-0.5894726	8.90E-06	CD8+ Tc1
CD5	2.87E-08	0.57704534	1.07E-05	CD8+ Tc1
KLRC4	3.08E-08	1.301062	1.14E-05	CD8+ Tc1
ADA	4.09E-08	0.83600987	1.52E-05	CD8+ Tc1
CCR2	6.46E-08	-2.899847	2.40E-05	CD8+ Tc1
TNFSF13B	1.13E-07	-2.8201107	4.20E-05	CD8+ Tc1
RORC	1.18E-07	-3.5646468	4.36E-05	CD8+ Tc1
KLRC1	1.78E-07	-0.9683508	6.62E-05	CD8+ Tc1
IL2RA	2.32E-07	-2.4907353	8.60E-05	CD8+ Tc1
BTLA	2.48E-07	-1.1680062	9.20E-05	CD8+ Tc1
RNASE6	2.60E-07	-2.5422403	9.64E-05	CD8+ Tc1
FCER2	3.28E-07	-1.5865631	0.00012159	CD8+ Tc1
GIMAP2	3.59E-07	-0.3068087	0.00013335	CD8+ Tc1
IRF4	4.02E-07	1.04103807	0.00014923	CD8+ Tc1
CD86	4.53E-07	-2.7736876	0.00016792	CD8+ Tc1
KIAA0101	6.49E-07	2.51534184	0.00024059	CD8+ Tc1
CXCR5	6.74E-07	-2.9383746	0.00025019	CD8+ Tc1
CCR4	7.24E-07	-3.6462977	0.00026867	CD8+ Tc1
CD1C	1.10E-06	-2.4405413	0.00040933	CD8+ Tc1
NAMPT	1.31E-06	-1.0776676	0.00048702	CD8+ Tc1
IGKC	1.52E-06	-2.3632994	0.00056334	CD8+ Tc1
CD63	2.30E-06	0.20487201	0.00085256	CD8+ Tc1
CD24	2.82E-06	-2.401639	0.00104736	CD8+ Tc1

IL18R1	3.00E-06	-0.9526556	0.00111245	CD8+ Tc1
BLNK	3.58E-06	-1.7968789	0.00132801	CD8+ Tc1
IL12RB2	3.73E-06	-5.2440844	0.00138522	CD8+ Tc1
FCN1	5.39E-06	-4.9699949	0.00199839	CD8+ Tc1
FAM65B	5.63E-06	-0.2367181	0.00209018	CD8+ Tc1
BCL2	6.08E-06	-0.3776107	0.00225664	CD8+ Tc1
CD33	6.24E-06	-5.4334705	0.00231399	CD8+ Tc1
PDIA6	6.97E-06	0.48622205	0.00258401	CD8+ Tc1
CD40	7.65E-06	-1.6446944	0.00283934	CD8+ Tc1
LTA	9.31E-06	-1.5123201	0.00345262	CD8+ Tc1
CD244	1.47E-05	0.58101405	0.00546864	CD8+ Tc1
PTGDR2	1.82E-05	-5.3192388	0.00673851	CD8+ Tc1
LILRB4	1.84E-05	-3.2069433	0.00682673	CD8+ Tc1
IGHA1-secreted	2.36E-05	-1.9835968	0.00877256	CD8+ Tc1
S100A9	2.56E-05	-3.9019632	0.00949308	CD8+ Tc1
ADGRE1	4.47E-05	-2.2201884	0.01658188	CD8+ Tc1
JCHAIN	4.76E-05	-2.8796012	0.01766075	CD8+ Tc1
IL18	5.18E-05	-0.480876	0.01923576	CD8+ Tc1
TYMS	5.59E-05	3.11436497	0.02075672	CD8+ Tc1
FYB	6.79E-05	-0.2514758	0.0251892	CD8+ Tc1
FAM129C	6.87E-05	-1.8019708	0.02548077	CD8+ Tc1
GAB2	7.47E-05	-1.135649	0.02771397	CD8+ Tc1
CD300A	7.53E-05	-0.3792492	0.02794961	CD8+ Tc1
TNFSF13	7.55E-05	-1.3018053	0.02800426	CD8+ Tc1
IGLC3	0.00011195	-3.3083584	0.04153402	CD8+ Tc1
IKZF2	0.00011555	-1.302054	0.04286804	CD8+ Tc1
IL12RB1	0.00012305	0.84539144	0.04565246	CD8+ Tc1
IGBP1	0.00013509	-0.2445194	0.05011775	CD8+ Tc1
CR2	0.00014282	-2.3083346	0.05298509	CD8+ Tc1
KIT	0.000148	-4.2942196	0.05490924	CD8+ Tc1
TCL1A	0.0001579	-0.4955414	0.05858241	CD8+ Tc1
BTG1	0.00016739	-0.1510116	0.06210036	CD8+ Tc1
SLC7A7	0.00017051	-0.8950696	0.06325896	CD8+ Tc1
KCNE3	0.00018343	-4.2718959	0.06805148	CD8+ Tc1
RPN2	0.00025237	0.29809192	0.09362943	CD8+ Tc1
F5	0.00025296	-2.6916121	0.09384635	CD8+ Tc1
VNN2	0.00025716	0.95925237	0.09540563	CD8+ Tc1
CD69	0.00025772	-0.1419154	0.09561275	CD8+ Tc1
FOXP3	0.00026491	-2.3800044	0.09828127	CD8+ Tc1
TLR2	0.00028216	-2.2203953	0.1046831	CD8+ Tc1
STAT6	0.00030873	-0.1289079	0.11453831	CD8+ Tc1
FOSB	0.0003222	-0.5362216	0.11953616	CD8+ Tc1

CD36	0.00034951	-4.6354484	0.12966999	CD8+ Tc1
GNLY	0.00036142	-0.5837902	0.13408768	CD8+ Tc1
STAT4	0.00038422	0.70747694	0.14254497	CD8+ Tc1
IL2RB	0.00039582	-0.5598949	0.14684952	CD8+ Tc1
CD14	0.00042101	-5.041584	0.15619586	CD8+ Tc1
IFNGR1	0.00045849	-0.5038105	0.17009932	CD8+ Tc1
IFITM3	0.0005568	0.2413818	0.20657316	CD8+ Tc1
MZB1	0.00062434	-1.4827902	0.23162845	CD8+ Tc1
STAT1	0.00062921	0.55220201	0.23343682	CD8+ Tc1
TNFRSF13C	0.00066378	-2.1830301	0.24626346	CD8+ Tc1
TCF4	0.00073821	-2.0219611	0.27387709	CD8+ Tc1
IGHM-membrane	0.00074859	-2.2650765	0.27772793	CD8+ Tc1
HLA-DMA	0.00083503	-0.8557205	0.3097969	CD8+ Tc1
IER3	0.0008393	-1.5094734	0.31137972	CD8+ Tc1
RORA	0.00088525	0.41783548	0.32842774	CD8+ Tc1
CASP5	0.00091958	0.38854632	0.34116417	CD8+ Tc1
TSPAN32	0.00097237	0.62413176	0.36075033	CD8+ Tc1
CXCR3	0.00100427	-1.0860078	0.37258574	CD8+ Tc1
CD200	0.00158442	-2.3645585	0.58782029	CD8+ Tc1
YBX3	0.00175122	0.46442535	0.64970172	CD8+ Tc1
ENTPD1	0.00184479	-1.3485848	0.68441881	CD8+ Tc1
CMKLR1	0.00202221	1.24050481	0.75024124	CD8+ Tc1
LIPA	0.00213324	0.49053994	0.79143026	CD8+ Tc1
CCR8	0.00224793	-3.5443426	0.83398201	CD8+ Tc1
KDELR1	0.00236766	-0.371594	0.87840023	CD8+ Tc1
LAMP3	0.0024529	-3.7820676	0.91002755	CD8+ Tc1
CD163	0.00256238	-4.6715501	0.95064176	CD8+ Tc1
TNFRSF4	0.00256556	-2.018229	0.9518232	CD8+ Tc1
RGS1	0.00295484	0.30497839	1	CD8+ Tc1
TGFBI	0.00350023	-1.9363676	1	CD8+ Tc1
IFITM2	0.00394805	0.22435699	1	CD8+ Tc1
PIK3AP1	0.00464316	-0.3245857	1	CD8+ Tc1
CD70	0.00671017	1.02046113	1	CD8+ Tc1
CD247	0.00918983	0.13386039	1	CD8+ Tc1
GZMK	0	2.94816501	0	CD8+ Teff
CD8A	3.16E-296	1.56898799	1.17E-293	CD8+ Teff
CD8B	6.66E-238	1.79831609	2.47E-235	CD8+ Teff
DUSP2	8.33E-194	1.71882672	3.09E-191	CD8+ Teff
CCL5	8.32E-176	1.21649617	3.09E-173	CD8+ Teff
KLRK1	6.42E-113	1.01369972	2.38E-110	CD8+ Teff
CXCR4	4.69E-91	0.86189261	1.74E-88	CD8+ Teff
CD4	1.36E-84	-4.3102384	5.05E-82	CD8+ Teff

GZMB	2.58E-67	-3.4219001	9.57E-65	CD8+ Teff
BTG1	1.64E-52	0.60308154	6.08E-50	CD8+ Teff
CD3D	3.42E-52	0.54339858	1.27E-49	CD8+ Teff
FCGR3A	4.15E-52	-3.203609	1.54E-49	CD8+ Teff
TRAC	2.11E-51	0.5758434	7.84E-49	CD8+ Teff
GNLY	7.03E-51	-2.3732006	2.61E-48	CD8+ Teff
IL7R	1.25E-49	0.59066688	4.62E-47	CD8+ Teff
RGS1	3.21E-49	1.81240789	1.19E-46	CD8+ Teff
TRBC2	1.78E-47	0.7138004	6.61E-45	CD8+ Teff
IL32	2.10E-47	0.45448385	7.78E-45	CD8+ Teff
TIGIT	2.86E-44	1.77689286	1.06E-41	CD8+ Teff
LAG3	5.41E-42	1.54053974	2.01E-39	CD8+ Teff
LYN	3.84E-41	-3.6307865	1.43E-38	CD8+ Teff
CD3E	2.97E-39	0.4407884	1.10E-36	CD8+ Teff
FYN	6.36E-39	0.59457637	2.36E-36	CD8+ Teff
FCER1G	9.11E-37	-5.4992574	3.38E-34	CD8+ Teff
YBX3	2.11E-36	1.13965043	7.81E-34	CD8+ Teff
IL23R	3.55E-36	0.5459221	1.32E-33	CD8+ Teff
ITGAM	9.22E-32	-1.7257026	3.42E-29	CD8+ Teff
TRDC	1.24E-31	-2.9294193	4.61E-29	CD8+ Teff
KLRB1	1.88E-30	-1.7164648	6.99E-28	CD8+ Teff
LAT2	4.99E-30	-3.6583424	1.85E-27	CD8+ Teff
RUNX3	8.61E-30	0.38792625	3.19E-27	CD8+ Teff
CD2	4.14E-29	0.57820311	1.54E-26	CD8+ Teff
TARP-refseq	1.01E-28	0.34560452	3.76E-26	CD8+ Teff
LGALS9	2.58E-28	-1.7397631	9.56E-26	CD8+ Teff
PIK3AP1	3.93E-28	-1.7408892	1.46E-25	CD8+ Teff
ITGAX	3.67E-27	-3.522173	1.36E-24	CD8+ Teff
KLRF1	3.67E-24	-2.4032993	1.36E-21	CD8+ Teff
CX3CR1	6.02E-24	-2.8519546	2.23E-21	CD8+ Teff
HLA-A	2.25E-23	0.22562775	8.34E-21	CD8+ Teff
ITGA4	2.71E-23	0.78808453	1.00E-20	CD8+ Teff
CD27	1.48E-22	0.88638598	5.49E-20	CD8+ Teff
IL18RAP	1.50E-22	-2.1193144	5.58E-20	CD8+ Teff
IRF8	7.81E-22	-3.5907249	2.90E-19	CD8+ Teff
PRF1	1.45E-20	-1.8923768	5.38E-18	CD8+ Teff
GZMH	5.15E-20	-1.4467767	1.91E-17	CD8+ Teff
CD300A	1.98E-19	-1.2944869	7.34E-17	CD8+ Teff
ZBTB16	2.82E-19	-2.9524666	1.05E-16	CD8+ Teff
CD79A	1.43E-18	-3.2216337	5.29E-16	CD8+ Teff
SELL	5.00E-18	-0.5031279	1.85E-15	CD8+ Teff
S100A10	5.74E-18	0.29890578	2.13E-15	CD8+ Teff

CD79B	7.05E-18	-1.7368932	2.61E-15	CD8+ Teff
CD69	7.57E-18	0.62473758	2.81E-15	CD8+ Teff
CXCR3	9.44E-18	1.58775562	3.50E-15	CD8+ Teff
B3GAT1	5.08E-17	-2.6658148	1.89E-14	CD8+ Teff
JUNB	3.18E-16	0.59321527	1.18E-13	CD8+ Teff
CCR5	1.13E-15	1.6042094	4.19E-13	CD8+ Teff
IL2RB	1.48E-15	-0.3682178	5.51E-13	CD8+ Teff
CBLB	2.70E-15	0.77231138	1.00E-12	CD8+ Teff
CD247	9.86E-15	-0.8052985	3.66E-12	CD8+ Teff
CD48	1.01E-14	0.33570097	3.74E-12	CD8+ Teff
TNFSF8	1.11E-14	0.93502238	4.14E-12	CD8+ Teff
MYC	1.44E-14	-0.9886302	5.34E-12	CD8+ Teff
TXK	3.08E-14	-0.9665984	1.14E-11	CD8+ Teff
GZMA	9.42E-14	0.21342843	3.49E-11	CD8+ Teff
HAVCR2	1.95E-13	-2.6054758	7.23E-11	CD8+ Teff
IFITM3	3.19E-13	-0.5012123	1.18E-10	CD8+ Teff
EOMES	6.36E-13	1.6566807	2.36E-10	CD8+ Teff
LGALS1	6.81E-13	-0.7305825	2.53E-10	CD8+ Teff
PASK	8.46E-13	0.98972102	3.14E-10	CD8+ Teff
CD38	1.12E-12	-3.0840097	4.14E-10	CD8+ Teff
IGHD-membrane	1.99E-12	-3.0402171	7.40E-10	CD8+ Teff
LY86	2.04E-12	-3.0057783	7.57E-10	CD8+ Teff
IGLC3	6.08E-12	-3.8930884	2.26E-09	CD8+ Teff
BCL11B	7.95E-12	0.63028169	2.95E-09	CD8+ Teff
IFITM2	3.04E-11	-0.4056245	1.13E-08	CD8+ Teff
CD22	4.49E-11	-2.2504647	1.67E-08	CD8+ Teff
KIR2DL1	6.69E-11	-2.2692839	2.48E-08	CD8+ Teff
XBP1	1.29E-10	-0.5181697	4.80E-08	CD8+ Teff
NCR3	2.09E-10	-1.0135244	7.76E-08	CD8+ Teff
LAIR2	2.63E-10	-2.8150591	9.74E-08	CD8+ Teff
CD74	3.06E-10	-0.841838	1.14E-07	CD8+ Teff
POU2AF1	3.26E-10	-2.2061077	1.21E-07	CD8+ Teff
PAX5	3.50E-10	-2.3317598	1.30E-07	CD8+ Teff
CD37	4.92E-10	-0.3712928	1.83E-07	CD8+ Teff
CD44	1.11E-09	0.37585979	4.11E-07	CD8+ Teff
TBX21	1.66E-09	-0.9399795	6.17E-07	CD8+ Teff
IGKC	2.85E-09	-3.2088747	1.06E-06	CD8+ Teff
VPREB3	2.88E-09	-2.8463112	1.07E-06	CD8+ Teff
TRIB2	2.88E-09	-0.403551	1.07E-06	CD8+ Teff
KLRC4	3.17E-09	1.19611647	1.18E-06	CD8+ Teff
TCL1A	3.32E-09	-1.0431089	1.23E-06	CD8+ Teff
IGHM-secreted	4.47E-09	-2.3436393	1.66E-06	CD8+ Teff

HLA-DRA	1.01E-08	-2.5938351	3.75E-06	CD8+ Teff
RNASE6	1.51E-08	-2.5609188	5.61E-06	CD8+ Teff
TNFSF10	3.26E-08	-0.5846206	1.21E-05	CD8+ Teff
IGHG1-secreted	3.58E-08	-4.7000288	1.33E-05	CD8+ Teff
CD5	6.01E-08	0.42821529	2.23E-05	CD8+ Teff
CD24	7.40E-08	-3.0315191	2.74E-05	CD8+ Teff
IRF4	1.03E-07	-1.2903012	3.83E-05	CD8+ Teff
BLNK	1.05E-07	-2.0722921	3.91E-05	CD8+ Teff
CD86	1.10E-07	-3.1322544	4.09E-05	CD8+ Teff
TNFRSF25	1.69E-07	-0.8153141	6.26E-05	CD8+ Teff
CTSD	1.74E-07	-0.8940435	6.45E-05	CD8+ Teff
LILRB4	3.23E-07	-4.970374	0.00011993	CD8+ Teff
LIPA	4.34E-07	-0.2953063	0.0001612	CD8+ Teff
CD40	5.19E-07	-1.8668136	0.00019257	CD8+ Teff
CD1C	5.54E-07	-3.5715394	0.00020542	CD8+ Teff
BACH2	6.03E-07	-0.8484478	0.00022356	CD8+ Teff
LAT	6.70E-07	0.35669803	0.00024871	CD8+ Teff
FCN1	6.98E-07	-4.7933707	0.00025908	CD8+ Teff
TNFSF13	8.53E-07	-1.93724	0.00031655	CD8+ Teff
IL4R	9.48E-07	-0.5067587	0.00035177	CD8+ Teff
IGHM-membrane	1.15E-06	-2.5464346	0.00042516	CD8+ Teff
FCER2	1.47E-06	-1.5751498	0.0005436	CD8+ Teff
PSEN1	1.60E-06	-0.8760372	0.000594	CD8+ Teff
TNFSF13B	1.70E-06	-1.9140214	0.0006302	CD8+ Teff
CCL3	1.72E-06	0.82015094	0.00063895	CD8+ Teff
CXCR2	2.09E-06	-4.3010567	0.00077566	CD8+ Teff
ARL4C	3.48E-06	0.20909713	0.00129113	CD8+ Teff
PIK3IP1	3.68E-06	0.33233411	0.00136491	CD8+ Teff
CD33	3.79E-06	-4.6508321	0.00140685	CD8+ Teff
SELPLG	4.74E-06	-0.1866651	0.00175802	CD8+ Teff
CD244	5.67E-06	-0.9389666	0.00210535	CD8+ Teff
CCR7	8.94E-06	-0.3815375	0.00331643	CD8+ Teff
SLC7A7	1.03E-05	-2.9167335	0.00380277	CD8+ Teff
IL2RA	1.79E-05	-1.3936434	0.00665742	CD8+ Teff
ADGRE1	2.03E-05	-2.4382031	0.00751384	CD8+ Teff
F5	2.34E-05	-4.4065001	0.00866381	CD8+ Teff
CD52	2.63E-05	-0.1207338	0.00976978	CD8+ Teff
CR2	2.92E-05	-2.5634117	0.0108477	CD8+ Teff
RORC	4.19E-05	-2.1291226	0.01556231	CD8+ Teff
CXCR5	4.32E-05	-1.3208865	0.01601577	CD8+ Teff
LCK	4.38E-05	0.24429414	0.01624473	CD8+ Teff
PDIA4	5.66E-05	-0.3169874	0.02099643	CD8+ Teff

KCNE3	5.93E-05	-4.4763462	0.02200823	CD8+ Teff
TLR2	6.36E-05	-2.6298723	0.02357757	CD8+ Teff
TCF4	6.98E-05	-2.7223705	0.02591269	CD8+ Teff
STAT3	7.30E-05	-0.2404442	0.0270653	CD8+ Teff
FYB	8.93E-05	0.29582086	0.03311912	CD8+ Teff
S100A9	0.00010351	-4.7705748	0.03840229	CD8+ Teff
CD28	0.00010686	0.97283454	0.03964456	CD8+ Teff
PTGDR2	0.00010712	-2.737625	0.03974078	CD8+ Teff
IGHA1-secreted	0.00010925	-4.2011743	0.0405325	CD8+ Teff
CD36	0.000124	-4.8398987	0.04600402	CD8+ Teff
CMKLR1	0.00012634	-2.2425895	0.04687211	CD8+ Teff
IGBP1	0.00015882	-0.1471726	0.05892373	CD8+ Teff
FASLG	0.0001787	-1.5879808	0.06629656	CD8+ Teff
DUSP4	0.00018446	1.13929101	0.06843578	CD8+ Teff
MZB1	0.00019148	-1.2596353	0.07104053	CD8+ Teff
CCR4	0.00019486	-1.4849851	0.0722937	CD8+ Teff
BIRC3	0.00020079	-0.1844257	0.07449338	CD8+ Teff
LTB	0.00021496	-0.8387579	0.07975045	CD8+ Teff
CCR9	0.00022059	2.16970716	0.08183805	CD8+ Teff
JCHAIN	0.0002254	-3.8941216	0.08362277	CD8+ Teff
BTLA	0.00025599	-0.3209419	0.09497079	CD8+ Teff
FAM129C	0.00025638	-2.1496864	0.09511591	CD8+ Teff
HLA-DQB1	0.0002811	-1.1712427	0.10428933	CD8+ Teff
CD72	0.00030944	-0.9135501	0.11480365	CD8+ Teff
TNFRSF4	0.00031949	-2.8094501	0.11853243	CD8+ Teff
GAB2	0.00033945	-0.8735221	0.12593586	CD8+ Teff
ZAP70	0.00035476	-0.3098847	0.13161428	CD8+ Teff
ENTPD1	0.00045679	-1.0758246	0.16946962	CD8+ Teff
ADA	0.000467	-0.2468249	0.17325534	CD8+ Teff
ZNF683	0.00052646	0.45530131	0.19531509	CD8+ Teff
TSPAN32	0.00059908	-0.1844127	0.22225737	CD8+ Teff
IL12RB2	0.00069993	-1.2537831	0.2596755	CD8+ Teff
FAS	0.00077034	0.74702612	0.28579685	CD8+ Teff
CD14	0.00081005	-4.2620674	0.30052717	CD8+ Teff
CD3G	0.00086043	0.39796988	0.31922055	CD8+ Teff
EBF1	0.00089513	-3.6938688	0.33209299	CD8+ Teff
GNAI2	0.001047	-0.1223344	0.38843882	CD8+ Teff
CD63	0.00114101	-0.3001789	0.42331335	CD8+ Teff
CD163	0.00120654	-4.8760003	0.44762627	CD8+ Teff
CD200	0.00126613	-0.550453	0.46973605	CD8+ Teff
FOSB	0.00142074	-0.3175217	0.52709551	CD8+ Teff
IL3RA	0.00152532	-4.1075412	0.56589465	CD8+ Teff

FCER1A	0.00213742	-5.3725755	0.79298442	CD8+ Teff
CLEC4E	0.00219727	-4.4276963	0.81518851	CD8+ Teff
JUN	0.0022228	0.42315983	0.8246581	CD8+ Teff
VPS28	0.00223298	-0.1144797	0.82843561	CD8+ Teff
IKZF2	0.00238884	-0.1354319	0.88625807	CD8+ Teff
LTA	0.00261528	-0.6348099	0.97026746	CD8+ Teff
CLEC10A	0.00262739	-5.3094646	0.97476067	CD8+ Teff
ATF6B	0.00270165	-0.1939329	1	CD8+ Teff
KIT	0.00284037	-2.0852367	1	CD8+ Teff
NKG7	0.0031049	-0.90957	1	CD8+ Teff
ITGB2	0.00313439	-0.4118138	1	CD8+ Teff
PCNA	0.00328173	-0.4204676	1	CD8+ Teff
ICOS	0.0035814	-0.5056355	1	CD8+ Teff
LGALS3	0.00375076	0.3512088	1	CD8+ Teff
BAX	0.00408618	-0.1383405	1	CD8+ Teff
CD6	0.00533575	0.21428129	1	CD8+ Teff
LAP3	0.00583389	-0.2426418	1	CD8+ Teff
TNFRSF13C	0.00744943	-0.963983	1	CD8+ Teff
MS4A1	0.00750607	-1.3571998	1	CD8+ Teff
S100A12	0.00934497	-4.0625504	1	CD8+ Teff
IL15	0.00980652	0.8182715	1	CD8+ Teff
LEF1	0.00985815	-0.1362957	1	CD8+ Teff
NT5E	0.00997574	0.94421667	1	CD8+ Teff
CXCL16	0	5.79565928	0	CD11c+ CD16+
FCN1	0	4.07650901	0	CD11c+ CD16+
TGFBI	0	4.12655046	0	CD11c+ CD16+
CD86	0	4.67061322	0	CD11c+ CD16+
ADGRE1	0	5.6048716	0	CD11c+ CD16+
SLC7A7	0	5.65384053	0	CD11c+ CD16+
LILRB4	0	4.6738228	0	CD11c+ CD16+
CD33	0	4.1522884	0	CD11c+ CD16+
KCNE3	0	5.66294015	0	CD11c+ CD16+
VMO1	0	9.44301911	0	CD11c+ CD16+
TLR8	0	6.09219045	0	CD11c+ CD16+
TNFRSF8	0	7.33468207	0	CD11c+ CD16+
S100A9	1.87E-286	1.28683858	6.93E-284	CD11c+ CD16+
TLR2	2.05E-259	4.47037533	7.61E-257	CD11c+ CD16+
BCL2A1	5.19E-233	3.83170846	1.93E-230	CD11c+ CD16+
NAMPT	2.74E-232	4.16072399	1.02E-229	CD11c+ CD16+
C1QA	1.93E-219	8.32384741	7.17E-217	CD11c+ CD16+
GAB2	2.74E-203	3.92261357	1.02E-200	CD11c+ CD16+
ITGAX	2.22E-201	3.55838822	8.22E-199	CD11c+ CD16+

FCER1G	5.23E-198	3.96609845	1.94E-195	CD11c+ CD16+
FTH1	2.04E-193	3.57062193	7.57E-191	CD11c+ CD16+
LYN	3.20E-190	4.71947326	1.19E-187	CD11c+ CD16+
TNFSF13	1.16E-173	3.60218151	4.29E-171	CD11c+ CD16+
PIK3AP1	2.13E-130	3.24841899	7.88E-128	CD11c+ CD16+
FCGR3A	5.49E-128	3.95806052	2.04E-125	CD11c+ CD16+
LGALS3	1.45E-122	2.62511192	5.38E-120	CD11c+ CD16+
LGALS9	3.20E-118	2.91856281	1.19E-115	CD11c+ CD16+
IL3RA	3.24E-113	3.83238717	1.20E-110	CD11c+ CD16+
TNFSF13B	3.10E-105	2.98565185	1.15E-102	CD11c+ CD16+
C10orf54	1.04E-101	3.33185112	3.86E-99	CD11c+ CD16+
HLA-DRA	1.21E-99	1.87420666	4.50E-97	CD11c+ CD16+
HLA-DPA1	8.38E-85	2.28098865	3.11E-82	CD11c+ CD16+
PTGDR2	2.13E-78	2.44694385	7.90E-76	CD11c+ CD16+
ANXA5	4.04E-74	2.38081029	1.50E-71	CD11c+ CD16+
TRBC2	2.07E-72	-4.7705608	7.68E-70	CD11c+ CD16+
DUSP1	2.45E-64	2.84854291	9.10E-62	CD11c+ CD16+
IL32	3.08E-61	-4.4228033	1.14E-58	CD11c+ CD16+
LGALS1	1.38E-60	1.78769141	5.10E-58	CD11c+ CD16+
CD3E	2.24E-58	-4.5924853	8.30E-56	CD11c+ CD16+
FOSB	1.39E-56	2.30283048	5.15E-54	CD11c+ CD16+
CD4	2.37E-53	1.70190085	8.80E-51	CD11c+ CD16+
CD74	1.61E-52	1.24395273	5.96E-50	CD11c+ CD16+
TRAC	1.14E-51	-4.3750712	4.24E-49	CD11c+ CD16+
IFITM3	1.30E-51	1.95492281	4.81E-49	CD11c+ CD16+
AQP9	4.96E-51	4.80750276	1.84E-48	CD11c+ CD16+
CD3D	9.41E-50	-4.6133374	3.49E-47	CD11c+ CD16+
CXCL8	1.02E-49	2.54630686	3.78E-47	CD11c+ CD16+
LCK	6.92E-48	-5.0140822	2.57E-45	CD11c+ CD16+
CD79B	5.53E-42	1.36775855	2.05E-39	CD11c+ CD16+
CXCR4	6.59E-41	-2.6903933	2.45E-38	CD11c+ CD16+
CD2	1.70E-40	-4.4889366	6.30E-38	CD11c+ CD16+
ITGB2	1.31E-39	1.13118329	4.85E-37	CD11c+ CD16+
HLA-DQB1	1.63E-38	0.76067723	6.06E-36	CD11c+ CD16+
JUNB	2.79E-38	1.68332291	1.03E-35	CD11c+ CD16+
YBX3	3.69E-38	1.4828159	1.37E-35	CD11c+ CD16+
LAP3	6.52E-37	1.61220292	2.42E-34	CD11c+ CD16+
GNAI2	7.24E-36	1.57363077	2.69E-33	CD11c+ CD16+
CTSW	2.62E-35	-4.7461916	9.70E-33	CD11c+ CD16+
ADA	1.37E-34	1.51438835	5.09E-32	CD11c+ CD16+
CTSD	1.16E-33	1.61830051	4.30E-31	CD11c+ CD16+
CD6	2.08E-30	-3.9271966	7.72E-28	CD11c+ CD16+

IL7R	7.80E-30	-4.4304767	2.89E-27	CD11c+ CD16+
IFITM2	9.96E-30	1.26150638	3.70E-27	CD11c+ CD16+
CST7	1.23E-28	-4.4201969	4.56E-26	CD11c+ CD16+
HLA-DMA	5.75E-28	0.99235485	2.13E-25	CD11c+ CD16+
IRF8	2.96E-26	0.69055948	1.10E-23	CD11c+ CD16+
PSEN1	6.38E-26	1.65633036	2.37E-23	CD11c+ CD16+
STAT5A	7.29E-26	1.25314057	2.70E-23	CD11c+ CD16+
IFNGR1	4.19E-25	1.15399341	1.56E-22	CD11c+ CD16+
TNF	4.20E-25	1.41311251	1.56E-22	CD11c+ CD16+
GZMA	1.56E-24	-5.3090684	5.80E-22	CD11c+ CD16+
IL2RB	1.90E-24	-4.1131269	7.04E-22	CD11c+ CD16+
IL15	3.32E-24	2.01472992	1.23E-21	CD11c+ CD16+
TNFSF10	9.73E-24	1.43215222	3.61E-21	CD11c+ CD16+
ARL4C	1.42E-23	-2.6991671	5.28E-21	CD11c+ CD16+
SELPLG	1.51E-23	0.93289933	5.59E-21	CD11c+ CD16+
LAT	3.43E-23	-3.3580505	1.27E-20	CD11c+ CD16+
NINJ2	3.50E-23	1.90603759	1.30E-20	CD11c+ CD16+
CD36	2.43E-22	1.95004217	9.00E-20	CD11c+ CD16+
CCL5	4.14E-22	-4.0074284	1.53E-19	CD11c+ CD16+
FUT4	7.08E-22	2.68314867	2.62E-19	CD11c+ CD16+
HLA-A	1.37E-21	-0.7839304	5.09E-19	CD11c+ CD16+
KLRK1	1.41E-21	-4.1176619	5.24E-19	CD11c+ CD16+
TARP-refseq	2.82E-20	-4.7331665	1.05E-17	CD11c+ CD16+
CD69	4.88E-20	-4.2992869	1.81E-17	CD11c+ CD16+
CD5	5.27E-18	-5.0324279	1.95E-15	CD11c+ CD16+
DUSP2	5.78E-18	-3.4166978	2.14E-15	CD11c+ CD16+
S100A10	6.38E-18	0.71683574	2.37E-15	CD11c+ CD16+
BCL11B	8.38E-18	-4.5099843	3.11E-15	CD11c+ CD16+
CD37	9.77E-18	0.71097638	3.63E-15	CD11c+ CD16+
CD8A	4.06E-17	-5.1247837	1.51E-14	CD11c+ CD16+
CD247	6.15E-17	-3.7450838	2.28E-14	CD11c+ CD16+
LY86	2.00E-16	1.0534573	7.42E-14	CD11c+ CD16+
PRF1	1.10E-15	-4.5457587	4.10E-13	CD11c+ CD16+
IL23R	1.30E-15	-1.516732	4.82E-13	CD11c+ CD16+
LEF1	1.63E-15	-3.7037941	6.05E-13	CD11c+ CD16+
KLRB1	3.07E-15	-5.222628	1.14E-12	CD11c+ CD16+
DOCK8	3.64E-15	0.83671384	1.35E-12	CD11c+ CD16+
TIAF1	5.65E-15	0.91791496	2.10E-12	CD11c+ CD16+
SELL	9.51E-15	-2.0845353	3.53E-12	CD11c+ CD16+
NKG7	1.22E-14	-3.7375003	4.52E-12	CD11c+ CD16+
PTPRC	1.49E-14	0.57938686	5.53E-12	CD11c+ CD16+
C1QB	2.06E-14	7.02556344	7.63E-12	CD11c+ CD16+

CD300A	2.08E-14	0.53340856	7.70E-12	CD11c+ CD16+
GZMH	6.67E-14	-4.4777225	2.47E-11	CD11c+ CD16+
CD244	8.21E-14	0.70511046	3.04E-11	CD11c+ CD16+
BIN2	1.05E-13	0.72711342	3.88E-11	CD11c+ CD16+
CD3G	1.66E-13	-5.5531217	6.14E-11	CD11c+ CD16+
PRDM1	5.02E-13	-4.6982287	1.86E-10	CD11c+ CD16+
RORA	7.93E-13	-4.4846674	2.94E-10	CD11c+ CD16+
LIPA	8.97E-13	0.85112427	3.33E-10	CD11c+ CD16+
TBX21	1.73E-12	-4.9514171	6.43E-10	CD11c+ CD16+
GAPDH	2.37E-12	0.45201323	8.78E-10	CD11c+ CD16+
GZMB	4.00E-12	-4.4587928	1.48E-09	CD11c+ CD16+
VPS28	4.92E-12	0.88261966	1.83E-09	CD11c+ CD16+
BCL6	1.29E-11	1.83225704	4.79E-09	CD11c+ CD16+
CD27	2.55E-11	-3.6579309	9.45E-09	CD11c+ CD16+
TRIB2	3.88E-11	-4.1196129	1.44E-08	CD11c+ CD16+
ITGA4	5.15E-11	0.45472874	1.91E-08	CD11c+ CD16+
LAT2	9.05E-11	0.47353396	3.36E-08	CD11c+ CD16+
GNLY	9.23E-11	-4.8154663	3.43E-08	CD11c+ CD16+
TLR7	1.64E-10	3.54637721	6.08E-08	CD11c+ CD16+
CCND2	1.98E-10	-4.5874162	7.35E-08	CD11c+ CD16+
CCR7	2.86E-10	-3.6312511	1.06E-07	CD11c+ CD16+
STAT6	5.10E-10	0.96963112	1.89E-07	CD11c+ CD16+
TXK	7.93E-10	-5.7420054	2.94E-07	CD11c+ CD16+
STAT4	8.14E-10	-4.7419413	3.02E-07	CD11c+ CD16+
MYC	1.57E-09	-3.8857278	5.83E-07	CD11c+ CD16+
PIK3IP1	2.51E-09	-1.2551616	9.30E-07	CD11c+ CD16+
SLC25A37	4.79E-09	0.84071727	1.78E-06	CD11c+ CD16+
CD44	5.16E-09	0.46346731	1.91E-06	CD11c+ CD16+
VNN2	5.67E-09	1.17601108	2.10E-06	CD11c+ CD16+
CD8B	1.33E-08	-3.6563814	4.93E-06	CD11c+ CD16+
GZMK	1.42E-08	-7.3614587	5.29E-06	CD11c+ CD16+
TRAT1	1.81E-08	-4.0162893	6.72E-06	CD11c+ CD16+
PASK	2.09E-08	-3.8118491	7.75E-06	CD11c+ CD16+
GIMAP5	2.12E-08	-2.9575258	7.87E-06	CD11c+ CD16+
ICAM1	4.16E-08	1.23336313	1.55E-05	CD11c+ CD16+
BCL2	4.90E-08	-3.8549619	1.82E-05	CD11c+ CD16+
CD7	5.20E-08	-3.7818442	1.93E-05	CD11c+ CD16+
TRDC	1.07E-07	-5.8750872	3.99E-05	CD11c+ CD16+
MITF	1.55E-07	4.32111834	5.76E-05	CD11c+ CD16+
NCR3	1.78E-07	-3.2357082	6.60E-05	CD11c+ CD16+
KLRG1	1.95E-07	-3.6009409	7.22E-05	CD11c+ CD16+
IL1RN	3.96E-07	2.71090916	0.00014698	CD11c+ CD16+

CASP5	5.22E-07	0.42810993	0.00019363	CD11c+ CD16+
IL18RAP	5.82E-07	-4.1940814	0.00021583	CD11c+ CD16+
CXCL2	5.84E-07	2.51885036	0.00021683	CD11c+ CD16+
TCF7	7.45E-07	-3.7072193	0.00027636	CD11c+ CD16+
LAMP1	9.18E-07	0.43753606	0.00034062	CD11c+ CD16+
HAVCR2	1.26E-06	0.15574786	0.00046803	CD11c+ CD16+
CBLB	1.29E-06	-2.3624437	0.00047674	CD11c+ CD16+
BTG1	1.65E-06	-0.6334047	0.00061326	CD11c+ CD16+
CD28	1.68E-06	-3.8884014	0.00062279	CD11c+ CD16+
XBP1	3.44E-06	-1.8200205	0.00127676	CD11c+ CD16+
CX3CR1	4.26E-06	0.21875899	0.00158027	CD11c+ CD16+
KLRF1	8.04E-06	-4.0007592	0.00298309	CD11c+ CD16+
ATF6B	8.69E-06	0.53623673	0.00322424	CD11c+ CD16+
CCL4	9.17E-06	-3.2919243	0.00340295	CD11c+ CD16+
FYN	1.06E-05	-0.9568969	0.00392798	CD11c+ CD16+
FAM65B	1.33E-05	-1.3212688	0.00493349	CD11c+ CD16+
CXCL5	1.48E-05	0.54109569	0.00548142	CD11c+ CD16+
KLRC1	4.62E-05	-4.4665027	0.01713182	CD11c+ CD16+
ZAP70	6.53E-05	-2.4876073	0.02421317	CD11c+ CD16+
ITGAM	7.12E-05	-2.2832088	0.0264186	CD11c+ CD16+
DPP4	0.00010073	-4.4722884	0.03737242	CD11c+ CD16+
BTLA	0.00012301	0.74427847	0.045637	CD11c+ CD16+
BAX	0.00013592	0.19750993	0.05042798	CD11c+ CD16+
ICOS	0.00015874	-4.259719	0.05889113	CD11c+ CD16+
LTB	0.00016014	-3.994899	0.05941272	CD11c+ CD16+
TNFSF8	0.00017095	-2.0400295	0.06342093	CD11c+ CD16+
ZNF683	0.00021805	-3.9157839	0.08089501	CD11c+ CD16+
TNFRSF25	0.00028147	-3.3390191	0.10442596	CD11c+ CD16+
IGBP1	0.00028925	0.11885688	0.10731273	CD11c+ CD16+
IL4R	0.0005314	-1.5665811	0.19714797	CD11c+ CD16+
KLRC3	0.00086516	-4.3359603	0.32097311	CD11c+ CD16+
KIR2DL1	0.0009923	-4.3111397	0.36814263	CD11c+ CD16+
B3GAT1	0.00118325	-3.3584747	0.43898673	CD11c+ CD16+
IL18R1	0.00121512	-2.9383049	0.450811	CD11c+ CD16+
CD63	0.00130119	-0.6817479	0.48273985	CD11c+ CD16+
BACH2	0.0015717	-3.2351682	0.58309897	CD11c+ CD16+
TSPAN32	0.00181247	0.17320577	0.67242489	CD11c+ CD16+
POU2AF1	0.00207641	-3.6363327	0.77034942	CD11c+ CD16+
TIGIT	0.0022173	-2.9875407	0.82261844	CD11c+ CD16+
MS4A1	0.00269577	-3.1345734	1	CD11c+ CD16+
CCR10	0.00295913	2.49491069	1	CD11c+ CD16+
LAG3	0.00334514	-3.1040608	1	CD11c+ CD16+

CHI3L2	0.00369391	-3.4416734	1	CD11c+ CD16+
ZBTB16	0.00428854	-2.6634089	1	CD11c+ CD16+
FYB	0.00428997	0.12312269	1	CD11c+ CD16+
NT5E	0.00465521	-3.4938968	1	CD11c+ CD16+
GIMAP2	0.00520814	-0.2437441	1	CD11c+ CD16+
CD160	0.00551417	-3.7304068	1	CD11c+ CD16+
IGHM-secreted	0.00554493	-3.1890797	1	CD11c+ CD16+
IGHD-membrane	0.00602075	-3.4206085	1	CD11c+ CD16+
LAIR2	0.00661101	-3.6008838	1	CD11c+ CD16+
VPREB3	0.00715861	-3.5335949	1	CD11c+ CD16+
KLRC4	0.00769079	-3.4149345	1	CD11c+ CD16+
CD79A	0.00863448	-3.8180328	1	CD11c+ CD16+
CXCR3	0.00917139	-3.1056512	1	CD11c+ CD16+
KLRB1	3.41E-188	3.61133409	1.27E-185	CD8+ Tc17
GZMK	6.52E-185	3.02963849	2.42E-182	CD8+ Tc17
CXCR6	2.49E-175	5.80249341	9.22E-173	CD8+ Tc17
RORC	3.89E-167	4.87904487	1.44E-164	CD8+ Tc17
DUSP2	1.25E-120	2.87875942	4.63E-118	CD8+ Tc17
CXCR4	5.89E-109	2.31000587	2.18E-106	CD8+ Tc17
IL7R	6.79E-102	2.23579728	2.52E-99	CD8+ Tc17
IL18RAP	3.71E-99	2.68173889	1.38E-96	CD8+ Tc17
ARL4C	5.81E-90	2.09565358	2.16E-87	CD8+ Tc17
NCR3	1.87E-89	2.87681342	6.94E-87	CD8+ Tc17
BTG1	2.79E-88	1.71896373	1.03E-85	CD8+ Tc17
ZBTB16	7.38E-81	3.07353892	2.74E-78	CD8+ Tc17
DUSP1	2.42E-79	2.26149439	8.97E-77	CD8+ Tc17
IL32	1.12E-63	1.2322754	4.14E-61	CD8+ Tc17
TARP-refseq	9.10E-62	1.83518326	3.38E-59	CD8+ Tc17
HLA-A	1.52E-61	0.87928236	5.63E-59	CD8+ Tc17
KLRG1	1.79E-54	2.50055085	6.66E-52	CD8+ Tc17
CD69	1.06E-53	2.22525645	3.92E-51	CD8+ Tc17
DPP4	1.49E-53	3.10764551	5.53E-51	CD8+ Tc17
CD3E	4.36E-46	1.12563865	1.62E-43	CD8+ Tc17
IFNGR1	9.67E-43	2.45877137	3.59E-40	CD8+ Tc17
GZMA	8.99E-40	1.33943985	3.33E-37	CD8+ Tc17
CCL5	3.66E-39	1.05681135	1.36E-36	CD8+ Tc17
CCR2	1.39E-36	3.19121313	5.15E-34	CD8+ Tc17
CTSW	8.94E-31	0.91013401	3.32E-28	CD8+ Tc17
RUNX3	6.16E-30	1.04859388	2.28E-27	CD8+ Tc17
CCR1	7.30E-30	4.95621544	2.71E-27	CD8+ Tc17
FYN	2.76E-29	1.21949769	1.02E-26	CD8+ Tc17
SELL	6.16E-29	-1.5713196	2.29E-26	CD8+ Tc17

CD3D	9.25E-29	1.00154314	3.43E-26	CD8+ Tc17
RORA	1.07E-28	1.84926272	3.96E-26	CD8+ Tc17
CST7	1.52E-28	0.89041771	5.63E-26	CD8+ Tc17
IL18R1	6.49E-28	2.60544766	2.41E-25	CD8+ Tc17
CD48	1.80E-26	1.02797958	6.68E-24	CD8+ Tc17
CCR5	1.46E-25	3.09876867	5.41E-23	CD8+ Tc17
TRAC	1.61E-24	0.88223915	5.96E-22	CD8+ Tc17
PRF1	2.15E-24	0.7271785	7.96E-22	CD8+ Tc17
LEF1	6.59E-23	-2.3559358	2.44E-20	CD8+ Tc17
CD44	1.84E-22	1.1714025	6.84E-20	CD8+ Tc17
NKG7	6.17E-22	0.20057089	2.29E-19	CD8+ Tc17
CD4	7.01E-21	-2.7617519	2.60E-18	CD8+ Tc17
IL23R	1.51E-20	0.89392104	5.59E-18	CD8+ Tc17
PRDM1	7.41E-20	1.83742567	2.75E-17	CD8+ Tc17
GZMH	1.77E-19	-3.0100244	6.58E-17	CD8+ Tc17
PTPRC	3.29E-19	0.65799201	1.22E-16	CD8+ Tc17
LAG3	4.69E-19	2.25456986	1.74E-16	CD8+ Tc17
GZMB	5.87E-19	-2.8941973	2.18E-16	CD8+ Tc17
GAPDH	7.94E-19	0.62800479	2.94E-16	CD8+ Tc17
LGALS1	1.62E-18	-1.368634	6.03E-16	CD8+ Tc17
FCGR3A	2.30E-18	-3.2682699	8.53E-16	CD8+ Tc17
C10orf54	3.28E-18	1.09326675	1.22E-15	CD8+ Tc17
IL2RB	4.64E-17	0.49588373	1.72E-14	CD8+ Tc17
CD52	1.83E-15	0.49616889	6.79E-13	CD8+ Tc17
LGALS3	2.11E-15	1.88857007	7.83E-13	CD8+ Tc17
PSEN1	5.43E-15	2.29331595	2.01E-12	CD8+ Tc17
RPN2	1.27E-14	1.15888187	4.70E-12	CD8+ Tc17
THBS1	3.52E-14	2.86257067	1.31E-11	CD8+ Tc17
XBP1	1.80E-13	1.54401425	6.69E-11	CD8+ Tc17
PIK3AP1	2.57E-13	1.52893669	9.52E-11	CD8+ Tc17
CCR7	3.02E-13	-2.2413179	1.12E-10	CD8+ Tc17
BIN2	8.08E-13	0.73038878	3.00E-10	CD8+ Tc17
TRBC2	8.22E-13	0.58284065	3.05E-10	CD8+ Tc17
CD6	1.28E-12	0.97179374	4.73E-10	CD8+ Tc17
LGALS9	1.82E-12	-2.8220271	6.73E-10	CD8+ Tc17
CBLB	1.94E-12	1.52029099	7.20E-10	CD8+ Tc17
TNF	2.90E-12	2.74904336	1.07E-09	CD8+ Tc17
CD8A	1.49E-11	0.76477564	5.52E-09	CD8+ Tc17
JUNB	3.16E-11	1.24978232	1.17E-08	CD8+ Tc17
HLA-DRA	4.80E-11	-3.6714207	1.78E-08	CD8+ Tc17
CASP5	6.25E-11	1.33226564	2.32E-08	CD8+ Tc17
MYC	7.47E-11	1.41940224	2.77E-08	CD8+ Tc17

FCER1G	8.05E-11	-4.242024	2.99E-08	CD8+ Tc17
BAX	1.51E-09	1.22693708	5.61E-07	CD8+ Tc17
ITGAM	1.64E-09	-1.4067743	6.07E-07	CD8+ Tc17
CD28	2.03E-09	1.60759731	7.52E-07	CD8+ Tc17
CD74	2.36E-09	-0.8062629	8.76E-07	CD8+ Tc17
TNFSF14	5.26E-09	3.04275621	1.95E-06	CD8+ Tc17
YBX3	6.58E-09	-1.8682691	2.44E-06	CD8+ Tc17
LAMP1	7.26E-09	0.81315097	2.70E-06	CD8+ Tc17
LCK	1.04E-08	0.7403639	3.87E-06	CD8+ Tc17
HLA-DPA1	2.05E-08	-1.4873517	7.62E-06	CD8+ Tc17
CX3CR1	3.67E-08	-3.0880349	1.36E-05	CD8+ Tc17
GNLY	4.24E-08	-1.6079405	1.57E-05	CD8+ Tc17
ITGAX	5.34E-08	-2.8794348	1.98E-05	CD8+ Tc17
IFITM2	3.02E-07	0.68910857	0.00011203	CD8+ Tc17
STAT4	3.09E-07	1.51374623	0.00011455	CD8+ Tc17
FYB	7.37E-07	-0.3104415	0.00027352	CD8+ Tc17
BCL11B	1.03E-06	1.14669646	0.00038162	CD8+ Tc17
S100A10	1.04E-06	0.43175743	0.00038674	CD8+ Tc17
LYN	1.07E-06	-1.6686982	0.00039825	CD8+ Tc17
HLA-DQB1	1.26E-06	-1.6766987	0.00046791	CD8+ Tc17
IGHM-membrane	1.29E-06	-2.2788659	0.00047847	CD8+ Tc17
B3GAT1	1.48E-06	-4.1267626	0.00055021	CD8+ Tc17
CD79A	1.55E-06	-2.5787935	0.00057678	CD8+ Tc17
ZNF683	1.87E-06	-1.7300757	0.00069333	CD8+ Tc17
PDIA6	3.82E-06	1.03960493	0.00141902	CD8+ Tc17
CD8B	4.98E-06	-0.9101351	0.00184777	CD8+ Tc17
CD22	5.15E-06	-2.5455529	0.00191157	CD8+ Tc17
IRF8	5.62E-06	-2.473472	0.00208495	CD8+ Tc17
BCL2	6.29E-06	1.38321489	0.00233275	CD8+ Tc17
CTLA4	8.10E-06	-5.0046416	0.00300579	CD8+ Tc17
TNFSF8	1.06E-05	1.65074017	0.00392856	CD8+ Tc17
KIR2DL1	1.18E-05	-5.1355061	0.00437064	CD8+ Tc17
IL15	1.73E-05	2.54649798	0.00641618	CD8+ Tc17
HLA-DMA	2.35E-05	-1.0712012	0.00870459	CD8+ Tc17
IL12RB2	2.50E-05	2.07078884	0.00926396	CD8+ Tc17
LAT2	2.79E-05	-0.4787342	0.01036429	CD8+ Tc17
CD38	3.05E-05	-4.8326442	0.01131931	CD8+ Tc17
LAIR2	4.93E-05	-5.1398766	0.018294	CD8+ Tc17
PASK	5.37E-05	-0.5573386	0.01991863	CD8+ Tc17
CD63	9.09E-05	0.55880459	0.03370935	CD8+ Tc17
GIMAP5	9.88E-05	-0.2306572	0.03665085	CD8+ Tc17
LY86	0.00010887	-4.5891453	0.0403906	CD8+ Tc17

IGHM-secreted	0.00012387	-2.0692956	0.04595469	CD8+ Tc17
PAX5	0.00017727	-1.2478038	0.06576681	CD8+ Tc17
IFITM3	0.00030475	0.55893998	0.11306095	CD8+ Tc17
EOMES	0.00030873	2.15482186	0.11454053	CD8+ Tc17
MS4A1	0.0003437	-1.5635356	0.12751201	CD8+ Tc17
POU2AF1	0.00040301	-2.5339497	0.14951839	CD8+ Tc17
ITGAE	0.00044122	1.32215415	0.1636933	CD8+ Tc17
FCER2	0.00050223	-2.8304348	0.18632576	CD8+ Tc17
KLRC3	0.00065572	-1.6190173	0.24327253	CD8+ Tc17
TGFBI	0.00075446	-4.4121721	0.27990593	CD8+ Tc17
RNASE6	0.00093852	-4.3415426	0.34818952	CD8+ Tc17
ANXA5	0.00101668	0.75503486	0.37718927	CD8+ Tc17
FAM65B	0.00111461	0.84505075	0.41352154	CD8+ Tc17
CD24	0.0011185	-4.328212	0.4149634	CD8+ Tc17
CD70	0.0012782	2.39318531	0.47421292	CD8+ Tc17
TRDC	0.00147794	0.11218579	0.54831754	CD8+ Tc17
IRF4	0.00218471	-1.6730779	0.81052722	CD8+ Tc17
IGHG1-secreted	0.00265824	-4.2490312	0.98620592	CD8+ Tc17
KLRC4	0.00325444	-2.0013548	1	CD8+ Tc17
CD37	0.0033119	0.24293828	1	CD8+ Tc17
CCND2	0.00341521	1.32446462	1	CD8+ Tc17
ICOS	0.00345179	-0.6565415	1	CD8+ Tc17
APOBEC3G	0.00417012	0.99155936	1	CD8+ Tc17
BLNK	0.00468907	-2.9360484	1	CD8+ Tc17
IFNG	0.00480358	-2.6444328	1	CD8+ Tc17
CCR4	0.00493984	-3.3180603	1	CD8+ Tc17
KLRK1	0.00580777	0.30084825	1	CD8+ Tc17
CCL3	0.00602987	1.20123511	1	CD8+ Tc17
IGHD-membrane	0.00647505	-2.284561	1	CD8+ Tc17
CD86	0.00662375	-2.3252904	1	CD8+ Tc17
IL15RA	0.00691131	2.09581933	1	CD8+ Tc17
LILRB4	0.00712272	-3.660545	1	CD8+ Tc17
SLC7A7	0.00772733	-3.9142469	1	CD8+ Tc17
BACH2	0.008557	-0.784226	1	CD8+ Tc17
TIGIT	0.00894075	-0.5935483	1	CD8+ Tc17
FOXP3	0.0090967	-4.0395782	1	CD8+ Tc17
IGLC3	0.00933288	-3.2714757	1	CD8+ Tc17
FCN1	0.00951369	-4.5587756	1	CD8+ Tc17
TGFBI	0	6.14639535	0	CD11c+ CD14+
S100A9	0	9.22786673	0	CD11c+ CD14+
FCN1	0	7.45068177	0	CD11c+ CD14+
CD86	0	6.0316463	0	CD11c+ CD14+

RNASE6	0	5.67181343	0	CD11c+ CD14+
CD33	0	7.38994159	0	CD11c+ CD14+
CXCL16	0	4.45073337	0	CD11c+ CD14+
LY86	0	5.02276362	0	CD11c+ CD14+
S100A12	0	9.83387694	0	CD11c+ CD14+
TNFSF13	0	5.11116732	0	CD11c+ CD14+
CD14	0	9.77877036	0	CD11c+ CD14+
LILRB4	0	5.65688821	0	CD11c+ CD14+
TNFSF13B	0	4.65407081	0	CD11c+ CD14+
CD36	0	8.53836115	0	CD11c+ CD14+
CD163	0	12.1366834	0	CD11c+ CD14+
CD1C	0	5.98307641	0	CD11c+ CD14+
TLR2	0	5.89708384	0	CD11c+ CD14+
SLC7A7	0	5.18868981	0	CD11c+ CD14+
CLEC10A	0	10.6158493	0	CD11c+ CD14+
FCER1A	0	9.08053434	0	CD11c+ CD14+
ENTPD1	0	5.31824223	0	CD11c+ CD14+
CLEC4E	0	10.1138956	0	CD11c+ CD14+
KCNE3	0	5.92466514	0	CD11c+ CD14+
MGST1	0	8.07856134	0	CD11c+ CD14+
RNASE2	0	10.5444532	0	CD11c+ CD14+
VEGFA	0	7.53572571	0	CD11c+ CD14+
F13A1	0	10.4139584	0	CD11c+ CD14+
CXCL8	0	8.35378594	0	CD11c+ CD14+
TREM1	0	8.48529107	0	CD11c+ CD14+
FLT3	0	6.91753875	0	CD11c+ CD14+
QPCT	0	8.39681107	0	CD11c+ CD14+
IL1RN	0	7.81297116	0	CD11c+ CD14+
IL1B	0	8.90985299	0	CD11c+ CD14+
FCER1G	2.58E-273	3.37175833	9.58E-271	CD11c+ CD14+
CLEC4D	2.97E-273	9.6326248	1.10E-270	CD11c+ CD14+
LGALS3	3.36E-260	3.51843672	1.25E-257	CD11c+ CD14+
ITGAX	9.18E-234	3.17558296	3.41E-231	CD11c+ CD14+
ICAM1	1.50E-230	3.84183716	5.57E-228	CD11c+ CD14+
HLA-DMA	2.10E-224	4.17039388	7.81E-222	CD11c+ CD14+
HLA-DRA	3.84E-218	5.15440139	1.42E-215	CD11c+ CD14+
GAB2	4.76E-212	4.25518273	1.77E-209	CD11c+ CD14+
AQP9	1.64E-211	6.24244335	6.10E-209	CD11c+ CD14+
NAMPT	9.29E-198	3.56176921	3.45E-195	CD11c+ CD14+
LYN	1.77E-190	2.86220291	6.56E-188	CD11c+ CD14+
HLA-DQB1	8.88E-184	4.66758525	3.29E-181	CD11c+ CD14+
TLR8	4.61E-182	5.36761372	1.71E-179	CD11c+ CD14+

FTH1	1.62E-161	3.09029522	6.00E-159	CD11c+ CD14+
IER3	1.74E-149	3.98865051	6.47E-147	CD11c+ CD14+
IRF8	9.05E-145	4.25145909	3.36E-142	CD11c+ CD14+
LAP3	7.77E-144	3.12782871	2.88E-141	CD11c+ CD14+
LAT2	1.48E-142	2.71560084	5.48E-140	CD11c+ CD14+
LGALS9	6.09E-142	3.21246711	2.26E-139	CD11c+ CD14+
CD74	8.88E-130	3.89200201	3.30E-127	CD11c+ CD14+
BPI	4.31E-127	9.77521037	1.60E-124	CD11c+ CD14+
HLA-DPA1	8.59E-127	4.46548917	3.19E-124	CD11c+ CD14+
LGALS1	9.67E-124	2.79751053	3.59E-121	CD11c+ CD14+
SNCA	3.43E-123	4.66709397	1.27E-120	CD11c+ CD14+
FOSB	1.72E-119	2.82355223	6.37E-117	CD11c+ CD14+
C10orf54	5.86E-116	2.67058464	2.17E-113	CD11c+ CD14+
ANXA5	4.59E-105	2.52583834	1.70E-102	CD11c+ CD14+
TRBC2	4.62E-104	-4.0583046	1.71E-101	CD11c+ CD14+
VSIG4	4.99E-101	7.0952561	1.85E-98	CD11c+ CD14+
YBX3	4.73E-95	2.50357444	1.75E-92	CD11c+ CD14+
GAPDH	3.04E-91	2.2187426	1.13E-88	CD11c+ CD14+
CD3E	1.01E-89	-4.5799713	3.73E-87	CD11c+ CD14+
IL32	1.11E-89	-3.9576996	4.12E-87	CD11c+ CD14+
S100A10	2.40E-89	2.25163677	8.92E-87	CD11c+ CD14+
CD4	3.41E-89	2.19312256	1.27E-86	CD11c+ CD14+
CXCL2	1.43E-88	7.41787907	5.30E-86	CD11c+ CD14+
IL18	3.03E-88	2.83442362	1.12E-85	CD11c+ CD14+
TRAC	2.96E-81	-4.3264528	1.10E-78	CD11c+ CD14+
CD3D	2.84E-76	-4.3740394	1.06E-73	CD11c+ CD14+
IL1R2	1.10E-75	7.64589458	4.07E-73	CD11c+ CD14+
CCL3	2.04E-74	3.16680457	7.58E-72	CD11c+ CD14+
ITGB2	4.64E-71	1.55582605	1.72E-68	CD11c+ CD14+
LCK	1.40E-70	-4.0734101	5.18E-68	CD11c+ CD14+
PIK3AP1	3.96E-63	1.41667688	1.47E-60	CD11c+ CD14+
CMTM2	6.72E-62	5.18524696	2.49E-59	CD11c+ CD14+
CXCL1	1.18E-61	7.37709365	4.38E-59	CD11c+ CD14+
DUSP1	1.55E-60	2.25364892	5.76E-58	CD11c+ CD14+
SELL	7.26E-54	1.60076769	2.69E-51	CD11c+ CD14+
MITF	4.44E-52	6.40059611	1.65E-49	CD11c+ CD14+
HAVCR2	9.61E-51	2.15365545	3.57E-48	CD11c+ CD14+
CD63	1.36E-50	1.35781401	5.04E-48	CD11c+ CD14+
IL7R	7.86E-49	-4.8674893	2.91E-46	CD11c+ CD14+
IFNGR1	1.54E-48	1.71651234	5.71E-46	CD11c+ CD14+
VNN2	2.15E-44	2.70717999	7.98E-42	CD11c+ CD14+
GNAI2	3.53E-44	1.56849552	1.31E-41	CD11c+ CD14+

CTSW	1.44E-43	-3.802608	5.33E-41	CD11c+ CD14+
CD1B	1.44E-43	8.41377139	5.36E-41	CD11c+ CD14+
CD1A	7.62E-43	4.91893537	2.83E-40	CD11c+ CD14+
CD2	1.46E-42	-2.6200469	5.41E-40	CD11c+ CD14+
IL2RB	1.30E-39	-4.4512606	4.83E-37	CD11c+ CD14+
BCL6	4.15E-39	2.93450597	1.54E-36	CD11c+ CD14+
CD6	1.08E-37	-2.5305935	4.00E-35	CD11c+ CD14+
PIK3IP1	3.69E-37	-2.2387816	1.37E-34	CD11c+ CD14+
GZMA	5.33E-37	-4.8993419	1.98E-34	CD11c+ CD14+
NINJ2	5.42E-36	1.83007468	2.01E-33	CD11c+ CD14+
KLRK1	2.20E-34	-4.8510713	8.15E-32	CD11c+ CD14+
FUT4	3.40E-34	2.60837574	1.26E-31	CD11c+ CD14+
SLC25A37	2.28E-33	1.62800396	8.46E-31	CD11c+ CD14+
ITGAE	1.53E-32	1.33253379	5.68E-30	CD11c+ CD14+
LAT	1.88E-32	-2.7463479	6.96E-30	CD11c+ CD14+
TARP-refseq	5.94E-31	-4.4192478	2.20E-28	CD11c+ CD14+
CCL5	1.92E-29	-3.829124	7.11E-27	CD11c+ CD14+
CD247	2.59E-29	-4.3267764	9.61E-27	CD11c+ CD14+
THBS1	6.15E-29	3.97924125	2.28E-26	CD11c+ CD14+
BCL2A1	8.26E-29	2.03005629	3.07E-26	CD11c+ CD14+
CD69	8.50E-29	-3.7120392	3.15E-26	CD11c+ CD14+
CTSD	2.28E-28	2.05454796	8.45E-26	CD11c+ CD14+
CST7	2.48E-28	-3.0479955	9.22E-26	CD11c+ CD14+
CD37	6.32E-28	0.83112214	2.34E-25	CD11c+ CD14+
IL23R	7.34E-28	-1.4524152	2.72E-25	CD11c+ CD14+
CCR1	9.59E-28	3.90118339	3.56E-25	CD11c+ CD14+
NKG7	3.70E-26	-4.0583689	1.37E-23	CD11c+ CD14+
BCL11B	6.56E-26	-4.1691894	2.44E-23	CD11c+ CD14+
CCR2	1.00E-25	2.9007262	3.72E-23	CD11c+ CD14+
CD8A	1.04E-24	-5.0129988	3.87E-22	CD11c+ CD14+
KIAA0101	1.10E-23	2.2994481	4.08E-21	CD11c+ CD14+
JUNB	1.89E-23	1.01418768	7.00E-21	CD11c+ CD14+
PRF1	4.04E-23	-3.7453445	1.50E-20	CD11c+ CD14+
KLRB1	4.17E-23	-5.4327672	1.55E-20	CD11c+ CD14+
CD209	9.28E-22	6.69085397	3.44E-19	CD11c+ CD14+
LEF1	1.08E-21	-3.461432	4.01E-19	CD11c+ CD14+
CD5	5.21E-21	-2.9586142	1.93E-18	CD11c+ CD14+
CD3G	5.76E-21	-6.2957708	2.14E-18	CD11c+ CD14+
RGS1	9.03E-21	2.20676135	3.35E-18	CD11c+ CD14+
ADGRE1	9.39E-21	1.97494342	3.48E-18	CD11c+ CD14+
F5	3.01E-20	2.98467944	1.12E-17	CD11c+ CD14+
BTG1	3.59E-20	-0.8289096	1.33E-17	CD11c+ CD14+

THBD	2.47E-19	5.66865461	9.18E-17	CD11c+ CD14+
CD27	3.37E-19	-3.8573806	1.25E-16	CD11c+ CD14+
RORA	1.22E-18	-4.0270129	4.51E-16	CD11c+ CD14+
GZMH	1.32E-18	-4.6224445	4.91E-16	CD11c+ CD14+
VPS28	1.49E-18	1.0774665	5.53E-16	CD11c+ CD14+
RUNX3	2.07E-18	-1.3697543	7.67E-16	CD11c+ CD14+
CD44	2.93E-18	0.91967365	1.09E-15	CD11c+ CD14+
GZMB	3.67E-18	-2.3955059	1.36E-15	CD11c+ CD14+
TBX21	5.62E-18	-4.6263383	2.08E-15	CD11c+ CD14+
IGBP1	1.93E-16	0.88525083	7.15E-14	CD11c+ CD14+
CXCR4	1.96E-16	-1.0286198	7.25E-14	CD11c+ CD14+
CD8B	1.15E-15	-4.1711976	4.27E-13	CD11c+ CD14+
CCR7	1.49E-15	-2.9354835	5.52E-13	CD11c+ CD14+
JUN	3.07E-15	1.31277497	1.14E-12	CD11c+ CD14+
TRAT1	5.44E-15	-5.6745399	2.02E-12	CD11c+ CD14+
STAT5A	6.36E-15	0.94298404	2.36E-12	CD11c+ CD14+
DOCK8	1.33E-14	1.08216627	4.92E-12	CD11c+ CD14+
BTLA	1.87E-14	1.46505944	6.95E-12	CD11c+ CD14+
RPN2	6.98E-14	0.8340852	2.59E-11	CD11c+ CD14+
BAX	1.48E-13	0.67953509	5.48E-11	CD11c+ CD14+
CASP5	2.87E-13	0.76794492	1.06E-10	CD11c+ CD14+
PRDM1	3.22E-13	-2.9985187	1.19E-10	CD11c+ CD14+
CD7	5.08E-13	-4.5372535	1.89E-10	CD11c+ CD14+
GNLY	9.01E-13	-3.9554191	3.34E-10	CD11c+ CD14+
GIMAP5	1.56E-12	-2.5412732	5.80E-10	CD11c+ CD14+
TLR7	2.20E-12	3.30399105	8.14E-10	CD11c+ CD14+
PSEN1	4.06E-12	1.08485999	1.51E-09	CD11c+ CD14+
LIPA	9.99E-12	1.01885901	3.70E-09	CD11c+ CD14+
STAT4	1.41E-11	-3.0621835	5.23E-09	CD11c+ CD14+
IL15	4.07E-11	1.01729144	1.51E-08	CD11c+ CD14+
TCF7	4.57E-11	-3.5311259	1.70E-08	CD11c+ CD14+
MYC	7.86E-11	-2.1951802	2.92E-08	CD11c+ CD14+
GZMK	1.19E-10	-5.4706079	4.40E-08	CD11c+ CD14+
PDIA6	1.23E-10	0.6464063	4.57E-08	CD11c+ CD14+
TRDC	1.26E-10	-5.4640555	4.67E-08	CD11c+ CD14+
FOSL1	4.23E-10	4.02493516	1.57E-07	CD11c+ CD14+
NCR3	1.07E-09	-3.713304	3.96E-07	CD11c+ CD14+
ITGAM	1.40E-09	0.4838272	5.18E-07	CD11c+ CD14+
BCL2	1.40E-09	-2.221991	5.18E-07	CD11c+ CD14+
CD28	1.58E-09	-3.3143325	5.87E-07	CD11c+ CD14+
C1QB	3.36E-09	3.64688578	1.25E-06	CD11c+ CD14+
TXK	6.19E-09	-2.4847394	2.30E-06	CD11c+ CD14+

CD300A	9.33E-09	0.26068055	3.46E-06	CD11c+ CD14+
IL3RA	1.18E-08	2.14767176	4.38E-06	CD11c+ CD14+
FCGR3A	1.19E-08	-3.0115983	4.40E-06	CD11c+ CD14+
TNFRSF8	1.37E-08	2.60220765	5.06E-06	CD11c+ CD14+
KLRG1	1.50E-08	-3.0375894	5.55E-06	CD11c+ CD14+
IL18RAP	2.58E-08	-3.8571175	9.57E-06	CD11c+ CD14+
CBLB	2.78E-08	-2.1036918	1.03E-05	CD11c+ CD14+
ZAP70	4.42E-08	-2.2460911	1.64E-05	CD11c+ CD14+
CD244	4.76E-08	0.43327513	1.77E-05	CD11c+ CD14+
PASK	5.79E-08	-2.3141052	2.15E-05	CD11c+ CD14+
KLRC1	8.04E-08	-5.6253601	2.98E-05	CD11c+ CD14+
TRIB2	1.10E-07	-1.3552165	4.07E-05	CD11c+ CD14+
ZNF683	1.37E-07	-4.8119273	5.06E-05	CD11c+ CD14+
BIRC3	7.34E-07	-2.3874697	0.00027237	CD11c+ CD14+
CXCL5	1.19E-06	0.77795673	0.00044212	CD11c+ CD14+
CCND2	1.42E-06	-0.973268	0.00052569	CD11c+ CD14+
SELPLG	2.02E-06	0.52423264	0.00074933	CD11c+ CD14+
FAM65B	3.01E-06	-0.8689421	0.00111667	CD11c+ CD14+
TNFSF10	3.44E-06	0.53737625	0.00127733	CD11c+ CD14+
EGR1	3.46E-06	1.40226868	0.00128233	CD11c+ CD14+
IFITM3	4.53E-06	0.49547647	0.00167892	CD11c+ CD14+
IKZF1	6.85E-06	-1.5052149	0.00253966	CD11c+ CD14+
IRF4	6.98E-06	0.88210792	0.00258813	CD11c+ CD14+
TNFSF8	7.39E-06	0.68558446	0.00274126	CD11c+ CD14+
LAG3	8.75E-06	-4.9873717	0.00324621	CD11c+ CD14+
ARL4C	1.05E-05	-0.665104	0.00388595	CD11c+ CD14+
LTB	1.33E-05	-2.5374051	0.00491762	CD11c+ CD14+
ICOS	1.42E-05	-3.7878952	0.00526473	CD11c+ CD14+
KDELR1	2.42E-05	1.96948896	0.00897061	CD11c+ CD14+
FOXP1	2.81E-05	-1.366207	0.01040784	CD11c+ CD14+
STAT6	2.92E-05	0.65058664	0.0108467	CD11c+ CD14+
KLRF1	5.72E-05	-2.3978971	0.02123681	CD11c+ CD14+
LAIR2	0.00011483	-4.992607	0.0426025	CD11c+ CD14+
C1QA	0.00012159	2.95570639	0.04511143	CD11c+ CD14+
CD160	0.00015835	-3.6970144	0.05874863	CD11c+ CD14+
CTLA4	0.00018103	-3.4319114	0.06716063	CD11c+ CD14+
B3GAT1	0.00022693	-2.8879295	0.0841898	CD11c+ CD14+
CD79A	0.0002346	-3.2734036	0.08703604	CD11c+ CD14+
KIR2DL1	0.00024371	-3.7536922	0.09041491	CD11c+ CD14+
TMEM97	0.00028495	1.24787462	0.10571747	CD11c+ CD14+
TNFRSF25	0.00031526	-2.4600612	0.11696154	CD11c+ CD14+
TIGIT	0.00032949	-2.781043	0.12223933	CD11c+ CD14+

KLRC3	0.0005507	-2.7319194	0.2043092	CD11c+ CD14+
TIAF1	0.00058196	0.46164239	0.21590722	CD11c+ CD14+
IFITM2	0.000617	0.21013688	0.22890652	CD11c+ CD14+
ATF6B	0.00064005	0.57084018	0.2374572	CD11c+ CD14+
STAT3	0.00080517	0.15552644	0.29871748	CD11c+ CD14+
BLNK	0.00084762	0.98656907	0.31446561	CD11c+ CD14+
LTA	0.00096006	-3.790556	0.35618041	CD11c+ CD14+
NT5E	0.00099098	-3.8110829	0.36765481	CD11c+ CD14+
FOXO1	0.00124184	-1.8039473	0.46072433	CD11c+ CD14+
FYN	0.00152527	-0.5182169	0.5658766	CD11c+ CD14+
HLA-A	0.00187127	0.1691663	0.69424059	CD11c+ CD14+
KLRC4	0.00217787	-3.3576838	0.80799159	CD11c+ CD14+
PCNA	0.00225276	0.29284382	0.83577569	CD11c+ CD14+
PAX5	0.0024649	-2.5316322	0.91447644	CD11c+ CD14+
TGFB1	0.00266925	0.43351961	0.99029132	CD11c+ CD14+
ZBTB16	0.00303481	-2.0814256	1	CD11c+ CD14+
CD48	0.00307513	0.27651118	1	CD11c+ CD14+
APOBEC3G	0.00317375	-1.0391365	1	CD11c+ CD14+
RORC	0.00327636	-3.9370447	1	CD11c+ CD14+
PTGDR2	0.00348865	0.1398176	1	CD11c+ CD14+
IGKC	0.0034952	-2.3713421	1	CD11c+ CD14+
IFNG	0.00370152	-3.3317903	1	CD11c+ CD14+
CCL4	0.00380892	-1.2292988	1	CD11c+ CD14+
IGHM-secreted	0.00426421	-2.7904473	1	CD11c+ CD14+
IKZF2	0.00485005	-3.1601618	1	CD11c+ CD14+
CD52	0.00628486	-0.2490751	1	CD11c+ CD14+
CCR4	0.00756125	-3.1707907	1	CD11c+ CD14+
HLA-A	8.73E-46	-1.5216816	3.24E-43	NK
CD48	1.06E-41	-2.5946083	3.92E-39	NK
CD52	2.13E-41	-1.8466958	7.92E-39	NK
BTG1	1.96E-38	-2.0636052	7.29E-36	NK
CD37	4.99E-36	-2.7785142	1.85E-33	NK
GAPDH	1.79E-28	-1.9188234	6.64E-26	NK
IL23R	1.87E-27	-3.1596961	6.93E-25	NK
TRAC	5.33E-27	-2.6458714	1.98E-24	NK
PTPRC	8.33E-27	-1.5772109	3.09E-24	NK
CXCR4	2.19E-26	-2.3955047	8.12E-24	NK
S100A10	7.57E-25	-2.218978	2.81E-22	NK
CD3E	1.56E-23	-1.9842735	5.78E-21	NK
IL32	4.70E-21	-1.751166	1.75E-18	NK
IL7R	6.15E-21	-4.016948	2.28E-18	NK
TRBC2	8.29E-21	-1.8324094	3.08E-18	NK

CD74	4.45E-19	-2.845733	1.65E-16	NK
CD3D	5.97E-19	-1.9741619	2.22E-16	NK
PIK3IP1	3.33E-18	-2.6686329	1.24E-15	NK
CD44	3.50E-18	-2.8353278	1.30E-15	NK
KIR2DL1	1.24E-15	0.49195669	4.58E-13	NK
LCK	2.65E-15	-1.8593312	9.84E-13	NK
CD6	6.67E-15	-2.6501298	2.47E-12	NK
SELL	7.96E-14	-2.7860781	2.95E-11	NK
GZMB	1.84E-13	-0.2746617	6.84E-11	NK
FCGR3A	3.50E-13	-0.4149472	1.30E-10	NK
GNLY	3.97E-12	-0.1129336	1.47E-09	NK
IFITM2	5.79E-12	-1.7211238	2.15E-09	NK
CD2	4.57E-11	-1.8005082	1.70E-08	NK
SELPLG	5.08E-11	-1.5614324	1.88E-08	NK
FYN	1.07E-10	-1.5831718	3.99E-08	NK
KLRF1	1.73E-10	-0.4137926	6.41E-08	NK
IFITM3	2.18E-10	-1.7183809	8.10E-08	NK
LEF1	2.64E-10	-3.365194	9.79E-08	NK
LAT	3.13E-10	-2.497205	1.16E-07	NK
CD4	4.53E-10	-4.1116133	1.68E-07	NK
FAM65B	7.32E-10	-2.8373626	2.72E-07	NK
BIN2	1.46E-09	-1.4385375	5.43E-07	NK
CD27	6.43E-09	-4.0455684	2.39E-06	NK
ITGB2	1.60E-08	-1.1711544	5.92E-06	NK
CD5	1.61E-08	-3.0465471	5.98E-06	NK
RPN2	2.53E-08	-1.8886677	9.39E-06	NK
FYB	3.78E-08	-2.9618022	1.40E-05	NK
MYC	8.83E-08	-3.868427	3.28E-05	NK
DUSP1	1.14E-07	-2.0865166	4.24E-05	NK
GZMH	1.16E-07	-0.5464061	4.32E-05	NK
CCR7	1.17E-07	-3.6244584	4.34E-05	NK
CD69	2.43E-07	-2.6831451	9.01E-05	NK
LAMP1	6.47E-07	-1.4678283	0.00024021	NK
BCL11B	9.38E-07	-2.6171077	0.00034811	NK
PRF1	1.07E-06	-0.5814067	0.00039792	NK
CD244	1.29E-06	-0.6461284	0.00047774	NK
TCF7	2.07E-06	-4.8001941	0.00076899	NK
TRDC	2.28E-06	-0.9106368	0.00084529	NK
C10orf54	2.90E-06	-2.0667742	0.00107746	NK
TRAT1	3.10E-06	-4.0452682	0.00115014	NK
ITGAM	3.44E-06	-0.5925547	0.00127663	NK
CX3CR1	3.96E-06	-0.9612093	0.00147045	NK

FCER1G	6.94E-06	-1.2920564	0.00257627	NK
ANXA5	1.01E-05	-2.7210736	0.00373272	NK
JUNB	1.33E-05	-1.6767254	0.00494229	NK
FOXP1	1.77E-05	-2.8239918	0.00655709	NK
CD160	2.11E-05	-0.4855367	0.00784145	NK
IL4R	2.14E-05	-2.787656	0.007942	NK
GIMAP5	2.20E-05	-2.6715171	0.00814366	NK
ITGAX	3.62E-05	-1.035447	0.01342951	NK
GIMAP2	4.21E-05	-2.2323489	0.01563548	NK
ITGA4	4.36E-05	-2.0043043	0.01617178	NK
BIRC3	5.68E-05	-3.5833487	0.02108455	NK
PASK	7.69E-05	-2.8069235	0.02851836	NK
GNAI2	8.09E-05	-1.9305509	0.03000269	NK
KLRC1	9.44E-05	-0.8481622	0.0350178	NK
CD28	0.00010809	-3.7008399	0.04009988	NK
ZNF683	0.00015133	-0.8272829	0.05614409	NK
NKG7	0.00020555	-0.6184998	0.07625988	NK
BAX	0.00021058	-1.4967944	0.07812602	NK
CCL4	0.00025869	-0.4244764	0.09597436	NK
ARL4C	0.0003002	-1.3934317	0.11137522	NK
LTB	0.0003178	-4.1328902	0.11790272	NK
GZMK	0.00036554	-4.3642257	0.13561514	NK
IRF4	0.00038726	-0.174125	0.14367306	NK
HLA-DPA1	0.00048432	-2.7600497	0.17968173	NK
TNFSF8	0.0005493	-3.0717677	0.20379068	NK
TRIB2	0.00059549	-2.4510448	0.22092515	NK
VPS28	0.00092735	-2.0280317	0.34404551	NK
DOCK8	0.00102495	-2.1884427	0.3802563	NK
CXCL5	0.00171549	-3.0983691	0.63644646	NK
HLA-DMA	0.00229341	-3.0588776	0.85085653	NK
BCL2	0.00231525	-2.7493035	0.85895599	NK
CD3G	0.00234897	-2.3292881	0.87146618	NK
CD300A	0.00280384	-0.7998359	1	NK
CASP5	0.0028556	-1.8325434	1	NK
DPP4	0.00312838	-3.2736232	1	NK
PDIA6	0.00338039	-1.676874	1	NK
TIAF1	0.00361437	-2.3705666	1	NK
HLA-DQB1	0.00392117	-3.1000552	1	NK
FOXO1	0.00401357	-3.0639425	1	NK
RUNX3	0.00423182	-1.1238219	1	NK
MS4A1	0.00425084	-3.9143213	1	NK
LIPA	0.00429451	-2.0321705	1	NK

LAT2	0.00446975	-1.0171986	1	NK
ITGAE	0.00476965	-2.1226754	1	NK
CD22	0.00571619	-4.1434209	1	NK
POU2AF1	0.00599815	-3.8977057	1	NK
CTLA4	0.00706778	-2.7800027	1	NK
DUSP2	0.0080032	-1.8738497	1	NK
FASLG	0.00834327	-0.4046245	1	NK
CD79B	0.00838387	-2.5987522	1	NK
IKZF1	0.00968053	-2.0507997	1	NK
PAX5	0.00991517	-3.5599334	1	NK
IL3RA	0	8.8264307	0	Other
NRP1	0	10.1403597	0	Other
FCER1A	7.15E-212	4.22366441	2.65E-209	Other
TCF4	1.54E-165	6.68046505	5.71E-163	Other
FLT3	6.78E-165	5.52510952	2.52E-162	Other
LILRB4	1.66E-157	6.13979745	6.15E-155	Other
TLR9	2.46E-157	6.70482043	9.12E-155	Other
JCHAIN	9.93E-152	6.39721704	3.68E-149	Other
MZB1	4.38E-149	6.23050769	1.63E-146	Other
RNASE6	1.77E-124	5.32332194	6.57E-122	Other
TGFBI	9.15E-112	5.372862	3.39E-109	Other
TNFRSF17	3.65E-87	6.45373855	1.35E-84	Other
SNCA	2.46E-78	5.71972452	9.14E-76	Other
IRF4	1.96E-70	5.09754266	7.26E-68	Other
FAM129C	2.18E-59	4.80968871	8.08E-57	Other
TLR7	4.40E-58	6.45539861	1.63E-55	Other
IRF8	8.25E-55	6.32152554	3.06E-52	Other
BLNK	5.63E-47	4.67640948	2.09E-44	Other
CD36	8.55E-35	4.00885484	3.17E-32	Other
IGHM-secreted	1.63E-32	2.53392539	6.06E-30	Other
CCR2	1.36E-30	3.57501706	5.03E-28	Other
FCER1G	1.64E-30	3.00182345	6.07E-28	Other
IGKC	2.96E-27	2.20120465	1.10E-24	Other
HLA-DMA	6.31E-26	2.33392151	2.34E-23	Other
MGST1	9.70E-23	4.35982347	3.60E-20	Other
HLA-DRA	1.37E-22	2.45989185	5.08E-20	Other
CXCR3	6.34E-22	3.41230777	2.35E-19	Other
GZMB	7.25E-22	3.31264442	2.69E-19	Other
LYN	1.33E-18	2.39500026	4.93E-16	Other
CD4	2.48E-18	3.31979249	9.20E-16	Other
CD74	2.23E-17	2.93138541	8.28E-15	Other
FOSB	3.64E-17	2.27209646	1.35E-14	Other

GAB2	4.66E-17	3.52912184	1.73E-14	Other
RGS1	9.03E-16	3.46718695	3.35E-13	Other
HLA-DPA1	9.19E-16	1.68236408	3.41E-13	Other
IGHM-membrane	2.40E-15	0.19992521	8.89E-13	Other
TRBC2	5.72E-15	-4.7922376	2.12E-12	Other
IL32	7.66E-14	-5.2553317	2.84E-11	Other
PIK3AP1	9.61E-13	2.11398799	3.57E-10	Other
ICAM1	2.51E-12	2.69478055	9.33E-10	Other
TRAC	6.19E-12	-5.6362814	2.30E-09	Other
ADA	8.01E-12	1.88382863	2.97E-09	Other
TIAF1	8.35E-12	1.92999466	3.10E-09	Other
MME	1.79E-11	4.91032913	6.64E-09	Other
F13A1	2.01E-11	3.24457173	7.44E-09	Other
CD3D	9.25E-11	-4.6048727	3.43E-08	Other
ITGAE	2.20E-10	2.39025359	8.15E-08	Other
SELL	4.59E-10	1.61676642	1.70E-07	Other
LCK	6.43E-10	-4.4073022	2.39E-07	Other
CD3E	7.77E-10	-3.0769626	2.88E-07	Other
IL18R1	1.62E-09	1.89178663	6.01E-07	Other
CD48	2.08E-09	-2.124181	7.72E-07	Other
CCR1	3.70E-09	3.54700957	1.37E-06	Other
CD2	5.95E-09	-4.2979454	2.21E-06	Other
BTLA	8.54E-09	1.86855154	3.17E-06	Other
RPN2	5.15E-08	1.59099685	1.91E-05	Other
PIK3IP1	5.54E-08	-3.5991896	2.06E-05	Other
IL7R	5.70E-08	-5.6232667	2.12E-05	Other
RUNX3	7.79E-08	-3.4443379	2.89E-05	Other
HLA-A	1.12E-07	-0.8286846	4.17E-05	Other
FYN	1.18E-07	-2.7783581	4.39E-05	Other
CST7	1.68E-07	-5.7981	6.23E-05	Other
TNFSF13	2.19E-07	2.22065862	8.14E-05	Other
IL2RB	8.14E-07	-5.6399358	0.00030195	Other
LAT	9.70E-07	-4.3770154	0.00036004	Other
CCL5	1.43E-06	-4.4235867	0.00053147	Other
CD52	2.43E-06	-1.1762592	0.00090308	Other
KLRK1	3.93E-06	-5.692158	0.00145857	Other
GZMA	4.35E-06	-5.5454844	0.00161372	Other
LAP3	4.70E-06	1.84777873	0.00174457	Other
IGHG3-secreted	7.91E-06	4.07897684	0.00293275	Other
CTSW	9.15E-06	-3.3148175	0.00339423	Other
PDIA4	1.11E-05	2.53837011	0.00413135	Other
SELPLG	1.20E-05	1.20947592	0.00445291	Other

PTPRC	1.59E-05	-1.2305341	0.00591343	Other
MCM4	1.71E-05	2.71918408	0.0063384	Other
CD6	2.66E-05	-2.5277256	0.00988105	Other
CD8A	3.61E-05	-6.0224623	0.01338893	Other
TARP-refseq	3.85E-05	-5.1149983	0.01429126	Other
HLA-DQB1	4.01E-05	0.4404583	0.01488665	Other
BCL11B	7.79E-05	-4.3707421	0.02888997	Other
CD69	8.52E-05	-3.6778335	0.03161693	Other
ITGB2	0.0001404	-1.5578957	0.05208815	Other
KLRB1	0.00015899	-6.0198054	0.05898562	Other
PRF1	0.00016685	-4.9713445	0.06190277	Other
GNLY	0.00019006	-5.5955882	0.07051196	Other
S100A10	0.00024335	-1.4737993	0.09028427	Other
PDIA6	0.00027347	1.81294849	0.10145617	Other
TNFSF13B	0.00028833	1.778642	0.10696974	Other
CXCR4	0.00042841	-0.6211062	0.15894001	Other
NKG7	0.00050739	-4.8278364	0.18824109	Other
IL23R	0.00094988	-1.3525607	0.35240714	Other
CD3G	0.00123524	-3.9294661	0.45827575	Other
BTG1	0.00129818	-0.9863572	0.48162406	Other
BIN2	0.00145595	-1.3270259	0.54015561	Other
CD247	0.00206335	-2.5953753	0.76550337	Other
IGLC3	0.00232396	5.35171206	0.86218779	Other
GZMH	0.00249062	-4.1091693	0.9240184	Other
XBP1	0.00253821	1.11539813	0.94167626	Other
LEF1	0.0025823	-2.7852618	0.95803474	Other
CD5	0.00268083	-2.3849036	0.99458829	Other
RORA	0.00274637	-3.0940412	1	Other
TBX21	0.00310081	-3.6287948	1	Other
TSPAN32	0.0033893	-3.5613627	1	Other
GIMAP2	0.00350378	-2.6432303	1	Other
PTTG2	0.00355264	2.42501116	1	Other
CD8B	0.00360748	-4.1784617	1	Other
MYC	0.00450408	-3.0000291	1	Other
CD27	0.00477675	-0.8187396	1	Other
TCL1A	0.00483686	2.40443177	1	Other
FCGR3A	0.00539337	-4.1588979	1	Other
CD37	0.00574481	0.45539145	1	Other
CD63	0.00610892	0.37912274	1	Other
GIMAP5	0.00681639	-2.74871	1	Other
TRAT1	0.00689036	-3.2968594	1	Other
CASP5	0.00885323	-1.5772882	1	Other

CD44	0.00948901	-1.1755483	1	Other
IFITM3	0.00967544	-1.1940759	1	Other
BCL2	0.00980938	-3.2323201	1	Other
ARL4C	0.00991983	-1.5171026	1	Other

Table D.3 Differential gene expression between cell clusters enriched in PBMC derived from HC and melanoma patients including adjusted p-value and log2-fold change.

gene	p_val	log2FC	p_val_adj	cluster
NETO1	1.38E-30	6.38584399	3.27E-26	B
CD19	8.84E-254	6.25651089	2.09E-249	B
CNR2	1.16E-120	6.03860035	2.74E-116	B
PAX5	2.19E-206	5.96651979	5.20E-202	B
FCER2	9.52E-163	5.91848319	2.25E-158	B
KHDRBS2	2.50E-62	5.872851	5.92E-58	B
VPREB3	7.71E-156	5.84111434	1.83E-151	B
BANK1	2.21E-252	5.72862466	5.24E-248	B
KIAA0125	5.09E-85	5.63848489	1.20E-80	B
HLA-DOB	8.23E-120	5.61845813	1.95E-115	B
CD1C	1.95E-79	5.60221929	4.61E-75	B
BLK	6.09E-194	5.57469751	1.44E-189	B
WDFY4	7.11E-179	5.5348571	1.68E-174	B
TCL1A	1.13E-125	5.53367658	2.68E-121	B
PNOC	1.71E-48	5.52570154	4.04E-44	B
CR2	4.58E-113	5.52296319	1.09E-108	B
BLNK	2.75E-161	5.50083071	6.52E-157	B
FAM177B	5.01E-52	5.48327362	1.19E-47	B
FCRL5	3.93E-114	5.45435204	9.32E-110	B
MS4A1	2.53E-242	5.44953303	5.98E-238	B
FAM129C	2.99E-173	5.43742714	7.09E-169	B
GYLTL1B	4.13E-14	5.42721527	9.78E-10	B
FCRL2	3.75E-62	5.35332744	8.87E-58	B
CD22	7.41E-201	5.3305263	1.75E-196	B
CD180	1.96E-60	5.28373335	4.63E-56	B
CRIP3	3.34E-22	5.26667109	7.92E-18	B
COL4A3	1.89E-50	5.22814221	4.47E-46	B
BCL11A	8.64E-207	5.15604155	2.05E-202	B
FCRL1	3.51E-110	5.03952738	8.32E-106	B
KLHL14	6.89E-26	5.01868107	1.63E-21	B
VAV3-AS1	7.99E-18	5.00749718	1.89E-13	B
TNFRSF13C	4.70E-34	4.98434161	1.11E-29	B
BTK	1.15E-118	4.95791792	2.73E-114	B
ESPNL	1.53E-09	4.871338	3.62E-05	B
CD79A	9.51E-223	4.87047497	2.25E-218	B
STAP1	1.12E-111	4.84712695	2.65E-107	B
LINC00494	2.34E-23	4.80170941	5.55E-19	B
NAPSB	9.39E-149	4.79531033	2.22E-144	B
SLC38A11	5.26E-20	4.76402949	1.25E-15	B
MYO7B	3.50E-30	4.66815241	8.29E-26	B

IGLL5	1.54E-124	4.62513019	3.64E-120	B
LY86	3.90E-90	4.61250042	9.24E-86	B
GLYATL1	4.94E-14	4.60619031	1.17E-09	B
IGLL1	3.07E-67	4.56001381	7.27E-63	B
TREML2	2.33E-18	4.53683939	5.52E-14	B
LOC100506178	5.43E-13	4.52155983	1.29E-08	B
NCF1C	7.26E-146	4.52017691	1.72E-141	B
Mar-01	3.79E-94	4.42247594	8.99E-90	B
LOC283194	6.96E-11	4.39603471	1.65E-06	B
CYBB	1.71E-104	4.37414504	4.06E-100	B
ABCB4	3.19E-27	4.35070054	7.56E-23	B
ADAM28	7.10E-140	4.31431191	1.68E-135	B
IGLL3P	4.56E-59	4.30146766	1.08E-54	B
CR1	2.32E-60	4.27307487	5.50E-56	B
MIR650	2.59E-15	4.26655707	6.14E-11	B
KCNH8	7.03E-14	4.24873004	1.67E-09	B
NCF1	2.71E-152	4.20551401	6.42E-148	B
TNFRSF13B	1.56E-35	4.19572742	3.70E-31	B
SLC2A5	2.36E-15	4.16323924	5.59E-11	B
SNX29P1	1.46E-47	4.15429918	3.46E-43	B
CCSER1	5.61E-21	4.1442227	1.33E-16	B
IRF8	9.08E-169	4.14262564	2.15E-164	B
C12orf74	5.17E-14	4.13790718	1.22E-09	B
HVCN1	4.92E-107	4.13298835	1.16E-102	B
ALOX5	2.76E-65	4.13173552	6.53E-61	B
STAG3	8.20E-39	4.09608736	1.94E-34	B
NCF1B	1.49E-110	4.0887515	3.54E-106	B
PLCG2	8.07E-94	4.08773896	1.91E-89	B
GAPT	5.00E-33	4.08470244	1.18E-28	B
RNASE6	5.42E-69	4.08206839	1.28E-64	B
MPEG1	4.89E-61	4.06259284	1.16E-56	B
TBC1D26	3.27E-17	4.01770333	7.75E-13	B
PLD4	7.39E-36	3.95738024	1.75E-31	B
CD79B	1.31E-146	3.95296819	3.10E-142	B
IL6	1.47E-17	3.89867593	3.48E-13	B
SDK2	5.23E-21	3.89538368	1.24E-16	B
CLEC17A	5.88E-39	3.87485493	1.39E-34	B
WNT16	1.82E-09	3.86095184	4.32E-05	B
IGJ	1.14E-29	3.85897003	2.70E-25	B
COL4A4	1.85E-18	3.84823537	4.39E-14	B
KIAA0226L	2.80E-78	3.81290156	6.64E-74	B

FGD2	7.00E-71	3.80407217	1.66E-66	B
CD72	1.15E-78	3.79805677	2.73E-74	B
C12orf42	1.67E-30	3.79578691	3.97E-26	B
ADAMDEC1	8.31E-18	3.77331042	1.97E-13	B
SLC45A3	1.12E-12	3.76875466	2.65E-08	B
COL19A1	5.89E-44	3.74884254	1.40E-39	B
ICOSLG	7.89E-29	3.74349015	1.87E-24	B
PIK3AP1	1.15E-57	3.73508836	2.73E-53	B
CIITA	2.65E-70	3.72344043	6.29E-66	B
P2RY14	1.69E-13	3.71864089	4.01E-09	B
HHEX	8.38E-23	3.71454293	1.99E-18	B
FAM26F	2.16E-27	3.71301007	5.12E-23	B
HLA-DQB2	3.10E-99	3.68301795	7.34E-95	B
FAM167A	5.15E-11	3.68024895	1.22E-06	B
DNASE1L3	9.48E-15	3.6790943	2.25E-10	B
CBFA2T3	1.58E-14	3.67857211	3.74E-10	B
CD83	1.65E-116	3.66608047	3.92E-112	B
SIGLEC14	3.91E-53	3.66432087	9.27E-49	B
HDAC9	1.52E-30	3.6381212	3.61E-26	B
TLR9	1.01E-20	3.61811942	2.38E-16	B
CR1L	2.81E-12	3.61684642	6.65E-08	B
CD40	3.19E-62	3.61328364	7.54E-58	B
SNX29P2	1.53E-24	3.60928313	3.63E-20	B
KBTBD8	3.07E-46	3.57819075	7.28E-42	B
ZBTB16	8.74E-49	3.56600779	2.07E-44	B
C1orf186	1.52E-13	3.53137533	3.60E-09	B
SYK	8.39E-51	3.51953328	1.99E-46	B
PION	1.87E-49	3.49640344	4.42E-45	B
SPI1	1.61E-17	3.4761059	3.82E-13	B
MOB3B	8.62E-31	3.42354486	2.04E-26	B
BACH2	6.05E-41	3.42058426	1.43E-36	B
CXCR5	3.05E-88	3.41868583	7.22E-84	B
RASL11A	2.38E-09	3.40688771	5.65E-05	B
LYN	1.28E-63	3.37668744	3.02E-59	B
TFEB	2.53E-24	3.36453996	5.99E-20	B
EAF2	2.48E-22	3.33968535	5.88E-18	B
BEND5	1.87E-12	3.32417908	4.43E-08	B
HLA-DMB	4.58E-99	3.31527032	1.09E-94	B
ZNF165	3.03E-18	3.31185324	7.18E-14	B
ELK2AP	2.59E-38	3.30389237	6.13E-34	B
DERL3	2.09E-09	3.29664481	4.94E-05	B

P2RX5	5.82E-79	3.29486842	1.38E-74	B
POU2F2	1.42E-56	3.28580439	3.36E-52	B
FCGR2B	2.61E-25	3.26512628	6.19E-21	B
RASGRP3	3.32E-17	3.26404333	7.86E-13	B
CYSLTR1	4.97E-22	3.22399898	1.18E-17	B
LAT2	4.22E-41	3.2198602	1.00E-36	B
LYL1	2.74E-13	3.19915785	6.49E-09	B
C16orf74	6.57E-11	3.19885292	1.56E-06	B
DENND3	1.54E-46	3.18417725	3.64E-42	B
DOK3	1.89E-22	3.16827465	4.49E-18	B
HLA-DOA	5.57E-42	3.14544444	1.32E-37	B
LOC148696	5.19E-21	3.14121529	1.23E-16	B
MIR600HG	4.01E-11	3.13665048	9.50E-07	B
RALGPS2	6.46E-44	3.12930884	1.53E-39	B
ANGPTL1	7.43E-13	3.12323828	1.76E-08	B
LCN10	2.53E-09	3.1111988	5.98E-05	B
HLA-DQB1	3.07E-114	3.08482974	7.27E-110	B
HLA-DQA2	3.29E-100	3.0621001	7.80E-96	B
MEF2C	7.55E-52	3.06110403	1.79E-47	B
P2RX1	4.42E-12	3.03061337	1.05E-07	B
COBLL1	2.10E-23	2.98549432	4.97E-19	B
GPR18	2.47E-41	2.97173307	5.85E-37	B
TCF4	1.66E-52	2.93038529	3.93E-48	B
ARHGAP24	3.87E-35	2.92132075	9.17E-31	B
NCF4	2.75E-33	2.89901829	6.51E-29	B
LOC283663	1.62E-51	2.89203679	3.85E-47	B
HLA-DRA	4.78E-109	2.8805271	1.13E-104	B
ZNF318	1.20E-28	2.8701135	2.84E-24	B
FCRLA	9.90E-49	2.84989854	2.35E-44	B
HLA-DPB2	4.73E-13	2.83615144	1.12E-08	B
SCIMP	4.42E-24	2.81389423	1.05E-19	B
GATS	1.98E-15	2.81330823	4.70E-11	B
HLA-DRB6	3.16E-99	2.801886	7.47E-95	B
SIPA1L3	1.48E-23	2.77190952	3.50E-19	B
FLJ40292	2.13E-10	2.75535537	5.05E-06	B
HLA-DQA1	1.25E-95	2.72795583	2.97E-91	B
KMO	2.46E-11	2.71576533	5.83E-07	B
GRASP	7.64E-14	2.71343582	1.81E-09	B
NAPSA	1.36E-12	2.71271629	3.23E-08	B
LY9	1.44E-83	2.70230921	3.41E-79	B
RASGEF1B	2.27E-35	2.69727746	5.38E-31	B

AFF3	6.16E-51	2.69198376	1.46E-46	B
PLEKHG1	1.03E-13	2.68543913	2.43E-09	B
GBGT1	2.28E-10	2.65420858	5.41E-06	B
RIC3	1.03E-20	2.65350277	2.43E-16	B
DAPP1	6.65E-26	2.61859017	1.57E-21	B
FAM49A	8.91E-15	2.60921435	2.11E-10	B
NCR3	2.02E-09	2.60188679	4.79E-05	B
PIK3C2B	3.79E-30	2.59478571	8.98E-26	B
SPINT2	2.87E-22	2.5880573	6.80E-18	B
RLTPR	3.40E-09	2.57712276	8.05E-05	B
LILRB1	4.37E-15	2.57648864	1.04E-10	B
TMEM154	3.83E-30	2.56737622	9.07E-26	B
RASGRP2	4.63E-32	2.53635802	1.10E-27	B
CDCA7L	1.79E-18	2.53010158	4.25E-14	B
SNX29	2.82E-34	2.52914266	6.68E-30	B
EBF1	6.42E-25	2.52153156	1.52E-20	B
KLF2	4.16E-33	2.48972019	9.85E-29	B
GNG7	3.10E-26	2.48787958	7.34E-22	B
DGKD	1.02E-23	2.46275084	2.41E-19	B
FCHSD2	1.67E-22	2.44629646	3.95E-18	B
MYO15B	3.59E-22	2.44513629	8.50E-18	B
HLA-DRB5	6.55E-88	2.41743092	1.55E-83	B
IL4R	9.03E-24	2.40853129	2.14E-19	B
SNN	4.30E-11	2.4067044	1.02E-06	B
GRAP	1.05E-17	2.39251964	2.49E-13	B
FAM159A	4.24E-09	2.38300773	0.00010045	B
CCR7	7.37E-48	2.38076821	1.75E-43	B
MTSS1	2.02E-25	2.37788384	4.79E-21	B
LOC283070	1.20E-11	2.36064646	2.85E-07	B
MZB1	5.64E-13	2.36048315	1.34E-08	B
NFKBID	6.55E-23	2.36005353	1.55E-18	B
HLA-DMA	8.84E-61	2.35572771	2.09E-56	B
POU2AF1	1.93E-36	2.34827211	4.56E-32	B
TSPAN13	2.69E-11	2.34475855	6.38E-07	B
PARP15	1.80E-40	2.34033339	4.26E-36	B
TLR10	2.12E-23	2.32842889	5.03E-19	B
MBNL3	2.22E-09	2.31956045	5.25E-05	B
RABEP2	2.19E-14	2.31818747	5.18E-10	B
SELL	1.95E-60	2.30309304	4.62E-56	B
EIF1AY	4.30E-14	2.30148243	1.02E-09	B
LTB	4.73E-58	2.30054404	1.12E-53	B

ADAM19	5.37E-45	2.29097434	1.27E-40	B
PDLIM1	1.33E-22	2.26889037	3.16E-18	B
BTLA	8.93E-29	2.26153311	2.11E-24	B
S1PR1	1.29E-24	2.2522832	3.06E-20	B
HLA-DRB1	1.41E-88	2.24894297	3.35E-84	B
LPAR5	2.16E-14	2.24851248	5.11E-10	B
AKAP2	4.63E-29	2.22975369	1.10E-24	B
GPR183	5.32E-43	2.21753819	1.26E-38	B
SEL1L3	7.95E-26	2.21325155	1.88E-21	B
HLA-DPA1	2.26E-81	2.17490485	5.36E-77	B
KYNU	1.44E-10	2.16570608	3.41E-06	B
CCR6	1.51E-31	2.15693545	3.58E-27	B
HLA-DPB1	7.71E-74	2.15627896	1.83E-69	B
PRKCB	3.48E-27	2.15324466	8.24E-23	B
CD24	1.61E-22	2.12274877	3.82E-18	B
L3MBTL3	8.12E-13	2.11376089	1.92E-08	B
CD37	5.28E-83	2.1071046	1.25E-78	B
RBM38	1.54E-14	2.09659474	3.65E-10	B
ADRBK2	1.50E-12	2.08659384	3.56E-08	B
SWAP70	2.62E-38	2.08226649	6.22E-34	B
KDM6B	1.25E-21	2.06893408	2.96E-17	B
SIDT1	4.67E-14	2.061263	1.11E-09	B
ITPR1	1.75E-24	2.05933712	4.15E-20	B
HIP1R	6.95E-15	2.05915901	1.65E-10	B
TNFRSF10A	2.44E-10	2.05409481	5.77E-06	B
CLECL1	3.18E-09	2.01705129	7.53E-05	B
GSC	5.54E-103	9.65520394	1.31E-98	CAFs
CCL11	5.07E-20	8.57455611	1.20E-15	CAFs
PRRX2	4.22E-123	8.5448408	1.00E-118	CAFs
ANKRD2	9.33E-58	8.45497963	2.21E-53	CAFs
PTGER1	4.39E-85	8.41742896	1.04E-80	CAFs
COMP	1.51E-42	8.24290151	3.58E-38	CAFs
MIR2355	9.48E-11	8.11649823	2.24E-06	CAFs
OR4X2	9.48E-11	8.05082869	2.24E-06	CAFs
MIR4485	9.48E-11	7.96957763	2.24E-06	CAFs
TMEM35	7.42E-42	7.92738297	1.76E-37	CAFs
SNORD114-18	9.48E-11	7.8772567	2.24E-06	CAFs
MXRA5	1.91E-118	7.87169152	4.53E-114	CAFs
SNORD114-13	9.48E-11	7.86633915	2.24E-06	CAFs
TCEAL7	5.64E-119	7.85858409	1.34E-114	CAFs
CREB3L1	4.47E-191	7.83351431	1.06E-186	CAFs

FIBIN	5.28E-54	7.82340928	1.25E-49	CAFs
ISLR	2.00E-211	7.753744	4.73E-207	CAFs
TWIST2	5.10E-110	7.62439733	1.21E-105	CAFs
MIR1245B	9.48E-11	7.51468487	2.24E-06	CAFs
COL3A1	6.34E-219	7.46787778	1.50E-214	CAFs
SFRP2	9.51E-76	7.45497032	2.25E-71	CAFs
LOC100507632	4.95E-22	7.44973028	1.17E-17	CAFs
PSG5	3.76E-101	7.37065714	8.92E-97	CAFs
CRLF1	1.10E-48	7.3654633	2.61E-44	CAFs
PODN	3.55E-161	7.3306973	8.41E-157	CAFs
MIR4435-2	9.48E-11	7.32105319	2.24E-06	CAFs
ITGA11	1.96E-146	7.30479163	4.65E-142	CAFs
DPT	3.92E-68	7.30149907	9.29E-64	CAFs
PDGFRA	2.79E-247	7.27855385	6.61E-243	CAFs
MIR3916	9.48E-11	7.19172575	2.24E-06	CAFs
CPZ	2.57E-70	7.17849019	6.08E-66	CAFs
MIR103B2	9.48E-11	7.1778554	2.24E-06	CAFs
PAMR1	1.48E-103	7.17311183	3.50E-99	CAFs
DKK2	2.79E-19	7.1672348	6.61E-15	CAFs
FMO1	8.84E-33	7.16397073	2.09E-28	CAFs
ADH1B	5.45E-10	7.12419871	1.29E-05	CAFs
MIR3689E	9.48E-11	7.1138068	2.24E-06	CAFs
MXRA8	1.57E-254	7.09748184	3.71E-250	CAFs
MIR329-2	9.48E-11	7.09720556	2.24E-06	CAFs
COL1A1	3.49E-180	7.09341896	8.27E-176	CAFs
FNDC1	5.32E-89	7.08517135	1.26E-84	CAFs
LUM	8.62E-214	7.07652373	2.04E-209	CAFs
ACTL9	9.48E-11	7.05575759	2.24E-06	CAFs
PKDCC	4.35E-58	7.03062221	1.03E-53	CAFs
COL5A1	3.17E-212	7.00538149	7.51E-208	CAFs
FGF16	9.48E-11	6.98506374	2.24E-06	CAFs
HTRA3	4.90E-115	6.94392461	1.16E-110	CAFs
FGF7	3.43E-174	6.87803632	8.12E-170	CAFs
CXCL6	1.38E-13	6.87338215	3.26E-09	CAFs
MEG8	5.07E-20	6.87133924	1.20E-15	CAFs
GJB2	9.75E-40	6.86913097	2.31E-35	CAFs
BICC1	3.14E-90	6.8258579	7.43E-86	CAFs
MIR637	9.48E-11	6.80573415	2.24E-06	CAFs
RGMA	3.45E-44	6.80146814	8.17E-40	CAFs
HOXA9	5.70E-107	6.794699	1.35E-102	CAFs
MGARP	5.55E-63	6.7944535	1.32E-58	CAFs

GREM1	4.44E-104	6.77604987	1.05E-99	CAFs
DCN	4.12E-222	6.7733251	9.76E-218	CAFs
AADAC	9.48E-11	6.7629769	2.24E-06	CAFs
SFRP4	7.22E-63	6.76284465	1.71E-58	CAFs
SCARA5	6.97E-37	6.73982752	1.65E-32	CAFs
PCSK9	8.29E-31	6.72785752	1.96E-26	CAFs
EN1	6.42E-34	6.70755665	1.52E-29	CAFs
HAS1	1.43E-66	6.69636231	3.38E-62	CAFs
CCL26	1.30E-48	6.66863898	3.09E-44	CAFs
FOXS1	5.13E-22	6.65656488	1.22E-17	CAFs
LGR5	9.51E-42	6.64260546	2.25E-37	CAFs
CD248	1.76E-208	6.61809037	4.17E-204	CAFs
KRTAP2-4	9.48E-11	6.61281218	2.24E-06	CAFs
AOX1	1.52E-111	6.5893535	3.59E-107	CAFs
CILP	1.63E-46	6.58483596	3.87E-42	CAFs
ITGA8	3.84E-70	6.57465775	9.10E-66	CAFs
MMP1	1.61E-94	6.57406363	3.82E-90	CAFs
C4orf22	4.77E-22	6.56496621	1.13E-17	CAFs
OR4K13	9.48E-11	6.56082783	2.24E-06	CAFs
IGF2	2.09E-87	6.53723478	4.96E-83	CAFs
TMEM100	1.77E-30	6.46400714	4.20E-26	CAFs
COL14A1	5.80E-76	6.45446288	1.37E-71	CAFs
NID2	6.14E-116	6.43097077	1.46E-111	CAFs
LOC100130301	9.48E-11	6.41125491	2.24E-06	CAFs
WT1	2.42E-10	6.40910175	5.74E-06	CAFs
PENK	1.07E-17	6.37954854	2.55E-13	CAFs
TPD52L3	9.48E-11	6.37485313	2.24E-06	CAFs
CXCL12	5.27E-195	6.37086165	1.25E-190	CAFs
RERGL	9.48E-11	6.36640648	2.24E-06	CAFs
SH2D5	5.13E-22	6.35990381	1.22E-17	CAFs
CXCL14	8.94E-58	6.33177463	2.12E-53	CAFs
WFDC10B	9.48E-11	6.3250411	2.24E-06	CAFs
MFAP4	9.84E-97	6.3148785	2.33E-92	CAFs
LOC100505718	1.75E-42	6.30232169	4.15E-38	CAFs
SULF1	8.80E-138	6.29625777	2.08E-133	CAFs
KRT34	9.35E-87	6.29285314	2.21E-82	CAFs
CLEC3B	5.44E-33	6.28927477	1.29E-28	CAFs
ABI3BP	9.24E-166	6.28483423	2.19E-161	CAFs
CDH11	1.46E-183	6.281014	3.45E-179	CAFs
CRABP2	2.05E-101	6.25037866	4.85E-97	CAFs
DEFB103B	9.48E-11	6.24244756	2.24E-06	CAFs

GPC6-AS2	9.48E-11	6.23387269	2.24E-06	CAFs
EGFR	4.64E-119	6.18272693	1.10E-114	CAFs
GPC3	1.59E-27	6.1665313	3.76E-23	CAFs
KCNT2	3.95E-35	6.12754085	9.37E-31	CAFs
FAM101A	9.48E-11	6.10855794	2.24E-06	CAFs
IFNE	5.07E-20	6.10538573	1.20E-15	CAFs
PSG9	1.38E-13	6.10228127	3.26E-09	CAFs
PDGFRL	3.49E-65	6.09550217	8.27E-61	CAFs
COL13A1	2.31E-90	6.09226996	5.48E-86	CAFs
ASPN	1.88E-41	6.08252299	4.46E-37	CAFs
F10	1.71E-42	6.05698661	4.04E-38	CAFs
ROR2	1.56E-57	6.05403131	3.70E-53	CAFs
XPNPEP2	9.08E-59	6.04797456	2.15E-54	CAFs
DMRTA2	9.48E-11	6.04262562	2.24E-06	CAFs
HSD11B1	9.42E-43	6.02941864	2.23E-38	CAFs
SYNGR4	9.48E-11	6.02544876	2.24E-06	CAFs
SMOC2	6.86E-53	6.02396062	1.62E-48	CAFs
CYP1B1	3.43E-184	6.02235462	8.11E-180	CAFs
NGF	2.43E-83	6.01378786	5.75E-79	CAFs
PRG4	2.48E-21	6.01377682	5.87E-17	CAFs
CYP4F24P	3.00E-19	5.99487948	7.11E-15	CAFs
SLC8A2	1.42E-13	5.98792507	3.37E-09	CAFs
NLRP10	5.13E-22	5.98082301	1.22E-17	CAFs
ELN	4.01E-129	5.96995234	9.50E-125	CAFs
HGF	1.27E-41	5.96429729	3.01E-37	CAFs
DKK1	7.34E-104	5.94756852	1.74E-99	CAFs
KISS1	9.48E-11	5.92578414	2.24E-06	CAFs
KRT31	9.48E-11	5.91770866	2.24E-06	CAFs
PLA2G2A	3.82E-68	5.91632072	9.05E-64	CAFs
FBLN2	3.37E-149	5.91470668	7.99E-145	CAFs
WNT2	2.08E-30	5.9081849	4.92E-26	CAFs
OSR1	7.51E-93	5.88019642	1.78E-88	CAFs
PI16	4.10E-44	5.87412757	9.70E-40	CAFs
LRRC15	1.86E-29	5.86950943	4.42E-25	CAFs
OR2A14	9.48E-11	5.85099679	2.24E-06	CAFs
ADAM12	9.82E-114	5.83785025	2.33E-109	CAFs
SMTNL2	9.48E-11	5.82994455	2.24E-06	CAFs
INA	6.50E-58	5.82887431	1.54E-53	CAFs
PLAU	9.62E-92	5.81820702	2.28E-87	CAFs
KRTAP10-7	9.48E-11	5.81792257	2.24E-06	CAFs
FAM26E	6.97E-54	5.81651266	1.65E-49	CAFs

NXPE4	9.48E-11	5.8103098	2.24E-06	CAFs
ACAN	5.13E-54	5.80707821	1.22E-49	CAFs
COL6A3	6.33E-142	5.80343542	1.50E-137	CAFs
CNTN3	2.53E-22	5.79470925	5.99E-18	CAFs
EBF2	3.02E-132	5.79150675	7.16E-128	CAFs
CYP11A1	1.11E-17	5.79037902	2.62E-13	CAFs
CPXM1	1.14E-61	5.7849471	2.70E-57	CAFs
KRTAP1-5	6.99E-62	5.76472505	1.65E-57	CAFs
FOXG1	1.84E-21	5.76369829	4.35E-17	CAFs
MN1	8.97E-96	5.74764605	2.12E-91	CAFs
RBMXL2	9.48E-11	5.74581724	2.24E-06	CAFs
PID1	3.65E-60	5.7426134	8.63E-56	CAFs
CAMK2N2	9.48E-11	5.72791323	2.24E-06	CAFs
SLIT2	3.15E-79	5.71588061	7.46E-75	CAFs
DACT1	8.35E-46	5.71260015	1.98E-41	CAFs
KRT7	4.80E-24	5.70472633	1.14E-19	CAFs
SRPX2	9.34E-103	5.69683562	2.21E-98	CAFs
MRGPRF	1.84E-118	5.68330391	4.37E-114	CAFs
SSTR1	3.31E-19	5.67039048	7.83E-15	CAFs
LOX	1.78E-119	5.66769312	4.22E-115	CAFs
GGT5	1.61E-100	5.66605963	3.82E-96	CAFs
STC2	3.90E-66	5.66466756	9.23E-62	CAFs
BDKRB1	1.24E-55	5.66020276	2.94E-51	CAFs
CACNA2D1	4.25E-88	5.65628175	1.01E-83	CAFs
FBN1	1.99E-121	5.64895718	4.72E-117	CAFs
CDR1	5.90E-115	5.63702793	1.40E-110	CAFs
HHIP	1.00E-85	5.63110729	2.37E-81	CAFs
CCDC74B	3.59E-11	5.62226315	8.50E-07	CAFs
TNFRSF11B	3.32E-57	5.61689894	7.86E-53	CAFs
INHBA	4.03E-127	5.58866966	9.55E-123	CAFs
SERTAD4	1.08E-68	5.58395256	2.56E-64	CAFs
HHIP-AS1	2.13E-42	5.57659822	5.04E-38	CAFs
COL8A1	8.33E-98	5.55985865	1.97E-93	CAFs
TBX15	2.91E-91	5.55978807	6.88E-87	CAFs
TNNT3	2.01E-15	5.55708597	4.77E-11	CAFs
CFHR1	9.08E-35	5.54833893	2.15E-30	CAFs
GPR133	2.84E-39	5.54188204	6.73E-35	CAFs
GPC6	5.47E-83	5.53918487	1.30E-78	CAFs
TMEM47	3.46E-82	5.5131837	8.19E-78	CAFs
ITGBL1	7.38E-86	5.5117523	1.75E-81	CAFs
LPAR1	4.26E-120	5.48902694	1.01E-115	CAFs

HSPB6	3.61E-131	5.48704408	8.56E-127	CAFs
ADAMTSL1	7.61E-125	5.48579115	1.80E-120	CAFs
C5orf46	1.35E-25	5.47725948	3.19E-21	CAFs
BDKRB2	3.52E-48	5.4647538	8.33E-44	CAFs
SCARA3	1.19E-70	5.46433541	2.83E-66	CAFs
IGFBP6	8.19E-120	5.45926213	1.94E-115	CAFs
FMO2	4.79E-13	5.45838765	1.14E-08	CAFs
CLGN	1.61E-42	5.45828861	3.82E-38	CAFs
C11orf52	3.46E-11	5.44185073	8.20E-07	CAFs
PPAPDC1A	1.15E-57	5.44031487	2.73E-53	CAFs
KRT222	5.54E-10	5.43277996	1.31E-05	CAFs
CCDC80	1.54E-128	5.41707827	3.66E-124	CAFs
CA12	4.79E-55	5.41040719	1.13E-50	CAFs
PDGFRB	5.90E-108	5.40859705	1.40E-103	CAFs
TENM3	1.38E-97	5.39408634	3.26E-93	CAFs
MAGI1-AS1	2.48E-10	5.39371563	5.88E-06	CAFs
AMPH	6.45E-46	5.3916963	1.53E-41	CAFs
CHRD	5.37E-16	5.38690002	1.27E-11	CAFs
THY1	5.23E-142	5.38534105	1.24E-137	CAFs
C1S	8.22E-111	5.38374328	1.95E-106	CAFs
HGD	1.47E-13	5.37936083	3.49E-09	CAFs
ESM1	1.59E-39	5.37685701	3.77E-35	CAFs
LTBP2	3.58E-78	5.37270429	8.48E-74	CAFs
PLAC9	1.24E-158	5.3677031	2.93E-154	CAFs
ZFHX4-AS1	8.70E-15	5.35877462	2.06E-10	CAFs
ADAMTS15	1.28E-17	5.35560872	3.03E-13	CAFs
ADAMTS5	8.87E-21	5.35516332	2.10E-16	CAFs
MEIS3	4.62E-55	5.35288577	1.09E-50	CAFs
OLFML2B	2.99E-77	5.35049	7.08E-73	CAFs
MMP2	1.53E-117	5.32605629	3.63E-113	CAFs
BGN	6.00E-124	5.32245569	1.42E-119	CAFs
DACT3	3.39E-19	5.32133785	8.02E-15	CAFs
CCIN	2.60E-26	5.3212951	6.17E-22	CAFs
ALPL	4.77E-61	5.31506005	1.13E-56	CAFs
H19	1.90E-35	5.3079851	4.51E-31	CAFs
GALNT16	1.14E-19	5.30114747	2.71E-15	CAFs
LOXL1	4.29E-87	5.29826904	1.02E-82	CAFs
DNM3OS	1.86E-69	5.29787167	4.42E-65	CAFs
PCDH18	2.03E-90	5.26339204	4.80E-86	CAFs
MRC2	1.96E-96	5.26244916	4.63E-92	CAFs
DACT2	1.03E-12	5.25967687	2.44E-08	CAFs

FOXF1	4.58E-38	5.25778207	1.09E-33	CAFs
THBS2	7.51E-112	5.25723192	1.78E-107	CAFs
GLI2	1.66E-84	5.25571146	3.94E-80	CAFs
MASP1	9.95E-34	5.24720537	2.36E-29	CAFs
SVEP1	2.00E-54	5.24212042	4.74E-50	CAFs
LOC389033	1.35E-25	5.23851192	3.19E-21	CAFs
C3	2.64E-43	5.23343002	6.25E-39	CAFs
COL1A2	1.09E-97	5.19990204	2.59E-93	CAFs
WISP1	2.19E-52	5.19976863	5.19E-48	CAFs
VEGFC	1.30E-61	5.19564273	3.08E-57	CAFs
MEDAG	2.61E-105	5.19164238	6.18E-101	CAFs
PCOLCE2	1.54E-47	5.18765356	3.65E-43	CAFs
CNN1	5.40E-54	5.16863211	1.28E-49	CAFs
RARRES2	7.03E-53	5.1309293	1.67E-48	CAFs
MYOCD	3.96E-25	5.12126796	9.38E-21	CAFs
COLEC12	4.49E-32	5.09657333	1.06E-27	CAFs
KRT33B	2.48E-10	5.07736696	5.88E-06	CAFs
LOC339524	6.30E-18	5.07409093	1.49E-13	CAFs
LRRC17	1.51E-22	5.07253111	3.58E-18	CAFs
SERTAD4-AS1	1.41E-46	5.07050142	3.34E-42	CAFs
SCUBE3	1.65E-36	5.0610459	3.90E-32	CAFs
TMEM37	5.90E-10	5.05305041	1.40E-05	CAFs
DNM1	7.11E-23	5.05034063	1.68E-18	CAFs
LYPD6B	9.28E-34	5.04985291	2.20E-29	CAFs
NOTCH3	2.27E-119	5.04832806	5.37E-115	CAFs
FAM180A	3.22E-34	5.04495267	7.63E-30	CAFs
HOXD11	2.54E-10	5.0403731	6.03E-06	CAFs
CACNB4	4.09E-49	5.02588289	9.69E-45	CAFs
CHRDL1	2.11E-15	5.01431344	5.01E-11	CAFs
NTN4	2.34E-64	5.00834983	5.53E-60	CAFs
KRT19	2.64E-38	5.00036146	6.25E-34	CAFs
DGKI	1.85E-61	4.99796904	4.39E-57	CAFs
SERPINB7	6.18E-22	4.98658766	1.46E-17	CAFs
MDFI	1.04E-16	4.97655189	2.46E-12	CAFs
TMEM233	8.07E-37	4.97149116	1.91E-32	CAFs
HTRA1	1.62E-84	4.95045179	3.83E-80	CAFs
P4HA3	2.71E-55	4.94673323	6.43E-51	CAFs
GPR176	4.03E-74	4.93152245	9.54E-70	CAFs
WISP2	1.51E-39	4.91895822	3.58E-35	CAFs
PTGFR	1.35E-39	4.91740824	3.19E-35	CAFs
FNDC4	1.46E-52	4.90189359	3.45E-48	CAFs

SORCS2	4.15E-10	4.90046881	9.84E-06	CAFs
KRTAP2-3	1.13E-46	4.88742658	2.68E-42	CAFs
SERPINF1	3.28E-73	4.88721173	7.77E-69	CAFs
ADRA2C	8.92E-15	4.87815854	2.11E-10	CAFs
RARRES1	4.95E-25	4.87247198	1.17E-20	CAFs
FST	1.45E-56	4.87125621	3.44E-52	CAFs
LIN7A	1.36E-23	4.85997972	3.22E-19	CAFs
BOC	3.10E-31	4.85466367	7.35E-27	CAFs
THBS4	3.77E-10	4.84594746	8.93E-06	CAFs
HMSD	1.42E-29	4.84257459	3.36E-25	CAFs
COL5A2	1.10E-80	4.83907165	2.60E-76	CAFs
NTM	7.04E-67	4.83644055	1.67E-62	CAFs
OR10A2	2.54E-10	4.8316382	6.03E-06	CAFs
HSPB7	1.65E-77	4.82156031	3.90E-73	CAFs
PRRX1	3.33E-116	4.81916407	7.90E-112	CAFs
DENND2A	4.14E-18	4.8020054	9.82E-14	CAFs
ADAMTS12	1.93E-50	4.79702447	4.57E-46	CAFs
TNXB	1.07E-56	4.79053185	2.53E-52	CAFs
PITX2	8.56E-17	4.77824162	2.03E-12	CAFs
ABCA8	1.63E-33	4.77700896	3.85E-29	CAFs
GRB14	1.45E-26	4.76789371	3.43E-22	CAFs
OPCML	9.48E-14	4.7652444	2.25E-09	CAFs
GPR64	4.61E-11	4.7629915	1.09E-06	CAFs
SLC16A2	2.24E-87	4.73876369	5.31E-83	CAFs
EFEMP1	5.70E-110	4.73521313	1.35E-105	CAFs
CSMD2	1.31E-12	4.73269374	3.11E-08	CAFs
SPOCD1	1.02E-76	4.73126487	2.42E-72	CAFs
CDH13	1.38E-50	4.72517964	3.27E-46	CAFs
APCDD1L-AS1	5.89E-14	4.72343476	1.40E-09	CAFs
KCNK2	4.50E-40	4.72080428	1.07E-35	CAFs
GLT8D2	2.11E-56	4.71103007	5.00E-52	CAFs
TNFAIP6	6.07E-41	4.7092206	1.44E-36	CAFs
MMP19	8.07E-44	4.69153379	1.91E-39	CAFs
CAP2	2.50E-57	4.69055999	5.91E-53	CAFs
PTX3	7.82E-50	4.68330701	1.85E-45	CAFs
PRSS3	3.19E-36	4.67743994	7.56E-32	CAFs
SPOCK1	1.36E-72	4.67037333	3.22E-68	CAFs
CLMP	5.70E-42	4.6627329	1.35E-37	CAFs
FMOD	1.51E-74	4.66222886	3.57E-70	CAFs
COL11A1	1.15E-44	4.65383629	2.73E-40	CAFs
GREM2	2.45E-29	4.64442322	5.81E-25	CAFs

MIR31HG	1.84E-39	4.64219423	4.37E-35	CAFs
EML1	4.39E-56	4.63633097	1.04E-51	CAFs
C14orf37	3.85E-31	4.63270836	9.13E-27	CAFs
PTN	7.47E-57	4.62331412	1.77E-52	CAFs
LOC152742	5.33E-25	4.61561078	1.26E-20	CAFs
OGN	6.12E-32	4.61431966	1.45E-27	CAFs
FLNC	7.94E-80	4.61060739	1.88E-75	CAFs
FOXC2	1.47E-13	4.6060357	3.49E-09	CAFs
SMO	3.40E-14	4.60231687	8.06E-10	CAFs
GFRA1	3.86E-36	4.59593451	9.14E-32	CAFs
SPEG	1.15E-32	4.59249779	2.73E-28	CAFs
TFPI2	1.25E-44	4.59056953	2.96E-40	CAFs
KCNJ15	2.97E-30	4.58900374	7.05E-26	CAFs
PTHLH	2.11E-23	4.58839643	4.99E-19	CAFs
VIT	8.62E-43	4.57645806	2.04E-38	CAFs
LMX1A	2.39E-15	4.57363291	5.67E-11	CAFs
RUNX1T1	2.58E-60	4.57034648	6.11E-56	CAFs
Mar-04	9.14E-38	4.56912875	2.16E-33	CAFs
EMILIN1	1.59E-73	4.55740875	3.76E-69	CAFs
ANO1	2.17E-14	4.55265345	5.15E-10	CAFs
LRRC32	2.37E-72	4.5408599	5.62E-68	CAFs
SMAD6	9.53E-13	4.53131727	2.26E-08	CAFs
SH3RF2	2.97E-28	4.52404687	7.05E-24	CAFs
KAZALD1	1.21E-27	4.52365598	2.87E-23	CAFs
FAM20C	2.77E-48	4.51175359	6.57E-44	CAFs
ANGPTL2	8.39E-60	4.51016072	1.99E-55	CAFs
HOXC8	9.59E-35	4.50824891	2.27E-30	CAFs
NXPH4	9.82E-15	4.50671605	2.33E-10	CAFs
VCAN	3.51E-77	4.4896398	8.32E-73	CAFs
GNB3	1.35E-14	4.48914279	3.19E-10	CAFs
EBF3	5.31E-26	4.48837237	1.26E-21	CAFs
KRT33A	6.71E-22	4.48674643	1.59E-17	CAFs
CKB	1.62E-58	4.47252431	3.83E-54	CAFs
TAGLN	7.73E-71	4.46811428	1.83E-66	CAFs
RFX8	8.48E-35	4.46333122	2.01E-30	CAFs
DOK5	2.72E-62	4.46247645	6.45E-58	CAFs
MATN3	4.63E-18	4.45110881	1.10E-13	CAFs
SLC1A7	1.12E-12	4.45003667	2.65E-08	CAFs
GABRE	4.77E-27	4.44784678	1.13E-22	CAFs
BMPER	6.52E-37	4.44705622	1.54E-32	CAFs
PXDN	2.49E-88	4.43370324	5.89E-84	CAFs

NOVA1	6.96E-24	4.43207449	1.65E-19	CAFs
LARP6	2.05E-62	4.42721579	4.86E-58	CAFs
CFH	8.86E-67	4.42123714	2.10E-62	CAFs
PALM	6.67E-28	4.41843183	1.58E-23	CAFs
CACNA1C	5.69E-42	4.41530135	1.35E-37	CAFs
MEG3	9.63E-25	4.40859658	2.28E-20	CAFs
PALM2-AKAP2	9.23E-13	4.40506115	2.19E-08	CAFs
C1R	7.95E-64	4.40484177	1.88E-59	CAFs
NYNRIN	2.41E-38	4.40116722	5.71E-34	CAFs
C3orf55	5.33E-27	4.39574913	1.26E-22	CAFs
POSTN	1.73E-51	4.38210776	4.10E-47	CAFs
PAPSS2	3.35E-54	4.37931219	7.93E-50	CAFs
KCNJ8	5.56E-28	4.37528881	1.32E-23	CAFs
FXYD1	4.36E-11	4.3719248	1.03E-06	CAFs
A4GALT	2.28E-41	4.37017	5.40E-37	CAFs
ANPEP	1.17E-75	4.35623853	2.78E-71	CAFs
GPR39	9.36E-15	4.3476709	2.22E-10	CAFs
COL6A2	3.16E-82	4.34550699	7.49E-78	CAFs
HEPH	4.86E-26	4.34547178	1.15E-21	CAFs
PPFIA2	8.36E-19	4.34100676	1.98E-14	CAFs
TMEM176A	1.71E-35	4.33414635	4.05E-31	CAFs
NRXN2	1.87E-26	4.33063023	4.44E-22	CAFs
LOC100505633	7.92E-35	4.32467032	1.88E-30	CAFs
PPAP2B	2.73E-83	4.30195641	6.47E-79	CAFs
BMP4	3.58E-10	4.29954575	8.47E-06	CAFs
AKR1C1	6.24E-50	4.29354353	1.48E-45	CAFs
ADRA2A	1.52E-30	4.27880439	3.60E-26	CAFs
LTBP1	4.84E-43	4.27799582	1.15E-38	CAFs
HOXA7	8.34E-31	4.27376564	1.98E-26	CAFs
SFN	5.01E-17	4.2728717	1.19E-12	CAFs
ARHGAP22	1.56E-44	4.24922708	3.68E-40	CAFs
SLIT3	9.81E-30	4.24751797	2.32E-25	CAFs
ECM2	2.21E-24	4.24375291	5.22E-20	CAFs
AK5	5.17E-53	4.24059775	1.22E-48	CAFs
FBLN5	2.28E-80	4.23636234	5.40E-76	CAFs
NLGN2	1.50E-21	4.23046774	3.56E-17	CAFs
PTPRD	3.73E-19	4.22498897	8.83E-15	CAFs
MYL9	2.16E-82	4.2230799	5.11E-78	CAFs
GATA6	5.50E-46	4.22138157	1.30E-41	CAFs
PDGFC	3.92E-53	4.21379648	9.28E-49	CAFs
PRR16	9.74E-32	4.21192367	2.31E-27	CAFs

FLRT2	4.39E-76	4.20035069	1.04E-71	CAFs
FAM71A	2.68E-12	4.19914286	6.36E-08	CAFs
MIR100HG	3.44E-48	4.19321503	8.14E-44	CAFs
TPBG	1.63E-74	4.18822179	3.86E-70	CAFs
NPR3	3.00E-47	4.18804746	7.11E-43	CAFs
CACNA1A	6.91E-13	4.17824433	1.64E-08	CAFs
TRPC4	8.56E-17	4.17445071	2.03E-12	CAFs
CCDC74A	2.49E-37	4.16813668	5.90E-33	CAFs
GFPT2	6.41E-40	4.16516036	1.52E-35	CAFs
LOC100134259	2.41E-26	4.16298186	5.70E-22	CAFs
TMEM200A	1.05E-58	4.15735594	2.50E-54	CAFs
RGAG4	9.21E-12	4.14632824	2.18E-07	CAFs
SDC1	5.81E-62	4.14112686	1.38E-57	CAFs
EDNRA	7.82E-44	4.13648197	1.85E-39	CAFs
DDAH1	2.74E-57	4.13054446	6.50E-53	CAFs
ADAM33	2.23E-19	4.12471462	5.29E-15	CAFs
ZNF295-AS1	3.32E-26	4.12050722	7.86E-22	CAFs
AGTR1	2.61E-10	4.11700632	6.18E-06	CAFs
TNXA	3.64E-10	4.11485699	8.62E-06	CAFs
DCLK1	2.52E-59	4.10958738	5.98E-55	CAFs
HSPB2	1.33E-46	4.09306261	3.16E-42	CAFs
RIMS1	2.20E-17	4.08390979	5.20E-13	CAFs
B3GNT8	1.55E-16	4.0833108	3.67E-12	CAFs
LOC401164	9.21E-12	4.07907028	2.18E-07	CAFs
ADAMTS2	2.83E-31	4.06690098	6.71E-27	CAFs
CPE	2.59E-49	4.06446385	6.14E-45	CAFs
GLIS2	1.11E-22	4.06156152	2.62E-18	CAFs
AWAT2	2.61E-10	4.05553711	6.18E-06	CAFs
ANKRD1	3.28E-30	4.0551201	7.78E-26	CAFs
ZNF804A	1.00E-13	4.04360053	2.38E-09	CAFs
SPON1	9.23E-33	4.04086589	2.19E-28	CAFs
CCL2	3.98E-58	4.03911431	9.44E-54	CAFs
IGDCC4	1.08E-16	4.02790589	2.56E-12	CAFs
IGFBP5	1.39E-55	4.02325882	3.30E-51	CAFs
MEOX2	1.12E-34	4.0208827	2.66E-30	CAFs
LCE2A	5.07E-18	4.01759063	1.20E-13	CAFs
PDE1C	1.53E-16	4.01654184	3.62E-12	CAFs
PRR15	8.86E-14	4.01633102	2.10E-09	CAFs
ZFHX4	7.76E-54	4.01462854	1.84E-49	CAFs
TBX5	6.39E-13	4.01280578	1.51E-08	CAFs
CYGB	7.44E-56	4.00216046	1.76E-51	CAFs

FMN2	4.78E-21	3.99922886	1.13E-16	CAFs
BEND6	1.69E-16	3.99443433	3.99E-12	CAFs
PBX1	2.69E-57	3.99300401	6.37E-53	CAFs
KCND2	2.84E-29	3.9926031	6.74E-25	CAFs
MFSD7	1.04E-20	3.9834139	2.47E-16	CAFs
TNS1	2.59E-68	3.98062973	6.13E-64	CAFs
ARHGAP6	1.99E-30	3.97706494	4.70E-26	CAFs
PPIC	3.72E-67	3.97402234	8.80E-63	CAFs
MGC45800	1.52E-23	3.96354563	3.60E-19	CAFs
OXTR	2.42E-09	3.96158127	5.73E-05	CAFs
GPC4	1.69E-24	3.95296178	3.99E-20	CAFs
FHL1	6.53E-64	3.94932571	1.55E-59	CAFs
CDC42EP2	1.24E-46	3.94309761	2.94E-42	CAFs
LINC00312	3.97E-12	3.94182813	9.41E-08	CAFs
IGFBP4	6.49E-69	3.94149173	1.54E-64	CAFs
HAS2-AS1	4.77E-23	3.9361746	1.13E-18	CAFs
ACE	6.66E-20	3.93319089	1.58E-15	CAFs
MAP1A	1.52E-49	3.92529824	3.59E-45	CAFs
ZNF423	1.58E-12	3.9246171	3.73E-08	CAFs
THBS1	2.21E-56	3.91362169	5.24E-52	CAFs
THSD4	3.46E-37	3.90300727	8.19E-33	CAFs
PEAR1	6.01E-48	3.90225942	1.42E-43	CAFs
FGF14	6.41E-15	3.90210523	1.52E-10	CAFs
MGST1	6.77E-80	3.89746525	1.60E-75	CAFs
FER1L5	1.17E-12	3.89173137	2.76E-08	CAFs
ADAMTS7	1.88E-34	3.89096426	4.45E-30	CAFs
PLEK2	1.81E-20	3.89092874	4.29E-16	CAFs
EFCAB3	1.44E-11	3.88663342	3.40E-07	CAFs
LRP3	4.79E-36	3.88655682	1.13E-31	CAFs
COL6A1	3.88E-51	3.88088712	9.20E-47	CAFs
NFATC4	1.89E-53	3.87722271	4.47E-49	CAFs
NFASC	9.64E-31	3.87586108	2.28E-26	CAFs
PDCD1LG2	1.48E-34	3.86816861	3.50E-30	CAFs
LOXL2	3.05E-55	3.86545788	7.23E-51	CAFs
EGFLAM	1.17E-26	3.86002306	2.78E-22	CAFs
HOXA-AS4	4.50E-13	3.85817325	1.07E-08	CAFs
FAM225B	2.41E-12	3.85604731	5.70E-08	CAFs
SSC5D	8.77E-55	3.85303203	2.08E-50	CAFs
PLXDC2	2.26E-33	3.85240269	5.36E-29	CAFs
LMOD1	3.65E-29	3.84808379	8.64E-25	CAFs
PPP1R3C	7.84E-36	3.841896	1.86E-31	CAFs

PTGIR	3.10E-54	3.84143295	7.35E-50	CAFs
EFEMP2	1.32E-50	3.84084769	3.12E-46	CAFs
PAPPA	1.18E-50	3.8402172	2.80E-46	CAFs
TPM2	1.25E-54	3.83827657	2.96E-50	CAFs
LPHN2	2.56E-36	3.82975729	6.06E-32	CAFs
NFIX	1.18E-41	3.81684661	2.80E-37	CAFs
CEACAM19	5.46E-17	3.80700805	1.29E-12	CAFs
LEPREL2	2.98E-42	3.80512371	7.07E-38	CAFs
PRPH2	4.31E-12	3.80400594	1.02E-07	CAFs
CFD	3.80E-17	3.79836889	8.99E-13	CAFs
PTGDS	8.68E-15	3.79655981	2.06E-10	CAFs
TSHZ3	9.41E-59	3.79164324	2.23E-54	CAFs
MMP28	3.77E-10	3.79057779	8.93E-06	CAFs
CXCR7	2.17E-14	3.78965213	5.15E-10	CAFs
PIP5KL1	4.70E-13	3.78874346	1.11E-08	CAFs
SLC35G2	7.36E-34	3.78737311	1.74E-29	CAFs
LOC100288911	9.71E-21	3.77996731	2.30E-16	CAFs
ANTXR1	7.72E-44	3.77869807	1.83E-39	CAFs
DPYSL3	9.27E-39	3.77644259	2.20E-34	CAFs
KRTAP2-1	2.74E-15	3.77575722	6.49E-11	CAFs
KIRREL3	5.45E-25	3.77539427	1.29E-20	CAFs
HAS2	1.28E-33	3.77275645	3.04E-29	CAFs
NRP1	1.05E-71	3.77274594	2.48E-67	CAFs
TICAM2	2.31E-31	3.77217773	5.47E-27	CAFs
EGFR-AS1	4.59E-12	3.76505172	1.09E-07	CAFs
LGR4	2.47E-17	3.73317211	5.85E-13	CAFs
ASAP3	4.02E-30	3.72917003	9.51E-26	CAFs
NRG1	9.92E-30	3.726492	2.35E-25	CAFs
H2AFY2	2.74E-44	3.72530315	6.50E-40	CAFs
SERPING1	1.00E-43	3.72059653	2.38E-39	CAFs
ACTC1	1.28E-14	3.71215203	3.03E-10	CAFs
RAB31	3.42E-63	3.70276258	8.10E-59	CAFs
KLHL35	2.21E-10	3.70231375	5.23E-06	CAFs
PCOLCE	1.35E-61	3.7004658	3.21E-57	CAFs
RAI2	2.29E-30	3.68493359	5.43E-26	CAFs
TGFB3	4.97E-23	3.68402903	1.18E-18	CAFs
LRRC8E	2.04E-13	3.68365665	4.83E-09	CAFs
AGT	6.68E-10	3.66785183	1.58E-05	CAFs
CRISPLD2	5.44E-14	3.66326855	1.29E-09	CAFs
HHIPL1	6.92E-25	3.65777792	1.64E-20	CAFs
TPPP3	1.14E-11	3.63595957	2.71E-07	CAFs

C1orf54	1.17E-38	3.63188991	2.78E-34	CAFs
GNG11	3.60E-61	3.62873055	8.53E-57	CAFs
SUSD2	1.15E-09	3.62815124	2.71E-05	CAFs
EDIL3	1.42E-16	3.62319	3.37E-12	CAFs
EDA2R	2.85E-21	3.62218058	6.75E-17	CAFs
FAM171B	3.91E-32	3.61607944	9.27E-28	CAFs
PINLYP	3.58E-09	3.61517591	8.49E-05	CAFs
FAM225A	2.03E-25	3.61098974	4.81E-21	CAFs
DKK3	1.80E-52	3.60912828	4.26E-48	CAFs
KCNK1	6.81E-10	3.60166075	1.61E-05	CAFs
FGF2	1.82E-18	3.6000518	4.32E-14	CAFs
HIC1	2.50E-30	3.57662443	5.93E-26	CAFs
CFB	1.92E-25	3.57546582	4.56E-21	CAFs
NUAK1	6.02E-40	3.5616511	1.43E-35	CAFs
GJA1	6.63E-49	3.55656725	1.57E-44	CAFs
FRMPD4	1.66E-14	3.55152097	3.93E-10	CAFs
SGMS2	4.01E-20	3.54872197	9.50E-16	CAFs
TMEM176B	3.21E-17	3.53965158	7.60E-13	CAFs
WNT5A	6.91E-43	3.52250914	1.64E-38	CAFs
IL6	5.75E-32	3.51991223	1.36E-27	CAFs
PRKG1	3.91E-28	3.51881008	9.26E-24	CAFs
CDR2L	2.21E-35	3.51774871	5.25E-31	CAFs
ATOH8	3.21E-27	3.51039044	7.61E-23	CAFs
PRUNE2	2.79E-32	3.5101515	6.60E-28	CAFs
CEP55	6.13E-13	3.50552347	1.45E-08	CAFs
ESCO2	5.29E-13	3.50440555	1.25E-08	CAFs
TBX5-AS1	2.48E-10	3.5020837	5.88E-06	CAFs
TFPI	1.04E-44	3.48941167	2.45E-40	CAFs
HAAO	4.83E-12	3.48901658	1.14E-07	CAFs
KCTD16	1.24E-13	3.48378721	2.93E-09	CAFs
BASP1	2.38E-42	3.48341427	5.64E-38	CAFs
ABCC3	1.65E-20	3.48222195	3.90E-16	CAFs
TGFBI	1.01E-43	3.47723399	2.39E-39	CAFs
LAMA2	2.17E-32	3.47353513	5.13E-28	CAFs
NEXN	2.97E-31	3.47343202	7.03E-27	CAFs
OLFM1	1.95E-14	3.46930566	4.63E-10	CAFs
PDPN	3.59E-14	3.46557335	8.50E-10	CAFs
NUDT11	1.26E-30	3.46302395	2.97E-26	CAFs
KITLG	2.53E-30	3.45611275	6.00E-26	CAFs
CHAC1	3.50E-11	3.43786621	8.29E-07	CAFs
NT5E	2.06E-46	3.43703085	4.88E-42	CAFs

MOXD1	4.24E-31	3.43351213	1.01E-26	CAFs
RAB3IL1	6.38E-14	3.4297707	1.51E-09	CAFs
TPM1	3.70E-43	3.42516627	8.77E-39	CAFs
COX7A1	1.04E-41	3.42442376	2.46E-37	CAFs
DSE	1.39E-33	3.42126753	3.30E-29	CAFs
NDUFA4L2	1.91E-16	3.41562679	4.53E-12	CAFs
HIST1H1A	3.54E-14	3.41419427	8.40E-10	CAFs
OLFML3	5.53E-53	3.40398313	1.31E-48	CAFs
FOXD4L3	7.26E-10	3.39837782	1.72E-05	CAFs
SNAP25	2.85E-15	3.38039328	6.74E-11	CAFs
FBLN1	1.40E-28	3.37902379	3.31E-24	CAFs
SCG5	1.87E-12	3.3783669	4.43E-08	CAFs
KIAA1199	1.13E-14	3.37377172	2.68E-10	CAFs
PROCR	2.65E-38	3.37155586	6.27E-34	CAFs
FZD1	5.25E-17	3.36571635	1.24E-12	CAFs
KIF26B	2.76E-15	3.36365135	6.53E-11	CAFs
BCAT1	1.37E-29	3.36114547	3.25E-25	CAFs
STEAP3	7.79E-27	3.35945721	1.84E-22	CAFs
MYOF	1.51E-36	3.3592483	3.59E-32	CAFs
PPARG	3.32E-19	3.34519587	7.87E-15	CAFs
VGLL3	5.73E-13	3.33605569	1.36E-08	CAFs
GPR124	1.76E-30	3.33337618	4.16E-26	CAFs
MAGED4B	5.92E-34	3.32493408	1.40E-29	CAFs
DIAPH3	3.26E-23	3.32313764	7.73E-19	CAFs
GAS6	1.81E-33	3.31632373	4.28E-29	CAFs
FAM110B	4.42E-39	3.30600645	1.05E-34	CAFs
RCN3	2.83E-50	3.29452912	6.71E-46	CAFs
NREP	5.56E-43	3.28816829	1.32E-38	CAFs
PVRL1	2.52E-19	3.28654809	5.96E-15	CAFs
TNFAIP2	6.41E-14	3.28597321	1.52E-09	CAFs
ELTD1	1.09E-31	3.28215412	2.58E-27	CAFs
KLHL13	1.39E-11	3.27446777	3.29E-07	CAFs
MAGED4	4.50E-33	3.27437674	1.07E-28	CAFs
TMEM171	1.47E-25	3.27128989	3.49E-21	CAFs
ANGPTL1	4.62E-13	3.26540979	1.09E-08	CAFs
SLC8A1	2.00E-26	3.26016355	4.74E-22	CAFs
AKR1C3	4.95E-42	3.24511938	1.17E-37	CAFs
COL5A3	5.27E-15	3.24296242	1.25E-10	CAFs
LURAP1L	1.13E-22	3.24273777	2.67E-18	CAFs
PRICKLE1	4.43E-35	3.23721302	1.05E-30	CAFs
ADAMTS1	4.31E-35	3.23472553	1.02E-30	CAFs

IL33	3.20E-10	3.22931512	7.59E-06	CAFs
MPP3	8.83E-27	3.22724465	2.09E-22	CAFs
LIMCH1	3.76E-21	3.21629067	8.91E-17	CAFs
FSIP1	3.62E-09	3.20668525	8.57E-05	CAFs
RNF217	5.63E-11	3.20442505	1.33E-06	CAFs
CDC42EP1	7.35E-30	3.20055394	1.74E-25	CAFs
CLIP3	4.44E-37	3.19337126	1.05E-32	CAFs
ZNF469	4.58E-21	3.19272535	1.09E-16	CAFs
CYR61	3.72E-36	3.19150541	8.82E-32	CAFs
TCEA3	9.72E-19	3.1900024	2.30E-14	CAFs
WNK4	3.02E-15	3.18815363	7.15E-11	CAFs
NEGR1	1.42E-25	3.17369919	3.35E-21	CAFs
WNT5B	7.00E-11	3.16537532	1.66E-06	CAFs
TGFB1I1	7.86E-31	3.15682323	1.86E-26	CAFs
TGFBR3L	1.73E-14	3.14718479	4.10E-10	CAFs
CDKN2B	2.03E-24	3.14325988	4.82E-20	CAFs
NEIL3	1.11E-13	3.14323648	2.64E-09	CAFs
SPATA18	1.91E-09	3.14189655	4.53E-05	CAFs
GALNT5	3.93E-18	3.13774781	9.31E-14	CAFs
TUSC3	2.65E-31	3.12500143	6.29E-27	CAFs
TEAD3	1.34E-25	3.12310956	3.17E-21	CAFs
PALLD	5.98E-29	3.12214661	1.42E-24	CAFs
SPC24	8.41E-16	3.12171408	1.99E-11	CAFs
IGF2BP1	6.39E-13	3.12129464	1.51E-08	CAFs
SDC2	6.82E-35	3.11571322	1.62E-30	CAFs
CAMK2N1	2.07E-24	3.10046408	4.91E-20	CAFs
TRIP10	7.02E-27	3.09682853	1.66E-22	CAFs
TMEM45A	1.45E-26	3.09553241	3.43E-22	CAFs
FLJ23867	2.61E-12	3.09458785	6.19E-08	CAFs
AMOTL2	3.59E-25	3.09200156	8.51E-21	CAFs
FOXL1	1.19E-12	3.08477785	2.82E-08	CAFs
C1QTNF5	9.25E-28	3.08413763	2.19E-23	CAFs
MFRP	9.25E-28	3.08413763	2.19E-23	CAFs
SGIP1	3.38E-29	3.06637473	8.01E-25	CAFs
DSCC1	1.66E-10	3.06442513	3.93E-06	CAFs
LRP1	8.62E-34	3.05262059	2.04E-29	CAFs
CORO6	8.01E-10	3.04951064	1.90E-05	CAFs
SOD3	1.13E-25	3.04527157	2.68E-21	CAFs
OMD	1.06E-14	3.04515723	2.52E-10	CAFs
PLAGL1	4.88E-49	3.03957676	1.16E-44	CAFs
EHD2	7.12E-26	3.03826805	1.69E-21	CAFs

E2F7	1.24E-15	3.035096	2.93E-11	CAFs
OLFML1	1.57E-13	3.03370353	3.72E-09	CAFs
LOC400456	4.15E-14	3.03275423	9.83E-10	CAFs
VASN	1.37E-29	3.02263791	3.25E-25	CAFs
FAP	2.05E-31	3.01744539	4.85E-27	CAFs
GLRB	1.98E-13	3.01384169	4.69E-09	CAFs
OAF	2.47E-18	3.01292646	5.84E-14	CAFs
COL4A2	6.22E-33	3.00938873	1.47E-28	CAFs
TNFRSF6B	3.14E-10	3.00904875	7.44E-06	CAFs
SH2D4A	1.69E-18	2.99956148	4.00E-14	CAFs
SH3D19	5.26E-32	2.9754257	1.24E-27	CAFs
COCH	5.21E-15	2.97500657	1.23E-10	CAFs
PPP1R14A	4.45E-12	2.9739532	1.05E-07	CAFs
BST1	1.19E-18	2.97375175	2.81E-14	CAFs
CTGF	5.78E-36	2.96885954	1.37E-31	CAFs
FAM13C	5.34E-13	2.96788713	1.26E-08	CAFs
FSTL1	4.55E-39	2.96468154	1.08E-34	CAFs
DOK4	2.71E-19	2.96419558	6.42E-15	CAFs
CNRIP1	1.07E-33	2.96318739	2.54E-29	CAFs
PLA2R1	2.56E-13	2.95949332	6.07E-09	CAFs
SULF2	4.03E-11	2.9537394	9.54E-07	CAFs
RFX2	1.75E-20	2.95071134	4.15E-16	CAFs
SH3PXD2B	1.82E-24	2.95056633	4.30E-20	CAFs
MFAP5	1.15E-13	2.94453875	2.72E-09	CAFs
ABCA6	6.08E-13	2.930239	1.44E-08	CAFs
UCHL1	6.55E-29	2.92897418	1.55E-24	CAFs
THSD1	7.49E-12	2.92824606	1.77E-07	CAFs
ITGA5	7.74E-44	2.91496831	1.83E-39	CAFs
MYO1B	4.25E-20	2.90571354	1.01E-15	CAFs
SOBP	5.49E-14	2.90467909	1.30E-09	CAFs
SHOX2	8.74E-22	2.90240194	2.07E-17	CAFs
SEC16B	7.27E-10	2.89561415	1.72E-05	CAFs
FAT4	7.45E-22	2.89450461	1.77E-17	CAFs
PTGS1	2.67E-26	2.88549192	6.33E-22	CAFs
FN1	2.90E-34	2.88301135	6.87E-30	CAFs
LEPREL1	1.30E-12	2.88033011	3.08E-08	CAFs
COL12A1	1.80E-29	2.87956852	4.27E-25	CAFs
NUPR1	8.99E-29	2.87804572	2.13E-24	CAFs
EPHB1	1.49E-20	2.87652859	3.54E-16	CAFs
BAG2	2.58E-25	2.87501487	6.11E-21	CAFs
BACE1	1.28E-27	2.85799332	3.03E-23	CAFs

CKAP4	7.59E-29	2.85781971	1.80E-24	CAFs
COPZ2	1.60E-15	2.85443573	3.80E-11	CAFs
FZD7	2.03E-19	2.85215652	4.80E-15	CAFs
MEST	5.59E-26	2.8363014	1.32E-21	CAFs
FAM198B	4.76E-13	2.83457634	1.13E-08	CAFs
LOC400043	2.84E-19	2.83260218	6.73E-15	CAFs
FOSL1	1.52E-19	2.82391387	3.60E-15	CAFs
KCTD11	9.56E-18	2.82175328	2.27E-13	CAFs
C1orf233	4.88E-11	2.82137821	1.16E-06	CAFs
DOCK1	5.91E-24	2.82080408	1.40E-19	CAFs
EFS	8.75E-13	2.82066694	2.07E-08	CAFs
IRS1	2.82E-19	2.81640518	6.69E-15	CAFs
THRB	1.68E-12	2.81441673	3.98E-08	CAFs
RHOD	7.88E-19	2.81368103	1.87E-14	CAFs
LMO7	2.28E-23	2.81196791	5.41E-19	CAFs
EDA	2.99E-11	2.80283705	7.09E-07	CAFs
IGFBP3	3.97E-24	2.79782269	9.41E-20	CAFs
TMCO3	2.71E-24	2.79363441	6.43E-20	CAFs
NPAS1	1.80E-09	2.78822447	4.27E-05	CAFs
SCARNA22	2.63E-10	2.78566677	6.24E-06	CAFs
DEPTOR	5.57E-20	2.76964126	1.32E-15	CAFs
STEAP1	4.22E-20	2.76883254	9.98E-16	CAFs
MGP	2.52E-15	2.76832144	5.97E-11	CAFs
MSC	2.01E-25	2.76793586	4.76E-21	CAFs
RAB23	7.36E-28	2.76793393	1.74E-23	CAFs
ANKRD35	2.38E-13	2.76547335	5.63E-09	CAFs
ARHGAP20	4.75E-13	2.76447955	1.12E-08	CAFs
ANGPT1	3.28E-09	2.76325425	7.77E-05	CAFs
SETD7	2.25E-26	2.76189325	5.32E-22	CAFs
MEIS3P1	7.31E-10	2.75813732	1.73E-05	CAFs
LIMS2	1.61E-30	2.75331442	3.81E-26	CAFs
CACNB3	1.86E-21	2.75323247	4.42E-17	CAFs
LXN	5.21E-18	2.74748463	1.23E-13	CAFs
GPX3	1.69E-14	2.7462346	4.00E-10	CAFs
PKMYT1	2.97E-10	2.74007416	7.03E-06	CAFs
PRTFDC1	4.88E-12	2.73907483	1.16E-07	CAFs
FSCN1	2.90E-27	2.73418743	6.86E-23	CAFs
EBF1	2.10E-21	2.72558948	4.98E-17	CAFs
SNED1	3.15E-14	2.72539635	7.46E-10	CAFs
CLEC11A	9.60E-24	2.72002774	2.27E-19	CAFs
ARMCX2	1.02E-24	2.71084039	2.41E-20	CAFs

RIN2	1.21E-22	2.71030779	2.86E-18	CAFs
ANLN	9.97E-17	2.70832612	2.36E-12	CAFs
TP53I11	6.43E-35	2.70719519	1.52E-30	CAFs
C11orf82	5.15E-11	2.7070039	1.22E-06	CAFs
EPB41L3	8.49E-13	2.70661355	2.01E-08	CAFs
MAGI1	1.41E-19	2.70594648	3.35E-15	CAFs
ME3	2.12E-12	2.70574598	5.01E-08	CAFs
HOXA10	4.79E-16	2.70221994	1.14E-11	CAFs
FILIP1L	4.21E-25	2.70187684	9.96E-21	CAFs
LMCD1	1.31E-22	2.69582878	3.10E-18	CAFs
SH3RF1	7.12E-17	2.68985033	1.69E-12	CAFs
NMNAT2	5.34E-13	2.68829579	1.26E-08	CAFs
KDELC1	2.02E-16	2.68824889	4.78E-12	CAFs
SLC1A3	1.22E-15	2.68721	2.88E-11	CAFs
PHLDB2	1.25E-27	2.68654056	2.97E-23	CAFs
LIFR	6.41E-10	2.68472597	1.52E-05	CAFs
SH3PXD2A	1.62E-16	2.67976204	3.84E-12	CAFs
SHANK2	3.74E-14	2.67731267	8.86E-10	CAFs
ARHGAP28	1.36E-09	2.67520603	3.22E-05	CAFs
EMX2	6.38E-12	2.67357485	1.51E-07	CAFs
MGLL	5.93E-19	2.66900719	1.41E-14	CAFs
FAM171A1	4.86E-34	2.66597149	1.15E-29	CAFs
ID3	1.37E-28	2.6649082	3.25E-24	CAFs
LOC645638	4.13E-12	2.66346143	9.79E-08	CAFs
KIAA1462	4.06E-14	2.65809578	9.62E-10	CAFs
SERPINE1	4.02E-24	2.65026638	9.52E-20	CAFs
COL4A1	1.45E-25	2.64534572	3.43E-21	CAFs
ADAMTS10	1.79E-09	2.64503821	4.23E-05	CAFs
MICAL2	3.88E-23	2.63688543	9.18E-19	CAFs
ADIRF	2.64E-19	2.63603326	6.25E-15	CAFs
PSD3	1.44E-15	2.63587082	3.41E-11	CAFs
PPP1R13L	1.31E-25	2.63507392	3.10E-21	CAFs
TBC1D2	2.91E-17	2.63500946	6.89E-13	CAFs
RNASE4	5.40E-17	2.63466611	1.28E-12	CAFs
NCKAP5	1.61E-09	2.63074412	3.82E-05	CAFs
TP53I3	1.82E-16	2.62128296	4.32E-12	CAFs
DNMBP	6.53E-20	2.6207557	1.55E-15	CAFs
TMEM119	1.27E-09	2.62000948	3.01E-05	CAFs
CYBRD1	2.92E-31	2.61999349	6.92E-27	CAFs
FADS2	5.21E-18	2.61396012	1.23E-13	CAFs
LOC100505806	4.54E-11	2.61169527	1.08E-06	CAFs

KCTD12	1.61E-15	2.6110667	3.81E-11	CAFs
NCS1	1.36E-15	2.61051431	3.23E-11	CAFs
MARK1	3.24E-09	2.61034327	7.67E-05	CAFs
PTGFRN	1.58E-14	2.59537934	3.75E-10	CAFs
NET1	1.18E-17	2.59073893	2.80E-13	CAFs
CLCF1	5.71E-21	2.58692077	1.35E-16	CAFs
NFIL3	1.70E-16	2.58316004	4.03E-12	CAFs
WASF3	1.24E-28	2.57907627	2.94E-24	CAFs
NFIB	3.59E-15	2.57487692	8.50E-11	CAFs
KLF5	6.59E-10	2.57232249	1.56E-05	CAFs
SIX1	5.69E-12	2.57138208	1.35E-07	CAFs
TJP2	6.63E-10	2.55660656	1.57E-05	CAFs
GPC1	1.41E-19	2.55560048	3.34E-15	CAFs
BMP1	1.15E-20	2.5545532	2.72E-16	CAFs
PODXL	9.93E-16	2.53743626	2.35E-11	CAFs
CLDN11	2.80E-13	2.53665539	6.63E-09	CAFs
TPST1	1.39E-22	2.53625185	3.28E-18	CAFs
PARD3B	4.36E-09	2.53268192	0.00010319	CAFs
ARHGAP29	5.09E-23	2.52417788	1.21E-18	CAFs
LAMC1	6.52E-25	2.52370743	1.55E-20	CAFs
PCDHGA12	2.85E-11	2.52291571	6.75E-07	CAFs
SYDE1	1.21E-11	2.50935037	2.87E-07	CAFs
DCBLD1	1.27E-10	2.50459482	3.00E-06	CAFs
PLSCR4	1.58E-16	2.50082563	3.73E-12	CAFs
CCRL1	1.17E-09	2.49824113	2.76E-05	CAFs
EDN1	1.79E-09	2.49592276	4.23E-05	CAFs
C7orf10	1.18E-12	2.49506565	2.80E-08	CAFs
PRSS12	5.07E-14	2.49407127	1.20E-09	CAFs
HEG1	1.03E-25	2.49381078	2.44E-21	CAFs
RHOBTB1	3.60E-13	2.48991387	8.53E-09	CAFs
SNX21	3.18E-16	2.48824022	7.53E-12	CAFs
ADAMTS6	1.37E-14	2.48553634	3.25E-10	CAFs
TMEM91	1.08E-09	2.48302145	2.55E-05	CAFs
PTGES	2.40E-12	2.48065244	5.68E-08	CAFs
PDE3A	1.50E-19	2.47821875	3.56E-15	CAFs
SLC38A5	1.47E-23	2.47797507	3.49E-19	CAFs
CRIM1	1.71E-20	2.47523075	4.05E-16	CAFs
LACC1	2.15E-24	2.4718078	5.09E-20	CAFs
DBN1	1.36E-23	2.47029383	3.21E-19	CAFs
SNAI2	1.31E-22	2.4689668	3.11E-18	CAFs
WDR62	3.58E-09	2.45293038	8.48E-05	CAFs

CPED1	1.48E-17	2.44762527	3.49E-13	CAFs
Mar-02	1.07E-09	2.44640478	2.52E-05	CAFs
SMTN	1.74E-16	2.44505376	4.13E-12	CAFs
BEX1	1.60E-09	2.4390063	3.79E-05	CAFs
HIST1H3G	3.13E-09	2.43708179	7.41E-05	CAFs
RCAN2	1.76E-19	2.42515372	4.17E-15	CAFs
TBC1D8B	8.72E-17	2.41956	2.06E-12	CAFs
DDR2	3.03E-18	2.41808229	7.18E-14	CAFs
ARHGAP10	5.54E-17	2.41651707	1.31E-12	CAFs
DLG5	2.09E-26	2.41452319	4.96E-22	CAFs
NAV3	5.90E-11	2.40698911	1.40E-06	CAFs
KIAA1522	7.35E-15	2.40586047	1.74E-10	CAFs
NNMT	4.78E-29	2.40579501	1.13E-24	CAFs
C10orf10	1.18E-15	2.39892484	2.79E-11	CAFs
CTIF	5.02E-18	2.3949061	1.19E-13	CAFs
RIN1	3.16E-10	2.39309967	7.47E-06	CAFs
FAM57A	1.09E-14	2.39222413	2.58E-10	CAFs
C12orf75	1.03E-19	2.39161476	2.44E-15	CAFs
LHFP	2.18E-26	2.39104529	5.16E-22	CAFs
FERMT2	1.57E-20	2.37949246	3.71E-16	CAFs
NPR2	7.83E-11	2.37827249	1.86E-06	CAFs
WWC2	3.56E-13	2.37826079	8.42E-09	CAFs
RPS6KA2	3.78E-16	2.37765343	8.96E-12	CAFs
C11orf91	1.69E-09	2.37666368	4.01E-05	CAFs
HS6ST1	2.84E-17	2.3720515	6.74E-13	CAFs
TLN2	2.97E-16	2.37003049	7.03E-12	CAFs
CTTNBP2NL	1.52E-15	2.36622532	3.60E-11	CAFs
PLAUR	2.35E-17	2.3654968	5.57E-13	CAFs
TUBB6	4.06E-23	2.3640016	9.61E-19	CAFs
EXT1	9.19E-14	2.3603643	2.18E-09	CAFs
HDGFRP3	1.66E-09	2.35568727	3.94E-05	CAFs
ADCY4	9.15E-20	2.35322789	2.17E-15	CAFs
PRR24	2.34E-15	2.3479312	5.54E-11	CAFs
LATS2	3.66E-18	2.34561727	8.67E-14	CAFs
DHRS3	5.03E-12	2.34559391	1.19E-07	CAFs
PPAP2A	2.66E-25	2.34525061	6.29E-21	CAFs
RAB11FIP5	2.92E-15	2.33891762	6.90E-11	CAFs
MEIS1	6.28E-17	2.33743876	1.49E-12	CAFs
RGS4	6.52E-17	2.3362869	1.54E-12	CAFs
CTSK	2.16E-25	2.33564981	5.12E-21	CAFs
RUSC2	1.62E-17	2.32939555	3.83E-13	CAFs

ALDH2	1.05E-18	2.32543175	2.48E-14	CAFs
MB21D2	8.55E-19	2.30201951	2.03E-14	CAFs
BDNF	4.30E-09	2.29833873	0.00010194	CAFs
CALHM2	3.27E-22	2.29776593	7.75E-18	CAFs
PKIA	3.78E-17	2.29630973	8.96E-13	CAFs
TWSG1	1.01E-18	2.29432705	2.39E-14	CAFs
CLU	2.04E-15	2.29415279	4.84E-11	CAFs
ID1	7.78E-16	2.28447558	1.84E-11	CAFs
MARCKS	5.94E-28	2.28085937	1.41E-23	CAFs
POLE2	2.51E-09	2.27415673	5.94E-05	CAFs
DAB2	7.62E-23	2.26901146	1.80E-18	CAFs
AJUBA	1.87E-09	2.26795902	4.43E-05	CAFs
TRIM3	2.82E-09	2.26366176	6.67E-05	CAFs
UBE2E2	9.11E-19	2.25769852	2.16E-14	CAFs
PLOD2	1.11E-15	2.25761311	2.63E-11	CAFs
NR2F2	8.47E-15	2.25548842	2.01E-10	CAFs
RARB	4.23E-10	2.25505357	1.00E-05	CAFs
AGPAT4	5.56E-10	2.25231298	1.32E-05	CAFs
ERRFI1	1.44E-15	2.24886123	3.41E-11	CAFs
SPHK1	2.63E-15	2.24429095	6.23E-11	CAFs
GALNT10	2.73E-14	2.23939062	6.47E-10	CAFs
RARG	6.78E-13	2.23406129	1.61E-08	CAFs
FHL2	2.31E-17	2.23191139	5.48E-13	CAFs
DRAM1	1.34E-12	2.2318878	3.17E-08	CAFs
LRRK1	1.94E-09	2.22813782	4.59E-05	CAFs
CDCA8	1.49E-10	2.21820617	3.52E-06	CAFs
PTRF	1.13E-22	2.21462746	2.67E-18	CAFs
ANGPTL4	5.40E-12	2.21393434	1.28E-07	CAFs
KIRREL	6.54E-15	2.20137002	1.55E-10	CAFs
TRIO	2.94E-18	2.19886386	6.97E-14	CAFs
LOC100132891	6.54E-10	2.19773016	1.55E-05	CAFs
RGL1	5.26E-15	2.19683726	1.25E-10	CAFs
OSMR	2.61E-12	2.19000793	6.19E-08	CAFs
FAT1	8.84E-15	2.18941007	2.09E-10	CAFs
UAP1	9.06E-21	2.18706934	2.15E-16	CAFs
VEPH1	5.49E-10	2.18608793	1.30E-05	CAFs
TNFRSF10D	2.67E-14	2.18246379	6.33E-10	CAFs
NDST1	1.12E-14	2.17871544	2.65E-10	CAFs
MAP9	2.40E-17	2.1723151	5.69E-13	CAFs
PXDC1	3.79E-11	2.17132358	8.99E-07	CAFs
LAMB1	1.27E-16	2.16386871	3.00E-12	CAFs

NAV1	3.31E-12	2.16069054	7.83E-08	CAFs
MORC4	6.21E-10	2.15898364	1.47E-05	CAFs
PDIA5	2.23E-13	2.15848259	5.28E-09	CAFs
PDLIM4	1.03E-19	2.15142475	2.43E-15	CAFs
CBS	1.02E-10	2.15036789	2.41E-06	CAFs
RAI14	4.13E-16	2.1491058	9.78E-12	CAFs
SCHIP1	1.53E-09	2.14096003	3.62E-05	CAFs
TCF4	1.39E-25	2.13677649	3.30E-21	CAFs
RND3	1.94E-15	2.13639761	4.60E-11	CAFs
SCRN1	1.42E-14	2.13336807	3.37E-10	CAFs
ACTA2	5.15E-14	2.13139886	1.22E-09	CAFs
CYB561	8.59E-11	2.12934972	2.03E-06	CAFs
SOCS5	7.93E-17	2.12670848	1.88E-12	CAFs
SMARCA1	1.73E-15	2.12560741	4.09E-11	CAFs
KDELR3	8.43E-19	2.12537555	2.00E-14	CAFs
LIMA1	1.16E-20	2.12004455	2.76E-16	CAFs
ARSJ	4.90E-11	2.11968191	1.16E-06	CAFs
RRAS	4.31E-12	2.11603227	1.02E-07	CAFs
FAM109B	2.50E-13	2.11325897	5.91E-09	CAFs
TK1	7.67E-10	2.11127462	1.82E-05	CAFs
ZAK	2.92E-09	2.11091595	6.92E-05	CAFs
SORBS3	1.39E-15	2.10474157	3.29E-11	CAFs
N6AMT2	4.07E-09	2.10266319	9.64E-05	CAFs
MAP1B	1.14E-20	2.10066077	2.71E-16	CAFs
PHLDB1	9.98E-18	2.09856789	2.36E-13	CAFs
SCN8A	4.52E-21	2.09849812	1.07E-16	CAFs
NDN	4.60E-14	2.09702319	1.09E-09	CAFs
PIP5K1C	1.67E-14	2.09046121	3.96E-10	CAFs
LPPR2	7.56E-15	2.08638527	1.79E-10	CAFs
KIF20A	3.01E-10	2.08341432	7.14E-06	CAFs
GLIS3	2.41E-16	2.08057321	5.70E-12	CAFs
ELOVL6	7.99E-10	2.07717588	1.89E-05	CAFs
FAM189B	9.72E-13	2.07712535	2.30E-08	CAFs
ENG	2.81E-14	2.07567314	6.66E-10	CAFs
NEK11	3.73E-11	2.06978422	8.84E-07	CAFs
NT5DC2	7.25E-11	2.06886701	1.72E-06	CAFs
TCF7L2	6.69E-10	2.06642426	1.58E-05	CAFs
FAM127C	1.35E-17	2.06366887	3.20E-13	CAFs
FRMD6	4.66E-15	2.06338348	1.10E-10	CAFs
NFIC	4.89E-18	2.06239	1.16E-13	CAFs
ECM1	1.01E-22	2.05927136	2.39E-18	CAFs

SYNC	1.69E-15	2.0587975	4.00E-11	CAFs
FHL3	3.14E-18	2.05853551	7.44E-14	CAFs
MPZL1	4.26E-20	2.0567856	1.01E-15	CAFs
EPAS1	5.75E-12	2.0557993	1.36E-07	CAFs
SLC2A10	1.78E-10	2.04880417	4.23E-06	CAFs
FLJ35946	1.37E-12	2.04735551	3.25E-08	CAFs
B3GNT9	7.95E-14	2.04501293	1.88E-09	CAFs
TBX18	4.10E-10	2.03523929	9.70E-06	CAFs
STX1A	5.60E-10	2.03257416	1.33E-05	CAFs
SLC12A4	1.10E-14	2.02869836	2.60E-10	CAFs
NCEH1	9.48E-13	2.02741196	2.25E-08	CAFs
LRP11	1.41E-11	2.02361658	3.35E-07	CAFs
VCL	5.38E-15	2.01426117	1.27E-10	CAFs
SLC31A2	2.78E-12	2.01023237	6.59E-08	CAFs
PDLIM7	5.52E-19	2.00721927	1.31E-14	CAFs
GNAI1	7.46E-13	2.00141698	1.77E-08	CAFs
ITGB5	6.62E-12	2.00091732	1.57E-07	CAFs
IL2	4.89E-12	6.51789794	1.16E-07	CD4 T
IL21	5.10E-32	5.7523346	1.21E-27	CD4 T
LOC100128420	3.08E-74	5.17113077	7.29E-70	CD4 T
CD40LG	1.27E-131	5.04059967	3.01E-127	CD4 T
PVALB	4.35E-21	4.71237932	1.03E-16	CD4 T
ANKRD55	3.15E-27	4.01262284	7.47E-23	CD4 T
TNFRSF25	1.47E-76	3.74959724	3.48E-72	CD4 T
DOK6	4.80E-16	3.54717109	1.14E-11	CD4 T
CD4	5.65E-122	3.37582585	1.34E-117	CD4 T
FAAH2	4.49E-48	3.21772784	1.06E-43	CD4 T
MORN3	3.91E-11	3.13379321	9.27E-07	CD4 T
PRKCQ-AS1	2.01E-35	3.13274608	4.76E-31	CD4 T
FBLN7	5.56E-39	3.09776686	1.32E-34	CD4 T
ANK3	1.29E-39	3.07846304	3.05E-35	CD4 T
CD226	1.20E-43	3.05007602	2.84E-39	CD4 T
CCR4	7.04E-34	2.99195315	1.67E-29	CD4 T
AQP3	5.10E-24	2.91648329	1.21E-19	CD4 T
IL7R	6.84E-104	2.90910234	1.62E-99	CD4 T
LOC285740	1.65E-35	2.87827194	3.90E-31	CD4 T
MDS2	4.55E-10	2.66393479	1.08E-05	CD4 T
BFSP2	2.24E-10	2.64639949	5.31E-06	CD4 T
RASGRF2	1.28E-09	2.64359163	3.03E-05	CD4 T
TENM1	9.72E-35	2.64157588	2.30E-30	CD4 T
LGALS9C	1.23E-09	2.64019433	2.91E-05	CD4 T

CD28	7.93E-75	2.56763638	1.88E-70	CD4 T
LOC286442	5.35E-13	2.53875241	1.27E-08	CD4 T
LOC100288122	1.08E-17	2.52989101	2.56E-13	CD4 T
TCF7	5.57E-77	2.47356919	1.32E-72	CD4 T
SH2D3A	3.65E-11	2.4523035	8.66E-07	CD4 T
PASK	2.86E-36	2.44718567	6.78E-32	CD4 T
SUSD3	2.95E-34	2.4347386	7.00E-30	CD4 T
CAMK4	1.35E-28	2.41608762	3.20E-24	CD4 T
LRIG1	4.60E-10	2.41035485	1.09E-05	CD4 T
CD6	9.50E-75	2.39061758	2.25E-70	CD4 T
MAL	2.37E-21	2.37811131	5.61E-17	CD4 T
KLRB1	7.51E-27	2.34820296	1.78E-22	CD4 T
HS3ST3B1	2.31E-20	2.3403084	5.47E-16	CD4 T
SLAMF1	1.41E-29	2.3197461	3.35E-25	CD4 T
RGCC	1.05E-24	2.3078132	2.49E-20	CD4 T
APBA2	1.13E-10	2.30562569	2.68E-06	CD4 T
LDLRAD4	1.91E-26	2.29504867	4.52E-22	CD4 T
TC2N	5.95E-68	2.29247366	1.41E-63	CD4 T
ICOS	1.33E-56	2.26591671	3.16E-52	CD4 T
C1orf228	6.16E-12	2.23129387	1.46E-07	CD4 T
CD5	1.46E-53	2.21702154	3.47E-49	CD4 T
TNFSF8	7.31E-57	2.21513736	1.73E-52	CD4 T
TNFRSF4	6.22E-16	2.17092772	1.47E-11	CD4 T
ITGB2-AS1	5.55E-47	2.15953278	1.31E-42	CD4 T
SORL1	4.98E-38	2.15107703	1.18E-33	CD4 T
CCDC109B	7.82E-34	2.14342236	1.85E-29	CD4 T
GIMAP1-GIMAP5	7.75E-14	2.13200798	1.84E-09	CD4 T
CCR7	1.73E-42	2.12088713	4.10E-38	CD4 T
SPOCK2	1.72E-86	2.11009216	4.08E-82	CD4 T
DGKA	1.83E-67	2.10997914	4.33E-63	CD4 T
ICA1	8.61E-19	2.08952966	2.04E-14	CD4 T
PRKCQ	5.16E-37	2.08137877	1.22E-32	CD4 T
PBX4	5.82E-17	2.07335685	1.38E-12	CD4 T
TOX2	6.04E-19	2.0711847	1.43E-14	CD4 T
ITK	2.40E-66	2.05397254	5.68E-62	CD4 T
MPP7	9.03E-18	2.04189521	2.14E-13	CD4 T
KCNA3	8.06E-19	2.03892291	1.91E-14	CD4 T
LAT	4.01E-58	2.03078915	9.50E-54	CD4 T
LTB	6.43E-49	2.01050537	1.52E-44	CD4 T
FAM163B	1.58E-09	7.2467353	3.75E-05	CD8 T
ITGAD	3.84E-56	6.26729821	9.10E-52	CD8 T

KLRC4-KLRK1	4.71E-66	5.85663758	1.12E-61	CD8 T
CD8A	4.52E-251	5.75421687	1.07E-246	CD8 T
TIMD4	8.46E-32	5.58628647	2.00E-27	CD8 T
KIR2DL4	3.65E-64	5.56309317	8.66E-60	CD8 T
TMEM155	3.87E-59	5.3999883	9.18E-55	CD8 T
CD8B	6.74E-197	5.17111745	1.60E-192	CD8 T
PP12613	1.22E-20	5.13051878	2.88E-16	CD8 T
CCL3L3	1.77E-139	5.08005303	4.18E-135	CD8 T
FASLG	5.82E-80	4.80613285	1.38E-75	CD8 T
KLRK1	1.03E-262	4.80469355	2.45E-258	CD8 T
NKG7	3.22E-269	4.78921603	7.63E-265	CD8 T
KLRC4	5.21E-108	4.62458378	1.24E-103	CD8 T
CCL4L1	2.23E-227	4.61603177	5.28E-223	CD8 T
CCL4L2	2.23E-227	4.61603177	5.28E-223	CD8 T
GZMH	2.28E-99	4.60920782	5.40E-95	CD8 T
VCAM1	9.76E-82	4.58407469	2.31E-77	CD8 T
LAG3	1.53E-107	4.54014289	3.63E-103	CD8 T
JAKMIP1	2.21E-77	4.43946173	5.23E-73	CD8 T
GZMA	6.01E-231	4.34954451	1.42E-226	CD8 T
XCL2	2.18E-57	4.3178861	5.16E-53	CD8 T
TTC16	2.95E-16	4.27957276	6.99E-12	CD8 T
GZMK	4.20E-236	4.2522905	9.94E-232	CD8 T
IFNG	4.79E-104	4.20761524	1.13E-99	CD8 T
CCL4	1.24E-235	4.18250712	2.93E-231	CD8 T
PRF1	4.33E-199	4.14422584	1.02E-194	CD8 T
EOMES	3.86E-78	4.11213843	9.15E-74	CD8 T
CXCR6	1.24E-95	4.06973155	2.94E-91	CD8 T
TARP	2.53E-91	4.04060653	5.99E-87	CD8 T
GTSF1L	2.75E-11	4.02803473	6.52E-07	CD8 T
DTHD1	2.51E-140	4.0168934	5.94E-136	CD8 T
KIR3DL1	2.77E-14	3.97566632	6.55E-10	CD8 T
CXCL13	1.59E-86	3.97413337	3.77E-82	CD8 T
KLRC2	1.64E-34	3.87728936	3.89E-30	CD8 T
CTSW	2.46E-150	3.86027224	5.83E-146	CD8 T
GZMB	4.50E-71	3.8208102	1.07E-66	CD8 T
CCL3L1	3.31E-12	3.73453044	7.83E-08	CD8 T
TTC24	1.96E-38	3.66030953	4.64E-34	CD8 T
CST7	1.53E-235	3.65251013	3.63E-231	CD8 T
FCRL6	2.91E-28	3.62375724	6.88E-24	CD8 T
CCR5	2.03E-113	3.6136861	4.80E-109	CD8 T
C17orf66	9.96E-16	3.57000149	2.36E-11	CD8 T

FAM179A	1.30E-22	3.56332088	3.08E-18	CD8 T
GFI1	1.20E-16	3.54704003	2.84E-12	CD8 T
KLRC3	2.30E-32	3.54105906	5.46E-28	CD8 T
XCL1	5.54E-44	3.50509322	1.31E-39	CD8 T
KRT86	1.52E-11	3.50431576	3.61E-07	CD8 T
CCL3	3.78E-92	3.48115539	8.96E-88	CD8 T
ZNF683	3.88E-10	3.46409374	9.19E-06	CD8 T
TRIM69	4.70E-13	3.43906184	1.11E-08	CD8 T
NCR1	1.01E-23	3.35092778	2.39E-19	CD8 T
RASGEF1A	5.71E-16	3.28978468	1.35E-11	CD8 T
ATP1A3	1.13E-18	3.23063923	2.67E-14	CD8 T
SALL4	1.81E-10	3.20192918	4.29E-06	CD8 T
KLRC1	2.88E-24	3.17494059	6.83E-20	CD8 T
PLCXD2	1.46E-23	3.12049735	3.46E-19	CD8 T
NEBL	7.73E-11	3.11296819	1.83E-06	CD8 T
LGR6	2.79E-09	3.10871885	6.61E-05	CD8 T
CD200R1	3.31E-42	3.10810116	7.85E-38	CD8 T
CCDC141	6.28E-84	3.10808215	1.49E-79	CD8 T
SEMA4A	6.57E-22	3.04683423	1.56E-17	CD8 T
GNLY	4.32E-28	3.02245447	1.02E-23	CD8 T
FCRL3	2.37E-102	3.012605	5.62E-98	CD8 T
AMICA1	3.75E-79	2.99826729	8.88E-75	CD8 T
MATK	1.36E-19	2.99219615	3.23E-15	CD8 T
NLRP6	5.69E-13	2.98222102	1.35E-08	CD8 T
GNGT2	2.24E-13	2.98138037	5.30E-09	CD8 T
PDCD1	1.64E-129	2.93106204	3.89E-125	CD8 T
SLFN12L	2.79E-29	2.89788846	6.61E-25	CD8 T
EDARADD	2.12E-11	2.89690783	5.01E-07	CD8 T
CD7	1.22E-119	2.8914856	2.90E-115	CD8 T
RGS9	1.74E-12	2.85335066	4.11E-08	CD8 T
AMIGO2	5.50E-21	2.8442277	1.30E-16	CD8 T
SIRPG	2.04E-124	2.83714936	4.83E-120	CD8 T
CD38	3.31E-55	2.82286939	7.85E-51	CD8 T
HOPX	2.93E-31	2.80013299	6.94E-27	CD8 T
C11orf21	8.32E-11	2.79253581	1.97E-06	CD8 T
PRR5L	7.18E-23	2.79069259	1.70E-18	CD8 T
SYTL3	1.25E-106	2.78894375	2.97E-102	CD8 T
OASL	1.94E-40	2.77289505	4.60E-36	CD8 T
SAMD3	1.67E-44	2.76668296	3.94E-40	CD8 T
PRDM1	4.21E-128	2.75829252	9.96E-124	CD8 T
SH2D2A	1.02E-89	2.75510379	2.41E-85	CD8 T

TOX	1.52E-121	2.75359204	3.59E-117	CD8 T
ADORA2A	8.74E-31	2.75118202	2.07E-26	CD8 T
PPP2R2B	1.81E-16	2.74017824	4.29E-12	CD8 T
AOAH	2.53E-54	2.71446937	6.00E-50	CD8 T
TSPAN32	2.72E-19	2.71044699	6.43E-15	CD8 T
CD244	7.85E-23	2.70869503	1.86E-18	CD8 T
CLIC3	9.84E-19	2.7025435	2.33E-14	CD8 T
DGKH	1.24E-29	2.66999306	2.93E-25	CD8 T
CCDC64	7.22E-31	2.65399524	1.71E-26	CD8 T
ABCD2	2.58E-20	2.64778392	6.12E-16	CD8 T
GPR171	2.39E-44	2.64543247	5.67E-40	CD8 T
LINC00612	6.88E-25	2.62511046	1.63E-20	CD8 T
MYO7A	5.99E-26	2.61989467	1.42E-21	CD8 T
THEMIS	1.39E-68	2.60110349	3.29E-64	CD8 T
ZBED2	7.04E-25	2.59870477	1.67E-20	CD8 T
ATP8B4	8.48E-12	2.59845522	2.01E-07	CD8 T
ITGB7	4.35E-39	2.57923127	1.03E-34	CD8 T
CDYL2	1.18E-09	2.5726166	2.80E-05	CD8 T
MTMR8	8.74E-11	2.56728002	2.07E-06	CD8 T
APOBEC3H	8.45E-15	2.55733566	2.00E-10	CD8 T
HAVCR2	4.31E-91	2.54366012	1.02E-86	CD8 T
KLRG1	8.65E-35	2.53841947	2.05E-30	CD8 T
RGS4	1.42E-11	2.53651208	3.36E-07	CD8 T
CXCR3	1.90E-58	2.52505803	4.50E-54	CD8 T
PSTPIP1	3.66E-79	2.5227971	8.67E-75	CD8 T
CRTAM	2.47E-50	2.50270039	5.84E-46	CD8 T
TTN	2.49E-72	2.50140111	5.89E-68	CD8 T
SLC27A2	2.72E-14	2.49048737	6.44E-10	CD8 T
ABCB1	3.32E-30	2.49009733	7.87E-26	CD8 T
HCST	8.89E-126	2.48951758	2.11E-121	CD8 T
IL2RB	7.63E-107	2.46367167	1.81E-102	CD8 T
ARRDC5	8.16E-14	2.45436724	1.93E-09	CD8 T
CD27	2.10E-114	2.44118085	4.96E-110	CD8 T
ASB2	3.84E-25	2.44099584	9.10E-21	CD8 T
CPA5	1.56E-12	2.43351263	3.69E-08	CD8 T
GZMM	2.42E-53	2.41993959	5.73E-49	CD8 T
TNFSF9	4.93E-25	2.4182408	1.17E-20	CD8 T
TIGIT	5.37E-92	2.41660982	1.27E-87	CD8 T
PZP	1.31E-16	2.41483451	3.11E-12	CD8 T
TNIP3	1.08E-21	2.41323643	2.57E-17	CD8 T
MIR155HG	4.45E-32	2.40856965	1.05E-27	CD8 T

CD3E	5.76E-160	2.40666638	1.37E-155	CD8 T
PLCH2	7.36E-14	2.40579834	1.74E-09	CD8 T
UBASH3A	1.22E-57	2.40495479	2.88E-53	CD8 T
PTGDR	3.58E-12	2.40462171	8.49E-08	CD8 T
PTPN22	9.29E-68	2.39618615	2.20E-63	CD8 T
PCED1B	1.91E-66	2.39541226	4.53E-62	CD8 T
CD2	1.94E-158	2.39083838	4.59E-154	CD8 T
VNN2	1.57E-17	2.3865612	3.73E-13	CD8 T
RAB37	5.70E-37	2.37438422	1.35E-32	CD8 T
PATL2	2.26E-27	2.36989845	5.35E-23	CD8 T
ETV1	4.32E-12	2.3651864	1.02E-07	CD8 T
SARDH	2.46E-23	2.36249792	5.83E-19	CD8 T
TRAT1	9.45E-68	2.31729742	2.24E-63	CD8 T
PYHIN1	3.33E-90	2.31437777	7.89E-86	CD8 T
GFOD1	1.27E-22	2.31178931	3.00E-18	CD8 T
CD3D	4.56E-158	2.2988217	1.08E-153	CD8 T
ITGAE	2.40E-23	2.28695118	5.68E-19	CD8 T
ITM2A	2.85E-109	2.2789626	6.75E-105	CD8 T
PRKCH	4.44E-124	2.26882501	1.05E-119	CD8 T
PTPN7	2.11E-80	2.26645582	4.99E-76	CD8 T
MPZL3	1.91E-09	2.25913967	4.51E-05	CD8 T
CASZ1	1.29E-12	2.25138963	3.05E-08	CD8 T
GATA3	2.16E-35	2.24979257	5.13E-31	CD8 T
BZRAP1	4.79E-21	2.24598535	1.13E-16	CD8 T
MIAT	5.09E-33	2.23671751	1.20E-28	CD8 T
MYO1G	3.40E-59	2.22895904	8.06E-55	CD8 T
SPNS3	1.51E-12	2.22079668	3.59E-08	CD8 T
SLA	2.65E-127	2.20714471	6.27E-123	CD8 T
TBX21	7.61E-10	2.20419519	1.80E-05	CD8 T
ABI3	1.38E-35	2.2040139	3.26E-31	CD8 T
GPR114	7.91E-22	2.19880241	1.87E-17	CD8 T
TRERF1	4.38E-47	2.19160444	1.04E-42	CD8 T
ITGA1	2.20E-09	2.19082425	5.21E-05	CD8 T
NELL2	7.90E-27	2.18269963	1.87E-22	CD8 T
PARP8	5.86E-71	2.17899586	1.39E-66	CD8 T
CLECL1	6.55E-16	2.17841175	1.55E-11	CD8 T
GIMAP7	9.52E-87	2.17769465	2.26E-82	CD8 T
SIT1	1.31E-52	2.173666	3.11E-48	CD8 T
C12orf75	1.25E-20	2.17013332	2.97E-16	CD8 T
UBASH3B	2.46E-15	2.1690184	5.83E-11	CD8 T
PLEK	8.12E-40	2.16836469	1.92E-35	CD8 T

SLAMF6	7.15E-74	2.1669859	1.69E-69	CD8 T
GAB3	1.33E-12	2.16194922	3.15E-08	CD8 T
DOK2	1.48E-57	2.15932596	3.51E-53	CD8 T
BCL11B	6.64E-80	2.15001936	1.57E-75	CD8 T
IL32	1.38E-152	2.14842254	3.28E-148	CD8 T
CD3G	6.32E-129	2.14435695	1.50E-124	CD8 T
DENND2D	1.53E-102	2.13390325	3.62E-98	CD8 T
IL10RA	2.62E-82	2.12350823	6.20E-78	CD8 T
ATHL1	1.58E-56	2.11704006	3.75E-52	CD8 T
SH2D1A	4.63E-63	2.10679775	1.10E-58	CD8 T
LINC00324	2.19E-09	2.10354402	5.19E-05	CD8 T
PVRIG	1.09E-57	2.09873152	2.59E-53	CD8 T
TNFRSF1B	2.70E-69	2.09026158	6.40E-65	CD8 T
GBP5	3.27E-61	2.08939543	7.75E-57	CD8 T
ARL4C	1.99E-58	2.05162999	4.72E-54	CD8 T
MYO1F	1.12E-33	2.05159494	2.65E-29	CD8 T
SLA2	1.63E-47	2.03368357	3.87E-43	CD8 T
RASAL3	5.13E-55	2.03343645	1.21E-50	CD8 T
DUSP2	6.12E-100	2.02004759	1.45E-95	CD8 T
ZAP70	4.20E-92	2.01499626	9.95E-88	CD8 T
LCK	6.11E-95	2.01380191	1.45E-90	CD8 T
PTPLAD2	7.88E-20	2.01058603	1.87E-15	CD8 T
SOX18	4.01E-146	9.830092	9.49E-142	Endo
CLEC14A	2.08E-223	9.72355654	4.94E-219	Endo
CCL14	7.41E-235	9.09220035	1.76E-230	Endo
CDH5	1.35E-287	8.955265	3.21E-283	Endo
CLDN5	4.38E-273	8.58706948	1.04E-268	Endo
CLEC4M	1.28E-105	8.26779738	3.03E-101	Endo
MIR548A2	1.60E-10	8.25573172	3.79E-06	Endo
USHBP1	3.81E-102	8.21633005	9.03E-98	Endo
SNORD7	1.60E-10	8.05990821	3.79E-06	Endo
MIR620	1.60E-10	8.05413979	3.79E-06	Endo
ROBO4	1.42E-221	8.00127223	3.35E-217	Endo
ERICH1-AS1	1.53E-21	7.89336541	3.63E-17	Endo
FGF20	1.60E-10	7.872012	3.79E-06	Endo
RNU6-83	1.60E-10	7.80053381	3.79E-06	Endo
ADAMTS18	6.82E-61	7.79953965	1.61E-56	Endo
ERG	2.78E-216	7.77550926	6.59E-212	Endo
MIR551A	1.60E-10	7.7328057	3.79E-06	Endo
GPR182	1.05E-124	7.71533346	2.48E-120	Endo
MIR1277	1.60E-10	7.70769956	3.79E-06	Endo

DSCAM-IT1	1.60E-10	7.67451448	3.79E-06	Endo
ECSCR	5.66E-295	7.65211372	1.34E-290	Endo
PLVAP	3.60E-121	7.62736193	8.53E-117	Endo
ARHGEF15	1.05E-153	7.61239435	2.50E-149	Endo
BCL6B	7.05E-101	7.57466789	1.67E-96	Endo
CLEC1A	3.66E-101	7.54748598	8.66E-97	Endo
TLL1	1.08E-161	7.54285459	2.55E-157	Endo
TPO	1.59E-21	7.52795088	3.76E-17	Endo
LY6H	4.42E-25	7.51604403	1.05E-20	Endo
SLCO2A1	2.88E-182	7.50206071	6.83E-178	Endo
NTS	3.19E-133	7.4962985	7.57E-129	Endo
CCM2L	1.46E-61	7.48016018	3.47E-57	Endo
PREX2	2.66E-146	7.46574408	6.29E-142	Endo
TFF3	8.95E-154	7.46418739	2.12E-149	Endo
MIR2277	1.60E-10	7.43065794	3.79E-06	Endo
LMO2	1.30E-84	7.39538592	3.08E-80	Endo
GDF3	1.43E-19	7.36523562	3.38E-15	Endo
TIE1	3.80E-210	7.3262863	9.01E-206	Endo
LOC147646	1.60E-10	7.26536411	3.79E-06	Endo
MACC1-AS1	1.60E-10	7.25420463	3.79E-06	Endo
BET3L	1.60E-10	7.24866158	3.79E-06	Endo
SEMA3F	9.21E-17	7.24848647	2.18E-12	Endo
SELE	1.15E-47	7.24495154	2.73E-43	Endo
TEK	3.34E-162	7.23997304	7.91E-158	Endo
DEFB112	1.60E-10	7.21914939	3.79E-06	Endo
LINC00642	1.60E-10	7.20732176	3.79E-06	Endo
FAM110D	2.76E-13	7.19412383	6.54E-09	Endo
CALCRL	4.87E-203	7.18786798	1.15E-198	Endo
VWF	1.09E-177	7.16759571	2.59E-173	Endo
SDPR	1.81E-199	7.16061439	4.28E-195	Endo
TSPAN12	8.41E-125	7.14745683	1.99E-120	Endo
GNAT3	1.60E-10	7.1369462	3.79E-06	Endo
CCL21	3.99E-154	7.13659419	9.45E-150	Endo
LOC100506388	2.18E-37	7.12364005	5.15E-33	Endo
FABP4	2.11E-186	7.11584089	5.01E-182	Endo
CCL15-CCL14	1.60E-10	7.08689196	3.79E-06	Endo
MMRN1	6.89E-175	7.08509084	1.63E-170	Endo
LYVE1	6.49E-154	7.02343514	1.54E-149	Endo
COL23A1	3.77E-33	6.98885095	8.94E-29	Endo
PDE2A	1.58E-154	6.97713129	3.73E-150	Endo
ZNF385D	2.48E-137	6.95412905	5.88E-133	Endo

PGM5	1.00E-132	6.92888149	2.38E-128	Endo
ELTD1	2.62E-116	6.90320624	6.22E-112	Endo
DARC	1.75E-45	6.89073684	4.15E-41	Endo
MOV10L1	1.55E-41	6.86156506	3.67E-37	Endo
MYCT1	4.24E-157	6.81238412	1.01E-152	Endo
FGD5	5.65E-137	6.80640829	1.34E-132	Endo
RELN	4.43E-81	6.80366744	1.05E-76	Endo
NDNF	8.73E-41	6.78269619	2.07E-36	Endo
KIAA1211L	1.73E-14	6.77633217	4.10E-10	Endo
STAB2	2.21E-63	6.76845543	5.24E-59	Endo
SPINK13	1.60E-10	6.74601721	3.79E-06	Endo
EXOC3L1	1.59E-63	6.74287816	3.76E-59	Endo
SNTG2	4.00E-10	6.70619527	9.47E-06	Endo
LOC388849	2.59E-17	6.68728224	6.13E-13	Endo
ELSPBP1	1.60E-10	6.6810642	3.79E-06	Endo
GATA2	2.71E-92	6.6776394	6.42E-88	Endo
DLL4	3.38E-84	6.66311872	8.01E-80	Endo
SHANK3	8.79E-114	6.61337299	2.08E-109	Endo
CYP46A1	2.43E-37	6.61330509	5.76E-33	Endo
HSPA12B	1.17E-49	6.57632145	2.76E-45	Endo
KIF17	3.04E-50	6.57172028	7.19E-46	Endo
SCNN1B	2.00E-68	6.54984272	4.73E-64	Endo
RASSF9	3.60E-112	6.54394231	8.53E-108	Endo
SULT1C4	1.57E-72	6.51037295	3.73E-68	Endo
REEP1	2.70E-74	6.49789133	6.39E-70	Endo
C2CD4B	2.68E-19	6.46128604	6.34E-15	Endo
KDR	1.52E-114	6.45732882	3.59E-110	Endo
FAM81B	1.60E-10	6.45311944	3.79E-06	Endo
ACR	1.60E-10	6.44314715	3.79E-06	Endo
FAM107A	3.66E-32	6.40984495	8.67E-28	Endo
RET	3.88E-33	6.40432135	9.20E-29	Endo
MYRIP	9.16E-42	6.38862875	2.17E-37	Endo
PCDH17	6.75E-104	6.37842667	1.60E-99	Endo
ABCA4	1.68E-51	6.3637415	3.99E-47	Endo
KIF26A	1.29E-52	6.35385784	3.04E-48	Endo
SNCAIP	3.51E-32	6.33029772	8.31E-28	Endo
LOC284933	1.60E-10	6.32667969	3.79E-06	Endo
SNCG	5.47E-100	6.29942828	1.30E-95	Endo
CAPN11	1.71E-21	6.29830098	4.06E-17	Endo
COL17A1	1.44E-13	6.26147536	3.42E-09	Endo
LTF	4.83E-21	6.23843241	1.14E-16	Endo

FAT4	2.24E-136	6.23637768	5.31E-132	Endo
PKHD1L1	5.74E-72	6.22947472	1.36E-67	Endo
CETP	6.62E-52	6.22162804	1.57E-47	Endo
RGS7BP	4.19E-10	6.21358161	9.94E-06	Endo
ITIH3	4.73E-21	6.20684484	1.12E-16	Endo
STAB1	1.06E-203	6.1994394	2.52E-199	Endo
UNC5A	3.92E-33	6.19379226	9.29E-29	Endo
KLHL4	1.86E-57	6.17955165	4.40E-53	Endo
FAM99A	1.60E-10	6.15852397	3.79E-06	Endo
PEAR1	8.61E-112	6.15658697	2.04E-107	Endo
ADCY4	3.64E-159	6.1249551	8.62E-155	Endo
TDRD10	5.04E-21	6.07310105	1.19E-16	Endo
GJA4	7.69E-52	6.07031234	1.82E-47	Endo
UNC5B	3.35E-91	6.05345904	7.94E-87	Endo
CLEC4G	3.07E-85	6.05053308	7.28E-81	Endo
GPR116	1.00E-148	6.04832332	2.38E-144	Endo
ART4	2.00E-73	6.01978774	4.73E-69	Endo
ITGB4	2.07E-86	6.01658379	4.91E-82	Endo
APLNR	4.72E-34	6.01491316	1.12E-29	Endo
CD34	2.29E-116	6.01338342	5.42E-112	Endo
GP1BB	1.55E-20	6.01323251	3.66E-16	Endo
SNAP25	4.66E-15	6.00321331	1.10E-10	Endo
RAMP2	7.90E-148	5.99257936	1.87E-143	Endo
ANKRD29	8.36E-28	5.98447536	1.98E-23	Endo
INS-IGF2	1.60E-10	5.96314013	3.79E-06	Endo
AOC3	1.27E-60	5.96004573	3.00E-56	Endo
CARD10	7.66E-87	5.9429158	1.81E-82	Endo
CYYR1	6.16E-61	5.93605179	1.46E-56	Endo
MYZAP	9.43E-72	5.93573874	2.23E-67	Endo
SHC2	8.81E-43	5.93068198	2.09E-38	Endo
TM4SF18	4.94E-108	5.91201604	1.17E-103	Endo
RAPGEF4	1.24E-52	5.88450498	2.94E-48	Endo
TMEM255B	1.41E-139	5.87051125	3.34E-135	Endo
ARHGAP29	8.79E-116	5.86617256	2.08E-111	Endo
LRRC70	2.26E-119	5.84721906	5.34E-115	Endo
ABO	5.04E-34	5.8383455	1.19E-29	Endo
LOC100131825	3.45E-36	5.8352458	8.18E-32	Endo
LINC00636	4.61E-34	5.83291514	1.09E-29	Endo
ZNF366	3.74E-23	5.82757809	8.86E-19	Endo
FXYD6	4.94E-90	5.82730762	1.17E-85	Endo
LDB2	3.60E-151	5.82199598	8.52E-147	Endo

CD93	1.87E-127	5.8029251	4.43E-123	Endo
FAM162B	1.07E-29	5.79724369	2.53E-25	Endo
OLFM1	5.47E-67	5.77604565	1.30E-62	Endo
ESAM	8.09E-78	5.76551143	1.92E-73	Endo
IL33	1.37E-123	5.76443136	3.24E-119	Endo
NPR1	1.20E-41	5.75941053	2.84E-37	Endo
PROX1	1.53E-59	5.75531622	3.61E-55	Endo
RADIL	1.93E-45	5.74173322	4.57E-41	Endo
CCL23	1.90E-12	5.73261712	4.49E-08	Endo
SLC38A4	2.57E-37	5.72983599	6.09E-33	Endo
DLL1	1.00E-69	5.70842463	2.37E-65	Endo
ADM5	9.90E-35	5.68322785	2.34E-30	Endo
KIAA1045	2.97E-19	5.64222263	7.04E-15	Endo
RAB3C	1.70E-21	5.62824835	4.04E-17	Endo
INHBB	8.83E-32	5.62270767	2.09E-27	Endo
EGFL7	9.08E-138	5.62207465	2.15E-133	Endo
WSCD1	5.38E-21	5.61802649	1.27E-16	Endo
ZNF467	4.66E-47	5.60789573	1.10E-42	Endo
RSPO3	1.36E-11	5.60569975	3.22E-07	Endo
PALMD	5.55E-40	5.59027385	1.31E-35	Endo
CCDC68	1.84E-11	5.58006419	4.35E-07	Endo
A4GALT	1.21E-68	5.57689131	2.87E-64	Endo
ABLIM2	1.07E-32	5.54417631	2.54E-28	Endo
ADAMTSL3	1.34E-11	5.54018107	3.17E-07	Endo
LOC100271832	1.86E-14	5.5258736	4.40E-10	Endo
LHX6	5.33E-32	5.51996726	1.26E-27	Endo
MYLK2	1.94E-12	5.51597693	4.59E-08	Endo
BMP6	1.10E-26	5.51305727	2.61E-22	Endo
ZNF521	6.83E-101	5.51117124	1.62E-96	Endo
COL4A1	8.84E-135	5.51080859	2.09E-130	Endo
TMEM150C	1.87E-58	5.48673024	4.42E-54	Endo
CCDC178	2.82E-17	5.47976385	6.67E-13	Endo
SP6	4.19E-10	5.4730175	9.94E-06	Endo
IQCA1	6.06E-63	5.44748581	1.44E-58	Endo
STARD8	1.56E-57	5.43484986	3.69E-53	Endo
ANO2	1.18E-13	5.43156336	2.79E-09	Endo
P4HA3	1.73E-54	5.4264236	4.09E-50	Endo
SMOC1	6.32E-33	5.42372978	1.50E-28	Endo
ZNF423	6.95E-58	5.41840253	1.65E-53	Endo
EDN1	2.65E-18	5.40827677	6.28E-14	Endo
HID1	6.36E-105	5.40723356	1.51E-100	Endo

C19orf80	1.98E-12	5.40574698	4.68E-08	Endo
ADIRF	6.59E-78	5.39224246	1.56E-73	Endo
WNT5A	6.22E-19	5.37970291	1.47E-14	Endo
GPR146	2.76E-78	5.37104892	6.54E-74	Endo
FGF11	9.96E-18	5.3412916	2.36E-13	Endo
C8orf4	7.05E-22	5.33645375	1.67E-17	Endo
TGFA	6.88E-29	5.32502865	1.63E-24	Endo
EPHB4	3.09E-95	5.31779224	7.31E-91	Endo
EMID1	2.94E-34	5.3173734	6.96E-30	Endo
TNFRSF11A	8.43E-27	5.31317434	2.00E-22	Endo
BMP2	5.51E-44	5.3039835	1.31E-39	Endo
PCDH15	8.26E-15	5.29495537	1.96E-10	Endo
KBTBD11	2.55E-38	5.28696613	6.04E-34	Endo
BCAM	1.92E-57	5.2856682	4.55E-53	Endo
LOC400456	8.77E-39	5.28137484	2.08E-34	Endo
SGIP1	1.12E-44	5.26794028	2.66E-40	Endo
ADAMTS9	2.18E-88	5.25480442	5.16E-84	Endo
COL4A2	2.84E-127	5.24570829	6.74E-123	Endo
COLEC12	1.21E-84	5.23888066	2.87E-80	Endo
PCDHB7	9.40E-11	5.22001919	2.23E-06	Endo
ALPK3	3.09E-44	5.21585257	7.33E-40	Endo
TSPAN18	1.05E-94	5.21166863	2.49E-90	Endo
THSD1	3.51E-48	5.21036625	8.31E-44	Endo
LOC100288911	2.19E-14	5.20798345	5.18E-10	Endo
CXCR7	1.78E-122	5.19255579	4.22E-118	Endo
FILIP1	6.22E-56	5.1874357	1.47E-51	Endo
ASGR1	3.81E-51	5.16935787	9.02E-47	Endo
CDH26	5.16E-26	5.16658058	1.22E-21	Endo
GJA1	6.82E-79	5.16569296	1.61E-74	Endo
MAGI1	1.42E-84	5.1538994	3.36E-80	Endo
C6orf141	2.74E-20	5.15362444	6.48E-16	Endo
KALRN	4.69E-67	5.1514449	1.11E-62	Endo
PDE1A	5.09E-37	5.14557023	1.20E-32	Endo
FMOD	6.59E-54	5.14477975	1.56E-49	Endo
GGTA1P	1.06E-53	5.11188172	2.52E-49	Endo
CCDC3	1.99E-23	5.11119107	4.72E-19	Endo
IL3RA	9.13E-57	5.11014117	2.16E-52	Endo
MDFI	3.42E-36	5.09426947	8.10E-32	Endo
EFEMP1	7.78E-84	5.08452147	1.84E-79	Endo
CA2	1.89E-34	5.08058905	4.47E-30	Endo
DCHS1	7.24E-101	5.07304638	1.72E-96	Endo

GALNT18	3.77E-99	5.06911507	8.92E-95	Endo
MRC1	1.49E-93	5.065548	3.52E-89	Endo
PLXNA2	2.22E-61	5.06374528	5.25E-57	Endo
KRT222	1.22E-25	5.05711665	2.89E-21	Endo
HOXD9	3.15E-39	5.05345174	7.45E-35	Endo
EGLN3	6.45E-53	5.05074798	1.53E-48	Endo
DACH1	2.16E-23	5.041225	5.11E-19	Endo
PALM	3.87E-54	5.028138	9.16E-50	Endo
GNG11	2.39E-119	5.01974148	5.66E-115	Endo
SEMA3D	7.63E-45	5.01404199	1.81E-40	Endo
NR2F1	1.76E-42	5.00172997	4.17E-38	Endo
MPZL2	1.84E-34	4.99588271	4.36E-30	Endo
SELP	5.63E-53	4.99059348	1.33E-48	Endo
LIFR	1.66E-43	4.98759427	3.92E-39	Endo
LRCH2	8.78E-17	4.98018321	2.08E-12	Endo
CPXM2	4.58E-35	4.97591966	1.08E-30	Endo
GPR97	8.23E-33	4.97203281	1.95E-28	Endo
FLRT2	1.18E-71	4.95566249	2.80E-67	Endo
PCLO	9.56E-29	4.95229968	2.26E-24	Endo
RAPGEF3	4.70E-43	4.95065909	1.11E-38	Endo
GIPC2	2.58E-41	4.94459274	6.11E-37	Endo
NOSTRIN	1.94E-14	4.94073056	4.59E-10	Endo
NHSL2	9.21E-65	4.93766897	2.18E-60	Endo
TSPEAR	1.64E-12	4.93645984	3.88E-08	Endo
PDPN	1.44E-40	4.92309769	3.41E-36	Endo
RHCE	2.62E-15	4.91941696	6.21E-11	Endo
SLC10A6	5.21E-15	4.89321112	1.23E-10	Endo
NDRG4	6.38E-23	4.88671333	1.51E-18	Endo
PDGFB	1.39E-39	4.84612229	3.29E-35	Endo
MBL1P	1.03E-09	4.84416412	2.44E-05	Endo
DOCK6	1.74E-67	4.82590558	4.12E-63	Endo
PCDH12	1.17E-55	4.82579829	2.78E-51	Endo
DYSF	1.34E-70	4.81701524	3.18E-66	Endo
CYP4X1	6.60E-11	4.79800967	1.56E-06	Endo
FLNC	7.59E-61	4.78093375	1.80E-56	Endo
ZNF454	1.01E-12	4.77278226	2.40E-08	Endo
CPLX1	4.19E-10	4.77239303	9.94E-06	Endo
HOXA7	1.76E-30	4.77020044	4.18E-26	Endo
EFNB2	2.15E-46	4.75592484	5.10E-42	Endo
SLC4A11	2.14E-09	4.75430546	5.07E-05	Endo
EFCC1	5.02E-15	4.75274644	1.19E-10	Endo

LIMCH1	3.68E-42	4.74967579	8.71E-38	Endo
RAMP3	1.33E-50	4.74774625	3.14E-46	Endo
C1orf64	4.19E-10	4.74541114	9.94E-06	Endo
SLPI	3.51E-23	4.73775586	8.32E-19	Endo
PALD1	3.09E-62	4.7138523	7.32E-58	Endo
MMP28	4.91E-10	4.71340048	1.16E-05	Endo
GABRE	6.53E-21	4.70199001	1.55E-16	Endo
VWA1	6.52E-22	4.70077904	1.54E-17	Endo
PDE9A	2.58E-15	4.69862743	6.11E-11	Endo
TACR1	4.13E-16	4.69822742	9.79E-12	Endo
LRRC55	5.41E-15	4.6921454	1.28E-10	Endo
PXDN	4.20E-88	4.68840086	9.95E-84	Endo
CLIC2	7.62E-70	4.68812587	1.80E-65	Endo
ALDH1A2	3.09E-20	4.67978588	7.31E-16	Endo
GLRB	1.37E-13	4.66316915	3.26E-09	Endo
THSD7A	5.79E-31	4.65956046	1.37E-26	Endo
TMEM252	2.04E-14	4.64585192	4.84E-10	Endo
TNXA	1.54E-39	4.64371657	3.66E-35	Endo
LOC100505933	2.97E-15	4.6414359	7.02E-11	Endo
TNXB	9.08E-56	4.63427187	2.15E-51	Endo
LTC4S	6.63E-21	4.62702739	1.57E-16	Endo
EPB49	1.24E-25	4.62052466	2.93E-21	Endo
PODXL	9.62E-66	4.61871736	2.28E-61	Endo
TFPI	1.04E-57	4.61638603	2.46E-53	Endo
FAM74A4	2.14E-12	4.61028334	5.07E-08	Endo
SEMA3A	3.08E-53	4.60004649	7.30E-49	Endo
HOXD10	1.02E-09	4.57187687	2.41E-05	Endo
GPR17	1.16E-16	4.5656823	2.75E-12	Endo
THSD4	6.56E-32	4.56511078	1.55E-27	Endo
WASF3	1.11E-25	4.56350332	2.64E-21	Endo
PBX1	1.56E-40	4.56156638	3.70E-36	Endo
ADAMTS7	1.97E-26	4.54960477	4.67E-22	Endo
MID1	7.76E-58	4.54741473	1.84E-53	Endo
EMCN	1.05E-22	4.54246296	2.49E-18	Endo
RNF180	7.10E-23	4.52598417	1.68E-18	Endo
GLT8D2	8.48E-44	4.52393769	2.01E-39	Endo
GP1BA	7.27E-11	4.5024756	1.72E-06	Endo
ACVRL1	8.54E-29	4.49324384	2.02E-24	Endo
SULF2	1.51E-80	4.45738467	3.58E-76	Endo
CASP12	1.33E-13	4.4557196	3.14E-09	Endo
NEURL1B	1.14E-12	4.43708767	2.69E-08	Endo

LIMS3-LOC440895	2.21E-12	4.43118386	5.25E-08	Endo
KCTD12	2.19E-39	4.42626659	5.19E-35	Endo
NTN4	2.07E-15	4.41182451	4.90E-11	Endo
SYNPO	1.38E-50	4.4099691	3.27E-46	Endo
C1QTNF5	1.08E-16	4.40596427	2.57E-12	Endo
MFRP	1.08E-16	4.40596427	2.57E-12	Endo
ITGA9	4.78E-22	4.39567974	1.13E-17	Endo
SMAD1	4.26E-67	4.39565315	1.01E-62	Endo
ADAMTS9-AS2	3.48E-15	4.37792592	8.24E-11	Endo
CHRDL1	6.65E-15	4.37590652	1.58E-10	Endo
GNA14	3.98E-27	4.3674632	9.43E-23	Endo
VEGFC	2.27E-17	4.34798671	5.39E-13	Endo
PLA2R1	1.18E-13	4.34553752	2.79E-09	Endo
KCNIP1	4.53E-17	4.34481598	1.07E-12	Endo
PPARG	6.32E-19	4.33951707	1.50E-14	Endo
B3GNT3	8.76E-12	4.338243	2.07E-07	Endo
TAL1	1.37E-20	4.32672396	3.24E-16	Endo
DOK5	9.46E-31	4.32561348	2.24E-26	Endo
GUCY1A3	1.99E-12	4.3068476	4.71E-08	Endo
FAM171A1	2.24E-40	4.28965718	5.30E-36	Endo
NUAK1	5.01E-20	4.28729453	1.19E-15	Endo
PLA2G4C	1.45E-51	4.27166598	3.43E-47	Endo
LRCOL1	5.69E-10	4.25078257	1.35E-05	Endo
PDGFC	1.12E-15	4.24484853	2.65E-11	Endo
ME3	6.61E-27	4.24288212	1.57E-22	Endo
RHOD	3.16E-19	4.23188108	7.48E-15	Endo
QRICH2	7.68E-15	4.2192611	1.82E-10	Endo
FLT4	6.29E-32	4.21779204	1.49E-27	Endo
MIR3654	4.80E-14	4.21367384	1.14E-09	Endo
C8orf42	1.23E-10	4.19832517	2.90E-06	Endo
GCOM1	1.08E-09	4.19610363	2.56E-05	Endo
NR5A2	8.75E-48	4.19053384	2.07E-43	Endo
DENND2A	1.68E-11	4.18763523	3.98E-07	Endo
NRARP	1.10E-09	4.17838719	2.60E-05	Endo
MEGF6	2.09E-54	4.1562684	4.94E-50	Endo
LOC440895	5.51E-12	4.15247012	1.30E-07	Endo
ELN	3.13E-42	4.14950357	7.40E-38	Endo
KANK3	4.16E-35	4.14677936	9.86E-31	Endo
IL7	1.26E-43	4.14659758	2.99E-39	Endo
ZFPM2	1.84E-17	4.13535109	4.36E-13	Endo
TJP2	2.62E-18	4.13419436	6.20E-14	Endo

PLEKHG5	8.73E-22	4.13042163	2.07E-17	Endo
MAGED4B	1.28E-55	4.12432483	3.04E-51	Endo
BGN	1.03E-60	4.11792094	2.45E-56	Endo
HTRA1	4.04E-45	4.11727544	9.57E-41	Endo
MAGED4	2.44E-54	4.10708799	5.78E-50	Endo
FAM171B	2.45E-16	4.10097436	5.80E-12	Endo
HECW2	2.83E-37	4.09163587	6.71E-33	Endo
ACE	8.24E-12	4.08244679	1.95E-07	Endo
CHST15	7.78E-36	4.07629943	1.84E-31	Endo
KIAA1199	1.24E-14	4.06801746	2.95E-10	Endo
LPHN2	1.80E-16	4.06692529	4.26E-12	Endo
KCNJ8	1.37E-16	4.06535899	3.24E-12	Endo
ACHE	5.01E-17	4.05370414	1.19E-12	Endo
GAS6	1.18E-52	4.05318039	2.79E-48	Endo
IPO11-LRRC70	1.43E-43	4.04541377	3.38E-39	Endo
DKK3	1.52E-48	4.03623392	3.61E-44	Endo
EPHA2	1.20E-35	4.03415964	2.83E-31	Endo
IL34	2.28E-18	4.03406588	5.39E-14	Endo
SPARCL1	9.96E-14	4.02689387	2.36E-09	Endo
DLGAP2	2.22E-13	4.02028722	5.26E-09	Endo
TLR4	1.14E-40	4.01196838	2.71E-36	Endo
PKP1	5.42E-10	4.0063004	1.28E-05	Endo
CDH13	1.54E-21	4.00129118	3.64E-17	Endo
CCRL1	2.69E-12	3.99852541	6.38E-08	Endo
PLEKHA7	4.69E-28	3.99842437	1.11E-23	Endo
TGM2	1.51E-38	3.99132274	3.59E-34	Endo
RAB3IL1	3.20E-10	3.98711935	7.58E-06	Endo
MEOX2	3.35E-27	3.9852734	7.92E-23	Endo
KIAA1462	1.67E-31	3.97946163	3.96E-27	Endo
LRRC15	2.28E-11	3.97939385	5.41E-07	Endo
TRAM1L1	2.93E-09	3.97725276	6.94E-05	Endo
TSPAN15	4.51E-41	3.9735054	1.07E-36	Endo
PDGFA	5.75E-40	3.97236226	1.36E-35	Endo
RND1	1.32E-09	3.9691888	3.13E-05	Endo
ETS2	5.17E-64	3.96207648	1.22E-59	Endo
MEOX1	1.33E-22	3.96107787	3.15E-18	Endo
PRSS48	1.32E-16	3.95773075	3.13E-12	Endo
KLHL3	9.47E-56	3.95322308	2.24E-51	Endo
BEND7	6.13E-10	3.95165433	1.45E-05	Endo
RPS6KA2	3.25E-67	3.95077542	7.69E-63	Endo
SAMD14	1.38E-11	3.9388919	3.28E-07	Endo

TSPAN11	1.78E-33	3.93737185	4.22E-29	Endo
GPR124	2.61E-28	3.93616089	6.18E-24	Endo
CSF2RB	1.74E-54	3.93495216	4.12E-50	Endo
GPM6A	2.67E-10	3.93320295	6.32E-06	Endo
RASGRP3	1.51E-60	3.93042917	3.57E-56	Endo
CNKSR3	9.28E-43	3.93023173	2.20E-38	Endo
HP	3.38E-14	3.92673669	8.00E-10	Endo
EFCAB4A	3.13E-28	3.89645541	7.41E-24	Endo
TSPAN9	3.30E-34	3.88122164	7.82E-30	Endo
PCDHB5	1.35E-10	3.87372237	3.21E-06	Endo
GGT5	1.79E-25	3.87283734	4.25E-21	Endo
THY1	1.50E-44	3.86339436	3.56E-40	Endo
RHOU	1.21E-14	3.85461787	2.86E-10	Endo
TMEM74B	7.20E-11	3.85164324	1.71E-06	Endo
FAM196A	2.56E-15	3.84661176	6.07E-11	Endo
CDA	2.32E-13	3.84169916	5.49E-09	Endo
RARRES2	6.74E-40	3.83889677	1.60E-35	Endo
ZBTB46	3.95E-16	3.82865716	9.36E-12	Endo
AQP1	6.38E-28	3.82570727	1.51E-23	Endo
HYAL2	4.31E-55	3.81811269	1.02E-50	Endo
SLC35G2	2.11E-24	3.81166142	5.00E-20	Endo
HDGFRP3	4.42E-24	3.80889281	1.05E-19	Endo
ADAMTS5	3.58E-12	3.80759848	8.49E-08	Endo
NFIB	1.79E-49	3.80324911	4.23E-45	Endo
NYNRIN	7.75E-18	3.79830371	1.84E-13	Endo
LRP5	3.64E-24	3.79785089	8.62E-20	Endo
ADAMTSL1	1.77E-21	3.79688036	4.19E-17	Endo
TMEM204	2.95E-63	3.78949912	6.99E-59	Endo
PHLDB2	3.57E-42	3.78788745	8.45E-38	Endo
ADAM23	4.41E-13	3.78564513	1.05E-08	Endo
RUNX1T1	9.54E-22	3.7774954	2.26E-17	Endo
TCF7L1	3.70E-29	3.77645948	8.75E-25	Endo
C17orf67	2.98E-14	3.77595148	7.06E-10	Endo
ID1	1.33E-47	3.7729531	3.15E-43	Endo
CCL2	1.54E-34	3.76538715	3.66E-30	Endo
PTGDS	3.83E-11	3.75744741	9.06E-07	Endo
DSP	1.02E-51	3.75598652	2.42E-47	Endo
NMNAT2	1.43E-09	3.73394388	3.40E-05	Endo
PLGLA	1.75E-12	3.73371813	4.15E-08	Endo
ITGA5	4.22E-72	3.73304733	1.00E-67	Endo
PGF	1.01E-16	3.73240685	2.39E-12	Endo

NINL	3.98E-35	3.72627262	9.43E-31	Endo
FLI1-AS1	6.54E-14	3.72611565	1.55E-09	Endo
HOXD8	5.12E-18	3.7194618	1.21E-13	Endo
SPNS2	1.09E-21	3.7173676	2.58E-17	Endo
PLCE1	9.03E-20	3.70396605	2.14E-15	Endo
MMRN2	1.03E-13	3.70199536	2.44E-09	Endo
CD36	5.24E-22	3.69265043	1.24E-17	Endo
TMEM44	4.20E-12	3.68984691	9.95E-08	Endo
FBN1	1.98E-51	3.6821688	4.69E-47	Endo
SLC40A1	2.64E-50	3.67564712	6.25E-46	Endo
PM20D1	1.19E-33	3.66880774	2.81E-29	Endo
SOCS2	5.77E-32	3.66013615	1.37E-27	Endo
ALDH2	4.35E-49	3.65666434	1.03E-44	Endo
NOTCH4	4.26E-12	3.65220126	1.01E-07	Endo
PPIC	6.02E-55	3.65152267	1.43E-50	Endo
P2RY6	2.89E-10	3.65017426	6.84E-06	Endo
C1orf115	2.23E-17	3.6176511	5.29E-13	Endo
ROBO3	6.28E-16	3.61563565	1.49E-11	Endo
FAM198B	9.66E-35	3.61550001	2.29E-30	Endo
NR2F2	1.65E-38	3.61524591	3.90E-34	Endo
PLXNA4	7.18E-19	3.6033431	1.70E-14	Endo
TNFAIP2	6.88E-27	3.58909879	1.63E-22	Endo
COL18A1	1.97E-38	3.58616221	4.67E-34	Endo
SLC52A3	2.54E-11	3.58512194	6.02E-07	Endo
TMEM88	2.44E-14	3.58024904	5.78E-10	Endo
THBS1	2.86E-45	3.5777212	6.78E-41	Endo
PCSK6	1.19E-26	3.57665345	2.83E-22	Endo
JAG2	2.51E-13	3.57292104	5.94E-09	Endo
PCDH1	1.53E-13	3.55756059	3.62E-09	Endo
IGFBP4	4.85E-62	3.55332898	1.15E-57	Endo
FBXL7	1.97E-18	3.52474191	4.66E-14	Endo
NOS3	2.47E-17	3.52118988	5.85E-13	Endo
ARHGAP23	6.38E-28	3.51327642	1.51E-23	Endo
RAB11FIP5	2.92E-23	3.50648286	6.91E-19	Endo
HHEX	2.27E-33	3.50479318	5.37E-29	Endo
FSCN1	4.03E-42	3.4930958	9.55E-38	Endo
ENG	2.83E-47	3.47874586	6.71E-43	Endo
JUP	5.25E-38	3.47611758	1.24E-33	Endo
DPYSL3	8.02E-29	3.47502306	1.90E-24	Endo
PPP1R13B	3.10E-27	3.45888427	7.34E-23	Endo
LRRC32	1.96E-23	3.45661998	4.64E-19	Endo

FOXP2	3.22E-13	3.45520554	7.63E-09	Endo
CXCL2	3.31E-26	3.45464227	7.84E-22	Endo
PRICKLE4	2.06E-16	3.45093307	4.88E-12	Endo
CRTAC1	6.13E-10	3.44354879	1.45E-05	Endo
BDKRB2	7.37E-14	3.43878507	1.75E-09	Endo
PPAP2B	1.33E-38	3.4373263	3.14E-34	Endo
PLSCR4	5.99E-29	3.43539657	1.42E-24	Endo
LAMA5	2.18E-21	3.43444991	5.17E-17	Endo
CFH	2.82E-25	3.43254585	6.68E-21	Endo
SLC16A14	1.06E-14	3.42865568	2.50E-10	Endo
EPHB1	6.31E-10	3.4263557	1.49E-05	Endo
AKR1C3	2.85E-42	3.42008208	6.75E-38	Endo
RGS16	4.66E-32	3.4159014	1.10E-27	Endo
SLCO2B1	2.95E-16	3.41547805	6.98E-12	Endo
C1R	1.23E-49	3.41242361	2.91E-45	Endo
PIEZO2	6.26E-12	3.41136923	1.48E-07	Endo
RAI14	2.42E-41	3.393722	5.73E-37	Endo
PROCR	2.39E-22	3.39132386	5.67E-18	Endo
LOC650226	1.94E-24	3.38330381	4.60E-20	Endo
RAI2	2.76E-13	3.37364231	6.53E-09	Endo
RHOJ	8.21E-35	3.3694633	1.94E-30	Endo
ZFP28	1.89E-10	3.36641519	4.49E-06	Endo
MCTP1	1.01E-19	3.36067907	2.39E-15	Endo
HOXD1	2.76E-12	3.35723351	6.55E-08	Endo
TCF4	1.28E-50	3.34764287	3.04E-46	Endo
CDC42EP2	2.80E-21	3.33729944	6.62E-17	Endo
BCAR1	1.67E-26	3.33011872	3.96E-22	Endo
RBP5	4.99E-12	3.30843073	1.18E-07	Endo
GPX3	7.21E-31	3.3076419	1.71E-26	Endo
GIMAP8	1.02E-51	3.3055617	2.41E-47	Endo
PTPRB	3.71E-19	3.29367697	8.80E-15	Endo
MGST2	1.24E-40	3.293162	2.94E-36	Endo
TM6SF1	3.26E-14	3.29127355	7.71E-10	Endo
AKR1C1	8.00E-17	3.29008961	1.90E-12	Endo
KIF26B	2.72E-12	3.28330444	6.45E-08	Endo
EPAS1	1.17E-37	3.27751503	2.77E-33	Endo
PDLIM1	8.06E-54	3.27655668	1.91E-49	Endo
HEPH	3.43E-13	3.2755499	8.11E-09	Endo
SERPING1	1.14E-39	3.27502364	2.71E-35	Endo
COX7A1	3.62E-25	3.26753292	8.58E-21	Endo
TMEM176B	5.15E-26	3.2661386	1.22E-21	Endo

MFAP4	4.59E-20	3.26587577	1.09E-15	Endo
F8	4.73E-30	3.26264627	1.12E-25	Endo
LPHN1	2.91E-11	3.26007885	6.90E-07	Endo
CRIM1	1.87E-50	3.25679161	4.42E-46	Endo
MAN1A1	7.46E-24	3.2560023	1.77E-19	Endo
FAM189A2	1.90E-11	3.24178951	4.50E-07	Endo
SLC9A3R2	6.72E-10	3.2409721	1.59E-05	Endo
TACSTD2	3.44E-12	3.21347659	8.14E-08	Endo
TNS1	4.85E-41	3.2093309	1.15E-36	Endo
UBTD1	1.13E-13	3.20634235	2.67E-09	Endo
STON2	5.85E-10	3.20445794	1.39E-05	Endo
PLXDC2	1.22E-38	3.20350647	2.88E-34	Endo
TEAD4	1.12E-15	3.19875713	2.66E-11	Endo
IL1R1	2.03E-19	3.19632798	4.81E-15	Endo
CNTNAP3	1.17E-17	3.19519795	2.76E-13	Endo
CNRIP1	7.78E-34	3.19455532	1.84E-29	Endo
CXorf36	1.34E-29	3.18923633	3.17E-25	Endo
MGLL	6.89E-33	3.18196723	1.63E-28	Endo
DOCK9	4.65E-42	3.16782265	1.10E-37	Endo
PVRL2	1.12E-31	3.15646057	2.64E-27	Endo
NRN1	8.05E-22	3.13873723	1.91E-17	Endo
CTIF	1.35E-18	3.13132156	3.20E-14	Endo
CCDC80	1.46E-27	3.13056417	3.46E-23	Endo
DDAH1	7.20E-25	3.12483713	1.70E-20	Endo
SCARA3	6.38E-18	3.12191368	1.51E-13	Endo
MIR4426	3.49E-09	3.10114283	8.27E-05	Endo
LAYN	5.08E-25	3.09851357	1.20E-20	Endo
SH3BGRL2	5.05E-18	3.09019154	1.20E-13	Endo
DNM3	3.48E-09	3.07234176	8.24E-05	Endo
NPDC1	1.49E-32	3.06616946	3.52E-28	Endo
PRTFDC1	3.89E-09	3.06241145	9.22E-05	Endo
TNFRSF10D	5.65E-17	3.06077013	1.34E-12	Endo
ABI3BP	3.30E-20	3.05887156	7.83E-16	Endo
MYO15B	5.19E-29	3.05882744	1.23E-24	Endo
STC2	6.28E-15	3.05439249	1.49E-10	Endo
CFI	3.72E-43	3.0501826	8.82E-39	Endo
PRKAR1B	1.57E-28	3.04566243	3.72E-24	Endo
CDH11	6.89E-14	3.03759323	1.63E-09	Endo
CNTNAP3B	1.44E-19	3.03280912	3.41E-15	Endo
MMP2	4.61E-23	3.03104691	1.09E-18	Endo
PRUNE2	3.84E-11	3.01896486	9.09E-07	Endo

ANGPTL2	1.00E-29	3.01349496	2.38E-25	Endo
UBD	1.83E-24	3.00027285	4.34E-20	Endo
MALL	3.08E-16	2.99764998	7.30E-12	Endo
EPHB2	1.95E-09	2.98844605	4.62E-05	Endo
TPBG	4.91E-17	2.95831147	1.16E-12	Endo
ITGA1	1.52E-22	2.95626291	3.61E-18	Endo
EHD2	1.52E-26	2.95597629	3.60E-22	Endo
SHE	4.98E-13	2.95302996	1.18E-08	Endo
HSPG2	5.98E-30	2.95275755	1.42E-25	Endo
NEIL1	6.23E-22	2.9519424	1.48E-17	Endo
OAF	2.54E-11	2.95022578	6.01E-07	Endo
SLC22A23	4.08E-15	2.94383363	9.68E-11	Endo
RAPGEF5	1.57E-27	2.92225051	3.72E-23	Endo
ARAP3	1.43E-16	2.92160068	3.38E-12	Endo
RALGAPA2	5.76E-34	2.92024492	1.37E-29	Endo
ID3	3.30E-32	2.91135034	7.81E-28	Endo
LOX	1.67E-11	2.90994942	3.97E-07	Endo
PDK4	3.00E-15	2.89028789	7.10E-11	Endo
COL6A2	6.17E-31	2.88380177	1.46E-26	Endo
ABLIM3	2.67E-22	2.86225284	6.31E-18	Endo
FILIP1L	2.93E-25	2.85725653	6.95E-21	Endo
PLAC9	3.83E-11	2.85546338	9.08E-07	Endo
FHL1	8.19E-22	2.85245519	1.94E-17	Endo
DNMBP	1.53E-22	2.84386767	3.61E-18	Endo
PDLIM3	1.11E-11	2.84130025	2.62E-07	Endo
CCDC102B	5.18E-13	2.83975929	1.23E-08	Endo
CASKIN2	4.88E-12	2.82826885	1.16E-07	Endo
SLC43A2	1.21E-14	2.82627726	2.87E-10	Endo
MID2	2.56E-16	2.82254539	6.05E-12	Endo
LIMS2	7.47E-21	2.81207983	1.77E-16	Endo
SLCO3A1	1.28E-14	2.80757172	3.04E-10	Endo
RASIP1	4.11E-11	2.80482788	9.73E-07	Endo
TP53I11	3.89E-21	2.80352854	9.21E-17	Endo
PLXND1	3.13E-29	2.79713134	7.41E-25	Endo
BMX	5.49E-14	2.79701331	1.30E-09	Endo
CYR61	1.88E-23	2.79328966	4.45E-19	Endo
C1S	2.64E-16	2.77429363	6.26E-12	Endo
VSIG10	2.40E-10	2.76821476	5.69E-06	Endo
IL15RA	2.63E-19	2.76808054	6.24E-15	Endo
NREP	1.52E-24	2.76364929	3.60E-20	Endo
S1PR1	7.44E-44	2.76291543	1.76E-39	Endo

SPHK1	1.17E-22	2.76069231	2.76E-18	Endo
PPP1R13L	5.23E-11	2.75717222	1.24E-06	Endo
ARHGAP28	1.54E-11	2.75551526	3.65E-07	Endo
FES	1.47E-14	2.75037562	3.48E-10	Endo
MLLT4	2.34E-24	2.74911504	5.54E-20	Endo
LTBP1	4.84E-10	2.74523126	1.15E-05	Endo
TMEM246	1.68E-11	2.74076405	3.97E-07	Endo
EFNA1	3.79E-26	2.73600352	8.97E-22	Endo
AFAP1L1	3.03E-19	2.73577337	7.18E-15	Endo
CEP112	1.49E-19	2.73525051	3.52E-15	Endo
NDST1	4.70E-21	2.7308009	1.11E-16	Endo
KIAA1217	3.11E-23	2.72921139	7.38E-19	Endo
PECAM1	1.52E-27	2.72900295	3.60E-23	Endo
LOC375295	4.56E-11	2.72613391	1.08E-06	Endo
PLCB4	9.14E-12	2.72143358	2.17E-07	Endo
TGFB1I1	1.60E-22	2.72071144	3.79E-18	Endo
Mar-03	1.05E-13	2.70126566	2.48E-09	Endo
LTBP2	1.10E-09	2.68454172	2.61E-05	Endo
APP	1.44E-39	2.67220975	3.40E-35	Endo
PKN3	3.48E-11	2.65393856	8.25E-07	Endo
ASS1	6.77E-10	2.65287876	1.60E-05	Endo
RBP1	6.12E-11	2.65025379	1.45E-06	Endo
RBPMS	7.10E-16	2.65016547	1.68E-11	Endo
THBD	3.95E-24	2.64184216	9.36E-20	Endo
EPB41L4A	1.06E-18	2.63377767	2.52E-14	Endo
NID1	6.25E-31	2.62782978	1.48E-26	Endo
POSTN	4.61E-11	2.62638478	1.09E-06	Endo
TNFSF10	3.47E-30	2.61774639	8.23E-26	Endo
HEG1	2.14E-17	2.6137873	5.06E-13	Endo
MARCKS	3.95E-29	2.60207791	9.35E-25	Endo
C10orf11	2.92E-09	2.59371809	6.93E-05	Endo
MGP	2.86E-24	2.58899642	6.76E-20	Endo
TP53I3	1.08E-14	2.58549005	2.56E-10	Endo
TBC1D9	1.79E-12	2.57765016	4.25E-08	Endo
DYNC1I1	2.66E-10	2.5630158	6.31E-06	Endo
MICAL2	1.38E-22	2.55622765	3.26E-18	Endo
NEDD4	6.60E-10	2.55447853	1.56E-05	Endo
ABCA3	1.87E-12	2.54858336	4.42E-08	Endo
CFB	1.39E-10	2.52478686	3.30E-06	Endo
EXD3	2.20E-09	2.52399702	5.20E-05	Endo
JAG1	1.44E-12	2.50704001	3.41E-08	Endo

LATS2	6.46E-17	2.49580715	1.53E-12	Endo
LAMB1	7.87E-29	2.4935597	1.86E-24	Endo
PLD2	7.88E-13	2.49213385	1.87E-08	Endo
SLC25A29	2.49E-10	2.47716917	5.89E-06	Endo
LOXL2	9.01E-18	2.47526437	2.13E-13	Endo
TSPAN5	4.73E-19	2.47524069	1.12E-14	Endo
TUBB6	4.07E-30	2.47457349	9.63E-26	Endo
WFS1	9.69E-13	2.47205799	2.30E-08	Endo
FAM174B	1.66E-13	2.47134825	3.92E-09	Endo
LMCD1	6.57E-13	2.4672614	1.56E-08	Endo
USP31	5.71E-13	2.46722046	1.35E-08	Endo
SH2D3C	6.73E-32	2.46024972	1.59E-27	Endo
CDC42BPB	1.62E-13	2.45889198	3.84E-09	Endo
SCARF1	1.37E-14	2.44885805	3.25E-10	Endo
TSPAN7	5.94E-26	2.4433798	1.41E-21	Endo
GRAPL	3.79E-13	2.44265277	8.97E-09	Endo
SOX7	4.55E-12	2.42843949	1.08E-07	Endo
LHFP	9.42E-30	2.42757317	2.23E-25	Endo
NT5E	6.35E-12	2.41858373	1.50E-07	Endo
NRP1	2.08E-09	2.40054293	4.92E-05	Endo
SEMA4C	8.46E-12	2.39876392	2.00E-07	Endo
C10orf10	7.93E-10	2.38693335	1.88E-05	Endo
TMCO3	8.04E-12	2.37267071	1.90E-07	Endo
TNFAIP1	1.67E-20	2.36425643	3.97E-16	Endo
ANKRD20A5P	2.35E-13	2.35799057	5.57E-09	Endo
CLU	1.24E-22	2.35604192	2.94E-18	Endo
RIN2	9.01E-18	2.35584235	2.13E-13	Endo
ABCG1	3.33E-21	2.35238453	7.89E-17	Endo
CRYBG3	1.26E-09	2.3488474	2.97E-05	Endo
FAM43A	9.35E-17	2.34781208	2.21E-12	Endo
MAP1LC3A	3.16E-21	2.34557908	7.48E-17	Endo
AGPAT4	8.47E-12	2.32905358	2.01E-07	Endo
ALDH1A3	3.44E-17	2.32741054	8.15E-13	Endo
IGFBP7	1.59E-33	2.32713337	3.76E-29	Endo
CTTNBP2NL	2.69E-17	2.32430303	6.38E-13	Endo
FLNB	2.54E-23	2.31725778	6.02E-19	Endo
SFRP1	2.88E-13	2.31631339	6.82E-09	Endo
SEMA6A	2.81E-20	2.31469404	6.66E-16	Endo
PRCP	6.30E-30	2.31110556	1.49E-25	Endo
LOC100506178	2.42E-09	2.29858878	5.73E-05	Endo
GRPEL2	6.88E-13	2.2975379	1.63E-08	Endo

LYN	6.31E-17	2.29559279	1.49E-12	Endo
LOC100505495	1.80E-15	2.28852795	4.27E-11	Endo
ARHGEF12	2.63E-15	2.28599855	6.23E-11	Endo
FCGRT	3.34E-29	2.27581854	7.92E-25	Endo
GPR68	2.76E-13	2.27017872	6.55E-09	Endo
MVB12B	1.27E-09	2.26620884	3.00E-05	Endo
NNMT	1.52E-29	2.26205728	3.61E-25	Endo
COL5A2	5.40E-11	2.2571903	1.28E-06	Endo
SH3TC1	3.19E-19	2.25707196	7.55E-15	Endo
FRMD4B	8.15E-17	2.25446339	1.93E-12	Endo
CCBP2	5.26E-14	2.24127322	1.25E-09	Endo
NOD1	2.53E-10	2.22596309	6.00E-06	Endo
LAMC1	1.61E-17	2.22445474	3.80E-13	Endo
ABCA1	6.23E-10	2.22428676	1.47E-05	Endo
TSHZ1	1.86E-09	2.20633632	4.42E-05	Endo
ARRB1	1.71E-12	2.19054612	4.06E-08	Endo
VCAN	8.10E-10	2.18605794	1.92E-05	Endo
CELSR1	1.96E-10	2.18182459	4.65E-06	Endo
DOCK1	2.50E-10	2.17918676	5.93E-06	Endo
NFIA	3.54E-23	2.17909515	8.39E-19	Endo
TINAGL1	5.07E-10	2.17102409	1.20E-05	Endo
PLCD1	2.07E-12	2.16555495	4.91E-08	Endo
SMTN	1.65E-09	2.16112936	3.91E-05	Endo
RGS3	9.55E-21	2.15842764	2.26E-16	Endo
TANC2	1.70E-09	2.15176169	4.02E-05	Endo
PTRF	2.57E-22	2.15125619	6.10E-18	Endo
NUPR1	3.04E-11	2.14599626	7.20E-07	Endo
LIMS3	4.51E-10	2.14350864	1.07E-05	Endo
LIMS3L	4.83E-10	2.14113061	1.15E-05	Endo
HAPLN3	5.40E-20	2.14095258	1.28E-15	Endo
PPM1F	7.67E-17	2.13766994	1.82E-12	Endo
FLI1	7.80E-24	2.1356654	1.85E-19	Endo
ITPRIP	2.00E-15	2.13421525	4.74E-11	Endo
RNASE1	2.63E-09	2.13192	6.23E-05	Endo
FN1	4.87E-23	2.13091534	1.15E-18	Endo
ICAM2	1.16E-20	2.12731301	2.75E-16	Endo
TENC1	2.22E-17	2.11016544	5.25E-13	Endo
ST6GALNAC3	1.91E-09	2.10545187	4.51E-05	Endo
AKAP12	4.88E-11	2.09672796	1.16E-06	Endo
TGFBR3	6.68E-14	2.09271475	1.58E-09	Endo
BCR	4.73E-16	2.0848369	1.12E-11	Endo

MPDZ	4.58E-13	2.07385963	1.09E-08	Endo
S100A16	6.26E-29	2.07179925	1.48E-24	Endo
GRAP	1.49E-15	2.07167092	3.53E-11	Endo
HSD3B7	9.95E-10	2.05724966	2.36E-05	Endo
RPGR	1.28E-11	2.04901142	3.02E-07	Endo
WWTR1	9.01E-22	2.0463772	2.13E-17	Endo
TXNDC5	1.14E-12	2.04451093	2.69E-08	Endo
CRIP2	7.18E-26	2.03501767	1.70E-21	Endo
CD302	4.87E-10	2.01874774	1.15E-05	Endo
ZFYVE21	6.97E-15	2.01763463	1.65E-10	Endo
PTPRE	8.22E-14	2.00393397	1.95E-09	Endo
PPAP2A	2.07E-12	2.00198269	4.89E-08	Endo
MIR618	1.04E-21	9.7112127	2.47E-17	Macrophage
IL36G	2.07E-11	9.31281514	4.91E-07	Macrophage
MIR3945	1.04E-21	9.2593949	2.47E-17	Macrophage
SPAG11A	1.04E-21	9.16948409	2.47E-17	Macrophage
SNORA36A	1.04E-21	8.84735519	2.47E-17	Macrophage
CD163	6.87E-185	8.83577748	1.63E-180	Macrophage
DEFB1	1.04E-21	8.66712698	2.47E-17	Macrophage
CLEC6A	8.46E-42	8.62278031	2.00E-37	Macrophage
CD300LD	1.04E-21	8.49436146	2.47E-17	Macrophage
ASGR2	7.29E-57	8.45759817	1.73E-52	Macrophage
IGSF21	8.46E-42	8.29674051	2.00E-37	Macrophage
GPR84	5.35E-123	8.22746988	1.27E-118	Macrophage
VSIG4	8.53E-123	8.13217402	2.02E-118	Macrophage
FCGR1A	1.12E-137	7.91517151	2.65E-133	Macrophage
CD300LF	1.92E-72	7.8704146	4.55E-68	Macrophage
HCAR2	2.28E-91	7.81991942	5.40E-87	Macrophage
NR1I3	1.04E-21	7.77585428	2.47E-17	Macrophage
RNASE2	9.77E-57	7.75466705	2.31E-52	Macrophage
FCN1	1.63E-82	7.70717362	3.86E-78	Macrophage
AQP9	1.46E-76	7.69946593	3.46E-72	Macrophage
OR2B11	3.24E-73	7.6814885	7.66E-69	Macrophage
HCAR3	2.42E-88	7.66457125	5.73E-84	Macrophage
S100A12	1.66E-39	7.61727176	3.94E-35	Macrophage
FOLR2	6.76E-50	7.59498464	1.60E-45	Macrophage
SIGLEC1	1.38E-47	7.53709978	3.28E-43	Macrophage
F13A1	2.85E-93	7.46992368	6.75E-89	Macrophage
CCL13	2.07E-11	7.45138227	4.91E-07	Macrophage
CACNA2D3	3.04E-43	7.44335279	7.20E-39	Macrophage
CCL8	2.81E-31	7.43757639	6.66E-27	Macrophage

C19orf59	9.62E-43	7.36572935	2.28E-38	Macrophage
CCKAR	1.04E-21	7.28375934	2.47E-17	Macrophage
MS4A4A	2.73E-94	7.25887767	6.46E-90	Macrophage
CSF1R	1.50E-129	7.21471377	3.56E-125	Macrophage
LINC00433	1.04E-21	7.20247328	2.47E-17	Macrophage
FCGR1C	3.93E-81	7.2010485	9.31E-77	Macrophage
CD300C	4.33E-61	7.17784251	1.03E-56	Macrophage
OCM2	2.07E-11	7.15140704	4.91E-07	Macrophage
HK3	2.01E-97	7.13823005	4.76E-93	Macrophage
SLCO2B1	4.89E-86	7.1136783	1.16E-81	Macrophage
LIPN	4.17E-73	7.09807298	9.87E-69	Macrophage
FPR3	3.42E-88	7.08279158	8.11E-84	Macrophage
LGALS16	2.07E-11	7.07712083	4.91E-07	Macrophage
CD300LB	6.51E-72	7.04114823	1.54E-67	Macrophage
IL1RN	1.88E-117	7.01518933	4.45E-113	Macrophage
MARCO	3.53E-43	6.96025795	8.35E-39	Macrophage
RETN	4.58E-51	6.95898522	1.09E-46	Macrophage
C1QA	2.36E-93	6.9568477	5.59E-89	Macrophage
TTTY12	1.04E-21	6.9292226	2.47E-17	Macrophage
CLEC4D	6.95E-27	6.92304789	1.65E-22	Macrophage
SDS	1.15E-42	6.91894099	2.71E-38	Macrophage
IL1B	6.53E-115	6.91767886	1.55E-110	Macrophage
OLR1	2.98E-82	6.90893061	7.05E-78	Macrophage
C1orf127	2.07E-11	6.89755818	4.91E-07	Macrophage
CEACAM4	2.15E-55	6.8723285	5.10E-51	Macrophage
CSF3R	4.71E-105	6.87131882	1.12E-100	Macrophage
FPR2	1.06E-74	6.86863403	2.50E-70	Macrophage
LILRB4	9.36E-147	6.86008455	2.22E-142	Macrophage
TNFSF12-TNFSF13	1.64E-14	6.85037633	3.87E-10	Macrophage
DSC2	2.74E-52	6.81509942	6.49E-48	Macrophage
LGALS2	3.62E-66	6.79614483	8.56E-62	Macrophage
MSR1	8.26E-86	6.77272216	1.96E-81	Macrophage
CLEC10A	4.01E-75	6.76161059	9.49E-71	Macrophage
LILRA3	8.53E-65	6.75244875	2.02E-60	Macrophage
C1QC	7.99E-79	6.71568633	1.89E-74	Macrophage
CXCL9	2.51E-17	6.6881297	5.95E-13	Macrophage
RGS18	3.74E-86	6.66747239	8.86E-82	Macrophage
CD1B	3.21E-17	6.65467329	7.60E-13	Macrophage
SIGLEC12	4.48E-41	6.64831313	1.06E-36	Macrophage
HCK	1.57E-121	6.63848407	3.72E-117	Macrophage
FPR1	7.91E-112	6.62808398	1.87E-107	Macrophage

C15orf48	1.63E-74	6.61792396	3.85E-70	Macrophage
TREM1	7.34E-101	6.60539075	1.74E-96	Macrophage
FCGR1B	2.06E-81	6.58810655	4.87E-77	Macrophage
ECRP	2.07E-11	6.55632779	4.91E-07	Macrophage
EMR3	5.67E-21	6.54253706	1.34E-16	Macrophage
SUPT20HL2	2.07E-11	6.53370259	4.91E-07	Macrophage
CHST13	1.75E-14	6.52381957	4.16E-10	Macrophage
CGB7	2.07E-11	6.51953516	4.91E-07	Macrophage
S100A9	1.58E-114	6.51903045	3.73E-110	Macrophage
CD14	9.59E-86	6.49797725	2.27E-81	Macrophage
CARD9	2.78E-54	6.49282168	6.59E-50	Macrophage
SNORD23	2.19E-11	6.48943149	5.18E-07	Macrophage
OR6C2	2.19E-11	6.48224654	5.18E-07	Macrophage
LILRA2	6.38E-63	6.47701559	1.51E-58	Macrophage
IL27	3.29E-31	6.42888355	7.80E-27	Macrophage
APOBEC3A-B	6.29E-16	6.3933029	1.49E-11	Macrophage
LILRA1	2.43E-65	6.36543806	5.75E-61	Macrophage
OR51L1	2.19E-11	6.35310457	5.18E-07	Macrophage
CCDC105	2.19E-11	6.35164472	5.18E-07	Macrophage
CXCL3	3.27E-60	6.31537649	7.73E-56	Macrophage
CLEC5A	1.72E-27	6.31032048	4.07E-23	Macrophage
LILRB2	1.79E-46	6.3019252	4.24E-42	Macrophage
DNAAF1	1.56E-56	6.28467793	3.69E-52	Macrophage
FBP1	5.79E-72	6.26925143	1.37E-67	Macrophage
CAPNS2	3.49E-17	6.2361179	8.27E-13	Macrophage
CXCR2P1	1.95E-18	6.16424476	4.61E-14	Macrophage
TLR8	3.99E-30	6.15674028	9.44E-26	Macrophage
AZU1	2.19E-11	6.15136065	5.18E-07	Macrophage
SAG	2.19E-11	6.1398709	5.18E-07	Macrophage
PILRA	4.77E-75	6.13386313	1.13E-70	Macrophage
VSTM1	3.35E-17	6.09735095	7.93E-13	Macrophage
PLB1	3.76E-33	6.07119832	8.91E-29	Macrophage
TFEC	1.37E-94	6.07064044	3.25E-90	Macrophage
CSTA	9.21E-81	6.06826206	2.18E-76	Macrophage
HAMP	7.95E-27	6.05534746	1.88E-22	Macrophage
TREM2	2.30E-28	5.9592666	5.44E-24	Macrophage
LOC100128568	3.35E-17	5.93772189	7.93E-13	Macrophage
PADI6	1.65E-12	5.92583945	3.91E-08	Macrophage
PADI4	1.65E-12	5.90973205	3.91E-08	Macrophage
KCNMB1	1.20E-48	5.90199283	2.84E-44	Macrophage
CFP	7.71E-32	5.8834113	1.83E-27	Macrophage

IL1A	1.42E-49	5.87027326	3.35E-45	Macrophage
GPBAR1	2.09E-11	5.86193572	4.95E-07	Macrophage
GPR162	4.90E-11	5.85544389	1.16E-06	Macrophage
SEMA6B	1.68E-24	5.85398547	3.99E-20	Macrophage
PRAM1	3.70E-56	5.84214599	8.75E-52	Macrophage
FCGR3B	6.26E-48	5.8277215	1.48E-43	Macrophage
OR52K1	1.88E-14	5.79574866	4.46E-10	Macrophage
CCDC164	1.70E-12	5.78455349	4.03E-08	Macrophage
SIGLEC9	3.89E-38	5.77076414	9.22E-34	Macrophage
RAB20	1.02E-59	5.76870113	2.41E-55	Macrophage
C19orf38	1.30E-49	5.75976317	3.08E-45	Macrophage
G0S2	8.45E-57	5.74327741	2.00E-52	Macrophage
ASGR1	9.17E-40	5.74237423	2.17E-35	Macrophage
ST14	7.36E-27	5.71076313	1.74E-22	Macrophage
S100A8	1.68E-50	5.69886829	3.97E-46	Macrophage
ICAM5	5.67E-21	5.6776476	1.34E-16	Macrophage
MNDA	3.20E-91	5.661849	7.57E-87	Macrophage
IGSF6	8.82E-63	5.6526164	2.09E-58	Macrophage
CMKLR1	3.40E-28	5.61966393	8.04E-24	Macrophage
SLC7A7	8.01E-62	5.54676014	1.90E-57	Macrophage
CD1E	1.41E-23	5.53639156	3.35E-19	Macrophage
CPA6	1.70E-12	5.52457931	4.03E-08	Macrophage
TLR2	1.15E-39	5.52032079	2.73E-35	Macrophage
SIGLEC7	5.21E-43	5.49775767	1.23E-38	Macrophage
P2RY13	1.07E-31	5.49484364	2.55E-27	Macrophage
NLRC4	2.40E-21	5.48727444	5.67E-17	Macrophage
VMO1	6.69E-32	5.46715499	1.59E-27	Macrophage
SLED1	4.42E-22	5.46350897	1.05E-17	Macrophage
OR52K2	1.88E-14	5.46267555	4.46E-10	Macrophage
GGTA1P	3.49E-18	5.43626614	8.27E-14	Macrophage
CGB8	2.19E-11	5.40649841	5.18E-07	Macrophage
CLEC4A	4.15E-63	5.38340316	9.82E-59	Macrophage
GSTO2	4.05E-10	5.36947034	9.60E-06	Macrophage
CD86	4.17E-98	5.35012249	9.87E-94	Macrophage
GRIN2C	4.05E-10	5.33366166	9.60E-06	Macrophage
CECR6	5.16E-11	5.33105511	1.22E-06	Macrophage
C3AR1	4.56E-63	5.31217114	1.08E-58	Macrophage
TNFSF13	3.01E-55	5.28296637	7.14E-51	Macrophage
CXCL10	2.70E-28	5.26584517	6.39E-24	Macrophage
MRC1	3.83E-40	5.26416519	9.08E-36	Macrophage
IL4I1	6.67E-31	5.22075803	1.58E-26	Macrophage

EMR1	6.50E-19	5.2183469	1.54E-14	Macrophage
TYROBP	5.55E-75	5.19688665	1.31E-70	Macrophage
SLC11A1	3.64E-18	5.19030597	8.61E-14	Macrophage
ZNF385A	7.07E-27	5.18732432	1.67E-22	Macrophage
TMEM176A	1.35E-58	5.18146652	3.19E-54	Macrophage
RGAG4	1.28E-14	5.17419582	3.04E-10	Macrophage
ADAP2	9.70E-29	5.17300983	2.30E-24	Macrophage
ADRA2B	3.53E-23	5.16895409	8.36E-19	Macrophage
PRAMEF8	2.19E-11	5.15135291	5.18E-07	Macrophage
CXCL2	1.12E-41	5.14697724	2.65E-37	Macrophage
IL8	7.91E-38	5.13165527	1.87E-33	Macrophage
TMEM176B	3.30E-41	5.12396659	7.82E-37	Macrophage
STAC3	1.94E-17	5.11690997	4.59E-13	Macrophage
NCF2	3.59E-46	5.1157404	8.50E-42	Macrophage
FCGR3A	1.63E-69	5.08730905	3.86E-65	Macrophage
P2RY6	1.84E-25	5.08693194	4.35E-21	Macrophage
MLXIPL	5.73E-11	5.08269803	1.36E-06	Macrophage
SLC8A1-AS1	3.74E-17	5.06712766	8.86E-13	Macrophage
LOC100288432	1.30E-16	5.03996751	3.08E-12	Macrophage
ANKRD22	9.92E-10	4.99547976	2.35E-05	Macrophage
PLXDC2	1.14E-56	4.98379749	2.69E-52	Macrophage
AIF1	2.97E-69	4.97542159	7.04E-65	Macrophage
MS4A6A	5.53E-62	4.97225491	1.31E-57	Macrophage
MS4A14	9.68E-27	4.93887465	2.29E-22	Macrophage
LOC100506585	9.49E-30	4.93281722	2.25E-25	Macrophage
STAB1	2.41E-51	4.92185287	5.70E-47	Macrophage
GNA15	2.67E-32	4.92049741	6.33E-28	Macrophage
LINC00515	5.58E-12	4.92013012	1.32E-07	Macrophage
SPI1	1.89E-39	4.89121996	4.49E-35	Macrophage
ITGAM	1.29E-41	4.89012105	3.06E-37	Macrophage
FCER1G	1.13E-57	4.88438357	2.68E-53	Macrophage
SLAMF8	4.89E-46	4.85763783	1.16E-41	Macrophage
CYP2S1	2.27E-19	4.78361145	5.37E-15	Macrophage
LST1	4.11E-57	4.73502067	9.74E-53	Macrophage
PTGS2	1.24E-23	4.65965623	2.94E-19	Macrophage
CHGA	2.04E-12	4.65588441	4.82E-08	Macrophage
CFD	2.32E-34	4.65495835	5.50E-30	Macrophage
C6orf223	1.48E-14	4.65373535	3.51E-10	Macrophage
PTGS1	2.83E-28	4.64550836	6.71E-24	Macrophage
C5AR1	1.55E-18	4.61461201	3.66E-14	Macrophage
TDRD9	6.52E-12	4.61417438	1.54E-07	Macrophage

LILRA5	1.01E-18	4.61286631	2.38E-14	Macrophage
CRB2	9.76E-13	4.60082424	2.31E-08	Macrophage
MAFB	2.77E-34	4.59261118	6.55E-30	Macrophage
CLEC12A	3.36E-18	4.59237527	7.96E-14	Macrophage
MYCL1	1.27E-09	4.57276508	3.02E-05	Macrophage
DSE	2.25E-27	4.56135683	5.32E-23	Macrophage
OSM	2.44E-30	4.55488536	5.77E-26	Macrophage
CEACAM3	5.88E-11	4.53957546	1.39E-06	Macrophage
FAM26F	3.23E-32	4.53116672	7.66E-28	Macrophage
SLC8A1	5.72E-45	4.52759224	1.36E-40	Macrophage
TRPM5	8.11E-10	4.5260561	1.92E-05	Macrophage
PLBD1	4.27E-27	4.44787397	1.01E-22	Macrophage
ANPEP	1.91E-33	4.4424423	4.53E-29	Macrophage
RAB31	2.18E-44	4.42846412	5.17E-40	Macrophage
PLAU	1.21E-11	4.40488248	2.86E-07	Macrophage
CCRL2	5.08E-45	4.39841254	1.20E-40	Macrophage
FLJ34208	2.95E-13	4.38038287	6.99E-09	Macrophage
FAM157B	8.16E-18	4.35756749	1.93E-13	Macrophage
CCL3L1	8.64E-24	4.3209446	2.05E-19	Macrophage
TNFAIP2	1.24E-24	4.30480029	2.93E-20	Macrophage
EMILIN2	3.15E-25	4.29165172	7.45E-21	Macrophage
PLAUR	1.29E-24	4.27557459	3.06E-20	Macrophage
CD33	6.64E-22	4.272247	1.57E-17	Macrophage
CD300E	1.13E-12	4.26586762	2.68E-08	Macrophage
CD93	6.84E-53	4.23872823	1.62E-48	Macrophage
SLC43A2	1.74E-27	4.16970921	4.11E-23	Macrophage
C1orf54	2.99E-15	4.16082126	7.07E-11	Macrophage
FGR	1.88E-33	4.16031594	4.45E-29	Macrophage
OLFML2B	1.58E-20	4.15952903	3.74E-16	Macrophage
ETS2	4.70E-33	4.14288921	1.11E-28	Macrophage
C1QB	2.51E-19	4.13648579	5.95E-15	Macrophage
CYBB	2.07E-36	4.12873361	4.91E-32	Macrophage
C3	8.49E-14	4.12834874	2.01E-09	Macrophage
TBXAS1	1.28E-24	4.12615166	3.02E-20	Macrophage
ALDH2	3.70E-34	4.11076916	8.76E-30	Macrophage
LINC00207	2.19E-11	4.10792598	5.18E-07	Macrophage
PLSCR2	9.90E-22	4.10045113	2.34E-17	Macrophage
GPR34	1.75E-14	4.09911602	4.14E-10	Macrophage
ARHGAP22	8.32E-10	4.08185946	1.97E-05	Macrophage
TLR4	1.35E-25	4.06726653	3.20E-21	Macrophage
FAM157A	5.31E-21	4.05272532	1.26E-16	Macrophage

TNFRSF10C	4.01E-09	4.05197139	9.51E-05	Macrophage
PLD4	1.76E-32	4.0048324	4.18E-28	Macrophage
LILRA6	5.79E-16	4.00073553	1.37E-11	Macrophage
CD300A	1.30E-35	3.99551244	3.08E-31	Macrophage
ACPP	1.50E-12	3.99430494	3.55E-08	Macrophage
MPEG1	9.43E-29	3.98404953	2.23E-24	Macrophage
TGFBI	3.89E-29	3.9682316	9.21E-25	Macrophage
ATP8B4	7.99E-42	3.93589153	1.89E-37	Macrophage
GPR35	4.82E-14	3.89350155	1.14E-09	Macrophage
CX3CR1	3.28E-30	3.88366495	7.77E-26	Macrophage
NLRP3	3.80E-12	3.84629693	9.01E-08	Macrophage
CD1D	1.08E-12	3.83747884	2.57E-08	Macrophage
IFI30	8.09E-27	3.82955254	1.92E-22	Macrophage
FES	7.81E-11	3.80111712	1.85E-06	Macrophage
ITGAX	3.33E-16	3.79798497	7.89E-12	Macrophage
SIGLEC5	6.38E-14	3.79303785	1.51E-09	Macrophage
CCR1	1.66E-25	3.79103237	3.93E-21	Macrophage
TLR5	1.44E-10	3.78634971	3.41E-06	Macrophage
NFAM1	1.61E-09	3.74658524	3.81E-05	Macrophage
CCL2	3.32E-09	3.72935428	7.87E-05	Macrophage
ALOX5	2.06E-30	3.68244019	4.88E-26	Macrophage
SLC31A2	2.27E-21	3.66808954	5.38E-17	Macrophage
CHST15	3.04E-11	3.66199189	7.21E-07	Macrophage
GAS6	5.32E-11	3.66147459	1.26E-06	Macrophage
OSCAR	6.51E-10	3.65750943	1.54E-05	Macrophage
LY86	5.05E-35	3.65484092	1.20E-30	Macrophage
HBEGF	8.06E-15	3.63144297	1.91E-10	Macrophage
IRF5	9.39E-23	3.6155963	2.22E-18	Macrophage
BRE-AS1	2.49E-26	3.61407521	5.89E-22	Macrophage
SH2B2	1.58E-09	3.61083528	3.74E-05	Macrophage
FCGR2B	1.87E-13	3.57921881	4.43E-09	Macrophage
RBM47	1.51E-15	3.57663231	3.59E-11	Macrophage
FGL2	2.03E-15	3.55730895	4.81E-11	Macrophage
TMPRSS13	1.55E-09	3.54166997	3.68E-05	Macrophage
LILRB1	2.44E-17	3.53014005	5.77E-13	Macrophage
LAT2	1.55E-23	3.5065481	3.67E-19	Macrophage
RNASE6	1.22E-27	3.46512778	2.88E-23	Macrophage
LOC338758	7.92E-15	3.45846515	1.88E-10	Macrophage
BST1	4.31E-11	3.44909502	1.02E-06	Macrophage
SECTM1	1.23E-09	3.42144794	2.90E-05	Macrophage
TNFSF13B	6.72E-18	3.40352271	1.59E-13	Macrophage

CXCL1	3.75E-11	3.38666734	8.88E-07	Macrophage
CRLF2	8.22E-12	3.38065235	1.95E-07	Macrophage
TNFAIP8L2	8.24E-21	3.36395433	1.95E-16	Macrophage
C11orf75	1.07E-20	3.35630653	2.54E-16	Macrophage
ADAMTSL4	2.02E-22	3.34224619	4.78E-18	Macrophage
NPL	1.53E-10	3.31499549	3.61E-06	Macrophage
SERPING1	3.53E-15	3.30966592	8.36E-11	Macrophage
STARD8	2.22E-09	3.29144015	5.27E-05	Macrophage
PAK1	1.15E-10	3.27635883	2.72E-06	Macrophage
VCAN	2.18E-11	3.25248067	5.17E-07	Macrophage
ASTL	1.26E-20	3.25085523	2.99E-16	Macrophage
C1orf162	2.11E-19	3.22538326	4.99E-15	Macrophage
CD101	4.84E-14	3.19369039	1.15E-09	Macrophage
CCL3	5.93E-20	3.16861743	1.41E-15	Macrophage
FAM49A	1.63E-12	3.15300694	3.86E-08	Macrophage
KYNU	1.78E-26	3.1500745	4.21E-22	Macrophage
CD302	1.15E-12	3.09697777	2.72E-08	Macrophage
THAP2	6.96E-15	3.06759786	1.65E-10	Macrophage
PLEK	1.02E-19	3.05838026	2.41E-15	Macrophage
RASSF4	1.87E-17	3.04900164	4.44E-13	Macrophage
HLA-DMB	7.03E-22	3.03758289	1.67E-17	Macrophage
ZSWIM6	2.13E-09	3.01676222	5.06E-05	Macrophage
SCIMP	1.49E-09	2.99842716	3.54E-05	Macrophage
TYMP	9.62E-16	2.99679892	2.28E-11	Macrophage
FGD2	6.30E-12	2.98816109	1.49E-07	Macrophage
NOD2	2.60E-14	2.94809214	6.15E-10	Macrophage
HLA-DQB2	1.97E-20	2.9345074	4.66E-16	Macrophage
SERPINA1	3.60E-19	2.92622348	8.53E-15	Macrophage
ASAP1-IT1	6.16E-11	2.91962228	1.46E-06	Macrophage
CERS6-AS1	2.43E-09	2.91343418	5.75E-05	Macrophage
DOK1	2.02E-10	2.90775763	4.78E-06	Macrophage
LYN	7.50E-21	2.89925712	1.78E-16	Macrophage
METRNL	4.24E-10	2.88400839	1.00E-05	Macrophage
CSF2RB	3.37E-11	2.85909362	7.97E-07	Macrophage
AOAH	1.63E-19	2.85339082	3.86E-15	Macrophage
DHRS3	2.44E-12	2.85196164	5.77E-08	Macrophage
KCTD12	8.96E-12	2.83804159	2.12E-07	Macrophage
LGALS9	1.39E-17	2.8371114	3.30E-13	Macrophage
RELT	2.27E-09	2.83208879	5.39E-05	Macrophage
LILRP2	2.62E-16	2.82664448	6.22E-12	Macrophage
BCL2A1	3.73E-18	2.82152297	8.84E-14	Macrophage

FCGRT	4.06E-13	2.80350854	9.61E-09	Macrophage
ZFP2	5.88E-10	2.80337449	1.39E-05	Macrophage
CD68	1.64E-13	2.76098904	3.89E-09	Macrophage
CD4	5.37E-20	2.73321055	1.27E-15	Macrophage
NAPSB	4.52E-16	2.7109634	1.07E-11	Macrophage
CD83	1.12E-16	2.69989758	2.65E-12	Macrophage
CXCL16	2.83E-09	2.69090284	6.71E-05	Macrophage
MAP3K8	5.38E-14	2.68980316	1.27E-09	Macrophage
MPP1	3.80E-11	2.68839329	9.00E-07	Macrophage
FCGR2A	5.78E-12	2.68094444	1.37E-07	Macrophage
DOK3	3.16E-12	2.67464036	7.49E-08	Macrophage
BTK	2.93E-17	2.66846083	6.93E-13	Macrophage
GCA	2.52E-09	2.65086334	5.96E-05	Macrophage
TLR1	5.34E-11	2.62578115	1.27E-06	Macrophage
CPVL	3.03E-13	2.62115965	7.18E-09	Macrophage
NCF1C	2.83E-17	2.60418469	6.71E-13	Macrophage
HLA-DQA1	6.39E-15	2.59669416	1.51E-10	Macrophage
STX11	3.72E-10	2.58990576	8.81E-06	Macrophage
AMPD3	3.75E-09	2.5779807	8.89E-05	Macrophage
NCF1	8.23E-11	2.57348622	1.95E-06	Macrophage
SYK	1.30E-10	2.56554362	3.08E-06	Macrophage
FAM65C	3.34E-09	2.56166431	7.91E-05	Macrophage
SEMA4A	2.76E-11	2.55672586	6.54E-07	Macrophage
FCGR2C	1.74E-10	2.53572049	4.12E-06	Macrophage
ARRB2	5.87E-13	2.52712932	1.39E-08	Macrophage
HLA-DQB1	6.48E-16	2.49980153	1.53E-11	Macrophage
NAAA	1.02E-11	2.49270848	2.43E-07	Macrophage
SOD2	9.23E-14	2.48630624	2.19E-09	Macrophage
RIPK2	1.62E-11	2.47874913	3.84E-07	Macrophage
AMICA1	3.05E-11	2.4481149	7.22E-07	Macrophage
DENND3	1.17E-16	2.44330944	2.77E-12	Macrophage
GLIPR2	2.21E-12	2.44312343	5.23E-08	Macrophage
ACSL1	3.26E-13	2.43960616	7.72E-09	Macrophage
CD80	3.88E-14	2.43233513	9.20E-10	Macrophage
THEMIS2	3.34E-12	2.42865351	7.91E-08	Macrophage
C17orf107	1.20E-11	2.42429651	2.84E-07	Macrophage
PTPRE	1.33E-11	2.42250259	3.15E-07	Macrophage
SCO2	4.67E-12	2.42192736	1.11E-07	Macrophage
RNF130	8.30E-12	2.40986776	1.97E-07	Macrophage
HLA-DMA	2.94E-14	2.40915699	6.97E-10	Macrophage
HLA-DRB5	4.79E-16	2.39729417	1.13E-11	Macrophage

HLA-DRA	4.03E-16	2.3963263	9.55E-12	Macrophage
NINJ1	3.67E-13	2.37275163	8.69E-09	Macrophage
NFKBID	2.03E-12	2.36356107	4.81E-08	Macrophage
GALC	6.75E-11	2.3608709	1.60E-06	Macrophage
MYO1F	5.76E-13	2.35674231	1.37E-08	Macrophage
SOCS3	1.99E-11	2.2803761	4.72E-07	Macrophage
VAMP5	1.39E-11	2.25881768	3.29E-07	Macrophage
PIK3AP1	1.06E-09	2.24332146	2.50E-05	Macrophage
PFKFB3	7.14E-10	2.23472499	1.69E-05	Macrophage
RASGEF1B	1.79E-12	2.23466852	4.24E-08	Macrophage
Mar-01	5.60E-15	2.23340732	1.33E-10	Macrophage
HLA-DRB1	8.59E-16	2.22340219	2.03E-11	Macrophage
EPSTI1	3.74E-10	2.20972068	8.85E-06	Macrophage
JAK2	1.68E-09	2.19883737	3.97E-05	Macrophage
PYCARD	1.68E-12	2.15212302	3.99E-08	Macrophage
MAN2B1	1.87E-11	2.13726249	4.42E-07	Macrophage
IRF8	7.96E-14	2.13682756	1.89E-09	Macrophage
CLEC7A	8.37E-10	2.11614557	1.98E-05	Macrophage
GLUL	2.08E-12	2.08208476	4.94E-08	Macrophage
RHOG	2.56E-09	2.0671353	6.07E-05	Macrophage
HLA-DRB6	3.77E-13	2.0463022	8.94E-09	Macrophage
HLA-DPB1	1.52E-12	2.02095597	3.59E-08	Macrophage
MAEL	1.03E-52	8.93056112	2.43E-48	Melanoma
ST3GAL6-AS1	1.07E-61	8.07515915	2.53E-57	Melanoma
LOC100127888	9.98E-74	7.67737365	2.36E-69	Melanoma
NR0B1	4.58E-20	7.35274317	1.08E-15	Melanoma
ANKRD7	1.43E-17	7.27700639	3.39E-13	Melanoma
CPN1	2.19E-25	7.2666892	5.18E-21	Melanoma
CITED1	6.13E-71	7.21575904	1.45E-66	Melanoma
ITIH6	2.30E-24	7.16962108	5.45E-20	Melanoma
MAGEA2	1.98E-44	7.14060423	4.69E-40	Melanoma
CMTM5	4.58E-20	7.07497696	1.08E-15	Melanoma
TRIM63	7.66E-60	7.01847951	1.81E-55	Melanoma
FOXD3	3.07E-47	6.98375774	7.27E-43	Melanoma
NAT8L	4.53E-34	6.90869955	1.07E-29	Melanoma
ESRP1	6.56E-39	6.90212343	1.55E-34	Melanoma
TSPAN10	1.43E-17	6.88599943	3.39E-13	Melanoma
CSAG4	4.23E-51	6.87142171	1.00E-46	Melanoma
NKAIN4	4.49E-17	6.8100793	1.06E-12	Melanoma
GPR143	4.78E-179	6.7602556	1.13E-174	Melanoma
LINC00473	1.13E-117	6.75752668	2.67E-113	Melanoma

HOXC10	2.52E-60	6.69974099	5.97E-56	Melanoma
GJB1	3.13E-178	6.67351889	7.41E-174	Melanoma
CTAG1A	6.83E-13	6.64176903	1.62E-08	Melanoma
CTAG1B	6.83E-13	6.64176903	1.62E-08	Melanoma
COX7B2	1.73E-09	6.62550663	4.11E-05	Melanoma
BIRC7	1.11E-129	6.60187357	2.63E-125	Melanoma
RAB17	3.39E-115	6.40672978	8.03E-111	Melanoma
UCN2	2.05E-54	6.37539905	4.85E-50	Melanoma
MMP8	2.46E-35	6.35826033	5.84E-31	Melanoma
ROPN1B	6.47E-140	6.35095989	1.53E-135	Melanoma
LOC146481	2.36E-71	6.3145292	5.60E-67	Melanoma
MKRN9P	1.79E-38	6.31098424	4.24E-34	Melanoma
AZGP1	5.56E-77	6.30636523	1.32E-72	Melanoma
MAGEA2B	1.77E-77	6.25493575	4.20E-73	Melanoma
GYG2	5.29E-115	6.25016781	1.25E-110	Melanoma
GJC3	1.98E-36	6.23746814	4.70E-32	Melanoma
MLIP	3.96E-25	6.21454611	9.38E-21	Melanoma
SLC24A5	1.09E-141	6.19693352	2.58E-137	Melanoma
GPR37	6.63E-26	6.17104042	1.57E-21	Melanoma
B3GALT1	1.32E-14	6.1179602	3.12E-10	Melanoma
MAGEA1	6.67E-37	6.10503673	1.58E-32	Melanoma
MAGEB1	3.25E-10	6.10233684	7.70E-06	Melanoma
ALX1	3.39E-60	6.07036861	8.03E-56	Melanoma
MAGEC1	2.94E-36	5.96002776	6.96E-32	Melanoma
KIF6	2.95E-80	5.9425959	6.98E-76	Melanoma
CCNO	2.02E-33	5.90893851	4.79E-29	Melanoma
TRIML2	7.29E-100	5.86614938	1.73E-95	Melanoma
FABP7	8.82E-20	5.8653605	2.09E-15	Melanoma
TOM1L1	2.34E-97	5.85051299	5.55E-93	Melanoma
LOC100130370	1.23E-83	5.84832523	2.92E-79	Melanoma
OLIG1	7.74E-16	5.84537704	1.83E-11	Melanoma
CSAG2	1.15E-53	5.84198836	2.73E-49	Melanoma
MYH14	3.11E-30	5.82021022	7.36E-26	Melanoma
ETV4	5.76E-131	5.80170652	1.36E-126	Melanoma
TNNT1	8.88E-20	5.79948318	2.10E-15	Melanoma
PAEP	4.67E-54	5.78832237	1.11E-49	Melanoma
RIPK4	2.25E-64	5.77562025	5.34E-60	Melanoma
LAD1	4.77E-29	5.75521534	1.13E-24	Melanoma
PLP1	6.66E-239	5.73549255	1.58E-234	Melanoma
MAGEA3	9.52E-100	5.73442153	2.25E-95	Melanoma
CDH19	2.47E-219	5.73251249	5.86E-215	Melanoma

CSAG1	5.59E-127	5.72218055	1.32E-122	Melanoma
CSAG3	3.12E-104	5.71219436	7.39E-100	Melanoma
APOC2	6.17E-171	5.67566055	1.46E-166	Melanoma
STK32A	1.32E-81	5.67302578	3.13E-77	Melanoma
TCN1	1.34E-58	5.64314144	3.18E-54	Melanoma
FAM178B	2.34E-48	5.62318934	5.55E-44	Melanoma
LINC00602	1.19E-20	5.61139138	2.83E-16	Melanoma
SOX10	1.34E-217	5.59406216	3.18E-213	Melanoma
ARSE	4.84E-27	5.59164268	1.15E-22	Melanoma
TFAP2C	3.68E-39	5.58505719	8.72E-35	Melanoma
ELOVL2	1.34E-41	5.58182999	3.17E-37	Melanoma
SLC6A15	8.73E-122	5.55925581	2.07E-117	Melanoma
SLC45A2	3.94E-104	5.54522586	9.34E-100	Melanoma
PAX3	1.69E-145	5.5385922	3.99E-141	Melanoma
VGF	9.92E-10	5.52639119	2.35E-05	Melanoma
RGL3	1.97E-22	5.51381413	4.66E-18	Melanoma
AIF1L	6.34E-127	5.5138065	1.50E-122	Melanoma
PCDHB13	7.57E-26	5.50681558	1.79E-21	Melanoma
RAB38	2.31E-117	5.49670332	5.47E-113	Melanoma
MAGEA6	2.85E-128	5.49417028	6.74E-124	Melanoma
SEMA3B	5.72E-132	5.49195465	1.35E-127	Melanoma
ROPN1	2.52E-110	5.4890716	5.96E-106	Melanoma
MFI2	1.36E-151	5.48248845	3.23E-147	Melanoma
SLC13A3	1.76E-39	5.46436686	4.18E-35	Melanoma
SCGB1D2	6.26E-14	5.45786771	1.48E-09	Melanoma
RDH5	1.17E-94	5.44294709	2.76E-90	Melanoma
OCA2	4.83E-15	5.43069181	1.14E-10	Melanoma
CTAG2	1.22E-27	5.41061784	2.89E-23	Melanoma
BFSP1	5.75E-46	5.40815593	1.36E-41	Melanoma
SAMD13	3.92E-17	5.40654118	9.28E-13	Melanoma
RLBP1	2.57E-47	5.3844294	6.09E-43	Melanoma
PRAME	1.05E-263	5.36299674	2.49E-259	Melanoma
LOC285000	1.18E-18	5.35774007	2.79E-14	Melanoma
PKNOX2	1.77E-36	5.35578573	4.19E-32	Melanoma
DAAM2	2.41E-183	5.35236912	5.71E-179	Melanoma
MAGEA12	2.89E-96	5.33406396	6.85E-92	Melanoma
KIAA1211	1.10E-27	5.32041574	2.61E-23	Melanoma
MAGEC2	2.56E-39	5.304645	6.05E-35	Melanoma
BCAN	6.63E-44	5.29307411	1.57E-39	Melanoma
PCDHGB4	5.07E-20	5.29160904	1.20E-15	Melanoma
LHFPL3-AS1	1.89E-59	5.28101577	4.49E-55	Melanoma

TFF2	5.65E-12	5.27936406	1.34E-07	Melanoma
TMEM255A	3.88E-118	5.2787159	9.18E-114	Melanoma
SERPINA5	4.27E-45	5.27027208	1.01E-40	Melanoma
XAGE1E	5.89E-156	5.26776181	1.39E-151	Melanoma
XAGE1A	2.60E-156	5.25790451	6.17E-152	Melanoma
XAGE1C	6.92E-156	5.2556432	1.64E-151	Melanoma
XAGE1D	7.11E-156	5.2540676	1.68E-151	Melanoma
XAGE1B	6.96E-156	5.25107042	1.65E-151	Melanoma
ECHDC3	3.58E-16	5.24774515	8.47E-12	Melanoma
MIA-RAB4B	1.58E-23	5.24596441	3.73E-19	Melanoma
EYA1	5.00E-33	5.24234361	1.18E-28	Melanoma
ENTHD1	1.94E-75	5.2373357	4.59E-71	Melanoma
ZNF280A	8.91E-11	5.20990755	2.11E-06	Melanoma
ATP6V0A4	6.62E-17	5.20571126	1.57E-12	Melanoma
CERS1	3.63E-21	5.20234768	8.60E-17	Melanoma
LOC100126784	5.17E-146	5.19586781	1.23E-141	Melanoma
CYP1A1	5.35E-21	5.18514821	1.27E-16	Melanoma
CSPG4	5.37E-222	5.17680183	1.27E-217	Melanoma
PTPRR	2.77E-34	5.17340066	6.57E-30	Melanoma
LOC100506451	6.09E-62	5.15768017	1.44E-57	Melanoma
S100A1	2.76E-147	5.15451507	6.53E-143	Melanoma
PTPRZ1	2.40E-49	5.14720216	5.68E-45	Melanoma
IGSF11	1.57E-123	5.10550717	3.72E-119	Melanoma
ZRANB2-AS2	3.15E-13	5.08800191	7.47E-09	Melanoma
XKR3	1.59E-15	5.06478365	3.76E-11	Melanoma
FBXO16	3.16E-20	5.05992026	7.48E-16	Melanoma
TYR	3.32E-239	5.05624197	7.86E-235	Melanoma
SCUBE2	7.16E-58	5.05324929	1.69E-53	Melanoma
HR	3.75E-24	5.04417867	8.88E-20	Melanoma
BAMBI	4.90E-89	5.04333694	1.16E-84	Melanoma
HILS1	1.93E-26	5.03909648	4.57E-22	Melanoma
DSCR8	1.56E-45	5.03374874	3.68E-41	Melanoma
SORT1	2.39E-206	5.03289759	5.66E-202	Melanoma
LGI4	1.01E-28	5.0324126	2.39E-24	Melanoma
GDF15	3.69E-149	5.02587749	8.75E-145	Melanoma
KCNS3	8.42E-37	5.01602777	1.99E-32	Melanoma
MIA	2.18E-217	5.00355554	5.16E-213	Melanoma
FN3K	4.15E-33	5.00306418	9.82E-29	Melanoma
XAGE3	2.14E-17	4.98385884	5.07E-13	Melanoma
HOXD13	1.16E-14	4.9705318	2.76E-10	Melanoma
FXYD3	3.67E-184	4.95499307	8.70E-180	Melanoma

RNF128	6.03E-33	4.93187625	1.43E-28	Melanoma
LOC100130275	2.30E-17	4.91993212	5.44E-13	Melanoma
GAD1	9.73E-12	4.91943216	2.30E-07	Melanoma
C10orf90	1.93E-46	4.91711406	4.56E-42	Melanoma
MAGEB2	2.81E-25	4.89814123	6.65E-21	Melanoma
MPZ	3.13E-88	4.8964115	7.42E-84	Melanoma
TP53TG3C	6.23E-55	4.89122698	1.48E-50	Melanoma
SSX2	2.08E-42	4.88683705	4.92E-38	Melanoma
TRIM51	2.55E-37	4.86931207	6.04E-33	Melanoma
RXRG	1.68E-58	4.86889005	3.99E-54	Melanoma
SYCE3	5.08E-15	4.86573096	1.20E-10	Melanoma
KHDRBS3	7.84E-31	4.86036328	1.86E-26	Melanoma
BMPR1B	1.80E-107	4.85937065	4.26E-103	Melanoma
CAMK1G	5.59E-20	4.85587744	1.32E-15	Melanoma
LOC340357	4.82E-75	4.85529726	1.14E-70	Melanoma
SOX6	1.64E-65	4.84275675	3.89E-61	Melanoma
PRR26	3.17E-71	4.83722127	7.51E-67	Melanoma
LEF1-AS1	2.02E-90	4.83683779	4.78E-86	Melanoma
LOC100302640	3.27E-12	4.83539319	7.75E-08	Melanoma
LINGO1	1.01E-18	4.82700813	2.40E-14	Melanoma
MT1G	4.84E-23	4.8209003	1.15E-18	Melanoma
PODXL2	7.65E-44	4.81986639	1.81E-39	Melanoma
ITGA7	5.07E-137	4.81540066	1.20E-132	Melanoma
HSD17B3	2.61E-09	4.81440748	6.18E-05	Melanoma
PMEL	1.36E-237	4.81419071	3.23E-233	Melanoma
SOX8	1.07E-38	4.81137922	2.53E-34	Melanoma
CNTN1	3.00E-25	4.81087133	7.10E-21	Melanoma
ST6GALNAC2	1.17E-122	4.80625112	2.77E-118	Melanoma
SORCS1	1.49E-58	4.80594324	3.52E-54	Melanoma
KLK6	5.93E-18	4.80281397	1.41E-13	Melanoma
BPI	1.13E-09	4.80226605	2.67E-05	Melanoma
C3orf67	2.09E-41	4.77689395	4.94E-37	Melanoma
EXTL1	1.39E-48	4.76118832	3.29E-44	Melanoma
ETV5	1.58E-216	4.75817112	3.73E-212	Melanoma
SAMD15	9.22E-11	4.75305792	2.18E-06	Melanoma
SGCD	1.11E-156	4.74412356	2.62E-152	Melanoma
TYRP1	9.28E-29	4.7399665	2.20E-24	Melanoma
EVA1A	8.96E-118	4.73471784	2.12E-113	Melanoma
PHYHIP	1.81E-17	4.73307111	4.28E-13	Melanoma
GPR158	1.80E-35	4.73213291	4.26E-31	Melanoma
RAC3	2.25E-30	4.71467859	5.33E-26	Melanoma

LINC00622	7.84E-29	4.7101942	1.86E-24	Melanoma
MITF	3.16E-209	4.70709005	7.49E-205	Melanoma
CLDN12	2.87E-112	4.70420509	6.79E-108	Melanoma
IRX6	2.22E-23	4.69993732	5.26E-19	Melanoma
SYT6	8.97E-18	4.69951009	2.12E-13	Melanoma
CLDN14	1.99E-13	4.69369483	4.71E-09	Melanoma
OR7A5	2.36E-38	4.68770336	5.59E-34	Melanoma
SHC4	7.07E-150	4.68764309	1.68E-145	Melanoma
ARC	3.61E-37	4.68099408	8.54E-33	Melanoma
SSX2B	4.00E-35	4.68040415	9.48E-31	Melanoma
KLHL38	1.14E-13	4.67955712	2.69E-09	Melanoma
SYT12	1.33E-11	4.66912336	3.15E-07	Melanoma
CA6	3.45E-09	4.65399077	8.17E-05	Melanoma
TRNP1	1.19E-12	4.63938167	2.82E-08	Melanoma
SH3BGR	1.17E-28	4.6382159	2.77E-24	Melanoma
EN2	1.15E-30	4.62651507	2.73E-26	Melanoma
PTPRH	2.35E-22	4.62630077	5.56E-18	Melanoma
TFAP2A	1.07E-169	4.61961627	2.53E-165	Melanoma
ZNF300P1	1.79E-16	4.60572065	4.24E-12	Melanoma
SHROOM2	5.29E-88	4.5771137	1.25E-83	Melanoma
ALDH3B2	1.03E-37	4.5725573	2.45E-33	Melanoma
PLXNB3	2.18E-102	4.57015154	5.16E-98	Melanoma
SPRY4	2.27E-148	4.56376883	5.39E-144	Melanoma
PAGE5	3.78E-37	4.55480274	8.95E-33	Melanoma
HEY2	4.94E-24	4.5520144	1.17E-19	Melanoma
GAS2L3	1.88E-85	4.54826567	4.46E-81	Melanoma
NSG1	1.87E-214	4.54408952	4.43E-210	Melanoma
DNAH14	2.78E-63	4.5364406	6.59E-59	Melanoma
SNCA	7.75E-227	4.53430585	1.84E-222	Melanoma
CA8	1.92E-74	4.53317049	4.54E-70	Melanoma
ADPRHL1	4.06E-20	4.5306071	9.63E-16	Melanoma
FAM224A	8.11E-20	4.52947258	1.92E-15	Melanoma
MAPK4	6.52E-14	4.52469657	1.54E-09	Melanoma
SPP1	8.54E-133	4.52468044	2.02E-128	Melanoma
PIR	5.55E-144	4.52263875	1.32E-139	Melanoma
GFRA3	2.27E-19	4.52242315	5.37E-15	Melanoma
LOXL4	1.05E-144	4.5211206	2.48E-140	Melanoma
CTTNBP2	2.40E-63	4.51634022	5.68E-59	Melanoma
GAREM	1.54E-41	4.51538069	3.65E-37	Melanoma
CYP39A1	4.75E-27	4.50550051	1.12E-22	Melanoma
SOX13	3.05E-127	4.49674642	7.24E-123	Melanoma

QPCT	7.92E-151	4.49514228	1.88E-146	Melanoma
LAMA1	7.75E-46	4.48850884	1.84E-41	Melanoma
SLC44A3	6.26E-38	4.4734991	1.48E-33	Melanoma
MLPH	2.22E-181	4.47339142	5.25E-177	Melanoma
XYLB	1.74E-81	4.46885373	4.12E-77	Melanoma
RAP1GAP	7.09E-32	4.46093196	1.68E-27	Melanoma
CT47A2	7.70E-27	4.45693829	1.82E-22	Melanoma
COL22A1	3.60E-29	4.45290978	8.53E-25	Melanoma
CELSR2	1.32E-120	4.44530813	3.14E-116	Melanoma
LOC100270746	2.69E-22	4.44508728	6.37E-18	Melanoma
LINC00511	5.49E-41	4.4419122	1.30E-36	Melanoma
BCHE	4.23E-75	4.43590995	1.00E-70	Melanoma
NUDT12	1.77E-30	4.43406521	4.20E-26	Melanoma
Sep-04	3.44E-49	4.42704382	8.14E-45	Melanoma
LINC00518	1.25E-75	4.41878269	2.95E-71	Melanoma
CYP27A1	2.06E-180	4.41712208	4.89E-176	Melanoma
VLDLR	1.17E-47	4.40791849	2.77E-43	Melanoma
CRNDE	1.06E-93	4.40493552	2.52E-89	Melanoma
UGT2B7	2.69E-16	4.40367542	6.38E-12	Melanoma
MOCOS	4.35E-26	4.39056464	1.03E-21	Melanoma
CST2	6.65E-15	4.38771933	1.57E-10	Melanoma
ARSI	1.57E-24	4.38030684	3.71E-20	Melanoma
BAGE2	4.23E-12	4.37184178	1.00E-07	Melanoma
BAGE3	4.23E-12	4.37184178	1.00E-07	Melanoma
NAV2	6.87E-170	4.36650403	1.63E-165	Melanoma
APOE	1.25E-195	4.36565472	2.95E-191	Melanoma
S100B	5.81E-253	4.36128031	1.38E-248	Melanoma
ASPHD1	1.62E-17	4.3552022	3.85E-13	Melanoma
SLC7A8	1.20E-113	4.35413222	2.84E-109	Melanoma
CT47A3	7.61E-27	4.35205725	1.80E-22	Melanoma
LZTS1-AS1	2.40E-11	4.35054785	5.68E-07	Melanoma
NELL1	4.91E-24	4.34455789	1.16E-19	Melanoma
NLGN1	1.28E-96	4.3442534	3.02E-92	Melanoma
EDNRB	4.78E-147	4.34397132	1.13E-142	Melanoma
LYPD1	6.02E-24	4.34267383	1.43E-19	Melanoma
HTA	1.50E-12	4.34161807	3.55E-08	Melanoma
LINC00520	1.55E-20	4.33522374	3.66E-16	Melanoma
FAM3B	3.24E-24	4.32877816	7.67E-20	Melanoma
ZNF214	3.52E-09	4.32688148	8.33E-05	Melanoma
MT1A	2.30E-22	4.32146883	5.44E-18	Melanoma
FIBCD1	2.81E-16	4.31523421	6.67E-12	Melanoma

Sep-03	6.13E-30	4.31497021	1.45E-25	Melanoma
GRIN2B	1.92E-14	4.31336959	4.55E-10	Melanoma
LINC00589	1.69E-44	4.31335373	4.01E-40	Melanoma
ZNF697	5.16E-59	4.31055264	1.22E-54	Melanoma
KIAA1549L	7.57E-72	4.30947015	1.79E-67	Melanoma
NOV	6.80E-55	4.3085232	1.61E-50	Melanoma
SERPINA3	1.69E-172	4.29963648	4.00E-168	Melanoma
MCHR1	1.15E-23	4.28425184	2.74E-19	Melanoma
ATP10B	6.25E-61	4.27699566	1.48E-56	Melanoma
TBX2	4.32E-28	4.27557446	1.02E-23	Melanoma
SPESP1	1.23E-26	4.27202774	2.92E-22	Melanoma
PCDHGA2	7.22E-18	4.26411179	1.71E-13	Melanoma
GRIK2	3.83E-33	4.26107657	9.07E-29	Melanoma
LINC00479	5.42E-18	4.25235342	1.28E-13	Melanoma
COL9A3	1.72E-69	4.24436296	4.08E-65	Melanoma
CT47A6	7.74E-27	4.24011885	1.83E-22	Melanoma
CT47A1	7.83E-27	4.23790966	1.85E-22	Melanoma
PCDH7	2.75E-86	4.23757616	6.52E-82	Melanoma
HEY1	3.47E-50	4.23630699	8.23E-46	Melanoma
P2RX6	1.87E-22	4.22179821	4.43E-18	Melanoma
CT47A11	7.79E-27	4.22025708	1.85E-22	Melanoma
HSF4	4.28E-45	4.21646959	1.01E-40	Melanoma
GLUD2	3.43E-54	4.20101704	8.13E-50	Melanoma
CLVS1	1.16E-09	4.19483499	2.76E-05	Melanoma
CT47A10	7.77E-27	4.19302225	1.84E-22	Melanoma
SDC3	9.63E-194	4.19172394	2.28E-189	Melanoma
CA14	2.68E-24	4.19005277	6.34E-20	Melanoma
FOLH1	2.90E-10	4.18396632	6.87E-06	Melanoma
CT47A4	7.81E-27	4.18057494	1.85E-22	Melanoma
CDH3	5.25E-45	4.17935203	1.24E-40	Melanoma
LINC00472	1.03E-21	4.17418065	2.45E-17	Melanoma
CT47A12	7.81E-27	4.17017692	1.85E-22	Melanoma
LOC100130700	2.32E-13	4.16755028	5.50E-09	Melanoma
RGS20	4.41E-77	4.16741644	1.04E-72	Melanoma
TF	3.00E-21	4.16066211	7.09E-17	Melanoma
TNFRSF19	4.21E-62	4.15290193	9.97E-58	Melanoma
CT47A5	7.79E-27	4.15098356	1.85E-22	Melanoma
PCDHGB5	1.83E-32	4.15029566	4.34E-28	Melanoma
CT47A8	7.83E-27	4.1459671	1.85E-22	Melanoma
LOC100505865	4.98E-80	4.1435667	1.18E-75	Melanoma
WISP3	1.20E-11	4.14328405	2.84E-07	Melanoma

RTN4R	4.81E-10	4.12769262	1.14E-05	Melanoma
TRIM2	1.16E-151	4.11228246	2.74E-147	Melanoma
ST3GAL4	1.04E-199	4.11184679	2.47E-195	Melanoma
THNSL2	4.01E-47	4.11168878	9.49E-43	Melanoma
APOC1	1.81E-143	4.11146914	4.30E-139	Melanoma
HPGD	1.51E-51	4.10847366	3.57E-47	Melanoma
CT47A9	7.81E-27	4.10845457	1.85E-22	Melanoma
TRPM3	4.47E-27	4.10223392	1.06E-22	Melanoma
NES	1.76E-113	4.10150256	4.17E-109	Melanoma
MGAT5B	5.36E-11	4.09435203	1.27E-06	Melanoma
HSPA4L	1.88E-37	4.09380246	4.46E-33	Melanoma
POPDC3	6.27E-45	4.09241345	1.49E-40	Melanoma
LINC00277	1.15E-18	4.07704889	2.73E-14	Melanoma
RHBDF1	9.98E-80	4.07351918	2.36E-75	Melanoma
SLC6A8	1.19E-79	4.07215348	2.81E-75	Melanoma
TCERG1L	7.42E-13	4.07058918	1.76E-08	Melanoma
MAGEA4	6.55E-10	4.06723089	1.55E-05	Melanoma
CDH7	1.27E-25	4.06262344	3.00E-21	Melanoma
TUBB2B	6.48E-113	4.05911239	1.53E-108	Melanoma
ARHGAP5-AS1	2.99E-39	4.05431988	7.08E-35	Melanoma
PABPC5	2.05E-15	4.05193857	4.86E-11	Melanoma
GPNMB	5.52E-241	4.04948464	1.31E-236	Melanoma
VENTXP1	4.85E-10	4.04614284	1.15E-05	Melanoma
TPTE	5.30E-16	4.03797493	1.26E-11	Melanoma
ITGB3	1.54E-128	4.03647454	3.65E-124	Melanoma
IGSF3	6.50E-167	4.02598063	1.54E-162	Melanoma
FRZB	1.72E-25	4.01900103	4.08E-21	Melanoma
NME5	8.08E-22	4.01516791	1.91E-17	Melanoma
FLJ46906	9.08E-29	4.00897331	2.15E-24	Melanoma
DCT	8.84E-45	4.00764778	2.09E-40	Melanoma
CECR7	4.15E-74	4.00438022	9.83E-70	Melanoma
SOX5	1.33E-68	4.00139919	3.16E-64	Melanoma
METTL7B	3.11E-49	4.00045896	7.37E-45	Melanoma
GSTT2	1.83E-33	3.99990177	4.34E-29	Melanoma
STXBP1	6.91E-206	3.99509401	1.64E-201	Melanoma
BAGE4	2.23E-21	3.99413222	5.29E-17	Melanoma
FAM167B	6.71E-78	3.99265576	1.59E-73	Melanoma
RNF175	1.36E-12	3.98430817	3.22E-08	Melanoma
KIT	2.11E-23	3.98417898	5.00E-19	Melanoma
SYNGR1	6.77E-156	3.97643578	1.60E-151	Melanoma
RAMP1	4.87E-38	3.97574694	1.15E-33	Melanoma

ANGPTL7	5.02E-18	3.97264105	1.19E-13	Melanoma
TMEM198	1.45E-14	3.97097192	3.44E-10	Melanoma
ASB9	2.40E-34	3.96637262	5.68E-30	Melanoma
SEMA3C	1.11E-107	3.96455144	2.64E-103	Melanoma
CCR10	9.50E-65	3.96425449	2.25E-60	Melanoma
DFNB59	1.68E-10	3.95820263	3.99E-06	Melanoma
KLKB1	5.53E-14	3.95416587	1.31E-09	Melanoma
ZC2HC1C	5.06E-19	3.95034203	1.20E-14	Melanoma
PMP2	3.20E-26	3.94923374	7.57E-22	Melanoma
LHFPL1	1.68E-10	3.94608634	3.97E-06	Melanoma
RTKN	3.38E-139	3.939302	8.02E-135	Melanoma
SH3D21	1.60E-55	3.93601287	3.79E-51	Melanoma
DCSTAMP	5.67E-10	3.928848	1.34E-05	Melanoma
IL17B	2.90E-10	3.9146494	6.87E-06	Melanoma
LINC00462	2.69E-12	3.91171525	6.37E-08	Melanoma
ITGA3	8.24E-122	3.90300196	1.95E-117	Melanoma
GSTT2B	9.44E-47	3.89835432	2.24E-42	Melanoma
NOL3	7.91E-53	3.89795101	1.87E-48	Melanoma
GRIA4	8.93E-18	3.89117459	2.12E-13	Melanoma
PLCB1	2.98E-63	3.8890303	7.06E-59	Melanoma
ACSM5	1.22E-24	3.87709703	2.88E-20	Melanoma
TMEM98	2.12E-170	3.87422061	5.03E-166	Melanoma
KCNH5	1.33E-12	3.87142936	3.16E-08	Melanoma
ZNF462	1.20E-91	3.86988547	2.85E-87	Melanoma
CRYAB	4.88E-153	3.8685598	1.16E-148	Melanoma
PC	8.88E-69	3.86501448	2.10E-64	Melanoma
LY6K	1.13E-22	3.86467981	2.68E-18	Melanoma
LOC100506368	2.46E-11	3.86229464	5.83E-07	Melanoma
KIAA1598	2.54E-130	3.85469747	6.03E-126	Melanoma
PKD1L2	7.06E-24	3.85099418	1.67E-19	Melanoma
FGF1	1.51E-38	3.84612618	3.59E-34	Melanoma
NKX2-5	6.94E-20	3.84151589	1.64E-15	Melanoma
CHL1	3.39E-97	3.83836032	8.04E-93	Melanoma
DPP6	2.73E-19	3.83726583	6.46E-15	Melanoma
HOMER2	1.08E-24	3.83706563	2.56E-20	Melanoma
MFAP3L	5.69E-41	3.83687176	1.35E-36	Melanoma
FSTL5	3.62E-21	3.8360342	8.58E-17	Melanoma
KCNK15	2.68E-30	3.83475212	6.36E-26	Melanoma
PCDHB8	1.01E-09	3.82861512	2.38E-05	Melanoma
OTOA	2.12E-13	3.82250338	5.03E-09	Melanoma
BAGE	1.14E-48	3.82233942	2.70E-44	Melanoma

MYADML	6.87E-25	3.81774465	1.63E-20	Melanoma
SNX7	2.67E-47	3.80894491	6.33E-43	Melanoma
TMEM51	3.02E-52	3.80336106	7.14E-48	Melanoma
AATK	2.37E-33	3.79779371	5.61E-29	Melanoma
SPIRE1	1.77E-60	3.79674272	4.18E-56	Melanoma
TBX3	3.45E-42	3.79079749	8.18E-38	Melanoma
DCBLD2	1.07E-128	3.78479438	2.53E-124	Melanoma
GLI3	4.96E-73	3.77708173	1.18E-68	Melanoma
KIAA0895	2.46E-21	3.77428385	5.83E-17	Melanoma
CYB5R2	8.22E-15	3.77335307	1.95E-10	Melanoma
NRG3	6.26E-19	3.76725276	1.48E-14	Melanoma
LOXL3	3.11E-97	3.76573588	7.37E-93	Melanoma
CAPN3	2.98E-204	3.753644	7.05E-200	Melanoma
HOXC11	1.63E-10	3.75307078	3.87E-06	Melanoma
ARHGEF40	9.52E-92	3.74950493	2.25E-87	Melanoma
OR56A1	1.25E-11	3.74871999	2.97E-07	Melanoma
STXBP6	2.37E-24	3.74550639	5.61E-20	Melanoma
LOC344887	5.04E-11	3.74254332	1.19E-06	Melanoma
BANCR	2.98E-34	3.7421432	7.06E-30	Melanoma
PRKD1	5.01E-33	3.73483185	1.19E-28	Melanoma
PPARGC1A	2.29E-22	3.73302833	5.43E-18	Melanoma
C5orf4	4.06E-63	3.73163587	9.61E-59	Melanoma
GAPDHS	8.40E-31	3.72980827	1.99E-26	Melanoma
ABCB9	5.43E-48	3.72866758	1.29E-43	Melanoma
APOD	4.95E-232	3.72799565	1.17E-227	Melanoma
INTU	7.12E-20	3.72508877	1.69E-15	Melanoma
IL13RA2	6.24E-15	3.72480291	1.48E-10	Melanoma
C1orf53	9.73E-18	3.72424903	2.31E-13	Melanoma
CNIH3	1.94E-38	3.72035477	4.59E-34	Melanoma
DDR1	6.97E-121	3.71966782	1.65E-116	Melanoma
CAMK2A	4.15E-15	3.71521443	9.83E-11	Melanoma
C8orf46	5.65E-22	3.70912288	1.34E-17	Melanoma
CADM4	4.94E-14	3.70743553	1.17E-09	Melanoma
HOXC9	7.27E-20	3.70712663	1.72E-15	Melanoma
SSX1	4.07E-11	3.69766251	9.64E-07	Melanoma
CPS1	5.07E-23	3.69218147	1.20E-18	Melanoma
PRKG2	1.58E-14	3.6880526	3.74E-10	Melanoma
LRP12	7.19E-50	3.68114077	1.70E-45	Melanoma
HOXB7	2.25E-78	3.6804364	5.34E-74	Melanoma
PPL	6.56E-71	3.67418997	1.55E-66	Melanoma
NRCAM	5.45E-18	3.67203798	1.29E-13	Melanoma

C4B	5.58E-43	3.66796189	1.32E-38	Melanoma
C4B-2	5.58E-43	3.66796189	1.32E-38	Melanoma
LSAMP	2.09E-82	3.66754655	4.95E-78	Melanoma
ITGA10	3.32E-56	3.66490688	7.86E-52	Melanoma
MAT1A	3.72E-11	3.66341311	8.81E-07	Melanoma
PLEKHB1	5.55E-173	3.65400616	1.31E-168	Melanoma
SMPDL3B	2.42E-11	3.65236123	5.73E-07	Melanoma
SERPINE2	6.21E-249	3.65138712	1.47E-244	Melanoma
RRAGD	1.40E-33	3.64417029	3.31E-29	Melanoma
TP53TG3	1.08E-42	3.64388714	2.57E-38	Melanoma
TP53TG3B	1.08E-42	3.64388714	2.57E-38	Melanoma
RASGRF1	7.34E-26	3.63505329	1.74E-21	Melanoma
COL11A2	7.08E-19	3.63154234	1.68E-14	Melanoma
EFCAB6	4.51E-13	3.62585207	1.07E-08	Melanoma
KCTD15	1.29E-43	3.62351234	3.06E-39	Melanoma
LOC254896	1.54E-16	3.62196005	3.65E-12	Melanoma
COL24A1	1.03E-18	3.61829239	2.43E-14	Melanoma
TOB2P1	1.94E-12	3.61119906	4.59E-08	Melanoma
PPP1R9A	5.31E-112	3.61029207	1.26E-107	Melanoma
CYP2J2	1.57E-32	3.60977972	3.71E-28	Melanoma
DLGAP1	4.46E-54	3.60801328	1.06E-49	Melanoma
ST5	3.16E-105	3.60422315	7.49E-101	Melanoma
KLHDC8A	6.10E-12	3.60418179	1.44E-07	Melanoma
EPDR1	2.34E-57	3.60077572	5.54E-53	Melanoma
SPATA17	2.51E-11	3.59667552	5.95E-07	Melanoma
PYGL	7.81E-72	3.59666024	1.85E-67	Melanoma
OSGIN1	1.06E-20	3.59063102	2.52E-16	Melanoma
ANXA3	6.16E-16	3.59037022	1.46E-11	Melanoma
COL16A1	9.09E-112	3.58252623	2.15E-107	Melanoma
KRT27	2.09E-20	3.57462335	4.95E-16	Melanoma
BHLHE41	1.55E-127	3.56870489	3.67E-123	Melanoma
RNF215	3.88E-13	3.56624478	9.20E-09	Melanoma
CD5L	6.87E-15	3.56574238	1.63E-10	Melanoma
RASEF	6.30E-24	3.56241917	1.49E-19	Melanoma
TIMP2	3.60E-216	3.56141092	8.53E-212	Melanoma
MYO1D	2.91E-126	3.56107778	6.89E-122	Melanoma
HES6	1.90E-16	3.56047015	4.51E-12	Melanoma
SRPX	1.54E-150	3.5555968	3.65E-146	Melanoma
PROS1	8.70E-159	3.55505209	2.06E-154	Melanoma
LBX2-AS1	4.60E-69	3.55486586	1.09E-64	Melanoma
TTC8	3.02E-69	3.54732192	7.16E-65	Melanoma

KRBOX1	2.30E-24	3.5355575	5.45E-20	Melanoma
ZNF704	5.30E-86	3.531407	1.26E-81	Melanoma
TEAD1	7.96E-102	3.52860787	1.89E-97	Melanoma
SH3BP4	4.63E-48	3.52115966	1.10E-43	Melanoma
MFGE8	9.82E-197	3.51430557	2.33E-192	Melanoma
TMPRSS5	3.09E-18	3.51084371	7.32E-14	Melanoma
LDLRAD3	1.26E-108	3.50706025	2.98E-104	Melanoma
CYTH3	8.83E-112	3.50408083	2.09E-107	Melanoma
GPRC5A	6.31E-52	3.50187653	1.50E-47	Melanoma
PHLDA3	3.58E-67	3.50136699	8.48E-63	Melanoma
MIPOL1	7.43E-20	3.50067428	1.76E-15	Melanoma
ROBO1	1.75E-129	3.49808145	4.15E-125	Melanoma
SLITRK2	2.47E-35	3.49132935	5.86E-31	Melanoma
TNFRSF21	9.44E-91	3.48571038	2.24E-86	Melanoma
ERBB3	2.44E-203	3.48144784	5.79E-199	Melanoma
NFE2	4.25E-11	3.46623481	1.01E-06	Melanoma
ATP1B1	1.93E-161	3.46361908	4.58E-157	Melanoma
C4A	1.92E-75	3.46113509	4.54E-71	Melanoma
GPRIN1	4.23E-20	3.45646305	1.00E-15	Melanoma
LOC257358	7.65E-27	3.45513664	1.81E-22	Melanoma
PPP1R1C	1.27E-09	3.45424426	3.00E-05	Melanoma
TSKU	1.61E-68	3.453314	3.81E-64	Melanoma
CX3CL1	1.16E-38	3.44434906	2.74E-34	Melanoma
PFN2	4.15E-114	3.43897826	9.84E-110	Melanoma
AEBP1	1.09E-186	3.4352432	2.59E-182	Melanoma
SHISA4	2.60E-53	3.43047122	6.17E-49	Melanoma
HRK	4.95E-31	3.43042785	1.17E-26	Melanoma
C1orf51	1.22E-18	3.43028206	2.88E-14	Melanoma
NRP2	1.87E-180	3.42527691	4.44E-176	Melanoma
FBXL2	2.35E-39	3.42506873	5.57E-35	Melanoma
EPS8	7.29E-141	3.42333945	1.73E-136	Melanoma
B9D1	2.29E-45	3.41864675	5.43E-41	Melanoma
PCDHGA3	4.53E-11	3.41435472	1.07E-06	Melanoma
LRRIQ3	2.38E-14	3.41053818	5.63E-10	Melanoma
WBSCR27	1.79E-18	3.4065588	4.24E-14	Melanoma
SPATA12	8.98E-12	3.40521824	2.13E-07	Melanoma
SPATA31A1	6.48E-16	3.40448006	1.53E-11	Melanoma
TP53TG3D	2.77E-30	3.40303351	6.57E-26	Melanoma
CRISPLD1	8.02E-30	3.39307655	1.90E-25	Melanoma
HMGA2	2.02E-32	3.38957218	4.78E-28	Melanoma
FLJ39051	5.52E-36	3.38837143	1.31E-31	Melanoma

CPVL	9.27E-102	3.38389885	2.20E-97	Melanoma
ETNK2	1.46E-34	3.38045965	3.47E-30	Melanoma
FAXC	8.86E-31	3.37918115	2.10E-26	Melanoma
C8orf48	2.18E-17	3.37761135	5.15E-13	Melanoma
FLJ39080	5.36E-10	3.37331762	1.27E-05	Melanoma
MNS1	4.25E-21	3.37308278	1.01E-16	Melanoma
FMNL2	3.14E-61	3.36690536	7.43E-57	Melanoma
OSCP1	1.96E-24	3.36621717	4.64E-20	Melanoma
IL17RE	5.70E-12	3.36514136	1.35E-07	Melanoma
P4HA2	1.19E-111	3.36167295	2.82E-107	Melanoma
ARNT2	7.33E-68	3.35517012	1.74E-63	Melanoma
MMP14	4.06E-126	3.35437814	9.62E-122	Melanoma
INSC	1.13E-12	3.35334224	2.69E-08	Melanoma
GMPR	2.85E-52	3.35149398	6.74E-48	Melanoma
KCNJ10	2.68E-24	3.35015535	6.35E-20	Melanoma
CDC42EP4	4.98E-79	3.34855419	1.18E-74	Melanoma
MMP17	3.37E-24	3.34350943	7.98E-20	Melanoma
LINC00673	2.72E-143	3.34268951	6.43E-139	Melanoma
SCG2	2.53E-19	3.34056094	5.98E-15	Melanoma
CDK18	2.00E-35	3.34001653	4.74E-31	Melanoma
PPM1H	1.64E-43	3.33594744	3.89E-39	Melanoma
SPR	3.64E-74	3.33039661	8.63E-70	Melanoma
S100A2	3.71E-14	3.32982665	8.79E-10	Melanoma
TYRO3	1.60E-55	3.32772532	3.80E-51	Melanoma
KCNJ2-AS1	3.59E-15	3.32400952	8.51E-11	Melanoma
NPAS2	5.25E-61	3.32353136	1.24E-56	Melanoma
SELENBP1	3.59E-56	3.31789094	8.51E-52	Melanoma
ALDH1A1	6.75E-112	3.31542284	1.60E-107	Melanoma
MORN2	1.49E-83	3.31215018	3.53E-79	Melanoma
PEG10	1.14E-125	3.31066543	2.70E-121	Melanoma
IFITM10	4.50E-22	3.31009201	1.07E-17	Melanoma
CDH2	1.01E-55	3.30836163	2.40E-51	Melanoma
TBC1D16	5.62E-102	3.30598243	1.33E-97	Melanoma
DOK7	7.74E-12	3.3041508	1.83E-07	Melanoma
TANC1	7.93E-133	3.30062438	1.88E-128	Melanoma
LAPTM4B	1.69E-96	3.29993991	3.99E-92	Melanoma
MUC15	1.47E-20	3.29676252	3.47E-16	Melanoma
LBX2	8.62E-12	3.29124401	2.04E-07	Melanoma
ARRDC4	1.49E-33	3.28791828	3.53E-29	Melanoma
KLHDC8B	6.45E-48	3.28706432	1.53E-43	Melanoma
PACSIN3	9.44E-20	3.28551742	2.24E-15	Melanoma

DOCK7	9.85E-95	3.28417282	2.33E-90	Melanoma
SEMA6D	3.41E-24	3.27933928	8.08E-20	Melanoma
S100A13	2.79E-192	3.27714118	6.62E-188	Melanoma
BEST1	6.06E-82	3.27682299	1.43E-77	Melanoma
CHCHD6	6.40E-137	3.27235722	1.51E-132	Melanoma
C7orf63	2.16E-16	3.26194862	5.13E-12	Melanoma
PLS1	1.78E-12	3.26067256	4.22E-08	Melanoma
TRIM9	7.04E-48	3.25894823	1.67E-43	Melanoma
ST8SIA6	3.67E-09	3.25694269	8.69E-05	Melanoma
PFKFB4	3.09E-37	3.25655105	7.32E-33	Melanoma
LRGUK	2.63E-21	3.25388577	6.23E-17	Melanoma
LOC344595	3.97E-30	3.25350214	9.40E-26	Melanoma
PCDHGA8	3.14E-09	3.25307262	7.45E-05	Melanoma
LZTS1	5.03E-107	3.25053986	1.19E-102	Melanoma
SLC6A10P	1.64E-24	3.24610425	3.89E-20	Melanoma
MAPK10	1.00E-14	3.24519773	2.37E-10	Melanoma
RNF150	1.03E-15	3.24205511	2.44E-11	Melanoma
DDO	9.49E-11	3.24200835	2.25E-06	Melanoma
CTDSPL	5.13E-67	3.23790454	1.21E-62	Melanoma
TTC39A	1.70E-34	3.23502797	4.02E-30	Melanoma
RAB34	1.62E-152	3.23365429	3.85E-148	Melanoma
SERPINA1	2.25E-89	3.22691477	5.33E-85	Melanoma
PLA1A	1.42E-32	3.22536998	3.35E-28	Melanoma
GULP1	2.91E-62	3.22524282	6.88E-58	Melanoma
C9orf9	5.76E-22	3.22462964	1.36E-17	Melanoma
PLEKHA4	5.62E-100	3.22367279	1.33E-95	Melanoma
RFTN2	6.38E-30	3.21972335	1.51E-25	Melanoma
NPHP1	1.63E-38	3.21714935	3.87E-34	Melanoma
MICALL2	2.06E-78	3.21621558	4.89E-74	Melanoma
LOC730101	1.97E-25	3.20883505	4.66E-21	Melanoma
SLC22A4	1.13E-24	3.20713826	2.68E-20	Melanoma
PLAT	1.97E-80	3.20271405	4.66E-76	Melanoma
SMOX	9.04E-31	3.1992317	2.14E-26	Melanoma
PTGR1	7.63E-84	3.19819496	1.81E-79	Melanoma
ECM1	1.17E-113	3.19719751	2.77E-109	Melanoma
HOXD-AS1	2.56E-31	3.19294258	6.07E-27	Melanoma
DMKN	1.17E-24	3.18854448	2.78E-20	Melanoma
COBL	2.28E-09	3.18725991	5.39E-05	Melanoma
PYCR1	5.84E-92	3.18182066	1.38E-87	Melanoma
SULT1C2	1.92E-24	3.17497854	4.55E-20	Melanoma
MAMDC2	4.03E-19	3.17310796	9.54E-15	Melanoma

C11orf74	9.83E-47	3.16956466	2.33E-42	Melanoma
DDIT4L	4.74E-14	3.16840141	1.12E-09	Melanoma
C6orf52	6.36E-16	3.16022622	1.51E-11	Melanoma
DHRS11	4.58E-17	3.15117959	1.08E-12	Melanoma
LOC100130776	3.15E-42	3.15098728	7.46E-38	Melanoma
ARHGEF11	2.52E-67	3.13983912	5.97E-63	Melanoma
RAB6B	2.52E-23	3.13766628	5.96E-19	Melanoma
HSPA12A	7.56E-51	3.13481047	1.79E-46	Melanoma
KIF3C	2.76E-64	3.13373417	6.54E-60	Melanoma
FAM19A5	3.93E-14	3.13326875	9.31E-10	Melanoma
MDK	4.65E-102	3.12726081	1.10E-97	Melanoma
ITGB5	8.06E-66	3.1269364	1.91E-61	Melanoma
LINGO2	8.62E-15	3.12277687	2.04E-10	Melanoma
IQCD	2.14E-10	3.12175347	5.07E-06	Melanoma
RNF182	8.91E-19	3.11844946	2.11E-14	Melanoma
FAH	2.58E-76	3.11656283	6.11E-72	Melanoma
ANO4	1.85E-13	3.11281597	4.38E-09	Melanoma
CEP170B	5.71E-24	3.11203912	1.35E-19	Melanoma
ASPA	3.31E-12	3.11189687	7.84E-08	Melanoma
C2	4.66E-50	3.11137609	1.10E-45	Melanoma
PTPRS	1.37E-155	3.10931675	3.24E-151	Melanoma
PPT2	3.33E-112	3.10606754	7.89E-108	Melanoma
REEP6	6.94E-28	3.10451469	1.64E-23	Melanoma
TPD52L1	4.58E-35	3.10286253	1.09E-30	Melanoma
GNG12-AS1	4.83E-10	3.09756949	1.14E-05	Melanoma
KCTD3	2.78E-64	3.09245689	6.58E-60	Melanoma
TMEM177	1.58E-59	3.08983318	3.75E-55	Melanoma
RASAL2	4.19E-65	3.08678697	9.92E-61	Melanoma
LOC100507299	1.67E-17	3.0751631	3.95E-13	Melanoma
LOC100507564	7.78E-10	3.07413141	1.84E-05	Melanoma
DZIP1L	1.07E-31	3.07370485	2.53E-27	Melanoma
DNAJC6	1.05E-19	3.07271009	2.48E-15	Melanoma
FIGN	4.40E-25	3.07131677	1.04E-20	Melanoma
PCDHB14	6.85E-12	3.06885037	1.62E-07	Melanoma
COL4A5	5.99E-24	3.06789674	1.42E-19	Melanoma
TTC26	1.22E-24	3.06557542	2.89E-20	Melanoma
CHRNA6	5.04E-20	3.06424432	1.19E-15	Melanoma
KANK1	5.51E-84	3.06275288	1.31E-79	Melanoma
PLXNA1	5.07E-134	3.06184877	1.20E-129	Melanoma
SGCE	5.89E-128	3.06000996	1.40E-123	Melanoma
SCARB1	9.40E-72	3.05905878	2.23E-67	Melanoma

L1CAM	7.65E-37	3.05519378	1.81E-32	Melanoma
LAMC3	9.23E-15	3.05457953	2.19E-10	Melanoma
PRRT3-AS1	2.00E-20	3.04998283	4.73E-16	Melanoma
EFHD1	1.81E-30	3.04903124	4.29E-26	Melanoma
MATN2	1.52E-120	3.04889898	3.60E-116	Melanoma
KCTD1	1.04E-15	3.04886691	2.47E-11	Melanoma
NAALADL2	8.98E-25	3.0443392	2.13E-20	Melanoma
GPR125	3.42E-19	3.04175819	8.10E-15	Melanoma
GPM6B	7.12E-146	3.04037731	1.69E-141	Melanoma
PRR4	6.91E-36	3.03971028	1.64E-31	Melanoma
DIP2C	3.21E-147	3.03967597	7.61E-143	Melanoma
LIF	1.80E-37	3.03389386	4.27E-33	Melanoma
FKBP1B	1.90E-11	3.03279682	4.50E-07	Melanoma
TM4SF1	6.92E-139	3.03052462	1.64E-134	Melanoma
EMP1	3.59E-142	3.02848309	8.49E-138	Melanoma
DMXL2	2.22E-103	3.02825905	5.25E-99	Melanoma
LRP2	6.79E-17	3.02749789	1.61E-12	Melanoma
CERCAM	1.48E-101	3.02555195	3.51E-97	Melanoma
SATB2	3.71E-21	3.0224332	8.79E-17	Melanoma
B3GNT1	3.23E-84	3.0214512	7.65E-80	Melanoma
PRKAR2B	5.41E-40	3.02022812	1.28E-35	Melanoma
TEX14	1.11E-14	3.01935106	2.63E-10	Melanoma
KAZN	1.01E-31	3.01881141	2.39E-27	Melanoma
AGRN	4.05E-90	3.01195241	9.59E-86	Melanoma
LOC100128822	7.77E-13	3.00913144	1.84E-08	Melanoma
DHCR24	3.68E-95	3.00680124	8.72E-91	Melanoma
TNFRSF12A	1.14E-105	3.00499684	2.70E-101	Melanoma
PRTG	6.32E-12	2.99976812	1.50E-07	Melanoma
SPATA6	3.15E-51	2.99823608	7.45E-47	Melanoma
IFI27	7.64E-174	2.99714232	1.81E-169	Melanoma
FRMD5	3.42E-11	2.99619643	8.10E-07	Melanoma
GLT25D2	8.73E-29	2.99156094	2.07E-24	Melanoma
GLCE	1.00E-86	2.99104452	2.37E-82	Melanoma
IL17RC	9.75E-67	2.98993759	2.31E-62	Melanoma
ACTR3B	2.11E-28	2.98513271	4.99E-24	Melanoma
OSBPL1A	1.06E-89	2.97819169	2.51E-85	Melanoma
PPAPDC3	1.42E-16	2.976179	3.36E-12	Melanoma
ARHGEF17	3.03E-51	2.97605049	7.18E-47	Melanoma
B4GALT6	7.45E-27	2.97518066	1.76E-22	Melanoma
METRN	2.16E-29	2.97243169	5.10E-25	Melanoma
SPINT1	1.34E-36	2.97203429	3.18E-32	Melanoma

MAML3	1.20E-82	2.97164536	2.83E-78	Melanoma
DAPK1	6.36E-69	2.96750667	1.51E-64	Melanoma
HEXIM2	8.31E-33	2.96320738	1.97E-28	Melanoma
ERBB2	7.66E-68	2.95907566	1.81E-63	Melanoma
FAT1	1.18E-80	2.95862465	2.80E-76	Melanoma
NHSL1	1.24E-132	2.94893299	2.94E-128	Melanoma
GOLM1	2.61E-89	2.94260518	6.19E-85	Melanoma
AHNAK2	3.29E-54	2.9355878	7.79E-50	Melanoma
OSBPL6	3.14E-33	2.93374531	7.45E-29	Melanoma
FARP1	1.71E-72	2.93368483	4.04E-68	Melanoma
SLMO1	2.96E-21	2.93362052	7.02E-17	Melanoma
IGF2BP3	9.19E-30	2.93028666	2.18E-25	Melanoma
STRA6	8.38E-10	2.92838462	1.98E-05	Melanoma
GATSL3	1.61E-79	2.92664376	3.82E-75	Melanoma
GTF2IRD1	5.42E-19	2.9228176	1.28E-14	Melanoma
TSPAN6	1.23E-61	2.92159439	2.91E-57	Melanoma
WLS	7.11E-74	2.920802	1.68E-69	Melanoma
CABLES1	6.01E-36	2.92071833	1.42E-31	Melanoma
MCAM	1.56E-119	2.91889282	3.68E-115	Melanoma
TUBB3	9.69E-78	2.91741607	2.29E-73	Melanoma
PI15	9.39E-33	2.91710278	2.22E-28	Melanoma
LOC100289361	5.14E-12	2.91543676	1.22E-07	Melanoma
AVIL	9.02E-22	2.91297831	2.14E-17	Melanoma
BAIAP2	6.82E-134	2.9129499	1.62E-129	Melanoma
GSTZ1	9.64E-48	2.91160338	2.28E-43	Melanoma
PARD3	4.08E-30	2.91155668	9.66E-26	Melanoma
DGCR6	3.30E-47	2.90601829	7.81E-43	Melanoma
FKBP10	9.80E-93	2.9030421	2.32E-88	Melanoma
FNTB	3.49E-49	2.90261253	8.26E-45	Melanoma
COPRS	2.59E-49	2.90203923	6.13E-45	Melanoma
PCGF2	4.73E-47	2.90034142	1.12E-42	Melanoma
TRIM47	4.85E-58	2.89999684	1.15E-53	Melanoma
IQSEC2	1.58E-18	2.89993417	3.74E-14	Melanoma
YAP1	1.31E-37	2.89937853	3.10E-33	Melanoma
FSTL3	4.88E-35	2.89634978	1.16E-30	Melanoma
TMCC2	1.59E-17	2.89574743	3.76E-13	Melanoma
KCNH1	8.46E-13	2.89495951	2.00E-08	Melanoma
PCDHGC3	1.50E-116	2.88949008	3.55E-112	Melanoma
ABTB2	1.54E-74	2.88789914	3.65E-70	Melanoma
CHPF	4.72E-135	2.887723	1.12E-130	Melanoma
GRHL1	1.92E-12	2.88721143	4.55E-08	Melanoma

MKRN3	1.86E-15	2.88532194	4.40E-11	Melanoma
ST7	5.36E-80	2.88458558	1.27E-75	Melanoma
C5orf54	1.86E-26	2.88427548	4.42E-22	Melanoma
MOK	1.13E-108	2.88278805	2.68E-104	Melanoma
CDK2	7.78E-131	2.8816771	1.84E-126	Melanoma
LOC100506474	3.01E-17	2.88114812	7.13E-13	Melanoma
FAM133A	9.37E-10	2.88009569	2.22E-05	Melanoma
PRICKLE2	4.88E-19	2.87760342	1.16E-14	Melanoma
CD276	4.18E-91	2.86974192	9.89E-87	Melanoma
CBS	1.04E-10	2.86635856	2.47E-06	Melanoma
LCA5	3.38E-14	2.86411453	8.01E-10	Melanoma
EGFL8	2.50E-52	2.86375265	5.91E-48	Melanoma
UNC13B	9.20E-30	2.86287576	2.18E-25	Melanoma
SPARC	3.80E-193	2.86258268	8.99E-189	Melanoma
ARHGAP39	5.72E-18	2.86235074	1.35E-13	Melanoma
GPR126	6.48E-22	2.86171267	1.53E-17	Melanoma
RCAN1	1.33E-98	2.86153607	3.15E-94	Melanoma
CBR3	1.62E-60	2.86060895	3.83E-56	Melanoma
PHGDH	8.79E-57	2.85799006	2.08E-52	Melanoma
C3orf65	3.19E-12	2.85571671	7.56E-08	Melanoma
SH3TC2	2.70E-46	2.85479477	6.40E-42	Melanoma
C19orf57	3.45E-12	2.85221471	8.17E-08	Melanoma
FAM129B	1.26E-47	2.8459863	2.98E-43	Melanoma
NME4	2.11E-96	2.8450481	5.01E-92	Melanoma
MOCS1	2.62E-33	2.84462981	6.21E-29	Melanoma
YPEL4	1.01E-17	2.84456492	2.39E-13	Melanoma
LIPH	8.25E-10	2.84244461	1.96E-05	Melanoma
KDM5B-AS1	3.86E-20	2.8411445	9.15E-16	Melanoma
ID4	1.90E-19	2.84006471	4.50E-15	Melanoma
GCSH	2.01E-105	2.83775918	4.75E-101	Melanoma
TIMP3	3.07E-169	2.832323	7.26E-165	Melanoma
LHFPL2	8.87E-86	2.83039845	2.10E-81	Melanoma
GNG12	1.19E-139	2.82197658	2.83E-135	Melanoma
C16orf93	1.58E-14	2.82108012	3.73E-10	Melanoma
ZNF280B	2.20E-66	2.82019861	5.22E-62	Melanoma
SLC19A2	3.60E-102	2.8201788	8.52E-98	Melanoma
CCND1	1.39E-145	2.81947039	3.30E-141	Melanoma
DST	7.74E-148	2.81847584	1.83E-143	Melanoma
SNX24	1.25E-31	2.81587212	2.96E-27	Melanoma
LONRF1	1.87E-60	2.81410114	4.43E-56	Melanoma
PLS3	2.10E-127	2.81171281	4.97E-123	Melanoma

TTYH2	1.06E-68	2.81035739	2.51E-64	Melanoma
LRP6	1.61E-61	2.80944338	3.81E-57	Melanoma
RANBP17	4.03E-25	2.8078454	9.56E-21	Melanoma
GSN	1.32E-200	2.80752305	3.13E-196	Melanoma
ANKRD50	7.42E-49	2.80478169	1.76E-44	Melanoma
MMP16	7.29E-24	2.80302781	1.73E-19	Melanoma
RND3	2.23E-76	2.79981508	5.28E-72	Melanoma
GABRP	2.02E-09	2.79859713	4.79E-05	Melanoma
TBX18	3.85E-15	2.79705539	9.12E-11	Melanoma
GRB10	2.73E-31	2.79616351	6.46E-27	Melanoma
CADPS	3.06E-12	2.79303398	7.25E-08	Melanoma
CHI3L1	7.60E-32	2.7929846	1.80E-27	Melanoma
HMCN1	5.88E-72	2.79141445	1.39E-67	Melanoma
HES1	1.56E-50	2.7912679	3.71E-46	Melanoma
SLITRK1	1.34E-13	2.79086835	3.18E-09	Melanoma
DYNC2LI1	5.57E-55	2.78516745	1.32E-50	Melanoma
PRKCDBP	2.44E-99	2.77809994	5.78E-95	Melanoma
MFAP2	8.37E-70	2.77770618	1.98E-65	Melanoma
MXI1	7.80E-97	2.77315033	1.85E-92	Melanoma
DYNC1I1	2.37E-24	2.77058553	5.63E-20	Melanoma
DCLK2	5.25E-18	2.7685708	1.24E-13	Melanoma
WBP5	2.79E-110	2.76224869	6.60E-106	Melanoma
FARP2	2.49E-117	2.75922206	5.91E-113	Melanoma
PLOD3	4.22E-176	2.75660971	9.99E-172	Melanoma
CDK20	6.96E-24	2.75608057	1.65E-19	Melanoma
CCDC149	1.52E-10	2.7556082	3.61E-06	Melanoma
POLR3G	2.34E-41	2.75423513	5.55E-37	Melanoma
PLOD1	8.10E-153	2.75287296	1.92E-148	Melanoma
TRIQK	1.39E-57	2.75212192	3.29E-53	Melanoma
MAGI2	1.24E-14	2.75008747	2.93E-10	Melanoma
CLIP2	1.98E-36	2.74993555	4.70E-32	Melanoma
OTUD7B	1.32E-71	2.74964633	3.12E-67	Melanoma
GPRC5B	2.93E-68	2.74841444	6.93E-64	Melanoma
GSTA4	1.56E-55	2.74608786	3.69E-51	Melanoma
PCDHGA5	2.13E-12	2.7412202	5.05E-08	Melanoma
PSEN2	4.13E-81	2.73952038	9.78E-77	Melanoma
ME1	1.94E-25	2.73931906	4.61E-21	Melanoma
ATL1	9.20E-27	2.7373468	2.18E-22	Melanoma
ENPP2	1.08E-61	2.73700587	2.56E-57	Melanoma
SERPINI1	1.42E-50	2.73506743	3.35E-46	Melanoma
LOC654342	6.21E-47	2.73506643	1.47E-42	Melanoma

AKR1E2	7.36E-13	2.73448505	1.74E-08	Melanoma
NR2F6	3.16E-26	2.73148133	7.47E-22	Melanoma
BTBD3	6.42E-46	2.72813041	1.52E-41	Melanoma
SPATA7	4.12E-16	2.71955364	9.75E-12	Melanoma
PTDSS2	9.27E-19	2.71666429	2.20E-14	Melanoma
KIRREL	9.83E-47	2.71657744	2.33E-42	Melanoma
MYLK-AS1	4.57E-12	2.71615759	1.08E-07	Melanoma
PSRC1	1.84E-37	2.71385053	4.35E-33	Melanoma
RAB13	1.29E-151	2.71377448	3.04E-147	Melanoma
MYO10	2.78E-104	2.71306501	6.58E-100	Melanoma
LAMB2	1.27E-148	2.70995808	3.00E-144	Melanoma
MST1P2	9.56E-25	2.70961243	2.26E-20	Melanoma
RAB40B	3.11E-44	2.70870286	7.37E-40	Melanoma
CCDC103	1.43E-09	2.7079064	3.39E-05	Melanoma
A2M	2.68E-150	2.70746359	6.34E-146	Melanoma
POMT2	6.88E-42	2.70621637	1.63E-37	Melanoma
SLC16A5	1.94E-24	2.70567262	4.60E-20	Melanoma
CADPS2	1.95E-25	2.70430879	4.62E-21	Melanoma
SIPA1L2	6.44E-47	2.70362981	1.53E-42	Melanoma
CCDC40	2.10E-17	2.70346538	4.97E-13	Melanoma
PFKFB2	3.78E-52	2.7030552	8.94E-48	Melanoma
ACSBG1	2.14E-09	2.70240529	5.07E-05	Melanoma
SNAI2	5.35E-40	2.70181583	1.27E-35	Melanoma
CAMSAP2	2.24E-39	2.70096166	5.31E-35	Melanoma
PDZRN3	2.14E-12	2.69775991	5.07E-08	Melanoma
SORBS1	1.35E-42	2.6932803	3.20E-38	Melanoma
MEIS2	2.44E-43	2.69288194	5.77E-39	Melanoma
CHST10	2.14E-23	2.69272503	5.07E-19	Melanoma
C14orf79	1.09E-20	2.69250294	2.58E-16	Melanoma
SIRPA	9.22E-103	2.69249516	2.18E-98	Melanoma
ROBO2	1.56E-09	2.69149668	3.69E-05	Melanoma
TRIP6	1.07E-40	2.68842794	2.53E-36	Melanoma
ACY1	1.74E-62	2.68737502	4.11E-58	Melanoma
PMP22	1.90E-127	2.68549645	4.50E-123	Melanoma
KIAA1755	1.83E-49	2.68255373	4.34E-45	Melanoma
STOX2	2.10E-23	2.68223406	4.97E-19	Melanoma
EXTL2	1.08E-55	2.67927751	2.56E-51	Melanoma
TUBB4A	4.94E-37	2.67818741	1.17E-32	Melanoma
PFKM	6.37E-103	2.67663462	1.51E-98	Melanoma
BCL2L2	1.38E-28	2.67659151	3.27E-24	Melanoma
QDPR	2.47E-130	2.67616758	5.86E-126	Melanoma

TSPAN7	7.40E-73	2.67431924	1.75E-68	Melanoma
ACOT7	1.87E-107	2.67321497	4.44E-103	Melanoma
C1orf85	7.77E-146	2.67235061	1.84E-141	Melanoma
ZBTB47	5.68E-25	2.67161317	1.34E-20	Melanoma
FCGR2A	5.89E-104	2.66818428	1.40E-99	Melanoma
GABRA3	4.31E-12	2.6673296	1.02E-07	Melanoma
MC1R	3.49E-50	2.66706401	8.27E-46	Melanoma
HDAC11	1.14E-37	2.66676001	2.71E-33	Melanoma
DPCD	7.53E-29	2.66490411	1.78E-24	Melanoma
ASAP2	7.92E-53	2.66307963	1.88E-48	Melanoma
PLXNB2	2.05E-136	2.6630184	4.86E-132	Melanoma
SOCS6	1.56E-63	2.66301185	3.69E-59	Melanoma
LOC401010	2.01E-14	2.6608719	4.77E-10	Melanoma
CALD1	6.23E-186	2.65840707	1.47E-181	Melanoma
PLA2G4A	6.30E-29	2.65833359	1.49E-24	Melanoma
WIPI1	1.50E-126	2.65446021	3.55E-122	Melanoma
BAIAP2L1	4.92E-28	2.65347242	1.16E-23	Melanoma
SMARCA1	1.60E-63	2.65150217	3.78E-59	Melanoma
TTLL4	3.33E-100	2.64453735	7.90E-96	Melanoma
SLC26A2	1.39E-126	2.64006173	3.29E-122	Melanoma
PHLDB1	7.66E-85	2.63651183	1.81E-80	Melanoma
FNBP1L	4.92E-64	2.63493792	1.16E-59	Melanoma
FMO5	3.46E-35	2.6333963	8.20E-31	Melanoma
BAGE5	1.25E-22	2.63208711	2.96E-18	Melanoma
MAPRE3	1.79E-30	2.63010218	4.24E-26	Melanoma
TMEM133	3.85E-09	2.62953509	9.11E-05	Melanoma
BMX	2.59E-22	2.62437599	6.14E-18	Melanoma
SMIM10	2.38E-25	2.62302497	5.64E-21	Melanoma
MT1M	2.80E-20	2.61950536	6.64E-16	Melanoma
LRRC23	4.77E-29	2.61247649	1.13E-24	Melanoma
GAS2L1	1.25E-24	2.61063605	2.95E-20	Melanoma
VEGFA	4.46E-26	2.60991934	1.06E-21	Melanoma
NUDT8	4.24E-23	2.60763929	1.00E-18	Melanoma
MPDZ	1.82E-62	2.60686	4.32E-58	Melanoma
CDK2AP1	2.47E-96	2.60395705	5.84E-92	Melanoma
LINC00340	4.24E-12	2.60137001	1.00E-07	Melanoma
MROH6	1.90E-10	2.60104281	4.50E-06	Melanoma
NAV3	8.77E-39	2.60093729	2.08E-34	Melanoma
NRBP2	3.30E-55	2.60054016	7.82E-51	Melanoma
CREB5	1.72E-70	2.6000815	4.08E-66	Melanoma
LGALS3BP	3.22E-188	2.59992124	7.62E-184	Melanoma

DLC1	2.66E-99	2.59840013	6.29E-95	Melanoma
KCNJ13	1.40E-21	2.59759819	3.32E-17	Melanoma
LTBR	3.76E-131	2.59738066	8.91E-127	Melanoma
CYSTM1	1.37E-150	2.59733151	3.26E-146	Melanoma
CNN3	2.71E-166	2.596733	6.42E-162	Melanoma
VAT1	9.67E-211	2.59586402	2.29E-206	Melanoma
FBXW9	1.92E-23	2.59378535	4.55E-19	Melanoma
IQCK	8.56E-37	2.58894958	2.03E-32	Melanoma
ETV2	1.56E-09	2.58631331	3.70E-05	Melanoma
STEAP1B	7.17E-43	2.58442874	1.70E-38	Melanoma
BACE2	3.07E-137	2.58416566	7.28E-133	Melanoma
C15orf38-AP3S2	3.03E-26	2.58118973	7.17E-22	Melanoma
SMIM1	5.12E-20	2.58112934	1.21E-15	Melanoma
FAM27A	1.88E-52	2.57948659	4.46E-48	Melanoma
HP07349	6.05E-13	2.57730058	1.43E-08	Melanoma
TJP1	2.24E-117	2.57651304	5.31E-113	Melanoma
KDELR3	5.09E-66	2.57414448	1.21E-61	Melanoma
CDH1	2.41E-91	2.57293096	5.70E-87	Melanoma
PEX10	3.79E-63	2.57086356	8.99E-59	Melanoma
HYDIN	9.04E-14	2.57028984	2.14E-09	Melanoma
RAPH1	3.04E-68	2.56894853	7.20E-64	Melanoma
IGF2BP2	6.81E-70	2.56794388	1.61E-65	Melanoma
CPEB1	8.42E-37	2.56641046	1.99E-32	Melanoma
IMPA2	1.18E-11	2.56606469	2.80E-07	Melanoma
LOC150568	5.34E-13	2.56557498	1.27E-08	Melanoma
C11orf96	2.55E-19	2.56425246	6.05E-15	Melanoma
TEX2	1.39E-92	2.56143248	3.29E-88	Melanoma
CCDC171	1.13E-22	2.56114862	2.68E-18	Melanoma
NEO1	2.96E-44	2.56068092	7.01E-40	Melanoma
ARHGAP32	3.91E-57	2.56040147	9.27E-53	Melanoma
ALG14	6.90E-59	2.56025115	1.64E-54	Melanoma
DLL3	1.58E-16	2.55667578	3.75E-12	Melanoma
AMOT	1.82E-16	2.55535209	4.30E-12	Melanoma
H1F0	7.96E-102	2.55419807	1.88E-97	Melanoma
PRSS23	1.33E-114	2.55297432	3.16E-110	Melanoma
METTL1	1.25E-42	2.55015656	2.96E-38	Melanoma
PDXP	2.18E-28	2.54652951	5.17E-24	Melanoma
LOC286297	1.57E-09	2.54519653	3.73E-05	Melanoma
CTSL1	2.16E-157	2.5443922	5.11E-153	Melanoma
LOC100127983	4.30E-12	2.54376141	1.02E-07	Melanoma
RTN2	2.98E-12	2.54351846	7.05E-08	Melanoma

LOC645166	9.04E-62	2.53895069	2.14E-57	Melanoma
PLTP	2.05E-65	2.53856338	4.87E-61	Melanoma
DDR2	5.26E-55	2.53807492	1.25E-50	Melanoma
PLK2	5.61E-110	2.53549852	1.33E-105	Melanoma
ZNF771	2.51E-27	2.53453716	5.95E-23	Melanoma
CLIC4	2.75E-141	2.53329863	6.51E-137	Melanoma
TTC30A	7.01E-13	2.53289511	1.66E-08	Melanoma
CST3	3.29E-185	2.52685195	7.79E-181	Melanoma
HSBP1L1	6.79E-52	2.52682301	1.61E-47	Melanoma
CHPT1	3.53E-59	2.52659004	8.37E-55	Melanoma
ABCD1	2.01E-68	2.52447074	4.76E-64	Melanoma
CHST3	1.09E-19	2.52054909	2.58E-15	Melanoma
RPP25	6.44E-30	2.51911695	1.53E-25	Melanoma
GPR153	2.47E-19	2.51799492	5.85E-15	Melanoma
ALDH7A1	1.74E-61	2.51737649	4.12E-57	Melanoma
GALE	2.63E-76	2.51732467	6.23E-72	Melanoma
NEDD4L	1.46E-68	2.51596484	3.45E-64	Melanoma
RAB32	2.12E-26	2.51336098	5.02E-22	Melanoma
AGAP3	8.97E-72	2.51242516	2.12E-67	Melanoma
HSPB8	2.60E-57	2.50550326	6.17E-53	Melanoma
PTCHD3P1	3.04E-76	2.50457425	7.21E-72	Melanoma
PCSK1	4.96E-13	2.503432	1.17E-08	Melanoma
FAM86DP	1.97E-65	2.50275837	4.66E-61	Melanoma
DTNA	7.77E-15	2.50062495	1.84E-10	Melanoma
FAM86B1	1.72E-12	2.49997073	4.08E-08	Melanoma
MT1E	1.70E-83	2.49893069	4.03E-79	Melanoma
TLCD1	3.70E-15	2.49564639	8.76E-11	Melanoma
TMEM246	7.11E-15	2.49560832	1.68E-10	Melanoma
PTPN21	1.52E-17	2.49529458	3.60E-13	Melanoma
MTSS1L	2.93E-16	2.49367275	6.93E-12	Melanoma
ST3GAL6	7.37E-124	2.49367199	1.75E-119	Melanoma
BOK	1.99E-32	2.48822236	4.71E-28	Melanoma
LRP11	2.15E-18	2.48651834	5.09E-14	Melanoma
LCN2	3.22E-15	2.48624084	7.62E-11	Melanoma
TUBB2A	2.82E-105	2.48216347	6.67E-101	Melanoma
TIGD4	1.33E-11	2.48135835	3.15E-07	Melanoma
LAMA4	3.53E-101	2.48082743	8.37E-97	Melanoma
LOC100130015	1.42E-18	2.48052771	3.37E-14	Melanoma
LINC00467	1.70E-41	2.47408397	4.03E-37	Melanoma
Sep-10	5.16E-77	2.47010064	1.22E-72	Melanoma
AP1S2	7.01E-201	2.46961138	1.66E-196	Melanoma

PRR19	1.60E-12	2.46762656	3.80E-08	Melanoma
MTMR9LP	7.98E-47	2.46717927	1.89E-42	Melanoma
ACSL3	4.22E-154	2.464832	1.00E-149	Melanoma
NGFR	1.24E-11	2.46402864	2.94E-07	Melanoma
VEPH1	6.55E-22	2.46242538	1.55E-17	Melanoma
SCCPDH	1.86E-141	2.46063372	4.40E-137	Melanoma
TWIST1	2.20E-19	2.46048093	5.22E-15	Melanoma
PLOD2	9.68E-54	2.46021225	2.29E-49	Melanoma
ZCWPW2	2.64E-12	2.46015648	6.25E-08	Melanoma
CAV1	3.80E-159	2.45843914	8.99E-155	Melanoma
SYNM	4.37E-43	2.45669025	1.03E-38	Melanoma
DAG1	1.25E-141	2.45095254	2.97E-137	Melanoma
BATF2	1.92E-10	2.45014348	4.54E-06	Melanoma
IL1RAP	4.33E-80	2.44936009	1.03E-75	Melanoma
ANGPTL4	3.24E-25	2.44699669	7.68E-21	Melanoma
CTSF	1.18E-62	2.44565703	2.80E-58	Melanoma
GLB1L2	7.25E-12	2.44543495	1.72E-07	Melanoma
ROR1	5.83E-19	2.44486797	1.38E-14	Melanoma
WASF1	1.07E-23	2.44486722	2.53E-19	Melanoma
SGK1	4.61E-156	2.44453729	1.09E-151	Melanoma
DMD	2.25E-36	2.44450191	5.32E-32	Melanoma
ARHGEF10L	5.15E-19	2.44338415	1.22E-14	Melanoma
IGF1R	1.23E-145	2.44119296	2.90E-141	Melanoma
LOC100128881	4.51E-19	2.43953523	1.07E-14	Melanoma
ACOT11	6.97E-16	2.43629683	1.65E-11	Melanoma
LARGE	2.23E-52	2.43614957	5.28E-48	Melanoma
LOC401397	1.19E-110	2.43386662	2.82E-106	Melanoma
SLC25A4	1.97E-119	2.43281955	4.68E-115	Melanoma
GNAI1	1.50E-38	2.43212829	3.55E-34	Melanoma
PLCB4	7.56E-22	2.43173978	1.79E-17	Melanoma
IFT140	6.90E-32	2.43053932	1.63E-27	Melanoma
GAS8	3.33E-44	2.4304852	7.89E-40	Melanoma
CD9	5.35E-123	2.43034979	1.27E-118	Melanoma
FAM127C	2.98E-31	2.42939299	7.06E-27	Melanoma
PCDHGA7	6.68E-11	2.42889272	1.58E-06	Melanoma
ITGB8	1.18E-80	2.42473183	2.79E-76	Melanoma
FZD7	2.81E-16	2.42443632	6.66E-12	Melanoma
MAP2	7.35E-24	2.42428727	1.74E-19	Melanoma
FSD1L	3.93E-22	2.42382407	9.31E-18	Melanoma
MEIS1	7.19E-36	2.42161603	1.70E-31	Melanoma
MRAS	1.03E-52	2.41916659	2.45E-48	Melanoma

SNX33	2.53E-15	2.41820864	5.99E-11	Melanoma
OPN3	7.25E-14	2.41781186	1.72E-09	Melanoma
GPC1	6.55E-23	2.41624201	1.55E-18	Melanoma
PHLDA2	3.91E-25	2.41549443	9.25E-21	Melanoma
G6PC3	5.25E-134	2.4054538	1.24E-129	Melanoma
SRC	2.61E-37	2.40466624	6.17E-33	Melanoma
GPR3	1.49E-11	2.39979885	3.52E-07	Melanoma
CCDC36	3.58E-15	2.39828891	8.48E-11	Melanoma
EPHA3	7.18E-19	2.39815464	1.70E-14	Melanoma
UBXN10	6.25E-16	2.39729284	1.48E-11	Melanoma
NENF	5.93E-56	2.3964861	1.40E-51	Melanoma
ASRGL1	7.41E-44	2.3949133	1.75E-39	Melanoma
EFNA1	1.83E-42	2.39489804	4.33E-38	Melanoma
SETD9	7.83E-28	2.39305531	1.86E-23	Melanoma
RENBP	6.55E-21	2.39288604	1.55E-16	Melanoma
LNP1	4.40E-15	2.38921007	1.04E-10	Melanoma
SLC2A13	9.73E-43	2.38493087	2.30E-38	Melanoma
LAMB3	1.03E-11	2.38445034	2.45E-07	Melanoma
TTC30B	9.56E-21	2.38371274	2.27E-16	Melanoma
JPH1	2.87E-09	2.3815949	6.80E-05	Melanoma
FADS1	2.68E-76	2.38115224	6.34E-72	Melanoma
EVA1B	4.75E-17	2.37971284	1.12E-12	Melanoma
PDLIM4	3.33E-32	2.37621651	7.90E-28	Melanoma
KIF9	9.66E-36	2.37464488	2.29E-31	Melanoma
RASIP1	5.90E-16	2.37422202	1.40E-11	Melanoma
DYRK3	6.36E-17	2.37202524	1.51E-12	Melanoma
HPDL	1.21E-10	2.37192049	2.86E-06	Melanoma
CDC42BPA	9.13E-63	2.37114376	2.16E-58	Melanoma
ATP6V0A1	6.02E-112	2.37059839	1.43E-107	Melanoma
FASN	2.57E-113	2.36991302	6.09E-109	Melanoma
MME	5.21E-27	2.36639816	1.23E-22	Melanoma
TENC1	1.24E-68	2.36335285	2.95E-64	Melanoma
RNF43	3.92E-29	2.36143961	9.28E-25	Melanoma
ACSS2	3.25E-35	2.35575759	7.70E-31	Melanoma
NUDT17	1.70E-18	2.35294035	4.02E-14	Melanoma
POMGNT1	1.25E-76	2.35264034	2.97E-72	Melanoma
SLC1A1	3.74E-24	2.35150334	8.85E-20	Melanoma
CEP70	1.91E-31	2.35083841	4.53E-27	Melanoma
FAM86B2	1.10E-10	2.34945251	2.60E-06	Melanoma
MET	2.68E-42	2.34683663	6.34E-38	Melanoma
AHCYL2	4.08E-38	2.34624518	9.67E-34	Melanoma

C17orf58	2.27E-42	2.34539124	5.37E-38	Melanoma
PPT2-EGFL8	2.46E-23	2.34290063	5.83E-19	Melanoma
ADM	6.49E-46	2.3428493	1.54E-41	Melanoma
BAHCC1	2.17E-26	2.34237848	5.14E-22	Melanoma
SLC44A1	3.59E-93	2.33855602	8.49E-89	Melanoma
CEACAM1	2.29E-66	2.33482684	5.42E-62	Melanoma
PTK2	1.04E-95	2.33273624	2.47E-91	Melanoma
RNASE1	9.87E-30	2.32937375	2.34E-25	Melanoma
LOC100507547	3.23E-15	2.32883465	7.65E-11	Melanoma
PTPRM	3.83E-96	2.32729705	9.08E-92	Melanoma
TNC	2.50E-40	2.32629595	5.92E-36	Melanoma
ATRNL1	1.38E-11	2.32502171	3.27E-07	Melanoma
SLC25A33	3.27E-22	2.32478078	7.74E-18	Melanoma
SERINC2	5.42E-35	2.32211327	1.28E-30	Melanoma
AVPI1	7.33E-73	2.31762607	1.74E-68	Melanoma
CTNNAL1	1.42E-76	2.31539601	3.37E-72	Melanoma
LRRC1	6.59E-15	2.31250524	1.56E-10	Melanoma
PERP	1.03E-99	2.31220252	2.45E-95	Melanoma
SOX4	2.73E-84	2.31173871	6.47E-80	Melanoma
PAX8	3.46E-21	2.31047123	8.18E-17	Melanoma
DUSP3	3.65E-92	2.31018045	8.64E-88	Melanoma
TSPAN4	7.56E-121	2.30940061	1.79E-116	Melanoma
TBC1D7	7.48E-98	2.30509451	1.77E-93	Melanoma
SLC25A27	2.48E-32	2.3046403	5.86E-28	Melanoma
DGKG	2.49E-24	2.30455293	5.89E-20	Melanoma
ZNF703	1.51E-16	2.30410999	3.59E-12	Melanoma
SOD3	4.26E-11	2.30406981	1.01E-06	Melanoma
ACVR2B	3.17E-35	2.29971488	7.52E-31	Melanoma
HSD11B1L	1.26E-18	2.29881783	2.98E-14	Melanoma
PYGB	5.80E-149	2.2982059	1.37E-144	Melanoma
FBXO15	1.96E-13	2.29564402	4.64E-09	Melanoma
DYNC2H1	3.07E-56	2.29288218	7.27E-52	Melanoma
CLCN2	6.23E-19	2.29258448	1.48E-14	Melanoma
ALDH4A1	4.01E-27	2.29130885	9.50E-23	Melanoma
ISYNA1	7.20E-75	2.28706855	1.70E-70	Melanoma
TNKS1BP1	1.65E-46	2.28288666	3.90E-42	Melanoma
HSD3B1	3.57E-09	2.2816217	8.45E-05	Melanoma
NCKAP1	8.54E-62	2.28068385	2.02E-57	Melanoma
SDC4	5.75E-85	2.28015275	1.36E-80	Melanoma
BNC2	5.13E-71	2.2781371	1.22E-66	Melanoma
TXNRD3	1.29E-09	2.27747863	3.05E-05	Melanoma

B4GALNT3	9.98E-17	2.27746985	2.36E-12	Melanoma
SSPN	2.81E-26	2.27503366	6.65E-22	Melanoma
FADS3	3.05E-59	2.27463008	7.22E-55	Melanoma
NT5DC2	3.27E-21	2.27423934	7.75E-17	Melanoma
GAS7	2.03E-103	2.27221315	4.81E-99	Melanoma
ANKS1A	1.25E-59	2.2719122	2.97E-55	Melanoma
PIGV	1.52E-47	2.26981986	3.61E-43	Melanoma
CCDC24	1.11E-18	2.2678063	2.62E-14	Melanoma
FREM2	8.24E-11	2.26698784	1.95E-06	Melanoma
WDR34	2.98E-70	2.26684581	7.05E-66	Melanoma
NPHP4	1.08E-39	2.26488843	2.56E-35	Melanoma
AKAP12	1.05E-106	2.26481577	2.48E-102	Melanoma
C7orf55-LUC7L2	1.62E-28	2.26392951	3.83E-24	Melanoma
ACSS3	3.18E-10	2.26365058	7.53E-06	Melanoma
PCDHGA12	9.99E-13	2.25972228	2.37E-08	Melanoma
LYRM9	1.58E-72	2.25924645	3.73E-68	Melanoma
KEL	2.62E-10	2.25689272	6.21E-06	Melanoma
PHACTR1	2.19E-85	2.25429185	5.19E-81	Melanoma
LOC284889	2.29E-49	2.25370695	5.43E-45	Melanoma
EXOSC4	8.26E-87	2.24880334	1.96E-82	Melanoma
WDR19	1.29E-48	2.2428378	3.07E-44	Melanoma
DBNDD1	6.77E-37	2.24147629	1.60E-32	Melanoma
ENDOD1	1.89E-112	2.24008977	4.48E-108	Melanoma
CD151	8.36E-123	2.23869594	1.98E-118	Melanoma
PTPLA	5.35E-33	2.2373553	1.27E-28	Melanoma
DNAL4	7.18E-46	2.23643232	1.70E-41	Melanoma
FRMD6	4.40E-56	2.23617858	1.04E-51	Melanoma
PTPRG	1.99E-33	2.23533979	4.72E-29	Melanoma
SLC39A14	1.00E-97	2.23520353	2.37E-93	Melanoma
AGPAT2	7.11E-72	2.2349734	1.68E-67	Melanoma
SPRED2	5.29E-59	2.23115898	1.25E-54	Melanoma
CREG1	8.84E-99	2.23031241	2.09E-94	Melanoma
TCN2	1.85E-27	2.23018056	4.39E-23	Melanoma
PDE10A	5.54E-10	2.22651637	1.31E-05	Melanoma
DUSP14	1.01E-69	2.2256217	2.40E-65	Melanoma
NRSN2	6.19E-51	2.22512593	1.47E-46	Melanoma
DVL1	3.46E-23	2.22456357	8.20E-19	Melanoma
C16orf95	8.79E-14	2.22415198	2.08E-09	Melanoma
CD59	1.06E-180	2.22283901	2.51E-176	Melanoma
FAM27C	6.04E-32	2.22203249	1.43E-27	Melanoma
PYROXD2	1.65E-24	2.22105392	3.91E-20	Melanoma

LDLRAD2	7.64E-17	2.22046389	1.81E-12	Melanoma
NCS1	5.70E-11	2.21573626	1.35E-06	Melanoma
GAB2	2.15E-38	2.21446361	5.10E-34	Melanoma
PLD1	4.99E-33	2.2124835	1.18E-28	Melanoma
STPG1	1.85E-26	2.21124173	4.37E-22	Melanoma
PHC2	4.70E-59	2.21032413	1.11E-54	Melanoma
IMMP2L	2.03E-77	2.20872426	4.80E-73	Melanoma
CCDC51	7.75E-33	2.20796157	1.84E-28	Melanoma
RBMS3	6.28E-65	2.2072556	1.49E-60	Melanoma
RSPH3	1.16E-28	2.2061034	2.75E-24	Melanoma
ANKRD30B	2.62E-12	2.20365946	6.21E-08	Melanoma
LPL	3.99E-26	2.20207966	9.46E-22	Melanoma
CTSK	1.57E-66	2.1989665	3.72E-62	Melanoma
KIF7	1.85E-10	2.19831735	4.38E-06	Melanoma
ZCCHC24	8.31E-53	2.19754714	1.97E-48	Melanoma
NDN	2.61E-12	2.19674778	6.19E-08	Melanoma
ANK2	5.75E-36	2.1962826	1.36E-31	Melanoma
SIX5	8.08E-11	2.19480629	1.91E-06	Melanoma
WEE1	6.57E-62	2.19123835	1.56E-57	Melanoma
PLEKHH3	2.84E-11	2.19098061	6.74E-07	Melanoma
MARVELD1	1.35E-24	2.18847845	3.20E-20	Melanoma
UBTD2	2.38E-17	2.18637089	5.63E-13	Melanoma
ENTPD6	1.18E-111	2.18608238	2.79E-107	Melanoma
CCDC88A	3.16E-93	2.18450521	7.48E-89	Melanoma
FAM127B	2.37E-103	2.18146488	5.61E-99	Melanoma
CCDC86	4.65E-51	2.17909318	1.10E-46	Melanoma
CARD14	4.03E-22	2.17879129	9.54E-18	Melanoma
RBFOX2	2.38E-64	2.17559639	5.63E-60	Melanoma
UGGT2	3.93E-39	2.17544968	9.31E-35	Melanoma
ANKRD28	1.07E-81	2.16628333	2.54E-77	Melanoma
MYH10	1.55E-71	2.16578669	3.67E-67	Melanoma
BCL9	3.65E-47	2.16279302	8.65E-43	Melanoma
SOX12	4.08E-14	2.16201326	9.67E-10	Melanoma
IER3	2.74E-91	2.15947198	6.49E-87	Melanoma
PLXNB1	1.01E-26	2.15942924	2.40E-22	Melanoma
LOC729013	3.80E-67	2.15905043	8.99E-63	Melanoma
CBY1	4.63E-53	2.15826448	1.10E-48	Melanoma
CTTN	6.61E-160	2.15801068	1.57E-155	Melanoma
FAM92A1	4.35E-31	2.15664644	1.03E-26	Melanoma
ZNF596	1.54E-10	2.15644325	3.65E-06	Melanoma
OBSL1	8.39E-26	2.15447703	1.99E-21	Melanoma

JAM3	6.76E-46	2.15323855	1.60E-41	Melanoma
TCTN1	2.22E-61	2.15111614	5.25E-57	Melanoma
PEX12	3.53E-23	2.14850697	8.37E-19	Melanoma
CBR1	7.97E-115	2.14807945	1.89E-110	Melanoma
FAM86HP	2.15E-13	2.14736099	5.09E-09	Melanoma
FAM195A	7.14E-40	2.14697028	1.69E-35	Melanoma
RARB	6.96E-13	2.1449334	1.65E-08	Melanoma
CRIP2	4.76E-86	2.14418973	1.13E-81	Melanoma
C7orf53	8.40E-11	2.14260377	1.99E-06	Melanoma
HSD3BP4	1.53E-26	2.14088796	3.62E-22	Melanoma
FNIP2	1.17E-30	2.13970186	2.77E-26	Melanoma
AAMDC	1.10E-47	2.1378865	2.60E-43	Melanoma
TMEM97	2.47E-34	2.13751582	5.84E-30	Melanoma
ECE2	1.31E-16	2.13654985	3.11E-12	Melanoma
LYSMD1	2.79E-31	2.13619684	6.60E-27	Melanoma
GAA	1.16E-103	2.1356001	2.75E-99	Melanoma
SEZ6L2	1.64E-09	2.13513886	3.89E-05	Melanoma
ARMCX1	8.28E-33	2.13319988	1.96E-28	Melanoma
PRKAB2	2.77E-67	2.13295773	6.56E-63	Melanoma
C1orf21	5.96E-91	2.13216347	1.41E-86	Melanoma
MAP1B	1.81E-90	2.13092331	4.29E-86	Melanoma
CHURC1-FNTB	2.55E-37	2.13057014	6.03E-33	Melanoma
LGALS3	3.84E-175	2.12932172	9.10E-171	Melanoma
LOC100505679	3.83E-10	2.12830467	9.07E-06	Melanoma
CTHRC1	1.63E-105	2.12782068	3.86E-101	Melanoma
HOXD4	9.99E-13	2.127649	2.37E-08	Melanoma
TMEM54	6.13E-14	2.12733655	1.45E-09	Melanoma
SLC5A3	3.86E-108	2.12696458	9.15E-104	Melanoma
FKBPL	1.97E-16	2.12430546	4.66E-12	Melanoma
ENPP5	3.73E-11	2.12400743	8.84E-07	Melanoma
LOC440297	2.20E-32	2.12375953	5.22E-28	Melanoma
NME1-NME2	1.24E-23	2.12365548	2.93E-19	Melanoma
TIMP1	2.78E-149	2.12345961	6.58E-145	Melanoma
ADAM9	6.41E-70	2.1222674	1.52E-65	Melanoma
FLG	5.11E-18	2.12201172	1.21E-13	Melanoma
TMEM132A	7.14E-12	2.1199368	1.69E-07	Melanoma
STEAP1	2.30E-19	2.11390415	5.46E-15	Melanoma
CBX2	2.42E-13	2.11366701	5.73E-09	Melanoma
HEBP1	4.02E-55	2.11220298	9.53E-51	Melanoma
HMGN5	2.40E-38	2.10999286	5.69E-34	Melanoma
SPON2	1.35E-72	2.10982237	3.19E-68	Melanoma

TCEAL4	1.52E-109	2.10967113	3.59E-105	Melanoma
SEMA6A	7.84E-71	2.10916438	1.86E-66	Melanoma
PLEKHG4	2.34E-37	2.10847245	5.55E-33	Melanoma
PACSIN2	3.62E-126	2.10718802	8.57E-122	Melanoma
PIGP	2.26E-77	2.10647918	5.36E-73	Melanoma
BOD1	4.71E-27	2.10578516	1.12E-22	Melanoma
NFE2L1	2.59E-92	2.10469814	6.13E-88	Melanoma
RNF24	2.91E-56	2.10387305	6.90E-52	Melanoma
CDK5	9.95E-56	2.10284876	2.36E-51	Melanoma
C1orf74	7.13E-11	2.10082948	1.69E-06	Melanoma
EIF4EBP1	8.52E-94	2.09900603	2.02E-89	Melanoma
IQCH	2.22E-13	2.09882058	5.25E-09	Melanoma
ITGA6	2.39E-65	2.09462742	5.66E-61	Melanoma
UBXN8	5.27E-36	2.09320202	1.25E-31	Melanoma
GUCY1B3	1.59E-13	2.09102016	3.76E-09	Melanoma
EGR3	7.91E-64	2.08703105	1.87E-59	Melanoma
PGRMC1	1.52E-101	2.08682576	3.60E-97	Melanoma
SLC39A4	1.34E-60	2.08535353	3.18E-56	Melanoma
AQP7P1	5.60E-11	2.08509141	1.33E-06	Melanoma
CTNND1	4.14E-121	2.08463878	9.80E-117	Melanoma
XG	1.75E-19	2.08451065	4.14E-15	Melanoma
MTUS1	3.43E-90	2.08322353	8.13E-86	Melanoma
C16orf46	1.54E-14	2.08148819	3.65E-10	Melanoma
ASB13	1.63E-36	2.08114206	3.86E-32	Melanoma
CTH	1.28E-22	2.08016965	3.03E-18	Melanoma
TMEM99	8.06E-53	2.07986578	1.91E-48	Melanoma
MCOLN3	3.14E-28	2.07921181	7.43E-24	Melanoma
AMOTL1	4.29E-50	2.07887665	1.02E-45	Melanoma
GPT2	1.03E-10	2.07854142	2.43E-06	Melanoma
ANKRD20A12P	2.64E-60	2.07807373	6.26E-56	Melanoma
FAHD2A	6.09E-63	2.07591562	1.44E-58	Melanoma
CMTM4	9.51E-12	2.0746826	2.25E-07	Melanoma
CSRP2	2.54E-28	2.07353447	6.02E-24	Melanoma
USP6NL	4.91E-69	2.07261575	1.16E-64	Melanoma
MCAT	1.81E-33	2.07216698	4.28E-29	Melanoma
BLVRB	7.08E-75	2.07065481	1.68E-70	Melanoma
ITFG3	3.96E-107	2.07028797	9.38E-103	Melanoma
FAM109B	1.35E-31	2.0684404	3.21E-27	Melanoma
AK4	3.27E-63	2.06764003	7.75E-59	Melanoma
LOC100133920	4.03E-13	2.06468017	9.54E-09	Melanoma
PLEKHA6	1.26E-10	2.06359177	2.99E-06	Melanoma

IRS2	1.52E-86	2.06302765	3.60E-82	Melanoma
NAGLU	6.35E-35	2.06271401	1.50E-30	Melanoma
FAM89A	9.61E-12	2.06180945	2.28E-07	Melanoma
HRNR	5.12E-20	2.06125406	1.21E-15	Melanoma
S100A16	2.64E-76	2.0607664	6.26E-72	Melanoma
MT1L	9.29E-14	2.05276275	2.20E-09	Melanoma
RCN1	6.06E-122	2.05253919	1.44E-117	Melanoma
CNTNAP1	9.70E-18	2.05051373	2.30E-13	Melanoma
PCDHGA4	1.10E-09	2.05025765	2.61E-05	Melanoma
HIST1H4H	4.44E-14	2.05006882	1.05E-09	Melanoma
DAAM1	4.80E-62	2.04950914	1.14E-57	Melanoma
MLF1	5.25E-42	2.04942807	1.24E-37	Melanoma
MFSD12	3.23E-63	2.04888399	7.65E-59	Melanoma
PXDC1	3.08E-23	2.04852137	7.29E-19	Melanoma
PRDX4	7.61E-120	2.04705772	1.80E-115	Melanoma
AKAP6	4.36E-20	2.0456653	1.03E-15	Melanoma
DECR2	8.98E-29	2.04481058	2.13E-24	Melanoma
CSRP1	5.58E-140	2.0427053	1.32E-135	Melanoma
MON1A	8.48E-18	2.04175039	2.01E-13	Melanoma
FAM86JP	6.77E-14	2.04096329	1.60E-09	Melanoma
CXXC5	2.35E-62	2.04080068	5.56E-58	Melanoma
APOO	6.21E-61	2.03928165	1.47E-56	Melanoma
NT5C3B	3.73E-56	2.03844597	8.83E-52	Melanoma
LMNA	2.30E-162	2.03838279	5.45E-158	Melanoma
DCAKD	2.08E-77	2.03794405	4.92E-73	Melanoma
LOC100506714	4.13E-41	2.03661599	9.77E-37	Melanoma
CEBPD	7.67E-28	2.03269938	1.82E-23	Melanoma
IGFBP7	4.09E-101	2.03267066	9.68E-97	Melanoma
BIN3	8.12E-96	2.03158927	1.92E-91	Melanoma
ZNF629	3.04E-16	2.0295381	7.19E-12	Melanoma
C10orf11	2.93E-25	2.02899856	6.95E-21	Melanoma
ZNF516	8.14E-44	2.02551655	1.93E-39	Melanoma
Sep-05	8.94E-11	2.02541413	2.12E-06	Melanoma
APITD1	1.34E-32	2.02381999	3.18E-28	Melanoma
ABHD12	1.94E-67	2.02127554	4.60E-63	Melanoma
TMEM45A	6.62E-20	2.02052562	1.57E-15	Melanoma
PCBP4	4.34E-47	2.01665645	1.03E-42	Melanoma
KLF4	2.86E-70	2.01524693	6.79E-66	Melanoma
AGPAT9	3.97E-15	2.01475083	9.40E-11	Melanoma
HIST1H2BD	1.68E-69	2.0136524	3.98E-65	Melanoma
BCAR3	4.14E-21	2.01166061	9.81E-17	Melanoma

CYTL1	2.56E-09	2.01081577	6.07E-05	Melanoma
FAP	4.02E-33	2.01032382	9.53E-29	Melanoma
TULP3	1.50E-45	2.00563337	3.56E-41	Melanoma
DOCK4	2.36E-21	2.00374858	5.58E-17	Melanoma
PLXNC1	1.43E-70	2.00296681	3.39E-66	Melanoma
SEPP1	4.91E-51	2.00147027	1.16E-46	Melanoma
ACTRT2	4.25E-24	10.1689793	1.01E-19	NK
MIR572	4.25E-24	9.08817985	1.01E-19	NK
DEFB107A	4.25E-24	8.90571402	1.01E-19	NK
DEFB107B	4.25E-24	8.90571402	1.01E-19	NK
MIR3974	4.25E-24	8.82571614	1.01E-19	NK
MIR3188	4.25E-24	8.79797472	1.01E-19	NK
MIR4296	4.25E-24	8.61586941	1.01E-19	NK
LRIT2	1.28E-12	8.38965833	3.04E-08	NK
ESX1	1.28E-12	8.2458554	3.04E-08	NK
BCL2L10	4.25E-24	7.76792313	1.01E-19	NK
RTDR1	3.47E-19	7.66515546	8.22E-15	NK
CIB3	4.25E-24	7.39050335	1.01E-19	NK
ACMSD	9.74E-24	7.19402215	2.31E-19	NK
KRTAP10-10	1.28E-12	7.19047028	3.04E-08	NK
PRSS57	2.37E-26	6.91484747	5.61E-22	NK
PRR5-ARHGAP8	1.03E-23	6.63021033	2.45E-19	NK
ARL5C	1.36E-12	6.52105583	3.22E-08	NK
LINC00301	1.36E-12	6.33248039	3.22E-08	NK
ORM1	3.76E-21	6.30212464	8.90E-17	NK
KLRF1	3.50E-86	6.29839178	8.30E-82	NK
SLC39A12	1.36E-12	6.27549289	3.22E-08	NK
MLC1	2.39E-34	6.22889151	5.65E-30	NK
SPTSSB	5.37E-11	6.22727395	1.27E-06	NK
SH2D1B	2.35E-55	5.86420701	5.56E-51	NK
KCNV1	4.65E-16	5.60357482	1.10E-11	NK
LRRC37A5P	1.36E-12	5.50116554	3.22E-08	NK
REG3A	6.15E-10	5.47728141	1.46E-05	NK
RLN1	5.96E-11	5.41025572	1.41E-06	NK
FAM224B	1.36E-12	5.32934521	3.22E-08	NK
SNORA68	7.78E-14	5.22759671	1.84E-09	NK
GPR97	8.03E-14	5.1420271	1.90E-09	NK
LINC00299	3.52E-31	4.98168828	8.34E-27	NK
OR2F1	1.36E-12	4.96641572	3.22E-08	NK
UGT2A3	5.44E-16	4.92726398	1.29E-11	NK
KRT86	4.78E-12	4.85853029	1.13E-07	NK

CD160	7.26E-13	4.85431146	1.72E-08	NK
NCR1	6.84E-38	4.6904511	1.62E-33	NK
FCGR3A	6.98E-33	4.65161635	1.65E-28	NK
TYROBP	2.16E-44	4.58473136	5.10E-40	NK
KLRC1	2.30E-45	4.55537238	5.46E-41	NK
ALAS2	7.07E-10	4.48503403	1.67E-05	NK
S1PR5	2.79E-13	4.47140005	6.60E-09	NK
IL18RAP	2.52E-19	4.4562244	5.97E-15	NK
PTGDR	2.01E-33	4.4443269	4.75E-29	NK
FGR	1.78E-27	4.35613914	4.23E-23	NK
SIGLEC7	5.89E-16	4.32951515	1.40E-11	NK
RAB27B	7.76E-10	4.28663186	1.84E-05	NK
GNLY	7.47E-30	4.27179594	1.77E-25	NK
FCER1G	8.60E-34	4.22992456	2.04E-29	NK
KLRC3	2.01E-25	4.13749686	4.75E-21	NK
IFITM4P	2.58E-13	4.04609669	6.11E-09	NK
B3GNT7	2.25E-11	4.02415199	5.34E-07	NK
LOC100652909	9.24E-12	4.00379943	2.19E-07	NK
KLRB1	2.81E-40	3.97057469	6.65E-36	NK
KLRC2	2.42E-36	3.93785584	5.73E-32	NK
CLIC3	3.98E-16	3.83306139	9.44E-12	NK
XCL1	1.87E-13	3.82644508	4.42E-09	NK
NCAM1	8.39E-11	3.81821064	1.99E-06	NK
NCR3	3.72E-11	3.72992008	8.82E-07	NK
TBX21	1.05E-14	3.72338016	2.48E-10	NK
CDHR1	6.92E-10	3.70838639	1.64E-05	NK
MATK	2.66E-11	3.6635832	6.31E-07	NK
PTGER2	1.42E-15	3.63616364	3.36E-11	NK
CD244	1.65E-24	3.62392896	3.92E-20	NK
RAP1GAP2	1.26E-12	3.61620241	2.98E-08	NK
HOPX	3.45E-18	3.57344171	8.17E-14	NK
FCRL6	2.13E-18	3.54897139	5.04E-14	NK
CD300A	2.45E-16	3.51766928	5.80E-12	NK
GZMB	9.96E-25	3.45983409	2.36E-20	NK
ZBTB16	1.33E-16	3.34013543	3.15E-12	NK
MYBL1	3.04E-10	3.2571297	7.19E-06	NK
AOAH	2.33E-24	3.20818172	5.53E-20	NK
DHRS3	2.58E-10	3.13417304	6.10E-06	NK
CTSW	8.62E-23	3.0196362	2.04E-18	NK
SAMD3	5.35E-14	2.94869002	1.27E-09	NK
GZMM	6.42E-17	2.94371033	1.52E-12	NK

GZMH	2.22E-13	2.86353107	5.26E-09	NK
MAP3K8	5.19E-10	2.80707289	1.23E-05	NK
PLCG2	3.06E-11	2.80335626	7.26E-07	NK
CCL3	3.73E-09	2.62117956	8.82E-05	NK
IL2RB	4.24E-16	2.61425523	1.00E-11	NK
PRF1	4.19E-16	2.59554356	9.93E-12	NK
CD247	7.25E-17	2.5523185	1.72E-12	NK
TXK	3.46E-10	2.55028506	8.19E-06	NK
AREG	2.19E-11	2.51752856	5.19E-07	NK
KLRC4	4.11E-16	2.47378387	9.72E-12	NK
NKG7	5.32E-16	2.42911778	1.26E-11	NK
MCTP2	1.56E-09	2.42268477	3.70E-05	NK
GZMA	1.48E-15	2.33910492	3.51E-11	NK
CCL4	2.01E-13	2.33423299	4.77E-09	NK
KLRK1	1.36E-13	2.18566945	3.23E-09	NK
PREX1	2.47E-09	2.17129624	5.86E-05	NK
KLRC4-KLRK1	2.35E-09	2.16920031	5.56E-05	NK
CD7	1.15E-13	2.12886974	2.73E-09	NK
PTPN22	2.53E-09	2.0771034	5.99E-05	NK
SLAMF7	1.69E-09	2.02876037	4.01E-05	NK
KRTAP21-2	5.74E-18	8.36157082	1.36E-13	Treg
KISS1R	5.74E-18	8.12885267	1.36E-13	Treg
MIR302C	1.03E-09	8.09329555	2.45E-05	Treg
CRYGA	5.74E-18	8.02515558	1.36E-13	Treg
FOXP3	6.36E-301	7.95246359	1.51E-296	Treg
OR6S1	1.03E-09	7.82764807	2.45E-05	Treg
SNORD56	1.03E-09	7.7702343	2.45E-05	Treg
HNRNPCL1	1.03E-09	7.66300682	2.45E-05	Treg
SCARNA11	1.03E-09	7.61856387	2.45E-05	Treg
SCGB1C1	1.03E-09	7.58220474	2.45E-05	Treg
MIR32	1.03E-09	7.49639579	2.45E-05	Treg
VWC2L	1.03E-09	7.47739519	2.45E-05	Treg
MYO16-AS1	1.03E-09	7.31809896	2.45E-05	Treg
TTTY18	1.03E-09	7.30705708	2.45E-05	Treg
MIR330	1.03E-09	7.12038824	2.45E-05	Treg
MS4A13	1.03E-09	7.06970715	2.45E-05	Treg
POU6F2-AS1	1.03E-09	6.97755926	2.45E-05	Treg
LOC285547	1.03E-09	6.90307133	2.45E-05	Treg
FOXR1	1.03E-09	6.86599415	2.45E-05	Treg
TTTY1	1.03E-09	6.80473823	2.45E-05	Treg
STOML3	1.03E-09	6.7525616	2.45E-05	Treg

C1orf105	1.03E-09	6.70400046	2.45E-05	Treg
OR1M1	1.03E-09	6.52713283	2.45E-05	Treg
LCN9	1.03E-09	6.51201901	2.45E-05	Treg
PITX1	1.03E-09	6.50975767	2.45E-05	Treg
TAS2R1	2.90E-13	5.92453161	6.87E-09	Treg
AFP	2.61E-09	5.91251705	6.18E-05	Treg
C2orf78	2.73E-09	5.69216082	6.46E-05	Treg
SERTM1	3.03E-13	5.66100798	7.17E-09	Treg
DPPA2P3	1.03E-09	5.64145984	2.45E-05	Treg
MNX1	1.03E-09	5.63135005	2.45E-05	Treg
CCR8	2.28E-50	5.5128104	5.40E-46	Treg
BARX1	2.73E-09	5.47337391	6.46E-05	Treg
CD177	3.58E-09	5.40713067	8.49E-05	Treg
CFC1	2.73E-09	5.39626709	6.46E-05	Treg
IL1R2	1.84E-17	4.85306829	4.35E-13	Treg
ARMS2	2.85E-09	4.74588168	6.74E-05	Treg
LOC732275	2.26E-11	4.47659134	5.36E-07	Treg
IL2RA	5.30E-27	4.2380562	1.26E-22	Treg
CCL20	1.51E-14	4.14702346	3.58E-10	Treg
LAIR2	2.06E-22	4.09022131	4.88E-18	Treg
RTKN2	7.64E-29	4.08684008	1.81E-24	Treg
DNAH8	8.11E-24	3.59994795	1.92E-19	Treg
TNFRSF18	1.50E-29	3.44215566	3.54E-25	Treg
ZBTB32	1.16E-09	3.35750313	2.74E-05	Treg
DPP4	4.94E-16	3.330676	1.17E-11	Treg
LOC256021	2.09E-09	3.31220019	4.96E-05	Treg
IL18R1	1.10E-15	3.24016639	2.61E-11	Treg
CCR4	4.43E-16	3.00898782	1.05E-11	Treg
TNFRSF4	1.81E-15	3.00118388	4.28E-11	Treg
AQP3	2.74E-15	2.84765637	6.48E-11	Treg
CSF2RB	6.16E-11	2.80531319	1.46E-06	Treg
SLAMF1	1.58E-24	2.80517518	3.73E-20	Treg
CISH	3.57E-11	2.7343473	8.45E-07	Treg
PBX4	6.91E-10	2.66991332	1.64E-05	Treg
IKZF2	8.31E-24	2.64223341	1.97E-19	Treg
MICAL2	1.37E-09	2.63942631	3.24E-05	Treg
F5	1.01E-11	2.51041222	2.39E-07	Treg
CD4	4.24E-29	2.50283083	1.01E-24	Treg
BATF	3.45E-21	2.44534544	8.17E-17	Treg
DUSP16	3.02E-16	2.39539868	7.14E-12	Treg
NCF4	7.52E-14	2.39170587	1.78E-09	Treg

RORA	1.39E-18	2.37207437	3.30E-14	Treg
CTLA4	8.92E-23	2.31840889	2.11E-18	Treg
HS3ST3B1	3.53E-10	2.3025063	8.37E-06	Treg
MAST4	1.22E-09	2.30163236	2.88E-05	Treg
MAL	5.02E-11	2.27298445	1.19E-06	Treg
ICOS	4.87E-17	2.27175319	1.15E-12	Treg
FLT3LG	1.01E-11	2.11425943	2.39E-07	Treg
IL2RB	8.13E-25	2.10904505	1.93E-20	Treg
CD5	8.99E-20	2.02019971	2.13E-15	Treg

Table D.4 Differential gene expression between cell clusters enriched in TILs derived from treatment-naïve melanoma patients including adjusted p-value and log_2-fold change.

gene	p_val	log2FC	p_val_adj	cluster
CAMK1D	1.01E-36	2.00364007	5.63E-32	B
FICD	2.07E-43	2.00612039	1.15E-38	B
SLC44A1	2.93E-48	2.01594375	1.63E-43	B
XXbac-BPG181M17.5	8.76E-45	2.01603876	4.88E-40	B
QPRT	1.70E-25	2.02753145	9.46E-21	B
PLTP	1.25E-16	2.02766612	6.95E-12	B
RP11-77H9.2	3.51E-31	2.03049818	1.96E-26	B
PIK3C2B	2.03E-74	2.03406777	1.13E-69	B
IFT57	4.81E-66	2.0470628	2.68E-61	B
SPINT2	7.30E-63	2.0535309	4.07E-58	B
HIST1H2BJ	2.58E-26	2.05943214	1.44E-21	B
RP11-134P9.3	9.89E-14	2.06021234	5.51E-09	B
TMEM19	3.97E-51	2.06655064	2.21E-46	B
IGHV1-3	5.50E-12	2.07401137	3.06E-07	B
ORAI2	1.67E-109	2.07566481	9.29E-105	B
TRIB1	1.03E-54	2.07671919	5.73E-50	B
CD72	8.44E-51	2.07762598	4.70E-46	B
SYVN1	1.57E-145	2.07969527	8.75E-141	B
RP11-325K4.2	1.84E-29	2.08176158	1.02E-24	B
TAF4B	1.64E-30	2.08380287	9.15E-26	B
SNX29	1.11E-82	2.08616488	6.19E-78	B
7SK	3.77E-20	2.08678972	2.10E-15	B
CIITA	1.39E-99	2.09453328	7.73E-95	B
HYI	5.88E-21	2.09515538	3.27E-16	B
CTC-244M17.1	1.21E-10	2.10778026	6.76E-06	B
IRF8	6.50E-137	2.10958466	3.62E-132	B
RP13-188A5.1	1.54E-14	2.11169173	8.58E-10	B
CDCA7L	3.94E-36	2.11350882	2.19E-31	B
AC017116.11	1.10E-09	2.12182087	6.14E-05	B
RP11-417L19.4	8.20E-10	2.12344332	4.57E-05	B
CYBB	4.29E-125	2.12394924	2.39E-120	B
SNX22	2.04E-14	2.12491652	1.14E-09	B
RP11-302F12.10	2.70E-22	2.13039848	1.51E-17	B
LYN	2.63E-65	2.14349912	1.47E-60	B
CD83	2.92E-133	2.14711987	1.63E-128	B
RP11-390F4.3	3.18E-10	2.15321085	1.77E-05	B
POU2F2	9.92E-130	2.15412669	5.53E-125	B
FAM63A	1.58E-20	2.16252901	8.79E-16	B
SIPA1L3	2.80E-74	2.16540885	1.56E-69	B
LRRC16A	3.78E-61	2.16964515	2.11E-56	B
AC104134.2	2.08E-20	2.16995513	1.16E-15	B

ZSCAN18	5.16E-13	2.17563213	2.88E-08	B
CLMN	4.14E-16	2.17717858	2.30E-11	B
SIGLEC14	2.39E-35	2.1792902	1.33E-30	B
UBE2E2	5.30E-46	2.18141557	2.95E-41	B
LAT2	3.32E-88	2.18401997	1.85E-83	B
INSR	2.68E-71	2.18656556	1.50E-66	B
ABCB9	4.38E-24	2.18766864	2.44E-19	B
C11orf24	9.88E-81	2.18779831	5.50E-76	B
TCTN1	6.55E-16	2.18856379	3.65E-11	B
PPP1R9A	4.41E-11	2.19859032	2.46E-06	B
GM2A	2.34E-91	2.20383428	1.30E-86	B
GABRR2	1.50E-09	2.21984993	8.35E-05	B
EVI5	4.83E-33	2.22580421	2.69E-28	B
CAV1	5.90E-34	2.22791378	3.29E-29	B
IFNGR2	1.74E-109	2.23254425	9.67E-105	B
HSPG2	4.44E-16	2.23824495	2.48E-11	B
EFHC1	1.54E-29	2.23900707	8.60E-25	B
SLC2A11	1.19E-33	2.24231597	6.64E-29	B
RP11-561C5.5	2.11E-17	2.24676439	1.18E-12	B
AC074289.1	8.31E-27	2.25384002	4.63E-22	B
RPL32P1	1.18E-09	2.26386048	6.57E-05	B
ITGA6	1.17E-51	2.26809517	6.54E-47	B
ZNF318	9.70E-28	2.27296604	5.41E-23	B
PTGS1	9.05E-16	2.27768272	5.04E-11	B
TSPAN3	7.54E-117	2.27790316	4.20E-112	B
AKAP2	1.33E-166	2.27871411	7.39E-162	B
LRRK2	9.71E-27	2.28024454	5.41E-22	B
KDM4B	1.21E-50	2.28137729	6.75E-46	B
C11orf80	2.56E-37	2.31211307	1.43E-32	B
WDR19	3.14E-16	2.31241441	1.75E-11	B
FKBP14	3.37E-29	2.31388237	1.88E-24	B
PPAPDC1B	1.90E-154	2.31778237	1.06E-149	B
EMILIN3	7.09E-11	2.32882433	3.95E-06	B
BACH2	2.55E-69	2.33953686	1.42E-64	B
MGAT5	4.16E-62	2.34096727	2.32E-57	B
CNKSR2	1.95E-11	2.34191104	1.09E-06	B
RNASE4	3.03E-10	2.35913958	1.69E-05	B
UGGT2	2.05E-10	2.36077042	1.14E-05	B
RP1-257A7.5	1.04E-84	2.364832	5.80E-80	B
GAPT	1.08E-22	2.38022044	6.01E-18	B
PDK1	1.15E-133	2.38327295	6.42E-129	B
KRT18	7.77E-11	2.38387201	4.33E-06	B

CD1C	3.21E-16	2.38782036	1.79E-11	B
MICAL3	1.02E-88	2.38993321	5.66E-84	B
MTMR9LP	4.91E-10	2.39310856	2.74E-05	B
KMO	6.31E-31	2.40177321	3.52E-26	B
PAIP2B	3.71E-27	2.40590666	2.07E-22	B
SGCE	1.80E-11	2.41133723	1.00E-06	B
STRBP	3.21E-69	2.41138524	1.79E-64	B
BMP2K	5.59E-35	2.42059062	3.11E-30	B
AC007952.5	4.69E-13	2.42183917	2.61E-08	B
METTL7A	6.27E-120	2.42268205	3.50E-115	B
TPST1	1.47E-18	2.42704439	8.18E-14	B
HS3ST1	3.73E-13	2.4275421	2.08E-08	B
RASL11A	4.10E-14	2.43277291	2.28E-09	B
GSTT1	7.25E-44	2.43282343	4.04E-39	B
L3MBTL4	1.02E-17	2.43717719	5.70E-13	B
RP11-293I14.2	7.02E-22	2.4386011	3.91E-17	B
GAS6	1.45E-52	2.44487266	8.09E-48	B
PHACTR1	1.14E-52	2.45873437	6.38E-48	B
RABEP2	5.23E-117	2.46703211	2.92E-112	B
CTSH	2.51E-184	2.46999924	1.40E-179	B
XXbac-B461K10.4	1.52E-34	2.48869989	8.48E-30	B
CTA-384D8.35	3.43E-46	2.49171769	1.91E-41	B
TSPAN33	3.73E-12	2.49193006	2.08E-07	B
CBFA2T3	1.59E-42	2.51269917	8.84E-38	B
HLA-DOA	8.96E-94	2.52265624	4.99E-89	B
KCNA2	8.62E-10	2.52718689	4.80E-05	B
FAM47E-STBD1	8.62E-22	2.52840759	4.81E-17	B
AC022182.1	4.30E-19	2.53380039	2.40E-14	B
IGLV2-14	2.22E-38	2.54230374	1.24E-33	B
SCRN1	5.38E-24	2.54298536	3.00E-19	B
ACY3	3.14E-11	2.55095885	1.75E-06	B
C1orf186	3.02E-83	2.55542144	1.69E-78	B
PXDC1	3.42E-12	2.55685776	1.91E-07	B
CCR6	1.07E-65	2.55989133	5.97E-61	B
DTX1	1.90E-23	2.56487565	1.06E-18	B
TXLNB	5.09E-17	2.56517273	2.84E-12	B
RP11-347C18.3	1.64E-09	2.56579263	9.13E-05	B
RNU4-1	4.83E-11	2.56958489	2.69E-06	B
HDAC9	4.66E-86	2.5752137	2.59E-81	B
PRDX4	1.11E-112	2.57525762	6.20E-108	B
IFNG-AS1	1.12E-83	2.58553484	6.24E-79	B
RP11-876N24.2	2.58E-37	2.58853888	1.44E-32	B

TSPAN13	8.54E-91	2.5887008	4.76E-86	B
FADS3	9.22E-38	2.5900129	5.14E-33	B
NT5DC2	2.56E-19	2.59463764	1.43E-14	B
FGD2	3.92E-287	2.59497414	2.19E-282	B
RP11-861A13.4	1.00E-27	2.59869921	5.59E-23	B
PLAG1	1.19E-16	2.59899028	6.61E-12	B
CTB-133G6.1	9.19E-32	2.60151656	5.12E-27	B
MIR600HG	1.01E-17	2.60790124	5.64E-13	B
U51244.2	4.82E-14	2.62198893	2.69E-09	B
AP001056.1	2.33E-15	2.62223446	1.30E-10	B
RP11-428G5.5	8.04E-10	2.6234913	4.48E-05	B
MARCKS	9.49E-138	2.62587816	5.29E-133	B
NUAK2	1.86E-70	2.62654718	1.03E-65	B
DENND2C	2.81E-18	2.6338229	1.57E-13	B
RP11-430C7.4	1.63E-12	2.63476061	9.09E-08	B
B4GALT2	5.70E-12	2.63944359	3.17E-07	B
PIP5K1B	1.92E-33	2.64879777	1.07E-28	B
TEC	1.09E-33	2.65152697	6.08E-29	B
PDLIM1P1	5.77E-24	2.65770049	3.22E-19	B
ISL2	1.34E-11	2.65830708	7.46E-07	B
RP11-188C12.2	1.92E-12	2.66010849	1.07E-07	B
CTD-2509G16.5	9.90E-13	2.67212784	5.52E-08	B
CTA-293F17.1	4.78E-11	2.6733727	2.66E-06	B
FAM212A	2.42E-10	2.67621615	1.35E-05	B
RP1-313I6.12	1.84E-81	2.68738664	1.03E-76	B
GPT2	5.06E-14	2.68784631	2.82E-09	B
CD1D	4.15E-51	2.69208268	2.32E-46	B
ALOX5	5.43E-134	2.69235208	3.03E-129	B
COCH	2.44E-16	2.69925206	1.36E-11	B
HIST1H2BG	6.59E-49	2.70030212	3.67E-44	B
RP11-44D5.1	9.96E-28	2.71160126	5.55E-23	B
HES1	9.22E-22	2.71361914	5.14E-17	B
CHST2	5.66E-45	2.71368085	3.15E-40	B
PTK2	1.10E-32	2.71416027	6.13E-28	B
ZNF667-AS1	1.93E-11	2.71858753	1.07E-06	B
RP11-81H14.2	3.46E-117	2.71935508	1.93E-112	B
RAB30	1.08E-268	2.73892553	6.00E-264	B
ELL3	6.02E-13	2.74255887	3.35E-08	B
SYK	6.85E-155	2.74523561	3.82E-150	B
NAPSB	2.25E-140	2.74678181	1.25E-135	B
GPLD1	4.60E-12	2.75111016	2.56E-07	B
RP11-568N6.1	2.92E-10	2.75409298	1.63E-05	B

RP11-38J22.6	2.43E-69	2.75749497	1.35E-64	B
HOOK1	9.09E-13	2.76467193	5.06E-08	B
EHD3	7.87E-54	2.76552795	4.39E-49	B
TPD52	1.00E-256	2.76584794	5.57E-252	B
CXXC5	3.85E-48	2.76931475	2.14E-43	B
ICOSLG	6.19E-62	2.77860028	3.45E-57	B
ZNF532	2.49E-58	2.78033862	1.39E-53	B
VAV2	5.52E-26	2.78880947	3.07E-21	B
PLCG2	2.09E-279	2.79273886	1.17E-274	B
RP11-96H19.1	4.07E-49	2.79354178	2.27E-44	B
LY86	1.16E-70	2.80330554	6.44E-66	B
RP11-160E2.19	3.23E-28	2.81496445	1.80E-23	B
PDLIM1	1.11E-118	2.8247099	6.18E-114	B
NOL3	1.75E-15	2.82693283	9.75E-11	B
GRAMD1C	1.81E-32	2.82907148	1.01E-27	B
FAM114A1	7.28E-21	2.83715027	4.06E-16	B
CABLES1	1.29E-23	2.8440056	7.18E-19	B
MRPS31P2	6.97E-11	2.84777256	3.89E-06	B
CTD-2545M3.6	3.69E-24	2.84794382	2.06E-19	B
SPINK2	1.26E-12	2.85131485	7.00E-08	B
CHODL	5.93E-13	2.8535273	3.31E-08	B
E2F5	2.95E-63	2.85466061	1.64E-58	B
PNPLA7	4.34E-39	2.85526851	2.42E-34	B
AC093818.1	3.62E-88	2.8626107	2.02E-83	B
NCF1B	1.04E-264	2.86628517	5.81E-260	B
AC007952.6	5.77E-10	2.86776386	3.22E-05	B
CXCR5	1.06E-133	2.87202626	5.92E-129	B
CTD-2516F10.2	1.80E-20	2.87398034	1.00E-15	B
RN7SL798P	5.52E-31	2.88707469	3.08E-26	B
RP11-444D3.1	1.07E-28	2.89025674	5.94E-24	B
OSBPL10	7.58E-43	2.89217316	4.22E-38	B
IGHV1-8	2.49E-31	2.90159994	1.39E-26	B
SPATS2	9.41E-112	2.90160949	5.24E-107	B
RP11-98L5.2	2.71E-10	2.90278761	1.51E-05	B
MNS1	6.73E-10	2.90299652	3.75E-05	B
LPIN3	1.29E-15	2.90395417	7.18E-11	B
LINC00173	1.65E-11	2.90962278	9.20E-07	B
UCHL1	2.68E-10	2.91406583	1.49E-05	B
ZNF165	1.19E-85	2.9236242	6.65E-81	B
CKAP4	2.71E-54	2.93066769	1.51E-49	B
FBXO16	1.37E-11	2.9330527	7.65E-07	B
RP11-160E2.11	1.76E-18	2.93338223	9.80E-14	B

HVCN1	5.09E-132	2.94413985	2.84E-127	B
KDELR3	1.80E-27	2.9540214	1.01E-22	B
MACC1	3.41E-37	2.95997598	1.90E-32	B
NCF1	1.80E-306	2.96203863	1.01E-301	B
CELSR1	4.34E-21	2.96696131	2.42E-16	B
MEF2B	3.35E-39	2.98652544	1.87E-34	B
PPFIBP2	2.75E-62	2.98714727	1.53E-57	B
AL590710.1	2.36E-23	2.99353702	1.32E-18	B
TRPV3	1.13E-20	2.99637417	6.29E-16	B
GPR160	3.02E-50	3.00807195	1.69E-45	B
RP11-102N12.3	1.02E-14	3.01242551	5.67E-10	B
BCL7A	2.66E-39	3.01480048	1.48E-34	B
SLC38A4	7.41E-10	3.01792735	4.13E-05	B
TEX14	8.55E-22	3.02197211	4.77E-17	B
RP1-152L7.5	2.33E-24	3.02298581	1.30E-19	B
MZB1	5.32E-180	3.02629333	2.96E-175	B
SLC47A1	1.65E-15	3.03660895	9.17E-11	B
RP11-330C7.3	8.01E-19	3.03919073	4.46E-14	B
ADAMDEC1	1.77E-37	3.04089259	9.88E-33	B
LINC01023	4.13E-14	3.04719575	2.30E-09	B
KIF19	3.86E-46	3.05285	2.15E-41	B
AC078883.3	5.37E-45	3.06123535	2.99E-40	B
C12orf42	5.38E-59	3.06234494	3.00E-54	B
PTPRK	7.43E-48	3.06654086	4.14E-43	B
ILDR1	4.62E-17	3.06875159	2.57E-12	B
GPR15	5.17E-32	3.06906261	2.88E-27	B
CD79B	0.00E+00	3.07758396	0.00E+00	B
IGLL3P	2.69E-25	3.07864545	1.50E-20	B
EFCAB13	2.55E-49	3.07899837	1.42E-44	B
RP11-430C7.5	1.33E-13	3.08545005	7.41E-09	B
CHST15	1.25E-124	3.11510489	6.95E-120	B
SMIM14	5.91E-164	3.11518696	3.29E-159	B
MAGED4B	1.56E-11	3.12562147	8.69E-07	B
PEG10	8.57E-11	3.12568782	4.77E-06	B
IGHV1-2	4.76E-42	3.12615647	2.65E-37	B
WDR64	6.57E-10	3.13169442	3.66E-05	B
TRIO	7.55E-114	3.14115845	4.21E-109	B
SLC15A2	7.35E-62	3.15196042	4.10E-57	B
LRRK1	1.11E-68	3.15551831	6.20E-64	B
CTA-384D8.34	3.90E-62	3.15790723	2.17E-57	B
SLCO5A1	2.48E-21	3.16686437	1.38E-16	B
AICDA	2.64E-10	3.17651112	1.47E-05	B

CD180	4.97E-92	3.19250482	2.77E-87	B
SLC17A9	1.29E-205	3.19382449	7.19E-201	B
NCMAP	1.00E-16	3.2046778	5.59E-12	B
NEIL1	2.54E-86	3.20510586	1.42E-81	B
CRNDE	1.01E-10	3.2103553	5.64E-06	B
LDLRAD2	4.13E-15	3.22112865	2.30E-10	B
ICAM4	5.48E-18	3.23868855	3.06E-13	B
TLR6	3.18E-43	3.23963203	1.77E-38	B
C2orf88	4.70E-38	3.24275081	2.62E-33	B
BASP1	4.34E-62	3.24763423	2.42E-57	B
RP11-290F5.2	1.66E-23	3.26197461	9.26E-19	B
SPIB	2.26E-136	3.26666967	1.26E-131	B
LINC00309	2.78E-11	3.2799692	1.55E-06	B
RP11-558F24.4	2.11E-24	3.2814198	1.18E-19	B
ACSM3	7.13E-17	3.2830008	3.97E-12	B
PRSS16	1.16E-22	3.28646927	6.48E-18	B
FCGR2B	1.35E-142	3.31061368	7.55E-138	B
IGKV1OR2-9	1.64E-13	3.31143664	9.16E-09	B
LRRC18	8.06E-15	3.32004789	4.49E-10	B
RP11-87G24.3	3.31E-24	3.32620614	1.84E-19	B
IGHV1-45	4.45E-21	3.33030817	2.48E-16	B
RP11-523O18.5	3.51E-10	3.34772555	1.96E-05	B
CCL25	5.93E-13	3.35556577	3.30E-08	B
HTR4	1.02E-10	3.35567203	5.66E-06	B
TMEM45A	1.95E-15	3.36595145	1.09E-10	B
P2RX1	3.29E-153	3.37652205	1.83E-148	B
TLE1P1	3.48E-21	3.38481807	1.94E-16	B
GNB3	2.15E-15	3.38707291	1.20E-10	B
TBC1D9	1.63E-74	3.39408967	9.11E-70	B
RP11-370B11.1	1.63E-18	3.39646077	9.10E-14	B
SDK2	9.91E-41	3.39875714	5.52E-36	B
TCF4	0.00E+00	3.40488723	0.00E+00	B
CCNJP2	4.77E-12	3.40995364	2.66E-07	B
NCF1C	0.00E+00	3.41423016	0.00E+00	B
C4B	8.56E-48	3.41761675	4.77E-43	B
BCAR3	3.28E-81	3.42414524	1.83E-76	B
ZNF418	6.52E-22	3.42684167	3.63E-17	B
OR7M1P	5.50E-10	3.43814366	3.06E-05	B
GAB1	2.83E-144	3.44078644	1.58E-139	B
BEND5	5.30E-27	3.44771585	2.96E-22	B
IGKV1OR2-11	1.00E-11	3.45102296	5.60E-07	B
C4A	2.74E-48	3.45379555	1.53E-43	B

C1orf220	2.19E-15	3.45392153	1.22E-10	B
TRAM2	7.70E-190	3.45464976	4.29E-185	B
CD40	1.76E-212	3.45730135	9.80E-208	B
PRCD	1.92E-12	3.46903577	1.07E-07	B
SPAG4	3.41E-136	3.4780798	1.90E-131	B
TREML2	6.46E-23	3.4807024	3.60E-18	B
MYO1D	1.60E-83	3.48188639	8.94E-79	B
COLCA1	6.13E-11	3.48507553	3.42E-06	B
MOB3B	1.41E-44	3.4862832	7.84E-40	B
POF1B	1.08E-09	3.49745031	6.04E-05	B
WDFY4	1.14E-251	3.50274434	6.36E-247	B
AF127936.5	1.58E-19	3.50902805	8.79E-15	B
CCSER1	3.67E-30	3.51335461	2.05E-25	B
RP11-301L8.2	3.81E-15	3.51367939	2.12E-10	B
HHEX	2.34E-28	3.5147217	1.30E-23	B
SMIM1	6.57E-22	3.51755929	3.66E-17	B
RGMB	2.51E-34	3.51766154	1.40E-29	B
CHAC1	1.92E-38	3.52199419	1.07E-33	B
PLEKHG1	2.07E-107	3.52835287	1.16E-102	B
IGF1	1.23E-35	3.53137168	6.86E-31	B
IGLV3-9	2.75E-20	3.54005703	1.53E-15	B
WASIR2	7.81E-16	3.54136432	4.35E-11	B
OR2T3	2.66E-10	3.55185424	1.49E-05	B
CDK14	1.28E-147	3.55815021	7.11E-143	B
USP6NL	6.11E-124	3.56657723	3.40E-119	B
EAF2	4.28E-238	3.57806683	2.39E-233	B
CH17-132F21.1	2.69E-18	3.59443102	1.50E-13	B
KRT19P2	5.65E-11	3.60183301	3.15E-06	B
AC097658.1	3.06E-63	3.60840469	1.71E-58	B
FAM177B	1.03E-15	3.62415667	5.75E-11	B
ADM2	2.93E-26	3.63327422	1.63E-21	B
IGKV1OR2-118	3.17E-21	3.64321647	1.76E-16	B
PDIA5	2.32E-58	3.64579226	1.29E-53	B
AC104024.1	4.69E-36	3.65686302	2.61E-31	B
RP11-259G18.1	1.01E-11	3.65805056	5.62E-07	B
TPTE2	1.68E-14	3.65811028	9.38E-10	B
CCR10	1.68E-68	3.67964894	9.39E-64	B
BTK	6.18E-188	3.691738	3.44E-183	B
WFS1	4.48E-78	3.69220321	2.50E-73	B
TLE1	1.77E-80	3.7083038	9.88E-76	B
CTD-2215E18.1	3.66E-11	3.70924034	2.04E-06	B
KB-1980E6.3	2.00E-36	3.71606858	1.12E-31	B

AP001058.3	5.91E-21	3.72241482	3.29E-16	B
AFF3	1.78E-145	3.72489945	9.91E-141	B
PYCR1	1.81E-96	3.7356325	1.01E-91	B
CLIC4	1.37E-231	3.74117001	7.65E-227	B
ZYG11A	1.63E-16	3.74532426	9.10E-12	B
CTD-2313J17.5	1.08E-16	3.74607845	6.04E-12	B
LINC00494	6.61E-22	3.74705628	3.69E-17	B
RP11-318K15.2	2.18E-35	3.74996951	1.22E-30	B
AC092667.2	1.24E-15	3.7582178	6.94E-11	B
LIX1	1.49E-13	3.75917252	8.29E-09	B
DOK3	1.31E-184	3.76063261	7.27E-180	B
AC016906.1	1.65E-13	3.76433289	9.18E-09	B
DCC	2.55E-10	3.76459723	1.42E-05	B
CERCAM	4.11E-55	3.7647201	2.29E-50	B
RP11-624C23.1	3.17E-83	3.77205049	1.77E-78	B
C15orf65	3.84E-15	3.77501913	2.14E-10	B
MGAT3	7.36E-35	3.77726395	4.10E-30	B
IGLV2-8	6.85E-45	3.77977623	3.82E-40	B
BCL11A	0.00E+00	3.78058474	0.00E+00	B
AC074212.5	7.68E-40	3.79037226	4.28E-35	B
RP11-512N21.1	2.66E-10	3.79353042	1.48E-05	B
RASGRP3	1.56E-240	3.80064734	8.68E-236	B
RP11-282E4.1	5.20E-15	3.80171133	2.90E-10	B
SLC2A5	1.52E-118	3.80550875	8.50E-114	B
RP11-1334A24.6	1.80E-72	3.81743861	1.00E-67	B
LCN10	1.15E-20	3.83086352	6.40E-16	B
ENAM	3.52E-36	3.83533662	1.96E-31	B
AC074389.9	4.27E-21	3.84082506	2.38E-16	B
RP11-43D2.2	6.62E-11	3.84543026	3.69E-06	B
AC121251.1	7.18E-12	3.84748405	4.00E-07	B
COLCA2	7.44E-11	3.84779678	4.15E-06	B
RP11-284F21.7	3.17E-26	3.84968289	1.77E-21	B
LY86-AS1	4.09E-22	3.85621994	2.28E-17	B
PRAMENP	3.88E-15	3.8578379	2.16E-10	B
SIX5	1.52E-26	3.85998041	8.45E-22	B
OR2T2	5.38E-10	3.8625067	3.00E-05	B
PLA2G2D	1.87E-12	3.87272461	1.04E-07	B
STAP1	1.83E-234	3.87318753	1.02E-229	B
CNTNAP2	3.99E-11	3.88600546	2.22E-06	B
CNN3	1.60E-37	3.88977009	8.90E-33	B
ADAM28	0.00E+00	3.89880507	0.00E+00	B
ALDH1L2	1.23E-56	3.90044375	6.83E-52	B

RP11-138I18.2	1.62E-13	3.9293148	9.02E-09	B
AP001057.1	1.34E-12	3.95463084	7.48E-08	B
RP11-498C9.13	5.69E-114	3.9664716	3.17E-109	B
CNKSR1	3.92E-91	3.97284747	2.19E-86	B
PAWR	1.81E-30	3.97408907	1.01E-25	B
RP11-136K14.1	7.64E-17	3.97411533	4.26E-12	B
RP11-469E19.1	3.82E-21	3.97912286	2.13E-16	B
NT5E	1.11E-60	3.98171616	6.20E-56	B
IGHV4OR15-8	1.58E-56	3.98514373	8.78E-52	B
PKIG	8.05E-160	4.00802899	4.48E-155	B
MEF2C	0.00E+00	4.00886718	0.00E+00	B
ACSM1	2.67E-16	4.03511536	1.49E-11	B
TCEB1P28	4.26E-10	4.03770107	2.38E-05	B
RP11-761I4.3	3.52E-69	4.05885845	1.96E-64	B
EYA2	2.82E-11	4.06363879	1.57E-06	B
TXNDC5	5.51E-283	4.06400913	3.07E-278	B
ANKRD36BP2	7.66E-110	4.06591366	4.27E-105	B
MYL2	6.63E-11	4.07460718	3.70E-06	B
ABCB4	1.67E-26	4.0753801	9.32E-22	B
HTR3A	2.95E-20	4.08365189	1.64E-15	B
C16orf74	1.89E-117	4.08384495	1.05E-112	B
IGJ	8.28E-304	4.08902473	4.61E-299	B
LINC01055	5.76E-12	4.0951129	3.21E-07	B
BHLHE41	5.34E-145	4.10744999	2.97E-140	B
FAM129C	2.71E-203	4.11904773	1.51E-198	B
ZNF608	2.35E-27	4.12913323	1.31E-22	B
SNX29P1	8.65E-81	4.13533345	4.82E-76	B
COL9A3	2.01E-32	4.14153377	1.12E-27	B
RP11-328C8.4	3.09E-15	4.14164168	1.72E-10	B
IGLL1	1.42E-42	4.14222164	7.89E-38	B
SLC6A9	7.57E-35	4.14498166	4.22E-30	B
ACOXL	8.01E-53	4.17274959	4.46E-48	B
RP5-1033H22.2	4.89E-28	4.17546745	2.72E-23	B
KLK1	3.06E-26	4.17663128	1.71E-21	B
IGKV1OR2-6	2.81E-19	4.18681404	1.56E-14	B
LINC00571	7.28E-11	4.18991372	4.06E-06	B
RP11-380I10.4	7.22E-12	4.19075938	4.03E-07	B
AC007879.2	7.64E-17	4.19281719	4.26E-12	B
IGHV1OR15-4	8.73E-26	4.20503486	4.87E-21	B
RP11-367G18.1	1.52E-25	4.21289174	8.49E-21	B
ADD2	9.91E-22	4.22016125	5.52E-17	B
ZNF215	2.78E-121	4.22157995	1.55E-116	B

SYT1	1.16E-17	4.23884323	6.46E-13	B
ESAM	1.45E-19	4.24045918	8.10E-15	B
CNR2	2.95E-123	4.25438527	1.64E-118	B
SNORA70F	5.31E-10	4.26153493	2.96E-05	B
RP11-131L23.1	8.64E-14	4.2637733	4.81E-09	B
DSP	4.84E-12	4.28139559	2.70E-07	B
SWAP70	6.63E-253	4.28879585	3.70E-248	B
B9D1	2.77E-63	4.29345504	1.55E-58	B
RP11-329N22.1	1.69E-16	4.30322298	9.44E-12	B
RP11-138I18.1	4.40E-34	4.30434764	2.45E-29	B
ARHGAP24	3.27E-221	4.30994693	1.82E-216	B
IGKC	0.00E+00	4.31544337	0.00E+00	B
BLNK	0.00E+00	4.34444224	0.00E+00	B
POU2AF1	0.00E+00	4.3553477	0.00E+00	B
EPN2-AS1	1.40E-20	4.38105787	7.79E-16	B
DUSP26	1.43E-12	4.3836726	7.96E-08	B
UGT8	5.26E-59	4.38457554	2.93E-54	B
STEAP1	1.36E-14	4.40698602	7.58E-10	B
CR1	8.90E-108	4.40757199	4.96E-103	B
AC129778.7	4.57E-25	4.40793809	2.55E-20	B
RP11-318K12.1	8.21E-29	4.41168238	4.57E-24	B
GNG7	0.00E+00	4.4216105	0.00E+00	B
DERL3	0.00E+00	4.42443835	0.00E+00	B
TLR10	2.98E-116	4.44190438	1.66E-111	B
RAPGEF5	1.54E-31	4.44241686	8.60E-27	B
IGKV1OR-2	4.95E-21	4.45742084	2.76E-16	B
CTA-250D10.23	0.00E+00	4.46424283	0.00E+00	B
RP11-511B23.1	5.64E-18	4.46497803	3.14E-13	B
IGHV4-4	1.76E-75	4.46652655	9.78E-71	B
TCL1A	1.60E-225	4.4694796	8.94E-221	B
KIAA0226L	2.80E-307	4.47462509	1.56E-302	B
AC012123.1	4.06E-19	4.47581128	2.26E-14	B
LAMC1	6.66E-25	4.49219214	3.71E-20	B
IGHV1-67	2.90E-20	4.50200758	1.61E-15	B
IGHM	0.00E+00	4.51445714	0.00E+00	B
GYLTL1B	1.99E-26	4.52206572	1.11E-21	B
SLC9C1	1.31E-12	4.53443693	7.27E-08	B
IGKV1OR10-1	6.52E-33	4.5414666	3.63E-28	B
AC019181.2	1.99E-13	4.55521967	1.11E-08	B
TNFRSF13B	1.48E-166	4.56143381	8.26E-162	B
RP11-768B22.2	3.98E-39	4.57466311	2.22E-34	B
GH1	5.65E-18	4.58309275	3.15E-13	B

RP13-514E23.2	1.87E-22	4.59094747	1.04E-17	B
RP5-1098D14.1	9.70E-12	4.6014781	5.41E-07	B
RP11-325F22.5	9.72E-12	4.63170979	5.42E-07	B
MEF2C-AS1	8.71E-97	4.66107664	4.86E-92	B
SYNPO	1.76E-18	4.6624878	9.81E-14	B
CNR1	2.49E-21	4.68613782	1.39E-16	B
WNT5B	9.08E-41	4.70575626	5.06E-36	B
TEX9	1.37E-61	4.71039525	7.62E-57	B
HLA-DOB	0.00E+00	4.72424686	0.00E+00	B
RP11-297B17.2	3.83E-16	4.72475639	2.14E-11	B
CTC-265F19.3	1.05E-27	4.72864129	5.83E-23	B
IGKV5-2	1.01E-17	4.73749238	5.62E-13	B
RP11-436H11.6	4.20E-10	4.75268059	2.34E-05	B
RP11-460N11.2	8.25E-35	4.76816656	4.60E-30	B
LARGE	1.70E-106	4.77920152	9.49E-102	B
BHLHA15	9.77E-22	4.78988329	5.44E-17	B
AMPD1	5.16E-36	4.79241792	2.88E-31	B
IGHG1	0.00E+00	4.80406188	0.00E+00	B
AC096579.7	0.00E+00	4.81756518	0.00E+00	B
PHF16	2.52E-39	4.82195065	1.40E-34	B
PRKCG	1.29E-24	4.82862821	7.19E-20	B
IGLV1-41	1.67E-16	4.8334529	9.30E-12	B
RP11-689B22.2	1.95E-233	4.85773967	1.09E-228	B
DENND5B	1.44E-206	4.89035538	8.02E-202	B
COL4A4	1.31E-97	4.89463197	7.28E-93	B
RP11-136K14.3	1.35E-25	4.92273697	7.52E-21	B
KHDRBS2	6.20E-47	4.92515753	3.46E-42	B
RP11-31F19.1	6.11E-33	4.92640246	3.41E-28	B
TBC1D27	2.62E-116	4.97595335	1.46E-111	B
AC002480.2	3.89E-30	5.00798543	2.17E-25	B
KCNH8	2.08E-47	5.01056452	1.16E-42	B
BTN1A1	6.06E-25	5.01108177	3.38E-20	B
IGLV1-51	1.66E-50	5.01952773	9.25E-46	B
AC103563.2	8.16E-17	5.0268715	4.55E-12	B
CLDN14	1.69E-31	5.03017168	9.44E-27	B
RP11-554D14.2	1.79E-22	5.03063703	9.97E-18	B
CTC-265F19.2	7.72E-32	5.03509752	4.31E-27	B
BLK	0.00E+00	5.03616156	0.00E+00	B
AC002480.3	2.78E-20	5.05135358	1.55E-15	B
IGLV3-10	4.33E-25	5.05433974	2.42E-20	B
IGLV3-21	1.93E-66	5.05932423	1.08E-61	B
TNFRSF13C	4.38E-25	5.06538031	2.44E-20	B

HID1	5.37E-234	5.0773389	2.99E-229	B
HCG23	2.91E-11	5.09156406	1.62E-06	B
RP11-148O21.4	1.52E-52	5.10474297	8.45E-48	B
CTD-2509G16.3	4.15E-10	5.10684212	2.31E-05	B
CADPS2	1.05E-23	5.1202128	5.86E-19	B
PNOC	3.84E-239	5.13454029	2.14E-234	B
IGHV3-65	1.14E-29	5.16503169	6.38E-25	B
C12orf74	7.87E-41	5.18405135	4.38E-36	B
IGKV1-5	2.69E-119	5.19142496	1.50E-114	B
CRIP3	1.21E-44	5.19365536	6.75E-40	B
RP11-1070N10.3	3.07E-56	5.21830185	1.71E-51	B
RP11-554D14.4	5.17E-21	5.22676015	2.88E-16	B
IGKV2-40	2.90E-11	5.23090349	1.62E-06	B
AL122127.25	1.56E-72	5.2343432	8.71E-68	B
AC026202.3	2.44E-58	5.23480516	1.36E-53	B
IGKV1-33	1.08E-120	5.23943551	6.03E-116	B
RP11-158I9.5	5.70E-143	5.24509584	3.17E-138	B
OSBPL10-AS1	1.60E-29	5.25066939	8.92E-25	B
PRICKLE1	1.03E-62	5.25294443	5.77E-58	B
RP11-87G24.6	6.87E-14	5.25669454	3.83E-09	B
BMP6	1.04E-23	5.26310295	5.82E-19	B
TMEM56	1.29E-32	5.26708801	7.22E-28	B
IGLC2	8.19E-296	5.26898005	4.57E-291	B
SCN3A	3.42E-37	5.27308493	1.91E-32	B
IGLV4-69	9.16E-18	5.27388368	5.10E-13	B
IGKV1D-27	7.92E-59	5.27915048	4.41E-54	B
IGHV3-16	4.56E-40	5.28693255	2.54E-35	B
IGKV2-4	3.97E-23	5.2938966	2.21E-18	B
BACE2	1.36E-37	5.29865975	7.57E-33	B
IGLV3-25	1.05E-36	5.30376712	5.83E-32	B
RP11-428K3.1	7.57E-24	5.30428382	4.22E-19	B
PARM1	5.21E-237	5.31266858	2.90E-232	B
IGLV1-40	5.94E-47	5.32686728	3.31E-42	B
IGKV3-20	3.46E-189	5.3459211	1.93E-184	B
IGLV4-3	2.97E-17	5.36249024	1.65E-12	B
AC007386.2	4.17E-12	5.37275778	2.32E-07	B
IGKV1-17	5.53E-109	5.39111957	3.08E-104	B
IGHV4-31	3.85E-104	5.39336404	2.15E-99	B
IGLC3	0.00E+00	5.39976384	0.00E+00	B
RP11-568J23.4	6.49E-11	5.42466128	3.62E-06	B
IGHV4-34	6.96E-137	5.43301301	3.88E-132	B
IGHV1-46	8.20E-96	5.43685532	4.57E-91	B

VAV3-AS1	3.12E-45	5.4605604	1.74E-40	B
IGKV3OR2-268	4.40E-200	5.46411151	2.46E-195	B
SSPN	2.44E-110	5.47571945	1.36E-105	B
COBLL1	0.00E+00	5.47747073	0.00E+00	B
RP11-116A1.1	1.88E-14	5.48326763	1.05E-09	B
IGHV2OR16-5	5.17E-30	5.48767569	2.88E-25	B
RP11-290F5.1	1.45E-192	5.49219281	8.08E-188	B
COL4A3	5.21E-67	5.50065553	2.90E-62	B
CD79A	0.00E+00	5.50168448	0.00E+00	B
RP11-142C4.6	2.44E-39	5.50521552	1.36E-34	B
IGLV5-45	3.11E-13	5.51141637	1.73E-08	B
ZNF587P1	1.20E-42	5.52394427	6.70E-38	B
IGHV2-5	8.39E-24	5.54997639	4.68E-19	B
OR2T34	7.32E-24	5.58278824	4.08E-19	B
RP11-693J15.5	8.82E-129	5.58679929	4.92E-124	B
IGKV2-18	6.52E-19	5.58976875	3.63E-14	B
CTD-2232E5.2	3.09E-15	5.59955123	1.72E-10	B
RP11-148O21.2	6.26E-154	5.61477258	3.49E-149	B
CTC-265F19.1	3.11E-60	5.62243401	1.73E-55	B
SMPDL3B	6.40E-80	5.64018006	3.57E-75	B
RP11-960L18.1	2.75E-201	5.65251735	1.53E-196	B
ANGPTL1	1.00E-74	5.65293294	5.60E-70	B
IGHV3-73	1.92E-37	5.65422277	1.07E-32	B
IGLV3-19	1.14E-38	5.65891565	6.34E-34	B
RP11-693J15.4	2.57E-83	5.66423842	1.43E-78	B
RP11-654D12.2	7.98E-17	5.66432945	4.45E-12	B
LARGE-AS1	1.24E-80	5.66992359	6.93E-76	B
RP11-164H13.1	9.80E-76	5.67699883	5.46E-71	B
IGLV3-27	1.37E-16	5.67948857	7.62E-12	B
RP5-1104E15.6	1.35E-27	5.68627595	7.54E-23	B
IGHA1	0.00E+00	5.68971521	0.00E+00	B
MS4A1	0.00E+00	5.71087408	0.00E+00	B
IGHV3-43	3.59E-140	5.72222869	2.00E-135	B
AC002480.4	5.05E-30	5.72823235	2.81E-25	B
IGHV4-55	1.36E-88	5.75038495	7.57E-84	B
IGHV3-30	5.57E-225	5.76044749	3.11E-220	B
IGHV4-59	4.38E-104	5.77056216	2.44E-99	B
IGHV3-49	4.03E-68	5.79985336	2.25E-63	B
RP11-731F5.1	2.74E-45	5.8022018	1.53E-40	B
IGHV3-62	1.70E-74	5.81069031	9.48E-70	B
IGHA2	0.00E+00	5.81341778	0.00E+00	B
IGHV1-18	1.35E-101	5.82564267	7.52E-97	B

IGLV2-23	4.06E-87	5.82702417	2.26E-82	B
UBE2QL1	4.81E-10	5.83661894	2.68E-05	B
IGHV3-33	1.77E-196	5.8464027	9.89E-192	B
IGHV2-26	5.98E-27	5.84858447	3.33E-22	B
IGHV3-35	6.73E-64	5.87821676	3.75E-59	B
IGLV2-18	4.51E-63	5.88577	2.51E-58	B
IGKV3-11	2.19E-177	5.8876039	1.22E-172	B
RP11-445F6.2	1.04E-55	5.89434323	5.80E-51	B
IL6	1.16E-116	5.89968113	6.47E-112	B
TNFRSF17	0.00E+00	5.91219564	0.00E+00	B
AC104699.1	2.76E-222	5.91478273	1.54E-217	B
IGKV3D-15	4.26E-230	5.91963907	2.38E-225	B
KIAA0125	0.00E+00	5.92728846	0.00E+00	B
GLYATL1P3	1.08E-29	5.93337719	6.02E-25	B
IGKV2D-18	5.07E-21	5.93530217	2.83E-16	B
ALPL	2.39E-14	5.95052196	1.33E-09	B
FCRLA	0.00E+00	5.95630417	0.00E+00	B
IGKV1D-33	5.40E-87	5.98317954	3.01E-82	B
AC079767.4	8.74E-94	5.98498762	4.87E-89	B
TAS1R3	1.58E-98	5.99279741	8.78E-94	B
IGKV3-15	4.75E-139	5.9947803	2.65E-134	B
RN7SL627P	1.24E-53	6.01006682	6.91E-49	B
RN7SL639P	1.24E-53	6.01006682	6.91E-49	B
CAMP	6.42E-19	6.01073036	3.58E-14	B
IGHE	2.61E-45	6.01580974	1.46E-40	B
IGHV1-12	1.34E-27	6.01630012	7.47E-23	B
IGKV2OR22-4	7.04E-36	6.04700837	3.93E-31	B
RP11-175K6.1	1.74E-22	6.0561154	9.68E-18	B
RP11-794P6.1	9.80E-13	6.05702359	5.46E-08	B
IGKV1D-39	8.86E-168	6.06027545	4.94E-163	B
IGKV2-28	1.87E-62	6.06727154	1.04E-57	B
LARGE-IT1	8.46E-32	6.06787299	4.72E-27	B
RALGPS2	0.00E+00	6.06899452	0.00E+00	B
COL19A1	1.17E-190	6.07651046	6.55E-186	B
IGHV7-81	3.51E-34	6.08617527	1.96E-29	B
ITGA8	7.46E-101	6.1176704	4.16E-96	B
IGKV4-1	2.93E-194	6.18302592	1.63E-189	B
IGHV5-51	2.61E-56	6.18561888	1.45E-51	B
CLEC17A	0.00E+00	6.1866035	0.00E+00	B
OR4C6	1.30E-14	6.19862849	7.23E-10	B
IGHV1-69	1.82E-166	6.21235322	1.02E-161	B
IGLC1	0.00E+00	6.22126061	0.00E+00	B

IGHV1OR15-9	1.09E-38	6.2279637	6.06E-34	B
RP11-820K3.2	6.94E-123	6.23951223	3.87E-118	B
RN7SL842P	1.33E-27	6.25583037	7.41E-23	B
IGHV4-39	4.89E-122	6.26948421	2.73E-117	B
IGKV3D-20	8.45E-187	6.27110808	4.71E-182	B
IGLV3-16	1.45E-34	6.28019333	8.10E-30	B
IGLV2-34	1.47E-42	6.28142279	8.21E-38	B
FCER2	0.00E+00	6.29860012	0.00E+00	B
IGKV2-30	1.25E-94	6.30473861	6.99E-90	B
AC073072.5	2.18E-24	6.31259152	1.22E-19	B
IGHV3-23	5.96E-298	6.31309072	3.32E-293	B
CTD-2227E11.1	8.77E-41	6.32215581	4.89E-36	B
IGHV3-74	2.99E-238	6.32383562	1.67E-233	B
IGHV4-61	4.10E-125	6.32397368	2.29E-120	B
IGLV1-50	1.98E-23	6.32803499	1.10E-18	B
IGLV1-44	2.36E-91	6.32937377	1.31E-86	B
FER1L4	0.00E+00	6.33260154	0.00E+00	B
RP11-403N16.3	5.26E-10	6.34937195	2.93E-05	B
IGKV2D-28	1.43E-106	6.3856083	7.95E-102	B
AC096579.13	3.47E-34	6.39230048	1.93E-29	B
IGKV3D-11	1.05E-165	6.41670527	5.85E-161	B
IGLV1-47	6.34E-81	6.41960248	3.53E-76	B
IGHV3-47	1.80E-59	6.4333821	1.00E-54	B
OSTN-AS1	4.65E-66	6.43359056	2.59E-61	B
IGHV1OR16-3	1.35E-16	6.43359436	7.52E-12	B
IGKV2D-24	1.25E-46	6.43947208	6.97E-42	B
CD22	0.00E+00	6.4654872	0.00E+00	B
IGKV2D-29	1.06E-38	6.49093373	5.91E-34	B
RNU4-38P	4.99E-21	6.5001934	2.78E-16	B
CTB-43E15.3	1.87E-102	6.50478562	1.05E-97	B
RP11-297B17.3	8.77E-41	6.50590858	4.89E-36	B
KCNN3	1.65E-183	6.51834608	9.19E-179	B
IGHV3OR16-6	4.25E-86	6.530897	2.37E-81	B
LINC00582	2.67E-72	6.53872697	1.49E-67	B
IGKV1-12	9.29E-159	6.54353768	5.18E-154	B
IGKV2-24	2.77E-51	6.54779347	1.54E-46	B
IGHV1OR15-2	3.51E-70	6.55684101	1.96E-65	B
BANK1	0.00E+00	6.56062805	0.00E+00	B
IGLV2-33	1.91E-44	6.59221523	1.06E-39	B
IGHV3-60	9.92E-64	6.6073246	5.53E-59	B
hsa-mir-5195	1.37E-61	6.60873616	7.64E-57	B
IGLV2-11	2.57E-94	6.64857358	1.43E-89	B

IGHEP1	2.84E-40	6.67033098	1.58E-35	B
IGHV3OR16-7	1.70E-55	6.67898155	9.46E-51	B
SLC38A11	3.87E-133	6.67934302	2.16E-128	B
IGHG3	0.00E+00	6.68733345	0.00E+00	B
MIXL1	3.13E-96	6.70610956	1.74E-91	B
IGHV6-1	3.75E-38	6.72086103	2.09E-33	B
IGLV2-28	1.50E-44	6.72507721	8.33E-40	B
RP11-279O9.4	1.24E-31	6.7600669	6.92E-27	B
IGHV1-24	1.29E-116	6.7659249	7.17E-112	B
IGHV3OR16-12	6.78E-36	6.84277696	3.78E-31	B
IGHV5-78	3.70E-126	6.8511051	2.06E-121	B
LINC00926	0.00E+00	6.87152173	0.00E+00	B
IGHV3-66	7.54E-260	6.87358761	4.20E-255	B
IGKV2D-26	6.17E-36	6.87521272	3.44E-31	B
RP11-713N11.5	9.66E-19	6.8791542	5.39E-14	B
IGHV4-28	6.31E-114	6.88038197	3.52E-109	B
CD24P4	8.10E-182	6.88382947	4.51E-177	B
IGKV1-9	3.40E-178	6.89143189	1.90E-173	B
IGHG2	0.00E+00	6.90968862	0.00E+00	B
DPEP1	3.28E-68	6.91689084	1.83E-63	B
IGHV2-70	1.37E-42	6.92693461	7.64E-38	B
UGT2B17	8.22E-32	6.93104348	4.58E-27	B
RP11-812E19.9	1.74E-59	6.93247362	9.67E-55	B
IGKV1D-12	4.43E-68	6.94808698	2.47E-63	B
IGHV3-38	1.61E-130	6.95660376	8.95E-126	B
IGKV1-39	3.11E-139	6.96678646	1.73E-134	B
SCNN1B	4.15E-98	6.99732905	2.31E-93	B
RN7SL337P	2.23E-27	7.0243778	1.24E-22	B
RASSF6	9.30E-105	7.04676043	5.18E-100	B
IGHG4	0.00E+00	7.05147423	0.00E+00	B
RP11-438F14.3	2.89E-17	7.05821462	1.61E-12	B
FCRL1	0.00E+00	7.0717153	0.00E+00	B
IGHV3-41	1.14E-104	7.0724772	6.35E-100	B
IGLV3-1	0.00E+00	7.08900254	0.00E+00	B
AC002480.5	4.62E-66	7.09289594	2.57E-61	B
IGKV1OR22-5	3.02E-40	7.1013577	1.68E-35	B
IGKV1-27	1.34E-74	7.1129119	7.49E-70	B
IGHV3-11	2.70E-282	7.12602236	1.51E-277	B
FCRL5	0.00E+00	7.129678	0.00E+00	B
IGHV3-9	3.04E-178	7.14489109	1.70E-173	B
IGHV3-6	8.66E-34	7.16088184	4.83E-29	B
AC123023.1	1.35E-16	7.16355089	7.52E-12	B

CTD-2363C16.2	8.66E-34	7.16959363	4.83E-29	B
CTD-2363C16.1	1.75E-29	7.18221245	9.75E-25	B
IGHV3-21	0.00E+00	7.19564612	0.00E+00	B
CPNE5	0.00E+00	7.19912286	0.00E+00	B
IGLV6-57	3.39E-165	7.21886316	1.89E-160	B
IGHV3-22	7.02E-79	7.23685291	3.92E-74	B
IGHV3OR16-13	2.83E-226	7.28344455	1.58E-221	B
RP11-295P22.2	2.42E-55	7.31895375	1.35E-50	B
KLHL14	1.82E-86	7.3237211	1.01E-81	B
PKHD1L1	3.45E-128	7.3242056	1.92E-123	B
FAM92B	4.56E-47	7.32668071	2.54E-42	B
IGHV3-53	1.12E-248	7.32977594	6.26E-244	B
STEAP1B	1.18E-72	7.34347068	6.60E-68	B
CR2	0.00E+00	7.35380879	0.00E+00	B
IGKV2-29	4.64E-53	7.36078586	2.59E-48	B
IGLC7	1.07E-304	7.37036163	5.98E-300	B
IGHV3-20	7.91E-244	7.3727749	4.41E-239	B
CTB-43E15.4	3.48E-40	7.40521997	1.94E-35	B
IGLV9-49	3.86E-23	7.431489	2.15E-18	B
RP11-731F5.2	0.00E+00	7.43471576	0.00E+00	B
IGLVI-70	1.35E-16	7.43763124	7.50E-12	B
IGHV3OR15-7	2.21E-85	7.46110608	1.23E-80	B
IGKV1D-37	9.30E-49	7.50439539	5.19E-44	B
IGLV4-60	8.63E-34	7.55464562	4.81E-29	B
IGHGP	0.00E+00	7.56483858	0.00E+00	B
RP11-170L3.7	1.72E-167	7.57476735	9.57E-163	B
IGHV3-7	1.10E-307	7.58207456	6.12E-303	B
IGLJ1	2.96E-40	7.59238907	1.65E-35	B
IGKV1D-17	2.04E-154	7.62067464	1.14E-149	B
AC007386.4	3.79E-187	7.64704649	2.11E-182	B
IGHV3-15	4.28E-150	7.64824353	2.39E-145	B
IGKV1-6	7.03E-183	7.73918411	3.92E-178	B
IGHV3-72	4.68E-198	7.76174103	2.61E-193	B
IGHV3-64	9.68E-207	7.78450564	5.39E-202	B
IGLV1-36	2.97E-40	7.78884351	1.66E-35	B
RP11-15J10.3	9.76E-17	7.79363185	5.44E-12	B
IGLV7-43	1.35E-16	7.80630724	7.50E-12	B
EBF1	0.00E+00	7.8065779	0.00E+00	B
IGKV2D-30	1.40E-89	7.85242872	7.79E-85	B
IGHV3OR16-9	8.36E-240	7.87776645	4.66E-235	B
IGLL5	0.00E+00	7.89571228	0.00E+00	B
IGKV3-7	1.77E-178	7.93532949	9.88E-174	B

IGKV1D-16	1.11E-130	7.93768712	6.19E-126	B
IGKV1-16	5.99E-133	7.93898443	3.34E-128	B
FCRL2	0.00E+00	7.94172642	0.00E+00	B
IGLV2-5	1.65E-57	7.9834215	9.17E-53	B
IGKV1D-13	1.03E-115	8.00226015	5.76E-111	B
PAX5	0.00E+00	8.07980789	0.00E+00	B
IGKV1-13	2.90E-111	8.12567936	1.62E-106	B
U62631.5	9.88E-47	8.17504258	5.51E-42	B
IGLC6	1.16E-202	8.17794837	6.47E-198	B
CD19	0.00E+00	8.20615808	0.00E+00	B
IGHV3-48	7.61E-302	8.25939564	4.24E-297	B
AL928768.3	0.00E+00	8.26646363	0.00E+00	B
IGKV1-37	4.04E-96	8.32650245	2.25E-91	B
IGKV1D-8	2.97E-161	8.41747208	1.65E-156	B
IGHD	0.00E+00	8.4223127	0.00E+00	B
RP11-108P20.4	3.03E-23	8.4310684	1.69E-18	B
IGHV1OR21-1	1.11E-59	8.44781787	6.17E-55	B
IGHV3-63	9.75E-30	8.47319113	5.43E-25	B
IGHV3OR16-11	5.58E-77	8.47445574	3.11E-72	B
SDC1	0.00E+00	8.58580466	0.00E+00	B
VPREB3	0.00E+00	8.58748475	0.00E+00	B
IGLC5	5.71E-77	8.6187251	3.18E-72	B
IGKV2D-40	6.97E-49	8.6394282	3.88E-44	B
IGLJ3	9.76E-17	8.64752224	5.44E-12	B
IGHV4-80	9.76E-17	8.6567772	5.44E-12	B
RP11-394O9.1	6.57E-19	8.66490449	3.66E-14	B
RP11-498M5.2	2.85E-83	8.67192656	1.59E-78	B
IGHV3-13	4.18E-181	8.70280067	2.33E-176	B
IGKV1OR22-1	2.19E-38	8.80957237	1.22E-33	B
RP11-344B23.2	4.46E-21	8.81586355	2.48E-16	B
IGHV1-58	1.42E-27	8.88150628	7.92E-23	B
IGKV1-8	7.32E-144	8.91659027	4.08E-139	B
RP5-887A10.1	1.75E-152	8.91928535	9.73E-148	B
IGKV1D-43	3.23E-131	8.9472911	1.80E-126	B
AC142381.1	1.90E-146	8.95584989	1.06E-141	B
IGKV1OR2-108	3.82E-79	8.99380828	2.13E-74	B
IGHV3OR16-10	1.04E-42	9.14112055	5.82E-38	B
RP11-685N3.1	3.31E-53	9.21988241	1.84E-48	B
RP11-1084E5.1	6.70E-32	9.22374912	3.74E-27	B
IGHV3OR16-8	2.55E-194	9.2404888	1.42E-189	B
IGHV3-71	1.29E-174	9.26520872	7.18E-170	B
IGHV3-19	8.17E-88	9.34529796	4.55E-83	B

MTND5P5	6.70E-32	9.78640263	3.74E-27	B
IGLJ2	1.04E-42	9.91708015	5.82E-38	B
IGKV2-26	4.62E-34	9.94949908	2.57E-29	B
RP11-16E12.2	5.51E-300	9.98270124	3.07E-295	B
AC103563.5	6.70E-32	10.0857694	3.74E-27	B
IGKV1D-42	1.21E-81	10.1779056	6.77E-77	B
IGHV3-52	1.77E-92	10.641529	9.89E-88	B
IGKV3D-7	2.35E-116	11.4764159	1.31E-111	B
TSHZ2	1.09E-67	2.00410684	6.08E-63	CD4 T
RHPN1	1.03E-15	2.03135081	5.76E-11	CD4 T
RP11-330A16.1	6.72E-13	2.0323032	3.74E-08	CD4 T
FAAH2	1.39E-88	2.04305146	7.75E-84	CD4 T
ESPN	3.99E-110	2.06091853	2.23E-105	CD4 T
RP11-345M22.2	7.40E-15	2.08409546	4.12E-10	CD4 T
LOXL1-AS1	1.23E-10	2.11364663	6.83E-06	CD4 T
PTPN14	5.42E-13	2.11912877	3.02E-08	CD4 T
ACVR2A	4.12E-30	2.15729764	2.30E-25	CD4 T
HSD11B1	3.72E-10	2.19022463	2.07E-05	CD4 T
CHRM3-AS2	3.63E-41	2.20852178	2.03E-36	CD4 T
MFHAS1	3.16E-50	2.21278157	1.76E-45	CD4 T
RPS20P22	1.22E-09	2.22024551	6.79E-05	CD4 T
LIF	4.44E-12	2.22319669	2.48E-07	CD4 T
RP11-350N15.4	5.34E-19	2.22372549	2.98E-14	CD4 T
LINC00402	4.53E-17	2.29576857	2.52E-12	CD4 T
RP11-403A21.2	4.66E-16	2.31640015	2.60E-11	CD4 T
SLC28A3	1.53E-09	2.31875719	8.53E-05	CD4 T
CCR4	7.19E-88	2.32597981	4.01E-83	CD4 T
RP11-15M15.1	5.72E-12	2.35032572	3.19E-07	CD4 T
RORC	5.66E-10	2.37144055	3.16E-05	CD4 T
LEF1	6.30E-105	2.38965491	3.51E-100	CD4 T
RASGRF2	1.31E-30	2.44547935	7.33E-26	CD4 T
BTBD11	1.26E-21	2.47410368	7.01E-17	CD4 T
RP4-781K5.8	2.40E-10	2.52005532	1.33E-05	CD4 T
ZG16B	2.71E-11	2.55228386	1.51E-06	CD4 T
FHL1	7.48E-24	2.55362225	4.17E-19	CD4 T
RP11-513O17.2	5.58E-10	2.56222729	3.11E-05	CD4 T
LYPD3	4.21E-17	2.57534957	2.35E-12	CD4 T
TRABD2A	1.09E-68	2.59003717	6.07E-64	CD4 T
AC006042.6	2.57E-19	2.60330366	1.43E-14	CD4 T
AC020571.3	3.51E-31	2.61305722	1.96E-26	CD4 T
SHISA2	6.82E-13	2.61810566	3.80E-08	CD4 T
CHGB	9.96E-10	2.62401116	5.55E-05	CD4 T

ARL4P	2.67E-11	2.73216687	1.49E-06	CD4 T
MAL	3.50E-91	2.74267797	1.95E-86	CD4 T
RP11-345M22.1	8.40E-26	2.76072941	4.68E-21	CD4 T
FBLN7	1.87E-87	2.7979501	1.04E-82	CD4 T
KIAA1217	3.26E-13	2.85463151	1.82E-08	CD4 T
PLAT	3.86E-42	2.85647084	2.15E-37	CD4 T
NTRK2	2.52E-20	2.89290589	1.40E-15	CD4 T
TUBA3D	2.68E-11	2.90412141	1.49E-06	CD4 T
PTPN3	8.72E-22	3.00671092	4.86E-17	CD4 T
CACNA1I	3.37E-14	3.07544929	1.88E-09	CD4 T
VSIG1	2.77E-12	3.12980401	1.54E-07	CD4 T
RP5-1158E12.3	1.15E-56	3.27814133	6.39E-52	CD4 T
CSF2	2.83E-34	3.28728171	1.58E-29	CD4 T
IL21-AS1	2.00E-45	3.41538682	1.11E-40	CD4 T
RFX8	2.19E-10	3.44167894	1.22E-05	CD4 T
PI16	3.75E-10	3.448339	2.09E-05	CD4 T
LINC00892	1.93E-107	3.5635943	1.07E-102	CD4 T
PTPN13	3.02E-137	3.7268807	1.68E-132	CD4 T
CD40LG	7.97E-272	3.7638295	4.44E-267	CD4 T
IL2	6.22E-24	3.89681813	3.47E-19	CD4 T
IL21	4.34E-72	4.02203619	2.42E-67	CD4 T
ANKRD55	4.96E-34	4.02821134	2.76E-29	CD4 T
CDO1	2.56E-12	4.7719722	1.43E-07	CD4 T
RP11-554D20.1	3.45E-12	4.86229477	1.92E-07	CD4 T
IGFL2	1.87E-44	5.03075545	1.04E-39	CD4 T
NEFL	4.98E-11	5.09034855	2.78E-06	CD4 T
PVALB	3.96E-16	5.23895968	2.21E-11	CD4 T
ADAM23	4.28E-21	5.48342827	2.38E-16	CD4 T
KRT1	4.04E-16	5.62938246	2.25E-11	CD4 T
TRAV30	3.96E-11	2.03400323	2.20E-06	CD8 T
TRBV4-2	5.79E-32	2.08718645	3.23E-27	CD8 T
GZMH	1.21E-280	2.10515295	6.75E-276	CD8 T
KLRC4	3.62E-164	2.11029621	2.02E-159	CD8 T
STYK1	9.37E-14	2.11065254	5.22E-09	CD8 T
RP11-328K2.1	7.26E-12	2.12597719	4.05E-07	CD8 T
RYR2	5.49E-13	2.12837798	3.06E-08	CD8 T
ANAPC1P1	1.09E-14	2.13253619	6.07E-10	CD8 T
GLDCP1	8.18E-15	2.1708189	4.56E-10	CD8 T
ITGAD	4.38E-16	2.17526933	2.44E-11	CD8 T
TRBV9	1.87E-41	2.18162925	1.04E-36	CD8 T
TRBV4-1	3.35E-16	2.18522613	1.87E-11	CD8 T
ITGA2	3.34E-38	2.20123592	1.86E-33	CD8 T

TRBV27	2.22E-34	2.20187954	1.24E-29	CD8 T
AC069363.1	4.30E-112	2.22054216	2.40E-107	CD8 T
HMGB3P32	2.34E-11	2.2959855	1.31E-06	CD8 T
RP11-146I2.1	5.68E-10	2.37739697	3.16E-05	CD8 T
TRAV12-2	1.08E-35	2.40562387	6.01E-31	CD8 T
TRAV24	1.80E-18	2.4470285	1.00E-13	CD8 T
RP11-291B21.2	1.22E-154	2.4577782	6.78E-150	CD8 T
LINC00158	5.91E-24	2.46876759	3.30E-19	CD8 T
RP11-383H13.1	4.14E-25	2.47518145	2.31E-20	CD8 T
AC131056.3	2.38E-27	2.5178045	1.32E-22	CD8 T
VCAM1	3.42E-186	2.55900814	1.91E-181	CD8 T
KIR2DL4	3.39E-107	2.65407777	1.89E-102	CD8 T
RP11-493L12.5	5.05E-33	2.67942511	2.82E-28	CD8 T
TNFSF4	4.18E-60	2.78236202	2.33E-55	CD8 T
ETV1	1.53E-89	2.80787871	8.52E-85	CD8 T
RP11-493L12.6	6.03E-16	2.84862286	3.36E-11	CD8 T
CTD-2288O8.1	4.76E-15	2.96760948	2.65E-10	CD8 T
PON3	6.01E-10	3.04772058	3.35E-05	CD8 T
TRAV1-2	8.20E-36	3.18099337	4.57E-31	CD8 T
AP000233.4	1.13E-26	3.23113924	6.29E-22	CD8 T
SH3BGRL2	4.37E-33	3.23334395	2.44E-28	CD8 T
RP11-109E24.1	5.62E-25	3.42931431	3.13E-20	CD8 T
CD8A	0	3.68658774	0	CD8 T
CD8B	0	3.89470268	0	CD8 T
CD8BP	3.42E-280	3.91217691	1.91E-275	CD8 T
MAOB	5.28E-11	4.59585668	2.94E-06	CD8 T
FAM49A	6.75E-173	2.00178935	3.76E-168	DC
SCRN1	2.20E-44	2.00318248	1.23E-39	DC
SPG20	1.25E-82	2.00320544	6.99E-78	DC
AMPD2	8.43E-148	2.00430685	4.70E-143	DC
SNX10	2.95E-123	2.00491841	1.64E-118	DC
KLF11	2.06E-24	2.0060036	1.15E-19	DC
DPYSL2	2.43E-197	2.00711525	1.36E-192	DC
ZNF839P1	6.07E-13	2.01340852	3.38E-08	DC
TOMM40L	9.45E-37	2.01654389	5.27E-32	DC
DFNA5	3.96E-13	2.01745863	2.21E-08	DC
IL18BP	5.73E-122	2.01941463	3.19E-117	DC
MFI2	1.23E-13	2.02366125	6.83E-09	DC
SPINT2	8.29E-145	2.02447442	4.62E-140	DC
SOD2	8.21E-184	2.02658939	4.58E-179	DC
RN7SL402P	2.05E-23	2.02860779	1.14E-18	DC
DEXI	3.65E-85	2.0310723	2.03E-80	DC

TMX2-CTNND1	3.61E-22	2.03286631	2.01E-17	DC
NAGK	8.40E-173	2.03382163	4.68E-168	DC
NCF1	1.89E-177	2.03846767	1.06E-172	DC
DPEP2	7.41E-68	2.04278693	4.13E-63	DC
SLC25A37	1.47E-151	2.04325934	8.18E-147	DC
BTK	2.54E-121	2.0444846	1.41E-116	DC
HES4	1.41E-14	2.04493295	7.86E-10	DC
TNFRSF1A	4.04E-201	2.04530498	2.25E-196	DC
BCO2	7.78E-15	2.04717032	4.34E-10	DC
TANC2	4.74E-36	2.04801027	2.64E-31	DC
HTATSF1P2	3.52E-21	2.05184865	1.96E-16	DC
RIPK2	2.85E-210	2.05278625	1.59E-205	DC
ARSB	9.30E-129	2.05413351	5.18E-124	DC
GAPT	2.15E-44	2.05509534	1.20E-39	DC
MPZL1	4.82E-64	2.06055159	2.68E-59	DC
GNS	3.46E-221	2.06173751	1.93E-216	DC
PRKACA	1.61E-75	2.0621266	8.96E-71	DC
SH2B3	7.25E-154	2.06324942	4.04E-149	DC
SESTD1	1.11E-37	2.06360245	6.20E-33	DC
TTC7B	2.39E-13	2.06521281	1.33E-08	DC
SCARB2	3.40E-112	2.06767727	1.89E-107	DC
CORO1C	1.51E-179	2.07442011	8.39E-175	DC
ROGDI	1.58E-65	2.07563676	8.78E-61	DC
KIFC3	1.44E-37	2.08059231	8.04E-33	DC
SLC16A5	1.28E-39	2.08128906	7.11E-35	DC
FTH1P12	1.01E-163	2.08536698	5.65E-159	DC
RP11-400F19.18	1.13E-18	2.08582899	6.29E-14	DC
PTK2	1.13E-55	2.0869561	6.33E-51	DC
HLA-DMB	4.87E-244	2.08827697	2.71E-239	DC
RAB3D	7.94E-57	2.08850338	4.43E-52	DC
PLA2G15	1.40E-46	2.09060729	7.82E-42	DC
P4HA2	1.46E-17	2.09071007	8.15E-13	DC
AP1S2	4.53E-213	2.09475507	2.52E-208	DC
HSPA6	1.15E-163	2.09714431	6.43E-159	DC
RP4-673M15.1	5.49E-10	2.09853112	3.06E-05	DC
PLOD1	3.16E-71	2.09972831	1.76E-66	DC
AC009093.1	9.28E-13	2.1002161	5.17E-08	DC
GAPDHP46	2.45E-12	2.10084804	1.37E-07	DC
THEMIS2	6.64E-263	2.10105696	3.70E-258	DC
RHOQ	8.32E-87	2.10440687	4.64E-82	DC
ITGA7	3.70E-13	2.10520699	2.06E-08	DC
TTYH3	1.01E-167	2.10594765	5.64E-163	DC

TRIM36-IT1	2.72E-10	2.10608154	1.52E-05	DC
RP11-254F7.2	5.00E-18	2.10676198	2.79E-13	DC
CCDC147-AS1	2.73E-10	2.10759914	1.52E-05	DC
CDH13	8.54E-10	2.109011	4.76E-05	DC
PHLDB1	4.55E-28	2.11280686	2.53E-23	DC
RP11-295K3.1	2.24E-14	2.11298298	1.25E-09	DC
CTIF	2.86E-20	2.1144234	1.59E-15	DC
C9orf72	1.37E-251	2.11603856	7.64E-247	DC
IL3RA	1.99E-80	2.11778789	1.11E-75	DC
CTC-510F12.6	1.20E-52	2.12238204	6.66E-48	DC
SPG21	6.14E-138	2.1236862	3.42E-133	DC
RP11-11N9.4	1.18E-09	2.12424489	6.59E-05	DC
RP4-798P15.3	1.63E-13	2.12734646	9.10E-09	DC
AFMID	2.25E-124	2.12837418	1.25E-119	DC
ALPK1	4.12E-83	2.13855004	2.30E-78	DC
DISC1-IT1	1.64E-09	2.13952389	9.15E-05	DC
FAM214B	9.71E-64	2.14100467	5.41E-59	DC
AKT1S1	7.42E-42	2.14604725	4.14E-37	DC
CD80	1.73E-49	2.14653084	9.65E-45	DC
CTD-2353F22.1	9.77E-22	2.14713884	5.45E-17	DC
RBMS2	2.51E-31	2.14879948	1.40E-26	DC
SCARB1	1.05E-56	2.15106287	5.85E-52	DC
RP11-333E1.1	3.27E-41	2.15250745	1.82E-36	DC
ASAH1	4.12E-236	2.15511917	2.29E-231	DC
PTGR1	1.04E-10	2.15634257	5.79E-06	DC
SLC12A7	1.20E-106	2.15757907	6.69E-102	DC
LAT2	7.44E-208	2.1583956	4.15E-203	DC
RP11-737O24.5	6.20E-21	2.15919881	3.46E-16	DC
RP11-69H7.3	3.16E-12	2.15992979	1.76E-07	DC
TMEM88	2.44E-30	2.16137805	1.36E-25	DC
PTPN12	3.92E-92	2.16461452	2.18E-87	DC
MYO15B	2.18E-100	2.16479908	1.21E-95	DC
TMED7-TICAM2	7.21E-19	2.16515187	4.02E-14	DC
SLC2A6	1.96E-85	2.17004161	1.09E-80	DC
FRY	2.70E-45	2.17060902	1.50E-40	DC
PLXND1	2.15E-154	2.17446186	1.20E-149	DC
TNFRSF10D	1.10E-56	2.17471457	6.15E-52	DC
ZBED3	2.56E-15	2.17548885	1.43E-10	DC
RP11-1198D22.3	1.25E-29	2.17993497	6.94E-25	DC
RP1-90J20.11	1.17E-12	2.18144947	6.50E-08	DC
TSHZ3	2.33E-11	2.18174075	1.30E-06	DC
RHEBP2	1.08E-30	2.18360566	6.01E-26	DC

XXbac-BPG181M17.5	2.08E-177	2.18400429	1.16E-172	DC
RP1-90J20.12	3.02E-28	2.18535066	1.68E-23	DC
S100B	8.93E-39	2.18915695	4.98E-34	DC
RNU2-59P	1.17E-75	2.19105245	6.53E-71	DC
CLIC4	2.42E-101	2.19256408	1.35E-96	DC
NCEH1	6.27E-58	2.19437121	3.49E-53	DC
PDCD1LG2	2.20E-30	2.19955226	1.23E-25	DC
ENG	9.68E-143	2.20192887	5.39E-138	DC
GUCY1A3	1.00E-17	2.20248733	5.60E-13	DC
GPX1P1	4.90E-169	2.20274943	2.73E-164	DC
CTBP2	5.20E-56	2.20279607	2.90E-51	DC
RCAN1	3.69E-21	2.20285168	2.06E-16	DC
RP11-417F21.1	7.13E-55	2.20349699	3.98E-50	DC
TCEA3	3.06E-20	2.20590207	1.71E-15	DC
IL15	8.04E-81	2.20732119	4.48E-76	DC
CCSER1	3.53E-35	2.20928026	1.96E-30	DC
TIMM8BP2	1.68E-13	2.21187924	9.37E-09	DC
LACC1	2.18E-49	2.21383348	1.22E-44	DC
ZGLP1	1.38E-18	2.21545772	7.68E-14	DC
AC026310.1	2.66E-12	2.21592639	1.48E-07	DC
OLFML3	2.18E-20	2.21632032	1.21E-15	DC
AP000240.9	1.71E-23	2.21679768	9.53E-19	DC
CCL22	1.51E-14	2.21743977	8.42E-10	DC
RP11-254F7.3	1.47E-25	2.2178101	8.20E-21	DC
MBOAT2	3.85E-12	2.22517925	2.15E-07	DC
CTD-2562J15.6	3.62E-10	2.2274541	2.02E-05	DC
KRT8P46	5.92E-27	2.22960671	3.30E-22	DC
RP11-76E17.3	2.56E-13	2.22988454	1.43E-08	DC
NCF1C	5.67E-209	2.23275704	3.16E-204	DC
PLD4	3.09E-99	2.2329504	1.72E-94	DC
GAL3ST4	1.70E-18	2.23685939	9.45E-14	DC
PALD1	4.61E-39	2.24138956	2.57E-34	DC
HILPDA	2.44E-30	2.24221571	1.36E-25	DC
RP11-54O7.17	1.08E-11	2.24671497	6.00E-07	DC
HLA-DRB9	1.50E-32	2.24800534	8.39E-28	DC
MFSD1	6.54E-259	2.24811459	3.65E-254	DC
CTD-2306M10.1	1.03E-09	2.24924871	5.76E-05	DC
CD300A	2.15E-221	2.25110515	1.20E-216	DC
RP11-10L12.2	1.63E-28	2.25325227	9.08E-24	DC
CD40	4.01E-159	2.25833806	2.24E-154	DC
MGAM	2.39E-14	2.25845021	1.33E-09	DC
SLC2A5	5.13E-41	2.25900176	2.86E-36	DC

PROCR	2.64E-14	2.25903044	1.47E-09	DC
LRRK1	2.26E-56	2.25926099	1.26E-51	DC
FLT1	6.12E-23	2.25982246	3.41E-18	DC
IRF5	9.13E-181	2.26054442	5.09E-176	DC
DENND1A	1.11E-148	2.26193807	6.19E-144	DC
RP11-356C4.5	7.27E-32	2.26447803	4.05E-27	DC
FGD6	6.61E-26	2.26560604	3.68E-21	DC
TSPAN33	7.47E-41	2.26656223	4.16E-36	DC
RNU2-61P	9.36E-45	2.26680713	5.22E-40	DC
RNF135	5.10E-137	2.26861683	2.84E-132	DC
RPS10-NUDT3	3.19E-30	2.2718565	1.78E-25	DC
SEMA3C	4.07E-20	2.27213631	2.27E-15	DC
NPC2	0	2.27336263	0	DC
ENPP2	1.21E-41	2.27851686	6.77E-37	DC
TUBB6	9.78E-100	2.28341168	5.45E-95	DC
TMCC3	3.27E-49	2.29286214	1.83E-44	DC
SAMD4A	1.34E-41	2.29396723	7.48E-37	DC
CACNA2D4	1.87E-62	2.29507813	1.04E-57	DC
GNB4	1.39E-79	2.29721299	7.77E-75	DC
OCRL	2.51E-22	2.30014814	1.40E-17	DC
SULT1A1	1.81E-61	2.3012122	1.01E-56	DC
CTD-3032J10.2	2.83E-13	2.30126551	1.58E-08	DC
TLN2	1.69E-09	2.3031022	9.40E-05	DC
GAS7	1.89E-122	2.30406803	1.05E-117	DC
CTD-2015H6.3	2.31E-10	2.30459019	1.29E-05	DC
IFITM10	8.27E-30	2.30490646	4.61E-25	DC
ASRGL1	6.05E-24	2.3056113	3.37E-19	DC
ROBO3	8.37E-38	2.30776893	4.66E-33	DC
NRP1	3.10E-56	2.30782441	1.73E-51	DC
SPECC1	4.11E-114	2.31162125	2.29E-109	DC
SERPINB6	1.06E-174	2.31529923	5.88E-170	DC
CTA-384D8.36	8.87E-75	2.31924092	4.94E-70	DC
CHRFAM7A	1.28E-15	2.32135952	7.16E-11	DC
IL6R	7.19E-154	2.32169319	4.01E-149	DC
ADAM15	1.11E-127	2.32762074	6.19E-123	DC
UNC93B1	6.24E-67	2.32922925	3.48E-62	DC
SCML1	5.64E-84	2.33066514	3.14E-79	DC
SOGA1	2.43E-78	2.33598513	1.35E-73	DC
CPQ	2.54E-133	2.33600838	1.42E-128	DC
GRASP	2.35E-163	2.34158243	1.31E-158	DC
BEST1	6.62E-262	2.34173869	3.69E-257	DC
FSTL3	9.67E-11	2.3421863	5.39E-06	DC

TBC1D9	7.86E-66	2.34220217	4.38E-61	DC
GPR133	6.28E-13	2.34471507	3.50E-08	DC
NADK	5.74E-155	2.34625689	3.20E-150	DC
TRPM2	4.85E-86	2.34695236	2.71E-81	DC
FTCDNL1	4.72E-26	2.34719344	2.63E-21	DC
TNFRSF11A	1.29E-21	2.35008766	7.18E-17	DC
CKB	1.40E-22	2.35012812	7.81E-18	DC
RCBTB2	2.32E-134	2.35208846	1.30E-129	DC
SMOX	3.39E-22	2.35224783	1.89E-17	DC
MMP9	4.57E-28	2.35332356	2.55E-23	DC
ARHGAP31	1.37E-117	2.35396797	7.65E-113	DC
STARD13	6.84E-33	2.355521	3.81E-28	DC
DOCK7	4.03E-48	2.3572192	2.25E-43	DC
NHSL2	2.62E-21	2.35912988	1.46E-16	DC
RP5-1160K1.6	3.04E-56	2.36153631	1.69E-51	DC
APOBR	5.67E-113	2.36629487	3.16E-108	DC
TNFRSF21	1.14E-66	2.36733772	6.33E-62	DC
PLBD2	1.48E-108	2.37179602	8.26E-104	DC
RP11-626G11.3	2.38E-79	2.37234343	1.33E-74	DC
STK3	1.69E-61	2.37388081	9.42E-57	DC
FSCN1	1.01E-83	2.37542532	5.63E-79	DC
CAMKK1	1.19E-37	2.37664079	6.65E-33	DC
ANXA2P1	5.81E-52	2.38047704	3.24E-47	DC
ZNF710	1.21E-106	2.38549373	6.74E-102	DC
TLR7	5.12E-82	2.38660701	2.85E-77	DC
GLB1L	3.79E-14	2.38722319	2.11E-09	DC
C4orf45	7.87E-13	2.38794214	4.39E-08	DC
BACH1-IT1	3.18E-28	2.38843194	1.77E-23	DC
AVPI1	8.03E-148	2.39057382	4.48E-143	DC
CUEDC1	1.19E-13	2.39107819	6.63E-09	DC
LSM3P2	3.61E-25	2.39309929	2.01E-20	DC
PRUNE2	4.73E-11	2.39364569	2.64E-06	DC
RP11-497H16.6	1.32E-50	2.39395333	7.35E-46	DC
C10orf128	6.56E-128	2.39455209	3.66E-123	DC
RP11-553A21.3	2.38E-11	2.3972622	1.33E-06	DC
DKFZP761J1410	7.40E-43	2.39936697	4.12E-38	DC
CTA-407F11.6	5.13E-10	2.39975289	2.86E-05	DC
PIPOX	2.62E-15	2.39982718	1.46E-10	DC
PPM1L	2.74E-26	2.40113443	1.53E-21	DC
MSRB2	1.33E-19	2.40245655	7.43E-15	DC
SNX24	5.05E-25	2.40587822	2.82E-20	DC
RP4-607J23.2	2.31E-12	2.40613925	1.29E-07	DC

NAPSB	4.85E-196	2.40667567	2.70E-191	DC
GRN	0	2.40770112	0	DC
ADRBK2	5.51E-166	2.40834985	3.07E-161	DC
OR5B21	4.36E-13	2.41311092	2.43E-08	DC
CTD-2369P2.5	2.95E-51	2.41495578	1.65E-46	DC
EPB41L2	2.01E-97	2.4160076	1.12E-92	DC
LAIR1	1.01E-218	2.41734035	5.64E-214	DC
MFSD2A	2.88E-45	2.41845396	1.61E-40	DC
ARHGAP26-AS1	2.84E-15	2.41887804	1.58E-10	DC
RP11-443B7.1	1.39E-10	2.42119279	7.72E-06	DC
SLC4A3	6.12E-18	2.42185403	3.41E-13	DC
AC005083.1	5.36E-22	2.42264772	2.99E-17	DC
PHC2	5.09E-95	2.42432438	2.84E-90	DC
CRISPLD2	3.35E-47	2.43123392	1.87E-42	DC
RN7SL798P	3.53E-61	2.43334458	1.97E-56	DC
GK-IT1	4.34E-32	2.43513232	2.42E-27	DC
SLC22A13	1.12E-13	2.43526353	6.26E-09	DC
SLC9A3R2	2.19E-11	2.43743183	1.22E-06	DC
RP11-347C12.10	2.43E-12	2.44008877	1.35E-07	DC
CDC42EP4	3.26E-38	2.44239202	1.82E-33	DC
RP11-667K14.3	8.36E-66	2.44474438	4.66E-61	DC
RP11-1149M10.2	2.90E-13	2.44919023	1.62E-08	DC
SMCO4	2.84E-158	2.44983046	1.58E-153	DC
PPP1R14A	3.31E-22	2.45177832	1.85E-17	DC
AC000003.2	1.15E-48	2.45231395	6.42E-44	DC
SORBS3	8.67E-104	2.45237825	4.83E-99	DC
STAC3	2.26E-18	2.4597472	1.26E-13	DC
GNAI1	1.45E-11	2.46291392	8.10E-07	DC
LTC4S	1.43E-25	2.46433071	7.95E-21	DC
RP11-10L12.1	3.87E-22	2.46805716	2.15E-17	DC
TLR6	1.48E-79	2.46810667	8.25E-75	DC
DNMBP	4.92E-64	2.46878617	2.74E-59	DC
ZEB2-AS1	1.72E-110	2.46944569	9.61E-106	DC
IL10	6.06E-72	2.47086392	3.38E-67	DC
RP11-1H15.1	1.75E-20	2.47431693	9.78E-16	DC
CCDC154	1.10E-20	2.47472147	6.16E-16	DC
ERMAP	2.45E-29	2.47514289	1.37E-24	DC
FGD2	0	2.47709985	0	DC
PPFIBP2	5.83E-81	2.48373035	3.25E-76	DC
FLI1-AS1	5.16E-19	2.48386155	2.88E-14	DC
HYAL2	2.63E-17	2.48772664	1.47E-12	DC
NEU4	1.30E-18	2.48853284	7.26E-14	DC

RILP	8.37E-32	2.49100585	4.67E-27	DC
AC079210.1	1.16E-19	2.49717161	6.48E-15	DC
CLDN7	4.48E-12	2.50722426	2.50E-07	DC
SPIRE1	3.48E-12	2.50938472	1.94E-07	DC
ITGA5	1.34E-225	2.51131986	7.44E-221	DC
RP3-522P13.1	1.03E-12	2.51254226	5.71E-08	DC
OPN3	1.32E-36	2.51268987	7.34E-32	DC
TICAM2	2.32E-41	2.51332242	1.29E-36	DC
MRVI1-AS1	4.48E-14	2.51606809	2.50E-09	DC
NRIP3	2.16E-38	2.51651741	1.21E-33	DC
ZNF358	1.37E-21	2.52503001	7.66E-17	DC
HEBP1	8.16E-84	2.52521008	4.55E-79	DC
LY96	5.02E-146	2.52787316	2.80E-141	DC
VASH1	1.65E-86	2.52893302	9.18E-82	DC
ZNF618	1.77E-27	2.52912109	9.88E-23	DC
RP11-108M9.4	2.98E-59	2.53033505	1.66E-54	DC
AF213884.2	1.87E-12	2.53185701	1.04E-07	DC
CFB	2.35E-30	2.53414034	1.31E-25	DC
FAM71A	3.21E-19	2.53429666	1.79E-14	DC
CSF2RB	1.99E-183	2.53533753	1.11E-178	DC
TSPAN15	2.38E-20	2.5367641	1.33E-15	DC
GLUL	0	2.5405248	0	DC
RP11-145M9.4	3.17E-50	2.54755689	1.76E-45	DC
VPS37C	3.34E-79	2.54771548	1.86E-74	DC
FTLP2	2.56E-152	2.54920271	1.43E-147	DC
SECTM1	2.94E-125	2.5497186	1.64E-120	DC
TMEM119	4.14E-13	2.55018235	2.31E-08	DC
SLC31A1	1.74E-135	2.55185018	9.70E-131	DC
ATF5	6.18E-133	2.55343791	3.44E-128	DC
BCAT1	1.44E-117	2.55965223	8.02E-113	DC
CCND1	4.10E-40	2.56370657	2.29E-35	DC
CTD-2587H19.1	2.67E-23	2.56715041	1.49E-18	DC
SLC40A1	3.11E-38	2.56750644	1.73E-33	DC
RP11-603J24.7	3.92E-40	2.56797522	2.18E-35	DC
EEPD1	2.54E-46	2.56936835	1.41E-41	DC
FCGR3A	7.99E-264	2.57223421	4.45E-259	DC
MCOLN1	3.28E-145	2.57400033	1.83E-140	DC
HESX1	5.38E-12	2.5820639	3.00E-07	DC
FBLN2	4.44E-12	2.58533032	2.48E-07	DC
TRIM36	5.49E-20	2.59502549	3.06E-15	DC
ICAM4	4.60E-26	2.59537383	2.56E-21	DC
RP11-295G20.2	4.04E-29	2.60034953	2.25E-24	DC

TBC1D8	1.34E-117	2.60225409	7.46E-113	DC
EFNB1	2.63E-23	2.60545659	1.47E-18	DC
GPX1P2	7.98E-25	2.60750776	4.45E-20	DC
NCKAP5L	2.32E-169	2.60828629	1.29E-164	DC
ACTN1	6.55E-73	2.60870463	3.65E-68	DC
PSD3	2.51E-20	2.61362059	1.40E-15	DC
LRRC37A15P	5.20E-47	2.61393111	2.90E-42	DC
STX3	1.73E-53	2.61439646	9.62E-49	DC
GPR34	4.57E-66	2.61585459	2.55E-61	DC
DPRXP4	5.43E-12	2.61900456	3.03E-07	DC
MPZL2	7.36E-13	2.62044221	4.10E-08	DC
AC067852.1	8.11E-31	2.62160354	4.52E-26	DC
EEF1DP3	2.21E-22	2.622085	1.23E-17	DC
RP4-535B20.4	8.32E-16	2.62266538	4.64E-11	DC
RENBP	4.14E-40	2.62575958	2.31E-35	DC
ATP6V0A1	2.24E-163	2.62582357	1.25E-158	DC
TNFAIP8L2	7.15E-113	2.62676537	3.98E-108	DC
GLT1D1	1.10E-20	2.62926817	6.14E-16	DC
LINC00937	5.99E-33	2.62971363	3.34E-28	DC
SIRPB1	2.85E-171	2.63333487	1.59E-166	DC
RP11-863P13.3	1.12E-12	2.63418899	6.26E-08	DC
GRINA	6.10E-287	2.6445842	3.40E-282	DC
ADAMDEC1	3.64E-19	2.64669205	2.03E-14	DC
FAM110B	2.03E-26	2.64834503	1.13E-21	DC
ADAMTSL4	8.63E-210	2.65260275	4.81E-205	DC
EMR1	5.33E-34	2.65353104	2.97E-29	DC
GPER1	1.02E-19	2.65389608	5.70E-15	DC
GPR141	1.74E-63	2.65724742	9.70E-59	DC
JHDM1D-AS1	1.87E-24	2.65969882	1.04E-19	DC
DNAJB5	6.09E-27	2.66407967	3.39E-22	DC
CTSH	0	2.66626144	0	DC
OSM	1.64E-116	2.66919557	9.11E-112	DC
NLN	7.27E-25	2.67237145	4.05E-20	DC
RP11-83B20.1	1.17E-15	2.67436839	6.52E-11	DC
CCDC112	9.21E-68	2.67789465	5.13E-63	DC
HMOX1	1.70E-177	2.68163895	9.45E-173	DC
HS3ST1	1.52E-47	2.68618305	8.47E-43	DC
DST	3.47E-95	2.69252799	1.94E-90	DC
ACSL1	6.48E-283	2.69285845	3.61E-278	DC
CRYBG3	7.01E-97	2.69321384	3.91E-92	DC
GNAQP1	9.31E-24	2.6983744	5.19E-19	DC
RP11-638I2.10	5.23E-193	2.69877644	2.92E-188	DC

GLULP4	9.84E-28	2.70003767	5.49E-23	DC
TNFSF15	4.06E-15	2.70232412	2.26E-10	DC
CD180	2.56E-101	2.70352248	1.43E-96	DC
RP11-268J15.5	2.36E-22	2.70775309	1.31E-17	DC
RP11-488C13.6	4.19E-10	2.70835383	2.33E-05	DC
DOK3	2.97E-153	2.71094573	1.66E-148	DC
CHN2	5.06E-162	2.7124555	2.82E-157	DC
PRKCDBP	1.06E-26	2.71345197	5.89E-22	DC
UACA	2.87E-31	2.71440744	1.60E-26	DC
PRKCD	3.27E-176	2.71574982	1.82E-171	DC
NRARP	1.10E-42	2.71660875	6.16E-38	DC
RP1-257A7.4	1.44E-45	2.7197001	8.00E-41	DC
PPARGC1B	1.21E-70	2.72669952	6.73E-66	DC
RP11-8H2.1	6.02E-12	2.7309232	3.35E-07	DC
ACER3	3.05E-145	2.73117038	1.70E-140	DC
FCGR3B	2.54E-233	2.7325524	1.41E-228	DC
WDR49	9.51E-11	2.7394208	5.30E-06	DC
FRRS1	4.09E-13	2.73978306	2.28E-08	DC
CNFN	9.44E-20	2.74094537	5.26E-15	DC
DGKG	1.05E-29	2.74284058	5.85E-25	DC
CCR1	7.33E-185	2.74373112	4.09E-180	DC
REPS2	1.08E-10	2.74460861	6.04E-06	DC
C5orf20	2.09E-20	2.75112466	1.16E-15	DC
RP11-38L15.8	9.38E-23	2.75248348	5.23E-18	DC
LYNX1	2.43E-16	2.75257028	1.36E-11	DC
PLEKHG6	4.68E-22	2.75371186	2.61E-17	DC
RXRA	1.09E-151	2.75489964	6.06E-147	DC
MLTK	8.91E-83	2.75717264	4.96E-78	DC
ANG	1.67E-23	2.76161817	9.29E-19	DC
MPP1	2.02E-243	2.76275456	1.13E-238	DC
RP11-1334A24.6	3.58E-76	2.76540539	1.99E-71	DC
PLA2G2D	3.31E-12	2.76613938	1.85E-07	DC
GNAQ	2.14E-166	2.76977386	1.19E-161	DC
TENM4	4.30E-19	2.77169978	2.40E-14	DC
AC009892.10	2.38E-12	2.7725273	1.33E-07	DC
AK4P1	1.17E-31	2.77255211	6.50E-27	DC
LINC00085	5.23E-26	2.7793031	2.91E-21	DC
RP11-732A19.5	9.49E-11	2.77965706	5.29E-06	DC
MGST2	8.42E-150	2.77995207	4.69E-145	DC
RXFP4	7.69E-12	2.78098418	4.28E-07	DC
PELI2	3.53E-57	2.78098751	1.97E-52	DC
SCHIP1	1.20E-09	2.78337204	6.70E-05	DC

IL1RAP	9.72E-100	2.78713898	5.42E-95	DC
RP11-414H17.5	3.84E-14	2.79045363	2.14E-09	DC
ZBTB47	1.32E-25	2.79095918	7.37E-21	DC
DGAT2	4.16E-24	2.79113798	2.32E-19	DC
CPPED1	2.42E-226	2.79216102	1.35E-221	DC
GCA	3.79E-220	2.79284986	2.11E-215	DC
AP003774.4	4.39E-10	2.79517745	2.45E-05	DC
CTD-2267D19.2	8.39E-42	2.79927507	4.68E-37	DC
ULK4P2	1.62E-23	2.8001534	9.03E-19	DC
HAL	1.97E-11	2.80073945	1.10E-06	DC
LONRF3	1.73E-78	2.80688596	9.64E-74	DC
GAA	1.22E-299	2.8086737	6.78E-295	DC
SYK	0	2.80951056	0	DC
FP15737	7.47E-52	2.8096655	4.16E-47	DC
SBF2	1.55E-141	2.80969018	8.64E-137	DC
RN7SKP78	4.42E-43	2.81170101	2.46E-38	DC
RP11-834C11.4	9.07E-16	2.8124058	5.06E-11	DC
PTPRO	3.11E-46	2.81580567	1.73E-41	DC
CTD-2583P5.3	7.91E-15	2.81846506	4.41E-10	DC
CTD-2033D15.1	3.64E-16	2.82209798	2.03E-11	DC
CDK2AP1	5.15E-65	2.82238281	2.87E-60	DC
CTB-83J4.1	5.60E-13	2.82269367	3.12E-08	DC
DRAM1	2.18E-172	2.82340404	1.21E-167	DC
SERPINF2	2.27E-42	2.82488763	1.26E-37	DC
SULF2	2.76E-226	2.82511011	1.54E-221	DC
PTGIR	6.77E-60	2.82902193	3.77E-55	DC
PAK1	2.92E-282	2.83112145	1.63E-277	DC
RP11-289H16.1	4.64E-22	2.83124886	2.58E-17	DC
PRSS36	1.53E-33	2.83318465	8.55E-29	DC
TMEM255A	2.25E-11	2.83353656	1.26E-06	DC
CTD-2616J11.3	7.81E-20	2.83465301	4.35E-15	DC
NR1H3	5.15E-68	2.8353829	2.87E-63	DC
INSR	2.15E-189	2.83650715	1.20E-184	DC
BCL2L14	4.39E-38	2.8365307	2.44E-33	DC
RNASE4	8.79E-24	2.84047514	4.90E-19	DC
RP11-261C10.5	3.16E-11	2.8409597	1.76E-06	DC
SMPDL3A	6.53E-59	2.84227016	3.64E-54	DC
LINC01023	1.17E-18	2.8422786	6.50E-14	DC
AC097461.4	3.87E-18	2.8425541	2.16E-13	DC
SGK1	4.41E-293	2.84903335	2.46E-288	DC
CYSLTR2	3.27E-62	2.85226308	1.82E-57	DC
RP11-876N24.4	2.51E-19	2.85343	1.40E-14	DC

ULK4P3	7.40E-21	2.85459555	4.13E-16	DC
IMPA2	2.98E-33	2.85666872	1.66E-28	DC
BCL2A1	0	2.85679722	0	DC
DUSP3	3.78E-211	2.85759887	2.10E-206	DC
ASCL2	6.02E-27	2.85901667	3.35E-22	DC
GAB2	5.25E-201	2.85994883	2.93E-196	DC
MGLL	4.28E-116	2.86099009	2.39E-111	DC
OTOA	1.06E-16	2.86169068	5.91E-12	DC
LGMN	5.97E-200	2.86264194	3.33E-195	DC
LINC00984	2.24E-48	2.86432089	1.25E-43	DC
PDGFB	1.08E-68	2.87031717	6.00E-64	DC
ACKR3	1.09E-18	2.87085699	6.07E-14	DC
RP11-8L8.2	3.70E-30	2.87170412	2.06E-25	DC
PVR	9.74E-54	2.87243563	5.43E-49	DC
CPM	7.59E-152	2.8768731	4.23E-147	DC
SMAD6	1.63E-12	2.87983352	9.10E-08	DC
LINC00936	1.41E-116	2.88222998	7.85E-112	DC
AL031602.1	6.75E-13	2.88263213	3.76E-08	DC
MT1G	4.87E-15	2.88323558	2.71E-10	DC
RP1-257A7.5	4.35E-298	2.884222	2.42E-293	DC
CALCRL	8.49E-41	2.8863695	4.73E-36	DC
CREG1	7.60E-261	2.88976634	4.23E-256	DC
BASP1	2.24E-80	2.89009956	1.25E-75	DC
UGGT2	1.64E-29	2.89746592	9.15E-25	DC
FAM127C	2.30E-10	2.90313128	1.28E-05	DC
FRMD3	4.42E-21	2.90358174	2.46E-16	DC
ACVR1B	1.07E-53	2.90549209	5.98E-49	DC
PIWIL4	6.06E-16	2.90665564	3.38E-11	DC
RN7SL698P	3.27E-15	2.90884087	1.83E-10	DC
PIK3R6	1.81E-94	2.90963532	1.01E-89	DC
LINC00884	6.50E-44	2.91144886	3.62E-39	DC
WBP5	1.79E-51	2.91146236	9.97E-47	DC
XCR1	3.62E-16	2.91556825	2.02E-11	DC
RP1-266L20.2	1.70E-09	2.91845416	9.50E-05	DC
RP11-272L13.2	1.73E-09	2.91862901	9.65E-05	DC
OGFRL1	2.10E-137	2.92416483	1.17E-132	DC
TP53I3	5.74E-42	2.92434415	3.20E-37	DC
CLIP2	2.64E-51	2.92452814	1.47E-46	DC
DNAJC5B	4.08E-26	2.92912507	2.27E-21	DC
HMGB3P9	4.82E-10	2.93027339	2.69E-05	DC
RP11-452H21.4	2.51E-18	2.93164073	1.40E-13	DC
LYN	0	2.93839887	0	DC

MOB3B	3.60E-115	2.93981788	2.00E-110	DC
AP001053.11	3.47E-11	2.94271857	1.93E-06	DC
PSTPIP2	7.05E-221	2.94370929	3.93E-216	DC
U52111.14	3.12E-11	2.94473348	1.74E-06	DC
FKBP9	2.23E-42	2.94810337	1.24E-37	DC
TBXAS1	0	2.95224845	0	DC
CLEC11A	1.46E-68	2.95686029	8.15E-64	DC
CCRL2	1.74E-190	2.95823825	9.70E-186	DC
CTD-2653D5.1	7.18E-18	2.95951842	4.00E-13	DC
RP11-368J21.3	2.92E-27	2.96105345	1.63E-22	DC
LATS2	6.69E-62	2.96374809	3.73E-57	DC
P2RY6	2.14E-100	2.96968818	1.19E-95	DC
GATM	1.32E-63	2.97782852	7.34E-59	DC
PALLD	1.65E-73	2.98061534	9.21E-69	DC
CLCN1	6.77E-11	2.98291618	3.77E-06	DC
DOCK5	0	2.98471549	0	DC
H1F0	5.92E-109	2.98573761	3.30E-104	DC
FAM151B	1.14E-25	2.98623424	6.35E-21	DC
F2RL1	1.76E-12	2.9863726	9.80E-08	DC
JUP	1.07E-83	2.98789661	5.99E-79	DC
CPED1	5.87E-55	2.98792368	3.27E-50	DC
ITGAX	0	2.9895831	0	DC
CAHM	2.24E-16	2.99220024	1.25E-11	DC
HRH2	1.87E-107	2.99635415	1.04E-102	DC
TLR1	6.75E-143	2.99676757	3.76E-138	DC
CLMN	7.04E-90	3.00120613	3.92E-85	DC
RP11-1415C14.2	2.23E-77	3.00478509	1.24E-72	DC
RP11-1415C14.1	2.23E-77	3.00478509	1.24E-72	DC
CEBPB	0	3.00613442	0	DC
ELAVL4	2.11E-14	3.00856403	1.18E-09	DC
RP11-102N12.3	8.69E-20	3.01115911	4.84E-15	DC
HIF1A-AS2	5.33E-44	3.01176697	2.97E-39	DC
AC011515.2	7.43E-12	3.01241143	4.14E-07	DC
RHOQP2	6.91E-11	3.01410691	3.85E-06	DC
BTBD3	6.45E-16	3.01538956	3.60E-11	DC
CNRIP1	1.69E-10	3.01819691	9.41E-06	DC
PPARG	5.67E-40	3.02050556	3.16E-35	DC
ECHDC3	1.10E-14	3.02228036	6.15E-10	DC
CDKN1C	1.74E-28	3.02235963	9.67E-24	DC
ABL2	2.08E-153	3.02531674	1.16E-148	DC
CTTNBP2NL	4.38E-167	3.02537081	2.44E-162	DC
RP11-408H1.3	2.25E-11	3.03061516	1.25E-06	DC

FCGR2B	4.88E-258	3.03195492	2.72E-253	DC
TMEM132A	7.21E-15	3.03507275	4.02E-10	DC
SCN1B	8.27E-32	3.040833	4.61E-27	DC
RP11-446E9.2	2.50E-15	3.04754071	1.39E-10	DC
PDPN	1.24E-09	3.05270847	6.90E-05	DC
RPL32P26	2.23E-11	3.05293855	1.24E-06	DC
LACTB	2.79E-116	3.06127497	1.55E-111	DC
FAM20A	2.03E-79	3.06239292	1.13E-74	DC
PHACTR1	0	3.06719147	0	DC
CHST15	2.63E-171	3.06722591	1.47E-166	DC
RP11-342D11.2	5.40E-13	3.06907238	3.01E-08	DC
BRI3	2.80E-189	3.06977495	1.56E-184	DC
BLVRB	2.33E-285	3.08448686	1.30E-280	DC
SH2B2	1.13E-37	3.08723757	6.29E-33	DC
HLA-DPA2	3.22E-17	3.08802311	1.80E-12	DC
KCTD15	9.58E-14	3.0916149	5.34E-09	DC
FRY-AS1	2.45E-11	3.1001267	1.37E-06	DC
CCDC88A	4.05E-304	3.10098822	2.26E-299	DC
RP11-219E7.1	3.08E-15	3.10209589	1.72E-10	DC
PGA3	1.00E-15	3.1025421	5.60E-11	DC
IGSF21	3.25E-11	3.10299058	1.81E-06	DC
RAB13	2.97E-93	3.10650703	1.66E-88	DC
CD1A	2.15E-20	3.10766822	1.20E-15	DC
ITGAM	0	3.10855622	0	DC
DENND5A	0	3.10924688	0	DC
GLDN	1.06E-34	3.11114065	5.92E-30	DC
APBA1	6.49E-21	3.11258108	3.62E-16	DC
FLVCR2	8.44E-120	3.11540098	4.71E-115	DC
PRKAG2-AS1	1.19E-75	3.11663603	6.62E-71	DC
UNC13B	2.20E-11	3.11713117	1.23E-06	DC
DOCK1	4.43E-37	3.11929207	2.47E-32	DC
GBGT1	6.28E-99	3.12147896	3.50E-94	DC
CTNND1	0	3.12148969	0	DC
ULK4P1	1.73E-21	3.12352128	9.66E-17	DC
ADAM9	4.89E-205	3.13480661	2.73E-200	DC
CTTNBP2	8.21E-16	3.13807287	4.58E-11	DC
CTD-2369P2.8	5.75E-123	3.14258073	3.21E-118	DC
AP005530.2	1.44E-11	3.1429865	8.03E-07	DC
RAB34	5.96E-179	3.14392853	3.32E-174	DC
MYCL	9.21E-43	3.14427234	5.13E-38	DC
RNASE6	0	3.14921513	0	DC
RP11-286E11.1	5.99E-58	3.1505233	3.34E-53	DC

HSPA7	1.59E-172	3.15556521	8.85E-168	DC
RP11-338C15.5	2.57E-46	3.15601361	1.43E-41	DC
IL1RL2	3.49E-22	3.15633051	1.95E-17	DC
OPLAH	2.25E-16	3.1584417	1.26E-11	DC
GPR42	1.60E-13	3.15868107	8.90E-09	DC
DDC8	2.27E-31	3.16159876	1.26E-26	DC
RP11-63P12.6	6.28E-49	3.1663561	3.50E-44	DC
UBE2E2	5.52E-270	3.16704727	3.07E-265	DC
ZNF516	1.04E-214	3.16800389	5.78E-210	DC
PLEK2	1.33E-17	3.16876529	7.40E-13	DC
TREML3P	4.44E-12	3.16971686	2.47E-07	DC
MB21D2	1.80E-52	3.1729387	1.01E-47	DC
FAM114A1	5.12E-51	3.17838757	2.85E-46	DC
IFI30	0	3.17843726	0	DC
RRAD	1.22E-09	3.17932532	6.80E-05	DC
INHBA-AS1	5.22E-12	3.18508696	2.91E-07	DC
DNM1	1.39E-16	3.18841388	7.77E-12	DC
TM6SF1	2.42E-124	3.19032577	1.35E-119	DC
WWC2	1.79E-20	3.19179056	9.99E-16	DC
AC108676.1	3.63E-11	3.19274929	2.02E-06	DC
LILRB1	0	3.19328339	0	DC
FOSL1	7.05E-75	3.19357793	3.93E-70	DC
RGAG4	4.73E-29	3.19447245	2.64E-24	DC
ASB13	1.26E-47	3.19778067	7.02E-43	DC
FHAD1	7.04E-35	3.19958296	3.92E-30	DC
LGMNP1	1.60E-92	3.20013241	8.94E-88	DC
ZNF185	2.59E-57	3.20141855	1.45E-52	DC
RRAS	1.66E-50	3.20330287	9.26E-46	DC
MPP3	6.34E-11	3.2083186	3.54E-06	DC
RP11-22N19.2	1.04E-49	3.21169929	5.79E-45	DC
RP5-1125K23.1	1.44E-10	3.21927902	8.04E-06	DC
RP11-408O19.5	9.49E-12	3.22240823	5.29E-07	DC
SERPINE1	6.21E-36	3.22278165	3.46E-31	DC
ARRDC4	1.02E-10	3.23339196	5.70E-06	DC
LYL1	2.75E-23	3.23347833	1.53E-18	DC
TACSTD2	2.21E-12	3.24001692	1.23E-07	DC
PPFIA4	3.23E-22	3.2400796	1.80E-17	DC
RNASE3	4.32E-14	3.24881776	2.41E-09	DC
ACSS2	1.44E-126	3.25024632	8.05E-122	DC
AC114730.2	6.55E-39	3.25187014	3.65E-34	DC
ARL11	3.52E-105	3.25213493	1.96E-100	DC
LATS2-AS1	2.56E-24	3.25238516	1.42E-19	DC

AP001056.1	1.26E-69	3.25260953	7.05E-65	DC
B3GNT8	7.12E-24	3.25596183	3.97E-19	DC
TOR4A	8.17E-33	3.25622787	4.55E-28	DC
CDH23	4.06E-195	3.25625732	2.26E-190	DC
PLD1	6.40E-80	3.25739134	3.57E-75	DC
GPX3	2.05E-77	3.25859069	1.14E-72	DC
SIGLEC18P	3.88E-15	3.26020792	2.16E-10	DC
KMO	2.89E-172	3.26439114	1.61E-167	DC
AC096677.1	1.49E-27	3.26513003	8.32E-23	DC
OPRL1	9.77E-27	3.26803361	5.45E-22	DC
AC012314.19	4.44E-32	3.27084163	2.48E-27	DC
RP11-545N8.3	1.01E-11	3.27740758	5.62E-07	DC
ETS2	0	3.27877396	0	DC
RP11-848P1.2	1.98E-39	3.28012063	1.10E-34	DC
RGS12	2.02E-113	3.28020353	1.13E-108	DC
MCTP1	4.93E-298	3.28075724	2.75E-293	DC
PRKAR2B	8.92E-38	3.2862658	4.97E-33	DC
RP11-748C4.1	1.44E-10	3.29015282	8.02E-06	DC
C3	9.90E-67	3.2905476	5.52E-62	DC
RP13-452N2.1	1.06E-48	3.29270308	5.89E-44	DC
TRIQK	8.43E-46	3.29366509	4.70E-41	DC
ALPK3	1.86E-14	3.29451054	1.04E-09	DC
RP11-1008C21.1	1.20E-09	3.3001252	6.67E-05	DC
RP11-365O16.3	4.28E-12	3.30072303	2.38E-07	DC
ZNF703	7.65E-43	3.30324914	4.26E-38	DC
SRC	5.07E-206	3.30482435	2.82E-201	DC
THBS1	3.03E-119	3.30691785	1.69E-114	DC
CXCR2P1	4.58E-66	3.31071873	2.55E-61	DC
CYBRD1	6.28E-81	3.3126605	3.50E-76	DC
RP11-10C24.1	1.04E-12	3.31271875	5.82E-08	DC
CDC42BPB	6.62E-82	3.31715089	3.69E-77	DC
RASSF4	0	3.32001451	0	DC
RP11-552D4.1	5.61E-18	3.32023322	3.12E-13	DC
IL1R2	1.87E-121	3.32455463	1.04E-116	DC
PLA1A	1.14E-53	3.32496227	6.38E-49	DC
MAML3	2.66E-146	3.32661728	1.48E-141	DC
OAF	1.15E-33	3.33127286	6.41E-29	DC
CNTLN	8.94E-128	3.33468695	4.98E-123	DC
TTLL9	3.07E-17	3.33498034	1.71E-12	DC
TGFA	1.43E-21	3.33909362	7.97E-17	DC
KAL1	4.07E-10	3.34092353	2.27E-05	DC
PDE2A	6.83E-40	3.34328711	3.80E-35	DC

MS4A6A	0	3.34505076	0	DC
SCIN	3.48E-49	3.35231522	1.94E-44	DC
CMKLR1	1.69E-114	3.35844978	9.40E-110	DC
LIN7A	7.26E-10	3.36589966	4.05E-05	DC
HES1	1.35E-80	3.36666276	7.51E-76	DC
SNORA56	5.07E-17	3.36756823	2.83E-12	DC
TMEM86A	2.84E-41	3.37001526	1.58E-36	DC
EGFL7	6.95E-15	3.37556819	3.87E-10	DC
FFAR3	6.57E-22	3.37584197	3.66E-17	DC
RP4-576H24.4	3.97E-61	3.37700533	2.21E-56	DC
ARHGAP32	1.01E-22	3.38242027	5.64E-18	DC
GTF2IRD1	1.78E-20	3.38278123	9.94E-16	DC
SPINT1	2.50E-112	3.3829589	1.39E-107	DC
PPM1H	1.89E-13	3.38550112	1.05E-08	DC
TNFSF13B	0	3.38749715	0	DC
ARRB1	1.00E-172	3.38790913	5.58E-168	DC
AC021016.6	3.47E-25	3.39066941	1.93E-20	DC
FGR	0	3.39435892	0	DC
ASAP2	1.69E-28	3.39493765	9.41E-24	DC
TBC1D2	1.90E-222	3.4011842	1.06E-217	DC
CASP5	8.21E-19	3.40274317	4.58E-14	DC
SYNDIG1	4.34E-12	3.40897104	2.42E-07	DC
RP11-848G14.5	2.43E-142	3.41331138	1.35E-137	DC
RP11-489O18.1	1.04E-09	3.41462226	5.77E-05	DC
LOXL3	6.14E-44	3.41951209	3.42E-39	DC
CTD-2616J11.2	1.96E-116	3.4206638	1.09E-111	DC
CES1	8.98E-58	3.42348088	5.01E-53	DC
SLAMF8	1.53E-288	3.42603537	8.53E-284	DC
CTSZ	5.61E-92	3.42650442	3.12E-87	DC
CTD-2545M3.8	6.62E-46	3.42740939	3.69E-41	DC
MN1	7.80E-23	3.43115522	4.35E-18	DC
PLXNB2	0	3.43291243	0	DC
PXDC1	9.70E-78	3.43353236	5.41E-73	DC
CD9	2.51E-185	3.43544438	1.40E-180	DC
TBC1D30	2.12E-11	3.43647323	1.18E-06	DC
CECR6	1.40E-17	3.44217154	7.82E-13	DC
TIMP1	0	3.44689141	0	DC
SH3RF1	3.53E-67	3.44976026	1.97E-62	DC
CD276	1.39E-65	3.45174398	7.77E-61	DC
HK2P1	2.21E-35	3.45281986	1.23E-30	DC
FAM109A	1.51E-55	3.45893362	8.44E-51	DC
RP11-293M10.6	3.13E-21	3.45945895	1.74E-16	DC

RP11-426L16.8	3.01E-11	3.46570986	1.68E-06	DC
SEPP1	8.47E-42	3.46966628	4.72E-37	DC
RP11-24F11.2	1.79E-102	3.47212026	9.99E-98	DC
MPO	1.38E-19	3.47247916	7.69E-15	DC
ENPP1	1.36E-24	3.47400989	7.56E-20	DC
MLK7-AS1	5.29E-17	3.48209838	2.95E-12	DC
TIFAB	1.03E-44	3.48954894	5.72E-40	DC
TSPAN4	3.24E-195	3.49459528	1.81E-190	DC
FN1	8.75E-50	3.49462225	4.88E-45	DC
PDE6G	3.01E-39	3.49518246	1.68E-34	DC
AC007182.6	1.28E-51	3.49704379	7.14E-47	DC
RP3-522D1.1	1.42E-11	3.49771935	7.92E-07	DC
NDRG2	3.33E-166	3.50253446	1.86E-161	DC
GUCY1B3	3.27E-26	3.50749853	1.82E-21	DC
FCGRT	0	3.50827045	0	DC
SIGLEC5	2.02E-281	3.50956299	1.13E-276	DC
ADORA2B	1.50E-45	3.51154609	8.36E-41	DC
KRT8P42	4.15E-14	3.51234579	2.31E-09	DC
KIF17	1.68E-23	3.5192995	9.39E-19	DC
JPH4	2.07E-26	3.51962018	1.15E-21	DC
SUCNR1	8.53E-27	3.52904373	4.75E-22	DC
FLT3	3.09E-104	3.53254121	1.72E-99	DC
PLTP	6.76E-102	3.5340529	3.77E-97	DC
SIRPD	4.18E-35	3.53520557	2.33E-30	DC
PROS1	4.02E-23	3.53734383	2.24E-18	DC
OSBPL1A	6.81E-79	3.53790243	3.80E-74	DC
PIR	5.12E-13	3.53924992	2.85E-08	DC
EMILIN2	0	3.54235097	0	DC
C1orf54	8.81E-135	3.54387492	4.91E-130	DC
C1orf162	0	3.54498397	0	DC
TTYH2	2.85E-204	3.55921485	1.59E-199	DC
DSE	2.46E-218	3.55967356	1.37E-213	DC
HPGDS	6.01E-23	3.55999246	3.35E-18	DC
RP11-139K1.2	2.08E-68	3.56082371	1.16E-63	DC
SPATA6	1.85E-35	3.56527826	1.03E-30	DC
ALOX5	0	3.56965216	0	DC
MRVI1	8.85E-30	3.57260802	4.93E-25	DC
CLEC4A	3.40E-292	3.57277685	1.89E-287	DC
LHFPL2	1.32E-126	3.57420089	7.38E-122	DC
AIFM3	2.10E-26	3.5811989	1.17E-21	DC
MILR1	3.99E-157	3.587324	2.22E-152	DC
SOCS6	7.91E-85	3.58771068	4.41E-80	DC

CA2	1.33E-107	3.58831307	7.43E-103	DC
GJB2	1.11E-12	3.58969709	6.21E-08	DC
RP11-362F19.2	6.95E-12	3.59230126	3.87E-07	DC
C11orf45	1.04E-17	3.59584603	5.82E-13	DC
HK2	1.13E-265	3.59641873	6.32E-261	DC
MYBPC3	9.01E-23	3.59851444	5.02E-18	DC
QPCT	2.98E-172	3.59956718	1.66E-167	DC
ARHGEF40	7.20E-108	3.60134774	4.01E-103	DC
RP11-351I24.1	1.02E-09	3.60264417	5.67E-05	DC
SPR	7.34E-46	3.60622365	4.09E-41	DC
C2orf62	3.57E-16	3.60737108	1.99E-11	DC
DEPTOR	3.00E-41	3.60740658	1.67E-36	DC
AATK	1.42E-17	3.60927213	7.94E-13	DC
RAB42P1	7.80E-14	3.61189899	4.35E-09	DC
NAV1	5.42E-156	3.61632557	3.02E-151	DC
RP11-8P13.1	9.33E-13	3.61757494	5.20E-08	DC
CYBB	0	3.61784188	0	DC
RP11-1055B8.4	1.17E-21	3.61991173	6.51E-17	DC
RP11-346C20.3	3.40E-16	3.62393631	1.89E-11	DC
G0S2	1.52E-254	3.62843256	8.45E-250	DC
SNCA	9.08E-103	3.62864021	5.06E-98	DC
CTD-2514K5.4	6.57E-137	3.63245272	3.66E-132	DC
IFNGR2	0	3.63254539	0	DC
RP11-327F22.6	2.42E-11	3.63419818	1.35E-06	DC
CYFIP1	0	3.63430237	0	DC
SLC16A10	4.17E-40	3.63615988	2.32E-35	DC
FBN2	2.80E-20	3.63834557	1.56E-15	DC
RP11-638I2.9	2.16E-28	3.64108084	1.20E-23	DC
ABCA1	0	3.64142563	0	DC
BANF1P1	1.43E-10	3.64787972	7.96E-06	DC
LL22NC03-86G7.1	1.53E-47	3.64964485	8.53E-43	DC
SLC2A9	4.58E-113	3.65412685	2.55E-108	DC
APOC2	3.09E-36	3.65664166	1.72E-31	DC
ST14	8.63E-114	3.65828148	4.81E-109	DC
MLXIPL	3.57E-34	3.65878127	1.99E-29	DC
LINC00877	1.87E-110	3.66239917	1.04E-105	DC
CD300LD	1.41E-10	3.66316725	7.85E-06	DC
ZFHX3	3.79E-230	3.66679281	2.11E-225	DC
RP11-589N15.2	1.24E-98	3.66907805	6.90E-94	DC
RRAGD	2.86E-55	3.67074184	1.59E-50	DC
FXYD6	3.37E-53	3.67410891	1.88E-48	DC
FCHO2	1.42E-137	3.67686814	7.90E-133	DC

RP11-443B7.3	2.12E-22	3.67732964	1.18E-17	DC
SDPR	7.18E-16	3.67750332	4.00E-11	DC
RP3-454B23.1	9.15E-13	3.67908804	5.10E-08	DC
AL022328.1	5.24E-146	3.68015262	2.92E-141	DC
GSN-AS1	3.68E-47	3.68062299	2.05E-42	DC
RP11-5L12.1	2.13E-238	3.68220657	1.19E-233	DC
AC002456.2	1.65E-18	3.68429335	9.18E-14	DC
CCDC26	4.15E-14	3.68680074	2.31E-09	DC
CTD-3187F8.14	2.74E-37	3.69355828	1.53E-32	DC
PHLDA2	1.72E-202	3.69775984	9.58E-198	DC
ZNF697	1.88E-09	3.70150171	0.00010467	DC
TPRG1-AS1	7.70E-14	3.70878773	4.29E-09	DC
CTD-2195B23.3	7.70E-14	3.70921661	4.29E-09	DC
KB-1507C5.4	2.92E-56	3.71201835	1.63E-51	DC
RP11-57C13.3	1.94E-23	3.71244085	1.08E-18	DC
KIF13A	3.20E-84	3.7139931	1.78E-79	DC
RP11-293M10.5	4.04E-32	3.71545558	2.25E-27	DC
ITGB5	1.53E-58	3.71857826	8.54E-54	DC
LA16c-444G7.2	9.53E-12	3.72191331	5.31E-07	DC
LRG1	4.55E-51	3.72489755	2.54E-46	DC
TYROBP	0	3.72775324	0	DC
SPHK1	2.87E-116	3.73049759	1.60E-111	DC
SLC43A2	0	3.73294397	0	DC
TBC1D12	3.59E-45	3.73620571	2.00E-40	DC
RP11-863P13.1	1.01E-11	3.73691048	5.63E-07	DC
GSN	0	3.73702337	0	DC
TNNI2	5.29E-65	3.74506136	2.95E-60	DC
ACRBP	5.41E-91	3.74528293	3.02E-86	DC
WI2-1896O14.1	1.17E-46	3.74680018	6.50E-42	DC
GPR126	4.53E-24	3.7469174	2.53E-19	DC
TFEC	1.77E-202	3.75300313	9.88E-198	DC
APOE	5.79E-71	3.76220024	3.23E-66	DC
RP11-497H16.2	5.71E-109	3.765885	3.18E-104	DC
RP1-93H18.7	1.60E-18	3.76668905	8.92E-14	DC
RP11-1275H24.1	1.12E-10	3.76683987	6.24E-06	DC
NR6A1	3.79E-60	3.76761057	2.11E-55	DC
COL4A2	5.91E-30	3.76976565	3.29E-25	DC
IL4I1	0	3.77032328	0	DC
LY86	0	3.77160595	0	DC
AC005162.4	1.01E-11	3.77245276	5.63E-07	DC
RP11-1391J7.1	3.94E-23	3.77506728	2.20E-18	DC
IER3	0	3.77717761	0	DC

FES	1.46E-306	3.77914045	8.11E-302	DC
LPL	1.37E-24	3.77945989	7.61E-20	DC
IL18	1.10E-229	3.77967225	6.10E-225	DC
FABP3	5.96E-24	3.78037445	3.32E-19	DC
KCNQ1	1.48E-65	3.78108063	8.26E-61	DC
ITSN1	3.27E-63	3.78322346	1.82E-58	DC
EPHB2	5.17E-35	3.78825799	2.88E-30	DC
AC093627.10	5.72E-33	3.79364582	3.19E-28	DC
RP11-1275H24.3	8.28E-50	3.79501473	4.61E-45	DC
CTC-205M6.5	1.79E-87	3.80369889	9.98E-83	DC
NPL	1.46E-211	3.8042141	8.15E-207	DC
B3GNT5	7.28E-186	3.80713045	4.06E-181	DC
FAM225B	6.19E-11	3.81125196	3.45E-06	DC
RP11-403I13.9	1.41E-17	3.81281322	7.85E-13	DC
CCL18	7.91E-52	3.81601091	4.41E-47	DC
AXL	2.81E-261	3.81664512	1.57E-256	DC
RP11-728F11.4	1.36E-32	3.81881298	7.60E-28	DC
CTC-564N23.2	9.29E-13	3.81939995	5.18E-08	DC
TNFSF13	0	3.83227059	0	DC
RP11-799B12.4	6.20E-13	3.83684601	3.46E-08	DC
UBTD1	1.48E-13	3.83807206	8.27E-09	DC
KLHDC8B	2.49E-45	3.838243	1.39E-40	DC
TREML4	8.42E-22	3.83996056	4.69E-17	DC
APOC1	3.12E-100	3.84075869	1.74E-95	DC
ANGPTL4	1.58E-16	3.84223163	8.80E-12	DC
RNF130	0	3.84502252	0	DC
ALDH3B2	5.00E-41	3.85069129	2.79E-36	DC
RPL36AP41	4.43E-16	3.85840456	2.47E-11	DC
ECM1	1.54E-38	3.86027584	8.59E-34	DC
MRC2	1.81E-102	3.86271554	1.01E-97	DC
RP11-848G14.2	0	3.8632853	0	DC
C3AR1	0	3.8639519	0	DC
RP11-141M1.1	2.42E-18	3.86693934	1.35E-13	DC
RP11-16K12.1	3.21E-11	3.86792864	1.79E-06	DC
NDST1	9.60E-131	3.87717756	5.35E-126	DC
ANKRD50	6.90E-21	3.87775983	3.85E-16	DC
SERINC2	1.05E-41	3.8810887	5.83E-37	DC
RP11-478K15.6	1.98E-19	3.89185175	1.10E-14	DC
AC008738.1	2.56E-56	3.8925162	1.43E-51	DC
DTNA	1.53E-47	3.89252028	8.51E-43	DC
CD86	0	3.89520571	0	DC
RP11-426K3.1	3.45E-55	3.89792681	1.92E-50	DC

PTGS1	1.84E-216	3.90634796	1.03E-211	DC
Z83851.1	4.58E-25	3.90856292	2.55E-20	DC
LRRK2	0	3.90876141	0	DC
XXbac-BPG252P9.10	0	3.91211821	0	DC
CXCL12	6.76E-28	3.91444759	3.77E-23	DC
IQSEC2	1.20E-73	3.91451135	6.68E-69	DC
M1AP	3.50E-14	3.91672549	1.95E-09	DC
SIGLEC8	6.87E-38	3.91728013	3.83E-33	DC
OXER1	1.12E-59	3.93030953	6.26E-55	DC
F3	1.05E-35	3.9304109	5.83E-31	DC
SLC7A8	3.50E-85	3.93125195	1.95E-80	DC
RP11-497H16.7	0	3.93310275	0	DC
ZNF503-AS2	1.12E-10	3.93555555	6.23E-06	DC
ARHGAP22	7.54E-96	3.93723538	4.20E-91	DC
NID1	1.78E-40	3.93972919	9.93E-36	DC
MARCKS	0	3.94539525	0	DC
RP11-474O21.5	3.60E-16	3.94734277	2.01E-11	DC
PPP1R3G	3.05E-26	3.94827857	1.70E-21	DC
CTD-2373H9.5	2.43E-18	3.95019304	1.35E-13	DC
GAS2L3	3.54E-70	3.95572699	1.97E-65	DC
RP11-933H2.4	6.13E-24	3.9558389	3.42E-19	DC
MPEG1	0	3.96890302	0	DC
RP11-760H22.2	3.83E-15	3.97437378	2.13E-10	DC
TCF7L2	2.42E-207	3.97493827	1.35E-202	DC
FFAR4	6.80E-12	3.97574293	3.79E-07	DC
CD302	0	3.97774407	0	DC
DPYSL3	1.25E-13	3.9782284	6.97E-09	DC
DZIP1L	1.23E-37	3.97934379	6.87E-33	DC
CTD-2540B15.11	1.11E-92	3.97992465	6.21E-88	DC
WLS	2.10E-12	3.99972625	1.17E-07	DC
SLC22A16	1.55E-12	4.00578736	8.65E-08	DC
TMEM51-AS1	6.58E-11	4.00632675	3.67E-06	DC
CEACAM3	2.02E-22	4.00705303	1.13E-17	DC
FNIP2	0	4.01152058	0	DC
SIGLEC10	2.95E-301	4.0120821	1.64E-296	DC
SIGLEC14	0	4.01413099	0	DC
KCNJ2	2.15E-155	4.01468012	1.20E-150	DC
RP11-61J19.4	1.00E-36	4.015582	5.57E-32	DC
OSGIN1	6.48E-24	4.01645358	3.61E-19	DC
AC003080.4	9.27E-12	4.01709138	5.17E-07	DC
SNAI1	3.73E-132	4.01718581	2.08E-127	DC
GPR157	1.08E-93	4.024318	6.01E-89	DC

CST6	4.55E-16	4.02846843	2.53E-11	DC
FCER1G	0	4.0288611	0	DC
RP11-701P16.2	7.75E-255	4.03017486	4.32E-250	DC
TGFBI	0	4.0301871	0	DC
SLC9A7P1	1.55E-38	4.03051146	8.66E-34	DC
RIN1	1.65E-44	4.03643274	9.21E-40	DC
B3GALNT1	6.99E-31	4.04769234	3.89E-26	DC
RP11-598F7.3	2.03E-44	4.04793657	1.13E-39	DC
RP4-593C16.3	7.46E-24	4.05199048	4.16E-19	DC
NRGN	5.35E-42	4.05220268	2.98E-37	DC
CDC42EP1	7.87E-57	4.05344486	4.39E-52	DC
CTD-3187F8.15	6.40E-16	4.05443623	3.57E-11	DC
ARHGAP6	2.34E-23	4.06090172	1.30E-18	DC
UNC93B2	4.17E-14	4.06188932	2.32E-09	DC
FGL2	0	4.06361706	0	DC
MFSD7	1.15E-44	4.06407014	6.42E-40	DC
NLRP3	0	4.0652989	0	DC
DAB2	1.20E-195	4.06951412	6.67E-191	DC
ZDHHC1	8.67E-31	4.07635838	4.83E-26	DC
HAMP	2.29E-61	4.0802063	1.27E-56	DC
PGA4	8.53E-19	4.08438181	4.76E-14	DC
RHOU	2.02E-60	4.08777812	1.13E-55	DC
RP11-6I2.3	3.81E-15	4.09381904	2.12E-10	DC
TCN2	1.83E-301	4.09772999	1.02E-296	DC
LILRB4	0	4.09869813	0	DC
CLEC4G	5.99E-15	4.10089448	3.34E-10	DC
SEZ6L	1.54E-43	4.10248779	8.59E-39	DC
ACSM5	6.66E-16	4.10436388	3.71E-11	DC
AC117834.1	5.26E-20	4.10441166	2.93E-15	DC
RP11-467L20.10	4.11E-14	4.10757291	2.29E-09	DC
CTD-2240H23.2	1.52E-18	4.10948458	8.45E-14	DC
RP11-274J7.3	1.91E-10	4.11527541	1.06E-05	DC
AC051649.16	1.30E-20	4.12282492	7.26E-16	DC
FAM26F	0	4.12340772	0	DC
RCN3	2.65E-115	4.12392944	1.48E-110	DC
CYTL1	2.23E-24	4.13666177	1.24E-19	DC
HSD3B7	1.75E-92	4.13744857	9.76E-88	DC
CD1D	0	4.13838106	0	DC
TMEM170B	2.32E-110	4.1396689	1.29E-105	DC
CTD-2514K5.2	7.81E-41	4.14139034	4.36E-36	DC
EMR4P	9.79E-30	4.14343003	5.46E-25	DC
MS4A4E	6.63E-41	4.14415645	3.70E-36	DC

EPHB3	5.84E-24	4.14929051	3.25E-19	DC
SLC24A4	2.48E-55	4.15273968	1.38E-50	DC
ST18	3.63E-52	4.15425042	2.02E-47	DC
EPS8	1.36E-126	4.15505031	7.59E-122	DC
MAMDC2	3.13E-38	4.15575119	1.74E-33	DC
RP11-389C8.2	4.20E-35	4.15618967	2.34E-30	DC
ZMYND15	3.99E-49	4.16780405	2.22E-44	DC
TRPM4	4.61E-137	4.16938976	2.57E-132	DC
RP4-684O24.5	3.26E-17	4.16964693	1.82E-12	DC
AC008440.10	7.70E-14	4.17293102	4.29E-09	DC
TRPV4	7.21E-32	4.17400266	4.02E-27	DC
NUDT16P	2.98E-72	4.17536356	1.66E-67	DC
COL8A2	5.60E-24	4.17958429	3.12E-19	DC
RP11-379F4.9	7.52E-14	4.18178933	4.19E-09	DC
BATF3	1.51E-118	4.18601158	8.43E-114	DC
FMN1	1.26E-226	4.18607117	7.03E-222	DC
HTR7	7.45E-33	4.18613627	4.15E-28	DC
ETV5	3.85E-183	4.19295659	2.15E-178	DC
APOL4	1.27E-70	4.19351618	7.11E-66	DC
MEP1A	1.55E-12	4.19385415	8.65E-08	DC
CD68	0	4.1986869	0	DC
GAPDHP14	1.78E-16	4.20230331	9.93E-12	DC
RP11-356N1.2	3.83E-15	4.20346283	2.13E-10	DC
C10orf55	6.73E-24	4.20923198	3.75E-19	DC
HAAO	2.28E-81	4.21165191	1.27E-76	DC
RP11-498E2.9	4.68E-20	4.21650143	2.61E-15	DC
RP11-575A19.2	5.60E-21	4.21664849	3.12E-16	DC
RP11-153M7.3	2.83E-24	4.21746283	1.58E-19	DC
IGF2BP2	1.48E-74	4.21746468	8.24E-70	DC
SLC8A1-AS1	5.21E-285	4.21853519	2.90E-280	DC
CCDC149	5.43E-64	4.22018173	3.03E-59	DC
JDP2	6.43E-269	4.22253947	3.59E-264	DC
KCNMA1	1.21E-82	4.22306614	6.75E-78	DC
ACOX2	3.82E-24	4.22539203	2.13E-19	DC
SLC31A2	0	4.22549819	0	DC
ICAM5	3.14E-36	4.22573637	1.75E-31	DC
AC015969.3	1.88E-158	4.22798348	1.05E-153	DC
FCGR2C	0	4.23781946	0	DC
GAS2L1	4.11E-77	4.23936017	2.29E-72	DC
TNFRSF10C	1.70E-66	4.24174642	9.48E-62	DC
AC135048.1	3.58E-16	4.24398846	1.99E-11	DC
RGS18	5.33E-254	4.24791538	2.97E-249	DC

ARMCX1	2.11E-82	4.25179537	1.18E-77	DC
SLC25A47	2.09E-27	4.2536469	1.16E-22	DC
EMP1	1.19E-187	4.2540844	6.65E-183	DC
RNF217	1.67E-50	4.27127829	9.30E-46	DC
OR51R1P	4.47E-20	4.27401183	2.49E-15	DC
PKP2	9.51E-49	4.28215085	5.30E-44	DC
XXbac-B135H6.15	4.41E-25	4.28846398	2.46E-20	DC
PPP1R17	1.39E-11	4.28927581	7.76E-07	DC
PMP22	9.93E-162	4.29355296	5.54E-157	DC
TMEM144	2.75E-141	4.2938915	1.53E-136	DC
MTMR11	9.76E-116	4.29543056	5.44E-111	DC
IL1A	2.80E-45	4.30099582	1.56E-40	DC
SRGAP1	4.76E-79	4.30306562	2.65E-74	DC
RP11-196G18.3	2.66E-25	4.30750094	1.48E-20	DC
NHSL1	3.60E-179	4.31829423	2.00E-174	DC
AC007362.1	4.98E-25	4.31944395	2.78E-20	DC
C11orf74	8.06E-51	4.32084919	4.49E-46	DC
CD1C	3.22E-237	4.32311022	1.80E-232	DC
UBD	9.86E-86	4.32315001	5.50E-81	DC
CDS1	7.73E-19	4.32685432	4.31E-14	DC
ZNF812	6.93E-21	4.32785948	3.86E-16	DC
MMP14	5.31E-73	4.32884165	2.96E-68	DC
LST1	0	4.33373611	0	DC
NUS1P2	6.08E-13	4.34042618	3.39E-08	DC
RP11-483P21.2	1.27E-71	4.34370806	7.06E-67	DC
AGPAT9	9.70E-281	4.34728903	5.41E-276	DC
DYSF	1.46E-170	4.34796623	8.12E-166	DC
PLB1	1.30E-185	4.34833768	7.25E-181	DC
CTD-2319I12.2	1.52E-34	4.34916724	8.50E-30	DC
SCIMP	0	4.35072242	0	DC
RAPH1	5.02E-189	4.35170662	2.80E-184	DC
RP1-60N8.1	9.27E-12	4.35905673	5.17E-07	DC
RP13-128O4.3	5.73E-38	4.36518727	3.19E-33	DC
MERTK	8.68E-150	4.36744718	4.84E-145	DC
UNC5A	2.38E-18	4.36793288	1.33E-13	DC
PILRA	0	4.36847546	0	DC
SPP1	1.32E-159	4.37028254	7.38E-155	DC
AC008984.7	7.41E-85	4.38891655	4.13E-80	DC
ALDH2	0	4.38950306	0	DC
RP3-460G2.2	2.25E-26	4.39291134	1.25E-21	DC
LAMB3	7.84E-51	4.39824423	4.37E-46	DC
FMNL2	3.33E-160	4.40297986	1.86E-155	DC

CXCL10	6.01E-145	4.40732904	3.35E-140	DC
PVRL2	1.73E-177	4.4096543	9.67E-173	DC
AC068580.5	1.89E-10	4.41125812	1.05E-05	DC
RP13-395E19.3	1.39E-36	4.41406158	7.72E-32	DC
RP11-568K15.1	5.96E-20	4.42090678	3.32E-15	DC
RNF144B	0	4.42787867	0	DC
RP11-588L15.2	5.77E-40	4.437095	3.22E-35	DC
RBM47	0	4.43779944	0	DC
RP1-228H13.2	1.01E-83	4.44395304	5.64E-79	DC
KYNU	0	4.44999623	0	DC
MGST1	2.67E-97	4.45635837	1.49E-92	DC
AC104809.3	5.10E-24	4.45656401	2.84E-19	DC
THBD	0	4.46837155	0	DC
UNC5B	1.69E-31	4.47033622	9.40E-27	DC
CLIC2	2.72E-253	4.47517574	1.52E-248	DC
RN7SL862P	1.87E-23	4.47745877	1.04E-18	DC
RP11-701P16.1	2.20E-59	4.47929054	1.23E-54	DC
CES1P1	1.23E-53	4.4818481	6.88E-49	DC
PADI2	1.01E-218	4.48706426	5.62E-214	DC
FAM129B	8.32E-199	4.49684679	4.64E-194	DC
AIF1	0	4.49998278	0	DC
SIRPAP1	7.09E-85	4.5072164	3.95E-80	DC
TIMP2	1.47E-260	4.51153847	8.19E-256	DC
CD163L1	1.76E-16	4.5120911	9.79E-12	DC
KLF4	0	4.52195706	0	DC
RP11-481A20.11	5.56E-34	4.52307166	3.10E-29	DC
AC034228.7	8.83E-30	4.53019705	4.92E-25	DC
LIPM	3.40E-31	4.53122391	1.89E-26	DC
CLEC1B	1.80E-45	4.53141902	1.00E-40	DC
S100Z	6.96E-41	4.53478069	3.88E-36	DC
LAMB2	8.43E-58	4.53731485	4.70E-53	DC
DAPK1	0	4.53844352	0	DC
TMEM37	5.00E-34	4.54366374	2.79E-29	DC
RNA5SP151	1.16E-273	4.56281058	6.45E-269	DC
GPBAR1	3.64E-171	4.5647436	2.03E-166	DC
RP11-290F20.1	6.06E-13	4.56797832	3.38E-08	DC
CEBPD	0	4.5705987	0	DC
MYZAP	9.80E-13	4.57328051	5.46E-08	DC
CD36	0	4.58567699	0	DC
HLX	1.84E-113	4.58883128	1.02E-108	DC
HOMER3	9.88E-87	4.5906388	5.51E-82	DC
RP11-439A17.9	9.26E-40	4.60666008	5.16E-35	DC

ZNF467	6.24E-85	4.60717571	3.48E-80	DC
RP11-588L15.1	2.50E-238	4.61024877	1.39E-233	DC
RUSC2	5.75E-76	4.61119124	3.20E-71	DC
PPAP2B	7.88E-51	4.61435665	4.39E-46	DC
SORT1	5.31E-194	4.62373647	2.96E-189	DC
PKIB	8.90E-123	4.63074313	4.96E-118	DC
FGD4	0	4.63830969	0	DC
RP3-393E18.2	3.53E-31	4.65439994	1.97E-26	DC
RP11-323N12.5	3.84E-111	4.66135621	2.14E-106	DC
FAM3B	6.78E-21	4.6644924	3.78E-16	DC
LILRB5	2.35E-269	4.66720981	1.31E-264	DC
RP11-128M1.1	7.81E-27	4.66825718	4.35E-22	DC
BATF2	2.08E-59	4.66953698	1.16E-54	DC
CST3	0	4.67695857	0	DC
SLC15A3	0	4.69057314	0	DC
ARHGEF11	2.70E-110	4.70354644	1.51E-105	DC
SLC7A7	0	4.7065386	0	DC
DCSTAMP	3.44E-31	4.71826478	1.92E-26	DC
SERPING1	0	4.72974691	0	DC
STARD8	0	4.7347405	0	DC
SGMS2	9.94E-76	4.73655997	5.54E-71	DC
RP11-404O13.5	1.69E-28	4.73806155	9.43E-24	DC
RP11-41O4.1	9.87E-12	4.74066033	5.50E-07	DC
ADAMTS2	6.07E-32	4.74723799	3.38E-27	DC
CTSL	0	4.74951812	0	DC
AC087269.1	7.49E-22	4.75031281	4.17E-17	DC
CTB-55O6.10	1.88E-23	4.7509287	1.05E-18	DC
LYVE1	1.59E-45	4.7512858	8.84E-41	DC
RAB31	0	4.75168104	0	DC
SLITRK4	1.83E-10	4.75730208	1.02E-05	DC
MYOF	0	4.75786239	0	DC
SLC1A3	2.44E-225	4.75907452	1.36E-220	DC
SLC22A18AS	8.62E-46	4.76490732	4.80E-41	DC
RP11-190C22.9	1.97E-27	4.78273506	1.10E-22	DC
CTC-510F12.4	5.93E-26	4.78295781	3.31E-21	DC
CSF2RA	0	4.786804	0	DC
TNS1	1.97E-199	4.79152565	1.10E-194	DC
NRP2	2.35E-162	4.7949912	1.31E-157	DC
STON2	2.70E-41	4.79890602	1.50E-36	DC
CXCL16	0	4.799934	0	DC
ADORA3	3.87E-179	4.80333874	2.16E-174	DC
PLA2G4A	3.21E-96	4.80712928	1.79E-91	DC

VNN1	1.72E-54	4.80840883	9.59E-50	DC
STARD13-AS	3.46E-33	4.81226634	1.93E-28	DC
CTB-113D17.1	6.39E-85	4.81664385	3.56E-80	DC
MITF	2.84E-141	4.81807226	1.58E-136	DC
PLAUR	0	4.82637692	0	DC
SLC22A4	7.99E-44	4.82657657	4.45E-39	DC
EXOC3L1	1.73E-14	4.82839986	9.67E-10	DC
KIAA1598	0	4.83239996	0	DC
HGF	1.15E-70	4.83579947	6.41E-66	DC
GDF15	7.44E-61	4.84323293	4.15E-56	DC
AP003733.1	3.72E-84	4.84917009	2.08E-79	DC
ALDH1A1	7.79E-123	4.85277161	4.34E-118	DC
MARVELD1	2.77E-66	4.8598597	1.54E-61	DC
CCDC170	2.66E-66	4.86638172	1.48E-61	DC
RP11-54C4.2	1.36E-22	4.86644509	7.57E-18	DC
STEAP4	1.33E-40	4.86794895	7.42E-36	DC
PFKFB4	2.06E-165	4.87075933	1.15E-160	DC
RP11-202G18.1	1.05E-27	4.87169421	5.88E-23	DC
COLEC12	3.87E-29	4.87394563	2.16E-24	DC
ANKRD22	1.44E-271	4.87538065	8.02E-267	DC
LPAR1	5.35E-52	4.87897148	2.98E-47	DC
RP11-390P2.4	1.38E-38	4.87934323	7.70E-34	DC
C2	1.69E-142	4.88167011	9.39E-138	DC
RP11-84C10.2	7.45E-27	4.88521016	4.15E-22	DC
CTD-2319I12.1	4.77E-75	4.89092622	2.66E-70	DC
SLCO2B1	3.08E-214	4.89254559	1.72E-209	DC
RP11-217B7.2	1.55E-54	4.89628174	8.62E-50	DC
AP001007.1	5.87E-137	4.89701746	3.27E-132	DC
IDO2	8.85E-50	4.91065009	4.93E-45	DC
CTC-558O19.1	9.73E-66	4.91343352	5.42E-61	DC
MRAS	6.38E-121	4.91505801	3.56E-116	DC
RP11-4C20.3	4.45E-20	4.915077	2.48E-15	DC
RP11-672A2.5	1.35E-17	4.91633189	7.50E-13	DC
RP11-47G11.2	1.86E-10	4.93259552	1.04E-05	DC
CARD9	1.20E-233	4.93807505	6.69E-229	DC
P2RY12	7.77E-103	4.94044862	4.33E-98	DC
LUCAT1	1.84E-149	4.94929381	1.02E-144	DC
ZNF366	8.86E-67	4.95385203	4.94E-62	DC
FCER1A	9.02E-128	4.9538957	5.03E-123	DC
CDC42EP2	4.43E-192	4.95638091	2.47E-187	DC
GPR162	5.57E-42	4.9586326	3.10E-37	DC
CLEC1A	2.20E-17	4.96035096	1.23E-12	DC

PTGES	4.76E-24	4.97426549	2.66E-19	DC
NUPR1	3.42E-78	4.99702819	1.90E-73	DC
TMEM150B	2.43E-73	4.99865138	1.35E-68	DC
STEAP3	4.03E-76	4.9986518	2.25E-71	DC
RP11-12A2.1	1.07E-56	5.00236422	5.95E-52	DC
DMXL2	0	5.00256789	0	DC
TNFAIP6	1.29E-71	5.00539528	7.20E-67	DC
AP002954.4	2.82E-58	5.0057296	1.57E-53	DC
TREML5P	1.06E-16	5.01484397	5.90E-12	DC
CTD-2331C18.5	2.47E-13	5.02318484	1.38E-08	DC
IL31RA	3.18E-49	5.02752985	1.77E-44	DC
PLAU	4.57E-164	5.02801539	2.55E-159	DC
VEGFA	0	5.0289057	0	DC
LILRB3	0	5.04856994	0	DC
RAB42	9.98E-22	5.05586764	5.56E-17	DC
AC187652.1	1.44E-18	5.05995675	8.05E-14	DC
SDSL	2.04E-216	5.06393682	1.14E-211	DC
CATSPER1	1.63E-87	5.06398602	9.07E-83	DC
KCNJ15	1.35E-24	5.06834904	7.53E-20	DC
RP11-212I21.4	3.57E-72	5.08027199	1.99E-67	DC
FAM225A	3.09E-42	5.08238426	1.72E-37	DC
CYP1B1	4.06E-43	5.0946163	2.26E-38	DC
ENHO	1.72E-28	5.09491474	9.60E-24	DC
CTB-114C7.4	1.27E-52	5.09686903	7.07E-48	DC
HBEGF	0	5.10000037	0	DC
RAB39A	7.48E-97	5.10470975	4.17E-92	DC
MS4A14	1.46E-106	5.10640441	8.16E-102	DC
ST3GAL6	4.87E-293	5.10660007	2.71E-288	DC
SPI1	0	5.11845977	0	DC
ME1	2.47E-83	5.11910744	1.38E-78	DC
LILRP1	0	5.12185283	0	DC
CCL24	1.29E-43	5.1281212	7.22E-39	DC
NRG1	1.16E-55	5.13698355	6.46E-51	DC
AF124730.4	2.18E-15	5.14366441	1.21E-10	DC
ACVRL1	5.35E-64	5.14518963	2.98E-59	DC
CTB-83J4.2	1.36E-10	5.14531103	7.57E-06	DC
PAPSS2	2.78E-243	5.14633338	1.55E-238	DC
OLIG1	2.17E-25	5.15133355	1.21E-20	DC
RP11-792D21.2	3.07E-78	5.1710067	1.71E-73	DC
RP11-848P1.3	2.71E-30	5.17564395	1.51E-25	DC
LINC01010	3.00E-40	5.17787344	1.67E-35	DC
FFAR2	1.32E-100	5.18111084	7.38E-96	DC

TREML1	5.78E-26	5.18863839	3.22E-21	DC
FZD1	1.82E-43	5.19111489	1.01E-38	DC
KCTD12	0	5.19414461	0	DC
RGL1	1.38E-277	5.2071051	7.71E-273	DC
UPK3A	1.02E-80	5.2100126	5.69E-76	DC
RP11-470B22.1	3.71E-46	5.21804136	2.07E-41	DC
DHRS9	2.56E-181	5.22852005	1.43E-176	DC
RASGRP4	5.46E-284	5.2306698	3.04E-279	DC
RP11-736N17.4	1.37E-11	5.23195531	7.64E-07	DC
TDRD6	2.41E-46	5.24269064	1.35E-41	DC
CLEC12B	4.88E-40	5.24296221	2.72E-35	DC
SH3PXD2B	8.52E-105	5.25907872	4.75E-100	DC
TMEM255B	3.84E-38	5.26796341	2.14E-33	DC
SPRED1	5.38E-67	5.27328679	3.00E-62	DC
RP11-519G16.5	1.35E-61	5.2773039	7.54E-57	DC
TMEM158	1.46E-18	5.28798807	8.14E-14	DC
SIGLEC7	0	5.30919086	0	DC
FBP1	0	5.32516005	0	DC
SLC6A12	1.21E-106	5.32861974	6.74E-102	DC
IL13RA1	0	5.32893711	0	DC
CEACAM4	4.29E-139	5.33221418	2.39E-134	DC
C19orf38	0	5.33377174	0	DC
DAPK1-IT1	7.48E-69	5.33418277	4.17E-64	DC
C10orf11	1.86E-179	5.33864677	1.03E-174	DC
RP11-44K6.4	9.58E-102	5.34144669	5.34E-97	DC
GFRA2	1.04E-81	5.34650902	5.78E-77	DC
DAGLA	3.49E-52	5.35116775	1.94E-47	DC
ASB9	1.37E-10	5.35791755	7.61E-06	DC
RP11-65J3.1	5.44E-80	5.36374472	3.03E-75	DC
F13A1	0	5.37564652	0	DC
APOC4	1.49E-18	5.39332894	8.28E-14	DC
RNF175	3.67E-90	5.39521954	2.04E-85	DC
P2RY2	5.54E-33	5.40060196	3.09E-28	DC
IGSF6	0	5.40156865	0	DC
RP11-324E6.6	3.15E-133	5.40176579	1.75E-128	DC
TNFAIP2	0	5.40243655	0	DC
IRAK3	0	5.40363824	0	DC
SIGLEC19P	6.26E-16	5.41455252	3.49E-11	DC
CREB5	0	5.42142709	0	DC
ABCC3	1.01E-141	5.42769786	5.63E-137	DC
RP5-998N21.4	6.10E-41	5.42925239	3.40E-36	DC
RP11-707P17.2	1.07E-48	5.43436001	5.97E-44	DC

ALOX15B	7.55E-70	5.44158393	4.21E-65	DC
IDO1	3.07E-236	5.44506984	1.71E-231	DC
MMP19	5.92E-231	5.45630088	3.30E-226	DC
NCF2	0	5.47485093	0	DC
TREM2	1.58E-167	5.48230636	8.81E-163	DC
VN1R105P	3.47E-36	5.49637086	1.93E-31	DC
WDFY3	1.29E-218	5.49961763	7.19E-214	DC
SLC8A1	0	5.49963638	0	DC
RP1-229K20.5	9.82E-43	5.51489034	5.47E-38	DC
ALDH1A2	2.92E-198	5.53404022	1.63E-193	DC
RP5-899E9.1	6.57E-33	5.53440042	3.66E-28	DC
PDLIM1P4	1.65E-79	5.54142973	9.18E-75	DC
FCGR2A	0	5.54222066	0	DC
FZD2	9.84E-56	5.54508936	5.49E-51	DC
AC104809.4	3.16E-33	5.54837823	1.76E-28	DC
CD300LB	0	5.55075793	0	DC
NLRP12	3.32E-61	5.55118018	1.85E-56	DC
LILRA5	0	5.55956971	0	DC
SIGLEC12	6.11E-120	5.56833398	3.40E-115	DC
CDCP1	0	5.56937868	0	DC
PTAFR	0	5.57517863	0	DC
SCARF1	1.44E-201	5.57576033	8.02E-197	DC
LTBR	0	5.5780874	0	DC
KCNMB1	3.33E-266	5.57960161	1.86E-261	DC
RP11-77A13.1	9.71E-12	5.60355072	5.41E-07	DC
CCL17	3.78E-25	5.60596497	2.10E-20	DC
EPB41L3	0	5.61464847	0	DC
C15orf38	1.85E-154	5.61572223	1.03E-149	DC
PDGFC	1.13E-62	5.62562464	6.28E-58	DC
RP11-221J22.1	4.68E-27	5.6257628	2.61E-22	DC
NOV	1.36E-10	5.63181009	7.57E-06	DC
SLC46A2	1.68E-44	5.64010295	9.37E-40	DC
CLEC6A	6.68E-67	5.64591005	3.72E-62	DC
RP11-221J22.2	3.07E-35	5.66067558	1.71E-30	DC
CLEC7A	0	5.67329665	0	DC
CFD	0	5.69054171	0	DC
PDK4	1.26E-209	5.69236664	7.04E-205	DC
BST1	0	5.69237663	0	DC
CLEC12A	0	5.69432293	0	DC
APOA2	3.11E-65	5.70391973	1.73E-60	DC
ZNF503	6.25E-32	5.70554442	3.48E-27	DC
CSF1R	0	5.7100543	0	DC

AF064858.11	1.55E-26	5.71069076	8.64E-22	DC
RP1-240K6.3	9.19E-58	5.71920871	5.12E-53	DC
RP5-1120P11.1	1.06E-20	5.72290245	5.90E-16	DC
C5AR2	4.61E-74	5.72584406	2.57E-69	DC
S100A8	0	5.7284975	0	DC
RP11-212I21.2	1.41E-86	5.73064418	7.88E-82	DC
GGT5	8.98E-76	5.73422053	5.01E-71	DC
PYGL	0	5.73768677	0	DC
NFE2	6.91E-44	5.74738407	3.85E-39	DC
C1QB	0	5.75949789	0	DC
LMO2	9.81E-116	5.76713122	5.47E-111	DC
MS4A4A	0	5.7689061	0	DC
FOLR3	1.80E-42	5.77866287	1.00E-37	DC
SYN1	2.79E-40	5.78549897	1.55E-35	DC
RP1-122P22.2	2.95E-19	5.80113622	1.64E-14	DC
RP11-274J7.2	1.47E-18	5.80356867	8.19E-14	DC
RNASE1	3.59E-193	5.80478856	2.00E-188	DC
RP3-522P13.3	6.95E-65	5.82224654	3.87E-60	DC
NLRC4	9.67E-216	5.83887882	5.39E-211	DC
TLR5	2.57E-225	5.84229486	1.43E-220	DC
LINC00968	5.18E-23	5.84234034	2.89E-18	DC
TGM2	0	5.8563543	0	DC
S100A9	0	5.85966313	0	DC
RP11-597D13.9	1.77E-90	5.86389469	9.86E-86	DC
CYP27A1	2.32E-233	5.86852513	1.29E-228	DC
FAM20C	1.86E-164	5.87300316	1.04E-159	DC
RAB20	0	5.87302712	0	DC
FAM198B	2.22E-183	5.88721575	1.24E-178	DC
C1QC	0	5.88759367	0	DC
RP11-701P16.5	1.82E-214	5.89066614	1.02E-209	DC
CDA	6.06E-105	5.89148772	3.38E-100	DC
APOBEC3B-AS1	7.35E-134	5.90821812	4.10E-129	DC
ADAP2	0	5.90824354	0	DC
RP11-701P16.4	4.20E-18	5.91212663	2.34E-13	DC
LILRB2	0	5.91686544	0	DC
RP11-695J4.2	1.08E-29	5.9177555	6.02E-25	DC
RN7SL297P	2.16E-15	5.92203305	1.20E-10	DC
IL1RN	0	5.92648241	0	DC
PTGS2	2.13E-279	5.93990067	1.19E-274	DC
CXCL2	0	5.94150677	0	DC
MNDA	0	5.94451911	0	DC
CD93	0	5.94521469	0	DC

SERPINB2	7.76E-28	5.94697826	4.33E-23	DC
RP11-807H22.6	1.53E-23	5.9542029	8.52E-19	DC
CD209	2.88E-54	5.95420573	1.61E-49	DC
RP11-362F19.1	1.98E-123	5.9579892	1.10E-118	DC
AC004837.3	3.32E-21	5.9608668	1.85E-16	DC
SDC2	1.44E-89	5.97602298	8.00E-85	DC
OR2B11	2.19E-85	5.98701223	1.22E-80	DC
INHBA	6.79E-83	5.98765794	3.79E-78	DC
SASH1	1.15E-80	5.98832927	6.38E-76	DC
AC015871.1	3.66E-25	5.98864095	2.04E-20	DC
MS4A7	0	6.00717107	0	DC
RNASE2	4.00E-169	6.02595807	2.23E-164	DC
SLC11A1	0	6.02816212	0	DC
LILRA1	0	6.0494874	0	DC
C15orf48	0	6.05138241	0	DC
RP11-519G16.3	7.46E-141	6.05567749	4.16E-136	DC
CTD-3214H19.16	3.17E-29	6.06276401	1.77E-24	DC
ACPP	8.22E-158	6.0650543	4.58E-153	DC
RTN1	2.10E-119	6.07242401	1.17E-114	DC
PLBD1	0	6.07531291	0	DC
OLFML2B	6.21E-117	6.07540074	3.46E-112	DC
CFP	0	6.0785305	0	DC
DSC2	1.55E-176	6.08008673	8.65E-172	DC
AP003774.6	3.55E-38	6.08842255	1.98E-33	DC
PLXDC2	0	6.09023453	0	DC
CSF3R	0	6.09053278	0	DC
LRP1	0	6.09607851	0	DC
RBP7	4.04E-59	6.09926782	2.25E-54	DC
SIRPA	0	6.11981551	0	DC
RFPL4A	2.14E-15	6.12240802	1.20E-10	DC
SIGLEC11	2.39E-98	6.13431162	1.33E-93	DC
C1QA	0	6.13974688	0	DC
LINC00189	8.52E-58	6.14620231	4.75E-53	DC
SIGLEC9	0	6.15315343	0	DC
RP11-310J24.3	2.40E-32	6.15659739	1.34E-27	DC
SDC3	4.20E-215	6.15776393	2.34E-210	DC
RP11-472N13.3	2.85E-26	6.15921976	1.59E-21	DC
CD207	9.21E-33	6.17442725	5.13E-28	DC
MRC1L1	0	6.18149253	0	DC
PRAM1	0	6.19496149	0	DC
DOCK4	1.70E-249	6.21456213	9.45E-245	DC
ADM	0	6.21929621	0	DC

GGTA1P	1.34E-222	6.22438704	7.48E-218	DC
SLAMF9	6.29E-60	6.22726162	3.51E-55	DC
RP11-367B6.2	2.51E-37	6.23560526	1.40E-32	DC
VENTX	1.56E-156	6.23704451	8.71E-152	DC
TPPP3	3.29E-126	6.23913225	1.83E-121	DC
CTD-2337J16.1	1.28E-67	6.24494808	7.16E-63	DC
SIGLEC16	7.87E-135	6.2473735	4.39E-130	DC
LRRC25	0	6.25298715	0	DC
CD1B	6.52E-85	6.26108122	3.64E-80	DC
RP11-213H15.4	3.84E-54	6.27545483	2.14E-49	DC
SIRPB2	0	6.2760563	0	DC
VSTM1	8.38E-39	6.27908435	4.67E-34	DC
P2RY13	0	6.28295645	0	DC
RP3-473L9.4	4.17E-18	6.29643965	2.33E-13	DC
FOLR2	6.39E-203	6.30023156	3.56E-198	DC
CLEC9A	2.10E-68	6.31019916	1.17E-63	DC
IL8	0	6.31312047	0	DC
CD300C	0	6.31507176	0	DC
ALDH3B1	0	6.31667092	0	DC
CD163	0	6.32097909	0	DC
CCL19	3.10E-29	6.32681366	1.73E-24	DC
RN7SKP283	2.84E-26	6.3275446	1.58E-21	DC
ZNF385A	0	6.33997577	0	DC
RP11-1143G9.4	0	6.3410429	0	DC
CXCL3	4.16E-269	6.34246221	2.32E-264	DC
CLEC4F	2.08E-34	6.35332251	1.16E-29	DC
CACNA2D3	2.49E-120	6.37118487	1.39E-115	DC
CTD-2330J20.1	3.72E-109	6.37365289	2.08E-104	DC
RIN2	0	6.37831777	0	DC
AC074011.2	6.01E-40	6.38204147	3.35E-35	DC
LDLRAD3	1.29E-111	6.38225859	7.17E-107	DC
RP11-344B5.2	2.35E-40	6.38371834	1.31E-35	DC
LILRA2	0	6.38513537	0	DC
EREG	0	6.3864753	0	DC
CCL8	2.58E-40	6.3955218	1.44E-35	DC
RP11-191A15.4	6.27E-32	6.39747166	3.50E-27	DC
CTD-2006K23.1	1.53E-88	6.41517894	8.50E-84	DC
APOBEC3A	0	6.42868912	0	DC
CLEC5A	2.83E-220	6.43972611	1.58E-215	DC
RP11-624L4.2	6.12E-65	6.44841451	3.41E-60	DC
OSCAR	0	6.46044642	0	DC
CPVL	0	6.46168099	0	DC

HCK	0	6.46421378	0	DC
AL590714.1	1.23E-53	6.47092967	6.85E-49	DC
IL27	3.94E-96	6.48015106	2.20E-91	DC
S100A12	2.55E-139	6.48674157	1.42E-134	DC
KCNK13	1.71E-23	6.50118118	9.56E-19	DC
CXCL9	1.25E-211	6.51281195	6.95E-207	DC
NFAM1	0	6.53135632	0	DC
CYP2S1	0	6.53397807	0	DC
FCGR1C	0	6.55856	0	DC
CD1E	5.80E-175	6.56072744	3.23E-170	DC
LYZ	0	6.56394131	0	DC
SLC37A2	0	6.56941699	0	DC
MRC1	5.10E-213	6.56976899	2.84E-208	DC
KCNE1	1.95E-223	6.57032178	1.09E-218	DC
FCGR1A	0	6.57067047	0	DC
RN7SL138P	1.50E-23	6.59107043	8.38E-19	DC
IRG1	2.33E-18	6.60066126	1.30E-13	DC
HCAR3	3.49E-298	6.60208453	1.95E-293	DC
KCNE3	2.36E-247	6.60311586	1.32E-242	DC
METTL7B	4.50E-76	6.60491966	2.51E-71	DC
TMEM52B	1.39E-256	6.62053048	7.75E-252	DC
CD33	0	6.637158	0	DC
SIGLEC1	0	6.63935234	0	DC
LPCAT2	0	6.65042734	0	DC
LILRA6	0	6.65798263	0	DC
VSIG4	0	6.6780532	0	DC
GPNMB	0	6.679334	0	DC
EMR3	7.36E-108	6.6913716	4.10E-103	DC
RFPL4AL1	2.14E-15	6.76431994	1.19E-10	DC
MEFV	0	6.76868021	0	DC
CXCL1	8.70E-98	6.7766584	4.85E-93	DC
SIGLEC22P	9.61E-128	6.77791615	5.36E-123	DC
RP11-925D8.6	7.82E-41	6.81051919	4.36E-36	DC
AF064858.8	9.65E-28	6.81931558	5.38E-23	DC
IL1B	0	6.84465753	0	DC
MT1H	1.50E-26	6.84854823	8.35E-22	DC
STAB1	0	6.8555525	0	DC
AC009469.1	1.71E-106	6.87438122	9.55E-102	DC
TLR4	0	6.90436442	0	DC
OR52K3P	1.22E-33	6.9067407	6.78E-29	DC
AC092653.5	4.15E-18	6.91815435	2.31E-13	DC
CLEC4E	0	6.93693585	0	DC

RAB32	8.85E-178	6.9454548	4.93E-173	DC
CSTA	0	6.94779596	0	DC
TMEM176A	0	6.97039107	0	DC
RP11-191A15.1	3.30E-48	6.97686973	1.84E-43	DC
VCAN	0	6.9930888	0	DC
HCAR2	0	6.99743116	0	DC
CXCL11	7.78E-91	7.02067758	4.34E-86	DC
AC011899.9	7.29E-157	7.02266915	4.06E-152	DC
LILRA3	0	7.05549287	0	DC
MSR1	0	7.09356124	0	DC
ARHGEF10L	0	7.09986119	0	DC
AC091177.1	7.59E-54	7.10242953	4.23E-49	DC
CCL7	1.09E-37	7.1318779	6.06E-33	DC
C5AR1	0	7.13644799	0	DC
SEMA6B	0	7.14507325	0	DC
TMEM51	9.13E-214	7.15579493	5.09E-209	DC
MAFB	0	7.16350296	0	DC
CLEC4D	1.99E-110	7.16628757	1.11E-105	DC
FPR2	0	7.16773252	0	DC
TNNT1	8.31E-98	7.17096495	4.63E-93	DC
PTX3	1.29E-50	7.1768119	7.20E-46	DC
VMO1	1.12E-297	7.19385766	6.27E-293	DC
TLR2	0	7.20526256	0	DC
SERPINA1	0	7.21575357	0	DC
RP11-925D8.2	1.69E-86	7.22600245	9.42E-82	DC
CD300LF	0	7.23523684	0	DC
RP11-925D8.5	1.67E-138	7.25329247	9.29E-134	DC
WDFY3-AS1	5.87E-40	7.25483702	3.27E-35	DC
VCAN-AS1	9.07E-161	7.28007869	5.06E-156	DC
CD14	0	7.28592349	0	DC
RP11-925D8.3	6.06E-109	7.28696679	3.38E-104	DC
FPR1	0	7.29218134	0	DC
ANPEP	0	7.32503234	0	DC
TMEM176B	0	7.35269769	0	DC
ASGR1	1.97E-284	7.35528848	1.10E-279	DC
FCGR1B	0	7.36472806	0	DC
RN7SL368P	0	7.38508438	0	DC
CHST13	1.94E-58	7.38553207	1.08E-53	DC
C19orf59	2.94E-235	7.39724922	1.64E-230	DC
HNMT	0	7.42949913	0	DC
OLR1	0	7.43729326	0	DC
MS4A6E	2.77E-26	7.44524922	1.54E-21	DC

SDS	5.15E-284	7.47477283	2.87E-279	DC
RP11-750H9.5	0	7.47601325	0	DC
LGALS2	0	7.47620678	0	DC
RP11-702H23.6	4.99E-147	7.5058799	2.78E-142	DC
GPR84	0	7.50622627	0	DC
FCN2	1.15E-174	7.52390933	6.40E-170	DC
HK3	0	7.58296123	0	DC
LINC00676	1.16E-23	7.63003187	6.49E-19	DC
TREM1	0	7.63790328	0	DC
TLR8	3.87E-253	7.721435	2.15E-248	DC
RP11-290F20.3	0	7.73760042	0	DC
ASGR2	6.97E-256	7.95554844	3.88E-251	DC
FCAR	1.25E-251	7.99676631	6.97E-247	DC
CCL2	2.66E-283	8.04179779	1.48E-278	DC
RP11-286N3.1	3.57E-29	8.0475959	1.99E-24	DC
LIPN	7.33E-139	8.15485704	4.08E-134	DC
PLA2G7	0	8.15726871	0	DC
FCN1	0	8.22246497	0	DC
CD300E	0	8.27158765	0	DC
MSLN	3.15E-37	8.28315868	1.76E-32	DC
CLEC10A	0	8.30721056	0	DC
PID1	0	8.34633492	0	DC
AL118508.1	2.04E-26	8.39361693	1.13E-21	DC
CTB-61M7.2	3.75E-242	8.46408304	2.09E-237	DC
MARCO	0	8.46829506	0	DC
AQP9	0	8.50633101	0	DC
FPR3	0	8.71873844	0	DC
HAS1	2.07E-56	8.82366998	1.15E-51	DC
RP11-338C15.3	1.11E-34	8.87046176	6.20E-30	DC
RP11-25K21.6	4.92E-164	8.95621957	2.74E-159	DC
RETN	2.01E-78	9.43456214	1.12E-73	DC
RNA5SP498	1.11E-34	9.5059933	6.20E-30	DC
DEFB1	3.33E-73	10.1978241	1.86E-68	DC
AC079325.6	2.33E-164	11.4421842	1.30E-159	DC
EEF2K	8.93E-48	2.00166796	4.97E-43	Mono and Mac
FAM65C	6.37E-32	2.00313752	3.55E-27	Mono and Mac
GNAQ	2.56E-43	2.00544213	1.43E-38	Mono and Mac
VAV2	1.40E-20	2.00589428	7.80E-16	Mono and Mac
ATP6V0A1	1.53E-37	2.00814815	8.54E-33	Mono and Mac
RP11-1000B6.3	2.82E-48	2.00963574	1.57E-43	Mono and Mac
RP11-1100L3.7	2.17E-82	2.01276369	1.21E-77	Mono and Mac
CIDECP	2.27E-48	2.01441056	1.27E-43	Mono and Mac

RAB13	9.27E-17	2.02021623	5.16E-12	Mono and Mac
RUNX2	1.34E-101	2.02458307	7.45E-97	Mono and Mac
ASPH	1.11E-59	2.02601595	6.21E-55	Mono and Mac
SPHK1	2.69E-12	2.02684877	1.50E-07	Mono and Mac
AC012615.1	2.56E-16	2.02772666	1.43E-11	Mono and Mac
RP11-115H15.2	1.35E-13	2.02905887	7.53E-09	Mono and Mac
NPC2	3.60E-126	2.02991611	2.01E-121	Mono and Mac
MFSD12	6.95E-52	2.03298169	3.87E-47	Mono and Mac
CDCA7L	9.09E-58	2.03302595	5.06E-53	Mono and Mac
PADI4	1.20E-10	2.03394991	6.69E-06	Mono and Mac
SORT1	3.11E-16	2.03395512	1.74E-11	Mono and Mac
FMN1	4.89E-38	2.03826869	2.73E-33	Mono and Mac
AC141586.5	8.96E-65	2.04525734	4.99E-60	Mono and Mac
AC010226.4	3.23E-22	2.04559469	1.80E-17	Mono and Mac
HIVEP1	7.62E-91	2.04671633	4.25E-86	Mono and Mac
RP11-383F6.1	9.15E-48	2.04786754	5.10E-43	Mono and Mac
ETV3	6.60E-101	2.04977133	3.68E-96	Mono and Mac
SERHL2	4.26E-10	2.0520818	2.38E-05	Mono and Mac
RP11-141O15.1	5.60E-14	2.05242477	3.12E-09	Mono and Mac
GPR160	6.91E-20	2.05436034	3.85E-15	Mono and Mac
CCR2	2.24E-44	2.05813813	1.25E-39	Mono and Mac
RP11-932O9.9	5.26E-18	2.05969813	2.93E-13	Mono and Mac
AP000476.1	2.80E-29	2.06227557	1.56E-24	Mono and Mac
RNVU1-13	3.00E-28	2.06301901	1.67E-23	Mono and Mac
GOLGA8Q	3.51E-13	2.06474128	1.96E-08	Mono and Mac
IL4I1	5.51E-29	2.06729821	3.07E-24	Mono and Mac
RP11-293I14.2	9.25E-12	2.0682835	5.15E-07	Mono and Mac
CD83	1.85E-116	2.06832838	1.03E-111	Mono and Mac
NCF1	7.53E-117	2.07380971	4.20E-112	Mono and Mac
C3orf58	2.21E-87	2.07621802	1.23E-82	Mono and Mac
RP13-104F24.1	7.64E-16	2.07628656	4.26E-11	Mono and Mac
GPX1P1	1.57E-75	2.07805307	8.77E-71	Mono and Mac
AREGB	3.12E-41	2.07989323	1.74E-36	Mono and Mac
CTBP2	5.50E-24	2.08051993	3.07E-19	Mono and Mac
PBX3	1.52E-45	2.08143141	8.50E-41	Mono and Mac
RP11-1114A5.4	2.84E-11	2.0817993	1.58E-06	Mono and Mac
GRN	3.72E-131	2.08332161	2.07E-126	Mono and Mac
SOCS5	5.42E-32	2.084767	3.02E-27	Mono and Mac
PLEKHG4	9.42E-10	2.08997857	5.25E-05	Mono and Mac
KHDRBS2	1.59E-13	2.09162046	8.89E-09	Mono and Mac
RN7SL672P	2.97E-14	2.09781321	1.66E-09	Mono and Mac
TRIT1	1.20E-29	2.0987721	6.66E-25	Mono and Mac

TSPAN3	2.03E-102	2.10010256	1.13E-97	Mono and Mac
RASSF2	2.32E-110	2.10371038	1.29E-105	Mono and Mac
BYSL	2.25E-20	2.10569416	1.25E-15	Mono and Mac
RP11-110I1.6	1.97E-90	2.11293811	1.10E-85	Mono and Mac
RELL1	4.44E-57	2.11653144	2.48E-52	Mono and Mac
GNMT	1.39E-11	2.11811948	7.73E-07	Mono and Mac
LILRB1	2.18E-135	2.12036785	1.21E-130	Mono and Mac
AC109826.1	1.46E-15	2.12312209	8.13E-11	Mono and Mac
SUZ12P	2.11E-49	2.12324476	1.18E-44	Mono and Mac
HLA-DOA	1.21E-89	2.12337911	6.75E-85	Mono and Mac
PLAUR	2.32E-78	2.12556773	1.29E-73	Mono and Mac
CTA-384D8.35	2.70E-30	2.1262599	1.50E-25	Mono and Mac
MYOM1	2.18E-14	2.12802903	1.21E-09	Mono and Mac
RNF11	3.28E-64	2.13164003	1.83E-59	Mono and Mac
WDFY2	7.26E-92	2.13211807	4.05E-87	Mono and Mac
DHTKD1	2.10E-73	2.13493361	1.17E-68	Mono and Mac
ALCAM	7.82E-45	2.1355461	4.36E-40	Mono and Mac
RP4-647C14.3	2.55E-15	2.14139592	1.42E-10	Mono and Mac
EFHC1	1.36E-33	2.14745179	7.58E-29	Mono and Mac
RAB34	1.37E-31	2.14805556	7.62E-27	Mono and Mac
C20orf96	1.67E-12	2.14818745	9.30E-08	Mono and Mac
RP11-453F18--B.1	2.53E-10	2.14928763	1.41E-05	Mono and Mac
MED26	3.27E-39	2.15159637	1.82E-34	Mono and Mac
FGD2	1.90E-141	2.15383184	1.06E-136	Mono and Mac
TMED7-TICAM2	5.66E-11	2.15870734	3.15E-06	Mono and Mac
ST6GALNAC4	1.62E-106	2.16026666	9.02E-102	Mono and Mac
UCK2	4.84E-43	2.16355672	2.70E-38	Mono and Mac
TBC1D32	5.83E-41	2.16399035	3.25E-36	Mono and Mac
MRPS18AP1	1.73E-33	2.16519786	9.66E-29	Mono and Mac
ALDH1L2	5.53E-21	2.16715152	3.08E-16	Mono and Mac
CIITA	2.31E-136	2.16792197	1.29E-131	Mono and Mac
KCTD5	3.71E-48	2.16828954	2.07E-43	Mono and Mac
CTA-357J21.1	1.14E-10	2.16894195	6.36E-06	Mono and Mac
SERPIND1	5.19E-13	2.17136373	2.89E-08	Mono and Mac
TNFRSF17	1.60E-27	2.17234331	8.94E-23	Mono and Mac
NEURL	3.00E-12	2.17235482	1.67E-07	Mono and Mac
CCDC138	1.51E-60	2.17449929	8.41E-56	Mono and Mac
RP11-20I23.6	6.16E-19	2.1754072	3.44E-14	Mono and Mac
CAMKK1	6.01E-18	2.17566287	3.35E-13	Mono and Mac
INF2	1.06E-50	2.17610959	5.92E-46	Mono and Mac
WBP5	2.57E-18	2.17649911	1.43E-13	Mono and Mac
RP4-781K5.2	9.88E-63	2.17745078	5.50E-58	Mono and Mac

TNFSF13B	2.32E-81	2.17858335	1.30E-76	Mono and Mac
TNK2-AS1	1.46E-11	2.18447698	8.12E-07	Mono and Mac
TMEM88	1.65E-16	2.18549734	9.19E-12	Mono and Mac
P2RY1	6.30E-11	2.18612952	3.51E-06	Mono and Mac
ADAT3	7.07E-13	2.187036	3.94E-08	Mono and Mac
TTC28	9.98E-16	2.18730543	5.56E-11	Mono and Mac
DPYSL2	8.26E-121	2.19150661	4.60E-116	Mono and Mac
LILRB2	1.16E-54	2.194784	6.47E-50	Mono and Mac
ZDHHC4	2.31E-65	2.19491916	1.29E-60	Mono and Mac
SIGLEC5	1.11E-29	2.19528843	6.19E-25	Mono and Mac
HHEX	5.31E-19	2.19687055	2.96E-14	Mono and Mac
MZB1	1.39E-140	2.19820803	7.76E-136	Mono and Mac
SH3PXD2A	7.05E-34	2.20588664	3.93E-29	Mono and Mac
TATDN3	4.72E-72	2.20866687	2.63E-67	Mono and Mac
GPATCH11	1.43E-43	2.20977173	7.99E-39	Mono and Mac
RNU5A-1	6.62E-10	2.21183787	3.69E-05	Mono and Mac
DEXI	9.27E-59	2.21337813	5.16E-54	Mono and Mac
RP11-588L15.1	1.68E-23	2.2154573	9.34E-19	Mono and Mac
RP11-288H12.4	2.25E-15	2.21837334	1.25E-10	Mono and Mac
RP11-39K24.14	2.23E-10	2.21984819	1.24E-05	Mono and Mac
CTSZ	2.59E-13	2.22062092	1.44E-08	Mono and Mac
CTD-2012K14.4	3.13E-51	2.22193173	1.74E-46	Mono and Mac
SLC35A2	2.93E-90	2.22293109	1.63E-85	Mono and Mac
THEMIS2	3.30E-139	2.22370711	1.84E-134	Mono and Mac
PAPD7	2.94E-73	2.22698858	1.64E-68	Mono and Mac
RP11-300J18.3	2.03E-15	2.22737709	1.13E-10	Mono and Mac
NCF1B	7.95E-117	2.23296163	4.43E-112	Mono and Mac
RAP1GAP2	6.14E-70	2.23849895	3.42E-65	Mono and Mac
LAIR1	1.08E-109	2.23984019	6.02E-105	Mono and Mac
VASH1	1.30E-38	2.24329718	7.25E-34	Mono and Mac
PPP1R3B	2.55E-45	2.24664152	1.42E-40	Mono and Mac
IGHM	5.55E-172	2.25168924	3.10E-167	Mono and Mac
TMX2-CTNND1	4.61E-18	2.25170399	2.57E-13	Mono and Mac
CTD-2349P21.10	1.56E-29	2.25233313	8.68E-25	Mono and Mac
NEXN	1.95E-15	2.25434579	1.09E-10	Mono and Mac
FAM65A	1.64E-121	2.2545375	9.17E-117	Mono and Mac
ARL11	1.20E-17	2.25637906	6.71E-13	Mono and Mac
FOXRED2	1.88E-14	2.25655144	1.05E-09	Mono and Mac
GARNL3	8.50E-13	2.25660483	4.74E-08	Mono and Mac
RRBP1	1.16E-127	2.25714344	6.47E-123	Mono and Mac
RP11-108P20.1	5.38E-28	2.25784416	3.00E-23	Mono and Mac
SPNS3	1.23E-45	2.26375341	6.85E-41	Mono and Mac

SLC23A1	3.32E-26	2.26784308	1.85E-21	Mono and Mac
ITM2C	1.33E-151	2.27184002	7.44E-147	Mono and Mac
GPM6B	2.24E-69	2.2782391	1.25E-64	Mono and Mac
EIF2AK4	1.53E-114	2.27943579	8.51E-110	Mono and Mac
TXNDC5	3.77E-93	2.28385365	2.10E-88	Mono and Mac
PLAC8	1.14E-153	2.284235	6.36E-149	Mono and Mac
TLR10	1.50E-48	2.28583235	8.36E-44	Mono and Mac
C15orf39	3.47E-104	2.28674415	1.93E-99	Mono and Mac
C10orf129	1.19E-10	2.28758999	6.63E-06	Mono and Mac
RNU12	6.64E-72	2.29049654	3.70E-67	Mono and Mac
CTD-2012K14.3	3.83E-19	2.29104918	2.14E-14	Mono and Mac
EIF4EBP3	3.82E-33	2.29257236	2.13E-28	Mono and Mac
PTGES3L	1.04E-11	2.29446181	5.81E-07	Mono and Mac
DENND5B	2.85E-28	2.29588686	1.59E-23	Mono and Mac
FUZ	7.81E-64	2.29921826	4.36E-59	Mono and Mac
RNU2-6P	1.95E-18	2.30088656	1.09E-13	Mono and Mac
FCGRT	3.03E-111	2.30116822	1.69E-106	Mono and Mac
RP11-832A4.5	1.23E-09	2.30650079	6.86E-05	Mono and Mac
RP11-147L13.2	2.29E-78	2.30858215	1.28E-73	Mono and Mac
CTD-2545M3.6	3.20E-19	2.30897452	1.78E-14	Mono and Mac
TAX1BP3	7.96E-72	2.31204225	4.44E-67	Mono and Mac
POLB	2.71E-136	2.31563579	1.51E-131	Mono and Mac
DFNB59	2.02E-12	2.31668621	1.12E-07	Mono and Mac
RP11-20I23.8	3.01E-35	2.32130676	1.68E-30	Mono and Mac
KIRREL2	6.82E-13	2.3225644	3.80E-08	Mono and Mac
MOXD1	1.85E-24	2.32480397	1.03E-19	Mono and Mac
PKIB	4.85E-14	2.32529444	2.71E-09	Mono and Mac
PPT2	6.67E-37	2.32647784	3.72E-32	Mono and Mac
MOB1B	1.10E-85	2.3300667	6.14E-81	Mono and Mac
IFIT2	5.14E-56	2.33047776	2.86E-51	Mono and Mac
MYO1E	1.26E-80	2.33064742	7.03E-76	Mono and Mac
MPZL1	2.13E-49	2.3342757	1.19E-44	Mono and Mac
CDYL	2.74E-54	2.33899049	1.52E-49	Mono and Mac
RP11-11N7.4	6.08E-10	2.34016375	3.39E-05	Mono and Mac
FCHSD2	1.37E-143	2.34460249	7.63E-139	Mono and Mac
MEF2C	6.07E-138	2.34603174	3.38E-133	Mono and Mac
FEZ2	6.82E-27	2.34650208	3.80E-22	Mono and Mac
MCC	4.86E-36	2.34667918	2.71E-31	Mono and Mac
GPR157	5.94E-13	2.34956215	3.31E-08	Mono and Mac
IGSF6	5.76E-60	2.35193345	3.21E-55	Mono and Mac
DPY19L1P1	4.50E-14	2.35413	2.51E-09	Mono and Mac
MYO15B	2.31E-85	2.35694296	1.29E-80	Mono and Mac

RPS6KA2	1.13E-57	2.35739762	6.32E-53	Mono and Mac
SEPHS1	1.28E-64	2.35972118	7.14E-60	Mono and Mac
UGCG	4.92E-150	2.36241514	2.74E-145	Mono and Mac
IDH3A	2.08E-126	2.36253168	1.16E-121	Mono and Mac
TP53I11	4.79E-102	2.36279131	2.67E-97	Mono and Mac
EFNB1	2.28E-12	2.36402866	1.27E-07	Mono and Mac
FES	1.58E-43	2.36708172	8.83E-39	Mono and Mac
SLC2A6	7.68E-64	2.36752014	4.28E-59	Mono and Mac
AC017116.11	3.11E-30	2.36982321	1.73E-25	Mono and Mac
ARHGAP24	5.41E-77	2.37099195	3.01E-72	Mono and Mac
RECQL5	2.05E-78	2.37251618	1.14E-73	Mono and Mac
CLN8	1.30E-131	2.37921965	7.27E-127	Mono and Mac
MYB	3.18E-30	2.38490489	1.77E-25	Mono and Mac
MORN1	2.94E-16	2.38662221	1.64E-11	Mono and Mac
RP11-126K1.6	1.54E-09	2.38664498	8.57E-05	Mono and Mac
RAB40B	1.39E-27	2.38677383	7.76E-23	Mono and Mac
RP3-508I15.14	1.63E-12	2.3876757	9.10E-08	Mono and Mac
TMEM170B	1.48E-09	2.39307235	8.25E-05	Mono and Mac
SRD5A1	1.78E-48	2.39665667	9.90E-44	Mono and Mac
RNU5D-1	1.48E-10	2.39669459	8.25E-06	Mono and Mac
C16orf86	1.77E-15	2.39758948	9.88E-11	Mono and Mac
RP11-1020A11.2	1.61E-09	2.4008288	8.97E-05	Mono and Mac
TBX19	1.02E-31	2.4011963	5.67E-27	Mono and Mac
ALG2	3.46E-117	2.4027532	1.93E-112	Mono and Mac
EFCAB2	5.87E-19	2.40475595	3.27E-14	Mono and Mac
AC010761.9	1.92E-13	2.40814023	1.07E-08	Mono and Mac
IRF8	6.42E-166	2.40860372	3.58E-161	Mono and Mac
TGFBR1	3.77E-94	2.40861187	2.10E-89	Mono and Mac
MAML3	2.22E-17	2.40869525	1.24E-12	Mono and Mac
LYN	4.52E-118	2.41074466	2.52E-113	Mono and Mac
CERS6	2.55E-40	2.41163128	1.42E-35	Mono and Mac
AC026150.8	6.65E-31	2.42179847	3.71E-26	Mono and Mac
RP11-793I11.1	4.08E-18	2.42449269	2.27E-13	Mono and Mac
CD302	1.60E-50	2.42925295	8.92E-46	Mono and Mac
CDH23	4.11E-32	2.43257789	2.29E-27	Mono and Mac
TRIP10	5.63E-34	2.43610482	3.14E-29	Mono and Mac
MS4A4A	8.97E-28	2.43648827	5.00E-23	Mono and Mac
ZNF891	2.60E-24	2.43738642	1.45E-19	Mono and Mac
DST	1.79E-42	2.43849595	1.00E-37	Mono and Mac
PRKAR2B	7.27E-16	2.44254713	4.05E-11	Mono and Mac
AC005488.11	2.15E-13	2.44435705	1.20E-08	Mono and Mac
BTK	6.98E-98	2.45395865	3.89E-93	Mono and Mac

COBLL1	2.54E-129	2.45512874	1.42E-124	Mono and Mac
LILRB5	6.24E-164	2.45779743	3.48E-159	Mono and Mac
DUSP3	8.38E-63	2.45810716	4.67E-58	Mono and Mac
NME4	1.27E-32	2.46381285	7.10E-28	Mono and Mac
GALNT3	8.62E-82	2.46448297	4.81E-77	Mono and Mac
LINC01059	4.90E-34	2.46556921	2.73E-29	Mono and Mac
PHF16	3.39E-15	2.46579464	1.89E-10	Mono and Mac
EEPD1	4.70E-27	2.46735898	2.62E-22	Mono and Mac
CXorf21	5.92E-65	2.46803418	3.30E-60	Mono and Mac
MS4A6A	2.83E-129	2.47043237	1.58E-124	Mono and Mac
MYOF	1.38E-45	2.47579665	7.70E-41	Mono and Mac
PDXP	1.50E-19	2.47669161	8.38E-15	Mono and Mac
ARHGEF10	8.33E-13	2.47670412	4.64E-08	Mono and Mac
PTP4A3	1.95E-60	2.47670704	1.09E-55	Mono and Mac
RNU1-60P	4.84E-67	2.47793273	2.70E-62	Mono and Mac
SCARB2	1.08E-109	2.47822361	6.00E-105	Mono and Mac
HDAC9	2.70E-98	2.48406138	1.51E-93	Mono and Mac
SH3D19	1.99E-25	2.48587579	1.11E-20	Mono and Mac
NIPSNAP3B	1.09E-15	2.48653321	6.09E-11	Mono and Mac
RP11-632K20.2	3.17E-10	2.48698812	1.77E-05	Mono and Mac
HVCN1	2.29E-140	2.48718119	1.28E-135	Mono and Mac
RP11-861A13.4	1.42E-43	2.48839492	7.91E-39	Mono and Mac
SMIM14	2.81E-137	2.48907739	1.57E-132	Mono and Mac
LSM3P2	1.91E-26	2.49105011	1.07E-21	Mono and Mac
NCF1C	9.11E-163	2.49657904	5.08E-158	Mono and Mac
TRPM4	5.46E-17	2.50038404	3.05E-12	Mono and Mac
RN7SL402P	3.51E-26	2.50177284	1.96E-21	Mono and Mac
TMCC3	9.08E-35	2.50508043	5.06E-30	Mono and Mac
CTA-384D8.34	3.81E-41	2.50957152	2.12E-36	Mono and Mac
DNAH11	1.71E-18	2.50995036	9.53E-14	Mono and Mac
DYRK3	7.66E-10	2.51963091	4.27E-05	Mono and Mac
CXXC5	9.31E-45	2.52056816	5.19E-40	Mono and Mac
CD300LB	2.08E-27	2.52430885	1.16E-22	Mono and Mac
C9orf91	1.94E-34	2.5276579	1.08E-29	Mono and Mac
RP13-977J11.5	5.29E-16	2.52826909	2.95E-11	Mono and Mac
RP3-475N16.1	8.57E-43	2.53147757	4.78E-38	Mono and Mac
RP11-20I23.13	7.25E-46	2.53177702	4.04E-41	Mono and Mac
SIRPB1	1.32E-84	2.53193567	7.33E-80	Mono and Mac
GNA12	1.03E-82	2.53425627	5.73E-78	Mono and Mac
GMPR	1.93E-25	2.53463379	1.07E-20	Mono and Mac
RP3-402G11.25	4.03E-21	2.53849361	2.25E-16	Mono and Mac
SPATC1	3.35E-12	2.53916177	1.87E-07	Mono and Mac

CCR3	4.84E-21	2.53922511	2.70E-16	Mono and Mac
CYB561A3	2.28E-177	2.54229051	1.27E-172	Mono and Mac
PTGIR	1.39E-16	2.54432445	7.74E-12	Mono and Mac
BEND5	5.78E-19	2.54460187	3.22E-14	Mono and Mac
RBM47	1.36E-79	2.54473092	7.60E-75	Mono and Mac
AC016700.5	1.48E-17	2.55073777	8.24E-13	Mono and Mac
RP1-257A7.5	4.41E-159	2.55654936	2.46E-154	Mono and Mac
RP11-661A12.5	1.43E-13	2.56183146	7.94E-09	Mono and Mac
SNX29P1	8.07E-30	2.56764758	4.50E-25	Mono and Mac
PLCB3	1.01E-52	2.56889365	5.61E-48	Mono and Mac
TUBB6	1.00E-69	2.57318539	5.58E-65	Mono and Mac
SLC29A1	2.23E-53	2.57387399	1.24E-48	Mono and Mac
RP13-395E19.3	1.16E-10	2.57779364	6.48E-06	Mono and Mac
GOLGA8R	2.45E-13	2.57926299	1.37E-08	Mono and Mac
KYNU	4.74E-95	2.58365881	2.64E-90	Mono and Mac
FLJ00273	1.51E-10	2.5850658	8.43E-06	Mono and Mac
MRPL37P1	3.20E-29	2.58877766	1.79E-24	Mono and Mac
H1F0	1.32E-35	2.59063798	7.38E-31	Mono and Mac
PAIP2B	1.80E-24	2.59288765	1.00E-19	Mono and Mac
AC067852.1	3.88E-10	2.59525587	2.16E-05	Mono and Mac
GHRL	2.21E-42	2.59658393	1.23E-37	Mono and Mac
PINLYP	8.83E-11	2.61286338	4.92E-06	Mono and Mac
PTK2	2.88E-65	2.61298392	1.61E-60	Mono and Mac
PHACTR1	5.55E-106	2.62255679	3.09E-101	Mono and Mac
CORO1C	1.60E-173	2.62352765	8.92E-169	Mono and Mac
ATP13A2	2.10E-75	2.62551119	1.17E-70	Mono and Mac
MROH8	5.98E-16	2.6256354	3.33E-11	Mono and Mac
FADS2	1.35E-70	2.62739899	7.54E-66	Mono and Mac
RP11-523O18.5	5.64E-15	2.62990015	3.14E-10	Mono and Mac
ALG1L2	9.33E-12	2.63349821	5.20E-07	Mono and Mac
CCDC106	2.09E-27	2.63444119	1.16E-22	Mono and Mac
ST3GAL2	1.42E-87	2.63557009	7.93E-83	Mono and Mac
SYK	1.77E-150	2.63642784	9.86E-146	Mono and Mac
CERS6-AS1	1.10E-48	2.63870771	6.14E-44	Mono and Mac
FNBP1L	6.15E-11	2.63937278	3.43E-06	Mono and Mac
TICAM2	4.63E-17	2.6409488	2.58E-12	Mono and Mac
AP001056.1	1.88E-16	2.64183398	1.05E-11	Mono and Mac
RP11-426K3.1	3.53E-12	2.6422863	1.97E-07	Mono and Mac
GNA15	1.40E-166	2.64276204	7.79E-162	Mono and Mac
RP11-325K4.2	1.29E-44	2.64402822	7.18E-40	Mono and Mac
NUDT17	5.80E-27	2.64634525	3.23E-22	Mono and Mac
RP11-8L8.2	1.88E-12	2.64676115	1.05E-07	Mono and Mac

AC012314.19	1.52E-12	2.64829328	8.48E-08	Mono and Mac
ZDHHC17	7.58E-145	2.65199621	4.22E-140	Mono and Mac
TFEC	4.99E-48	2.6529638	2.78E-43	Mono and Mac
CLIC3	7.36E-198	2.6530327	4.10E-193	Mono and Mac
BSPRY	1.42E-17	2.65856982	7.91E-13	Mono and Mac
TBC1D9	6.06E-51	2.65971761	3.37E-46	Mono and Mac
ULK4P2	3.21E-12	2.66264249	1.79E-07	Mono and Mac
TYROBP	1.31E-220	2.67108271	7.31E-216	Mono and Mac
TEX14	3.91E-18	2.67429205	2.18E-13	Mono and Mac
KLF4	3.36E-78	2.67452656	1.88E-73	Mono and Mac
KCNH8	9.18E-19	2.67504969	5.12E-14	Mono and Mac
AKR1C3	2.99E-39	2.68761711	1.67E-34	Mono and Mac
PRRT1	1.90E-12	2.6888247	1.06E-07	Mono and Mac
ZRANB2-AS2	3.22E-10	2.68901174	1.80E-05	Mono and Mac
LINC00877	1.68E-27	2.68903906	9.36E-23	Mono and Mac
MGLL	2.86E-75	2.69089027	1.60E-70	Mono and Mac
STAP1	8.20E-141	2.69096852	4.57E-136	Mono and Mac
MFSD2A	5.64E-27	2.69195836	3.14E-22	Mono and Mac
C5orf34	2.30E-18	2.69454636	1.28E-13	Mono and Mac
GLCE	3.78E-44	2.69685573	2.11E-39	Mono and Mac
RP11-54O7.17	1.48E-17	2.69792743	8.24E-13	Mono and Mac
LINC00106	8.50E-28	2.69821089	4.74E-23	Mono and Mac
SLC9A7	2.87E-42	2.69952437	1.60E-37	Mono and Mac
FCER1G	2.86E-209	2.69959191	1.60E-204	Mono and Mac
RP11-432J24.3	1.66E-09	2.70028271	9.23E-05	Mono and Mac
SLC2A9	3.08E-28	2.70169161	1.72E-23	Mono and Mac
HOMER1	1.21E-28	2.70394357	6.76E-24	Mono and Mac
RIMS3	3.37E-20	2.70478724	1.88E-15	Mono and Mac
LRRK1	3.18E-64	2.70610664	1.77E-59	Mono and Mac
RP1-111C20.3	3.87E-16	2.7174512	2.15E-11	Mono and Mac
FZD3	2.03E-94	2.71808505	1.13E-89	Mono and Mac
HIGD1AP1	1.60E-26	2.722547	8.94E-22	Mono and Mac
FAM95B1	7.21E-15	2.72391841	4.02E-10	Mono and Mac
GRAMD1B	1.19E-76	2.7254178	6.61E-72	Mono and Mac
PNLDC1	6.54E-10	2.72615215	3.64E-05	Mono and Mac
KB-1507C5.4	1.31E-09	2.7278561	7.28E-05	Mono and Mac
BAIAP2	6.51E-90	2.72808716	3.63E-85	Mono and Mac
RPS6KL1	2.39E-11	2.72878903	1.33E-06	Mono and Mac
LILRA5	8.42E-109	2.73080213	4.69E-104	Mono and Mac
AC005532.5	1.77E-11	2.73514805	9.89E-07	Mono and Mac
TTTY14	8.35E-11	2.73531461	4.66E-06	Mono and Mac
TJP2	2.20E-22	2.7374689	1.23E-17	Mono and Mac

CD2AP	1.16E-145	2.73763161	6.48E-141	Mono and Mac
SPINT2	3.30E-169	2.73810894	1.84E-164	Mono and Mac
RP11-126O1.4	9.15E-17	2.74098823	5.10E-12	Mono and Mac
SLIT1	6.60E-11	2.7459577	3.68E-06	Mono and Mac
REPIN1	1.71E-78	2.74715475	9.56E-74	Mono and Mac
RPPH1	9.72E-45	2.74962074	5.42E-40	Mono and Mac
RP11-325K4.3	2.42E-42	2.75506234	1.35E-37	Mono and Mac
MYOM2	4.10E-36	2.76438655	2.29E-31	Mono and Mac
ARID3A	4.26E-128	2.76948072	2.37E-123	Mono and Mac
PNOC	1.41E-53	2.77020622	7.86E-49	Mono and Mac
RPS6KA4	1.65E-155	2.7710063	9.21E-151	Mono and Mac
RP11-726G1.1	5.38E-58	2.771639	3.00E-53	Mono and Mac
AC005776.1	5.02E-11	2.77165132	2.80E-06	Mono and Mac
IFNLR1	2.31E-85	2.77220612	1.29E-80	Mono and Mac
KIAA1984-AS1	6.16E-43	2.7723561	3.44E-38	Mono and Mac
CLMN	1.87E-39	2.77640257	1.04E-34	Mono and Mac
RBPMS	3.03E-29	2.77708007	1.69E-24	Mono and Mac
CD180	1.42E-64	2.77757771	7.91E-60	Mono and Mac
RP11-24F11.2	2.81E-48	2.77954699	1.57E-43	Mono and Mac
C2orf81	1.25E-17	2.78132628	6.97E-13	Mono and Mac
RP11-512H23.2	7.14E-12	2.78206233	3.98E-07	Mono and Mac
DCLK2	4.59E-16	2.78832007	2.56E-11	Mono and Mac
HES4	1.19E-09	2.78943167	6.65E-05	Mono and Mac
RNF144B	9.38E-124	2.7900638	5.23E-119	Mono and Mac
RP5-827C21.6	1.58E-10	2.79488326	8.82E-06	Mono and Mac
AXL	4.53E-52	2.79877492	2.52E-47	Mono and Mac
SEPHS1P1	6.91E-12	2.80212676	3.85E-07	Mono and Mac
AP001046.5	1.22E-52	2.80794639	6.82E-48	Mono and Mac
MROH6	7.90E-11	2.81361411	4.40E-06	Mono and Mac
RP11-642P15.1	4.72E-21	2.81408508	2.63E-16	Mono and Mac
C11orf74	3.82E-10	2.81764515	2.13E-05	Mono and Mac
HS3ST1	2.37E-24	2.82015419	1.32E-19	Mono and Mac
ZNF467	1.14E-14	2.82076969	6.36E-10	Mono and Mac
KIAA1377	1.15E-25	2.82270889	6.39E-21	Mono and Mac
ARHGAP31	1.36E-93	2.82635838	7.59E-89	Mono and Mac
GSN	1.12E-141	2.83524974	6.24E-137	Mono and Mac
F13A1	7.70E-55	2.83981948	4.29E-50	Mono and Mac
C16orf93	1.29E-29	2.84681213	7.19E-25	Mono and Mac
C12orf45	4.32E-119	2.85094012	2.41E-114	Mono and Mac
KMO	5.83E-63	2.85101606	3.25E-58	Mono and Mac
RP4-791C19.1	3.69E-16	2.85509418	2.05E-11	Mono and Mac
PMP22	4.09E-41	2.85657982	2.28E-36	Mono and Mac

NRROS	1.54E-81	2.85763249	8.60E-77	Mono and Mac
UBE2E2	1.91E-133	2.8593968	1.06E-128	Mono and Mac
ENTPD7	1.37E-64	2.86645633	7.65E-60	Mono and Mac
CLIC2	1.69E-35	2.867566	9.43E-31	Mono and Mac
SLC22A1	1.35E-22	2.86836757	7.52E-18	Mono and Mac
ASAP2	6.68E-26	2.86870667	3.72E-21	Mono and Mac
RP11-449P15.1	1.77E-11	2.86989522	9.87E-07	Mono and Mac
SH2B3	2.81E-190	2.87014715	1.57E-185	Mono and Mac
GPRC5B	2.50E-12	2.87153748	1.39E-07	Mono and Mac
LINC00984	1.53E-28	2.87832171	8.52E-24	Mono and Mac
RNF130	1.64E-194	2.88424695	9.15E-190	Mono and Mac
RP11-229P13.20	2.48E-15	2.88618729	1.38E-10	Mono and Mac
UNC93B1	1.04E-80	2.88776292	5.81E-76	Mono and Mac
RUFY4	3.86E-106	2.8970816	2.15E-101	Mono and Mac
RP11-395G23.3	5.60E-10	2.89769648	3.12E-05	Mono and Mac
AP000783.1	1.08E-33	2.89990877	6.03E-29	Mono and Mac
SLC41A2	2.06E-159	2.90499318	1.15E-154	Mono and Mac
MIR181A2HG	2.67E-18	2.91133073	1.49E-13	Mono and Mac
KPTN	1.74E-53	2.91443317	9.70E-49	Mono and Mac
AL022328.1	3.60E-57	2.91729343	2.01E-52	Mono and Mac
TSPYL5	5.14E-15	2.91771173	2.87E-10	Mono and Mac
RDH12	2.22E-12	2.91997446	1.24E-07	Mono and Mac
CCDC50	4.88E-215	2.92128137	2.72E-210	Mono and Mac
HLX	4.04E-18	2.92600596	2.25E-13	Mono and Mac
MAP2K6	5.71E-106	2.92611829	3.18E-101	Mono and Mac
CYBB	1.38E-246	2.92946673	7.69E-242	Mono and Mac
AFF3	3.64E-171	2.93006518	2.03E-166	Mono and Mac
RNF165	4.21E-17	2.93071273	2.34E-12	Mono and Mac
ZNF816-ZNF321P	4.89E-17	2.93384837	2.73E-12	Mono and Mac
TBC1D8	1.82E-93	2.93454045	1.02E-88	Mono and Mac
GPR146	1.11E-33	2.93523741	6.18E-29	Mono and Mac
MTSS1L	1.08E-17	2.9380798	6.00E-13	Mono and Mac
SLC12A7	1.46E-125	2.94006597	8.15E-121	Mono and Mac
INSR	4.31E-112	2.94196786	2.40E-107	Mono and Mac
CTD-3222D19.5	4.30E-41	2.9507303	2.39E-36	Mono and Mac
OSBPL1A	1.53E-17	2.95189461	8.55E-13	Mono and Mac
SOX15	3.39E-13	2.95583123	1.89E-08	Mono and Mac
FLNB	5.25E-176	2.96158784	2.93E-171	Mono and Mac
BCYRN1	1.82E-09	2.96488115	1.01E-04	Mono and Mac
AMIGO3	9.43E-140	2.96530573	5.26E-135	Mono and Mac
KIAA1598	6.93E-79	2.96897887	3.86E-74	Mono and Mac
SIRPD	3.30E-22	2.96993533	1.84E-17	Mono and Mac

SLC47A1	7.63E-13	2.97200721	4.25E-08	Mono and Mac
DAPK1	4.55E-96	2.97945964	2.54E-91	Mono and Mac
AL122127.25	4.58E-14	2.9894999	2.56E-09	Mono and Mac
RP11-589N15.2	5.70E-40	2.99360583	3.17E-35	Mono and Mac
IGFBP3	2.79E-71	2.99453103	1.55E-66	Mono and Mac
RP11-341G23.4	9.28E-10	2.99627509	5.17E-05	Mono and Mac
VEGFB	1.12E-119	2.99799047	6.22E-115	Mono and Mac
LPAR1	2.59E-11	2.99888178	1.44E-06	Mono and Mac
RP11-425I13.3	6.40E-15	2.99988526	3.57E-10	Mono and Mac
TRAF4	2.46E-228	3.00609906	1.37E-223	Mono and Mac
CNTNAP1	1.50E-35	3.01305002	8.37E-31	Mono and Mac
CCR10	2.61E-52	3.01962445	1.46E-47	Mono and Mac
PLAU	1.25E-27	3.01978835	6.95E-23	Mono and Mac
C9orf139	1.36E-14	3.02557847	7.56E-10	Mono and Mac
PTPRO	7.51E-39	3.03116732	4.18E-34	Mono and Mac
C20orf26	3.23E-12	3.03265178	1.80E-07	Mono and Mac
CD68	1.89E-256	3.04361695	1.05E-251	Mono and Mac
CTD-3222D19.2	1.72E-11	3.04635952	9.58E-07	Mono and Mac
RP11-302F12.10	4.29E-79	3.05093252	2.39E-74	Mono and Mac
AC068282.3	1.18E-38	3.05386484	6.56E-34	Mono and Mac
AC096579.7	0.00E+00	3.05590629	0.00E+00	Mono and Mac
PLXNB2	4.57E-185	3.06353899	2.54E-180	Mono and Mac
BLNK	1.00E-229	3.06382929	5.57E-225	Mono and Mac
FAM177B	2.26E-67	3.06780631	1.26E-62	Mono and Mac
FADS1	7.66E-100	3.06814726	4.27E-95	Mono and Mac
RP11-385F7.1	8.08E-20	3.07463903	4.50E-15	Mono and Mac
KIAA0226L	7.70E-239	3.07733217	4.29E-234	Mono and Mac
ABCA9	4.66E-12	3.07879231	2.60E-07	Mono and Mac
RGS13	1.02E-73	3.07914652	5.71E-69	Mono and Mac
SPRED2	1.16E-69	3.08250253	6.48E-65	Mono and Mac
GNG7	9.29E-192	3.08458096	5.18E-187	Mono and Mac
TTYH2	9.15E-89	3.08565799	5.10E-84	Mono and Mac
IQSEC3	5.67E-26	3.09036466	3.16E-21	Mono and Mac
KANK1	2.55E-35	3.09636377	1.42E-30	Mono and Mac
PDGFB	1.33E-27	3.09643312	7.41E-23	Mono and Mac
ICOSLG	2.18E-130	3.09882355	1.22E-125	Mono and Mac
TREML2	2.83E-68	3.10084505	1.58E-63	Mono and Mac
CPED1	1.28E-35	3.10709015	7.11E-31	Mono and Mac
RP11-300J18.1	2.62E-10	3.11166698	1.46E-05	Mono and Mac
FAAH	5.62E-37	3.11432917	3.13E-32	Mono and Mac
ALDH7A1	1.62E-12	3.11560688	9.05E-08	Mono and Mac
FTCDNL1	2.47E-25	3.11589203	1.38E-20	Mono and Mac

RP4-536B24.4	6.53E-12	3.11977813	3.64E-07	Mono and Mac
SPG20	5.51E-176	3.12191197	3.07E-171	Mono and Mac
TTC26	2.17E-19	3.12255959	1.21E-14	Mono and Mac
FLG-AS1	2.00E-14	3.12274605	1.11E-09	Mono and Mac
P2RX1	7.12E-151	3.1272987	3.97E-146	Mono and Mac
WDFY4	1.76E-265	3.13288365	9.81E-261	Mono and Mac
CTD-2514K5.4	2.40E-64	3.13736982	1.34E-59	Mono and Mac
VNN1	2.23E-11	3.13807556	1.24E-06	Mono and Mac
AMZ1	1.07E-49	3.14139438	5.97E-45	Mono and Mac
AC009404.2	4.32E-42	3.14185505	2.41E-37	Mono and Mac
RP11-282I1.1	1.67E-09	3.14294009	9.29E-05	Mono and Mac
RP11-141J13.4	6.64E-12	3.14460057	3.70E-07	Mono and Mac
MFI2	1.18E-16	3.1454911	6.56E-12	Mono and Mac
SOGA1	4.52E-97	3.15251542	2.52E-92	Mono and Mac
CTD-2165H16.3	2.48E-11	3.1640842	1.38E-06	Mono and Mac
TRPM2	3.29E-137	3.16621292	1.84E-132	Mono and Mac
TMIGD2	4.90E-130	3.16989073	2.73E-125	Mono and Mac
CTD-2349P21.5	2.46E-11	3.17167619	1.37E-06	Mono and Mac
RP4-576H24.4	3.39E-28	3.17250629	1.89E-23	Mono and Mac
ABHD15	7.19E-136	3.17472061	4.01E-131	Mono and Mac
AC010761.10	3.79E-78	3.17954318	2.11E-73	Mono and Mac
MME	1.90E-10	3.18345664	1.06E-05	Mono and Mac
DERL3	6.39E-284	3.18785108	3.56E-279	Mono and Mac
UPK3A	2.33E-22	3.18912875	1.30E-17	Mono and Mac
RP11-68I3.2	4.05E-30	3.19931682	2.26E-25	Mono and Mac
RP11-123J14.2	2.47E-47	3.20492227	1.38E-42	Mono and Mac
BAIAP2-AS1	1.29E-19	3.20674416	7.20E-15	Mono and Mac
CST3	4.82E-303	3.20911811	2.68E-298	Mono and Mac
RP11-505E24.2	2.35E-10	3.20971368	1.31E-05	Mono and Mac
MED12L	1.06E-40	3.21064846	5.91E-36	Mono and Mac
AC009495.2	5.12E-45	3.21628758	2.85E-40	Mono and Mac
CCDC88A	2.02E-220	3.22072523	1.13E-215	Mono and Mac
DCBLD2	1.99E-10	3.2313488	1.11E-05	Mono and Mac
SCARB1	1.03E-118	3.23270774	5.74E-114	Mono and Mac
NAPSA	8.26E-168	3.23359641	4.61E-163	Mono and Mac
RP11-105N14.1	4.58E-11	3.23570978	2.55E-06	Mono and Mac
RP11-122A3.2	4.71E-15	3.23864852	2.63E-10	Mono and Mac
TFPI	2.65E-10	3.24040761	1.48E-05	Mono and Mac
HRH2	6.42E-93	3.24056994	3.58E-88	Mono and Mac
RP11-235E17.6	2.52E-18	3.24485424	1.40E-13	Mono and Mac
CHML	7.74E-52	3.24593897	4.32E-47	Mono and Mac
SULF2	1.85E-217	3.2486357	1.03E-212	Mono and Mac

RPP25	1.54E-47	3.24926526	8.59E-43	Mono and Mac
AMN	7.60E-12	3.25286372	4.24E-07	Mono and Mac
RP11-443B7.1	7.66E-26	3.25408324	4.27E-21	Mono and Mac
UNC93B2	8.95E-10	3.25507122	4.99E-05	Mono and Mac
ATF5	1.06E-172	3.26726686	5.92E-168	Mono and Mac
CTD-2643K12.3	2.42E-11	3.26732567	1.35E-06	Mono and Mac
CYCSP52	3.70E-30	3.26872923	2.06E-25	Mono and Mac
LY6G6C	5.48E-11	3.2705525	3.05E-06	Mono and Mac
CRYBG3	1.81E-96	3.27145126	1.01E-91	Mono and Mac
HSPG2	1.11E-38	3.27402431	6.18E-34	Mono and Mac
RNVU1-6	5.41E-40	3.27478216	3.02E-35	Mono and Mac
RGS18	2.14E-70	3.27535445	1.19E-65	Mono and Mac
GRASP	1.26E-211	3.27583645	7.02E-207	Mono and Mac
ULK4P1	4.75E-13	3.27676033	2.65E-08	Mono and Mac
DMD	2.59E-31	3.27854727	1.44E-26	Mono and Mac
RNU6-672P	9.16E-10	3.28307202	5.10E-05	Mono and Mac
LHFPL2	1.66E-72	3.28308164	9.28E-68	Mono and Mac
FCER1A	1.17E-34	3.28462763	6.53E-30	Mono and Mac
ZNF618	2.93E-27	3.28530778	1.63E-22	Mono and Mac
SCRN1	4.67E-104	3.2881587	2.60E-99	Mono and Mac
KCNG2	6.71E-12	3.29292258	3.74E-07	Mono and Mac
WNT10A	2.33E-53	3.30212254	1.30E-48	Mono and Mac
FSTL3	2.11E-15	3.30825853	1.18E-10	Mono and Mac
TEX2	3.05E-149	3.31263548	1.70E-144	Mono and Mac
STARD4-AS1	2.59E-50	3.31364407	1.44E-45	Mono and Mac
ADC	8.82E-92	3.32032253	4.92E-87	Mono and Mac
SLC15A4	2.14E-275	3.32213197	1.19E-270	Mono and Mac
C4orf19	6.70E-21	3.32724604	3.73E-16	Mono and Mac
ALDH2	2.23E-192	3.32953131	1.24E-187	Mono and Mac
RP11-843A23.1	1.70E-23	3.33644696	9.45E-19	Mono and Mac
CTD-2044J15.2	1.17E-29	3.35345949	6.50E-25	Mono and Mac
TMEM144	1.88E-56	3.36100093	1.05E-51	Mono and Mac
RP11-603J24.6	1.68E-09	3.36164401	9.37E-05	Mono and Mac
SH3RF3	1.12E-33	3.36321127	6.23E-29	Mono and Mac
RP11-354M1.2	2.61E-10	3.36731725	1.45E-05	Mono and Mac
CXCR2	1.22E-31	3.37413801	6.80E-27	Mono and Mac
MGST1	1.82E-36	3.37938778	1.01E-31	Mono and Mac
MEIS1	1.26E-14	3.38026227	7.05E-10	Mono and Mac
PLA2G4A	1.21E-44	3.38751783	6.76E-40	Mono and Mac
RP11-803P9.1	1.63E-23	3.39613665	9.09E-19	Mono and Mac
TCEB1P28	5.46E-11	3.39847748	3.04E-06	Mono and Mac
AC019181.2	6.36E-14	3.40592657	3.54E-09	Mono and Mac

DAB2	2.98E-109	3.40975824	1.66E-104	Mono and Mac
CTNS	6.82E-180	3.41744123	3.80E-175	Mono and Mac
TGFBI	0.00E+00	3.4180501	0.00E+00	Mono and Mac
RP1-168P16.1	7.36E-20	3.42622011	4.10E-15	Mono and Mac
RP11-534L6.3	6.45E-13	3.43524276	3.60E-08	Mono and Mac
PMEPA1	1.17E-155	3.43693949	6.49E-151	Mono and Mac
AC097658.1	2.49E-78	3.43776625	1.39E-73	Mono and Mac
RP11-356J5.12	6.74E-47	3.44378376	3.75E-42	Mono and Mac
MGST2	2.33E-191	3.45150234	1.30E-186	Mono and Mac
RP11-108P20.2	2.30E-10	3.45267697	1.28E-05	Mono and Mac
RP1-244F24.1	6.61E-23	3.46386318	3.68E-18	Mono and Mac
IGJ	0.00E+00	3.4650979	0.00E+00	Mono and Mac
CTD-2306M10.1	1.12E-25	3.46855564	6.25E-21	Mono and Mac
CTB-50L17.5	4.42E-25	3.4746865	2.47E-20	Mono and Mac
AC005264.2	1.67E-77	3.47662418	9.30E-73	Mono and Mac
ELOVL2	1.53E-12	3.47670536	8.53E-08	Mono and Mac
SEMA7A	1.34E-250	3.48087667	7.49E-246	Mono and Mac
APCDD1	8.10E-23	3.48935	4.51E-18	Mono and Mac
CTD-2287O16.5	7.77E-64	3.49172417	4.33E-59	Mono and Mac
RNASE6	0.00E+00	3.49229265	0.00E+00	Mono and Mac
BCL7A	9.93E-142	3.4938985	5.53E-137	Mono and Mac
DPPA3P2	5.36E-11	3.49632353	2.99E-06	Mono and Mac
RP4-536B24.3	3.44E-13	3.49721422	1.91E-08	Mono and Mac
LGMN	1.09E-265	3.49801618	6.09E-261	Mono and Mac
CCDC102B	2.41E-45	3.5195637	1.34E-40	Mono and Mac
CSF2RA	2.48E-243	3.5239613	1.38E-238	Mono and Mac
SERPING1	5.13E-174	3.52572689	2.86E-169	Mono and Mac
BCL11A	0.00E+00	3.5274058	0.00E+00	Mono and Mac
RYR3	5.43E-16	3.54964059	3.02E-11	Mono and Mac
CRLF2	4.65E-61	3.54977568	2.59E-56	Mono and Mac
PHEX	7.56E-212	3.5503996	4.22E-207	Mono and Mac
ARL5C	4.67E-22	3.55965788	2.60E-17	Mono and Mac
RP11-219E7.1	2.20E-23	3.56652329	1.23E-18	Mono and Mac
ZBTB18	1.11E-109	3.57265286	6.17E-105	Mono and Mac
NAPSB	0.00E+00	3.57591648	0.00E+00	Mono and Mac
RP11-830F9.5	1.30E-29	3.57739635	7.25E-25	Mono and Mac
TNFSF13	5.80E-247	3.59030845	3.23E-242	Mono and Mac
CTD-2353F22.1	8.95E-40	3.59191222	4.99E-35	Mono and Mac
NTM	7.07E-12	3.59962748	3.94E-07	Mono and Mac
SDK2	5.53E-204	3.60152683	3.08E-199	Mono and Mac
AC104024.2	2.56E-10	3.60310469	1.43E-05	Mono and Mac
PTPN20A	1.04E-10	3.60850805	5.80E-06	Mono and Mac

TCF4	0.00E+00	3.62244844	0.00E+00	Mono and Mac
LRGUK	2.15E-15	3.62815542	1.20E-10	Mono and Mac
RP11-638I2.6	1.47E-88	3.63179273	8.18E-84	Mono and Mac
RP11-190C22.8	2.84E-11	3.63834859	1.58E-06	Mono and Mac
GPM6A	1.52E-11	3.63934885	8.47E-07	Mono and Mac
RP11-216L13.18	3.15E-19	3.64856215	1.75E-14	Mono and Mac
AC010441.1	9.84E-239	3.65251778	5.49E-234	Mono and Mac
LINC00494	3.73E-30	3.65304808	2.08E-25	Mono and Mac
CTD-2011F17.2	6.75E-36	3.65391336	3.76E-31	Mono and Mac
RP11-359E7.2	6.39E-13	3.66262329	3.56E-08	Mono and Mac
RP11-542M13.3	4.31E-52	3.66317539	2.40E-47	Mono and Mac
LRRC18	8.05E-73	3.667536	4.49E-68	Mono and Mac
RBMS3	1.16E-53	3.669575	6.45E-49	Mono and Mac
ZNF629	1.08E-17	3.68706826	6.00E-13	Mono and Mac
TCL1A	3.94E-254	3.6892556	2.20E-249	Mono and Mac
ENAM	3.45E-41	3.70654643	1.92E-36	Mono and Mac
RASD1	2.96E-219	3.70852566	1.65E-214	Mono and Mac
HHAT	8.65E-115	3.71221445	4.82E-110	Mono and Mac
PDZRN3	5.22E-32	3.71650546	2.91E-27	Mono and Mac
RP11-598F7.6	1.65E-09	3.7274007	9.19E-05	Mono and Mac
Z95704.4	5.94E-12	3.73481645	3.31E-07	Mono and Mac
RP11-69H7.4	8.74E-21	3.73568314	4.87E-16	Mono and Mac
AC006028.11	1.68E-25	3.75255411	9.36E-21	Mono and Mac
RP11-443B7.3	3.90E-17	3.75484615	2.18E-12	Mono and Mac
GAL3ST4	9.53E-49	3.75941952	5.31E-44	Mono and Mac
HRNR	2.84E-55	3.76053375	1.58E-50	Mono and Mac
NEK8	2.72E-274	3.7632674	1.52E-269	Mono and Mac
RP11-342D11.2	3.58E-19	3.76491991	2.00E-14	Mono and Mac
MILR1	1.55E-115	3.76566632	8.64E-111	Mono and Mac
PLEKHG4B	2.53E-13	3.76719228	1.41E-08	Mono and Mac
MYO7B	1.16E-96	3.76876073	6.45E-92	Mono and Mac
GAB1	1.89E-289	3.76895646	1.05E-284	Mono and Mac
AC010127.3	3.81E-22	3.77121432	2.12E-17	Mono and Mac
TIGD3	7.50E-44	3.77416866	4.18E-39	Mono and Mac
EPB41L1	1.25E-21	3.77597117	6.99E-17	Mono and Mac
TSKS	1.01E-11	3.78196488	5.64E-07	Mono and Mac
ST14	1.14E-101	3.78420753	6.33E-97	Mono and Mac
CTD-2587H19.1	2.27E-95	3.78560667	1.27E-90	Mono and Mac
KRT6A	7.00E-39	3.79195865	3.90E-34	Mono and Mac
RP11-77H9.8	4.85E-31	3.79209656	2.70E-26	Mono and Mac
AC009495.4	2.86E-36	3.79492456	1.59E-31	Mono and Mac
ST3GAL4	1.08E-179	3.79783766	6.05E-175	Mono and Mac

RP11-11N9.4	2.84E-44	3.7992677	1.58E-39	Mono and Mac
TMEM8B	8.46E-126	3.80586816	4.72E-121	Mono and Mac
SRC	2.32E-240	3.81142154	1.29E-235	Mono and Mac
FLJ00418	4.47E-13	3.81202673	2.49E-08	Mono and Mac
PRKD1	1.99E-12	3.81345227	1.11E-07	Mono and Mac
CHAF1A	4.60E-273	3.81506275	2.56E-268	Mono and Mac
RP11-164P12.3	1.82E-25	3.81697104	1.01E-20	Mono and Mac
CD36	1.21E-210	3.83008438	6.74E-206	Mono and Mac
IQSEC2	2.60E-35	3.83444275	1.45E-30	Mono and Mac
GAS6	1.70E-269	3.84158472	9.45E-265	Mono and Mac
RP11-158M2.4	2.57E-10	3.84806128	1.43E-05	Mono and Mac
LGMNP1	3.00E-174	3.84844804	1.67E-169	Mono and Mac
CTD-3193K9.4	3.26E-36	3.84913245	1.82E-31	Mono and Mac
SUCNR1	4.76E-20	3.86802496	2.66E-15	Mono and Mac
PCDHGB4	2.79E-21	3.87334209	1.56E-16	Mono and Mac
MMP23B	2.09E-78	3.87677687	1.16E-73	Mono and Mac
LPAR3	8.93E-20	3.88153984	4.98E-15	Mono and Mac
FAM129C	0.00E+00	3.88259597	0.00E+00	Mono and Mac
NEGR1	1.44E-17	3.88664133	8.02E-13	Mono and Mac
RP11-1151B14.4	5.54E-23	3.89289091	3.09E-18	Mono and Mac
RP11-701H16.4	1.94E-45	3.89670905	1.08E-40	Mono and Mac
RP11-275F13.1	2.58E-10	3.90398181	1.44E-05	Mono and Mac
RP11-523O18.7	1.01E-16	3.90773217	5.61E-12	Mono and Mac
ARPP21	1.35E-10	3.91058213	7.51E-06	Mono and Mac
TCL6	1.74E-71	3.91567981	9.68E-67	Mono and Mac
RP13-494C23.1	4.29E-31	3.91908334	2.39E-26	Mono and Mac
SLC25A29	2.67E-122	3.93129306	1.49E-117	Mono and Mac
ZFAT	0.00E+00	3.93809636	0.00E+00	Mono and Mac
MTND4P9	5.21E-11	3.93895855	2.91E-06	Mono and Mac
RP11-309M23.1	1.63E-09	3.94503032	9.07E-05	Mono and Mac
MPEG1	0.00E+00	3.95074543	0.00E+00	Mono and Mac
AC008984.7	2.90E-60	3.9525826	1.62E-55	Mono and Mac
SOX4	1.18E-301	3.9650255	6.57E-297	Mono and Mac
PCSK4	1.37E-17	3.96642138	7.64E-13	Mono and Mac
CMKLR1	3.20E-135	3.97142593	1.78E-130	Mono and Mac
RP11-59H7.3	5.62E-17	3.97405593	3.13E-12	Mono and Mac
ZNF321P	3.36E-13	3.99595701	1.87E-08	Mono and Mac
RP11-588K22.2	3.31E-13	4.00636438	1.85E-08	Mono and Mac
AC024592.9	1.95E-14	4.00851254	1.09E-09	Mono and Mac
FLNB-AS1	2.19E-21	4.01199685	1.22E-16	Mono and Mac
RP11-1036E20.7	2.46E-24	4.01339667	1.37E-19	Mono and Mac
SNCA	1.33E-88	4.01519134	7.44E-84	Mono and Mac

SCHIP1	4.32E-15	4.01583208	2.41E-10	Mono and Mac
BEND3P2	4.83E-14	4.02013565	2.69E-09	Mono and Mac
ARHGEF17	8.02E-23	4.02124303	4.47E-18	Mono and Mac
RP11-4O1.2	1.67E-84	4.02702064	9.28E-80	Mono and Mac
CSF2RB	0.00E+00	4.03219609	0.00E+00	Mono and Mac
AC051649.16	5.93E-14	4.0357554	3.31E-09	Mono and Mac
DOCK1	2.25E-42	4.04589541	1.25E-37	Mono and Mac
ZNF521	2.87E-30	4.05007898	1.60E-25	Mono and Mac
RN7SKP69	3.16E-69	4.05702697	1.76E-64	Mono and Mac
THBD	7.01E-248	4.06021881	3.91E-243	Mono and Mac
OPN3	1.34E-100	4.06320142	7.46E-96	Mono and Mac
RP11-216L13.19	1.09E-67	4.07520511	6.10E-63	Mono and Mac
PPP1R14BP3	2.18E-50	4.07818819	1.21E-45	Mono and Mac
CXCR2P1	1.61E-153	4.08612158	8.98E-149	Mono and Mac
ENPP2	2.62E-150	4.08703515	1.46E-145	Mono and Mac
EBF4	2.20E-49	4.08860723	1.23E-44	Mono and Mac
CBFA2T3	1.67E-266	4.08924689	9.33E-262	Mono and Mac
RP11-20E24.1	2.31E-10	4.08992783	1.29E-05	Mono and Mac
RP11-475O6.1	5.28E-23	4.10423182	2.94E-18	Mono and Mac
RP11-162P23.2	7.33E-11	4.10510108	4.09E-06	Mono and Mac
MMRN1	9.81E-27	4.10750395	5.47E-22	Mono and Mac
BAI3	5.93E-12	4.11445079	3.30E-07	Mono and Mac
OR9H1P	2.30E-10	4.11450537	1.28E-05	Mono and Mac
WDR66	1.83E-66	4.11531675	1.02E-61	Mono and Mac
CTD-2653D5.1	2.65E-40	4.11796291	1.47E-35	Mono and Mac
SETP11	4.48E-30	4.11939259	2.50E-25	Mono and Mac
TSPAN1	2.07E-21	4.11988965	1.15E-16	Mono and Mac
SNORA70F	3.15E-19	4.1203028	1.75E-14	Mono and Mac
RP11-504I13.3	2.31E-10	4.12264903	1.29E-05	Mono and Mac
TNNI2	3.16E-99	4.14906643	1.76E-94	Mono and Mac
KB-1958F4.1	2.80E-11	4.15152164	1.56E-06	Mono and Mac
PPP1R14B	1.57E-295	4.15255942	8.76E-291	Mono and Mac
PTK7	1.49E-139	4.15386751	8.31E-135	Mono and Mac
AP001631.9	1.39E-29	4.1629332	7.73E-25	Mono and Mac
CTB-50L17.7	7.45E-31	4.17157432	4.15E-26	Mono and Mac
KIAA1984	4.47E-101	4.17252443	2.49E-96	Mono and Mac
GAPDHP59	1.26E-23	4.17832682	7.03E-19	Mono and Mac
PVRL1	1.94E-186	4.19074222	1.08E-181	Mono and Mac
NPTX2	1.05E-14	4.19737501	5.84E-10	Mono and Mac
KCNE1L	5.96E-14	4.20164282	3.32E-09	Mono and Mac
APP	0.00E+00	4.20575874	0.00E+00	Mono and Mac
CUEDC1	7.36E-34	4.21510518	4.10E-29	Mono and Mac

SPIB	0.00E+00	4.22031384	0.00E+00	Mono and Mac
MMP15	2.06E-15	4.2216217	1.15E-10	Mono and Mac
RP4-799P18.5	7.87E-16	4.22319496	4.39E-11	Mono and Mac
DPPA3	5.07E-20	4.23668219	2.83E-15	Mono and Mac
C10orf112	2.78E-23	4.23843778	1.55E-18	Mono and Mac
LILRB4	0.00E+00	4.24207885	0.00E+00	Mono and Mac
RP11-563N6.6	1.52E-12	4.24362675	8.48E-08	Mono and Mac
RP11-239H6.2	2.48E-10	4.24584818	1.38E-05	Mono and Mac
RP11-598F7.3	5.95E-58	4.24862713	3.32E-53	Mono and Mac
HHIP	9.29E-10	4.25143012	5.18E-05	Mono and Mac
AP000349.1	2.31E-10	4.25217902	1.29E-05	Mono and Mac
UNC93B7	7.94E-14	4.27466255	4.43E-09	Mono and Mac
RP11-619L19.2	1.97E-43	4.28258637	1.10E-38	Mono and Mac
MYBL2	1.95E-270	4.29135105	1.08E-265	Mono and Mac
VASH2	2.84E-84	4.30314349	1.58E-79	Mono and Mac
AC008984.2	9.63E-115	4.30412739	5.37E-110	Mono and Mac
LINC00996	1.45E-289	4.31018745	8.06E-285	Mono and Mac
KLHL33	1.32E-27	4.31163534	7.35E-23	Mono and Mac
RP11-426L16.10	1.65E-31	4.31306324	9.22E-27	Mono and Mac
C6orf25	2.56E-49	4.31529105	1.43E-44	Mono and Mac
TSPAN13	0.00E+00	4.31704877	0.00E+00	Mono and Mac
GAPT	0.00E+00	4.31783272	0.00E+00	Mono and Mac
AC013268.5	3.29E-13	4.32057698	1.83E-08	Mono and Mac
CCR12P	2.31E-10	4.33612284	1.29E-05	Mono and Mac
CTD-3049M7.1	4.94E-14	4.33785099	2.75E-09	Mono and Mac
AC104024.1	2.40E-94	4.33828816	1.34E-89	Mono and Mac
CLLU1OS	4.64E-12	4.34064494	2.58E-07	Mono and Mac
RP11-302F12.5	1.97E-12	4.3449812	1.10E-07	Mono and Mac
CTD-2547E10.3	6.91E-54	4.34584799	3.85E-49	Mono and Mac
AC010761.6	1.56E-153	4.36063364	8.68E-149	Mono and Mac
PAPLN	5.29E-223	4.36663942	2.95E-218	Mono and Mac
BICC1	1.32E-17	4.37520602	7.37E-13	Mono and Mac
HMGB1P21	2.74E-11	4.38423012	1.53E-06	Mono and Mac
RP1-288H2.2	2.31E-10	4.38599602	1.29E-05	Mono and Mac
RP11-379K17.9	1.94E-12	4.38723451	1.08E-07	Mono and Mac
AP001442.2	2.59E-98	4.38813263	1.44E-93	Mono and Mac
RP11-525A16.4	1.48E-29	4.39553356	8.26E-25	Mono and Mac
HOXA9	1.70E-13	4.40610571	9.47E-09	Mono and Mac
CDHR5	2.78E-52	4.40709033	1.55E-47	Mono and Mac
RP11-164P12.4	4.64E-12	4.41105949	2.58E-07	Mono and Mac
NREP	2.47E-246	4.42905296	1.38E-241	Mono and Mac
ATG10-AS1	7.72E-14	4.43344063	4.30E-09	Mono and Mac

AR	7.76E-18	4.43490106	4.32E-13	Mono and Mac
NLRP7	1.26E-87	4.43666941	7.03E-83	Mono and Mac
RP11-478K7.2	3.87E-26	4.43786266	2.16E-21	Mono and Mac
NOTCH4	4.85E-270	4.43978597	2.70E-265	Mono and Mac
RP11-551L14.1	4.72E-145	4.44273407	2.63E-140	Mono and Mac
GPR39	9.49E-27	4.44516815	5.29E-22	Mono and Mac
AC011893.3	2.51E-81	4.45722176	1.40E-76	Mono and Mac
RP11-566K19.6	2.72E-21	4.45765868	1.52E-16	Mono and Mac
AC005307.1	5.12E-11	4.46096019	2.85E-06	Mono and Mac
RHPN1-AS1	1.57E-09	4.46303936	8.78E-05	Mono and Mac
RP11-799B12.4	1.10E-15	4.4720283	6.12E-11	Mono and Mac
CLCN5	5.15E-212	4.48663925	2.87E-207	Mono and Mac
LRP5	1.61E-64	4.48904336	8.98E-60	Mono and Mac
OPRK1	3.28E-13	4.49627627	1.83E-08	Mono and Mac
GUCY1A3	1.81E-82	4.50114372	1.01E-77	Mono and Mac
ZNF556	3.34E-22	4.50285118	1.86E-17	Mono and Mac
P2RY14	0.00E+00	4.50801018	0.00E+00	Mono and Mac
SLC9C2	6.51E-17	4.51069062	3.63E-12	Mono and Mac
RP4-799P18.3	7.93E-16	4.52870009	4.42E-11	Mono and Mac
CDH1	7.16E-214	4.53338985	3.99E-209	Mono and Mac
CYP4F59P	4.02E-30	4.53349075	2.24E-25	Mono and Mac
AC023347.1	2.30E-10	4.54178678	1.28E-05	Mono and Mac
PROC	1.25E-80	4.54253956	6.98E-76	Mono and Mac
RP4-742J24.2	1.53E-12	4.5817975	8.53E-08	Mono and Mac
KDR	1.61E-26	4.58545215	8.95E-22	Mono and Mac
ABCA6	6.35E-62	4.59252473	3.54E-57	Mono and Mac
TDRD1	5.21E-44	4.6000197	2.91E-39	Mono and Mac
WASF1	5.01E-41	4.60450725	2.79E-36	Mono and Mac
GPR87	6.47E-18	4.60939315	3.61E-13	Mono and Mac
SERPINI2	1.60E-09	4.61044922	8.94E-05	Mono and Mac
IGLON5	6.49E-18	4.62698096	3.62E-13	Mono and Mac
AC007327.5	1.92E-12	4.63452714	1.07E-07	Mono and Mac
TNFSF15	3.91E-59	4.66969754	2.18E-54	Mono and Mac
TLR7	0.00E+00	4.67550382	0.00E+00	Mono and Mac
WDR49	3.25E-49	4.67688734	1.81E-44	Mono and Mac
RP11-87C12.5	7.72E-14	4.68359814	4.30E-09	Mono and Mac
FLT3	6.78E-216	4.68406408	3.78E-211	Mono and Mac
GPRC5C	2.08E-58	4.70366456	1.16E-53	Mono and Mac
RP4-799P18.4	1.94E-12	4.70442418	1.08E-07	Mono and Mac
AC018643.4	1.29E-22	4.71016499	7.17E-18	Mono and Mac
CA8	3.31E-30	4.71156167	1.85E-25	Mono and Mac
PPP1R2P4	2.77E-38	4.71557601	1.54E-33	Mono and Mac

OR7E47P	1.67E-13	4.71677978	9.29E-09	Mono and Mac
GLOD5	2.27E-10	4.71747575	1.26E-05	Mono and Mac
RP11-491H9.3	2.69E-11	4.72924439	1.50E-06	Mono and Mac
SUSD1	0.00E+00	4.73218948	0.00E+00	Mono and Mac
PRSS48	1.08E-30	4.73868088	6.04E-26	Mono and Mac
CTD-2315E11.1	4.59E-12	4.7450432	2.56E-07	Mono and Mac
SMIM3	4.04E-47	4.7455594	2.25E-42	Mono and Mac
DTX4	1.06E-143	4.74568445	5.91E-139	Mono and Mac
C5orf20	3.79E-52	4.75179195	2.11E-47	Mono and Mac
IGSF10	1.43E-93	4.75442318	7.96E-89	Mono and Mac
PTPN20CP	7.84E-16	4.75443311	4.37E-11	Mono and Mac
LCN12	8.93E-56	4.7576124	4.98E-51	Mono and Mac
GLDN	2.29E-64	4.76216436	1.27E-59	Mono and Mac
RP11-830F9.6	2.71E-34	4.76237164	1.51E-29	Mono and Mac
VIPR2	2.96E-96	4.76666576	1.65E-91	Mono and Mac
FAM81A	3.29E-57	4.77500877	1.83E-52	Mono and Mac
RP11-104E19.1	3.36E-98	4.77511437	1.87E-93	Mono and Mac
AP003774.4	6.10E-30	4.77626709	3.40E-25	Mono and Mac
DACH1	4.17E-58	4.78225677	2.33E-53	Mono and Mac
FUT7	6.53E-177	4.78927333	3.64E-172	Mono and Mac
ZNF385C	6.66E-61	4.79111868	3.71E-56	Mono and Mac
SMPD3	0.00E+00	4.79463511	0.00E+00	Mono and Mac
NKD2	1.40E-14	4.80662389	7.81E-10	Mono and Mac
FMO3	5.91E-42	4.81431384	3.29E-37	Mono and Mac
ANKRD53	7.99E-128	4.82166401	4.46E-123	Mono and Mac
SCML2	3.42E-46	4.83626465	1.91E-41	Mono and Mac
RP11-1055B8.7	2.22E-43	4.84186483	1.24E-38	Mono and Mac
RP11-163G10.4	1.38E-15	4.84508079	7.67E-11	Mono and Mac
CIB2	4.71E-69	4.84679358	2.62E-64	Mono and Mac
RP3-449M8.6	3.21E-28	4.84742008	1.79E-23	Mono and Mac
AC009970.1	7.77E-18	4.88132605	4.33E-13	Mono and Mac
RP11-3D4.3	2.44E-10	4.88483204	1.36E-05	Mono and Mac
AVPR1B	1.94E-12	4.88753774	1.08E-07	Mono and Mac
RP11-146E23.2	2.27E-10	4.89032517	1.26E-05	Mono and Mac
TIFAB	2.70E-80	4.89800286	1.50E-75	Mono and Mac
BEND6	3.08E-46	4.90374523	1.71E-41	Mono and Mac
AC011515.2	5.45E-47	4.92407568	3.04E-42	Mono and Mac
CTD-3193K9.3	1.18E-45	4.9254734	6.57E-41	Mono and Mac
MMP11	1.62E-57	4.93089161	9.01E-53	Mono and Mac
C17orf99	6.88E-53	4.9325425	3.83E-48	Mono and Mac
KLRF2	2.65E-24	4.93737228	1.48E-19	Mono and Mac
AC023590.1	5.16E-295	4.94258046	2.88E-290	Mono and Mac

RP11-483F11.7	1.96E-14	4.94377968	1.09E-09	Mono and Mac
RP4-593M8.1	4.62E-12	4.94633741	2.57E-07	Mono and Mac
TLR9	0.00E+00	4.95424414	0.00E+00	Mono and Mac
RP5-1092L12.2	1.38E-14	4.96770311	7.68E-10	Mono and Mac
FTLP14	7.63E-14	4.98392842	4.25E-09	Mono and Mac
NRP1	0.00E+00	4.9845524	0.00E+00	Mono and Mac
HESX1	1.10E-71	4.98538705	6.11E-67	Mono and Mac
MMP23A	3.65E-68	4.98658016	2.04E-63	Mono and Mac
FAM221B	1.67E-81	4.99056649	9.31E-77	Mono and Mac
RP11-162D9.3	2.29E-10	5.00023088	1.27E-05	Mono and Mac
P2RY6	0.00E+00	5.00354267	0.00E+00	Mono and Mac
MYCL	2.12E-136	5.01177603	1.18E-131	Mono and Mac
RP11-619L19.1	4.11E-69	5.01220833	2.29E-64	Mono and Mac
CTD-2195B23.3	1.41E-14	5.02242567	7.86E-10	Mono and Mac
AC007092.1	3.16E-19	5.02288212	1.76E-14	Mono and Mac
DNAJC12	4.43E-40	5.07239003	2.47E-35	Mono and Mac
TLCD1	8.11E-86	5.0798068	4.52E-81	Mono and Mac
CALCRL	2.90E-231	5.07996352	1.62E-226	Mono and Mac
FAM213A	0.00E+00	5.08508128	0.00E+00	Mono and Mac
SHROOM2	4.23E-13	5.08999992	2.36E-08	Mono and Mac
GNA11	2.00E-139	5.09397916	1.12E-134	Mono and Mac
RP11-65J21.3	7.84E-21	5.09576981	4.37E-16	Mono and Mac
RP4-647C14.2	1.36E-130	5.10203533	7.60E-126	Mono and Mac
SLC4A3	2.11E-102	5.11583597	1.18E-97	Mono and Mac
RP11-381K20.5	4.55E-12	5.11627425	2.54E-07	Mono and Mac
RP11-332J15.3	5.51E-18	5.11762666	3.07E-13	Mono and Mac
RP4-737E23.2	1.66E-37	5.12336798	9.28E-33	Mono and Mac
SLC35F3	5.46E-82	5.12722192	3.04E-77	Mono and Mac
RP11-75N4.2	6.54E-48	5.13406022	3.65E-43	Mono and Mac
SEMA5A	1.78E-55	5.13923026	9.94E-51	Mono and Mac
PALD1	0.00E+00	5.14164881	0.00E+00	Mono and Mac
C1orf186	0.00E+00	5.1456577	0.00E+00	Mono and Mac
KRT8P5	4.89E-32	5.15815167	2.73E-27	Mono and Mac
LTK	2.29E-184	5.16673215	1.28E-179	Mono and Mac
FGF13	7.57E-14	5.18017755	4.22E-09	Mono and Mac
TUBB3P1	2.47E-10	5.18436806	1.37E-05	Mono and Mac
RP5-826L7.1	1.35E-15	5.19685559	7.50E-11	Mono and Mac
KCTD19	6.35E-84	5.1996531	3.54E-79	Mono and Mac
TTC39A	2.56E-174	5.22656118	1.43E-169	Mono and Mac
SERPINF2	1.18E-239	5.24076719	6.55E-235	Mono and Mac
TMEM210	4.04E-19	5.24933593	2.25E-14	Mono and Mac
INSM1	1.38E-14	5.27113533	7.68E-10	Mono and Mac

CTD-2287O16.4	1.76E-65	5.28525273	9.82E-61	Mono and Mac
FMO6P	5.02E-11	5.28562602	2.80E-06	Mono and Mac
ZFAT-AS1	3.25E-61	5.2946218	1.81E-56	Mono and Mac
NAT8L	1.36E-33	5.32403146	7.60E-29	Mono and Mac
RP4-584D14.5	1.91E-30	5.32909089	1.06E-25	Mono and Mac
FECHP1	4.55E-12	5.33704111	2.54E-07	Mono and Mac
RP11-397C12.1	7.46E-63	5.34984386	4.16E-58	Mono and Mac
PPP1R14A	1.48E-220	5.35233454	8.27E-216	Mono and Mac
AEBP1	1.72E-266	5.3584613	9.61E-262	Mono and Mac
COBL	4.11E-117	5.35950831	2.29E-112	Mono and Mac
AGR2	3.84E-26	5.36069325	2.14E-21	Mono and Mac
RP11-154H12.3	1.96E-14	5.37286674	1.09E-09	Mono and Mac
PFKFB2	0.00E+00	5.37381734	0.00E+00	Mono and Mac
PCDHGC3	8.52E-81	5.40201838	4.75E-76	Mono and Mac
RP11-38J22.6	0.00E+00	5.40263668	0.00E+00	Mono and Mac
RP11-1036E20.9	2.08E-80	5.40335469	1.16E-75	Mono and Mac
RP11-439L8.4	1.06E-40	5.40613989	5.89E-36	Mono and Mac
KLHL13	3.77E-21	5.40871601	2.10E-16	Mono and Mac
NME8	5.40E-285	5.41292075	3.01E-280	Mono and Mac
PLD4	0.00E+00	5.4146175	0.00E+00	Mono and Mac
RN7SL436P	2.58E-27	5.41863292	1.44E-22	Mono and Mac
GLT1D1	1.55E-252	5.43696957	8.65E-248	Mono and Mac
SH3BP4	2.35E-236	5.46453343	1.31E-231	Mono and Mac
LYPD8	7.61E-18	5.4656438	4.24E-13	Mono and Mac
OR52N3P	7.51E-14	5.47206623	4.18E-09	Mono and Mac
AOX2P	1.19E-29	5.47804201	6.63E-25	Mono and Mac
HHIP-AS1	3.60E-33	5.48791892	2.01E-28	Mono and Mac
SLC7A11	2.25E-263	5.50574781	1.25E-258	Mono and Mac
IL3RA	0.00E+00	5.51870983	0.00E+00	Mono and Mac
DPPA4	7.20E-118	5.52505789	4.02E-113	Mono and Mac
CTSE	3.08E-104	5.52936587	1.72E-99	Mono and Mac
AC024580.1	5.10E-24	5.55218954	2.84E-19	Mono and Mac
TNFRSF11B	3.39E-16	5.55254694	1.89E-11	Mono and Mac
PTGDS	0.00E+00	5.5598459	0.00E+00	Mono and Mac
RP11-2O17.2	2.14E-24	5.5623268	1.19E-19	Mono and Mac
IGHVII-74-1	1.95E-14	5.56365919	1.09E-09	Mono and Mac
AC008984.6	3.47E-40	5.57338445	1.93E-35	Mono and Mac
KCNA5	6.74E-63	5.5819804	3.76E-58	Mono and Mac
PACSIN1	0.00E+00	5.59009288	0.00E+00	Mono and Mac
SEMA3C	6.06E-230	5.64627781	3.38E-225	Mono and Mac
CTB-50L17.9	1.82E-104	5.66352625	1.02E-99	Mono and Mac
MSRB3	2.52E-89	5.67174512	1.40E-84	Mono and Mac

RP3-416J7.4	2.12E-126	5.67673795	1.18E-121	Mono and Mac
OR3A3	1.85E-30	5.68304006	1.03E-25	Mono and Mac
GP5	7.97E-35	5.69188192	4.44E-30	Mono and Mac
SIGLEC6	1.02E-277	5.69924277	5.69E-273	Mono and Mac
AC007880.1	6.91E-194	5.70587385	3.85E-189	Mono and Mac
RP11-306K13.1	1.87E-30	5.71759115	1.04E-25	Mono and Mac
S100A3	3.95E-19	5.72704855	2.20E-14	Mono and Mac
HOXA-AS4	4.53E-12	5.72877594	2.53E-07	Mono and Mac
RP5-1031D4.2	1.42E-94	5.73574884	7.93E-90	Mono and Mac
PTPRS	0.00E+00	5.76789668	0.00E+00	Mono and Mac
SMOC1	1.89E-84	5.77714263	1.05E-79	Mono and Mac
AC007319.1	1.04E-30	5.78250447	5.82E-26	Mono and Mac
PLXNA4	0.00E+00	5.79571946	0.00E+00	Mono and Mac
RP11-356M20.1	2.21E-50	5.79923279	1.23E-45	Mono and Mac
CYP46A1	1.56E-180	5.80331912	8.71E-176	Mono and Mac
MAP1A	0.00E+00	5.80804628	0.00E+00	Mono and Mac
CTD-3073N11.9	3.28E-263	5.81726622	1.83E-258	Mono and Mac
AC005262.3	8.06E-66	5.81984659	4.49E-61	Mono and Mac
PPM1J	4.06E-265	5.82148865	2.26E-260	Mono and Mac
GRIN1	1.41E-14	5.8249357	7.84E-10	Mono and Mac
EGLN3	0.00E+00	5.89885723	0.00E+00	Mono and Mac
RP11-1036E20.10	2.37E-53	5.92140147	1.32E-48	Mono and Mac
AC005262.2	2.50E-41	5.93298178	1.39E-36	Mono and Mac
SYCP2L	8.36E-103	5.95381246	4.66E-98	Mono and Mac
AC007381.3	3.08E-194	5.95496806	1.72E-189	Mono and Mac
C4BPB	1.58E-87	5.97900973	8.79E-83	Mono and Mac
TNFRSF21	0.00E+00	5.97925678	0.00E+00	Mono and Mac
SLITRK5	1.47E-12	6.00680394	8.20E-08	Mono and Mac
SCAMP5	0.00E+00	6.02615183	0.00E+00	Mono and Mac
RP11-76E17.3	0.00E+00	6.04023008	0.00E+00	Mono and Mac
RP3-436N22.3	2.40E-27	6.06622065	1.34E-22	Mono and Mac
RP11-137H2.6	2.50E-107	6.07674463	1.39E-102	Mono and Mac
ASIP	2.63E-178	6.09644851	1.47E-173	Mono and Mac
TPM2	0.00E+00	6.09705973	0.00E+00	Mono and Mac
SERPINF1	0.00E+00	6.10622117	0.00E+00	Mono and Mac
RP11-17P16.2	5.00E-25	6.12885687	2.79E-20	Mono and Mac
RP11-418J17.3	2.13E-94	6.15073068	1.19E-89	Mono and Mac
LRRC36	7.63E-175	6.15337863	4.25E-170	Mono and Mac
AC011625.1	7.61E-21	6.25371035	4.24E-16	Mono and Mac
AC018634.9	6.94E-273	6.29109007	3.87E-268	Mono and Mac
RP11-100G15.10	5.00E-25	6.30477678	2.79E-20	Mono and Mac
KIRREL3	2.84E-138	6.33171585	1.58E-133	Mono and Mac

SMIM5	0.00E+00	6.38326781	0.00E+00	Mono and Mac
LEPREL1	8.51E-296	6.40494075	4.74E-291	Mono and Mac
FAM160A1	2.80E-292	6.41868686	1.56E-287	Mono and Mac
RN7SL794P	1.04E-50	6.42451247	5.81E-46	Mono and Mac
AHNAK2	1.20E-247	6.4272241	6.70E-243	Mono and Mac
RET	2.22E-170	6.43102945	1.24E-165	Mono and Mac
RP1-302G2.5	1.79E-152	6.44001541	9.99E-148	Mono and Mac
RP11-117D22.2	0.00E+00	6.44752589	0.00E+00	Mono and Mac
RP11-151H2.1	7.47E-21	6.4563744	4.16E-16	Mono and Mac
AC007381.2	1.71E-242	6.49595678	9.56E-238	Mono and Mac
DNASE1L3	0.00E+00	6.49671632	0.00E+00	Mono and Mac
SCARA5	7.69E-159	6.49895842	4.29E-154	Mono and Mac
RP11-637O19.3	1.63E-44	6.50000408	9.07E-40	Mono and Mac
RP11-61E11.1	5.44E-18	6.5164284	3.03E-13	Mono and Mac
CTD-2003C8.2	2.46E-104	6.54123397	1.37E-99	Mono and Mac
RP11-240E2.2	6.96E-149	6.55223081	3.88E-144	Mono and Mac
LCNL1	2.44E-124	6.58125636	1.36E-119	Mono and Mac
CTD-2117L12.3	5.40E-18	6.62736405	3.01E-13	Mono and Mac
SCN9A	0.00E+00	6.64441724	0.00E+00	Mono and Mac
C5orf64	1.08E-117	6.65058089	5.99E-113	Mono and Mac
COL24A1	0.00E+00	6.6653364	0.00E+00	Mono and Mac
SMIM6	6.69E-138	6.66938298	3.73E-133	Mono and Mac
DSG2	1.36E-118	6.70716913	7.60E-114	Mono and Mac
CRYM	1.04E-192	6.71088455	5.78E-188	Mono and Mac
RP11-542M13.2	4.87E-86	6.71294541	2.71E-81	Mono and Mac
RP5-1119D9.4	1.75E-30	6.71949545	9.76E-26	Mono and Mac
PLVAP	0.00E+00	6.7242175	0.00E+00	Mono and Mac
RN7SL854P	1.16E-46	6.7331405	6.46E-42	Mono and Mac
GUCY2D	0.00E+00	6.78027366	0.00E+00	Mono and Mac
SLC25A47P1	7.71E-79	6.81666874	4.30E-74	Mono and Mac
SLC12A3	0.00E+00	6.84023768	0.00E+00	Mono and Mac
FAM196A	3.36E-214	6.90480934	1.87E-209	Mono and Mac
LILRA4	0.00E+00	6.90687503	0.00E+00	Mono and Mac
LINC00865	1.22E-264	6.90991508	6.80E-260	Mono and Mac
NEFLP1	1.54E-27	6.91212246	8.60E-23	Mono and Mac
RGS7	1.15E-120	6.94900448	6.40E-116	Mono and Mac
CTD-2132N18.4	2.06E-48	6.97190895	1.15E-43	Mono and Mac
RP11-731D1.4	8.96E-135	7.0055399	5.00E-130	Mono and Mac
CRYM-AS1	0.00E+00	7.05688183	0.00E+00	Mono and Mac
PLEKHD1	0.00E+00	7.05850653	0.00E+00	Mono and Mac
CADM4	9.38E-115	7.13400558	5.23E-110	Mono and Mac
PLCB4	2.45E-91	7.15186213	1.36E-86	Mono and Mac

EPHA2	0.00E+00	7.16426669	0.00E+00	Mono and Mac
AP001631.10	5.10E-81	7.16976658	2.84E-76	Mono and Mac
RP11-783K16.5	1.25E-123	7.17758406	6.97E-119	Mono and Mac
RP11-76E17.4	2.44E-109	7.29114943	1.36E-104	Mono and Mac
RP3-322L4.2	2.42E-100	7.31427031	1.35E-95	Mono and Mac
EPHB1	0.00E+00	7.33157138	0.00E+00	Mono and Mac
KCNK10	0.00E+00	7.34065486	0.00E+00	Mono and Mac
LAMP5	0.00E+00	7.45075727	0.00E+00	Mono and Mac
RP11-248C1.3	3.32E-205	7.47111503	1.85E-200	Mono and Mac
CUX2	0.00E+00	7.5299452	0.00E+00	Mono and Mac
LRCOL1	4.70E-149	7.56350647	2.62E-144	Mono and Mac
P2RX2	1.04E-64	7.64609855	5.81E-60	Mono and Mac
RP11-456A14.1	4.86E-25	7.66039063	2.71E-20	Mono and Mac
CYYR1	3.26E-262	7.73644431	1.81E-257	Mono and Mac
CTC-782O7.1	2.61E-205	7.76695169	1.45E-200	Mono and Mac
AC114494.1	2.60E-31	7.87739374	1.45E-26	Mono and Mac
DRD4	1.26E-136	8.07225024	7.02E-132	Mono and Mac
SRPX	5.16E-63	8.12243901	2.88E-58	Mono and Mac
RP11-610P16.1	7.16E-165	8.13174954	3.99E-160	Mono and Mac
RP11-439L8.3	1.03E-273	8.42229971	5.73E-269	Mono and Mac
RP11-350O14.18	1.61E-135	8.47055848	9.00E-131	Mono and Mac
KCNK17	4.84E-299	8.5141856	2.70E-294	Mono and Mac
RP1-288H2.4	6.83E-24	8.5400124	3.81E-19	Mono and Mac
RP11-775A1.2	6.83E-24	8.59872396	3.81E-19	Mono and Mac
RP11-476B1.1	9.43E-247	8.70118796	5.26E-242	Mono and Mac
RP11-203M5.6	7.19E-292	8.72568476	4.01E-287	Mono and Mac
KRT5	0.00E+00	8.73308893	0.00E+00	Mono and Mac
CLEC4C	0.00E+00	8.78419608	0.00E+00	Mono and Mac
LRRC26	0.00E+00	8.95346784	0.00E+00	Mono and Mac
PTCRA	0.00E+00	9.11263612	0.00E+00	Mono and Mac
COL26A1	2.56E-306	9.11374421	1.43E-301	Mono and Mac
RP1-45C12.1	4.04E-46	9.18261442	2.25E-41	Mono and Mac
SHD	2.61E-234	9.19455797	1.46E-229	Mono and Mac
EGLN3-AS1	4.09E-120	9.42004126	2.28E-115	Mono and Mac
RP11-71G12.1	0.00E+00	9.70448997	0.00E+00	Mono and Mac
RN7SKP143	2.65E-68	9.74910895	1.47E-63	Mono and Mac
SCT	0.00E+00	9.84774533	0.00E+00	Mono and Mac
SLC32A1	0.00E+00	10.0133803	0.00E+00	Mono and Mac
RP11-73G16.2	0.00E+00	10.2650274	0.00E+00	Mono and Mac
RNU1-32P	1.07E-75	10.4932346	5.97E-71	Mono and Mac
LGR6	1.26E-15	2.03930505	7.01E-11	NK/NKT
TXK	3.37E-60	2.07831548	1.88E-55	NK/NKT

GS1-115G20.1	1.62E-13	2.11606076	9.03E-09	NK/NKT
TMEM232	1.78E-15	2.11889615	9.90E-11	NK/NKT
GNLY	3.44E-157	2.13344673	1.92E-152	NK/NKT
KIR2DL3	1.31E-34	2.15261523	7.28E-30	NK/NKT
SIGLEC17P	4.04E-13	2.16362675	2.25E-08	NK/NKT
KIR2DP1	2.14E-21	2.1810139	1.19E-16	NK/NKT
OSBPL5	9.64E-34	2.20410898	5.37E-29	NK/NKT
NCR1	3.61E-55	2.23408051	2.01E-50	NK/NKT
RP11-20I20.4	2.24E-15	2.25561384	1.25E-10	NK/NKT
C1orf21	9.84E-93	2.26069505	5.49E-88	NK/NKT
MYOM2	7.75E-10	2.29578326	4.32E-05	NK/NKT
HRASLS2	4.30E-28	2.30561843	2.39E-23	NK/NKT
KIR2DS4	1.01E-35	2.38319585	5.62E-31	NK/NKT
NMUR1	7.88E-36	2.40475475	4.39E-31	NK/NKT
KIR3DP1	1.73E-10	2.43111453	9.64E-06	NK/NKT
TRGV8	8.02E-117	2.46819861	4.47E-112	NK/NKT
BNC2	4.65E-13	2.46847369	2.59E-08	NK/NKT
TRGV9	1.42E-101	2.47470911	7.91E-97	NK/NKT
KLRC1	9.42E-109	2.48131897	5.25E-104	NK/NKT
PRSS23	3.47E-34	2.5356801	1.93E-29	NK/NKT
KIR2DL1	5.93E-26	2.5555145	3.31E-21	NK/NKT
RP11-121A8.1	4.08E-12	2.61026005	2.28E-07	NK/NKT
FGFBP2	9.96E-79	2.62216418	5.55E-74	NK/NKT
FEZ1	5.49E-15	2.63193275	3.06E-10	NK/NKT
PDGFRB	5.84E-15	2.7082424	3.26E-10	NK/NKT
C1orf177	1.19E-09	2.73094417	6.62E-05	NK/NKT
AKR1C3	1.48E-20	2.75146909	8.26E-16	NK/NKT
KIR3DL1	4.01E-42	2.77353391	2.24E-37	NK/NKT
KIR3DL2	6.66E-84	2.81036894	3.71E-79	NK/NKT
LIM2	4.58E-11	2.8168037	2.55E-06	NK/NKT
LINGO2	1.22E-12	2.82167818	6.82E-08	NK/NKT
PPP1R9A	1.01E-11	2.87877195	5.65E-07	NK/NKT
AC017104.6	3.39E-21	2.88196057	1.89E-16	NK/NKT
S1PR5	1.61E-86	2.89582938	9.00E-82	NK/NKT
SLC1A7	5.32E-10	3.01324211	2.97E-05	NK/NKT
B3GNT7	1.54E-80	3.02537434	8.61E-76	NK/NKT
LDB2	1.94E-10	3.08631078	1.08E-05	NK/NKT
SLCO4C1	3.80E-12	3.09778	2.12E-07	NK/NKT
SH2D1B	1.06E-77	3.20907909	5.89E-73	NK/NKT
DLL1	7.43E-12	3.23301834	4.14E-07	NK/NKT
GPR97	1.26E-15	3.34620873	7.03E-11	NK/NKT
KRT81	1.40E-09	3.36286935	7.80E-05	NK/NKT

CXCR1	8.84E-11	3.44908598	4.93E-06	NK/NKT
AC092566.1	1.21E-23	3.53208644	6.73E-19	NK/NKT
NCAM1	1.05E-90	4.02290568	5.87E-86	NK/NKT
PRSS57	1.99E-11	4.26129527	1.11E-06	NK/NKT
TRGV11	6.66E-14	4.29269672	3.71E-09	NK/NKT
MLC1	2.71E-70	4.38464308	1.51E-65	NK/NKT
KLRF1	1.60E-163	4.40334185	8.89E-159	NK/NKT
NCAM1-AS1	2.06E-34	4.84597932	1.15E-29	NK/NKT
TRDV3	1.08E-60	4.99595455	6.03E-56	NK/NKT
AE000661.37	0.00E+00	5.11205045	0.00E+00	NK/NKT
TRDV1	0.00E+00	5.4909503	0.00E+00	NK/NKT
SPTSSB	1.07E-33	6.21382172	5.94E-29	NK/NKT
TRDC	0.00E+00	6.47506391	0.00E+00	NK/NKT
TRDV2	2.25E-194	8.50628436	1.25E-189	NK/NKT
IL7	3.29E-18	2.02656903	1.84E-13	Treg
TNFRSF18	1.04E-146	2.05266015	5.82E-142	Treg
ADTRP	1.56E-17	2.06783709	8.72E-13	Treg
BTNL9	1.36E-09	2.07604923	7.57E-05	Treg
EBI3	8.00E-24	2.1037627	4.46E-19	Treg
TBC1D4	7.57E-146	2.10577831	4.22E-141	Treg
RP11-53B2.5	1.10E-21	2.11012511	6.12E-17	Treg
LTA	1.51E-55	2.13877637	8.44E-51	Treg
CCL20	1.67E-21	2.14333222	9.34E-17	Treg
MIR146A	2.25E-28	2.18681008	1.26E-23	Treg
LAYN	2.93E-82	2.18920276	1.63E-77	Treg
COL9A2	1.58E-28	2.21185474	8.83E-24	Treg
RP11-691H4.4	3.69E-12	2.21259737	2.06E-07	Treg
RP11-265P11.2	4.37E-18	2.22592913	2.43E-13	Treg
RP11-242C19.2	1.16E-25	2.22850132	6.49E-21	Treg
RP11-624L4.1	3.63E-17	2.23050961	2.02E-12	Treg
CEACAM1	1.99E-32	2.23878656	1.11E-27	Treg
SETD7	2.28E-23	2.24438689	1.27E-18	Treg
ECSCR	6.97E-10	2.24737289	3.88E-05	Treg
PPP1R3F	8.89E-17	2.2474139	4.96E-12	Treg
NGFRAP1	9.42E-27	2.26828243	5.25E-22	Treg
ZG16B	3.85E-11	2.27518705	2.15E-06	Treg
RP11-53B2.4	4.81E-13	2.29217229	2.68E-08	Treg
XKR9	2.17E-12	2.29524272	1.21E-07	Treg
LOXL1-AS1	2.03E-19	2.29744773	1.13E-14	Treg
HPGD	1.74E-30	2.29823452	9.70E-26	Treg
SAMSN1-AS1	1.40E-09	2.30040878	7.79E-05	Treg
ARHGEF10	1.77E-10	2.31462343	9.85E-06	Treg

EPHX2	2.50E-56	2.32385857	1.39E-51	Treg
CCR4	6.20E-98	2.32646647	3.46E-93	Treg
PDGFA	1.91E-41	2.33524398	1.06E-36	Treg
NTNG2	1.33E-32	2.35567257	7.40E-28	Treg
PRKCDBP	3.42E-12	2.3565174	1.91E-07	Treg
TRIM16	4.41E-27	2.36896362	2.46E-22	Treg
LAIR2	1.33E-46	2.39448385	7.40E-42	Treg
IKZF2	1.78E-161	2.3971794	9.93E-157	Treg
RP11-316P17.2	1.58E-30	2.40369624	8.83E-26	Treg
PTP4A3	2.62E-65	2.40588963	1.46E-60	Treg
ANKRD30B	6.65E-13	2.40809432	3.71E-08	Treg
SERPINE2	3.06E-31	2.41309886	1.71E-26	Treg
RP11-214O1.2	8.99E-14	2.43059242	5.01E-09	Treg
MCAM	3.89E-26	2.43832847	2.17E-21	Treg
ZC2HC1A	6.16E-30	2.44204173	3.43E-25	Treg
RP11-53B2.1	2.80E-24	2.46421696	1.56E-19	Treg
TNFRSF4	7.97E-171	2.48585976	4.44E-166	Treg
LDLRAD4-AS1	2.25E-37	2.53810278	1.26E-32	Treg
RP11-214O1.3	2.25E-56	2.57160469	1.25E-51	Treg
FBLN7	8.04E-87	2.57721897	4.48E-82	Treg
RP11-62H7.2	2.01E-19	2.61021796	1.12E-14	Treg
PDE9A	2.67E-13	2.61616742	1.49E-08	Treg
AC074289.1	2.28E-33	2.62647262	1.27E-28	Treg
AC007182.6	1.15E-20	2.67206051	6.40E-16	Treg
EMR1	2.39E-21	2.72326557	1.33E-16	Treg
STAC	2.92E-23	2.72413889	1.63E-18	Treg
ICA1	3.59E-94	2.75057029	2.00E-89	Treg
CCL22	6.66E-18	2.76900867	3.71E-13	Treg
IKZF4	2.00E-99	2.77686824	1.11E-94	Treg
RP11-887P2.6	2.32E-26	2.78107171	1.29E-21	Treg
FTH1P24	3.36E-10	2.79096479	1.87E-05	Treg
PTGIR	6.97E-18	2.81755549	3.88E-13	Treg
IL23R	1.04E-26	2.82210181	5.78E-22	Treg
RP11-345M22.1	6.32E-25	2.83209004	3.52E-20	Treg
AF165138.7	1.19E-09	2.83260402	6.63E-05	Treg
ACTG2	2.80E-13	2.85854419	1.56E-08	Treg
GRPEL2-AS1	3.21E-14	2.86117611	1.79E-09	Treg
RP11-469A15.2	1.22E-12	2.86660838	6.81E-08	Treg
CTSV	1.15E-09	2.87248958	6.43E-05	Treg
HOXA1	9.92E-11	2.87684647	5.53E-06	Treg
TMEM136	3.61E-10	2.95295067	2.01E-05	Treg
RP11-62C7.2	4.21E-22	2.98604688	2.35E-17	Treg

BCAS1	3.26E-18	3.00241628	1.82E-13	Treg
COL5A1	1.70E-12	3.01153708	9.46E-08	Treg
MYO5C	1.48E-11	3.02891519	8.27E-07	Treg
C15orf53	6.55E-45	3.03093378	3.65E-40	Treg
AC002331.1	1.97E-48	3.05532882	1.10E-43	Treg
RP11-345M22.2	2.05E-28	3.1016059	1.14E-23	Treg
DLGAP1-AS5	2.88E-10	3.14187801	1.61E-05	Treg
RN7SL630P	1.65E-23	3.15961334	9.21E-19	Treg
ANK1	9.09E-41	3.16581027	5.07E-36	Treg
TNFRSF8	3.50E-51	3.2085229	1.95E-46	Treg
CYP7B1	5.08E-33	3.25462984	2.83E-28	Treg
FAM78B	5.07E-10	3.29235612	2.83E-05	Treg
TWIST1	6.15E-18	3.32536729	3.43E-13	Treg
RP11-98G13.1	4.30E-20	3.34119181	2.39E-15	Treg
IL12RB2	1.47E-303	3.34722456	8.21E-299	Treg
SELP	3.88E-30	3.35642013	2.17E-25	Treg
TMPRSS6	9.53E-33	3.36766587	5.31E-28	Treg
CDKL2	2.61E-21	3.42064352	1.45E-16	Treg
PTPLA	3.79E-42	3.46648017	2.11E-37	Treg
RTKN2	1.51E-253	3.50741799	8.44E-249	Treg
CHRNA6	3.37E-15	3.52664694	1.88E-10	Treg
RP11-603B24.1	5.97E-109	3.67934608	3.33E-104	Treg
IL1R2	1.57E-124	3.68778819	8.72E-120	Treg
RP5-1170K4.7	2.92E-20	3.74508722	1.63E-15	Treg
PLCL1	1.45E-24	3.75168901	8.08E-20	Treg
DLGAP1	3.20E-90	3.85557343	1.79E-85	Treg
IL2RA	0.00E+00	3.86966915	0.00E+00	Treg
RP11-1060G2.1	4.04E-10	3.8883389	2.25E-05	Treg
ADAM12	2.47E-61	3.89553931	1.38E-56	Treg
RP11-944C7.1	3.36E-11	3.92887272	1.87E-06	Treg
F5	1.13E-291	3.9466364	6.30E-287	Treg
AE000658.31	3.37E-11	3.98986232	1.88E-06	Treg
HNRNPA1P21	2.94E-110	4.06932839	1.64E-105	Treg
IL17REL	2.98E-17	4.07283632	1.66E-12	Treg
IL1RL1	8.19E-56	4.07956845	4.57E-51	Treg
RP11-21J7.1	1.68E-69	4.09474483	9.39E-65	Treg
LAPTM4B	9.55E-41	4.10963378	5.32E-36	Treg
RP11-94H18.1	3.66E-20	4.14437379	2.04E-15	Treg
RP11-856F16.2	1.24E-11	4.15126884	6.90E-07	Treg
LRRC32	2.55E-122	4.18846432	1.42E-117	Treg
DNAH8	9.32E-76	4.22638387	5.20E-71	Treg
AC007271.3	6.81E-13	4.23921449	3.80E-08	Treg

RN7SL89P	1.25E-13	4.29188686	6.98E-09	Treg
HLF	1.66E-60	4.30444163	9.26E-56	Treg
RP11-536K7.5	1.31E-52	4.30971153	7.33E-48	Treg
IL1R1	1.89E-139	4.31355018	1.05E-134	Treg
GNG8	2.13E-31	4.55804397	1.18E-26	Treg
CASP1P2	2.24E-130	4.59389501	1.25E-125	Treg
AC145110.1	5.08E-169	4.63212797	2.83E-164	Treg
SNORA14	5.89E-33	4.83156746	3.28E-28	Treg
CCR8	0.00E+00	4.8927286	0.00E+00	Treg
LINC00519	2.26E-41	5.005753	1.26E-36	Treg
AC011997.1	7.79E-16	5.04523481	4.34E-11	Treg
LINC00589	1.45E-41	5.21408247	8.06E-37	Treg
AKR1C6P	2.19E-34	5.39128345	1.22E-29	Treg
RP11-138C24.2	8.44E-24	5.55576161	4.70E-19	Treg
FANK1	2.27E-86	5.60119052	1.26E-81	Treg
CTC-490G23.2	8.91E-37	5.82691405	4.97E-32	Treg
RPL23AP22	1.62E-15	6.08714257	9.03E-11	Treg
CD177	6.99E-79	6.13527823	3.89E-74	Treg
RP1-207H1.3	1.58E-96	6.16641416	8.82E-92	Treg
CD177P1	1.11E-83	6.57226778	6.18E-79	Treg
FOXP3	0	8.13409715	0	Treg
RP11-462G2.1	3.49E-22	9.21712869	1.94E-17	Treg

Table D.5 Differential gene expression between cell clusters enriched in TILs derived from melanoma patients at baseline/ anti-PD-1-treated conditions including adjusted p-value and log_2-fold change.

Appendix E

WT and *Pd1*$^{-/-}$ mice were subcutaneously injected with B16F10 melanoma cells on d0 and the TILs were harvested from tumours on d14 for BD Rhapsody scRNA-seq (n=5/cohort). An unsupervised clustering of data was performed by using PhenoGraph plugin in SeqGeq™ with a k value of 87 applied. By using iCellR plugin, differential expression analysis was performed between cell clusters, and genes were considered differentially expressed when they achieved fold change ≥ 1.5 and a q-value cutoff of 0.05 in cluster 01 **(Table E.1)**, cluster 05 **(Table E.2)** and cluster 10 **(Table E.3)**.

Genes	**Fold-Change**	**q-Value**
CD335 (Ab)	8.539192448	2.34E-102
NK-1.1 (Ab)	6.116636848	1.02E-119
Bcl2	2.524708553	1.41E-21
Cd244	2.100546478	1.30E-06
Eomes	9.764703795	2.05E-81
Gzma	40.53598285	4.32E-121
Gzmb	3.72726915	3.57E-20
Ifng	2.276813913	7.86E-12
Il18rap	3.359760017	8.83E-87
Klra1	7.339119151	7.84E-46
Klra21	21.31431755	9.61E-32
Klra3	9.601043941	1.38E-16
Klra6	2.926724282	5.38E-08
Klra7	14.06593596	3.01E-87
Klrb1	12.06313835	5.38E-05
Klrc1	6.202240635	2.83E-121
Klrc3	19.8001857	1.04E-05
Klrg1	2.48630128	5.41E-06
Klrk1	4.703514701	1.18E-119
Prf1	4.451682023	1.23E-13
Stat4	2.209646679	2.85E-47
Tbx21	3.617020043	2.46E-52
Tnfsf14	2.15392834	5.57E-05
Xcl1	11.99625944	3.91E-33

Table E.1 Marker gene details for the Cluster 01 enriched in TILs derived from murine including adjusted q-value and log_2-fold change.

Genes	Fold-Change	q-Value
CD3:145-2C11 (Ab)	4.96555237	1.17E-65
Bach2	2.15638876	0.00139794
Il7r	2.78485279	2.36E-19
Tcf7	4.05092914	8.96E-64
Tnfsf8	2.12935051	0.01620748

Table E.2 Marker gene details for the Cluster 05 enriched in TILs derived from murine including adjusted q-value and log_2-fold change.

Genes	Fold-Change	q-Value
CD223 (Ab)	11.62154814	7.09E-06
CD279:J43 (Ab)	4.118801242	0.001536206
Bax	2.627713697	1.19E-11
Bcl2a1a	6.465066203	3.46E-23
Cd247	4.728934863	5.33E-21
Cd28	3.440226789	5.25E-08
Ctla4	4.182252673	2.25E-06
Eomes	2.683573708	7.01E-06
Gzmb	8.499340215	2.28E-13
Gzmk	21.93989374	3.19E-16
Ifng	9.481308258	4.08E-07
Klrc1	2.750404159	1.33E-06
Lag3	24.10510323	2.30E-17
Prf1	12.84582186	5.45E-08
Stat4	2.232826133	7.61E-08
Tbx21	2.849084918	1.18E-07
Tigit	10.21080457	4.19E-22
Tnfrsf18	2.385246729	2.23E-06
Tnfrsf1b	3.533903183	4.30E-14
Tnfrsf4	3.816779548	0.000804157
Tnfrsf9	6.903898642	4.88E-16
Tnfsf10	4.462782678	0.001536206
Tnfsf13b	11.81004684	0.010407342

Table E.3 Marker gene details for the Cluster 10 enriched in TILs derived from murine including adjusted q-value and log_2-fold change.

Appendix F

Publications

Lim JX, McTaggart T, Jung SK, Smith KJ, Hulme G, Laba S, Ng YQ, Williams A, Hussain R, Coxhead J, Cosgarea I. PD-1 receptor deficiency enhances CD30+ Treg cell function in melanoma. Nature Immunology. 2025 Jun 2:1-3.

Resistance to anti-PD-1 therapy is driven by CD30+ regulatory T cell activity. Nature Immunology Research Briefing. 2025 Jun 10.

McTaggart T, **Lim JX**, Smith KJ, Heaney B, McDonald D, Hulme G, Hussain R, Coxhead J, Mann DA, Sayer AA, Granic A. Deciphering novel communication patterns in T regulatory cells from very old adults. Aging Cell. 2025 Mar 18:e70044.

McTaggart T*, **Lim JX***, Smith KJ, Heaney B, McDonald D, Hulme G, Hussain R, Coxhead J, Degnan AE, Isaacs J, Pratt A. Deep phenotyping of T regulatory cells in psoriatic arthritis highlights targetable mechanisms of disease. Journal of Biological Chemistry. 2025 Jan 1;301(1).

Lim JX, Lai CY, Mallett GE, McDonald D, Hulme G, Laba S, Shapanis A, Payne M, Patterson W, Alexander M, Coxhead J. Programmed cell death-1 receptor-mediated regulation of Tbet+ NK1. 1− innate lymphoid cells within the tumor microenvironment. Proceedings of the National Academy of Sciences. 2023 May 2;120(18):e2216587120.

Posters and Presentations

53rd Annual European Society for Dermatological Research Meeting. 5 September 2024. Oral and Poster presentations: Resistance to anti-PD1 therapy is driven by CD30+ T regulatory cells in melanoma.

Nature Conferences for Cancer Immunotherapy: From bench to bedside and back. 10 Jun 2024. Poster: Programmed cell death-1 receptor deficiency drives non-redundant regulatory mechanisms in T regulatory cells in melanoma.

British Society Immunology Meeting: Revealing and tackling complexities of the tumour microenvironment. 14 March 2024. Poster: Programmed cell death-1 receptor deficiency drives non-redundant regulatory mechanisms in T regulatory cells.

Newcastle University Centre for Cancer for Research-in-Progress Talk. 05 January 2024. Oral presentation: Resistance to immune checkpoint inhibitor is driven by CD30.

Newcastle University Centre for Cancer for PGR Conference 2023. 01 December 2023. Oral presentation: Hyper-progressive disease after checkpoint therapy is driven by CD30.

British Society Immunology for BSI Congress 2022. 05 December 2022. Poster: Programmed cell death-1 receptor controls a multi-layered regulatory axis in T regulatory cells within the tumour microenvironment.

Newcastle University Centre for Cancer for Research-in-Progress Talk. 20 October 2022. Oral presentation: Artificially imprinted antibodies against checkpoint receptor PD1.